NEW DRUG TARGETS FOR PROTEOTOXICITY IN CARDIOMETABOLIC DISEASES

EDITED BY: Jun Ren, Xin Wang and Ying Mei Zhang

PUBLISHED IN: Frontiers in Physiology, Frontiers in Cardiovascular Medicine and Frontiers in Pharmacology

frontiers Research Topics

Frontiers eBook Copyright Statement

The copyright in the text of individual articles in this eBook is the property of their respective authors or their respective institutions or funders. The copyright in graphics and images within each article may be subject to copyright of other parties. In both cases this is subject to a license granted to Frontiers.

The compilation of articles constituting this eBook is the property of Frontiers.

Each article within this eBook, and the eBook itself, are published under the most recent version of the Creative Commons CC-BY licence. The version current at the date of publication of this eBook is CC-BY 4.0. If the CC-BY licence is updated, the licence granted by Frontiers is automatically updated to the new version.

When exercising any right under the CC-BY licence, Frontiers must be attributed as the original publisher of the article or eBook, as applicable.

Authors have the responsibility of ensuring that any graphics or other materials which are the property of others may be included in the CC-BY licence, but this should be checked before relying on the CC-BY licence to reproduce those materials. Any copyright notices relating to those materials must be complied with.

Copyright and source acknowledgement notices may not be removed and must be displayed in any copy, derivative work or partial copy which includes the elements in question.

All copyright, and all rights therein, are protected by national and international copyright laws. The above represents a summary only. For further information please read Frontiers' Conditions for Website Use and Copyright Statement, and the applicable CC-BY licence.

ISSN 1664-8714
ISBN 978-2-88971-583-1
DOI 10.3389/978-2-88971-583-1

About Frontiers

Frontiers is more than just an open-access publisher of scholarly articles: it is a pioneering approach to the world of academia, radically improving the way scholarly research is managed. The grand vision of Frontiers is a world where all people have an equal opportunity to seek, share and generate knowledge. Frontiers provides immediate and permanent online open access to all its publications, but this alone is not enough to realize our grand goals.

Frontiers Journal Series

The Frontiers Journal Series is a multi-tier and interdisciplinary set of open-access, online journals, promising a paradigm shift from the current review, selection and dissemination processes in academic publishing. All Frontiers journals are driven by researchers for researchers; therefore, they constitute a service to the scholarly community. At the same time, the Frontiers Journal Series operates on a revolutionary invention, the tiered publishing system, initially addressing specific communities of scholars, and gradually climbing up to broader public understanding, thus serving the interests of the lay society, too.

Dedication to Quality

Each Frontiers article is a landmark of the highest quality, thanks to genuinely collaborative interactions between authors and review editors, who include some of the world's best academicians. Research must be certified by peers before entering a stream of knowledge that may eventually reach the public - and shape society; therefore, Frontiers only applies the most rigorous and unbiased reviews.
Frontiers revolutionizes research publishing by freely delivering the most outstanding research, evaluated with no bias from both the academic and social point of view. By applying the most advanced information technologies, Frontiers is catapulting scholarly publishing into a new generation.

What are Frontiers Research Topics?

Frontiers Research Topics are very popular trademarks of the Frontiers Journals Series: they are collections of at least ten articles, all centered on a particular subject. With their unique mix of varied contributions from Original Research to Review Articles, Frontiers Research Topics unify the most influential researchers, the latest key findings and historical advances in a hot research area! Find out more on how to host your own Frontiers Research Topic or contribute to one as an author by contacting the Frontiers Editorial Office: frontiersin.org/about/contact

NEW DRUG TARGETS FOR PROTEOTOXICITY IN CARDIOMETABOLIC DISEASES

Topic Editors:
Jun Ren, University of Washington, United States
Xin Wang, The University of Manchester, United Kingdom
Ying Mei Zhang, Fudan University, China

Citation: Ren, J., Wang, X., Zhang, Y. M., eds. (2021). New Drug Targets for Proteotoxicity in Cardiometabolic Diseases. Lausanne: Frontiers Media SA.
doi: 10.3389/978-2-88971-583-1

Table of Contents

05 ***Editorial: New Drug Targets for Proteotoxicity in Cardiometabolic Diseases***
Jun Ren, Xin Wang and Yingmei Zhang

08 ***Cardioprotective Role of Melatonin in Acute Myocardial Infarction***
Zhenhong Fu, Yang Jiao, Jihang Wang, Ying Zhang, Mingzhi Shen, Russel J. Reiter, Qing Xi and Yundai Chen

23 ***Metformin Ameliorates Diabetic Cardiomyopathy by Activating the PK2/PKR Pathway***
Zhen Yang, Min Wang, Yuchen Zhang, Fei Cai, Botao Jiang, Wenliang Zha and Wei Yu

35 ***Critical Roles of ELVOL4 and IL-33 in the Progression of Obesity-Related Cardiomyopathy via Integrated Bioinformatics Analysis***
Jun Tao, Yajing Wang, Ling Li, Junmeng Zheng and Shi Liang

46 ***Regulation of Long Non-coding RNAs and MicroRNAs in Heart Disease: Insight Into Mechanisms and Therapeutic Approaches***
Lucy Collins, Pablo Binder, Hongshan Chen and Xin Wang

66 ***Novel Therapeutic Targets for Hypoxia-Related Cardiovascular Diseases: The Role of HIF-1***
Minxuan Liu, Gina Galli, Yilin Wang, Qiru Fan, Zhenzhong Wang, Xin Wang and Wei Xiao

74 ***Transient Receptor Potential Ankyrin Type-1 Channels as a Potential Target for the Treatment of Cardiovascular Diseases***
Song Gao, Keneilwe Kenny Kaudimba, Shanshan Guo, Shuang Zhang, Tiemin Liu, Peijie Chen and Ru Wang

88 ***GEO Data Sets Analysis Identifies COX-2 and Its Related Micro RNAs as Biomarkers for Non-Ischemic Heart Failure***
Youyou Yan, Dandan Song, Xiaoling Zhang, Gang Hui and Junnan Wang

95 ***Role of Histone Deacetylases in Skeletal Muscle Physiology and Systemic Energy Homeostasis: Implications for Metabolic Diseases and Therapy***
Haili Tian, Sujuan Liu, Jun Ren, Jason Kai Wei Lee, Ru Wang and Peijie Chen

106 ***SHANK3 Co-ordinately Regulates Autophagy and Apoptosis in Myocardial Infarction***
Wanrong Man, Jing Gu, Bo Wang, Mingming Zhang, Jianqiang Hu, Jie Lin, Dong Sun, Zhenyu Xiong, Xiaoming Gu, Kaikai Hao, Baolin Guo, Gaoli Wei, Liang Zhang, Rui Song, Congye Li, Haichang Wang and Dongdong Sun

116 ***Farnesoid X Receptor Agonists as Therapeutic Target for Cardiometabolic Diseases***
Chao Li, Jie Yang, Yu Wang, Yingzi Qi, Wenqing Yang and Yunlun Li

131 ***MAP4 as a New Candidate in Cardiovascular Disease***
Lingfei Li, Qiong Zhang, Xia Lei, Yuesheng Huang and Jiongyu Hu

140 ***Targeting Ca^{2+} Handling Proteins for the Treatment of Heart Failure and Arrhythmias***
Alexandra Njegic, Claire Wilson and Elizabeth J. Cartwright

170 ***Repurposing Antidiabetic Drugs for Cardiovascular Disease***
Mario Schubert, Sinah Hansen, Julian Leefmann and Kaomei Guan

190 ***Circulating Ceramide: A New Cardiometabolic Biomarker in Patients With Comorbid Acute Coronary Syndrome and Type 2 Diabetes Mellitus***
Ruihua Cao, Zhiyi Fang, Sulei Li, Mengqi Xu, Jibin Zhang, Dong Han, Wenchao Hu, Liqiu Yan, Yabin Wang, Li Fan and Feng Cao

200 ***Angiotensin II Decreases Endothelial Nitric Oxide Synthase Phosphorylation* via *AT_1R Nox/ROS/PP2A Pathway***
Jing Ding, Min Yu, Juncai Jiang, Yanbei Luo, Qian Zhang, Shengnan Wang, Fei Yang, Alei Wang, Lingxiao Wang, Mei Zhuang, Shan Wu, Qifang Zhang, Yong Xia and Deqin Lu

212 ***Disruption of STAT6 Signal Promotes Cardiac Fibrosis Through the Mobilization and Transformation of $CD11b^+$ Immature Myeloid Cells***
Weiwei Zhang, Baoling Zhu, Suling Ding, Xiangfei Wang, Jian Wu, Xiaowei Zhu, Yunzeng Zou, Junbo Ge, Minghong Tong and Xiangdong Yang

225 ***Drug Discovery and Development of Novel Therapeutics for Inhibiting TMAO in Models of Atherosclerosis and Diabetes***
Ian Steinke, Nila Ghanei, Manoj Govindarajulu, Sieun Yoo, Juming Zhong and Rajesh H. Amin

233 ***Unraveling the Mystery of Cold Stress-Induced Myocardial Injury***
Xue Kong, Haitao Liu, Xiaole He, Yang Sun and Wei Ge

242 ***Functioning of Long Noncoding RNAs Expressed in Macrophage in the Development of Atherosclerosis***
Xirui Ma, Huifang Liu and Fengling Chen

257 ***The Cardioprotective Mechanism of Phenylaminoethyl Selenides (PAESe) Against Doxorubicin-Induced Cardiotoxicity Involves Frataxin***
Xiaoyu Fu, Mathew Eggert, Sieun Yoo, Nikhil Patel, Juming Zhong, Ian Steinke, Manoj Govindarajulu, Emine Akyuz Turumtay, Shravanthi Mouli, Peter Panizzi, Ronald Beyers, Thomas Denney, Robert Arnold and Rajesh H. Amin

271 ***Early Passive Leg Movement Prevents Against the Development of Heart Failure With Preserved Ejection Fraction in Rats***
Jian Liu, Xi-xin Ji, Yang Fu, Wen-chao Zhang, Hui-fang Ji, Jian-wei Liu, Xiao-shu Cheng and Yi-Fei Dong

283 ***Heat Shock Proteins: Potential Modulators and Candidate Biomarkers of Peripartum Cardiomyopathy***
Graham Chakafana, Timothy F. Spracklen, Stephen Kamuli, Tawanda Zininga, Addmore Shonhai, Ntobeko A. B. Ntusi and Karen Sliwa

301 ***Cross-Sectional Survey of Clinical Trials of Stem Cell Therapy for Heart Disease Registered at ClinicalTrials.gov***
Rong Yang, Yonggang Zhang, Xiaoyang Liao, Ru Guo, Yi Yao, Chuanying Huang and Li Qi

frontiers in Physiology

EDITORIAL
published: 16 September 2021
doi: 10.3389/fphys.2021.745296

Editorial: New Drug Targets for Proteotoxicity in Cardiometabolic Diseases

Jun Ren[1,2]*, *Xin Wang*[3]* and *Yingmei Zhang*[1]*

[1] Department of Cardiology and Shanghai Institute of Cardiovascular Diseases, Zhongshan Hospital, Fudan University, Shanghai, China, [2] Department of Laboratory Medicine and Pathology, University of Washington, Seattle, WA, United States, [3] Faculty of Biology, Medicine and Health, The University of Manchester, Manchester, United Kingdom

Keywords: non-coding RNA, ischemia, metabolic, drug target, cardiometabolic

OPEN ACCESS

Edited and reviewed by:
Johannes Van Lieshout, University of Amsterdam, Netherlands

Correspondence:
Jun Ren
jren@uw.edu
Xin Wang
xin.wang@manchester.ac.uk
Yingmei Zhang
zhangym197951@126.com

Specialty section:
This article was submitted to Clinical and Translational Physiology, a section of the journal Frontiers in Physiology

Received: *21 July 2021*
Accepted: *20 August 2021*
Published: *16 September 2021*

Citation:
Ren J, Wang X and Zhang Y (2021) Editorial: New Drug Targets for Proteotoxicity in Cardiometabolic Diseases. Front. Physiol. 12:745296. doi: 10.3389/fphys.2021.745296

Editorial on the Research Topic

New Drug Targets for Proteotoxicity in Cardiometabolic Diseases

We are honored to serve as lead editors for this Frontier theme issue of "*New drug targets for proteotoxicity in cardiometabolic diseases*." Our enthusiasm for this special topic rooted from the recent surge of novel medications and therapeutic modalities in cardiometabolic diseases in particular obesity, diabetes mellitus, insulin resistance, hypertension, ischemic/reperfusion injury and myocardial infarction (Ceylan-Isik et al., 2008; Ren and Zhang, 2018; Zhang et al., 2018; Aguilar-Ballester et al., 2021). Although development of medical technology has significantly advanced clinical diagnosis and management for cardiometabolic diseases, the ever-rising risks of metabolic diseases impose a main threat for health care in the 21st century (Onat, 2011; Kaur, 2014; Ren and Anversa, 2015; Zhang et al., 2018). Up-to-date, a number of theories have been suggested for the etiology of cardiometabolic anomalies including disturbed glucose/lipid metabolism, endoplasmic reticulum (ER) stress, oxidative and nitrosative/nitrative stress, mitochondrial injury, inflammation, and programmed cell death (apoptosis, necroptosis, pyroptosis, and ferroptosis) (Ren and Kelley, 2009; Ren et al., 2010, 2021; Onat, 2011; Ceylan-Isik et al., 2013; Kaur, 2014; Ren and Anversa, 2015). More evidence has noted an essential role for proteotoxicity or protein quality control in the pathogenesis of cardiometabolic diseases (Sandri and Robbins, 2014; Zhang et al., 2018). In general, protein quality control is governed by ubiquitin-proteasome system (UPS) and autophagy-lysosomal systems, two major albeit distinct machineries for degradation and removal of damaged and/or long-lived intracellular macromolecules (nucleic acids, proteins, carbohydrates, lipids) and organelles (e.g., mitochondria, ribosomes, peroxisomes, and ER) (Zhang et al., 2018; Ren et al., 2021). Interruption of UPS and autophagy evokes detrimental proteotoxic sequalae and is drawing much attention in the pathophysiology and pharmacotherapies in cardiometabolic diseases (Sandri and Robbins, 2014; Wang and Wang, 2014). In this context, this issue tackles some of the burning issues in cardiometabolic diseases with a particular focus on proteotoxicity and protein quality control.

In this issue, Li C. et al. discussed the role of Farnesoid X receptor (FXR) agonists as a possible target for the management of cardiometabolic diseases (Li C. et al.). FXR, a metabolic nuclear receptor, is mainly turned on by primary bile acids (BAs) such as chenodeoxycholic acid, cholic acid and synthetic agonists such as obeticholic acid. Recent evidence suggests that FXR agonists help to maintain regulation of cholesterol, lipid metabolism, glucose metabolism, and intestinal microorganism, with promises in the management of cardiometabolic diseases (Li C. et al.). Next, Tao et al. analyzed co-expression module genes from GSE18897 and GSE47022 to reveal 6 upregulated genes. These authors then validated upregulated levels of elongation of very-long-chain fatty

acids protein 4, matrix metalloproteinase-8, and interleukin-33 in peripheral bloods from patients with obesity heart diseases. Given the poorly defined molecular machineries underneath obesity cardiomyopathy, findings from this integrated bioinformatics analysis favored a role for these hub genes as potential biomarkers for diagnosis and therapeutic targets in obesity heart diseases (Tao et al.). In this theme issue, Yang et al. discussed the benefits of antidiabetics metformin in the management of diabetic cardiomyopathy. These authors found that metformin activates prokineticin 2 (PK2), a small-molecule secreted protein governing survival and angiogenesis, to mediate Akt/GSK3β signaling, improve cardiac function and alleviate apoptosis in diabetic mice (Yang et al.). In this theme issue, Tian et al. provided insights into the complex interplay between histone acetyltransferases (HATs) and histone deacetylases (HDACs), two enzyme families controlling biological processes of histone acetylation and deacetylation, in the regulation of skeletal muscle physiology and energy homeostasis during exercise. Balance between these two enzymes plays a major role in mitochondrial remodeling, insulin sensitivity, on/off metabolic fuel switching and physiological homeostasis of skeletal muscles (Tian et al.). Type 2 diabetic patients usually display high levels of metabolic products such as trimethylamine N-oxide (TMAO) associated with gut dysbiosis. Here Steinke et al. discussed the value of TMAO levels in reference to cardiovascular risk. Next, Cao et al. examined levels of circulating ceramide in 761 patients with comorbid acute coronary syndrome (ACS) and type 2 diabetes mellitus, and noted that circulating ceramides are correlated with the risk of ACS-type 2 diabetes comorbidity. These innovative results suggested the utility of ceramide levels in the risk assessment of ACS- diabetes mellitus comorbidity (Cao et al.). Next, Schubert et al. summarized the possible cardiac benefits of new antidiabetic agents, including sodium-glucose cotransporter 2 (SGLLT2) inhibitor and glucagon-like peptide-1 receptor agonist, dipeptidyl peptidase-4 (DPP) inhibitor and metformin in patients with high cardiovascular risk with or without type 2 diabetes (Schubert et al.).

Myocardial ischemia injury and acute myocardial infarction remain the leading causes of mortality in patients with cardiovascular diseases (Zhang and Ren, 2014, 2016; Ren and Zhang, 2017). In this theme issue, Man et al. tackled the role of Shank3 in post-infarction cardiac dysfunction. They found that Shank3 knockout aggravated, while Shank3 overexpression alleviated, cardiac dysfunction following myocardial infarction. These findings revealed a novel role for Shank3 as a new therapeutic target for cardiac dysfunction following myocardial infarction through induction of autophagy (Man et al.). Next, Fu et al. succinctly dissected the compelling roles for melatonin in acute myocardial infarction. These authors elaborated the current well-perceived mechanisms underneath beneficial effects of melatonin against oxidative stress, promoting autophagic repair of cells, regulating immune and inflammatory responses, engaging mitochondrial function, and relieving ER stress, in the pathology of myocardial infraction injury (Fu Z. et al.). Microtubule and mitochondrial dysfunction are involved in cardiovascular disease etiology, including cardiac remodeling, heart failure, and hypoxic/ischemic injury. In this issue, Li L. et al. discussed MAP4 phosphorylation in microtubule instability. Phosphorylation of MAP4 triggers mitochondrial apoptosis, en route to cardiac injury, denoting a novel role for MAP4 as a candidate in cardiovascular pathologies (Li L. et al.). Next, Liu M. et al. discussed the therapeutic options for hypoxia-related cardiovascular disease. Hypoxia-inducible factor (HIF) is turned on in hypoxia to modulate diverse target genes. The authors recapitulated pathophysiology of hypoxic injury in cardiovascular disease, and provided convincing evidence for HIF-evoked cardioprotective signaling (Liu M. et al.). Cold stress is often associated with ischemia heart injury involving disturbed endothelin (ET-A) receptor, ER stress, transient receptor potential (TRP) vanilloid, mitochondrial damage. Here Kong et al. discussed various aspects of cold stress-induced cardiac injury, in particular dysregulated autophagy (Kong et al.). Next, Gao et al. introduced structural and functional characteristics of TRPA1 in cardiovascular diseases. They discussed evidence where TRPA1 is correlated to cardiovascular disease risk factors (Gao et al.). Exercising evokes benefits on heart failure with preserved ejection fraction (HFpEF). Then, Liu J. et al. designed a device to perform early passive leg movement (ePLM) and noted benefit of ePLM in alleviating high salt diet-induced HFpEF through inhibition of fibrosis in a TGF-β1/Smad3-dependdent manner in conjunction to Akt/eNOS signaling activation. These findings implied the benefit of ePLM as a novel non-pharmacological approach for HFpEF (Liu J. et al.). Chronic inflammation is part of ischemic heart disease process with overt atherosclerosis. Due to overwhelmed accumulation of monocytes/macrophages within arterial plaques, monocytes/macrophages are deemed critical cellular targets in the management of atherosclerosis. Many long non-coding RNAs (LncRNAs) were found to exert regulatory roles on metabolism and plasticity in macrophages, consequently stimulating or inhibiting atherosclerotic inflammation. Next, Ma et al. provided a balanced viewpoint of lncRNAs in macrophage biology, pathogenesis and therapeutics of atherosclerosis (Ma et al.). Furthermore, Chakafana et al. have carefully assessed the role of heat shock proteins in peripartum cardiomyopathy, and explored the possibility of given heat shock proteins as novel candidate biomarkers and drug targets in peripartum cardiomyopathy (Chakafana et al.). Next, Amin and team discovered a cardioprotective property of an orally active selenium based compound phenylaminoethyl selenides against doxorubicin cardiomyopathy possibly through preserving the stability of the iron-sulfur cluster biogenesis protein Frataxin (FXN) (Fu X. et al.). Moreover, Zhang et al. suggest that STAT6 plays a vital role in isoproterenol-induced β1-AR overactivation and inflammatory response, en route to cardiac fibrogenesis. Their findings denoted a novel role for STAT6 as a promising target against myocardial fibrosis and heart failure (Zhang et al.). Next, Njegic et al. addressed the molecular changes to proteins associated with Ca^{2+}-handling and -signaling. These authors made an in-depth analysis on these potential novel therapeutic targets from the perspective of both pre-clinical and, clinical settings (Njegic et al.). In this series of collection, Ding et al. reported a novel mechanism where angiotensin (AngII) evokes endothelial dysfunction likely via AT1R-mediated protein phosphatase 2A (PP2A) activation to suppress endothelial nitric oxide

synthase (eNOS) phosphorylation *via* Nox/ROS pathway (Ding et al.).

Given the advances in science and technology, non-coding (LncRNA) or microRNAs (miRNA) are considered as important regulators of cellular processes, and serve as an important platform for therapeutic regimen of cardiovascular disease. Nonetheless, many questions remain unanswered for LncRNA and miRNA, such as consequences of targeting, refinement of targeting systems. Here Collins et al. summarized the level of genomic regulation strategy for the treatment of cardiovascular disease (Collins et al.). Furthermore, Yan et al. identified COX-2 and related microRNA as possible biomarkers for non-ischemic heart failure. These authors analyzed genomic and transcription information from peripheral blood mononuclear cells of heart failure patients and found enrichment of prostaglandin-endoperoxide synthase 2 (PTGS2, or cyclooxygenase-2 - COX-2), as well as its related micro RNAs including miR-1297 and miR-4649-3p as potential biomarkers for non-ischemic heart failure. These authors noted overtly elevated plasma COX-2 and miR-4649-3p I conjunction with downregulated plasma miR-1297. Moreover, these authors suggested that miR-4649-3p possessed high predictive power for non-ischemic heart failure (Yan et al.). Although this theme issue did not touch too much on clinical trials, Yang et al. did a cross-sectional survey of 241 trials conducted on stem cell therapy. These authors shared their "disappointment" on the outcome of these registered clinical applications (Yang et al.).

Although this theme issue has shed some insights toward a more thorough knowledge on possible drug targets in cardiometabolic diseases, we regret to say we have failed in a large part identifying specific target(s) or drug(s) on autophagy or mitophagy molecules (the benchmarks for proteotoxic issue). This may reflect the overall challenge and difficulty in drug development targeting autophagy/mitophagy. Nonetheless, the recent advances in computer-based biological modeling and bioinformatic system should help us to better achieve desirable chemicals to target a given protein or signaling molecule in cardiometabolic diseases. We hope that this theme issue will aid to unveil novel therapeutic targets to launch better intervention regimens for cardiometabolic diseases.

AUTHOR CONTRIBUTIONS

JR, XW, and YZ contributed to drafting and editing of this editorial. All authors contributed to the article and approved the submitted version.

REFERENCES

Aguilar-Ballester, M., Hurtado-Genoves, G., Taberner-Cortes, A., Herrero-Cervera, A., Martinez-Hervas, S., and Gonzalez-Navarro, H. (2021). Therapies for the treatment of cardiovascular disease associated with type 2 diabetes and dyslipidemia. *Int. J. Mol. Sci*. 22:20660. doi: 10.3390/ijms22020660

Ceylan-Isik, A. F., Fliethman, R. M., Wold, L. E., and Ren, J. (2008). Herbal and traditional Chinese medicine for the treatment of cardiovascular complications in diabetes mellitus. *Curr. Diabetes Rev*. 4, 320–328. doi: 10.2174/157339908786241142

Ceylan-Isik, A. F., Kandadi, M. R., Xu, X., Hua, Y., Chicco, A. J., Ren, J., et al. (2013). Apelin administration ameliorates high fat diet-induced cardiac hypertrophy and contractile dysfunction. *J. Mol. Cell Cardiol*. 63, 4–13. doi: 10.1016/j.yjmcc.2013.07.002

Kaur, J. (2014). A comprehensive review on metabolic syndrome. *Cardiol. Res. Pract*. 2014:943162. doi: 10.1155/2014/943162

Onat, A. (2011). Metabolic syndrome: nature, therapeutic solutions and options. *Exp. Opin. Pharmacother*. 12, 1887–1900. doi: 10.1517/14656566.2011.585462

Ren, J., and Anversa, P. (2015). The insulin-like growth factor I system: physiological and pathophysiological implication in cardiovascular diseases associated with metabolic syndrome. *Biochem. Pharmacol*. 93, 409–417. doi: 10.1016/j.bcp.2014.12.006

Ren, J., Bi, Y., Sowers, J. R., Hetz, C., and Zhang, Y. (2021). Endoplasmic reticulum stress and unfolded protein response in cardiovascular diseases. *Nat. Rev. Cardiol*. 18, 499–521. doi: 10.1038/s41569-021-00511-w

Ren, J., and Kelley, R. O. (2009). Cardiac health in women with metabolic syndrome: clinical aspects and pathophysiology. *Obesity*. 17, 1114–1123. doi: 10.1038/oby.2009.8

Ren, J., Pulakat, L., Whaley-Connell, A., and Sowers, J. R. (2010). Mitochondrial biogenesis in the metabolic syndrome and cardiovascular disease. *J. Mol. Med*. 88, 993–1001. doi: 10.1007/s00109-010-0663-9

Ren, J., and Zhang, Y. (2017). Editorial: new therapetic approaches in the management of ischemia reperfusion injury and cardiometabolic diseases: opportunities and challenges. *Curr. Drug Targets*. 18, 1687–1688. doi: 10.2174/1389450118151710190927 03

Ren, J., and Zhang, Y. (2018). Targeting autophagy in aging and aging-related cardiovascular diseases. *Trends Pharmacol. Sci*. 39, 1064–1076. doi: 10.1016/j.tips.2018.10.005

Sandri, M., and Robbins, J. (2014). Proteotoxicity: an underappreciated pathology in cardiac disease. *J. Mol. Cell. Cardiol*. 71, 3–10. doi: 10.1016/j.yjmcc.2013.12.015

Wang, C., and Wang, X. (2014). The interplay between autophagy and the ubiquitin-proteasome system in cardiac proteotoxicity. *Biochim. Biophys. Acta* 1852, 188–194. doi: 10.1016/j.bbadis.2014.07.028

Zhang, Y., and Ren, J. (2014). Targeting autophagy for the therapeutic application of histone deacetylase inhibitors in ischemia/reperfusion heart injury. *Circulation* 129, 1088–1091. doi: 10.1161/CIRCULATIONAHA.113.008115

Zhang, Y., and Ren, J. (2016). Bridging the gap, facing the challenge-the 26(th) great wall international congress of cardiology (GW-ICC). *Cardiovasc. Diagn. Ther*. 6, 97–100. doi: 10.3978/j.issn.2223-3652.2016.01.01

Zhang, Y., Whaley-Connell, A. T., Sowers, J. R., and Ren, J. (2018). Autophagy as an emerging target in cardiorenal metabolic disease: from pathophysiology to management. *Pharmacol. Ther*. 191, 1–22. doi: 10.1016/j.pharmthera.2018.06.004

Conflict of Interest: The authors declare that the research was conducted in the absence of any commercial or financial relationships that could be construed as a potential conflict of interest.

Publisher's Note: All claims expressed in this article are solely those of the authors and do not necessarily represent those of their affiliated organizations, or those of the publisher, the editors and the reviewers. Any product that may be evaluated in this article, or claim that may be made by its manufacturer, is not guaranteed or endorsed by the publisher.

Copyright © 2021 Ren, Wang and Zhang. This is an open-access article distributed under the terms of the Creative Commons Attribution License (CC BY). The use, distribution or reproduction in other forums is permitted, provided the original author(s) and the copyright owner(s) are credited and that the original publication in this journal is cited, in accordance with accepted academic practice. No use, distribution or reproduction is permitted which does not comply with these terms.

frontiers in Physiology

REVIEW
published: 29 April 2020
doi: 10.3389/fphys.2020.00366

Cardioprotective Role of Melatonin in Acute Myocardial Infarction

Zhenhong Fu[1]†, Yang Jiao[1]†, Jihang Wang[1], Ying Zhang[1], Mingzhi Shen[1], Russel J. Reiter[2,3], Qing Xi[4]* and Yundai Chen[1]**

[1] Department of Cardiology, The First Medical Center, Chinese PLA General Hospital, Beijing, China, [2] Department of Cellular and Structural Biology, UT Health San Antonio, San Antonio, TX, United States, [3] San Antonio Cellular Therapeutics Institute, Department of Biology, College of Sciences, University of Texas at San Antonio, San Antonio, TX, United States, [4] The First Medical Center, Chinese PLA General Hospital, Beijing, China

OPEN ACCESS

Edited by:
Jun Ren,
University of Washington,
United States

Reviewed by:
Ying Tan,
Southern Medical University, China
Ana Beatriz Rodríguez,
University of Extremadura, Spain
Jian Yang,
Fourth Military Medical University,
China

***Correspondence:**
Zhenhong Fu
fuzhenh@126.com
Qing Xi
xiqing301@163.com
Yundai Chen
yundaic@163.com

† These authors have contributed equally to this work

Specialty section:
This article was submitted to Integrative Physiology, a section of the journal Frontiers in Physiology

Received: 07 February 2020
Accepted: 30 March 2020
Published: 29 April 2020

Citation:
Fu Z, Jiao Y, Wang J, Zhang Y, Shen M, Reiter RJ, Xi Q and Chen Y (2020) Cardioprotective Role of Melatonin in Acute Myocardial Infarction. Front. Physiol. 11:366. doi: 10.3389/fphys.2020.00366

Melatonin is a pleiotropic, indole secreted, and synthesized by the human pineal gland. Melatonin has biological effects including anti-apoptosis, protecting mitochondria, anti-oxidation, anti-inflammation, and stimulating target cells to secrete cytokines. Its protective effect on cardiomyocytes in acute myocardial infarction (AMI) has caused widespread interest in the actions of this molecule. The effects of melatonin against oxidative stress, promoting autophagic repair of cells, regulating immune and inflammatory responses, enhancing mitochondrial function, and relieving endoplasmic reticulum stress, play crucial roles in protecting cardiomyocytes from infarction. Mitochondrial apoptosis and dysfunction are common occurrence in cardiomyocyte injury after myocardial infarction. This review focuses on the targets of melatonin in protecting cardiomyocytes in AMI, the main molecular signaling pathways that melatonin influences in its endogenous protective role in myocardial infarction, and the developmental prospect of melatonin in myocardial infarction treatment.

Keywords: melatonin, cardioprotective, cardiomyocyte, myocardial infarction, mitochondrion

INTRODUCTION

With the general improvement of the human living standard, the change of living habits and the prolongation of life span, the prevalence rate of cardiovascular diseases has risen sharply. According to *China Cardiovascular Disease Report in 2018*, the population with cardiovascular diseases in China has reached up to 290 million, and the number of patients with acute myocardial infarction (AMI) is about 2.5 million annually. AMI has become a disease seriously affecting people's life span and quality. Despite great progress of modern medicine, science and technology, iterative new anticoagulants and antiplatelet drug, improvements in the management of AMI patients (Amanakis et al., 2019; Heusch, 2019), including the more frequent coronary reperfusion using fibrinolysis, primary percutaneous coronary intervention (PCI) or coronary artery bypass grafting (CABG), the prognosis of AMI has improved, yet, there are frequent occurrences of malignant arrhythmia events, a decline of cardiac function following AMI leading to the development of heart failure and a poor prognosis (Botker et al., 2018; Davidson et al., 2018; Joshi et al., 2019). Due to ischemia and hypoxia of the infarct area, a large number of inflammatory cells

infiltrate the lesion, cardiomyocyte apoptosis is frequent and scar repair is common (Li et al., 2010; Galluzzi et al., 2018). Due to the non-regenerative feature of cardiomyocytes, irreversible cardiomyocyte apoptosis and infarction caused by acute ischemia are main factors for poor prognosis of AMI (Abukar et al., 2018; Beckendorf et al., 2018). After myocardial infarction, the myocardial tissue in the infarcted area and its adjacent non-infarcted areas undergoes apoptosis and necrosis due to ischemia, hypoxia and inflammatory response (Zhou et al., 2018c; Hu et al., 2019). Thus, the hemodynamic parameters and electrical nerve conduction of the myocardium are changed, and bring about cardiac systolic, diastolic dysfunction and dysrhythmia, and result in ventricular remodeling and electrocardiogram (ECG) changes (Zhang et al., 2014; Joshi et al., 2019). Mitochondria are organelles that generate ATP (Kowaltowski, 2019; Lee B.W.L. et al., 2019). They play a significant role in myocardial injury after myocardial infarction (Zhou et al., 2018h; Zhou et al., 2020). Stabilizing the structure and function of mitochondria effectively inhibits cardiomyocyte injury and necrosis (Audia et al., 2018; Lu J. et al., 2019). Melatonin, an indoleamine secreted by pineal gland, is a highly effective antioxidant and beneficial to many diseases including diabetes, infectious diseases, metabolic syndrome, depression, and neurodegenerative diseases (Zaouali et al., 2011; de Oliveira Junior et al., 2019). The value of melatonin in the treatment of myocardial infarction has drawn wide-spread attention in recent years. Highly compatible with mitochondrial membrane receptors, melatonin effectively reduces mitochondrial dysfunction, thus inhibiting post-myocardial infarction damage of cardiomyocytes. This review summarizes the effect of melatonin in protecting cardiomyocytes and improving prognosis after myocardial infarction by enhancing the adaptability of cardiomyocytes to ischemia and hypoxia via stabilizing mitochondrial function. We hope this introduction will be helpful to the research of melatonin in the treatment of myocardial infarction.

PATHOPHYSIOLOGICAL CHANGES OF HEART DURING MYOCARDIAL INFARCTION

Lipid Deposition and Atherosclerotic Plaque Formation

The direct cause of AMI is myocardial necrosis caused by prolonged ischemia and hypoxia resulting from coronary artery occlusion or spasm. The key factor leading to acute myocardial ischemia is the rupture of an atherosclerotic plaque in the coronary artery and the gradual formation of a thrombus (Zhou et al., 2018e; Bacmeister et al., 2019). The pathogenesis of atherosclerosis includes lipid deposition, inflammation, thrombosis, endothelial dysfunction, smooth muscle cell cloning and other processes (Nofe et al., 2010; Zhou et al., 2018b; Zhao J. et al., 2019). The most important risk factors are lipid metabolism disorder and endothelial cell injury. Under long-term lipid metabolism abnormality, low density lipoprotein cholesterol (LDL-C) enters intima through damaged arterial endothelium where it is converted to oxidized LDL cholesterol (Ox LDL-C), causing further damage to the intima of the coronary artery (Liu et al., 2019; Aimo et al., 2020). Ox LDL-C is engulfed by macrophages, gradually forming foam cells; there after, atherosclerotic plaques gradually develop along with the aggregation of foam cells and lipids (Abdelnaseer et al., 2016; Wu et al., 2019). If the intima of a coronary artery ruptures, the atheromatous plaque substance enters the lumen and becomes an embolus which completely occludes the blood vessel (Yuqi et al., 2015; Tian et al., 2018; Xiong et al., 2019). Thus, regulating the lipid metabolism balance, delaying the formation of atherosclerotic plaques and inhibiting plaque rupture are key measures in preventing myocardial infarction.

Platelet Activation Aggregation and Thrombosis

When atherosclerotic plaques are formed and protrude into the lumen, local arterial stenosis causes changes in blood flow turbulence and shear force, leading to an interruption of arterial intima continuity, contraction of endothelial cells, exposure of tissues such as subendothelial collagen, and activation of platelets; this causes further adhesion and aggregation of platelets on the arterial intima, and finally formation of atherosclerotic thrombotic disease (Cohen et al., 2019; Trindade et al., 2019). Reports show that the mural thrombosis plays a vital role in pathophysiological changes of myocardial infarction progression (Hu S.Y. et al., 2017; Zhou et al., 2017b). At present, there are three types of antiplatelet drugs used in the clinic: (1) cyclooxygenase-1 (COX-1) inhibitor: aspirin. (2) ADP receptor antagonists: clopidogrel, prasugrel, ticagrelor. (3) platelet glycoprotein IIb/IIIa (GP IIb/IIIa) receptor antagonists: tirofiban, etibadin, abciximab. Among these, aspirin is a first-line antiplatelet drug and can irreversibly inactivate COX-1, an enzyme expressed in platelets, which moderates the synthesis of thromboxane; thromboxane is a potent platelet aggregation agent (Davidson et al., 2018; Merz et al., 2018).

Inflammatory Cell Infiltration and Inflammatory Response

The microenvironment of the infarcted cardiomyocyte is a dynamic and complex area. Inflammation and immune responses play important roles in the initiation and progression of myocardial infarction. After myocardial infarction, inflammatory cells such as neutrophils, monocytes, and macrophages are activated, causing their number to increase sharply (Basalay et al., 2018; Wang Z. et al., 2019; Faghfouri et al., 2020). A large amount of inflammatory cytokines are released and move toward the injured area, and the permeability of endothelial cells increases, which results in the infiltration of inflammatory cells (Chen et al., 2016; Thieltges et al., 2018). Cytokine release and the inflammatory response are important conditions for tissue healing after myocardial infarction, but an excessive inflammatory response leads to myocardial tissue remodeling, activating apoptosis signals in cardiomyocytes with destruction

of the integrity of extracellular matrix, which is not conducive to the survival of cardiomyocytes and the recovery of cardiac function (Nahrendorf et al., 2010; Krause et al., 2018). Apoptosis and the inflammatory response are initiated by myocardial tissue injury in the ischemic area. Specific cytokines and mediators including interleukin-1 (IL-1), IL-6, nuclear transcription factor kB (NF-κB) p65, NF-κB p50, Toll-like receptor 4(TLR4), Tenascin-C (TNC) and other inflammatory response regulatory proteins, as well as apoptosis regulatory proteins caspase-3, Bcl-2, etc. are produced. Excessive inflammatory response and fiber proliferation lead to ventricular remodeling (Nokik et al., 2017; Crist et al., 2018; Bocci et al., 2019; Chen M. et al., 2019). TLRs are a major reaction pathway of the inflammatory response after myocardial infarction. Recognition receptors are expressed by inflammatory cells and recognize the danger signal released by injured cells (Jager and Hoefer, 2019; Sircana et al., 2019; Yang M.Y. et al., 2019). Studies have shown that adjusting the activity of TLRs enhances the positive effect of the inflammatory response on myocardial tissue healing and limits damage to tissue, thus providing a new therapeutic process for promoting myocardial tissue recovery after myocardial infarction (Dominguez-Rodriguez et al., 2010b; Cao et al., 2019). Protein kinase D1 (PKD1) mediates the processes of myocardial remodeling, angiogenesis and myocardial contraction (Ren, 2016; Serocki et al., 2018), but the mechanism of PKD1 in the processes of the inflammatory response and cell injury in the microenvironment after myocardial infarction has not been determined.

Cardiomyocyte Death

Cardiomyocyte injury following AMI is a very complex with multi-linked pathophysiological processes, including not only an inflammatory response, immune response, and cell signal transduction, but also complex processes such as apoptosis, necrosis, autophagy, and mitochondrial dysfunction (Westman et al., 2016; Hockings et al., 2018; Heckmann et al., 2019). Immunological studies show that cardiomyocyte in the myocardial infarction region is seriously damaged, apoptosis is severe, the expressions of Bax and caspase-3 are significantly increased, while the expression of Bcl-2 is reduced (Jin et al., 2018). It is reported that, caspase-8 is involved in fatty acid synthase (Fas)/FasL-related death receptor pathway, caspase-9 is depended on mitochondrial damage, and caspase-12 is related to endoplasmic reticulum stress (Fuhrmann and Brune, 2017; Karwi et al., 2018; Jiang et al., 2019). These are associated with cardiomyocyte apoptosis following myocardial infarction. After AMI, the focal area mainly consists of a peripheral ischemic penumbra and inner infarct area. The ischemic penumbra is mainly composed of apoptotic cardiomyocytes, and the inner infarcted area contains numerous dead cardiomyocytes (Niccoli et al., 2016; Hadebe et al., 2018). Studies reveal that the number of necrotic cells is seven times that of apoptotic cells; thus apoptosis plays only a minor role in the progression of myocardial infarction (Adameova et al., 2016; Zhou et al., 2018a; Zhu P. et al., 2018). Mitochondrial reactive oxygen species (ROS) and xanthine oxidase activity in ischemic areas lead to oxidative stress, and the calcium-induced calcium release (CICR) leads to intracellular calcium overload (Zollbrecht et al., 2016; Espinosa-Diez et al., 2018; Graczyk-Jarzynka et al., 2019; Guidarelli et al., 2019). Oxidative stress and inflammatory response activate receptor interaction protein kinase 3 (Ripk3) via interaction with cell death receptors; the common receptors are the Fas receptor, TRAIL receptor and TNFR1 (Zhou et al., 2017e; Zhou and Toan, 2020). Ripk3 destroys cell membrane integrity by mediating cell membrane-related chromosome translocation, resulting in cell necrosis (Kohlstedt et al., 2018; Zhong et al., 2019).

Mitochondrial Dysfunction and Mitophagy

As organelles with important functions in eukaryotic cells, mitochondria mainly generate ATP, moderating apoptosis and oxidative stress reactions and exhibit dynamic changes. Their development and degradation, fusion and fission, and their quantity and morphology are precisely regulated and controlled based on changes in the environment where the cells are located (Zhou et al., 2017a,f; Chen S. et al., 2019; Mayorov et al., 2019; Simula et al., 2019). Mitochondrial dynamics include mitochondrial fission, fusion and mitophagy. Mitochondrial fission aggravates the damage to mitochondrial structure and function by inducing mitochondrial fragmentation. The fission process is considered as an initiation event for mitochondrial apoptosis (Zhou et al., 2017c; Xu Z. et al., 2019; Zhou et al., 2019). Mitochondrial fusion reduces mitochondrial damage and maintains function of these organelles by promoting the integration of mitochondrial fragments, enhancing the stability of mitochondrial genes, and promoting the exchange of mitochondrial contents (Filadi et al., 2018; Kanaan et al., 2018; Yao et al., 2019). As a process of organelle autophagy, mitophagy removes and digests damaged mitochondria fragment via mitochondrial degradation moderated by lysosomes (Zhou et al., 2018d,e; Breda et al., 2019; Mei et al., 2019). Mitophagy is specific and a main pathway of mitochondrial metabolism, and plays a key role in maintaining cell function stability (Liu et al., 2012; Bhandari et al., 2014; Kang et al., 2016).

When cellular damage causes mitochondrial structural dysfunction, cells firstly maintain their original structure through antioxidant factors, DNA repair, protein folding, and so on. If this first line of defense is breached, autophagy, fusion, and biogenesis of the mitochondria are activated, which is a more effective and extensive quality control system (Yang M. et al., 2019). The process of mitophagy is closely related to ubiquitin/proteasome system (UPS). First, the damaged mitochondria are ubiquitinated through modification and then recognized by ubiquitin receptors. The substrates are induced to mitophagy degradation by binding to LC3 on phages, and finally the components after degradation are released to the cytoplasm for recycling, providing nutrients and energy for cell survival (Ji and Kwon, 2017). Recent studies reveal that mitophagy participates in mitochondrial protection induced by mitochondrial fusion (Kornicka et al., 2019). Mitochondrial fusion initially promotes the integration of fragmented mitochondria, and then "cleans" mitochondria

by proteolysis in lysosomes to moderately degrade damaged mitochondrial fragments, thus maintaining the stability of mitochondrial quality and quantity (Tahrir et al., 2019; Wang et al., 2020). In most cases, mitophagy can remove defective mitochondria from AMI injuries, playing a protective and adaptive role. The experimental results of Siddall et al. (2013) show that the enhancement of mitophagy activity protects cardiomyocytes by reducing the production of mitochondrial ROS and inhibiting calcium overload (Reddy et al., 2018). The role of mitophagy in myocardial infarction cell injury, however, is still controversial. However, experimental data of Yang et al. (2017) indicates that the rise of mitophagy reduces the energy supply of cells, thus aggravating cell injury (Koentges et al., 2018; Zhou et al., 2018g).

The heart has a very high demand for energy. There are a large number of mitochondria in cardiomyocytes. Their total volume of mitochondria in a cardiomyocyte accounts for approximately 22–37%. The energy is used to maintain the normal blood pumping function of the heart. The distribution and supply of energy are related closely to the functional state of mitochondria (Battogtokh et al., 2018; Joshi and Mochly-Rosen, 2018; Zhong et al., 2019). The mitochondrial membrane is a bilayer structure, with a non-specific ion channel in the inner membrane. This channel is known as the mitochondrial permeability transition pore (MPTP), which plays a critical role in maintaining Ca^{2+} dynamic balance and apoptosis (Meyer and Leuschner, 2018; Venugopal et al., 2018). The opening of MPTP leads to an increase of mitochondrial intimal permeability, resulting in imbalance of electrochemical driving force of ions inside and outside the membrane, a decrease of Na^{+}-K^{+}-ATP enzyme activity, and transmembrane transport barrier of sodium and potassium ions, which further leads to mitochondrial dysfunction, a drop of the mitochondrial inner membrane potential with the release of cytochrome c (Cyt c), and activation of the apoptosis program (Xiao et al., 2018; Xu T. et al., 2019). Under normal circumstances, MPTP is closed state and is activated when the concentration of oxygen-derived free radicals and Ca^{2+} is elevated (Yang et al., 2016; Xu S.F. et al., 2019). During AMI, cardiomyocytes are in a microenvironment of ischemia and hypoxia, with an extensive infiltration of inflammatory cells and oxygen-derived free radicals. Mitochondria then release apoptosis-inducing factors, Cyt c, pro-interleukin 1, and other mediators that induce apoptosis in this harsh microenvironment; this mediates the release of IL-1 through an inflammatory cascade reaction resulting in cardiomyocyte injury and necrosis (Teixeira et al., 2018; Lee E. et al., 2019). In addition, a large number of free radicals and inflammatory agents destroy the structure and function of mitochondria, causing inactivation of various enzymes, destruction of double membrane barrier and opening of the MPTP, causing mitochondrial edema, disintegration, and dysfunction of energy generation, and eventually leading to cardiomyocyte death and cardiac function damage. During the process of AMI, opening of MPTP plays an important role (Boengler et al., 2018; Schreiber et al., 2019). The cardiomyocyte injury in ischemia is reduced by inhibiting opening of the MPTP, lowering the release of Cyt c and limiting oxygen-derived free radicals and Ca^{2+} overload (Seidlmayer et al., 2015; Morell et al., 2018).

TARGET THE MELATONIN PROTECTS CARDIOMYOCYTES IN ACUTE MYOCARDIAL INFARCTION

Melatonin Plays Anti-oxidative Stress Effect and Inhibits Inflammatory Response

Melatonin was originally discovered in the bovine pineal gland and was named after its ability to change pigmentation (melanin) in amphibian skin. Controlled by sympathetic nervous system, the synthesis and secretion of melatonin are in phase with the fluctuations in the light:dark cycle with little secretion during the day and high amounts of secretion at night (Perez-Gonzalez et al., 2019). Some of the biological effects of melatonin are related to its ability to effectively scavenge free radicals and enhance the activity of antioxidant enzymes; melatonin's metabolites also exhibit high radical scavenging activity (Galano et al., 2013). Melatonin is highly potent free radical scavenger due to multiple mechanisms (Galano and Reiter, 2018). Free radicals that are eliminated include nitric oxide (NO·), superoxide anion radical (O_2^{-}·) and hydroxyl radical (OH·), etc. Its hydrophilicity and high lipophilicity, allows melatonin to pass through the cell membrane and the nuclear membrane easily, thus exerting strong antioxidant effects in cytoplasm and nucleus (Garcia et al., 2015). In addition to directly scavenging free radicals, melatonin also induces the expression of antioxidant enzymes to achieve indirect antioxidant effects (Kleszczynski et al., 2016). Nrf2 (NF-E2-related factor2), a transcription factor, plays a key role in cell oxidative stress response, and controls the expression of various antioxidant response genes after linking to the DNA antioxidant response element (ARE), while melatonin mainly influences the pathway through a nuclear retinoid-related orphan receptor (RZR/RORα) (Giudice et al., 2010).

Melatonin also plays an antioxidant role in coordination with reduced glutathione, nicotinamide adenine dinucleotide phosphate (NADPH), vitamin C, vitamin E, etc. (Yang C.H. et al., 2019). Its synergistic anti-inflammatory effects are mainly realized by up-regulating the activity of enzymes synthesizing such antioxidants so as to increase total content of antioxidants in the organism (Yoon et al., 2019). The anti-inflammatory mechanisms of melatonin include inhibiting the aggregation of inflammatory cells and the release of inflammatory cytokines including TNF-α, IL-1β, and IL-6 all of which are important inflammatory mediators of the inflammatory response. These inflammatory factors directly cause tissue injury and also stimulate other inflammatory cells to release inflammatory mediators, causing a chain reaction (Amin et al., 2019). Experiments show that melatonin increases the release of anti-inflammatory mediators such as IL-10 and while inhibiting the release of inflammatory mediators such as TNF-α, IL-1β, and IL-6, thus achieving an anti-inflammatory effect. In addition, animal experiments show that anti-inflammatory actives of melatonin

are related to its inhibition of adhesion molecule related gene expression (Hu C. et al., 2017).

The TLRs mentioned above are the main response pathway of the inflammatory response after myocardial infarction. In a rat myocardial infarction model (Zhao Y. et al., 2019), the expression of the TLR4 signaling pathway is inhibited when melatonin is injected into the heart before ischemic injury. In addition, melatonin also blocks upstream signals (e.g., lipopolysaccharide binding protein CD14) of TLR4. This process can significantly reduce the release of inflammatory factors such as Granulocyte-Monocyte Colony-Stimulating Factor (GM-CSF), TNF-α, C-C Motif Chemokine Ligand 2 (CCL 2), IL-1β, IL-6, C-reactive protein (CRP), serum amyloid A, α-1 antitrypsin, while the content of Nrf2, IL-1α, heme oxygenase-1, and other anti-inflammatory cytokines rise significantly (Ter Horst et al., 2018; Ostjen et al., 2019; Tang et al., 2019).

Dyslipidemia is an independent risk factor for attack of coronary heart disease (CHD). It is reported that (Tengattini et al., 2008) melatonin regulates blood lipid, and reduces the Ox LDL-C, both of which are helpful for reducing the overall incidence of myocardial infarction injury. In terms of protecting vascular endothelial cells, melatonin reduces the degree of injury of endothelial cells in the process of myocardial infarction by inhibiting the activity of myosin light streptokinase, thus delaying the progression of atherosclerosis (Rezzani et al., 2013). In addition, several studies demonstrate that melatonin induces calcium overload and ROS generation in platelets, and activates caspase pathway and depolarizes mitochondrial membrane to mediate platelet inactivation, and this process also involves peroxisome proliferator-activated receptor γ(PPARγ)/FUN14 domain containing 1 (FUNDC1) /mitophagy pathways (Zhou et al., 2017b; NaveenKumar et al., 2019). In addition to directly mediating platelet dysfunction, melatonin also down-regulates adhesion molecules and delays NO metabolism, thus indirectly inhibiting platelet aggregation (Girish et al., 2013). This antithrombotic effect reduces cardiomyocyte injury after myocardial infarction, and plays a role in protecting the myocardium (Dominguez-Rodriguez et al., 2010a). The circadian rhythm of melatonin release significantly reduces the activity of platelets at night, while the early morning with low melatonin levels is often the time for the occurrence of cardiovascular events. Therefore, supplementation of melatonin through external sources may effectively prevent cardiovascular events (Arushanian, 2013; Lansink et al., 2016).

Melatonin Mediates Myocardial Protection Through Receptor and Non-receptor Pathways

In rat models of myocardial infarction, melatonin concentrations in plasma and left ventricle tissue increase sharply within 1 day, and mRNA levels of the MT1, a member of melatonin receptor, rise significantly after 2 weeks, indicating that melatonin may play an endogenous protective role in myocardial infarction (Sallinen et al., 2007). Melatonin has a biological role mainly by being bound to receptors including both membrane and nuclear binding sites. Among them, membrane receptors include melatonin receptor, TNF receptor and Notch receptor. Melatonin nuclear receptors are members of the retinoic acid related orphan nuclear receptor / retinoic acid Z receptor (ROR/RZR) family, including three subtypes: α, β, γ. The subtype α is referred to as novel endogenous myocardial infarction injury defense agent in new development progress. In rats that lack RORα receptors, the size of the myocardial infarct and degree of cardiac dysfunction after cell injury increases significantly (He et al., 2016). The related pathways by which melatonin executes its cardiac protective role via the receptor pathway includes the reperfusion injury salvage kinase (RISK) pathway, SAFE pathway and Notch pathway, with a complex association among the downstream signaling molecules (Botker et al., 2018; Coverstone et al., 2018; Shanmugam et al., 2019; Yarana et al., 2019).

The RISK pathway has an intracellular biological role primarily through the best known melatonin receptors including MT1, MT2, and MT3, all of which belong to G-protein coupled receptor family (GPCR). MT1 and MT2 have a high affinity with melatonin, while MT3 has a low affinity (Cho et al., 2019). Researchers have discovered a large number of MT1 and MT2 in the heart of rats, ducks, and coronary arteries of chicken and human beings, indicating that the cardiovascular system is a major target organ of melatonin (Hukic et al., 2017). A non-specific melatonin receptor antagonist Luzindole, eliminates the protective action of melatonin on cardiomyocytes, thus confirming their role in mediating the protective effect of melatonin on the heart (Pan et al., 2015). There are three downstream signal pathways of MT1/2, namely MAPK-ERK signal pathway, AMP-dependent protein kinase (AMPK) signal pathway and PI3K-Akt signal pathway. The three routes transmit MT1/2 activation signals from extracellular to intracellular level and mediate intracellular second messenger transmission. The downstream signaling molecules of the three pathways are crossed and connected. (a) The MAPK-ERK signaling pathway is mediated by MT1/2, the activation of MAPK-ERK up-regulates of the level of antioxidant factor Nrf2, and Nrf2 couples with DNA antioxidant reaction elements (ARE) to up-regulate the expressions of HO-1, NADPH, quinone oxidoreductase 1 (NQO1), and glutathione s-transferase 1 (GST1), and reduces the expressions of apoptotic proteins, p21 and p38 (Audia et al., 2018; Canugovi et al., 2019; Kim C.Y. et al., 2019; Liu et al., 2019). The activity of the voltage dependent anion channel (VDAC) and the transcription factor of IP3R-cAMP response element binding protein (CREB) are inhibited by activated extracellular signal regulating kinase (ERK), while excessive activation of VDAC and CREB leads to intracellular calcium overload and then causes mitochondrial dysfunction, eventually bringing about cardiomyocyte necrosis (Li et al., 2018; Zhu H. et al., 2018). Activation of this pathway also leads to inactivation of glycogen synthase kinase-3β (GSK-3β) (Nduhirabandi et al., 2012). The downstream effects also involve the activation of endothelial nitric oxide synthase (eNOS), PKC, and p70 ribosomal protein S6 (p70S6), and down-regulation of the expression of apoptosis related factors such as Bax, Bad, and phosphorylation of caspases (Paradies et al., 2015; Eid et al., 2018; Wang S. et al., 2019; Xu N. et al., 2019). In addition, the activation of MAPK-ERK signaling pathway directly inhibits the

opening of MPTP. (b) In the AMPK signaling pathway, Nrf2 is also a downstream signaling molecule of AMPK-PKG1α pathway (Wu et al., 2018b; Lu M. et al., 2019). The AMPK pathway and MAPK-ERK pathways are interrelated through Nrf2 and have a synergistic role in antioxidative stress processes and reducing apoptosis (Yu et al., 2018). In addition, the activation of AMPK inhibits the activity of mitochondrial motility related protein Drp1, which promotes mitochondrial fission, thereby activating VDAC-HK opening and ultimately promoting the MPTP opening (Singhanat et al., 2018). SIRT1 and SIRT3 are both important downstream signaling molecules that aid melatonin in its cardioprotective role. SIRT3 is the downstream target of peroxisome proliferator-activated receptor γ co-activator 1α (PGC-1α) which is stimulated by AMPK. The effect of this pathway is to reduce the transfer of Bax to mitochondria, promote the deacetylation of mitochondrial antioxidant enzyme GPX, boost the biosynthesis of mitochondria, and enhance the activity of superoxide dismutase (SOD) (Lombard and Zwaans, 2014; Lochner et al., 2018). (c) The primary downstream molecular effect of the PI3K-Akt signaling pathway is the reduction of cellular oxidative stress. The activation of Akt promotes phosphorylation of signal transducer and activator of transcription 3 (STAT3), thereby elevating TNFα release for cardiac protection (Yu et al., 2016; Kim E.H. et al., 2019). The enhanced activity of GPX and SOD raises the level of Nrf2, thus promoting the Akt signaling pathway (Song et al., 2017; Zhang H. et al., 2019). Melatonin regulates the activity of ERK through the Akt pathway. Signaling molecules in this pathway include Zrt/Irt-like protein 1 (Zip1), brain-derived neurotrophic factor (BDNF) and PPARγ. In the nuclear receptor signaling pathway, melatonin regulates autophagy and Cyt c release through ROR α, and also enhances the expression of the myocardial sarcoplasmic reticulum Ca^{2+}-ATPase (SERCA)2α, sodium-calcium exchange 1 (NCX1), Ryanodine receptor 2 (RyR2), Ca^{2+}-calmodulin-dependent kinase II (CAMKII) and other protein-related genes, thus enhancing the ability of cells to process calcium ions and reduce the stress injury to and apoptosis of the cardiomyocytes (Gebhard et al., 2018; Na et al., 2019).

In addition to the conventional melatonin receptor pathway, melatonin also binds to other receptors on the cell membrane for signal transduction, including the SAFE pathway and the Notch pathway. In the SAFE pathway, melatonin plays a role in phosphorylation of JAK2-STAT3 through TNF receptor on the cell membrane. Downstream molecular effects include the promotion of expression of BCL-2, antioxidant genes, TNFα, mcl 1, FAS and the inhibition of Bax, caspase-3, Cyt c, cyclin-dependent kinase (cyclin D1), P21 and GSK-3β (Yang et al., 2013). Melatonin also directly inhibits MPTP opening through this pathway. Phosphorylation of STAT3 activates the ERK and Akt pathways, which also promote phosphorylation of STAT3. In the Notch pathway, melatonin promotes the expression of Hairy and enhancer of split 1 (Hes 1) through Notch 1-Notch Intracellular area (NICD), while Hes1 inhibits the negative regulatory effect of chromosome 10 (PTEN) on phosphatidylinositol 3-kinase (PI3K). Notch pathway also reduces the effects of cardiomyocyte apoptosis by regulating mitophagy with mitochondrial fusion related protein (Mfn2) (Pei et al., 2016).

In addition to binding to receptors, melatonin also enters cells where it has direct biological effects (Mauriz et al., 2013). Melatonin enters the cytosol to promote the release of NO, enhances the activity of nitric oxide synthase (iNOS) and boosts the expression of SIRT3 via the activation of PKB-Akt. Activated by melatonin, SIRT1 regulates oxidative stress in cardiomyocytes, mitophagy and apoptosis by enhancing the expression of Bcl-2 and weakening Bax and caspase-3. Studies have shown that SIRT1 is an important upstream molecule of Nrf2 and can also be bound to the SIRT3 promoter to enhance the expression of SIRT3. However, whether melatonin regulates the expression of SIRT3 through the SIRT1-Nrf2 pathway requires verification (**Figure 1**).

Melatonin Stabilizes the Structure and Function of Mitochondria After AMI

Mitochondria are the site of ATP and oxygen-derived free radical production, and the target of attack by various free radicals (Connolly et al., 2018; Boengler et al., 2019; Yuan et al., 2019). Melatonin protects cardiomyocytes by stabilizing the structure and function of mitochondria and regulates mitochondrial oxidative stress, raises mitochondrial antioxidant enzyme levels, restores mitochondrial energy metabolism (Soto-Heras et al., 2019), maintains mitochondrial membrane potential stability, reduces mitochondrial injury, and inhibits mitochondrial apoptosis (Yan et al., 2018) through receptors including MT1/2. In addition, mitochondrial biosynthesis, DNA homeostasis and regulation of SIRT3 system are closely related to the function of melatonin (Reiter et al., 2017; Zhou et al., 2017d). After myocardial infarction, injured tissue releases a large quantity of oxygen-derived free radicals, inflammatory mediators and other harmful substances, which cause direct injury to mitochondria (Kalkavan and Green, 2018; Riehle and Bauersachs, 2018; Nanadikar et al., 2019). Mitochondrial dysfunction aggravates cell injury, which then becomes a vicious cycle. Melatonin breaks this vicious cycle by virtue of its potent free radical scavenging ability and antioxidant effects, thus playing a protective role in myocardium such as in ischemia-reperfusion injury (Reina and Martínez, 2018). Studies show that melatonin, as a potent free radical scavenger, is abundant in mitochondria (Venegas et al., 2012). This shows that melatonin likely prevents mitochondrial injury during the oxidative stress response (Ma et al., 2016). Melatonin also up-regulates the activity of the four respiratory complexes, thus reducing electron leakage and the generation of oxygen-derived free radicals (Nair et al., 2011). Melatonin inhibits mitochondrion fission, prevents disintegration of VDAC1 and hexokinase 2 (HK2), inhibits MTPT opening, limits endothelial cell injury, improves endothelial barrier function, reduces inflammatory cell infiltration, restores eNOS content and blood flow, lowers infarct size, preserves myocardial microvasculature, and improve prognosis (Zhang and Zhang, 2014; Li et al., 2019). Based on published reports (Wang et al., 2016), activation of MT1/2 receptor strengthens AMPK signaling pathway, up-regulates optic atrophy 1 (OPA1) level and then modulates mitophagy during myocardial infarction. Mitophagy degrades injured mitochondria so as to maintain the structure and function of normal mitochondria, reduces cardiomyocyte apoptosis and lowers the degree of myocardial

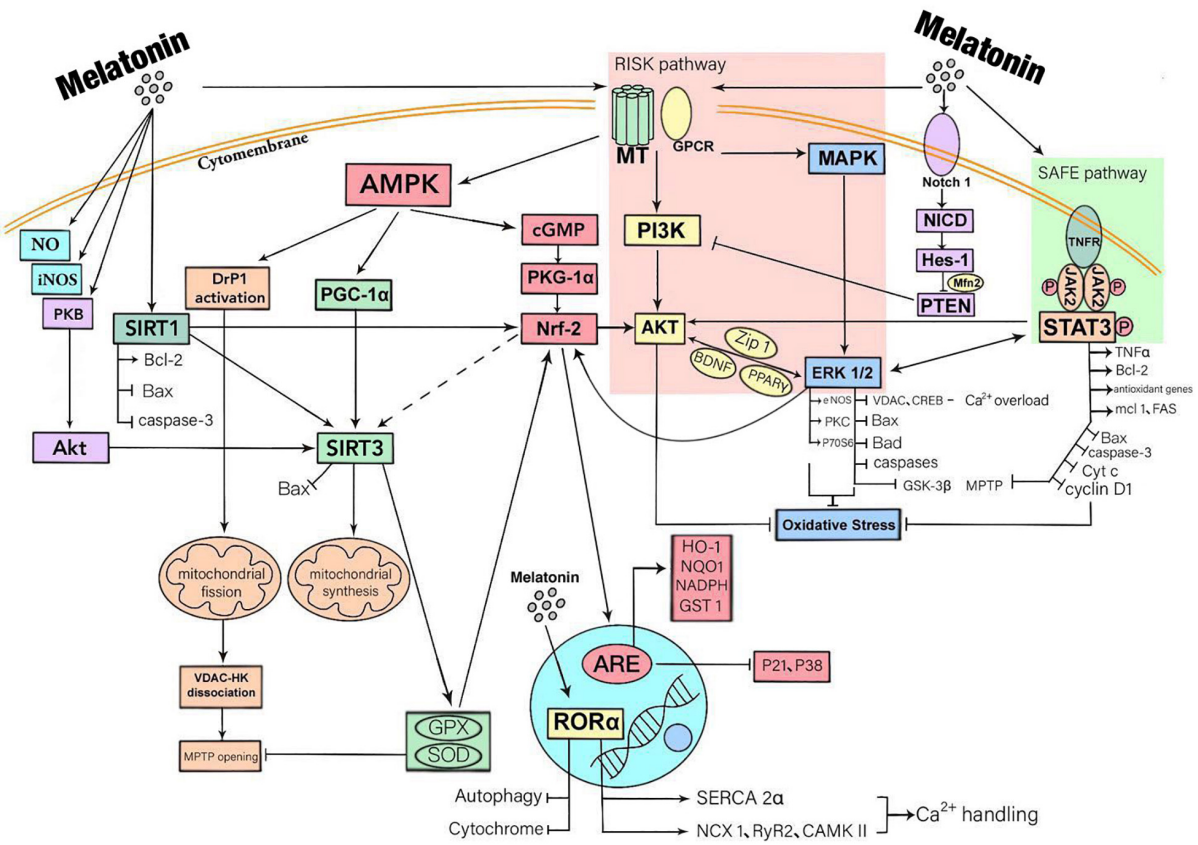

FIGURE 1 | A summary of the mechanisms that myocardial protection mediated by melatonin through receptor and non-receptor pathways. Melatonin has a biological role mainly by being bound to receptors. There are three downstream signal pathways of MT1/2, namely MAPK-ERK signal pathway, AMP-dependent protein kinase (AMPK) signal pathway and PI3K-Akt signal pathway. Melatonin also activates STAT3, a signal transducer and activator of transcription factor for antioxidant enzymes, by activating SAFE pathway. Besides, melatonin activates the Notch1 pathway, thus inhibiting PIK3 function. These downstream signaling molecules are crossed and connected within the cell. In addition, melatonin also enters cells where it has direct biological effects. It promotes the release of NO, enhances the activity of iNOS and boosts the expression of SIRT3 via the activation of PKB-Akt. The ultimate effects of these responses are to reduce oxidative stress, inflammatory responses, and to protect mitochondrial function, thereby reducing cardiomyocyte apoptosis.

injury during infarction (Dominguez-Rodriguez et al., 2017a; Zhang Y. et al., 2019).

CLINICAL APPLICATION AND PROSPECT OF MELATONIN USE IN ACUTE MYOCARDIAL INFARCTION

Due to the non-renewability of cardiomyocytes, it is essential to reduce cardiac damage and improve long-term prognosis of patients with myocardial infarction by clarifying the mechanisms of injury and necrosis of cardiomyocytes after a cardiovascular episode (Gaspar et al., 2018; Wu et al., 2018a; Heusch, 2019). In addition to the mechanisms of inflammatory cell infiltration and oxidative stress injury which have been reported many times, mitochondrial injury and apoptosis are the key initiating processes of myocardial injury following myocardial infarction (Hofmann, 2018; Villalobos et al., 2018; Wang Y. et al., 2018; Boengler et al., 2019; Phan et al., 2019). There is an urgent need to find a method which can effectively reduce mitochondrial injury and to improve cardiomyocyte function following myocardial infarction and provide a new target for clinical treatment.

As an indole and age-related molecule secreted by the human pineal gland, melatonin has remarkable functions including antioxidant, anti-apoptosis, anti-fibrosis, direct free radical scavenging, and mitochondrial protection (Jumnongprakhon et al., 2016). Melatonin receptors also play a role in reducing cardiac damage (Liu et al., 2016). In models of myocardial reperfusion injury, melatonin promotes mitochondrial fusion through AMPK/OPA1 signaling pathway and OPA1 binds with lysine 70 residues of mitophagy receptor FUNDC1 to mediate mitophagy (Del Dotto et al., 2018; Wang B. et al., 2018). Recent studies reveal that mitochondria exhibit biological rhythms, which may be regulated by the melatonin cycle. However, studies have not been conducted to clarify the role of melatonin in the mitochondrial biological clock and the myocardial protective effects that involve these rhythms. As mentioned above, melatonin is secreted in large quantities at night according to its circadian rhythm. Studies illustrates that the nocturnal secretion of melatonin in patients with CHD

TABLE 1 | A summary of the results of some clinical trials (there are many more), which illustrate the beneficial effects of melatonin in clinical acute myocardial infarction.

Type of study	Study population	Administration route	Results	Possible mechanism
Unicenter, randomized, double-blind, parallel-group, placebo-controlled study (Dominguez-Rodriguez et al., 2007a)	272 patients with AMI and be expected to undergo primary angioplasty (PA); melatonin group (n = 136), placebo group (n = 136).	Patients received a total intravenous melatonin dose of 11.61 mg (approximately 166 μg/kg) or placebo. The temporal distribution of perfusion was: 30 min previous to percutaneous revascularization and remainder doses in a subsequent 120 min (1 h during the angioplasty + 60 min post-intervention).	The infarction size of melatonin group and placebo group was 9.0% and 19.5%, respectively ($P < 0.05$).	The cardiac-protection effect of melatonin was most likely through its direct free radical scavenging activities, indirect antioxidant activity and its ability to increase mitochondrial bioenergetics.
Case-control study (Dominguez-Rodriguez et al., 2008)	90 patients with STEMI and 70 healthy humans.	No melatonin was administered.	Melatonin value kept adiurnal variation but with a significantly lower dose in STEMI patients ($P < 0.001$). The mean nocturnal melatonin levels in these patients was lower than in the control group ($P < 0.001$).	The lower melatonin production rate in AMI patients was correlated with the stage of the disease, and some immunological factors, such as CRP and cytokines, could play an important role in the pathogenesis.
Prospective cohort study (Dominguez-Rodriguez et al., 2010a)	180 patients with first STEMI who underwent PCI within 6 h from onset of symptoms. 63 patients (35%) were angiographic no-reflow after PCI.	No melatonin was administered.	Patients with angiographic no-reflow had lower intraplatelet melatonin levels compared to patients without no-reflow (12.32 ± 3.64 vs. 18.62 ± 3.88 ng/100,000 platelets, $P < 0.0001$)	Platelets have Melatonin inhibits platelet cyclooxygenase and decreases arachidonic acid-induced aggregation and thromboxane B2 production and thus inhibits platelet aggregation.
Prospective cohort study (Dominguez-Rodriguez et al., 2012)	161 patients with AMI.	No melatonin was administered.	Melatonin levels (OR = 2.10, CI 95% 1.547–2.870, $P < 0.001$) were an independent predictor of LV remodeling.	The anti-fibrotic and antioxidant effect of melatonin.
Nested case-control study (McMullan et al., 2017)	209 women with incident cases of fatal and non-fatal MI and were matched to 209 controls.	No melatonin was administered.	Lower melatonin secretion was significantly associated with a higher risk of MI. Women in the highest concentration had an estimated absolute risk of MI of 84 cases per 100,000 person-years compared with 197 cases per 100,000 person-years in the lowest concentration, and the association was strongly modified by body mass index (BMI) (p = 0.02).	Melatonin reduces platelet aggregation, against plaque rupture, and regulates the immune system and inflammation.
Prospective, multicenter, randomized, double blind, placebo-controlled study (Dominguez-Rodriguez et al., 2017b)	146 patients with STEMI; melatonin group (n = 73), placebo group (n = 73).	The experimental drug was a formulation of melatonin in polyethylene glycol solution. Patients in the melatonin group received a dose of 51.7 μmol intravenously given by a time period of 60 min starting immediately before PCI and a bolus of 8.6 μmol of intracoronary melatonin given through the PCI-guiding catheter after restoring the blood flow to the infarct related artery. The placebo group received a matching placebo formulation.	No significant differences in the myocardial infarct size between the two group. Both left ventricular end-diastolic and end-systolic volumes were lower in the placebo group (P = 0.01). No significant differences in the incidence of adverse events at 1 year in both groups (P = 0.150).	The median pain-to-balloon time (200 min) was so long that it likely negated the benefits of melatonin in reducing lethal IRI.

(Continued)

TABLE 1 | Continued

Type of study	Study population	Administration route	Results	Possible mechanism
Unicenter, randomized, double-blinded, placebo controlled (Ekeloef et al., 2017)	48 patients with STEMI; melatonin group (n = 24), placebo group (n = 24).	Patients were randomized to receive either intracoronary or intravenous melatonin (total 50 mg) or placebo (isotonic saline)	Melatonin did not exert a significant effect on myocardial salvage index after PCI. The myocardial salvage index at day 4 (±1 day) after PCI was similar in the melatonin group (n = 22) at 55.3% (95% CI 47.0–63.6) and the placebo group (n = 19) at 61.5% (95% CI 57.5–65.5), p = 0.21.	The cardioprotective effects of melatonin might be largely dependent on a clinically effective distribution of the drug in the myocardial area at risk, prior to ischemia and definitely prior to reperfusion
Prospective, multicenter, randomized, double blind, placebo-controlled study (Dominguez-Rodriguez et al., 2017a)	146 patients with STEMI; melatonin group (n = 73), placebo group (n = 73). Randomized patients were divided into tertiles according to symptoms onset to balloon time: first tertile (136 ± 23 min), second tertile (196 ± 19 min), and third tertile (249 ± 41 min).	The experimental drug was a formulation of melatonin in polyethylene glycol solution. Patients in the melatonin group received a dose of 51.7 μmol intravenously given by a time period of 60 min starting immediately before PCI and a bolus of 8.6 μmol of intracoronary melatonin given through the PCI-guiding catheter after restoring the blood flow to the infarct related artery. The placebo group received a matching placebo formulation.	In the first tertile, the infarct size was significantly smaller in the melatonin-treated subjects compared with placebo (14.6 ± 14.2 vs. 24.9 ± 9.0%; P = 0.003). Treatment with melatonin was associated with a larger infarct size in the group of patients included in the third tertile (20.5 ± 8.7% vs. 11.2 ± 5.2%; P = 0.001), resulting in a significant interaction (P = 0.001).	Melatonin administered earlier may result in a greater cardioprotective effect compared with delayed administration. Treatments that are able to reduce mitochondrial dysfunction appear to be more effective after shorter ischemic periods.

AMI, acute myocardial infarction; PCI, percutaneous coronary intervention; STEMI, ST-segment elevation myocardial infarction.

decreases significantly compared with healthy people and it may be associated with various disease risk factors in these patients which can explain why AMI always happen (at a peak) in early morning when melatonin levels are adequate (Dominguez-Rodriguez et al., 2006, 2007a).

In terms of clinical disease treatment, most studies on melatonin-induced cardiovascular effect are in phase 2a of clinical trials, and according to literatures, melatonin has a beneficial therapeutic effect on hypertension, atherosclerosis, CHD, and other chronic cardiovascular diseases (Yang et al., 2014; Simko et al., 2016; Baltatu et al., 2019) (**Table 1**). Since it is an age-related molecule, it declines with age. Because of its high safety profile, it has important potential clinical applications. Clinical trials demonstrate that melatonin significantly reduce the area of myocardial infarction when used in the treatment of STEMI (ST-elevation myocardial infarction) patients after PCI (Dominguez-Rodriguez et al., 2017a). In addition, the use of melatonin before surgery significantly reduces CABG related oxidative stress and cardiac injury, and on the other hand increase the activity of Nrf2 in patients (Haghjooy Javanmard et al., 2013; Shafiei et al., 2018). Melatonin plays a role in reducing nocturnal hypertension in patients by affecting circadian cardiovascular rhythms of blood pressure (Grossman et al., 2011). The experimental results of Ma et al. (2018) show that melatonin eliminates ROS by regulating the mitophagy in macrophages, thus inhibiting the activation of NLRP3 (nucleotide-binding domain and leucine-rich repeat pyrin domain containing 3) inflammasome and ultimately inhibiting the progression of atherosclerosis, which is mediated at least in part through the Sirt3 signaling pathway.

Studies reveal that (Dominguez-Rodriguez et al., 2017a), from the onset of myocardial infarction symptoms to the beginning of interventional therapy, the application of melatonin in a short time window can effectively reduce the size of a myocardial infarct. Repair after a myocardial infarction is a complex process involved with multiple factors, but whether melatonin is involved with these repair processes have not been investigated. The combination of melatonin with other myocardial protective drugs (e.g., antithrombotic drugs and new-type myocardial metabolic regulation drug GLP1) has not yet been reported, and further research is required to confirm the myocardial protective actions of melatonin treatment.

AUTHOR CONTRIBUTIONS

ZF conceived and designed the review. ZF, YJ, JW, YZ, and MS collected the literatures. YJ and ZF wrote the manuscript. ZF, RR, and YC reviewed and edited the manuscript. QX revised the manuscript and the language. All authors read and approved the manuscript.

FUNDING

This study was supported by National Natural Science Foundation of China (fund numbers 81500269, 81500202, and 81570383).

REFERENCES

Abdelnaseer, M., Elfayomi, N., Esmail, E. H., Kamal, M. M., Hamdy, A., Samie, R. M. A., et al. (2016). Relationship between matrix metalloproteinase-9 and common carotid artery intima media thickness. *Neurol. Sci.* 37, 117–122. doi: 10.1007/s10072-015-2358-z

Abukar, Y., Ramchandra, R., Hood, S. G., McKinley, M. J., Booth, L. C., Yao, S. T., et al. (2018). Increased cardiac sympathetic nerve activity in ovine heart failure is reduced by lesion of the area postrema, but not lamina terminalis. *Basic Res. Cardiol.* 113:35.

Adameova, A., Goncalvesova, E., Szobi, A., and Dhalla, N. S. (2016). Necroptotic cell death in failing heart: relevance and proposed mechanisms. *Heart Fail. Rev.* 21, 213–221. doi: 10.1007/s10741-016-9537-8

Aimo, A., Cerbai, E., Bartolucci, G., Adamo, L., Barison, A., Lo Surdo, G., et al. (2020). Pirfenidone is a cardioprotective drug: mechanisms of action and preclinical evidence. *Pharmacol. Res.* 155:104694. doi: 10.1016/j.phrs.2020.104694

Amanakis, G., Kleinbongard, P., Heusch, G., and Skyschally, A. (2019). Attenuation of ST-segment elevation after ischemic conditioning maneuvers reflects cardioprotection online. *Basic Res. Cardiol.* 114:22. doi: 10.1007/s00395-019-0732-3

Amin, N., Shafabakhsh, R., Reiter, R. J., and Asemi, Z. (2019). Melatonin is an appropriate candidate for breast cancer treatment: based on known molecular mechanisms. *J. Cell. Biochem.* 120, 12208–12215. doi: 10.1002/jcb.28832

Arushanian, E. B. (2013). Effect of melatonin on the thrombocyte hemostasis and its circadian organization. *Eksp. Klin. Farmakol.* 76, 32–36.

Audia, J. P., Yang, X. M., Crockett, E. S., Housley, N., Haq, E. U., O'Donnell, K., et al. (2018). Caspase-1 inhibition by VX-765 administered at reperfusion in P2Y12 receptor antagonist-treated rats provides long-term reduction in myocardial infarct size and preservation of ventricular function. *Basic Res. Cardiol.* 113:32. doi: 10.1007/s00395-018-0692-z

Bacmeister, L., Schwarzl, M., Warnke, S., Stoffers, B., Blankenberg, S., Westermann, D., et al. (2019). Inflammation and fibrosis in murine models of heart failure. *Basic Res. Cardiol.* 114:19.

Baltatu, O. C., Senar, S., Campos, L. A., and Cipolla-Neto, J. (2019). Cardioprotective melatonin: translating from proof-of-concept studies to therapeutic use. *Int. J. Mol. Sci.* 20:4342. doi: 10.3390/ijms20184342

Basalay, M. V., Davidson, S. M., Gourine, A. V., and Yellon, D. M. (2018). Neural mechanisms in remote ischaemic conditioning in the heart and brain: mechanistic and translational aspects. *Basic Res. Cardiol.* 113:25. doi: 10.1007/s00395-018-0684-z

Battogtokh, G., Choi, Y. S., Kang, D. S., Park, S. J., Shim, M. S., Huh, K. M., et al. (2018). Mitochondria-targeting drug conjugates for cytotoxic, anti-oxidizing and sensing purposes: current strategies and future perspectives. *Acta Pharm. Sin. B* 8, 862–880. doi: 10.1016/j.apsb.2018.05.006

Beckendorf, J., van den Hoogenhof, M. M. G., and Backs, J. (2018). Physiological and unappreciated roles of CaMKII in the heart. *Basic Res. Cardiol.* 113:29.

Bhandari, P., Song, M., Chen, Y., Burelle, Y., and Dorn, G. W. (2014). Mitochondrial contagion induced by Parkin deficiency in *Drosophila* hearts and its containment by suppressing mitofusin. *Circ. Res.* 114, 257–265. doi: 10.1161/CIRCRESAHA.114.302734

Bocci, M., Sjolund, J., Kurzejamska, E., Lindgren, D., Marzouka, N. A., Bartoschek, M., et al. (2019). Activin receptor-like kinase 1 is associated with immune cell infiltration and regulates CLEC14A transcription in cancer. *Angiogenesis* 22, 117–131. doi: 10.1007/s10456-018-9642-5

Boengler, K., Bornbaum, J., Schluter, K. D., and Schulz, R. (2019). P66shc and its role in ischemic cardiovascular diseases. *Basic Res. Cardiol.* 114:29. doi: 10.1007/s00395-019-0738-x

Boengler, K., Lochnit, G., and Schulz, R. (2018). Mitochondria "THE" target of myocardial conditioning. *Am. J. Physiol. Heart Circ. Physiol.* 315, H1215–H1231. doi: 10.1152/ajpheart.00124.2018

Botker, H. E., Hausenloy, D., Andreadou, I., Antonucci, S., Boengler, K., Davidson, S. M., et al. (2018). Practical guidelines for rigor and reproducibility in preclinical and clinical studies on cardioprotection. *Basic Res. Cardiol.* 113:39.

Breda, C. N. S., Davanzo, G. G., Basso, P. J., Saraiva Camara, N. O., and Moraes-Vieira, P. M. M. (2019). Mitochondria as central hub of the immune system. *Redox Biol.* 26:101255. doi: 10.1016/j.redox.2019.101255

Canugovi, C., Stevenson, M. D., Vendrov, A. E., Hayami, T., Robidoux, J., Xiao, H., et al. (2019). Increased mitochondrial NADPH oxidase 4 (NOX4) expression in aging is a causative factor in aortic stiffening. *Redox Biol.* 26:101288. doi: 10.1016/j.redox.2019.101288

Cao, T., Fan, S., Zheng, D., Wang, G., Yu, Y., Chen, R., et al. (2019). Increased calpain-1 in mitochondria induces dilated heart failure in mice: role of mitochondrial superoxide anion. *Basic Res. Cardiol.* 114:17.

Chen, M., Ye, K., Zhang, B., Xin, Q., Li, P., Kong, A. N., et al. (2019). Paris Saponin II inhibits colorectal carcinogenesis by regulating mitochondrial fission and NF-kappaB pathway. *Pharmacol. Res.* 139, 273–285. doi: 10.1016/j.phrs.2018.11.029

Chen, S., Dong, G., Wu, S., Liu, N., Zhang, W., and Sheng, C. (2019). Novel fluorescent probes of 10-hydroxyevodiamine: autophagy and apoptosis-inducing anticancer mechanisms. *Acta Pharm. Sin. B* 9, 144–156. doi: 10.1016/j.apsb.2018.08.003

Chen, W., Spitzl, A., Mathes, D., Nikolaev, V. O., Werner, F., Weirather, J., et al. (2016). Endothelial actions of ANP enhance myocardial inflammatory infiltration in the early phase after acute infarction. *Circ. Res.* 119, 237–248. doi: 10.1161/CIRCRESAHA.115.307196

Cho, J. H., Tae, H. J., Kim, I. S., Song, M., Kim, H., Lee, T. K., et al. (2019). Melatonin alleviates asphyxial cardiac arrest-induced cerebellar Purkinje cell death by attenuation of oxidative stress. *Exp. Neurol.* 320:112983. doi: 10.1016/j.expneurol.2019.112983

Cohen, A. T., Berger, S. E., Milenkovic, D., Hill, N. R., and Lister, S. (2019). Anticoagulant selection for patients with VTE-Evidence from a systematic literature review of network meta-analyses. *Pharmacol. Res.* 143, 166–177. doi: 10.1016/j.phrs.2019.03.017

Connolly, N. M. C., Theurey, P., Adam-Vizi, V., Bazan, N. G., Bernardi, P., Bolanos, J. P., et al. (2018). Guidelines on experimental methods to assess mitochondrial dysfunction in cellular models of neurodegenerative diseases. *Cell Death Differ.* 25, 542–572.

Coverstone, E. D., Bach, R. G., Chen, L., Bierut, L. J., Li, A. Y., Lenzini, P. A., et al. (2018). A novel genetic marker of decreased inflammation and improved survival after acute myocardial infarction. *Basic Res. Cardiol.* 113:38.

Crist, A. M., Lee, A. R., Patel, N. R., Westhoff, D. E., and Meadows, S. M. (2018). Vascular deficiency of Smad4 causes arteriovenous malformations: a mouse model of Hereditary Hemorrhagic Telangiectasia. *Angiogenesis* 21, 363–380. doi: 10.1007/s10456-018-9602-0

Davidson, S. M., Arjun, S., Basalay, M. V., Bell, R. M., Bromage, D. I., Botker, H. E., et al. (2018). The 10th biennial hatter cardiovascular institute workshop: cellular protection-evaluating new directions in the setting of myocardial infarction, ischaemic stroke, and cardio-oncology. *Basic Res. Cardiol.* 113:43. doi: 10.1007/s00395-018-0704-z

de Oliveira Junior, E. R., Nascimento, T. L., Salomao, M. A., da Silva, A. C. G., Valadares, M. C., and Lima, E. M. (2019). Increased nose-to-brain delivery of melatonin mediated by polycaprolactone nanoparticles for the treatment of glioblastoma. *Pharm. Res.* 36:131. doi: 10.1007/s11095-019-2662-z

Del Dotto, V., Fogazza, M., Lenaers, G., Rugolo, M., Carelli, V., and Zanna, C. (2018). OPA1: how much do we know to approach therapy? *Pharmacol. Res.* 131, 199–210. doi: 10.1016/j.phrs.2018.02.018

Dominguez-Rodriguez, A., Abreu-Gonzalez, P., Arroyo-Ucar, E., and Reiter, R. J. (2012). Decreased level of melatonin in serum predicts left ventricular remodelling after acute myocardial infarction. *J. Pineal Res.* 53, 319–323. doi: 10.1111/j.1600-079X.2012.01001.x

Dominguez-Rodriguez, A., Abreu-Gonzalez, P., de la Torre-Hernandez, J. M., Consuegra-Sanchez, L., Piccolo, R., Gonzalez-Gonzalez, J., et al. (2017a). Usefulness of early treatment with melatonin to reduce infarct size in patients with ST-segment elevation myocardial infarction receiving percutaneous coronary intervention (from the melatonin adjunct in the acute myocardial infarction treated with angioplasty trial). *Am. J. Cardiol.* 120, 522–526. doi: 10.1016/j.amjcard.2017.05.018

Dominguez-Rodriguez, A., Abreu-Gonzalez, P., de la Torre-Hernandez, J. M., Gonzalez-Gonzalez, J., Garcia-Camarero, T., Consuegra-Sanchez, L., et al. (2017b). Effect of intravenous and intracoronary melatonin as an adjunct to primary percutaneous coronary intervention for acute ST-elevation myocardial infarction: results of the Melatonin Adjunct in the acute myocaRdial Infarction treated with Angioplasty trial. *J. Pineal Res.* 62:e12374. doi: 10.1111/jpi.12374

Dominguez-Rodriguez, A., Abreu-Gonzalez, P., Garcia-Gonzalez, M., and Reiter, R. J. (2006). Prognostic value of nocturnal melatonin levels as a novel marker in patients with ST-segment elevation myocardial infarction. *Am. J. Cardiol.* 97, 1162–1164. doi: 10.1016/j.amjcard.2005.11.033

Dominguez-Rodriguez, A., Abreu-Gonzalez, P., Garcia-Gonzalez, M. J., Kaski, J. C., Reiter, R. J., and Jimenez-Sosa, A. (2007a). A unicenter, randomized, double-blind, parallel-group, placebo-controlled study of melatonin as an adjunct in patients with acute myocardial infarction undergoing primary angioplasty the melatonin adjunct in the acute myocardial infarction treated with angioplasty (MARIA) trial: study design and rationale. *Contemp. Clin. Trials* 28, 532–539. doi: 10.1016/j.cct.2006.10.007

Dominguez-Rodriguez, A., Abreu-Gonzalez, P., Garcia-Gonzalez, M. J., and Reiter, R. J. (2007b). Relation of nocturnal melatonin levels to serum matrix metalloproteinase-9 concentrations in patients with myocardial infarction. *Thromb. Res.* 120, 361–366. doi: 10.1016/j.thromres.2006.10.010

Dominguez-Rodriguez, A., Abreu-Gonzalez, P., Garcia-Gonzalez, M. J., Samimi-Fard, S., Kaski, J. C., and Reiter, R. J. (2008). Light/dark patterns of soluble vascular cell adhesion molecule-1 in relation to melatonin in patients with ST-segment elevation myocardial infarction. *J. Pineal Res.* 44, 65–69. doi: 10.1111/j.1600-079X.2007.00529.x

Dominguez-Rodriguez, A., Abreu-Gonzalez, P., Jimenez-Sosa, A., Avanzas, P., Bosa-Ojeda, F., and Kaski, J. C. (2010a). Usefulness of intraplatelet melatonin levels to predict angiographic no-reflow after primary percutaneous coronary intervention in patients with ST-segment elevation myocardial infarction. *Am. J. Cardiol.* 106, 1540–1544. doi: 10.1016/j.amjcard.2010.07.030

Dominguez-Rodriguez, A., Abreu-Gonzalez, P., Sanchez-Sanchez, J. J., Kaski, J. C., et al. (2010b). Melatonin and circadian biology in human cardiovascular disease. *J. Pineal Res.* 49, 14–22. doi: 10.1111/j.1600-079X.2010.00773.x

Eid, R. A., Alkhateeb, M. A., Eleawa, S., Al-Hashem, F. H., Al-Shraim, M., El-Kott, A. F., et al. (2018). Cardioprotective effect of ghrelin against myocardial infarction-induced left ventricular injury via inhibition of SOCS3 and activation of JAK2/STAT3 signaling. *Basic Res. Cardiol.* 113:13.

Ekeloef, S., Halladin, N., Fonnes, S., Jensen, S. E., Zaremba, T., Rosenberg, J., et al. (2017). Effect of intracoronary and intravenous melatonin on myocardial salvage index in patients with ST-elevation myocardial infarction: a randomized placebo controlled trial. *J. Cardiovasc. Transl. Res.* 10, 470–479. doi: 10.1007/s12265-017-9768-7

Espinosa-Diez, C., Miguel, V., Vallejo, S., Sanchez, F. J., Sandoval, E., Blanco, E., et al. (2018). Role of glutathione biosynthesis in endothelial dysfunction and fibrosis. *Redox Biol.* 14, 88–99. doi: 10.1016/j.redox.2017.08.019

Faghfouri, A. H., Zarrin, R., Maleki, V., Payahoo, L., and Khajebishak, Y. (2020). A comprehensive mechanistic review insight into the effects of micronutrients on toll-like receptors functions. *Pharmacol. Res.* 152:104619. doi: 10.1016/j.phrs.2019.104619

Filadi, R., Greotti, E., and Pizzo, P. (2018). Highlighting the endoplasmic reticulum-mitochondria connection: focus on mitofusin 2. *Pharmacol. Res.* 128, 42–51. doi: 10.1016/j.phrs.2018.01.003

Fuhrmann, D. C., and Brune, B. (2017). Mitochondrial composition and function under the control of hypoxia. *Redox Biol.* 12, 208–215. doi: 10.1016/j.redox.2017.02.012

Galano, A., and Reiter, R. J. (2018). Melatonin and its metabolites vs oxidative stress: from individual actions to collective protection. *J. Pineal Res.* 65:e12514. doi: 10.1111/jpi.12514

Galano, A., Tan, D. X., and Reiter, R. J. (2013). On the free radical scavenging activities of melatonin's metabolites, AFMK and AMK. *J. Pineal Res.* 54, 245–257. doi: 10.1111/jpi.12010

Galluzzi, L., Vitale, I., Aaronson, S. A., Abrams, J. M., Adam, D., Agostinis, P., et al. (2018). Molecular mechanisms of cell death: recommendations of the nomenclature committee on cell death 2018. *Cell Death Differ.* 25, 486–541.

Garcia, J. A., Volt, H., Venegas, C., Doerrier, C., Escames, G., Lopez, L. C., et al. (2015). Disruption of the NF-kappaB/NLRP3 connection by melatonin requires retinoid-related orphan receptor-alpha and blocks the septic response in mice. *FASEB J.* 29, 3863–3875. doi: 10.1096/fj.15-273656

Gaspar, A., Lourenco, A. P., Pereira, M. A., Azevedo, P., Roncon-Albuquerque, R. Jr., et al. (2018). Randomized controlled trial of remote ischaemic conditioning in ST-elevation myocardial infarction as adjuvant to primary angioplasty (RIC-STEMI). *Basic Res. Cardiol.* 113:14.

Gebhard, C., Maafi, F., Stahli, B. E., Dang, J., Nachar, W., de Oliveira Moraes, A. B., et al. (2018). Apolipoprotein A-I proteolysis in aortic valve stenosis: role of cathepsin S. *Basic Res. Cardiol.* 113:30. doi: 10.1007/s00395-018-0689-7

Girish, K. S., Paul, M., Thushara, R. M., Hemshekhar, M., Shanmuga Sundaram, M., Rangappa, K. S., et al. (2013). Melatonin elevates apoptosis in human platelets via ROS mediated mitochondrial damage. *Biochem. Biophys. Res. Commun.* 438, 198–204. doi: 10.1016/j.bbrc.2013.07.053

Giudice, A., Arra, C., and Turco, M. C. (2010). Review of molecular mechanisms involved in the activation of the Nrf2-ARE signaling pathway by chemopreventive agents. *Methods Mol. Biol.* 647, 37–74. doi: 10.1007/978-1-60761-738-9_3

Graczyk-Jarzynka, A., Goral, A., Muchowicz, A., Zagozdzon, R., Winiarska, M., Bajor, M., et al. (2019). Inhibition of thioredoxin-dependent H2O2 removal sensitizes malignant B-cells to pharmacological ascorbate. *Redox Biol.* 21:101062. doi: 10.1016/j.redox.2018.11.020

Grossman, E., Laudon, M., and Zisapel, N. (2011). Effect of melatonin on nocturnal blood pressure: meta-analysis of randomized controlled trials. *Vasc. Health Risk Manag.* 7, 577–584. doi: 10.2147/VHRM.S24603

Guidarelli, A., Fiorani, M., Cerioni, L., and Cantoni, O. (2019). Calcium signals between the ryanodine receptor- and mitochondria critically regulate the effects of arsenite on mitochondrial superoxide formation and on the ensuing survival vs apoptotic signaling. *Redox Biol.* 20, 285–295. doi: 10.1016/j.redox.2018.10.015

Hadebe, N., Cour, M., and Lecour, S. (2018). The SAFE pathway for cardioprotection: is this a promising target? *Basic Res. Cardiol.* 113:9. doi: 10.1007/s00395-018-0670-5

Haghjooy Javanmard, S., Ziaei, A., Ziaei, S., Ziaei, E., and Mirmohammad-Sadeghi, M. (2013). The effect of preoperative melatonin on nuclear erythroid 2-related factor 2 activation in patients undergoing coronary artery bypass grafting surgery. *Oxid. Med. Cell. Longev.* 2013:676829. doi: 10.1155/2013/676829

He, B., Zhao, Y. C., Xu, L. W., Gao, L. C., Su, Y. Y., Lin, N., et al. (2016). The nuclear melatonin receptor RORα is a novel endogenous defender against myocardial ischemia/reperfusion injury. *J. Pineal Res.* 60, 313–326. doi: 10.1111/jpi.12312

Heckmann, B. L., Tummers, B., and Green, D. R. (2019). Crashing the computer: apoptosis vs. necroptosis in neuroinflammation. *Cell Death Differ.* 26, 41–52. doi: 10.1038/s41418-018-0195-3

Heusch, G. (2019). Coronary microvascular obstruction: the new frontier in cardioprotection. *Basic Res. Cardiol.* 114:45. doi: 10.1007/s00395-019-0756-8

Hockings, C., Alsop, A. E., Fennell, S. C., Lee, E. F., Fairlie, W. D., Dewson, G., et al. (2018). Mcl-1 and Bcl-xL sequestration of Bak confers differential resistance to BH3-only proteins. *Cell Death Differ.* 25, 719–732. doi: 10.1038/s41418-017-0010-6

Hofmann, F. (2018). A concise discussion of the regulatory role of cGMP kinase I in cardiac physiology and pathology. *Basic Res. Cardiol.* 113:31. doi: 10.1007/s00395-018-0690-1

Hu, C., Wang, P., Zhang, S., Ren, L., Lv, Y., Yin, R., et al. (2017). Neuroprotective effect of melatonin on soluble Abeta1-42-induced cortical neurodegeneration via Reelin-Dab1 signaling pathway. *Neurol. Res.* 39, 621–631. doi: 10.1080/01616412.2017.1312805

Hu, S. Y., Zhang, Y., Zhu, P. J., Zhou, H., and Chen, Y. D. (2017). Liraglutide directly protects cardiomyocytes against reperfusion injury possibly via modulation of intracellular calcium homeostasis. *Geriatr. Cardiol.* 14, 57–66. doi: 10.11909/j.issn.1671-5411.2017.01.008

Hu, C., Zhang, X., Wei, W., Zhang, N., Wu, H., Ma, Z., et al. (2019). Matrine attenuates oxidative stress and cardiomyocyte apoptosis in doxorubicin-induced cardiotoxicity via maintaining AMPKalpha/UCP2 pathway. *Acta Pharm. Sin. B* 9, 690–701. doi: 10.1016/j.apsb.2019.03.003

Hukic, D. S., Lavebratt, C., Olsson, E., Ostenson, C. G., Eriksson, S. V., Erlinge, D., et al. (2017). Troponin T levels associated with genetic variants in NOTCH2 and MTNR1B in women with psychosis. *Psychiatry Res.* 250, 217–220. doi: 10.1016/j.psychres.2017.01.030

Jager, S. C. A. D., and Hoefer, I. E. (2019). Local inflammatory responses take their toll on the heart. *Int. J. Cardiol.* 293, 254–255. doi: 10.1016/j.ijcard.2019.07.055

Ji, C. H., and Kwon, Y. T. (2017). Crosstalk and interplay between the ubiquitin-proteasome system and autophagy. *Mol. Cells* 40, 441–449. doi: 10.14348/molcells.2017.0115

Jiang, Q., Xiang, B., Wang, H., Huang, K., Kong, H., and Hu, S. (2019). Remote ischaemic preconditioning ameliorates sinus rhythm restoration rate through Cox maze radiofrequency procedure associated with inflammation reaction reduction. *Basic Res. Cardiol.* 114:14. doi: 10.1007/s00395-019-0723-4

Jin, Q., Li, R., Hu, N., Xin, T., Zhu, P., Hu, S., et al. (2018). DUSP1 alleviates cardiac ischemia/reperfusion injury by suppressing the Mff-required mitochondrial fission and Bnip3-related mitophagy via the JNK pathways. *Redox Biol.* 14, 576–587. doi: 10.1016/j.redox.2017.11.004

Joshi, A. U., and Mochly-Rosen, D. (2018). Mortal engines: mitochondrial bioenergetics and dysfunction in neurodegenerative diseases. *Pharmacol. Res.* 138, 2–15. doi: 10.1016/j.phrs.2018.08.010

Joshi, C., Bapat, R., Anderson, W., Dawson, D., Hijazi, K., and Cherukara, G. (2019). Detection of periodontal microorganisms in coronary atheromatous plaque specimens of myocardial infarction patients: a systematic review and meta-analysis. *Trends Cardiovasc. Med.* [Epub ahead of print].

Jumnongprakhon, P., Govitrapong, P., Tocharus, C., and Tocharus, J. (2016). Inhibitory effect of melatonin on cerebral endothelial cells dysfunction induced by methamphetamine via NADPH oxidase-2. *Brain Res.* 1650, 84–92. doi: 10.1016/j.brainres.2016.08.045

Kalkavan, H., and Green, D. R. (2018). MOMP, cell suicide as a BCL-2 family business. *Cell Death Differ.* 25, 46–55. doi: 10.1038/cdd.2017.179

Kanaan, G. N., Ichim, B., Gharibeh, L., Maharsy, W., Patten, D. A., Xuan, J. Y., et al. (2018). Glutaredoxin-2 controls cardiac mitochondrial dynamics and energetics in mice, and protects against human cardiac pathologies. *Redox Biol.* 14, 509–521. doi: 10.1016/j.redox.2017.10.019

Kang, J. W., Hong, J. M., and Lee, S. M. (2016). Melatonin enhances mitophagy and mitochondrial biogenesis in rats with carbon tetrachloride-induced liver fibrosis. *J. Pineal Res.* 60, 383–393. doi: 10.1111/jpi.12319

Karwi, Q. G., Bice, J. S., and Baxter, G. F. (2018). Pre- and postconditioning the heart with hydrogen sulfide (H2S) against ischemia/reperfusion injury in vivo: a systematic review and meta-analysis. *Basic Res. Cardiol.* 113:6. doi: 10.1007/s00395-017-0664-8

Kim, C. Y., Kang, B., Suh, H. J., and Choi, H. S. (2019). Parthenolide, a feverfew-derived phytochemical, ameliorates obesity and obesity-induced inflammatory responses via the Nrf2/Keap1 pathway. *Pharmacol. Res.* 145:104259. doi: 10.1016/j.phrs.2019.104259

Kim, E. H., Wong, S. W., and Martinez, J. (2019). Programmed necrosis and disease:we interrupt your regular programming to bring you necroinflammation. *Cell Death Differ.* 26, 25–40. doi: 10.1038/s41418-018-0179-3

Kleszczynski, K., Zillikens, D., and Fischer, T. W. (2016). Melatonin enhances mitochondrial ATP synthesis, reduces reactive oxygen species formation, and mediates translocation of the nuclear erythroid 2-related factor 2 resulting in activation of phase-2 antioxidant enzymes (gamma-GCS, HO-1, NQO1) in ultraviolet radiation-treated normal human epidermal keratinocytes (NHEK). *J. Pineal Res.* 61, 187–197. doi: 10.1111/jpi.12338

Koentges, C., Pepin, M. E., Musse, C., Pfeil, K., Alvarez, S. V. V., Hoppe, N., et al. (2018). Gene expression analysis to identify mechanisms underlying heart failure susceptibility in mice and humans. *Basic Res. Cardiol.* 113:8. doi: 10.1007/s00395-017-0666-6

Kohlstedt, K., Trouvain, C., Fromel, T., Mudersbach, T., Henschler, R., and Fleming, I. (2018). Role of the angiotensin-converting enzyme in the G-CSF-induced mobilization of progenitor cells. *Basic Res. Cardiol.* 113:18. doi: 10.1007/s00395-018-0677-y

Kornicka, K., Szlapka-Kosarzewska, J., Smieszek, A., and Marycz, K. (2019). 5-Azacytydine and resveratrol reverse senescence and ageing of adipose stem cells via modulation of mitochondrial dynamics and autophagy. *J. Cell. Mol. Med.* 23, 237–259. doi: 10.1111/jcmm.13914

Kowaltowski, A. J. (2019). Strategies to detect mitochondrial oxidants. *Redox Biol.* 21:101065. doi: 10.1016/j.redox.2018.101065

Krause, J., Loser, A., Lemoine, M. D., Christ, T., Scherschel, K., Meyer, C., et al. (2018). Rat atrial engineered heart tissue: a new in vitro model to study atrial biology. *Basic Res. Cardiol.* 113:41. doi: 10.1007/s00395-018-0701-2

Lansink, M. O., Görlinger, K., Hartmann, M., de Groot, H., and Effenberger-Neidnicht, K. (2016). Melatonin does not affect disseminated intravascular coagulation but diminishes decreases in platelet count during subacute endotoxaemia in rats. *Thromb. Res.* 139, 38–43. doi: 10.1016/j.thromres.2015.10.025

Lee, B. W. L., Ghode, P., and Ong, D. S. T. (2019). Redox regulation of cell state and fate. *Redox Biol.* 25:101056. doi: 10.1016/j.redox.2018.11.014

Lee, E., Hwang, I., Park, S., Hong, S., Hwang, B., Cho, Y., et al. (2019). MPTP-driven NLRP3 inflammasome activation in microglia plays a central role in dopaminergic neurodegeneration. *Cell Death Differ.* 26, 213–228. doi: 10.1038/s41418-018-0124-5

Li, J. Y., Zheng, X. Y., Ma, X. Y., Xu, X. Y., Du, Y., Lv, Q. J., et al. (2019). Melatonin protects against chromium(VI)-induced cardiac injury via activating the AMPK/Nrf2 pathway. *J. Inorg. Biochem.* 197:110698. doi: 10.1016/j.jinorgbio.2019.110698

Li, Q., Turdi, S., Thomas, D. P., Zhou, T., and Ren, J. (2010). Intra-myocardial delivery of mesenchymal stem cells ameliorates left ventricular and cardiomyocyte contractile dysfunction following myocardial infarction. *Toxicol. Lett.* 195, 119–126. doi: 10.1016/j.toxlet.2010.03.009

Li, R., Xin, T., Li, D., Wang, C., Zhu, H., and Zhou, H. (2018). Therapeutic effect of Sirtuin 3 on ameliorating nonalcoholic fatty liver disease: the role of the ERK-CREB pathway and Bnip3-mediated mitophagy. *Redox Biol.* 18, 229–243. doi: 10.1016/j.redox.2018.07.011

Liu, J. B., Clough, S. J., Hutchinson, A. J., Adamah-Biassi, E. B., Popovska-Gorevski, M., and Dubocovich, M. L. (2016). MT1 and MT2 melatonin receptors: a therapeutic perspective. *Annu. Rev. Pharmacol. Toxicol.* 56, 361–383. doi: 10.1146/annurev-pharmtox-010814-124742

Liu, L., Feng, D., Chen, G., Chen, M., Zheng, Q., Song, P., et al. (2012). Mitochondrial outer-membrane protein FUNDC1 mediates hypoxia-induced mitophagy in mammalian cells. *Nat. Cell Biol.* 14, 177–185. doi: 10.1038/ncb2422

Liu, Y., Xu, W., Zhai, T., You, J., and Chen, Y. (2019). Silibinin ameliorates hepatic lipid accumulation and oxidative stress in mice with non-alcoholic steatohepatitis by regulating CFLAR-JNK pathway. *Acta Pharm. Sin. B* 9, 745–757. doi: 10.1016/j.apsb.2019.02.006

Lochner, A., Marais, E., and Huisamen, B. (2018). Melatonin and cardioprotection against ischaemia/reperfusion injury: what's new? A review. *J. Pineal Res.* 65:e12490. doi: 10.1111/jpi.12490

Lombard, D. B., and Zwaans, B. M. M. (2014). SIRT3: as simple as it seems? *Gerontology* 60, 56–64. doi: 10.1159/000354382

Lu, J., Li, J., Hu, Y., Guo, Z., Sun, D., Wang, P., et al. (2019). Chrysophanol protects against doxorubicin-induced cardiotoxicity by suppressing cellular PARylation. *Acta Pharm. Sin. B* 9, 782–793. doi: 10.1016/j.apsb.2018.10.008

Lu, M., Wang, P., Qiao, Y., Jiang, C., Ge, Y., Flickinger, B., et al. (2019). GSK3beta-mediated Keap1-independent regulation of Nrf2 antioxidant response: a molecular rheostat of acute kidney injury to chronic kidney disease transition. *Redox Biol.* 26:101275. doi: 10.1016/j.redox.2019.101275

Ma, S., Chen, J., Feng, J., Zhang, R., Fan, M., Han, D., et al. (2018). Melatonin ameliorates the progression of atherosclerosis via mitophagy activation and NLRP3 inflammasome inhibition. *Oxid. Med. Cell. Longev.* 2018:9286458. doi: 10.1155/2018/9286458

Ma, Z. Q., Yang, Y., Fan, C. X., Han, J., Wang, D. J., Di, S. Y., et al. (2016). Melatonin as a potential anticarcinogen for non-small-cell lung cancer. *Oncotarget* 7, 46768–46784. doi: 10.18632/oncotarget.8776

Mauriz, J. L., Collado, P. S., Veneroso, C., Reiter, R. J., and Gonzalez-Gallego, J. (2013). A review of the molecular aspects of melatonin's anti-inflammatory actions: recent insights and new perspectives. *J. Pineal Res.* 54, 1–14. doi: 10.1111/j.1600-079X.2012.01014.x

Mayorov, V., Uchakin, P., Amarnath, V., Panov, A. V., Bridges, C. C., Uzhachenko, R., et al. (2019). Targeting of reactive isolevuglandins in mitochondrial dysfunction and inflammation. *Redox Biol.* 26:101300. doi: 10.1016/j.redox.2019.101300

McMullan, C. J., Rimm, E. B., Schernhammer, E. S., and Forman, J. P. (2017). A nested case-control study of the association between melatonin secretion and incident myocardial infarction. *Heart* 103, 694–701. doi: 10.1136/heartjnl-2016-310098

Mei, D., Chen, B., He, B., Liu, H., Lin, Z., Lin, J., et al. (2019). Actively priming autophagic cell death with novel transferrin receptor-targeted nanomedicine for synergistic chemotherapy against breast cancer. *Acta Pharm. Sin. B* 9, 1061–1077. doi: 10.1016/j.apsb.2019.03.006

Merz, J., Albrecht, P., von Garlen, S., Ahmed, I., Dimanski, D., Wolf, D., et al. (2018). Purinergic receptor Y2 (P2Y2)- dependent VCAM-1 expression promotes immune cell infiltration in metabolic syndrome. *Basic Res. Cardiol.* 113:45. doi: 10.1007/s00395-018-0702-1

Meyer, I. S., and Leuschner, F. (2018). The role of Wnt signaling in the healing myocardium: a focus on cell specificity. *Basic Res. Cardiol.* 113:44. doi: 10.1007/s00395-018-0705-y

Morell, M., Burgos, J. I., Gonano, L. A., and Vila Petroff, M. (2018). AMPK-dependent nitric oxide release provides contractile support during hyperosmotic stress. *Basic Res. Cardiol.* 113:7. doi: 10.1007/s00395-017-0665-7

Na, H. J., Yeum, C. E., Kim, H. S., Lee, J., Kim, J. Y., and Cho, Y. S. (2019). TSPYL5-mediated inhibition of p53 promotes human endothelial cell function. *Angiogenesis* 22, 281–293. doi: 10.1007/s10456-018-9656-z

Nahrendorf, M., Pittet, M. J., and Swirski, F. K. (2010). Monocytes: protagonists of infarct inflammation and repair after myocardial infarction. *Circulation* 121, 2437–2445. doi: 10.1161/CIRCULATIONAHA.109.916346

Nair, S. M., Rahman, R. M., Clarkson, A. N., Sutherland, B. A., Taurin, S., Sammut, I. A., et al. (2011). Melatonin treatment following stroke induction modulates L-arginine metabolism. *J. Pineal Res.* 51, 313–323. doi: 10.1111/j.1600-079X.2011.00891.x

Nanadikar, M. S., Vergel Leon, A. M., Borowik, S., Hillemann, A., Zieseniss, A., Belousov, V. V., et al. (2019). O2 affects mitochondrial functionality ex vivo. *Redox Biol.* 22:101152. doi: 10.1016/j.redox.2019.101152

NaveenKumar, S. K., Hemshekhar, M., Kemparaju, K., and Girish, K. S. (2019). Hemin-induced platelet activation and ferroptosis is mediated through ROS-driven proteasomal activity and inflammasome activation: protection by melatonin. *Biochim. Biophys. Acta* 1865, 2303–2316. doi: 10.1016/j.bbadis.2019.05.009

Nduhirabandi, F., du Toit, E. F., and Lochner, A. (2012). Melatonin and the metabolic syndrome: a tool for effective therapy in obesity-associated abnormalities? *Acta Physiol.* 205, 209–223. doi: 10.1111/j.1748-1716.2012.02410.x

Niccoli, G., Scalone, G., Lerman, A., and Crea, F. (2016). Coronary microvascular obstruction in acute myocardial infarction. *Eur. Heart J.* 37, 1024–1033. doi: 10.1093/eurheartj/ehv484

Nofe, J. R., Brodde, M. F., and Kehrel, B. E. (2010). High-density lipoproteins, platelets and the pathogenesis of atherosclerosis. *Clin. Exp. Pharmacol. Physiol.* 37, 726–735. doi: 10.1111/j.1440-1681.2010.05377.x

Nokik, S. E., Nobuyuki, M., Kazuko, T., Dongzhu, X., Taizo, K., Rujie, Q., et al. (2017). Rev-erb agonist improves adverse cardiac remodeling and survival in myocardial infarction through an anti-inflammatory mechanism. *PLoS One* 12:e0189330. doi: 10.1371/journal.pone.0189330

Ostjen, C. A., Rosa, C. G. S., Hartmann, R. M., Schemitt, E. G., Colares, J. R., and Marroni, N. P. (2019). Anti-inflammatory and antioxidant effect of melatonin on recovery from muscular trauma induced in rats. *Exp. Mol. Pathol.* 106, 52–59. doi: 10.1016/j.yexmp.2018.12.001

Pan, S., Wever-Pinzon, O., Rao, S., Levin, A., Garan, A., Takeda, K., et al. (2015). Myocardial recovery from short- and long-term cardiac support devices: results from the UNOS registry. *J. Heart Lung Transplant.* 34:S41.

Paradies, G., Paradies, V., Ruggiero, F. M., and Petrosillo, G. (2015). Protective role of melatonin in mitochondrial dysfunction and related disorders. *Arch. Toxicol.* 89, 923–939. doi: 10.1007/s00204-015-1475-z

Pei, H. F., Du, J., Song, X. F., He, L., Zhang, Y. F., Li, X. C., et al. (2016). Melatonin prevents adverse myocardial infarction remodeling via Notch1/Mfn2 pathway. *Free Radic. Biol. Med.* 97, 408–417. doi: 10.1016/j.freeradbiomed.2016.06.015

Perez-Gonzalez, A., Castaneda-Arriaga, R., Alvarez-Idaboy, J. R., Reiter, R. J., and Galano, A. (2019). Melatonin and its metabolites as chemical agents capable of directly repairing oxidized DNA. *J. Pineal Res.* 66:e12539. doi: 10.1111/jpi.12539

Phan, T. K., Williams, S. A., Bindra, G. K., Lay, F. T., Poon, I. K. H., and Hulett, M. D. (2019). Phosphoinositides: multipurpose cellular lipids with emerging roles in cell death. *Cell Death Differ.* 26, 781–793. doi: 10.1038/s41418-018-0269-2

Reddy, K. R. K., Dasari, C., Duscharla, D., Supriya, B., Ram, N. S., Surekha, M. V., et al. (2018). Dimethylarginine dimethylaminohydrolase-1 (DDAH1) is frequently upregulated in prostate cancer, and its overexpression conveys tumor growth and angiogenesis by metabolizing asymmetric dimethylarginine (ADMA). *Angiogenesis* 21, 79–94. doi: 10.1007/s10456-017-9587-0

Reina, M., and Martínez, A. (2018). A new free radical scavenging cascade involving melatonin and three of its metabolites (3OHM, AFMK and AMK). *Comput. Theor. Chem.* 1123, 111–118. doi: 10.1016/j.comptc.2017.11.017

Reiter, R. J., Rosales-Corral, S., Tan, D. X., Jou, M. J., Galano, A., and Xu, B. (2017). Melatonin as a mitochondria-targeted antioxidant: one of evolution's best ideas. *Cell. Mol. Life Sci.* 74, 3863–3881. doi: 10.1007/s00018-017-2609-7

Ren, B. (2016). Protein kinase D1 signaling in angiogenic gene expression and VEGF-mediated angiogenesis. *Front. Cell Dev. Biol.* 4:37. doi: 10.3389/fcell.2016.00037

Rezzani, R., Favero, G., Stacchiotti, A., and Rodella, L. F. (2013). Endothelial and vascular smooth muscle cell dysfunction mediated by cyclophylin A and the atheroprotective effects of melatonin. *Life Sci.* 92, 875–882. doi: 10.1016/j.lfs.2012.11.011

Riehle, C., and Bauersachs, J. (2018). Of mice and men: models and mechanisms of diabetic cardiomyopathy. *Basic Res. Cardiol.* 114:2. doi: 10.1007/s00395-018-0711-0

Sallinen, P., Manttari, S., Leskinen, H., Ilves, M., Vakkuri, O., Ruskoaho, H., et al. (2007). The effect of myocardial infarction on the synthesis, concentration and receptor expression of endogenous melatonin. *J. Pineal Res.* 42, 254–260. doi: 10.1111/j.1600-079X.2006.00413.x

Schreiber, T., Salhofer, L., Quinting, T., and Fandrey, J. (2019). Things get broken: the hypoxia-inducible factor prolyl hydroxylases in ischemic heart disease. *Basic Res. Cardiol.* 114:16. doi: 10.1007/s00395-019-0725-2

Seidlmayer, L. K., Juettner, V. V., Kettlewell, S., Pavlov, E. V., Blatter, L. A., and Dedkova, E. N. (2015). Distinct mPTP activation mechanisms in ischaemia-reperfusion: contributions of Ca2+, ROS, pH, and inorganic polyphosphate. *Cardiovasc. Res.* 106, 237–248. doi: 10.1093/cvr/cvv097

Serocki, M., Bartoszewska, S., Janaszak-Jasiecka, A., Ochocka, R. J., Collawn, J. F., and Bartoszewski, R. (2018). miRNAs regulate the HIF switch during hypoxia: a novel therapeutic target. *Angiogenesis* 21, 183–202. doi: 10.1007/s10456-018-9600-2

Shafiei, E., Bahtoei, M., Raj, P., Ostovar, A., Iranpour, D., Akbarzadeh, S., et al. (2018). Effects of N-acetyl cysteine and melatonin on early reperfusion injury in patients undergoing coronary artery bypass grafting: a randomized, open-labeled, placebo-controlled trial. *Medicine* 97:e11383. doi: 10.1097/MD.0000000000011383

Shanmugam, G., Challa, A. K., Litovsky, S. H., Devarajan, A., Wang, D., Jones, D. P., et al. (2019). Enhanced Keap1-Nrf2 signaling protects the myocardium from isoproterenol-induced pathological remodeling in mice. *Redox Biol.* 27:101212. doi: 10.1016/j.redox.2019.101212

Siddall, H. K., Yellon, D. M., Ong, S. B., Mukherjee, U. A., Burke, N., Hall, A. R., et al. (2013). Loss of PINK1 increases the heart's vulnerability to ischemia-reperfusion injury. *PLoS One* 8:e62400. doi: 10.1371/journal.pone.0062400

Simko, F., Baka, T., Paulis, L., and Reiter, R. J. (2016). Elevated heart rate and nondipping heart rate as potential targets for melatonin: a review. *J. Pineal Res.* 61, 127–137. doi: 10.1111/jpi.12348

Simula, L., Campanella, M., and Campello, S. (2019). Targeting Drp1 and mitochondrial fission for therapeutic immune modulation. *Pharmacol. Res.* 146:104317. doi: 10.1016/j.phrs.2019.104317

Singhanat, K., Apaijai, N., Chattipakorn, S. C., and Chattipakorn, N. (2018). Roles of melatonin and its receptors in cardiac ischemia-reperfusion injury. *Cell. Mol. Life Sci.* 75, 4125–4149. doi: 10.1007/s00018-018-2905-x

Sircana, A., De Michieli, F., Parente, R., Framarin, L., Leone, N., Berrutti, M., et al. (2019). Gut microbiota, hypertension and chronic kidney disease: recent advances. *Pharmacol. Res.* 144, 390–408. doi: 10.1016/j.phrs.2018.01.013

Song, C., Zhao, J., Fu, B., Li, D., Mao, T., Peng, W., et al. (2017). Melatonin-mediated upregulation of Sirt3 attenuates sodium fluoride-induced hepatotoxicity by activating the MT1-PI3K/AKT-PGC-1alpha signaling pathway. *Free Radic. Biol. Med.* 112, 616–630. doi: 10.1016/j.freeradbiomed.2017.09.005

Soto-Heras, S., Catala, M. G., Roura, M., Menendez-Blanco, I., Piras, A. R., Izquierdo, D., et al. (2019). Effects of melatonin on oocyte developmental competence and the role of melatonin receptor 1 in juvenile goats. *Reprod. Domest. Anim.* 54, 381–390. doi: 10.1111/rda.13378

Tahrir, F. G., Langford, D., Amini, S., Mohseni Ahooyi, T., and Khalili, K. (2019). Mitochondrial quality control in cardiac cells: mechanisms and role in cardiac cell injury and disease. *J. Cell. Physiol.* 234, 8122–8133. doi: 10.1002/jcp.27597

Tang, V., Fu, S., Rayner, B. S., and Hawkins, C. L. (2019). 8-Chloroadenosine induces apoptosis in human coronary artery endothelial cells through the activation of the unfolded protein response. *Redox Biol.* 26:101274. doi: 10.1016/j.redox.2019.101274

Teixeira, J., Basit, F., Swarts, H. G., Forkink, M., Oliveira, P. J., Willems, P., et al. (2018). Extracellular acidification induces ROS- and mPTP-mediated death in HEK293 cells. *Redox Biol.* 15, 394–404. doi: 10.1016/j.redox.2017.12.018

Tengattini, S., Reiter, R. J., Tan, D. X., Terron, M. P., Rodella, L. F., and Rezzani, R. (2008). Cardiovascular diseases: protective effects of melatonin. *J. Pineal Res.* 44, 16–25. doi: 10.1111/j.1600-079X.2007.00518.x

Ter Horst, E. N., Krijnen, P. A. J., Hakimzadeh, N., Robbers, L., Hirsch, A., Nijveldt, R., et al. (2018). Elevated monocyte-specific type I interferon signalling correlates positively with cardiac healing in myocardial infarct patients but

interferon alpha application deteriorates myocardial healing in rats. *Basic Res. Cardiol.* 114:1. doi: 10.1007/s00395-018-0709-7

Thieltges, K. M., Avramovic, D., Piscitelli, C. L., Markovic-Mueller, S., Binz, H. K., and Ballmer-Hofer, K. (2018). Characterization of a drug-targetable allosteric site regulating vascular endothelial growth factor signaling. *Angiogenesis* 21, 533–543. doi: 10.1007/s10456-018-9606-9

Tian, L., Lu, L., Feng, J., and Melancon, M. P. (2018). Radiopaque nano and polymeric materials for atherosclerosis imaging, embolization and other catheterization procedures. *Acta Pharm. Sin. B* 8, 360–370. doi: 10.1016/j.apsb.2018.03.002

Trindade, F., Vitorino, R., Leite-Moreira, A., and Falcao-Pires, I. (2019). Pericardial fluid: an underrated molecular library of heart conditions and a potential vehicle for cardiac therapy. *Basic Res. Cardiol.* 114:10. doi: 10.1007/s00395-019-0716-3

Venegas, C., Garcia, J. A., Escames, G., Ortiz, F., Lopez, A., Doerrier, C., et al. (2012). Extrapineal melatonin: analysis of its subcellular distribution and daily fluctuations. *J. Pineal Res.* 52, 217–227. doi: 10.1111/j.1600-079X.2011.00931.x

Venugopal, S., Kao, C., Chandna, R., Sulochana, K. N., Subramanian, V., Chen, M., et al. (2018). Angio-3, a 10-residue peptide derived from human plasminogen kringle 3, suppresses tumor growth in mice via impeding both angiogenesis and vascular permeability. *Angiogenesis* 21, 653–665. doi: 10.1007/s10456-018-9616-7

Villalobos, C., Gutierrez, L. G., Hernandez-Morales, M., Del Bosque, D., and Nunez, L. (2018). Mitochondrial control of store-operated Ca(2+) channels in cancer: pharmacological implications. *Pharmacol. Res.* 135, 136–143. doi: 10.1016/j.phrs.2018.08.001

Wang, B., Nie, J. L., Wu, L. J., Hu, Y. Y., Wen, Z., Dong, L. L., et al. (2018). AMPKα2 protects against the development of heart failure by enhancing mitophagy via PINK1 phosphorylation. *Circ. Res.* 122, 712–729. doi: 10.1161/circresaha.117.312317

Wang, J., Zhu, P., Li, R., Ren, J., and Zhou, H. (2020). Fundc1-dependent mitophagy is obligatory to ischemic preconditioning-conferred renoprotection in ischemic AKI via suppression of Drp1-mediated mitochondrial fission. *Redox Biol.* 30:101415. doi: 10.1016/j.redox.2019.101415

Wang, S., Dong, G., and Sheng, C. (2019). Structural simplification: an efficient strategy in lead optimization. *Acta Pharm. Sin. B* 9, 880–901. doi: 10.1016/j.apsb.2019.05.004

Wang, X. N., Shu, H., Wang, M. W., Sun, Y. Y., Liu, C. F., Liu, W. L., et al. (2016). Melatonin alleviates lipopolysaccharide-compromised integrity of blood brain barrier by activation of AMP-activated protein kinase in old mice. *Chin. J. Pharmacol. Toxicol.* 30, 1021–1022. doi: 10.1111/acel.12572

Wang, Y., Lei, T., Yuan, J., Wu, Y., Shen, X., Gao, J., et al. (2018). GCN2 deficiency ameliorates doxorubicin-induced cardiotoxicity by decreasing cardiomyocyte apoptosis and myocardial oxidative stress. *Redox Biol.* 17, 25–34. doi: 10.1016/j.redox.2018.04.009

Wang, Z., Xu, G., Gao, Y., Zhan, X., Qin, N., Fu, S., et al. (2019). Cardamonin from a medicinal herb protects against LPS-induced septic shock by suppressing NLRP3 inflammasome. *Acta Pharm. Sin. B* 9, 734–744. doi: 10.1016/j.apsb.2019.02.003

Westman, P. C., Lipinski, M. J., Luger, D., Waksman, R., Bonow, R. O., Wu, E., et al. (2016). Inflammation as a driver of adverse left ventricular remodeling after acute myocardial infarction. *J. Am. Coll. Cardiol.* 67, 2050–2060. doi: 10.1016/j.jacc.2016.01.073

Wu, C., Xi, C., Tong, J., Zhao, J., Jiang, H., Wang, J., et al. (2019). Design, synthesis, and biological evaluation of novel tetrahydroprotoberberine derivatives (THPBs) as proprotein convertase subtilisin/kexin type 9 (PCSK9) modulators for the treatment of hyperlipidemia. *Acta Pharm. Sin. B* 9, 1216–1230. doi: 10.1016/j.apsb.2019.06.006

Wu, D., Hu, Q., Tan, B., Rose, P., Zhu, D., and Zhu, Y. Z. (2018a). Amelioration of mitochondrial dysfunction in heart failure through S-sulfhydration of Ca(2+)/calmodulin-dependent protein kinase II. *Redox Biol.* 19, 250–262. doi: 10.1016/j.redox.2018.08.008

Wu, D., Wang, H., Teng, T., Duan, S., Ji, A., and Li, Y. (2018b). Hydrogen sulfide and autophagy: a double edged sword. *Pharmacol. Res.* 131, 120–127. doi: 10.1016/j.phrs.2018.03.002

Xiao, Y., Karam, C., Yi, J., Zhang, L., Li, X., Yoon, D., et al. (2018). ROS-related mitochondrial dysfunction in skeletal muscle of an ALS mouse model during the disease progression. *Pharmacol. Res.* 138, 25–36. doi: 10.1016/j.phrs.2018.09.008

Xiong, Q., Wang, Z., Yu, Y., Wen, Y., Suguro, R., Mao, Y., et al. (2019). Hydrogen sulfide stabilizes atherosclerotic plaques in apolipoprotein E knockout mice. *Pharmacol. Res.* 144, 90–98. doi: 10.1016/j.phrs.2019.04.006

Xu, N., Wang, Q., Jiang, S., Wang, Q., Hu, W., Zhou, S., et al. (2019). Fenofibrate improves vascular endothelial function and contractility in diabetic mice. *Redox Biol.* 20, 87–97. doi: 10.1016/j.redox.2018.09.024

Xu, S. F., Zhang, Y. H., Wang, S., Pang, Z. Q., Fan, Y. G., Li, J. Y., et al. (2019). Lactoferrin ameliorates dopaminergic neurodegeneration and motor deficits in MPTP-treated mice. *Redox Biol.* 21:101090. doi: 10.1016/j.redox.2018.101090

Xu, T., Ding, W., Ao, X., Chu, X., Wan, Q., Wang, Y., et al. (2019). ARC regulates programmed necrosis and myocardial ischemia/reperfusion injury through the inhibition of mPTP opening. *Redox Biol.* 20, 414–426. doi: 10.1016/j.redox.2018.10.023

Xu, Z., Fu, T., Guo, Q., Sun, W., and Gan, Z. (2019). Mitochondrial quality orchestrates muscle-adipose dialog to alleviate dietary obesity. *Pharmacol. Res.* 141, 176–180. doi: 10.1016/j.phrs.2018.12.020

Yan, G. G., Yu, L. Z., Jiang, S. M., and Zhu, J. F. (2018). Melatonin antagonizes oxidative stress-induced mitochondrial dysfunction in retinal pigmented epithelium cells via melatonin receptor 1 (MT1). *J. Toxicol. Sci.* 43, 659–669. doi: 10.2131/jts.43.659

Yang, C. H., Xu, J. H., Ren, Q. C., Duan, T., Mo, F., and Zhang, W. (2019). Melatonin promotes secondary hair follicle development of early postnatal cashmere goat and improves cashmere quantity and quality by enhancing antioxidant capacity and suppressing apoptosis. *J. Pineal Res.* 67:e12569. doi: 10.1111/jpi.12569

Yang, M., Linn, B. S., Zhang, Y., and Ren, J. (2019). Mitophagy and mitochondrial integrity in cardiac ischemia-reperfusion injury. *Biochim. Biophys. Acta* 1865, 2293–2302. doi: 10.1016/j.bbadis.2019.05.007

Yang, M. Y., Yu, Q. L., Huang, Y. S., and Yang, G. (2019). Neuroprotective effects of andrographolide derivative CX-10 in transient focal ischemia in rat: involvement of Nrf2/AE and TLR/NF-kappaB signaling. *Pharmacol. Res.* 144, 227–234. doi: 10.1016/j.phrs.2019.04.023

Yang, Q., He, G. W., Underwood, M. J., and Yu, C. M. (2016). Cellular and molecular mechanisms of endothelial ischemia/reperfusion injury: perspectives and implications for postischemic myocardial protection. *Am. J. Transl. Res.* 8, 765–777.

Yang, X., Wang, H., Ni, H.-M., Xiong, A., Wang, Z., Sesaki, H., et al. (2017). Inhibition of Drp1 protects against senecionine-induced mitochondria-mediated apoptosis in primary hepatocytes and in mice. *Redox Biol.* 12, 264–273. doi: 10.1016/j.redox.2017.02.020

Yang, Y., Duan, W., Jin, Z., Yi, W., Yan, J., Zhang, S., et al. (2013). JAK2/STAT3 activation by melatonin attenuates the mitochondrial oxidative damage induced by myocardial ischemia/reperfusion injury. *J. Pineal Res.* 55, 275–286. doi: 10.1111/jpi.12070

Yang, Y., Sun, Y., Yi, W., Li, Y., Fan, C. X., Xin, Z. L., et al. (2014). A review of melatonin as a suitable antioxidant against myocardial ischemia–reperfusion injury and clinical heart diseases. *J. Pineal Res.* 57, 357–366. doi: 10.1111/jpi.12175

Yao, X., Zhang, J., Jing, X., Ye, Y., Guo, J., Sun, K., et al. (2019). Fibroblast growth factor 18 exerts anti-osteoarthritic effects through PI3K-AKT signaling and mitochondrial fusion and fission. *Pharmacol. Res.* 139, 314–324. doi: 10.1016/j.phrs.2018.09.026

Yarana, C., Thompson, H., Chaiswing, L., Butterfield, D. A., Weiss, H., Bondada, S., et al. (2019). Extracellular vesicle-mediated macrophage activation: an insight into the mechanism of thioredoxin-mediated immune activation. *Redox Biol.* 26:101237. doi: 10.1016/j.redox.2019.101237

Yoon, Y. M., Kim, H. J., Lee, J. H., and Lee, S. H. (2019). Melatonin enhances mitophagy by upregulating expression of heat shock 70 kDa protein 1L in human mesenchymal stem cells under oxidative stress. *Int. J. Mol. Sci.* 20:4545. doi: 10.3390/ijms20184545

Yu, L. M., Di, W. C., Dong, X., Li, Z., Zhang, Y., Xue, X. D., et al. (2018). Melatonin protects diabetic heart against ischemia-reperfusion injury, role of membrane receptor-dependent cGMP-PKG activation. *Biochim. Biophys. Acta* 1864, 563–578. doi: 10.1016/j.bbadis.2017.11.023

Yu, L. M., Li, B. Y., Zhang, M., Jin, Z. X., Duan, W. X., Zhao, G. L., et al. (2016). Melatonin reduces PERK-eIF2α-ATF4-mediated endoplasmic reticulum stress during myocardial ischemia-reperfusion injury: role of RISK and SAFE pathways interaction. *Apoptosis* 21, 809–824. doi: 10.1007/s10495-016-1246-1

Yuan, T., Yang, T., Chen, H., Fu, D., Hu, Y., Wang, J., et al. (2019). New insights into oxidative stress and inflammation during diabetes mellitus-accelerated atherosclerosis. *Redox Biol.* 20, 247–260. doi: 10.1016/j.redox.2018.09.025

Yuqi, L., Lei, G., Yanqiu, S., Qiao, X., Yu, W., and Yundai, C. (2015). Efficacy and safety of limus-eluting versus paclitaxel-eluting coronary artery stents in patients with diabetes mellitus: a meta-analysis. *Int. J. Cardiol.* 64, 680–691. doi: 10.1016/j.ijcard.2015.02.002

Zaouali, M. A., Reiter, R. J., Padrissa-Altes, S., Boncompagni, E., Garcia, J. J., Ben Abnennebi, H., et al. (2011). Melatonin protects steatotic and nonsteatotic liver grafts against cold ischemia and reperfusion injury. *J. Pineal Res.* 50, 213–221. doi: 10.1111/j.1600-079X.2010.00831.x

Zhang, H., Jin, B., and Faber, J. E. (2019). Mouse models of Alzheimer's disease cause rarefaction of pial collaterals and increased severity of ischemic stroke. *Angiogenesis* 22, 263–279. doi: 10.1007/s10456-018-9655-0

Zhang, H. M., and Zhang, Y. (2014). Melatonin: a well-documented antioxidant with conditional pro-oxidant actions. *J. Pineal Res.* 57, 131–146. doi: 10.1111/jpi.12162

Zhang, Y., Mi, S. L., Hu, N., Doser, T. A., Sun, A., Ge, J., et al. (2014). Mitochondrial aldehyde dehydrogenase 2 accentuates aging-induced cardiac remodeling and contractile dysfunction: role of AMPK, Sirt1, and mitochondrial function. *Free Radic. Biol. Med.* 71, 208–220. doi: 10.1016/j.freeradbiomed.2014.03.018

Zhang, Y., Wang, Y., Xu, J. N., Tian, F., Hu, S. Y., Chen, Y. D., et al. (2019). Melatonin attenuates myocardial ischemia-reperfusion injury via improving mitochondrial fusion/mitophagy and activating the AMPK-OPA1 signaling pathways. *J. Pineal Res.* 66:e12542. doi: 10.1111/jpi.12542

Zhao, J., Gao, J. L., Zhu, J. X., Zhu, H. B., Peng, X., Jiang, M., et al. (2019). The different response of cardiomyocytes and cardiac fibroblasts to mitochondria inhibition and the underlying role of STAT3. *Basic Res. Cardiol.* 114:12. doi: 10.1007/s00395-019-0721-6

Zhao, Y., Wang, H. Y., Chen, W., Chen, L. F., Liu, D. M., Wang, X., et al. (2019). Melatonin attenuates white matter damage after focal brain ischemia in rats by regulating the TLR4/NF-kappaB pathway. *Brain Res. Bull.* 150, 168–178. doi: 10.1016/j.brainresbull.2019.05.019

Zhong, J., Tan, Y., Lu, J., Liu, J., Xiao, X., Zhu, P., et al. (2019). Therapeutic contribution of melatonin to the treatment of septic cardiomyopathy: a novel mechanism linking Ripk3-modified mitochondrial performance and endoplasmic reticulum function. *Redox Biol.* 26:101287. doi: 10.1016/j.redox.2019.101287

Zhou, H., Hu, S., Jin, Q., Shi, C., Zhang, Y., Zhu, P., et al. (2017a). Mff-dependent mitochondrial fission contributes to the pathogenesis of cardiac microvasculature ischemia/reperfusion injury via induction of mROS-mediated cardiolipin oxidation and HK2/VDAC1 disassociation-involved mPTP opening. *J. Am. Heart Assoc.* 6:e005328. doi: 10.1161/JAHA.116.005328

Zhou, H., Li, D., Zhu, P., Hu, S., Hu, N., Ma, S., et al. (2017b). Melatonin suppresses platelet activation and function against cardiac ischemia/reperfusion injury via PPARgamma/FUNDC1/mitophagy pathways. *J. Pineal Res.* 63:e12438. doi: 10.1111/jpi.12438

Zhou, H., Zhang, Y., Hu, S., Shi, C., Zhu, P., Ma, Q., et al. (2017c). Melatonin protects cardiac microvasculature against ischemia/reperfusion injury via suppression of mitochondrial fission-VDAC1-HK2-mPTP-mitophagy axis. *J. Pineal Res.* 63:e12413. doi: 10.1111/jpi.12413

Zhou, H., Zhang, Y., Hu, S. Y., Shi, C., Zhu, P. J., Ma, Q., et al. (2017d). Melatonin protects cardiac microvasculature against ischemia/reperfusion injury via suppression of mitochondrial fission-VDAC1-HK2-mPTP-mitophagy axis. *J. Pineal Res.* 63;e12413. doi: 10.1111/jpi.12413

Zhou, H., Zhu, P., Guo, J., Hu, N., Wang, S., Li, D., et al. (2017e). Ripk3 induces mitochondrial apoptosis via inhibition of FUNDC1 mitophagy in cardiac IR injury. *Redox Biol.* 13, 498–507. doi: 10.1016/j.redox.2017.07.007

Zhou, H., Li, D., Zhu, P., Ma, Q., Toan, S., Wang, J., et al. (2018a). Inhibitory effect of melatonin on necroptosis via repressing the Ripk3-PGAM5-CypD-mPTP pathway attenuates cardiac microvascular ischemia-reperfusion injury. *J. Pineal Res.* 65:e12503. doi: 10.1111/jpi.12503

Zhou, H., Li, N., Yuan, Y., Jin, Y. G., Guo, H., Deng, W., et al. (2018b). Activating transcription factor 3 in cardiovascular diseases: a potential therapeutic target. *Basic Res. Cardiol.* 113:37.

Zhou, H., Ma, Q., Zhu, P., Ren, J., Reiter, R. J., and Chen, Y. (2018c). Protective role of melatonin in cardiac ischemia-reperfusion injury: from pathogenesis to targeted therapy. *J. Pineal Res.* 64:e12471. doi: 10.1111/jpi.12471

Zhou, H., Shi, C., Hu, S., Zhu, H., Ren, J., and Chen, Y. (2018d). BI1 is associated with microvascular protection in cardiac ischemia reperfusion injury via repressing Syk-Nox2-Drp1-mitochondrial fission pathways. *Angiogenesis* 21, 599–615. doi: 10.1007/s10456-018-9611-z

Zhou, H., Wang, J., Zhu, P., Zhu, H., Toan, S., Hu, S., et al. (2018e). NR4A1 aggravates the cardiac microvascular ischemia reperfusion injury through suppressing FUNDC1-mediated mitophagy and promoting Mff-required mitochondrial fission by CK2alpha. *Basic Res. Cardiol.* 113:23. doi: 10.1007/s00395-018-0682-1

Zhou, H., Wang, S., Hu, S., Chen, Y., and Ren, J. (2018f). ER-mitochondria microdomains in cardiac ischemia-reperfusion injury: a fresh perspective. *Front. Physiol.* 9:755. doi: 10.3389/fphys.2018.00755

Zhou, H., Wang, S., Zhu, P., Hu, S., Chen, Y., and Ren, J. (2018g). Empagliflozin rescues diabetic myocardial microvascular injury via AMPK-mediated inhibition of mitochondrial fission. *Redox Biol.* 15, 335–346. doi: 10.1016/j.redox.2017.12.019

Zhou, H., Zhu, P., Wang, J., Zhu, H., Ren, J., and Chen, Y. (2018h). Pathogenesis of cardiac ischemia reperfusion injury is associated with CK2alpha-disturbed mitochondrial homeostasis via suppression of FUNDC1-related mitophagy. *Cell Death Differ.* 25, 1080–1093. doi: 10.1038/s41418-018-0086-7

Zhou, H., and Toan, S. (2020). Pathological roles of mitochondrial oxidative stress and mitochondrial dynamics in cardiac microvascular ischemia/reperfusion injury. *Biomolecules* 10:85. doi: 10.3390/biom10010085

Zhou, H., Toan, S., Zhu, P., Wang, J., Ren, J., and Zhang, Y. (2020). DNA-PKcs promotes cardiac ischemia reperfusion injury through mitigating BI-1-governed mitochondrial homeostasis. *Basic Res. Cardiol.* 115:11. doi: 10.1007/s00395-019-0773-7

Zhou, H., Wang, J., Hu, S., Zhu, H., Toanc, S., and Ren, J. (2019). BI1 alleviates cardiac microvascular ischemia-reperfusion injury via modifying mitochondrial fission and inhibiting XO/ROS/F-actin pathways. *J. Cell Physiol.* 234, 5056–5069. doi: 10.1002/jcp.27308

Zhu, H., Jin, Q., Li, Y., Ma, Q., Wang, J., Li, D., et al. (2018). Melatonin protected cardiac microvascular endothelial cells against oxidative stress injury via suppression of IP3R-[Ca(2+)]c/VDAC-[Ca(2+)]m axis by activation of MAPK/ERK signaling pathway. *Cell Stress Chaperones* 23, 101–113. doi: 10.1007/s12192-017-0827-4

Zhu, P., Hu, S., Jin, Q., Li, D., Tian, F., Toan, S., et al. (2018). Ripk3 promotes ER stress-induced necroptosis in cardiac IR injury: a mechanism involving calcium overload/XO/ROS/mPTP pathway. *Redox Biol.* 16, 157–168. doi: 10.1016/j.redox.2018.02.019

Zollbrecht, C., Persson, A. E. G., Lundberg, J. O., Weitzberg, E., and Carlström, M. (2016). Nitrite-mediated reduction of macrophage NADPH oxidase activity is dependent on xanthine oxidoreductase-derived nitric oxide but independent of S-nitrosation. *Redox Biol.* 10, 119–127. doi: 10.1016/j.redox.2016.09.015

Conflict of Interest: The authors declare that the research was conducted in the absence of any commercial or financial relationships that could be construed as a potential conflict of interest.

Copyright © 2020 Fu, Jiao, Wang, Zhang, Shen, Reiter, Xi and Chen. This is an open-access article distributed under the terms of the Creative Commons Attribution License (CC BY). The use, distribution or reproduction in other forums is permitted, provided the original author(s) and the copyright owner(s) are credited and that the original publication in this journal is cited, in accordance with accepted academic practice. No use, distribution or reproduction is permitted which does not comply with these terms.

frontiers in Physiology

ORIGINAL RESEARCH
published: 19 May 2020
doi: 10.3389/fphys.2020.00425

Metformin Ameliorates Diabetic Cardiomyopathy by Activating the PK2/PKR Pathway

Zhen Yang[1†], Min Wang[1†], Yuchen Zhang[1], Fei Cai[2], Botao Jiang[3], Wenliang Zha[4,5] and Wei Yu[1]**

[1] Department of Pharmacology, School of Pharmacy, Hubei University of Science and Technology, Xianning, China, [2] Hubei Province Key Laboratory on Cardiovascular, Cerebrovascular, and Metabolic Disorders, Hubei University of Science and Technology, Xianning, China, [3] Department of Urology, Xianning Central Hospital, Xianning, China, [4] Department of Surgery, Clinic Medical College, Hubei University of Science and Technology, Xianning, China, [5] National Demonstration Center for Experimental General Medicine Education, Hubei University of Science and Technology, Xianning, China

OPEN ACCESS

Edited by:
Jun Ren,
University of Washington,
United States

Reviewed by:
Christian Cadeddu Dessalvi,
University of Cagliari, Italy
Naifeng Liu,
Southeast University, China

***Correspondence:**
Wenliang Zha
xyzwl800@163.com
Wei Yu
yuwei0805@163.com

[†] These authors have contributed equally to this work

Specialty section:
This article was submitted to Vascular Physiology, a section of the journal Frontiers in Physiology

Received: 21 December 2019
Accepted: 07 April 2020
Published: 19 May 2020

Citation:
Yang Z, Wang M, Zhang Y, Cai F, Jiang B, Zha W and Yu W (2020) Metformin Ameliorates Diabetic Cardiomyopathy by Activating the PK2/PKR Pathway. Front. Physiol. 11:425. doi: 10.3389/fphys.2020.00425

Diabetic cardiomyopathy (DCM) is a complication of diabetes that can cause damage to myocardial structure and function. Metformin (Met) is a widely used type 2 diabetes treatment drug that exerts cardioprotective effects through multiple pathways. Prokineticin 2 (PK2) is a small-molecule secreted protein that plays pivotal parts in cardiomyocyte survival and angiogenesis. However, the role of Met in regulating the PK2 signaling pathway in DCM remains unclear. This experiment explored the effects of Met on high glucose (HG)-induced injury through the PK2/PKR pathway *in vivo* and *in vitro*. Cardiomyocytes isolated from adult or AKT-knockout mice were treated with HG (33 mmol/L) and PK2 or AKT1/2 kinase inhibitor (AKT inhibitor). Heart contraction properties based on cell shortening were evaluated; these properties included the resting cell length, peak shortening (PS), maximum speed of shortening/relengthening (±dL/dt), time to 90% relengthening (TR_{90}), and time to peak shortening (TPS). Mice with streptozotocin-induced diabetes were treated with Met to evaluate cardiac function, myocardial structure, and the PK2/PKR and AKT/GSK3β pathways. Moreover, H9c2 cardiomyocytes were exposed to HG in the absence or presence of Met with or without the PK2 antagonist PKRA7 or the AKT inhibitor, and apoptotic proteins such as Bax and Bcl-2 and the PK2/PKR and AKT/GSK3β pathways were evaluated using western blot analysis. The prolongation of TR_{90} and decreases in PS and ±dL/dt caused by HG were ameliorated by PK2 in cardiomyocytes, but the effects of PK2 were ameliorated or negated by the AKT inhibitor and in AKT-knockout mice. Diabetic mice showed metabolic abnormalities, aberrant myocardial enzyme levels, declines in myocardial systolic and diastolic function associated with myocardial fibrosis, and pronounced apoptosis, but these effects were greatly rescued by Met treatment. Moreover, PK2, PKR1, and PKR2 expression and p-AKT/AKT and p-GSK3β/GSK3β ratios were decreased in diabetic mice, and these decreases were attenuated by Met. Likewise, H9c2 cells exposed to HG showed reduced PK2/PKR expression and decreased p-AKT/AKT and p-GSK3β/GSK3β ratios, and these effects were nullified by Met. In addition, the effects of Met on cardiomyocytes exposed to HG were abolished

after intervention with PKRA7 or the AKT inhibitor. These results suggest that Met can activate the PK2/PKR-mediated AKT/GSK3β pathway, thus improving cardiac function and alleviating apoptosis in DM mice.

Keywords: diabetic cardiomyopathy, prokineticin 2, prokineticin 2 receptors, AKT/GSK3β signaling pathway, apoptosis

INTRODUCTION

Diabetes mellitus (DM) is a metabolic disease caused by a combination of genetic and environmental factors that is characterized by persistent hyperglycemia and insulin deficiency. Currently, the diabetic population is becoming younger, and the International Diabetes Federation has reported that the total number of people with diabetes is expected to reach 642 million by 2040 (von Scholten et al., 2015; Ogurtsova et al., 2017). Diabetes is a strong risk factor for cardiovascular morbidity and mortality (Agrawal et al., 2006). Nowadays, the combinations of traditional Chinese medicines and modern Western medicine are widely used in clinical treatment to prevent or ameliorate the development of diabetic complications (Ceylan Isik et al., 2008). Diabetic cardiomyopathy (DCM) is a structural and functional disorder of the heart caused by diabetes (Rubler et al., 1972). Alterations in mitochondrial, apoptotic, intracellular Ca^{2+} anomalies, oxidative stress, as well as the expression of p-AKT, GSK3β all lead to damaged myocardial structure and function in diabetics (Wold et al., 2005; Zhang et al., 2012). In the current work, the specific or tissue selective PI3K modulators and AKT activation were considered as the potential treatment targets of DCM (Bi et al., 2020). However, the mechanisms underlying DCM remain unclear. Therefore, clinical studies are urgently needed to explore these mechanisms.

Prokineticin 2 (PK2) is an 8-kDa small-molecule secreted protein (Mollay et al., 1999). PK2 belongs to the prokineticin protein family, which participates in many biological processes, such as angiogenesis, hematopoiesis, and inflammation, by activating downstream signaling pathways (Martin et al., 2011; Maftei et al., 2014; Kurebayashi et al., 2015; Arora et al., 2016; Gordon et al., 2016). PK2 participates in myocardial diseases by binding to two agonist receptors, prokineticin receptor 1 (PKR1) and prokineticin receptor 2 (PKR2) (Negri et al., 2009). Insulin resistance, cardiac lipid deposition, interstitial fibrosis, and myocardial systolic diastolic function have been observed in PKR1-knockout mice (Boulberdaa et al., 2011a; Dormishian et al., 2013). In addition, AKT plays crucial roles in cardiac growth, coronary angiogenesis, and metabolic regulation (De Los Santos et al., 2017; Qi et al., 2017; Landa-Galvan et al., 2020). Recently, Su et al. (2020) demonstrated that PK2 relieves hypoxia/reoxygenation-induced injury in H9c2 cardiomyocytes by activating the AKT pathway. In our recent study, the role of the PK2-mediated AKT/GSK3β pathway in the development of DCM was investigated.

Metformin (Met) is a well-known therapeutic drug for diabetes. Met reduces blood glucose mainly by activating AMP-activated protein kinase (AMPK) and non-AMPK pathways. Met is thought to exert its primary antidiabetic action through the suppression of hepatic glucose production (Foretz et al., 2019). Met is also used in the treatment of diabetes complications such as DCM. Metformin ameliorates metabolic disorders, reduces ROS production and cardiac cell death, and improves myocardial structure and function on DCM (Sanit et al., 2019; Yang et al., 2019). Met also protects against brain and liver injury by activating AKT phosphorylation (Naicker et al., 2016; Xu et al., 2016). However, whether Met exerts a positive effect on DCM by regulating the AKT/GSK3β signaling pathway via PK2 is still unclear. Therefore, this study was conducted to elucidate the effects and the possible mechanisms of action of Met in high glucose (HG)-treated cardiomyocytes and DM mice myocardium.

MATERIALS AND METHODS

Animals

Male C57BL/6J mice (22 ± 2 g, 5–6 weeks of age) were purchased from Jinan Pengyue Experimental Animal Breeding Co., Ltd. (China). AKT-knockout mice were provided by the University of Wyoming (Laramie, WY, United States). The animal protocols were in accordance with the Guide for the Care and Use of Laboratory Animals, and the use of the animals was approved by the Institutional Animal Care and Use Committee at Hubei University of Science and Technology.

Cardiomyocyte Isolation and Mechanical Analyses

Hearts from adult wild-type or AKT-knockout mice were immediately perfused and then digested for 15 min. Then, the left ventricles were removed, and Ca^{2+} was added to a concentration of 1.25 mmol/L. The cardiomyocytes were used for shortening experiments. The mechanical properties of myocytes were evaluated with an IonOptix SoftEdge system. The resting cell length, time to peak shortening (TPS), peak shortening (PS), time to 90% relengthening (TR_{90}), and maximum speed of shortening/relengthening (±dL/dt) were measured to evaluate cell shortening and relengthening after stimulation at 0.5 Hz (Aberle et al., 2004). The cells were incubated with Krebs–Henseleit bicarbonate solution containing HG (33 mmol/L) with or without PK2 (10 nmol/L, Sigma) for 4 h to observe the effect of PK2 on cardiac functional impairment induced by HG.

Experimental DM Model Establishment and Met Treatment

Mice were randomized into three groups: a control group (n = 20), a DM group (n = 25), and a DM-Met group (n = 25).

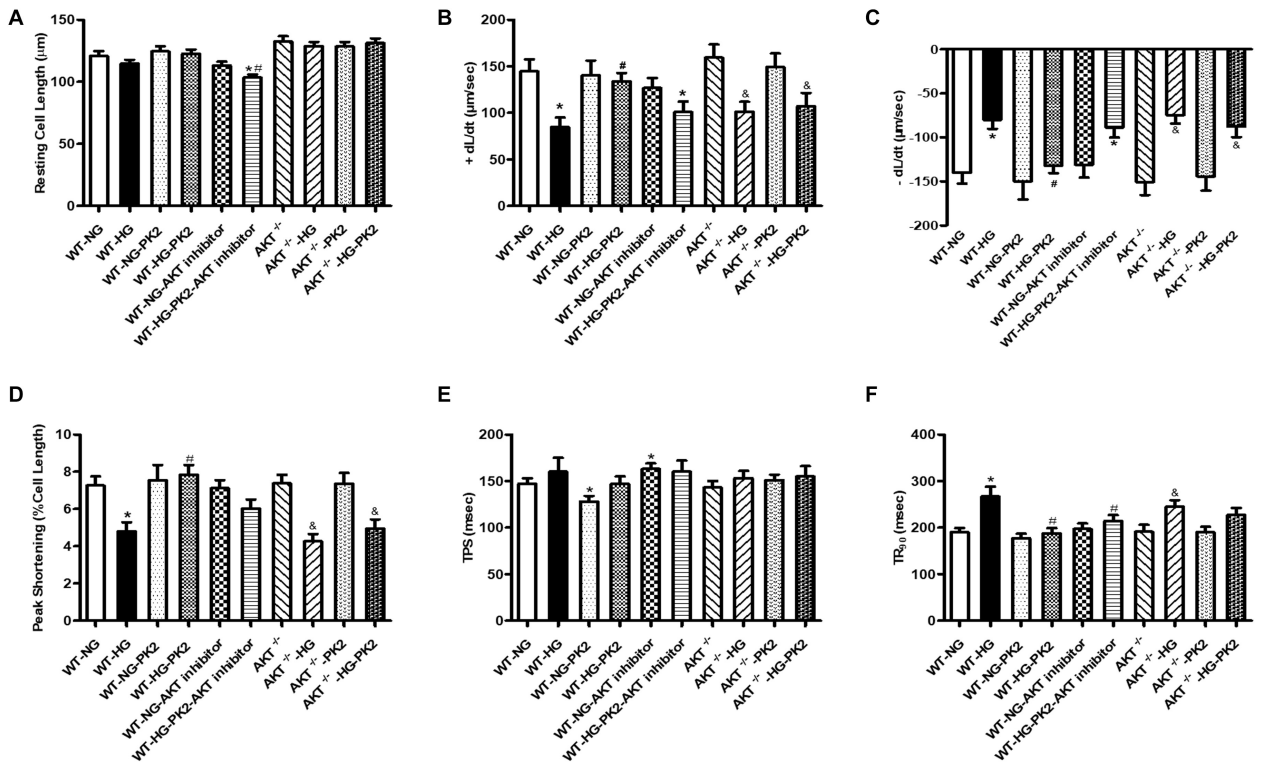

FIGURE 1 | Effect of PK2 on cardiomyocyte shortening. WT, wild-type mouse cardiomyocytes; $AKT^{-/-}$, AKT-knockout mouse cardiomyocytes; NG, normal glucose; HG, high glucose; NG-PK2, normal glucose plus PK2; HG-PK2, high glucose plus PK2. **(A)** Resting cell length. **(B)** +dL/dt. **(C)** –dL/dt. **(D)** PS. **(E)** TPS. **(F)** TR_{90}. The data are mean ± SEM; * *P* value less than 0.05 versus the WT-NG; #*P* value less than 0.05 versus the WT-HG; &P value less than 0.05 versus the $AKT^{-/-}$ group; *n* = 35–75 cells per group.

The mice in the DM group and the DM-Met group were injected intraperitoneally with 50 mg/kg/day streptozotocin (STZ, Sigma, United States) for five consecutive days. The control mice were administered with citrate buffer. Mice with blood glucose levels higher than 16.7 mmol/L were considered diabetic. The mice in the DM-Met group were given 250 mg/kg/day Met (Sino-American Shanghai Squibb Pharmaceuticals Ltd., China) in drinking water for 16 weeks.

Cell Culture and Treatment

The H9c2 cell line was purchased from the China Center for Type Culture Collection (CCTCC, China), and the cells were cultured and maintained in Dulbecco's modified Eagle's medium (DMEM, HyClone, United States) supplemented with fetal bovine serum (FBS, 10%, Gibco, United States), penicillin (1%, Gibco), and streptomycin at 37°C in a humidified atmosphere (5% CO_2 and 95% air). H9c2 cells were incubated with normal glucose (NG, 5.5 mmol/L) or HG (33 mmol/L) for 72 h with or without Met (2.5 mmol/L, Meilunbio, China), a PK2 antagonist (PKRA7, 10 μmol/L, Sigma), and an AKT1/2 kinase inhibitor (AKT inhibitor, 10 μmol/L, Sigma).

Echocardiographic Assessment

Mice were anesthetized with isoflurane. Each rat was fixed on a rat plate, and the chest area was shaved. Cardiac function was evaluated using a two-dimensional guided M-mode echocardiography. Basic hemodynamic parameters, such as the heart rate (HR), left ventricular ejection fraction (LVEF), left ventricular fractional shortening (LVFS), left ventricular posterior wall thickness in diastole (LVPWD), and left ventricular internal dimension in end-diastole (LVIDD), were measured and calculated.

Histopathologic Analysis

Cardiac tissue was fixed in 4% paraformaldehyde for 24 h and then embedded and sectioned. The sections were stained with hematoxylin and eosin (HE) and Masson's trichrome. Myocardial microstructure was observed under a light microscope. Additional cardiac tissue was fixed in electron microscopy fixative and embedded in an acetone-812 embedding agent. The tissues were cut into 60-nm-thick sections and stained with uranyl acetate and lead citrate. Myocardial ultramicrostructure was observed by electron microscopy.

Biochemical Indicators

Blood was collected from each group of animals, stored at 4°C overnight, and centrifuged at 3000 r/min for 15 min at 4°C in a low-temperature ultracentrifuge. The levels of lactic dehydrogenase (LDH), aspartate aminotransferase (AST), creatine kinase (CK), total cholesterol (TC), and triglyceride

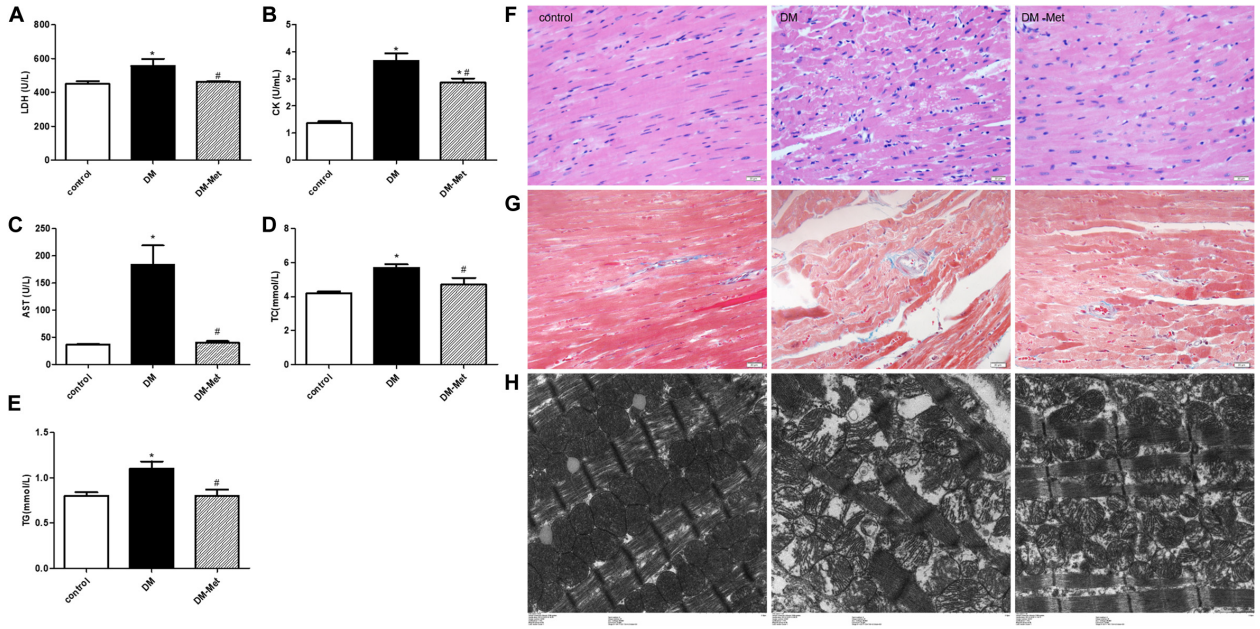

FIGURE 2 | Met protected against myocardial injury in DM mice. **(A)** LDH, **(B)** CK, **(C)** AST, **(D)** TC, and **(E)** TG levels. n = 8–22 per group. **(F)** HE staining of cardiomyopathy tissue. **(G)** Masson's trichrome staining of cardiomyopathy tissue. **(H)** Transmission electron microscopy images of the left ventricle. The data are mean ± SEM; * P value less than 0.05 versus the control group; # P value less than 0.05 versus the DM group; magnification = 400×; scale bar = 20 μm; n = 5 per group.

TABLE 1 | Primer sequences.

Primers	Forward sequence	Reverse sequence
PKR1	5′-GGCTTCCAGACAGAGCAG ATC-3′	5′-GACAGTCACAAAGCAGA GCGTA-3′
PKR2	5′-CTACTTCCTCTTCGTCTT CGGG-3′	5′-AGAAGTCTCGCACTATGG TAAAGC-3′

(TG) in the serum were tested according to procedures from the Nanjing Jiancheng Institute of Biological Engineering (China).

Real-Time Quantitative Fluorescence PCR Analysis

Total RNA was extracted from heart tissues with TRIzol reagent. Reverse transcription was performed to synthesize cDNA. The samples were incubated at 65°C for 5 min and then cooled on ice. Reaction buffer (5×), mixed dNTPs, RiboLock RNase inhibitor, and RevertAid M-MuLV reverse transcriptase were sequentially added. The samples were incubated at 42°C for 60 min in a PCR instrument, and the reverse transcriptase was inactivated at 70°C for 5 min. The PCR amplification reaction conditions were as follows: 95°C for 10 min, 95°C for 15 s, and annealing at 60°C for 60 s for 40 cycles. Melting curve analysis was performed from 60°C to 95°C in 0.3°C increments over 15 s. The results were analyzed by the ΔΔCT method. **Table 1** shows the primer sequences used for the PCR experiment.

Immunohistochemistry

After dewaxing and hydration of the conventionally prepared paraffin slices, the samples were incubated with primary antibodies (working concentration: 1:1000) at 4°C for 12 h and then incubated with secondary antibodies for 1 h. A solution of diaminobenzidine was added dropwise, and the slices were observed under a microscope. The procedure was carried out according to the kit instructions.

TUNEL Assay

Apoptosis was tested with a terminal deoxynucleotidyl transferase-mediated dUTP-biotin nick end labeling (TUNEL) assay in paraffin-embedded heart sections. Ten fields were analyzed for each slice, and the number of positive cells among cardiomyocytes was determined for each field. The apoptosis rates were calculated as the percentages of positive cells (Long et al., 2018).

Western Blot Analysis

Fifty milligrams of myocardial tissue was weighed, and RIPA lysis buffer was added. A BCA Protein Assay Kit (Beyotime, China) was used to test the protein concentration. Protein (50 mg) was added to each lane of a 12% SDS-polyacrylamide gel, and the proteins were separated and transferred to a polyvinylidene fluoride (PVDF) membrane. The membrane was blocked and incubated overnight at 4°C with AKT, p-AKT, GSK3β, p-GSK3β, Bax, Bcl-2 (1:1000, Cell Signaling Technology, United States), PK2 (1:1000, Abcam, United States), PKR1, and PKR2 (1:2000, Santa Cruz) antibodies. After incubation with

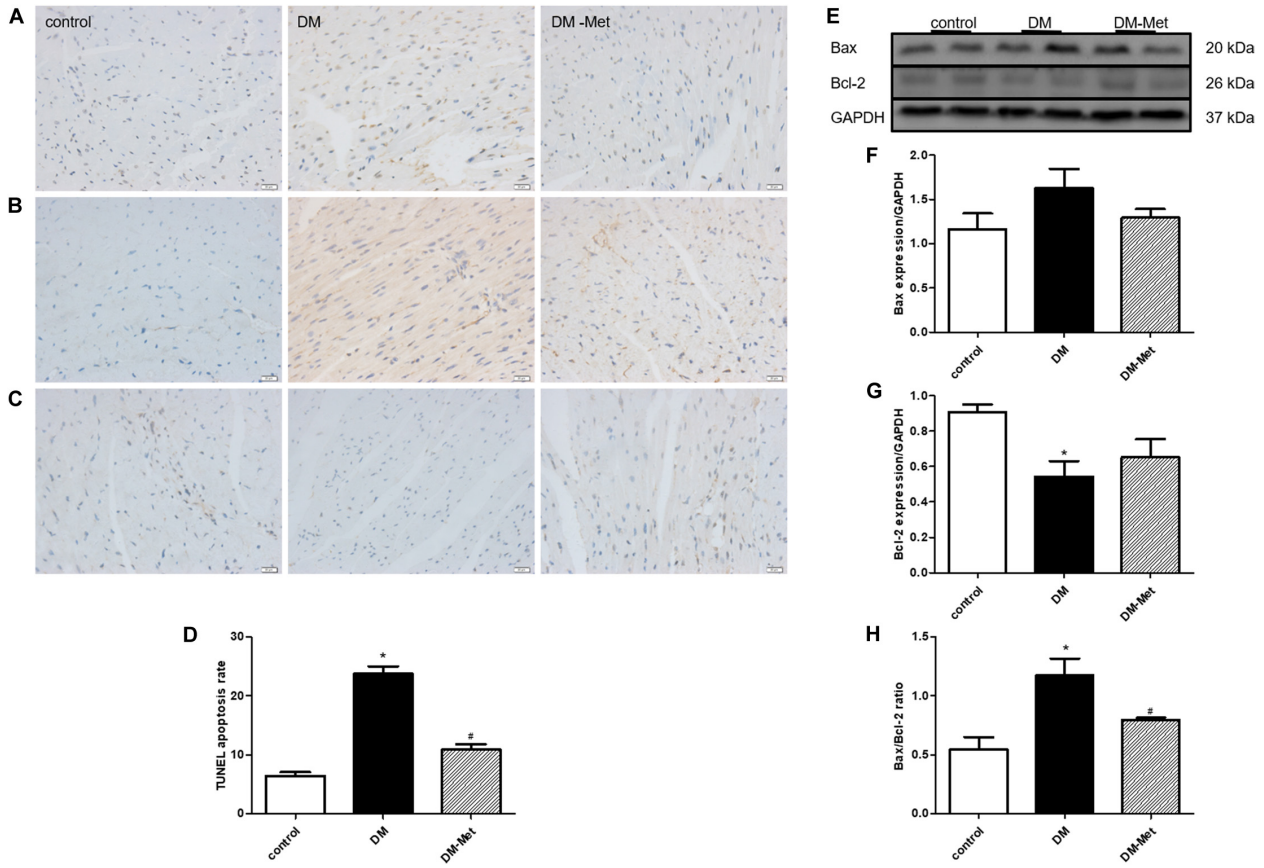

FIGURE 3 | Met prevented diabetes-induced cardiomyocyte apoptosis. **(A)** TUNEL staining. **(B)** Immunohistochemical staining for Bax. **(C)** Immunohistochemical staining for Bcl-2. **(D)** Analysis of TUNEL-positive cells. **(E)** Images of Bcl-2 and Bax protein levels. **(F)** Analysis of Bax. **(G)** Analysis of Bcl-2. **(H)** Analysis of the Bax/Bcl-2 ratio. The data are mean ± SEM; * *P* value less than 0.05 versus the control group; # *P* value less than 0.05 versus the DM group; *n* = 3–5 per group.

secondary antibodies for an hour, the analysis was completed using an Enhanced Chemiluminescence Kit (Meilunbio, China).

Statistical Analysis

The data are presented as the mean ± standard error of the mean (SEM). *T*-tests or one-way ANOVA was performed for all statistical analyses. *T*-tests were applied to analyze differences between two groups, and one-way ANOVA (Student–Newman–Keuls) was used to analyze differences among three or more groups. A *P* value less than 0.05 was considered to indicate statistical significance.

RESULTS

Effect of PK2 on Cardiomyocyte Shortening

As shown in **Figure 1**, compared with NG exposure, HG (33 mmol/L) exposure decreased the ±dL/dt and PS and prolonged the TR_{90} significantly but did not affect the resting cell length or TPS. PK2 significantly alleviated the HG-induced abnormalities in PS, ±dL/dt, and TR_{90} but had no effect on TPS or resting cell length. The effects were ameliorated or negated in AKT-knockout mouse cardiomyocytes and by AKT inhibitor treatment. These data strongly indicate that PK2 plays a pivotal role in the diabetic heart and that the important roles of AKT in PK2 provide benefits against glucose toxicity.

Met Improved General Features and Echocardiographic Properties in DM Mice

Body weight (BW), heart weight (HW), and blood glucose levels reflect the general health state of mice. The results showed that BW and HW were significantly decreased and that the heart-to-body weight ratio (HW/BW) was significantly increased in the DM group compared with the control group; these changes were overtly reversed by Met treatment (**Table 2**). In addition, diabetic mice displayed significantly higher blood glucose levels than control mice. Treatment with Met improved the blood glucose levels in diabetic mice but did not restore them to normal levels. We have published the data of BW and blood glucose (Liu et al., 2019).

Echocardiography is a technique for examining the anatomy and function of the heart. Echocardiographic evaluation revealed

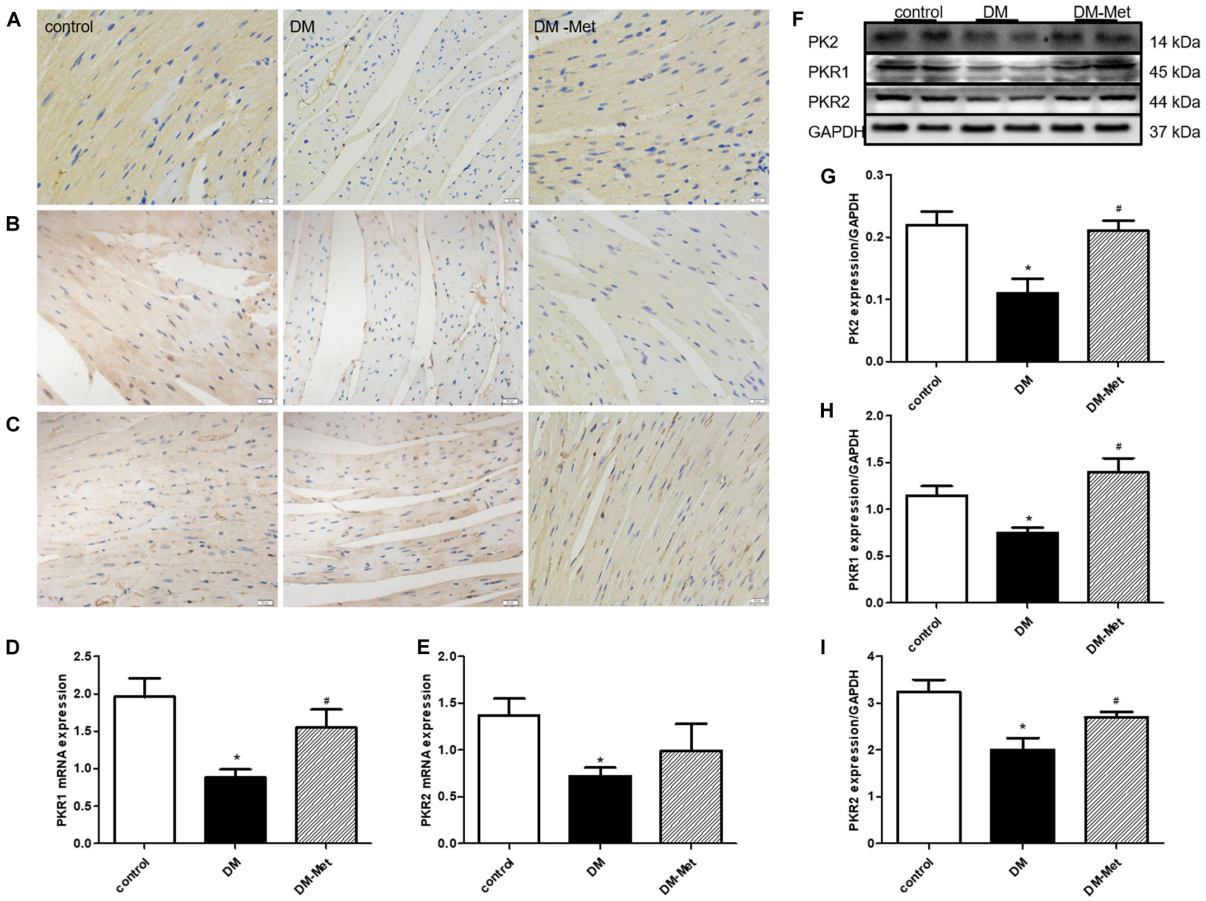

FIGURE 4 | Met increased the expression of PK2/PKR signaling pathway members in DM mice. **(A)** Immunohistochemical staining for PK2. **(B)** Immunohistochemical staining for PKR1. **(C)** Immunohistochemical staining for PKR2. n = 4–5 per group. **(D)** Expression of PKR1 mRNA, as determined by RT-PCR. **(E)** Expression of PKR2 mRNA, as determined by RT-PCR. **(F)** Images of PK2, PKR1, and PKR2 protein levels. **(G)** Analysis of PK2. **(H)** Analysis of PKR1. **(I)** Analysis of PKR2. The data are mean ± SEM; * P value less than 0.05 versus the control group; # P value less than 0.05 versus the DM group; n = 4–8 per group.

that LVPWD and LVIDD were slightly increased in DM mice, but these increases were mitigated by Met. Moreover, HR was significantly reduced in DM mice, and the reduction was partly eliminated by Met. Moreover, DM mice showed remarkable reductions in both LVEF and LVFS that were notably nullified by Met (**Table 2**).

TABLE 2 | Met improved general features and echocardiographic properties in DM mice.

Parameter	control	DM	DM-Met
HW (mg)	144.9 ± 2.8	99.9 ± 6.3*	111.6 ± 4.9*
HW/BW (mg/g)	4.6 ± 0.1	5.2 ± 0.2*	4.0 ± 0.2*#
HR (bpm)	505.21 ± 36.84	372.71 ± 34.22*	462.25 ± 6.24
LVPWD (mm)	0.68 ± 0.06	0.72 ± 0.04	0.58 ± 0.01
LVIDD (mm)	3.38 ± 0.12	3.57 ± 0.06	3.43 ± 0.05
LVEF (%)	72.13 ± 3.17	58.31 ± 4.18*	71.32 ± 2.64#
LVFS (%)	40.64 ± 2.66	30.37 ± 2.75*	39.72 ± 2.24#

*HR, heart rate; LVPWD, left ventricular posterior wall thickness; LVIDD, left ventricular internal dimension in end-diastole; LVEF, left ventricular ejection fraction; LVFS, left ventricular fractional shortening. The data are mean ± SEM; *P value less than 0.05 versus the control group; #P value less than 0.05 versus the DM group; n = 4–11 per group.*

Met Protected Against Myocardial Injury in DM Mice

Myocardial zymograms are recognized as effective indicators of cardiac function. The levels of LDH, CK, and AST in serum were significantly increased in the DM group compared to the control group, the effects of which were reversed by Met administration (**Figures 2A–C**). Moreover, TC and TG levels were significantly elevated in DM mice, indicating that DM mice had abnormal blood lipid metabolism, the effects of which were ameliorated by Met (**Figures 2D,E**).

Hematoxylin and eosin staining showed that the myocardial cells in the control group were clearly visible and arranged neatly, while those in the DM group showed disordered myocardial fiber arrangement and vacuolization. Interestingly, the myocardial fibers were denser in the Met treatment group than in the DM group, and less vacuolization was observed (**Figure 2F**).

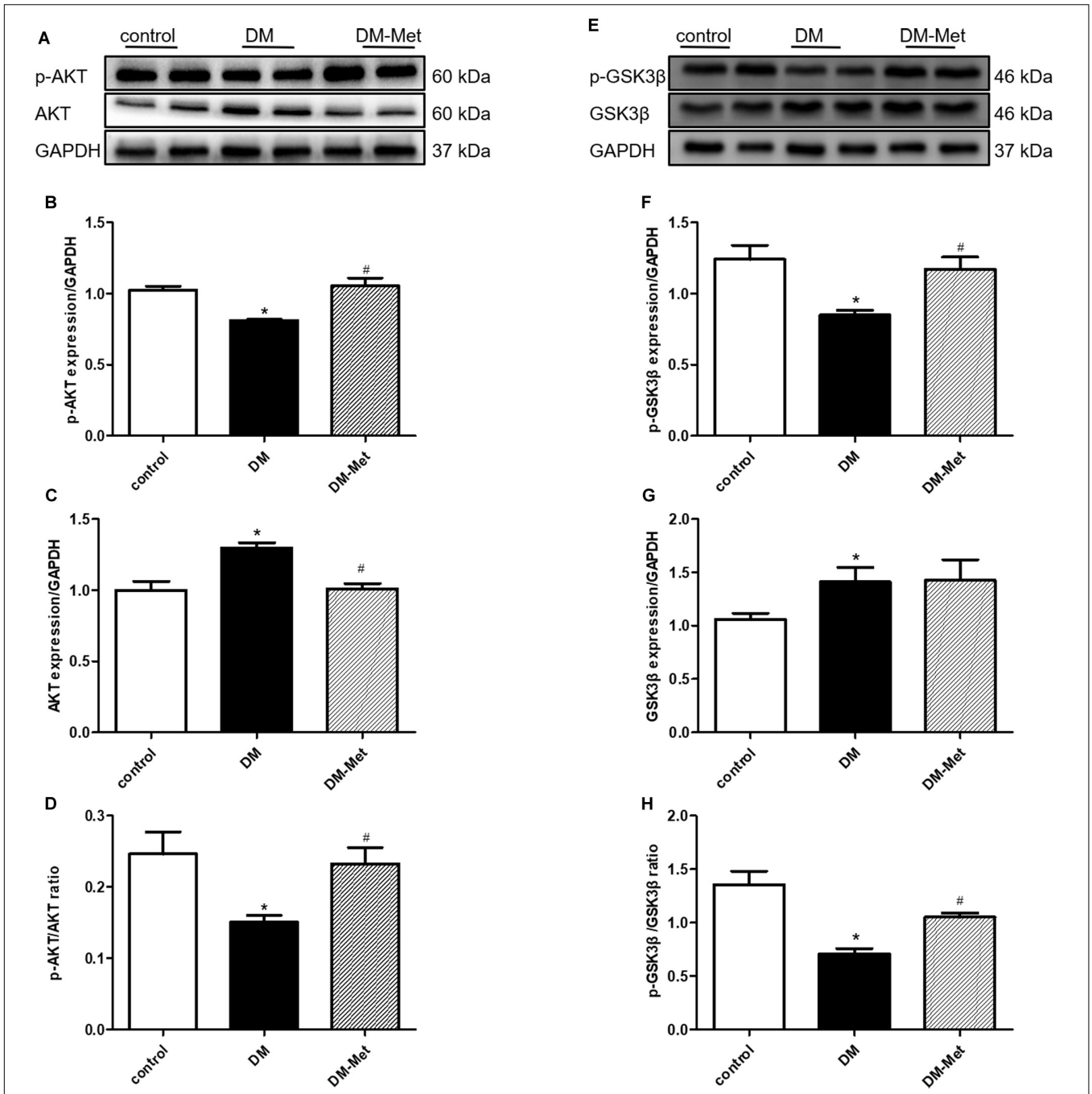

FIGURE 5 | Met activated the AKT/GSK3β signaling pathway in DM mice. **(A)** Images of p-AKT and AKT protein levels. **(B)** Analysis of p-AKT. **(C)** Analysis of AKT. **(D)** Analysis of the p-AKT/AKT ratio. **(E)** Images of p-GSK3β and GSK3β protein levels. **(F)** Analysis of p-GSK3β. **(G)** Analysis of GSK3β. **(H)** Analysis of the p-GSK3β/GSK3β ratio. The data are mean ± SEM; * *P* value less than 0.05 versus the control group; # *P* value less than 0.05 versus the DM group; *n* = 4 per group.

Masson's trichrome staining showed that there was less blue collagen in the myocardial interstitium in the control group than in the other groups. In contrast, increased interstitial fibrosis was evident in the DM mice hearts, and the fibrotic changes were significantly attenuated after Met administration (**Figure 2G**).

Electron microscopy revealed that in the control group, the mitochondria were intact, the myofilaments were neat and complete, and the Z-line and M-line were clear. However, in the DM group, the myocardial cells were arranged in a disorderly manner, the mitochondria were swollen, and myofilament fracture was present. Met ameliorated these abnormalities, causing the myofilament arrangement to be more regular and the mitochondrial structure to be more complete and reducing myofilament fracture (**Figure 2H**).

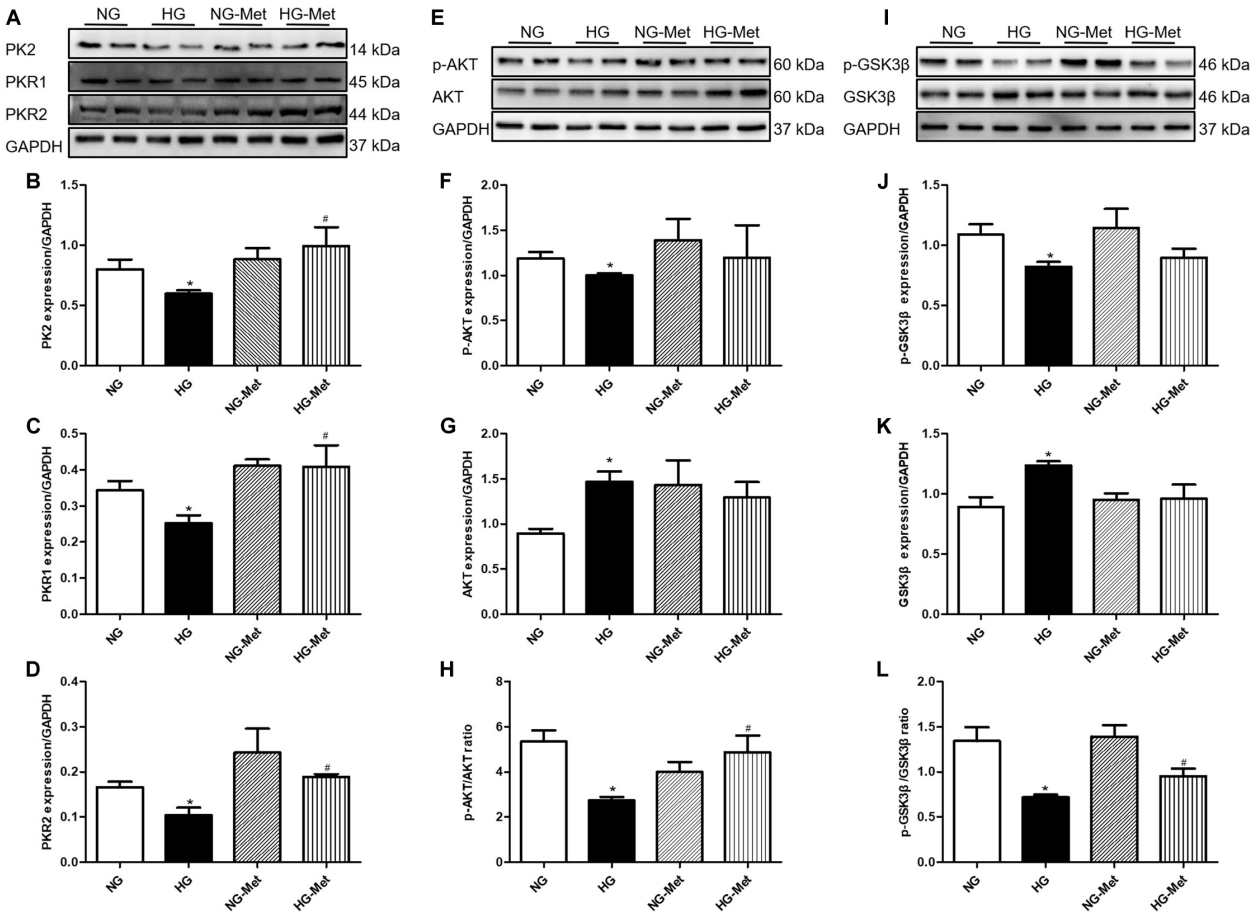

FIGURE 6 | Effects of Met on the PK2/PKR and AKT/GSK3β signaling pathways in HG-treated cardiomyocytes. NG-Met, normal glucose plus metformin; HG-Met, high glucose plus metformin. **(A)** Images of PK2, PKR1, and PKR2 protein levels. **(B)** Analysis of PK2. **(C)** Analysis of PKR1. **(D)** Analysis of PKR2. **(E)** Images of p-AKT and AKT protein levels. **(F)** Analysis of p-AKT. **(G)** Analysis of AKT. **(H)** Analysis of the p-AKT/AKT ratio. **(I)** Images of p-GSK3β and GSK3β protein levels. **(J)** Analysis of p-GSK3β. **(K)** Analysis of GSK3β. **(L)** Analysis of the p-GSK3β/GSK3β ratio. The data are mean ± SEM; * *P* value less than 0.05 versus the NG group; # *P* value less than 0.05 versus the HG group; *n* = 3–4 per group.

Met Prevented Diabetes-Induced Cardiomyocyte Apoptosis

TUNEL staining was used to detect apoptotic cardiomyocytes. The data showed that there were many more apoptotic cardiomyocytes (stained in brown) in the DM group than in the control group, but Met treatment significantly decreased DM-induced myocardial cell apoptosis (**Figures 3A,D**).

Apoptosis-related proteins play important roles in apoptosis progression. We thus carried out a more in-depth experiment to investigate whether apoptosis-related proteins affected the amelioration of DM-induced cardiomyocyte apoptosis by Met. As shown in **Figures 3B,C**, Bax protein upregulation and Bcl-2 protein downregulation (as assessed using immunohistochemical staining) were evident in the DM group compared with the control group, and these effects were reversed by Met. Consistent with the immunohistochemical staining results, the western blot results showed that Bax expression was enhanced in the DM group, whereas Bcl-2 expression was remarkably reduced; these changes were partly attenuated by Met administration. Furthermore, the Bax/Bcl-2 ratio was elevated in the DM group compared to that in the control group, the effect of which was markedly abrogated by Met administration (**Figures 3E–H**).

Met Increased the Expression of PK2/PKR Signaling Pathway Members in DM Mice

Previous studies have suggested that PK2 plays essential roles in the survival, proliferation, and apoptosis of cardiomyocytes. To further elucidate the role of PK2 in Met-mediated cardioprotection, we measured the effects of Met on PK2/PKR signaling pathway members. The results of immunohistochemical staining showed that the expression of PK2, PKR1, and PKR2 (brown labeling) was lower in the DM group than in the control group, the effects of which were ablated by Met treatment (**Figures 4A–C**). Constant to immunohistochemical results, the levels of PKR1 and PKR2 mRNA were also significantly downregulated, the effects of which were partly or considerably reversed by Met treatment

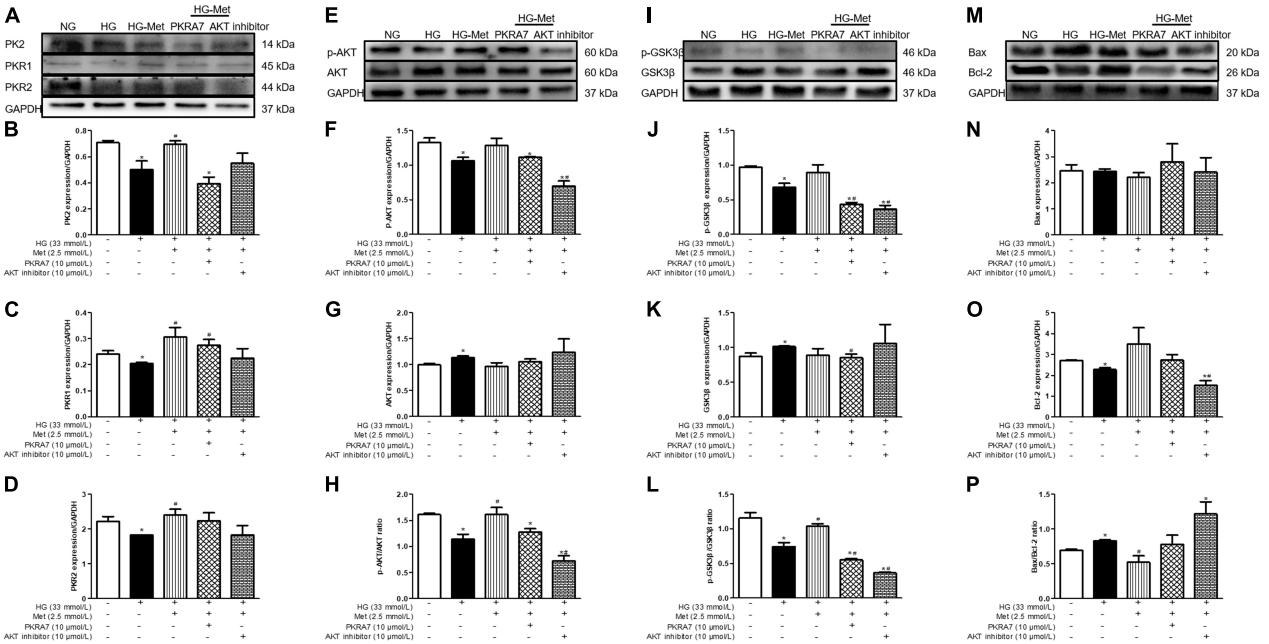

FIGURE 7 | A PK2 antagonist and an AKT inhibitor blocked the effects of Met on HG-treated cardiomyocytes. **(A)** Images of PK2, PKR1, and PKR2 protein levels. **(B)** Analysis of PK2. **(C)** Analysis of PKR1. **(D)** Analysis of PKR2. **(E)** Images of p-AKT and AKT protein levels. **(F)** Analysis of p-AKT. **(G)** Analysis of AKT. **(H)** Analysis of the p-AKT/AKT ratio. **(I)** Images of p-GSK3β and GSK3β protein levels. **(J)** Analysis of p-GSK3β. **(K)** Analysis of GSK3β. **(L)** Analysis of the p-GSK3β/GSK3β ratio. **(M)** Images of Bcl-2 and Bax protein levels. **(N)** Analysis of Bax. **(O)** Analysis of Bcl-2. **(P)** Analysis of the Bax/Bcl-2 ratio. The data are mean ± SEM; * *P* value less than 0.05 versus the NG group; # *P* value less than 0.05 versus the HG group; *n* = 3–4 per group.

(**Figures 4D,E**). Furthermore, the western blot results showed that the levels of PK2, PKR1, and PKR2 protein were markedly lower in the DM group than in the control group, but higher in the DM-Met group than in the DM group (**Figures 4F–I**). The data suggest that Met exerts a positive effect against diabetes-induced cardiac injury primarily by increasing the expression of PK2/PKR pathway members.

Met Activated the AKT/GSK3β Signaling Pathway in DM Mice

Previously obtained evidence has revealed that the cardioprotective actions of PK2/PKR may involve the phosphorylation of AKT, and impaired AKT activity in response to insulin is a common feature of DM (Wang C.Y. et al., 2016; Su et al., 2020). We therefore assessed the effect of Met on the AKT/GSK3β signaling pathway. As shown in **Figure 5**, the p-AKT/AKT and p-GSK3β/GSK3β ratios were significantly declined in the DM group, the effects of which were notably reversed by Met treatment.

Effects of Met on the PK2/PKR Signaling Pathway in HG-Treated Cardiomyocytes

To further validate the role of the PK2/PKR pathway in Met-induced cardiomyocyte mechanical responses against HG *in vitro*, the PK2/PKR signaling pathway was examined using western blot analysis. The data showed that PK2, PKR1, and PKR2 expression levels were overtly decreased in H9c2 cardiomyocytes exposed to HG, but the changes were significantly abrogated by Met treatment (**Figures 6A–D**).

Met Activated the AKT/GSK3β Signaling Pathway in HG-Treated Cardiomyocytes

To determine whether Met activates the PK2-mediated AKT/GSK3β signaling pathway in HG-treated cardiomyocytes, AKT and GSK3β signaling was examined using western blot analysis. As demonstrated in **Figures 6E–L**, HG incubation markedly decreased the ratio of p-AKT/AKT and p-GSK3β/GSK3β, the effects of which were negated by Met treatment.

A PK2 Antagonist and an AKT Inhibitor Blocked the Effects of Met on HG-Treated Cardiomyocytes

To clarify whether PK2 and PK2-mediated AKT play key roles in the Met-induced beneficial response to HG challenge, cardiomyocytes were incubated with NG or HG medium in the absence or presence of Met and PKRA7 or an AKT inhibitor. As shown in **Figures 7A–P**, incubation with PKRA7 partially or overtly reversed the Met-induced increases in PK2, PKR1, and PKR2 expression. In parallel, the Met-induced elevations in the p-AKT/AKT and p-GSK3β/GSK3β ratios were abolished by treatment with PKRA7. In addition, the AKT inhibitor effectively eliminated the effects of Met on the p-AKT/AKT and p-GSK3β/GSK3β ratios and partially attenuated the effects of

Met on PK2 and PKR expression. Furthermore, Met failed to regulate the expression of Bcl-2 and Bax when PKRA7 or the AKT inhibitor was applied. These results illustrate that Met exerts protective effects against glucose toxicity through the PK2/PKR-mediated AKT/GSK3β pathway.

DISCUSSION

The salient findings from our current study suggest that the PK2/PKR pathway plays a crucial role in the pathogenesis of DCM and that Met treatment prevents diabetes-induced glucose and lipid metabolism dysfunction, cardiomyocyte apoptosis, fibrosis, and cardiac insufficiency by stimulating PK2/PKR and the downstream AKT/GSK3β pathway. Glucose toxicity is considered to be the key factor in cardiovascular complications caused by diabetes, but the clinical treatment of DCM is still challenging. Our data reveal a likely role for the PK2/PKR pathway in the anti-DCM effects of Met.

It is well known that myocardial fibrosis and apoptosis contribute to the development of DCM (Gao et al., 2019). Several studies have also shown that left ventricular dysfunction and myocardial apoptosis are closely related, which indicates that inhibition of cardiomyocyte apoptosis can restore cardiac function (Yu et al., 2016). Various apoptotic stimuli, such as hyperglycemia and lipid metabolism dysfunction, can lead to enormous cardiomyocyte loss, which is proven to facilitate contractile dysfunction, fibrosis, and remodeling. Therefore, inhibition of cardiomyocyte fibrosis and apoptosis is thought to be a valid strategy for treating DCM. In the current work, disturbance of glucose and lipid metabolism, overt remodeling mainly presented as disorderly arrangement of myocardial cells, considerable deposition of collagen fibers in the myocardial interstitium, elevated HW/BW, and compromised cardiac function were observed in diabetic mice. However, long-term administration of Met rescued against DM-induced cardiac remodeling and functional anomalies. Notably, apoptosis-related Bcl-2 family members regulate apoptosis progression. Bax and Bcl-2 are members of the Bcl-2 family, and Bax binds with Bcl-2 to block upstream apoptotic signal transduction and promote cell survival and growth (Thandavarayan et al., 2011; Jafri et al., 2019). We discovered diabetes triggered cardiomyocytes apoptosis and increased Bax/Bcl-2 ratios in DM mice compared with control mice. However, Met reduced the diabetes-induced increases in cardiomyocyte apoptosis and the Bax/Bcl-2 ratio. Thus, it is plausible to speculate that repair of cardiac function upon Met treatment is conducive to the inhibition of cardiomyocyte apoptosis.

Prokineticin 2 expression has been observed in a variety of tissues, such as the brain, heart, and testes. PK2 affects various biological processes, including neuronal survival, olfactory bulb morphogenesis, testis development, and circadian rhythms (Boulberdaa et al., 2011b; Neal et al., 2018). In recent years, evidence has demonstrated that PK2 protects against oxidative stress in cardiomyocytes and H9c2 cells, suggesting that PK2 is inversely related to apoptosis (Gao et al., 2019). In addition, PK2 treatment can reduce food intake and BW in lean and obesity models (Gardiner et al., 2010). However, the precise functions of PK2 in diabetic-induced cardiac injury have not been determined to date. In this study, we found that PK2 ameliorated HG-induced cardiac contractile dysfunction by elevating PS and ±dL/dt and decreasing TR_{90} in cardiomyocytes, supporting that PK2 may be the key factor in DCM. Prokineticins exert multiple biological effects by activating PKR1 and PKR2 and mostly differ in their N-terminal sequences. Previous studies have revealed that PK2 and PKR1 levels are reduced in the late stage of heart failure, but PKR1 overexpression can protect cardiomyocytes from hypoxia injury-elicited apoptosis (Urayama et al., 2007; Gasser et al., 2015). Moreover, accumulating studies have demonstrated that PK2/PKR is associated with many types of cardiometabolic risk factors and exerts a vital role in cardiovascular disease development (Wang Y. et al., 2016). Upregulation of PK2 manipulates epicardium-derived progenitor cells involved in tissue repair/regeneration in heart diseases, whereas PKR1 knockout in the epicardium results in ventricular hypoplasia, ventricular septal defects, and even embryo necrosis (Curtis et al., 2013). Similarly, PK2 induces the growth of myocardium derived from mice, but the effect is abolished in PKR1-knockout myocardium (Gasser et al., 2015). In addition, PKR1-null mice exhibit cardiomyocyte apoptosis and contractile defects (Boulberdaa et al., 2011a). Recently, numerous studies have explored the cardioprotective effect of Met in the DCM myocardium, but whether Met can activate PK2 and its pathway in DCM remains unclear. Since our data showed that PK2 treatment protected against HG-induced cardiac function compromise *in vitro*, we made further efforts to investigate the protective effect of Met on HG-induced cardiac damage mediated via regulation of the PK2/PKR pathway *in vitro* and *in vivo*. As expected, our current results suggested that PK2, PKR1, and PKR2 expression was remarkably dampened both in diabetic mouse hearts and H9c2 cardiomyocytes exposure to HG, which further confirmed that a decrease in PK2 may be the main contributor to myocardial apoptosis in DCM. Interestingly, after administration of Met, PK2, PKR1, and PKR2 expression was significantly increased *in vivo* and *in vitro*. In addition, PKRA7 partly or considerably counteracted the beneficial effects of Met against glucose toxicity. Our observations favored a role for activation PK2/PKR pathway in the Met-offered beneficial mechanical effects against HG-induced cardiac damage.

Cumulative evidence suggests that PK2/PKR participates in myocardial survival, angiogenesis, and the hematopoietic system through the AKT and STAT3 signaling pathways (Urayama et al., 2007; Xin et al., 2013). AKT appears to regulate cell survival, growth, apoptosis, and angiogenesis. Abnormal AKT regulation leads to impaired glucose tolerance in diabetic patients (Chen et al., 2001). GSK3β, one of the downstream substrates of AKT, is involved in physiological processes including cell death (Wang et al., 2009). It is now recognized that glucose utilization and abnormal free fatty acid oxidation are involved in the development of DCM (Neglia et al., 2007). Thus, activating AKT and inhibiting GSK3β activity can be considered effective treatment strategies for DCM. Our study clearly shows that regulation of the PK2-mediated AKT/GSK3β pathway may be a potential mechanism of the cardioprotective role of Met.

This possibility is supported by several pieces of experimental data. First, we found that the protective effect of PK2 against HG challenge was completely negated in AKT-knockout mice and AKT inhibitor-treated isolated cardiomyocytes. Second, the results revealed that the p-AKT/AKT and p-GSK3β/GSK3β ratios were notably decreased not only in diabetic mice but also in HG-challenged H9c2 cardiomyocytes, the effects of which were significantly reversed by Met treatment. Third, the effects of Met on cardiomyocytes with HG-induced injury, such as the Met-mediated promotion of AKT and GSK3β phosphorylation and the regulation of apoptosis-related protein expression, were abolished after treatment with an AKT inhibitor. Therefore, Met-mediated reductions in diabetes-induced apoptosis might be attributable to activation of the PK2-mediated AKT/GSK3β pathway.

Limitations of the Experiment

Our current studies have elucidated the important role of PK2 signaling cascade in DCM and Met ameliorates HG-induced cardiac damage through the PK2-mediated AKT/GSK3β pathway using *in vivo* diabetes animal models and *in vitro* HG-exposed cardiomyocytes. Any conclusions about the exact role of the Met activated PK2-AKT signaling cascade in DCM must be taken with caution. As proof of concept evidence is still lacking from genetically engineered mouse models of PK2 and AKT, it is quite challenging to better understand the role of PK2 signaling in biological process.

In summary, our data suggest that PK2 may participate in pathophysiological changes in DCM and that Met protects against diabetes-induced cardiac and remodeling, apoptosis, and dysfunction via activation of the PK2/PKR signaling, thereby regulating the AKT/GSK3β pathway. These findings suggest new strategies for the prevention and treatment of DCM, which are worthy of further clinical study.

DATA AVAILABILITY STATEMENT

The raw data supporting the conclusions of this article will be made available by the authors, without undue reservation, to any qualified researcher.

ETHICS STATEMENT

The animal study was reviewed and approved by the Institutional Animal Care and Use Committee at Hubei University of Science and Technology.

AUTHOR CONTRIBUTIONS

ZY, MW, YZ, FC, and BJ performed the experiments. WZ and WY contributed to analysis and interpretation of the data, and responsible for critically revising the manuscript. All authors read and approved the final manuscript.

FUNDING

This work was supported by grants from the National Natural Science Foundation of China (81500296 and 81870576), Xianning City of Science and Technology Fund Project (2018-52), and Research Innovation Team Project of Hubei University of Science and Technology (2018).

REFERENCES

Aberle, N. S., Lee, K. J., and Ren, J. (2004). Korean anti-inflammatory compound allergina enhances cardiac contractile function in isolated ventricular cardiomyocytes. *J. Altern. Complement. Med.* 10, 514–518. doi: 10.1089/1075553041323858

Agrawal, R. P., Sharma, P., Pal, M., Kochar, A., and Kochar, D. K. (2006). Magnitude of dyslipedemia and its association with micro and macro vascular complications in type 2 diabetes: a hospital based study from Bikaner (Northwest India). *Diabetes Res. Clin. Pract.* 73, 211–214. doi: 10.1016/j.diabres.2006.01.006

Arora, H., Boulberdaa, M., Qureshi, R., Bitirim, V., Gasser, A., Messaddeq, N., et al. (2016). Prokineticin receptor-1 signaling promotes epicardial to mesenchymal transition during heart development. *Sci. Rep.* 6:25541. doi: 10.1038/srep25541

Bi, Y., Zhang, Y., and Ren, J. (2020). Phosphoinositide 3-Kinase therapy in diabetic cardiomyopathy: unravelling an enigma. *Am. J. Physiol. Heart Circ. Physiol.* 13:160. doi: 10.1152/ajpheart.00160.2020

Boulberdaa, M., Turkeri, G., Urayama, K., Dormishian, M., Szatkowski, C., Zimmer, L., et al. (2011a). Genetic inactivation of prokineticin receptor-1 leads to heart and kidney disorders. *Arterioscler. Thromb. Vasc. Biol.* 31, 842–850. doi: 10.1161/ATVBAHA.110.222323

Boulberdaa, M., Urayama, K., and Nebigil, C. G. (2011b). Prokineticin receptor 1 (PKR1) signalling in cardiovascular and kidney functions. *Cardiovasc. Res.* 92, 191–198. doi: 10.1093/cvr/cvr228

Ceylan Isik, A. F., Fliethman, R. M., Wold, L. E., and Ren, J. (2008). Herbal and traditional Chinese medicine for the treatment of cardiovascular complications in diabetes mellitus. *Curr. Diabetes Rev.* 4, 320–328. doi: 10.2174/157339908786241142

Chen, W. S., Xu, P. Z., Gottlob, K., Chen, M. L., Sokol, K., Shiyanova, T., et al. (2001). Growth retardation and increased apoptosis in mice with homozygous disruption of the Akt1 gene. *Genes Dev.* 15, 2203–2208. doi: 10.1101/gad.913901

Curtis, V. F., Wang, H., Yang, P., McLendon, R. E., Li, X., Zhou, Q. Y., et al. (2013). A PK2/Bv8/PROK2 antagonist suppresses tumorigenic processes by inhibiting angiogenesis in glioma and blocking myeloid cell infiltration in pancreatic cancer. *PLoS One* 8:e54916. doi: 10.1371/journal.pone.0054916

De Los Santos, S., García-Pérez, V., Hernández-Reséndiz, S., Palma-Flores, C., González-Gutiérrez, C. J., Zazueta, C., et al. (2017). (-)-Epicatechin induces physiological cardiac growth by activation of the PI3K/Akt pathway in mice. *Mol. Nutr. Food Res.* 61:343. doi: 10.1002/mnfr.201600343

Dormishian, M., Turkeri, G., Urayama, K., Nguyen, T. L., Boulberdaa, M., Messaddeq, N., et al. (2013). Prokineticin receptor-1 is a new regulator of endothelial insulin uptake and capillary formation to control insulin sensitivity and cardiovascular and kidney functions. *J. Am. Heart Assoc.* 2:e000411. doi: 10.1161/JAHA.113.000411

Foretz, M., Guigas, B., and Viollet, B. (2019). Understanding the glucoregulatory mechanisms of metformin in type 2 diabetes mellitus. *Nat. Rev. Endocrinol.* 15, 569–589. doi: 10.1038/s41574-019-0242-2

Gao, Y., Yang, Z. G., Ren, Y., Liu, X., Jiang, L., Xie, L. J., et al. (2019). Evaluation of myocardial fibrosis in diabetes with cardiac magnetic resonance T1-mapping:

correlation with the high-level hemoglobin A1c. *Diabetes Res. Clin. Pract.* 150, 72–80. doi: 10.1016/j.diabres.2019.03.004

Gardiner, J. V., Bataveljic, A., Patel, N. A., Bewick, G. A., Roy, D., Campbell, D., et al. (2010). Prokineticin 2 is a hypothalamic neuropeptide that potently inhibits food intake. *Diabetes Metab. Res. Rev.* 59, 397–406. doi: 10.2337/db09-1198

Gasser, A., Brogi, S., Urayama, K., Nishi, T., Kurose, H., Tafi, A., et al. (2015). Discovery and cardioprotective effects of the first non-Peptide agonists of the G protein-coupled prokineticin receptor-1. *PLoS One* 10:e0121027. doi: 10.1371/journal.pone.0121027

Gordon, R., Neal, M. L., Luo, J., Langley, M. R., Harischandra, D. S., Panicker, N., et al. (2016). Prokineticin-2 upregulation during neuronal injury mediates a compensatory protective response against dopaminergic neuronal degeneration. *Nat. Commun.* 7:12932. doi: 10.1038/ncomms12932

Jafri, A., Siddiqui, S., Rais, J., Ahmad, M. S., Kumar, S., Jafar, T., et al. (2019). Induction of apoptosis by piperine in human cervical adenocarcinoma via ROS mediated mitochondrial pathway and caspase-3 activation. *EXCLI J.* 18, 154–164. doi: 10.17179/excli2018-1928

Kurebayashi, H., Goi, T., Shimada, M., Tagai, N., Naruse, T., Nakazawa, T., et al. (2015). Prokineticin 2 (PROK2) is an important factor for angiogenesis in colorectal cancer. *Oncotarget* 6, 26242–26251. doi: 10.18632/oncotarget.4385

Landa-Galvan, H. V., Rios-Castro, E., Romero-Garcia, T., Rueda, A., and Olivares-Reyes, J. A. (2020). Metabolic syndrome diminishes insulin-induced Akt activation and causes aredistribution of Akt-interacting proteins in cardiomyocytes. *PLoS One* 15:e0228115. doi: 10.1371/journal.pone.0228115

Liu, Y., Yang, Z., Kong, D., Zhang, Y., Yu, W., and Zha, W. (2019). Metformin ameliorates testicular damage in male mice with streptozotocin-induced type 1 diabetes through the PK2/PKR pathway. *Oxid. Med. Cell. Longev* 18:5681701. doi: 10.1155/2019/5681701

Long, L., Qiu, H., Cai, B., Chen, N., Lu, X., Zheng, S., et al. (2018). Hyperglycemia induced testicular damage in type 2 diabetes mellitus rats exhibiting microcirculation impairments associated with vascular endothelial growth factor decreased via PI3K/Akt pathway. *Oncotarget* 9, 5321–5336. doi: 10.18632/oncotarget.23915

Maftei, D., Marconi, V., Florenzano, F., Giancotti, L. A., Castelli, M., Moretti, S., et al. (2014). Controlling the activation of the Bv8/prokineticin system reduces neuroinflammation and abolishes thermal and tactile hyperalgesia in neuropathic animals. *Br. J. Pharmacol.* 171, 4850–4865. doi: 10.1111/bph.12793

Martin, C., Balasubramanian, R., Dwyer, A. A., Au, M. G., Sidis, Y., Kaiser, U. B., et al. (2011). The role of the prokineticin 2 pathway in human reproduction: evidence from the study of human and murine gene mutations. *Endocr. Rev.* 32, 225–246. doi: 10.1210/er.2010-0007

Mollay, C., Wechselberger, C., Mignogna, G., Negri, L., Melchiorri, P., Barra, D., et al. (1999). Bv8, a small protein from frog skin and its homologue from snake venom induce hyperalgesia in rats. *Eur. J. Pharmacol.* 374, 189–196. doi: 10.1016/s0014-2999(99)00229-0

Naicker, N., Nagiah, S., Phulukdaree, A., and Chuturgoon, A. (2016). Trigonella foenum-graecum seed extract, 4-hydroxyisoleucine, and metformin stimulate proximal insulin signaling and increase expression of glycogenic enzymes and GLUT2 in HepG2 cells. *Metab. Syndr. Relat. Disord.* 14, 114–120. doi: 10.1089/met.2015.0081

Neal, M., Luo, J., Harischandra, D. S., Gordon, R., Sarkar, S., Jin, H., et al. (2018). Prokineticin-2 promotes chemotaxis and alternative A2 reactivity of astrocytes. *Glia* 66, 2137–2157. doi: 10.1002/glia.23467

Neglia, D., De Caterina, A., Marraccini, P., Natali, A., Ciardetti, M., Vecoli, C., et al. (2007). Impaired myocardial metabolic reserve and substrate selection flexibility during stress in patients with idiopathic dilated cardiomyopathy. *Am. J. Physiol. Heart Circ. Physiol.* 293, H3270–H3278. doi: 10.1152/ajpheart.00887.2007

Negri, L., Lattanzi, R., Giannini, E., Canestrelli, M., Nicotra, A., and Melchiorri, P. (2009). Bv8/Prokineticins and their receptors: a new pronociceptive system. *Int. Rev. Neurobiol.* 85, 145–157. doi: 10.1016/S0074-7742(09)85011-3

Ogurtsova, K., da Rocha Fernandes, J. D., Huang, Y., Linnenkamp, U., Guariguata, L., Cho, N. H., et al. (2017). IDF diabetes atlas: global estimates for the prevalence of diabetes for 2015 and 2040. *Diabetes Res. Clin. Pract.* 128, 40–50. doi: 10.1016/j.diabres.2017.03.024

Qi, X., Liu, H., Mao, L., Sun, P., and Kong, D. (2017). Combination of exendin-4 and DPP-4 silencing promoted angigenesis of human cornary artery endothelial cells via acrivation of PI3K/Akt pathway. *Pak. J. Pharm. Sci.* 30, 555–560.

Rubler, S., Dlugash, J., Yuceoglu, Y. Z., Kumral, T., Branwood, A. W., and Grishman, A. (1972). New type of cardiomyopathy associated with diabetic glomerulosclerosis. *Am. J. Cardiol.* 30, 595–602. doi: 10.1016/0002-9149(72)90595-4

Sanit, J., Prompunt, E., Adulyaritthikul, P., Nokkaew, N., Mongkolpathumrat, P., Kongpol, K., et al. (2019). Combination of metformin and p38 MAPK inhibitor, SB203580, reduced myocardial ischemia/reperfusion injury in non-obese type 2 diabetic Goto-Kakizaki rats. *Exp. Ther. Med.* 18, 2701–2714. doi: 10.3892/etm.2019.7763

Su, G., Sun, G., Liu, H., Shu, L., Zhang, E., and Liang, Z. (2020). Prokineticin a relieves hypoxiaoxia/reoxygenation-induced injury through activation of Akt/mTOR pathway in H9c2 cardiomyocytes. *Artif. Cells Nanomed. Biotechnol.* 48, 345–352. doi: 10.1080/21691401.2019.1709850

Thandavarayan, R. A., Giridharan, V. V., Watanabe, K., and Konishi, T. (2011). Diabetic cardiomyopathy and oxidative stress: role of antioxidants. *Cardiovasc. Hematol. Agents Med. Chem.* 9, 225–230. doi: 10.2174/187152511798120877

Urayama, K., Guilini, C., Messaddeq, N., Hu, K., Steenman, M., Kurose, H., et al. (2007). The prokineticin receptor-1 (GPR73) promotes cardiomyocyte survival and angiogenesis. *FASEB J.* 21, 2980–2993. doi: 10.1096/fj.07-8116com

von Scholten, B. J., Hansen, T. W., Goetze, J. P., Persson, F., and Rossing, P. (2015). Glucagon-like peptide 1 receptor agonist (GLP-1 RA): long-term effect on kidney function in patients with type 2 diabetes. *J. Diabetes Complicat.* 29, 670–674. doi: 10.1016/j.jdiacomp.2015.04.004

Wang, C. Y., Li, X. D., Hao, Z. H., and Xu, D. (2016). Insulin-like growth factor-1 improves diabetic cardiomyopathy through antioxidative and anti-inflammatory processes along with modulation of Akt/GSK-3β signaling in rats. *Korean J. Physiol. Pharmacol.* 20:613. doi: 10.4196/kjpp.2016.20.6.613

Wang, Y., Guo, X., Ma, H., Lu, L., and Zhang, R. (2016). Prokineticin-2 is associated with metabolic syndrome in a middle-aged and elderly Chinese population. *Lipids Health Dis.* 15:1. doi: 10.1186/s12944-015-0172-5

Wang, Y., Feng, W., Xue, W., Tan, Y., Hein, D. W., Li, X. K., et al. (2009). Inactivation of GSK-3beta by metallothionein prevents diabetes-related changes in cardiac energy metabolism, inflammation, nitrosative damage, and remodeling. *Diabetes Metab. Res. Rev.* 58, 1391–1402. doi: 10.2337/db08-1697

Wold, L. E., Ceylan-Isik, A. F., and Ren, J. (2005). Oxidative stress and stress signaling: menace of diabetic cardiomyopathy. *Acta Pharmacol. Sin.* 26, 908–917. doi: 10.1111/j.1745-7254.2005.00146.x

Xin, H., Lu, R., Lee, H., Zhang, W., Zhang, C., Deng, J., et al. (2013). G-protein-coupled receptor agonist BV8/prokineticin-2 and STAT3 protein form a feed-forward loop in both normal and malignant myeloid cells. *J. Biol. Chem.* 288, 13842–13849. doi: 10.1074/jbc.M113.450049

Xu, H., Zhou, Y., Liu, Y., Ping, J., Shou, Q., Chen, F., et al. (2016). Metformin improves hepatic IRS2/PI3K/Akt signaling in insulin-resistant rats of NASH and cirrhosis. *J. Endocrinol.* 229, 133–144. doi: 10.1530/JOE-15-0409

Yang, F., Qin, Y., Wang, Y., Meng, S., Xian, H., Che, H., et al. (2019). Metformin inhibits the NLRP3 inflammasome via AMPK/mTOR-dependent effects in diabetic cardiomyopathy. *Int. J. Biol. Sci.* 15, 1010–1019. doi: 10.7150/ijbs.29680

Yu, W., Zha, W., Ke, Z., Min, Q., Li, C., Sun, H., et al. (2016). Curcumin protects neonatal rat cardiomyocytes against high glucose-induced apoptosis via PI3K/Akt signalling pathway. *J. Diabetes Res.* 2016:4158591. doi: 10.1155/2016/4158591

Zhang, Y., Babcock, S. A., Hu, N., Maris, J. R., Wang, H., and Ren, J. (2012). Mitochondrial aldehyde dehydrogenase (ALDH2) protects against streptozotocin-induced diabetic cardiomyopathy: role of GSK3β and mitochondrial function. *BMC Med.* 10:40. doi: 10.1186/1741-7015-10-40

Conflict of Interest: The authors declare that the research was conducted in the absence of any commercial or financial relationships that could be construed as a potential conflict of interest.

Copyright © 2020 Yang, Wang, Zhang, Cai, Jiang, Zha and Yu. This is an open-access article distributed under the terms of the Creative Commons Attribution License (CC BY). The use, distribution or reproduction in other forums is permitted, provided the original author(s) and the copyright owner(s) are credited and that the original publication in this journal is cited, in accordance with accepted academic practice. No use, distribution or reproduction is permitted which does not comply with these terms.

frontiers in Physiology

ORIGINAL RESEARCH
published: 05 June 2020
doi: 10.3389/fphys.2020.00542

Critical Roles of ELVOL4 and IL-33 in the Progression of Obesity-Related Cardiomyopathy via Integrated Bioinformatics Analysis

Jun Tao[1†], Yajing Wang[2†], Ling Li[1], Junmeng Zheng[1] and Shi Liang[1*]*

[1] Department of Cardiovascular Surgery, Sun Yat-sen Memorial Hospital, Sun Yat-sen University, Guangzhou, China,
[2] Department of Otorhinolaryngology, Sun Yat-sen Memorial Hospital, Sun Yat-sen University, Guangzhou, China

The molecular mechanisms underlying obesity-related cardiomyopathy (ORCM) progression involve multiple signaling pathways, and the pharmacological treatment for ORCM is still limited. Thus, it is necessary to explore new targets and develop novel therapies. Microarray analysis for gene expression profiles using different bioinformatics tools has been an effective strategy for identifying novel targets for various diseases. In this study, we aimed to explore the potential genes related to ORCM using the integrated bioinformatics analysis. The GSE18897 (whole blood expression profiling of obese diet-sensitive, obese diet-resistant, and lean human subjects) and GSE47022 (regular weight C57BL/6 and diet-induced obese C57BL/6 mice) were used for bioinformatics analysis. Weighted gene co-expression network analysis (WGCNA) of GSE18897 was employed to investigate gene modules that were strongly correlated with clinical phenotypes. Gene Ontology (GO) functional enrichment analysis and Kyoto Encyclopedia of Genes and Genomes (KEGG) pathway analysis were performed on the co-expression genes. The expression levels of the hub genes were validated in the clinical samples. Yellow co-expression module of WGCNA in GSE18897 was found to be significantly related to the caloric restriction treatment. In addition, GO functional enrichment analysis and KEGG pathway analysis were performed on the co-expression genes in yellow co-expression module, which showed an association with oxygen transport and the porphyrins pathway. Overlap analysis of yellow co-expression module genes from GSE18897 andGSE47022 revealed six upregulated genes, and further experimental validation results showed that elongation of very-long-chain fatty acids protein 4 (ELOVL4), matrix metalloproteinase-8 (MMP-8), and interleukin-33 (IL-33) were upregulated in the peripheral blood from patients with ORCM compared to that in the controls. The bioinformatics analysis revealed that ELOVL4 expression levels are positively correlated with that of IL-33. Collectively, using WGCNA in combination with integrated bioinformatics analysis, the hub genes of ELVOL4 and IL-33 might serve as potential biomarkers for diagnosis and/or therapeutic targets for ORCM. The detailed roles of ELVOL4 and IL-33 in the pathophysiology of ORCM still require further investigation.

Keywords: ORCM, WGCNA, yellow co-expression module, ELOVL4, IL-33

OPEN ACCESS

Edited by:
Jun Ren,
University of Washington,
United States

Reviewed by:
Ying Tan,
Southern Medical University, China
Ne Natalie Wu,
Fudan University, China

****Correspondence:***
Junmeng Zheng
zhengjunmeng@126.com
Shi Liang
md02ls@mail2.sysu.edu.cn

† These authors have contributed equally to this work

Specialty section:
This article was submitted to Integrative Physiology, a section of the journal Frontiers in Physiology

Received: *19 March 2020*
Accepted: *30 April 2020*
Published: *05 June 2020*

Citation:
Tao J, Wang Y, Li L, Zheng J and Liang S (2020) Critical Roles of ELVOL4 and IL-33 in the Progression of Obesity-Related Cardiomyopathy via Integrated Bioinformatics Analysis. Front. Physiol. 11:542. doi: 10.3389/fphys.2020.00542

INTRODUCTION

The number of overweight and obese individuals has dramatically increased. In China, more than 10% of the adult population is obese (He et al., 2017; Qasim et al., 2018; Wang and Ren, 2018). While in America, the prevalence of obesity among adults is about 39.6% (Hales et al., 2018). China is the most populous country with a total population of 1.4 billion compared to 0.32 billion in America (in 2018). Although the prevalence of obesity is much higher in America than in China, the obese population is comparable in these two countries. In 2014, China ranked first worldwide, with 43.2 million obese men and 46.4 million obese women (Collaboration, 2016).

According to the WHO classification, individuals with a body mass index (BMI) $\geq$ 30 kg/m^2 are defined as obese (WHO, 2000). However, the universal BMI criteria are not suitable among diverse Asian populations, as Asian populations show different associations between BMI, percentage of body fat, and health risks than European populations (Consultation, 2004). According to the classification of the Chinese Ministry of Public Health, Chinese individuals with a BMI $\geq$ 28 kg/m^2 are defined as obese. Waist circumference is another important indicator for obesity, which provides both independent and additive information to BMI for predicting morbidity and risk of death. As BMI alone is not sufficient to properly assess or manage the cardiometabolic risk, the combination of BMI and waist circumference can identify the highest-risk phenotype of obesity far better than either measure alone (Ross et al., 2020).

Obesity is the second leading cause of preventable death and has been identified as a risk factor for heart diseases, type 2 diabetes, certain types of cancers, and metabolic syndromes (Qasim et al., 2018). Overweight and obesity adversely affect cardiovascular (CV) function and serve as an independent risk factor for both systolic and diastolic heart dysfunction, resulting in heart failure (HF) (Wang and Ren, 2018). Obese women are at higher risk of CV disease (CVD), as increased aldosterone and mineralocorticoid receptor activation, aberrant estrogenic signaling, and elevated levels of androgens are among some of the proposed mechanisms explaining the heightened CVD risk. Except for the traditional CV risk factors, excess weight gain during pregnancy, preeclampsia, gestational diabetes, and menopause are central to designing personalized interventions aimed to curb the epidemic of CVD (Manrique-Acevedo et al., 2020). Maternal obesity (MO) during pregnancy exhibits intergenerational effects by programming offspring to CVD. The animal experiment indicates that MO impairs fetal cardiomyocyte contractility through altered intracellular Ca^{2+} handling, overloading fetal cardiomyocyte intracellular Ca^{2+}, and aberrant myofilament protein composition (Wang Q. et al., 2019).

In obesity-related cardiomyopathy (ORCM), obesity affects the cardiac function and remodeling in the aspects of myocardial fibrosis, hemodynamic load, and impaired ventricular contractility, which eventually results in HF (Alpert et al., 2014; Carbone et al., 2017). Leptin exerts profound functions in the regulation of food intake, energy expenditure, glucose metabolism, reproduction, and immune response. Therapeutic applications of leptin in the management of obesity and metabolic syndrome are also discussed (Zhang and Ren, 2015). Autophagy pathway may play a pivotal role in the development of cardiac anomalies induced by obesity (Xu and Ren, 2013; Zhang and Ren, 2016).

In vivo study revealed high-fat intake downregulated leptin receptor and PPARγ, insulin signaling, phosphorylation of AMPK, ACC, upregulated GATA-4, ANP, NFATc3, PPARα, m-TOR/p70s6k signaling in obesity cardiomyopathy, while knocking out ET-1 receptor A (ET_A) attenuated the exception of AMPK/ACC. *In vitro* study indicated high-fat diet-induced hypertrophic and autophagic responses can be abolished by the ETA receptor antagonist (Ceylan et al., 2018). However, direct and indirect pathophysiologic factors related to obesity interplay in ORCM, the underling mechanism of ORCM had not been full studied. Meanwhile, current pharmacological treatments have limited curative effects on the clinical outcomes of ORCM. It is essential to broaden our understanding for the precise mechanisms behind these therapeutic modalities in the management of cardiometabolic diseases (Ren and Zhang, 2018). In this regard, it is urgent to explore the molecular mechanisms underlying ORCM progression and to develop novel therapeutic strategies to prevent the progression of ORCM.

Recently, the system biology analysis of microarrays has become an efficient tool for deciphering possible meaningful genes and pathophysiological pathways of various diseases. Sonne et al. (2017) performed microarray analysis to examine the gene expression profiles in adipocytes from diet-induced obese mice and obese ob/ob mice, and identified nine genes in epididymal adipocytes that are possibly involved in immune type1/type2 balance. Rendo-Urteaga et al. (2015) analyzed 28,869 genes using microarray analysis in peripheral blood mononuclear cells (PBMCs) of obese boys and suggested that changes in the gene expression profile of PBMCs in obese boys may help to understand the weight-loss response. Keustermans et al. (2017) used an Illumina microarray platform to analyze gene expression profiles in sorted monocytes from obese and lean children and revealed that monocyte gene expression in childhood obesity might be correlated with obesity and complexity of atherosclerosis in adults. In terms of cardiomyopathy, Zhao et al. (2018) analyzed the gene expression profiles (GSE3585 and GSE42955) of patients with cardiomyopathy and healthy controls and revealed that 89 differentially expressed genes (DEGs) might be associated with cardiomyopathy. In addition, Li et al. (2018) used four data profiles (GSE5406, GSE26887, GSE42955, and GSE57338) for microarray analysis and revealed a common differential gene expression signature in ischemic cardiomyopathy. However, the systematic and thorough microarray analysis for ORCM is still lacking.

In this study, we constructed a co-expression correlation network using the expression data from GSE18897 (whole blood expression profiling of obese diet-sensitive, obese diet-resistant, and lean human subjects) and identified the DEGs from murine datasets (GSE47022, regular weight C57BL/6, and diet-induced obese C57BL/6 mice) using linear models for microarray (LIMMA) data. Selected co-expression modules and DEGs were further subjected to enrichment analysis of Gene

Ontology (GO) and Kyoto Encyclopedia of Genes and Genome (KEGG) pathway. Furthermore, the hub genes derived from bioinformatics analysis were validated in the clinical samples from ORCM patients and lean controls. The present study provides preliminary insights into the molecular mechanisms underlying the progression of ORCM.

MATERIALS AND METHODS

Data Collection and Processing

The dataset (GSE18897) including 80-whole-genome expression profiles of the whole blood of obese diet-sensitive, obese diet-resistant, and lean human subjects; and the dataset (GSE47022) including lean individuals and murine data, including the cardiac samples of parallel regular weight C57BL/6, and diet-induced obese C57BL/6 mice, were downloaded from the GEO database. The GSE18897 series were performed on the GPL570 [HG U133_Plus_2] Affymetrix Human Genome U133 Plus 2.0 Array platform (Affymetrix, Santa Clara, CA, United States); the GSE47022 series were performed on GPL8321 [Mouse430A_2] Affymetrix Mouse Genome 430A 2.0 Array (Affymetrix). The raw data were extracted from the CEL files using the oligo package in the Bioconductor[1] and subsequently processed using the robust multiarray average algorithm (Carvalho and Irizarry, 2010). The human and mouse genes were matched by Gene database[2]. The gene symbols of probes were annotated using the annotation profiles provided by Affymetrix. The DEGs were detected using the R package LIMMA (Ritchie et al., 2015). The cut-off criteria were set as log2-fold change (log2 FC) ≥ 0.5 and $P < 0.05$.

Construction of Co-expression Network

Global gene expression profiles and co-expressed genes were identified using weighted gene co-expression network analysis (WGCNA; v1.49) package downloaded from Bioconductor. The possibility of two transcripts to construct a weighted network was determined using the soft-threshold method of the Pearson correlation analysis. Average linkage hierarchical clustering was performed to group transcripts based on the topological overlap dissimilarities in the network connection strengths. The restricted minimum gene number was set to 30 for each module, and a threshold of 0.25 was used to merge the similar modules.

Enrichment Analysis Using GO and KEGG Pathway Analysis

Functional enrichment analysis of the selected genes was performed using the cluster Profiler package (Ritchie et al., 2015). $P < 0.05$ was considered statistically significant, and the identified significant analyses were sorted by gene counts.

Protein–Protein Interaction (PPI) Network Construction

The protein–protein interaction (PPI) network of the selected genes was constructed using the search tool for the retrieval of interacting genes (STRING) database, and the threshold of medium confidence ≥ 0.4 was applied in the analysis. The constructed PPI network was visualized using Cytoscape software (v3.6.1[3]).

Blood Sample Collection

A total of six ORCM patients were recruited between July 2018 and June 2019 in the Sun Yat-sen Memorial Hospital of Sun Yat-sen University. The diagnosis of ORCM was based on previous reports (Lavie et al., 2013). The inclusion criteria for ORCM patients were: (1) age > 18 years old; (2) patients with BMI $\geq$ 28 kg/m^2 (Chinese classification of obesity) and class II cardiac function according to the NYHA functional classification; and (3) color Doppler ultrasound examination indicating myocardial injury, including diastolic dysfunction, myocardial hypertrophy, or systolic dysfunction (EF < 60%). Healthy volunteers (six) were recruited during routine physical examination. The inclusion criteria for healthy subjects were: (1) age > 18 years; (2) 18.5 < BMI < 23.9; (3) no hyperlipidemia; and (4) color Doppler ultrasound examination indicating no myocardial injury. Exclusion criteria were: (1) pregnancy or breastfeeding; (2) patients with tumors or infection; and (3) patients having heart valve disease. The peripheral blood was collected from both ORCM patients and healthy controls. The serum was extracted from the peripheral blood and was stored at −80°C until further analysis. All the procedures were approved by the Ethics Committee of Sun Yat-sen Memorial Hospital of Sun Yat-sen University (Ethics approval#:SYSEC-KY-KS-2019-019), and each patient submitted written informed consent in accordance with the Declaration of Helsinki. Clinical characteristics of all patients enrolled are summarized in **Tables 1**, **2**.

Quantitative Real-Time PCR Analysis (qRT-PCR)

The RNA from the serum was extracted using TRIzol reagent (Invitrogen, Carlsbad, CA, United States) according to the manufacturer's instructions. The mRNA was reverse transcribed into cDNA using the First Strand Synthesis kit (Thermo Fisher Scientific, Waltham, MA, United States). Real-time PCR was performed on an ABI7900 Real-time PCR system (Applied Biosystems, Foster City, CA, United States) using the SYBR Green Master Mix kit (Takara, Dalian, China). GAPDH was used as the control for mRNA expression. The relevant gene expression levels were calculated using the comparative Ct method. The primers for the relevant genes are summarized in **Table 3**.

Enzyme-Linked Immunosorbent Assay (ELISA) Analysis

The protein levels of elongation of very-long-chain fatty acids protein 4 (ELOVL4), matrix metalloproteinase-8 (MMP8), and interleukin-33 (IL-33) were determined by respective enzyme-linked immunosorbent assay (ELISA) kits (Abcam, Cambridge, MA, United States) according to the manufacturer's instructions.

[1]http://bioconductor.org/biocLite.R

[2]https://www.ncbi.nlm.nih.gov/gene/

[3]http://www.cytoscape.org/

TABLE 1 | Clinical characteristics of patients enrolled.

Characteristics	ORCM (*N* = 6)	Control (*n* = 6)
Age (years)	51.8 ± 14.8	51.5 ± 10.5
Men (*N*,%)	5 (83.3%)	3 (50%)
Women (*N*,%)	1 (16.7%)	3 (50%)
CAD (*N*,%)	1 (16.6%)	0 (0%)
Hypertension (*N*,%)	2 (33.3%)	0 (0%)
Diabetes (*N*,%)	0 (0%)	0 (0%)
BMI (kg/m^2)	30.9 ± 3.5	24.2 ± 3.5
Echocardiography parameters		
LA (mm)	40 ± 4.4	35 ± 4.9
LVDd (mm)	58.1 ± 5.4	49.3 ± 5.0
IVSTd (mm)	10.5 ± 1.5	8.8 ± 1.1
EF (%)	54.8 ± 16.7	70.3 ± 2.8
Diastolic dysfunction (*N*,%)	2 (33.3%)	0 (0%)
NYHA grading		
Grade I (*N*,%)	2 (33.3%)	6 (100%)
Grade II (*N*,%)	4 (66.7%)	0 (0%)
Grade III (*N*,%)	(0%)	0 (0%)
Grade IV (*N*,%)	(0%)	0 (0%)

Data are present as mean ± SD; CAD, coronary artery disease; BMI, body mass index; EF, ejection fraction; LA, left atrial; LVDd, left ventricular end diastolic diameter; IVSTd, intel-ventricular scptum end-diastolic thickness; EF, ejection fraction.

TABLE 3 | Primer sequences for qRT-PCR.

Genes	Forward (5′–3′)	Reverse (5′–3′)
KCTD12	GCTCGGGCTACATCACCATC	GGTCCCGGCTTTCGTTCAG
CD45	ACCACAAGTTTACTAACGCAAGT	TTTGAGGGGGATTCCAGGTAAT
ZNF383	ATGGCTGAGGGATCAGTGATG	GAAACCAGATTGCCGTAGTTCT
C7orf33	CGGTCCAGGTCAATTTAACTTGT	TTTGGTGGGAGCTGATACAGG
MMP8	TGCTCTTACTCCATGTGCAGA	TCCAGGTAGTCCTGAACAGTTT
CYPB	AAGTCACCGTCAAGGTGTATTTT	TGCTGTTTTTGTAGCCAAATCCT
ELOVL4	GAGCCGGGTAGTGTCCTAAAC	CACACGCTTATCTGCGATGG
SNCA	AAGAGGGTGTTCTCTATGTAGGC	GCTCCTCCAACATTTGTCACTT
IL33	GTGACGGTGTTGATGGTAAGAT	AGCTCCACAGAGTGTTCCTTG
GAPDH	AGGTGAAGGTCGGAGTCAAC	CGCTCCTGGAAGATGGTGAT

Statistical Analysis

qRT-PCR and ELISA data were analyzed using GraphPad Prism 5 (GraphPad Software, La Jolla, CA, United States). The data were presented as mean ± standard deviation. Significant differences between groups were analyzed using unpaired *t*-test. $^*P < 0.05$ was considered statistically significant.

RESULTS

The Workflow of Study Strategies

Figure 1 illustrates the workflow of the experimental design and data processing. One microarray-based gene expression dataset (GSE18897) included 80-whole-genome expression profiling of the whole blood from obese diet-sensitive, obese diet-resistant, and lean human subjects. The human datasets were used for constructing gene networks with WGCNA, and the expression models were subjected to GO term enrichment and KEGG pathway enrichment analysis. The top highest degree genes were chosen to overlap with the murine heart DEGs. The murine GSE47022 datasets include the cardiac samples of parallel regular weight C57BL/6 and diet induced obese C57BL/6 mice. The GSE47022 datasets were processed using LIMMA to reveal the DEGs in the heart samples. In addition, the overlap hub genes were verified in the clinical samples.

Construction and Analysis of Gene Co-expression Network With DEGs in Obese Individuals

The co-expression network of 5121 genes was analyzed using WGCNA to explore the gene expression network in obesity. First, as shown in **Figure 2A**, sample clustering was undertaken to detect outliers. The sample clusters were summarized based on the flash-cluster method by combining a heuristic cut-off, and the top 25% most variably expressed genes were selected for analysis (**Figure 2A**). The power value is a critical parameter and

TABLE 2 | Anthropometric information of patient enrolled.

Group	Sex	CAD	Hypertension	DM	Hight (cm)	Weight (kg)	BMI (kg/m^2)	LA (mm)	LVDd (mm)	IVSTd (mm)	EF (%)	DS
ORCM group	Male	Yes	Yes	No	168	86	30.47	43	55	9	74	No
	Male	No	Yes	No	175	88	28.73	39	55	12	73	Yes
	Male	No	No	Yes	172	89.5	30.25	38	68	10	30	No
	Female	No	Yes	No	144	60	28.94	46	63	13	38	No
	Male	Yes	Yes	No	160	99	38.67	42	54	9	51	No
	Male	No	Yes	No	175	88	28.73	32	54	10	63	Yes
Control group	Female	No	Yes	No	153	60	25.63	38	48	9	73	No
	Female	No	No	No	150	37	16.44	25	39	7	69	No
	Male	No	No	No	158	64	25.64	35	52	8	70	No
	Male	No	No	No	178	79	24.93	35	54	9	67	No
	Male	No	Yes	No	167	72.5	26.00	36	50	10	75	No
	Female	No	No	No	151	61	26.75	41	53	10	68	No

CAD, coronary artery disease; DM, diabetes mellitus; BMI, body mass index; LA, left atrial; LVDd, left ventricular end diastolic diameter; IVSTd, intel-ventricular scptum end-diastolic thickness; EF, ejection fraction; DS, diastolic dysfunction.

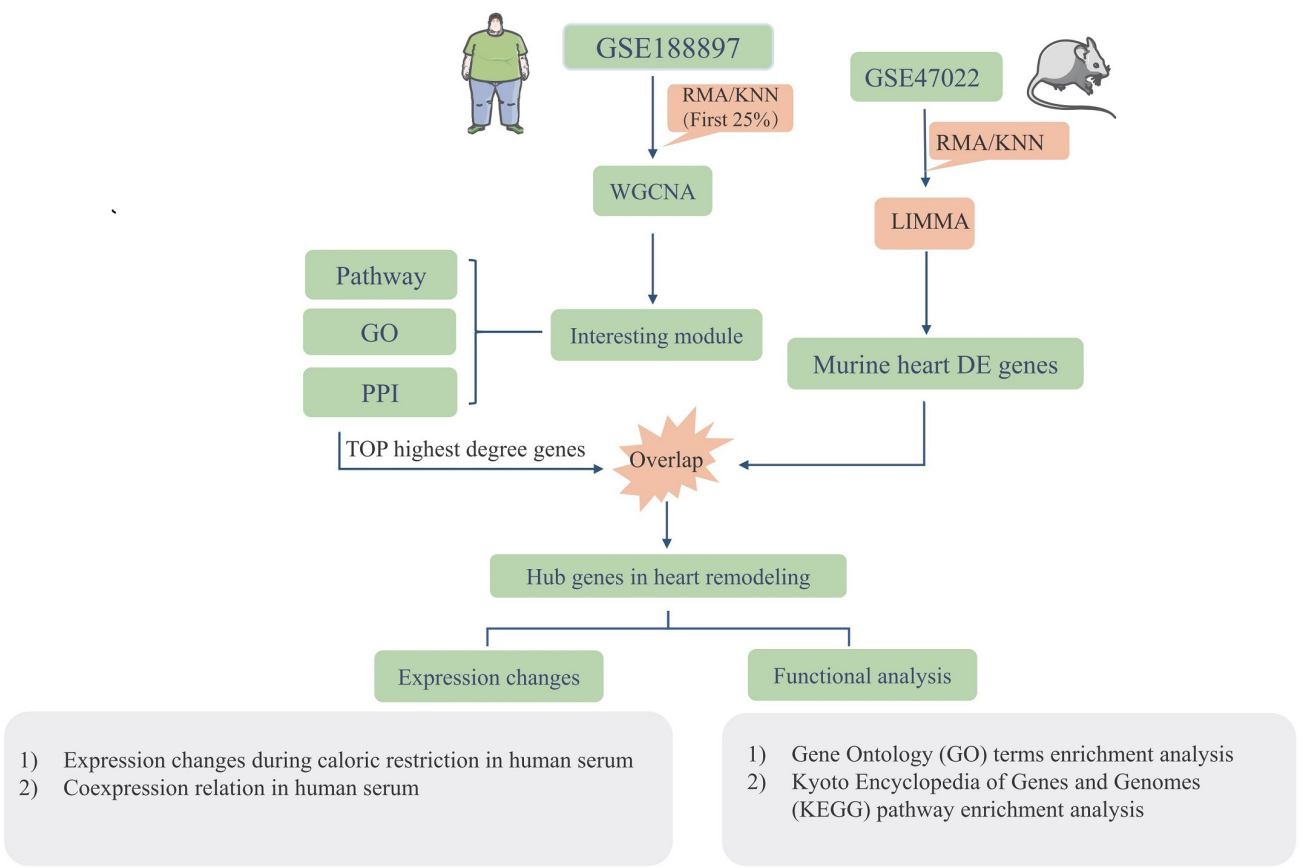

FIGURE 1 | Workflow of the study strategies using datasets including GSE18897 and GSE47022.

affects the average connectivity degree and independence of the co-expression modules. In this regard, we screened the network topology using different soft thresholding powers, and $\beta = 16$ was chosen for further analysis (**Figure 2B**). Provided that the appropriate soft power parameter was chosen, the eigengenes were used as representative profiles to quantify module similarity by the eigengene correlation (**Figure 2C**).

Figure 3A demonstrates the construction of co-expression modules with no merge and merge cut height at 0.25, and the WGCNA analysis, which produced a hierarchical clustering tree (dendrogram) of 5121 genes. A total of eight co-expression modules were generated based on the analysis (**Figure 3B**). The smallest co-expression module contained 50 genes, while the largest co-expression module contained 3000 genes, and on average, each co-expression module contained 1250 genes. We further determined if any co-expression module was associated with the caloric restriction treatment and investigated the relevance between each module and traits of the caloric restriction treatment. Among eight modules, the co-expression module significance of the yellow co-expression module was higher than that of any other, suggesting it had a greater correlation with the caloric restriction treatment (**Figure 3B**). The yellow co-expression module showed a positive correlation with the caloric restriction treatment ($r = 0.74$, $p = 4e\text{-}7$) and was chosen for further investigation. GO function and KEGG pathway enrichment analyses were performed using DAVID functional annotation to determine the function of these genes in the yellow module. For GO biological processes, genes in the co-expression module were significantly enriched in oxygen transport (**Figure 3D**); for the KEGG analysis, the genes were mainly enriched in the metabolism of porphyrins (**Figure 3D**) and the datas can be found in **Supplementary Tables S1, S2** in **Supplementary Material**.

The yellow co-expression module genes were used on the STRING database to clarify high confidence hub genes. The genes were ranked by the PPI nodes, and the top 50 genes were selected (**Figure 3E**). Among these genes, FECH, SNCA, GLRX5, BPGM, SENSN, BNIP3L, and RAB2B showed the highest connectivity (**Figures 3C,E**).

Overlap Analysis of Hub Genes From Human and Mouse DEGs

The genes in the yellow co-expression module and DEGs from the murine datasets were subjected to KEGG pathway enrichment analysis and the datas can be found in **Supplementary Table S3** in **Supplementary Material**. As shown in **Figure 4A**, for the murine datasets, metabolic, AMPK,

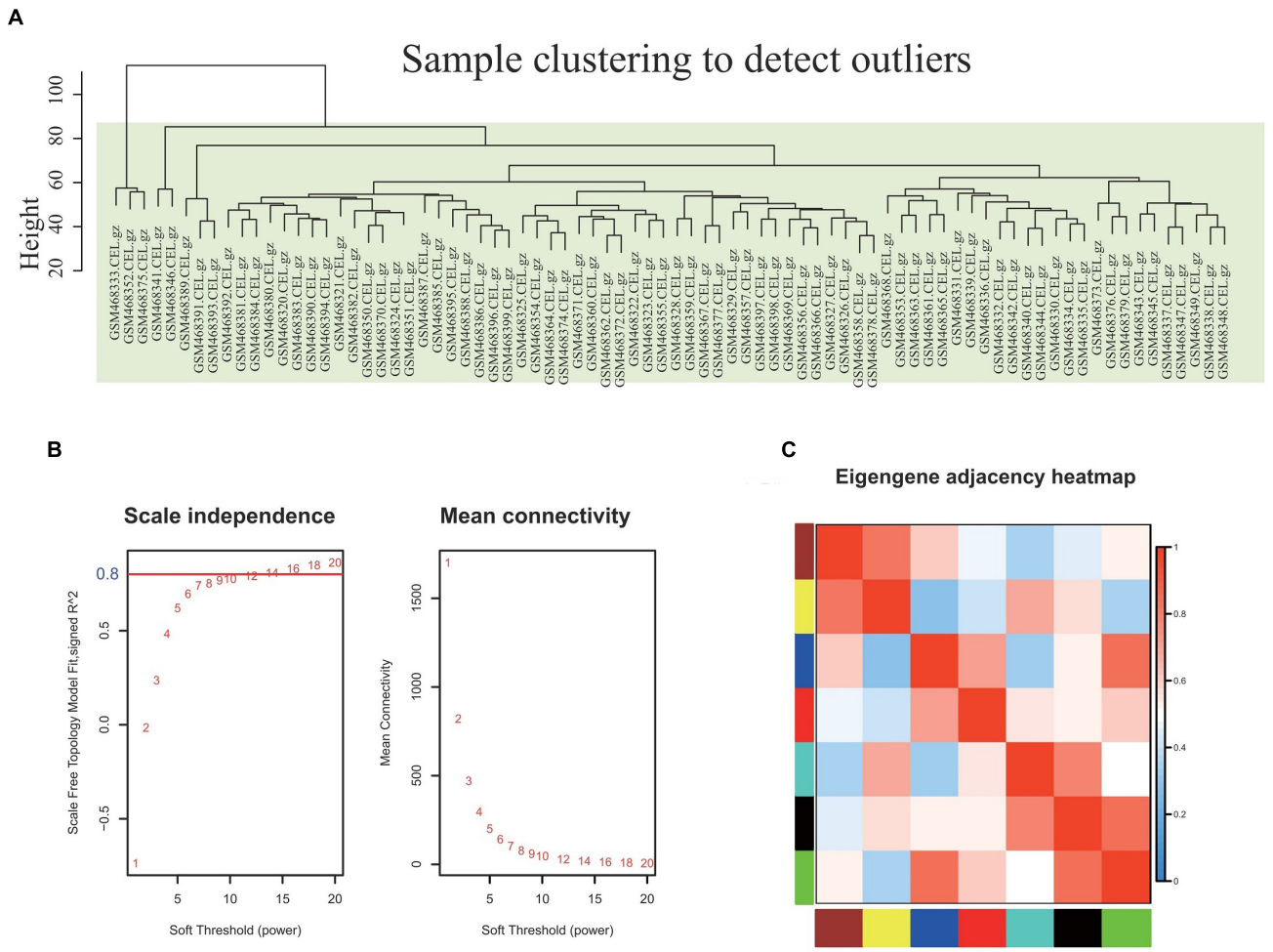

FIGURE 2 | Selection of the proper soft-threshold power β for WGCNA. **(A)** Outliers were determined using sample clustering method, and the analysis was performed according to the expression data of DEGs from whole blood of well-matched obesity and lean individuals. **(B)** The scale-free fit index of network topology was determined by soft-thresholding power analysis. **(C)** Heatmap plot of the adjacencies in the hub gene network. The trait weight was included. Each column and row correspond to one co-expression module hub gene (labeled by color) or weight. In the heatmap, red represents high adjacency (positive correlation) and blue represents low adjacency (negative correlation). Red squares along the diagonal are the meta-modules.

fatty acid, PPAR signaling, insulin signaling, biosynthesis of antibiotics, biosynthesis of unsaturated fatty acids, glucagon signaling, insulin resistance pathways were enriched; for the yellow co-expression module genes, Alzheimer's disease, MAPK signaling, oxidative phosphorylation, ABC transporters cardiac muscle contraction signaling pathways were enriched. The overlap showed that six common hub genes (ELOVL4, CYPB, SNCA, ZFN383, MMP8, and IL-33) were detected (**Figure 4B**). The volcano plot results showed that the six common hub genes were all upregulated (**Figure 4C**).

Validation of Hub Genes in the Human Clinical Samples

To validate the results from bioinformatics analysis, we examined the gene expression levels of these hub genes in human peripheral blood from patients with ORCM and healthy controls. As shown in **Figure 5A**, the expression levels of ELOVL4, MMP8, and IL-33 were significantly upregulated in the ORCM group compared to normal controls, while no significant difference was detected in the other hub genes. Furthermore, the increased protein levels of ELOVL4, MMP8, and IL-33 in the peripheral blood from patients with ORCM were confirmed using ELISA (**Figure 5B**).

Correlation Analysis of ELOVL4 and IL33 Gene Expression Levels Using GEO Database

The KEGG pathway analysis revealed that the hub genes derived from the overlap analysis were involved in the fatty acid metabolism and IL33/sST2 signaling pathways (**Figure 6A**). The correlation analysis showed that ELOVL4 expression levels were positively correlated with IL-33 expression levels (**Figure 6B**). More importantly, analysis of ELOLV4 and IL-33 using GEO

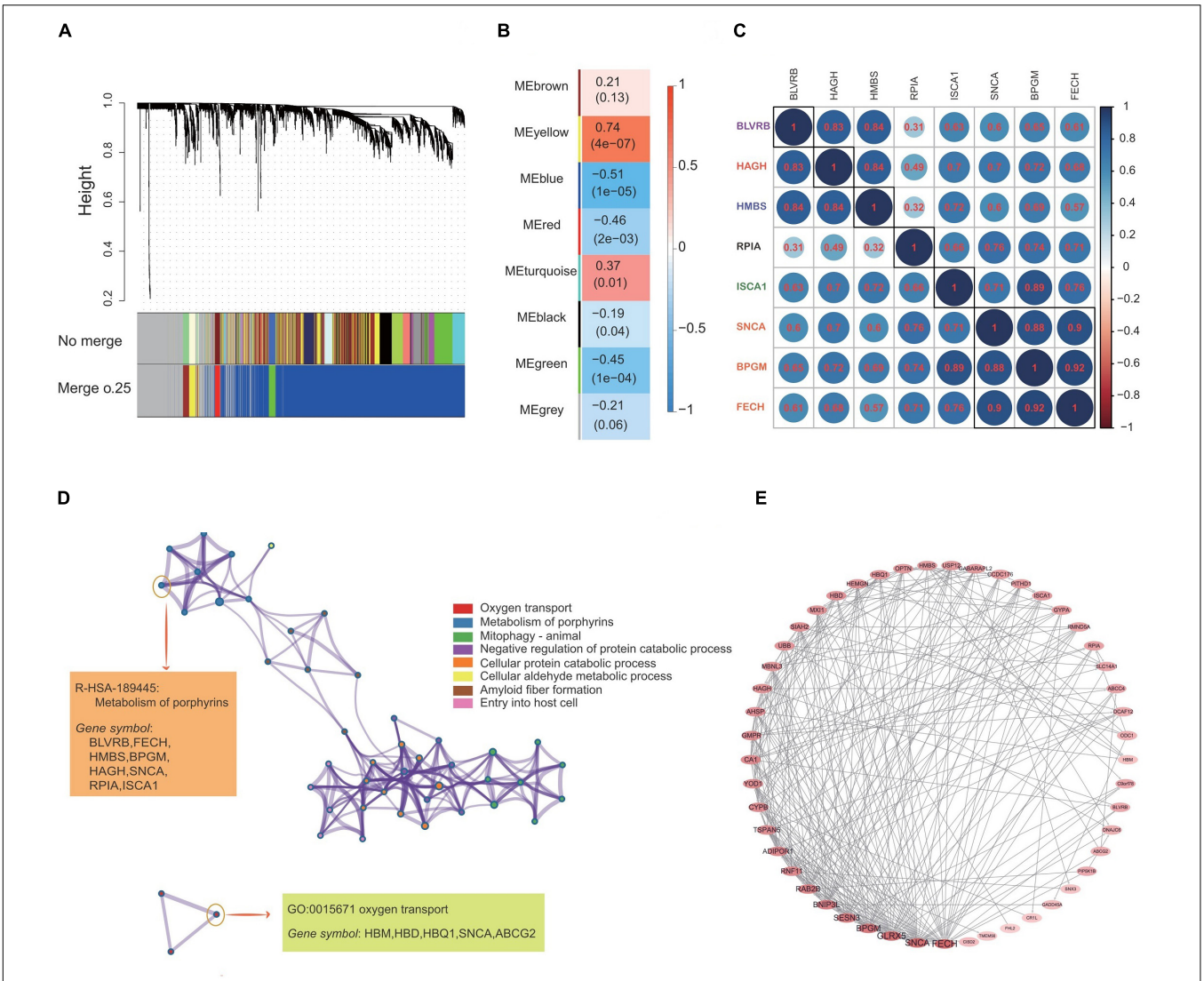

FIGURE 3 | Construction of the co-expression network and identification of the most related co-expression modules. **(A)** Clustering of genes together with assigned module colors. The dissimilarity was based on the topological overlap. The *y*-axis is the distance determined by the extent of the topological overlap. **(B)** Heatmap with each cell containing the *p*-value correlation from linear mixed effects model. Row corresponds to different co-expression modules; column corresponds to traits of caloric restriction treatment. **(C)** The gene correlation heatmap of the genes in yellow co-expression module. Each color circle represents the distance between different genes. **(D)** GO enrichment and KEGG pathway analysis of 633 genes in the yellow co-expression module. **(E)** PPI network construction of the top 50 genes in the yellow co-expression module.

database showed that ELOVL4 and IL33 expression were both upregulated in the obese group when compared to the lean group. Caloric restriction for 3 and 6 months significantly attenuated the increased expression levels of ELOVL4 in the obesity group, while a significant reduction of IL-33 expression levels was observed in the obese patients with a 6-month period of caloric restriction treatment (**Figure 6C**).

DISCUSSION

The molecular mechanisms underlying ORCM progression involve multiple signaling pathways and the pharmacological treatment for ORCM is still limited (Khan and Movahed, 2013; Alpert et al., 2014; Tiwari and Ndisang, 2014; Bhatheja et al., 2016). Thus, it is necessary to explore new targets and develop novel therapies. Microarray analysis for gene expression profiles using different bioinformatics tools has been an effective strategy for identifying novel targets for various diseases. In the present study, we performed WGCNA on the series GSE188897 combined with routine bioinformatics analysis and revealed six potential target genes that might be involved in the development of obesity. In addition, the DEGs from GSE47022 were analyzed. The overlap analysis of the hub genes from the WGCNA analysis of GSE188897 and DEGs from GSE47022 revealed six potential genes that may be associated with ORCM. qRT-PCR and ELISA

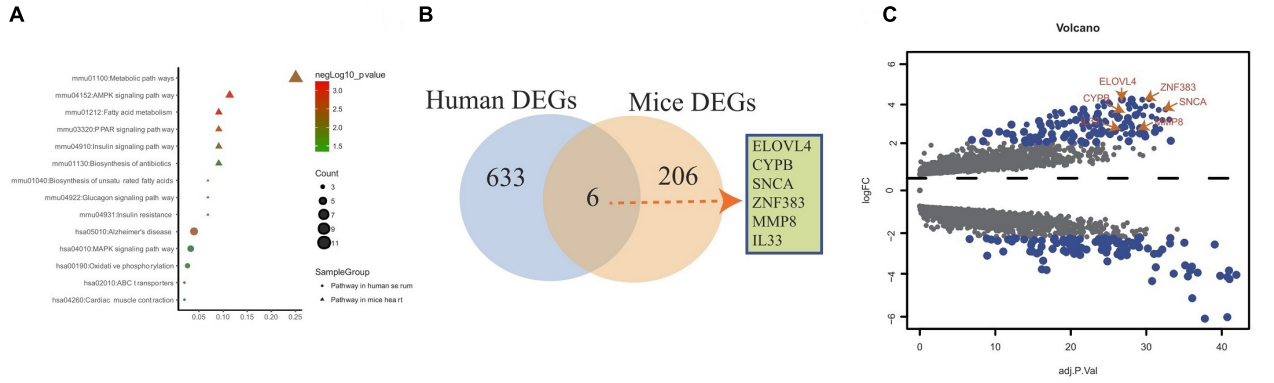

FIGURE 4 | Overlap analysis of hub genes from human and mouse DEGs. **(A)** KEGG pathway analysis of genes from yellow co-expression module and DEGs from mice. **(B)** Venn diagram shows common hub genes between yellow co-expression module and DEGs from mice. **(C)** Volcano plot of yellow co-expression module and DEGs from murine datasets.

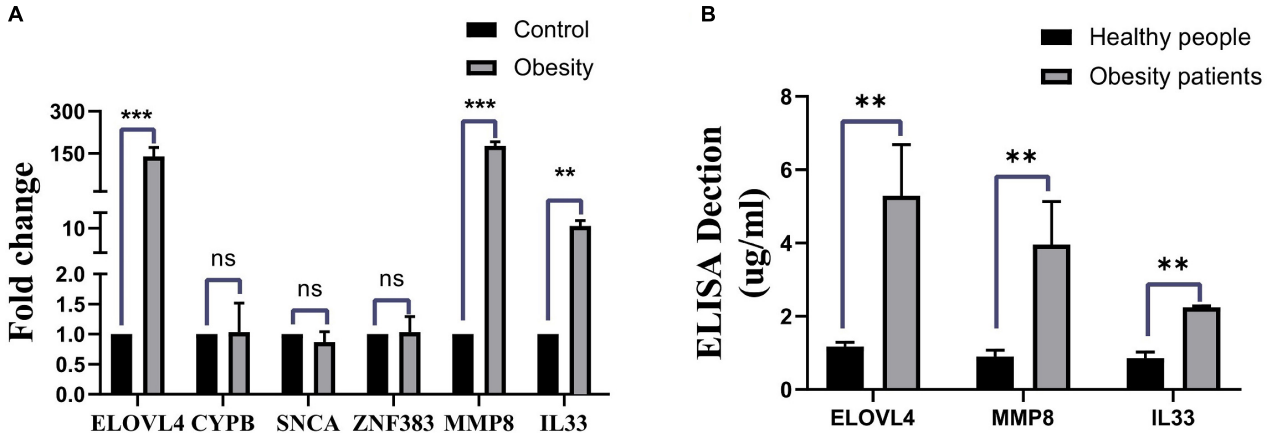

FIGURE 5 | Validation of hub genes in the clinical human samples. **(A)** Gene expression levels of the hub genes (ELOVL4, CYPB, SNCA, ZFN383, MMP8, and IL33) in the human peripheral blood from ORCM patients and healthy controls were determined by qRT-PCR. **(B)** Protein levels of ELOVL4, MMP8, and IL33 in the human peripheral blood from ORCM patients and healthy controls were determined by ELISA assay. $N = 6$; ns = non-significant; $^{**}P < 0.01$.

further validated the upregulation of ELOVL4, MMP8, and IL-33 in the patients with ORCM when compared to healthy lean controls. Collectively, in the present study, we used different bioinformatics analytical strategies to explore the potential hub genes related to ORCM development. Further validation studies indicated that ELOVL4, MMP8, and IL-33 might participate in the progression of ORCM.

WGCNA is a newly developed method to identify highly correlated genes in microarrays (Langfelder and Horvath, 2008; Pei et al., 2017). In contrast with the traditional gene-gene correlation co-expression matrices by setting a hard threshold, WGCNA can identify correlated genes using a soft-threshold algorithm and determine the relationship between co-expression modules and phenotypes (Kakati et al., 2019). Thus, WGCNA has been widely used in the study of various diseases, including CVDs (Chen et al., 2016; Wang Y. et al., 2019). Kang et al. (2020) performed the WGCNA in GSE79962 and revealed the potential critical roles of NDUFB5, TIMMDC1, and VDAC3 in the septic cardiomyopathy progression. Using microarray data of coronary artery diseases (CADs; GSE23561), studies detected a co-expression module associated with hypertrophic cardiomyopathy pathway in CAD and found that G6PD and S100A7 were the potential targets (Liu et al., 2016). The GSE18897 datasets were originally generated by Ghosh et al. (2010), and further pathway analysis by gene-set enrichment showed increased transcript levels for genes classified in the oxidative phosphorylation, apoptosis, and ribosome pathways in the obese cohort. In the present study, WGCNA was performed in GSE18897 datasets, and yellow co-expression module was chosen for further GO function and KEGG pathway enrichment analyses. GO function enrichment revealed the genes related to oxygen transport, which was consistent with previous studies showing that transcripts associated with oxygen transport were elevated with the increasing BMI (Rai et al., 2014). Moreover, the genes related to oxygen transport are also upregulated in the peripheral blood from patients with pulmonary hypertension (Cheadle et al., 2012), suggesting the potential involvement of these genes in the ORCM. The KEGG pathway analysis

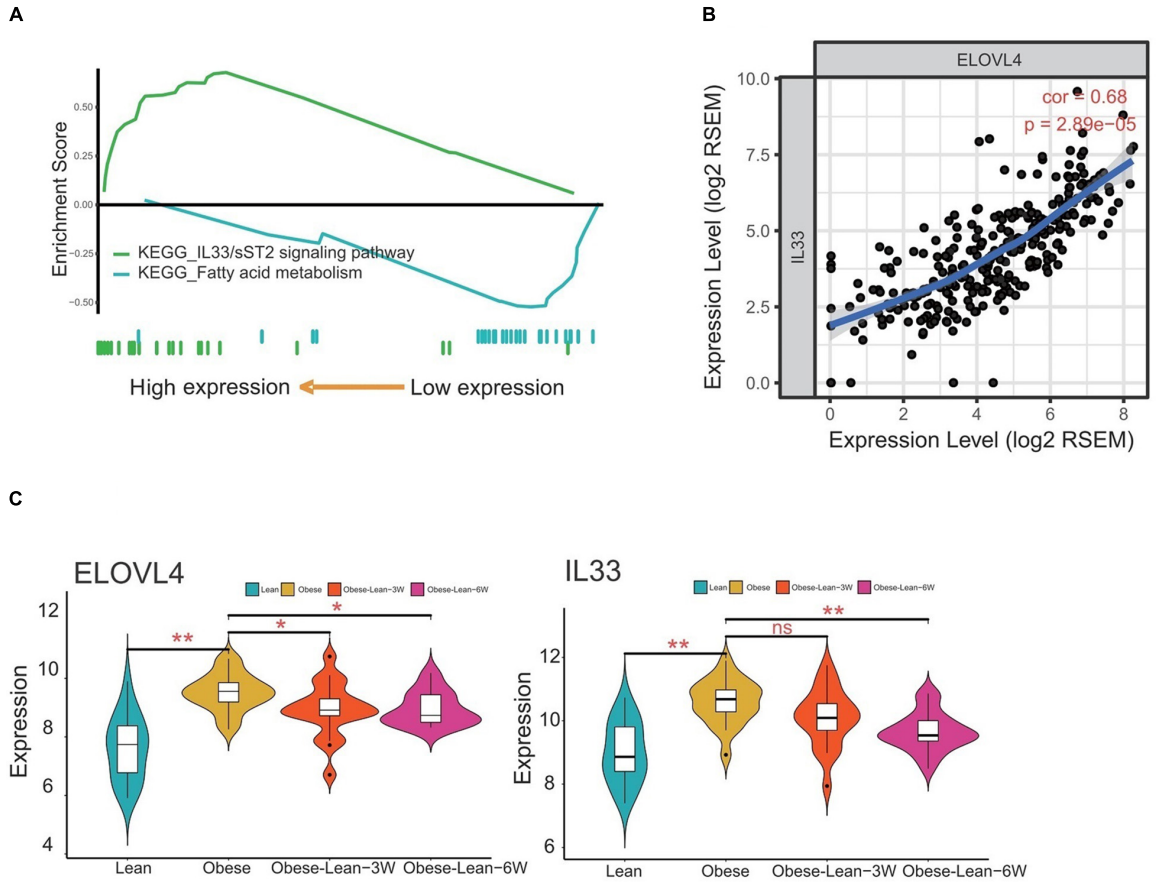

FIGURE 6 | Correlation analysis of ELOVL4 and IL33 gene expression levels. **(A)** KEGG pathway analysis of the hub genes. **(B)** The correlation between ELOVL4 and IL33 expression levels were analyzed using Pearson correlation analysis. **(C)** Analysis of ELOVL4 and IL33 expression levels in lean controls, obese patients, and obese patients received 3- or 6-month period of caloric restriction treatment.

identified enriched genes related to porphyrin metabolism. The porphyrins metabolism is associated with the heme biosynthesis, which is functionally linked to adipogenesis via mitochondrial respiratory activity (Moreno-Navarrete et al., 2017). Our analysis strategies enabled us to identify important genes related to obesity development.

Overlap analysis of hub genes from the yellow co-expression module and DEGs from the murine datasets revealed six upregulated genes. Further experimental validation results showed that ELOVL4, MMP8, and IL-33 were upregulated in the peripheral blood from patients with ORCM compared to the lean controls. The bioinformatics analysis revealed that ELOVL4 expression levels were positively correlated with IL-33 expression levels. These data suggest the potential involvement of ELOVL4 and IL-33 in the pathophysiology of ORCM. ELOVL4 is an elongase that participates in the biosynthesis of very-long-chain (VLC, $\geq$ C28) saturated fatty acid (VLC-SFA) and polyunsaturated fatty acid (VLC-PUFA) in different tissues (Hopiavuori et al., 2019), and plays a key role in the retinal function (Harkewicz et al., 2012). The increased deposition of long-chain fatty acids in adipocytes is one of the main characteristics of obesity (Walewski et al., 2010). In addition, ELOVL4 is involved in the biosynthesis of VLC fatty acids in the cardiomyocytes (Agbaga et al., 2008). Ge et al. (2012) demonstrated that accumulation of the cardiomyocyte triglyceride and reduction in the ventricular function in obese mice reflected enhanced VLC fatty acid uptake and *de novo* fatty acid synthesis. The involvement of ELOV4 in ORCM might be due to its regulatory effects on the VLC fatty acid synthesis. IL-33 belongs to the IL-1 family of cytokines and acts as an ST2 receptor ligand, and the IL-33/ST2 signaling plays an important role in regulating the progression of cardiomyopathy (Demyanets et al., 2013). Upregulation of IL-33 has been detected in the obese adipose tissues (de Oliveira et al., 2019). Nevertheless, the interaction between ELOVL4 and IL-33 has not been determined, which requires further investigation.

LIMITATIONS

There are several limitations to this study. First, the clinical sample size for validation is relatively small, and future studies are required to increase the sample size and recruit human subjects from multiple clinical centers to confirm the findings. Second,

the microarray data were retrieved from diet-induced obese mice, and whether the obese mice had cardiomyopathy is not known, which may lessen the significance of our findings. In terms of the database selection, only one database was chosen for the data analysis, which may have the selection bias, and future studies should consider including more datasets to validate our current findings. Third, whether the caloric restriction treatment in patients with ORCM could restore the expression levels of ELOVL4 and IL-33 requires further determination. Finally, the present study lacks the mechanistic studies regarding the role of ELOVL4 and IL-33 in the ORCM pathophysiology, which may be considered in the future investigation.

CONCLUSION

Using WGCNA in combination with integrated bioinformatics analysis, the hub genes of ELVOL4 and IL-33 might serve as potential biomarkers for diagnosis and/or therapeutic targets for ORCM. The detailed roles of ELVOL4 and IL-33 in the pathophysiology of ORCM still require further investigation.

DATA AVAILABILITY STATEMENT

The datasets generated for this study can be found in the Gene Expression Omnibus (accession: GSE18897, GSE47022).

ETHICS STATEMENT

The studies involving human participants were reviewed and approved by the Ethics Committee of Sun Yat-sen Memorial Hospital of Sun Yat-sen university. The patients/participants provided their written informed consent to participate in this study. Written informed consent was obtained from the individual(s) for the publication of any potentially identifiable images or data included in this article.

AUTHOR CONTRIBUTIONS

JZ and SL contributed to study conception and design. JT and YW performed the experiments and analyzed the data. LL interpreted the results. JT prepared figures and drafted the manuscript. All authors edited and revised the manuscript.

FUNDING

This work was supported by grants from Youth Program of National Natural Science Foundation of China (No. 81702618).

ACKNOWLEDGMENTS

We would like to thank our colleagues, especially Chang Liu, for his help in collecting the blood samples.

SUPPLEMENTARY MATERIAL

The Supplementary Material for this article can be found online at: https://www.frontiersin.org/articles/10.3389/fphys.2020.00542/full#supplementary-material

REFERENCES

Agbaga, M. P., Brush, R. S., Mandal, M. N., Henry, K., Elliott, M. H., and Anderson, R. E. (2008). Role of Stargardt-3 macular dystrophy protein (ELOVL4) in the biosynthesis of very long chain fatty acids. *Proc. Natl. Acad. Sci. U.S.A.* 105, 12843–12848. doi: 10.1073/pnas.0802607105

Alpert, M. A., Lavie, C. J., Agrawal, H., Aggarwal, K. B., and Kumar, S. A. (2014). Obesity and heart failure: epidemiology, pathophysiology, clinical manifestations, and management. *Transl. Res.* 164, 345–356. doi: 10.1016/j.trsl.2014.04.010

Bhatheja, S., Panchal, H. B., Ventura, H., and Paul, T. K. (2016). Obesity cardiomyopathy: pathophysiologic factors and nosologic reevaluation. *Am. J. Med. Sci.* 352, 219–222. doi: 10.1016/j.amjms.2016.05.014

Carbone, S., Lavie, C. J., and Arena, R. (2017). Obesity and heart failure: focus on the obesity paradox. *Mayo. Clin. Proc.* 92, 266–279. doi: 10.1016/j.mayocp.2016.11.001

Carvalho, B. S., and Irizarry, R. A. (2010). A framework for oligonucleotide microarray preprocessing. *Bioinformatics* 26, 2363–2367. doi: 10.1093/bioinformatics/btq431

Ceylan, A. F., Wang, S., Kandadi, M. R., Chen, J., Hua, Y., Pei, Z., et al. (2018). Cardiomyocyte-specific knockout of endothelin receptor a attenuates obesity cardiomyopathy. *Biochim. Biophys. Acta Mol. Basis Dis.* 1864, 3339–3352. doi: 10.1016/j.bbadis.2018.07.020

Cheadle, C., Berger, A. E., Mathai, S. C., Grigoryev, D. N., Watkins, T. N., Sugawara, Y., et al. (2012). Erythroid-specific transcriptional changes in PBMCs from pulmonary hypertension patients. *PLoS One* 7:e34951. doi: 10.1371/journal.pone.0034951

Chen, J., Yu, L., Zhang, S., and Chen, X. (2016). Network analysis-based approach for exploring the potential diagnostic biomarkers of acute myocardial infarction. *Front. Physiol.* 7:615. doi: 10.3389/fphys.2016.00615

Collaboration, N. C. D. R. F. (2016). Trends in adult body-mass index in 200 countries from 1975 to 2014: a pooled analysis of 1698 population-based measurement studies with 19.2 million participants. *Lancet* 387, 1377–1396. doi: 10.1016/S0140-6736(16)30054-X

Consultation, W. H. O. E. (2004). Appropriate body-mass index for Asian populations and its implications for policy and intervention strategies. *Lancet* 363, 157–163. doi: 10.1016/S0140-6736(03)15268-3

de Oliveira, M. F. A., Talvani, A., and Rocha-Vieira, E. (2019). IL-33 in obesity: where do we go from here? *Inflamm. Res.* 68, 185–194. doi: 10.1007/s00011-019-01214-2

Demyanets, S., Kaun, C., Pentz, R., Krychtiuk, K. A., Rauscher, S., Pfaffenberger, S., et al. (2013). Components of the interleukin-33/ST2 system are differentially expressed and regulated in human cardiac cells and in cells of the cardiac vasculature. *J. Mol. Cell Cardiol.* 60, 16–26. doi: 10.1016/j.yjmcc.2013.03.020

Ge, F., Hu, C., Hyodo, E., Arai, K., Zhou, S., Lobdell, H. T., et al. (2012). Cardiomyocyte triglyceride accumulation and reduced ventricular function in mice with obesity reflect increased long chain Fatty Acid uptake and de novo Fatty Acid synthesis. *J. Obes.* 2012:205648. doi: 10.1155/2012/205648

Ghosh, S., Dent, R., Harper, M. E., Gorman, S. A., Stuart, J. S., and McPherson, R. (2010). Gene expression profiling in whole blood identifies distinct biological pathways associated with obesity. *BMC Med. Genomics* 3:56. doi: 10.1186/1755-8794-3-56

Hales, C. M., Fryar, C. D., Carroll, M. D., Freedman, D. S., and Ogden, C. L. (2018). Trends in obesity and severe obesity prevalence in US youth and adults by sex

and age, 2007-2008 to 2015-2016. *JAMA* 319, 1723–1725. doi: 10.1001/jama.2018.3060

Harkewicz, R., Du, H., Tong, Z., Alkuraya, H., Bedell, M., Sun, W., et al. (2012). Essential role of ELOVL4 protein in very long chain fatty acid synthesis and retinal function. *J. Biol. Chem.* 287, 11469–11480. doi: 10.1074/jbc.M111.256073

He, Y., Pan, A., Wang, Y., Yang, Y., Xu, J., Zhang, Y., et al. (2017). Prevalence of overweight and obesity in 15.8 million men aged 15-49 years in rural China from 2010 to 2014. *Sci. Rep* 7:5012. doi: 10.1038/s41598-017-04135-4

Hopiavuori, B. R., Anderson, R. E., and Agbaga, M. P. (2019). ELOVL4: Very long-chain fatty acids serve an eclectic role in mammalian health and function. *Prog. Retin. Eye Res.* 69, 137–158. doi: 10.1016/j.preteyeres.2018.10.004

Kakati, T., Bhattacharyya, D. K., Barah, P., and Kalita, J. K. (2019). Comparison of methods for differential co-expression analysis for disease biomarker prediction. *Comput. Biol. Med.* 113:103380. doi: 10.1016/j.compbiomed.2019.103380

Kang, K., Li, J., Li, R., Xu, X., Liu, J., Qin, L., et al. (2020). Potentially critical Roles of NDUFB5, TIMMDC1, and VDAC3 in the progression of septic cardiomyopathy through integrated bioinformatics analysis. *DNA Cell Biol.* 39, 105–117. doi: 10.1089/dna.2019.4859

Keustermans, G. C., Kofink, D., Eikendal, A., de Jager, W., Meerding, J., Nuboer, R., et al. (2017). Monocyte gene expression in childhood obesity is associated with obesity and complexity of atherosclerosis in adults. *Sci. Rep.* 7:16826. doi: 10.1038/s41598-017-17195-3

Khan, M. F., and Movahed, M. R. (2013). Obesity cardiomyopathy and systolic function: obesity is not independently associated with dilated cardiomyopathy. *Heart Fail Rev.* 18, 207–217. doi: 10.1007/s10741-012-9320-4

Langfelder, P., and Horvath, S. (2008). WGCNA: an R package for weighted correlation network analysis. *BMC Bioinformatics* 9:559. doi: 10.1186/1471-2105-9-559

Lavie, C. J., Alpert, M. A., Arena, R., Mehra, M. R., Milani, R. V., and Ventura, H. O. (2013). Impact of obesity and the obesity paradox on prevalence and prognosis in heart failure. *JACC Heart Fail* 1, 93–102. doi: 10.1016/j.jchf.2013.01.006

Li, Y., Jiang, Q., Ding, Z., Liu, G., Yu, P., Jiang, G., et al. (2018). Identification of a common different gene expression signature in ischemic cardiomyopathy. *Genes (Basel)* 9:56. doi: 10.3390/genes9010056

Liu, J., Jing, L., and Tu, X. (2016). Weighted gene co-expression network analysis identifies specific modules and hub genes related to coronary artery disease. *BMC Cardiovasc. Disord.* 16:54. doi: 10.1186/s12872-016-0217-3

Manrique-Acevedo, C., Chinnakotla, B., Padilla, J., Martinez-Lemus, L. A., and Gozal, D. (2020). Obesity and cardiovascular disease in women. *Int. J. Obes. (Lond.)* 2020. doi: 10.1038/s41366-020-0548-0

Moreno-Navarrete, J. M., Rodriguez, A., Ortega, F., Becerril, S., Girones, J., Sabater-Masdeu, M., et al. (2017). Heme biosynthetic pathway is functionally linked to adipogenesis via mitochondrial respiratory activity. *Obesity (Silver Spring)* 25, 1723–1733. doi: 10.1002/oby.21956

Pei, G., Chen, L., and Zhang, W. (2017). WGCNA application to proteomic and metabolomic data analysis. *Methods Enzymol.* 585, 135–158. doi: 10.1016/bs.mie.2016.09.016

Qasim, A., Turcotte, M., de Souza, R. J., Samaan, M. C., Champredon, D., Dushoff, J., et al. (2018). On the origin of obesity: identifying the biological, environmental and cultural drivers of genetic risk among human populations. *Obes. Rev.* 19, 121–149. doi: 10.1111/obr.12625

Rai, M. F., Patra, D., Sandell, L. J., and Brophy, R. H. (2014). Relationship of gene expression in the injured human meniscus to body mass index: a biologic connection between obesity and osteoarthritis. *Arthr. Rheumatol.* 66, 2152–2164. doi: 10.1002/art.38643

Ren, J., and Zhang, Y. (2018). New therapeutic approaches in the management of cardiometabolic diseases: bringing the concepts together. *Curr. Drug Targets* 19, 987–988. doi: 10.2174/1389450119091806290957 09

Rendo-Urteaga, T., Garcia-Calzon, S., Gonzalez-Muniesa, P., Milagro, F. I., Chueca, M., Oyarzabal, M., et al. (2015). Peripheral blood mononuclear cell gene expression profile in obese boys who followed a moderate energy-restricted diet: differences between high and low responders at baseline and after the intervention. *Br. J. Nutr.* 113, 331–342. doi: 10.1017/S0007114514003584

Ritchie, M. E., Phipson, B., Wu, D., Hu, Y., Law, C. W., Shi, W., et al. (2015). limma powers differential expression analyses for RNA-sequencing and microarray studies. *Nucleic Acids Res.* 43:e47. doi: 10.1093/nar/gkv007

Ross, R., Neeland, I. J., Yamashita, S., Shai, I., Seidell, J., Magni, P., et al. (2020). Waist circumference as a vital sign in clinical practice: a consensus Statement from the IAS and ICCR working group on visceral obesity. *Nat. Rev. Endocrinol.* 16, 177–189. doi: 10.1038/s41574-019-0310-7

Sonne, S. B., Yadav, R., Yin, G., Dalgaard, M. D., Myrmel, L. S., Gupta, R., et al. (2017). Obesity is associated with depot-specific alterations in adipocyte DNA methylation and gene expression. *Adipocyte* 6, 124–133. doi: 10.1080/21623945.2017.1320002

Tiwari, S., and Ndisang, J. F. (2014). The role of obesity in cardiomyopathy and nephropathy. *Curr. Pharm. Des.* 20, 1409–1417. doi: 10.2174/1381612811319999056 2

Walewski, J. L., Ge, F., Gagner, M., Inabnet, W. B., Pomp, A., Branch, A. D., et al. (2010). Adipocyte accumulation of long-chain fatty acids in obesity is multifactorial, resulting from increased fatty acid uptake and decreased activity of genes involved in fat utilization. *Obes. Surg.* 20, 93–107. doi: 10.1007/s11695-009-0002-9

Wang, Q., Zhu, C., Sun, M., Maimaiti, R., Ford, S. P., Nathanielsz, P. W., et al. (2019). Maternal obesity impairs fetal cardiomyocyte contractile function in sheep. *FASEB J.* 33, 2587–2598. doi: 10.1096/fj.201800988R

Wang, S., and Ren, J. (2018). Obesity paradox in aging: from prevalence to pathophysiology. *Prog. Cardiovasc. Dis.* 61, 182–189. doi: 10.1016/j.pcad.2018.07.011

Wang, Y., Liu, T., Liu, Y., Chen, J., Xin, B., Wu, M., et al. (2019). Coronary artery disease associated specific modules and feature genes revealed by integrative methods of WGCNA. *Metade Mach. Learn. Gene* 710, 122–130. doi: 10.1016/j.gene.2019.05.010

WHO (2000). Obesity: preventing and managing the global epidemic. Report of a WHO consultation. *World Health Organ. Tech. Rep. Ser.* 894, 1–253.

Xu, X. H., and Ren, J. (2013). "Regulation of autophagy in obesity-induced cardiac dysfunction," in *Autophagy: Caner, Other Pathologies, Inflammation, Immunity, and Infection*, ed. M. A. Hayat (Cambridge, MA: Academic Press), 329–340.

Zhang, Y., and Ren, J. (2016). Epigenetics and obesity cardiomyopathy: From pathophysiology to prevention and management. *Pharmacol. Ther.* 161, 52–66. doi: 10.1016/j.pharmthera.2016.03.005

Zhang, Y. Y., and Ren, J. (2015). "Leptin and obesity," in *Obesity – A practical Guide*, ed. S. A. I. Ahmad (Berlin: Springer Press), 45–58.

Zhao, J., Lv, T., Quan, J., Zhao, W., Song, J., Li, Z., et al. (2018). Identification of target genes in cardiomyopathy with fibrosis and cardiac remodeling. *J. Biomed. Sci.* 25:63. doi: 10.1186/s12929-018-0459-8

Conflict of Interest: The authors declare that the research was conducted in the absence of any commercial or financial relationships that could be construed as a potential conflict of interest.

Copyright © 2020 Tao, Wang, Li, Zheng and Liang. This is an open-access article distributed under the terms of the Creative Commons Attribution License (CC BY). The use, distribution or reproduction in other forums is permitted, provided the original author(s) and the copyright owner(s) are credited and that the original publication in this journal is cited, in accordance with accepted academic practice. No use, distribution or reproduction is permitted which does not comply with these terms.

frontiers in Physiology

REVIEW
published: 10 July 2020
doi: 10.3389/fphys.2020.00798

Regulation of Long Non-coding RNAs and MicroRNAs in Heart Disease: Insight Into Mechanisms and Therapeutic Approaches

Lucy Collins[1†], Pablo Binder[1†], Hongshan Chen[2] and Xin Wang[1*]*

[1] Division of Cardiovascular Sciences, Faculty of Biology, Medicine and Health, The University of Manchester, Manchester, United Kingdom, [2] Key Laboratory of Cardiovascular and Cerebrovascular Medicine, Nanjing Medical University, Nanjing, China

Cardiovascular disease is the leading cause of mortality worldwide and there is an increasing need to identify new therapeutic targets that could be used to prevent or treat these diseases. Due to recent scientific advances, non-coding RNAs are widely accepted as important regulators of cellular processes, and the identification of an axis of interaction between long non-coding RNAs (lncRNAs) and micro RNAs (miRNAs) has provided another platform through which cardiovascular disease could be targeted therapeutically. Increasing evidence has detailed the importance of these non-coding RNAs, both individually and in an axis of regulation, in the processes and diseases involving the heart. However, further investigation into the consequences of targeting this mechanism, as well as refinement of how the system is targeted, are required before a treatment can be provided in clinic. This level of genomic regulation provides an exciting potential novel therapeutic strategy for the treatment of cardiovascular disease.

Keywords: microRNAs, long non-coding RNAs, cardiovascular disease, therapy, proteostasis

OPEN ACCESS

Edited by:
Gaetano Santulli,
Columbia University, United States

Reviewed by:
Jason N. Peart,
Griffith University, Australia
Meijing Wang,
Indiana University Bloomington School of Medicine, United States

****Correspondence:***
Pablo Binder
pablo.binder@manchester.ac.uk
Xin Wang
xin.wang@manchester.ac.uk

† These authors have contributed equally to this work

Specialty section:
This article was submitted to Clinical and Translational Physiology, a section of the journal Frontiers in Physiology

Received: *17 March 2020*
Accepted: *15 June 2020*
Published: *10 July 2020*

Citation:
Collins L, Binder P, Chen H and Wang X (2020) Regulation of Long Non-coding RNAs and MicroRNAs in Heart Disease: Insight Into Mechanisms and Therapeutic Approaches. Front. Physiol. 11:798. doi: 10.3389/fphys.2020.00798

INTRODUCTION

Cardiovascular disease is the leading cause of mortality worldwide. In 2016, it is estimated that cardiovascular disease caused 17.6 million deaths globally, an increase of 14.5% since 2006 (Benjamin et al., 2019). It is predicted that, without further medical innovation, by 2030 over 23.6 million people are expected to die from cardiovascular disease (AHA, 2019) the majority of which will be due to stroke and heart disease. Stress conditions cause alterations in cardiac homeostasis and result in pathological conditions such as cardiac hypertrophy, myocardial infarction, and heart failure. During the development and progression of these conditions, various cellular changes occur including cell death through both necrosis and apoptosis, extra cellular matrix deposition leading to cardiac fibrosis, and increased protein load that results in endoplasmic reticulum (ER) stress and proteotoxicity. Novel therapies are required to target these cellular events that occur during these conditions, both to prevent their occurrence and as treatment.

The majority (98%) of the genome consists of non-coding DNA, which was once considered 'junk DNA.' However, the finding that around three quarters of the genome has the potential to be transcribed (Djebali et al., 2012) demonstrated both the importance and potential of non-coding RNAs, and revolutionized how this part of the genome is viewed, bringing about new potential

therapeutic strategies to treat disease. As will be discussed, numerous studies have identified regulatory roles of these non-coding RNAs in cardiovascular disease. More recently, the regulatory interplay between non-coding RNAs, specifically between long non-coding RNAs and micro-RNAs, has been identified, and this review will explore the potential therapeutic approaches which could target this regulatory system in diseases of the heart, focusing predominantly on those with evidence of their impact in animal models.

OVERVIEW OF lncRNAs AND miRNAs

Non-coding RNAs were first identified in the 1960s though it took many more years to realize their potential in the cell (Cech and Steitz, 2014). They are functional RNAs that, unlike coding RNA, do not undergo translation, and it appears that their predominant role is gene expression regulation. MicroRNAs and long non-coding RNAs are the two most understood members of the non-coding RNA family and will be the focus of this review.

MicroRNAs

MicroRNAs (miRNAs) are small, single-stranded, non-coding RNAs around 18–25 nucleotides in length which were first discovered in 1993 (Lee et al., 1993) in *Caenorhabditis elegans*. They regulate gene expression at the post-transcriptional level, either by directing their target mRNA to be degraded or inhibiting its translation. Over 2000 miRNAs have been identified in the human genome (Alles et al., 2019) and these are thought to regulate around one third of all genes.

Most miRNAs are transcribed by RNA polymerase II into primary miRNA (pri-miRNA) with a hairpin loop structure which often have a poly-A tail. Following this they undergo processing in the nucleus, which is enabled by interaction with DGCR8 and DROSHA, a ribonuclease, leading to the generation of a hairpin structure known as the pre-miRNA. This is subsequently translocated into the cytoplasm where it is further processed by DICER into miRNA duplexes. Duplexes unwind; one strand, known as the passenger strand, is degraded, whilst the other remains as the mature miRNA which is incorporated into the RNA-induced silencing complex (RISC), along with other proteins such as Ago-2, to form a multiprotein complex through which the miRNA interacts with mRNA.

MiRNAs function by binding to mRNA sequences with complementary base-pairs. The majority of miRNAs bind to the 3′ untranslated region of target mRNAs; however, interactions with other sites, such as promoters and 5′ regions have been described (O'Brien et al., 2018). Once bound, miRNAs cause silencing through multiple mechanisms including; (1) translational inhibition, often through interfering with ribosomal processes, (2) site-specific mRNA cleavage, commonly known as RNA interference (RNAi), and (3) destabilizing the mRNA through deadenylation leading to enhanced degradation. Whether mRNA is targeted for irreversible degradation or reversible translational inhibition is determined by the level of sequence complementarity. On top of their silencing capability, recent research in the past decade has identified that miRNAs can also function as ligands for toll-like receptors (TLRs), leading to their activation. This has been particularly investigated in cancer, where paracrine miRNA-TLR activation leads to cytokine production by local immune cells, promoting cancer proliferation and metastatic potential (Fabbri et al., 2013). Furthermore, miRNAs have been shown to regulate gene expression independent of RISC, demonstrating the complexity in their functions (Catalanotto et al., 2016).

MiRNAs are highly evolutionarily conserved and play key roles in various biological processes including cell survival, proliferation, angiogenesis, and insulin secretion, as well as many others, and as such, are key regulators of, and thus therapeutic approaches for, diseases such as cancer and cardiovascular disease (Di Leva and Croce, 2015; Oliveira et al., 2016; da Silva et al., 2018).

Long Non-coding RNAs

Long non-coding RNAs (LncRNAs) are characterized as RNAs longer than 200 nucleotides. Unlike miRNAs, lncRNAs often have poor sequence conservation and expression, and are more numerous. The first eukaryotic lncRNA was identified in the 1990s - H19 (Brannan et al., 1990). Potentially a reason for its early discovery is that H19, unlike many other lncRNAs, has high sequence conservation among mammals. However, H19's functional ability was not determined at this time, and the first lncRNA to be identified with a specific function was Xist, which is involved in X chromosome inactivation (Brockdorff et al., 1991; Brown et al., 1991). The publishing of the human genome in 2001 led to a greater focus on non-coding RNAs, which in turn led to a substantial increase in the number of lncRNAs identified (Jarroux et al., 2017).

LncRNA synthesis, much like that of mRNA, occurs by RNA polymerase II dependent transcription and can then be further processed, for instance by splicing and polyadenylation. Their structure, too, is similar to that of mRNA, so much so that they were originally known as 'mRNA-like' (Erdmann et al., 1999), though they lack a stable open reading frame. As a whole, they have no specific localization, and can be localized in the nucleus and/or the cytosol. LncRNAs are a heterogeneous group, grouped into classes with varying functions, which are explored further in other reviews (Jarroux et al., 2017). The majority of lncRNAs appear to function as gene regulators, influencing both peri- and post-transcriptional gene expression.

LncRNAs can directly bind or interact with mRNA leading to translational suppression (Yoon et al., 2012) or mRNA decay (Gong and Maquat, 2011). LncRNAs can also bind proteins, altering their localization, activity, stability, and can also sequester them (Paneru et al., 2018). There are five main mechanisms through which lncRNAs have been identified to function and alter gene expression, and individual lncRNAs are not restricted to one mode of action.

Scaffolds

Scaffold lncRNAs provide a platform at a specific genomic locus. They contain multiple binding sites, allowing the recruitment of numerous molecules that can form a functional complex, known as a ribonucleoprotein (RNP) complex. TUG1 can bind

to the methylated polycomb 2 protein, leading to assembly of a transcription repressor complex, which is believed to be important for grown-control gene repression (Yang et al., 2011).

Decoy

LncRNAs can also act as decoys for transcription factors or other regulatory proteins, competing for binding sites, preventing them from acting on the loci of interest. The lncRNA p21-associated ncRNA DNA damage activated (PANDA) is a well-studied lncRNA acting as a decoy following DNA damage. PANDA binds to the transcription factor NF-YA, which causes its sequestration, preventing it from binding and promoting the transcription of pro-apoptotic genes (Hung et al., 2011).

Signals

Signal lncRNAs are transcribed following a specific stimulus, acting in a time- and space-dependent signaling pathway. This mechanism is evident in phenomena such as gene imprinting (Pandey et al., 2008; Mohammad et al., 2009). It appears that the benefit of this mechanism is that, as it is RNA-dependent, it allows for a faster response due to the lack of need for protein translation.

Guides

LncRNAs that act as guides are required to direct transcription-related factors to the correct genomic loci. They can act in either a *cis* or *trans* fashion. For instance, the lncRNA HOTAIR directs PRC2, a chromatin modifier with histone methyltransferase activity, to the HOXD locus, leading to gene silencing of these transcription factors. HOTAIR has been identified as an oncogene, promoting cancer metastasis through this guide capability (Gupta et al., 2010). As well as acting as guides to supress transcription, lncRNAs can also promote transcription by guiding transcription factors and histone modifiers to gene targets. For instance, the lncRNA HOTTIP has been identified as recruiting the MLL protein to the 5′HOXA locus through binding to the WDR5 adaptor protein, leading to H3 lysin 4 trimethylation, and subsequent gene transcription (Wang et al., 2011).

Enhancers

A less understood mechanism of lncRNAs in altering gene expression is by acting as enhancers. These lncRNAs have been shown in human cell lines to Ørom et al. (2010) to regulate gene expression distant to the lncRNA location. More research is required into the exact mechanism, though one study suggests that this occurs through DNA looping to bring the enhancer and the target site into closer proximity, and promoting the recruitment of RNA polymerase II and transcription factors leading to target gene expression (Lai et al., 2013).

THE lncRNA–miRNA–mRNA AXIS

Whilst many lncRNAs and miRNAs have been identified separately as being involved in biological functions and disease, they have also been shown to be involved through interacting with one another, resulting in another level of gene regulation. This has been termed the lncRNA–miRNA–mRNA axis. This regulation is bi-directional, with miRNAs influencing lncRNA expression, and vice versa. Multiple mechanisms of lncRNA–miRNA interaction have been reported (Yoon et al., 2014) (**Figure 1**) and are discussed below.

LncRNAs Acting as Sponges

LncRNAs can bind miRNAs, preventing them from interacting with their target mRNA, therefore acting as positive regulators of transcription. Those that do this are known as competitive endogenous RNAs (ceRNAs), decoys, or sponges as this review will call them. Most sponge lncRNAs bind to miRNAs through complementary interaction between the Ago binding sites on miRNAs and the 3′ ends of lncRNAs. Cardiac hypertrophy related factor (CHRF) was the first lncRNA described as able to act as a sponge, directly binding to miR489 to downregulate its expression, with enforced CHRF overexpression leading to reduced miR-489 expression and a hypertrophic response in neonatal cardiomyocytes regardless of the presence of a pro-hypertrophy stimulus (Wang et al., 2014a). Since this discovery, other lncRNAs have been demonstrated to have this ability, such as SNHG7 which was found to sponge miR-216b in order to promote proliferation and metastasis of cancerous colorectal cells (Shan et al., 2018). However, on top of directly binding to miRNAs to prevent their interaction with mRNA, lncRNAs have also been identified as able to bind mRNAs to prevent miRNA-mediated degradation of both the mRNA and lncRNA (Barbagallo et al., 2018).

Competition Between miRNAs and lncRNAs

It has been noted that miRNAs and lncRNAs can compete to bind the same target mRNA. Faghihi et al. (2010) identified this phenomenon *in vitro* in the regulation of the *BACE1* gene. They demonstrated that miR-485-5p and the lncRNA BACE1AS, which is partially antisense to *BACE1* mRNA, compete to bind the same mRNA region of BACE1, with BACE1AS overexpression protecting BACE1 from mRNA-mediated silencing. This suggests that the cellular stimulus and the ratio between miRNAs and lncRNAs may determine whether a gene is expressed or silenced.

MiRNA Generation by lncRNAs

As well as acting antagonistically, lncRNAs have been shown as able to be processed to produce miRNAs. The first exon of lncRNA H19 contains the transcript for miR-675, and H19 has been shown to effectively act as a pri-mRNA for miR-675. Processing of H19 to release this miRNA is regulated by the RNA binding protein HuR, upregulated during stress, with HuR inhibiting miR-675's processing by binding to full-length H19 (Keniry et al., 2012). Removal of HuR allowed the processing of H19, and it is believed to be due to the removal of HuR's inhibition of the endonuclease Drosha. This allows for temporal- and spatial-specific regulation, with this miRNA released prior to birth to prevent placental overgrowth. It has also been shown to be important in skeletal muscle differentiation and regeneration (Dey et al., 2014). Further to this, the lncRNA

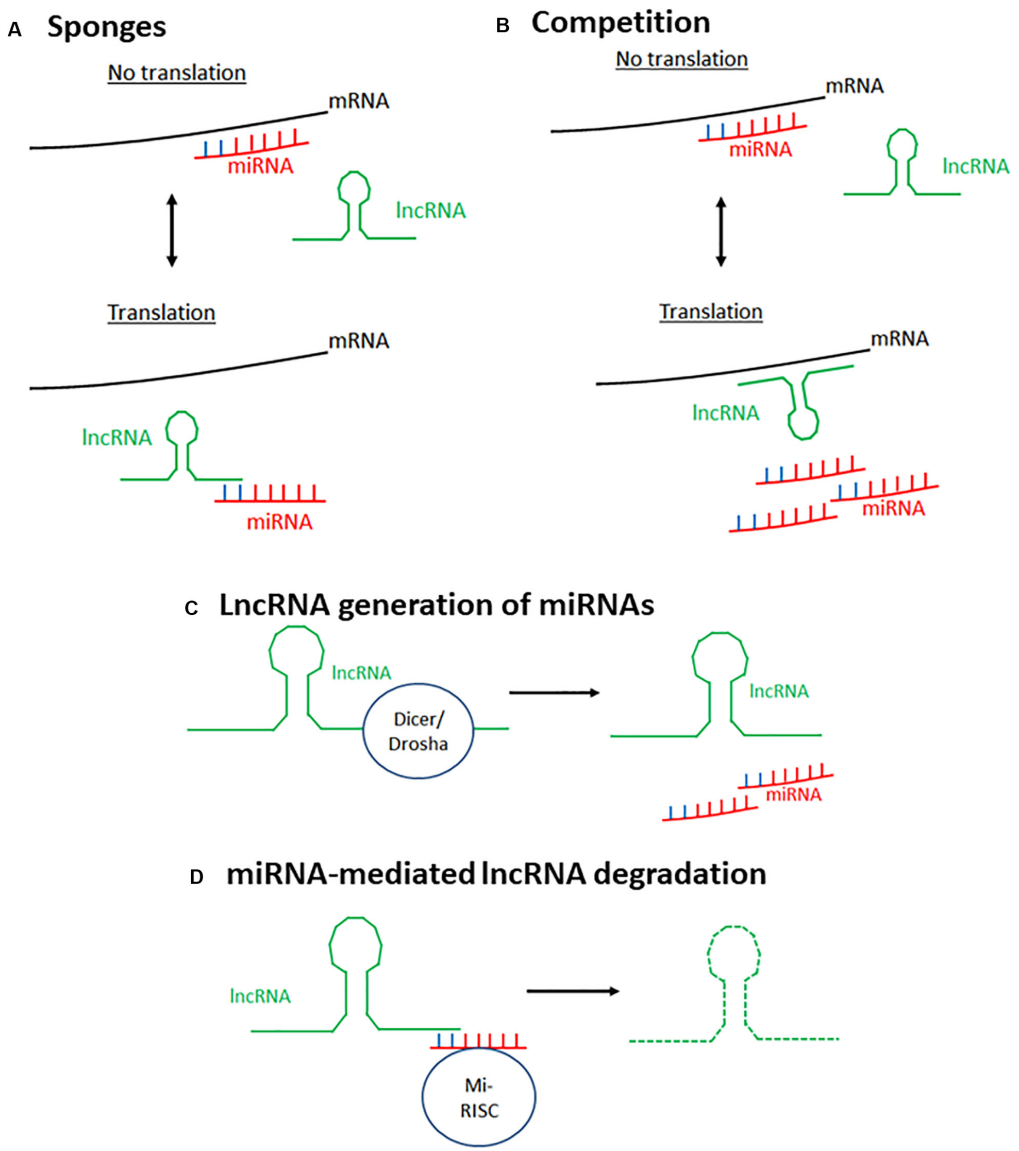

FIGURE 1 | Mechanisms of lncRNA–miRNA interaction to affect mRNA expression. There are four main known mechanisms through which lncRNAs and miRNAs interact to alter gene expression. **(A)** LncRNAs can act as sponges for miRNAs. LncRNAs bind miRNAs preventing their interaction with their target mRNA, thus preventing silencing of this gene. **(B)** LncRNAs and miRNAs compete to bind the same target mRNA, thus, depending on the stimulus, gene expression can be differentially expressed. **(C)** miRNAs can be generated from lncRNAs through spicing of the lncRNA by endoribonucleases such as Dicer and Drosha. **(D)** MiRNAs silence lncRNA activity by targeting lncRNAs for degradation using the same mechanism through which they target mRNAs. Mi-RISC, miRNA-induced silencing complex.

Ang-362 and miR-221/222 were shown to be co-transcribed in vascular smooth muscle cells (Leung et al., 2013) with these microRNAs transcribed as part of the larger transcript of Ang-362 that lies proximal. Using siRNA-mediated knockdown of the lncRNA, this group confirmed that expression of Ang-362 is required for expression of these miRNAs, and this is important for Angiotensin II-mediated cellular proliferation. The finding that lncRNAs can positively regulate miRNAs led to the re-analysis of our understanding of the relationship between non-coding RNAs.

MiRNA-Triggered lncRNA Decay

As previously described, miRNAs can initiate mRNA decay by recruiting the RNA-induced silencing complex (RISC). Similarly, miRNAs can trigger lncRNA decay. As with mRNA decay, the miRNA binds the lncRNA as part of the RISC due to imperfect base-pair complementarity. This interaction targets the lincRNA for degradation. MALAT1, one of the most abundant and conserved lncRNAs, is degraded through direct binding with miR9 in the nucleus (Leucci et al., 2013). Knockdown of Ago2 led to elevated levels of MALAT1, indicating that this degradation is

through interaction with RISC. The let-7 family of miRNAs has been shown to promote the degradation of multiple lncRNAs, including HOTAIR (Yoon et al., 2013) and lincRNA-p21 (Yoon et al., 2012) through the RBP HuR.

Novel Mechanisms of Interaction

As well as the more developed concepts of lncRNA–miRNA–mRNA interaction described above, other ways in which lncRNAs and miRNA have been shown to interact have been identified. Yu et al. (2017) identified that the lncRNA CCAT2 could regulate miR-145 expression by selectively blocking its maturation. This demonstrates that there are potentially other mechanisms of RNA-mediated regulation, suggesting that this axis may be more complex than first thought.

ROLE OF LONG NON-CODING RNAs AND MICRO RNAs IN HEART DISEASE

Emerging evidence has highlighted the important roles of miRNAs and lncRNAs in heart development, physiology and disease. Transcriptome and functional analyses have identified numerous miRNAs and lncRNAs whose expressions are altered in heart pathology, and revealed that while the expression of some of these non-coding RNAs show negative effects in the progression of disease, others appear to play protective roles (Thum et al., 2008; Di Mauro et al., 2018). Therefore, greater understanding is required on the relationship between non-coding RNAs and the pathogenesis and development of heart disease. This, together with discovery of novel approaches to manipulate their expression and activity, will aid the design and development of novel diagnostic and therapeutic strategies to ameliorate cardiac dysfunction and diminish the pathological progression of heart failure.

The role of miRNAs and lncRNAs in cardiovascular disease has previously been described in detail (Uchida and Dimmeler, 2015; Wronska et al., 2015) and both lncRNAs and miRNAs have been shown to act as both positive and negative regulators of cardiovascular disease (Sardu et al., 2014).

Role of Non-coding RNAs in Cardiac Hypertrophy

Cardiac hypertrophy is the adaptive response to stress-induced injury due to pathological pressure overload or neurohormonal stimulation (Frey and Olson, 2003). This response is initially compensatory and aims to reduce wall stress through thickening of the ventricular wall in order to maintain normal cardiac function. However, sustained hypertrophy often leads to maladaptive cardiac remodeling which can progress into heart failure.

During heart hypertrophy and dysfunction diverse signaling pathways are activated resulting in increased cardiomyocyte size, protein synthesis, organelle alterations, and expression of fetal genes (Nakamura and Sadoshima, 2018). However, the molecular mechanisms responsible for the development of cardiac hypertrophy are still not fully understood. Several studies have shown miRNAs and lncRNAs to be key players in the regulation of cell differentiation, growth, survival and proliferation. Particularly, many of these non-coding RNAs have been reported to be critical regulators in heart hypertrophy and failure in *in vivo* and *in vitro* disease models (Kumarswamy and Thum, 2013).

The involvement of miRNAs in heart hypertrophy was firstly described in cardiac tissue from mice in response to pressure overload and activated calcineurin overexpression, which result in pathological cardiac remodeling. Initially, more than a dozen miRNAs showing up- or down-regulation were identified, many of which were similarly altered in failing human hearts (van Rooij et al., 2006). One of these, miRNA-195, is up-regulated during cardiac hypertrophy and its cardiac overexpression appears to be sufficient to drive cardiac pathological hypertrophy leading to heart failure in mice. This revealed a crucial role for miRNAs in hypertrophic growth leading to remodeling of the heart as a result of pathological signaling. The same group reported that the cardiac-specific miRNA, miR-208, conserved among humans, mice, rats, and dogs is required for hypertrophy, fibrosis, and βMHC upregulation in cardiomyocytes under stress conditions (van Rooij et al., 2007, 2008).

On the other hand, miR-133 and miR-1 are downregulated in mouse and human models of cardiac hypertrophy. Overexpression of both miRNAs inhibits cardiac hypertrophy, and inhibition of miR-133 causes significant cardiac hypertrophy and cardiac dysfunction via upregulation of the miR-133 targets Rho1, Cdc42, and Nelf-A/WHSC2 *in vivo*, suggesting miR-133 is cardioprotective in the context of hypertrophy (Carè et al., 2007). Several other miRNAs have been described as modulators of cardiac hypertrophy, either by protecting cardiac tissue from pathological hypertrophy such as miR-1 and miR-541 (Liu et al., 2014) or by contributing to hypertrophy, such as miR-23a and miR-34 (Li et al., 2015a). This further highlights the importance of the regulation of miRNAs as potential targets for therapeutic application in heart disease.

LncRNAs have also been shown to have a role in the development of cardiac hypertrophy. Viereck et al. (2016) identified the lncRNA cardiac hypertrophy-associated transcript (Chast) and showed it to be increased in mice in response to pressure overload. This group showed, both *in vitro* and *in vivo*, that Chast can induce cardiac hypertrophy. Furthermore, the human homolog CHAST is upregulated in human samples of hypertrophic cardiac tissue, thus suggesting a conserved role. Interestingly, as well as lncRNAs being able to interact with chromatin remodeling factors and alter chromatin structure, chromatin remodeling factors have been shown to alter lncRNA expression, demonstrating a feedback loop that creates another level of regulation, and one such feedback loop, involving the lncRNA Mhrt and chromatin has been shown to be important for heart function and protecting the heart from pathological cardiac hypertrophy (Han et al., 2014). Mhrt is a cardiac-specific lncRNA that antagonizes the chromatin-remodeling factor Brg1. During hypertrophy, stress causes Brg1 activation, stimulating the Brg1-Hdac-Parp chromatin repressor complex, which results in reduced cardiac Mhrt expression. Restoration of Mhrt expression protects the heart from cardiac hypertrophy and heart failure.

Role of Non-coding RNAs in Arrhythmias

As well as influencing structural cardiac changes, lncRNAs and miRNAs have also been implicated in the development of arrhythmias (Kim, 2013; Zhang Y. et al., 2019). MiRNAs in particular have been implicated in the development of atrial fibrillation (AF) (Santulli et al., 2014) the most common sustained cardiac arrhythmia seen in clinic (Lee et al., 2014). Overexpression of miR-328, which is upregulated in tissue samples from AF patients, leads to AF in mice due to a reduced L-type Ca^{2+} current (Lu et al., 2010). AntagomiR-mediated reduction in miR-328 levels reverses the AF phenotype, demonstrating its importance in regulating calcium signaling and atrial electrical conduction during AF. Alternatively, some miRNAs become downregulated during certain cardiac arrhythmias. Downregulation of mir-1 during disease results in tachyarrhythmia due to loss of its ability to regulate Connexin 43 (Cx43), leading to Cx43 hyperphosphorylation and displacement (Curcio et al., 2013). This demonstrates the varied roles that miRNAs play in regulating the electrical remodeling that occurs in the heart during disease, and the varied ways in which they could be manipulated for therapeutic purposes.

However, the ability of miRNAs to alter cellular processes leading to arrhythmias has presented difficulties when targeting miRNAs for treatment. In one study, overexpression of human miRNA-199a in pig hearts following myocardial infarction initially seemed to be a therapeutic success, with treated animals showing improved contractility and reduced infarct size due to the ability of this miRNA to promote cardiomyocyte proliferation (Gabisonia et al., 2019). However, the continued expression of miR-199a resulted in sudden arrhythmic death in the majority of animals. Evidently, this must be taken into account and doses carefully monitored should these molecules be targeted for therapeutic benefit, in order to reduce adverse effects.

Role of Exosomal miRNAs in Cardiovascular Disease

As well as the canonical pathway for miRNA gene regulation, miRNAs can also be secreted and transported throughout the body in extracellular vesicles known as exosomes; these are known as exosomal miRNAs Valadi et al., 2007). Encapsulation in exosomes protect these miRNAs from degradation by RNases (Mitchell et al., 2008; Koga et al., 2011). These miRNAs are important in cell–cell communications and regulate gene expression in recipient cells. Exosomal miRNAs have been implicated in the development of diseases such as cancer (Melo et al., 2014) and diabetes (Santulli, 2018), and viruses can promote their release in order to dampen the immune response (Pegtel et al., 2010). Similarly, exosomal miRNAs have been shown to prevent against cardiac injury induced during sepsis (Wang et al., 2015c). The exact mechanism by which miRNAs are sorted and transported into exosomes within a cell is unclear; however, it appears that this is a regulated process and not random, considering that miRNAs in exosomes differ to the general miRNA content in the parent cell (Goldie et al., 2014). Exosomal miRNAs have been implicated in CVDs (Chistiakov et al., 2016) as will be discussed below, but the complexity in how they are regulated, and the low exosomal yield, means that much more research is required to allow for effective therapeutic strategies involving them (Gangadaran et al., 2018).

Exosomal miRNAs have been shown to regulate development of fibrosis following myocardial infarction. Morelli et al. (2019) identified that exposure of fibroblasts to cardiomyocyte-derived exosomes isolated from a murine model of myocardial infarction were sufficient to initiate myofibroblast differentiation and activation, whilst exosomes derived from sham mice had no effect. They identified that exosomal transport of miR-195 was significantly upregulated, and inhibition of miR-195 using a miRNA mimic prevented the upregulation of periostin, a myofibroblast marker, in cultured fibroblasts. Other exosomal miRNAs have also shown to influence fibrotic development following MI. Exosomes isolated from mice subjected to ligation of the left anterior descending coronary artery (LAD) contained the miR-92a, which was also found to be upregulated in isolated cardiac myofibroblasts (Wang et al., 2020). These exosomes were shown to be cardiomyocyte-derived and, when introduced to isolated fibroblasts led to suppression of SMAD-7, a known inhibitor of alpha-smooth muscle actin (αSMA) which is crucial for myofibroblast differentiation and activation post-MI. The importance of exosomal miRNA secretion was confirmed *in vitro* using an inhibitor of exosome secretion. However, cardiac exosomes have also been shown to be enriched for miRNAs that have anti-fibrotic roles, such as miR-29a (Yamaguchi et al., 2015) and miR-144 (Li et al., 2014) and have shown to be cardioprotective during remote ischemic conditioning. These findings demonstrate the importance of investigating exosomal miRNAs as potential therapeutic targets for targeting cardiac fibrosis. Considering that this structural change in the heart is found in many cardiac pathologies, including myocardial infarction and cardiac hypertrophy, and since its occurrence is strongly related to progression to heart failure, it could provide an important therapeutic approach to prevent the development of this disease.

Other studies have demonstrated the involvement of exosomal miRNAs in other cellular responses during CVD. Pro-angiogenic miRNAs have been identified in exosomes from patient-derived cardiac progenitor cells (Barile et al., 2014), and rats injected with these exosomes had improved cardiac function, reduced cardiomyocyte apoptosis and increased angiogenesis after MI compared to controls. However, as with other cellular processes and with cell-resident miRNAs, miRNAs can have opposing effects, and some have been shown to promote cell death in the heart. The serum of acute myocardial infarction (AMI) patients had elevated levels of miR-30a, and *in vitro* investigation showed that upon exposure to hypoxic conditions this miRNA is upregulated and packaged into exosomes (Yang et al., 2016). Inhibition of exosome release, or miR-30a itself, led to autophagy of cultured cardiomyoblasts but attenuated apoptosis, demonstrating that this miRNA is important in regulating the cell survival response in cardiomyocytes following AMI. Considering that following AMI up to 1 billion cardiomyocytes are thought

to undergo cell death (Murry et al., 2006) further investigation into the mechanism of this exosomal miRNA and how it might be targeted therapeutically could prove beneficial in reducing cardiac damage following AMI.

Exosomal miRNAs also influence CVDs of the vasculature and targeting their release could prove beneficial in treating pulmonary arterial hypertension (PAH). Sindi et al. (2020) identified that during the pre-clinical phase of PAH downregulation in the release of exosomal miRNAs miR-181a-5p and miR-324-5p occurs. These exosomal miRNAs are secreted in a paracrine fashion from endothelial cells and act to suppress vascular remodeling associated with PAH, such as increased proliferation and angiogenesis. In PAH mice, addition of these miRNAs assuaged disease progression. Crucially, this study identified that exosomal release of the miRNAs is mediated by the transcription factor KLF2, and as such provides a further information that could be used to target this pathway therapeutically.

The ability of exosomal transport of RNAs demonstrates the potential for miRNA–lncRNA axis interaction in cell types in which one component of the axis is not normally expressed. This presents a potential increased level of complexity in the regulation of gene expression across various cell types, and must be taken into account when investigating the possibility to exploit this axis for therapeutic benefit.

Role of Non-coding RNAs as Biomarkers

Due to their involvement in cardiovascular disease, and their stability in plasma because of their ability to be confined in exosomes, greater interest is being placed on using miRNAs as biomarkers for disease (Zhou et al., 2018) and could also be used to influence treatment decisions (Kiyosawa et al., 2020). For instance, circulating levels of miRNAs -27a, -16b, -30e, 18b, and others are reduced in patients with heart failure, and some have been associated with an increased risk of mortality (Colpaert and Calore, 2019). This is not a unique phenomenon and, similarly, changes in circulating miRNAs have been shown to occur in other cardiovascular diseases such as acute myocardial infarction (Chistiakov et al., 2016) and cardiogenic shock (Jäntti et al., 2019). The increased use of bioinformatic modeling has aided the identification of potential miRNAs that may prove to act as biomarkers for multiple cardiovascular diseases (Kayvanpour et al., 2020).

A large body of research has focused on the investigation of miRNAs as potential biomarkers for myocardial infarction and related events. In patients with ST-segment elevation myocardial infarction (STEMI) following a type 1 MI, miR-331 and miR-151-3p were identified as significantly upregulated in these patients, and it appeared that their upregulation occurred as early as plaque rupture, suggesting that these could be used to predict STEMI development soon after the event, allowing for early intervention (Horváth et al., 2020). miRNAs have also been identified as predictive markers for cellular changes and remodeling following MI and reperfusion therapies such as percutaneous coronary intervention (PCI) and coronary artery bypass grafting (CABG). For instance, an increase in circulating levels of miR-320a has been noted to be correlated with development of adverse remodeling, such as wall thinning and dilation of the LV after PCI, which can promote the progression to heart failure (Galeano-Otero et al., 2020). Khan et al. (2020) have carried out a thorough analytical review of research to date surrounding the levels of miRNAs in blood or tissue extracted during CABP to predict the development of atrial fibrillation after CABG. Whilst many small studies have found increased levels of certain miRNAs correlated to arrhythmia development, the authors recognize that these have not been validated elsewhere in the literature, and many do not take into account changes in miRNA levels that may occur upon reperfusion. Evidently, further research is required to validate these miRNAs as biomarkers.

LncRNAs have also been investigated for their potential use as biomarkers of cardiovascular disease (Chen C. et al., 2019) and levels of lncRNAs have been shown to be identifiable in urine and blood plasma samples (Zhou et al., 2015; Terracciano et al., 2017) as they too can be encapsulated in exosomes (Li et al., 2015b). The lncRNAs NRON and MHRT have been identified as potential predictive biomarkers of heart failure (Xuan et al., 2017) and lncRNAs have also been identified as novel biomarkers for atrial fibrillation (Xu et al., 2016). Plasma levels of the lncRNA long intergenic non-coding RNA predicting cardiac remodeling (LIPCAR) were shown to predict survival in patients with heart failure, and higher levels of LIPCAR were associated with increased levels of left ventricular remodeling (Kumarswamy et al., 2014). LIPCAR also been associated with increased risk of coronary artery disease alongside the lncRNA H19 (Zhang et al., 2017). However, like studies into miRNAs, due to the novel exploration into this many studies have been conducted on small cohorts and thus need to be validated in larger cohort studies.

Role of Non-coding RNAs in Cardiac Proteotoxicity

Due to the poor replicative ability of cardiomyocytes, it is highly important that cellular homeostasis is maintained, and as such there is a reliance on the protein quality control system. In recent years, alterations in proteostasis have received substantial attention and there is growing evidence for its role in the pathogenesis and progression of many forms of cardiovascular disease (Henning and Brundel, 2017). During cardiac remodeling, there is sustained alteration in protein homeostasis as a result of enhanced protein translation, oxidative stress, hypoxia and altered glucose metabolism, and this can result in the accumulation of misfolded protein, proteotoxicity and ER stress, and ultimately impacts cardiomyocyte function (Schirone et al., 2017). To cope with unfolded and misfolded proteins, activation of the unfolded protein response (UPR) takes place. The UPR acts as a defensive mechanism, that can protect cardiac cells functions by maintaining ER and protein homoeostasis by restoring its protein folding and clearance capacity and promoting cell survival. However, if the UPR fails to restore homeostasis, prolonged ER stress will eventually result in cardiomyocyte dysfunction and apoptosis, ultimately leading to cardiac disease (Kim et al., 2008).

There is substantial evidence of alterations in protein homeostasis resulting in ER stress in hearts exposed to pressure-overload and ischemic injury, and several studies in both mice and humans have provided evidence to suggest that the UPR response is essential in the development of these cardiac conditions. For example, ATF6 activation found to occur in cardiac hypertrophy is a protective cardiomyocyte response (Toko et al., 2010). Conversely, in mouse models of heart hypertrophy by pressure overload, elevated CHOP (Fu et al., 2010) and ASK1 (Liu et al., 2009) the downstream apoptotic effectors of the PERK and IRE1 branches of the UPR, respectively, have been reported. Similarly, under sustained ischemia or hypoxia, UPR related proteins ATF6, Bip, XBP1, ATF4, eIF2α, Tribbles 3, PUMA and CHOP are upregulated at both the mRNA and protein levels in cardiac cells, and in failing human hearts activation of the IRE1 and Perk branches can be observed (Wang et al., 2018a). Increased ER stress and alterations in the UPR have been reported in many cardiomyopathies including diabetic cardiomyopathy, alcoholic cardiomyopathy, cancer chemotherapy-induced cardiotoxicity, obesity-induced cardiomyopathy and autoimmune cardiomyopathy. Ultimately, chronic UPR activation contributes to the progression from compensatory hypertrophy to dilated cardiomyopathy and ER stress- dependent cell death participates in cardiac tissue decline in the progression of heart failure (Minamino et al., 2010).

Evidently, understanding the regulation of the signaling pathways involved in the UPR and the discovery of novel approaches to alleviate ER stress represents a promising strategy to prevent and treat cardiac dysfunction. Genetic and pharmacological regulation of these pathways have been shown be promising alternatives in the treatment of cardiac hypertrophy, MI and heart failure (Wang et al., 2018a). However, despite the great progress in understanding the role of ER stress in heart disease, the molecular mechanisms involved in the regulation of the pro-survival UPR pathway are still poorly understood. The recent discovery of non-coding RNAs as key players in the regulation of ER function in the heart suggests that further knowledge of regulatory mechanisms of non-coding RNAs in protein homeostasis could provide not only novel insight into the pathogenesis of cardiac disease under stress conditions but also lead to new therapeutic approaches.

It has been postulated that non-coding RNAs might be responsible for the regulation of the pro-survival/pro-apoptotic molecular switch observed in the UPR under sustained ER stress (Byrd and Brewer, 2013). Thus, modulation of miRNAs and lncRNAs particularly involved in the modulation of ER stress responses has the potential to be targeted to treat cardiovascular diseases. For instance, forced expression of miR-93 results in a decrease in ER stress-associated cell death and protects cardiomyocytes during I/R injury through suppression of PTEN and enhancement of Akt activity (Ke et al., 2016). In contrast, in an MI model, MiR-711 appears to increase ER-dependent apoptosis via downregulation of calnexin. Increased miR-711 results in an enhanced UPR response evidenced by upregulation of GRP78, ATF6, and spliced XBP1, and sustained expression of miR-711 eventually results in the increase of ER-stress-regulated apoptotic effectors, highlighting the substantial effect that miR-711 has as a ER stress-mediated apoptosis regulator in cardiac remodeling after MI (Zhao et al., 2018). Additionally, it has been shown that, *in vitro*, I/R triggers the expression of the lncRNA UCA1 which is accompanied by increased ROS production and ER stress, which leads to increased cardiomyocyte apoptosis (Chen J. et al., 2019). Overexpression of UCA1 seems to have a protective effect in cells subjected to I/R by modulating the ER stress response, resulting in reduced mitochondria dysfunction and apoptosis. Overall, this evidence suggests that modulation of non-coding RNAs have the potential to serve as therapeutic approach for the regulation of ER stress responses in the heart.

The impact of the dysregulation of non-coding RNAs on cardiac hypertrophy and MI, I/R and heart failure confirms that any imbalance or alterations in the expression and activity can have detrimental effects on cardiac function. It also highlights the potential non-coding RNAs present as future therapeutic targets in cardiovascular disease.

ROLE OF THE lncRNA–miRNA AXIS IN CARDIOVASCULAR DISEASE

Increasing evidence has demonstrated that the functional interaction between miRNAs and lncRNAs has a critical role in cardiovascular disease (**Table 1**), some of which have been described elsewhere (Guduric-Fuchs et al., 2012; Li et al., 2019). As described above, there are several ways in which these types of non-coding RNAs can regulate each other's activities and multiple mechanisms of lncRNA–miRNA interaction have been reported (Yoon et al., 2014). Unfortunately, information from research in cellular and animal models are so far limited and only a small number of lncRNA–miRNA–mRNA axis regulation and their molecular mechanism have been well studied. Here, we discuss some examples on miRNA–lncRNA interactions, focusing on their role in cardiac hypertrophy and ischaemic heart disease.

LncRNA–miRNA Interactions in Cardiac Hypertrophy

With the recent finding that lncRNAs can modulate miRNA function, this appears as a novel target for their regulation in the heart. Furthermore, these lncRNA–miRNA interactions have been observed in different *in vivo* and *in vitro* models of cardiac hypertrophy. In this context, as previously mentioned, the lncRNA cardiac hypertrophy-related factor (CHRF) is upregulated *in vivo* in response to angiotensin II (Ang II) treatment and it is increased in human tissue from patients with heart failure (Wang et al., 2014b). The role of CHRF in cardiac hypertrophy is through its ability to act as a miRNA sponge to supress miR-489 activity. In the heart, the expression of miR-489 is profoundly reduced in response to Ang II and this results in the upregulation of its target, hypertrophic gene myeloid differentiation primary response gene 88 (Myd88), which has a pro-hypertrophic effect in the heart (Singh et al., 2012; Masè et al., 2019). Consistent with this, miR-489 forced overexpression *in vivo* shows reduced hypertrophic response under angiotensin II (Wang et al., 2014a). Additionally, CHRF is also upregulated

TABLE 1 | Examples of miRNA–lncRNA–mRNA axis interactions in Cardiac disease.

	Experimental disease model	lncRNA, response	miRNA	Interaction	Target	Function	References
Hypertrophic heart disease	TAC angiotensin II	CHAR downregulated	miR-20b	Competitive RNA	PTEN	Anti-hypertrophic response in the heart	Zhang M. et al., 2019
	Angiotensin II heart failure	CHRF upregulated	miR-489	miRNA sponge	Myd88	Pro-hypertrophic response in the heart	Wang et al., 2014a
	ISO injection	CHRF upregulated	miR-93	Competitive RNA	AKT3	Pro-hypertrophic response in the heart	Wo et al., 2018
	TAC	CYTOR upregulated	miR-155	miRNA sponge	IKBKE	Anti-hypertrophic response in the heart	Yuan et al., 2019
	TAC ISO	H19 upregulated	miR-675	miRNA coding lncRNA	CaMKIIδ	Anti-hypertrophic response in the heart	Liu et al., 2016
	Angiotensin II	MIAT upregulated	miR-93	miRNA sponge	TLR4	Pro-hypertrophic response in the heart	Zhu et al., 2016
	ISO	MIAT upregulated	miR-150p	Not specified	P3000	Pro-hypertrophic response in the heart	Zhu et al., 2016
	TAC angiotensin II	Plscr4 upregulated	miR-214	miRNA sponge	Mfn2	Anti-hypertrophic response in the heart	Lv et al., 2018
	TAC PE	ROR upregulated	miR-133	miRNA sponge	ANP/BNP*	Pro-hypertrophic response in the heart	Jiang et al., 2016
Ischemic heart disease	MI	CARL upregulated	miR-539	miRNA sponge	PHB2	Enhanced Cardiac apoptosis and mitochondrial dynamics	Wang et al., 2014b
		H19, downregulated	miR-103/107	miRNA sponge	FADD	Inhibition of myocardial necrosis	Wang et al., 2015a
		MALAT1, upregulated	miR-145	miRNA sponge	Furin	Pro-fibrotic response in the heart	Huang et al., 2019
		MIAT, upregulated	miR-24	miRNA sponge	Furin	Pro-fibrotic response in the heart	Qu et al., 2017
		n379519, upregulated	miR-30	miRNA sponge	Collagen I/III*	Pro-fibrotic response in the heart	Wang et al., 2018c
		PFL, upregulated	Let-7d	competitive endogenous RNA	Ptafr	Pro-fibrotic response in the heart	Liang et al., 2018
	I/R	APF, upregulated	miR-188-3p	Competitive RNA	ATG7	Increased autophagy and myocardial injury	Wang et al., 2015b
		NRF, upregulated	miR-873	miRNA sponge	RIPK1/RIPK3	Enhanced myocardial necrosis	Wang et al., 2016
		RMRP, upregulated	miR-206	miRNA sponge	ATG3	Increased apoptosis and myocardial injury	Kong et al., 2019
Metabolic heart disease	Diabetic cardiomyopathy	H19 upregulated	miR-455	Competitive RNA	CTGF	Pro-fibrotic response in the heart	Huang et al., 2017

**Correlation, not confirmed as a direct miRNA target. APF, autophagy-promoting factor; ANP, atrial natriuretic peptide; BNP, brain natriuretic peptide; CaMKIIδ, Ca(2+)/calmodulin-dependent protein kinase II delta; CARL, cardiac apoptosis-related LncRNA; CHAR, cardiac hypertrophy-associated regulator; CHRF, cardiac hypertrophy related factor; CTGF, connective tissue growth factor; CYTOR, cytoskeleton regulator RNA; FADD, Fas-associated death domain; IKBKE, inhibitor of nuclear factor kappa-B kinase epsilon; Let-7d, Lethal 7 d; MIAT, myocardial infarction associated transcript; Mfn2, mitofusin 2; Myd88, myeloid differentiation primary response gene 88; NRF, necrosis-related factor; PFL, pro-fibrotic lncRNA PHB2: prohibitin 2; Ptafr, platelet-activating factor receptor; PTEN, phosphatase and tensin homolog; RIPK, receptor interacting protein kinase; TLR4, toll-like receptor 4; TAC, transverse aortic constriction; MI, myocardial infarction; I/R, ischemia/reperfusion; ISO, isoproterenol; PE, phenylephrine.*

in mice subjected to ISO injection. Interestingly, the increase of CHRF under hypertrophic stimulus correlates with an upregulation of miR-93, and ablation of CHRF in cardiomyocytes is sufficient to attenuate the ISO-induced hypertrophic responses via restoration of miR-93 expression. Furthermore, the kinase Akt3 was identified as the direct target for miR-93 in this model. Hence, the pro-hypertrophic activity of CHRF could be due to its sponging of miR-93, resulting in the upregulation of Akt3 activity and blunting miR-489 expression and activity, thus promoting the expression of hypertrophic genes such as Myd88 in response to hypertrophic stimuli (Wo et al., 2018).

Similarly, the lncRNA Plscr4 is also found to be upregulated in hypertrophic mice hearts (Lv et al., 2018). However, overexpression of Plscr4, in this case, leads to attenuation of cardiac hypertrophy, which appears to occur through altering the miR-214-Mitofusin 2 (Mfn2) pathway and maintaining mitochondrial homeostasis in mice subjected to pressure overload via Transverse Aortic Constriction (TAC) surgery. This was also shown in cardiomyocytes treated with angiotensin II. In response to pathological stimuli, upregulation of Plscr4 exerts an anti-hypertrophy effect by sponging miR-214, resulting in the attenuation of the inhibition of Mfn2 by miR-214 (Lv et al., 2018). Alterations in mitochondrial dynamics have been associated with pathological cardiac hypertrophy (Wüst et al., 2016) and recent reports have revealed that Mfn2 has a crucial role in the regulation of cardiac hypertrophy by regulating these processes under stress (Guan et al., 2016).

A recent study also identified the lncRNA cardiac hypertrophy-associated regulator (CHAR) as regulator of cardiac disease by acting as a competitive RNA *in vivo* (Zhang M. et al., 2019). CHAR expression is significantly decreased in hypertrophic conditions such as mouse models of pressure overload and *in vitro* angiotensin II-induced cardiomyocyte hypertrophy. Downregulation of CHAR by shRNA is sufficient to induce hypertrophic phenotypes, and this downregulation greatly exacerbated cardiac dysfunction induced by TAC. Conversely, forced overexpression of CHAR prevented hypertrophy. Mechanistically, CHAR acts by targeting miR-20b, a pro-hypertrophic factor which acts through inhibiting phosphatase and tensin homolog (PTEN), a known negative regulator of cardiac hypertrophy. PTEN downregulation AKT leading to hypertrophic responses to pathological stimulation (Zhang M. et al., 2019). In a similar fashion, the long non-coding RNA cytoskeleton regulator RNA (CYTOR) has also been described as a novel anti-hypertrophic modulator in the heart. However, unlike CHAR, CYTOR expression is markedly upregulated in response to pressure overload induced cardiac hypertrophy. CYTOR expression in the heart appears to be positively correlated with IKBKE expression, which has been reported to protect the heart from developing pathological cardiac hypertrophy through the IKKi and NF-κB signaling pathway (Yuan et al., 2019). Mechanistically, CYTOR functions as a 'sponge' for miR-155 to release IKBKE from miR-155-induced downregulation.

Several other lncRNAs have also been shown to regulate cardiac hypertrophy by functioning as miRNA sponges. Although most of the literature available on these corresponds to *in vitro* studies, the mechanistic insights provided by these will contribute to the understanding of cardiac pathology at the cellular level. The lncRNA myocardial infarction-associated transcript (MIAT) appears to be upregulated and act as a pro-hypertrophic factor after AngII and ISO treatment in cardiomyocytes. In response to AngII, MIAT acts as a molecular sponge of miR-93 which participates in the inactivation of the PI3K/Akt/mTOR pathway via targeting TLR4 in AngII-induced cardiac hypertrophy. Consistent with its hypertrophic effects, silencing MIAT results in a decreased expression of atrial natriuretic peptide and brain natriuretic peptide in ISO-treated NRVM cardiomyocytes. Under ISO treatment, MIAT acts by increasing P3000 expression levels via downregulation of miR-150p, resulting in cellular hypertrophy (Li et al., 2018c). MIAT has also been shown to promote the progression of AngII and isoproterenol induced cell hypertrophy *in vitro* by targeting miR-150 (Zhu et al., 2016). Similarly, ROR acts as a pro-hypertrophic factor via attenuation of miR-133 expression which results in augmented cardiac cell growth and ANP and BNP increased expression (Jiang et al., 2016), and H19 protects cardiomyocytes from phenylephrine-induced hypertrophy by targeting CaMKIIδ via miR-675 upregulation as miR-675 is encoded by H19 (Liu et al., 2016). These findings highlight the versatility of the functions of lncRNAs and miRNA-controlled cellular events. Thus, understanding these lncRNA–miRNA interactions and the modulation of different non-coding RNAs will help in the development of new cardiac hypertrophy treatments.

LncRNAs–miRNA Interactions in Ischaemic Heart Disease

Acute myocardial infarction (MI) is caused by coronary artery occlusion. Insufficient blood supply results in the massive loss of cardiomyocytes by apoptotic and necrotic cell death (Krijnen et al., 2002) which results in impaired cardiac contractility due to pathological remodeling, such as fibrosis. Additionally, following MI, acute ischemia/reperfusion (I/R) injury leads to further cardiomyocyte death, triggered by reactive oxygen species (ROS) and metabolic dysfunction, leading to impaired cardiac function (Kalogeris et al., 2012). Several studies have highlighted the regulatory involvement of non-coding RNAs such as miRNAs, and more recently lncRNAs, as well as their interactions in the setting of myocardial infarction and reperfusion induced cardiac injury (Choi et al., 2014; Andreassi, 2018). The following sections review how these interactions are involved in MI-related events.

Among the pathological changes after MI, cardiac fibrosis is a characteristic and inevitable event. Cardiac fibrosis, although initially beneficial for heart function, results ultimately in impaired heart function (Kong et al., 2014). Generation and maintenance of the scar is key for the prevention of heart dilation at the infarct region. However, extracellular matrix deposition in the heart might lead to excessive collagen accumulation and ventricular wall stiffness which will greatly contribute to the development of heart failure (Frangogiannis, 2017). Fibrosis is finely regulated by various signaling pathways.

Different SNPs within the coding region for the lncRNA myocardial infarction associated transcript (MIAT) have been

associated with increased MI risk (Ishii et al., 2006). *In vivo* studies showed that MI promotes the up-regulation of MIAT, which promotes fibrosis by reducing the availability of functional miR-24 in the heart through acting as a molecular sponge for miR-24 in cardiac fibroblasts (Qu et al., 2017). Further investigation showed that this pro-fibrotic effect is due to an increased expression of Furin, an activating factor of TGF-β1 that promotes cardiac fibrosis. Furin shows an reverse expression pattern compared to miR-24 and was identified as a miR-24 target. Consistently, *in vivo* models of MIAT knockdown show reduced infarct size and fibrosis and exhibit improved cardiac function in infarcted hearts. MIAT has also been shown to target several other anti-fibrotic miRNAs, including miR-29, miR-30, and miR-133 (Hobuß et al., 2019) further supporting its role in the promotion of cardiac fibrosis and remodeling.

Additionally, as described previously, MIAT expression is upregulated in cardiomyocytes under AngII treatment, participating as an inducer of cardiac hypertrophy by activation of the PI3K/Akt/mTOR pathway via TLR4 upregulation by sponging miR-93 in cardiomyocytes (Li et al., 2018b). Overall, MIAT-regulated fibrosis might be a promising therapeutic target for the alleviation of cardiac injury. Similarly, the lncRNA MALAT1 is upregulated in murine hearts in response to MI and in cardiac fibroblasts treated with angiotensin II. MALAT1, like MIAT1, shows a pro-fibrotic effect in the heart, and its knockdown via lentivirus-delivered MALAT1 siRNA is able to ameliorate the observed MI-impaired cardiac function, infarct size and ECM deposition *in vivo*. MALAT1 ablation also prevents AngII-induced fibrogenesis by halting fibroblast proliferation, collagen production, and α-SMA expression in neonatal cardiac fibroblasts. Mechanistically, MALAT1 acts as molecular sponge of miR-145. Similar to the MIAT-miR-24 axis, miR-145 inhibits the activation of TGF-β1 by decreasing the expression of Furin. Thus, MALAT1 promotes cardiac fibrosis by activating TGF-β1 dependent on miR 145 (Huang et al., 2019).

A recent study identified the lncRNA NONMMUT022555, or Pro-fibrotic lncRNA (PFL), as a novel fibrosis regulator. The expression of PFL is significantly higher in cardiac fibroblasts compared to cardiomyocytes and it is upregulated in mice subjected to MI promoting cardiac fibrogenesis mediated by fibroblasts. Mechanistically, PFL binds to the anti-fibrotic miRNA Let-7d acting as a sponge. Inhibition of Let-7d results in fibrogenesis via release of platelet-activating factor receptor (Ptafr) repression which leads to an increase in the expression of collagen1, α-SMA, FN1, and CTGF. Importantly, knockdown of PFL or forced expression of let-7d in MI mice markedly decreased the expression of profibrotic proteins and results in a decrease in collagen deposition and improved heart function in mice subjected to MI (Liang et al., 2018). Similarly, the expression of the lncRNA n379519 is significantly upregulated in the hearts of mice subjected to MI surgery and in TGF-b1-induced cardiac fibroblasts. Suppression of n379519 improves heart function and attenuates fibrosis in the myocardium. n379519 acts as a profibrotic lncRNA acting as a miR-30 sponge, which results in an upregulation of collagen I and collagen III expression. Interestingly, n379519 expression is also decreased when miR-30 is inhibited, suggesting a mutual regulation between the miR-30 and n379519 (Wang et al., 2018c).

Furthermore, in a model of diabetic cardiomyopathy, the antifibrotic miRNA, miR-455 was found to be significantly downregulated in both diabetic mice and in cardiac fibroblasts treated with AngII. *In vitro* studies revealed that miR-455 acts as an antifibrotic factor by targeting CTGF which results in a downregulation of proteins participating in fibrosis in cardiac fibroblasts. In primary mouse cardiac fibroblasts, the accumulation of collagen I and III observed after AngII treatment can be prevented by inhibiting miR-455 activity. The lncRNA H19 appears to have a regulatory role in this pathway as its expression is inversely correlated to that of miR-455. MiR-455 downregulation and expression of fibrosis associated proteins after AngII treatment can be recovered by ablation of H19 expression via siRNA in AngII-induced CFs. Thus, H19 could potentially modulate myocardial extracellular matrix accumulation through negative regulation of miR-455 by targeting CTGF (Huang et al., 2017).

During myocardial infarction, oxygen deficiency induces substantial cardiomyocyte loss by triggering apoptosis and necrosis (Krijnen et al., 2002). Several studies have highlighted the regulatory roles of non-coding RNAs in apoptosis in cancer and growing evidence have placed lncRNAs as crucial novel regulator of apoptosis and necroptosis in the infarcted heart. The role of lncRNAs such as MALAT1, UCA1, NRF, and H19 in survival has been discussed elsewhere (Zhou H. et al., 2019). Here we discuss the role of the lnRNA–miRNA axis in the regulation of cell death during MI, I/R and the failing heart.

The lncRNA Cardiac Apoptosis-Related LncRNA (CARL) regulates apoptosis by decreasing the expressions of Bax and the activity of Caspase-3, and by increasing Bcl-2 expression (Li et al., 2018d). CARL plays a critical role in cardiac apoptosis and mitochondrial dynamics regulating cardiac dysfunction via modulation of PHB2 expression in response to anoxia. PHB2 is important for maintaining the homeostasis of mitochondrial dynamics, and its expression is reduced during anoxia and ischemia-reperfusion in mitochondria (Wang et al., 2014b). PHB2 function is negatively regulated by miR-539. Furthermore, CARL was found to bind to miR-539 *in vivo*, acting as a functional sponge for miR-539, thus participating in maintaining the integrity of mitochondrial network dynamics via the CARL/miR-539/PHB2 axis. Consistent with this, adenoviral overexpression of CARL and the consequent downregulation of miR-539 results in increased PHB2 levels, which in turn is able to inhibit mitochondrial fission and apoptosis leading to smaller infarct size upon I/R *in vivo* (Wang et al., 2014b). Similarly, HOX antisense intergenic RNA (HOTAIR), downregulated by cardiac hypoxia or ischemia, was reported as a cardioprotective lncRNA (Gao et al., 2017). HOTAIR overexpression inhibits hypoxia/ischemia-induced apoptosis. Conversely, HOTAIR ablation results in a significant increase in cell death. Mechanistically, the cardioprotective role of HOTAIR might be explained by its interaction with miR-125 and miR-1, inhibiting their pro-apoptotic effects (Li et al., 2018a). In contrast, the lncRNA XIST was found to be upregulated in cardiomyocytes after infarction, protecting them from cell death by targeting miR-130a-3p, which

has been linked to increased apoptosis and reduced proliferation (Zhou T. et al., 2019).

In addition to apoptosis, the induction of necrosis is prominent in the ischaemic heart (McCully et al., 2004). Recent studies have shown the importance of non-coding RNAs in necrosis. Fas-associated protein with death domain (FADD) triggers apoptosis through binding to death domain of members of the TNF family death receptors, including Fas and TNFR1 (Nagata, 1997). Additionally, FADD was shown to prevent formation of the RIPK1-RIPK3 complex, resulting in the inhibition of necrosis. The microRNA miR-103/107 participates in the downregulation of FADD-mediated necrosis in cardiomyocytes under oxidative stress, and in I/R injury in animal models (Wang et al., 2015a). In response to ischemic conditions, the lncRNA H19 inhibits myocardial necrosis by downregulating miR-103/107, relieving FADD downregulation (Wang et al., 2015a). In a similar fashion, the lncRNA necrosis-related factor (NRF) facilitates the programmed necrosis of myocardial cells under I/R condition by acting as a sponge to miR-873, and by doing so promotes RIPK1/RIPK3-dependent necrosis. Conversely, NRF ablation shows cardioprotective effects by preventing necrosis (Wang et al., 2016).

Abnormalities in the regulation of autophagy has also been linked to the pathogenesis of cardiovascular disease (Levine and Kroemer, 2008). The autophagy promoting gene ATG7 has also been reported to promote I/R-induced myocardial injury. *In vivo* and *in vitro* research has demonstrated that ATG7 is targeted by miR-188-3p, which results in the inhibition of autophagy and apoptosis. Under ischemia/reperfusion conditions, increased levels of the long non-coding RNA, autophagy-promoting factor (APF) regulates ATG7 expression by directly binding to miR-188-3p and inhibiting its activity. Furthermore, APF regulates autophagy through targeting miR-188-3p, which results in increased injury following MI *in vivo* (Wang et al., 2015b). Similarly, the lncRNA AK139328 modulates autophagy and apoptosis via inhibition of miR-204-3p during myocardial ischaemia/reperfusion injury in diabetic mice. Knockdown of lncRNA AK139328 relieved hypoxia/reoxygenation injury and protects against cardiac dysfunction in mice via inhibiting cardiomyocyte autophagy (Yu et al., 2018). In rats subjected to I/R, the upregulation of lncRNA RMRP is shown to aggravate myocardial injury and suppression of RMPR improves cardiac function and reduces levels of apoptosis. RMRP upregulates ATG3 expression and results in the activation of PI3K/AKT/mTOR pathway. Mechanistically, lncRNA RMPR acts by sponging miR-206, which targets ATG3, resulting in the subsequent ATG3 upregulation (Kong et al., 2019).

miRNAs AND lncRNAs AS POTENTIAL THERAPEUTIC TARGETS IN CVD

As described above, cardiovascular disease still represents the number one cause of death worldwide (World Health Organization). With the recent advances in the understanding of the role of non-coding RNAs in physiology and pathology, and based on the growing evidence of the participation of non-coding RNAs in the pathogenesis of heart disease, their potential as novel therapeutic targets has become a matter of great interest not only for basic research, but also for pharmaceutical companies (Di Mauro et al., 2018). Cardiac remodeling is a progressive process accompanied by abnormal cell metabolism and function, remodeling of matrix components, and ultimately results in organ and systemic dysfunction (Schirone et al., 2017). As described above, several *in vitro* and *in vivo* studies have confirmed the critical roles of non-coding RNAs in cardiac remodeling. Cardiac-specific gene modulation experiments have shown a great potential to prevent and attenuate cardiac dysfunction or pathological progression in heart disease, thus highlighting the potential of non-coding RNAs as therapeutic targets. Here we will discuss the strategies currently available for non-coding RNA modulation and the potential issues that exist regarding the effectiveness of non-coding RNA-based therapies.

Drug and cell-based therapies in cardiac hypertrophy and ischemic injury have been found as effective intervention strategies (Machaj et al., 2019). However, the exact mechanisms and pathways involved are not always clear. Interestingly, some pharmacological agents have been described to act by regulating non-coding RNA expression and activities. An example of this is Losartan, an angiotensin II receptor antagonist used to treat hypertension. Losartan appears to diminish the effects of Ang II-induced fibrosis by restoring the lncRNA-NR024118 and Cdkn1c expression in cardiac fibroblasts (Jiang et al., 2015). It has also been shown that Atorvastatin, a hydroxymethylglutaryl coenzyme A reductase inhibitor used to treat dyslipidemia, possesses beneficial effects in patients with ischemic and non-ischemic induced heart failure. In a hypoxic cardiac progenitor cell (CPC) model, Atorvastatin treatment can protect progenitor cells from hypoxia-induced injury by inhibiting the expression of the lncRNA MEG3. MEG3 plays a role in CPC viability and proliferation by regulating HMGB1 expression through the inhibition of miR-22 (Su et al., 2018). These studies highlight the relevance of non-coding RNAs in the molecular mechanism of drugs currently used in the treatment of cardiovascular disease by protecting cardiac cells. Additionally, the direct modulation of the activity of non-coding RNA might present novel opportunities to develop more targeted and fine-tuned therapeutic approaches. Manipulation of the expression of miRNAs or lncRNAs with gene-based technologies has been effectively performed in animals, confirming the feasibility to ameliorate cardiac remodeling, myocardial inflammation and cell death, and heart hypertrophy using these genetic tools (Wang et al., 2018b).

It is possible to modulate the expression of non-coding RNAs in settings of disease progression in a tissue and cell-type specific fashion, which is promising for precision therapy. However, the challenge to transform the existing knowledge and methodologies used in research into therapies of relevance for clinical trials still persists. As non-coding RNAs are, compared to proteins, new potential therapeutic targets, the information about the effects of non-coding RNA based therapies is also limited and no extensive clinical data is available. Additionally, a key issue that needs to be addressed is that, particularly lncRNAs, have poor sequence conservation, presenting a clear challenge to extrapolate the

findings observed in *in vivo* models to clinical based strategies requiring further optimization to ensure target selectivity and overall long term safety of non-coding RNA-based approaches (Poller and Fechner, 2010).

Another issue is that non-coding RNAs usually are degraded quickly and, as with other types of RNA, are damage prone (Amaral et al., 2013). Thus, exogenous gene delivery vectors, such as viruses are required for *in vivo* experiments (Di Mauro et al., 2018). Moreover, in the translation into clinical interventions, additional factors such as determination of bioavailability, optimization of delivery and distribution, safety, efficiency, concentration, stability, timing, etc. should be taken into consideration.

NON-CODING RNA MODULATION STRATEGIES

In general, silencing of RNA is achieved by inhibitors, such as sequence-specific RNA interference (RNAi), antisense oligonucleotides (ASO) or the use of small molecule inhibitors. On the other hand, the overexpression or upregulation of non-coding RNA activities can be achieved by synthetic non-coding RNA mimics and other gene delivery strategies such as adeno-associated virus (Poller et al., 2010).

The use of antisense molecules has already been used in clinical trials targeting protein-coding mRNAs. An example, approved by the Food and Drug Administration, is Eteplirsen, a drug used to treat Duchenne muscular dystrophy caused by loss-of-function mutations in the *DMD* gene coding for dystrophin. Eteplirsen restores the translational reading frame of *DMD* through specific skipping of exon 51 in defective gene variants (Lim et al., 2017). In contrast to mRNAs and miRNAs, lncRNAs functions depend on their subcellular localization (Lennox and Behlke, 2016). Thus, for targeting lncRNAs this must be taken into consideration. For example, RNAi strategies will target RNA molecules in the cytoplasm, thus this approach might not be useful targeting nuclear lncRNAs. Additionally, tissue and cell type dependent expression has to be considered for targeted lncRNA modulation using specific delivery of antisense based therapies in different cardiovascular diseases.

Non-coding RNAs Down-Regulation Strategies

miRNA target inhibitors and small molecule inhibitors: The binding of an inhibitor or protector interferes with the interaction of an miRNA with its target mRNA and therefore inhibits its silencing (Choi et al., 2007). Additionally, miRNA inhibition can be achieved with the use of low molecular weight compounds, known as small molecule inhibitors, that impair miRNA function by interfering with the miRNA maturation, processing and degradation machinery. An example of the use of these molecules in miRNA down-regulation is the use of diazobenzene 1 to inhibit the action of miR-21 (Gumireddy et al., 2008).

lncRNA small molecule inhibitors: As with miRNAs, use of small molecule inhibitors as an alternative strategy has to be taken into consideration for lncRNA modulation. Small compounds can inhibit the lncRNA activity by interfering with its binding to their targets (Colley and Leedman, 2009). The use of small molecules to modulate miRNA and lncRNA is currently being studied in cancer with promising results in the regulation of lncRNAs such as *HOTAIR* and MALAT1 (Arun et al., 2018). Interestingly, both these lncRNAs have been described to be implicated in cardiomyocyte survival and cardiac pathology, thus highlighting the potential use of this approach to treat lncRNA dysregulation in heart disease.

miRNA sponges and competitors: Similar to lncRNAs, artificial miRNA sponges can be generated using vectors with specific miRNAs binding sites. This will prevent the target miRNA activity by either sponging and decreasing the miRNA availability, competing for its binding target genes, or acting by interfering the miRNA–mRNA (or lncRNA) binding (Ebert et al., 2007).

Anti-miRNA Oligodeoxyribonucleotides (ASOs)

This strategy relies on small antisense oligonucleotides that act as miRNAs inhibitors by annealing to their guide strand. This results in either conformational changes that alter their function, or the degradation of the target miRNA (Broderick and Zamore, 2011). This approach has been extensively used in research and ASOs have been modified in order to improve their uptake, stability, and binding specificity. Addition of a 2′-*O*-methyl or 2′-*O*-methoxyethyl group to the RNA 2′-ribose results in the prevention of RISC nuclease degradation (Krützfeldt et al., 2005). Another important chemical modification, locked-nucleotide (LNA), enables an increased affinity and target specificity toward complementary single-stranded RNA molecules, by the formation of a methylene bridge between the 2′ oxygen with the 4′ carbon of the ribose ring (Thayer et al., 2019). However, the use of LNA oligonucleotides has been linked with liver damage (Burdick et al., 2014). This highlights the need for chemical refinement of ASOs before their use in the clinic.

LncRNA RNA-Interference (RNAi)

Although, RNAi-based technology is widely used for lncRNA downregulation, as mentioned above, it has to be taken into consideration that RNAi will mainly act in the cytoplasm. Thus, this approach will not be effective targeting lncRNAs that are active in the nucleus. The use of GapmeRs are a way to overcome this issue since they are able to block lncRNA activity in the nucleus via the nuclear endonuclease RNase H–dependent degradation (Lennox and Behlke, 2016). Structurally, GapmeRs consist of a DNA core flanked by two LNA sequences, which are complementary to the target RNA sequence. The chemical "lock" in the ribose backbone provides LNA with higher stability and increased endonuclease activity, resulting in greater knockdown efficiency (Swayze et al., 2006).

GapmeR-mediated silencing has been used to downregulate the lncRNA Chast, which mediates cardiac hypertrophy *in vivo* in mice and human cells *in vitro* (Viereck et al., 2016). The use of a GapmeR complimentary to Chast prevented and ameliorated pressure overload induced cardiac remodeling with no toxicological side effects. Similarly, *in vivo*, GapmeR-induced

knockdown of the conserved lncRNA Wisp2 super-enhancer–associated RNA (Wisper) in mice subjected to MI results in reduced fibrosis and overall infarct size, and preserved cardiac function, further highlighting the potential use of lncRNA manipulation via GapmeRs for translation into clinics (Micheletti et al., 2017). Currently, the main limitations of these technologies are the formation of secondary structures that impair RNAi and GapmeR activity.

Virus-Mediated Gene Silencing

The adeno-associated virus (AAV) system has been used as a silencing strategy by carrying shRNA designed to specifically target lncRNAs in cardiac cells. An example of this is Meg3, a lncRNA which is highly conserved and enriched in both mouse and human hearts; increased expression of the lncRNA *Meg3* leads to profound cardiomyocyte apoptosis (Wu et al., 2018). *Meg3* inactivation by injection of an AAV9 system carrying *Meg3* shRNA into mouse hearts after MI preserved significantly cardiac function, suggesting that knockdown in a cardiomyocytes-specific manner can be achieved using AAV9 systems presenting a promising tool to treat cardiac disease in preclinical models.

Non-coding RNAs Upregulation Strategies

In addition to inhibition or down-regulation of harmful non-coding RNAs, restoration of miRNA and lncRNA expression and activity has become a potential strategy for treatment in cardiac disease. The use of viral-mediated gene delivery, nanoparticles, or RNA mimics can be used to restore their expression when it is decreased in pathological contexts (Hobuß et al., 2019).

miRNA Mimics

miRNA mimics are synthetic small RNA molecules designed to be identical to a specific miRNA, thus restoring the expression of a miRNA that might be downregulated in a given pathological setting. This approach is the most widely used strategy for miRNA activity restoration. Similar to ASOs, mimics can also be modified to improve their activity, safety, delivery, and stability (Rupaimoole and Slack, 2017).

Virus-mediated gene expression: As a novel alternative, there is growing interest in the use of miRNA-expressing viral vectors (Xie et al., 2015). Lentivirus and adeno-associated virus (AAV) allow efficient gene delivery in a tissue specific manner. However, this approach still presents safety risks due to potential random viral DNA insertions into the genome or dysregulated overexpression of the delivered miRNA (Williams, 2007). Similar to the limitations in miRNA up-regulation strategies, lncRNA over-expression technologies are not fully developed. For example, the AAV vectors used for gene therapy in animal models have low packaging capacity and are not suited for lncRNA longer than 4 kb. Thus, more efforts are needed to develop novel strategies for lncRNA upregulation and restoration *in vivo*. Nevertheless, some studies have provided proof of principle for cardioprotective non-coding RNA upregulation via virus gene delivery in a preventative therapeutic approach in MI (Wang et al., 2014b).

Adeno-associated viruses (AAV) provide long-term, and efficient gene delivery into the heart. Furthermore, AAV systems have been used in clinical trials, such as the Calcium upregulation by percutaneous administration of gene therapy in cardiac disease (CUPID) trial which aims to restore SERCA2a by enzyme replacement via gene therapy (Jessup et al., 2011). However, less promising results have been observed in larger clinical trials. It is possible that modulation of single targets is not the optimal approach for treatment of many multifactorial diseases such as heart disease. Adenoviral overexpression of the previously described lncRNA Carl in MI models inhibits mitochondrial fission and cardiomyocyte loss via inhibition of miR-539 resulting in smaller infarct sizes *in vivo* (Wang et al., 2014b). However, overexpression of lncRNAs using viral gene delivery is still challenging and needs to overcome different limitations including the efficiency of infection and regulation of the lncRNA expression, which may differ depending on the pathological context. Considerations, such as whether transient or stable overexpression of a particular gene is needed, the magnitude of the response needed, the timing of the expression and cell specificity, have to be taken into consideration for therapeutic treatment.

FUTURE PERSPECTIVES

Despite the evidence of the role of lncRNAs and miRNAs in the regulation of ER stress in the heart, to date the interaction between these regulatory RNAs in the context of cardiac disease remains unknown. Evidence from other disease models highlights the potential relevance of this new level of regulation in the promotion of the UPR in order to alleviate ER stress. We propose that the study of lncRNA–miRNA–mRNA axis and other forms of non-coding RNA interactions in the context of ER stress in cardiomyocytes could give insights into new levels of regulation of the progression of cardiac hypertrophy and ischemic damage.

For instance, the lncRNA MIAT, previously described in models of MI and hypertrophy, participates in the regulation of the ER chaperone, GRP78. Both MIAT and GRP78 levels are increased in Müller cells under high-glucose treatment (Xu et al., 2019). Mechanistically, MIAT acts as a molecular sponge for microRNA-379, which targets GRP78 mRNA for its degradation. Similarly, another study in a high glucose diabetic model shows an upregulation of around 40 miRNAs within the miR-379 megacluster. Interestingly, this megacluster is hosted by the lncRNA lnc-MGC which is upregulated by ER stress (Kato et al., 2016). The miRNAs in the cluster, as mentioned above, target different groups of genes participating in fibrosis, protein synthesis, and ER stress, resulting in hypertrophy via dysregulation of protein synthesis and extracellular matrix accumulation related to diabetic nephropathy. Thus, in pathological conditions, the increase in lncRNA MGC and the miR-379 cluster further enhance ER stress and nephropathy phenotypes by inhibiting the miR-379 cluster targets. Additionally, Xbp1 splicing and Atf3 downregulation occurs via upregulation of miR-494, one of the miR-379 cluster

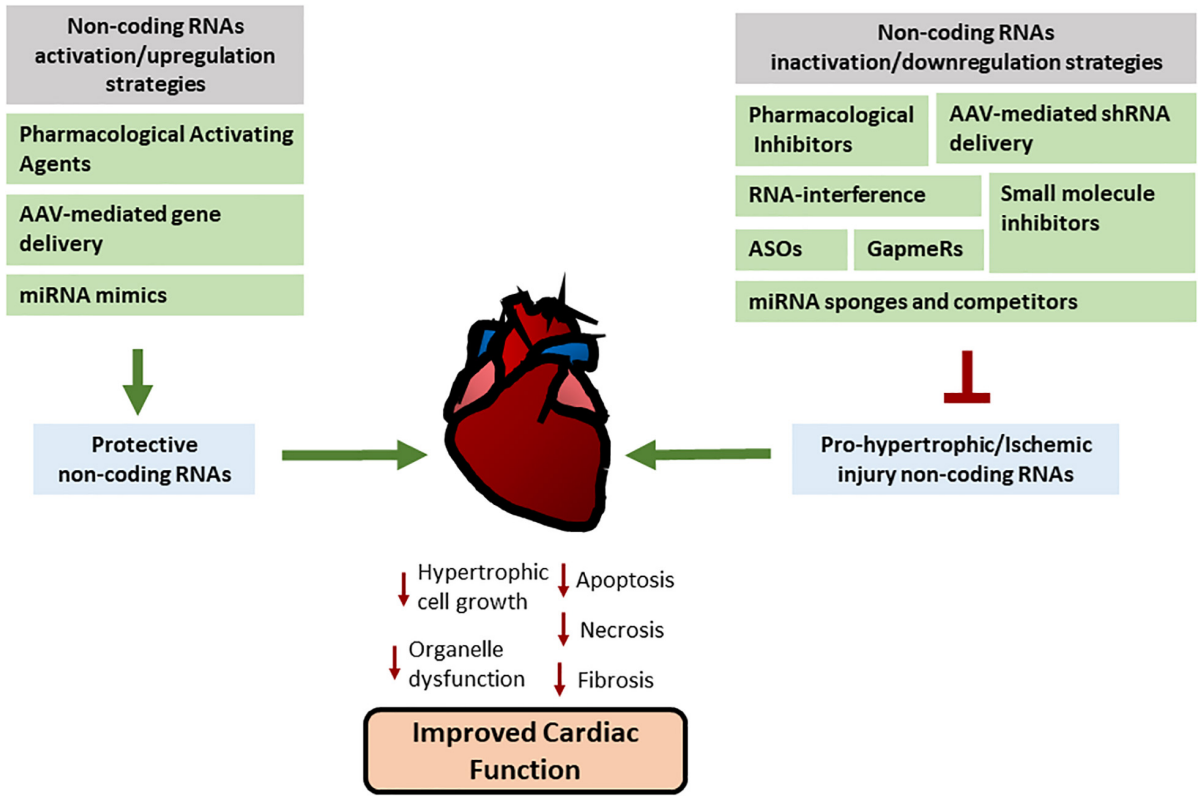

FIGURE 2 | Therapeutic approaches used for non-coding RNA modulation. Different pharmacological and genetic approaches are being developed in order to regulate miRNAs and lncRNAs activities or manipulate their expression. Their main aim is to increase the activity or upregulate/restore the expression of non-coding RNAs with cardiac protective effects (on the left) or inhibit or downregulate the expression of non-coding RNAs that have a detrimental effect in heart pathology (on the right) in order to reduce the progression of pathological processes. See text for more details.

miRNAs, which participates in the upregulation of Chop in response to high glucose or TGF-β1 in mouse mesangial cells (Kato et al., 2016). Furthermore, it was observed that miR-379 cluster upregulation in diabetes contributes to ER stress via loss of Edem3. Therapeutically, as previously described, the use of GapmeRs is an attractive and effective strategy for the regulation of cellular functions mediated by LncRNAs. Inhibition of the miRNA cluster by targeting its host lnc-MGC using the GapmeR MGC10 was able to ameliorate matrix accumulation and glomerular hypertrophy in mice by restoring the expression of the cluster miRNA targets.

In a diabetic nephropathy model the ER stress response can be regulated by the lncRNA LINC01619 acting as a molecular sponge for miR-27a (Bai et al., 2018). miR-27a targets forkhead box protein O1 (FOXO1) for its degradation leading to ER stress activation and resulting in podocyte injury. Inhibition of miR-27a can effectively increase the expression level of FOXO1 and decrease the ER stress markers CHOP and GRP78 in podocytes under high glucose-triggered ER stress, further highlighting the role of lncRNA–miRNA–mRNA regulation in metabolic disease. Additionally, modulation of the ER stress response has also shown to be beneficial in a model of osteosarcoma. The transcription factor ZBTB7A appears to have a pro-survival role in cells undergoing ER stress via suppression of the lncRNA GAS5 by binding to its promoter region and transcriptionally suppressing its expression. Pharmacological induction of ER stress results in the downregulation of ZBTB7A accompanied by sustained apoptosis. Mechanistically, ER stress triggers the induction of miR-663a which targets the 3′UTR of ZBTB7A for its downregulation, resulting in an upregulation of GAS5 leading to ER stress-induced cell apoptosis (Zhang L. et al., 2019).

Overall, since ER stress plays an essential role in cardiac physiology and pathology, finding new approaches to modulate the ER stress responses in the heart is essential to develop novel therapeutic approaches. The further study of the modulation of key stress pathways via the genetic or pharmacological regulation of non-coding RNAs could provide the ability to fine tune these responses in order to enhance pro-survival mechanisms and to minimize the cell and tissue damage in the progression of disease.

CONCLUSION

In summary, a great number of non-coding RNAs are dynamically regulated upon initiation and progression of cardiovascular disease. Many non-coding RNAs have important biological functions and several *in vivo* experiments have revealed that modulation of miRNAs and lncRNAs offers promising

new therapeutic approaches (**Figure 2**). However, inhibition or activation of non-coding RNA function and its consequences still requires further investigation. Refinement on the current approaches and the development of novel strategies will allow in the future clinical translation for non-coding RNA-based therapy and its use in the treatment of different pathologies including cardiovascular disease.

AUTHOR CONTRIBUTIONS

LC and PB development of conceptual ideas and general outline and writing and edition of the manuscript. HC provided critical feedback and editing of the manuscript. XW development of conceptual ideas and provided critical feedback. All authors contributed to the article and approved the submitted version.

REFERENCES

AHA (2019). *Heart Disease and Stroke Statistics-2019 At-a-Glance Heart Disease, Stroke and other Cardiovascular Diseases.* Dallas, TX: AHA.

Alles, J., Fehlmann, T., Fischer, U., Backes, C., Galata, V., Minet, M., et al. (2019). An estimate of the total number of true human miRNAs. *Nucleic Acids Res.* 47, 3353–3364. doi: 10.1093/nar/gkz097

Amaral, P. P., Dinger, M. E., and Mattick, J. S. (2013). Non-coding RNAs in homeostasis, disease and stress responses: an evolutionary perspective. *Brief. Funct. Genomics* 12, 254–278. doi: 10.1093/bfgp/elt016

Andreassi, M. G. (2018). Non-coding RNA in cardiovascular disease: a general overview on microRNAs, long non-coding RNAs and circular RNAs. *Non Coding RNA Investig.* 2:63. doi: 10.21037/ncri.2018.11.03

Arun, G., Diermeier, S. D., and Spector, D. L. (2018). Therapeutic targeting of long non-coding RNAs in cancer. *Trends Mol. Med.* 24, 257–277. doi: 10.1016/j.molmed.2018.01.001

Bai, X., Geng, J., Li, X., Wan, J., Liu, J., Zhou, Z., et al. (2018). Long Noncoding RNA LINC01619 regulates MicroRNA-27a/Forkhead Box Protein O1 and endoplasmic reticulum stress-mediated podocyte injury in diabetic nephropathy. *Antioxid. Redox Signal.* 29, 355–376. doi: 10.1089/ars.2017.7278

Barbagallo, C., Brex, D., Caponnetto, A., Cirnigliaro, M., Scalia, M., Magnano, A., et al. (2018). LncRNA UCA1, upregulated in CRC biopsies and downregulated in serum exosomes, controls mRNA expression by RNA-RNA interactions. *Mol. Ther. Nucleic Acids* 12, 229–241. doi: 10.1016/j.omtn.2018.05.009

Barile, L., Lionetti, V., Cervio, E., Matteucci, M., Gherghiceanu, M., Popescu, L. M., et al. (2014). Extracellular vesicles from human cardiac progenitor cells inhibit cardiomyocyte apoptosis and improve cardiac function after myocardial infarction. *Cardiovasc. Res.* 103, 530–541. doi: 10.1093/cvr/cvu167

Benjamin, E. J., Muntner, P., Alonso, A., Bittencourt, M. S., Callaway, C. W., Carson, A. P., et al. (2019). Heart disease and stroke statistics-2019 update: a report from the american heart association. *Circulation* 139, e56–e528.

Brannan, C. I., Dees, E. C., Ingram, R. S., and Tilghman, S. M. (1990). The product of the H19 gene may function as an RNA. *Mol. Cell. Biol.* 10, 28–36. doi: 10.1128/mcb.10.1.28

Brockdorff, N., Ashworth, A., Kay, G. F., Cooper, P., Smith, S., McCabe, V. M., et al. (1991). Conservation of position and exclusive expression of mouse Xist from the inactive X chromosome. *Nature.* 351, 329–331. doi: 10.1038/351329a0

Broderick, J. A., and Zamore, P. D. (2011). MicroRNA therapeutics. *Gene Ther.* 18, 1104–1110.

Brown, C. J., Ballabio, A., Rupert, J. L., Lafreniere, R. G., Grompe, M., Tonlorenzi, R., et al. (1991). A gene from the region of the human X inactivation centre is expressed exclusively from the inactive X chromosome. *Nature* 349, 38–44. doi: 10.1038/349038a0

Burdick, A. D., Sciabola, S., Mantena, S. R., Hollingshead, B. D., Stanton, R., Warneke, J. A., et al. (2014). Sequence motifs associated with hepatotoxicity of locked nucleic acid–modified antisense oligonucleotides. *Nucleic Acids Res.* 42, 4882–4891. doi: 10.1093/nar/gku142

Byrd, A. E., and Brewer, J. W. (2013). Micro(RNA)managing endoplasmic reticulum stress. *IUBMB Life* 65, 373–381. doi: 10.1002/iub.1151

Carè, A., Catalucci, D., Felicetti, F., Bonci, D., Addario, A., Gallo, P., et al. (2007). MicroRNA-133 controls cardiac hypertrophy. *Nat. Med.* 13, 613–618.

Catalanotto, C., Cogoni, C., and Zardo, G. (2016). MicroRNA in control of gene expression: an overview of nuclear functions. *Int. J. Mol. Sci.* 17:1712. doi: 10.3390/ijms17101712

Cech, T. R., and Steitz, J. A. (2014). The noncoding RNA revolution - Trashing old rules to forge new ones. *Cell* 157, 77–94. doi: 10.1016/j.cell.2014.03.008

Chen, C., Tang, Y., Sun, H., Lin, X., and Jiang, B. (2019). The roles of long noncoding RNAs in myocardial pathophysiology. *Biosci. Rep.* 39, BSR20190966.

Chen, J., Hu, Q., Zhang, B.-F., Liu, X.-P., Yang, S., and Jiang, H. (2019). Long noncoding RNA UCA1 inhibits ischaemia/reperfusion injury induced cardiomyocytes apoptosis via suppression of endoplasmic reticulum stress. *Genes Genomics* 41, 803–810. doi: 10.1007/s13258-019-00806-w

Chistiakov, D. A., Orekhov, A. N., and Bobryshev, Y. V. (2016). Cardiac extracellular vesicles in normal and infarcted heart. *Int. J. Mol. Sci.* 17:63. doi: 10.3390/ijms17010063

Choi, E., Cha, M. J., and Hwang, K. C. (2014). Roles of calcium regulating microRNAs in cardiac ischemia-reperfusion injury. *Cells* 3, 899–913. doi: 10.3390/cells3030899

Choi, W.-Y., Giraldez, A. J., and Schier, A. F. (2007). Target protectors reveal dampening and balancing of nodal agonist and antagonist by miR-430. *Science* 318, 271–274. doi: 10.1126/science.1147535

Colley, S. M., and Leedman, P. J. (2009). SRA and its binding partners: an expanding role for RNA-binding coregulators in nuclear receptor-mediated gene regulation. *Crit. Rev. Biochem. Mol. Biol.* 44, 25–33. doi: 10.1080/10409230802661719

Colpaert, R. M. W., and Calore, M. (2019). MicroRNAs in cardiac diseases. *Cells* 8:737. doi: 10.3390/cells8070737

Curcio, A., Torella, D., Iaconetti, C., Pasceri, E., Sabatino, J., Sorrentino, S., et al. (2013). MicroRNA-1 downregulation increases connexin 43 displacement and induces ventricular tachyarrhythmias in rodent hypertrophic hearts. *PLoS One* 8:e70158. doi: 10.1371/journal.pone.0070158

da Silva, D. C. P., Carneiro, F. D., de Almeida, K. C., and Bottino, C. F. D. S. (2018). Role of miRNAs on the pathophysiology of cardiovascular diseases. *Arq. Bras. Cardiol.* 738–746.

Dey, B. K., Pfeifer, K., and Dutta, A. (2014). The H19 long noncoding RNA gives rise to microRNAs miR-675-3p and miR-675-5p to promote skeletal muscle differentiation and regeneration. *Genes Dev.* 28, 491–501. doi: 10.1101/gad.234419.113

Di Leva, G., and Croce, C. M. (2015). The role of microRNAs in cancer. *Target. Ther. Transl. Cancer Res.* 79, 80–88.

Di Mauro, V., Barandalla-Sobrados, M., and Catalucci, D. (2018). The noncoding-RNA landscape in cardiovascular health and disease. *Non Coding RNA Res.* 3, 12–19. doi: 10.1016/j.ncrna.2018.02.001

Djebali, S., Davis, C. A., Merkel, A., Dobin, A., Lassmann, T., Mortazavi, A., et al. (2012). Landscape of transcription in human cells. *Nature* 489, 101–108.

Ebert, M. S., Neilson, J. R., and Sharp, P. A. (2007). MicroRNA sponges: competitive inhibitors of small RNAs in mammalian cells. *Nat. Methods* 4, 721–726. doi: 10.1038/nmeth1079

Erdmann, V. A., Szymanski, M., Hochberg, A., De Groot, N., and Barciszewski, J. (1999). Collection of mRNA-like non-coding RNAs. *Nucleic Acids Res.* 27, 192–195. doi: 10.1093/nar/27.1.192

Fabbri, M., Paone, A., Calore, F., Galli, R., and Croce, C. M. (2013). A new role for microRNAs, as ligands of Toll-like receptors. *RNA Biol.* 10, 169–174. doi: 10.4161/rna.23144

Faghihi, M. A., Zhang, M., Huang, J., Modarresi, F., Van der Brug, M. P., Nalls, M. A., et al. (2010). Evidence for natural antisense transcript-mediated inhibition of microRNA function. *Genome Biol.* 11:R56.

Frangogiannis, N. G. (2017). The extracellular matrix in myocardial injury, repair, and remodeling. *J. Clin. Invest.* 127, 1600–1612. doi: 10.1172/jci87491

Frey, N., and Olson, E. N. (2003). Cardiac hypertrophy: the good, the bad, and the ugly. *Annu. Rev. Physiol.* 65, 45–79. doi: 10.1146/annurev.physiol.65.092101.142243

Fu, H. Y., Okada, K.-I., Liao, Y., Tsukamoto, O., Isomura, T., Asai, M., et al. (2010). Ablation of C/EBP homologous protein attenuates endoplasmic reticulum-mediated apoptosis and cardiac dysfunction induced by pressure overload. *Circulation* 122, 361–369. doi: 10.1161/circulationaha.109.917914

Gabisonia, K., Prosdocimo, G., Aquaro, G. D., Carlucci, L., Zentilin, L., Secco, I., et al. (2019). MicroRNA therapy stimulates uncontrolled cardiac repair after myocardial infarction in pigs. *Nature* 569, 418–422. doi: 10.1038/s41586-019-1191-6

Galeano-Otero, I., Del Toro, R., Guisado, A., Díaz, I., Mayoral-González, I., Guerrero-Márquez, F., et al. (2020). Circulating miR-320a as a predictive biomarker for left ventricular remodelling in STEMI patients undergoing primary percutaneous coronary intervention. *J. Clin. Med.* 9:E1051.

Gangadaran, P., Hong, C. M., and Ahn, B. C. (2018). An update on *in vivo* imaging of extracellular vesicles as drug delivery vehicles. *Front. Pharmacol.* 9:169. doi: 10.3389/fphar.2018.00169

Gao, L., Liu, Y., Guo, S., Yao, R., Wu, L., Xiao, L., et al. (2017). Circulating long noncoding RNA HOTAIR is an essential mediator of acute myocardial infarction. *Cell. Physiol. Biochem.* 44, 1497–1508.

Goldie, B. J., Dun, M. D., Lin, M., Smith, N. D., Verrills, N. M., Dayas, C. V., et al. (2014). Activity-associated miRNA are packaged in Map1b-enriched exosomes released from depolarized neurons. *Nucleic Acids Res.* 42, 9195–9208. doi: 10.1093/nar/gku594

Gong, C., and Maquat, L. E. (2011). LncRNAs transactivate STAU1-mediated mRNA decay by duplexing with 39 UTRs via Alu eleme. *Nature* 470, 284–290.

Guan, X., Wang, L., Liu, Z., Guo, X., Jiang, Y., Lu, Y., et al. (2016). miR-106a promotes cardiac hypertrophy by targeting mitofusin 2. *J. Mol. Cell. Cardiol.* 99, 207–217. doi: 10.1016/j.yjmcc.2016.08.016

Guduric-Fuchs, J., O'Connor, A., Camp, B., O'Neill, C. L., Medina, R. J., and Simpson, D. A. (2012). Selective extracellular vesicle-mediated export of an overlapping set of microRNAs from multiple cell types'. *BMC Genomics* 13:357. doi: 10.1186/1471-2164-13-357

Gumireddy, K., Young, D. D., Xiong, X., Hogenesch, J. B., Huang, Q., and Deiters, A. (2008). Small-molecule inhibitors of microrna miR-21 function. *Angew. Chem.* 47, 7482–7484. doi: 10.1002/anie.200801555

Gupta, R. A., Shah, N., Wang, K. C., Kim, J., Horlings, H. M., Wong, D. J., et al. (2010). Long non-coding RNA HOTAIR reprograms chromatin state to promote cancer metastasis. *Nature* 464, 1071–1076. doi: 10.1038/nature08975

Han, P., Li, W., Lin, C. H., Yang, J., Shang, C., Nurnberg, S. T., et al. (2014). A long noncoding RNA protects the heart from pathological hypertrophy. *Nature* 514, 102–106. doi: 10.1038/nature13596

Henning, R. H., and Brundel, B. J. J. M. (2017). Proteostasis in cardiac health and disease. *Nat. Rev. Cardiol.* 14, 637–653. doi: 10.1038/nrcardio.2017.89

Hobuß, L., Bär, C., and Thum, T. (2019). Long non-coding RNAs: At the heart of cardiac dysfunction? *Front. Physiol.* 10:30. doi: 10.3389/fphys.2019.00030

Horváth, M., Horváthová, V., Hájek, P., Štìchovský, C., Honěk, J., Šenolt, L., et al. (2020). MicroRNA-331 and microRNA-151-3p as biomarkers in patients with ST-segment elevation myocardial infarction. *Sci. Rep.* 10:5845.

Huang, S., Zhang, L., Song, J., Wang, Z., Huang, X., Guo, Z., et al. (2019). Long noncoding RNA MALAT1 mediates cardiac fibrosis in experimental postinfarct myocardium mice model'. *J. Cell. Physiol.* 234, 2997–3006. doi: 10.1002/jcp.27117

Huang, Z. W., Tian, L. H., Yang, B., and Guo, R. M. (2017). Long NONCODING RNA H19 acts as a competing endogenous RNA to mediate CTGF expression by sponging miR-455 in cardiac fibrosis. *DNA Cell Biol.* 36, 759–766. doi: 10.1089/dna.2017.3799

Hung, T., Wang, Y., Lin, M. F., Koegel, A. K., Kotake, Y., Grant, G. D., et al. (2011). Extensive and coordinated transcription of noncoding RNAs within cell-cycle promoters. *Nat. Genet.* 43, 621–629. doi: 10.1038/ng.848

Ishii, N., Ozaki, K., Sato, H., Mizuno, H., Susumu, S., Takahashi, A., et al. (2006). Identification of a novel non-coding RNA, MIAT, that confers risk of myocardial infarction. *J. Hum. Genet.* 51, 1087–1099. doi: 10.1007/s10038-006-0070-9

Jäntti, T., Segersvärd, H., Tolppanen, H., Tarvasmäki, T., Lassus, J., Devaux, Y., et al. (2019). Circulating levels of microRNA 423-5p are associated with 90 day mortality in cardiogenic shock. *ESC Heart Fail.* 6, 98–102. doi: 10.1002/ehf2.12377

Jarroux, J., Morillon, A., and Pinskaya, M. (2017). History, discovery, and classification of lncRNAs. *Adv. Exp. Med. Biol.* 1008, 1–46. doi: 10.1007/978-981-10-5203-3_1

Jessup, M., Greenberg, B., Mancini, D., Cappola, T., Pauly, D. F., Jaski, B., et al. (2011). Calcium Upregulation by Percutaneous Administration of Gene Therapy in Cardiac Disease (CUPID): a phase 2 trial of intracoronary gene therapy of sarcoplasmic reticulum Ca2+-ATPase in patients with advanced heart failure. *Circulation* 124, 304–313. doi: 10.1161/circulationaha.111.022889

Jiang, F., Zhou, X., and Huang, J. (2016). Long non-coding RNA-ROR mediates the reprogramming in cardiac hypertrophy. *PLoS One* 11:e0152767. doi: 10.1371/journal.pone.0152767

Jiang, X., Zhang, F., and Ning, Q. (2015). Losartan reverses the down-expression of long noncoding RNA-NR024118 and Cdkn1c induced by angiotensin II in adult rat cardiac fibroblasts. *Pathol. Biol.* 63, 122–125. doi: 10.1016/j.patbio.2015.04.001

Kalogeris, T., Baines, C. P., Krenz, M., and Korthuis, R. J. (2012). Cell biology of ischemia/reperfusion injury. *Int. Rev. Cell Mol. Biol.* 298, 229–317. doi: 10.1016/b978-0-12-394309-5.00006-7

Kato, M., Wang, M., Chen, Z., Bhatt, K., Oh, H. J., Lanting, L., et al. (2016). An endoplasmic reticulum stress-regulated lncRNA hosting a microRNA megacluster induces early features of diabetic nephropathy. *Nat. Commun.* 7, 12864–12864.

Kayvanpour, E., Gi, W. T., Sedaghat-Hamedani, F., Lehmann, D. H., Frese, K. S., Haas, J., et al. (2020). microRNA neural networks improve diagnosis of acute coronary syndrome (ACS). *J. Mol. Cell. Cardiol.* 30097–30093. doi: 10.1016/j.yjmcc.2020.04.014 [Epub ahead of print].

Ke, Z.-P., Xu, P., Shi, Y., and Gao, A.-M. (2016). MicroRNA-93 inhibits ischemia-reperfusion induced cardiomyocyte apoptosis by targeting PTEN. *Oncotarget* 7, 28796–28805. doi: 10.18632/oncotarget.8941

Keniry, A., Oxley, D., Monnier, P., Kyba, M., Dandolo, L., Smits, G., et al. (2012). The H19 lincRNA is a developmental reservoir of miR-675 that suppresses growth and Igf1r. *Nat. Cell Biol.* 14, 659–665. doi: 10.1038/ncb2521

Khan, M. S., Yamashita, K., Sharma, V., Ranjan, R., and Dosdall, D. J. (2020). RNAs and gene expression predicting postoperative atrial fibrillation in cardiac surgery patients undergoing coronary artery bypass grafting. *J. Clin. Med.* 9:E1139.

Kim, G. H. (2013). MicroRNA regulation of cardiac conduction and arrhythmias. *Transl. Res.* 161, 381–392. doi: 10.1016/j.trsl.2012.12.004

Kim, I., Xu, W., and Reed, J. C. (2008). Cell death and endoplasmic reticulum stress: disease relevance and therapeutic opportunities. *Nat. Rev. Drug Discov.* 7, 1013–1030. doi: 10.1038/nrd2755

Kiyosawa, N., Watanabe, K., Morishima, Y., Yamashita, T., Yagi, N., Arita, T., et al. (2020). Exploratory analysis of circulating miRNA signatures in atrial fibrillation patients determining potential biomarkers to support decision-making in anticoagulation and catheter ablation. *Int. J. Mol. Sci.* 21:2444. doi: 10.3390/ijms21072444

Koga, Y., Yasunaga, M., Moriya, Y., Akasu, T., Fujita, S., Yamamoto, S., et al. (2011). 'Exosome can prevent RNase from degrading microRNA in feces. *J. Gastrointest. Oncol.* 2, 215–222.

Kong, F., Jin, J., Lv, X., Han, Y., Liang, X., Gao, Y., et al. (2019). Long noncoding RNA RMRP upregulation aggravates myocardial ischemia-reperfusion injury by sponging miR-206 to target ATG3 expression. *Biomed. Pharmacother.* 109, 716–725. doi: 10.1016/j.biopha.2018.10.079

Kong, P., Christia, P., and Frangogiannis, N. G. (2014). The pathogenesis of cardiac fibrosis. *Cell. Mol. Life Sci.* 71, 549–574.

Krijnen, P. A. J., Nijmeijer, R., Meijer, C. M., Visser, C. A., Hack, C. E., and Niessen, H. W. M. (2002). Apoptosis in myocardial ischaemia and infarction. *J. Clin. Pathol.* 55, 801–811. doi: 10.1136/jcp.55.11.801

Krützfeldt, J., Rajewsky, N., Braich, R., Rajeev, K. G., Tuschl, T., Manoharan, M., et al. (2005). Silencing of microRNAs *in vivo* with 'antagomirs'. *Nature* 438, 685–689. doi: 10.1038/nature04303

Kumarswamy, R., Bauters, C., Volkmann, I., Maury, F., Fetisch, J., Holzmann, A., et al. (2014). Circulating long noncoding RNA. LIPCAR, predicts survival in patients with heart failure. *Circ. Res.* 114, 1569–1575. doi: 10.1161/circresaha.114.303915

Kumarswamy, R., and Thum, T. (2013). Non-coding RNAs in cardiac remodeling and heart failure. *Circ. Res.* 113, 676–689. doi: 10.1161/circresaha.113.300226

Lai, F., Orom, U. A., Cesaroni, M., Beringer, M., Taatjes, D. J., Blobel, G. A., et al. (2013). Activating RNAs associate with Mediator to enhance chromatin architecture and transcription. *Nature* 494, 497–501. doi: 10.1038/nature11884

Lee, R. C., Feinbaum, R. L., and Ambros, V. (1993). The *C. elegans* heterochronic gene lin-4 encodes small RNAs with antisense complementarity to lin-14. *Cell* 75, 843–854. doi: 10.1016/0092-8674(93)90529-y

Lee, S., Choi, E., Cha, M. J., and Hwang, K. C. (2014). Looking into a conceptual framework of ROS-miRNA-atrial fibrillation. *Int. J. Mol. Sci.* 15, 21754–21776. doi: 10.3390/ijms151221754

Lennox, K. A., and Behlke, M. A. (2016). Cellular localization of long non-coding RNAs affects silencing by RNAi more than by antisense oligonucleotides. *Nucleic Acids Res.* 44, 863–877. doi: 10.1093/nar/gkv1206

Leucci, E., Patella, F., Waage, J., Holmstrøm, K., Lindow, M., Porse, B., et al. (2013). MicroRNA-9 targets the long non-coding RNA MALAT1 for degradation in the nucleus. *Sci. Rep.* 3:2535.

Leung, A., Trac, C., Jin, W., Lanting, L., Akbany, A., Sætrom, P., et al. (2013). Novel long noncoding RNAs are regulated by angiotensin II in vascular smooth muscle cells. *Circ. Res.* 113, 266–278. doi: 10.1161/circresaha.112.300849

Levine, B., and Kroemer, G. (2008). Autophagy in the pathogenesis of disease. *Cell* 132, 27–42. doi: 10.1016/j.cell.2007.12.018

Li, J., Rohailla, S., Gelber, N., Rutka, J., Sabah, N., Gladstone, R. A., et al. (2014). MicroRNA-144 is a circulating effector of remote ischemic preconditioning. *Basic Res. Cardiol.* 109:423.

Li, L., Zhang, M., Chen, W., Wang, R., Ye, Z., Wang, Y., et al. (2018a). LncRNA-HOTAIR inhibition aggravates oxidative stress-induced H9c2 cells injury through suppression of MMP2 by miR-125. *Acta Biochim. Biophys. Sin.* 50, 996–1006. doi: 10.1093/abbs/gmy102

Li, L., Wang, J. J., and Zhang, H. S. (2018d). LncRNA-CARl in a rat model of myocardial infarction'. *Eur. Rev. Med. Pharmacol. Sci.* 22, 4332–4340.

Li, M., Duan, L., Li, Y., and Liu, B. (2019). Long noncoding RNA/circular noncoding RNA-miRNA-mRNA axes in cardiovascular diseases. *Life Sci.* 233:116440.

Li, N., Wang, K., and Li, P.-F. (2015a). MicroRNA-34 family and its role in cardiovascular disease. *Crit. Rev. Eukaryot. Gene Expr.* 25, 293–297. doi: 10.1615/critreveukaryotgeneexpr.2015015396

Li, Q., Shao, Y., Zhang, X., Zheng, T., Miao, M., Qin, L., et al. (2015b). Plasma long noncoding RNA protected by exosomes as a potential stable biomarker for gastric cancer. *Tumour Biol.* 36, 2007–2012. doi: 10.1007/s13277-014-2807-y

Li, Y., Wang, J., Sun, L., and Zhu, S. (2018b). LncRNA myocardial infarction-associated transcript (MIAT) contributed to cardiac hypertrophy by regulating TLR4 via miR-93. *Eur. J. Pharmacol.* 818, 508–517. doi: 10.1016/j.ejphar.2017.11.031

Li, Z., Liu, Y., Guo, X., Sun, G., Ma, Q., Dai, Y., et al. (2018c). Long noncoding RNA myocardial infarction-associated transcript is associated with the microRNA-150-5p/P300 pathway in cardiac hypertrophy'. *Int. J. Mol. Med.* 42, 1265–1272.

Liang, H., Pan, Z., Zhao, X., Liu, L., Sun, J., Su, X., et al. (2018). LncRNA PFL contributes to cardiac fibrosis by acting as a competing endogenous RNA of let-7d. *Theranostics* 8, 1180–1194. doi: 10.7150/thno.20846

Lim, K. R. Q., Maruyama, R., and Yokota, T. (2017). Eteplirsen in the treatment of Duchenne muscular dystrophy. *Drug Des. Dev. Ther.* 11, 533–545. doi: 10.2147/dddt.s97635

Liu, F., Li, N., Long, B., Fan, Y. Y., Liu, C. Y., Zhou, Q. Y., et al. (2014). Cardiac hypertrophy is negatively regulated by miR-541. *Cell Death Dis.* 5:e1171. doi: 10.1038/cddis.2014.141

Liu, L., An, X., Li, Z., Song, Y., Li, L., Zuo, S., et al. (2016). The H19 long noncoding RNA is a novel negative regulator of cardiomyocyte hypertrophy. *Cardiovasc. Res.* 111, 56–65. doi: 10.1093/cvr/cvw078

Liu, Q., Sargent, M. A., York, A. J., and Molkentin, J. D. (2009). ASK1 regulates cardiomyocyte death but not hypertrophy in transgenic mice. *Circ. Res.* 105, 1110–1117. doi: 10.1161/circresaha.109.200741

Lu, Y., Zhang, Y., Wang, N., Pan, Z., Gao, X., Zhang, F., et al. (2010). MicroRNA-328 contributes to adverse electrical remodeling in atrial fibrillation'. *Circulation* 122, 2378–2387. doi: 10.1161/circulationaha.110.958967

Lv, L., Li, T., Li, X., Xu, C., Liu, Q., Jiang, H., et al. (2018). The lncRNA Plscr4 controls cardiac hypertrophy by regulating miR-214. *Mol. Ther. Nucleic Acids* 10, 387–397. doi: 10.1016/j.omtn.2017.12.018

Machaj, F., Dembowska, E., Rosik, J., Szostak, B., Mazurek-Mochol, M., and Pawlik, A. (2019). New therapies for the treatment of heart failure: a summary of recent accomplishments. *Ther. Clin. Risk Manage.* 15, 147–155. doi: 10.2147/tcrm.s179302

Masè, M., Grasso, M., Avogaro, L., Nicolussi Giacomaz, M., D'Amato, E., Tessarolo, F., et al. (2019). Upregulation of miR-133b and miR-328 in patients with atrial dilatation: implications for stretch-induced atrial fibrillation. *Front. Physiol.* 10:1133. doi: 10.3389/fphys.2019.01133

McCully, J. D., Wakiyama, H., Hsieh, Y.-J., Jones, M., and Levitsky, S. (2004). Differential contribution of necrosis and apoptosis in myocardial ischemia-reperfusion injury. *Am. J. Physiol. Heart Circul. Physiol.* 286, H1923–H1935.

Melo, S. A., Sugimoto, H., O'Connell, J. T., Kato, N., Villanueva, A., Vidal, A., et al. (2014). Cancer exosomes perform cell-independent microRNA biogenesis and promote tumorigenesis. *Cancer Cell* 26, 707–721. doi: 10.1016/j.ccell.2014.09.005

Micheletti, R., Plaisance, I., Abraham, B. J., Sarre, A., Ting, C.-C., Alexanian, M., et al. (2017). The long noncoding RNA Wisper controls cardiac fibrosis and remodeling. *Sci. Transl. Med.* 9:eaai9118. doi: 10.1126/scitranslmed.aai9118

Minamino, T., Komuro, I., and Kitakaze, M. (2010). Endoplasmic reticulum stress as a therapeutic target in cardiovascular disease. *Circ. Res.* 107, 1071–1082. doi: 10.1161/circresaha.110.227819

Mitchell, P. S., Parkin, R. K., Kroh, E. M., Fritz, B. R., Wyman, S. K., Pogosova-Agadjanyan, E. L., et al. (2008). Circulating microRNAs as stable blood-based markers for cancer detection. *Proc. Natl. Acad. Sci. U.S.A.* 105, 10513–10518.

Mohammad, F., Mondal, T., and Kanduri, C. (2009). 'Epigenetics of imprinted long noncoding RNAs. *Epigenetics* 4, 277–286. doi: 10.4161/epi.4.5.9242

Morelli, M. B., Shu, J., Sardu, C., Matarese, A., and Santulli, G. (2019). Cardiosomal microRNAs are essential in post-infarction myofibroblast phenoconversion. *Int. J. Mol. Sci.* 21:201. doi: 10.3390/ijms21010201

Murry, C. E., Reinecke, H., and Pabon, L. M. (2006). Regeneration gaps: observations on stem cells and cardiac repair. *J. Am. Coll. Cardiol.* 47, 1777–1785.

Nagata, S. (1997). Apoptosis by death factor. *Cell* 88, 355–365. doi: 10.1016/s0092-8674(00)81874-7

Nakamura, M., and Sadoshima, J. (2018). Mechanisms of physiological and pathological cardiac hypertrophy. *Nat. Rev. Cardiol.* 15, 387–407. doi: 10.1038/s41569-018-0007-y

O'Brien, J., Hayder, H., Zayed, Y., and Peng, C. (2018). Overview of microRNA biogenesis, mechanisms of actions, and circulation. *Front. Endocrinol.* 9:402. doi: 10.3389/fendo.2018.00402

Oliveira, K. C. D. S., Araújo, T. M. T., Albuquerque, C. I., Barata, G. A., Gigek, C. O., Leal, M. F., et al. (2016). Role of miRNAs and their potential to be useful as diagnostic and prognostic biomarkers in gastric cancer. *World J. Gastroenterol.* 22, 7951–7962.

Ørom, U. A., Derrien, T., Beringer, M., Gumireddy, K., Gardini, A., Bussotti, G., et al. (2010). Long noncoding RNAs with enhancer-like function in human cells. *Cell* 143, 46–58. doi: 10.1016/j.cell.2010.09.001

Pandey, R. R., Mondal, T., Mohammad, F., Enroth, S., Redrup, L., Komorowski, J., et al. (2008). Kcnq1ot1 antisense noncoding RNA Mediates lineage-specific transcriptional silencing through chromatin-level regulation. *Mol. Cell* 32, 232–246. doi: 10.1016/j.molcel.2008.08.022

Paneru, B., Ali, A., Al-Tobasei, R., Kenney, B., and Salem, M. (2018). Crosstalk among lncRNAs, microRNAs and mRNAs in the muscle "degradome" of rainbow trout. *Sci. Rep.* 8:8416.

Pegtel, D. M., Cosmopoulos, K., Thorley-Lawson, D. A., van Eijndhoven, M. A., Hopmans, E. S., Lindenberg, J. L., et al. (2010). Functional delivery of viral miRNAs via exosomes. *Proc. Natl. Acad. Sci. U.S.A.* 107, 6328–6333. doi: 10.1073/pnas.0914843107

Poller, W., and Fechner, H. (2010). Development of novel cardiovascular therapeutics from small regulatory RNA molecules - an outline of key requirements. *Curr. Pharm. Des.* 16, 2252–2268. doi: 10.2174/138161210791792813

Poller, W., Hajjar, R., Schultheiss, H.-P., and Fechner, H. (2010). Cardiac-targeted delivery of regulatory RNA molecules and genes for the treatment of heart failure. *Cardiovasc. Res.* 86, 353–364. doi: 10.1093/cvr/cvq056

Qu, X., Du, Y., Shu, Y., Gao, M., Sun, F., Luo, S., et al. (2017). MIAT Is a pro-fibrotic long non-coding RNA governing cardiac fibrosis in post-infarct myocardium. *Sci. Rep.* 7:42657.

Rupaimoole, R., and Slack, F. J. (2017). MicroRNA therapeutics: towards a new era for the management of cancer and other diseases. *Nat. Rev. Drug Discov.* 16, 203–222. doi: 10.1038/nrd.2016.246

Santulli, G. (2018). Exosomal microRNA: the revolutionary endogenous Innerspace nanotechnology. *Sci. Transl. Med.* 10:eaav9141. doi: 10.1126/scitranslmed.aav9141

Santulli, G., Iaccarino, G., De Luca, N., Trimarco, B., and Condorelli, G. (2014). Atrial fibrillation and microRNAs. *Front. Physiol.* 5:15. doi: 10.3389/fphys.2014.00015

Sardu, C., Marfella, R., Santulli, G., and Paolisso, G. (2014). Functional role of miRNA in cardiac resynchronization therapy. *Pharmacogenomics* 15, 1159–1168. doi: 10.2217/pgs.14.76

Schirone, L., Forte, M., Palmerio, S., Yee, D., Nocella, C., Angelini, F., et al. (2017). A review of the molecular mechanisms underlying the development and progression of cardiac remodeling. *Oxid. Med. Cell. Longev.* 2017:3920195.

Shan, Y., Ma, J., Pan, Y., Hu, J., Liu, B., and Jia, L. (2018). LncRNA SNHG7 sponges MIR-216b to promote proliferation and liver metastasis of colorectal cancer through upregulating GALNT1. *Cell Death Dis.* 9:722.

Sindi, H. A., Russomanno, G., Satta, S., Abdul-Salam, V. B., Jo, K. B., Qazi-Chaudhry, B., et al. (2020). Therapeutic potential of KLF2-induced exosomal microRNAs in pulmonary hypertension. *Nat. Commun.* 11:1185.

Singh, M. V., Swaminathan, P. D., Luczak, E. D., Kutschke, W., Weiss, R. M., and Anderson, M. E. (2012). MyD88 mediated inflammatory signaling leads to CaMKII oxidation, cardiac hypertrophy and death after myocardial infarction. *J. Mol. Cell. Cardiol.* 52, 1135–1144. doi: 10.1016/j.yjmcc.2012.01.021

Su, J., Fang, M., Tian, B., Luo, J., Jin, C., Wang, X., et al. (2018). Atorvastatin protects cardiac progenitor cells from hypoxia-induced cell growth inhibition via MEG3/miR-22/HMGB1 pathway. *Acta Biochim. Biophys. Sin.* 50, 1257–1265. doi: 10.1093/abbs/gmy133

Swayze, E. E., Siwkowski, A. M., Wancewicz, E. V., Migawa, M. T., Wyrzykiewicz, T. K., Hung, G., et al. (2006). Antisense oligonucleotides containing locked nucleic acid improve potency but cause significant hepatotoxicity in animals. *Nucleic Acids Res.* 35, 687–700. doi: 10.1093/nar/gkl1071

Terracciano, D., Ferro, M., Terreri, S., Lucarelli, G., D'Elia, C., Musi, G., et al. (2017). Urinary long noncoding RNAs in nonmuscle-invasive bladder cancer: new architects in cancer prognostic biomarkers. *Transl. Res.* 184, 108–117. doi: 10.1016/j.trsl.2017.03.005

Thayer, M. B., Lade, J. M., Doherty, D., Xie, F., Basiri, B., Barnaby, O. S., et al. (2019). Application of locked nucleic acid oligonucleotides for siRNA preclinical bioanalytics. *Sci. Rep.* 9:3566.

Thum, T., Gross, C., Fiedler, J., Fischer, T., Kissler, S., Bussen, M., et al. (2008). MicroRNA-21 contributes to myocardial disease by stimulating MAP kinase signalling in fibroblasts. *Nature* 456, 980–984. doi: 10.1038/nature07511

Toko, H., Takahashi, H., Kayama, Y., Okada, S., Minamino, T., Terasaki, F., et al. (2010). ATF6 is important under both pathological and physiological states in the heart. *J. Mol. Cell. Cardiol.* 49, 113–120. doi: 10.1016/j.yjmcc.2010.03.020

Uchida, S., and Dimmeler, S. (2015). Long noncoding RNAs in cardiovascular diseases. *Circ. Res.* 116, 737–750. doi: 10.1161/circresaha.116.302521

Valadi, H., Ekström, K., Bossios, A., Sjöstrand, M., Lee, J. J., and Lötvall, J. O. (2007). Exosome-mediated transfer of mRNAs and microRNAs is a novel mechanism of genetic exchange between cells. *Nat. Cell Biol.* 9, 654–659. doi: 10.1038/ncb1596

van Rooij, E., Sutherland, L. B., Liu, N., Williams, A. H., McAnally, J., Gerard, R. D., et al. (2006). A signature pattern of stress-responsive microRNAs that can evoke cardiac hypertrophy and heart failure. *Proc. Natl. Acad. Sci. U.S.A.* 103, 18255–18260. doi: 10.1073/pnas.0608791103

van Rooij, E., Sutherland, L. B., Qi, X., Richardson, J. A., Hill, J., and Olson, E. N. (2007). Control of stress-dependent cardiac growth and gene expression by a microRNA. *Science* 316, 575–579. doi: 10.1126/science.1139089

van Rooij, E., Sutherland, L. B., Thatcher, J. E., DiMaio, J. M., Naseem, R. H., Marshall, W. S., et al. (2008). Dysregulation of microRNAs after myocardial infarction reveals a role of miR-29 in cardiac fibrosis. *Proc. Natl. Acad. Sci. U.S.A.* 105, 13027–13032. doi: 10.1073/pnas.0805038105

Viereck, J., Kumarswamy, R., Foinquinos, A., Xiao, K., Avramopoulos, P., Kunz, M., et al. (2016). Long noncoding RNA Chast promotes cardiac remodeling. *Sci. Transl. Med.* 8, ra22–ra326.

Wang, J.-X., Zhang, X.-J., Li, Q., Wang, K., Wang, Y., Jiao, J.-Q., et al. (2015a). MicroRNA-103/107 regulate programmed necrosis and myocardial ischemia/reperfusion injury through targeting FADD. *Circ. Res.* 117, 352–363. doi: 10.1161/circresaha.117.305781

Wang, K., Liu, C.-Y., Zhou, L.-Y., Wang, J.-X., Wang, M., Zhao, B., et al. (2015b). APF lncRNA regulates autophagy and myocardial infarction by targeting miR-188-3p. *Nat. Commun.* 6:6779.

Wang, K., Liu, F., Liu, C. Y., An, T., Zhang, J., Zhou, L. Y., et al. (2016). The long noncoding RNA NRF regulates programmed necrosis and myocardial injury during ischemia and reperfusion by targeting miR-873. *Cell Death Differ.* 23, 1394–1405. doi: 10.1038/cdd.2016.28

Wang, K., Liu, F., Zhou, L.-Y., Long, B., Yuan, S.-M., Wang, Y., et al. (2014a). The long noncoding RNA CHRF regulates cardiac hypertrophy by targeting miR-489. *Circ. Res.* 114, 1377–1388. doi: 10.1161/circresaha.114.302476

Wang, K., Long, B., Zhou, L.-Y., Liu, F., Zhou, Q.-Y., Liu, C.-Y., et al. (2014b). CARL lncRNA inhibits anoxia-induced mitochondrial fission and apoptosis in cardiomyocytes by impairing miR-539-dependent PHB2 downregulation. *Nat. Commun.* 5, 3596.

Wang, K. C., Yang, Y. W., Liu, B., Sanyal, A., Corces-Zimmerman, R., Chen, Y., et al. (2011). A long noncoding RNA maintains active chromatin to coordinate homeotic gene expression. *Nature* 472, 120–126.

Wang, S., Binder, P., Fang, Q., Wang, Z., Xiao, W., Liu, W., et al. (2018a). Endoplasmic reticulum stress in the heart: insights into mechanisms and drug targets. *Br. J. Pharmacol.* 175, 1293–1304. doi: 10.1111/bph.13888

Wang, S., Yu, W., Chen, J., Yao, T., and Deng, F. (2018b). LncRNA MALAT1 sponges miR-203 to promote inflammation in myocardial ischemia-reperfusion injury. *Int. J. Cardiol.* 268:245. doi: 10.1016/j.ijcard.2018.03.085

Wang, X., Yong, C., Yu, K., Yu, R., Zhang, R., Yu, L., et al. (2018c). 'Long Noncoding RNA (lncRNA) n379519 promotes cardiac fibrosis in post-infarct myocardium by targeting miR-30'. *Med. Sci. Monit.* 24, 3958–3965. doi: 10.12659/msm.910000

Wang, X., Gu, H., Qin, D., Yang, L., Huang, W., Essandoh, K., et al. (2015c). Exosomal miR-223 contributes to mesenchymal stem cell-elicited cardioprotection in polymicrobial sepsis. *Sci. Rep.* 5:13721.

Wang, X., Morelli, M. B., Matarese, A., Sardu, C., and Santulli, G. (2020). Cardiomyocyte-derived exosomal microRNA-92a mediates post-ischemic myofibroblast activation both in vitro and ex vivo. *ESC Heart Fail.* 7, 284–288.

Williams, D. A. (2007). AAV and insertional mutagenesis. *Mol. Ther.* 15:P1737.

Wo, Y., Guo, J., Li, P., Yang, H., and Wo, J. (2018). Long non-coding RNA CHRF facilitates cardiac hypertrophy through regulating Akt3 via miR-93. *Cardiovasc. Pathol.* 35, 29–36. doi: 10.1016/j.carpath.2018.04.003

Wronska, A., Kurkowska-Jastrzebska, I., and Santulli, G. (2015). Application of microRNAs in diagnosis and treatment of cardiovascular disease. *Acta Physiol.* 213, 60–83. doi: 10.1111/apha.12416

Wu, H., Zhao, Z.-A., Liu, J., Hao, K., Yu, Y., Han, X., et al. (2018). Long noncoding RNA Meg3 regulates cardiomyocyte apoptosis in myocardial infarction. *Gene Ther.* 25, 511–523. doi: 10.1038/s41434-018-0045-4

Wüst, R. C. I., de Vries, H. J., Wintjes, L. T., Rodenburg, R. J., Niessen, H. W. M., and Stienen, G. J. M. (2016). Mitochondrial complex I dysfunction and altered NAD(P)H kinetics in rat myocardium in cardiac right ventricular hypertrophy and failure. *Cardiovasc. Res.* 111, 362–372. doi: 10.1093/cvr/cvw176

Xie, J., Burt, D. R., and Gao, G. (2015). Adeno-associated virus-mediated microRNA delivery and therapeutics. *Semin. Liver Dis.* 35, 81–88.

Xu, Y., Huang, R., Gu, J., and Jiang, W. (2016). Identification of long non-coding RNAs as novel biomarker and potential therapeutic target for atrial fibrillation in old adults. *Oncotarget* 7, 10803–10811. doi: 10.18632/oncotarget.7514

Xu, Y., Wang, X., and Zhang, Y. (2019). Myocardial infarction-related transcripts (MIAT) participate in diabetic optic nerve injury by regulating heart shock protein 5 (HSPA5) via competitively binding to microRNA-379. *Med. Sci. Monit.* 25, 2096–2103. doi: 10.12659/msm.911930

Xuan, L., Sun, L., Zhang, Y., Huang, Y., Hou, Y., Li, Q., et al. (2017). Circulating long non-coding RNAs NRON and MHRT as novel predictive biomarkers of heart failure. *J. Cell. Mol. Med.* 21, 1803–1814. doi: 10.1111/jcmm.13101

Yamaguchi, T., Izumi, Y., Nakamura, Y., Yamazaki, T., Shiota, M., Sano, S., et al. (2015). Repeated remote ischemic conditioning attenuates left ventricular remodeling via exosome-mediated intercellular communication on chronic heart failure after myocardial infarction. *Int. J. Cardiol.* 178, 239–246. doi: 10.1016/j.ijcard.2014.10.144

Yang, L., Lin, C., Liu, W., Zhang, J., Ohgi, K. A., Grinstein, J. D., et al. (2011). NcRNA- and Pc2 methylation-dependent gene relocation between nuclear structures mediates gene activation programs. *Cell* 147, 773–788. doi: 10.1016/j.cell.2011.08.054

Yang, Y., Li, Y., Chen, X., Cheng, X., Liao, Y., and Yu, X. (2016). Exosomal transfer of miR-30a between cardiomyocytes regulates autophagy after hypoxia. *J. Mol. Med.* 94, 711–724. doi: 10.1007/s00109-016-1387-2

Yoon, J. H., Abdelmohsen, K., and Gorospe, M. (2014). Functional interactions among microRNAs and long noncoding RNAs. *Semin. Cell Dev. Biol.* 34, 9–14. doi: 10.1016/j.semcdb.2014.05.015

Yoon, J. H., Abdelmohsen, K., Kim, J., Yang, X., Martindale, J. L., Tominaga-Yamanaka, K., et al. (2013). Scaffold function of long non-coding RNA HOTAIR in protein ubiquitination. *Nat. Commun.* 4:2939.

Yoon, J. H., Abdelmohsen, K., Srikantan, S., Yang, X., Martindale, J. L., De, S., et al. (2012). LincRNA-p21 Suppresses Target mRNA Translation. *Mol. Cell* 47, 648–655. doi: 10.1016/j.molcel.2012.06.027

Yu, S.-Y., Dong, B., Fang, Z.-F., Hu, X.-Q., Tang, L., and Zhou, S.-H. (2018). Knockdown of lncRNA AK139328 alleviates myocardial ischaemia/reperfusion injury in diabetic mice via modulating miR-204-3p and inhibiting autophagy. *J. Cell. Mol. Med.* 22, 4886–4898. doi: 10.1111/jcmm.13754

Yu, Y., Nangia-Makker, P., Farhana, L., and Majumdar, A. P. N. (2017). A novel mechanism of lncRNA and miRNA interaction: CCAT2 regulates miR-145 expression by suppressing its maturation process in colon cancer cells. *Mol. Cancer* 16:155.

Yuan, Y., Wang, J., Chen, Q., Wu, Q., Deng, W., Zhou, H., et al. (2019). Long non-coding RNA cytoskeleton regulator RNA (CYTOR) modulates pathological cardiac hypertrophy through miR-155-mediated IKKi signaling. *Biochim. Biophys. Acta* 1865, 1421–1427. doi: 10.1016/j.bbadis.2019.02.014

Zhang, L., Wang, Y., Zhang, L., Xia, X., Chao, Y., He, R., et al. (2019). ZBTB7A, a miR-663a target gene, protects osteosarcoma from endoplasmic reticulum stress-induced apoptosis by suppressing LncRNA GAS5 expression. *Cancer Lett.* 448, 105–116. doi: 10.1016/j.canlet.2019.01.046

Zhang, M., Jiang, Y., Guo, X., Zhang, B., Wu, J., Sun, J., et al. (2019). Long non-coding RNA cardiac hypertrophy-associated regulator governs cardiac hypertrophy via regulating miR-20b and the downstream PTEN/AKT pathway. *J. Cell. Mol. Med.* 23, 7685–7698. doi: 10.1111/jcmm.14641

Zhang, Y., Du, W., and Yang, B. (2019). Long non-coding RNAs as new regulators of cardiac electrophysiology and arrhythmias: molecular mechanisms, therapeutic implications and challenges. *Pharmacol. Ther.* 203:107389. doi: 10.1016/j.pharmthera.2019.06.011

Zhang, Z., Gao, W., Long, Q. Q., Zhang, J., Li, Y. F., Liu, D. C., et al. (2017). Increased plasma levels of lncRNA H19 and LIPCAR are associated with increased risk of coronary artery disease in a Chinese population. *Sci. Rep.* 7:7491.

Zhao, N., Mi, L., Zhang, X. J., Xu, M. Y., Yu, H. Y., Liu, Z. W., et al. (2018). Enhanced MiR-711 transcription by PPARγ induces endoplasmic reticulum stress-mediated apoptosis targeting calnexin in rat cardiomyocytes after myocardial infarction. *J. Mol. Cell. Cardiol.* 118, 36–45. doi: 10.1016/j.yjmcc.2018.03.006

Zhou, H., Wang, B., Yang, Y.-X., Jia, Q.-J., Zhang, A., et al. (2019). Long noncoding RNAs in pathological cardiac remodeling: a review of the update literature. *Biomed Res. Int.* 2019:7159592.

Zhou, T., Qin, G., Yang, L., Xiang, D., and Li, S. (2019). LncRNA XIST regulates myocardial infarction by targeting miR-130a-3p. *J. Cell. Physiol.* 234, 8659–8667. doi: 10.1002/jcp.26327

Zhou, S. S., Jin, J. P., Wang, J. Q., Zhang, Z. G., Freedman, J. H., Zheng, Y., et al. (2018). MiRNAS in cardiovascular diseases: potential biomarkers, therapeutic targets and challenges review-article. *Acta Pharmacol. Sin.* 39, 1073–1084.

Zhou, X., Yin, C., Dang, Y., Ye, F., and Zhang, G. (2015). Identification of the long non-coding RNA H19 in plasma as a novel biomarker for diagnosis of gastric cancer'. *Sci. Rep.* 5:11516.

Zhu, X. H., Yuan, Y. X., Rao, S. L., and Wang, P. (2016). LncRNA MIAT enhances cardiac hypertrophy partly through sponging miR-150'. *Eur. Rev. Med. Pharmacol. Sci.* 20, 3653–3660.

Conflict of Interest: The authors declare that the research was conducted in the absence of any commercial or financial relationships that could be construed as a potential conflict of interest.

Copyright © 2020 Collins, Binder, Chen and Wang. This is an open-access article distributed under the terms of the Creative Commons Attribution License (CC BY). The use, distribution or reproduction in other forums is permitted, provided the original author(s) and the copyright owner(s) are credited and that the original publication in this journal is cited, in accordance with accepted academic practice. No use, distribution or reproduction is permitted which does not comply with these terms.

frontiers in Physiology

REVIEW
published: 15 July 2020
doi: 10.3389/fphys.2020.00774

Novel Therapeutic Targets for Hypoxia-Related Cardiovascular Diseases: The Role of HIF-1

Minxuan Liu[1], Gina Galli[2], Yilin Wang[3], Qiru Fan[1,4], Zhenzhong Wang[1], Xin Wang[2] and Wei Xiao[1]**

[1] State Key Laboratory of New-tech for Chinese Medicine Pharmaceutical Process, Lianyungang, China, [2] Faculty of Life Sciences, The University of Manchester, Manchester, United Kingdom, [3] Pharmaceutical Sciences, University of Maryland, Baltimore, Baltimore, MD, United States, [4] Life Science and Technology, China Pharmaceutical University, Nanjing, China

Insufficient oxygen availability (hypoxia) is a precursor to numerous cardiovascular diseases, including atherosclerosis, pulmonary hypertension, and heart failure. The main site of hypoxic injury in the human body is the mitochondria, where oxygen acts as the final electron acceptor in the process of oxidative phosphorylation. Hypoxia-inducible factor (HIF) is activated in hypoxic conditions and acts as an important modulator of diverse target genes in the human body. The downstream genes of HIF include vital modulators of cardiovascular-related signaling pathways. Therefore, it is hypothesized that HIF represents a potential therapeutic target for the treatment and prevention of cardiovascular diseases. In this short review, we introduce the pathophysiology of hypoxic injury in cardiovascular disease, and we conclude from convincing evidence that HIF can modulate relevant cardioprotective signaling pathways.

Keywords: hypoxia, cardiovascular disease, therapeutic target, HIF, myocardial infarction, atherosclerosis

OPEN ACCESS

Edited by:
Tommaso Angelone, University of Calabria, Italy

Reviewed by:
Kiichi Hirota, Kansai Medical University, Japan
Giuseppe Pignataro, University of Naples Federico II, Italy
Claudia Penna, University of Turin, Italy

***Correspondence:**
Xin Wang
xin.wang@manchester.ac.uk
Wei Xiao
xw_kanion@163.com

Specialty section:
This article was submitted to Vascular Physiology, a section of the journal Frontiers in Physiology

Received: *27 February 2020*
Accepted: *12 June 2020*
Published: *15 July 2020*

Citation:
Liu M, Galli G, Wang Y, Fan Q, Wang Z, Wang X and Xiao W (2020) Novel Therapeutic Targets for Hypoxia-Related Cardiovascular Diseases: The Role of HIF-1. Front. Physiol. 11:774. doi: 10.3389/fphys.2020.00774

INTRODUCTION

Oxygen is essential for most eukaryotic organisms to maintain normal cellular function and survival. As an important prerequisite for aerobic respiration, oxygen helps to generate ATP which provides the energy for organisms to maintain cellular homeostasis (Waypa et al., 2016). Mitochondria are the site of aerobic respiration and the largest consumer of cellular oxygen; they produce ATP via the tricarboxylic acid (TCA) cycle and the process of oxidative phosphorylation (OXPHOS) (Kim et al., 2006). However, when oxygen supply does not meet cellular ATP demand, termed hypoxia, cells are forced to employ anaerobic respiration which produces less than 1/10th of the aerobic ATP supply. Therefore, hypoxia is usually synonymous with cellular dysfunction and it may lead to cell death under chronic circumstances (Sendoel and Hengartner, 2014). It is well-known that this condition is a major cause of several severe cardiovascular diseases (Han et al., 2014).

In response to hypoxia and its direct impact on cell metabolism, the cell induces the expression of a large number of genes. In particular, hypoxia-inducible factor 1 (HIF-1) is a transcriptional heterodimer composed of an α-subunit (HIF-1α) and a β-subunit (HIF-1β) (Sousa Fialho et al., 2019). In normoxic conditions, the HIF-1α subunit is generated in the cytosol and degraded in an oxygen-dependent manner (Salceda, 1997). However, in hypoxic conditions, the degradation process is suppressed and HIF-1α is transferred into the nucleus to form a heterodimer with the β-subunit (Benson Ham and Raju, 2017). It is well-known that HIF-1 acts as a regulator of hundreds

of target genes that can initiate distinct responses to low oxygen availability. While these regulated gene signaling pathways are known to mediate protective pathways in the short term, they can eventually lead to cardiovascular dysfunction (Abe et al., 2017). In this short review, we highlight the importance of HIF-1 cellular hypoxia and the pathophysiology of cardiovascular disease, and we offer insight into potential clinical therapies involving the modulation of HIF-1 pathways. Before we turn to the role of HIF-1 in cardiovascular disease, it is instructive to review the sequence of events leading to cellular dysfunction during hypoxia.

THE CELLULAR RESPONSE TO HYPOXIA

Under normoxic conditions, eukaryotes adopt aerobic respiration. In brief, glucose is broken down into pyruvate via glycolysis which yields 2 molecules of ATP. Pyruvate is then transported to the mitochondrial matrix and dehydrogenated by pyruvate dehydrogenase (PDH). The resulting product, acetyl coenzyme A, feeds into the citric acid cycle and is broken down into NADH and $FADH_2$, which are the electron providers for OXPHOS. In the mitochondrial inner membrane, the electron transport chain (ETC) is the main stage for OXPHOS (Supinski et al., 2019). Electrons are transported from NADH and $FADH_2$ to complex I (NADH CoQ reductase) and complex II (succinate CoQ reductase), respectively, where they are shuttled to complex III (ubiquinol cytochrome c reductase) by diffusible ubiquinone CoQ, and finally to complex IV (cytochrome c oxidase) by diffusible cytochrome c (Fuhrmann and Brune, 2017). Here, oxygen contributes to energy production by acting as the terminal electron acceptor. The electron transportation through the inner membrane provides the energy for complexes I, III, and IV to pump protons against their electrochemical gradient and create a proton motive force between the mitochondrial matrix and intermembrane space; this gradient provides the energy for complex V (ATP synthase) to convert ADP to ATP (Ham and Raju, 2017).

Under hypoxic conditions, mitochondrial function is severely impacted because the terminal electron acceptor, oxygen, becomes limiting. The lack of oxygen inhibits electron transport and OXPHOS, which reduces ATP production. In order to survive hypoxia, cells must adapt to the hypoxic condition and remodel aspects of the ETC. For example, the original ETC can be altered into supercomplexes, formed by complexes I, III, and IV. The remodeled supercomplexes maintain normal transportation of electrons, and they also help to inhibit the overproduction of reactive oxygen species (ROS) (Chaban et al., 2014). Under normal conditions, mitochondria generate ROS species, including superoxide and H_2O_2, from the leakage of electrons from the ETC; this process contributes to cellular signaling and does not cause damage to the cell (McElroy and Chandel, 2017). However, in hypoxic conditions, the lack of oxygen causes more electron slip, and ROS accumulates, leading to serious oxidative damage to numerous cellular components. The accumulation of superoxide radicals has a direct impact on the mitochondrial membrane; membrane permeability is increased and membrane potential is decreased. This instability of the mitochondrial membrane causes the leakage of cytochrome c and apoptotic protease activating factor into the cytosol (Ham and Raju, 2017). Therefore, the overproduction of superoxide radicals eventually causes cell death via apoptosis.

Cardioprotective conditioning is a series of mechanisms involving various signaling pathways. Once ischemia occurs, conditioning progress will be induced to reduce damage to the cardiovascular system. An ischemia-induced myocardial stretch can be a physical stimulation to cardioprotection conditioning. As shown in **Figure 1**, the signaling pathway of protein kinase C (PKC) and ATP-dependent potassium (KATP) channel will be activated to retard energy metabolism to achieve sustaining protection during prolonged ischemia and to decrease the infarct size (IS) (Gysembergh et al., 1998). Chemical metabolites generated from ischemia can also be activators of conditioning. Although ROS can bring severe damage to myocardial cells, a small quantity of ROS can stimulate protective signaling through the oxidation of protective cytosolic kinases (Tullio et al., 2013). Adenosine is a crucial chemical involved in ischemia conditioning. There are 4 kinds of adenosine receptors, A_1, A_{2A}, A_{2B}, and A_3, on cardiomyocyte sarcolemma. The A_1 and A_3 receptors are essential parts of the ischemic preconditioning (IPC) and their activation function is performed with the combination of K_{ATP} channel (McCully et al., 2001). However, receptors A_{2A} and A_{2B} are related to ischemic postconditioning (POC), which should be activated at early stage of ischemia to preserve the protective function (Methner et al., 2010). All the adenosine receptor protective conditioning will be ceased if the receptor signaling such as TNFα is blocked (Lacerda et al., 2009). Remote ischemic conditioning (RIC) can be activated by stromal cell-derived factor-1α (SDF-1α). It has been confirmed that SDF-1α may perform a MI treatment by increasing long-term, stem cell migration, and homing to the heart (Davidson et al., 2013).

HYPOXIA-RELATED CARDIOVASCULAR DISEASES

The human body can experience hypoxia under a wide variety of circumstances. We may encounter problems with oxygen extraction due to environmental or physiological reasons. Alternatively, there are pathophysiological circumstances that impair oxygen delivery to the cells, such as respiration system dysfunction, unreached peripheral areas by blood, and occlusion of blood flow by vascular plaques (Thomas and Ashcroft, 2019). In either case, a lack of cellular oxygen has negative consequences for the cardiovascular function which eventually manifests in disease.

A typical example of a hypoxia-related cardiovascular disease is atherosclerosis; a potentially fatal disorder that is characterized by the formation of arterial plaques by the deposition of lipids, macrophages, and other cells in the vessel wall (Weber and Noels, 2011). Endothelial dysfunction is the main cause of atherosclerosis, which is thought to be related to hypoxic conditions. The generation of ROS during hypoxia has a direct effect on the initiation of endothelial dysfunction, especially

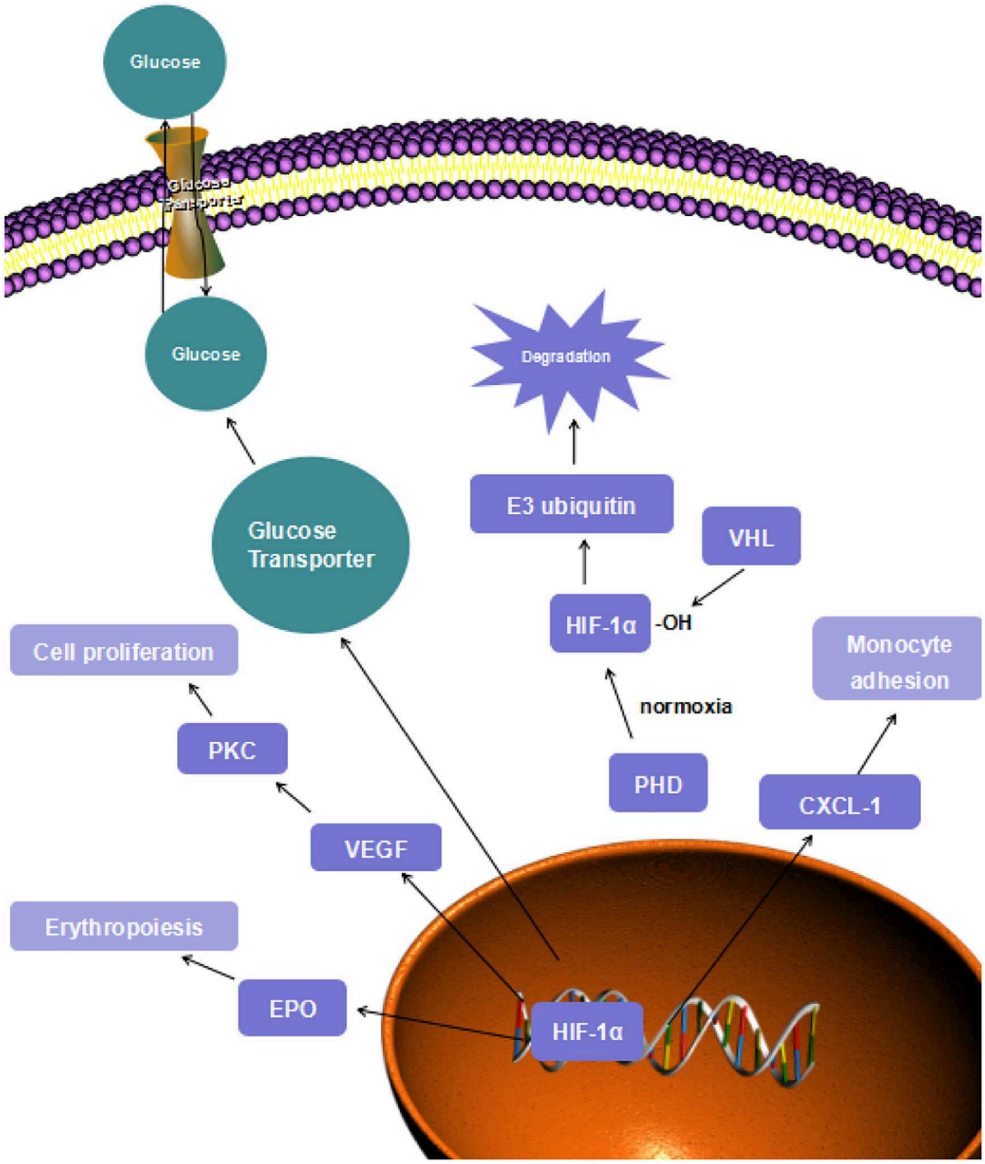

FIGURE 1 | HIF-1α signaling.

superoxide (Douglas and Channon, 2014). Superoxide can combine with nitric oxide (NO) and form the harmful product peroxynitrite, which has a damaging effect on lipids and proteins, causing endothelial injuries. As an inflammatory site, endothelial injury can represent a bed for plaque formation (Wang et al., 2012).

Low-density lipoprotein (LDL) is an unstable cholesterol transporter that can easily be oxidized into oxidized LDL (oxLDL). Monocytes migrating to the plaque lesion will differentiate into macrophages and take up oxLDL, thereby turning intofoam cells. Foam cells can exacerbate the inflammatory process and form fatty streak (Insull, 2009). This process can be seen as the initiation of atherosclerosis. Afterward, if chronic hypoxia persists, the fatty streak will generate an atheroma and eventually cause atherosclerosis (Negre-Salvayre et al., 2019).

Another cardiovascular disease that can be induced by hypoxia is pulmonary hypertension. Pulmonary hypertension is defined as mean pulmonary blood pressure sustained over 25mmHg at rest (Humbert et al., 2013). Pulmonary hypertension is induced by hypoxic pulmonary vasoconstriction (HPV) and vascular remodeling (Rimoldi et al., 2012). In a low oxygen environment, HPV is adopted by the lungs as the main strategy to improve oxygen delivery. This response is mechanistically achieved by a rise in calcium influx triggered by ROS signaling. An increase in ROS activates the sarcoplasmic reticulum which leads to the release of Ca^{2+} that enters pulmonary arterial smooth muscle cells and causes vasoconstriction (Siques et al.,

2018). This process leads to an increase in pulmonary vasculature blood pressure in order to maintain normal cardiac output, and alongside this, the right ventricle must enhance systolic pressure. The enhanced right ventricular systolic pressure will lead to an increase in both vascular stress and oxygen demand, and a decrease in right coronary artery flow, which is a known compensatory mechanism in pulmonary hypertension (PH) (Oliveira et al., 2020).

The thickness of the pulmonary artery can also be mediated by hypoxic stress. This parameter is normally maintained by the dynamic equilibrium between proliferation and apoptosis of vessel wall cells (Welsh and Peacock, 2013). However, this balance can be interrupted in hypoxic conditions due to the consequent oxidative stress. Oxidative stress can both inhibit the anti-mitogenic factor and lead to the release of mitogenic stimuli (Stenmark and Mecham, 1997). These processes play a vital role in enhancing the proliferation of vessel wall cells, which disturbs the dynamic balance of vessel wall thickness, leading to vascular remodeling (Renna et al., 2013). The blockage of lumen blood flow by hypoxic vascular remodeling is also a contributor to the PH. Moreover, if PH persists, the condition will deteriorate further into another cardiovascular problem, heart failure (Guazzi and Naeije, 2017).

Heart failure is not a single myocardial disease but a progressive disorder where the heart is incapable of filling the left ventricle and/or ejecting sufficient blood to meet the body's metabolic demands (Kiyuna et al., 2018). Heart failure represents the end-stage of almost all kinds of cardiac diseases, including myocardial infarction, hypertrophy, and hypertension; all of which are associated with high mortality (Garg et al., 2005). According to extensive studies on the pathophysiology of heart failure, mitochondrial abnormalities resulting from hypoxia are a major contributor and a hallmark of heart failure (Okonko and Shah, 2015). The lack of oxygen and subsequent mitochondrial dysfunction causes a sudden decrease in energy supply which can strikingly impair the metabolism of cardiomyocytes. Moreover, the increased generation of ROS can have damaging effects on cell function and integrity that may eventually trigger cardiomyocyte apoptosis. The severe loss of myocardial cells can lead to ventricular remodeling and contractile impairment (Hilfiker-Kleiner et al., 2005). As a consequence, left ventricle dysfunction will lead to decreased cardiac output and may even cause myocardial infarction, which is a critical stage in the progression of heart failure (Struthers, 2005).

THE ROLES OF HYPOXIC HIF-1 SIGNALING IN CARDIOVASCULAR DISEASES

In response to hypoxia, protective mechanisms will be modulated by activation of the transcriptional factor HIF-1 (Garg et al., 2005). HIF-1 regulates target genes related to inflammation, vascular remodeling, and angiogenesis, which all help the organism respond and adapt to a low oxygen environment. However, these responses are also major contributors to cardiovascular dysfunction (Semenza, 2014a), and once initiated, they can manifest as severe cardiovascular diseases (Abe et al., 2017).

HIF-1 transcriptional factor is a heterodimer consisting of the α-subunit, which includes HIF-1α, HIF-2α, and HIF-3α isoforms, and the HIF-β subunit (Halligan et al., 2016). Under normoxic conditions, the HIF-α subunits are not stabilized and do not modulate their target genes because the subunits are degraded through oxygen-dependent mechanisms (Masoud and Li, 2015). The degradation process starts with hydroxylation of HIF-α. Once the HIF-α is generated, the prolyl hydroxylase domains (PHD) will hydroxylate its highly conserved specific proline residue and form a binding site. Subsequently, the von Hippel-Lindau (VHL) tumor suppressor protein will bind to this binding site, and this reaction makes HIF-α a target for the multiprotein E3 ubiquitin ligase complex to recognize (Semenza Gregg, 2012). Finally, the proteasomal degradation of HIF-α will be induced. However, the hydroxylation process of proline residue by PHD employs oxygen as a reaction substrate, so that the VHL degradation will be inhibited under hypoxic conditions (**Figure 1**) (Hewitson and Schofield, 2004).

Another HIF degradation process is asparaginyl hydroxylation. This hydroxylase was first identified as a factor inhibiting HIF (FIH). When HIF-α binds to p300-CBP co-activator family, a hydrophobic region will be formed. In this hydrophobic region, an asparagine residue (Asn803 in HIF-α; Asn850 in HIF-2α) is located in the C-terminal of the HIF-α, which is the target of FIH (Kaelin and Ratcliffe, 2008). After the hydroxylation of this asparagine residue, the combination reaction of HIF-α and p300-CBP co-activator will be inhibited. This inhibition will cause the inactivation of HIF transcriptional modulation of downstream target genes (Schodel and Ratcliffe, 2019). However, this hydroxylation is also oxygen-dependent, so that HIF transcription factors can exhibit the regulation effect on target genes.

The beta subunits of HIF are highly conserved and stabilized in the cell nucleus (Metzen, 2003). Under low oxygen conditions, the proteasomal degradation of HIF-α subunits is ceased, the alpha subunits are stabilized and transferred to the nucleus, allowing binding to HIF-β (Liu and Semenza, 2007). When the beta subunits bind to the 1α subunits, the complex forms the HIF-1 transcription factor. Furthermore, it can form HIF-2 when the beta subunits bind to 2α subunits. As the HIF-α/β stabilization is achieved, this transcriptional factor will exhibit its transcriptional function and regulate diverse target genes (Schönenberger and Kovacs, 2015).

Hypoxia-inducible factorHIF transcription factor regulates the expression of target genes by binding to their specific hypoxia response elements (HREs) at the gene loci (Pugh and Ratcliffe, 2003). In response to hypoxia, the protective mechanisms are activated by a network of hundreds of downstream target genes to adapt the body to a low oxygen environment. These responses include a coordinated reduction in oxygen-consuming processes and the promotion of anaerobic metabolic processes (Semenza, 2011). In addition to maintaining ATP balance, the cell must also avoid the overproduction of toxic ROS due to inefficient mitochondrial aerobic respiration (Okamoto et al., 2017). To

TABLE 1 | Experimental models used, the protocols, and the role exercised by HIF in studies involved in the article.

Model of the study	Methods	Outcome and experimental evidence	References
Mouse model with high-fat diet induced atherosclerosis	The lesion formation of EC-Hif1a-/- mice and wild type were determined after partial carotid ligation and HFD feeding.	EC-Hif1a-/- mice generated reduced lesion area compared to EC-Hif1a + / + mice.	Akhtar et al., 2015
Mouse aortae endothelial cell model after HFD feeding	Monocyte adhesion to MAECs was determined after the stimulation of LPA20:4, LPA18:0, moxLDL or nLDL.	The moxLDL-and LPA20:4-induced monocyte adhesion was abolished by silencing Hif-1a in MAECs. Upregulation of HIF1a helps MoxLDL-derived unsaturated LPAs promote CXCL1-dependent monocytes adhesion.	Akhtar et al., 2015
Mouse aortae endothelial cell model after HFD feeding	Endothelial cell proliferation was measured between Hif-1a silencing group and the control group.	The proliferation of ECs was decreased in gene silencing group, demonstrating that EC proliferation is regulated by Hif-1a.	Feng et al., 2017
Mouse pulmonary hypertension model induced by hypoxia-induced mitogenic factor (HIMF) injection	The level of medial thickening was determined between HIF-1$\alpha^{+/+}$ and HIF-1$\alpha^{\pm}$ group after HIMF injection.	An obvious medial thickening was induced by HIMF in the HIF-1$\alpha^{+/+}$ group, while the process was dismissedin the HIF-1$\alpha^{\pm}$ group, indicating the regulation effect of HIF-1α in the PH development.	Johns et al., 2016
Mouse model by normoxia or chronic hypoxia (10% O_2) for 30 days	HIF-1α deletion was performed in 2 ways on model group mice, followed by normoxia and chronic hypoxia exposure to all groups.	HIF-1α-SMM-Cre mice generated decreased arterial wall thickness, while the control group mice developed significant vascular remodeling in arteries, showing HIF-1α as an important part in vascular remodeling regulation.	Ball et al., 2014

attenuate the cell-damaging effects of ROS, OXPHOS processes are downregulated, while the anaerobic respiration process, glycolysis, is upregulated (Thomas and Ashcroft, 2019).

As the essential substrate of OXPHOS process, pyruvate must first be reduced to acetyl coenzyme A. This step is catalyzed by pyruvate dehydrogenase, and acetyl coenzyme A is supplied to the TCA cycle (Iyer et al., 1998). A PDH inhibitor, PDK-1, is activated by the HIF-1 transcription under hypoxic circumstances (Wigfield et al., 2008). PDK-1 phosphorylases and inhibits the catalytic domain of PDH. As a result, PDH is driven away from the mitochondria, and the TCA cycle is impaired (Papandreou et al., 2006). In a previous study, HIF-1α null (Hifa^{-}/$^{-}$) mouse embryo fibroblasts (MEFs) were unable to activate PDK1, compared to the dramatic increase of PDK1 in isogenic wild-type MEFs (Kim et al., 2006); the decrease of PDH expression is related to HIF-1α but not HIF-2α (Eguchi and Nakayama, 2019).

While the aerobic respiration substrate is reduced, the glycolysis substrates are upregulated by HIF-1 transcription. The expressions of SLC2A1 and SLC2A3 genes are activated by HIF-1 modulation. These genes encode glucose transporters, GLUT1 and GLUT3 (Nishimura et al., 2017). These transporters are upregulated to transfer more glucose to enhance the process of glycolysis. In mouse chondrocytes, GLUT-1 and GLUT-3 expressions were remarkably increased after hypoxic treatment, compared with cells treated in normoxic conditions (Ren et al., 2008). In **Figure 1**, the increase in the "fast" transporter GLUT-3 can be considered adaptive in hypoxia because this is a more efficient glucose carrier in chondrocytes, compared to other members of this transporter family. Moreover, lactate dehydrogenase A is also upregulated by HIF-1 due to its role in converting pyruvate into lactate (Lee Dong et al., 2015). Hexokinase is the first enzyme to initiate the glycolysis process. This enzyme is encoded by HK-1 and HK-3 gene, which are targets of HIF-1 protective mechanisms as well (Riddle et al., 2000). As the glycolysis process can be carried out smoothly, sufficient ATP will be supplied to maintain normal cell function and metabolism.

During prolonged hypoxia, the generation of ROS becomes a major threat to cell survival (Chi et al., 2010). The overproduction of ROS can trigger several mechanisms that effectively disrupt the proton gradient and lead to the rupture of mitochondrial membrane (Suski et al., 2012). The leakage of mitochondrial content can cause cell death (Bock and Tait, 2019). In order to preserve cell viability, mitochondrial autophagy is activated through the HIF-1 signaling pathway. The selective autophagy regulator, Beclin 1, originally binds to Bcl 2, but when hypoxia occurs, HIF-1 modulation activates BNIP3. The BNIP3 protein has a competitive effect on Beclin 1 on the bond to Bcl 2. The detached Beclin 1 from Bcl 2 triggers selective autophagy (Lu et al., 2018). This autophagy pathway is an adaptive mechanism that protects cell viability during prolonged hypoxic exposure.

HIF-1α, as an important gene modulator to hypoxia, the expression of which has been detected in atherosclerotic lesions from different cell types (Akhtar et al., 2015). Development of atherosclerosis can be promoted by endothelial dysfunction, inflammation, macrophages, and proliferation of smooth muscle cells. Interestingly, all features mentioned above can be induced by HIF regulated pathways (Semenza, 2014b). In **Table 1**, the contribution of HIF-1α on atherosclerosis has been demonstrated by Shamima's research (Akhtar et al., 2015). After partial ligation of carotid arteries and high-fat diet (HFD) feeding for over 6 weeks, mice from EC-HIF-1$\alpha^{-/-}$ group and EC-HIF-1$\alpha^{+/+}$group were conducted to atherosclerosis lesion quantification. It was determined that, compared to EC-HIF-1$\alpha^{+/+}$ group mice, the lesion area was reduced in gene silencing group. Endothelial dysfunction and proliferation is a vital feature of atherosclerosis formation, and it has proven to be upregulated by HIF1-α. Cultured endothelial cells were conducted to proliferation measurement, PCNA [proliferating cell nuclear antigen], and Ki67 staining. The level of EC proliferation in HIF-1$\alpha^{+/+}$ group was much higher than that in the HIF-1α gene deletion group (Feng et al., 2017). The accumulation

and adhesion of monocytes in endothelial cells also promote the formation of atherosclerosis. The adhesion process can be enhanced depending on upregulated (C–X–C motif) ligand 1 (CXCL1) expression (Zhou et al., 2011). In Shamima's study, moxLDL and LPA 20:4 were used to induce monocyte adhesion in mouse aortic EC (MAECs). As the monocyte adhesion cannot be induced in the HIF-1α silencing group, it is indicated that the adhesion-depending CXCL-1 expression is regulated by HIF-1α (**Table 1**) (Akhtar et al., 2015).

During the development of pulmonary hypertension and heart failure, HIF-1α-induced vascular remodeling also plays an important role (Schultz et al., 2006). Hypoxia-induced mitogenic factor (HIMF) regulation is a crucial part of the EC proliferation phase in pulmonary hypertension. Johns' group used HIMF to induced medial thickness on mouse model, to compare the level of EC proliferation between HIF-1α ± group and wild type (WT) group. The result turned out that the vessel wall thickness process was abolished in the HIF-1α ± group compared to the WT group. This outcome indicated that HIF-1α is a vital downstream regulator in the process of HIMF-induced pulmonary hypertension, which means HIF-1α plays an important part in PH development (Johns et al., 2016). Ball's group performed two ways, homozygous conditional deletion of HIF-1 a combined with tamoxifen-inducible smooth muscle-specific Cre recombinase expression, to achieve the gene silencing of HIF-1α. Both the HIF-1α-SMM-Cre group and WT group mice were exposed to either normoxia or chronic hypoxia (CH, 10% O_2). In normoxic situation, both groups exhibited no vascular remodeling, while in CH situation, the obvious vessel wall thickness induced in WT group was significantly reduced in gene negative group (**Table 1**) (Ball et al., 2014).

According to the researches above, HIF-1α is closely correlated with the developing process of several cardiovascular diseases, such as endothelial dysfunction, smooth muscle proliferation, inflammation, and angiogenesis through the transcription of vascular endothelial growth factor (VEGF), erythropoietin (EPO), CXCL1, etc (**Figure 1**). The important role of HIF-1α in CVD development makes it a convincing target of cardioprotective treatment.

HYPOXIA-INDUCIBLE FACTORS AND POTENTIAL THERAPEUTIC TARGETS

A lack of blood flow (ischemia) underlies numerous cardiovascular, including myocardial infarction and atherosclerosis. Furthermore, ischemia not only underlies cardiovascular diseases but also diabetes and other chronic diseases (Howell and Tennant, 2014). To treat the ischemic myocardium in myocardial infarction, the standard therapy is to reperfuse the ischemic area. This standard treatment may paradoxically cause additional injury to the myocardium, which is termed ischemic-reperfusion injury (IRI) (Martin-Puig et al., 2015). IRI can trigger a sudden increase in ROS and intracellular calcium overload at the reperfusion site, which can eventually cause mitochondrial dysfunction and even cell death. To protect the cell from this cascade of events, researchers have adopted the process of ischemic preconditioning, whereby the cell is subjected to short cycles of ischemia-reperfusion before the longer, chronic phase of IRI. Due to its short period, this process is not lethal, and it is known to adapt and protect the myocardium to the later damaging effects of IRI. Because of the differences in the partial pressure of oxygen between the ischemic and reperfusion periods, it can be hypothesized that the HIF signaling pathway may participate in the mechanisms underlying ischemic preconditioning.

Previous studies have demonstrated that HIF transcription factor and its downstream target genes have cardioprotective abilities through the modulation of mitochondrial metabolism, cell function, and angiogenesis. All these reactions adjust cellular function in the hypoxic area to the low oxygen environment and maintain normal cell homeostasis, which is vital for the human body when facing hypoxic stress. Therefore, the HIF pathway provides a new target to develop strategies for treating ischemic diseases and reducing reperfusion injury.

As a promoter of atherosclerosis development, HIF may not be considered for therapeutic treatment of this disease. While protective in the short term, the angiogenesis induced by HIF-1 transcription that forms collateral vessels may result in terrible consequences in atherosclerosis patients (Jain et al., 2018). However, this conclusion is based on current research results, which are mostly focusing on the HIF-1 signaling pathway, particularly the HIF-α subunits. More study is needed on other members of the hypoxia-inducible factor family and the HIF-β subunits. The physiological mechanisms behind the modulation of these transcription factors may possess great potential for treating cardiovascular diseases such as atherosclerosis.

Pulmonary hypertension is another cardiovascular disease associated with HIF modulation. The proliferation of pulmonary arterial smooth muscle cells (PASMCs) and endothelial cells (ECs) which are activated by HIF-1 and HIF-2 transcription, respectively, contributes toward the increase in pulmonary blood pressure (Ahmad et al., 2013). Strategies that target the inhibition of HIF transcription in PH patients could be an interesting new perspective in the treatment of hypertension. For example, it has been demonstrated that HIF-2 inhibited by C76 is capable of relieving pulmonary artery blood pressure in different models (Dai et al., 2018).

In summary, according to current researchers, the complicated mechanisms of HIF transcription have yet be completely revealed. Further research is necessary in order to obtain a complete therapeutic picture of HIF in the treatment of cardiovascular diseases (Burgueno et al., 2013).

AUTHOR CONTRIBUTIONS

ML and GG contributed to the drafting and revision of the manuscript. YW and ZW contributed to the critical revision of the manuscript. QF contributed to the substantial contributions to conception and design. WX and XW contributed to the critical revision of the manuscript and final approval of the version for submission. All authors contributed to the article and approved the submitted version.

REFERENCES

Abe, H., Semba, H., and Takeda, N. (2017). The roles of hypoxia signaling in the pathogenesis of cardiovascular diseases. *J. Atheroscler. Thromb.* 24, 884–894. doi: 10.5551/jat.RV17009

Ahmad, A., Ahmad, S., Malcolm, K. C., Miller, S. M., Hendry-Hofer, T., Schaack, J. B., et al. (2013). Differential regulation of pulmonary vascular cell growth by hypoxia-inducible transcription factor-1alpha and hypoxia-inducible transcription factor-2alpha. *Am. J. Respir. Cell Mol. Biol.* 49, 78–85. doi: 10.1165/rcmb.2012-0107OC

Akhtar, S., Hartmann, P., Karshovska, E., Rinderknecht, F.-A., Subramanian, P., Gremse, F., et al. (2015). Endothelial hypoxia-inducible factor-1α promotes atherosclerosis and monocyte recruitment by upregulating MicroRNA-19a. *Hypertension* 66, 1220–1226. doi: 10.1161/HYPERTENSIONAHA.115.05886

Ball, M. K., Waypa, G. B., Mungai, P. T., Nielsen, J. M., Czech, L., Dudley, V. J., et al. (2014). Regulation of hypoxia-induced pulmonary hypertension by vascular smooth muscle hypoxia-inducible factor-1alpha. *Am. J. Respir. Crit. Care Med.* 189, 314–324. doi: 10.1164/rccm.201302-0302OC

Benson Ham, H. P., and Raju, R. (2017). Mitochondrial function in hypoxic ischemic injury and influence of aging. *Prog. Neurobiol.* 157, 92–116. doi: 10.1016/j.pneurobio.2016.06.006

Bock, F. J., and Tait, S. W. G. (2019). Mitochondria as multifaceted regulators of cell death. *Nat. Rev. Mol. Cell Biol.* 21, 85–100. doi: 10.1038/s41580-019-0173-8

Burgueno, A. L., Gianotti, T. F., Mansilla, N. G., Pirola, C. J., and Sookoian, S. (2013). Cardiovascular disease is associated with high-fat-diet-induced liver damage and up-regulation of the hepatic expression of hypoxia-inducible factor 1alpha in a rat model. *Clin. Sci. (Lond.)* 124, 53–63. doi: 10.1042/CS20120151

Chaban, Y., Boekema, E. J., and Dudkina, N. V. (2014). Structures of mitochondrial oxidative phosphorylation supercomplexes and mechanisms for their stabilisation. *Biochim. Biophys. Acta Bioenerget.* 1837, 418–426. doi: 10.1016/j.bbabio.2013.10.004

Chi, A. Y., Waypa, G. B., Mungai, P. T., and Schumacker, P. T. (2010). Prolonged hypoxia increases ROS signaling and RhoA activation in pulmonary artery smooth muscle and endothelial cells. *Antioxid. Redox Signal.* 12, 603–610. doi: 10.1089/ars.2009.2861

Dai, Z., Zhu, M. M., Peng, Y., Machireddy, N., Evans, C. E., Machado, R., et al. (2018). Therapeutic targeting of vascular remodeling and right heart failure in pulmonary arterial hypertension with a HIF-2alpha inhibitor. *Am. J. Respir. Crit. Care Med.* 198, 1423–1434. doi: 10.1164/rccm.201710-2079OC

Davidson, S. M., Selvaraj, P., He, D., Boi-Doku, C., Yellon, R. L., Vicencio, J. M., et al. (2013). Remote ischaemic preconditioning involves signalling through the SDF-1α/CXCR4 signalling axis. *Basic Res. Cardiol.* 108:377. doi: 10.1007/s00395-013-0377-6

Douglas, G., and Channon, K. M. (2014). The pathogenesis of atherosclerosis. *Medicine* 42, 480–484. doi: 10.1016/j.mpmed.2014.06.011

Eguchi, K., and Nakayama, K. (2019). Prolonged hypoxia decreases nuclear pyruvate dehydrogenase complex and regulates the gene expression. *Biochem. Biophys. Res. Commun.* 520, 128–135. doi: 10.1016/j.bbrc.2019.09.109

Feng, S., Bowden, N., Fragiadaki, M., Souilhol, C., Hsiao, S., Mahmoud, M., et al. (2017). Mechanical activation of hypoxia-inducible factor 1alpha drives endothelial dysfunction at atheroprone sites. *Arteriosc. Thromb. Vasc. Biol.* 37, 2087–2101. doi: 10.1161/ATVBAHA.117.309249

Fuhrmann, D. C., and Brune, B. (2017). Mitochondrial composition and function under the control of hypoxia. *Redox Biol.* 12, 208–215. doi: 10.1016/j.redox.2017.02.012

Garg, S., Narula, J., and Chandrashekhar, Y. (2005). Apoptosis and heart failure: clinical relevance and therapeutic target. *J. Mol. Cell. Cardiol.* 38, 73–79. doi: 10.1016/j.yjmcc.2004.11.006

Guazzi, M., and Naeije, R. (2017). Pulmonary hypertension in heart failure. *J. Am. Coll. Cardiol.* 69:1718. doi: 10.1016/j.jacc.2017.01.051

Gysembergh, A., Margonari, H., Loufoua, J., Ovize, A., André-Fouët, X., Minaire, Y., et al. (1998). Stretch-induced protection shares a common mechanism with ischemic preconditioning in rabbit heart. *Am. J. Physiol. Heart Circulat. Physiol.* 274, H955–H964. doi: 10.1152/ajpheart.1998.274.3.H955

Halligan, D. N., Murphy, S. J. E., and Taylor, C. T. (2016). The hypoxia-inducible factor (HIF) couples immunity with metabolism. *Semin. Immunol.* 28, 469–477. doi: 10.1016/j.smim.2016.09.004

Ham, P. B. and Raju, R. (2017). Mitochondrial function in hypoxic ischemic injury and influence of aging. *Prog. Neurobiol.* 157, 92–116. doi: 10.1016/j.pneurobio.2016.06.006

Han, M., Qing, H. E., Shi, Y., Feng, J., and Chen, B. (2014). The impact of intermittent hypoxia from obstructive sleep apnea on cardiovascular and cerebrovascular diseases. *Tianjin Med. J.* 946–949.

Hewitson, K. S., and Schofield, C. J. (2004). The HIF pathway as a therapeutic target. *Drug Discov. Today* 9, 704–711. doi: 10.1016/S1359-6446(04)03202-7

Hilfiker-Kleiner, D., Landmesser, U., and Drexler, H. (2005). Inflammation, angiogenesis, and apoptosis molecular mechanisms in heart failure: focus on cardiac hypertrophy. *J. Am. Coll. Cardiol.* 48(Suppl.), A56–A66.

Howell, N. J., and Tennant, D. A. (2014). The role of HIFs in ischemia-reperfusion injury. *Hypoxia (Auckl)* 2, 107–115. doi: 10.2147/HP.S49720

Humbert, M., Montani, D., Evgenov, O. V., and Simonneau, G. (2013). Definition and classification of pulmonary hypertension. *Handb. Exp. Pharmacol.* 218, 3–29. doi: 10.1007/978-3-642-38664-0_1

Insull, W. (2009). The pathology of atherosclerosis: plaque development and plaque responses to medical treatment. *Am. J. Med.* 122(1 Suppl.), S3–S14. doi: 10.1016/j.amjmed.2008.10.013

Iyer, N. V., Kotch, L. E., Agani, F., Leung, S. W., Laughner, E., Wenger, R. H., et al. (1998). Cellular and developmental control of O2 homeostasis by hypoxia-inducible factor 1 alpha. *Genes Dev.* 12, 149–162. doi: 10.1101/gad.12.2.149

Jain, T., Nikolopoulou, E. A., Xu, Q., and Qu, A. (2018). Hypoxia inducible factor as a therapeutic target for atherosclerosis. *Pharmacol. Ther.* 183, 22–33. doi: 10.1016/j.pharmthera.2017.09.003

Johns, R. A., Takimoto, E., Meuchel, L. W., Elsaigh, E., Zhang, A., Heller, N. M., et al. (2016). Hypoxia-inducible factor 1alpha is a critical downstream mediator for hypoxia-induced mitogenic factor (FIZZ1/RELMalpha)-induced pulmonary hypertension. *Arteriosc. Thromb. Vasc. Biol.* 36, 134–144. doi: 10.1161/ATVBAHA.115.306710

Kaelin, W. G., and Ratcliffe, P. J. (2008). Oxygen sensing by metazoans: the central role of the HIF hydroxylase pathway. *Mol. Cell* 30, 393–402. doi: 10.1016/j.molcel.2008.04.009

Kim, J. W., Tchernyshyov, I., Semenza, G. L., and Dang, C. V. (2006). HIF-1-mediated expression of pyruvate dehydrogenase kinase: a metabolic switch required for cellular adaptation to hypoxia. *Cell Metab.* 3, 177–185. doi: 10.1016/j.cmet.2006.02.002

Kiyuna, L. A., Albuquerque, R. P. E., Chen, C. H., Mochly-Rosen, D., and Ferreira, J. C. B. (2018). Targeting mitochondrial dysfunction and oxidative stress in heart failure: challenges and opportunities. *Free Radic. Biol. Med.* 129, 155–168. doi: 10.1016/j.freeradbiomed.2018.09.019

Lacerda, L., Somers, S., Opie, L. H., and Lecour, S. (2009). Ischaemic postconditioning protects against reperfusion injury via the SAFE pathway. *Cardiovasc. Res.* 84, 201–208. doi: 10.1093/cvr/cvp274

Lee Dong, C., Sohn Hyun, A., Park, Z.-Y., Oh, S., Kang Yun, K., Lee, K.-M., et al. (2015). A lactate-induced response to hypoxia. *Cell* 161, 595–609. doi: 10.1016/j.cell.2015.03.011

Liu, Y., and Semenza, G. (2007). RACK1 vs. HSP90: competition for HIF-1 alpha degradation vs. stabilization. *Cell Cycle (Georgetown, Tex)* 6, 656–659. doi: 10.4161/cc.6.6.3981

Lu, N., Li, X., Tan, R., An, J., Cai, Z., Hu, X., et al. (2018). HIF-1α/Beclin1-mediated autophagy is involved in neuroprotection induced by hypoxic preconditioning. *J. Mol. Neurosci.* 66, 238–250. doi: 10.1007/s12031-018-1162-7

Martin-Puig, S., Tello, D., and Aragonés, J. (2015). Novel perspectives on the PHD-HIF oxygen sensing pathway in cardioprotection mediated by IPC and RIPC. *Front. Physiol.* 6:137. doi: 10.3389/fphys.2015.00137

Masoud, G. N., and Li, W. (2015). HIF-1alpha pathway: role, regulation and intervention for cancer therapy. *Acta Pharm. Sin. B* 5, 378–389. doi: 10.1016/j.apsb.2015.05.007

McCully, J. D., Toyoda, Y., Uematsu, M., Stewart, R. D., and Levitsky, S. (2001). Adenosine-enhanced ischemic preconditioning: adenosine receptor involvement during ischemia and reperfusion. *Am. J. Physiol. Heart Circulat. Physiol.* 280, H591–H602. doi: 10.1152/ajpheart.2001.280.2.H591

McElroy, G. S., and Chandel, N. S. (2017). Mitochondria control acute and chronic responses to hypoxia. *Exp. Cell Res.* 356, 217–222. doi: 10.1016/j.yexcr.2017.03.034

Methner, C., Schmidt, K., Cohen, M. V., Downey, J. M., and Krieg, T. (2010). Both A2a and A2b adenosine receptors at reperfusion are necessary to reduce infarct

size in mouse hearts. *Am. J. Physiol. Heart Circulat. Physiol.* 299, H1262–H1264. doi: 10.1152/ajpheart.00181.2010

Metzen, E. (2003). Intracellular localisation of human HIF-1alpha hydroxylases: implications for oxygen sensing. *J. Cell Sci.* 116, 1319–1326. doi: 10.1242/jcs.00318

Negre-Salvayre, A., Guerby, P., Gayral, S., Laffargue, M., and Salvayre, R. (2019). Role of reactive oxygen species in atherosclerosis: lessons from murine genetic models. *Free Radic. Biol. Med.* 149, 8–22. doi: 10.1016/j.freeradbiomed.2019.10.011

Nishimura, R., Hasegawa, H., Yamashita, M., Ito, N., Okamoto, Y., Takeuchi, T., et al. (2017). Hypoxia increases glucose transporter 1 expression in bovine corpus luteum at the early luteal stage. *J. Vet. Med. Sci.* 79, 1878–1883. doi: 10.1292/jvms.17-0284

Okamoto, A., Sumi, C., Tanaka, H., Kusunoki, M., Iwai, T., Nishi, K., et al. (2017). HIF-1-mediated suppression of mitochondria electron transport chain function confers resistance to lidocaine-induced cell death. *Sci. Rep.* 7:3816. doi: 10.1038/s41598-017-03980-7

Okonko, D. O., and Shah, A. M. (2015). Mitochondrial dysfunction and oxidative stress in CHF. *Nat. Rev. Cardiol.* 12, 6–8. doi: 10.1038/nrcardio.2014.189

Oliveira, A. C., Richards, E. M., and Raizada, M. K. (2020). Pulmonary hypertension: pathophysiology beyond the lung. *Pharmacol. Res.* 151:104518. doi: 10.1016/j.phrs.2019.104518

Papandreou, I., Cairns, R. A., Fontana, L., Lim, A. L., and Denko, N. C. (2006). HIF-1 mediates adaptation to hypoxia by actively downregulating mitochondrial oxygen consumption. *Cell Metab.* 3, 187–197. doi: 10.1016/j.cmet.2006.01.012

Pugh, C. W., and Ratcliffe, P. J. (2003). Regulation of angiogenesis by hypoxia: role of the HIF system. *Nat. Med.* 9, 677–684. doi: 10.1038/nm0603-677

Ren, B.-F., Deng, L.-F., Wang, J., Zhu, Y.-P., Wei, L., and Zhou, Q. (2008). Hypoxia regulation of facilitated glucose transporter-1 and glucose transporter-3 in mouse chondrocytes mediated by HIF-1α. *Joint Bone Spine* 75, 176–181. doi: 10.1016/j.jbspin.2007.05.012

Renna, N. F., de Las Heras, N., and Miatello, R. M. (2013). Pathophysiology of vascular remodeling in hypertension. *Int. J. Hypertens.* 2013:808353. doi: 10.1155/2013/808353

Riddle, S., Ahmad, A., Ahmad, S., Malkki, M., Schneider, B., Allen, C., et al. (2000). Hypoxia induces hexokinase II gene expression in human lung cell line A549. *Am. J. Physiol. Lung Cell. Mol. Physiol.* 278, L407–L416. doi: 10.1152/ajplung.2000.278.2.L407

Rimoldi, S. F., Rexhaj, E., Pratali, L., Bailey, D. M., Hutter, D., Faita, F., et al. (2012). Systemic vascular dysfunction in patients with chronic mountain sickness. *Chest* 141, 139–146. doi: 10.1378/chest.11-0342

Salceda, S. (1997). Hypoxia-inducible factor 1alpha (HIF-1alpha) protein is rapidly degraded by the ubiquitin-proteasome system under normoxic conditions. Its stabilization by hypoxia depends on redox-induced changes. *J. Biol. Chem.* 272, 22642–22647. doi: 10.1074/jbc.272.36.22642

Schodel, J., and Ratcliffe, P. J. (2019). Mechanisms of hypoxia signalling: new implications for nephrology. *Nat. Rev. Nephrol.* 15, 641–659. doi: 10.1038/s41581-019-0182-z

Schönenberger, M., and Kovacs, W. (2015). Hypoxia signaling pathways: modulators of oxygen-related organelles. *Front. Cell Dev. Biol.* 3:42. doi: 10.3389/fcell.2015.00042

Schultz, K., Fanburg, B. L., and Beasley, D. (2006). Hypoxia and hypoxia-inducible factor-1α promote growth factor-induced proliferation of human vascular smooth muscle cells. *Am. J. Physiol. Heart Circulat. Physiol.* 290, H2528–H2534. doi: 10.1152/ajpheart.01077.2005

Semenza, G. L. (2011). Hypoxia-inducible factor 1: regulator of mitochondrial metabolism and mediator of ischemic preconditioning. *Biochim. Biophys. Acta* 1813, 1263–1268. doi: 10.1016/j.bbamcr.2010.08.006

Semenza, G. L. (2014a). Hypoxia-inducible factor 1 and cardiovascular disease. *Annu. Rev. Physiol.* 76, 39–56. doi: 10.1146/annurev-physiol-021113-170322

Semenza, G. L. (2014b). Oxygen sensing, hypoxia-inducible factors, and disease pathophysiology. *Annu. Rev. Pathol.* 9, 47–71. doi: 10.1146/annurev-pathol-012513-104720

Semenza Gregg, L. (2012). Hypoxia-inducible factors in physiology and medicine. *Cell* 148, 399–408. doi: 10.1016/j.cell.2012.01.021

Sendoel, A., and Hengartner, M. O. (2014). Apoptotic cell death under hypoxia. *Physiology (Bethesda)* 29, 168–176. doi: 10.1152/physiol.00016.2013

Siques, P., Brito, J., and Pena, E. (2018). Reactive oxygen species and pulmonary vasculature during hypobaric hypoxia. *Front. Physiol.* 9:865. doi: 10.3389/fphys.2018.00865

Sousa Fialho, M. D. L., Abd Jamil, A. H., Stannard, G. A., and Heather, L. C. (2019). Hypoxia-inducible factor 1 signalling, metabolism and its therapeutic potential in cardiovascular disease. *Biochim. Biophys. Acta Mol. Basis Dis.* 1865, 831–843. doi: 10.1016/j.bbadis.2018.09.024

Stenmark, K., and Mecham, R. (1997). Cellular and molecular mechanisms of pulmonary vascular remodeling. *Annu. Rev. Physiol.* 59, 89–144. doi: 10.1146/annurev.physiol.59.1.89

Struthers, A. D. (2005). Pathophysiology of heart failure following myocardial infarction. *Heart* 91(Suppl. 2), ii14–ii16; discussion ii31, ii43–ii48. doi: 10.1136/hrt.2005.062034

Supinski, G. S., Schroder, E. A., and Callahan, L. A. (2019). Mitochondria and critical illness. *Chest* 157, 310–322. doi: 10.1016/j.chest.2019.08.2182

Suski, J. M., Lebiedzinska, M., Bonora, M., Pinton, P., Duszynski, J., and Wieckowski, M. R. (2012). "Relation between mitochondrial membrane potential and ROS formation," in *Mitochondrial Bioenergetics: Methods and Protocols*, eds C. M. Palmeira, and A. J. Moreno (Totowa, NJ: Humana Press), 183–205. doi: 10.1007/978-1-61779-382-0_12

Thomas, L. W., and Ashcroft, M. (2019). Exploring the molecular interface between hypoxia-inducible factor signalling and mitochondria. *Cell. Mol. Life Sci.* 76, 1759–1777. doi: 10.1007/s00018-019-03039-y

Tullio, F., Angotti, C., Perrelli, M.-G., Penna, C., and Pagliaro, P. (2013). Redox balance and cardioprotection. *Basic Res. Cardiol.* 108:392. doi: 10.1007/s00395-013-0392-7

Wang, T., Palucci, D., Law, K., Yanagawa, B., Yam, J., and Butany, J. (2012). Atherosclerosis: pathogenesis and pathology. *Diagn. Histopathol.* 18, 461–467. doi: 10.1016/j.mpdhp.2012.09.004

Waypa, G. B., Smith, K. A., and Schumacker, P. T. (2016). O2 sensing, mitochondria and ROS signaling: the fog is lifting. *Mol. Aspects Med.* 47-48, 76–89. doi: 10.1016/j.mam.2016.01.002

Weber, C., and Noels, H. (2011). Atherosclerosis: current pathogenesis and therapeutic options. *Nat. Med.* 17, 1410–1422. doi: 10.1038/nm.2538

Welsh, D. J., and Peacock, A. J. (2013). Cellular responses to hypoxia in the pulmonary circulation. *High Alt. Med. Biol.* 14, 111–116. doi: 10.1089/ham.2013.1016

Wigfield, S. M., Winter, S. C., Giatromanolaki, A., Taylor, J., Koukourakis, M. L., and Harris, A. L. (2008). PDK-1 regulates lactate production in hypoxia and is associated with poor prognosis in head and neck squamous cancer. *Br. J. Cancer* 98, 1975–1984. doi: 10.1038/sj.bjc.6604356

Zhou, Z., Subramanian, P., Sevilmis, G., Globke, B., Soehnlein, O., Karshovska, E., et al. (2011). Lipoprotein-derived lysophosphatidic acid promotes atherosclerosis by releasing CXCL1 from the endothelium. *Cell Metab.* 13, 592–600. doi: 10.1016/j.cmet.2011.02.016

Conflict of Interest: The authors declare that the research was conducted in the absence of any commercial or financial relationships that could be construed as a potential conflict of interest.

Copyright © 2020 Liu, Galli, Wang, Fan, Wang, Wang and Xiao. This is an open-access article distributed under the terms of the Creative Commons Attribution License (CC BY). The use, distribution or reproduction in other forums is permitted, provided the original author(s) and the copyright owner(s) are credited and that the original publication in this journal is cited, in accordance with accepted academic practice. No use, distribution or reproduction is permitted which does not comply with these terms.

frontiers in Physiology

REVIEW
published: 30 July 2020
doi: 10.3389/fphys.2020.00836

Transient Receptor Potential Ankyrin Type-1 Channels as a Potential Target for the Treatment of Cardiovascular Diseases

Song Gao[1†], Keneilwe Kenny Kaudimba[1†], Shanshan Guo[1], Shuang Zhang[1,2], Tiemin Liu[1,3], Peijie Chen[1]* and Ru Wang[1]**

[1] School of Kinesiology, Shanghai University of Sport, Shanghai, China, [2] Institute of Sport Science, Harbin Sport University, Harbin, China, [3] State Key Laboratory of Genetic Engineering, Institute of Metabolism and Integrative Biology, Human Phenome Institute, Department of Endocrinology and Metabolism, and School of Life Sciences, Zhongshan Hospital, Fudan University, Shanghai, China

OPEN ACCESS

Edited by:
Ying Mei Zhang,
Zhongshan Hospital, Fudan University, China

Reviewed by:
Alexander Dietrich,
Ludwig Maximilian University of Munich, Germany
Jun Ren,
University of Washington, United States

***Correspondence:**
Tiemin Liu
tiemin_liu@fudan.edu.cn
Peijie Chen
chenpeijie@sus.edu.cn
Ru Wang
wangru@sus.edu.cn

[†] These authors have contributed equally to this work

Specialty section:
This article was submitted to Vascular Physiology, a section of the journal Frontiers in Physiology

Received: 19 January 2020
Accepted: 22 June 2020
Published: 30 July 2020

Citation:
Gao S, Kaudimba KK, Guo S, Zhang S, Liu T, Chen P and Wang R (2020) Transient Receptor Potential Ankyrin Type-1 Channels as a Potential Target for the Treatment of Cardiovascular Diseases. Front. Physiol. 11:836. doi: 10.3389/fphys.2020.00836

Cardiovascular disease is one of the chronic conditions with the highest mortality rate in the world. Underlying conditions such as hypertension, metabolic disorders, and habits like smoking are contributors to the manifestation of cardiovascular diseases. The treatment of cardiovascular diseases is inseparable from the development of drugs. Consequently, this has led to many researchers to focus on the search for effective drug targets. The transient receptor potential channel Ankyrin 1 (TRPA1) subtype is a non-selective cation channel, which belongs to the transient receptor potential (TRP) ion channel. Previous studies have shown that members of the TRP family contribute significantly to cardiovascular disease. However, many researchers have not explored the role of TRPA1 as a potential target for the treatment of cardiovascular diseases. Furthermore, recent studies revealed that TRPA1 is commonly expressed in the vascular endothelium. The endothelium is linked to the causes of some cardiovascular diseases, such as atherosclerosis, myocardial fibrosis, heart failure, and arrhythmia. The activation of TRPA1 has a positive effect on atherosclerosis, but it has a negative effect on other cardiovascular diseases such as myocardial fibrosis and heart failure. This review introduces the structural and functional characteristics of TRPA1 and its importance on vascular physiology and common cardiovascular diseases. Moreover, this review summarizes some evidence that TRPA1 is correlated to cardiovascular disease risk factors.

Keywords: TRPA1 channel, vascular physiology, atherosclerosis, heart failure, myocardial fibrosis, arrhythmia

INTRODUCTION

At present, the incidence of cardiovascular disease has increased significantly and has become a significant health issue of global concern (North and Sinclair, 2012; Alali et al., 2017). The rapid world economic growth has aggravated the double pressure of work coupled with unhealthy lifestyles, which increases the chance of being exposed to independent risk factors (Luan et al., 2019). Independent risk factors for cardiovascular diseases include smoking, diabetes, hypertension, dyslipidemia, and obesity (Guo et al., 2020; Wang R. et al., 2020). Long-term exposure to risk factors exacerbates the impacts of cardiovascular disease (Pei et al., 2014; Wu et al., 2019a). Common cardiovascular diseases include atherosclerosis, myocardial fibrosis, heart failure, and arrhythmia. Almost all cardiovascular diseases require long-term medication to correct their

physiological and pathological changes (Huddy et al., 2013). However, the side effects of long-term medication should be addressed aggressively (Ramkumar et al., 2016). Treating arrhythmia with some antiarrhythmic drugs can cause bradycardia and atrioventricular block (Sardar et al., 2016). Furthermore, long-term use of cardiotonic drugs can cause arrhythmia in addition to gastrointestinal symptoms (Ward et al., 1983; Hamlin, 2007; Sala and Bellin, 2017; Ivanov and Lagunin, 2019). Therefore, it is particularly important to explore new drug targets for the treatment of cardiovascular diseases. The discovery of drug targets is the basis of new drug development. The discovery of a new drug target is a breakthrough in the development of a series of new drugs. Currently, the targets of cardiovascular diseases are updated constantly. Researchers started with the pathogenesis of cardiovascular diseases looking for key receptors, ion channels, and signaling pathways that mediate the formation of cardiovascular diseases as targets for drug development (Overington et al., 2006; Maclay and MacNee, 2013; Mokou et al., 2017). Common drug targets for cardiovascular diseases are Rho kinase (Shimokawa et al., 2016), M3 receptor in functional muscarinic acetylcholine receptor (Kovacevic et al., 2015; Rhoden et al., 2019), S1P signaling pathway (sphingosine 1-phosphate) (Yung et al., 2017), and miR-145 (Massy et al., 2017; Sahu et al., 2017).

Transient receptor potential (TRP) channels are widely regarded as drug targets (Moran, 2018). TRP was first discovered when studying the visual conduction system of *Drosophila melanogaster* (Katz et al., 2013). In subsequent studies, more than 50 channel members of this family have been found from yeast, insects, fish, and mammals, of which more than 30 were found in mammals (Moran et al., 2004; Vriens et al., 2004; Nilius and Owsianik, 2011). Based on the differences in amino acid sequence homology of 33 TRP channels found in mammals, the TPR channels are divided into seven subfamilies, namely, TRPA, TRPC, TRPV, TRPM, TRPP, TRPML, and TRPN (Ramsey et al., 2006). Previous research has shown that members of the TRP family closely relate to cardiovascular disease (Ma et al., 2017). TRPV1 channel can regulate vascular smooth muscle and improve hypertension, causing heart dysfunction under cold exposure (Zhang et al., 2012; Shanks et al., 2019). The TRPV1 and TRPV4 channels are involved in the cardiovascular protection of hypoxia. TRPM7 is significantly upregulated in atrial fibroblasts from patients with atrial fibrillation (Yue et al., 2015). However, the role of TRPA1 in cardiovascular diseases is uncertain. In recent years, research on TRPA1 has been increasing, hence a close relationship between TRPA1 and cardiovascular diseases is established (Bodkin and Brain, 2011). Atherosclerosis causes chronic inflammation, and the activation of TRPA1 suppresses this inflammation (Bautista et al., 2006; Bonet et al., 2013). Moreover, some studies found that TRPA1 is also involved in the process of oxidative stress and myocardial fibrosis (Nilius and Szallasi, 2014; Wang et al., 2018).

In this review, researchers summarized the structure and the functions of TRPA1, which commonly uses agonists and inhibitors. Furthermore, the review summarizes the potential role of TRPA1 in regulating the pathophysiology of the cardiovascular system, including vascular physiology, atherosclerosis, myocardial fibrosis, heart failure, and arrhythmia (**Table 1**). Finally, this paper presents some evidence that TRPA1 is closely linked to cardiovascular disease risk factors.

The Structure and Function of TRPA1

TRP ion channel is a non-selective cation channel located on the cell membrane, which is essentially a tetrameric form of Ca^{2+} influx channel (Hardie and Minke, 1992; Hofmann et al., 2017). Minke et al. discovered TRP in visual cells of *Drosophila* for the first time when studying the *Drosophila* experiments that is related to visual conduction (Cosens and Manning, 1969). It was observed that TRP only induces transient Ca^{2+} influx after light stimulation, generating a transient potential (Kumar et al., 2015). The letter "A" in the TPRA subfamily represents ankyrin, which has only one member, TRPA1. Like other TRP channels, ankyrin is embedded in the cell membrane and has a six-time transmembrane structure. They have a stoma area between S5 and S6 for ions to enter and exit the cell membrane. The N terminus and C terminus of the channel protein are located inside the cell (Schaefer, 2005; MacPherson, 2007). TRPA1 has similar characteristics of ankyrin repeats at its N terminus, whereas other TRP subfamily ankyrin repeats have only three to four times (Bodkin and Brain, 2011; Benemei et al., 2013). Ankyrin repeats are 33-amino-acid motifs that regulate the interaction between proteins. The cysteine residues in these repeats act as TRPA1 agonists covalently modifying the binding target (Dietrich et al., 2017). After TRPA1 activation, extracellular cations, such as Na^{+} and H^{+}, are increased, especially Ca^{2+} influx, thereby mediating a series of physiological responses (Story et al., 2003). The structure of TRPA1 is shown in **Figure 1**. TRPA1 is best known as a sensor for environmental irritants giving rise to somatosensory modalities, such as pain, cold, itch, and other protective responses. TRPA1 plays an vital role in the pathological process of cough, oxidative stress, and inflammation (Chen et al., 2013; Benemei et al., 2014; Kurganov et al., 2014; Nassini et al., 2014; Winter et al., 2017). Recent studies have found that TRPA1 activation articulates in pancreatic islets, gastrointestinal tract, heart, and blood vessels (Pozsgai et al., 2010; Kun et al., 2014). Activation of TRPA1 in islet β cells can stimulate insulin secretion (Cao et al., 2012), in vascular cells it can improve endothelium-dependent diastolic function (Earley et al., 2009; Inoue et al., 2009), whereas in the intestine it can regulate the secretion of hunger hormones, GLP-1, and has effects on weight loss and regulating glucose and lipid metabolism (Derbenev and Zsombok, 2016). These studies concluded that TRPA1 might serve as a potential target to protect blood vessels and regulate metabolism.

TRPA1 is a non-selective cation channel and has the function of a receptor. TRPA1 channel activation includes multiple pathways. TRPA1 can be activated by a series of chemical stimuli, including cinnamaldehyde (Bandell et al., 2004), allicin (Bautista et al., 2005), allyl isothiocyanate (AITC) (Bandell et al., 2004; Jordt et al., 2004), ligustilide (Zhong et al., 2011), acrolein (Bautista et al., 2006), and nicotine (Andre et al., 2008; Talavera et al., 2009). In addition to exogenous agonists, recent studies found out that endogenous compounds released during tissue damage and oxidative stress can also activate

TABLE 1 | Role of the TRPA1 channel in the cardiovascular system.

Diseases	Animals	Expression in heart and vasculature	Effects	Mechanisms	References
Vascular physiology	Female CD1, C57BL/6, CGRP-/-, TRPV1-/-, and TRPA1-/- mice	–	4-ONE (1–30 nmol, intraplantar injection) triggers a vasodilation response, but not in TRPA1-/- mice	TRPA1-dependent neurogenic vasodilatation	Graepel et al., 2011
	Male Sprague–Dawley rats	Trigeminal root ganglia neurons	AITC (100 μM, intranasal administration) and acrolein (30 μM, intranasal administration) increase cerebral blood flow, but the effect is blocked by HC-030031 (50 μM, intranasal administration)	Neurogenic vasodilation	Kunkler et al., 2011
	Male CD1, CGRP-/-, TRPV1-/-, and TRPA1-/- mice (8–12 weeks old)	–	Cinnamaldehyde (1–30%) increases the blood flow, but not in HC-030031 (100 mg/kg)-treated and TRPA1 knockout mice	Neurogenic vasodilation	Aubdool et al., 2016
	Male Sprague–Dawley rats	Endothelial cells	AITC-induced (3–100 μM) cerebral artery dilation was abolished by the administration of HC-030031 (3 μM)	Endothelium-dependent vasodilation	Earley et al., 2009
	Adolescent rats	Endothelial cells	AITC (15–60 μM) evokes graded cerebral artery vasodilation	Endothelium-dependent vasodilation	Qian et al., 2013
	CD1, CGRP-/-, TRPV1-/-, and TRPA1-/- mice	–	Cinnamaldehyde (80–320 μM/kg) induces a transient hypotensive response followed by a sustained hypertensive response	Autonomic system reflexes	Pozsgai et al., 2010
Atherosclerosis	Male C57BL/6, apoE-/- and apoE-/-TRPA1-/- mice (8 weeks old)	Macrophages	AITC (10 mg/kg/day, 4 weeks, i.g.) suppresses atherosclerosis; HC-030031 (10 mg/kg/day, 4 weeks, i.g.) and TRPA1 knockout exacerbate atherosclerosis	Cholesterol metabolism and inflammation in macrophages	Zhao et al., 2016
	Male C57BL/6, apoE-/-, and apoE-/-TRPA1-/-mice (6–8 weeks old)	Macrophages	TRPA1-/-ApoE-/- mice showed a significant increase in atherosclerosis plaques; activation of TRPA1 by CIN sharply reduced atherosclerosis progression	Inflammation in macrophages	Wang Q. et al., 2020
Myocardial fibrosis	Male C57BL/6 mice (8–10 weeks old)	Cardiomyocytes and macrophages	HC-030031 (10 mg/kg/day, 4 weeks, i.g.) and TCS-5861528 (3 mg/kg/day, 4 weeks, i.g.) ameliorate cardiac hypertrophy and heart failure	Inhibits Ca^{2+}-dependent signal pathways and macrophage polarization	Wang et al., 2018
	–	Human adult ventricular cardiac fibroblasts	HC-030031 (100 μM) and siRNA targeting the TRPA1 channel inhibit methylglyoxal-induced (300 μM) proliferation of cardiac fibroblasts	Inhibits Ca^{2+} entry	Oguri et al., 2014
	–	Cardiac fibroblasts	Activating TRPA1 with a specific agonist AITC promoted the synthesis and secretion of CGRP, as well as intracellular Ca^{2+}	Increasing autocrine CGRP by activating TRPA1 can ameliorate cardiac fibrosis	Li et al., 2019
Heart failure	Male SD rats	Cardiomyocytes and dorsal root ganglia cell	The measured physiological response to topical application of AITC to both the lung and heart surface was blunted	*In vivo* reduction of TRPA1 expression was, in part, caused by CHF-related tissue ischemia and inflammation	Adam et al., 2019
Arrhythmia	Female B6129 mice (19–21 weeks old) and TRPA1-/- mice (21–28 weeks old)	–	Acrolein (537 ppm, 8 times/4 weeks, inhalation) increases heart rate variability and myocardial desynchrony in B6129 mice but not in TRPA1-/- mice	Influence the autonomic nervous system	Thompson et al., 2019
	Female C57BL/6 and TRPA1-/- mice (15–30 weeks old)	–	TRPA1 knockout decreases acrolein-induced (3 ppm, 3 h) heart rate variability and arrhythmias	Cardiac autonomic function	Kurhanewicz et al., 2017, 2018

(Continued)

TABLE 1 | Continued

Diseases	Animals	Expression in heart and vasculature	Effects	Mechanisms	References
	Male spontaneously hypertensive rats (18–20 weeks old)	–	HC-030031 (5 mg/kg, i.p.) reduces diesel exhaust (32 ppm, 4 h)–induced and aconitine (1.5 mg/kg, i.p.)–induced ventricular arrhythmias	Restrains the activity of sympathetic and autonomic imbalance	Hazari et al., 2011
	Male Sprague–Dawley rats (15 weeks old)	–	AITC (30 mM) inhalation causes bradycardia atrioventricular blockade and prolonged PR intervals	Activates the vagus nerve	Hooper et al., 2016

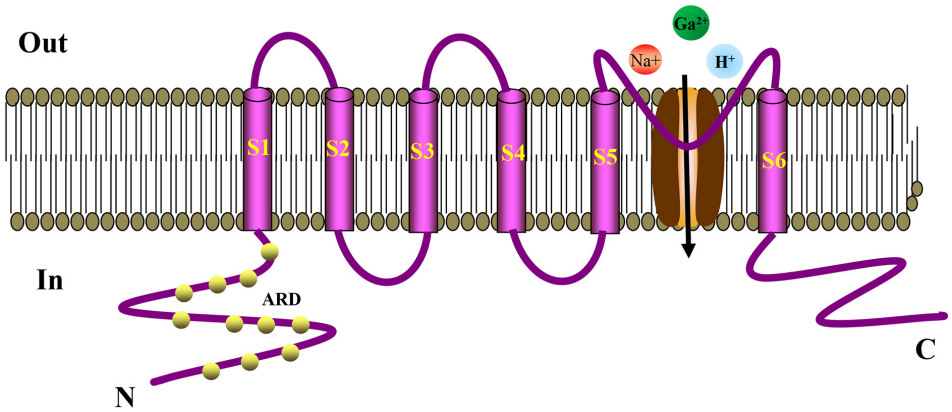

FIGURE 1 | Schematic diagram showing the structure of TRPA1 channel. The TRPA1 channel has a six-time transmembrane structure (S1–S6), and there is a minute opening between S5 and S6 for ions to enter and exit the cell membrane. The N-terminus and C-terminus of the channel protein are located inside the cell. The N-terminus has a large number of characteristic ankyrin repeats, and the cysteine residues in these repeats serve as binding targets for the covalent modification of TRPA1 agonists. TRPA1 can increase the influx of extracellular cations, such as Na^+, H^+, especially Ca^{2+}, thereby mediating a series of physiological reactions. ARD, Ankyrin Repeat Domain.

TRPA1 channels, such as nitric oxide (NO) and hydrogen sulfide (H_2S) (Andersson et al., 2008; Eberhardt et al., 2014), hydrogen peroxide (H_2O_2), 4-hydroxynon-enal (4-HNE), 4-oxoquinone (4-ONE), 4-hydroxyhexenal (4-HHE), and 15-deoxy-delta (12, 14)-prostaglandin J (2) (MacPherson et al., 2007b; Trevisani et al., 2007; Taylor-Clark et al., 2008). Besides, some synthetic compounds have also been reported, including ASP-7663 and Optovin (Kokel et al., 2013; Kojima et al., 2014). Low temperature is thought to activate the TRPA1 channel (Winter et al., 2017). However, TRPA1 is heat sensitive in snakes, lizards, and frogs (Kurganov et al., 2014). However, some agonists have a dual regulatory effect on TRPA1. For example, menthol activates TRPA1 at low concentrations and inhibits TRPA1 at high concentrations (MacPherson et al., 2006; Karashima et al., 2007; Alpizar et al., 2013). **Table 2** lists commonly used TRPA1 agonists.

TRPA1's exogenous antagonists are mainly complex organic or inorganic compounds. Previous studies have found some TRPA1 antagonists, such as ruthenium red, gentamicin, camphor, and high concentration menthol, but these antagonists also have regulatory effects on other certain ion channels (such as TRPV1, TRPV2); therefore, it is not specific. At present, the specific antagonists of TRPA1 mainly include xanthine derivatives, such as HC030031 and its derivatives (McNamara et al., 2007), TCS-5861528 (Wei et al., 2009), and GRC-17536 (Mukhopadhyay et al., 2014); and oxime derivatives, such as A-967079 (Chen et al., 2011) and AP-18 (Petrus et al., 2007; Defalco et al., 2010). The discovery of TRPA1 channel-specific antagonists has essential value for exploring the therapeutic uses of TRPA1. Therefore, researchers devote to finding TRPA1 channel-specific antagonists. **Table 3** lists commonly used TRPA1 inhibitors.

TRPA1 IN THE CARDIOVASCULAR SYSTEM

TRPA1 and Vascular Physiology

The contraction and relaxation of blood vessels form blood pressure, which provides impetus for the blood flow. Vascular smooth muscle regulates the tension of blood vessels under the joint control of vasoconstrictor nerve fibers and vasomotor nerve fibers, which in turn affects changes in blood pressure and blood flow. Long-term abnormal blood pressure is a key factor that causes cardiovascular disease (Earley, 2012). Vascular endothelial cells and vascular smooth muscle cells play an essential role in maintaining normal vascular physiology. K_{Ca} channels in endothelial cells and K_{IR} channels in cerebral arterial muscle cells are jointly mediated by vasodilation signals (Earley et al., 2009; Kohler and Ruth, 2010; Brunt et al., 2013). In addition, calcitonin gene–related peptides (CGRPs) secreted by vascular endothelial cells contribute to vasodilation (Aubdool et al., 2016).

TABLE 2 | TRPA1 agonists.

Agonists	Source	EC_{50}	References
Allyl isothiocyanate (AITC)	Mustard	33 μM (mice)	Bandell et al., 2004; Jordt et al., 2004
		11 ± 1 μM (rat)	
Cinnamaldehyde (CA)	Cinnamon	100 μM (mice)	Bandell et al., 2004
Ligustilide	*Angelica sinensis*	44 μM (mouse)	Zhong et al., 2011
Allicin	Garlic	1.9 μM (human)	Jordt et al., 2004
		1.3 μM (mice)	Bautista et al., 2005
Nicotine	Tobacco	10 μM (mice)	Talavera et al., 2009
Hydrogen peroxide (H_2O_2)	Oxidative stress	230 μM (mice)	Andersson et al., 2008
4-Hydroxynon-enal (4-HNE)	Oxidative stress	10–27 μM (mice)	MacPherson et al., 2007b; Andersson et al., 2008; Taylor-Clark et al., 2008
4-Oxonon-enal (4-ONE)	Oxidative stress	1.5–1.9 μM (mice)	Andersson et al., 2008; Taylor-Clark et al., 2008
4-Hydroxyhexenal (4-HHE)	Oxidative stress	39–50 μM (mice)	Andersson et al., 2008; Taylor-Clark et al., 2008
15-Deoxy-delta(12,14)-prostaglandin J(2) ([15d-PGJ(2)])	Oxidative stress	5.6 μM (mice)	Andersson et al., 2008
ASP-7663	Synthetic	0.51 μM (human)	Kokel et al., 2013
		0.50 μM (mice)	
		0.54 μM (rat)	
Optovin	Synthetic	2 μM (mice)	Kojima et al., 2014

TABLE 3 | TRPA1 antagonists.

Agonists	Structures	IC_{50}	References
HC-030031	Xanthine derivative	6.2 μM (human) 7.6 μM (rat)	McNamara et al., 2007
GRC-17536	Xanthine derivative	Not reported	Mukhopadhyay et al., 2014
TCS-5861528	Xanthine derivative	14.3 μM (human)	Wei et al., 2009
AP-18	Oxime	3.1 μM (human) 8.8 μM (rat) 4.5 μM (mice)	Petrus et al., 2007; Defalco et al., 2010
A-967079	Oxime	0.067 μM (human) 0.289 μM (rat)	Chen et al., 2011

In recent years, studies have demonstrated that TRPA1 has been explored in the vascular system and it was discovered that it has a vital role in the regulation of vascular tone (Earley et al., 2010; Aubdool et al., 2014). Formaldehyde activates the sensitive TRPA1 channel, causing the endothelium-dependent mechanism of Ca^{2+} influx and mediating the relaxation of isolated rat superior mesenteric artery. However, the same effect has not been found in the aorta (Jin et al., 2019). 4-ONE leads to obvious vasodilation, but this effect is not reflected in TRPA1-/- mice (Graepel et al., 2011). Both AITC and cinnamaldehyde significantly increased blood flow in the skin of anesthetized wild-type mice, but had no significant effect on TRPA1 knockout mice (Pozsgai et al., 2010). In cerebral circulation, the TRPA1 channel occurs in endothelial cells, and it is concentrated in the junction site of the endothelium muscle. Activation of the TRPA1 channel causes Ca^{2+} influx, mediating smooth muscle cell hyperpolarization and endothelium-dependent vasodilation (Sullivan et al., 2015). A study pointed out that stimulation of the TRPA1 channel causes vasodilation in a graded cerebral artery which is also caused by endothelial cell Ca^{2+} signaling (Qian et al., 2013). One study revealed that TRPA1 inhibitors and endothelial destruction antagonize AITC-induced cerebral artery vasodilation. AITC-induced arterial dilatation was blocked by treatment with small and medium-conductivity Ca^{2+}-activated K^+ channel blockers. Inwardly rectifying potassium channel treatment by blockers also blocked AITC-mediated vasodilation (Earley et al., 2009). The research indicated that Ca^{2+} influx via endothelial TRPA1 channels mediates cerebral artery vasodilation, which involves endothelial cell Ca^{2+}-activated K^+ channels and smooth muscle inward rectification K^+ channels leading to hyperpolarization of cell membranes.

Other studies showed that the TRPA1 channel present in the peripheral vascular nerve mediates the chemical agonist through the mechanism of CGRP release, thereby mediating peripheral arterial vasodilation (Peixoto-Neves et al., 2019). The exogenous agonist of TRPA1 stimulates the release of CGRP and increases cerebral blood flow; this effect is blocked by TRPA1 and CGRP receptor antagonists (Kunkler et al., 2011; Aubdool et al., 2016).

The effect of TRPA1 activity on vascular physiology is also reflected in the regulation of blood pressure (Pazienza et al., 2014). Systemic administration of TRPA1 agonists will cause a transient hypotensive response, and then the heart rate and blood pressure continue to increase as a result of increased sympathetic nerve activity. Cinnamaldehyde relaxes the mesenteric artery in mice in a TRPA1-dependent manner (Pozsgai et al., 2010); however, the effect of intravenous administration of cinnamaldehyde on blood pressure is more complicated. The low dose of cinnamaldehyde causes the mesenteric artery to relax, which in turn causes a hypotensive response. The high dose of cinnamaldehyde causes a boosting response, which may involve the regulatory mechanism of the vagus nerve. Studies have indicated that vasodilation and antihypertensive effects are mediated by TRPA1 and TRPV1 (Ma et al., 2019). Vasodilation often uses propofol as an anesthetic, which in turn causes a hypotensive effect (Sinharoy et al., 2017). Currently, researchers knocked out the genes of TRPA1 and TRPV1 in mice, and the antihypertensive effect of propofol was significantly weakened (Sinha et al., 2015). However, after knocking out the mouse TRPV1 gene alone, the antihypertensive effect of propofol was not affected. Therefore, the TRPA1 ion channel, which mediates propofol-induced vasodilation, had little significance on TRPV1 ion channel. TRPA1 is a cold-stress cation channel that is activated at low temperatures (<17°C). In low-temperature environments, skin blood vessels contract, and vasodilation occurs after continuous contraction. TRPA1 plays a vital role in changes in vascular tone mediated by low temperatures (Aubdool et al., 2014).

Therefore, TRPA1 causes vasodilation under the action of an agonist and increases blood flow, which in turn regulates blood pressure. TRPA1 channel regulates blood pressure in a

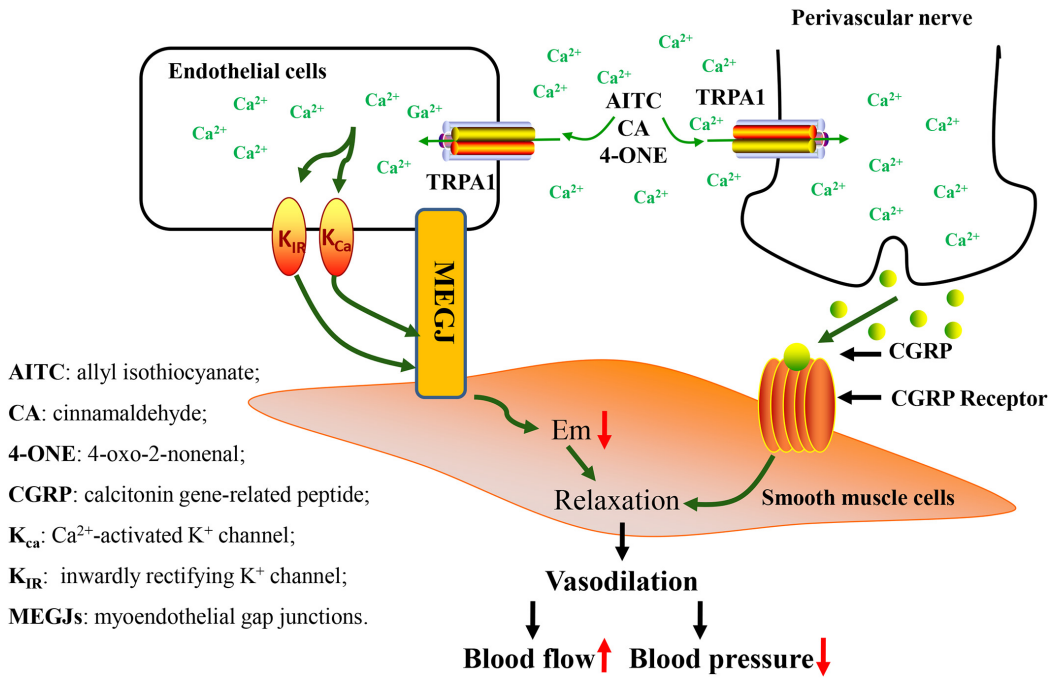

FIGURE 2 | Vascular physiological changes caused by activation of TRPA1 channel. Activation of the TRPA1 channel causes Ca^{2+} influx, leading to hyperpolarization of endothelial cell membranes. This change in potential causes hyperpolarization of smooth muscle cell membranes, causing relaxation of muscle cells. In addition, activation of the TRPA1 channel induces an increase in [Ca^{2+}], which leads to the release of the neuropeptide CGRP from perivascular nerve, thereby mediating vasodilation. Vasodilation causes changes in blood flow and blood pressure.

bidirectional manner, which is related to the dose of the agonist. In addition, the activation of the TRPA1 channel under low-temperature environment causes changes in the tension of blood vessels (**Figure 2**). In conclusion, TRPA1 activity affects vascular function, but the exact role and significance of this channel in the cardiovascular system is yet to be determined.

TRPA1 AND COMMON CARDIOVASCULAR DISEASES

TRPA1 and Atherosclerosis

Atherosclerosis is one of the main reasons that lead to the causes of various cardiovascular diseases. The key initial factor of atherosclerosis is the accumulation of cholesterol (Yu et al., 2016), which in turn causes the formation of atherosclerotic plaques. This plaque leads macrophages to trigger a chronic inflammatory response. Macrophages clear excess peripheral cholesterol and convert the intracellular cholesterol into high-density lipoprotein (HDL) for excretion or storage. Macrophages play an essential role in the immune response of atherosclerosis, and the excessive intake of cholesterol into foam cells is the main reason for the formation of atherosclerosis (Lin et al., 2015). The outflow of cholesterol derived from oxidized low-density lipoprotein (oxLDL) is destroyed, and then the lipid accumulates in macrophages. When the lipid is overloaded and exceeds the metabolic capacity of macrophages, a large amount of lipids accumulate in the macrophages, which promotes the growth of blood vessel intima and the formation of necrotic nuclei, increasing the risk of plaque rupture. Furthermore, macrophages transform into foam cells, which further activates the inflammatory response and exacerbates the risk factors of plaque formation.

Cholesterol accumulation in macrophages determines lipid phagocytosis and cholesterol efflux. When the cholesterol content in the macrophages is too high, the macrophages will start the cholesterol efflux system and expel cholesterol from the cells to synthesize HDL. The main factors involved in cholesterol efflux are ATP binding cassette subfamily A member 1 (ABCA1) and ABCG1. Oxidative modified LDL causes lipid peroxidation of macrophages, which reduces the amount of HDL binding and causes cholesterol outflow disorder. TRPA1 expression in macrophage foam cells in the atherosclerotic aorta of apolipoprotein E-deficient [apoE (-/-)] mice was increased. Administration of the TRPA1 channel antagonist HC030031 or knockout of the TRPA1 [TRPA1 (-/-)] gene in apoE (-/-) mice can exacerbate atherosclerotic lesions, hyperlipidemia, and systemic inflammation (Zhao et al., 2016). Moreover, treatment with allyl isothiocyanate (AITC, TRPA1 agonist) can inhibit the progression of atherosclerosis in apoE (-/-) mice, but the TRPA1 (-/-) gene knockout atherosclerosis has no effect on sclerotic mice. Mouse macrophages showed that TRPA1 channels were activated by oxidized low-density lipoprotein (oxLDL). TRPA1 antagonists or knocking out the TRPA1 gene will exacerbate OxLDL-induced lipid accumulation in macrophages. Whereas inhibiting TRPA1 activity damages cholesterol efflux

by downregulating the ATP binding cassette transporter, it does not change the internalization of oxLDL. Furthermore, macrophages activated by AITC weakens the inflammatory response induced by tumor necrosis factor-α, hence a recent study also reached a similar conclusion, TRPA1-/-ApoE-/- mice atherosclerotic plaque increased significantly (Wang Q. et al., 2020). The activation of TRPA1 by cinnamaldehyde significantly slows the progression of atherosclerosis. The researchers found out that inhibition of TRPA1 significantly stimulated the expression of M1 marker genes. TRPA1, which is upregulated in atherosclerotic plaques, can regulate the inflammatory phenotype of macrophages, thereby regulating the progress of atherosclerosis (Wang Q. et al., 2020). Therefore, TRPA1 plays a crucial role in the mechanism of atherosclerosis formation and it could be a therapeutic target for atherosclerosis and other metabolic diseases.

The current study confirmed that TRPA1 is associated with atherosclerosis, and it plays a key role in the macrophage cholesterol outflow and inflammation. However, it is not clear how the TRPA1 channel depends on the Ca^{2+} influx to mediate macrophage-derived foam cell formation. Lysophosphatidylcholine (LPC) is the main atherosclerotic lipid that stimulates the increase in mitochondrial reactive oxygen species (mtROS) and releases cytokines upon activation of the inflammatory body. A recent study examined the functional expression of TRPA1 in macrophages derived from the human acute monocytic leukemia cell line (THP-1). LPC induces the activation of THP-1-derived macrophages through Ca^{2+} influx, and TRPA1 inhibitors inhibit this activation. TRPA1 is involved in regulating Ca^{2+} influx caused by LPC. This result indicates that TRPA1 has important physiological functions in macrophages and is widely involved in the inflammation caused by LPC (Tian et al., 2020). This may be the early stage of macrophage foam cell. Further studies should be conducted to reveal the specific role of TRPA1 in the formation of macrophage foam cells.

TRPA1 and Myocardial Fibrosis

Myocardial fibrosis refers to the excessive deposition of collagen fibers in myocardial tissue, the imbalance of various types of collagen, and the disorder of arrangement. Abnormal activation of cardiac fibroblasts is closely related to the formation of myocardial fibrosis. Myocardial fibroblasts are directed to the injury site under the influence of various pathological factors such as pressure overload, endothelial injury, hypoxic–ischemic injury, and generate a large number of extracellular matrix (ECM) mediated by local inflammatory factors, cytokines, and neurohumoral factors (Ma et al., 2012). Changes in the composition of myocardial ECM are the pathological basis of myocardial fibrosis. The process of myocardial fibrosis causes abnormalities in myocardial function, metabolism, and transmission, which leads to heart failure, various arrhythmias, and other heart disorders. Studies have shown that endogenous bioactive substances produced by cardiac fibroblasts regulate their activation. Furthermore, Ca^{2+}-dependent signaling is essential for the proliferation of cardiac fibroblasts. Thus, understanding the effects and regulatory mechanisms of endogenous bioactive substances and Ca^{2+}-dependent signaling on cardiac fibroblasts, which will provide new targets for anti-fibrosis strategies.

The autocrine of calcitonin gene-related peptide (CGRP) in myocardial fibroblasts may cause a positive cardiovascular effect, which relates to the inhibition of myocardial fibrosis (Russell et al., 2014). TRPA1 has been proven to promote the synthesis and secretion of CGRP and intracellular Ca^{2+} under the action of non-specific agonist AITC, while TRPA1 specific antagonist HC030031 can reverse these effects. CGRP is abundant in rat, mouse, and human myocardium, and it shows that cardiac CGRP develops from cardiac fibroblasts. In an animal experiment, calcitonin/CGRP knockout (KO) mice showed significant cardiac phenotypes, including cardiac remodeling and myocardial fibrosis (Supowit et al., 2005). The TGF-β superfamily is an important multifunctional growth factor that not only mediates cell growth, proliferation, and differentiation but also plays an important role in wound healing and the formation of ECM. It was discovered that TGF-β1 induced the activation of cardiac fibroblasts, and found that TGF-β1 can increase the mRNA expression of cardiac fibroblasts and the secretion level of CGRP. CGRP8-37 (CGRP receptor antagonist) exacerbates TGF-β1-induced cardiac fibroblast proliferation, differentiation, collagen production, and inflammation, thus indicating the decisive role of CGRP secretion in the formation of myocardial fibrosis. CGRP of cardiac fibroblasts is also an endogenous inhibitor of cardiac fibrosis. Furthermore, monocrotaline (MCT) is used to induce pulmonary hypertension, which gradually led to right ventricular fibrosis. The non-toxic TRPA1 agonist cinnamaldehyde (CA) inhibits MCT-induced pulmonary hypertension, which increases the RVSP, RV/LV + S, and right ventricular collagen accumulation, and downregulation of CGRP (Li et al., 2019). This indicates that TRPA1 activation has potential benefits in inhibiting TGF-β1-induced myocardial fibrosis.

Methylglyoxal (MG), also known as pyruvaldehyde, can activate TRPA1, which is a toxic by-product of glycolysis. It is distributed in all cells of mammals and is associated with various vascular diseases (Wang et al., 2019). In an *in vitro* study, myocardial fibroblast differentiation showed that it closely relates to MG-induced Ca^{2+} influx, and this effect was attenuated with the inhibition of TRPA1 channels, and the study suggests that MG-induced cardiac fibroblasts require TRPA1-mediated Ca^{2+}-dependent signaling pathway (Oguri et al., 2014). In addition, inhibition of TRPA1 activity can significantly improve the degree of cardiac hypertrophy and myocardial fibrosis in mice, which may be related to weight loss and increase in aortic cross-sectional area (Wang et al., 2018).

Autocrine CGRP and Ca^{2+}-dependent signaling of cardiac fibroblasts play an important role in the process of myocardial fibrosis formation. TRPA1 promotes the secretion of CGRP under the action of agonists and then inhibit the formation of myocardial fibrosis. However, TRPA1 inhibition antagonizes MG-induced Ca^{2+} influx. Subsequently, TRPA1 has opposite roles in the two pathways. At least it is clear that TRPA1 plays an important role in the pathological process of myocardial fibrosis. Further research should be done to consider the role of TRPA1

in different stages of myocardial fibrosis formation and use this potential therapeutic target more accurately.

TRPA1 and Heart Failure

Heart failure is the ultimate destination of most cardiovascular diseases, which leads to heart circulation disorder caused by systolic or diastolic dysfunction. The activation of various neuroendocrine mechanisms such as the renin–angiotensin system, pro-inflammatory factors, and natriuretic peptide system closely relates to the development of heart failure (Geng et al., 2019; Hsu et al., 2020). Abnormal activation of the sympathetic nervous system is one of the most critical pathophysiological characteristics of heart failure (Sousa-Pinto et al., 2014). Excessive cardiac sympathetic reflex helps in nerve excitement. In an animal model experiment, capsaicin, as an agonist of TRPV1, enhanced cardiac sympathetic reflex. Capsaicin given after cutting off the vagus nerve in a rat heart failure model increased mean arterial pressure, heart rate, and renal sympathetic nerve activity (Adam et al., 2019). This suggests that TRPV1 activation enhances the degree of heart failure. Because of the similarity of TRPV1 and TRPA1 channels, TRPA1 activation may mediate cardiac sympathetic excitation. In addition, Ca^{2+} plays an important role in the myocardial excitation–contraction coupling mechanism, and myocardial cells in heart failure models show abnormal Ca^{2+} flow (Bers, 2006; Roe et al., 2015). The exact mechanism is unclear, however, as to the causes of abnormal sympathetic nerve excitement and heart muscle cell Ca^{2+} insufficiency. In the future, research must focus on these important targets for reducing heart failure.

The TRPA1 channel-mediated sympathetic reflex is unclear. It is worth noting that excessive sympathetic nerve excitation is a characteristic of chronic heart failure (CHF). In a recent study, the use of TRPA1 agonists to the surface of the heart and lungs increased heart rate and sympathetic nerve output in the control group of rats, on average arterial pressure, which changes in two phases. However, these effects are attenuated in CHF rats, thereby reducing the possibility of TRPA1 channel sensitization to CHF cardiopulmonary afferent (Adam et al., 2019). This shows that activation of the TRPA1 channel does not mediate an increase in sympathetic nerve reflexes and slightly decreases in CHF rats. In a mouse model experiment, the AITC stimulation of TRPA1 caused a dose-dependent increase in the peak $[Ca^{2+}]_I$ of isolated cardiomyocytes, time, and speed of reaching the peak of $[Ca^{2+}]_I$. However, no change in $[Ca^{2+}]_I$ was observed in cardiomyocytes pretreated with TRPA1 antagonist HC-030031 or cardiomyocytes obtained from TRPA1-/- mice (Andrei et al., 2017). TRPA1 stimulation leads to rapid phosphorylation of Ca^{2+}/calmodulin-dependent kinase II (CaMKII). The stimulation of TRPA1 ion channels in cardiomyocytes mediates the activation of CaMKII-dependent signaling pathways, which increases cardiomyocytes contractile function (Marks, 2013; Roe et al., 2015). This may suggest that TRPA1 is involved in the regulation of heart failure through a Ca^{2+}-dependent mechanism.

To our knowledge from previous studies, it seems that there is no direct evidence that TRPA1 activation causes sympathetic nerve excitation and that mediates heart failure. The current research results indicate that activation of the TRPA1 channel does not cause an increase in sympathetic reflex under heart failure. However, other studies suggest that the activation of TRPA1 channel helps to enhance cardiomyocyte contractility.

TRPA1 and Arrhythmia

Arrhythmia is caused by the abnormal sinus node activation or excitement which occurs outside the sinus node, resulting in abnormal heartbeat frequency or rhythm. It is an important group of cardiovascular diseases, which includes premature atrial complexes, premature ventricular complexes, atrial fibrillation, and ventricular tachycardia (Goudis et al., 2015). Genetic factors and other external factors can cause arrhythmia. Numerous studies have shown that there is a potential connection between air pollution and arrhythmia (Watkins et al., 2013; Monrad et al., 2017). In addition, the heart rhythm regulated by the autonomic nervous system (ANS) and air pollution increase the possibility of arrhythmia by interfering with the ANS balance (Wu et al., 2015).

ANS plays an important role in regulating arrhythmia. Some studies suggest that $PM_{2.5}$ interferes with the balance of ANS, thus resulting in increased heart rate, reduced heart rate variability, and increased risk of arrhythmia (Watkins et al., 2013; Shen and Zipes, 2014; Feng et al., 2019). In another study, exposure to automobile exhaust increased sympathetic excitability in hypertensive rats, and this sensitivity decreased with the application of TRPA1 inhibitors (Hazari et al., 2011). On the other hand, AITC increased the incidence of arrhythmia in rats, and this effect is inhibited by cholinergic antagonists (Hooper et al., 2016). Furthermore, acrolein, a smoke component, increases the heart rate variability and arrhythmia in mice, and this effect disappears after knocking out the TRPA1 gene or giving TRPA1 inhibitors (Kurhanewicz et al., 2017, 2018; Thompson et al., 2019). Continued exposure to air pollution, toxic chemicals, and particulate matter (PM) causes inflammation of the lungs, leading to cough, asthma, chronic obstructive pulmonary disease (COPD), and other diseases. Studies have indicated that PM activates TRPA1 activity in the respiratory tract, which induces human lung disease (Deering-Rice et al., 2011; Akopian et al., 2016). As the level of systemic inflammation increases, the risk of atrial fibrillation in COPD subjects increases (Grymonprez et al., 2019), and there is a negative relationship between the level of asthma control and the increased risk of atrial fibrillation (Cepelis et al., 2018). This seems to suggest that TRPA1 activation indirectly causes arrhythmia. These findings indicate that the TRPA1 channel may stimulate arrhythmia through an airway inflammation and ANS imbalance.

The ANS can be divided into the sympathetic nervous system and the parasympathetic nervous system. The autonomic nervous system mainly innervates the muscles and smooth muscles of the internal organs, glands, and blood vessel walls. Pain, fear, and temperature can cause stress regulation of ANS. Owing to different types of harmful components in air pollution, the effect of TRPA1 activation is not absolute, however, activation of the sympathetic nervous system or parasympathetic nervous system is different (Middlekauff et al., 2014; Perez et al., 2015), thus, the role of the TRPA1 channel on cardiac autonomic nerves needs further investigation. Furthermore, previous reports stated

that the activation of TRPA1 mediates the production of airway inflammation, causing lung inflammation, which increases the risk of arrhythmia to some extent. The activation of TRPA1 indirectly promotes the occurrence of arrhythmia.

Relationship Between TRPA1 and Other Cardiovascular Disease Risk Factors

In addition to the primary physiological and pathological changes of the cardiovascular system, the occurrence and development of cardiovascular diseases are often secondary to other risk factors. There are many risk factors for cardiovascular disease, including diabetes, hypertension, dyslipidemia, age, genetics, and lifestyle habits (Park et al., 2020; Ungar et al., 2020). TRPA1 closely relates to many risk factors of cardiovascular disease.

TRPA1 and Glycolipid Metabolism

Glycolipid metabolism disorder is a key factor in the formation of cardiovascular disease (Delitala et al., 2017). Metabolic diseases such as obesity and diabetes are important conditions for causing the development of cardiovascular diseases (Jokinen, 2015; Hansen, 2018). Diabetes manifests as insulin resistance and impaired insulin signaling. Hyperinsulinemia and hyperglycemia together accelerate the development of atherosclerosis (Bornfeldt and Tabas, 2011; Tabas, 2017). In particular, acute hyperglycemia weakens endothelial function and reduces the bioavailability of nitric oxide (Williams et al., 1998), increasing leukocyte adhesion (Perkins et al., 2015). In the state of hyperglycemia, the phenotype of vascular smooth muscle cells changes from a static, contracted state to an activated, proliferative state, which accelerates the progress of atherosclerosis (Zheng et al., 2007).

Atherosclerosis is the basis of other cardiovascular diseases; hence, many cardiovascular diseases develop from atherosclerosis (Frostegard, 2013). TRPA1 plays an important role in regulating glycolipid metabolism, which has important significance for the treatment of atherosclerosis (Zhao et al., 2016). Islet function, insulin level, and sensitivity are important factors that affect glucose metabolism. Studies have found that TRPA1 is abundant in rat islet β cells. AITC, H_2O_2, and 15d-PGJ2 activate TRPA1 in islet β cells and stimulate insulin secretion (Cao et al., 2012; Numazawa et al., 2012). Ghrelin, GLP-1, and other intestinal hormones affect the metabolism of glycolipids through various mechanisms. TRPA1 was present in endocrine cells in the mouse small intestine, and activating TRPA1 on these cells promoted GLP-1 secretion in a calcium-dependent manner (Shrestha et al., 2018). Cinnamaldehyde significantly inhibits the secretion of ghrelin by activating TRPA1 in the intestine to reduce food intake, and has the effect of weight loss and blood sugar reduction (Emery et al., 2015).

Cinnamaldehyde is a specific agonist of TRPA1 and has a moderate hypoglycemic effect on patients with type 2 diabetes (Rafehi et al., 2012). It has been confirmed that cinnamaldehyde promotes insulin and GLP-1 secretion (Numazawa et al., 2012; Shrestha et al., 2018), improves insulin sensitivity, and reduces liver fat deposition (Sartorius et al., 2014). The activation of pancreatic β-cell TRPA1 also promotes insulin secretion (Cao et al., 2012), as well as mesenteric adipose tissue which suggests that TRPA1 has a regulatory role in glucose metabolism. Intake of cinnamaldehyde has been shown to reduce visceral adipose tissue in high-fat and high-sugar fed mice (Tamura et al., 2012). This suggests that TRPA1 also has a potential regulatory role in lipid metabolism. In conclusion, the activation of TRPA1 indirectly reduces the incidence of cardiovascular diseases caused by glucose and lipid metabolism disorders.

TRPA1 and Oxidative Stress

Oxidative stress refers to the tissue damage caused by the excessive production of highly reactive molecular oxygen species (ROS) and reactive nitrogen species (RNS) or the inability to eliminate them in the body (Del Rio, 2015). Although the organism has established a relatively complete anti-oxidative stress system during evolution, the balance between oxidation and anti-oxidation will eventually be broken under the joint action of various risk factors. The products of oxidative stress lead to cardiovascular metabolic diseases (Sverdlov et al., 2016; Faria and Persaud, 2017; van der Pol et al., 2019). ROS, RNS, 4-hydroxynon-enal (4-HNE), H_2O_2, NO, H_2S, prostaglandin J2 (15d-PGJ2) are all TRPA1 direct or indirect agonists (Hinman et al., 2006; Taylor-Clark et al., 2009). This shows that oxidative stress metabolites can activate TRPA1, which is considered to be the endogenous substance that regulates TRPA1 in the body (Cao et al., 2012; Tamura et al., 2012). However, the relevant pathophysiological significance is currently unknown.

Previous studies confirmed that several TRPA1 agonists such as cinnamic aldehyde, artemisinol, and mustard oil have significant antioxidant activity, which activates the classic Nrf2/ARE antioxidant stress pathway (Huang et al., 2011; Zheng et al., 2011; Hsu et al., 2013). TRPA1 agonist cinnamaldehyde significantly antagonizes high glucose-mediated vascular endothelial oxidative stress through the Nrf2 pathway (Wang et al., 2015; Takahashi et al., 2018). Therefore, the role of TRPA1 and its agonists in the process of oxidative stress is worthy of further research. Among all subgroups of the TRP family, TRPA1 is the most sensitive to ROS. Its activation depends on the modification of the cysteine residue at the N-terminal end of the protein. Oxidation and peroxidation of cysteine residues cause residues to bind to disulfide bonds, which enhances TRPA1 activity (MacPherson et al., 2007a). TRPA1 is present in cardiomyocytes and is important in regulating myocardial reperfusion injury (Lu et al., 2016). A study showed that TRPA1 gene-knockout myocardial ischemia–reperfusion mice alleviated myocardial injury, indicating that TRPA1 channel activation mediates myocardial ischemia–reperfusion injury (Conklin et al., 2019). This may be related to the accumulation of free radicals and unsaturated aldehydes generated after myocardial ischemia and reperfusion to activate TRPA1 channel. The activated TRPA1 channel mediates a large amount of Ca^{2+} influx, aggravating inflammation and ischemia–reperfusion injury. Therefore, TRPA1 could be a potential drug target for reducing myocardial ischemia–reperfusion injury. In conclusion, the mechanism in which oxidative stress products activate TRPA1-mediated cardiovascular disease needs to be further discussed.

TRPA1 and Aging

With aging, the damage of molecules, cells, and tissues in the body leads to an imbalanced state, which makes the body's functions degenerate or cause diseases (Wu et al., 2019b). As a nutrient delivery channel of the human body, blood vessels play an important role in maintaining normal physiological functions. After entering old age, vascular aging becomes an independent risk factor for cardiovascular diseases (Costantino et al., 2016; He, 2016).

Current research reflects that mammalian lifespan is closely related to mitochondrial aging, oxidative stress, diet, insulin/IGF-1 signaling pathway, and UCP2 (Katic and Kahn, 2005; Duangjan et al., 2019), but the exact mechanism is still unclear. DAF-16 gene is a kind of lifespan regulator, called forkhead transcription factors of the O class (FOXO) in mammals (Jahn et al., 2020). Other studies revealed that hypothermia-activated TRPA1 regulates the downstream DAF-16/FOXO pathway through calcium-sensitive protein kinase C2 (PKC-2) signaling to extend lifespan (Xiao et al., 2013). However, low-temperature activation of TRPA1 failed to extend the lifespan of young individuals, which suggests that activation of TRPA1 plays a more important role in extending lifespan in adult and elderly individuals (Zhang et al., 2015). This is relatively related to the stable redox system in young individuals. These studies confirmed that low-temperature activation of TRPA1 could prolong the lifespan, but the specific mechanism still needs further clarification.

Aging is closely related to vascular aging; therefore, activating TRPA1 can significantly prolong life. Moreover, current research denotes that TRPA1 may have proper metabolic regulation and cardiovascular protection. Therefore, the role and mechanism of TRPA1 on age-related vascular damage should be explored further in combination with *in vitro* vascular culture and vascular endothelial-specific knockout mice.

CONCLUSION

TRPA1's role in cardiovascular diseases has received extensive attention, and it is directly or indirectly involved in the occurrence and development of cardiovascular diseases. This review describes the role of TRPA1 channels in common cardiovascular diseases. The TRPA1 channel is involved in mediating vascular physiological functions, which closely relates to the regulation of vasodilation and blood pressure. However, this regulation of blood pressure is biphasic. The activation of TRPA1 channel has a protective effect on the development of atherosclerosis; its channel blockade is beneficial for arrhythmia progression. The role of TRPA1 in the formation of heart failure and myocardial fibrosis is difficult to determine, and further experimental proof is needed. This review found evidence that TRPA1 channels relate closely to glucose and lipid metabolism, oxidative stress, and vascular aging. Considering the relationship between TRPA1 channel and various cardiovascular diseases, it may be a potential target for clinical treatment of cardiovascular diseases. In addition, according to the new drug design stage, the dual function of the TRPA1 channel should be fully considered.

AUTHOR CONTRIBUTIONS

SG and KK conceived the review and drafted the manuscript. SG and SZ revised the manuscript critically for important intellectual content. TL, PC, and RW provided funding for research. All authors approved the final version of the manuscript submitted.

FUNDING

This study was supported by the National Key R&D Program of China (No. 2018YFC1314701).

REFERENCES

Adam, R. J., Xia, Z., Pravoverov, K., Hong, J., and Case, A. J. (2019). Sympathoexcitation in response to cardiac and pulmonary afferent stimulation of TRPA1 channels is attenuated in rats with chronic heart failure. *Am. J. Physiol. Heart Circ. Physiol.* 316, H862–H872.

Akopian, A. N., Fanick, E. R., and Brooks, E. G. (2016). TRP channels and traffic-related environmental pollution-induced pulmonary disease. *Semin. Immunopathol.* 38, 331–338. doi: 10.1007/s00281-016-0554-4

Alali, F. Q., El-Elimat, T., Khalid, L., Hudaib, R., Al-Shehabi, T. S., and Eid, A. H. (2017). Garlic for cardiovascular disease: prevention or treatment? *Curr. Pharm. Des.* 23, 1028–1041. doi: 10.2174/1381612822666161010124530

Alpizar, Y. A., Gees, M., Sanchez, A., Apetrei, A., Voets, T., Nilius, B., et al. (2013). Bimodal effects of cinnamaldehyde and camphor on mouse TRPA1. *Pflugers Arch.* 465, 853–864. doi: 10.1007/s00424-012-1204-x

Andersson, D. A., Gentry, C., Moss, S., and Bevan, S. (2008). Transient receptor potential A1 is a sensory receptor for multiple products of oxidative stress. *J. Neurosci.* 28, 2485–2494. doi: 10.1523/jneurosci.5369-07.2008

Andre, E., Campi, B., Materazzi, S., Trevisani, M., Amadesi, S., Massi, D., et al. (2008). Cigarette smoke-induced neurogenic inflammation is mediated by alpha,beta-unsaturated aldehydes and the TRPA1 receptor in rodents. *J. Clin. Invest.* 118, 2574–2582.

Andrei, S. R., Ghosh, M., Sinharoy, P., Dey, S., Bratz, I. N., and Damron, D. S. (2017). TRPA1 ion channel stimulation enhances cardiomyocyte contractile function via a CaMKII-dependent pathway. *Channels* 11, 587–603. doi: 10.1080/19336950.2017.1365206

Aubdool, A. A., Graepel, R., Kodji, X., Alawi, K. M., Bodkin, J. V., Srivastava, S., et al. (2014). TRPA1 is essential for the vascular response to environmental cold exposure. *Nat. Commun.* 5:5732.

Aubdool, A. A., Kodji, X., Abdul-Kader, N., Heads, R., Fernandes, E. S., Bevan, S., et al. (2016). TRPA1 activation leads to neurogenic vasodilatation: involvement of reactive oxygen nitrogen species in addition to CGRP and NO. *Br. J. Pharmacol.* 173, 2419–2433. doi: 10.1111/bph.13519

Bandell, M., Story, G. M., Hwang, S. W., Viswanath, V., Eid, S. R., Petrus, M. J., et al. (2004). Noxious cold ion channel TRPA1 is activated by pungent compounds and bradykinin. *Neuron* 41, 849–857. doi: 10.1016/s0896-6273(04)00150-3

Bautista, D. M., Jordt, S. E., Nikai, T., Tsuruda, P. R., Read, A. J., Poblete, J., et al. (2006). TRPA1 mediates the inflammatory actions of environmental irritants and proalgesic agents. *Cell* 124, 1269–1282. doi: 10.1016/j.cell.2006.02.023

Bautista, D. M., Movahed, P., Hinman, A., Axelsson, H. E., Sterner, O., Hogestatt, E. D., et al. (2005). Pungent products from garlic activate the sensory ion channel TRPA1. *Proc. Natl. Acad. Sci. U.S.A.* 102, 12248–12252. doi: 10.1073/pnas.0505356102

Benemei, S., De Cesaris, F., Fusi, C., Rossi, E., Lupi, C., and Geppetti, P. (2013). TRPA1 and other TRP channels in migraine. *J. Headache Pain* 14, 71.

Benemei, S., Fusi, C., Trevisan, G., and Geppetti, P. (2014). The TRPA1 channel in migraine mechanism and treatment. *Br. J. Pharmacol.* 171, 2552–2567. doi: 10.1111/bph.12512

Bers, D. M. (2006). Altered cardiac myocyte Ca regulation in heart failure. *Physiology* 21, 380–387. doi: 10.1152/physiol.00019.2006

Bodkin, J. V., and Brain, S. D. (2011). Transient receptor potential ankyrin 1: emerging pharmacology and indications for cardiovascular biology. *Acta Physiol.* 203, 87–98. doi: 10.1111/j.1748-1716.2010.02203.x

Bonet, I. J., Fischer, L., Parada, C. A., and Tambeli, C. H. (2013). The role of transient receptor potential A 1 (TRPA1) in the development and maintenance of carrageenan-induced hyperalgesia. *Neuropharmacology* 65, 206–212. doi: 10.1016/j.neuropharm.2012.09.020

Bornfeldt, K. E., and Tabas, I. (2011). Insulin resistance, hyperglycemia, and atherosclerosis. *Cell Metab.* 14, 575–585. doi: 10.1016/j.cmet.2011.07.015

Brunt, V. E., Fujii, N., and Minson, C. T. (2013). No independent, but an interactive, role of calcium-activated potassium channels in human cutaneous active vasodilation. *J. Appl. Physiol.* 115, 1290–1296. doi: 10.1152/japplphysiol.00358.2013

Cao, D. S., Zhong, L., Hsieh, T. H., Abooj, M., Bishnoi, M., Hughes, L., et al. (2012). Expression of transient receptor potential ankyrin 1 (TRPA1) and its role in insulin release from rat pancreatic beta cells. *PLoS One* 7:e38005. doi: 10.1371/journal.pone.0038005

Cepelis, A., Brumpton, B. M., Malmo, V., Laugsand, L. E., Loennechen, J. P., Ellekjaer, H., et al. (2018). Associations of asthma and asthma control with atrial fibrillation risk: results from the nord-trondelag health study (HUNT). *JAMA Cardiol.* 3, 721–728.

Chen, J., Joshi, S. K., Didomenico, S., Perner, R. J., Mikusa, J. P., Gauvin, D. M., et al. (2011). Selective blockade of TRPA1 channel attenuates pathological pain without altering noxious cold sensation or body temperature regulation. *Pain* 152, 1165–1172. doi: 10.1016/j.pain.2011.01.049

Chen, J., Kang, D., Xu, J., Lake, M., Hogan, J. O., Sun, C., et al. (2013). Species differences and molecular determinant of TRPA1 cold sensitivity. *Nat. Commun.* 4:2501.

Conklin, D. J., Guo, Y., Nystoriak, M. A., Jagatheesan, G., Obal, D., Kilfoil, P. J., et al. (2019). TRPA1 channel contributes to myocardial ischemia-reperfusion injury. *Am. J. Physiol. Heart Circ. Physiol.* 316, H889–H899.

Cosens, D. J., and Manning, A. (1969). Abnormal electroretinogram from a *Drosophila* mutant. *Nature* 224, 285–287. doi: 10.1038/224285a0

Costantino, S., Paneni, F., and Cosentino, F. (2016). Ageing, metabolism and cardiovascular disease. *J. Physiol.* 594, 2061–2073. doi: 10.1113/jp270538

Deering-Rice, C. E., Romero, E. G., Shapiro, D., Hughen, R. W., Light, A. R., Yost, G. S., et al. (2011). Electrophilic components of diesel exhaust particles (DEP) activate transient receptor potential ankyrin-1 (TRPA1): a probable mechanism of acute pulmonary toxicity for DEP. *Chem. Res. Toxicol.* 24, 950–959. doi: 10.1021/tx200123z

Defalco, J., Steiger, D., Gustafson, A., Emerling, D. E., Kelly, M. G., and Duncton, M. A. (2010). Oxime derivatives related to AP18: agonists and antagonists of the TRPA1 receptor. *Bioorg. Med. Chem. Lett.* 20, 276–279. doi: 10.1016/j.bmcl.2009.10.113

Del Rio, L. A. (2015). ROS and RNS in plant physiology: an overview. *J. Exp. Bot.* 66, 2827–2837. doi: 10.1093/jxb/erv099

Delitala, A. P., Fanciulli, G., Maioli, M., and Delitala, G. (2017). Subclinical hypothyroidism, lipid metabolism and cardiovascular disease. *Eur. J. Intern. Med.* 38, 17–24. doi: 10.1016/j.ejim.2016.12.015

Derbenev, A. V., and Zsombok, A. (2016). Potential therapeutic value of TRPV1 and TRPA1 in diabetes mellitus and obesity. *Semin. Immunopathol.* 38, 397–406. doi: 10.1007/s00281-015-0529-x

Dietrich, A., Steinritz, D., and Gudermann, T. (2017). Transient receptor potential (TRP) channels as molecular targets in lung toxicology and associated diseases. *Cell Calcium* 67, 123–137. doi: 10.1016/j.ceca.2017.04.005

Duangjan, C., Rangsinth, P., Gu, X., and Wink, M. (2019). Lifespan extending and oxidative stress resistance properties of a leaf extracts from *Anacardium occidentale* L. in *Caenorhabditis elegans*. *Oxid. Med. Cell.* 2019:9012396.

Earley, S. (2012). TRPA1 channels in the vasculature. *Br. J. Pharmacol.* 167, 13–22. doi: 10.1111/j.1476-5381.2012.02018.x

Earley, S., Gonzales, A. L., and Crnich, R. (2009). Endothelium-dependent cerebral artery dilation mediated by TRPA1 and Ca2+-Activated K+ channels. *Circ. Res.* 104, 987–994. doi: 10.1161/circresaha.108.189530

Earley, S., Gonzales, A. L., and Garcia, Z. I. (2010). A dietary agonist of transient receptor potential cation channel V3 elicits endothelium-dependent vasodilation. *Mol. Pharmacol.* 77, 612–620. doi: 10.1124/mol.109.060715

Eberhardt, M., Dux, M., Namer, B., Miljkovic, J., Cordasic, N., Will, C., et al. (2014). H2S and NO cooperatively regulate vascular tone by activating a neuroendocrine HNO-TRPA1-CGRP signalling pathway. *Nat. Commun.* 5:4381.

Emery, E. C., Diakogiannaki, E., Gentry, C., Psichas, A., Habib, A. M., Bevan, S., et al. (2015). Stimulation of GLP-1 secretion downstream of the ligand-gated ion channel TRPA1. *Diabetes* 64, 1202–1210. doi: 10.2337/db14-0737

Faria, A., and Persaud, S. J. (2017). Cardiac oxidative stress in diabetes: mechanisms and therapeutic potential. *Pharmacol. Ther.* 172, 50–62. doi: 10.1016/j.pharmthera.2016.11.013

Feng, B., Song, X., Dan, M., Yu, J., Wang, Q., Shu, M., et al. (2019). High level of source-specific particulate matter air pollution associated with cardiac arrhythmias. *Sci. Total Environ.* 657, 1285–1293. doi: 10.1016/j.scitotenv.2018.12.178

Frostegard, J. (2013). Immunity, atherosclerosis and cardiovascular disease. *BMC Med.* 11:117. doi: 10.1186/1741-7015-11-117

Geng, Q., Li, S., Wang, Z., and Ren, Y. (2019). Efficacy and safety of combined neprilysin and RAS inhibition in heart failure: a meta-analysis of randomized controlled trials. *Int. J. Cardiol.* 293, 159–164. doi: 10.1016/j.ijcard.2019.05.048

Goudis, C. A., Konstantinidis, A. K., Ntalas, I. V., and Korantzopoulos, P. (2015). Electrocardiographic abnormalities and cardiac arrhythmias in chronic obstructive pulmonary disease. *Int. J. Cardiol.* 199, 264–273. doi: 10.1016/j.ijcard.2015.06.096

Graepel, R., Fernandes, E. S., Aubdool, A. A., Andersson, D. A., Bevan, S., and Brain, S. D. (2011). 4-oxo-2-nonenal (4-ONE): evidence of transient receptor potential ankyrin 1-dependent and -independent nociceptive and vasoactive responses in vivo. *J. Pharmacol. Exp. Ther.* 337, 117–124. doi: 10.1124/jpet.110.172403

Grymonprez, M., Vakaet, V., Kavousi, M., Stricker, B. H., Ikram, M. A., Heeringa, J., et al. (2019). Chronic obstructive pulmonary disease and the development of atrial fibrillation. *Int. J. Cardiol.* 276, 118–124.

Guo, S., Huang, Y., Zhang, Y., Huang, H., Hong, S., and Liu, T. (2020). Impacts of exercise interventions on different diseases and organ functions in mice. *J. Sport Health Sci.* 9, 53–73. doi: 10.1016/j.jshs.2019.07.004

Hamlin, R. L. (2007). Animal models of ventricular arrhythmias. *Pharmacol. Ther.* 113, 276–295. doi: 10.1016/j.pharmthera.2006.08.006

Hansen, P. R. (2018). Chronic inflammatory diseases and atherosclerotic cardiovascular disease: innocent bystanders or partners in crime? *Curr. Pharm. Des.* 24, 281–290.

Hardie, R. C., and Minke, B. (1992). The trp gene is essential for a light-activated Ca2+ channel in *Drosophila* photoreceptors. *Neuron* 8, 643–651. doi: 10.1016/0896-6273(92)90086-s

Hazari, M. S., Haykal-Coates, N., Winsett, D. W., Krantz, Q. T., King, C., Costa, D. L., et al. (2011). TRPA1 and sympathetic activation contribute to increased risk of triggered cardiac arrhythmias in hypertensive rats exposed to diesel exhaust. *Environ. Health Perspect.* 119, 951–957. doi: 10.1289/ehp.1003200

He, J. (2016). Hypertension in China: a large and increasing public health challenge. *J. Hypertens* 34, 29–31. doi: 10.1097/hjh.0000000000000818

Hinman, A., Chuang, H. H., Bautista, D. M., and Julius, D. (2006). TRP channel activation by reversible covalent modification. *Proc. Natl. Acad. Sci .U.S.A.* 103, 19564–19568. doi: 10.1073/pnas.0609598103

Hofmann, L., Wang, H., Zheng, W., Philipp, S. E., Hidalgo, P., Cavalie, A., et al. (2017). The S4—S5 linker - gearbox of TRP channel gating. *Cell Calcium* 67, 156–165. doi: 10.1016/j.ceca.2017.04.002

Hooper, J. S., Hadley, S. H., Morris, K. F., Breslin, J. W., Dean, J. B., and Taylor-Clark, T. E. (2016). Characterization of cardiovascular reflexes evoked by airway stimulation with allylisothiocyanate, capsaicin, and ATP in Sprague-Dawley rats. *J. Appl. Physiol.* 120, 580–591. doi: 10.1152/japplphysiol.00944.2015

Hsu, C. C., Fu, T. C., Huang, S. C., and Wang, J. S. (2020). High-intensity interval training recuperates capacity of endogenous thrombin generation in heart failure patients with reduced ejection fraction. *Thromb. Res.* 187, 159–165. doi: 10.1016/j.thromres.2020.01.013

Hsu, W. H., Lee, B. H., Li, C. H., Hsu, Y. W., and Pan, T. M. (2013). Monascin and AITC attenuate methylglyoxal-induced PPARgamma phosphorylation and degradation through inhibition of the oxidative stress/PKC pathway depending on Nrf2 activation. *J. Agric. Food Chem.* 61, 5996–6006. doi: 10.1021/jf401197r

Huang, T. C., Chung, Y. L., Wu, M. L., and Chuang, S. M. (2011). Cinnamaldehyde enhances Nrf2 nuclear translocation to upregulate phase II detoxifying enzyme

expression in HepG2 cells. *J. Agric. Food Chem.* 59, 5164–5171. doi: 10.1021/jf200579h

Huddy, K., Dhesi, P., and Thompson, P. D. (2013). Do the frequencies of adverse events increase, decrease, or stay the same with long-term use of statins? *Curr. Atheroscler. Rep.* 15:301.

Inoue, R., Jian, Z., and Kawarabayashi, Y. (2009). Mechanosensitive TRP channels in cardiovascular pathophysiology. *Pharmacol. Ther.* 123, 371–385. doi: 10.1016/j.pharmthera.2009.05.009

Ivanov, S., and Lagunin, A. (2019). Assessment of the cardiovascular adverse effects of drug-drug interactions through a combined analysis of spontaneous reports and predicted drug-target interactions. *PLoS Comput. Biol.* 15:e1006851. doi: 10.1371/journal.pcbi.1006851

Jahn, A., Scherer, B., Fritz, G., and Honnen, S. (2020). Statins Induce a DAF-16/Foxo-dependent Longevity Phenotype via JNK-1 through Mevalonate Depletion in *C. elegans*. *Aging Dis.* 11, 60–72.

Jin, L., Jagatheesan, G., Guo, L., Nystoriak, M., Malovichko, M., Lorkiewicz, P., et al. (2019). Formaldehyde induces mesenteric artery relaxation via a sensitive transient receptor potential ankyrin-1 (TRPA1) and endothelium-dependent mechanism: potential role in postprandial hyperemia. *Front. Physiol.* 10:277. doi: 10.3389/fphys.2019.00277

Jokinen, E. (2015). Obesity and cardiovascular disease. *Minerva Pediatr.* 67, 25–32.

Jordt, S. E., Bautista, D. M., Chuang, H. H., Mckemy, D. D., Zygmunt, P. M., Hogestatt, E. D., et al. (2004). Mustard oils and cannabinoids excite sensory nerve fibres through the TRP channel ANKTM1. *Nature* 427, 260–265. doi: 10.1038/nature02282

Karashima, Y., Damann, N., Prenen, J., Talavera, K., Segal, A., Voets, T., et al. (2007). Bimodal action of menthol on the transient receptor potential channel TRPA1. *J. Neurosci.* 27, 9874–9884. doi: 10.1523/jneurosci.2221-07.2007

Katic, M., and Kahn, C. R. (2005). The role of insulin and IGF-1 signaling in longevity. *Cell Mol. Life Sci.* 62, 320–343. doi: 10.1007/s00018-004-4297-y

Katz, B., Oberacker, T., Richter, D., Tzadok, H., Peters, M., Minke, B., et al. (2013). *Drosophila* TRP and TRPL are assembled as homomultimeric channels in vivo. *J. Cell Sci.* 126, 3121–3133. doi: 10.1242/jcs.123505

Kohler, R., and Ruth, P. (2010). Endothelial dysfunction and blood pressure alterations in K+-channel transgenic mice. *Pflugers Arch.* 459, 969–976. doi: 10.1007/s00424-010-0819-z

Kojima, R., Nozawa, K., Doihara, H., Keto, Y., Kaku, H., Yokoyama, T., et al. (2014). Effects of novel TRPA1 receptor agonist ASP7663 in models of drug-induced constipation and visceral pain. *Eur. J. Pharmacol.* 723, 288–293. doi: 10.1016/j.ejphar.2013.11.020

Kokel, D., Cheung, C. Y., Mills, R., Coutinho-Budd, J., Huang, L., Setola, V., et al. (2013). Photochemical activation of TRPA1 channels in neurons and animals. *Nat. Chem. Biol.* 9, 257–263. doi: 10.1038/nchembio.1183

Kovacevic, I., Muller, M., Kojonazarov, B., Ehrke, A., Randriamboavonjy, V., Kohlstedt, K., et al. (2015). The F-BAR protein NOSTRIN dictates the localization of the muscarinic m3 receptor and regulates cardiovascular function. *Circ. Res.* 117, 460–469. doi: 10.1161/circresaha.115.306187

Kumar, A., Kumari, S., Majhi, R. K., Swain, N., Yadav, M., and Goswami, C. (2015). Regulation of TRP channels by steroids: implications in physiology and diseases. *Gen. Comp. Endocrinol.* 220, 23–32. doi: 10.1016/j.ygcen.2014.10.004

Kun, J., Szitter, I., Kemeny, A., Perkecz, A., Kereskai, L., Pohoczky, K., et al. (2014). Upregulation of the transient receptor potential ankyrin 1 ion channel in the inflamed human and mouse colon and its protective roles. *PLoS One* 9:e108164. doi: 10.1371/journal.pone.0108164

Kunkler, P. E., Ballard, C. J., Oxford, G. S., and Hurley, J. H. (2011). TRPA1 receptors mediate environmental irritant-induced meningeal vasodilatation. *Pain* 152, 38–44. doi: 10.1016/j.pain.2010.08.021

Kurganov, E., Zhou, Y., Saito, S., and Tominaga, M. (2014). Heat and AITC activate green anole TRPA1 in a membrane-delimited manner. *Pflugers Arch.* 466, 1873–1884. doi: 10.1007/s00424-013-1420-z

Kurhanewicz, N., Ledbetter, A., Farraj, A., and Hazari, M. (2018). TRPA1 mediates the cardiac effects of acrolein through parasympathetic dominance but also sympathetic modulation in mice. *Toxicol. Appl. Pharmacol.* 347, 104–114. doi: 10.1016/j.taap.2018.03.027

Kurhanewicz, N., Mcintosh-Kastrinsky, R., Tong, H., Ledbetter, A., Walsh, L., Farraj, A., et al. (2017). TRPA1 mediates changes in heart rate variability and cardiac mechanical function in mice exposed to acrolein. *Toxicol. Appl. Pharmacol.* 324, 51–60. doi: 10.1016/j.taap.2016.10.008

Li, W., Zhang, Z., Li, X., Cai, J., Li, D., Du, J., et al. (2019). CGRP derived from cardiac fibroblasts is an endogenous suppressor of cardiac fibrosis. *Cardiovasc. Res.* 116, 1335–1348. doi: 10.1093/cvr/cvz234

Lin, Y. W., Liu, P. S., Adhikari, N., Hall, J. L., and Wei, L. N. (2015). RIP140 contributes to foam cell formation and atherosclerosis by regulating cholesterol homeostasis in macrophages. *J. Mol. Cell Cardiol.* 79, 287–294. doi: 10.1016/j.yjmcc.2014.12.009

Lu, Y., Piplani, H., Mcallister, S. L., Hurt, C. M., and Gross, E. R. (2016). Transient receptor potential ankyrin 1 activation within the cardiac myocyte limits ischemia-reperfusion injury in rodents. *Anesthesiology* 125, 1171–1180. doi: 10.1097/aln.0000000000001377

Luan, X., Tian, X., Zhang, H., Huang, R., Li, N., Chen, P. et al. (2019). Exercise as a prescription for patients with various diseases. *J. Sport Health Sci.* 8, 422–441. doi: 10.1016/j.jshs.2019.04.002

Ma, J., Chen, L., Fan, J., Cao, W., Zeng, G., Wang, Y., et al. (2019). Dual-targeting Rutaecarpine-NO donor hybrids as novel anti-hypertensive agents by promoting release of CGRP. *Eur. J. Med. Chem.* 168, 146–153. doi: 10.1016/j.ejmech.2019.02.037

Ma, J., Yang, L., Ma, Y., Wang, X., Ren, J., and Yang, J. (2017). Targeting transient receptor potential channels in cardiometabolic diseases and myocardial ischemia reperfusion injury. *Curr. Drug Targets* 18, 1733–1745.

Ma, Y., Halade, G. V., and Lindsey, M. L. (2012). Extracellular matrix and fibroblast communication following myocardial infarction. *J. Cardiovasc. Transl. Res.* 5, 848–857. doi: 10.1007/s12265-012-9398-z

Maclay, J. D., and MacNee, W. (2013). Cardiovascular disease in COPD: mechanisms. *Chest* 143, 798–807.

MacPherson, H. (2007). Acupuncture for hypertension: a tale of two trials. From the perspective of the acupuncturist–MacPherson, York, UK. *Forsch Komplementmed* 14, 371–373.

MacPherson, L. J., Dubin, A. E., Evans, M. J., Marr, F., Schultz, P. G., Cravatt, B. F., et al. (2007a). Noxious compounds activate TRPA1 ion channels through covalent modification of cysteines. *Nature* 445, 541–545. doi: 10.1038/nature05544

MacPherson, L. J., Xiao, B., Kwan, K. Y., Petrus, M. J., Dubin, A. E., Hwang, S., et al. (2007b). An ion channel essential for sensing chemical damage. *J. Neurosci.* 27, 11412–11415. doi: 10.1523/jneurosci.3600-07.2007

MacPherson, L. J., Hwang, S. W., Miyamoto, T., Dubin, A. E., Patapoutian, A., and Story, G. M. (2006). More than cool: promiscuous relationships of menthol and other sensory compounds. *Mol. Cell Neurosci.* 32, 335–343.

Marks, A. R. (2013). Calcium cycling proteins and heart failure: mechanisms and therapeutics. *J. Clin. Invest.* 123, 46–52.

Massy, Z. A., Metzinger-Le Meuth, V., and Metzinger, L. (2017). MicroRNAs are associated with uremic toxicity, cardiovascular calcification, and disease. *Contrib. Nephrol.* 189, 160–168.

McNamara, C. R., Mandel-Brehm, J., Bautista, D. M., Siemens, J., Deranian, K. L., Zhao, M., et al. (2007). TRPA1 mediates formalin-induced pain. *Proc. Natl. Acad. Sci. U.S.A.* 104, 13525–13530.

Middlekauff, H. R., Park, J., and Moheimani, R. S. (2014). Adverse effects of cigarette and noncigarette smoke exposure on the autonomic nervous system: mechanisms and implications for cardiovascular risk. *J. Am. Coll Cardiol.* 64, 1740–1750.

Mokou, M., Lygirou, V., Vlahou, A., and Mischak, H. (2017). Proteomics in cardiovascular disease: recent progress and clinical implication and implementation. *Expert Rev. Proteomics* 14, 117–136.

Monrad, M., Sajadieh, A., Christensen, J. S., Ketzel, M., Raaschou-Nielsen, O., Tjonneland, A., et al. (2017). Long-term exposure to traffic-related air pollution and risk of incident atrial fibrillation: a cohort study. *Environ. Health Perspect.* 125, 422–427.

Moran, M. M. (2018). TRP channels as potential drug targets. *Annu. Rev. Pharmacol. Toxicol.* 58, 309–330.

Moran, M. M., Xu, H., and Clapham, D. E. (2004). TRP ion channels in the nervous system. *Curr. Opin. Neurobiol.* 14, 362–369.

Mukhopadhyay, I., Kulkarni, A., Aranake, S., Karnik, P., Shetty, M., Thorat, S., et al. (2014). Transient receptor potential ankyrin 1 receptor activation in vitro and in vivo by pro-tussive agents: GRC 17536 as a promising anti-tussive therapeutic. *PLoS One* 9:e97005. doi: 10.1371/journal.pone.0097005

Nassini, R., Materazzi, S., Benemei, S., and Geppetti, P. (2014). The TRPA1 channel in inflammatory and neuropathic pain and migraine. *Rev. Physiol. Biochem. Pharmacol.* 167, 1–43.

Nilius, B., and Owsianik, G. (2011). The transient receptor potential family of ion channels. *Genome Biol.* 12:218.

Nilius, B., and Szallasi, A. (2014). Transient receptor potential channels as drug targets: from the science of basic research to the art of medicine. *Pharmacol. Rev.* 66, 676–814.

North, B. J., and Sinclair, D. A. (2012). The intersection between aging and cardiovascular disease. *Circ. Res.* 110, 1097–1108.

Numazawa, S., Takase, M., Ahiko, T., Ishii, M., Shimizu, S., and Yoshida, T. (2012). Possible involvement of transient receptor potential channels in electrophile-induced insulin secretion from RINm5F cells. *Biol. Pharm. Bull.* 35, 346–354.

Oguri, G., Nakajima, T., Yamamoto, Y., Takano, N., Tanaka, T., Kikuchi, H., et al. (2014). Effects of methylglyoxal on human cardiac fibroblast: roles of transient receptor potential ankyrin 1 (TRPA1) channels. *Am. J. Physiol. Heart Circ. Physiol.* 307, H1339–H1352.

Overington, J. P., Al-Lazikani, B., and Hopkins, A. L. (2006). How many drug targets are there? *Nat. Rev. Drug Discov.* 5, 993–996.

Park, E. O., Bae, E. J., Park, B. H., and Chae, S. W. (2020). The associations between liver enzymes and cardiovascular risk factors in adults with mild dyslipidemia. *J. Clin. Med.* 9:1147.

Pazienza, V., Pomara, C., Cappello, F., Calogero, R., Carrara, M., Mazzoccoli, G., et al. (2014). The TRPA1 channel is a cardiac target of mIGF-1/SIRT1 signaling. *Am. J. Physiol. Heart Circ. Physiol.* 307, H939–H944.

Pei, Z., Zhuang, Z., Sang, H., Wu, Z., Meng, R., He, E. Y., et al. (2014). α,β-unsaturated aldehyde crotonaldehyde triggers cardiomyocyte contractile dysfunction: role of TRPV1 and mitochondrial function. *J. Pharmacol Res.* 82, 40–50. doi: 10.1016/j.phrs.2014.03.010

Peixoto-Neves, D., Soni, H., and Adebiyi, A. (2019). CGRPergic nerve TRPA1 channels contribute to epigallocatechin gallate-induced neurogenic vasodilation. *ACS Chem. Neurosci.* 10, 216–220.

Perez, C. M., Hazari, M. S., and Farraj, A. K. (2015). Role of autonomic reflex arcs in cardiovascular responses to air pollution exposure. *Cardiovasc. Toxicol.* 15, 69–78.

Perkins, J. M., Joy, N. G., Tate, D. B., and Davis, S. N. (2015). Acute effects of hyperinsulinemia and hyperglycemia on vascular inflammatory biomarkers and endothelial function in overweight and obese humans. *Am. J. Physiol. Endocrinol. Metab.* 309, E168–E176.

Petrus, M., Peier, A. M., Bandell, M., Hwang, S. W., Huynh, T., Olney, N., et al. (2007). A role of TRPA1 in mechanical hyperalgesia is revealed by pharmacological inhibition. *Mol. Pain* 3:40.

Pozsgai, G., Bodkin, J. V., Graepel, R., Bevan, S., Andersson, D. A., and Brain, S. D. (2010). Evidence for the pathophysiological relevance of TRPA1 receptors in the cardiovascular system in vivo. *Cardiovasc. Res.* 87, 760–768.

Qian, X., Francis, M., Solodushko, V., Earley, S., and Taylor, M. S. (2013). Recruitment of dynamic endothelial Ca2+ signals by the TRPA1 channel activator AITC in rat cerebral arteries. *Microcirculation* 20, 138–148.

Rafehi, H., Ververis, K., and Karagiannis, T. C. (2012). Controversies surrounding the clinical potential of cinnamon for the management of diabetes. *Diabetes Obes Metab.* 14, 493–499.

Ramkumar, S., Raghunath, A., and Raghunath, S. (2016). Statin therapy: review of safety and potential side effects. *Acta Cardiol. Sin.* 32, 631–639.

Ramsey, I. S., Delling, M., and Clapham, D. E. (2006). An introduction to TRP channels. *Annu. Rev. Physiol.* 68, 619–647.

Rhoden, A., Speiser, J., Geertz, B., Uebeler, J., Schmidt, K., De Wit, C., et al. (2019). Preserved cardiovascular homeostasis despite blunted acetylcholine-induced dilation in mice with endothelial muscarinic M3 receptor deletion. *Acta Physiol.* 226:e13262.

Roe, A. T., Frisk, M., and Louch, W. E. (2015). Targeting cardiomyocyte Ca2+ homeostasis in heart failure. *Curr. Pharm. Des.* 21, 431–448.

Russell, F. A., King, R., Smillie, S. J., Kodji, X., and Brain, S. D. (2014). Calcitonin gene-related peptide: physiology and pathophysiology. *Physiol. Rev.* 94, 1099–1142.

Sahu, A., Jha, P. K., Prabhakar, A., Singh, H. D., Gupta, N., Chatterjee, T., et al. (2017). MicroRNA-145 impedes thrombus formation via targeting tissue factor in venous thrombosis. *EBioMedicine* 26, 175–186.

Sala, L., and Bellin, M. (2017). Integrating cardiomyocytes from human pluripotent stem cells in safety pharmacology: has the time come? *Br. J. Pharmacol.* 174, 3749–3765.

Sardar, M. R., Saeed, W., and Kowey, P. R. (2016). Antiarrhythmic drug therapy for atrial fibrillation. *Heart Fail. Clin.* 12, 205–221.

Sartorius, T., Peter, A., Schulz, N., Drescher, A., Bergheim, I., Machann, J., et al. (2014). Cinnamon extract improves insulin sensitivity in the brain and lowers liver fat in mouse models of obesity. *PLoS One* 9:e92358. doi: 10.1371/journal.pone.0092358

Schaefer, M. (2005). Homo- and heteromeric assembly of TRP channel subunits. *Pflugers Arch.* 451, 35–42.

Shanks, J., De Morais, S. D. B., Gao, L., Zucker, I. H., and Wang, H. J. (2019). TRPV1 (Transient Receptor Potential Vanilloid 1) cardiac spinal afferents contribute to hypertension in spontaneous hypertensive rat. *Hypertension* 74, 910–920.

Shen, M. J., and Zipes, D. P. (2014). Role of the autonomic nervous system in modulating cardiac arrhythmias. *Circ. Res.* 114, 1004–1021.

Shimokawa, H., Sunamura, S., and Satoh, K. (2016). RhoA/Rho-kinase in the cardiovascular system. *Circ. Res.* 118, 352–366.

Shrestha, N., Bouttefeux, O., Vanvarenberg, K., Lundquist, P., Cunarro, J., Tovar, S., et al. (2018). The stimulation of GLP-1 secretion and delivery of GLP-1 agonists via nanostructured lipid carriers. *Nanoscale* 10, 603–613.

Sinha, S., Sinharoy, P., Bratz, I. N., and Damron, D. S. (2015). Propofol causes vasodilation in vivo via TRPA1 ion channels: role of nitric oxide and BKCa channels. *PLoS One* 10:e0122189. doi: 10.1371/journal.pone.0122189

Sinharoy, P., Bratz, I. N., Sinha, S., Showalter, L. E., Andrei, S. R., and Damron, D. S. (2017). TRPA1 and TRPV1 contribute to propofol-mediated antagonism of U46619-induced constriction in murine coronary arteries. *PLoS One* 12:e0180106. doi: 10.1371/journal.pone.0180106

Sousa-Pinto, B., Ferreira-Pinto, M. J., Santos, M., and Leite-Moreira, A. F. (2014). Central nervous system circuits modified in heart failure: pathophysiology and therapeutic implications. *Heart Fail. Rev.* 19, 759–779.

Story, G. M., Peier, A. M., Reeve, A. J., Eid, S. R., Mosbacher, J., Hricik, T. R., et al. (2003). ANKTM1, a TRP-like channel expressed in nociceptive neurons, is activated by cold temperatures. *Cell* 112, 819–829.

Sullivan, M. N., Gonzales, A. L., Pires, P. W., Bruhl, A., Leo, M. D., Li, W., et al. (2015). Localized TRPA1 channel Ca2+ signals stimulated by reactive oxygen species promote cerebral artery dilation. *Sci. Signal.* 8:ra2.

Supowit, S. C., Rao, A., Bowers, M. C., Zhao, H., Fink, G., Steficek, B., et al. (2005). Calcitonin gene-related peptide protects against hypertension-induced heart and kidney damage. *Hypertension* 45, 109–114.

Sverdlov, A. L., Elezaby, A., Qin, F., Behring, J. B., Luptak, I., Calamaras, T. D., et al. (2016). Mitochondrial reactive oxygen species mediate cardiac structural, functional, and mitochondrial consequences of diet-induced metabolic heart disease. *J. Am. Heart Assoc.* 5:e002555.

Tabas, I. (2017). 2016 russell ross memorial lecture in vascular biology: molecular-cellular mechanisms in the progression of atherosclerosis. *Arterioscler. Thromb. Vasc. Biol.* 37, 183–189.

Takahashi, N., Chen, H. Y., Harris, I. S., Stover, D. G., Selfors, L. M., Bronson, R. T., et al. (2018). Cancer cells co-opt the neuronal redox-sensing channel trpa1 to promote oxidative-stress tolerance. *Cancer Cell* 33, 985.e7–1003.e7.

Talavera, K., Gees, M., Karashima, Y., Meseguer, V. M., Vanoirbeek, J. A., Damann, N., et al. (2009). Nicotine activates the chemosensory cation channel TRPA1. *Nat. Neurosci.* 12, 1293–1299.

Tamura, Y., Iwasaki, Y., Narukawa, M., and Watanabe, T. (2012). Ingestion of cinnamaldehyde, a TRPA1 agonist, reduces visceral fats in mice fed a high-fat and high-sucrose diet. *J. Nutr. Sci. Vitaminol.* 58, 9–13.

Taylor-Clark, T. E., Ghatta, S., Bettner, W., and Undem, B. J. (2009). Nitrooleic acid, an endogenous product of nitrative stress, activates nociceptive sensory nerves via the direct activation of TRPA1. *Mol. Pharmacol.* 75, 820–829.

Taylor-Clark, T. E., Mcalexander, M. A., Nassenstein, C., Sheardown, S. A., Wilson, S., Thornton, J., et al. (2008). Relative contributions of TRPA1 and TRPV1 channels in the activation of vagal bronchopulmonary C-fibres by the endogenous autacoid 4-oxononenal. *J. Physiol.* 586, 3447–3459.

Thompson, L. C., Walsh, L., Martin, B. L., Mcgee, J., Wood, C., Kovalcik, K., et al. (2019). Ambient particulate matter and acrolein co-exposure increases myocardial dyssynchrony in mice via TRPA1. *Toxicol. Sci.* 167, 559–572.

Tian, C., Huang, R., Tang, F., Lin, Z., Cheng, N., Han, X., et al. (2020). Transient receptor potential ankyrin 1 contributes to lysophosphatidylcholine-induced intracellular calcium regulation and THP-1-derived macrophage activation. *J. Membr. Biol.* 253, 43–55.

Trevisani, M., Siemens, J., Materazzi, S., Bautista, D. M., Nassini, R., Campi, B., et al. (2007). 4-Hydroxynonenal, an endogenous aldehyde, causes pain and neurogenic inflammation through activation of the irritant receptor TRPA1. *Proc. Natl. Acad. Sci. U.S.A.* 104, 13519–13524.

Ungar, A., Rivasi, G., Petrovic, M., Schonenberger, A., Martinez-Selles, M., Gasowski, J., et al. (2020). Toward a geriatric approach to patients with advanced age and cardiovascular diseases: position statement of the EuGMS Special Interest Group on cardiovascular medicine. *Eur. Geriatr. Med.* 11, 179–184.

van der Pol, A., Van Gilst, W. H., Voors, A. A., and Van Der Meer, P. (2019). Treating oxidative stress in heart failure: past, present and future. *Eur. J. Heart Fail.* 21, 425–435.

Vriens, J., Owsianik, G., Voets, T., Droogmans, G., and Nilius, B. (2004). Invertebrate TRP proteins as functional models for mammalian channels. *Pflugers Arch.* 449, 213–226.

Wang, F., Pu, C., Zhou, P., Wang, P., Liang, D., Wang, Q., et al. (2015). Cinnamaldehyde prevents endothelial dysfunction induced by high glucose by activating Nrf2. *Cell Physiol. Biochem.* 36, 315–324.

Wang, Q., Chen, K., Zhang, F., Peng, K., Wang, Z., Yang, D., et al. (2020). TRPA1 regulates macrophages phenotype plasticity and atherosclerosis progression. *Atherosclerosis* 301, 44–53.

Wang, R., Tian, H., Guo, D., Tian, Q., Yao, T., and Kong, X. (2020). Impacts of exercise intervention on various diseases in rats. *J. Sport Health Sci.* 9, 211–227. doi: 10.1016/j.jshs.2019.09.008

Wang, Z., Xu, Y., Wang, M., Ye, J., Liu, J., Jiang, H., et al. (2018). TRPA1 inhibition ameliorates pressure overload-induced cardiac hypertrophy and fibrosis in mice. *EBioMedicine* 36, 54–62.

Wang, Z., Ye, D., Ye, J., Wang, M., Liu, J., Jiang, H., et al. (2019). The TRPA1 channel in the cardiovascular system: promising features and challenges. *Front. Pharmacol.* 10:1253. doi: 10.3389/fphar.2019.01253

Ward, A., Brogden, R. N., Heel, R. C., Speight, T. M., and Avery, G. S. (1983). Amrinone. A preliminary review of its pharmacological properties and therapeutic use. *Drugs* 26, 468–502.

Watkins, A., Danilewitz, M., Kusha, M., Masse, S., Urch, B., Quadros, K., et al. (2013). Air pollution and arrhythmic risk: the smog is yet to clear. *Can. J. Cardiol.* 29, 734–741.

Wei, H., Hamalainen, M. M., Saarnilehto, M., Koivisto, A., and Pertovaara, A. (2009). Attenuation of mechanical hypersensitivity by an antagonist of the TRPA1 ion channel in diabetic animals. *Anesthesiology* 111, 147–154.

Williams, S. B., Goldfine, A. B., Timimi, F. K., Ting, H. H., Roddy, M. A., Simonson, D. C., et al. (1998). Acute hyperglycemia attenuates endothelium-dependent vasodilation in humans in vivo. *Circulation* 97, 1695–1701.

Winter, Z., Gruschwitz, P., Eger, S., Touska, F., and Zimmermann, K. (2017). Cold temperature encoding by cutaneous TRPA1 and TRPM8-carrying fibers in the mouse. *Front. Mol. Neurosci.* 10:209. doi: 10.3389/fnmol.2017.00209

Wu, Z., He, E. Y., Scott, G. I., and Ren, J. (2015). α,β-unsaturated aldehyde pollutant acrolein suppresses cardiomyocyte contractile function: role of TRPV1 and oxidative stress. *Environ. Toxicol.* 30, 638–647. doi: 10.1002/tox.21941

Wu, N. N., Tian, H., Chen, P., Wang, D., Ren, J., and Zhang, Y. (2019a). Physical exercise and selective autophagy: benefit and risk on cardiovascular health. *Cells* 8:1436. doi: 10.3390/cells8111436

Wu, N. N., Zhang, Y., and Ren, J. (2019b). Mitophagy, mitochondrial dynamics, and homeostasis in cardiovascular aging. *Oxid. Med. Cell. Longev.* 2019:9825061. doi: 10.1155/2019/9825061

Xiao, R., Zhang, B., Dong, Y., Gong, J., Xu, T., Liu, J., et al. (2013). A genetic program promotes *C. elegans* longevity at cold temperatures via a thermosensitive TRP channel. *Cell* 152, 806–817.

Yu, M., Jiang, M., Chen, Y., Zhang, S., Zhang, W., Yang, X., et al. (2016). Inhibition of Macrophage CD36 Expression and Cellular Oxidized Low Density Lipoprotein (oxLDL) Accumulation by Tamoxifen: a PEROXISOME PROLIFERATOR-ACTIVATED RECEPTOR (PPAR)gamma-DEPENDENT MECHANISM. *J. Biol. Chem.* 291, 16977–16989.

Yue, Z., Xie, J., Yu, A. S., Stock, J., Du, J., and Yue, L. (2015). Role of TRP channels in the cardiovascular system. *Am. J. Physiol. Heart Circ. Physiol.* 308, H157–H182.

Yung, B. S., Brand, C. S., Xiang, S. Y., Gray, C. B., Means, C. K., Rosen, H., et al. (2017). Selective coupling of the S1P3 receptor subtype to S1P-mediated RhoA activation and cardioprotection. *J. Mol. Cell Cardiol.* 103, 1–10.

Zhang, B., Xiao, R., Ronan, E. A., He, Y., Hsu, A. L., Liu, J., et al. (2015). Environmental temperature differentially modulates *C. elegans* Longevity through a Thermosensitive TRP Channel. *Cell Rep.* 11, 1414–1424.

Zhang, Y., Li, L., Hua, Y., Nunn, J. M., Dong, F., Yanagisawa, M., et al. (2012). Cardiac-specific knockout of ET(A) receptor mitigates low ambient temperature-induced cardiac hypertrophy and contractile dysfunction. *J. Mol. Cell Biol.* 4, 97–107.

Zhao, J. F., Shyue, S. K., Kou, Y. R., Lu, T. M., and Lee, T. S. (2016). Transient receptor potential ankyrin 1 channel involved in atherosclerosis and macrophage-foam cell formation. *Int. J. Biol. Sci.* 12, 812–823.

Zheng, H., Whitman, S. A., Wu, W., Wondrak, G. T., Wong, P. K., Fang, D., et al. (2011). Therapeutic potential of Nrf2 activators in streptozotocin-induced diabetic nephropathy. *Diabetes* 60, 3055–3066.

Zheng, X. L., Yuan, S. G., and Peng, D. Q. (2007). Phenotype-specific inhibition of the vascular smooth muscle cell cycle by high glucose treatment. *Diabetologia* 50, 881–890.

Zhong, J., Pollastro, F., Prenen, J., Zhu, Z., Appendino, G., and Nilius, B. (2011). Ligustilide: a novel TRPA1 modulator. *Pflugers Arch.* 462, 841–849.

Conflict of Interest: The authors declare that the research was conducted in the absence of any commercial or financial relationships that could be construed as a potential conflict of interest.

Copyright © 2020 Gao, Kaudimba, Guo, Zhang, Liu, Chen and Wang. This is an open-access article distributed under the terms of the Creative Commons Attribution License (CC BY). The use, distribution or reproduction in other forums is permitted, provided the original author(s) and the copyright owner(s) are credited and that the original publication in this journal is cited, in accordance with accepted academic practice. No use, distribution or reproduction is permitted which does not comply with these terms.

frontiers in Pharmacology

ORIGINAL RESEARCH
published: 05 August 2020
doi: 10.3389/fphar.2020.01155

GEO Data Sets Analysis Identifies COX-2 and Its Related Micro RNAs as Biomarkers for Non-Ischemic Heart Failure

*Youyou Yan[1], Dandan Song[2], Xiaoling Zhang[3], Gang Hui[4] and Junnan Wang[1]**

[1] Department of Cardiology, Second Hospital of Jilin University, Changchun, China, [2] Department of Clinical Laboratory, Second Hospital of Jilin University, Changchun, China, [3] Key Laboratory of Organ Regeneration and Transplantation of Ministry of Education, Institute of Immunology, The First Hospital, Jilin University, Changchun, China, [4] The Department of 31656 Troops of Chinese People's Liberation Army, Leshan, China

Heart failure (HF) is a heterogeneous clinical syndrome with a variety of causes, risk factors, and pathology. Clinically, only brain natriuretic peptide (BNP) or its precursor N-terminus proBNP (NTproBNP) has been validated for HF diagnosis, but they are also affected by other conditions, such as female gender, renal disease, and acute coronary syndromes, and false low levels in the setting of obesity or flash pulmonary edema. In addition, there is no one biomarker which could encompass all heart failure phenotypes. Advances in bioinformatics have provided us with large databases that characterize the complex genetic and epigenetic changes associated with human diseases. The use of data mining strategies on public access databases to identify previously unknown disease markers is an innovative approach to identify potential biomarkers or even new therapeutic targets in complex diseases such as heart failure (HF). In this study, we analyzed the genomic and transcription data of HF peripheral blood mononuclear cell (PBMC) samples obtained from the Gene Expression Omnibus data sets using Omicsbean online database (http://www.omicsbean.cn/) and found that the prostaglandin-endoperoxide synthase 2 (PTGS2), also named as cyclooxygenase-2 (COX-2), as well as its related micro RNAs including miR-1297 and miR-4649-3p might be used as potential biomarkers for non-ischemic heart failure. Our result showed that plasma COX-2 and miR-4649-3p were significantly up-regulated, whereas the plasma miR-1297 was significantly decreased, and miR-4649-3p displayed high predictive power for non-ischemic heart failure.

Keywords: heart failure, micro RNA, COX-2, biomarker, bioinformatics analysis

OPEN ACCESS

Edited by:
Ying Mei Zhang,
Fudan University, China

Reviewed by:
Jason Hellmann,
University of Louisville, United States
InKyeom Kim,
Kyungpook National University,
South Korea

***Correspondence:**
Junnan Wang
jdeywjn@163.com

Specialty section:
This article was submitted to Cardiovascular and Smooth Muscle Pharmacology, a section of the journal Frontiers in Pharmacology

Received: *03 January 2020*
Accepted: *15 July 2020*
Published: *05 August 2020*

Citation:
Yan Y, Song D, Zhang X, Hui G and Wang J (2020) GEO Data Sets Analysis Identifies COX-2 and Its Related Micro RNAs as Biomarkers for Non-Ischemic Heart Failure. Front. Pharmacol. 11:1155. doi: 10.3389/fphar.2020.01155

INTRODUCTION

Heart failure (HF) is a heterogeneous clinical syndrome with a variety of risk factors, and pathology and a leading cause of mortality in the world (Linsenmayer et al., 2019). Approximately 50% of patients with HF are expected to die within 5 years of diagnosis (Gathright et al., 2017). Clinically, only brain natriuretic peptide (BNP) or its precursor N-terminus proBNP (NTproBNP) has been

validated for HF diagnosis, and they were affected by many other conditions such as advanced age, female gender, renal disease and acute coronary syndromes, and obesity or flash pulmonary edema (Goetze et al., 2005). In addition, the diagnosis of heart failure is most frequently made at the time of presentation of symptoms, while advances in congestive heart failure (CHF) management depend on biomarkers for monitoring disease progression and therapeutic response (Inamdar and Inamdar, 2016). However, there is no biomarker that could encompass all heart failure phenotypes (Senthong et al., 2017). Hence, it is urgent to discover novel and reliable biomarkers for HF.

It was found that some inflammatory markers such as interleukin-33 (IL-33)/ST2 (suppressor of tumorigenicity 2; interleukin 1 receptor-like 1), IL-6, and tumor necrosis factor-alpha (TNF-α), were associated with HF, but they were not specific for HF and were often affected by other multiple comorbidities (Weinberg et al., 2002; Liu et al., 2014). In addition, microRNAs (miRNAs) are small non-coding RNA molecules that can regulate gene expression in many biological processes and stable in blood, those prepotencies make micro RNAs as potential biomarkers (Maegdefessel, 2014). Many studies have investigated the circulating micro RNAs as the biomarkers for cardiovascular diseases including HF (Dickinson et al., 2013; Endo et al., 2013).

Recently, gene expression profiling and the analysis of protein-protein interaction (PPI) networks have been widely used for identifying disease biomarkers and potential drug targets (Sakharkar et al., 2019). Some widely available open access databases such as Gene Expression Omnibus (GEO) provided abundant microarray resources for searching deregulated genes (Sakharkar et al., 2019). Therefore, data mining strategies on public access databases on identifying candidate gene or their related micro RNAs are used to find biomarkers for HF.

In this study, we explored the deregulated genes of non-ischemic heart failure based on Gene Expression Omnibus (GEO) data sets and predicted related micro RNAs using bioinformatics analyses. Furthermore, we tested their levels and evaluated their predictive power for non-ischemic heart failure.

METHODS

Analysis of Non-Ischemic Heart Failure From GEO Data

Gene Expression Omnibus database (http://www.ncbi.nlm.nih.gov/geo) is an open functional genomics database of high-throughput resource (Barrett et al., 2005). In this study, we downloaded the microarray data of GDS3115 including three non-ischemic heart failure patients and three normal subjects were obtained from the GEO. The microarray data of GDS3115 contained a total of 22214 known genes were then screened with the following criteria: differential expression ratio > 4 (log2FC > 2) or < _4 (log2FC >_2) and a p-value <0.05. The dysregulated gene-related micro RNA prediction and integrating protein-protein-micro RNA interaction were next analyzed by Omicsbean online database (http://www.omicsbean.cn/), which is a multi-omics data analysis tool that integrates biological data and analysis tools and provides a comprehensive set of functional annotation information of genes and proteins for users to extract biological information (Liu et al., 2018).

Sample Collection

In this study, we enrolled 70 patients that were diagnosed with non-ischemic heart failure at Second Hospital of Jilin University, Changchun, China, From January 2018 to August 2018. Inclusion criteria: Newly diagnosed HF within 12 months in stages B, C, and D according to the American College of Cardiology/American Heart Association 2005 Guidelines (Hunt et al., 2009; Dai et al., 2012), an elevated level (>200 pg. per milliliter) of N-terminal pro-brain natriuretic peptide (NT-proBNP) and a left ventricular ejection fraction (LVEF) ≤ 35%. Exclusion criteria: advanced HF needed the ongoing support or surgery within 6 months, or HF with prior ST-segment elevation myocardial infarction (STEMI) or non-STEMI in the left anterior descending coronary artery distribution. In addition, 77 matched control subjects without heart failure were used as control. All blood samples (5 ml per patient), collected before those received any treatments, were collected *via* a direct venous puncture and placed into tubes containing sodium citrate, centrifuged at 1,000×***g*** for 5 min and 3,000×***g*** for 10 min, the layer of the supernatant (plasma) was carefully transferred into other tubes and stored at −80°C. Written consent was obtained from all subjects, and the study protocol was approved by the ethics committee of Jilin University second hospital.

Assay for Plasma PTGS2 (COX-2), hsa-miR-4649-3p, and hsa-miR-1297

We test the plasma level of COX-2 using the ELISA kit from Elabscience, following the manufacturer's instructions. Absorbance was measured at 450 nm (primary wave length).

MiRNAs were extracted from the plasma samples contained 50 pmol/L *Caenorhabditis elegans* miR-39 (cel-miR-39), which was used as an external reference, following the instruction of miRcute miRNA Isolation kit (TRANS GEN, Beijing, China). Each sample was eluted in 100 μl of RNAse-free water. QPCR assay Poly-(A) tailing and reverse transcription were performed with the miScript reverse transcription kit (TRANS GEN, Beijing, China). QRT-PCR was performed to quantify the levels of miRNA using the SYBR Green PCR method (TRANS GEN, Beijing, China). Cel-miR39 was used as a stable exogenous control. Threshold cycle values (Ct values) were determined from amplification curves. Negative controls using nuclease-free water were included with every real-time PCR operation and Ct values >35 viewed as negative. All samples for miRs were run in one assay, and all reactions were run in triplicate. The $2^{-\Delta Ct}$ method was used to calculate relative quantitative expression (ΔCt = CtmiRNA−CtmiR39). The micro RNA assay primers used were miR-4649-3p forward: 5′-TCTGAGGCC TGCCTCTCCCA-3′, miR-1297 5′-TTCAAGTAATTCAGG TG-3′ and cel-miR-39 forward: 5′-TCACCGGGUGUAAATCA GCTTG-3′.

Statistical Analyses

SPSS version 26 (SPSS Inc., USA) was used to perform the statistical analyses. Data are presented as the mean ± SD and median for the general characteristics of the subjects. Differences between control and heart failure group were assessed using Two-tailed t-tests. The correlations of plasma COX-2 and hsa-miR-4649 and hsa-miR-1297 were also assayed using Spearman ranked correlations. Binary logistical regression analysis were also used to evaluate the predictive powers of plasma PTGS2 (COX-2), hsa-miR-4649 and hsa-miR-1297 for HF. Receiver operating characteristic (ROC) analysis containing the ROC curves and overall model quality were used to evaluate the individual predictive accuracy of the candidate biomarkers. As the validation cohort is relatively small, bootstrap analysis of 1000 iterations was used to correct the false positive findings. Values with a $p < 0.05$ were considered to indicate statistical significance.

RESULTS

Baseline Characteristics

70 patients with non-ischemic heart failure and 77 matched control subjects without cardiovascular disease were enrolled. Their clinical characteristics and biochemical parameters are listed in **Table 1**. Age, sex, hypertension, smoking history, drinking history were not different between non-ischemic heart failure and control groups.

Deferentially Expressed Genes and miRNAs Networks

The gene expression profiles of non-ischemic heart failure and control subjects were down-loaded from GEO data sets and analyzed using the Omicsbean online database (http://www.omicsbean.cn/). Based on the criterions ($p < 0.05$ and fold change 4), 9 genes were found to be deferentially expressed in non-ischemic heart failure, including 8 up- and 1 downregulated genes (**Figures 1A, B**). Among them, PTGS2 (COX-2) is a secreted protein with high expression levels in patients with non-ischemic heart failure, indicating it might be used as biomarker. As the miRNAs were also investigated as biomarker, the regulation networks of genes and their related miRNAs were constructed based on the gene expression profile. We predicted the dysregulated gene-related micro RNAs and constructed the PPI network to provide the interactions among various proteins and micro RNAs using the Omicsbean online database. Integrative bioinformatics analysis showed that hsa-miR-4649 and hsa-miR-1297 could target COX-2 and were not associated with other dysregulated genes (**Figure 1C**), suggesting they might be also used as the biomarker for no non-ischemic heart failure.

TABLE 1 | Clinical characteristics and biochemical parameters of the patients with non-ischemic heart failure.

Variable	Control n=77	Non-ischemic heart failure n=70	P value
Age (y)	60.79 ± 7.56	62.41 ± 7.23	0.16
Male, n (%)	15 (19.48)	11 (15.71)	0.55
Smoking, n (%)	34 (44.16)	21 (30.00)	0.08
Diabetes, n (%)	29 (37.66)	31 (44.29)	0.42
Hypertension, n (%)	39 (50.65)	44 (62.85)	0.19
Drinking (%)	36 (46.75)	35 (50.00)	0.70

The Plasma Levels of COX-2 and hsa-miR-4649-3p and hsa-miR-1297 and Their Correlations

We next measured the plasma levels of COX-2, hsa-miR-4649-3p, and hsa-miR-1297, and bootstrap analysis of 1000 iterations was used to correct the false positive findings. The results showed that the plasma level of COX-2 in the non-ischemic heart failure group was significantly higher than that in control group (36.67 ± 11.97ng/ml vs 27.84 ± 12.82 ng/ml, 95% CI, −12.88 to −4.78, p = 0.00) (bootstrapped 95% CI, −13.10 to 4.90; p = 0.001) (**Figure 2A**). hsa-miR-4649 was also significantly increased in the plasma of patients with non-ischemic heart failure, compared with control subjects (11.03 ± 10.05 vs 1.00 ± 0.79 fold, 95% CI, −12.43 to −7.63; p = 0.00) (bootstrapped 95% CI, −12.47 to −7.87; p = 0.001) (**Figure 2B**). However, hsa-miR-1297 was significantly decreased in the plasma of patients with non-ischemic heart failure, compared with control subjects (0.13 ± 0.30 vs 1.00 ± 1.33 fold, 95% CI: 0.56,1.18; p =0.00) (bootstrapped 95% CI: 0.56, 1.18; p =0.003) (**Figure 2C**). We further investigated the correlations of COX-2 with hsa-miR-4649 and hsa-miR-1297. The results showed that plasma COX-2 positively correlated with plasma hsa-miR-4649 (R = 0.227, p =0.006) (bootstrapped 95% CI: 0.078, 0.369) (**Figure 2D**). There was a negative correlation of COX-2 with hsa-miR-1297 in non-ischemic heart failure (R = −0.237, p = 0.004) (bootstrapped 95% CI, −0.390 to −0.069) (**Figure 2E**).

The Predictive Powers of COX-2 With Its Related miRNAs for Non-Ischemic Heart Failure

As plasma COX-2 and miR-4649-3p, miR-1297 were significantly dysregulated in patients with non-ischemic heart failure, we evaluated their predictive power by performing ROC analysis. As shown in **Figure 3A**, AUC of COX-2 is 0.693 (95% CI: 0.608, 0.778; p < 0.01), the optimal cutoff value is 31.06 ng/ml with sensitivity, and specificity were 70.0% and 62.3%, respectively. AUC of miR-4649 is 0.969 (95% CI: 0.947, 0.991; p<0.01), and the optimal cutoff value is 2.14 fold change with the sensitivity and specificity are 90.0% and 94.5%, respectively. The AUC of 1/miR-1297 is 0.897 (95% CI: 0.842, 0.951; p<0.01) and the optimal cut-off value is 0.16 fold change with the sensitivity and specificity are 85.7% and 84.4%, respectively. Overall model quality displays the value of the lower bound of the confidence interval of the estimated AUC, and predictive model is considered good when the value is over 0.5. As shown in **Figure 3B**, the overall model quality for COX-2, miR-4649-3p, or miR-1297 is over 0.61, 0.95, 0.84, respectively. Binary logistical regression analysis showed that plasma COX-2 (odds ratio, 1.292; 95% CI, 1.001−1.134; p = 0.047), miR-4649-3p (odds

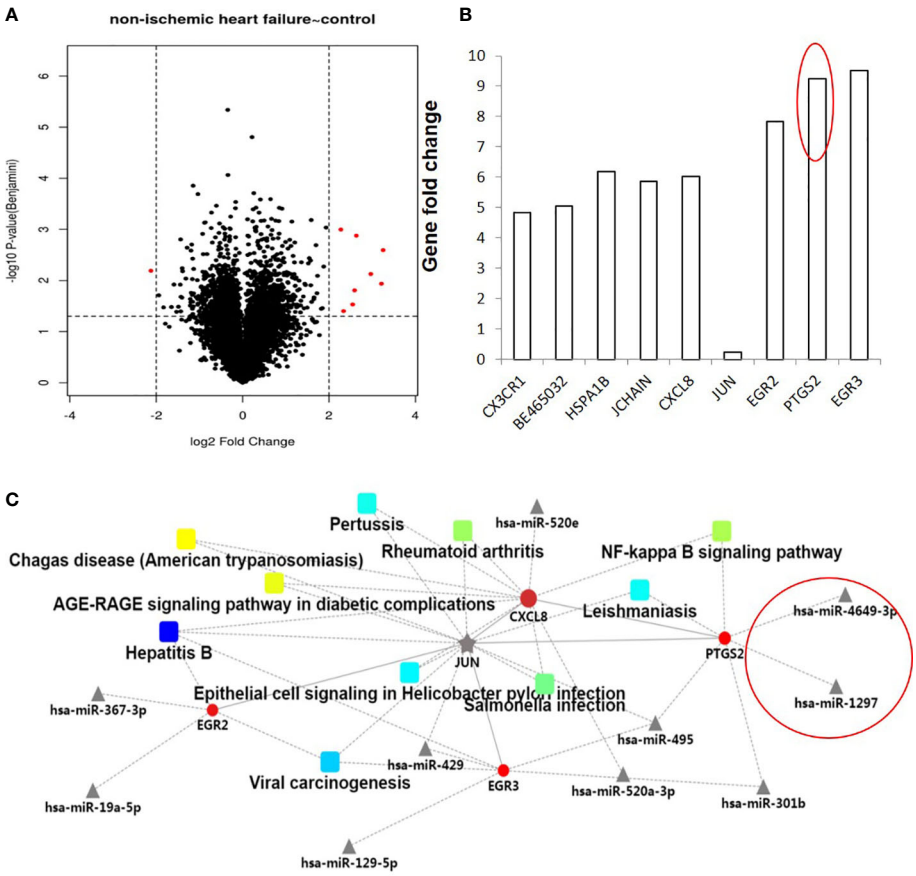

FIGURE 1 | Analysis of dysregulated genes and their micro RNAs between non-ischemic heart failure and control groups. **(A)** The volcano plot graph of genes was constructed according to fold change values and p values. The X axis represents the log2 (fold change) value of differential expression, and the Y axis represents the -log10 (padj) value of differential expression. The vertical lines correspond to 4-fold upregulation and downregulation between non-ischemic heart failure and control groups, and the horizontal line represents a p–value of 0.05. **(B)**. A Histogram of dysregulated genes between non-ischemic heart failure and control groups. **(C)** Construction and analysis of a PPI network.

ratio, 3.821; 95% CI, 2.010–7.263; p = 0.000), miR-1297 (odds ratio, 0.031; 95% CI, 0.002–0.514; p = 0.015) were significantly correlated with non-ischemic heart failure (**Table 2**). However, bootstrap analysis of 1000 iterations showed that there was no significant predictive power of plasma COX-2 for non-ischemic heart failure (bootstrapped 95% CI, −0.029 to 0.245; p=0.089) and plasma miR-4649-3p also displayed higher predictive power than miR-1297 ((bootstrapped 95% CI, 0.916–15.783; p=0.002) vs bootstrapped 95% CI: −80.258 to −1.420; p =0.041)).

DISCUSSION

Clinically, only BNP or NT-proBNP has been validated for heart failure diagnosis (Goetze et al., 2005), but they are also affected by other conditions and could not encompass all heart failure phenotypes. Recently, data mining strategies on public access databases and integrative bioinformatics analysis have been used to identify potential biomarkers or even new therapeutic targets in complex disease (Sakharkar et al., 2019). In this study, we analyzed GEO Datasets to screen dysregulated genes in whole blood from patients with non-ischemic heart failure for identifying the new biomarkers. We found that COX-2, a secreted protein, was highly expressed in the blood of patients with non-ischemic heart failure. Consistently, many studies showed that COX-2 played an important role in the development of heart failure (Camacho et al., 2011; Liu et al., 2012; Chien et al., 2015; Pang et al., 2016). Normally, the expression of COX-2 is very low and strongly induced by different stimuli, including hypoxia, mechanical stress, and proinflammatory cytokines (Camacho et al., 2011). For example, COX-2 was significantly stimulated by H/R in H9C2 cardiomyocytes by activating NF-κB and inhibition of COX-2 could attenuate H/R-induced cell apoptosis through blocking the expression of proinflammatory cytokines (Pang et al., 2016). In the ISO-induced cardiac hypertrophy rat model, COX-2 was highly expressed, accompanied by elevation of cardiac NF-κB, TNF-α, and IL-6 (Liu et al., 2012). Similarly, COX-2 expression was higher in thrombin-induced hypertrophy in primary human cardiomyocytes (Chien et al., 2015). In this study, the PPI network also showed that COX-2 was associated with the

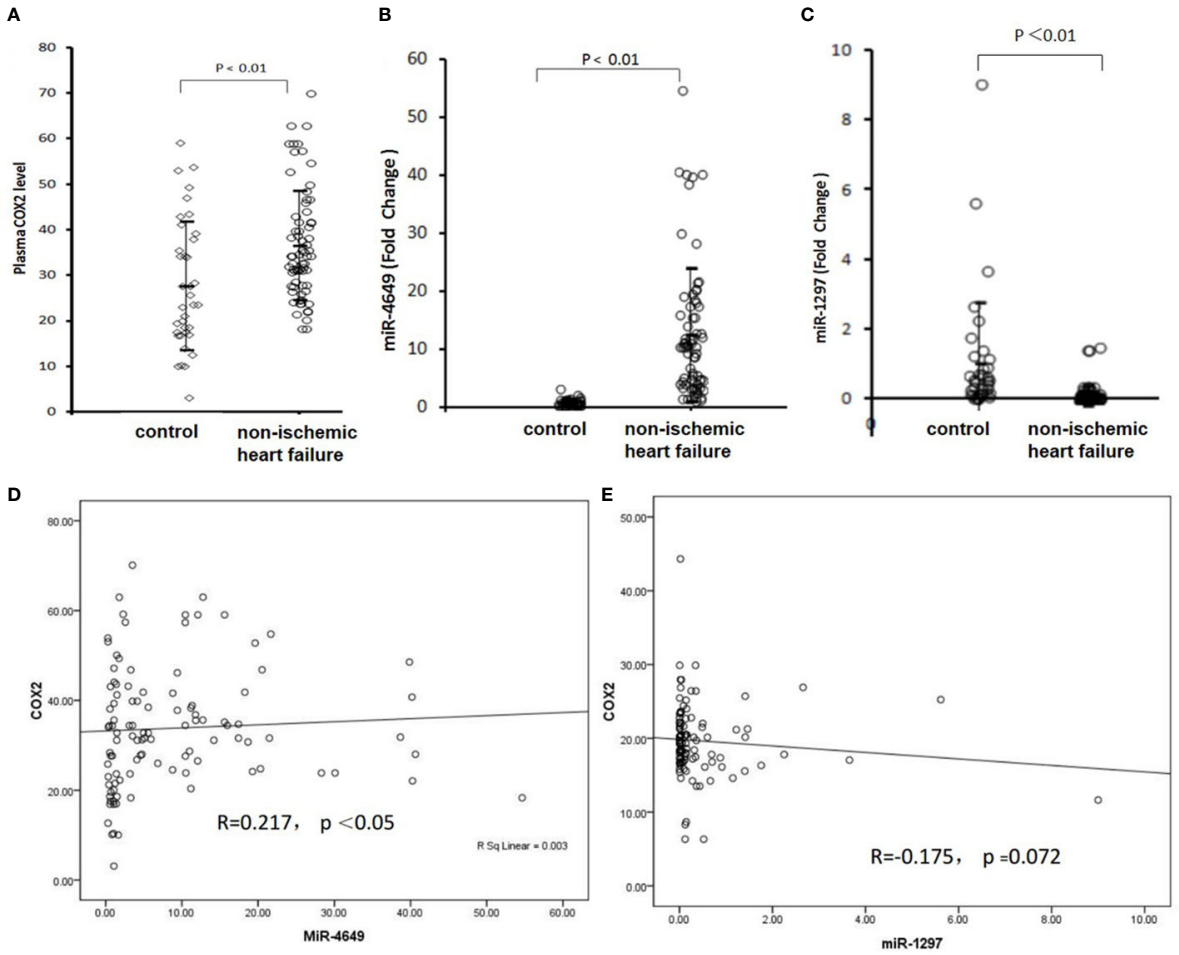

FIGURE 2 | The plasma levels of COX-2, miR-4649-3p, and miR-1297 as well as their correlations. **(A)** The plasma level of COX-2 in patients with non-ischemic heart failure or subjects without cardiovascular disease. **(B)** The plasma level of miR-4649-3p in patients with non-ischemic heart failure or subjects without cardiovascular disease. **(C)** The plasma level of miR-1297 in patients with non-ischemic heart failure or subjects without cardiovascular disease. **(D)** The correlation of COX-2 with miR-4649-3p. **(E)** The correlation of COX-2 with miR-1297.

NF-κB pathway and IL-8, indicating that COX-2 could induce persistent inflammation, which plays a pathogenic role in chronic heart failure by influencing heart contractility, inducing hypertrophy and promoting apoptosis, contributing to myocardial remodeling.

In this study, bioinformatics analysis showed that COX-2 was up-regulated in the blood sample of patients with non-ischemic heart failure, indicating it might be as a promising candidate for the diagnosis of HF. Our results showed the level of COX-2 was significantly up-regulated in the non-ischemic heart failure. Plasma COX-2 also displayed potent predictive power for non-ischemic heart failure, but its sensitivity and specificity were not high enough. Micro RNAs are also present in the circulation and stable, those properties make them be potential biomarkers. In this study, we predicted that miR-4649-3p and miR-1297 could target at COX-2 by using omics bean analysis which combined with the results from 5 databases; TargetScan, PicTar, RNA22, PITA, and miRanda. It has been found that miR-1297 suppressed colorectal cancer growth by targeting COX-2 *in vitro* and *in vivo* study (Chen et al., 2014). In this study, miR-1297 was decreased in the plasma of patients with non-ischemic heart failure and negatively correlated with COX-2. Although there was a week correlation of miR-1297 and COX-2 in the plasma, miR-1297 displayed higher predictive power than COX-2. MiR-4649 was also predicted to target COX-2 and increased in the plasma of patients with non-ischemic heart failure. There was a positive correlation of miR-4649 with COX-2 in the plasma of patients with non-ischemic heart failure, indicating that there was negative feedback regulation between miR-4649 with COX-2. Notably, the COX-2 is not constitutively present in tissues and not very stable in plasma (Mendes et al., 2012; Kirkby et al., 2013). Besides, the genes or micro RNAs in tissues and blood are not always consistent (An et al., 2019). Those might lead to the week correlation of miR-4649 with COX-2 in plasma of non-ischemic heart failure. However, miR-4649 displayed stronger predictive power than COX-2 and miR-

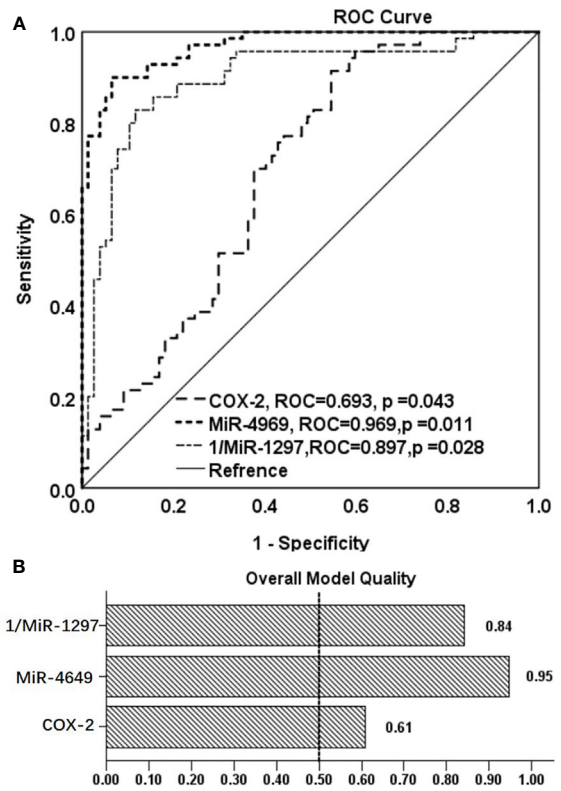

FIGURE 3 | The ROC analysis of the predictive powers of COX-2, miR-4649-3p, and miR-1297 for non-ischemic heart failure. **(A)** ROC curve of COX-2, miR-4649-3p, and 1/miR-12971 for non-ischemic heart failure, **(B)** Overall model quality of COX-2, miR-4649-3p, and 1/miR-12971 for non-ischemic heart failure.

TABLE 2 | Binary logistical regression analysis of COX-2, miR-4649-3p, miR-1297 in patients with non-ischemic heart failure.

Variable	P value	OR	95% CI		Bootstrap	Bootstrap 95% CI	
			Lower	Upper	P-value	Lower	Upper
COX-2	0.047	1.065	1.001	1.134	0.089	–0.029	0.245
MiR-4649-3p	0.000	3.821	2.010	7.263	0.002	0.916	15.783
MiR-1297	0.015	0.031	0.002	0.514	0.041	–80.258	–1.420

Bootstrap significance or 95% CI is two-tailed with 1000 iterations.

1297. Micro RNAs are also present in the circulation and stable, indicating that plasma miR-4649 and miR-1297 might be as biomarkers for non-ischemic heart failure.

Nonsteroidal anti-inflammatory drugs (NSAIDs), which inhibit the expression of COX-2, have been used to treat heart failure, but impair renal function (Bleumink et al., 2003). COX-2 selective inhibitors have similar effects on renal function as the traditional NSAIDs, and can likewise be expected to increase the risk of heart failure in susceptible patients (Patrono, 2016). The micro RNAs target COX-2 might be also used to treat heart failure. It was favored that therapeutic cardiac-targeted delivery of miR-1 reverses pressure overload-induced cardiac hypertrophy and attenuates pathological remodeling. Therefore, manipulation of miR-4649 or miR-1297 might be a strategy to cure the non-ischemic heart failure by targeting COX-2.

CONCLUSION

The COX-2 related micro RNAs miR-4649, miR-1297 could be used as biomarkers for non-ischemic heart failure.

Limitations

In this study, we used the mining strategy to identify the COX-2 and it micro RNAs, which might be used as biomarkers for non-ischemic heart failure. Although the miR-4649 and miR-1297 are predicted to target the COX-2, their correlations were week. Further studies were need to confirm that their direct correlations. In addition, the sample size was small and analyzed from a single-center, larger studies are needed to confirm the current results.

DATA AVAILABILITY STATEMENT

The raw data supporting the conclusions of this article will be made available by the authors, without undue reservation, to any qualified researcher.

ETHICS STATEMENT

The studies involving human participants were reviewed and approved by the study protocol was approved by the ethics committee of Jilin University second hospital. Written informed consent to participate in this study was provided by the participants' legal guardian/next of kin. Written informed consent was obtained from the individual(s), and minor(s)' legal guardian/next of kin, for the publication of any potentially identifiable images or data included in this article.

AUTHOR CONTRIBUTIONS

JW designed the study. YY analyzed the data for GEO data sets and drafted the manuscript. DS collected the samples and tested the plasma levels of COX-2. XZ tested the micro RNA levels. GH performed the statistical analyses.

FUNDING

This study was supported by the National Natural Science Foundation of China (31600728), Key Scientific and Technological Project of Science and Technology Department of Jilin Province (20170402032YY) and Special Fund Project of Jilin Provincial Innovation (2017C049).

REFERENCES

An, T., Fan, T., Zhang, X. Q., Liu, Y. F., Huang, J., Liang, C., et al. (2019). Comparison of Alterations in miRNA Expression in Matched Tissue and Blood Samples during Spinal Cord Glioma Progression. *Sci. Rep.* 9 (1), 9169. doi: 10.1038/s41598-019-42364-x

Barrett, T., Suzek, T. O., Troup, D. B., Wilhite, S. E., Ngau, W. C., Ledoux, P., et al. (2005). NCBI GEO: mining millions of expression profiles—database and tools. *Nucleic Acids Res.* 33 (suppl_1), D562–D566. doi: 10.1093/nar/gki022

Bleumink, G. S., Feenstra, J., Sturkenboom, M. C., and Stricker, B. H. C. (2003). Nonsteroidal anti-inflammatory drugs and heart failure. *Drugs* 63 (6), 525–534. doi: 10.2165/00003495-200363060-00001

Camacho, M., Rodríguez, C., Guadall, A., Alcolea, S., Orriols, M., Escudero, J. R., et al. (2011). Hypoxia upregulates PGI-synthase and increases PGI2 release in human vascular cells exposed to inflammatory stimuli. *J. Lipid Res.* 52 (4), 720–731. doi: 10.1194/jlr.M011007

Chen, P., Wang, B. L., Pan, B. S., and Guo, W. (2014). MiR-1297 regulates the growth, migration and invasion of colorectal cancer cells by targeting cyclooxygenase-2. *Asian Pac J. Cancer Prev.* 15 (21), 9185–9190. doi: 10.7314/APJCP.2014.15.21.9185

Chien, P. T. Y., Lin, C. C., Hsiao, L. D., and Yang, C. M. (2015). Induction of HO-1 by carbon monoxide releasing molecule-2 attenuates thrombin-induced COX-2 expression and hypertrophy in primary human cardiomyocytes. *Toxicol. Appl. Pharmacol.* 289 (2), 349–359. doi: 10.1016/j.taap.2015.09.009

Dai, Z., Aoki, T., Fukumoto, Y., and Shimokawa, H. (2012). Coronary perivascular fibrosis is associated with impairment of coronary blood flow in patients with non-ischemic heart failure. *J. Cardiol.* 60 (5), 416–421. doi: 10.1016/j.jjcc.2012.06.009

Dickinson, B. A., Semus, H. M., Montgomery, R. L., Stack, C., Latimer, P. A., Lewton, S. M., et al. (2013). Plasma microRNAs serve as biomarkers of therapeutic efficacy and disease progression in hypertension-induced heart failure. *Eur. J. Heart Failure* 15 (6), 650–659. doi: 10.1093/eurjhf/hft018

Endo, K., Naito, Y., Ji, X., Nakanishi, M., Noguchi, T., Goto, Y., et al. (2013). MicroRNA 210 as a biomarker for congestive heart failure. *Biol. Pharm. Bull.* 36 (1), 48–54. doi: 10.1248/bpb.b12-00578

Gathright, E. C., Goldstein, C. M., Josephson, R. A., and Hughes, J. W. (2017). Depression increases the risk of mortality in patients with heart failure: a meta-analysis. *J. Psychosomatic Res.* 94, 82–89. doi: 10.1016/j.jpsychores.2017.01.010

Goetze, J. P., Rehfeld, J. F., Videbaek, R., Friis-Hansen, L., and Kastrup, J. (2005). B-type natriuretic peptide and its precursor in cardiac venous blood from failing hearts. *Eur. J. Heart Failure* 7 (1), 69–74. doi: 10.1016/j.ejheart.2004.04.012

Hunt, S. A., Abraham, W. T., Chin, M. H., Feldman, A. M., Francis, G. S., Ganiats, T. G., et al. (2009). 2009 Focused update incorporated into the ACC/AHA 2005 Guidelines for the Diagnosis and Management of Heart Failure in Adults A Report of the American College of Cardiology Foundation/American Heart Association Task Force on Practice Guidelines Developed in Collaboration With the International Society for Heart and Lung Transplantation. *Circulation* 119 (14), e391–e479. doi: 10.1161/CIRCULATIONAHA.109.192065

Inamdar, A. A., and Inamdar, A. C. (2016). Heart failure: diagnosis, management and utilization. *J. Clin. Med.* 5 (7), 62. doi: 10.3390/jcm5070062

Kirkby, N. S., Lundberg, M. H., Harrington, L. S., Leadbeater, P. D., Milne, G. L., Potter, C. M., et al. (2013). Cyclooxygenase-1, not cyclooxygenase-2, is responsible for physiological production of prostacyclin in the cardiovascular system. *Proc. Natl. Acad. Sci. U. S. A.* 109 (43), 17597–17602. doi: 10.1073/pnas.1209192109

Linsenmayer, C., Hadi, A., Williams, G., Doyle, M., and Callihan, M. (2019). Polypharmacy Increases Heart Failure (HF) Readmission Rate. *J. Cardiac Failure* 25 (8), S26. doi: 10.1016/j.cardfail.2019.07.072

Liu, Q., Chen, Y., Auger-Messier, M., and Molkentin, J. D. (2012). Interaction between NFκB and NFAT coordinates cardiac hypertrophy and pathological remodeling. *Circ. Res.* 110 (8), 1077–1086. doi: 10.1161/CIRCRESAHA.111.260729

Liu, M., Chen, J., Huang, D., Ke, J., and Wu, W. (2014). A meta-analysis of proinflammatory cytokines in chronic heart failure. *Heart Asia* 6 (1), 130–136. doi: 10.1136/heartasia-2013-010484

Liu, S., Yao, X., Zhang, D., Sheng, J., Wen, X., Wang, Q., et al. (2018). Analysis of transcription factor-related regulatory networks based on bioinformatics analysis and validation in hepatocellular carcinoma. *BioMed. Res. Int.* 2018, 1431396. doi: 10.1155/2018/1431396

Maegdefessel, L. (2014). The emerging role of micro RNA s in cardiovascular disease. *J. Internal Med.* 276 (6), 633–644. doi: 10.1111/joim.12298

Mendes, R. T., Stanczyk, C. P., Sordi, R., Otuki, M. F., dos Santos, F. A., and Fernandes, D. (2012). Selective inhibition of cyclooxygenase-2: risks and benefits. *Rev. Bras Reumatol.* 52 (5), 767–782. doi: 10.1590/S0482-50042012000500011

Pang, L., Cai, Y., Tang, E. H. C., Yan, D., Kosuru, R., Li, H., et al. (2016). Cox-2 inhibition protects against hypoxia/reoxygenation-induced cardiomyocyte apoptosis via Akt-dependent enhancement of iNOS expression. *Oxid. Med. Cell. Longevity* 2016, 3453059. doi: 10.1155/2016/3453059

Patrono, C. (2016). Cardiovascular effects of cyclooxygenase-2 inhibitors: a mechanistic and clinical perspective. *Br. J. Clin. Pharmacol.* 82 (4), 957–964. doi: 10.1111/bcp.13048

Sakharkar, M. K., Singh, S. K. K., Rajamanickam, K., Essa, M. M., Yang, J., and Chidambaram, S. B. (2019). A systems biology approach towards the identification of candidate therapeutic genes and potential biomarkers for Parkinson's disease. *PLoS One* 14 (9), e0220995. doi: 10.1371/journal.pone.0220995

Senthong, V., Kirsop, J. L., and Tang, W. W. (2017). Clinical phenotyping of heart failure with biomarkers: current and future perspectives. *Curr. Heart Failure Rep.* 14 (2), 106–116. doi: 10.1007/s11897-017-0321-4

Weinberg, E. O., Shimpo, M., De Keulenaer, G. W., MacGillivray, C., Tominaga, S.II, Solomon, S. D., et al. (2002). Expression and regulation of ST2, an interleukin-1 receptor family member, in cardiomyocytes and myocardial infarction. *Circulation* 106 (23), 2961–2966. doi: 10.1161/01.CIR.0000038705.69871.D9

Conflict of Interest: The authors declare that the research was conducted in the absence of any commercial or financial relationships that could be construed as a potential conflict of interest.

Copyright © 2020 Yan, Song, Zhang, Hui and Wang. This is an open-access article distributed under the terms of the Creative Commons Attribution License (CC BY). The use, distribution or reproduction in other forums is permitted, provided the original author(s) and the copyright owner(s) are credited and that the original publication in this journal is cited, in accordance with accepted academic practice. No use, distribution or reproduction is permitted which does not comply with these terms.

frontiers in Physiology

REVIEW
published: 11 August 2020
doi: 10.3389/fphys.2020.00949

Role of Histone Deacetylases in Skeletal Muscle Physiology and Systemic Energy Homeostasis: Implications for Metabolic Diseases and Therapy

Haili Tian[1†], Sujuan Liu[2†], Jun Ren[3], Jason Kai Wei Lee[4,5,6], Ru Wang[1] and Peijie Chen[1*]*

[1] School of Kinesiology, Shanghai University of Sport, Shanghai, China, [2] Department of Anatomy and Histology, School of Basic Medical Sciences, Tianjin Medical University, Tianjin, China, [3] Department of Cardiology, Shanghai Institute of Cardiovascular Diseases, Zhongshan Hospital Fudan University, Shanghai, China, [4] Department of Physiology, Yong Loo Lin School of Medicine, National University of Singapore, Singapore, Singapore, [5] Global Asia Institute, National University of Singapore, Singapore, Singapore, [6] N.1 Institute for Health, National University of Singapore, Singapore, Singapore

OPEN ACCESS

Edited by:
Brian James Morris,
The University of Sydney, Australia

Reviewed by:
Sean L. McGee,
Deakin University, Australia
Viviana Moresi,
Sapienza University of Rome, Italy

***Correspondence:**
Ru Wang
wangru@ty.sus.edu.cn
Peijie Chen
chenpeijie@sus.edu.cn

[†] These authors have contributed equally to this work

Specialty section:
This article was submitted to Integrative Physiology, a section of the journal Frontiers in Physiology

Received: 27 May 2020
Accepted: 14 July 2020
Published: 11 August 2020

Citation:
Tian H, Liu S, Ren J, Lee JKW, Wang R and Chen P (2020) Role of Histone Deacetylases in Skeletal Muscle Physiology and Systemic Energy Homeostasis: Implications for Metabolic Diseases and Therapy. Front. Physiol. 11:949. doi: 10.3389/fphys.2020.00949

Skeletal muscle is the largest metabolic organ in the human body and is able to rapidly adapt to drastic changes during exercise. Histone acetyltransferases (HATs) and histone deacetylases (HDACs), which target histone and non-histone proteins, are two major enzyme families that control the biological process of histone acetylation and deacetylation. Balance between these two enzymes serves as an essential element for gene expression and metabolic and physiological function. Genetic KO/TG murine models reveal that HDACs possess pivotal roles in maintaining skeletal muscles' metabolic homeostasis, regulating skeletal muscles motor adaptation and exercise capacity. HDACs may be involved in mitochondrial remodeling, insulin sensitivity regulation, turn on/off of metabolic fuel switching and orchestrating physiological homeostasis of skeletal muscles from the process of myogenesis. Moreover, many myogenic factors and metabolic factors are modulated by HDACs. HDACs are considered as therapeutic targets in clinical research for treatment of cancer, inflammation, and neurological and metabolic-related diseases. This review will focus on physiological function of HDACs in skeletal muscles and provide new ideas for the treatment of metabolic diseases.

Keywords: histone deacetylases, exercise capacity, skeletal muscle, metabolism, muscle physiology

INTRODUCTION

Skeletal muscle is the largest metabolic organ in the human body, consuming about 18% of the entire body daily expenditure of energy (Durnin, 1981). It produces various secrete factors and participates in the interplay among multiple tissues and organs (Pedersen and Febbraio, 2012; Mizgier et al., 2019). Muscular contraction is one of the main physiological functions of skeletal muscles and plays a role in maintaining organ and systemic metabolic homeostasis (Guo et al., 2020). Proper exercises help build up body defense to combat various diseases including obesity, type 2 diabetes, Alzheimer disease, osteoarthritis, and so on (Luan et al., 2019). These important

functions require delicate regulations in muscle from the level of genome to signal transduction, establishing muscle plasticity, and responses to environmental stress. Acetyl-CoA as a central metabolite of amino acid/fatty acid/glucose not only serves as fuel for energy expenditure but also bridges the gap between environmental stress and organismal response (Lempradl et al., 2015; Liu et al., 2020). This control occurs through post-translational modification on nucleosomes histone lysine residues and other signal transducing proteins, which in turn controls accessibility of DNA to regulatory factors and protein activity. Acetylation, one of the most prevalent modifications of protein, is believed to function as a key modulator of chromatin structure and signal transduction, and provides an avenue to couple extracellular stimuli with genome during muscle metabolism process by regulating acetylation and deacetylation (Haberland et al., 2009).

histone deacetylases (HDACs) as a family of protein deacetylases have been demonstrated to moderate physiological homeostasis and development by deacetylation (Haberland et al., 2009) (**Table 1**). In humans, there are 18 types of HDACs, which are classified into four categories based on homologous proteins in yeast, namely: Class I Rpd3-like protein (HDAC1, -2, -3, -8); Class II Hda1-like proteins are classified as Class IIa (HDAC4, -5, -7, -9) and Class IIb (HDAC6, -10); Class III Sir2p-like, nicotinamide adenine dinucleotide (NAD^+)-dependent (SIRT1, -2, -3, -4, -5, -6, -7); and Class IV HDAC11, containing homologous domain with both Rpd3 and Hda1 (Seto and Yoshida, 2014). HDACs modulate gene expression and protein activity through deacetylating proteins. When histone lysine ε-amino acid in the nucleosome is acetylated, it can neutralize positive charge, before loosening chromatin structure, to promote binding of transcription factors to DNA and expression of downstream target genes. By contrast, histone deacetylation compresses chromatin structure, thereby inhibiting transcriptional gene expression (Shahbazian and Grunstein, 2007).

Biochemical properties of HDACs have been comprehensively reviewed (Shahbazian and Grunstein, 2007). However, the physiological functions of HDACs have yet to be well examined in skeletal muscles. A series of researches shed light on the potential of drugs targeting HDACs to improve muscle fitness and cardiac muscle disease, which needs further clarification of HDACs physiological function to understand the mechanisms (Bai et al., 2011; Galmozzi et al., 2013; Xie et al., 2014; Zhang and Ren, 2014; Gaur et al., 2016). Ample work has revealed the role of HDAC in muscle physiology such as skeletal muscles me olism and thus exercise capacity (McGee and Hargreaves, 2010) (**Table 1**). Class I HDACs can interact with myocyte enhancer factor 2 (MEF2), MyoD, regulating myogenesis, and exercise capacity (Mal et al., 2001; Puri et al., 2001; Ohkawa et al., 2006; Gregoire et al., 2007). HDAC3 participates in myocytes differentiation and is linked to skeletal muscles metabolic fuel switching (Gregoire et al., 2007; Hong et al., 2017). Class II HDACs can be phosphorylated by HDAC kinases and are transduced from nucleus to cytoplasm in response to cellular stress, mediating muscle fiber switch and affecting the pathway of insulin sensitivity such as *Glut4* and AKT (Haberland et al., 2009; McGee and Hargreaves, 2010). Class III HDACs target a crucial mitochondrial biogenesis factor peroxisome proliferator-activated receptor gamma, coactivator 1 alpha (PGC-1α) in skeletal muscles, liver and fat tissue (White and Schenk, 2012). Therefore, we will further discuss how these HDACs influence respective downstream targets, exercise capacity, and therapeutic effects in human diseases.

CLASS I HDAC: HDAC1/2/3

Regulation of Myogenesis by Class I HDACs

In previous studies, HDAC1/2/3 was shown to be associated with the process of myogenesis or myocyte differentiation (Mal et al., 2001; Puri et al., 2001; Ohkawa et al., 2006; Gregoire et al., 2007). HDAC1 tightly binds to MyoD and deacetylates specific sites to inhibit the expression of muscle-specific genes such as *MHC* and *MCK* in myoblasts. Mimicking muscle differentiation condition by serum deprivation, HDAC1 protein gradually decreases during myocyte differentiation and transfers to bind to the tumor suppressor pRb, accompanied by isolation of HDAC1-MyoD and transcriptional activation of muscle-specific genes (Puri et al., 2001). A HDAC1 (H141A) mutant incapable of binding with MyoD loses its inhibitory property on muscle-specific genes in myoblast state (Mal et al., 2001). In the late stage of myocyte differentiation, activating factor gradually switches from MyoD to myogenin, occurring with a decrease in the MEF2D inhibitory regulator HDAC2. Simultaneous overexpression of myogenin and MEF2D can enhance the expression of the muscle-specific gene *MHC* in the absence of MyoD (Ohkawa et al., 2006). MEF2D, a key factor that controls myocyte differentiation, can only be effectively deacetylated by HDAC3, rather than HDAC1/2/8 (Gregoire et al., 2007). In addition, HDAC3 can inhibit autoacetylation of acetyltransferases p300 and p300/CBP-associated factor (PCAF). Thus, HDAC3 impedes MyoD-MEF2-PCAF to form a multicomplex, disturbing MEF2-dependent myogenic transcription (Gregoire et al., 2007; **Figure 1**).

Redundant Roles of HDAC1/2 in Maintaining Sarcomere Homeostasis in Muscle

Loss of function of HDAC1/2 inhibits autophagy flux in skeletal muscles tissue, accompanied by decreased LC3 II/I ratio and p62 accumulation under fasting condition (Moresi et al., 2012). Toxic autophagy intermediates accumulate in muscle fibers in which class I HDACs deficiency led to impaired exercise capacity (Moresi et al., 2012). This offers convincing evidence on the role of HDAC1/2 in stabilizing basic structure and facilitating development in muscles. Genetic models suggest that Class I HDACs control the physiological homeostasis of skeletal muscles. A germline deletion shows that whole-body knockout of either HDAC1 or HDAC2 leads to mortality in mice prior to the perinatal period (Montgomery et al., 2007). However, a tissue-specific single deletion of HDAC1 or HDAC2 in myocardium does not cause any phenotype (Montgomery et al., 2007). Double knockout HDAC1/2 in the

TABLE 1 | The targets of HADCs in skeletal muscles and their physiological functions.

Class	Members	Down targets	Genetic KO/TG phenotype	References
I	HDAC1	MyoD↓, *PTEN*↓, FoxO?	Functionally redundant HDAC1/2 DKO mice causes mitochondrial abnormalities and sarcomere degeneration	Puri et al., 2001; Ohkawa et al., 2006; Beharry et al., 2014; Cho et al., 2015; Zhu et al., 2016; Bin et al., 2019
	HDAC2	MyoD↓, MEF2D↓, *NF-κBp65*↓		
	HDAC3	MEF2D, PCAF↓, *Ampd3*↓ RCAN1? MEF2A-*Cpt1b*↓	mKO mice: Enhanced amino acid\lipid metabolism and endurance exercise Causes IR under basal condition	Gregoire et al., 2007; Han et al., 2014; Yuan et al., 2014; Hong et al., 2017
	HDAC8	–	–	
IIA	HDAC4	MEF2↓, *Glut4*↓, Myosin Heavy Chain, PGC-1α, and Hsc70-, *Pax7*↓	Functionally redundant HDAC4/5 DKO, HDAC5/9 DKO, HDAC4/5/9 TKO increases type I fiber percentage and oxidation metabolism	McKinsey et al., 2000a; Choi et al., 2014; Niu et al., 2017; Luo et al., 2019
	HDAC5	MEF2↓, *Glut4*↓, *Baf60c*↓		Yuan et al., 2014; Meng et al., 2017; Niu et al., 2017
	HDAC9	*Atg7, Beclin1, LC3*↓ Dach2-*Myog, Gdf5*↓		Macpherson et al., 2015; Zhang et al., 2019
	HDAC7	MEF2↓	–	Dressel et al., 2001
IIB	HDAC6	*Pax7,* MFN1↓ Fam65b, dysferlin and MAFbx-	KO mice: Causes mitochondrial oxidative damage, mitofusion defect Protect against muscle wasting	Balasubramanian et al., 2014; Lee et al., 2014; Ratti et al., 2015
	HDAC10	–	–	
III	SIRT1	PGC-1α? STAT3↓	mKO mice: Mediates CR induced insulin sensitivity, has no effect on glucose homeostasis or exercise capacity TG mice: no effect on glucose homeostasis or exercise capacity	Rodgers et al., 2005; Schenk et al., 2011
	SIRT2	–	KO mice: Exacerbates obesity and IR in HFD	
	SIRT3	MnSOD?, Hexokinase II? PDH subunit E1α?	KO mice: Exacerbates obesity and IR in HFD	Boyle et al., 2013; Jing et al., 2013; Lantier et al., 2015
	SIRT4	Malonyl CoA decarboxylase↓	KO mice: Increased exercise tolerance and protect against HFD-induced obesity	Laurent et al., 2013
	SIRT5	–	–	
	SIRT6	NF-κB-*Mstn*	KO mice: Abnormal hypoglycemia TG mice: Protect against HFD mKO mice: Impaired insulin sensitivity, loss of muscle mass	Kanfi et al., 2010; Xiao et al., 2010; Cui et al., 2017; Samant et al., 2017
	SIRT7	–	–	–
IV	HDAC11	–	–	–

Activation?, inhibition↓, unknown. KO, whole-body deletion; TG, whole-body overexpression; DKO, double knockout; TKO, triple knockout; mKO, muscle-specific knockout; CR, caloric restriction; HFD, high fat diet; IR, insulin resistance.

heart leads to severe cardiomyopathy in mice, indicating the obligatory role for HDAC1/2 in specific tissues (Montgomery et al., 2007). In skeletal muscle, double knockout of HDAC1/2 by myogenin-Cre causes mitochondrial abnormalities and sarcomere degeneration, disrupting fundamental structural units of myofibers (Moresi et al., 2012). Therefore, these findings demonstrate that HDAC1/2 redundantly maintains sarcomere homeostasis in skeletal muscle.

HDAC3 Functions as a Fuel Switch in Muscle Energy Metabolism

Histone deacetylases 3 is the enzymatic core of nuclear receptor corepressor (N-CoR) and silencing mediator of retinoic acid and thyroid hormone receptors (SMRT) co-repressor; correspondingly, N-CoR and SMRT co-repressor activate HDAC3 through its SANT domain enzyme activity (Karagianni and Wong, 2007). Mice suffer from insulin resistance after specifically knocking out HDAC3 in skeletal muscles-mKO, while their endurance exercise abilities are enhanced (Hong et al., 2017). It seems a self-contradictory phenomenon because former studies pointed out that increased endurance exercise capacity enhances insulin sensitivity. The study shows that insulin signaling cascades including pAKT/AKT, pIRS1-S1101, and pGSK/GSK have no change in HDAC3 mKO muscle, while glucose uptake and insulin sensitivity are impaired in glucose tolerance test (GTT) and insulin tolerance test (ITT) (Hong et al., 2017), which is called the "dissociation effect" by researchers. Lipid tends to be used as energy fuel in HDAC mKO mice, which inhibits glucose absorption but does not influence insulin signaling sensitivity (Hong et al., 2017). Further work found that the HDAC3 knockout upregulates the expression of AMP deaminase 3 (AMPD3), the first rate-limiting enzyme in purine metabolism, in skeletal muscles (Fortuin et al., 1996; Hong et al., 2017). AMPD3 can deaminate AMP to form IMP, facilitating aspartic acid to transmit into fumarate and malate, the intermediate metabolites of tricarboxylic acid cycle (TCA cycle) (Hong et al., 2017). Research studies found that exercise induced glucose labeled 13C6 expressed a lower glycolysis flux rate in muscles of HDAC3 mKO but a higher expression in the TCA

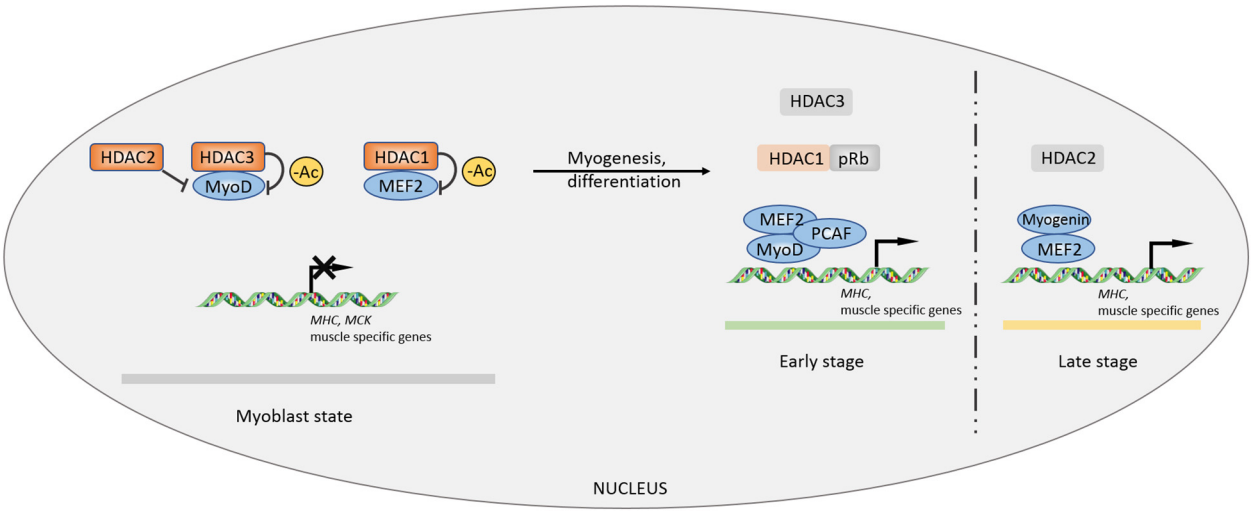

FIGURE 1 | Controls of myogenesis by Class I HDACs. The inhibitory effects of HDACs on myogenic factors MEF2 and MyoD maintain a primary myoblast state. During myocyte differentiation and myogenic process, the inhibition is lifted by other factors, facilitating MEF2-MyoD complex formation to promote myogenesis. –Ac, deacetylation.

cycle intermediates (Hong et al., 2017; Gong et al., 2018). Thus, a general increase in TCA cycle metabolites activates the oxidation in mitochondria. *In vitro* radioactive aspartic acid isotope tracer test showed that inhibiting HDAC3 or overexpressing AMPD3 can increase amino acid metabolism rate and enhance fatty acid metabolism, thereby downregulating glucose metabolism (Hong et al., 2017 **Figure 2**). In liver, knockout HDAC3 causes severe liver steatosis and can be rescued by wild-type or catalytically inactive mutants of HDAC3, indicating an enzymatic activity independent function (Sun et al., 2013). However, the muscle fuel switching in HDAC3 mKO mice cannot be rescued by an enzymatic inactivity mutant HDAC3 (Song et al., 2019). This finding demonstrates that HDAC3 controls the fuel utilization in skeletal muscles and is dependent on its enzymatic activity. The relationship between exercise and glucose uptake is far more complex than one could expect.

CLASS II HDACs: HDAC4/5/7/9/6

Phosphorylation and Nucleus-Cytoplasm Shuttle of Class II HDACs

The MEF2 family is a class of transcription factors that are closely associated with myogenic basic helix-loop-helix domains, including MyoD (Taylor and Hughes, 2017). MEF2 may interact with Class IIa histone deacetylase HDAC4/5 to inhibit the transcription of MEF2-dependent genes, thereby impeding the differentiation from myoblast to myotube (McKinsey et al., 2000a). During exercise, Ca^{2+} flows out from sarcoplasmic reticulum and activate calcium/calmodulin-dependent protein kinase (CaMK), which phosphorylates HDAC4/5 and mediates HDAC4/5 shuttle from the nucleus to the cytoplasm, thus releasing the repressive effect of HDAC4/5 on MEF2-dependent genes (McKinsey et al., 2000b; Yuan et al., 2014). Further research demonstrates that the nucleoplasmic shuttle of HDAC4 relies on 14-3-3 binding, while the shuttle of HDAC5 depends on CaMK phosphorylation at serine -259 and -498 sites first, and then exporting from the nucleus by binding with 14-3-3 (McKinsey et al., 2000b). As expected, HDAC7 in Class IIa also possesses the ability to be exported from nucleus to cytoplasm (Gao et al., 2010), suggesting that there may be redundant functions of Class IIa HDACs. Except for Class IIa, knocking out Class IIb HDAC6 in embryonic stem cells (ESCs) can promote ESCs to differentiate into myoblast cells, and transplantation of ESCs with HDAC6 knockdown can also help the regeneration of wound skeletal muscles (Lee et al., 2015).

Regulation of Class II HDACs on Fiber-Type Switch, Mitochondria Remodeling, and Energy Stress in Skeletal Muscle

Evidence shows that the proportion of type I fiber in skeletal muscles has no change in animal knocked out alone any member of Class IIa (Potthoff et al., 2007). However, the proportion of type I fiber is significantly increased in HDAC4/5 DKO, HDAC5/9 DKO, HDAC4/5/9 TKO mice as well as exercise capacity of skeletal muscles (Potthoff et al., 2007). Altogether, the finding indicated a functional redundant mechanism in Class II HDACs family. Previous study found that Class IIa HDACs are closely associated with the MEF2 family and can repress their downstream target genes (McKinsey et al., 2000a). Therefore, similar to Class IIa HDACs DKO, the proportion of type I fiber is decreased in the MEF2C and MEF2D knockout mouse models, overexpressing MEF2C results in increasing type I fiber and exercise capacity. HDAC4/5 not only regulates exercise capacity but also governs motor adaptation. Several studies had shown that exercise

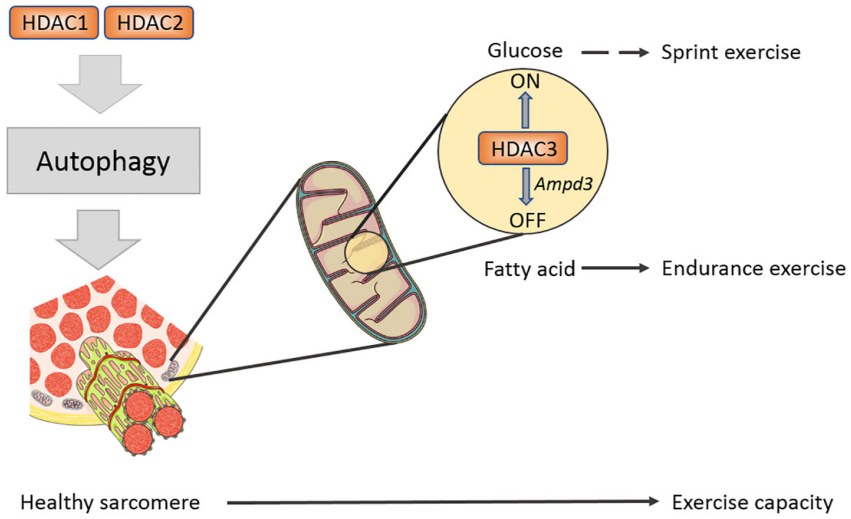

FIGURE 2 | Class I HDACs regulates sarcomere structure and exercise capacity in mature muscle. A schematic diagram shows Class I HDACs regulate exercise capacity on different levels. HDAC1/2 have redundant roles in modulating autophagy flux in muscle, eliminating toxic factors in muscle. HDAC3 serves as a fuel switch and promotes muscle to use fatty acid to adapt endurance exercise.

promotes phosphorylation of HDAC4/5 mediated by CaMK and adenosine monophosphate-activated protein kinase (AMPK), then increasing a MEF2-dependent transcription of *Glut4* and muscle-specific genes, which participates in the adaptation and plasticity of skeletal muscles (McGee et al., 2008, 2009; McGee and Hargreaves, 2011). Besides exercise, glucose can also activate K_{ATP} channel-dependent calcium signaling and CaMK, which induce phosphorylation-dependent nuclear-cytoplasm transportation of HDAC5 (Meng et al., 2017). The leaving HDAC5 releases its repressive effect on *Baf60c* and enhancing insulin-independent AKT activation (Meng et al., 2017). Using specific inhibitor of class IIa HDAC activity, myosin heavy chain, PGC-1α, and heat-shock cognate (HSC70) are confirmed to be one of the substrates of HDAC4 in denervation-induced atrophy muscle in comparison with acetylated protein enrichment with untreated group (Luo et al., 2019). Taken together, Class IIa HDACs play critical roles in exercise capacity, remodeling, and nutrient sensing of skeletal muscles (**Figure 3**).

For Class IIb, it was revealed that glucose deprivation-induced mitochondrial fusion mediated by mitofusion1 (MFN1) is significantly disrupted in HDAC6 KO mice, causing mitochondria degeneration, which is reversed following application of MFN1 acetylation-resistant mutant (Lee et al., 2014). This study suggested that MFN1 deacetylation by HDAC6 plays an important role in mitochondrial adaptive energy production and remodeling of skeletal muscles.

CLASS III HDACs/Sir2-HOMOLOG: SIRT1/6/3/4

Nuclear-Located SIRT1/6

Numerous studies have found that caloric restriction (CR) extends lifespan of mammals, *Caenorhabditis elegans*, and fruit flies, while such effect is lost in *SIR2* or *NPT1* mutant *C. elegans* strains (Imai et al., 2000; Lin et al., 2000). *SIR2* encodes the silencing protein, Sir2p, and NPT1 participates in the synthesis of NAD^+. NAD^+ is an essential cofactor for Sir2p-Class III HDACs to exert enzyme activity rather than Class I, II, and IV relaying on the zinc (Imai et al., 2000; Lin et al., 2000). In mammals, Sir2 has 7 homologous proteins and these proteins are essential to mitochondrial energy homeostasis, antioxidant defense, cell proliferation, and DNA repair (Vargas-Ortiz et al., 2019).

SIRT1 Mediates Energy Stress Adaptation in Skeletal Muscles

Rodgers et al. (2005) reported that SIRT1 promotes the transcriptional activity of PGC-1α by deacetylating the PGC-1α at K13 site and mediates CR-induced gluconeogenesis-related genes *G6P*, *PEPCK* expression in liver. Further research showed that the NAD^+/NADH ratio and the enzymatic activity of Sir2, a sensor of redox state, were decreased in differentiating myocytes, which relieved the inhibitory effect on MyoD and then promoted cell differentiation. Resveratrol (RSV), a compound that may target SIRT1-PGC-1α, can improve mitochondrial function and metabolic homeostasis, owning a potential to prolong lifespan. RSV loses its activating effect on PGC-1α in SIRT1 ($^{-/-}$) MEFs (Lagouge et al., 2006). Moreover, RSV-treated mice at a dose of 4 g/kg increased their exercise capacity, oxygen consumption, and improved insulin sensitivity against high-fat induced obesity (Lagouge et al., 2006). In addition, RSV could enhance the deacetylation of PGC-1α in brown fat tissue (BAT) and skeletal muscles, which promotes mitochondrial production, oxygen consumption, and thus improves metabolic syndrome (Lagouge et al., 2006). The function of SIRT1 in regulating skeletal muscles metabolic homeostasis and exercise capacity has attracted great attention from researchers. Researchers further generated skeletal muscle-specific SIRT1-mKO mice and found that mKO mice

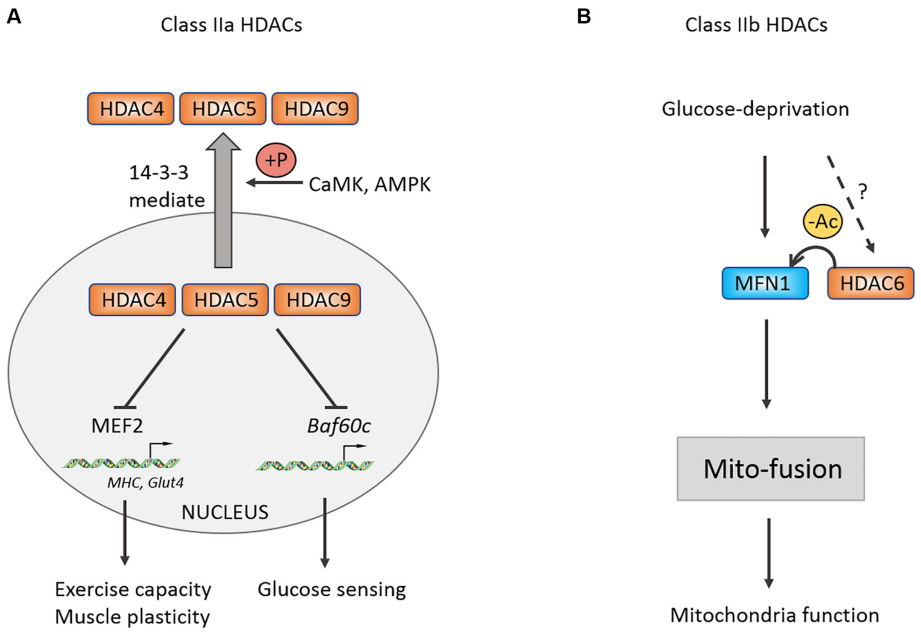

FIGURE 3 | Control of muscle exercise adaption and mitochondrial function by Class II HDACs. **(A)** Schematic of the Class IIa HDACs nucleoplasm shuttle. Under stress condition, CaMK and AMPK could be activated and phosphorylate Class IIa HDACs. Phosphorylated HDACs then bind with 14-3-3 and shuttle to cytoplasm, relieving inhibitory effects on MEF2 and *Baf60c*. **(B)** Class IIb HDAC6 can deacetylate MFN1 and facilitates its mito-fusion function. +P, phosphorylation.

lost the effect of CR-induced increasing insulin sensitivity and were unable to deacetylate and inactivate STAT3, resulting in upregulating the phosphatidylinositol-3-kinase (PI3K) inhibitory regulator p55α/p50α expression (Schenk et al., 2011). Although knockout or overexpression of SIRT1 in skeletal muscles has no effect on endurance capacity or glucose homeostasis in mice (Gurd et al., 2009; Philp et al., 2011; White et al., 2013; Svensson et al., 2020), some studies have shown that AMPK regulates energy metabolism of skeletal muscles partially mediated by SIRT1, and SIRT1 is significantly increased after endurance exercise (Suwa et al., 2008; Canto et al., 2009). Overexpression of Sirt1 in skeletal muscles by adeno-associated virus 1 (AAV1) promotes the expression of oxidation-related genes including *Ppargc1a*, *Tfam*, *Cpt1b*, and *Pdk4*, while it has no effect on insulin sensitivity of body (Vila et al., 2016). But overexpressing Sirt1 in liver by AAV8 can protect from fatty liver induced by high-carbohydrate food (HCD) (Vila et al., 2014). Taken together, the aforementioned studies suggest that SIRT1 possesses limited regulation capacity of skeletal muscles motility, and SIRT1 may modulate mitochondrial homeostasis and mediate skeletal muscles adaptation under certain physiological conditions, such as CR, aging, and regeneration (Gomes et al., 2013; Ryall et al., 2015; **Figure 4**). In addition, there may be more beneficial effects of SIRT1 on metabolism in the liver or fat tissue (Lagouge et al., 2006; Vila et al., 2014, 2016; Stefanowicz et al., 2018).

SIRT6 Improves Muscle Fitness and Exercise Capacity

SIRT6 is another Sir2-like deacetylase located in the nucleus. Whole body deletion of SIRT6 causes 60% mice death around 4 weeks owning to hypoglycemia (Xiao et al., 2010). Nevertheless, the skeletal muscle-specific knockout of SIRT6 causes insulin resistance and impairs glucose homeostasis of mKO mice (Cui et al., 2017). Because the activity of AMPK is reduced in SIRT6-mKO mice, the glycolipids absorption and utilization of skeletal muscles are impaired, and the exercise capacity of the mice was also attenuated (Cui et al., 2017). Furthermore, researchers constructed the overexpressing SIRT6 (Sirt6BAC) mice and found that their body weight and fat content were normal, but the Sirt6BAC mice could protect from HCD-induced hyperglycemia via increasing p-AKT/AKT induced by insulin stimulation and glucose absorption (Anderson et al., 2015). Vitro experiments further demonstrated that the ability of glucose uptake was enhanced mainly in skeletal muscles, not in brain, iWAT, eWAT tissues of Sirt6BAC mice (Anderson et al., 2015). These results shows the potential effects of SIRT6 targeted in skeletal muscles on improving exercise performance and treating metabolic diseases (**Figure 4**).

Mitochondria-Located SIRT3/4

SIRT3/4 Maintains Mitochondria Function in Skeletal Muscles

SIRT3/4 are mitochondria-localized deacetylases and responsible for regulating the deacetylation of proteins in mitochondria and maintaining mitochondrial homeostasis. After feeding high-fat-diet (HFD), accelerated obesity, attenuated insulin sensitivity, worsened fatty liver and increased acetylation of proteins in mitochondria were observed in SIRT3 KO mice (Hirschey et al., 2011). Multi-tissue proteomics and physiological examination reveals that SIRT3 is responsible for mitochondrial acetylated

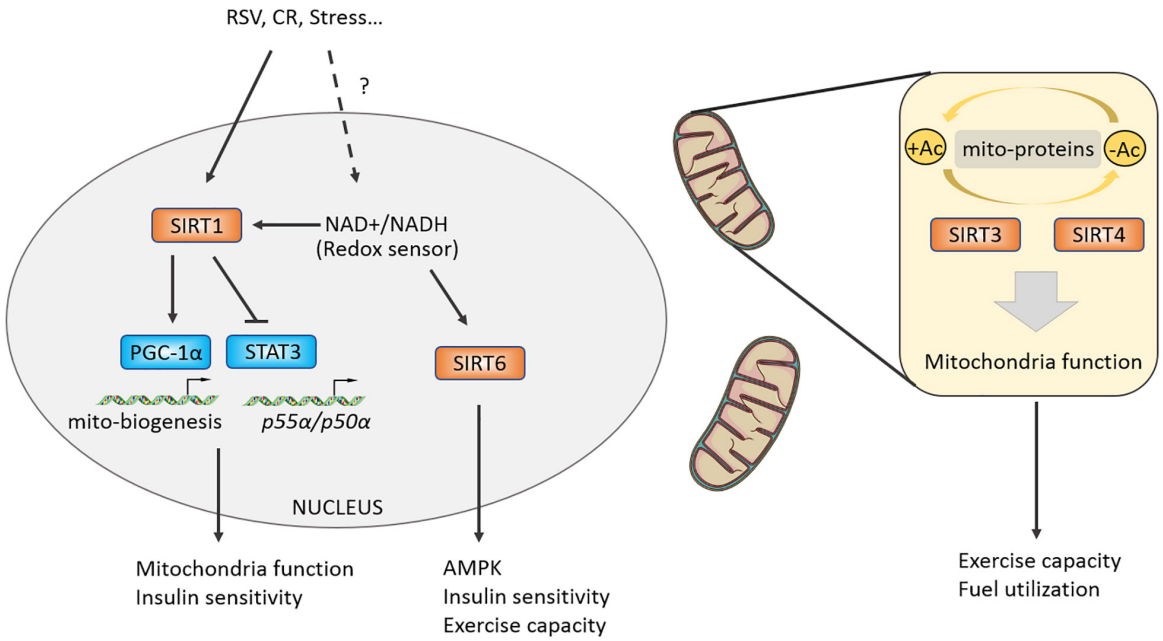

FIGURE 4 | Class III HDACs promote a stress-induced adaptation in muscle and regulate mitochondrial function. Class III HDACs are NAD^+-dependent deacetylases and may function as a redox sensor in muscle cell. SIRT1 could activate PGC-1alpha by directly deacetylasing K13 site and regulate insulin sensitivity by targeting STAT3. Mitochondria-located Class III HDACs control mitochondrial function by deacetylating certain mitochondrial proteins, modulating muscle fuel utilization and exercise capacity.

proteome regulation and metabolic fuel switching in brain, heart, kidney, liver, and skeletal muscles (Dittenhafer-Reed et al., 2015). Protein enrichment analysis discovers that its regulatory proteins were mainly concentrated in lipid metabolism (Dittenhafer-Reed et al., 2015). Knocking out SIRT3 leads to reduction in the levels of deacetylation of manganese superoxide dismutase (MnSOD) mitochondrial complex II and pyruvate dehydrogenase (PDH) subunit E1α, a downregulation of hexokinase II (HK II) binding with mitochondria, resulting in impaired glucose and lipid metabolism of skeletal muscles (Lantier et al., 2015). Interestingly, SIRT3 liver-specific knockout ($hep^{-/-}$) and skeletal muscle-specific knockout ($skm^{-/-}$) mice did not affect glucose homeostasis under chow or HFD conditions (Fernandez-Marcos et al., 2012). The above results indicate that SIRT3 has an important role in metabolic regulation, but in specific physiological processes such as redox state, exercise, and aging, and its regulatory mechanism is yet defined in skeletal muscles (Kong et al., 2010; Robin et al., 2020; Williams et al., 2020). A recent study found that SIRT4 knockout can resist HFD-induced obesity and increase endurance exercise in mice by repressing malonyl CoA decarboxylase, which was a key enzyme controlling fatty acid beta-oxidation and was reported to regulate muscle fuel switching between carbohydrates and fatty acids (Koves et al., 2008; Laurent et al., 2013). Moreover, knockdown of SIRT4 by adenoviral shRNA can increase the mRNA and protein content of SIRT1, thereby enhancing the expression of fatty acid oxidation genes and mitochondrial oxidation capacity in hepatocytes and myotubes (Nasrin et al., 2010) (**Table 1**).

THERAPEUTIC TARGETS OF HDACs AND THEIR POTENTIAL FOR METABOLIC DISEASES

A comparative analysis used HDAC pan-inhibitor SAHA, a class I HDAC selective inhibitor (MS275) and a class II HDAC selective inhibitor (MC1568) to treat C2C12 separately. It was found that only MS275 could significantly stimulate mitochondria biogenesis and oxygen consumption (Galmozzi et al., 2013). In obese diabetic mice, it was found that specifically inhibiting Class I rather than Class II HDACs improved GTT and insulin sensitivity, increased oxidative metabolism of skeletal muscles and adipose tissue, and reduced body weight (Galmozzi et al., 2013). Similar to the effect of MS275, knockdown HDAC3 in C2C12 could also increase *Pgc-1α*, *Glut4*, *Tfam*, *Idh3α* transcription, suggesting that HDAC3 and its target genes played an important role in the above events (Galmozzi et al., 2013).

For Class II HDACs, studies have found that scriptaid, a Class IIa HDAC inhibitor, has similar effects to exercise. Six weeks of scriptaid administration significantly improved endurance performance, and significantly increased the whole-body energy expenditure and the expression of lipid oxidation related genes (*Pdk4*, *Cpt1b*, *Pgc-1α*, *Pparδ*, etc.) of C57BL/6 mice (Gaur et al., 2016). One possible explanation of above observation is the potential target of scriptaid inhibition of titin (a structure protein of sarcomere) deacetylation and downstream genes of Class IIa HDACs (Gaur et al., 2016; Huang et al., 2019).

In mice treated with SPT1720, another activator of SIRT1, overtly enhanced endurance exercise ability was noted. Moreover, these mice were protected from HFD-induced obesity and insulin resistance, owing to an upregulation of the oxidative metabolism in skeletal muscles, liver, and BAT tissues (Pacholec et al., 2010). In order to further explore the principle of SIRT1 activation, the researchers purified SIRT1 *in vitro* and added SRT1720 and its analogs SRT2183, SRT1460, and RSV, and they found that the enzymatic activity of SIRT1 was not enhanced, suggesting that these drugs may indirectly activate SIRT1 (Pacholec et al., 2010). The enzymatic activity of SIRT1 largely depends on the content of cofactor NAD^+. This implied that the enhancement of SIRT1 activity may be achieved through indirect upregulation of NAD^+. Study has discovered that knocking out poly (ADP-ribose) polymerase-1 (PARP-1), which is a NAD^+ consuming enzyme, could increase NAD^+ content and enhance the activity of SIRT1 in BAT and skeletal muscles (Bai et al., 2011). PARP-1 inhibitors can upregulate the proteins of mitochondrial respiratory chain complexes in mice, enhance the aerobic oxidation capacity of mitochondria, and improve mitochondrial defects in the primary myotubes of obese humans (Bai et al., 2011; Pirinen et al., 2014).

Resveratrol was initially reported as an SIRT1 activator that improves mitochondrial function and exercise capacity in mice, and resists HFD-induced obesity (Lagouge et al., 2006). However, subsequent studies have discovered that administering the same dose of RSV to rats or mice does not increase mitochondrial protein content (Higashida et al., 2013). By contrast, overexpression of SIRT1 in the triceps muscle of rats decreases the mitochondrial protein content (Higashida et al., 2013). In a double-blind human trial, 11 healthy and obese men were supplied for 30-day RSV, in which the data showed that RSV can improve systolic blood pressure and homeostasis model assessment (HOMA) index-indicating glucose metabolism ability, simulating the effect of CR (Timmers et al., 2011). However, some researchers found that the overexpression of SIRT1 alone cannot mimic the CR effect in transgenic mice, and the transcriptomic changes in various tissues were quite different or even opposite (Boutant et al., 2016). Such an opposite situation may explain that the genetic model and compound stimulation are not completely consistent. RSV as a potential metabolic syndrome treatment drug still needs large-scale population sample verification.

CONCLUSION

The very first mammalian histone deacetylase HDAC1 was cloned and isolated by Taunton et al. (1996), and 15,000 articles about HDACs have been published in the last 20 years. Currently, we know at least 18 HDAC proteins. They are responsible for eradicating epigenetic modifications, establishing an epigenetic off chromatin state, and regulating heritable gene expression (Yang and Seto, 2008; Haberland et al., 2009). In these processes, each HDACs may play a different role (**Table 1**). What kind of gene/protein is the specific downstream target of these HDACs? Is its enzyme activity related to intracellular localization and the formation of multi-protein complex? It is still one of the key and difficult issues in this field. Based on previous research experience, some techniques may be used to further experiments as follows: (1) HDACs interacting proteins/complex co-IP; (2) Protein-acetylation western; (3) Histone acetylation target gene ChIP; (4) High through put proteomics/acetylome with specific HDACs inhibitor, etc.

Histone deacetylases are potential therapeutic targets, and clinical drugs such as SAHA (Vorinostat) and FK228 (romidepsin) have been used for antitumor treatment (Bolden et al., 2006). However, they have two disadvantages: (1) great toxic and side effects and (2) difficulty in specific inhibition of HDACs activity. With the development of computer simulation technology and structural biology, it is believed that more specific HDACs inhibitors/activators can be constructed. And researches should attach importance to HDACs regulatory factors like PARP-1 when direct targeting on HDACs fails to show its effects. Further development of their inhibitors with more specificity, and trials for the treatment of metabolic diseases, may have great potential as well. Additionally, with the further development of biotechnology, some RNA therapies presented by AAV can specifically inhibit/overexpression of certain protein in skeletal muscles tissue, which may be able to target HDACs and treat related diseases (Wang et al., 2005; Long et al., 2016). However, its safety and effectiveness still need further clinical trials. Future research can discover known or unknown HDACs targeted drugs for the treatment of metabolic diseases.

AUTHOR CONTRIBUTIONS

HT, SL, and JR designed the literature search and wrote the review. JL, RW, and PC critically analyzed and revised the manuscript. All authors contributed to the article and approved the submitted version.

FUNDING

This work was supported by grants from the China Postdoctoral Science Foundation (2019M661042 to SL and 2019M651553 to HT) and National Natural Science Foundation of China (81501071 to SL).

REFERENCES

Anderson, J. G., Ramadori, G., Ioris, R. M., Galie, M., Berglund, E. D., Coate, K. C., et al. (2015). Enhanced insulin sensitivity in skeletal muscle and liver by physiological overexpression of SIRT6. *Mol. Metab.* 4, 846–856. doi: 10.1016/j.molmet.2015.09.003

Bai, P., Canto, C., Oudart, H., Brunyanszki, A., Cen, Y., Thomas, C., et al. (2011). PARP-1 inhibition increases mitochondrial metabolism through SIRT1 activation. *Cell Metab.* 13, 461–468. doi: 10.1016/j.cmet.2011.03.004

Balasubramanian, A., Kawahara, G., Gupta, V. A., Rozkalne, A., Beauvais, A., Kunkel, L. M., et al. (2014). Fam65b is important for formation of the HDAC6-dysferlin protein complex during

myogenic cell differentiation. *Faseb J.* 28, 2955–2969. doi: 10.1096/fj.13-246470

Beharry, A. W., Sandesara, P. B., Roberts, B. M., Ferreira, L. F., Senf, S. M., and Judge, A. R. (2014). HDAC1 activates FoxO and is both sufficient and required for skeletal muscle atrophy. *J. Cell Sci.* 127(Pt 7), 1441–1453. doi: 10.1242/jcs.136390

Bin, Y., Xiao, Y., Huang, D., Ma, Z., Liang, Y., Bai, J., et al. (2019). Theophylline inhibits cigarette smoke-induced inflammation in skeletal muscle by upregulating HDAC2 expression and decreasing NF-kappaB activation. *Am. J. Physiol. Lung. Cell Mol. Physiol.* 316, L197–L205. doi: 10.1152/ajplung.00005.2018

Bolden, J. E., Peart, M. J., and Johnstone, R. W. (2006). Anticancer activities of histone deacetylase inhibitors. *Nat. Rev. Drug. Discov.* 5, 769–784. doi: 10.1038/nrd2133

Boutant, M., Kulkarni, S. S., Joffraud, M., Raymond, F., Metairon, S., Descombes, P., et al. (2016). SIRT1 gain of function does not mimic or enhance the adaptations to intermittent fasting. *Cell Rep.* 14, 2068–2075. doi: 10.1016/j.celrep.2016.02.007

Boyle, K. E., Newsom, S. A., Janssen, R. C., Lappas, M., and Friedman, J. E. (2013). Skeletal muscle MnSOD, mitochondrial complex II, and SIRT3 enzyme activities are decreased in maternal obesity during human pregnancy and gestational diabetes mellitus. *J. Clin .Endocrino.l Metab.* 98, E1601–E1609. doi: 10.1210/jc.2013-1943

Canto, C., Gerhart-Hines, Z., Feige, J. N., Lagouge, M., Noriega, L., Milne, J. C., et al. (2009). AMPK regulates energy expenditure by modulating NAD+ metabolism and SIRT1 activity. *Nature* 458, 1056–1060. doi: 10.1038/nature07813

Cho, O. H., Mallappa, C., Hernandez-Hernandez, J. M., Rivera-Perez, J. A., and Imbalzano, A. N. (2015). Contrasting roles for MyoD in organizing myogenic promoter structures during embryonic skeletal muscle development. *Dev. Dyn.* 244, 43–55. doi: 10.1002/dvdy.24217

Choi, M. C., Ryu, S., Hao, R., Wang, B., Kapur, M., Fan, C. M., et al. (2014). HDAC4 promotes Pax7-dependent satellite cell activation and muscle regeneration. *EMBO Rep.* 15, 1175–1183. doi: 10.15252/embr.201439195

Cui, X., Yao, L., Yang, X., Gao, Y., Fang, F., Zhang, J., et al. (2017). SIRT6 regulates metabolic homeostasis in skeletal muscle through activation of AMPK. *Am. J. Physiol. Endocrinol. Metab.* 313, E493–E505. doi: 10.1152/ajpendo.00122.2017

Dittenhafer-Reed, K. E., Richards, A. L., Fan, J., Smallegan, M. J., Fotuhi Siahpirani, A., Kemmerer, Z. A., et al. (2015). SIRT3 mediates multi-tissue coupling for metabolic fuel switching. *Cell Metab.* 21, 637–646. doi: 10.1016/j.cmet.2015.03.007

Dressel, U., Bailey, P. J., Wang, S. C., Downes, M., Evans, R. M., and Muscat, G. E. (2001). A dynamic role for HDAC7 in MEF2-mediated muscle differentiation. *J. Biol. Chem.* 276, 17007–17013. doi: 10.1074/jbc.M101508200

Durnin, J. (1981). *Basal Metabolic Rate in Man. Report to FAO/ WHO/UNU.* Vol. 15, Rome: FAO. 507–524. doi: 10.1038/s41574-019-0230-6

Fernandez-Marcos, P. J., Jeninga, E. H., Canto, C., Harach, T., de Boer, V. C., Andreux, P., et al. (2012). Muscle or liver-specific Sirt3 deficiency induces hyperacetylation of mitochondrial proteins without affecting global metabolic homeostasis. *Sci. Rep.* 2:425. doi: 10.1038/srep00425

Fortuin, F. D., Morisaki, T., and Holmes, E. W. (1996). Subunit composition of AMPD varies in response to changes in AMPD1 and AMPD3 gene expression in skeletal muscle. *Proc. Assoc. Am. Physicians* 108, 329–333.

Galmozzi, A., Mitro, N., Ferrari, A., Gers, E., Gilardi, F., Godio, C., et al. (2013). Inhibition of class I histone deacetylases unveils a mitochondrial signature and enhances oxidative metabolism in skeletal muscle and adipose tissue. *Diabetes* 62, 732–742. doi: 10.2337/db12-0548

Gao, C., Liu, Y., Lam, M., and Kao, H. Y. (2010). Histone deacetylase 7 (HDAC7) regulates myocyte migration and differentiation. *Biochim. Biophys. Acta* 1803, 1186–1197. doi: 10.1016/j.bbamcr.2010.06.008

Gaur, V., Connor, T., Sanigorski, A., Martin, S. D., Bruce, C. R., Henstridge, D. C., et al. (2016). Disruption of the Class IIa HDAC corepressor complex increases energy expenditure and lipid oxidation. *Cell Rep.* 16, 2802–2810. doi: 10.1016/j.celrep.2016.08.005

Gomes, A. P., Price, N. L., Ling, A. J., Moslehi, J. J., Montgomery, M. K., Rajman, L., et al. (2013). Declining NAD(+) induces a pseudohypoxic state disrupting nuclear-mitochondrial communication during aging. *Cell* 155, 1624–1638. doi: 10.1016/j.cell.2013.11.037

Gong, Y., Cao, R., Ding, G., Hong, S., Zhou, W., Lu, W., et al. (2018). Integrated omics approaches to characterize a nuclear receptor corepressor-associated histone deacetylase in mouse skeletal muscle. *Mol. Cell. Endocrinol.* 471, 22–32. doi: 10.1016/j.mce.2017.05.024

Gregoire, S., Xiao, L., Nie, J., Zhang, X., Xu, M., Li, J., et al. (2007). Histone deacetylase 3 interacts with and deacetylates myocyte enhancer factor 2. *Mol. Cell Biol.* 27, 1280–1295. doi: 10.1128/mcb.00882-06

Guo, S., Huang, Y., Zhang, Y., Huang, H., Hong, S., and Liu, T. (2020). Impacts of exercise interventions on different diseases and organ functions in mice. *J. Sport Health Sci.* 9, 53–73. doi: 10.1016/j.jshs.2019.07.004

Gurd, B. J., Yoshida, Y., Lally, J., Holloway, G. P., and Bonen, A. (2009). The deacetylase enzyme SIRT1 is not associated with oxidative capacity in rat heart and skeletal muscle and its overexpression reduces mitochondrial biogenesis. *J. Physiol.* 587(Pt 8), 1817–1828. doi: 10.1113/jphysiol.2008.168096

Haberland, M., Montgomery, R. L., and Olson, E. N. (2009). The many roles of histone deacetylases in development and physiology: implications for disease and therapy. *Nat. Rev. Genet.* 10, 32–42. doi: 10.1038/nrg2485

Han, K. A., Kang, H. S., Lee, J. W., Yoo, L., Im, E., Hong, A., et al. (2014). Histone deacetylase 3 promotes RCAN1 stability and nuclear translocation. *PLoS One* 9:e105416. doi: 10.1371/journal.pone.0105416

Higashida, K., Kim, S. H., Jung, S. R., Asaka, M., Holloszy, J. O., and Han, D. H. (2013). Effects of resveratrol and SIRT1 on PGC-1alpha activity and mitochondrial biogenesis: a reevaluation. *PLoS Biol.* 11:e1001603. doi: 10.1371/journal.pbio.1001603

Hirschey, M. D., Shimazu, T., Jing, E., Grueter, C. A., Collins, A. M., Aouizerat, B., et al. (2011). SIRT3 deficiency and mitochondrial protein hyperacetylation accelerate the development of the metabolic syndrome. *Mol. Cell* 44, 177–190. doi: 10.1016/j.molcel.2011.07.019

Hong, S., Zhou, W., Fang, B., Lu, W., Loro, E., Damle, M., et al. (2017). Dissociation of muscle insulin sensitivity from exercise endurance in mice by HDAC3 depletion. *Nat. Med.* 23, 223–234. doi: 10.1038/nm.4245

Huang, S., Liu, S., Niu, Y., and Fu, L. (2019). Scriptaid/exercise-induced lysine acetylation is another type of posttranslational modification occurring in titin. *J. Appl. Physiol.* 128, 276–285. doi: 10.1152/japplphysiol.00617.2019

Imai, S., Armstrong, C. M., Kaeberlein, M., and Guarente, L. (2000). Transcriptional silencing and longevity protein Sir2 is an NAD-dependent histone deacetylase. *Nature* 403, 795–800. doi: 10.1038/35001622

Jing, E., O'Neill, B. T., Rardin, M. J., Kleinridders, A., Ilkeyeva, O. R., Ussar, S., et al. (2013). Sirt3 regulates metabolic flexibility of skeletal muscle through reversible enzymatic deacetylation. *Diabetes* 62, 3404–3417. doi: 10.2337/db12-1650

Kanfi, Y., Peshti, V., Gil, R., Naiman, S., Nahum, L., Levin, E., et al. (2010). SIRT6 protects against pathological damage caused by diet-induced obesity. *Aging Cell* 9, 162–173. doi: 10.1111/j.1474-9726.2009.00544.x

Karagianni, P., and Wong, J. (2007). HDAC3: taking the SMRT-N-CoRrect road to repression. *Oncogene* 26, 5439–5449. doi: 10.1038/sj.onc.1210612

Kong, X., Wang, R., Xue, Y., Liu, X., Zhang, H., Chen, Y., et al. (2010). Sirtuin 3, a new target of PGC-1alpha, plays an important role in the suppression of ROS and mitochondrial biogenesis. *PLoS One* 5:e11707. doi: 10.1371/journal.pone.0011707

Koves, T. R., Ussher, J. R., Noland, R. C., Slentz, D., Mosedale, M., Ilkayeva, O., et al. (2008). Mitochondrial overload and incomplete fatty acid oxidation contribute to skeletal muscle insulin resistance. *Cell Metab.* 7, 45–56. doi: 10.1016/j.cmet.2007.10.013

Lagouge, M., Argmann, C., Gerhart-Hines, Z., Meziane, H., Lerin, C., Daussin, F., et al. (2006). Resveratrol improves mitochondrial function and protects against metabolic disease by activating SIRT1 and PGC-1alpha. *Cell* 127, 1109–1122. doi: 10.1016/j.cell.2006.11.013

Lantier, L., Williams, A. S., Williams, I. M., Yang, K. K., Bracy, D. P., Goelzer, M., et al. (2015). SIRT3 is crucial for maintaining skeletal muscle insulin action and protects against severe insulin resistance in high-fat-fed mice. *Diabetes* 64, 3081–3092. doi: 10.2337/db14-1810

Laurent, G., German, N. J., Saha, A. K., de Boer, V. C., Davies, M., Koves, T. R., et al. (2013). SIRT4 coordinates the balance between lipid synthesis and catabolism by repressing malonyl CoA decarboxylase. *Mol. Cell* 50, 686–698. doi: 10.1016/j.molcel.2013.05.012

Lee, J. Y., Kapur, M., Li, M., Choi, M. C., Choi, S., Kim, H. J., et al. (2014). MFN1 deacetylation activates adaptive mitochondrial fusion and protects

metabolically challenged mitochondria. *J. Cell Sci.* 127(Pt 22), 4954–4963. doi: 10.1242/jcs.157321

Lee, S. W., Yang, J., Kim, S. Y., Jeong, H. K., Lee, J., Kim, W. J., et al. (2015). MicroRNA-26a induced by hypoxia targets HDAC6 in myogenic differentiation of embryonic stem cells. *Nucleic Acids Res.* 43, 2057–2073. doi: 10.1093/nar/gkv088

Lempradl, A., Pospisilik, J. A., and Penninger, J. M. (2015). Exploring the emerging complexity in transcriptional regulation of energy homeostasis. *Nat. Rev. Genet.* 16, 665–681. doi: 10.1038/nrg3941

Lin, S. J., Defossez, P. A., and Guarente, L. (2000). Requirement of NAD and SIR2 for life-span extension by calorie restriction in *Saccharomyces cerevisiae*. *Science* 289, 2126–2128. doi: 10.1126/science.289.5487.2126

Liu, S., Niu, Y., and Fu, L. (2020). Metabolic adaptations to exercise training. *J. Sci. Sport Exerc.* 2, 1–6. doi: 10.1007/s42978-019-0018-3

Long, C., Amoasii, L., Mireault, A. A., McAnally, J. R., Li, H., Sanchez-Ortiz, E., et al. (2016). Postnatal genome editing partially restores dystrophin expression in a mouse model of muscular dystrophy. *Science* 351, 400–403. doi: 10.1126/science.aad5725

Luan, X., Tian, X., Zhang, H., Huang, R., Li, N., Chen, P., et al. (2019). Exercise as a prescription for patients with various diseases. *J. Sport Health Sci.* 8, 422–441. doi: 10.1016/j.jshs.2019.04.002

Luo, L., Martin, S. C., Parkington, J., Cadena, S. M., Zhu, J., Ibebunjo, C., et al. (2019). HDAC4 controls muscle homeostasis through deacetylation of myosin heavy Chain, PGC-1alpha, and Hsc70. *Cell Rep.* 29, 749.e12–763.e12. doi: 10.1016/j.celrep.2019.09.023

Macpherson, P. C., Farshi, P., and Goldman, D. (2015). Dach2-Hdac9 signaling regulates reinnervation of muscle endplates. *Development* 142, 4038–4048. doi: 10.1242/dev.125674

Mal, A., Sturniolo, M., Schiltz, R. L., Ghosh, M. K., and Harter, M. L. (2001). A role for histone deacetylase HDAC1 in modulating the transcriptional activity of MyoD: inhibition of the myogenic program. *Embo J.* 20, 1739–1753. doi: 10.1093/emboj/20.7.1739

McGee, S. L., Fairlie, E., Garnham, A. P., and Hargreaves, M. (2009). Exercise-induced histone modifications in human skeletal muscle. *J. Physiol.* 587(Pt 24), 5951–5958. doi: 10.1113/jphysiol.2009.181065

McGee, S. L., and Hargreaves, M. (2010). Histone modifications and skeletal muscle metabolic gene expression. *Clin. Exp. Pharmacol. Physiol.* 37, 392–396. doi: 10.1111/j.1440-1681.2009.05311.x

McGee, S. L., and Hargreaves, M. (2011). Histone modifications and exercise adaptations. *J. Appl. Physiol.* 110, 258–263. doi: 10.1152/japplphysiol.00979.2010

McGee, S. L., van Denderen, B. J., Howlett, K. F., Mollica, J., Schertzer, J. D., Kemp, B. E., et al. (2008). AMP-activated protein kinase regulates GLUT4 transcription by phosphorylating histone deacetylase 5. *Diabetes* 57, 860–867. doi: 10.2337/db07-0843

McKinsey, T. A., Zhang, C. L., Lu, J., and Olson, E. N. (2000a). Signal-dependent nuclear export of a histone deacetylase regulates muscle differentiation. *Nature* 408, 106–111. doi: 10.1038/35040593

McKinsey, T. A., Zhang, C. L., and Olson, E. N. (2000b). Activation of the myocyte enhancer factor-2 transcription factor by calcium/calmodulin-dependent protein kinase-stimulated binding of 14-3-3 to histone deacetylase 5. *Proc. Natl. Acad. Sci. U.S.A.* 97, 14400–14405. doi: 10.1073/pnas.260501497

Meng, Z. X., Gong, J., Chen, Z., Sun, J., Xiao, Y., Wang, L., et al. (2017). Glucose sensing by skeletal myocytes couples nutrient signaling to systemic homeostasis. *Mol. Cell* 66, 332.e4–344.e4. doi: 10.1016/j.molcel.2017.04.007

Mizgier, M. L., Fernandez-Verdejo, R., Cherfan, J., Pinget, M., Bouzakri, K., and Galgani, J. E. (2019). Insights on the role of putative muscle-derived factors on pancreatic beta cell function. *Front. Physiol.* 10:1024. doi: 10.3389/fphys.2019.01024

Montgomery, R. L., Davis, C. A., Potthoff, M. J., Haberland, M., Fielitz, J., Qi, X., et al. (2007). Histone deacetylases 1 and 2 redundantly regulate cardiac morphogenesis, growth, and contractility. *Genes Dev.* 21, 1790–1802. doi: 10.1101/gad.1563807

Moresi, V., Carrer, M., Grueter, C. E., Rifki, O. F., Shelton, J. M., Richardson, J. A., et al. (2012). Histone deacetylases 1 and 2 regulate autophagy flux and skeletal muscle homeostasis in mice. *Proc. Natl. Acad. Sci. U.S.A.* 109, 1649–1654. doi: 10.1073/pnas.1121159109

Nasrin, N., Wu, X., Fortier, E., Feng, Y., Bare, O. C., Chen, S., et al. (2010). SIRT4 regulates fatty acid oxidation and mitochondrial gene expression in liver and muscle cells. *J. Biol. Chem.* 285, 31995–32002. doi: 10.1074/jbc.M110.124164

Niu, Y., Wang, T., Liu, S., Yuan, H., Li, H., and Fu, L. (2017). Exercise-induced GLUT4 transcription via inactivation of HDAC4/5 in mouse skeletal muscle in an AMPKalpha2-dependent manner. *Biochim. Biophys. Acta* 1863, 2372–2381. doi: 10.1016/j.bbadis.2017.07.001

Ohkawa, Y., Marfella, C. G., and Imbalzano, A. N. (2006). Skeletal muscle specification by myogenin and Mef2D via the SWI/SNF ATPase Brg1. *Embo J.* 25, 490–501. doi: 10.1038/sj.emboj.7600943

Pacholec, M., Bleasdale, J. E., Chrunyk, B., Cunningham, D., Flynn, D., Garofalo, R. S., et al. (2010). SRT1720, SRT2183, SRT1460, and resveratrol are not direct activators of SIRT1. *J. Biol. Chem.* 285, 8340–8351. doi: 10.1074/jbc.M109.088682

Pedersen, B. K., and Febbraio, M. A. (2012). Muscles, exercise and obesity: skeletal muscle as a secretory organ. *Nat. Rev. Endocrinol.* 8, 457–465. doi: 10.1038/nrendo.2012.49

Philp, A., Chen, A., Lan, D., Meyer, G. A., Murphy, A. N., Knapp, A. E., et al. (2011). Sirtuin 1 (SIRT1) deacetylase activity is not required for mitochondrial biogenesis or peroxisome proliferator-activated receptor-gamma coactivator-1alpha (PGC-1alpha) deacetylation following endurance exercise. *J. Biol. Chem.* 286, 30561–30570. doi: 10.1074/jbc.M111.261685

Pirinen, E., Canto, C., Jo, Y. S., Morato, L., Zhang, H., Menzies, K. J., et al. (2014). Pharmacological Inhibition of poly(ADP-ribose) polymerases improves fitness and mitochondrial function in skeletal muscle. *Cell Metab.* 19, 1034–1041. doi: 10.1016/j.cmet.2014.04.002

Potthoff, M. J., Wu, H., Arnold, M. A., Shelton, J. M., Backs, J., McAnally, J., et al. (2007). Histone deacetylase degradation and MEF2 activation promote the formation of slow-twitch myofibers. *J. Clin. Invest.* 117, 2459–2467. doi: 10.1172/jci31960

Puri, P. L., Iezzi, S., Stiegler, P., Chen, T. T., Schiltz, R. L., Muscat, G. E., et al. (2001). Class I histone deacetylases sequentially interact with MyoD and pRb during skeletal myogenesis. *Mol. Cell* 8, 885–897. doi: 10.1016/s1097-2765(01)00373-2

Ratti, F., Ramond, F., Moncollin, V., Simonet, T., Milan, G., Mejat, A., et al. (2015). Histone deacetylase 6 is a FoxO transcription factor-dependent effector in skeletal muscle atrophy. *J. Biol. Chem.* 290, 4215–4224. doi: 10.1074/jbc.M114.600916

Robin, J. D., Jacome Burbano, M. S., Peng, H., Croce, O., Thomas, J. L., Laberthonniere, C., et al. (2020). Mitochondrial function in skeletal myofibers is controlled by a TRF2-SIRT3 axis over lifetime. *Aging Cell* 19:e13097. doi: 10.1111/acel.13097

Rodgers, J. T., Lerin, C., Haas, W., Gygi, S. P., Spiegelman, B. M., and Puigserver, P. (2005). Nutrient control of glucose homeostasis through a complex of PGC-1alpha and SIRT1. *Nature* 434, 113–118. doi: 10.1038/nature03354

Ryall, J. G., Dell'Orso, S., Derfoul, A., Juan, A., Zare, H., Feng, X., et al. (2015). The NAD(+)-dependent SIRT1 deacetylase translates a metabolic switch into regulatory epigenetics in skeletal muscle stem cells. *Cell Stem Cell* 16, 171–183. doi: 10.1016/j.stem.2014.12.004

Samant, S. A., Kanwal, A., Pillai, V. B., and Bao, R. (2017). The histone deacetylase SIRT6 blocks myostatin expression and development of muscle atrophy. *Sci. Rep.* 7:11877. doi: 10.1038/s41598-017-10838-5

Schenk, S., McCurdy, C. E., Philp, A., Chen, M. Z., Holliday, M. J., Bandyopadhyay, G. K., et al. (2011). Sirt1 enhances skeletal muscle insulin sensitivity in mice during caloric restriction. *J. Clin. Invest.* 121, 4281–4288. doi: 10.1172/jci58554

Seto, E., and Yoshida, M. (2014). Erasers of histone acetylation: the histone deacetylase enzymes. *Cold Spring Harb. Perspect. Biol.* 6:a018713. doi: 10.1101/cshperspect.a018713

Shahbazian, M. D., and Grunstein, M. (2007). Functions of site-specific histone acetylation and deacetylation. *Annu. Rev. Biochem.* 76, 75–100. doi: 10.1146/annurev.biochem.76.052705.162114

Song, S., Wen, Y., Tong, H., Loro, E., Gong, Y., Liu, J., et al. (2019). The HDAC3 enzymatic activity regulates skeletal muscle fuel metabolism. *J. Mol. Cell Biol.* 11, 133–143. doi: 10.1093/jmcb/mjy066

Stefanowicz, M., Nikolajuk, A., Matulewicz, N., and Karczewska-Kupczewska, M. (2018). Adipose tissue, but not skeletal muscle, sirtuin 1 expression is decreased in obesity and related to insulin sensitivity. *Endocrine* 60, 263–271. doi: 10.1007/s12020-018-1544-1

Sun, Z., Feng, D., Fang, B., Mullican, S. E., You, S. H., Lim, H. W., et al. (2013). Deacetylase-independent function of HDAC3 in transcription and metabolism requires nuclear receptor corepressor. *Mol. Cell.* 52, 769–782. doi: 10.1016/j.molcel.2013.10.022

Suwa, M., Nakano, H., Radak, Z., and Kumagai, S. (2008). Endurance exercise increases the SIRT1 and peroxisome proliferator-activated receptor gamma coactivator-1alpha protein expressions in rat skeletal muscle. *Metabolism* 57, 986–998. doi: 10.1016/j.metabol.2008.02.017

Svensson, K., Tahvilian, S., Martins, V. F., Dent, J. R., Lemanek, A., Barooni, N., et al. (2020). Combined overexpression of SIRT1 and knockout of GCN5 in adult skeletal muscle does not affect glucose homeostasis or exercise performance in mice. *Am. J. Physiol. Endocrinol. Metab.* 318, E145–E151. doi: 10.1152/ajpendo.00370.2019

Taunton, J., Hassig, C. A., and Schreiber, S. L. (1996). A mammalian histone deacetylase related to the yeast transcriptional regulator Rpd3p. *Science* 272, 408–411. doi: 10.1126/science.272.5260.408

Taylor, M. V., and Hughes, S. M. (2017). Mef2 and the skeletal muscle differentiation program. *Semin. Cell Dev. Biol.* 72, 33–44. doi: 10.1016/j.semcdb.2017.11.020

Timmers, S., Konings, E., Bilet, L., Houtkooper, R. H., van de Weijer, T., Goossens, G. H., et al. (2011). Calorie restriction-like effects of 30 days of resveratrol supplementation on energy metabolism and metabolic profile in obese humans. *Cell Metab.* 14, 612–622. doi: 10.1016/j.cmet.2011.10.002

Vargas-Ortiz, K., Perez-Vazquez, V., and Macias-Cervantes, M. H. (2019). Exercise and sirtuins: a way to mitochondrial health in skeletal muscle. *Int. J. Mol. Sci.* 20:2717. doi: 10.3390/ijms20112717

Vila, L., Elias, I., Roca, C., Ribera, A., Ferre, T., Casellas, A., et al. (2014). AAV8-mediated Sirt1 gene transfer to the liver prevents high carbohydrate diet-induced nonalcoholic fatty liver disease. *Mol. Ther. Methods Clin. Dev.* 1:14039. doi: 10.1038/mtm.2014.39

Vila, L., Roca, C., Elias, I., Casellas, A., Lage, R., Franckhauser, S., et al. (2016). AAV-mediated Sirt1 overexpression in skeletal muscle activates oxidative capacity but does not prevent insulin resistance. *Mol. Ther. Methods Clin. Dev.* 5:16072. doi: 10.1038/mtm.2016.72

Wang, Z., Zhu, T., Qiao, C., Zhou, L., Wang, B., Zhang, J., et al. (2005). Adeno-associated virus serotype 8 efficiently delivers genes to muscle and heart. *Nat. Biotechnol.* 23, 321–328. doi: 10.1038/nbt1073

White, A. T., McCurdy, C. E., Philp, A., Hamilton, D. L., Johnson, C. D., and Schenk, S. (2013). Skeletal muscle-specific overexpression of SIRT1 does not enhance whole-body energy expenditure or insulin sensitivity in young mice. *Diabetologia* 56, 1629–1637. doi: 10.1007/s00125-013-2912-2

White, A. T., and Schenk, S. (2012). NAD(+)/NADH and skeletal muscle mitochondrial adaptations to exercise. *Am. J. Physiol. Endocrinol. Metab.* 303, E308–E321. doi: 10.1152/ajpendo.00054.2012

Williams, A. S., Koves, T. R., Davidson, M. T., Crown, S. B., Fisher-Wellman, K. H., Torres, M. J., et al. (2020). Disruption of acetyl-lysine turnover in muscle mitochondria promotes insulin resistance and redox stress without overt respiratory dysfunction. *Cell Metab.* 31, 131.e11–147.e11. doi: 10.1016/j.cmet.2019.11.003

Xiao, C., Kim, H. S., Lahusen, T., Wang, R. H., Xu, X., Gavrilova, O., et al. (2010). SIRT6 deficiency results in severe hypoglycemia by enhancing both basal and insulin-stimulated glucose uptake in mice. *J. Biol. Chem.* 285, 36776–36784. doi: 10.1074/jbc.M110.168039

Xie, M., Kong, Y., Tan, W., May, H., Battiprolu, P. K., Pedrozo, Z., et al. (2014). Histone deacetylase inhibition blunts ischemia/reperfusion injury by inducing cardiomyocyte autophagy. *Circulation* 129, 1139–1151. doi: 10.1161/circulationaha.113.002416

Yang, X. J., and Seto, E. (2008). The Rpd3/Hda1 family of lysine deacetylases: from bacteria and yeast to mice and men. *Nat. Rev. Mol. Cell Biol.* 9, 206–218. doi: 10.1038/nrm2346

Yuan, H., Niu, Y., Liu, X., and Fu, L. (2014). Exercise increases the binding of MEF2A to the Cpt1b promoter in mouse skeletal muscle. *Acta Physiol.* 212, 283–292. doi: 10.1111/apha.12395

Zhang, Y., and Ren, J. (2014). Targeting autophagy for the therapeutic application of histone deacetylase inhibitors in ischemia/reperfusion heart injury. *Circulation* 129, 1088–1091. doi: 10.1161/circulationaha.113.008115

Zhang, Z., Zhang, L., Zhou, Y., Li, L., Zhao, J., Qin, W., et al. (2019). Increase in HDAC9 suppresses myoblast differentiation via epigenetic regulation of autophagy in hypoxia. *Cell Death Dis.* 10:552. doi: 10.1038/s41419-019-1763-2

Zhu, B., Zhang, M., Williams, E. M., Keller, C., Mansoor, A., and Davie, J. K. (2016). TBX2 represses PTEN in rhabdomyosarcoma and skeletal muscle. *Oncogene* 35, 4212–4224. doi: 10.1038/onc.2015.486

Conflict of Interest: The authors declare that the research was conducted in the absence of any commercial or financial relationships that could be construed as a potential conflict of interest.

Copyright © 2020 Tian, Liu, Ren, Lee, Wang and Chen. This is an open-access article distributed under the terms of the Creative Commons Attribution License (CC BY). The use, distribution or reproduction in other forums is permitted, provided the original author(s) and the copyright owner(s) are credited and that the original publication in this journal is cited, in accordance with accepted academic practice. No use, distribution or reproduction is permitted which does not comply with these terms.

frontiers in Physiology

ORIGINAL RESEARCH
published: 25 August 2020
doi: 10.3389/fphys.2020.01082

SHANK3 Co-ordinately Regulates Autophagy and Apoptosis in Myocardial Infarction

Wanrong Man[1†], Jing Gu[2†], Bo Wang[1†], Mingming Zhang[3], Jianqiang Hu[3], Jie Lin[1], Dong Sun[1], Zhenyu Xiong[1], Xiaoming Gu[4], Kaikai Hao[1], Baolin Guo[1], Gaoli Wei[1], Liang Zhang[1], Rui Song[1], Congye Li[1], Haichang Wang[5] and Dongdong Sun[1]**

[1] Department of Cardiology, Xijing Hospital, Fourth Military Medical University, Xi'an, China, [2] School of Basic Medicine, Fourth Military Medical University, Xi'an, China, [3] Department of Cardiology, Tangdu Hospital, Fourth Military Medical University, Xi'an, China, [4] Department of Physiology and Pathophysiology, Fourth Military Medical University, Xi'an, China, [5] Heart Hospital, Xi'an International Medical Center, Xi'an, China

OPEN ACCESS

Edited by:
Ying Mei Zhang,
Zhongshan Hospital, Fudan University, China

Reviewed by:
Xiang Cheng,
Huazhong University of Science and Technology, China
Mariann Gyöngyösi,
Medical University of Vienna, Austria
Ding Ai,
Tianjin Medical University, China

***Correspondence:**
Haichang Wang
wanghc@nwu.edu.cn
Dongdong Sun
wintersun3@gmail.com;
51483696@qq.com

[†] These authors have contributed equally to this work

Specialty section:
This article was submitted to Clinical and Translational Physiology, a section of the journal Frontiers in Physiology

Received: 20 May 2020
Accepted: 06 August 2020
Published: 25 August 2020

Citation:
Man W, Gu J, Wang B, Zhang M, Hu J, Lin J, Sun D, Xiong Z, Gu X, Hao K, Guo B, Wei G, Zhang L, Song R, Li C, Wang H and Sun D (2020) SHANK3 Co-ordinately Regulates Autophagy and Apoptosis in Myocardial Infarction. Front. Physiol. 11:1082. doi: 10.3389/fphys.2020.01082

Cardiac remodeling and dysfunction are responsible for the high mortality after myocardial infarction (MI). We assessed the potential for Shank3 to alleviate the post-infarction cardiac dysfunction. The experimental MI mice model was constructed by left anterior descending coronary artery ligation. Shank3 knockout aggravated cardiac dysfunction after MI, while Shank3 overexpression alleviated it. The histological examination showed that the infarct size was significantly increased in the acute phase of MI in the Shank3 knockout group, and the cardiac dysfunction of the Shank3 knockout group was even more severe than the Shank3 overexpression group, revealed by echocardiography analyses. *In vitro*, cultured neonatal cardiomyocytes were subjected to simulated MI. Shank3 downregulation curbed LC3 expression and autophagosome-lysosome fusion. Furthermore, Shank3 downregulation increased cardiomyocyte apoptosis. In contrast, Shank3 upregulation induced autophagy, and inhibited apoptosis under hypoxia. *In vivo*, western blot analysis showed decreased levels of Atg7, Beclin1, LC3-II, and Bcl-2 as well as increased expression of p62, cleaved caspase-3, and cleaved caspase-9 in the Shank3 knockout group which suffered from MI. On the other hand, it also revealed that Shank3 overexpression induced autophagy and inhibited apoptosis after MI. Shank3 may serve as a new target for improving cardiac function after MI by inducing autophagy while inhibiting apoptosis.

Keywords: SH3 and multiple ankyrin repeat domains 3, myocardial infarction, autophagy, apoptosis, cardiomyocytes

INTRODUCTION

Globally, myocardial infarction (MI) remains a big challenge (Likosky et al., 2018). Cardiac remodeling and progressive heart failure after MI have been a major cause of mortality (Arnold et al., 2014; Bucholz et al., 2016). Although many interventions have been reported to alleviate cardiac remodeling and dysfunction in animal models, the vast majority of them has proved clinically less effective against MI injury. Cardiac remodeling after MI is a complex process involving various mechanisms contributing to cardiac structural and functional injury (Prabhu and Frangogiannis, 2016; Gibb and Hill, 2018). Autophagy is a physiological and regulated process

in which a cell removes unnecessary or dysfunctional components via the lysosomal degradative pathway (Shirakabe et al., 2016a; Del Re et al., 2019; Wu et al., 2019). In response to MI, increased levels of autophagy can also promote cell survival (Shirakabe et al., 2016b; Sciarretta et al., 2018a). Uncontrolled apoptosis can worsen cardiac function after ischemia and hypoxia (Frangogiannis, 2015). Hence, the regulation of autophagy and apoptosis is essential for the restoration of cardiac function.

Shank proteins are post-synaptic scaffold proteins, which are crucial for proper synaptic development and function (Monteiro and Feng, 2017). The Shank3 gene is located on mouse chromosome 15E3 (human: 22q13.3) and spans 60 kilobases of genomic DNA (Monteiro and Feng, 2017). SHANK3 (or ProSAP2) regulates the synaptic formation, development, and plasticity (Mossa et al., 2018). Phelan–McDermid syndrome (PMS) symptoms such as autistic-like behaviors, hypotonia and delayed or absent speech are due to SHANK3 haploinsufficiency (Monteiro and Feng, 2017). The expression of Shank3 vary in different organs of rodents. It is highly expressed in the brain, heart and spleen (Lim et al., 1999). Shank3 has been reported to regulate autophagy, apoptosis, proliferation, and development (Grasselli et al., 2020). However, the role of Shank3 in post-infarction cardiac remodeling is not well understood. In this study, we constructed Shank3 knockout and transgenic mice to recapitulate MI pathogenesis and assessed the restoration of cardiac function after MI.

Our study revealed a novel molecular, Shank3, participated in MI pathology and identified Shank3 as a potential therapeutic target against MI injury.

MATERIALS AND METHODS

Genetically Modified Mice

Shank3 knockout (Shank3$^{-/-}$) and Shank3 transgenic (Tg-Shank3) mice were generated on the C57BL/6 background by K&D gene technology (Wuhan, China). Animals were genotyped by real-time PCR. Age-matched male mice (6–8 weeks, 20–25 *g*) were used in all animal experiments. The experimenters were blind to group assignment and outcome assessment. All mice procedures were performed in compliance with the Guide for the Care and Use of Laboratory Animals and the Guidelines for the Welfare of Experimental Animals issued by Ethics Committee on Animal Care of the Fourth Military Medical University.

The mice were randomly allocated into the following groups with n = 30 each: (1) wild-type (WT); (2) Shank3$^{-/-}$; (3) MI; (4) MI + Shank3$^{-/-}$; (5) non-transgenic mice (NTg); (6) Tg-Shank3; (7) MI + NTg; and (8) MI + Tg-Shank3.

Myocardial Infarction Surgical Procedures

The surgical procedures were carried out under anesthesia which was induced by 2% isoflurane inhalation. A left thoracotomy was performed at the level of the fifth intercostal space to expose the heart. The left anterior descending branch (LAD) of the coronary artery 2–3 mm from its origin was ligated permanently by a knot made around with a 6–0 silk suture. The heart was rapidly pushed back into the chest, and then the muscles were reclosed. The type of skin sutures was 5–0 nylon. Sham-operated animals received the same surgical procedures without LAD ligation. The mice recovered in a cage with the temperature maintained at 37°C under humane care. The survival status of each group after surgery was shown in the **Supplementary Material**. Myocardial death was evaluated by 2,3,5-triphenyltetrazolium chloride (TTC) staining (n = 4–7/group). For detailed procedures, please refer to the previous description (Gao et al., 2010; Valentin et al., 2016).

Echocardiography

After 28 days of MI, M-mode Echocardiography was conducted with the aid of an echocardiography system with a 15-MHz linear transducer (Visual Sonics Vevo 2100, Toronto, ON, Canada) (n = 4–8/group). Left ventricular end-diastolic diameter (LVEDD) and left ventricular end-systolic diameter (LVESD) were measured. Left ventricular ejection fraction (LVEF) and left ventricular fraction shortening (LVFS) were calculated by computer algorithms.

Immunoblotting

The following antibodies were used: Shank3 (#ab93607, Abcam), Beclin1 (#ab62472, Abcam), p62 (#ab91526, Abcam), cleaved caspase-3 (#ab2302, Abcam), cleaved caspase-9 (#a0281, ABclonal), Bax (#a19684, ABclonal), Bcl-2 (#a19693, Abclonal), LC3A/B (#12741S, CST), Atg7 (#67341-1-Ig, Proteintech); and the secondary antibodies (anti-mouse/rabbit IgG) conjugated with horseradish peroxidase. Details of the immunoblotting procedure were described previously (Hu et al., 2016).

Primary Neonatal Cardiomyocytes Culture

Primary cultures of cardiomyocytes were prepared from 1-day-old non-transgenic mice. Cells were cultured in DMEM supplemented with 10% fetal bovine serum (Hyclone SV30087.02, Logan, UT, United States) and 1% penicillin/streptomycin and maintained at 37°C in 5% CO^2 as previously described (Hu et al., 2016).

Construction and Transduction of Adenoviruses

Adenovirus encoding HBAD-mRFP-GFP-LC3 was purchased from Hanbio Technology Ltd. (Shanghai, China). Adenoviruses expressing a short hairpin (sh) RNA directed against Shank3 (Ad-sh-Shank3), and harboring Shank3 (Ad-Shank3) and control vectors (Ad-LacZ, Ad-sh-LacZ) were purchased from Hanbio Technology Ltd. (Shanghai, China). The titers of adenoviruses were 1×10^{10} PFU/ml. The multiplicity of infection used was 80:1. The shRNA sequence targeting mouse Shank3 was GACCACTGATGAGAATGGTTGGCAA.

Adenoviruses about Shank3 (Ad-sh-Shank3, Ad-Shank3, Ad-LacZ, and Ad-sh-LacZ) were transduced 24 h after the transduction of HBAD-mRFP-GFP-LC3. After 24 h, the

cardiomyocytes were treated with hypoxia for 8 h as previously described (Hu et al., 2016).

Detection of GFP-LC3 and Aggresomes

Fluorescence detection of GFP-LC3, autophagolysosomes (APL), and autophagosomes were observed under the Olympus (Japan) FV1000 laser confocal microscope as previously described (Hu et al., 2016).

Determination of Cardiomyocytes Apoptosis

Apoptosis was detected by the Cell Death Detection kit (Roche) after hypoxia for 8 hs as previously described (Hu et al., 2016). Olympus FV1000 laser confocal microscope was used. Apoptotic index = the number of TUNEL-positive cardiomyocytes/the total number of cardiomyocytes.

Hypoxia

Cardiomyocytes were transferred into an ischemic buffer and simulated ischemia was performed in a humidified cell culture incubator (5% O^2, 95% CO^2, 37°C) for 8 h.

Public Data and Statistical Analysis

To analyze gene expression, public repository data were employed such as BioGPS[1], NCBI Gene Expression Omnibus (GEO) profiles[2], and GeneNetwork (a free scientific web resource)[3]. Firstly, we visited BioGPS's homepage and searched for the target gene. Secondly, we selected the species of the mouse. Then we read the gene report and downloaded the raw data. Finally, we used R language software to analyze the original data and export figures. R language source code was provided in the **Supplementary Material**.

Statistical analyses were conducted with the aid of GraphPad Prism 7 (GraphPad Software, La Jolla, CA, United States). Data visualization was done using R (version 3.3.2, The R Foundation for Statistical Computing ISBN 3-900051-07-0). Statistical analyses of differences between groups were done by Student's *t* test, one-way ANOVA with a Fisher's *post hoc* comparison test or two-way ANOVA with multiple *post hoc* comparisons. Significant values were defined as $p < 0.05$.

RESULTS

Shank3 Alleviates Experimental MI Cardiac Injury

In line with the BioGPS profiles, NCBI GEO profiles also demonstrated that Shank3 expression existed in the heart of the mouse (**Figure 1I** and **Supplementary Material**). To gain insight into the function of Shank3 in MI cardiac injury, loss-of-function and gain-of-function approaches were used in the MI mice model. We first evaluated the final MI 1-day post-MI. Histological examination demonstrated a significantly increased infarct size in Shank3 KO mice in comparison to WT group after MI, but the infarct size of Shank3 TG group was smaller than NTg group (**Figures 1A–C**). No infarction was observed in sham-operated groups.

Then, echocardiography analyses were employed to evaluate the heart function. Four weeks of permanent coronary ligation caused severe cardiac dysfunction as evidenced by decreased LVEF, and LVFS with increased LVEDD and LVESD (**Figures 1D–H**). But LVEF and LVFS were significantly lower in the MI + Shank3$^{-/-}$ group compared with the MI group (**Figures 1E,F**). Shank3 knockout significantly promoted the increase in LVESD and LVEDD caused by MI (**Figures 1G,H**).

Shank3 Knockout Inhibits Autophagy and Autophagosome-Lysosome Fusion

Western blot analysis showed decreased Atg7, Beclin1, and LC3-II protein levels in the hypoxia group as compared with the control group. Besides, there was a significantly elevated level of p62 expression in the Shank3$^{-/-}$ group compared with the control group (**Figures 2A–F**).

In cardiomyocytes transduced with HBAD-mRFP-GFP-LC3, Ad-sh-Shank3 transfection decreased green puncta number as compared with the control group under normal or hypoxia condition (**Figure 2G**). Under hypoxia, Ad-sh-Shank3 transfection significantly decreased autophagosome-lysosome fusion (**Figures 2G–J**). There was a significant increase in SHANK3 after hypoxia culture and a significant decrease after Ad-sh-Shank3 transfection as evaluated by western blotting (**Figures 2H,I**).

Shank3 Knockout Induces Cardiomyocytes Apoptosis

Levels of cleaved caspase-3 and cleaved caspase-9 were upregulated by Shank3 knockout in the MI + Shank3$^{-/-}$ group (**Figures 3A–C**). Bcl-2 protein levels decreased after MI, but the levels of Bax showed no evident change (**Figures 3A–E**).

Concomitantly, photomicrograph images showed that TUNEL-positive cardiomyocytes were more abundant in the hypoxia groups than in the control groups; this effect was notable by Shank3 knockout (**Figures 3F,G**).

Shank3 Overexpression Induces Autophagy

In the hypoxia group, western blot analysis showed significantly increased Shank3, Atg7, Beclin1, and LC3-II protein levels as compared with the control group (**Figures 4A–F**). Meanwhile, the p62 expression of MI + Tg-Shank3 was lower than the control group (**Figures 4A–C**).

To investigate whether SHANK3 enhanced autophagy, we transduced the neonatal mice cardiomyocytes with adenoviruses harboring Shank3 (Ad-Shank3) and LacZ (Ad-LacZ). In cardiomyocytes transduced with HBAD-mRFP-GFP-LC3, Shank3 overexpression significantly increased the number of green puncta when compared with the control group under both normal and hypoxia conditions (**Figures 4G–J**). When

[1]http://biogps.org/

[2]http://www.ncbi.nlm.nih.gov/geoprofiles

[3]http://www.genenetwork.org/

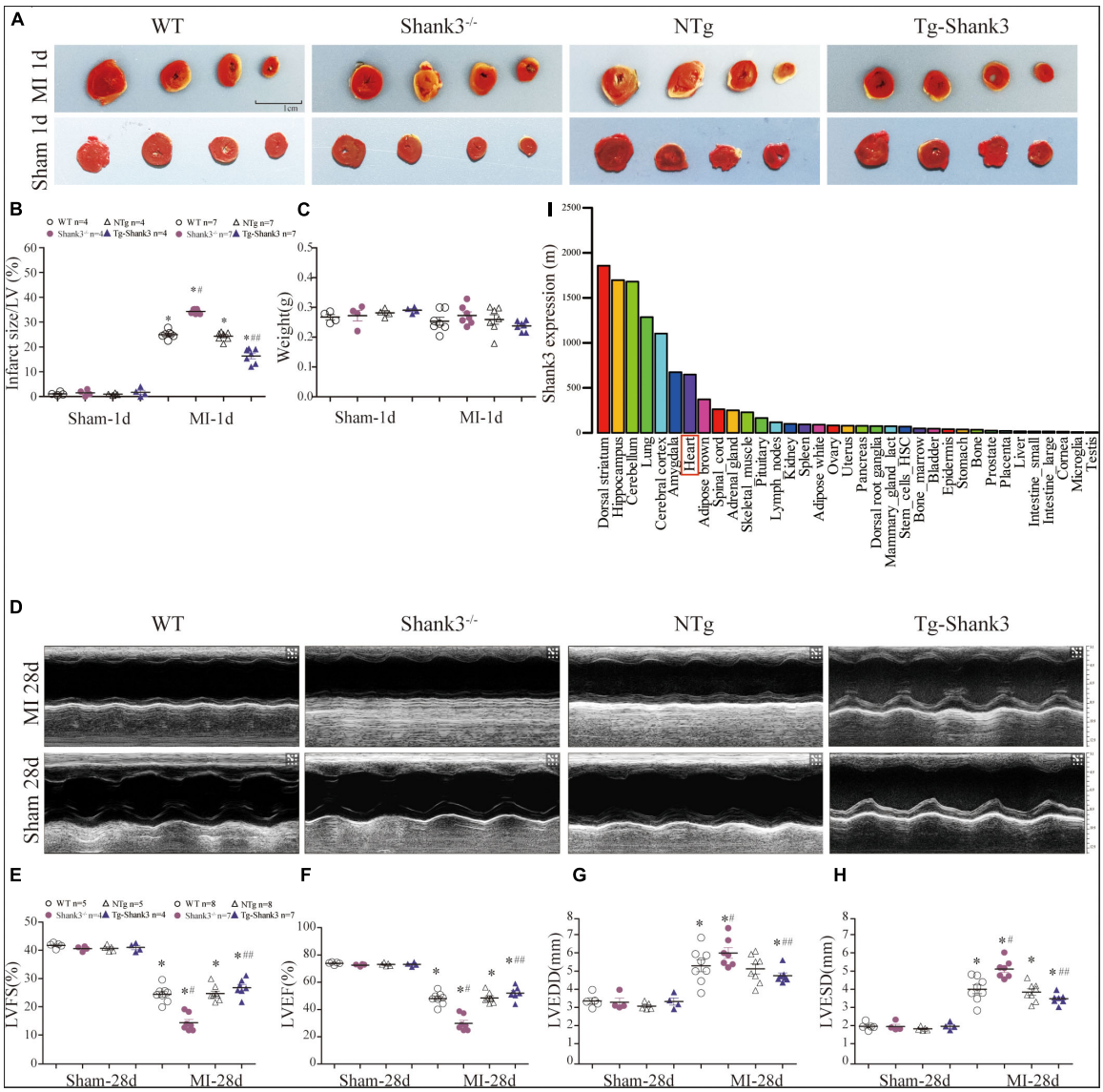

FIGURE 1 | Shank3 alleviates experimental MI cardiac injury. WT, Shank3 KO, and Shank3 TG mice were subjected to sham or MI injury (ischemia 1 day or 28 days). **(A)** Representative photographs of triphenyltetrazolium chloride (TTC) staining in WT, Shank3 KO, and Shank3 TG hearts; **(B)** Quantification of TTC-stained infarct; **(C)** weight of heart; **(D)** Representative echocardiographic images at 4 weeks after MI; **(E–H)** Measurements of LVFS, LVEF, LVEDD, and LVESD; **(I)** Protein differential expression in normal mice tissues for Shank3 Gene. *$p < 0.05$ vs. sham-operation control; #$p < 0.05$ vs. MI + WT; ##$p < 0.05$ vs. MI + NTg (n = 4–8/group). Data are means and SEM. LVFS, left ventricular fraction shortening; LVEF, left ventricular ejection fraction; LVESD, left ventricular end-systolic diameter; and LVEDD, Left ventricular end-diastolic diameter.

cardiomyocytes underwent hypoxic preconditioning, the autophagosome-lysosome fusion and the level of intracellular autophagy increased significantly (**Figures 4G–J**).

Shank3 Overexpression Inhibits Cardiomyocytes Apoptosis

Protein levels of cleaved caspase-3 and cleaved caspase-9 were increased after MI injury, but western blot analysis revealed a downward trend in Shank3 overexpressing transgenic mice (**Figures 5A–C**). The level of Bcl-2 significantly increased in MI + Tg-Shank3 (**Figures 5A–E**).

Furthermore, representative TUNEL images also demonstrated that Shank3 overexpression resulted in a decrease in the ratio of apoptotic cardiomyocytes cultured under hypoxia (**Figures 5F,G**).

DISCUSSION

SHANK proteins are a family of scaffold proteins organizing the postsynaptic density of excitatory synapses and are indispensable for normal brain function. Several studies

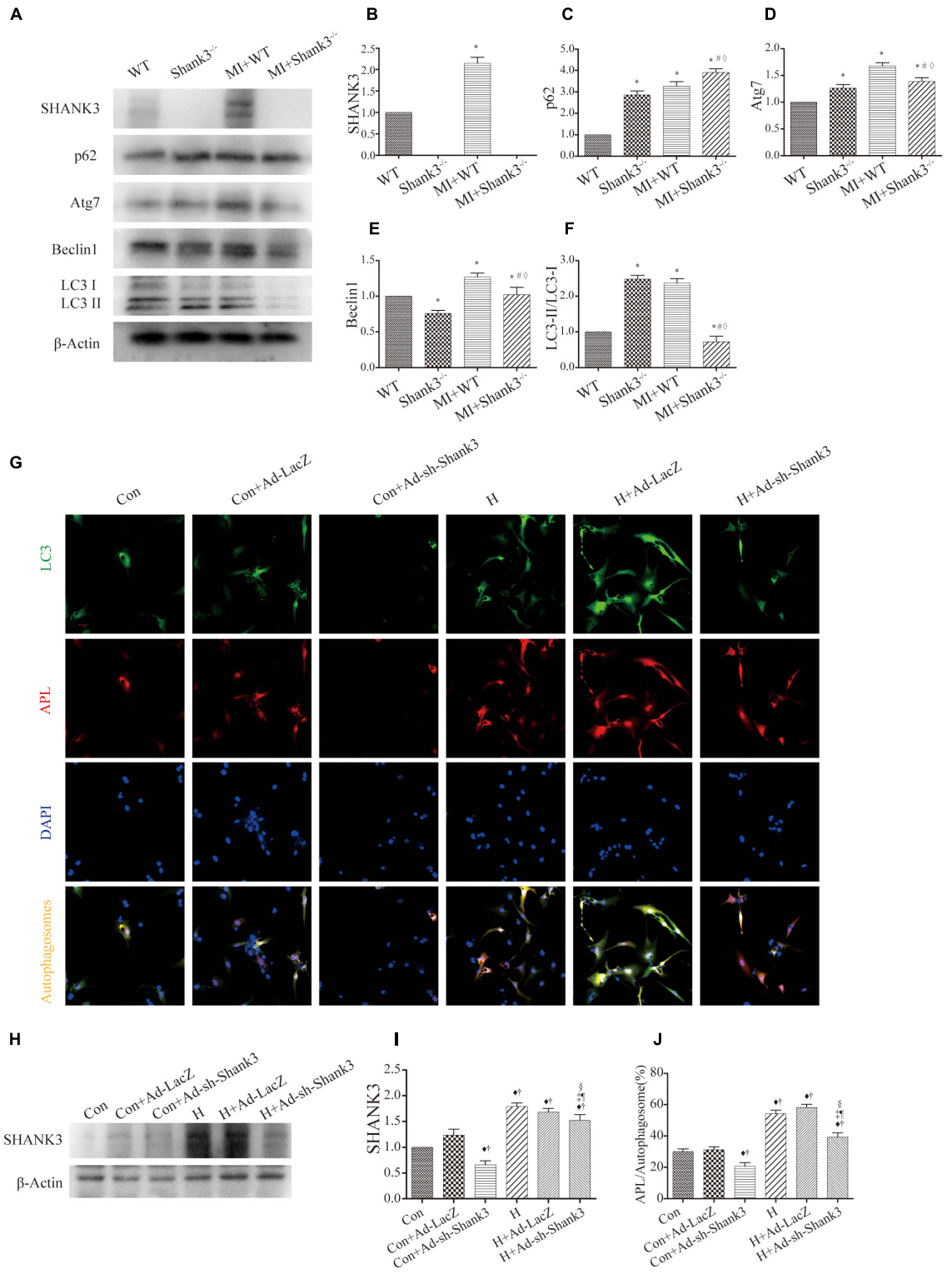

FIGURE 2 | Shank3 knockout inhibits autophagy and autophagosome-lysosome fusion in cardiomyocytes. **(A–F)** Immunoblots and quantitative analyses of SHANK3, p62, Atg7, Beclin1, LC3-II/LC3-I, and β-actin *in vivo*. [n = 4–8/group; **(G)**] Shank3 knockout decreased the numbers of red and green puncta in cardiomyocytes transduced with Ad-GFP-mRFP-LC3 after hypoxia. Immunofluorescence staining for LC3 (green), autophagolysosomes (APL, red), DAPI (blue), and autophagosomes (orange). **(H,I)** Immunoblots and quantitative analyses of SHANK3 *in vitro*. **(J)** Quantitative analyses of APL/autophagosomes. *$p < 0.05$ vs. WT; #$p < 0.05$ vs. MI + WT; ◊$p < 0.05$ vs. Shank3$^{-/-}$; ♦$p < 0.05$ vs. Con; †$p < 0.05$ vs. Con + Ad-LacZ; ‡$p < 0.05$ vs. Con + Ad-sh-Shank3; §$p < 0.05$ vs. H; ¶$p < 0.05$ vs. H + Ad-LacZ. Con, control and H, hypoxia.

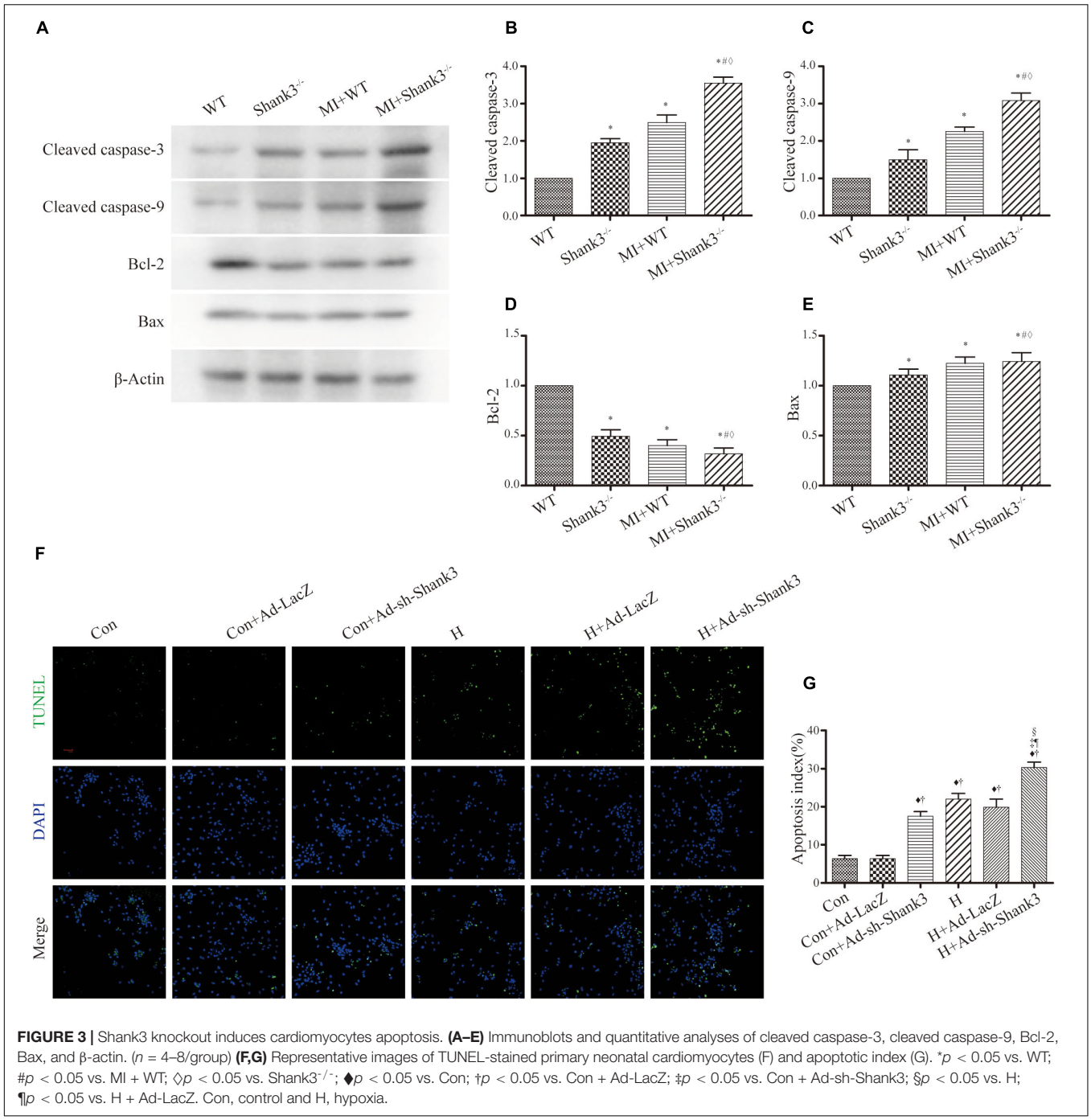

FIGURE 3 | Shank3 knockout induces cardiomyocytes apoptosis. **(A–E)** Immunoblots and quantitative analyses of cleaved caspase-3, cleaved caspase-9, Bcl-2, Bax, and β-actin. (n = 4–8/group) **(F,G)** Representative images of TUNEL-stained primary neonatal cardiomyocytes (F) and apoptotic index (G). *$p < 0.05$ vs. WT; #$p < 0.05$ vs. MI + WT; ◊$p < 0.05$ vs. Shank3$^{-/-}$; ♦$p < 0.05$ vs. Con; †$p < 0.05$ vs. Con + Ad-LacZ; ‡$p < 0.05$ vs. Con + Ad-sh-Shank3; §$p < 0.05$ vs. H; ¶$p < 0.05$ vs. H + Ad-LacZ. Con, control and H, hypoxia.

show that SHANK3 is responsible for autism spectrum disorders (ASDs), intellectual disability (ID), and schizophrenia (Durand et al., 2007; Moessner et al., 2007; Leblond et al., 2014). Recent research shows that Shank3 also plays an important role in metabolism and mitochondria function (Lee et al., 2017; Grasselli et al., 2020). *In vivo*, the metabolism of the heart and nervous system is relatively active, and both are more sensitive to hypoxia injury. We found that the expression level of Shank3 in the heart is only second to that in the nervous system through bioinformatics analysis (**Figure 1I** and ESM). Thus, we hypothesized that Shank3 may also play an essential role in the process of cardiac ischemia and hypoxia.

To investigate whether the Shank3 deficit affects cardiac function after MI, we used Shank3 knockout and transgenic mice to establish the experimental mouse model of MI.

Interestingly, we observed that Shank3 knockout in the experimental mouse model exacerbated the area of MI and cardiac function. However, the overexpression of Shank3 showed potential protection.

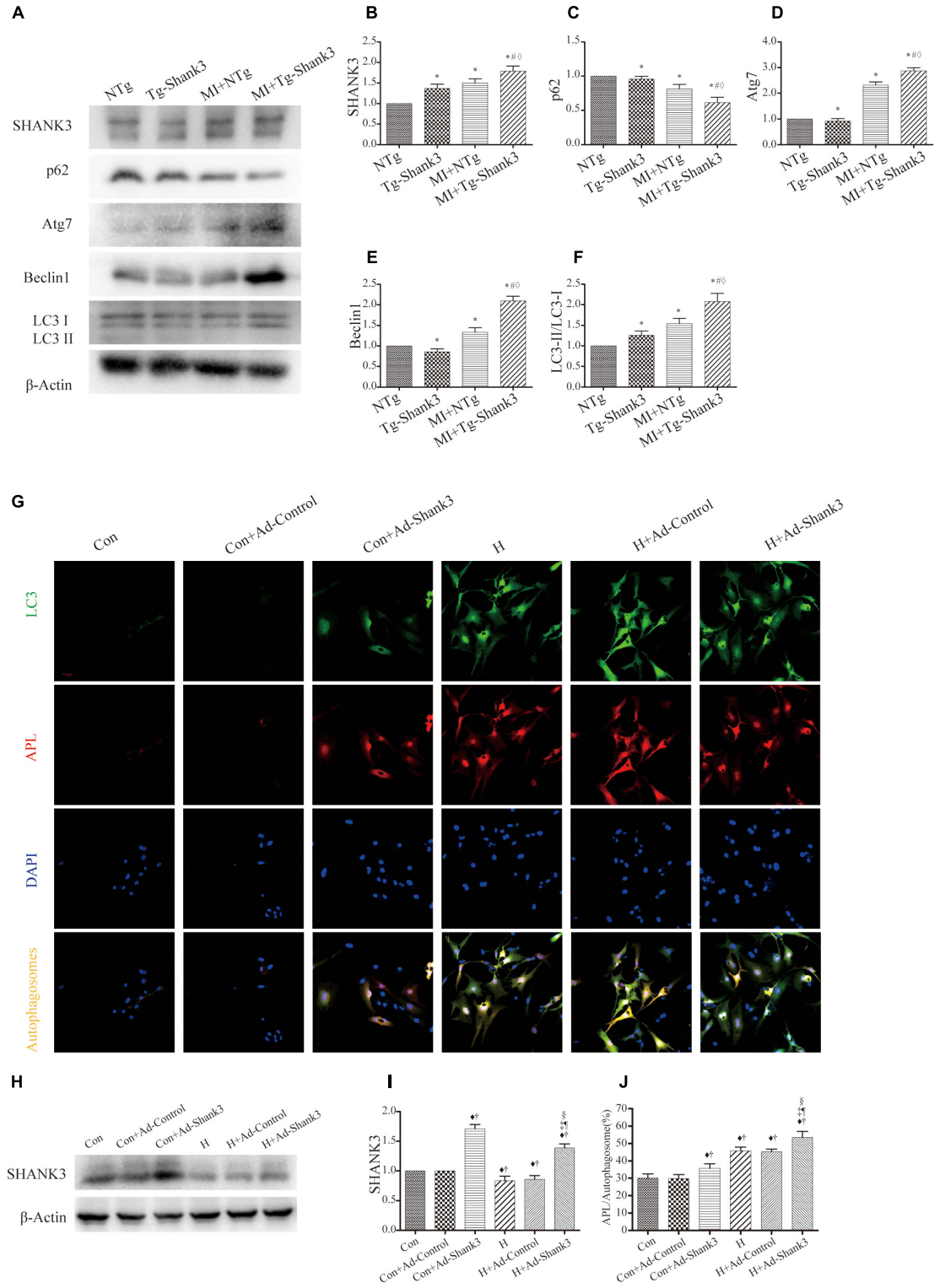

FIGURE 4 | Shank3 overexpression induces autophagy and increases the accumulation of protein aggresomes in cardiomyocytes. **(A–F)** Immunoblots and quantitative analyses of SHANK3, p62, Atg7, Beclin1, and LC3-II/LC3-I and β-actin *in vivo*. (n = 4–8/group) **(G)** Shank3 overexpression increased the numbers of red and green puncta in cardiomyocytes transduced with Ad-GFP-mRFP-LC3 after hypoxia. Immunofluorescence staining for LC3 (green), autophagolysosomes (APL, red), DAPI (blue), and autophagosomes (orange). **(H,I)** Immunoblots and quantitative analyses of SHANK3 *in vitro*. **(J)** Quantitative analyses of APL/autophagosomes. *$p < 0.05$ vs. NTg; #$p < 0.05$ vs. MI + NTg; ◊$p < 0.05$ vs. Tg-Shank3; ♦$p < 0.05$ vs. Con; †$p < 0.05$ vs. Con + Ad-Control; ‡$p < 0.05$ vs. Con + Ad-Shank3; §$p < 0.05$ vs. H; ¶$p < 0.05$ vs. H + Ad-Control. Con, control and H, hypoxia.

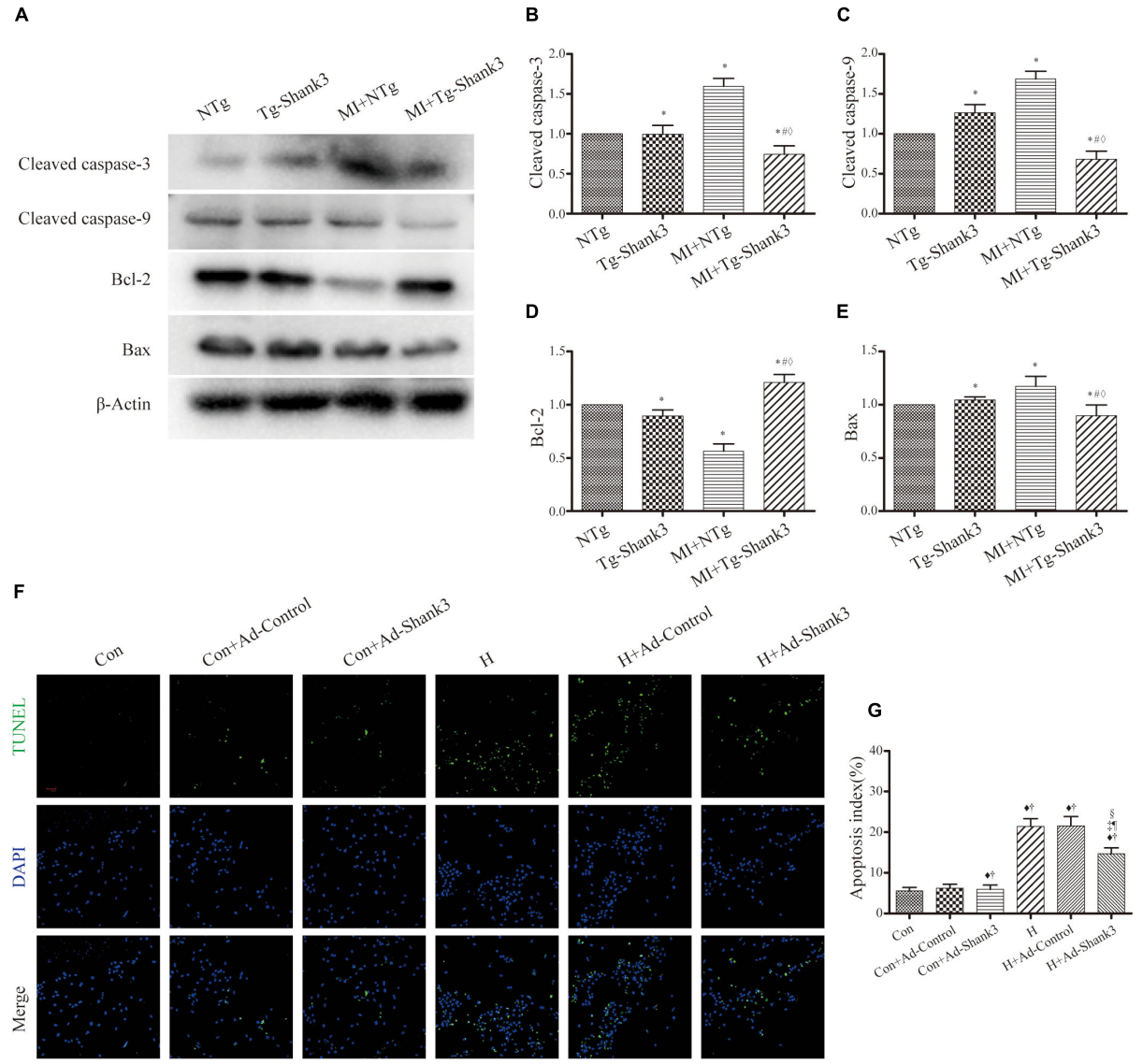

FIGURE 5 | Shank3 overexpression inhibits cardiomyocytes apoptosis. **(A–E)** Immunoblots and quantitative analyses of cleaved caspase-3, cleaved caspase-9, Bcl-2, Bax, and β-actin. (n = 4–8/group) **(F,G)** Representative images of TUNEL-stained primary neonatal cardiomyocytes **(F)** and apoptotic index **(G)**. *$p < 0.05$ vs. NTg; #$p < 0.05$ vs. MI + NTg; ◊$p < 0.05$ vs. Tg-Shank3; ♦$p < 0.05$ vs. Con; †$p < 0.05$ vs. Con + Ad-Control; ‡$p < 0.05$ vs. Con + Ad-Shank3; §$p < 0.05$ vs. H; ¶$p < 0.05$ vs. H + Ad-Control. Con, control and H, hypoxia.

Heart failure after MI has high morbidity and mortality, and cardiac remodeling is the main cause of heart failure, but the pathological mechanism of this process is not yet clear (Arnold et al., 2014; Bucholz et al., 2016; Prabhu and Frangogiannis, 2016; Wang et al., 2016; Gibb and Hill, 2018). Previous studies have shown that the levels of autophagy and apoptosis of cardiomyocytes after MI are directly involved in the recovery of cardiac function and cardiac remodeling (Kappel et al., 2016; Sciarretta et al., 2018b; Del Re et al., 2019).

In vitro, a reasonable level of autophagy can protect cells by removing harmful proteins from them (Wu et al., 2019). Our previous research proved that the increase of autophagy level helped to restore cardiac function and alleviate cardiac remodeling under hypoxic injury conditions (Hu et al., 2016). On the contrary, if the level of autophagy cannot be increased correspondingly after suffering the injury, it will lead to further deterioration of heart function (Hu et al., 2016; Packer, 2020).

In our study, both levels of LC-3 and autophagosome maturation showed a significant reduction in Shank3 deficit groups after MI. On the contrary, the level of autophagy in the Shank3 overexpression group was increased to deal with waste organelles and proteins after injury. The evidence above made us believe that Shank3 had an indispensable role in the autophagy of cardiomyocytes. Meanwhile, we hypothesized that Shank3, as a scaffold protein, may provide a platform for the biological

function of autophagy-related proteins (Shaw and Filbert, 2009). This viewpoint needs to be confirmed by further research.

In addition, our research also investigated cardiomyocyte apoptosis. *In vivo* or *in vitro*, the higher level of apoptosis was observed in the low expression of Shank3 groups as compared with the control groups. Several studies have shown that in the environment of nutritional deprivation and a lack of growth factors, the heart will induce autophagy and reduce apoptosis so that cardiomyocytes can survive (Del Re et al., 2019; Rabinovich-Nikitin et al., 2019; Cao et al., 2020; Davidson et al., 2020).

Our study first reports the key role Shank3 plays in functional recovery after cardiac ischemia and hypoxia by promoting autophagy and inhibiting apoptosis. Our results sheds light on a new research direction for cardiac remodeling and heart failure after MI, and Shank3 may also become a new therapeutic target for the diseases.

DATA AVAILABILITY STATEMENT

The raw data supporting the conclusions of this article will be made available by the authors, without undue reservation.

ETHICS STATEMENT

The animal study was reviewed and approved by the Fourth Military Medical University Ethics Committee on Animal Care.

AUTHOR CONTRIBUTIONS

DDS and HW defined the topic of this project and revised the manuscript carefully. WM, BW, MZ, and JH carried out the laboratory experiments and wrote the manuscript. JL, DS, ZX, KH, GW, LZ, RS, and BG analyzed the data. JG translated literature and polished the manuscript. CL and XG were responsible for the animal model establishment. All authors carried out the work, read, and approved the final manuscript.

FUNDING

This work was supported by the National Natural Science Foundation of China (Nos. 81922008, 81770224, and 81670204), National Key Research and Development Plan (2018YFA0107400), and Shaanxi Innovative Talent Promotion Plan (2018KJXX-013).

SUPPLEMENTARY MATERIAL

The Supplementary Material for this article can be found online at: https://www.frontiersin.org/articles/10.3389/fphys.2020.01082/full#supplementary-material

REFERENCES

Arnold, S. V., Masoudi, F. A., Rumsfeld, J. S., Li, Y., Jones, P. G., and Spertus, J. A. (2014). Derivation and validation of a risk standardization model for benchmarking hospital performance for health-related quality of life outcomes after acute myocardial infarction. *Circulation* 129, 313–320. doi: 10.1161/CIRCULATIONAHA.113.001773

Bucholz, E. M., Butala, N. M., Ma, S., Normand, S. T., and Krumholz, H. M. (2016). Life expectancy after myocardial infarction, according to hospital performance. *N. Engl. J. Med.* 375, 1332–1342. doi: 10.1056/NEJMoa1513223

Cao, X., Li, B., Han, X., Zhang, X., Dang, M., Wang, H., et al. (2020). Soluble receptor for advanced glycation end-products promotes angiogenesis through activation of STAT3 in myocardial ischemia/reperfusion injury. *Apoptosis* 25, 341–353. doi: 10.1007/s10495-020-01602-8

Davidson, S. M., Adameova, A., Barile, L., Cabrera-Fuentes, H. A., Lazou, A., Pagliaro, P., et al. (2020). Mitochondrial and mitochondrial-independent pathways of myocardial cell death during ischaemia and reperfusion injury. *J. Cell. Mol. Med.* 24, 3795–3806. doi: 10.1111/jcmm.15127

Del Re, D. P., Amgalan, D., Linkermann, A., Liu, Q., and Kitsis, R. N. (2019). Fundamental mechanisms of regulated cell death and implications for heart disease. *Physiol. Rev.* 99, 1765–1817. doi: 10.1152/physrev.00022.2018

Durand, C. M., Betancur, C., Boeckers, T. M., Bockmann, J., Chaste, P., Fauchereau, F., et al. (2007). Mutations in the gene encoding the synaptic scaffolding protein SHANK3 are associated with autism spectrum disorders. *Nat. Genet.* 39, 25–27. doi: 10.1038/ng1933

Frangogiannis, N. G. (2015). Pathophysiology of Myocardial Infarction. *Compr. Physiol.* 5, 1841–1875. doi: 10.1002/cphy.c150006

Gao, E., Hong Lei, Y., Shang, X., Huang, Z. M., Zuo, L., Boucher, M., et al. (2010). A novel and efficient model of coronary artery ligation and myocardial infarction in the mouse. *Circ. Res.* 107, 1445–1453. doi: 10.1161/CIRCRESAHA.110.223925

Gibb, A. A., and Hill, B. G. (2018). Metabolic coordination of physiological and pathological cardiac remodeling. *Circ. Res.* 123, 107–128. doi: 10.1161/CIRCRESAHA.118.312017

Grasselli, C., Carbone, A., Panelli, P., Giambra, V., Bossi, M., Mazzoccoli, G., et al. (2020). Neural stem cells from Shank3-ko mouse model autism spectrum disorders. *Mol. Neurobiol.* 57, 1502–1515. doi: 10.1007/s12035-019-01811-6

Hu, J., Man, W., Shen, M., Zhang, M., Lin, J., Wang, T., et al. (2016). Luteolin alleviates post-infarction cardiac dysfunction by up-regulating autophagy through Mst1 inhibition. *J. Cell. Mol. Med.* 20, 147–156. doi: 10.1111/jcmm.12714

Kappel, B. A., Stohr, R., De Angelis, L., Mavilio, M., Menghini, R., and Federici, M. (2016). Posttranslational modulation of FoxO1 contributes to cardiac remodeling in post-ischemic heart failure. *Atherosclerosis* 249, 148–156. doi: 10.1016/j.atherosclerosis.2016.04.001

Leblond, C. S., Nava, C., Polge, A., Gauthier, J., Huguet, G., Lumbroso, S., et al. (2014). Meta-analysis of SHANK mutations in autism spectrum disorders: a gradient of severity in cognitive impairments. *PLoS Genet.* 10:e1004580. doi: 10.1371/journal.pgen.1004580

Lee, Y., Ryu, J. R., Kang, H., Kim, Y., Kim, S., Zhang, Y., et al. (2017). Characterization of the zinc-induced Shank3 interactome of mouse synaptosome. *Biochem. Biophys. Res. Commun.* 494, 581–586. doi: 10.1016/j.bbrc.2017.10.143

Likosky, D. S., Van Parys, J., Zhou, W., Borden, W. B., Weinstein, M. C., and Skinner, J. S. (2018). Association between medicare expenditure growth and mortality rates in patients with acute myocardial infarction: a comparison from 1999 through 2014. *JAMA Cardiol.* 3, 114–122. doi: 10.1001/jamacardio.2017.4771

Lim, S., Naisbitt, S., Yoon, J., Hwang, J. I., Suh, P. G., Sheng, M., et al. (1999). Characterization of the Shank family of synaptic proteins. Multiple genes, alternative splicing, and differential expression in brain and development. *J. Biol. Chem.* 274, 29510–29518. doi: 10.1074/jbc.274.41.29510

Moessner, R., Marshall, C. R., Sutcliffe, J. S., Skaug, J., Pinto, D., Vincent, J., et al. (2007). Contribution of SHANK3 mutations to autism spectrum disorder. *Am. J. Hum. Genet.* 81, 1289–1297. doi: 10.1086/522590

Monteiro, P., and Feng, G. (2017). SHANK proteins: roles at the synapse and in autism spectrum disorder. *Nat. Rev. Neurosci.* 18, 147–157. doi: 10.1038/nrn.2016.183

Mossa, A., Giona, F., Pagano, J., Sala, C., and Verpelli, C. (2018). SHANK genes in autism: defining therapeutic targets. *Prog. Neuro Psychopharm. Biol. Psychiatry* 84 (Pt B), 416–423. doi: 10.1016/j.pnpbp.2017.11.019

Packer, M. (2020). Autophagy stimulation and intracellular sodium reduction as mediators of the cardioprotective effect of sodium-glucose cotransporter 2 inhibitors. *Eur. J. Heart Fail.* 22, 618–628. doi: 10.1002/ejhf.1732

Prabhu, S. D., and Frangogiannis, N. G. (2016). The biological basis for cardiac repair after myocardial infarction: from inflammation to fibrosis. *Circ. Res.* 119, 91–112. doi: 10.1161/CIRCRESAHA.116.303577

Rabinovich-Nikitin, I., Lieberman, B., Martino, T. A., and Kirshenbaum, L. A. (2019). Circadian-regulated cell death in cardiovascular diseases. *Circulation* 139, 965–980. doi: 10.1161/CIRCULATIONAHA.118.036550

Sciarretta, S., Maejima, Y., Zablocki, D., and Sadoshima, J. (2018a). The role of autophagy in the heart. *Annu. Rev. Physiol.* 80, 1–26. doi: 10.1146/annurev-physiol-021317-121427

Sciarretta, S., Yee, D., Nagarajan, N., Bianchi, F., Saito, T., Valenti, V., et al. (2018b). Trehalose-induced activation of autophagy improves cardiac remodeling after myocardial infarction. *J. Am. Coll. Cardiol.* 71, 1999–2010. doi: 10.1016/j.jacc.2018.02.066

Shaw, A. S., and Filbert, E. L. (2009). Scaffold proteins and immune-cell signalling. *Nat. Rev. Immunol.* 9, 47–56. doi: 10.1038/nri2473

Shirakabe, A., Ikeda, Y., Sciarretta, S., Zablocki, D. K., and Sadoshima, J. (2016a). Aging and autophagy in the heart. *Circ. Res.* 118, 1563–1576. doi: 10.1161/CIRCRESAHA.116.307474

Shirakabe, A., Zhai, P., Ikeda, Y., Saito, T., Maejima, Y., Hsu, C. P., et al. (2016b). Drp1-dependent mitochondrial autophagy plays a protective role against pressure overload-induced mitochondrial dysfunction and heart failure. *Circulation* 133, 1249–1263. doi: 10.1161/CIRCULATIONAHA.115.020502

Valentin, J., Frobert, A., Ajalbert, G., Cook, S., and Giraud, M. N. (2016). Histological quantification of chronic myocardial infarct in rats. *J. Vis. Exp.* 11:54914. doi: 10.3791/54914

Wang, N., Hung, C. L., Shin, S. H., Claggett, B., Skali, H., Thune, J. J., et al. (2016). Regional cardiac dysfunction and outcome in patients with left ventricular dysfunction, heart failure, or both after myocardial infarction. *Eur. Heart J.* 37, 466–472. doi: 10.1093/eurheartj/ehv558

Wu, D., Zhang, K., and Hu, P. (2019). The Role of Autophagy in Acute Myocardial Infarction. *Front. Pharmacol.* 10:551. doi: 10.3389/fphar.2019.00551

Conflict of Interest: The authors declare that the research was conducted in the absence of any commercial or financial relationships that could be construed as a potential conflict of interest.

Copyright © 2020 Man, Gu, Wang, Zhang, Hu, Lin, Sun, Xiong, Gu, Hao, Guo, Wei, Zhang, Song, Li, Wang and Sun. This is an open-access article distributed under the terms of the Creative Commons Attribution License (CC BY). The use, distribution or reproduction in other forums is permitted, provided the original author(s) and the copyright owner(s) are credited and that the original publication in this journal is cited, in accordance with accepted academic practice. No use, distribution or reproduction is permitted which does not comply with these terms.

frontiers in Pharmacology

REVIEW
published: 26 August 2020
doi: 10.3389/fphar.2020.01247

Farnesoid X Receptor Agonists as Therapeutic Target for Cardiometabolic Diseases

Chao Li[1], Jie Yang[2], Yu Wang[2], Yingzi Qi[3], Wenqing Yang[1] and Yunlun Li[1,2]**

[1] Experimental Center, Shandong University of Traditional Chinese Medicine, Jinan, China, [2] Cardiovascular Department, Affiliated Hospital of Shandong University of Traditional Chinese Medicine, Jinan, China, [3] School of Health, Shandong University of Traditional Chinese Medicine, Jinan, China

Cardiometabolic diseases are characterized as a combination of multiple risk factors for cardiovascular disease (CVD) and metabolic diseases including diabetes mellitus and dyslipidemia. Cardiometabolic diseases are closely associated with cell glucose and lipid metabolism, inflammatory response and mitochondrial function. Farnesoid X Receptor (FXR), a metabolic nuclear receptor, are found to be activated by primary BAs such as chenodeoxycholic acid (CDCA), cholic acid (CA) and synthetic agonists such as obeticholic acid (OCA). FXR plays crucial roles in regulating cholesterol homeostasis, lipid metabolism, glucose metabolism, and intestinal microorganism. Recently, emerging evidence suggests that FXR agonists are functional for metabolic syndrome and cardiovascular diseases and are considered as a potential therapeutic agent. This review will discuss the pathological mechanism of cardiometabolic disease and reviews the potential mechanisms of FXR agonists in the treatment of cardiometabolic disease.

Keywords: Farnesoid X Receptor, cardiometabolic diseases, lipid metabolism, diabetes mellitus, obesity

OPEN ACCESS

Edited by:
Ying Mei Zhang,
Fudan University, China

Reviewed by:
Roberta d'Emmanuele di Villa Bianca,
University of Naples Federico II, Italy
Jun Ren,
University of Washington,
United States

Correspondence:
Wenqing Yang
wenqing-yang@hotmail.com
Yunlun Li
yunlun.lee@hotmail.com

Specialty section:
This article was submitted to Cardiovascular and Smooth Muscle Pharmacology, a section of the journal Frontiers in Pharmacology

Received: *31 May 2020*
Accepted: *29 July 2020*
Published: *26 August 2020*

Citation:
Li C, Yang J, Wang Y, Qi Y, Yang W and Li Y (2020) Farnesoid X Receptor Agonists as Therapeutic Target for Cardiometabolic Diseases. Front. Pharmacol. 11:1247. doi: 10.3389/fphar.2020.01247

INTRODUCTION

Cardiometabolic diseases are reaching epidemic proportions in the world and the leading cause of death in both developed and developing countries (Matsuzawa et al., 2011). Cardiometabolic diseases are characterized by a combination of multiple risk factors for cardiovascular disease (CVD) and metabolic diseases including type 2 diabetes (T2D), obesity and dyslipidemia (Arnett et al., 2019; Ralston and Nugent, 2019). Individuals with cardiometabolic diseases face a higher risk of developing myocardial infarction, stroke and heart failure (Landsberg et al., 2013). According to a May 2017 report of the World Health Organization, CVD are the leading cause of death worldwide, with 17.9 million people dying from CVD in 2016, representing 31% of all global deaths. Cardiometabolic diseases are linked to several risk factors, in particular high-salt and high-fat diet (HFD), smoking, hypertension, and high cholesterol. Mounting evidence-based medical data indicates that hypercholesterolemia is an independent risk factor for CVD (Birbeck et al., 2015; Wald et al., 2016). Reducing abnormally high levels of cholesterol can effectively decrease the occurrence of cardiovascular events. Over the past few decades, the obesity rate and prevalence of T2D have increased significantly worldwide (Lascar et al., 2018; Bluher, 2019). The increase in the

prevalence of diabetes and obesity has further contributed to the increase in the incidence rate of cardiometabolic diseases and continues to undermine the management of CVD (Zhang et al., 2018). In addition, a major cause of increased morbidity and mortality of cardiometabolic diseases is the increasing population of aging. Projections indicate that the prevalence of CVD in the United States may escalate by 10% between 2010 and 2030. The estimated increase stems in part from the aging of the population (Vasan and Benjamin, 2016). Measures to achieve healthy aging and alleviate aging-related morbidity have become a burning issue for health care (Ren et al., 2018). Understanding mechanism of aging is of immense clinical importance to population-wide cardiovascular risk. Although statins and angiotensin converting enzyme inhibitors improve cardiovascular outcomes, there is still a percentage of patients with cardiometabolic diseases still face the risk of developing overt cardiovascular disease.

Farnesoid X receptor (FXR) is a member of the nuclear receptor superfamily, and was identified as a receptor of bile acids (BAs) (Li C. et al., 2019). There is one human gene for FXR (*NR1H4*) separately from the rodent genes (*Nr1h4* and *Nr1h5*), and human *NR1H5P* is a pseudogene. The human and rodent *Nr1h4* genes are conserved and encode four different protein isoforms (FXRα1, FXRα2, FXRα3, and FXRα4), which are produced by alternative promoters and RNA splicing (Teodoro et al., 2011). FXR is mainly expressed in various tissues, including the liver, intestine, and kidney. In recent years, FXR has been found to also be expressed in cells of the cardiovascular system, such as cardiomyocytes and endothelial cells. Besides being a bile acid receptor, FXR is also a bile acid synthesis biosensor, FXR participates in the synthesis, conjugation, absorption and secretion of BAs (Tu et al., 2000). FXR has also been shown to have a regulatory effect on glucose and lipid metabolism, intestinal flora metabolism, oxidative stress, and inflammation (Li H. et al., 2019; Schoeler and Caesar, 2019). Therefore, increasingly more attention has been paid lately to the therapeutic role of FXR in cardiovascular physiology and pathology. Moreover, FXR also showed effective therapeutic effect on nonalcoholic fatty liver disease (NAFLD) and metabolic diseases including obesity, diabetes, and hypercholesterolemia (Wang et al., 2018). In this review, we will focus on the potential mechanisms of FXR agonists in the treatment of cardiometabolic disease.

FXR MODULATORS

As other nuclear receptors, the FXR protein also exhibits a highly-conserved DNA binding domain (DBD) to bind to the ligand (Modica et al., 2010). BAs are a common agonist, including primary BAs, such as chenodeoxycholic acid (CDCA), and cholic acid (CA), and secondary BAs, such as lithocholic acid (LCA), and deoxycholic acid (DCA). Several non-BA agonists of FXR have also been discovered, and according to their chemical structure are classified as steroidal or non-steroidal (Carotti et al., 2014). Several FXR agonists have been investigated in phase II and phase III clinical trials, and some candidate compounds have also been found to regulate FXR activity in pre-clinical studies (**Table 1**).

Bile Acid Agonists and Its Analogues

Natural BAs and OCA

BAs are considered as important endogenous FXR agonists in different tissues. The potency of natural BAs to activate FXR follows the order CDCA>DCA>LCA>CA (Wang et al., 2018). Some studies have found that replacing the carboxylic group on the side chain of CDCA with 6α-alkyl significantly enhances its activating potency and efficacy on FXR, which is consistent with the hydrophobic nature of the pocket in FXR that is complementary to the 6α position (Pellicciari et al., 2006). The first FXR agonist that was investigated in clinical practice was obeticholic acid (OCA), which has an ethyl group substituted at the 6 position of CDCA, which is the most potent natural ligand activator of FXR (Pellicciari et al., 2002). OCA was approved by the United States (US) Food and Drug Administration for the treatment of primary biliary cholangitis (PBC) and evaluated in additional clinical trials for non-alcoholic steatohepatitis (NASH) (NCT01265498), alcoholic hepatitis (NCT02039219) and lipodystrophy (NCT02430077). However, besides its obvious therapeutic effect, OCA also has side effects, such as pruritus, and may participate in the regulation of blood lipids (Hirschfield et al., 2015; Neuschwander-Tetri et al., 2015). Future studies are needed to explore the effects of OCA on serum lipoprotein metabolism, which may be associated with CVD.

INT-767

INT-767, a semisynthetic BA that acts as a dual FXR and TGR5 (G-protein coupled receptor) agonist, has been found to be a slightly more potent activator of FXR, which also has the ability to alleviate liver injury and metabolic disorders (Baghdasaryan et al., 2011). It has been reported that INT-767 improves the NASH histopathological characteristics in a diet-induced *ob/ob* mouse model, showing greater efficacy than the treatment with OCA (Roth et al., 2018). Also, INT-767 has been shown to alleviate hypercholesterolemia and increase the expression of thermogenic genes through FXR and/or TGR5 activation, leading to the reversal of HFD-induced metabolic disorders (Jadhav et al., 2018). Moreover, since TGR5 is an important regulator of metabolism and energy homeostasis, INT-767 shows a broader and more effective therapeutic potency.

TC-100

TC-100 (3α,7α,11β-trihydroxy-6α-ethyl-5β-cholan-24-oic acid) is the first semisynthetic BA that combines the ability to specifically bind and activate FXR without TGR5 activation (Pellicciari et al., 2016). The study of the activation of FXR by TC-100 by cell-based analysis revealed that TC-100 is slightly more potent than OCA, and is highly effective in increasing the clearance of BAs from the liver to the bile canaliculus (Pellicciari et al., 2016).

Additionally, several other BA derivatives, including NIHS700 (Suzuki et al., 2008), 22(R)-OHC [oxysterol 22(R)-hydroxycholesterol] (Deng et al., 2006), androsterone [5α-androstan-3α-ol-17-one] (Wang et al., 2006), MFA-1 [17β-(4-hydroxybenzoyl) androsta-3,5-diene-3-carboxylic acid] (Soisson et al., 2008), have also been identified as FXR agonist.

TABLE 1 | Bile acid agonists and its derivatives.

Name	Chemical structures	Preclinical studies	Current clinical status	References
Obeticholic acid (OCA, INT-747)	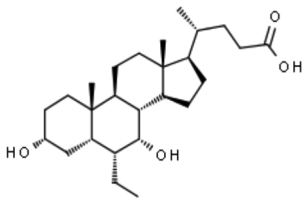	NASH mice; estrogen-induced cholestasis; rodent models of cholestasis.	Phase II for Lipodystrophy (NCT02430077); Phase IV for Primary Biliary Cholangitis (NCT02308111)	(Fiorucci et al., 2005; Carino et al., 2020; Li et al., 2020)
INT-767	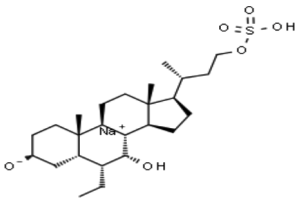	Chronic cholangiopathy (Mdr2$^{-/-}$ Abcb4$^{-/-}$ mice); *Lep*$^{ob/ob}$ mice with NASH; HFD induced metabolic disorders.	NA	(Baghdasaryan et al., 2011; Jadhav et al., 2018; Roth et al., 2018)
TC-100	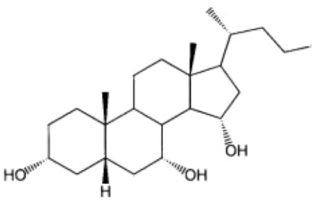	Bile fistula rats and bile duct ligation mice	NA	(Pellicciari et al., 2016)
GW4064	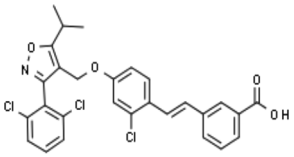	Short bowel resection rats associated with liver disease; endotoxin-induced hepatic inflammation; diet-induced obesity and hepatic steatosis.	NA	(Ma et al., 2013; Yao et al., 2014; Cao et al., 2019)
Px-102 (PX20606) and its eutomer Px-104 (GS-9674)	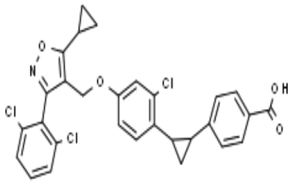	non-cirrhotic and cirrhotic portal hypertension; High-density lipoprotein-mediated transhepatic cholesterol efflux in mice.	Phase II for NAFLD (NCT01999101, completed). No current study	(Hambruch et al., 2012; Schwabl et al., 2017)
TERN-101 (LY2562175)	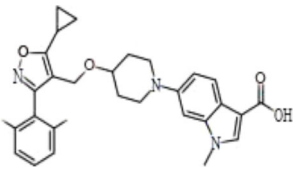	Dyslipidemia (LDLr-/- mice)	Phase II for NASH (NCT04328077)	(Genin et al., 2015)
Tropifexor (LJN452)	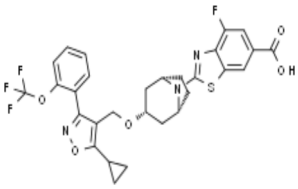	Amylin liver NASH model	Phase II for NAFLD and NASH (NCT03517540, NCT04147195)	(Hernandez et al., 2019)
WAY-362450	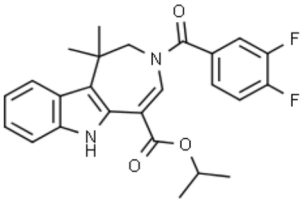	Maternal cholestasis; fructose-induced hepatic steatosis; murine model of alcoholic liver disease; murine model of non-alcoholic steatohepatitis.	Phase I (NCT00499629, completed; NCT00509756, terminated). No current study	(Zhang et al., 2009b; Liu et al., 2014; Wu et al., 2014; Wu et al., 2015)

(Continued)

TABLE 1 | Continued

Name	Chemical structures	Preclinical studies	Current clinical status	References
Fexaramine	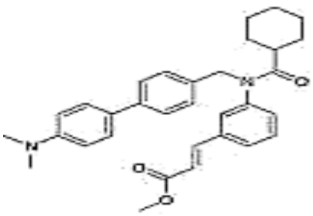	Alcoholic liver disease in mice; obese and diabetic mice, *Lep*$^{ob/ob}$ mice; obesity and metabolic syndrome.	NA	(Fang et al., 2015; Hartmann et al., 2018; Pathak et al., 2018)
LMB763	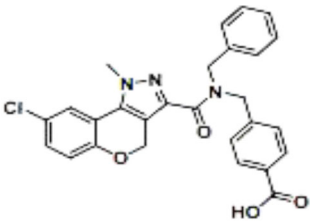	STAM and NASH murine mode	Phase II for Diabetic Nephropathy (NCT03804879)	(Chianelli et al., 2020)
EYP001	unknown	NA	Phase II for NASH (NCT03812029); Phase II for Chronic Hepatitis B (NCT04365933)	NA
EDP-305	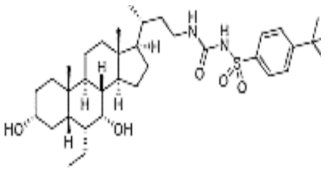	Biliary fibrosis and steatohepatitis mice; unilateral ureteral obstruction mice; choline-deficient, L-amino acid-defined, high-fat diet models of hepatic injury.	Phase II for Primary Biliary Cholangitis (NCT03394924); Phase II for NASH (NCT04378010)	(Erstad et al., 2018; Li S. et al., 2019; An et al., 2020)

NA, not available; NASH, non-alcoholic steatohepatitis; NAFLD, Nonalcoholic fatty liver disease; HFD, High-fat diet.

Non-Bile Acid Agonists

GW4064 and Its Derivatives

GW4064 is an agonist of FXR that belongs to a class of trisubstituted isoxazole core compounds with high affinity for FXR, which was reported in 2000 (GERARDUS et al.). GW4064 was reported to reverse BA dysmetabolism and alleviate hepatotoxicity in rats with short bowel resection associated with liver disease (Cao et al., 2019). GW4064 also attenuated lipopolysaccharide (LPS)-induced hepatic inflammation (Yao et al., 2014) and diet-induced hepatic steatosis and insulin resistance (Ma et al., 2013). However, GW4064 could only serve as a tool compound due to its poor bioavailability (Akwabi-Ameyaw et al., 2008) and potential hepatobiliary toxicity (Bass et al., 2011). A further study found that the chemical structure of GW4064 contains a stilbene olefin, which may be responsible for its poor bioavailability and photolabile properties. Px-102 (PX20606) and its eutomer Px-104 (GS-9674) are highly effective GW4064 derivatives, in which the stilbene olefin is replaced by a cyclopropyl moiety, with high affinity for FXR, which improved the aqueous solubility and membrane permeability. A phase I study with Px-102 was completed in healthy volunteers in 2011 and 2012 (NCT01998672, NCT01998659). Other studies have reported that Px-102 showed therapeutic potentials in the treatment of other diseases, including BA synthesis dysfunction (Al-Khaifi et al., 2018), vascular remodeling and sinusoidal dysfunction (Schwabl et al., 2017).

Px-104 (GS-9674, also called cilofexor) was considered as the best example of FXR agonist in the clinical development derivative. A single 100 -mg dose of cilofexor showed good tolerance in healthy volunteers and no grade 3 adverse effects were observed (Nelson et al., 2017). A Phase II trial with Px-104 (NCT01999101) was also conducted to evaluate the safety and tolerability of Px-104 in NAFLD patients. A Phase II randomized controlled trial (NCT02854605) with cilofexor in patients with NASH reported that cilofexor for 24 weeks was well tolerated and significantly reduced hepatic steatosis, liver biochemistry, and serum BAs (Patel et al., 2020). Another randomized, placebo-controlled trial (NCT02943460) also suggested that cilofexor significantly improved liver biochemistry and markers of cholestasis in patients with primary sclerosing cholangitis (Trauner et al., 2019).

LY2562175 and LJN452

LY2562175, a compound developed by Eli Lilly and Company, was evaluated in a European Phase I trial and subsequently licensed to Terns Pharmaceuticals and renamed TERN-101 (Genin et al., 2015). LJN452 (also called tropifexor) is a powerful and highly effective FXR agonist *in vivo*, which introduces a bicyclic nortropine-substituted benzothiazole carboxylic acid moiety into a trisubstituted isoxazole scaffold building on the chemistry structure of the Eli Lilly and Company compound LY2562175 compound (Tully et al., 2017). In healthy volunteers, tropifexor was well tolerated, had a pharmacokinetic curve indicating it was suitable for once daily administration and showed dose-dependent target binding without changing plasma lipids (Badman et al., 2020). Preclinical evaluation in animal

models has demonstrated that tropifexor is a promising investigational therapy and it is currently under phase II (CLJC242A2201J; NCT03517540) development for NASH and liver fibrosis (Hernandez et al., 2019; Pedrosa et al., 2020).

WAY-362450

WAY-362450 is a highly selective FXR agonist [EC(50)= 4nM, Eff=149%] without cross-reactivity with other nuclear receptors at concentrations up to 10 μM (Flatt et al., 2009). WAY-362450 was reported to decrease LPS-induced serum amyloid P component and have anti-inflammatory effects (Zhang et al., 2009a). Several animal studies have demonstrated that WAY-362450 has effective therapeutic effect on atherosclerotic lesion formation (Hartman et al., 2009), hepatic fibrosis and NASH (Zhang et al., 2009b), and regulation of triglyceride and cholesterol homeostasis (Evans et al., 2009). However, WAY-362450 exhibits insufficient aqueous solubility due to its planar structure and lack of free ionizable group (Wang et al., 2018).

Fexaramine

Fexaramine is one of the earliest synthetic nonsteroidal FXR agonists with a 100-fold increased affinity relative to natural compounds (Downes et al., 2003). Fexaramine has become the prototype of the intestine-restricted FXR agonist, and has been shown to elicit potent beneficial metabolic effects without the side effects due to the activation of liver FXR (Fang et al., 2015). In addition, it has also been found that fexaramine has effective therapeutic effect on stabilizing the gut barrier and modulating hepatic lipid metabolism (Hartmann et al., 2018). Further studies have shown that fexaramine improves lipid profiles, increases glucose and insulin tolerance, and promotes browning of adipose tissue (Fang et al., 2015; Pathak et al., 2018).

Others

LMB763 (nidufexor), a novel non-BA FXR agonist, is based on a tricyclic dihydrochromenopyrazole core, which has partial FXR agonistic activity *in vitro* and FXR-dependent gene modulation *in vivo* (Chianelli et al., 2020). LMB763 has advanced to Phase II clinical trials in patients with NASH and diabetic nephropathy. EYP001 is a synthetic FXR agonist developed by ENYO Pharma and currently in Phase II trial for hepatitis B virus (HBV) infection as well as for NASH treatment. However, the chemical structure of EYP001 is unknown and there are no peer-reviewed publications on this compound. EDP-305 is a non-BA FXR ligand, which contains steroidal and non-steroidal components without carboxylic acid group (Wang et al., 2018). Some studies have reported that EDP-305 reduced liver fibrosis progression in rat with bile duct ligation (Erstad et al., 2018), attenuated interstitial renal fibrosis in a mouse unilateral ureteral obstruction model (Li S. et al., 2019), and improved liver injury and fibrosis in mouse models of biliary and metabolic diseases (An et al., 2020).

FXR Antagonists

Bile Acid Antagonists

Although BAs are considered as FXR agonists, some less hydrophobic BAs were still identified as FXR antagonists. Tauro-β-muricholic acid (T-β-MCA), a naturally occurring FXR antagonist, was reported to inhibit the FXR activation, which induced by taurocholic acid (TCA) or GW4064 (Sayin et al., 2013). More studies have demonstrated that T-β-MCA is an endogenous FXR antagonist in the intestine, which can inhibit basal FXR signaling and TCA-activated signaling (Li et al., 2013; Liu et al., 2020). Moreover, taurochenodeoxycholic acid (TCDCA), a weak agonist of FXR, can also inhibit the FXR activation by TCA and inhibits Shp mRNA expression (Li et al., 2013). Glycoursodeoxycholic acid (GUDCA) was another BAs, which was identified as an intestinal FXR antagonist showing effective therapeutic potency on obesity and type 2 diabetes (Cherney and Lam, 2018; Sun et al., 2018). It was also reported that glycine-β-muricholic acid (Gly-MCA) inhibited FXR signaling exclusively in intestine, resulting in the decrease of serum and intestine ceramide level and the improvement of metabolic dysfunction in obesity mouse (Jiang et al., 2015b).

Non-Bile Acid Antagonists

Guggulsterone (4,17(20)-Pregnadiene-3,16-dione) is a phytosterol found in the resin of the guggul plant, which inhibited CDCA-induced FXR activation in concentrations above 10 μM and was identified as FXR antagonists (Urizar et al., 2002). Guggulsterone has a significantly inhibitory effect on NF-kB signaling and attenuated the expression of proinflammatory cytokines, showing the therapeutic potential on Graves' orbitopathy, colorectal cancer and atherosclerosis (Gautam et al., 2019; Leo et al., 2019; Kim et al., 2020). Epiallopregnanolone sulfate (PM5S) is closely associated with intrahepatic cholestasis of pregnancy (ICP) and elevates in the serum of ICP patients. PM5S can inhibited FXR activation resulting in the decrease of FXR-mediated bile acid efflux (Abu-Hayyeh et al., 2013). 3,5-disubstituted oxadiazole core (a new chemotype of FXR antagonists) (Festa et al., 2019), Stigmasterol (a Soy Lipid-Derived Phytosterol) (Carter et al., 2007), tuberatolides (isolated from the Korean marine tunicate Botryllus tuberatus) (Choi et al., 2011), andrographolide (representative active ingredient of Andrographis panniculata Nees) (Kumar et al., 2020) were also identified to have antagonistic activity on FXR. However, the effect and mechanism of FXR inhibition by these FXR antagonists also need further study and exact evidence.

ROLE OF FXR IN CARDIOVASCULAR DISEASES

Several studies reported that the relative risk for developing CVD is double that of the general population in patients suffering from cardiometabolic syndrome, accompanied with an increase in all-cause mortality (Ford, 2005; Galassi et al., 2006; Gami et al., 2007). At the beginning of the 21st century, CVD, including hypertension and atherosclerosis, were regarded as one of the main risk factors for developing cardiometabolic disease. China already has the largest absolute disease burden of hypertension in the world (Li et al., 2015). In 2010, approximately 265 million Chinese adults had hypertension. The development of essential hypertension is complex, particularly with obesity, glucose metabolism disorders, and inflammation involved. FXR has an

extensive role in regulating cholesterol, lipid and glucose metabolism (Li and G, 2015; Massafra et al., 2018). And FXR activation has been shown to limit the inflammatory response (Massafra et al., 2018). It is widely known that disorders involving the secretion of endothelial factors play important roles in the pathogenesis of hypertension. The regulatory effect of FXR on the secretion of endothelial factors suggests it plays a key role in mediating the pathophysiological effects of hypertension. Indeed, recent studies have revealed novel functions of FXR in hypertension. For instance, it was reported that FXR activation upregulates endothelial nitric oxide synthase (eNOS) expression (Li et al., 2008) and down-regulates endothelin-1 (ET-1) expression (He et al., 2006) by negatively interfering with the activator protein 1 (AP-1) signaling pathway in cultured human vascular endothelial cells. FXR activation also inhibited vascular contraction and induced concentration-dependent relaxation in normal aorta through nitric oxide (NO) mechanism (Zhang et al., 2012). In addition, it was found that treatment with the FXR agonist CDCA decreased blood pressure in spontaneously hypertensive rats (SHRs) by improving vasorelaxation and reducing vasoconstriction (Lin, 2015). Attenuation of the inflammatory response in mesenteric resistant arteries by altering eNOS and ET-1 levels could be a possible mechanism. These findings support a potential role for FXR as a regulator in vascular activities and the treatment of hypertension.

Since FXR regulates the expression of genes critical for BA and lipid homeostasis, research has long been focused on the role played by FXR in the initiation and progression of atherosclerosis. Many studies were undertaken to investigate the pathological consequences of the loss of FXR function on the risk and severity of atherosclerosis. Hanniman et al. (2005) reported that $Fxr^{-/-}$ $ApoE^{-/-}$ mice fed a high fat/high-cholesterol diet developed larger atherosclerotic lesions. This study on a mouse model of atherosclerotic disease suggested that loss of Fxr function is associated with decreased survival, increased severity of defects in lipid metabolism, and more extensive aortic plaque formation. However, two other studies found reduced atherosclerosis development in $Fxr^{-/-}Apoe^{-/-}$ mice and $Fxr^{-/-}$ $Ldlr^{-/-}$ mice (Guo et al., 2006; Zhang et al., 2006). In contrast, another study has reported that LDL receptor (*Ldlr*) knockout (KO) mice with Fxr and Tgr5 dual deficiency developed severe atherosclerosis and aortic inflammation through activation of the NF-κB signaling pathway (Miyazaki-Anzai et al., 2018). Due to inconsistent results from studies of FXR loss-of function models, the role of FXR in the development of atherosclerosis remains unclear. Despite these discrepancies, it is generally agreed that FXR activation is antiatherogenic. Many studies have shown that the synthetic FXR agonists, such as INT-767 (Jadhav et al., 2018; Miyazaki-Anzai et al., 2018), INT-747 (Mencarelli et al., 2009), WAY-362450 (Hartman et al., 2009), improved blood lipid and reduced aortic plaque formation. FXR agonists induced SHP expression and repressed cholesterol 7alpha-hydroxylase (CYP7A1) and sterol 12 alpha-hydroxylase (CYP8B1) expression (Hartman et al., 2009). FXR agonists were found to induce small heterodimer partner (SHP) expression and repress cholesterol 7alpha-hydroxylase (CYP7A1) and sterol 12 alpha-hydroxylase (CYP8B1) expression (Mencarelli et al., 2009). Interestingly, researcher also found that the effects of FXR agonist are different according to sex. Female but not male mice had reduced aortic lesion formation on treatment with the potent synthetic FXR agonist WAY-362450 (Hartman et al., 2009). FXR controls the expression of multiple genes that are key to many aspects of CVD. Li et al. (2019b) found that activation of FXR increased FNDC5 mRNA expression in human and increased the circulating level of irisin in Rhesus macaques and level of irisin is related to the degree of atherosclerosis in $Apoe^{-/-}$ mice.

During heart failure, decreased vascular bioavailability of NO leads to the attenuation of coronary or systemic vasodilatation (Chen et al., 2002; Chen et al., 2003; Chen et al., 2005). Asymmetric dimethylarginine (ADMA) can limit NO bioavailability and increase production of eNOS derived reactive oxygen species. High plasma ADMA levels are considered as an increased risk for cardiac death (Boger et al., 2009). Dimethylarginine dimethylaminohydrolase 1 (DDAH1) can cause ADMA degradation. DDAH1 plays an important role in regulating the cardiovascular function and risk factors of congestive heart failure (CHF) by maintaining cardiovascular NO/cGMP/PKG signaling. Current, research shows that the FXR agonist GW4064 increases DDAH1 expression in the liver and kidney and decreases plasma ADMA (Hu et al., 2006; Li et al., 2009). These findings indicate that activating FXR to increase DDAH1 activity could be a promising strategy for improving NO bioavailability and maintaining cardiovascular function in the failing heart. However, it is unclear whether FXR activation induces DDAH1 expression in the cardiovascular system.

ROLE OF FXR IN NAFLD AND CHOLESTEROL METABOLISM

NAFLD Is Associated With an Increased Risk of CVD

NAFLD is becoming the most common liver disease worldwide. In the US, approximately 25% of adults suffer from fatty liver without excessive drinking. In China, the incidence of fatty liver is increasing at a rate of 0.594% per year and it is anticipated that 20% of people in China will suffer from fatty liver by 2020 (Zhu et al., 2015). NAFLD includes a histological spectrum of conditions ranging from simple steatosis (SS) to steatosis plus necroinflammation (NASH). NAFLD is frequently associated with an increased risk of CVD and metabolic abnormalities, including obesity, diabetes, insulin resistance, hypertension, dyslipidemia, and atherosclerosis (Adams et al., 2017). A recent meta-analysis involving more than 8.5 million people in 22 countries showed that more than 80% of NASH patients were overweight or obese, 72% had dyslipidemia, and 44% had T2D, suggesting that NASH increased the incidence of CVD-related risk factors and metabolic diseases (Younossi et al., 2016). Further research has also confirmed that NAFLD is closely related to impaired left ventricular diastolic function, reduced myocardial energy metabolism and decreased coronary blood flow in patients with T2D (Rijzewijk et al., 2010; Mantovani et al., 2015). A clinical study suggested that NAFLD was independently

associated independently with CVD, after adjusting for major demographic, clinical, and metabolic confounders (odds ratio, 1.23; 95% confidence interval, 1.04–1.44) (Stepanova and Younossi, 2012). This finding is further supported by a meta-analysis revealing that NAFLD is associated with an increased risk of CVD, hypertension, and atherosclerosis (Wu et al., 2016).

Cholesterol Metabolism Disorder Plays a Key Role in NAFLD

Since NASH is closely related to the incidence of cardiometabolic diseases, they share many of the same pathological damage factors, including dyslipidaemia, oxidative stress, insulin resistance, inflammation, and endoplasmic reticulum (ER) stress (Lim et al., 2019). It should be noted that cholesterol metabolism disorder plays a key role in the pathological process of NAFLD, and a severe disturbance of cholesterol homeostasis in the cell leads to the accumulation of cholesterol and eventually cholesterol toxicity (Musso et al., 2010). It was reported that cholesterol accumulation or lipotoxicity induced oxidative injury, mitochondrial dysfunction, ER stress and inflammasome activation, which resulted in hepatocyte damage and liver fibrosis progression (Hager et al., 2012; Gan et al., 2014; Mridha et al., 2017). Dysregulation of cellular cholesterol homeostasis by increased activity of nuclear transcription factor-sterol regulatory binding protein 2 (SREBP2) and liver X receptor (LXR), and reduced activity of FXR plays a crucial role in in the accumulation of liver cholesterol in NASH (Musso et al., 2013).

Effects of FXR Activation on NAFLD and Cholesterol Metabolism

FXR activation mediates BA metabolism and cholesterol homeostasis. FXR activation could lead to inhibition of the expression of the *CYP7A1* gene (encoding the rate-limiting enzyme in BA biosynthesis) by activating fibroblast growth factor 15 (FGF15) (Inagaki et al., 2005) or SHP (De Fabiani et al., 2001; Lee et al., 2018), contributing to BA metabolism and cholesterol homeostasis. A recent clinical study reported that variations in the *CYP7A1* gene are associated with elevated low-density lipoprotein cholesterol levels, and with increased risk of myocardial infarction and symptomatic gallstone disease (Qayyum et al., 2018). Therefore, the FXR/CYP7A1 pathway could be consider as a therapeutic target for cardiometabolic disease. Since cholesterol metabolism is closely related to the occurrence of NASH and CVD, more and more studies are focusing on the therapeutic effect of FXR agonists on NASH. Numerous clinical studies have demonstrated that OCA (a FXR agonist) has a significant therapeutic effect on NASH by increasing insulin sensitivity and reducing markers of liver inflammation and fibrosis (Mudaliar et al., 2013; Neuschwander-Tetri et al., 2015; Younossi et al., 2019). Clinical research also has revealed that cilofexor significantly reduced hepatic steatosis, liver biochemistry, and serum BAs (Patel et al., 2020). Additionally, animal studies have also shown that INT-767 reduced the severity of steatohepatitis, inflammatory infiltrates and fibrosis by restoring insulin sensitivity and promoting visceral fat brown adipogenesis and mitochondrial function (Comeglio et al., 2018; Roth et al., 2018). Tropifexor was reported to markedly prevent liver steatohepatitis and fibrosis by reducing oxidative stress and inflammatory injury (Hernandez et al., 2019). Overall, FXR activation has effective therapeutic effect on NAFLD and cholesterol metabolism, which may become a breakthrough for FXR agonists to be used in the treatment of cardiometabolic diseases.

ROLE OF FXR IN HIGH-FAT DIETARY CONSUMPTION AND OBESITY

With the development of the social economy, the diet and lifestyle habits have changed drastically. The sharp increase in obesity rates worldwide poses a constant health challenge, which is associated with the morbidity and mortality of multiple diseases. At present, obesity is a leading risk factor for cardiometabolic diseases in the general population. Overweight and obesity lead to adverse metabolic effects on blood pressure, blood lipid and insulin resistance as well as increased occurrence of metabolic syndrome (Riobo Servan, 2013). Population-based epidemiological studies investigated the association of cardiometabolic risk factors with obesity indices, which can be used to aid screening for cardiometabolic risks in different population settings. A study of older adults in Colombia showed that the body roundness index (BRI) and waist-to-height ratio (WtHR), which are both obesity-related parameters, have a moderate discriminating power for detecting high cardiometabolic risks and are useful screening tools (Ramirez-Velez et al., 2019). Another study investigated the association of body mass index (BMI), waist circumference (WC) and body fat per cent (BF%) with cardiometabolic risk factors in Unguja Island, Zanzibar (Nyangasa et al., 2019). This study found that high BMI, WC and BF% were strongly associated with hypertension, with individuals with high WC being twice more likely to have hypertension. In the past, the importance of obesity as a risk factor for cardiometabolic diseases has been underestimated among children and adolescents. A recent study performed a cross-sectional analysis of data from overweight or obese children and young adults 3 to 19 years of age to assess the prevalence of multiple cardiometabolic risk factors according to the severity of obesity (Skinner et al., 2015). They found that severe obesity in children and young adults was associated with an increased prevalence of cardiometabolic risk factors, particularly among boys and young men. Accordingly, there is a need for effective interventions to create awareness as well as for primary prevention public health strategies aimed at preventing cardiometabolic diseases caused by obesity.

The FXR is an important regulator in the promotion of lipid metabolism and organismal energy metabolism, as well as in reducing inflammation. Based on these findings, the specific targeting of FXR may be an effective approach to treat obesity-induced cardiometabolic diseases. A central role of FXR in lipid homeostasis has been confirmed in mice with gene ablation or HFD-induced obesity. High-fat diet-fed intestine-specific Fxr-null mice were less obese compared with their wild-type counterparts (Li et al., 2013). Mice with intestine-specific FXR disruption had

reduced hepatic triglyceride accumulation in response to a HFD-induced (Jiang et al., 2015a). Meanwhile, researcher also found that sex specific expression of lipid-related genes, including Fas, Colla1, Timp1, and Smpd3, may be FXR-dependent (Jiang et al., 2015b). However, other studies have found that lack of FXR can adversely affect lipid metabolism. Fxr/Bar null mice and Fxr-deficient mice have increased hepatic cholesterol, triglycerides and high-density lipoprotein cholesterol, as well as a proatherogenic serum lipoprotein profile (Sinal et al., 2000; Lambert et al., 2003). And there is no gender-based difference in this adverse effect. FXR knockout mice do not display sex-specific expression of lipid- and bile acid-associated genes (Sheng et al., 2017). Lipid metabolism can be increased when FXR is activated. When CDCA is given to hamsters fed a HFD, it significantly reduces triglycerides and very-low-density cholesterol (Bilz et al., 2006). They also found that activation of FXR facilitates the clearance of very-low-density cholesterol and chylomicrons by repressing the expression of microsomal triglyceride transfer protein and apolipoprotein B (Zhang et al., 2004).

Despite recent advances in understanding the relationship between FXRs and obesity, the specific mechanism by which FXR regulates obesity requires further studies. Some studies analyzed the hepatic genome-wide binding sites of FXR in healthy mice and mice with diet-induced obesity. They found that more FXR-binding sites are likely functionally inactive in obesity and direct gene repression by agonist-activated FXR is common (Lee et al., 2012). In addition, the beneficial effect of bariatric surgical procedures, such as vertical sleeve gastrectomy (VSG), may also be related to FXR. Since FXR can maintain weight loss after VSG, it is considered as an important molecular underpinning for the beneficial effects of this weight-loss surgical procedure (Ryan et al., 2014). Although the different research studies reach different or even contrary conclusions, they suggest that inhibition of intestinal FXR is a potential target for anti-obesity drug development.

ROLE OF FXR IN INSULIN RESISTANCE AND DIABETES MELLITUS

Insulin resistance refers to a state of weakened insulin response, which is a common feature of T2D, obesity, and hypertension (Rask-Madsen and Kahn, 2012). T2D is associated with chronic inflammation, characterized by the release of excessive proinflammatory cytokines, acute-phase proteins and other mediators, all of which are important damage factors for CVD (Paneni et al., 2013). Insulin resistance is not only an important pathological factor of diabetes, but is also considered as the underlying cause of the development of the cardiometabolic syndrome. It has been reported that fasting insulin (an indicator of insulin resistance) contributed to the development of the metabolic syndrome, including hypertension, hypertriglyceridemia, reduced HDL-C, and T2D (Haffner et al., 1992). Insulin resistance is the direct cause of elevated fasting glucose and prediabetes (impaired glucose tolerance) contributing to glycotoxicity, lipotoxicity, and inflammation, all of which trigger and accelerate vascular damage, endothelial dysfunction, hypertension, atherosclerosis and CVD (Ouchi et al., 2011). There are many factors that cause insulin resistance, including dysfunctional binding to insulin receptor, abnormal insulin secretion, lipid oversupply and alterations in substrate metabolism (Roberts et al., 2013). Elevated plasma-free fatty acids played a key role in the development of insulin resistance and T2D, and the decrease in plasma-free fatty acids was closely correlated with improvement in insulin sensitivity in T2D ($r=0.76$) subjects ($P< 0.001$) (Daniele et al., 2014). Excess free fatty acid can simultaneously cause insulin resistance, activate oxidative stress and ER stress, ultimately leading to the secretion of a variety of proinflammatory cytokines, both of which could conversely produce the development of insulin resistance (Boden, 2011). As the key regulatory element of free fatty acid metabolism, FXR has effective therapeutic effect on insulin resistance and T2D.

A recent study in a rabbit model of HFD-induced metabolic syndrome indicated that long-term treatment with INT-767 decreased HFD-induced fatty acid synthesis and fibrosis, while increasing lipid handling and improving insulin resistance (Comeglio et al., 2018). Insulin resistance is associated with increased pro-inflammatory cytokines and decreased anti-inflammatory cytokines released by adipose tissue. FXR activation was found to increase the release of anti-inflammatory cytokines and insulin-sensitive adipokines (adiponectin and leptin), and then reversed insulin resistance (Shihabudeen et al., 2015). FXR agonist fexaramine (Fex) was reported to active white adipose tissue and reduce insulin resistance enhancing glucose tolerance and lowering inflammatory cytokine levels (Fang et al., 2015). FXR activation reduced liver expression of genes involved in fatty acid synthesis, lipogenesis, and gluconeogenesis, thereby reversing the development of insulin resistance and liver steatosis in *fa/fa* rats (Cipriani et al., 2010). A clinical study also has reported that administration of 25 or 50 mg of OCA for 6 weeks increased insulin sensitivity in patients with T2DM and NAFLD (Mudaliar et al., 2013). Recent studies indicate that FXR has the potential to be a therapeutic target for T2D. HS218, a new FXR specific antagonist, suppressed liver gluconeogenesis and effectively improved glucose homeostasis in db/db and HFD-induced T2D mice by inhibiting Fxr binding to PGC-1α promoter (Xu et al., 2018). FXR activation mitigated tacrolimus-induced DM by regulating gluconeogenesis as well as glucose uptake of renal in a PGC1α/Foxo1-dependent manner (Li L. et al., 2019). In summary, FXR has a significant regulatory effect on insulin resistance and T2D. However, further study is still needed to confirm the therapeutic potency and mechanism of FXR agonists on T2D.

ROLE OF FXR IN INTESTINAL MICROORGANISM

The human gut harbors more than 10 trillion microbial cells, which provide unique metabolic functions to the host. Commensal gut microbiota is said to act as a "signaling hub" in many pathophysiological functions of the mammalian host (Cani, 2018).

The gut microbiome plays a critical role in host susceptibility to and risk of disease (Sender et al., 2016). Among them, the association between gut microbiota and cardiometabolic diseases has attracted wide attention. Numerous studies have shown that intestinal bacteria are closely related to cardiometabolic diseases. Differences in microbial richness, species abundance, and microbial community structure might be involved in the pathogenesis of cardiometabolic diseases. Patients with symptomatic atherosclerosis were found to have increased number of the genus *Collinsella*, while the healthy controls had an increased abundance of *Eubacterium* and *Roseburia* (Karlsson et al., 2012). *Candida*, *Campylobacter*, and *Shigella* species apparently increased with the duration and aggravation of the disease. The importance of gut microbiota in CVD development is evident in germ-free animal models. For example, Li et al. (2017) transferred feces from hypertensive patients to germ-free mice and found elevated blood pressure in germ-free mice exposed to feces. Also, Stepankova et al. (2010) found that germ-free Apoe$^{-/-}$ mice fed the low-cholesterol standard diet had increased atherosclerotic plaques compared with their conventionally reared counterparts with defined microflora. However, it should be noted that other researchers have come to the opposite conclusion, and they suggested that gut microbiota could accelerate the formation of atherosclerosis (Kasahara et al., 2017). Although there is controversy about the precise molecular mechanisms by which gut microbiota influences cardiometabolic diseases, there is no doubt that targeting gut microbiota is an effective strategy for the treatment of cardiometabolic diseases. Numerous research studies have identified the gut microbiota as a novel regulator of cardiometabolic diseases. For instance, 12-week administration, *via* drinking water, of *E. coli* Nissle 1917 (pNAPE-EcN) expressing the endogenous lipid satiety factors N-acyl phosphatidylethanolamines (NAPEs), were found to improve various indices of cardiometabolic disease in Ldlr$^{-/-}$ mice (May-Zhang et al., 2019).

FXR and gut microbiota are closely linked. For instance, FXR alters the gut microbiota composition, and transplantation of the gut microbiota into germ-free mice changes the lean phenotype of *Fxr* knockout donor mice, indicating that Fxr may contribute to increased adiposity by altering the microbiota composition (Schoeler and Caesar, 2019). The FXR-gut microbiota interaction plays an important role in most forms of CVD. Trimethylamine N-oxide (TMAO) is an intestinal bacterial-related metabolite. Trimethylamine (TMA), the precursor of TMAO, is oxidized by the host hepatic enzyme flavin monooxygenase 3 (FMO3) to generate TMAO (Bennett et al., 2013). High levels of TMAO represent a strong prognostic biomarker of cardiovascular events (Wang et al., 2011). The study found FXR could induce FMO3 expression, thereby increasing plasma TMAO levels (Bennett et al., 2013).

About 95% of BAs are reabsorbed and transported back to the liver *via* the portal circulation, but the remaining 5% will be transformed into secondary BAs by intestinal microorganisms by microorganisms in the intestine. BA metabolism is modulated by BA biotransformation in the intestine. Gut microbiota-derived secondary BAs play important roles in the development of atherosclerosis through the modulation of FXR. Sayin et al. (2013) found that gut microbiota regulated expression of FGF15 in the ileum and CYP7A1 in the liver through FXR-dependent mechanisms so as to maintain the balance of cholesterol metabolism. Sun et al. (2018) found that *Bacteroides fragilis* was decreased and the BA glycoursodeoxycholic acid (GUDCA) was increased in the gut of patients with T2D after metformin treatment. These changes were accompanied by inhibition of intestinal FXR signaling, which indicated that metformin acts in part through a *Bacteroides fragilis*–GUDCA–intestinal FXR axis to improve metabolic dysfunction. These findings also suggest that microbiota-derived secondary BAs might be involved in signaling pathways that regulate lipid and glucose metabolism due to their binding affinity to FXR thereby playing a role in the regulation of cardiometabolic disease and vascular function. In addition, some studies suggest that there is sex-specific interplay among the gut microbiome, FXR, and BAs. Women reportedly produce higher concentrations of secondary BAs compared to men (Baars et al., 2018), therefore, perhaps, women harbor more gut microbiota that are capable of bile acid transformations. Secondary bile acids may then activate a number of downstream targets, including FXR, having potential mixed effects on CVD risk (Claudel et al., 2005).

ROLE OF FXR ON AGING

Aging is an inevitable natural process and also a complex process that takes place in all living organisms. At present, there is a growing population of elderly people. Aging population is a big challenge and a great economic burden all over the world. It is expected that the population over 65 years of age will reach 22% by 2040 (Heidenreich et al., 2011). The high incidence rate of age-related degenerative diseases brings impact to the social health system. Now people have realized that aging is an important risk factor in the development of CVD (North and Sinclair, 2012). To effectively halt the progression of cardiometabolic disease, researcher actively explore the molecular mechanisms behind declined organs function in aging. Inflammation (Cevenini et al., 2010) and cellular oxidative stress (Chen et al., 2007) are considered as key mechanisms that aging induced diseases. The inflammatory biomarkers related to aging, such as high-sensitivity C-reactive protein (hs-CRP), IL6 and TNF, presenting high circulating concentrations (Singh and Newman, 2011), leading to a chronic overproduction of ROS (Dinh et al., 2014) and mitochondrial dysfunction later in life (Anderson et al., 2018). These factors can lead to arterial dysfunction. And the main changes are increased stiffness of the large arteries and reduced vascular endothelial function (Lakatta and Levy, 2003). The vascular endothelial function dysfunction can aggravate inflammation and oxidative stress, forming a vicious circle. These pathological changes induced by aging which partially explains the pathogenesis of cardiometabolic disease include hypertension, atherosclerosis and T2D. In addition, it should be noted that aging presents a unique challenge to the prediction of cardiometabolic risk in men and women as both sex hormone-dependent and sex hormone-independent effects play various roles in the development of aging related cardiovascular diseases in men versus women (Faulkner and

Belin de Chantemele, 2019). Therefore, a better understanding mechanism of aging contributes to the formulation of new therapeutic strategies for age-related cardiovascular diseases and improvement the quality of life.

As aging progresses, chronic imbalance of energy intake and expenditure promote hepatic steatosis and muscle insulin resistance (Shulman, 2014). Many studies have shown increased body weight and decreased physical activity resulting in glucose intolerance and insulin resistance in aging mice (Kenyon, 2010; Houtkooper et al., 2011). FXR and SHP selectively expressed in liver and have pivotal functions in metabolic pathways such as bile acid homeostasis, fatty acid and glucose metabolism. Previous study has shown that FXR reduction was responsible for the hepatic TG accumulation in aging mice, suggesting that FXR dysfunction might be involved in the development of hepatosteatosis in aging mice (Xiong et al., 2014). On the other hand, research has found that combined deletion of the hepatic FXR/SHP axis improves glucose/fatty acid homeostasis in aged mice, reversing the aging phenotype of body weight gain, increased adiposity and glucose/insulin tolerance (Kim et al., 2017). Moreover, FXR-deficient C57BL/6 mice were more prone to spontaneous development of NASH than wild-type upon aging (Bjursell et al., 2013).

CONCLUSION

Cardiometabolic diseases are very complex diseases, which not only involve cardiovascular diseases, diabetes, and obesity, but also have complicated pathological mechanisms, including disorders of lipid metabolism, insulin resistance, abnormal glucose metabolism, oxidative stress, and inflammatory response. Intestinal microorganism also participates in the pathological process of cardiovascular disease through microbial metabolism. As the bile acids receptor, FXR plays a crucial role in bile acids metabolism and cholesterol homeostasis. Activating FXR could regulate lipid metabolism, maintain cardiovascular function, reduce insulin resistance, enhance glucose tolerance and decrease inflammatory cytokine levels. Therefore, more and more attention has been paid to the potential role of FXR as a regulatory factor in repairing damaged vessel, increasing insulin sensitivity and reducing markers of liver inflammation and so on. (As shown in **Figure 1**).

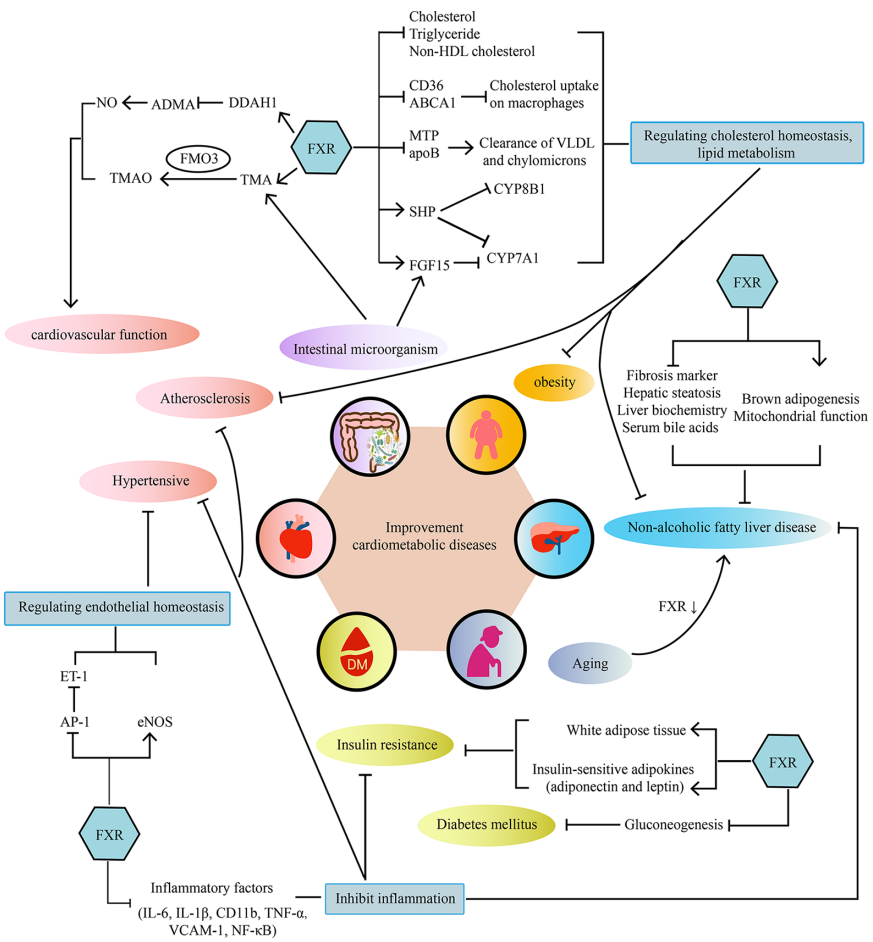

FIGURE 1 | The main mechanisms of the effect of FXR on cardiometabolic diseases. FXR acts on cardiometabolic diseases in a multi-organ and multifactorial manner.

Therefore, FXR agonists have the potential to become a new treatment strategy for cardiometabolic diseases. However, although FXR agonists have shown good clinical efficacy in the treatment of NAFLD/NASH, there is no definite clinical trial to confirm its benefit for cardiovascular disease. Further well-designed clinical trials of FXR agonists are required to prove their efficacy in cardiometabolic diseases and explore the underlying mechanism.

AUTHOR CONTRIBUTIONS

CL, JY, and WY searched for articles and wrote the paper. YW compiled the table. YQ drew the figure. YL proposed the topics and checked the whole manuscript. All authors contributed to the article and approved the submitted version.

FUNDING

This work received support by National Nature Science Foundation of China (81774242, 81804006), China Postdoctoral Science Foundation (2020M672125), the Major Science Natural Science Foundation of the Shandong Province (ZR2018ZC1157), and Taishan Scholar Post Construction Fund (ts201712042).

REFERENCES

Abu-Hayyeh, S., Papacleovoulou, G., Lovgren-Sandblom, A., Tahir, M., Oduwole, O., Jamaludin, N. A., et al. (2013). Intrahepatic cholestasis of pregnancy levels of sulfated progesterone metabolites inhibit farnesoid X receptor resulting in a cholestatic phenotype. *Hepatology* 57 (2), 716–726. doi: 10.1002/hep.26055

Adams, L. A., Anstee, Q. M., Tilg, H., and Targher, G. (2017). Non-alcoholic fatty liver disease and its relationship with cardiovascular disease and other extrahepatic diseases. *Gut* 66 (6), 1138–1153. doi: 10.1136/gutjnl-2017-313884

Akwabi-Ameyaw, A., Bass, J. Y., Caldwell, R. D., Caravella, J. A., Chen, L., Creech, K. L., et al. (2008). Conformationally constrained farnesoid X receptor (FXR) agonists: Naphthoic acid-based analogs of GW 4064. *Bioorg. Med. Chem. Lett.* 18 (15), 4339–4343. doi: 10.1016/j.bmcl.2008.06.073

Al-Khaifi, A., Rudling, M., and Angelin, B. (2018). An FXR Agonist Reduces Bile Acid Synthesis Independently of Increases in FGF19 in Healthy Volunteers. *Gastroenterology* 155 (4), 1012–1016. doi: 10.1053/j.gastro.2018.06.038

An, P., Wei, G., Huang, P., Li, W., Qi, X., Lin, Y., et al. (2020). A novel non-bile acid FXR agonist EDP-305 potently suppresses liver injury and fibrosis without worsening of ductular reaction. *Liver Int.* 40 (7), 1655–1669. doi: 10.1111/liv.14490

Anderson, R., Richardson, G. D., and Passos, J. F. (2018). Mechanisms driving the ageing heart. *Exp. Gerontol.* 109, 5–15. doi: 10.1016/j.exger.2017.10.015

Arnett, D. K., Blumenthal, R. S., Albert, M. A., Buroker, A. B., Goldberger, Z. D., Hahn, E. J., et al. (2019). 2019 ACC/AHA Guideline on the Primary Prevention of Cardiovascular Disease: A Report of the American College of Cardiology/American Heart Association Task Force on Clinical Practice Guidelines. *Circulation* 140 (11), e596–e646. doi: 10.1161/CIR.0000000000000678

Baars, A., Oosting, A., Lohuis, M., Koehorst, M., El Aidy, S., Hugenholtz, F., et al. (2018). Sex differences in lipid metabolism are affected by presence of the gut microbiota. *Sci. Rep.* 8 (1), 13426. doi: 10.1038/s41598-018-31695-w

Badman, M. K., Chen, J., Desai, S., Vaidya, S., Neelakantham, S., Zhang, J., et al. (2020). Safety, Tolerability, Pharmacokinetics, and Pharmacodynamics of the Novel Non-Bile Acid FXR Agonist Tropifexor (LJN452) in Healthy Volunteers. *Clin. Pharmacol. Drug Dev.* 9 (3), 395–410. doi: 10.1002/cpdd.762

Baghdasaryan, A., Claudel, T., Gumhold, J., Silbert, D., Adorini, L., Roda, A., et al. (2011). Dual farnesoid X receptor/TGR5 agonist INT-767 reduces liver injury in the Mdr2-/- (Abcb4-/-) mouse cholangiopathy model by promoting biliary HCO(-)(3) output. *Hepatology* 54 (4), 1303–1312. doi: 10.1002/hep.24537

Bass, J. Y., Caravella, J. A., Chen, L., Creech, K. L., Deaton, D. N., Madauss, K. P., et al. (2011). Conformationally constrained farnesoid X receptor (FXR) agonists: heteroaryl replacements of the naphthalene. *Bioorg. Med. Chem. Lett.* 21 (4), 1206–1213. doi: 10.1016/j.bmcl.2010.12.089

Bennett, B. J., de Aguiar Vallim, T. Q., Wang, Z., Shih, D. M., Meng, Y., Gregory, J., et al. (2013). Trimethylamine-N-oxide, a metabolite associated with atherosclerosis, exhibits complex genetic and dietary regulation. *Cell Metab.* 17 (1), 49–60. doi: 10.1016/j.cmet.2012.12.011

Bilz, S., Samuel, V., Morino, K., Savage, D., Choi, C. S., and Shulman, G. I. (2006). Activation of the farnesoid X receptor improves lipid metabolism in combined hyperlipidemic hamsters. *Am. J. Physiol. Endocrinol. Metab.* 290 (4), E716–E722. doi: 10.1152/ajpendo.00355.2005

Birbeck, G. L., Meyer, A. C., and Ogunniyi, A. (2015). Nervous system disorders across the life course in resource-limited settings. *Nature* 527 (7578), S167–S171. doi: 10.1038/nature16031

Bjursell, M., Wedin, M., Admyre, T., Hermansson, M., Böttcher, G., Göransson, M., et al. (2013). Ageing Fxr deficient mice develop increased energy expenditure, improved glucose control and liver damage resembling NASH. *PloS One* 8 (5), e64721. doi: 10.1371/journal.pone.0064721

Bluher, M. (2019). Obesity: global epidemiology and pathogenesis. *Nat. Rev. Endocrinol.* 15 (5), 288–298. doi: 10.1038/s41574-019-0176-8

Boden, G. (2011). Obesity, insulin resistance and free fatty acids. *Curr. Opin. Endocrinol. Diabetes Obes.* 18 (2), 139–143. doi: 10.1097/MED.0b013e3283444b09

Boger, R. H., Sullivan, L. M., Schwedhelm, E., Wang, T. J., Maas, R., Benjamin, E. J., et al. (2009). Plasma asymmetric dimethylarginine and incidence of cardiovascular disease and death in the community. *Circulation* 119 (12), 1592–1600. doi: 10.1161/CIRCULATIONAHA.108.838268

Cani, P. D. (2018). Human gut microbiome: hopes, threats and promises. *Gut* 67 (9), 1716–1725. doi: 10.1136/gutjnl-2018-316723

Cao, Y., Xiao, Y., Zhou, K., Yan, J., Wang, P., Yan, W., et al. (2019). FXR agonist GW4064 improves liver and intestinal pathology and alters bile acid metabolism in rats undergoing small intestinal resection. *Am. J. Physiol. Gastrointest Liver Physiol.* 317 (2), G108–G115. doi: 10.1152/ajpgi.00356.2017

Carino, A., Biagioli, M., Marchiano, S., Fiorucci, C., Bordoni, M., Roselli, R., et al. (2020). Opposite effects of the FXR agonist obeticholic acid on Mafg and Nrf2 mediate the development of acute liver injury in rodent models of cholestasis. *Biochim. Biophys. Acta Mol. Cell Biol. Lipids* 1865 (9), 158733. doi: 10.1016/j.bbalip.2020.158733

Carotti, A., Marinozzi, M., Custodi, C., Cerra, B., Pellicciari, R., Gioiello, A., et al. (2014). Beyond bile acids: targeting Farnesoid X Receptor (FXR) with natural and synthetic ligands. *Curr. Top. Med. Chem.* 14 (19), 2129–2142. doi: 10.2174/1568026614666141112094058

Carter, B. A., Taylor, O. A., Prendergast, D. R., Zimmerman, T. L., Von Furstenberg, R., Moore, D. D., et al. (2007). Stigmasterol, a soy lipid-derived phytosterol, is an antagonist of the bile acid nuclear receptor FXR. *Pediatr. Res.* 62 (3), 301–306. doi: 10.1203/PDR.0b013e3181256492

Cevenini, E., Caruso, C., Candore, G., Capri, M., Nuzzo, D., Duro, G., et al. (2010). Age-related inflammation: the contribution of different organs, tissues and systems. How to face it for therapeutic approaches. *Curr. Pharm. Des.* 16 (6), 609–618. doi: 10.2174/138161210790883840

Chen, Y., Traverse, J. H., Du, R., Hou, M., and Bache, R. J. (2002). Nitric oxide modulates myocardial oxygen consumption in the failing heart. *Circulation* 106 (2), 273–279. doi: 10.1161/01.cir.0000021120.90970.b9

Chen, Y., Park, S., Li, Y., Missov, E., Hou, M., Han, X., et al. (2003). Alterations of gene expression in failing myocardium following left ventricular assist device support. *Physiol. Genomics* 14 (3), 251–260. doi: 10.1152/physiolgenomics.00022.2003

Chen, Y., Li, Y., Zhang, P., Traverse, J. H., Hou, M., Xu, X., et al. (2005). Dimethylarginine dimethylaminohydrolase and endothelial dysfunction in failing hearts. *Am. J. Physiol. Heart Circ. Physiol.* 289 (5), H2212–H2219. doi: 10.1152/ajpheart.00224.2005

Chen, J. H., Hales, C. N., and Ozanne, S. E. (2007). DNA damage, cellular senescence and organismal ageing: causal or correlative? *Nucleic Acids Res.* 35 (22), 7417–7428. doi: 10.1093/nar/gkm681

Cherney, D. Z. I., and Lam, T. K. T. (2018). A Gut Feeling for Metformin. *Cell Metab.* 28 (6), 808–810. doi: 10.1016/j.cmet.2018.11.012

Chianelli, D., Rucker, P. V., Roland, J., Tully, D. C., Nelson, J., Liu, X., et al. (2020). Nidufexor (LMB763), a Novel FXR Modulator for the Treatment of Nonalcoholic Steatohepatitis. *J. Med. Chem.* 63 (8), 3868–3880. doi: 10.1021/acs.jmedchem.9b01621

Choi, H., Hwang, H., Chin, J., Kim, E., Lee, J., Nam, S. J., et al. (2011). Tuberatolides, potent FXR antagonists from the Korean marine tunicate Botryllus tuberatus. *J. Nat. Prod.* 74 (1), 90–94. doi: 10.1021/np100489u

Cipriani, S., Mencarelli, A., Palladino, G., and Fiorucci, S. (2010). FXR activation reverses insulin resistance and lipid abnormalities and protects against liver steatosis in Zucker (fa/fa) obese rats. *J. Lipid Res.* 51 (4), 771–784. doi: 10.1194/jlr.M001602

Claudel, T., Staels, B., and Kuipers, F. (2005). The Farnesoid X receptor: a molecular link between bile acid and lipid and glucose metabolism. *Arterioscler. Thromb. Vasc. Biol.* 25 (10), 2020–2030. doi: 10.1161/01.ATV.0000178994.21828.a7

Comeglio, P., Cellai, I., Mello, T., Filippi, S., Maneschi, E., Corcetto, F., et al. (2018). INT-767 prevents NASH and promotes visceral fat brown adipogenesis and mitochondrial function. *J. Endocrinol.* 238 (2), 107–127. doi: 10.1530/JOE-17-0557

Daniele, G., Eldor, R., Merovci, A., Clarke, G. D., Xiong, J., Tripathy, D., et al. (2014). Chronic reduction of plasma free fatty acid improves mitochondrial function and whole-body insulin sensitivity in obese and type 2 diabetic individuals. *Diabetes* 63 (8), 2812–2820. doi: 10.2337/db13-1130

De Fabiani, E., Mitro, N., Anzulovich, A. C., Pinelli, A., Galli, G., and Crestani, M. (2001). The negative effects of bile acids and tumor necrosis factor-alpha on the transcription of cholesterol 7alpha-hydroxylase gene (CYP7A1) converge to hepatic nuclear factor-4: a novel mechanism of feedback regulation of bile acid synthesis mediated by nuclear receptors. *J. Biol. Chem.* 276 (33), 30708–30716. doi: 10.1074/jbc.M103270200

Deng, R., Yang, D., Yang, J., and Yan, B. (2006). Oxysterol 22(R)-hydroxycholesterol induces the expression of the bile salt export pump through nuclear receptor farsenoid X receptor but not liver X receptor. *J. Pharmacol. Exp. Ther.* 317 (1), 317–325. doi: 10.1124/jpet.105.097758

Dinh, Q. N., Drummond, G. R., Sobey, C. G., and Chrissobolis, S. (2014). Roles of inflammation, oxidative stress, and vascular dysfunction in hypertension. *BioMed. Res. Int.* 2014, 406960. doi: 10.1155/2014/406960

Downes, M., Verdecia, M. A., Roecker, A. J., Hughes, R., Hogenesch, J. B., Kast-Woelbern, H. R., et al. (2003). A chemical, genetic, and structural analysis of the nuclear bile acid receptor FXR. *Mol. Cell* 11 (4), 1079–1092. doi: 10.1016/s1097-2765(03)00104-7

Erstad, D. J., Farrar, C. T., Ghoshal, S., Masia, R., Ferreira, D. S., Chen, Y. I., et al. (2018). Molecular magnetic resonance imaging accurately measures the antifibrotic effect of EDP-305, a novel farnesoid X receptor agonist. *Hepatol. Commun.* 2 (7), 821–835. doi: 10.1002/hep4.1193

Evans, M. J., Mahaney, P. E., Borges-Marcucci, L., Lai, K., Wang, S., Krueger, J. A., et al. (2009). A synthetic farnesoid X receptor (FXR) agonist promotes cholesterol lowering in models of dyslipidemia. *Am. J. Physiol. Gastrointest Liver Physiol.* 296 (3), G543–G552. doi: 10.1152/ajpgi.90585.2008

Fang, S., Suh, J. M., Reilly, S. M., Yu, E., Osborn, O., Lackey, D., et al. (2015). Intestinal FXR agonism promotes adipose tissue browning and reduces obesity and insulin resistance. *Nat. Med.* 21 (2), 159–165. doi: 10.1038/nm.3760

Faulkner, J. L., and Belin de Chantemele, E. J. (2019). Sex hormones, aging and cardiometabolic syndrome. *Biol. Sex Differ.* 10 (1), 30. doi: 10.1186/s13293-019-0246-6

Festa, C., Finamore, C., Marchiano, S., Di Leva, F. S., Carino, A., Monti, M. C., et al. (2019). Investigation around the Oxadiazole Core in the Discovery of a New Chemotype of Potent and Selective FXR Antagonists. *ACS Med. Chem. Lett.* 10 (4), 504–510. doi: 10.1021/acsmedchemlett.8b00534

Fiorucci, S., Clerici, C., Antonelli, E., Orlandi, S., Goodwin, B., Sadeghpour, B. M., et al. (2005). Protective effects of 6-ethyl chenodeoxycholic acid, a farnesoid X receptor ligand, in estrogen-induced cholestasis. *J. Pharmacol. Exp. Ther.* 313 (2), 604–612. doi: 10.1124/jpet.104.079665

Flatt, B., Martin, R., Wang, T. L., Mahaney, P., Murphy, B., Gu, X. H., et al. (2009). Discovery of XL335 (WAY-362450), a highly potent, selective, and orally active agonist of the farnesoid X receptor (FXR). *J. Med. Chem.* 52 (4), 904–907. doi: 10.1021/jm8014124

Ford, E. S. (2005). Risks for all-cause mortality, cardiovascular disease, and diabetes associated with the metabolic syndrome: a summary of the evidence. *Diabetes Care* 28 (7), 1769–1778. doi: 10.2337/diacare.28.7.1769

Galassi, A., Reynolds, K., and He, J. (2006). Metabolic syndrome and risk of cardiovascular disease: a meta-analysis. *Am. J. Med.* 119 (10), 812–819. doi: 10.1016/j.amjmed.2006.02.031

Gami, A. S., Witt, B. J., Howard, D. E., Erwin, P. J., Gami, L. A., Somers, V. K., et al. (2007). Metabolic syndrome and risk of incident cardiovascular events and death: a systematic review and meta-analysis of longitudinal studies. *J. Am. Coll. Cardiol.* 49 (4), 403–414. doi: 10.1016/j.jacc.2006.09.032

Gan, L. T., Van Rooyen, D. M., Koina, M. E., McCuskey, R. S., Teoh, N. C., and Farrell, G. C. (2014). Hepatocyte free cholesterol lipotoxicity results from JNK1-mediated mitochondrial injury and is HMGB1 and TLR4-dependent. *J. Hepatol.* 61 (6), 1376–1384. doi: 10.1016/j.jhep.2014.07.024

Gautam, A., Paudel, Y. N., Abidin, S., and Bhandari, U. (2019). Guggulsterone, a farnesoid X receptor antagonist lowers plasma trimethylamine-N-oxide levels: An evidence from in vitro and in vivo studies. *Hum. Exp. Toxicol.* 38 (3), 356–370. doi: 10.1177/0960327118817862

Genin, M. J., Bueno, A. B., Agejas Francisco, J., Manninen, P. R., Bocchinfuso, W. P., Montrose-Rafizadeh, C., et al. (2015). Discovery of 6-(4-{[5-Cyclopropyl-3-(2,6-dichlorophenyl)isoxazol-4-yl]methoxy}piperidin-1-yl)- 1-methyl-1H-indole-3-carboxylic Acid: A Novel FXR Agonist for the Treatment of Dyslipidemia. *J. Med. Chem.* 58 (24), 9768–9772. doi: 10.1021/acs.jmedchem.5b01161

Gerardus, B. S., Jus, P. D., and Bethus, S. J. "ASSAYS FOR LIGANDS FOR NUCLEAR RECEPTORS". EP).

Guo, G. L., Santamarina-Fojo, S., Akiyama, T. E., Amar, M. J., Paigen, B. J., Brewer, B.Jr., et al. (2006). Effects of FXR in foam-cell formation and atherosclerosis development. *Biochim. Biophys. Acta* 1761 (12), 1401–1409. doi: 10.1016/j.bbalip.2006.09.018

Haffner, S. M., Valdez, R. A., Hazuda, H. P., Mitchell, B. D., Morales, P. A., and Stern, M. P. (1992). Prospective analysis of the insulin-resistance syndrome (syndrome X). *Diabetes* 41 (6), 715–722. doi: 10.2337/diab.41.6.715

Hager, L., Li, L., Pun, H., Liu, L., Hossain, M. A., Maguire, G. F., et al. (2012). Lecithin:cholesterol acyltransferase deficiency protects against cholesterol-induced hepatic endoplasmic reticulum stress in mice. *J. Biol. Chem.* 287 (24), 20755–20768. doi: 10.1074/jbc.M112.340919

Hambruch, E., Miyazaki-Anzai, S., Hahn, U., Matysik, S., Boettcher, A., Perovic-Ottstadt, S., et al. (2012). Synthetic farnesoid X receptor agonists induce high-density lipoprotein-mediated transhepatic cholesterol efflux in mice and monkeys and prevent atherosclerosis in cholesteryl ester transfer protein transgenic low-density lipoprotein receptor (-/-) mice. *J. Pharmacol. Exp. Ther.* 343 (3), 556–567. doi: 10.1124/jpet.112.196519

Hanniman, E. A., Lambert, G., McCarthy, T. C., and Sinal, C. J. (2005). Loss of functional farnesoid X receptor increases atherosclerotic lesions in apolipoprotein E-deficient mice. *J. Lipid Res.* 46 (12), 2595–2604. doi: 10.1194/jlr.M500390-JLR200

Hartman, H. B., Gardell, S. J., Petucci, C. J., Wang, S., Krueger, J. A., and Evans, M. J. (2009). Activation of farnesoid X receptor prevents atherosclerotic lesion formation in LDLR-/- and apoE-/- mice. *J. Lipid Res.* 50 (6), 1090–1100. doi: 10.1194/jlr.M800619-JLR200

Hartmann, P., Hochrath, K., Horvath, A., Chen, P., Seebauer, C. T., Llorente, C., et al. (2018). Modulation of the intestinal bile acid/farnesoid X receptor/fibroblast growth factor 15 axis improves alcoholic liver disease in mice. *Hepatology* 67 (6), 2150–2166. doi: 10.1002/hep.29676

He, F., Li, J., Mu, Y., Kuruba, R., Ma, Z., Wilson, A., et al. (2006). Downregulation of endothelin-1 by farnesoid X receptor in vascular endothelial cells. *Circ. Res.* 98 (2), 192–199. doi: 10.1161/01.RES.0000200400.55539.85

Heidenreich, P. A., Trogdon, J. G., Khavjou, O. A., Butler, J., Dracup, K., Ezekowitz, M. D., et al. (2011). Forecasting the future of cardiovascular disease in the United States: a policy statement from the American Heart Association. *Circulation* 123 (8), 933–944. doi: 10.1161/CIR.0b013e31820a55f5

Hernandez, E. D., Zheng, L., Kim, Y., Fang, B., Liu, B., Valdez, R. A., et al. (2019). Tropifexor-Mediated Abrogation of Steatohepatitis and Fibrosis Is Associated With the Antioxidative Gene Expression Profile in Rodents. *Hepatol. Commun.* 3 (8), 1085–1097. doi: 10.1002/hep4.1368

Hirschfield, G. M., Mason, A., Luketic, V., Lindor, K., Gordon, S. C., Mayo, M., et al. (2015). Efficacy of obeticholic acid in patients with primary biliary cirrhosis and inadequate response to ursodeoxycholic acid. *Gastroenterology* 148 (4), 751–761 e758. doi: 10.1053/j.gastro.2014.12.005

Houtkooper, R. H., Argmann, C., Houten, S. M., Cantó, C., Jeninga, E. H., Andreux, P. A., et al. (2011). The metabolic footprint of aging in mice. *Sci. Rep.* 1, 134. doi: 10.1038/srep00134

Hu, T., Chouinard, M., Cox, A. L., Sipes, P., Marcelo, M., Ficorilli, J., et al. (2006). Farnesoid X receptor agonist reduces serum asymmetric dimethylarginine levels through hepatic dimethylarginine dimethylaminohydrolase-1 gene regulation. *J. Biol. Chem.* 281 (52), 39831–39838. doi: 10.1074/jbc.M606779200

Inagaki, T., Choi, M., Moschetta, A., Peng, L., Cummins, C. L., McDonald, J. G., et al. (2005). Fibroblast growth factor 15 functions as an enterohepatic signal to regulate bile acid homeostasis. *Cell Metab.* 2 (4), 217–225. doi: 10.1016/j.cmet.2005.09.001

Jadhav, K., Xu, Y., Xu, Y., Li, Y., Xu, J., Zhu, Y., et al. (2018). Reversal of metabolic disorders by pharmacological activation of bile acid receptors TGR5 and FXR. *Mol. Metab.* 9, 131–140. doi: 10.1016/j.molmet.2018.01.005

Jiang, C., Xie, C., Li, F., Zhang, L., Nichols, R. G., Krausz, K. W., et al. (2015a). Intestinal farnesoid X receptor signaling promotes nonalcoholic fatty liver disease. *J. Clin. Invest.* 125 (1), 386–402. doi: 10.1172/JCI76738

Jiang, C., Xie, C., Lv, Y., Li, J., Krausz, K. W., Shi, J., et al. (2015b). Intestine-selective farnesoid X receptor inhibition improves obesity-related metabolic dysfunction. *Nat. Commun.* 6, 10166. doi: 10.1038/ncomms10166

Karlsson, F. H., Fak, F., Nookaew, I., Tremaroli, V., Fagerberg, B., Petranovic, D., et al. (2012). Symptomatic atherosclerosis is associated with an altered gut metagenome. *Nat. Commun.* 3, 1245. doi: 10.1038/ncomms2266

Kasahara, K., Tanoue, T., Yamashita, T., Yodoi, K., Matsumoto, T., Emoto, T., et al. (2017). Commensal bacteria at the crossroad between cholesterol homeostasis and chronic inflammation in atherosclerosis. *J. Lipid Res.* 58 (3), 519–528. doi: 10.1194/jlr.M072165

Kenyon, C. J. (2010). The genetics of ageing. *Nature* 464 (7288), 504–512. doi: 10.1038/nature08980

Kim, K. H., Choi, S., Zhou, Y., Kim, E. Y., Lee, J. M., Saha, P. K., et al. (2017). Hepatic FXR/SHP axis modulates systemic glucose and fatty acid homeostasis in aged mice. *Hepatology* 66 (2), 498–509. doi: 10.1002/hep.29199

Kim, B. R., Kim, J., Lee, J. E., Lee, E. J., and Yoon, J. S. (2020). Therapeutic Effect of Guggulsterone in Primary Cultured Orbital Fibroblasts Obtained From Patients with Graves' Orbitopathy. *Invest. Ophthalmol. Vis. Sci.* 61 (3), 39. doi: 10.1167/iovs.61.3.39

Kumar, G., Singh, D., Tali, J. A., Dheer, D., and Shankar, R. (2020). Andrographolide: Chemical modification and its effect on biological activities. *Bioorg. Chem.* 95, 103511. doi: 10.1016/j.bioorg.2019.103511

Lakatta, E. G., and Levy, D. (2003). Arterial and cardiac aging: major shareholders in cardiovascular disease enterprises: Part I: aging arteries: a "set up". *Vasc. Dis. Circulation* 107 (1), 139–146. doi: 10.1161/01.cir.0000048892.83521.58

Lambert, G., Amar, M. J., Guo, G., Brewer, H. B.Jr., Gonzalez, F. J., and Sinal, C. J. (2003). The farnesoid X-receptor is an essential regulator of cholesterol homeostasis. *J. Biol. Chem.* 278 (4), 2563–2570. doi: 10.1074/jbc.M209525200

Landsberg, L., Aronne, L. J., Beilin, L. J., Burke, V., Igel, L. I., Lloyd-Jones, D., et al. (2013). Obesity-related hypertension: pathogenesis, cardiovascular risk, and treatment–a position paper of the The Obesity Society and The American Society of Hypertension. *Obes. (Silver Spring)* 21 (1), 8–24. doi: 10.1002/oby.20181

Lascar, N., Brown, J., Pattison, H., Barnett, A. H., Bailey, C. J., and Bellary, S. (2018). Type 2 diabetes in adolescents and young adults. *Lancet Diabetes Endocrinol.* 6 (1), 69–80. doi: 10.1016/S2213-8587(17)30186-9

Lee, J., Seok, S., Yu, P., Kim, K., Smith, Z., Rivas-Astroza, M., et al. (2012). Genomic analysis of hepatic farnesoid X receptor binding sites reveals altered binding in obesity and direct gene repression by farnesoid X receptor in mice. *Hepatology* 56 (1), 108–117. doi: 10.1002/hep.25609

Lee, E. A., Lee, D. I., Kim, H. Y., Ahn, S. H., Seong, H. R., Jung, W. H., et al. (2018). Cyp7a1 is continuously increased with disrupted Fxr-mediated feedback inhibition in hypercholesterolemic TALLYHO/Jng mice. *Biochim. Biophys. Acta Mol. Cell Biol. Lipids* 1863 (1), 20–25. doi: 10.1016/j.bbalip.2017.08.007

Leo, R., Therachiyil, L., Siveen, S. K., Uddin, S., Kulinski, M., Buddenkotte, J., et al. (2019). Protein Expression Profiling Identifies Key Proteins and Pathways Involved in Growth Inhibitory Effects Exerted by Guggulsterone in Human Colorectal Cancer Cells. *Cancers (Basel)* 11 (10), 1478. doi: 10.3390/cancers11101478

Li, J., Wilson, A., Kuruba, R., Zhang, Q., Gao, X., He, F., et al. (2008). FXR-mediated regulation of eNOS expression in vascular endothelial cells. *Cardiovasc. Res.* 77 (1), 169–177. doi: 10.1093/cvr/cvm016

Li, J., Wilson, A., Gao, X., Kuruba, R., Liu, Y., Poloyac, S., et al. (2009). Coordinated regulation of dimethylarginine dimethylaminohydrolase-1 and cationic amino acid transporter-1 by farnesoid X receptor in mouse liver and kidney and its implication in the control of blood levels of asymmetric dimethylarginine. *J. Pharmacol. Exp. Ther.* 331 (1), 234–243. doi: 10.1124/jpet.109.153510

Li, F., Jiang, C., Krausz, K. W., Li, Y., Albert, I., Hao, H., et al. (2013). Microbiome remodelling leads to inhibition of intestinal farnesoid X receptor signalling and decreased obesity. *Nat. Commun.* 4, 2384. doi: 10.1038/ncomms3384

Li, D., Lv, J., Liu, F., Liu, P., Yang, X., Feng, Y., et al. (2015). Hypertension burden and control in mainland China: Analysis of nationwide data 2003-2012. *Int. J. Cardiol.* 184, 637–644. doi: 10.1016/j.ijcard.2015.03.045

Li, J., Zhao, F., Wang, Y., Chen, J., Tao, J., Tian, G., et al. (2017). Gut microbiota dysbiosis contributes to the development of hypertension. *Microbiome* 5 (1), 14. doi: 10.1186/s40168-016-0222-x

Li, C., Li, Y., and Gai, Z. (2019). Bile Acids and Farnesoid X Receptor: Novel Target for the Treatment of Diabetic Cardiomyopathy. *Curr. Protein Pept. Sci.* 20 (10), 976–983. doi: 10.2174/1389203720666190726152847

Li, H., Shen, J., Wu, T., Kuang, J., Liu, Q., Cheng, S., et al. (2019). Irisin Is Controlled by Farnesoid X Receptor and Regulates Cholesterol Homeostasis. *Front. Pharmacol.* 10, 548. doi: 10.3389/fphar.2019.00548

Li, L., Zhao, H., Chen, B., Fan, Z., Li, N., Yue, J., et al. (2019). FXR activation alleviates tacrolimus-induced post-transplant diabetes mellitus by regulating renal gluconeogenesis and glucose uptake. *J. Transl. Med.* 17 (1), 418. doi: 10.1186/s12967-019-02170-5

Li, S., Ghoshal, S., Sojoodi, M., Arora, G., Masia, R., Erstad, D. J., et al. (2019). The farnesoid X receptor agonist EDP-305 reduces interstitial renal fibrosis in a mouse model of unilateral ureteral obstruction. *FASEB J.* 33 (6), 7103–7112. doi: 10.1096/fj.201801699R

Li, H., Xi, Y., Xin, X., Tian, H., and Hu, Y. (2020). Gypenosides regulate farnesoid X receptor-mediated bile acid and lipid metabolism in a mouse model of non-alcoholic steatohepatitis. *Nutr. Metab. (Lond)* 17, 34. doi: 10.1186/s12986-020-00454-y

Li, G., and G, L. G (2015). Farnesoid X receptor, the bile acid sensing nuclear receptor, in liver regeneration. *Acta Pharm. Sin. B.* 5 (2), 93–98. doi: 10.1016/j.apsb.2015.01.005

Lim, S., Taskinen, M. R., and Boren, J. (2019). Crosstalk between nonalcoholic fatty liver disease and cardiometabolic syndrome. *Obes. Rev.* 20 (4), 599–611. doi: 10.1111/obr.12820

Lin, H. H. (2015). In Vitro and in Vivo Atheroprotective Effects of Gossypetin against Endothelial Cell Injury by Induction of Autophagy. *Chem. Res. Toxicol.* 28 (2), 202–215. doi: 10.1021/tx5003518

Liu, X., Xue, R., Ji, L., Zhang, X., Wu, J., Gu, J., et al. (2014). Activation of farnesoid X receptor (FXR) protects against fructose-induced liver steatosis via inflammatory inhibition and ADRP reduction. *Biochem. Biophys. Res. Commun.* 450 (1), 117–123. doi: 10.1016/j.bbrc.2014.05.072

Liu, Y., Chen, K., Li, F., Gu, Z., Liu, Q., He, L., et al. (2020). Probiotic Lactobacillus rhamnosus GG Prevents Liver Fibrosis Through Inhibiting Hepatic Bile Acid Synthesis and Enhancing Bile Acid Excretion in Mice. *Hepatology* 71 (6), 2050–2066. doi: 10.1002/hep.30975

Ma, Y., Huang, Y., Yan, L., Gao, M., and Liu, D. (2013). Synthetic FXR agonist GW4064 prevents diet-induced hepatic steatosis and insulin resistance. *Pharm. Res.* 30 (5), 1447–1457. doi: 10.1007/s11095-013-0986-7

Mantovani, A., Pernigo, M., Bergamini, C., Bonapace, S., Lipari, P., Pichiri, I., et al. (2015). Nonalcoholic Fatty Liver Disease Is Independently Associated with Early Left Ventricular Diastolic Dysfunction in Patients with Type 2 Diabetes. *PloS One* 10 (8), e0135329. doi: 10.1371/journal.pone.0135329

Massafra, V., Pellicciari, R., Gioiello, A., and van Mil, S. W. C. (2018). Progress and challenges of selective Farnesoid X Receptor modulation. *Pharmacol. Ther.* 191, 162–177. doi: 10.1016/j.pharmthera.2018.06.009

Matsuzawa, Y., Funahashi, T., and Nakamura, T. (2011). The concept of metabolic syndrome: contribution of visceral fat accumulation and its molecular mechanism. *J. Atheroscler. Thromb.* 18 (8), 629–639. doi: 10.5551/jat.7922

May-Zhang, L. S., Chen, Z., Dosoky, N. S., Yancey, P. G., Boyd, K. L., Hasty, A. H., et al. (2019). Administration of N-Acyl-Phosphatidylethanolamine Expressing Bacteria to Low Density Lipoprotein Receptor(-/-) Mice Improves Indices of Cardiometabolic Disease. *Sci. Rep.* 9 (1), 420. doi: 10.1038/s41598-018-37373-1

Mencarelli, A., Renga, B., Distrutti, E., and Fiorucci, S. (2009). Antiatherosclerotic effect of farnesoid X receptor. *Am. J. Physiol. Heart Circ. Physiol.* 296 (2), H272–H281. doi: 10.1152/ajpheart.01075.2008

Miyazaki-Anzai, S., Masuda, M., Kohno, S., Levi, M., Shiozaki, Y., Keenan, A. L., et al. (2018). Simultaneous inhibition of FXR and TGR5 exacerbates atherosclerotic formation. *J. Lipid Res.* 59 (9), 1709–1713. doi: 10.1194/jlr.M087239

Modica, S., Gadaleta, R. M., and Moschetta, A. (2010). Deciphering the nuclear bile acid receptor FXR paradigm. *Nucl. Recept Signal* 8, e005. doi: 10.1621/nrs.08005

Mridha, A. R., Wree, A., Robertson, A. A. B., Yeh, M. M., Johnson, C. D., Van Rooyen, D. M., et al. (2017). NLRP3 inflammasome blockade reduces liver inflammation and fibrosis in experimental NASH in mice. *J. Hepatol.* 66 (5), 1037–1046. doi: 10.1016/j.jhep.2017.01.022

Mudaliar, S., Henry, R. R., Sanyal, A. J., Morrow, L., Marschall, H. U., Kipnes, M., et al. (2013). Efficacy and safety of the farnesoid X receptor agonist obeticholic acid in patients with type 2 diabetes and nonalcoholic fatty liver disease. *Gastroenterology* 145 (3), 574–582 e571. doi: 10.1053/j.gastro.2013.05.042

Musso, G., Gambino, R., and Cassader, M. (2010). Non-alcoholic fatty liver disease from pathogenesis to management: an update. *Obes. Rev.* 11 (6), 430–445. doi: 10.1111/j.1467-789X.2009.00657.x

Musso, G., Gambino, R., and Cassader, M. (2013). Cholesterol metabolism and the pathogenesis of non-alcoholic steatohepatitis. *Prog. Lipid Res.* 52 (1), 175–191. doi: 10.1016/j.plipres.2012.11.002

Nelson, C. H., Kirby, B. J., Lu, N., Mccolgan, B., Djedjos, C. S., Myers, R. P., et al. (2017). Pharmacokinetics of selonsertib, GS-9674, and/or GS-0976 in combination in healthy subjects. *J. Hepatol.* 66 (1), S151–S152. doi: 10.1016/S0168-8278(17)30575-5

Neuschwander-Tetri, B. A., Loomba, R., Sanyal, A. J., Lavine, J. E., Van Natta, M. L., Abdelmalek, M. F., et al. (2015). Farnesoid X nuclear receptor ligand obeticholic acid for non-cirrhotic, non-alcoholic steatohepatitis (FLINT): a multicentre, randomised, placebo-controlled trial. *Lancet* 385 (9972), 956–965. doi: 10.1016/S0140-6736(14)61933-4

North, B. J., and Sinclair, D. A. (2012). The intersection between aging and cardiovascular disease. *Circ. Res.* 110 (8), 1097–1108. doi: 10.1161/CIRCRESAHA.111.246876

Nyangasa, M. A., Buck, C., Kelm, S., Sheikh, M. A., Brackmann, K. L., and Hebestreit, A. (2019). Association between cardiometabolic risk factors and body mass index, waist circumferences and body fat in a Zanzibari cross-sectional study. *BMJ Open* 9 (7), e025397. doi: 10.1136/bmjopen-2018-025397

Ouchi, N., Parker, J. L., Lugus, J. J., and Walsh, K. (2011). Adipokines in inflammation and metabolic disease. *Nat. Rev. Immunol.* 11 (2), 85–97. doi: 10.1038/nri2921

Paneni, F., Beckman, J. A., Creager, M. A., and Cosentino, F. (2013). Diabetes and vascular disease: pathophysiology, clinical consequences, and medical therapy: part I. *Eur. Heart J.* 34 (31), 2436–2443. doi: 10.1093/eurheartj/eht149

Patel, K., Harrison, S. A., Elkashab, M., Trotter, J. F., Herring, R., Rojter, S., et al. (2020). Cilofexor, a Nonsteroidal FXR AgonistNon-Cirrhotic Patients with Nonalcoholic Steatohepatitis: A Phase 2 Randomized Controlled Trial. *Hepatology* 72 (1), 58–71. doi: 10.1002/hep.31205

Pathak, P., Xie, C., Nichols, R. G., Ferrell, J. M., Boehme, S., Krausz, K. W., et al. (2018). Intestine farnesoid X receptor agonist and the gut microbiota activate G-protein bile acid receptor-1 signaling to improve metabolism. *Hepatology* 68 (4), 1574–1588. doi: 10.1002/hep.29857

Pedrosa, M., Seyedkazemi, S., Francque, S., Sanyal, A., Rinella, M., Charlton, M., et al. (2020). A randomized, double-blind, multicenter, phase 2b study to evaluate the safety and efficacy of a combination of tropifexor and cenicriviroc in patients with nonalcoholic steatohepatitis and liver fibrosis: Study design of the TANDEM trial. *Contemp. Clin. Trials* 88, 105889. doi: 10.1016/j.cct.2019.105889

Pellicciari, R., Fiorucci, S., Camaioni, E., Clerici, C., Costantino, G., Maloney, P. R., et al. (2002). 6alpha-ethyl-chenodeoxycholic acid (6-ECDCA), a potent and selective FXR agonist endowed with anticholestatic activity. *J. Med. Chem.* 45 (17), 3569–3572. doi: 10.1021/jm025529g

Pellicciari, R., Gioiello, A., Costantino, G., Sadeghpour, B. M., Rizzo, G., Meyer, U., et al. (2006). Back door modulation of the farnesoid X receptor: design, synthesis, and biological evaluation of a series of side chain modified chenodeoxycholic acid derivatives. *J. Med. Chem.* 49 (14), 4208–4215. doi: 10.1021/jm060294k

Pellicciari, R., Passeri, D., De Franco, F., Mostarda, S., Filipponi, P., Colliva, C., et al. (2016). Discovery of 3alpha,7alpha,11beta-Trihydroxy-6alpha-ethyl-5beta-cholan-24-oic Acid (TC-100), a Novel Bile Acid as Potent and Highly Selective FXR Agonist for Enterohepatic Disorders. *J. Med. Chem.* 59 (19), 9201–9214. doi: 10.1021/acs.jmedchem.6b01126

Qayyum, F., Lauridsen, B. K., Frikke-Schmidt, R., Kofoed, K. F., Nordestgaard, B. G., and Tybjaerg-Hansen, A. (2018). Genetic variants in CYP7A1 and risk of myocardial infarction and symptomatic gallstone disease. *Eur. Heart J.* 39 (22), 2106–2116. doi: 10.1093/eurheartj/ehy068

Ralston, J., and Nugent, R. (2019). Toward a broader response to cardiometabolic disease. *Nat. Med.* 25 (11), 1644–1646. doi: 10.1038/s41591-019-0642-9

Ramirez-Velez, R., Perez-Sousa, M. A., Izquierdo, M., Cano-Gutierrez, C. A., Gonzalez-Jimenez, E., Schmidt-RioValle, J., et al. (2019). Validation of Surrogate Anthropometric Indices in Older Adults: What Is the Best Indicator of High Cardiometabolic Risk Factor Clustering? *Nutrients* 11 (8), 1701. doi: 10.3390/nu11081701

Rask-Madsen, C., and Kahn, C. R. (2012). Tissue-specific insulin signaling, metabolic syndrome, and cardiovascular disease. *Arterioscler. Thromb. Vasc. Biol.* 32 (9), 2052–2059. doi: 10.1161/ATVBAHA.111.241919

Ren, J., Sowers, J. R., and Zhang, Y. (2018). Metabolic Stress, Autophagy, and Cardiovascular Aging: from Pathophysiology to Therapeutics. *Trends Endocrinol. Metab.* 29 (10), 699–711. doi: 10.1016/j.tem.2018.08.001

Rijzewijk, L. J., Jonker, J. T., van der Meer, R. W., Lubberink, M., de Jong, H. W., Romijn, J. A., et al. (2010). Effects of hepatic triglyceride content on myocardial metabolism in type 2 diabetes. *J. Am. Coll. Cardiol.* 56 (3), 225–233. doi: 10.1016/j.jacc.2010.02.049

Riobo Servan, P. (2013). Obesity and diabetes. *Nutr. Hosp.* 28 Suppl 5, 138–143. doi: 10.3305/nh.2013.28.sup5.6929

Roberts, C. K., Hevener, A. L., and Barnard, R. J. (2013). Metabolic syndrome and insulin resistance: underlying causes and modification by exercise training. *Compr. Physiol.* 3 (1), 1–58. doi: 10.1002/cphy.c110062

Roth, J. D., Feigh, M., Veidal, S. S., Fensholdt, L. K., Rigbolt, K. T., Hansen, H. H., et al. (2018). INT-767 improves histopathological features in a diet-induced ob/ob mouse model of biopsy-confirmed non-alcoholic steatohepatitis. *World J. Gastroenterol.* 24 (2), 195–210. doi: 10.3748/wjg.v24.i2.195

Ryan, K. K., Tremaroli, V., Clemmensen, C., Kovatcheva-Datchary, P., Myronovych, A., Karns, R., et al. (2014). FXR is a molecular target for the effects of vertical sleeve gastrectomy. *Nature* 509 (7499), 183–188. doi: 10.1038/nature13135

Sayin, S. I., Wahlstrom, A., Felin, J., Jantti, S., Marschall, H. U., Bamberg, K., et al. (2013). Gut microbiota regulates bile acid metabolism by reducing the levels of tauro-beta-muricholic acid, a naturally occurring FXR antagonist. *Cell Metab.* 17 (2), 225–235. doi: 10.1016/j.cmet.2013.01.003

Schoeler, M., and Caesar, R. (2019). Dietary lipids, gut microbiota and lipid metabolism. *Rev. Endocr. Metab. Disord.* 20 (4), 461–472. doi: 10.1007/s11154-019-09512-0

Schwabl, P., Hambruch, E., Seeland, B. A., Hayden, H., Wagner, M., Garnys, L., et al. (2017). The FXR agonist PX20606 ameliorates portal hypertension by targeting vascular remodelling and sinusoidal dysfunction. *J. Hepatol.* 66 (4), 724–733. doi: 10.1016/j.jhep.2016.12.005

Sender, R., Fuchs, S., and Milo, R. (2016). Are We Really Vastly Outnumbered? Revisiting the Ratio of Bacterial to Host Cells in Humans. *Cell* 164 (3), 337–340. doi: 10.1016/j.cell.2016.01.013

Sheng, L., Jena, P. K., Liu, H. X., Kalanetra, K. M., Gonzalez, F. J., French, S. W., et al. (2017). Gender Differences in Bile Acids and Microbiota in Relationship with Gender Dissimilarity in Steatosis Induced by Diet and FXR Inactivation. *Sci. Rep.* 7 (1), 1748. doi: 10.1038/s41598-017-01576-9

Shihabudeen, M. S., Roy, D., James, J., and Thirumurugan, K. (2015). Chenodeoxycholic acid, an endogenous FXR ligand alters adipokines and reverses insulin resistance. *Mol. Cell Endocrinol.* 414, 19–28. doi: 10.1016/j.mce.2015.07.012

Shulman, G. I. (2014). Ectopic fat in insulin resistance, dyslipidemia, and cardiometabolic disease. *N. Engl. J. Med.* 371 (12), 1131–1141. doi: 10.1056/NEJMra1011035

Sinal, C. J., Tohkin, M., Miyata, M., Ward, J. M., Lambert, G., and Gonzalez, F. J. (2000). Targeted disruption of the nuclear receptor FXR/BAR impairs bile acid and lipid homeostasis. *Cell* 102 (6), 731–744. doi: 10.1016/s0092-8674(00)00062-3

Singh, T., and Newman, A. B. (2011). Inflammatory markers in population studies of aging. *Ageing Res. Rev.* 10 (3), 319–329. doi: 10.1016/j.arr.2010.11.002

Skinner, A. C., Perrin, E. M., Moss, L. A., and Skelton, J. A. (2015). Cardiometabolic Risks and Severity of Obesity in Children and Young Adults. *N. Engl. J. Med.* 373 (14), 1307–1317. doi: 10.1056/NEJMoa1502821

Soisson, S. M., Parthasarathy, G., Adams, A. D., Sahoo, S., Sitlani, A., Sparrow, C., et al. (2008). Identification of a potent synthetic FXR agonist with an unexpected mode of binding and activation. *Proc. Natl. Acad. Sci. U.S.A.* 105 (14), 5337–5342. doi: 10.1073/pnas.0710981105

Stepankova, R., Tonar, Z., Bartova, J., Nedorost, L., Rossman, P., Poledne, R., et al. (2010). Absence of microbiota (germ-free conditions) accelerates the atherosclerosis in ApoE-deficient mice fed standard low cholesterol diet. *J. Atheroscler. Thromb.* 17 (8), 796–804. doi: 10.5551/jat.3285

Stepanova, M., and Younossi, Z. M. (2012). Independent association between nonalcoholic fatty liver disease and cardiovascular disease in the US population. *Clin. Gastroenterol. Hepatol.* 10 (6), 646–650. doi: 10.1016/j.cgh.2011.12.039

Sun, L., Xie, C., Wang, G., Wu, Y., Wu, Q., Wang, X., et al. (2018). Gut microbiota and intestinal FXR mediate the clinical benefits of metformin. *Nat. Med.* 24 (12), 1919–1929. doi: 10.1038/s41591-018-0222-4

Suzuki, T., Tamehiro, N., Sato, Y., Kobayashi, T., Ishii-Watabe, A., Shinozaki, Y., et al. (2008). The novel compounds that activate farnesoid X receptor: the diversity of their effects on gene expression. *J. Pharmacol. Sci.* 107 (3), 285–294. doi: 10.1254/jphs.08006fp

Teodoro, J. S., Rolo, A. P., and Palmeira, C. M. (2011). Hepatic FXR: key regulator of whole-body energy metabolism. *Trends Endocrinol. Metab.* 22 (11), 458–466. doi: 10.1016/j.tem.2011.07.002

Trauner, M., Gulamhusein, A., Hameed, B., Caldwell, S., Shiffman, M. L., Landis, C., et al. (2019). The Nonsteroidal Farnesoid X Receptor Agonist Cilofexor (GS-9674) Improves Markers of Cholestasis and Liver Injury in Patients With Primary Sclerosing Cholangitis. *Hepatology* 70 (3), 788–801. doi: 10.1002/hep.30509

Tu, H., Okamoto, A. Y., and Shan, B. (2000). FXR, a bile acid receptor and biological sensor. *Trends Cardiovasc. Med.* 10 (1), 30–35. doi: 10.1016/s1050-1738(00)00043-8

Tully, D. C., Rucker, P. V., Chianelli, D., Williams, J., Vidal, A., Alper, P. B., et al. (2017). Discovery of Tropifexor (LJN452), a Highly Potent Non-bile Acid FXR Agonist for the Treatment of Cholestatic Liver Diseases and Nonalcoholic Steatohepatitis (NASH). *J. Med. Chem.* 60 (24), 9960–9973. doi: 10.1021/acs.jmedchem.7b00907

Urizar, N. L., Liverman, A. B., Dodds, D. T., Silva, F. V., Ordentlich, P., Yan, Y., et al. (2002). A natural product that lowers cholesterol as an antagonist ligand for FXR. *Science* 296 (5573), 1703–1706. doi: 10.1126/science.1072891

Vasan, R. S., and Benjamin, E. J. (2016). The Future of Cardiovascular Epidemiology. *Circulation* 133 (25), 2626–2633. doi: 10.1161/circulationaha.116.023528

Wald, D. S., Bestwick, J. P., Morris, J. K., Whyte, K., Jenkins, L., and Wald, N. J. (2016). Child-Parent Familial Hypercholesterolemia Screening in Primary Care. *N. Engl. J. Med.* 375 (17), 1628–1637. doi: 10.1056/NEJMoa1602777

Wang, S., Lai, K., Moy, F. J., Bhat, A., Hartman, H. B., and Evans, M. J. (2006). The nuclear hormone receptor farnesoid X receptor (FXR) is activated by androsterone. *Endocrinology* 147 (9), 4025–4033. doi: 10.1210/en.2005-1485

Wang, Z., Klipfell, E., Bennett, B. J., Koeth, R., Levison, B. S., Dugar, B., et al. (2011). Gut flora metabolism of phosphatidylcholine promotes cardiovascular disease. *Nature* 472 (7341), 57–63. doi: 10.1038/nature09922

Wang, H., He, Q., Wang, G., Xu, X., and Hao, H. (2018). FXR modulators for enterohepatic and metabolic diseases. *Expert Opin. Ther. Pat.* 28 (11), 765–782. doi: 10.1080/13543776.2018.1527906

Wu, W., Zhu, B., Peng, X., Zhou, M., Jia, D., and Gu, J. (2014). Activation of farnesoid X receptor attenuates hepatic injury in a murine model of alcoholic liver disease. *Biochem. Biophys. Res. Commun.* 443 (1), 68–73. doi: 10.1016/j.bbrc.2013.11.057

Wu, W. B., Xu, Y. Y., Cheng, W. W., Wang, Y. X., Liu, Y., Huang, D., et al. (2015). Agonist of farnesoid X receptor protects against bile acid induced damage and oxidative stress in mouse placenta–a study on maternal cholestasis model. *Placenta* 36 (5), 545–551. doi: 10.1016/j.placenta.2015.02.005

Wu, S., Wu, F., Ding, Y., Hou, J., Bi, J., and Zhang, Z. (2016). Association of non-alcoholic fatty liver disease with major adverse cardiovascular events: A systematic review and meta-analysis. *Sci. Rep.* 6, 33386. doi: 10.1038/srep33386

Xiong, X., Wang, X., Lu, Y., Wang, E., Zhang, Z., Yang, J., et al. (2014). Hepatic steatosis exacerbated by endoplasmic reticulum stress-mediated downregulation of FXR in aging mice. *J. Hepatol.* 60 (4), 847–854. doi: 10.1016/j.jhep.2013.12.003

Xu, X., Shi, X., Chen, Y., Zhou, T., Wang, J., Xu, X., et al. (2018). HS218 as an FXR antagonist suppresses gluconeogenesis by inhibiting FXR binding to PGC-1alpha promoter. *Metabolism* 85, 126–138. doi: 10.1016/j.metabol.2018.03.016

Yao, J., Zhou, C. S., Ma, X., Fu, B. Q., Tao, L. S., Chen, M., et al. (2014). FXR agonist GW4064 alleviates endotoxin-induced hepatic inflammation by repressing macrophage activation. *World J. Gastroenterol.* 20 (39), 14430–14441. doi: 10.3748/wjg.v20.i39.14430

Younossi, Z. M., Koenig, A. B., Abdelatif, D., Fazel, Y., Henry, L., and Wymer, M. (2016). Global epidemiology of nonalcoholic fatty liver disease-Meta-analytic assessment of prevalence, incidence, and outcomes. *Hepatology* 64 (1), 73–84. doi: 10.1002/hep.28431

Younossi, Z. M., Ratziu, V., Loomba, R., Rinella, M., Anstee, Q. M., Goodman, Z., et al. (2019). Obeticholic acid for the treatment of non-alcoholic steatohepatitis: interim analysis from a multicentre, randomised, placebo-controlled phase 3 trial. *Lancet* 394 (10215), 2184–2196. doi: 10.1016/S0140-6736(19)33041-7

Zhang, Y., Castellani, L. W., Sinal, C. J., Gonzalez, F. J., and Edwards, P. A. (2004). Peroxisome proliferator-activated receptor-gamma coactivator 1alpha (PGC-1alpha) regulates triglyceride metabolism by activation of the nuclear receptor FXR. *Genes Dev.* 18 (2), 157–169. doi: 10.1101/gad.1138104

Zhang, Y., Wang, X., Vales, C., Lee, F. Y., Lee, H., Lusis, A. J., et al. (2006). FXR deficiency causes reduced atherosclerosis in Ldlr-/- mice. *Arterioscler. Thromb. Vasc. Biol.* 26 (10), 2316–2321. doi: 10.1161/01.ATV.0000235697.35431.05

Zhang, S., Liu, Q., Wang, J., and Harnish, D. C. (2009a). Suppression of interleukin-6-induced C-reactive protein expression by FXR agonists. *Biochem. Biophys. Res. Commun.* 379 (2), 476–479. doi: 10.1016/j.bbrc.2008.12.117

Zhang, S., Wang, J., Liu, Q., and Harnish, D. C. (2009b). Farnesoid X receptor agonist WAY-362450 attenuates liver inflammation and fibrosis in murine model of non-alcoholic steatohepatitis. *J. Hepatol.* 51 (2), 380–388. doi: 10.1016/j.jhep.2009.03.025

Zhang, R., Ran, H. H., Zhang, Y. X., Liu, P., Lu, C. Y., Xu, Q., et al. (2012). Farnesoid X receptor regulates vascular reactivity through nitric oxide mechanism. *J. Physiol. Pharmacol.* 63 (4), 367–372.

Zhang, Y., Whaley-Connell, A. T., Sowers, J. R., and Ren, J. (2018). Autophagy as an emerging target in cardiorenal metabolic disease: From pathophysiology to management. *Pharmacol. Ther.* 191, 1–22. doi: 10.1016/j.pharmthera.2018.06.004

Zhu, J. Z., Zhou, Q. Y., Wang, Y. M., Dai, Y. N., Zhu, J., Yu, C. H., et al. (2015). Prevalence of fatty liver disease and the economy in China: A systematic review. *World J. Gastroenterol.* 21 (18), 5695–5706. doi: 10.3748/wjg.v21.i18.5695

Conflict of Interest: The authors declare that the research was conducted in the absence of any commercial or financial relationships that could be construed as a potential conflict of interest.

Copyright © 2020 Li, Yang, Wang, Qi, Yang and Li. This is an open-access article distributed under the terms of the Creative Commons Attribution License (CC BY). The use, distribution or reproduction in other forums is permitted, provided the original author(s) and the copyright owner(s) are credited and that the original publication in this journal is cited, in accordance with accepted academic practice. No use, distribution or reproduction is permitted which does not comply with these terms.

frontiers in Physiology

REVIEW
published: 26 August 2020
doi: 10.3389/fphys.2020.01044

MAP4 as a New Candidate in Cardiovascular Disease

*Lingfei Li[1], Qiong Zhang[2,3], Xia Lei[1], Yuesheng Huang[2,3] and Jiongyu Hu[3,4]**

[1] Department of Dermatology, Daping Hospital, Third Military Medical University (Army Medical University), Chongqing, China, [2] Institute of Burn Research, Southwest Hospital, Third Military Medical University (Army Medical University), Chongqing, China, [3] State Key Laboratory of Trauma, Burns and Combined Injury, Third Military Medical University (Army Medical University), Chongqing, China, [4] Department of Endocrinology, Southwest Hospital, Third Military Medical University (Army Medical University), Chongqing, China

Microtubule and mitochondrial dysfunction have been implicated in the pathogenesis of cardiovascular diseases (CVDs), including cardiac hypertrophy, fibrosis, heart failure, and hypoxic/ischemic related heart dysfunction. Microtubule dynamics instability leads to disrupted cell homeostasis and cell shape, decreased cell survival, and aberrant cell division and cell cycle, while mitochondrial dysfunction contributes to abnormal metabolism and calcium flux, increased cell death, oxidative stress, and inflammation, both of which causing cell and tissue dysfunction followed by CVDs. A cytosolic skeleton protein, microtubule-associated protein 4 (MAP4), belonging to the family of microtubule-associated proteins (MAPs), is widely expressed in non-neural cells and possesses an important role in microtubule dynamics. Increased MAP4 phosphorylation results in microtubule instability. In addition, MAP4 also expresses in mitochondria and reveals a crucial role in maintaining mitochondrial homeostasis. Phosphorylated MAP4 promotes mitochondrial apoptosis, followed by cardiac injury. The aim of the present review is to highlight the novel role of MAP4 as a potential candidate in multiple cardiovascular pathologies.

Keywords: microtubule-associated protein 4, microtubule-associated proteins, microtubule, mitochondria, cardiovascular disease

OPEN ACCESS

Edited by:
Jun Ren,
University of Washington,
United States

Reviewed by:
Ne Natalie Wu,
Zhongshan Hospital, Fudan University, China
Ying Tan,
Nanfang Hospital, Southern Medical University, China

***Correspondence:**
Jiongyu Hu
jiongyuhu@163.com

Specialty section:
This article was submitted to Clinical and Translational Physiology, a section of the journal Frontiers in Physiology

Received: *21 May 2020*
Accepted: *29 July 2020*
Published: *26 August 2020*

Citation:
Li L, Zhang Q, Lei X, Huang Y and Hu J (2020) MAP4 as a New Candidate in Cardiovascular Disease. Front. Physiol. 11:1044. doi: 10.3389/fphys.2020.01044

INTRODUCTION

Cardiovascular disease (CVD) is the leading cause of mortality worldwide, accounting for approximately 40% of all deaths (Schwalm et al., 2016). Hypoxia/ischemia, hypertension, inflammation, diabetes, cardiomyopathies, cardiometabolic syndrome, and obesity are the common risk factors for CVD, and these multiple comorbidities elevate the rates of mortality and morbidity in CVD (Koene et al., 2016; Ceylan et al., 2018; Ren and Zhang, 2018; Zhang et al., 2018; Zhou et al., 2018a; Caporizzo et al., 2019). Despite the advent of a number of drugs and techniques, only limited efficacy has been reached in CVD treatment. Considering these facts, novel interventions, with a broad scope to cover these multiple comorbidities, are necessary.

Cardiovascular dysfunction leads to the development and progress of CVD. Cardiomyocytes and endothelial cells are mainly involved in the maintenance of normal cardiovascular function. Accumulating evidence suggests that damaged microtubules (MT) and mitochondria are the key players in the pathogenesis of cardiomyocytes and endothelial dysfunction. As an important cytoskeletal component, MTs are involved in cell death, maintenance of cellular homeostasis,

and organelle transport, and the instability of MT dynamics induces cardiac hypertrophy/heart failure (Tagawa et al., 1996; Sato et al., 1997), myocardial ischemia–reperfusion injury (Sato et al., 1993), and catecholamine-induced myocardial injury. Since mitochondria are involved in cell metabolism, oxidative reactions, and energy supply, mitochondrial disruption reportedly leads to apoptosis, metabolic disorder, and excessive oxidative stress, which contribute to the dysfunction of cardiomyocytes and endothelial cells, and is followed by abnormal cardiovascular events (Bravo-San Pedro et al., 2017; Suomalainen and Battersby, 2018).

In the current review, we discuss a novel candidate intervention target in CVD and elucidate its evolutionary genetic history, basic characteristics, and function, and its correlation with MTs and mitochondria.

MICROTUBULE-ASSOCIATED PROTEIN 4 (MAP4)

Gene Evolutionary History

In mammals, microtubule-associated proteins (MAPs) are mainly consisted of MAP2, tau (also known as MAPT), and MAP4, all of which are crucial cytosolic skeletal proteins. Both MAP2 and tau are mainly distributed in neurons and have been reviewed elsewhere (Dehmelt and Halpain, 2005). MAP4 is a unique member of MAPs that is widely expressed in various tissues and cells, and recently, an increasing number of studies have suggested that MAP4 might play an important role in cardiovascular disorders. MAP4 is encoded by a single gene located in 3p21 and consists of 23 exons. Moreover, MAP4 gene has many isoforms, as well as three to five MT binding repeats (Dehmelt and Halpain, 2005). Following isolation of the cDNA sequence encoding human and mouse MAP4, three distinct regions consisting of related sequences with different motifs were identified in its open reading frames. Analysis of its amino acid sequence suggests that human, mouse, and bovine MAP4 are close homologs and their sequences reach 0–75% similarity, and have highly conserved domains, including the amino terminus, MT binding domain, and carboxyl terminus, thus inferring that they are members of the same class (West et al., 1991).

Characteristic Structural Features

The MAP4 protein is a ubiquitous, heat-stable protein composed of an asymmetrical structure similar to other MAPs and consists of an amino terminal projection domain and a carboxyl terminal MT binding domain (Mangan and Olmsted, 1996). Accumulating studies have shown that the MT binding domain contains a conserved phosphorylated KXGS motif (Lewis et al., 1988; Drewes et al., 1995; Illenberger et al., 1996; Ozer and Halpain, 2000). It has been reported that the phosphorylation sites, such as Ser696, Ser768, and Ser787 (corresponding to Ser667, Ser737, and Ser760 in mouse) in the proline-rich region of the human MT binding domains, are involved in the dissociation of MAP4 from MTs and regulate MT dynamics instability (Srsen et al., 1999; Kitazawa et al., 2000; Hu et al., 2010). MT dynamic is a process that depends on α and β subunits of tubulin, their post-translational modifications, and interaction of MT with MAPs, and is regulated by the balance between MT polymerization and disassembly, the disruption of which could lead to a series of diseases. Although a number of studies have concentrated on this region, the detailed mechanism of the regulation of MT dynamics remains unclear (Chapin and Bulinski, 1991; Tokuraku et al., 1999). In contrast, the amino terminal projection domain, which protrudes from the MT wall and does not bind to MTs, varies in length among different MAPs. The projection domain of MAP4 consists of three regions, including the amino terminal acidic region, the KDM-repeat sequence, and the b-regions. The region containing KDM-repeat sequence is a representative structure of the projection domain, and is a highly conserved unit composed of an imperfect 14 amino acid repeat (KD(M/V)X(L/P)(P/L)XETEVALA) starting with KD(M/V) (Aizawa et al., 1990; Chapin and Bulinski, 1991; Permana et al., 2005). Recent studies have indicated that the projection domain of MAP4 allows the separation of individual MTs by inhibiting the bundle-forming ability of the MT binding domain. Further, this suppressive activity of the projection domain is correlated with its length rather than its amino acid sequence. However, the detail process of the regulation of MT dynamics or their organization by the projection domain remains elusive (Faruki and Karsenti, 1994; Tokuraku et al., 1999; Iida et al., 2002; Permana et al., 2005).

Distribution

Microtubule-associated protein 4 is reported to be widely expressed in non-neuronal cells and tissues, such as the adrenal gland, liver, lung, heart, vascular tissues, and skin (Parysek et al., 1985; Kotani et al., 1988; Matsushima et al., 2005; Hu et al., 2010; Li et al., 2015; Xia and He, 2018; Zhang et al., 2019a).

Function

MAP4 and Cytoskeleton

Microtubules dynamics is affected by the balance between tubulin polymerization and depolymerization. As a cytoskeleton regulator, MAP4 regulates MT dynamics through its posttranscriptional phosphorylation modification (Chapin and Bulinski, 1991; Nguyen et al., 1997). Under normal conditions, MAP4 combines with MTs, resulting in the stability of MTs. Once phosphorylated, MAP4 dissociates from MTs, leading to MT disassembly and dynamic instability (Ebneth et al., 1999; Hu et al., 2014). Previous studies indicated that the MT binding domain of MAP4 contains a repeat region with tandemly organized repeat sequences, and different types of MAP4 contain a different number and arrangement of these repeat sequences. However, different isoform fragments of MAP4 exhibit similar degrees of MT polymerization activity and MT binding affinity, suggesting that variations in the repeat region are not essential for the regulation of MT dynamics, which is believed to be the main function of MAP4. In contrast, the MT bundle-forming activity is reported to differ among MAP4 isoform fragments, with the bundle formation being augmented by increasing the number of repeat sequences in the fragments, indicating that the role of MAP4 isoforms is to regulate the surface charge of MTs (Tokuraku et al., 2003). In addition, Tokuraku et al. (2003)

demonstrated that MAP4 isoforms may also affect kinesin motor activity by regulating MT surface properties. They analyzed MAP4 isoforms in an *in vitro* gliding assay and found that the five-repeat isoforms suppressed the movement of MTs in a concentration-dependent manner. Furthermore, they revealed that MAP4 isoforms did not compete with kinesin for binding to MTs in a sedimentation assay, suggesting that kinesin could bind to MAP4-bound MTs, although it could not move on them (Tokuraku et al., 2007).

Semenova et al. (2014) used *Xenopus melanophores* to test the regulation of MT transport by MAP4. They found that pigment granules moved along the MTs to the cell center or periphery by means of dynein and kinesin-2, respectively. They showed that aggregation signals induced phosphorylation of threonine residues in the MT binding domain; meanwhile, the binding of the protein to MTs was shown to be reduced. Whereas overexpression of *Xenopus* MAP4 suppressed pigment aggregation by shortening dynein-dependent MT runs of melanosomes, removal of *Xenopus* MAP4 from MTs was reported to decrease the length of kinesin-2-dependent runs, inhibiting pigment dispersion. Thus, their data indicated that the MAP4-MT binding promoted the kinesin-2-based movement in parallel with the suppression of dynein-dependent movement of melanosomes. In addition, phosphorylation led to the dissociation of *Xenopus* MAP4 from MTs, thereby raising dynein-dependent and reducing kinesin-2-dependent motility of melanosomes, which stimulates their accumulation in the cell center. Conversely, dephosphorylation of *Xenopus* MAP4 during dispersion triggered the opposite effect (Semenova et al., 2014).

On a separate note, Matsushima et al. (2012) tested the interaction of MAP4 with actin filaments. Their data demonstrated that MAP4 and its MT binding domain fragments bound to actin filaments under normal conditions. The apparent dissociation constant and binding stoichiometry of the fragments to actin have been demonstrated to be approximately 0.1 μM and 1:3 (MAP4/actin), respectively, with the actin binding site on MAP4 reported to be located at the carboxyl terminal part of the proline-rich region, consistent with the MT binding site. Besides, they showed that MAP4-bound actin filaments tended to be straighter and longer, with the number of actin bundles increasing when the MAP4 fragment was added, suggesting that MAP4 binding altered the properties of the actin filaments. A multiple sequence alignment of the proline-rich regions of MAP4 and tau also revealed the presence of two putative actin-binding consensus sequences (Matsushima et al., 2012).

MAP4 and Cell Cycle

Previous studies demonstrated that mutations in human MAP4 (Ser696 and Ser787) affect MT dynamics and subsequently mediate the progression of cell cycle, with p34cdc2/cyclin B being deemed an important kinase in this biological process. In addition, the phosphorylation of the human MAP4 at Ser787 is noted during mitosis, whereas the phosphorylation of MAP4 at Ser696 is shown to occur throughout the cell cycle in proliferating cells. Overexpression of dephosphorylated MAP4 did not affect cell doubling time; in contrast, expression of phosphorylated MAP4 may affect progression into or through cell division, indicating that MAP4 phosphorylation plays a crucial role in regulation of cell cycle (Tombes et al., 1991; Ookata et al., 1995, 1997; Nguyen et al., 1997; Chang et al., 2001).

MAP4 and Mitosis

The MAP4 protein is involved in the regulation of MT dynamics during the M-phase (Ookata et al., 1995; Dehmelt and Halpain, 2005). However, both the MT network and MT dynamics show little change when MAP4 is removed from MTs using a blocking antibody. In addition, absence of MAP4 binding to MTs results in maintenance of the normal structure of spindles in cells progressing to mitosis, and posttranslational modifications of tubulin subunits also remain unchanged, suggesting that MAP4 may just be a component of a functionally redundant system (Wang et al., 1996). Zahnleiter et al. (2015) found that MAP4 mutations lead to the development of a clinical spectrum of centrosomal defects and demonstrated that centrosomal proteins play a regulatory role in the centrosomes and ciliary and Golgi bodies related to severe short stature. Both MAP4 and MT rescue factor and cytoplasmic linker associated protein 1 (CLASP1) are necessary for maintaining spindle location and an accurate cell division axis. In human cells, CLASP1 is required for capturing astral MTs, whereas MAP4 prevents engagement of excess dynein motors (Samora et al., 2011). Consistent with this, MAP4 was observed to interact with dynein-dynactin, thereby suppressing dynein-induced MT sliding. In contrast, absence of MAP4 leads to spindle disorientation in the vertical plane, revealing that force generators are under spatial control. Collectively, these data showed an essential role of MAP4 during mitosis, as spindle positioning is considered to be crucial during embryogenesis and stem-cell homeostasis (Samora et al., 2011). Shiina and Tsukita (1999) reported that mutations of serine and threonine to alanine at p34cdc2 kinase-specific phosphorylation sites interfered with the mitosis-associated reduction in MT affinity of *Xenopus* MAP4, and their overexpression affected the chromosomal movement during anaphase A in mitotic cells.

Regulating Mechanisms

As already known, MT dynamics are affected by a variety of factors, including drugs (e.g., taxol and colchicine), temperature, GTP, free tubulin, and MAPs. Moreover, the effect of drugs and GTP on MT dynamics was also shown to be mediated by MAP4 (Holmfeldt et al., 2002, 2003; Delphin et al., 2012; Gombos et al., 2013; Ojeda-Lopez et al., 2014; Watanabe and Goshima, 2014).

Xiao et al. (2012) found that the MT binding domain of MAP4 binds to the outer and luminal surfaces of MTs, and taxol, an MT stabilizing drug, suppresses these interactions. Although taxol negatively regulated the interaction of MAP4 with MTs, its binding to the MT binding domain-MAP4-MT complex further decreased the overall deuterium incorporation, suggesting that a more stable complex was formed in the presence of the drug (Xiao et al., 2012). In addition, DNA-damaging agents could affect sensitivity to anti-MT drugs through the regulation of the expression of MAP4 (Zhang et al., 1998, 1999). Chapin and Bulinski (1994) revealed that MAP4 could bind to different types of MTs, including detyrosinated and tyrosinated tubulin, with the differential binding to these forms of tubulin not directly leading

to a mechanism of segregation of MAP4 on MTs. Additionally, they also suggested that in TC-7 cells, the absence of MAP4 may affect rapid growth of MTs to which MAP4 was not yet bound, or the presence of other MAPs may compete with MAP4 for MT binding sites. These observations indicate that different binding states of MAP4 on MTs directly regulate MT dynamics within single cells, as well as other MT functions such as those involving MT motor activity (Chapin and Bulinski, 1994).

Septins are a conserved family of GTPases forming heterooligomers and interacting with the actin-based cytoskeleton and MTs. Ghossoub et al. (2013) explored the effect of septins in the primary cilium of retinal pigmented epithelial cells and showed that septin2, septin7, and septin9 formed a 1:1:1 complex, colocalizing along the length of the axoneme. Similarly, knockdown of cilium-localized septins were reported to suppress ciliogenesis in kidney epithelial cells. As a binding partner of septin2, MAP4 regulated the accessibility of septins to MTs and was also localized to the axoneme, where it appeared to negatively control ciliary length. This study provided new insights into the functions and regulations of septins and MAP4 in the organization of the primary cilium and MT-based activities in cells (Ghossoub et al., 2013). Kremer et al. (2005) found that reduced septin in Hela cells leads to a robust elevation in MT stability, and they also identified MAP4 as the septin binding partner using mass spectroscopic analysis. Septin2, spetin6, and septin7 were shown to directly bind to the proline-rich region of MAP4 to form a heterotrimer and this binding suppressed the ability of the MAP4 fragment to bind and bundle MTs. In addition, the absence of septin increased the number of abnormal cell, whereas this effect was suppressed when MAP4 was knocked down. Thus, these data reveal a novel role of septins in mediating MT dynamics through interaction with MAP4 (Kremer et al., 2005).

Hoshi et al. (1992) reported that MAP4 might be a good substrate for MAPK, with its phosphorylation leading to inactivation of tubulin polymerization. In addition, Mori et al. (1991) demonstrated that protein kinase C regulated the activity of MAP4 and subsequently led to changes in the MT dynamics.

MICROTUBULES IN CVD

Microtubules, the major component of the cytoskeleton, are composed of α/β tubulin dimers and exhibit a crucial role in regulating many processes, including cell survival and death, cell migration and proliferation, cell shape maintenance, and organelle transport (Walczak, 2000; Birukova et al., 2004; Hu et al., 2010; Zhang et al., 2013, 2019a). In particular, MTs target focal adhesions to regulate extracellular matrix adhesion, and the attachment of MTs to special cortical regions of cells is required for cell polarization (Small et al., 2002). The functions of MTs are affected by MT dynamics as active polymerization and depolymerization indicate MT growth and shortening (Mitchison and Kirschner, 1984). Thus, the growth, shortening, catastrophe, and rescue of MTs are reflected by MT instability, induced cellular homeostasis, division, and movement. Based on the essential functions of MTs, many researchers have investigated the role of MT dysfunction in CVD, including cardiac hypertrophy/heart failure (Tagawa et al., 1996; Sato et al., 1997), myocardial ischemia–reperfusion injury (Sato et al., 1993), and catecholamine-induced myocardial injury (Hori et al., 1994). In addition, desmin intermediate filaments have been identified as a key component of an anchoring complex that links MTs to the sarcomere and imparts structural organization to the MT network. Mutations in the human desmin gene lead to an autosomal dominant, autosomal recessive, and sporadic forms of protein aggregation myopathies and cardiomyopathies (Clemen et al., 2015; Robison et al., 2016). Previous studies have also reported that a complex receptor dependent or independent kinase cascade regulates the transcription of MT deformation-sensitive genes, such as *PAI-1* and *CTGF*, which may provide novel targets to impede the development of CVD (Samarakoon and Higgins, 2018). These studies provided a phenomenological insight into the role of MTs in cardiovascular injury, but the detailed molecular perspective regarding their role has not yet been elucidated. In addition, other researchers have focused on tubulin posttranslational modifications, including detyrosination and tyrosination, which are currently emerging as key modulators of MTs. They demonstrated that tubulin detyrosination affected mechanotransduction in muscle cells and was crucial for load-bearing of buckling MTs during cardiomyocyte contraction (Kerr et al., 2015). Excess or reduced tubulin detyrosination was reported to affect the stiffness of cardiomyocytes, thereby contributing to cardiac dysfunction. Upregulation of tubulin detyrosination is also exhibited in patients with hypertrophic and dilated cardiomyopathies (Robison et al., 2016). These clinical links suggested that an imbalance in the levels of tubulin tyrosination and detyrosination may be a risk factor for heart failure, and could be linked to muscle dysfunctions in various other diseases. Thus, a better understanding of the posttranslational regulation of MTs might substantially change the way we perceive the roles of MTs in CVD (Magiera et al., 2018).

MITOCHONDRIA IN CVD

Mitochondria are double-membrane bound intracellular organelles responsible for energy production and regulation of cellular metabolism, and occupy a core role in eukaryotic cells, particularly cells of the cardiovascular system (Galluzzi et al., 2012, 2018; Lopez-Crisosto et al., 2017; Mehta et al., 2017). Mitochondrial dynamics (both fusion and fission), mitophagy, and homeostasis are crucial factors in the maintenance of mitochondrial integrity. Mitochondria are more prone to stress, including hypoxia and ischemia–reperfusion. Several studies have shown that accumulation of reactive oxygen species, inflammatory damage, molecular defects, and abnormal signal transduction pathways, including AMPK/ULK1, PI3K/Akt, and p38/MAPK/MAP4, lead to mitochondrial dysfunction and are at the root of numerous diseases. Alterations in the endogenous apoptotic pathway, acute exercise, impaired mitophagy, excessive or untimely mitochondrial fission or fusion, and aging are

also known to lead to mitochondrial dysfunction, followed by abnormal metabolism. Alteration in metabolism leads to defects in mitochondrial biogenesis and energy supply, cell death, and calcium fluxes, which are contributing factors toward the pathogenesis of multiple cardiovascular disorders such as myocardial infarction, cardiomyopathies of various etiologies, hypertension, and atherosclerosis (Hu et al., 2014; Bravo-San Pedro et al., 2017; Suomalainen and Battersby, 2018; Zhou et al., 2018b; Wu et al., 2019a,b). In addition, impaired mitochondria have been demonstrated to actively promote inflammatory responses and cell death, thereby contributing to the pathogenesis of CVD. Based on these studies, attempts were made to develop mitochondria-targeting drugs for the treatment of cardiovascular disorders in the clinical setting. The main direction of these interventions involved mitochondrial metabolism, mitochondrial dynamics, mitophagy, calcium homeostasis, oxidative stress, inflammation, regulated cell death, and mitochondrial microRNAs. Despite extraordinary efforts spanning three decades, results have been rather dismal and a small number of effective targeted drugs have been approved for the treatment of patients with CVD (Bonora et al., 2019). Thus, molecules with optimized pharmacological characteristics and precise mechanistic insights into mitochondrial processes, along with a reassessment of the pathogenesis of CVD, are essential for the development of new drugs with clinical utility.

TRENDS IN MAP4-MEDIATED CVD

Accumulating evidence has suggested that MT and mitochondria are crucial subcellular components involved in the pathogenesis of CVD. Moreover, MAP4 is a key mediator in regulating MTs and mitochondria (Li et al., 2018, 2019; Zhang et al., 2019b). Fang et al. (2011) demonstrated that hypoxia-induced MAP4 phosphorylation in cardiomyocytes leads to MT disassembly, whereas MAP4 overexpression promotes MT polymerization leading to the stabilization of MT networks. Besides, they found that MAP4 overexpression increased viability and ATP content of cardiomyocytes under hypoxia. In addition, MAP4 was shown to inhibit the increased permeability of the mitochondrial membrane under hypoxia via regulating the interaction between dynein light chain tctex-type (DYNLT1) and voltage-dependent anion channel 1 (VDAC1) (Fang et al., 2011). Our previous study suggested that p38/MAPK affected MT dynamics and the viability of cardiomyocytes by regulating MAP4 phosphorylation under hypoxic conditions. Following hypoxia, p38/MAPK and MAP4 phosphorylation increased, with activation of p38/MAPK leading to MAP4 phosphorylation, which in turn contributed to MT disassembly and cell viability reduction. We also revealed that p38/MAPK interacts with MAP4, and thus administration of the p38/MAPK inhibitor could increase MT polymerization and enhance the viability of cardiomyocytes after hypoxia. In contrast, MKK6 (Glu), the upstream activator of p38/MAPK, was shown to reduce cell viability and promote MT disassembly under the same conditions (Hu et al., 2010). We further showed that in hypoxic cardiomyocytes, MAP4 phosphorylation was notably increased with MAP4-MT dissociation, and MAP4 translocated to mitochondria where it induced mitochondrial permeability transition pore opening and cytochrome c release followed by endogenous mitochondrial apoptosis in cardiomyocytes (Hu et al., 2014). In our recent study, we showed that MAP4 phosphorylation was evident not only in cardiac tissues in right ventricular hypertrophy in tetralogy of Fallot, but was also increased in the hearts of both myocardial infraction and transverse aortic constriction mouse models. Briefly, mice exhibiting MAP4 phosphorylation exerted age-dependent effects such as pathological cardiac remodeling, cardiomyocyte mitochondrial apoptosis and disruption, and systolic and diastolic dysfunction. As such, MT disassembly, translocation of phosphorylated MAP4, and cardiomyocyte apoptosis are deemed important factors in initiating cardiac remodeling, with the activation of p38/MAPK being suggested as the crucial upstream kinase involved in the MAP4 phosphorylation (Li et al., 2018)

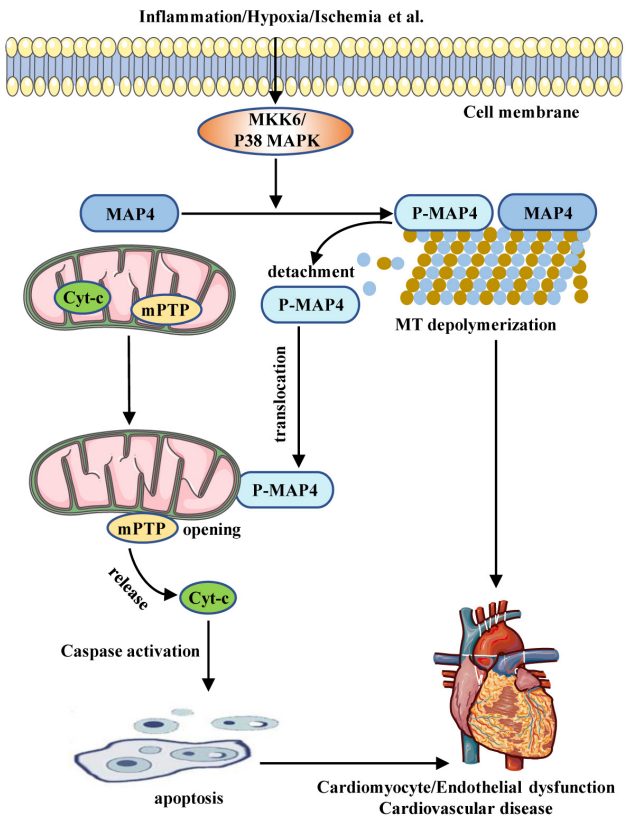

FIGURE 1 | Schematic illustrating the role of MAP4 in CVD. Inflammation, hypoxia, ischemia, etc., stimulate the activation of the MKK6/p38 MAPK pathway. The activated p38 MAPK induces MAP4 phosphorylation and, sequentially, the depolymerization of MT. The phosphorylated MAP4 detaches from MT and translocates to mitochondria from cytosol, leading to mitochondrial permeability transition pore (mPTP) opening and cytochrome c (cyt-c) release, which activates caspase pathway and promotes mitochondrial apoptosis. Increased apoptosis together with MT depolymerization causes cardiomyocyte/endothelial cell dysfunction, which is involved in the pathogenesis of CVD.

as shown in previous studies (Teiger et al., 1996; Choi et al., 2009; Dees et al., 2012). Interestingly, some other studies revealed that MAP4 (Ser472, Ser924, and Ser1056) phosphorylation increases in the model of pressure overload-induced cardiac hypertrophy. When these three sites were mutated to alanine and transfected into cardiomyocytes to obtain mutant MAP4 constructs, the dephosphorylated MAP4 (Ser924 and Ser1056) caused MT reorganization in the pressure overload model, similar to the hypertrophic cardiac MT phenotype, indicating that MAP4 (Ser924 and Ser1056) dephosphorylation might be the core process in mediating MT reorganization. Further, the underlying mechanism correlated with the activation of the serine/threonine phosphatase 1 and 2A, as well as the upstream p21 kinase (Cheng et al., 2010; Chinnakkannu et al., 2010). Takahashi et al. (2003) reported that MAP4 overexpression not only promoted tubulin expression and stability but also changed the characteristics of MT networks, which is considered a key factor in mediating the phenotype of the pressure overload-induced cardiac hypertrophy. Although there have been some inconsistencies in the proposed mechanisms of MAP4-mediated cardiac remodeling, this might be attributed to different models and phosphorylation sites used in these studies. Our focused sites were located in the proline-rich regions and were responsible for the longitudinal affinity between each tubulin dimer in a protofilament, whereas focused sites in other studies were located in the KXGS region, which is responsible for lateral protofilament–protofilament interactions (Katsuki et al., 1999). Even though both regions are located in the MT binding domain, the detailed functional mechanisms and resulting phenotypes may not be identical. Thus, further research is necessary to elucidate the mechanisms underlying these potential differences.

Another study revealed that the total expression of the cardiac MAP4 protein reached its highest level in the first week in neonatal rats, and then was shown to gradually reduce with aging. Likewise, MAP4 was also demonstrated to be involved in drug- and hypothermia-induced MT stability in cardiomyocytes of newborns, suggesting that the regulation of MAP4 plays an important role in MT functions during cardiac development (Webster and Bratcher, 2006). In addition, previous studies have demonstrated that MAP4 might be a potential regulator of vascular permeability. In microvascular endothelial cells, tumor necrosis-α (TNF-α)/lipopolysaccharides (LPS) induced MAP4 phosphorylation-dependent MT disassembly, followed by increased vascular permeability via activation of p38/MAPK (Li et al., 2015), providing a novel insight for MAP4 phosphorylation in regulating microvascular permeability. Furthermore, Zhou et al. (2015) found that LPS stimulation leads to disruption of MT dynamics through the activation of p38/MAPK in endothelial cells, which was shown to be blocked by a MT stabilizer. Moreover, p38/MAPK was observed to interact with MAP4 to form a complex, subsequently leading to MT disassembly, which could be suppressed by a p38/MAPK inhibitor (Zhou et al., 2015). These data indicate that MAP4 phosphorylation-dependent MT disassembly plays a key role in regulating the permeability of endothelial cells. Another study revealed that Down syndrome exhibits variable features, including heart defect, which is correlated with mitochondrial dysfunction. Overexpression of genes on chromosome-21 is responsible for the phenotypic features of Down syndrome either in a direct or in an indirect manner (Izzo et al., 2018). Our previous study showed that MAP4 phosphorylation is deemed a crucial factor in mediating mitochondrial apoptosis, morphological and functional disruption, and heart defects, which is partially similar to the mitochondrial phenotype of Down syndrome. However, whether MAP4 is involved in Down syndrome remains unclear and warrants further studies.

FUTURE RESEARCH FOCUSES

Conclusively, MAP4 has been demonstrated to regulate MTs or mitochondria in cardiomyocytes and endothelial cells, both of which play a key role in the pathogenesis of CVD (**Figure 1**). The correlation and interactions between MAP4 and MT/mitochondria, and MT/mitochondrial-targeting drugs may provide useful tools to analyze potential MAP4-related signaling pathways or molecular interactions among p38/MAPK, septins, DYNLT1, and VDAC1. Moreover, the elucidation of their association with pathological outcomes may provide novel targets for the development of MAP4-targeting drugs. In addition, MAP4 is a unique member of MAPs, which is expressed in both vascular tissues and the heart. Recent studies have shown an important role of MAP4 in the cardiovascular system, and interventions targeting the function of MAP4 may provide protection against cardiomyocyte or endothelial cell dysfunction. For these reasons, MAP4 may serve as a potential target for pharmacological interventions in CVD.

In contrast, although there has been some progress regarding MAP4 in both basic and clinical studies, more information on MAP4, including its detailed structure, function, and regulatory mechanism, remains elusive. Thus, future studies should focus on these issues and elucidate the role of MAP4 specific to CVD both *in vivo* and *in vitro*. Meanwhile, unraveling of related pathways, molecule–molecule interactions, and the role of MAP4 in other systems may provide us with substantial evidence for the development of novel drugs targeting MAP4.

AUTHOR CONTRIBUTIONS

LL, QZ, XL, and YH participated in research design. JH supervised in research design. LL, QZ, XL, YH, and JH wrote or contributed to the writing of the manuscript. All authors contributed to the article and approved the submitted version.

FUNDING

This work was supported by the Military Medical Innovation Program in Daping Hospital (2019CXJSC014) and the Innovation Research Program in Southwest Hospital (SWH2018BJKJ-11).

REFERENCES

Aizawa, H., Emori, Y., Murofushi, H., Kawasaki, H., Sakai, H., and Suzuki, K. (1990). Molecular cloning of a ubiquitously distributed microtubule-associated protein with Mr 190,000. *J. Biol. Chem.* 265, 13849–13855.

Birukova, A. A., Birukov, K. G., Smurova, K., Adyshev, D., Kaibuchi, K., Alieva, I., et al. (2004). Novel role of microtubules in thrombin-induced endothelial barrier dysfunction. *FASEB J.* 18, 1879–1890. doi: 10.1096/fj.04-2328com

Bonora, M., Wieckowski, M. R., Sinclair, D. A., Kroemer, G., Pinton, P., and Galluzzi, L. (2019). Targeting mitochondria for cardiovascular disorders: therapeutic potential and obstacles. *Nat. Rev. Cardiol.* 16, 33–55. doi: 10.1038/s41569-018-0074-0

Bravo-San Pedro, J. M., Kroemer, G., and Galluzzi, L. (2017). Autophagy and mitophagy in cardiovascular disease. *Circ. Res.* 120, 1812–1824. doi: 10.1161/circresaha.117.311082

Caporizzo, M. A., Chen, C. Y., and Prosser, B. L. (2019). Cardiac microtubules in health and heart disease. *Exp. Biol. Med.* 244, 1255–1272. doi: 10.1177/1535370219868960

Ceylan, A. F., Wang, S., Kandadi, M. R., Chen, J., Hua, Y., Pei, Z., et al. (2018). Cardiomyocyte-specific knockout of endothelin receptor a attenuates obesity cardiomyopathy. *Biochim. Biophys. Acta Mol. Basis Dis.* 1864, 3339–3352. doi: 10.1016/j.bbadis.2018.07.020

Chang, W., Gruber, D., Chari, S., Kitazawa, H., Hamazumi, Y., Hisanaga, S., et al. (2001). Phosphorylation of MAP4 affects microtubule properties and cell cycle progression. *J. Cell Sci.* 114, 2879–2887.

Chapin, S. J., and Bulinski, J. C. (1991). Non-neuronal 210 x 10(3) Mr microtubule-associated protein (MAP4) contains a domain homologous to the microtubule-binding domains of neuronal MAP2 and tau. *J. Cell Sci.* 98(Pt 1), 27–36.

Chapin, S. J., and Bulinski, J. C. (1994). Cellular microtubules heterogeneous in their content of microtubule-associated protein 4 (MAP4). *Cell Motil. Cytoskeleton* 27, 133–149. doi: 10.1002/cm.970270205

Cheng, G., Takahashi, M., Shunmugavel, A., Wallenborn, J. G., DePaoli-Roach, A. A., Gergs, U., et al. (2010). Basis for MAP4 dephosphorylation-related microtubule network densification in pressure overload cardiac hypertrophy. *J. Biol. Chem.* 285, 38125–38140. doi: 10.1074/jbc.m110.148650

Chinnakkannu, P., Samanna, V., Cheng, G., Ablonczy, Z., Baicu, C. F., Bethard, J. R., et al. (2010). Site-specific microtubule-associated protein 4 dephosphorylation causes microtubule network densification in pressure overload cardiac hypertrophy. *J. Biol. Chem.* 285, 21837–21848. doi: 10.1074/jbc.m110.120709

Choi, Y. H., Cowan, D. B., Moran, A. M., Colan, S. D., Stamm, C., Takeuchi, K., et al. (2009). Myocyte apoptosis occurs early during the development of pressure-overload hypertrophy in infant myocardium. *J. Thorac. Cardiovasc. Surg.* 1362, e1351–e1353.

Clemen, C. S., Stockigt, F., Strucksberg, K. H., Chevessier, F., Winter, L., Schutz, J., et al. (2015). The toxic effect of R350P mutant desmin in striated muscle of man and mouse. *Acta Neuropathol.* 129, 297–315. doi: 10.1007/s00401-014-1363-2

Dees, E., Miller, P. M., Moynihan, K. L., Pooley, R. D., Hunt, R. P., Galindo, C. L., et al. (2012). Cardiac-specific deletion of the microtubule-binding protein CENP-F causes dilated cardiomyopathy. *Dis. Model Mech.* 5, 468–480. doi: 10.1242/dmm.008680

Dehmelt, L., and Halpain, S. (2005). The MAP2/Tau family of microtubule-associated proteins. *Genome Biol.* 6:204.

Delphin, C., Bouvier, D., Seggio, M., Couriol, E., Saoudi, Y., Denarier, E., et al. (2012). MAP6-F is a temperature sensor that directly binds to and protects microtubules from cold-induced depolymerization. *J. Biol. Chem.* 287, 35127–35138. doi: 10.1074/jbc.m112.398339

Drewes, G., Trinczek, B., Illenberger, S., Biernat, J., Schmitt-Ulms, G., Meyer, H. E., et al. (1995). Microtubule-associated protein/microtubule affinity-regulating kinase (p110mark). A novel protein kinase that regulates tau-microtubule interactions and dynamic instability by phosphorylation at the Alzheimer-specific site serine 262. *J. Biol. Chem.* 270, 7679–7688. doi: 10.1074/jbc.270.13.7679

Ebneth, A., Drewes, G., Mandelkow, E. M., and Mandelkow, E. (1999). Phosphorylation of MAP2c and MAP4 by MARK kinases leads to the destabilization of microtubules in cells. *Cell Motil. Cytoskeleton* 44, 209–224. doi: 10.1002/(sici)1097-0169(199911)44:3<209::aid-cm6>3.0.co;2-4

Fang, Y. D., Xu, X., Dang, Y. M., Zhang, Y. M., Zhang, J. P., Hu, J. Y., et al. (2011). MAP4 mechanism that stabilizes mitochondrial permeability transition in hypoxia: microtubule enhancement and DYNLT1 interaction with VDAC1. *PLoS One* 6:e28052. doi: 10.1371/journal.pone.0028052

Faruki, S., and Karsenti, E. (1994). Purification of microtubule proteins from Xenopus egg extracts: identification of a 230K MAP4-like protein. *Cell Motil. Cytoskeleton* 28, 108–118. doi: 10.1002/cm.970280203

Galluzzi, L., Kepp, O., Trojel-Hansen, C., and Kroemer, G. (2012). Mitochondrial control of cellular life, stress, and death. *Circ. Res.* 111, 1198–1207. doi: 10.1161/circresaha.112.268946

Galluzzi, L., Vitale, I., Aaronson, S. A., Abrams, J. M., Adam, D., Agostinis, P., et al. (2018). Molecular mechanisms of cell death: recommendations of the nomenclature committee on cell death 2018. *Cell Death Differ.* 25, 486–541.

Ghossoub, R., Hu, Q., Failler, M., Rouyez, M. C., Spitzbarth, B., Mostowy, S., et al. (2013). Septins 2, 7 and 9 and MAP4 colocalize along the axoneme in the primary cilium and control ciliary length. *J. Cell Sci.* 126, 2583–2594. doi: 10.1242/jcs.111377

Gombos, L., Neuner, A., Berynskyy, M., Fava, L. L., Wade, R. C., Sachse, C., et al. (2013). GTP regulates the microtubule nucleation activity of gamma-tubulin. *Nat. Cell Biol.* 15, 1317–1327. doi: 10.1038/ncb2863

Holmfeldt, P., Brattsand, G., and Gullberg, M. (2002). MAP4 counteracts microtubule catastrophe promotion but not tubulin-sequestering activity in intact cells. *Curr. Biol.* 12, 1034–1039. doi: 10.1016/s0960-9822(02)00897-7

Holmfeldt, P., Brattsand, G., and Gullberg, M. (2003). Interphase and monoastral-mitotic phenotypes of overexpressed MAP4 are modulated by free tubulin concentrations. *J. Cell Sci.* 116, 3701–3711.

Hori, M., Sato, H., Kitakaze, M., Iwai, K., Takeda, H., Inoue, M., et al. (1994). Beta-adrenergic stimulation disassembles microtubules in neonatal rat cultured cardiomyocytes through intracellular Ca2+ overload. *Circ. Res.* 75, 324–334. doi: 10.1161/01.res.75.2.324

Hoshi, M., Ohta, K., Gotoh, Y., Mori, A., Murofushi, H., Sakai, H., et al. (1992). Mitogen-activated-protein-kinase-catalyzed phosphorylation of microtubule-associated proteins, microtubule-associated protein 2 and microtubule-associated protein 4, induces an alteration in their function. *Eur. J. Biochem.* 203, 43–52.

Hu, J., Chu, Z., Han, J., Zhang, Q., Zhang, D., Dang, Y., et al. (2014). Phosphorylation-dependent mitochondrial translocation of MAP4 is an early step in hypoxia-induced apoptosis in cardiomyocytes. *Cell Death Dis.* 5:e1424. doi: 10.1038/cddis.2014.369

Hu, J. Y., Chu, Z. G., Han, J., Dang, Y. M., Yan, H., Zhang, Q., et al. (2010). The p38/MAPK pathway regulates microtubule polymerization through phosphorylation of MAP4 and Op18 in hypoxic cells. *Cell Mol. Life Sci.* 67, 321–333. doi: 10.1007/s00018-009-0187-z

Iida, J., Itoh, T. J., Hotani, H., Nishiyama, K., Murofushi, H., Bulinski, J. C., et al. (2002). The projection domain of MAP4 suppresses the microtubule-bundling activity of the microtubule-binding domain. *J. Mol. Biol.* 320, 97–106. doi: 10.1016/s0022-2836(02)00402-3

Illenberger, S., Drewes, G., Trinczek, B., Biernat, J., Meyer, H. E., Olmsted, J. B., et al. (1996). Phosphorylation of microtubule-associated proteins MAP2 and MAP4 by the protein kinase p110mark. Phosphorylation sites and regulation of microtubule dynamics. *J. Biol. Chem.* 271, 10834–10843. doi: 10.1074/jbc.271.18.10834

Izzo, A., Mollo, N., Nitti, M., Paladino, S., Cali, G., Genesio, R., et al. (2018). Mitochondrial dysfunction in down syndrome: molecular mechanisms and therapeutic targets. *Mol. Med.* 24:2.

Katsuki, M., Tokuraku, K., Murofushi, H., and Kotani, S. (1999). Functional analysis of microtubule-binding domain of bovine MAP4. *Cell Struct. Funct.* 24, 337–344. doi: 10.1247/csf.24.337

Kerr, J. P., Robison, P., Shi, G., Bogush, A. I., Kempema, A. M., Hexum, J. K., et al. (2015). Detyrosinated microtubules modulate mechanotransduction in heart and skeletal muscle. *Nat. Commun.* 6:8526.

Kitazawa, H., Iida, J., Uchida, A., Haino-Fukushima, K., Itoh, T. J., Hotani, H., et al. (2000). Ser787 in the proline-rich region of human MAP4 is a critical phosphorylation site that reduces its activity to promote tubulin polymerization. *Cell Struct. Funct.* 25, 33–39. doi: 10.1247/csf.25.33

Koene, R. J., Prizment, A. E., Blaes, A., and Konety, S. H. (2016). Shared risk factors in cardiovascular disease and cancer. *Circulation* 133, 1104–1114. doi: 10.1161/circulationaha.115.020406

Kotani, S., Murofushi, H., Maekawa, S., Aizawa, H., and Sakai, H. (1988). Isolation of rat liver microtubule-associated proteins. Evidence for a family of microtubule-associated proteins with molecular mass of around 200,000 which distribute widely among mammalian cells. *J. Biol. Chem.* 263, 5385–5389.

Kremer, B. E., Haystead, T., and Macara, I. G. (2005). Mammalian septins regulate microtubule stability through interaction with the microtubule-binding protein MAP4. *Mol. Biol. Cell* 16, 4648–4659. doi: 10.1091/mbc.e05-03-0267

Lewis, S. A., Wang, D. H., and Cowan, N. J. (1988). Microtubule-associated protein MAP2 shares a microtubule binding motif with tau protein. *Science* 242, 936–939. doi: 10.1126/science.3142041

Li, L., Hu, J., He, T., Zhang, Q., Yang, X., Lan, X., et al. (2015). P38/MAPK contributes to endothelial barrier dysfunction via MAP4 phosphorylation-dependent microtubule disassembly in inflammation-induced acute lung injury. *Sci.Rep.* 5:8895.

Li, L., Zhang, J., Zhang, Q., Huang, Y., and Hu, J. (2019). Cardiac proteomics reveals the potential mechanism of microtubule associated protein 4 phosphorylation-induced mitochondrial dysfunction. *Burns Trauma* 7:8.

Li, L., Zhang, Q., Zhang, X., Zhang, J., Wang, X., Ren, J., et al. (2018). Microtubule associated protein 4 phosphorylation leads to pathological cardiac remodeling in mice. *EBioMedicine* 37, 221–235. doi: 10.1016/j.ebiom.2018.10.017

Lopez-Crisosto, C., Pennanen, C., Vasquez-Trincado, C., Morales, P. E., Bravo-Sagua, R., Quest, A. F. G., et al. (2017). Sarcoplasmic reticulum-mitochondria communication in cardiovascular pathophysiology. *Nat. Rev. Cardiol.* 14, 342–360. doi: 10.1038/nrcardio.2017.23

Magiera, M. M., Singh, P., Gadadhar, S., and Janke, C. (2018). Tubulin posttranslational modifications and emerging links to human disease. *Cell* 173, 1323–1327. doi: 10.1016/j.cell.2018.05.018

Mangan, M. E., and Olmsted, J. B. (1996). A muscle-specific variant of microtubule-associated protein 4 (MAP4) is required in myogenesis. *Development* 122, 771–781.

Matsushima, K., Aosaki, M., Tokuraku, K., Hasan, M. R., Nakagawa, H., and Kotani, S. (2005). Identification of a neural cell specific variant of microtubule-associated protein 4. *Cell Struct. Funct.* 29, 111–124. doi: 10.1247/csf.29.111

Matsushima, K., Tokuraku, K., Hasan, M. R., and Kotani, S. (2012). Microtubule-associated protein 4 binds to actin filaments and modulates their properties. *J. Biochem.* 151, 99–108. doi: 10.1093/jb/mvr119

Mehta, M. M., Weinberg, S. E., and Chandel, N. S. (2017). Mitochondrial control of immunity: beyond ATP. *Nat. Rev. Immunol.* 17, 608–620. doi: 10.1038/nri.2017.66

Mitchison, T., and Kirschner, M. (1984). Dynamic instability of microtubule growth. *Nature* 312, 237–242. doi: 10.1038/312237a0

Mori, A., Aizawa, H., Saido, T. C., Kawasaki, H., Mizuno, K., Murofushi, H., et al. (1991). Site-specific phosphorylation by protein kinase C inhibits assembly-promoting activity of microtubule-associated protein 4. *Biochemistry* 30, 9341–9346. doi: 10.1021/bi00102a029

Nguyen, H. L., Chari, S., Gruber, D., Lue, C. M., Chapin, S. J., and Bulinski, J. C. (1997). Overexpression of full- or partial-length MAP4 stabilizes microtubules and alters cell growth. *J. Cell Sci.* 110(Pt 2), 281–294.

Ojeda-Lopez, M. A., Needleman, D. J., Song, C., Ginsburg, A., Kohl, P. A., Li, Y., et al. (2014). Transformation of taxol-stabilized microtubules into inverted tubulin tubules triggered by a tubulin conformation switch. *Nat. Mater.* 13, 195–203. doi: 10.1038/nmat3858

Ookata, K., Hisanaga, S., Bulinski, J. C., Murofushi, H., Aizawa, H., Itoh, T. J., et al. (1995). Cyclin B interaction with microtubule-associated protein 4 (MAP4) targets p34cdc2 kinase to microtubules and is a potential regulator of M-phase microtubule dynamics. *J. Cell Biol.* 128, 849–862. doi: 10.1083/jcb.128.5.849

Ookata, K., Hisanaga, S., Sugita, M., Okuyama, A., Murofushi, H., Kitazawa, H., et al. (1997). MAP4 is the in vivo substrate for CDC2 kinase in HeLa cells: identification of an M-phase specific and a cell cycle-independent phosphorylation site in MAP4. *Biochemistry* 36, 15873–15883. doi: 10.1021/bi971251w

Ozer, R. S., and Halpain, S. (2000). Phosphorylation-dependent localization of microtubule-associated protein MAP2c to the actin cytoskeleton. *Mol. Biol. Cell* 11, 3573–3587. doi: 10.1091/mbc.11.10.3573

Parysek, L. M., del Cerro, M., and Olmsted, J. B. (1985). Microtubule-associated protein 4 antibody: a new marker for astroglia and oligodendroglia. *Neuroscience* 15, 869–875. doi: 10.1016/0306-4522(85)90084-3

Permana, S., Hisanaga, S., Nagatomo, Y., Iida, J., Hotani, H., and Itoh, T. J. (2005). Truncation of the projection domain of MAP4 (microtubule-associated protein 4) leads to attenuation of microtubule dynamic instability. *Cell Struct. Funct.* 29, 147–157. doi: 10.1247/csf.29.147

Ren, J., and Zhang, Y. (2018). New therapeutic approaches in the management of cardiometabolic diseases: bringing the concepts together. *Curr. Drug Targets* 19, 987–988. doi: 10.2174/1389450119091806290957 09

Robison, P., Caporizzo, M. A., Ahmadzadeh, H., Bogush, A. I., Chen, C. Y., Margulies, K. B., et al. (2016). Detyrosinated microtubules buckle and bear load in contracting cardiomyocytes. *Science* 352:aaf0659. doi: 10.1126/science.aaf0659

Samarakoon, R., and Higgins, P. J. (2018). The cytoskeletal network regulates expression of the profibrotic genes PAI-1 and CTGF in vascular smooth muscle cells. *Adv. Pharmacol.* 81, 79–94. doi: 10.1016/bs.apha.2017.08.006

Samora, C. P., Mogessie, B., Conway, L., Ross, J. L., Straube, A., and McAinsh, A. D. (2011). MAP4 and CLASP1 operate as a safety mechanism to maintain a stable spindle position in mitosis. *Nat. Cell Biol.* 13, 1040–1050. doi: 10.1038/ncb2297

Sato, H., Hori, M., Kitakaze, M., Iwai, K., Takashima, S., Kurihara, H., et al. (1993). Reperfusion after brief ischemia disrupts the microtubule network in canine hearts. *Circ. Res.* 72, 361–375. doi: 10.1161/01.res.72.2.361

Sato, H., Nagai, T., Kuppuswamy, D., Narishige, T., Koide, M., Menick, D. R., et al. (1997). Microtubule stabilization in pressure overload cardiac hypertrophy. *J. Cell Biol.* 139, 963–973. doi: 10.1083/jcb.139.4.963

Schwalm, J. D., McKee, M., Huffman, M. D., and Yusuf, S. (2016). Resource effective strategies to prevent and treat cardiovascular disease. *Circulation* 133, 742–755. doi: 10.1161/circulationaha.115.008721

Semenova, I., Ikeda, K., Resaul, K., Kraikivski, P., Aguiar, M., Gygi, S., et al. (2014). Regulation of microtubule-based transport by MAP4. *Mol. Biol. Cell* 25, 3119–3132. doi: 10.1091/mbc.e14-01-0022

Shiina, N., and Tsukita, S. (1999). Mutations at phosphorylation sites of Xenopus microtubule-associated protein 4 affect its microtubule-binding ability and chromosome movement during mitosis. *Mol. Biol. Cell* 10, 597–608. doi: 10.1091/mbc.10.3.597

Small, J. V., Geiger, B., Kaverina, I., and Bershadsky, A. (2002). How do microtubules guide migrating cells? *Nat. Rev. Mol. Cell Biol.* 3, 957–964. doi: 10.1038/nrm971

Srsen, V., Kitazawa, H., Sugita, M., Murofushi, H., Bulinski, J. C., Kishimoto, T., et al. (1999). Serum-dependent phosphorylation of human MAP4 at Ser696 in cultured mammalian cells. *Cell Struct. Funct.* 24, 321–327. doi: 10.1247/csf.24.321

Suomalainen, A., and Battersby, B. J. (2018). Mitochondrial diseases: the contribution of organelle stress responses to pathology. *Nat. Rev. Mol. Cell Biol.* 19, 77–92. doi: 10.1038/nrm.2017.66

Tagawa, H., Rozich, J. D., Tsutsui, H., Narishige, T., Kuppuswamy, D., Sato, H., et al. (1996). Basis for increased microtubules in pressure-hypertrophied cardiocytes. *Circulation* 93, 1230–1243. doi: 10.1161/01.cir.93.6.1230

Takahashi, M., Shiraishi, H., Ishibashi, Y., Blade, K. L., McDermott, P. J., Menick, D. R., et al. (2003). Phenotypic consequences of beta1-tubulin expression and MAP4 decoration of microtubules in adult cardiocytes. *Am. J. Physiol. Heart Circ. Physiol.* 285, H2072–H2083.

Teiger, E., Than, V. D., Richard, L., Wisnewsky, C., Tea, B. S., Gaboury, L., et al. (1996). Apoptosis in pressure overload-induced heart hypertrophy in the rat. *J. Clin. Invest.* 97, 2891–2897. doi: 10.1172/jci118747

Tokuraku, K., Katsuki, M., Nakagawa, H., and Kotani, S. (1999). A new model for microtubule-associated protein (MAP)-induced microtubule assembly. The Pro-rich region of MAP4 promotes nucleation of microtubule assembly in vitro. *Eur. J. Biochem.* 259, 158–166. doi: 10.1046/j.1432-1327.1999.00019.x

Tokuraku, K., Matsushima, K., Matui, T., Nakagawa, H., Katsuki, M., Majima, R., et al. (2003). The number of repeat sequences in microtubule-associated protein 4 affects the microtubule surface properties. *J. Biol. Chem.* 278, 29609–29618. doi: 10.1074/jbc.m302186200

Tokuraku, K., Noguchi, T. Q., Nishie, M., Matsushima, K., and Kotani, S. (2007). An isoform of microtubule-associated protein 4 inhibits kinesin-driven microtubule gliding. *J. Biochem.* 141, 585–591. doi: 10.1093/jb/mvm063

Tombes, R. M., Peloquin, J. G., and Borisy, G. G. (1991). Specific association of an M-phase kinase with isolated mitotic spindles and identification of two of its substrates as MAP4 and MAP1B. *Cell Regul.* 2, 861–874. doi: 10.1091/mbc.2.11.861

Walczak, C. E. (2000). Microtubule dynamics and tubulin interacting proteins. *Curr. Opin. Cell Biol.* 12, 52–56. doi: 10.1016/s0955-0674(99)00056-3

Wang, X. M., Peloquin, J. G., Zhai, Y., Bulinski, J. C., and Borisy, G. G. (1996). Removal of MAP4 from microtubules in vivo produces no observable phenotype at the cellular level. *J. Cell Biol.* 132, 345–357. doi: 10.1083/jcb.132.3.345

Watanabe, S., and Goshima, G. (2014). Friction on MAP determines its traveling direction on microtubules. *Dev. Cell* 29, 5–6. doi: 10.1016/j.devcel.2014.03.022

Webster, D. R., and Bratcher, J. M. (2006). Developmental regulation of cardiac MAP4 protein expression. *Cell Motil. Cytoskeleton* 63, 512–522. doi: 10.1002/cm.20140

West, R. R., Tenbarge, K. M., and Olmsted, J. B. (1991). A model for microtubule-associated protein 4 structure. Domains defined by comparisons of human, mouse, and bovine sequences. *J. Biol. Chem.* 266, 21886–21896.

Wu, N. N., Tian, H., Chen, P., Wang, D., Ren, J., and Zhang, Y. (2019a). Physical exercise and selective autophagy: benefit and risk on cardiovascular health. *Cells* 8:1436. doi: 10.3390/cells8111436

Wu, N. N., Zhang, Y., and Ren, J. (2019b). Mitophagy, mitochondrial dynamics, and homeostasis in cardiovascular aging. *Oxid Med. Cell Longev.* 2019:9825061.

Xia, X., and He, C. (2018). Microtubule-associated protein 4 is a prognostic factor and promotes tumor progression in lung adenocarcinoma. *Dis. Markers* 2018:8956072.

Xiao, H., Wang, H., Zhang, X., Tu, Z., Bulinski, C., Khrapunovich-Baine, M., et al. (2012). Structural evidence for cooperative microtubule stabilization by Taxol and the endogenous dynamics regulator MAP4. *ACS Chem. Biol.* 7, 744–752. doi: 10.1021/cb200403x

Zahnleiter, D., Hauer, N. N., Kessler, K., Uebe, S., Sugano, Y., Neuhauss, S. C., et al. (2015). MAP4-dependent regulation of microtubule formation affects centrosome, cilia, and Golgi architecture as a central mechanism in growth regulation. *Hum. Mutat.* 36, 87–97. doi: 10.1002/humu.22711

Zhang, C. C., Yang, J. M., Bash-Babula, J., White, E., Murphy, M., Levine, A. J., et al. (1999). DNA damage increases sensitivity to vinca alkaloids and decreases sensitivity to taxanes through p53-dependent repression of microtubule-associated protein 4. *Cancer Res.* 59, 3663–3670.

Zhang, C. C., Yang, J. M., White, E., Murphy, M., Levine, A., and Hait, W. N. (1998). The role of MAP4 expression in the sensitivity to paclitaxel and resistance to vinca alkaloids in p53 mutant cells. *Oncogene* 16, 1617–1624. doi: 10.1038/sj.onc.1201658

Zhang, J., Li, L., Zhang, Q., Wang, W., Zhang, D., Jia, J., et al. (2019a). Microtubule-associated protein 4 phosphorylation regulates epidermal keratinocyte migration and proliferation. *Int. J. Biol. Sci.* 15, 1962–1976. doi: 10.7150/ijbs.35440

Zhang, J., Li, L., Zhang, Q., Yang, X., Zhang, C., Zhang, X., et al. (2019b). Phosphorylation of microtubule- associated protein 4 promotes hypoxic endothelial cell migration and proliferation. *Front. Pharmacol.* 10:368. doi: 10.3389/fphar.2019.00368

Zhang, L., Shao, H., Zhu, T., Xia, P., Wang, Z., Liu, L., et al. (2013). DDA3 associates with microtubule plus ends and orchestrates microtubule dynamics and directional cell migration. *Sci. Rep.* 3:1681.

Zhang, Y., Whaley-Connell, A. T., Sowers, J. R., and Ren, J. (2018). Autophagy as an emerging target in cardiorenal metabolic disease: from pathophysiology to management. *Pharmacol. Ther.* 191, 1–22. doi: 10.1016/j.pharmthera.2018.06.004

Zhou, H., Wang, S., Hu, S., Chen, Y., and Ren, J. (2018a). ER-mitochondria microdomains in cardiac ischemia-reperfusion injury: a fresh perspective. *Front. Physiol.* 9:755. doi: 10.3389/fphys.2018.00755

Zhou, H., Wang, S., Zhu, P., Hu, S., Chen, Y., and Ren, J. (2018b). Empagliflozin rescues diabetic myocardial microvascular injury via AMPK-mediated inhibition of mitochondrial fission. *Redox Biol.* 15, 335–346. doi: 10.1016/j.redox.2017.12.019

Zhou, Z., Guo, F., Yi, L., Tang, J., Dou, Y., and Huan, J. (2015). The p38/mitogen-activated protein kinase pathway is implicated in lipopolysaccharide-induced microtubule depolymerization via up-regulation of microtubule-associated protein 4 phosphorylation in human vascular endothelium. *Surgery* 157, 590–598. doi: 10.1016/j.surg.2014.10.007

Conflict of Interest: The authors declare that the research was conducted in the absence of any commercial or financial relationships that could be construed as a potential conflict of interest.

Copyright © 2020 Li, Zhang, Lei, Huang and Hu. This is an open-access article distributed under the terms of the Creative Commons Attribution License (CC BY). The use, distribution or reproduction in other forums is permitted, provided the original author(s) and the copyright owner(s) are credited and that the original publication in this journal is cited, in accordance with accepted academic practice. No use, distribution or reproduction is permitted which does not comply with these terms.

frontiers in Physiology

REVIEW
published: 04 September 2020
doi: 10.3389/fphys.2020.01068

Targeting Ca^{2+} Handling Proteins for the Treatment of Heart Failure and Arrhythmias

Alexandra Njegic[1,2†], Claire Wilson[1,3†] and Elizabeth J. Cartwright[1]*

[1] Division of Cardiovascular Sciences, The University of Manchester, Manchester, United Kingdom, [2] Centre for Tumour Biology, Barts Cancer Institute, Queen Mary University of London, London, United Kingdom, [3] Institute of Translational Medicine, University of Liverpool, Liverpool, United Kingdom

Diseases of the heart, such as heart failure and cardiac arrhythmias, are a growing socio-economic burden. Calcium (Ca^{2+}) dysregulation is key hallmark of the failing myocardium and has long been touted as a potential therapeutic target in the treatment of a variety of cardiovascular diseases (CVD). In the heart, Ca^{2+} is essential for maintaining normal cardiac function through the generation of the cardiac action potential and its involvement in excitation contraction coupling. As such, the proteins which regulate Ca^{2+} cycling and signaling play a vital role in maintaining Ca^{2+} homeostasis. Changes to the expression levels and function of Ca^{2+}-channels, pumps and associated intracellular handling proteins contribute to altered Ca^{2+} homeostasis in CVD. The remodeling of Ca^{2+}-handling proteins therefore results in impaired Ca^{2+} cycling, Ca^{2+} leak from the sarcoplasmic reticulum and reduced Ca^{2+} clearance, all of which contributes to increased intracellular Ca^{2+}. Currently, approved treatments for targeting Ca^{2+} handling dysfunction in CVD are focused on Ca^{2+} channel blockers. However, whilst Ca^{2+} channel blockers have been successful in the treatment of some arrhythmic disorders, they are not universally prescribed to heart failure patients owing to their ability to depress cardiac function. Despite the progress in CVD treatments, there remains a clear need for novel therapeutic approaches which are able to reverse pathophysiology associated with heart failure and arrhythmias. Given that heart failure and cardiac arrhythmias are closely associated with altered Ca^{2+} homeostasis, this review will address the molecular changes to proteins associated with both Ca^{2+}-handling and -signaling; their potential as novel therapeutic targets will be discussed in the context of pre-clinical and, where available, clinical data.

Keywords: cardiovascular disease, heart failure, arrhythmia, calcium dysregulation, calcium

OPEN ACCESS

Edited by:
Jun Ren,
University of Washington,
United States

Reviewed by:
Marisol Ruiz-Meana,
University Hospital Vall d'Hebron-Universitat Autònoma de Barcelona, Spain
Haixia Xu,
Zhongshan Hospital, Fudan University, China

****Correspondence:***
Elizabeth J. Cartwright
elizabeth.j.cartwright@manchester.ac.uk

† These authors have contributed equally to this work

Specialty section:
This article was submitted to Clinical and Translational Physiology, a section of the journal Frontiers in Physiology

Received: *31 May 2020*
Accepted: *04 August 2020*
Published: *04 September 2020*

Citation:
Njegic A, Wilson C and Cartwright EJ (2020) Targeting Ca^{2+} Handling Proteins for the Treatment of Heart Failure and Arrhythmias. Front. Physiol. 11:1068. doi: 10.3389/fphys.2020.01068

Abbreviations: AC, adenylyl cyclase; AC6, adenylyl cyclase 6; ACE, angiotensin-converting enzyme; ACEI, ACE inhibitors; AF, atrial fibrillation; ANG-II, angiotensin II; AP, action potential; ARB, angiotensin receptor blocker; AVN, atrioventricular node; Ca^{2+}, calcium; CaM, calmodulin; CaMKII, Ca^{2+}/calmodulin-dependent protein kinase; CPVT, catecholaminergic polymorphic ventricular tachycardia; CVD, cardiovascular disease; DAD, delayed after depolarization; EAD, early after depolarization; ECC, excitation contraction coupling; GWAS, genome wide association studies; HF, heart failure; HFmEF, HF with mid-range ejection fraction; HFpEF, HF with preserved ejection fraction; HFrEF, HF with reduced ejection fraction; HNO/NO, nitroxyl; I_{Ca}, Ca^{2+} current; I_{CaL}, L-type Ca^{2+} current; I_K, K^+ current; I_{Na}, Na^+ current; I_{NCX}, NCX current; I_{to}, transient outward K^+ current; I/R, ischemia/reperfusion; LQTS, long QT syndrome; LTCC, L-type Ca^{2+} channel; MAPK, mitogen activated protein kinase; MCU, mitochondrial Ca^{2+} uniporter; MI, myocardial infarction; NCX, Na^+/Ca^{2+} exchanger; NFAT, nuclear factor of activated T-cell; PKA, protein kinase A; PLN, phospholamban; PMCA, plasma membrane Ca^{2+} ATPase; Pyr-3, pyrazole-3; RAAS, renin–angiotensin–aldosterone signaling; ROS, reactive oxygen species; RR, ruthenium red; RyR, ryanodine receptor; SAN, sino-atrial node; SERCA, SR Ca^{2+} ATPase; SNPs, single nucleotide polymorphisms; SR, sarcoplasmic reticulum; TAC, transverse aortic constriction; TdP, Torsades de Pointes; TRIC, trimeric intracellular cation.

INTRODUCTION

Cardiovascular diseases, such as ischemic heart disease, stroke, and arrhythmias, are the leading cause of death globally (Roth et al., 2017); with over 17 million fatalities attributed annually to CVD (Collaborators GBDCoD., 2018). Acquired CVD are thought to arise due to a combination of modifiable environmental causes and underlying genetic pre-dispositions (Kannel et al., 1961; Khot et al., 2003). CVDs lead to both functional and structural changes to the vasculature and myocardium. In the heart, cardiac dysfunction encompassing cardiac decompensation, arrhythmogenesis and impaired contractility are all closely associated with changes to calcium (Ca^{2+}) handling proteins, Ca^{2+} channels and Ca^{2+} pumps (Lou et al., 2012). Determining the full scope of changes to Ca^{2+}-handling proteins and mechanisms will aid in the development of novel therapeutics to reverse and/or prevent CVD. This review will focus on how changes to Ca^{2+}-handling proteins observed during cardiac arrhythmogenesis and HF have been therapeutically targeted, with emphasis placed on recent developments in the search for novel therapies.

Ca^{2+} AND Ca^{2+}-HANDLING PROTEINS IN THE HEART

Maintenance of Ca^{2+} Homeostasis

The initiation and control of each heartbeat is achieved by the cardiac conduction system consisting of the SAN, AVN, and His-Purkinje system. Electrical impulses, termed cardiac AP arise from the SAN, often referred to as the pacemaker of heart, and propagate throughout the heart (Boyett, 2009). During the cardiac AP, the electrical membrane potential rapidly rises and falls, referred to as depolarization and repolarization respectively, triggering ECC. The changes in membrane potential are driven by the movement of ions across the cell membrane (Grant, 2009). Generally, the cardiac AP is divided into five phases (**Figure 1**): (Phase 0) involves rapid depolarization of the membrane potential which is key to the propagation of cardiac impulse in the heart; (Phase 1) is a brief interval of rapid depolarization; (Phase 2) known as the plateau phase of the cardiac AP in which Ca^{2+} enters the cell to trigger ECC; (Phase 3) rapid repolarization restores the membrane potential; and (Phase 4) the membrane potential is stable at the resting potential (Grant, 2009). Following an AP, the cell enters a recovery state termed the refractory period. Here, the cell is unable to initiate an AP which allows the heart to prepare for the next contraction (Ramza et al., 1990). The key ionic currents involved in the generation and propagation of the cardiac AP are the Ca^{2+} (I_{Ca}), sodium (Na^+, I_{Na}), and potassium (K^+, I_K) currents (Grant, 2009). It is worth noting that different cell types within the cardiac conduction system exhibit specific cardiac AP relating to their function. Differences in ion channel expression results in regional specific APs (Monfredi et al., 2010).

In the heart, Ca^{2+} has an indispensable role in cardiomyocyte ECC; in addition, as a signaling molecule, Ca^{2+} also acts as an intracellular second messenger in cardiomyocytes and other cell types. ECC results in cardiac contraction and helps to maintain diastolic and systolic cardiac function (Lou et al., 2012). During ECC, four steps involving Ca^{2+} trigger cardiomyocyte contraction: (1) membrane depolarization causes a rapid influx of Ca^{2+} through the LTCC located on transverse (T)-tubules, which results in an intracellular Ca^{2+} gradient in the junctional zone; (2) Ca^{2+} diffusion activates RyR located on the SR resulting in Ca^{2+} sparks and an amplification of the Ca^{2+} signal in a process termed Ca^{2+}-induced Ca^{2+} release; (3) Ca^{2+} released via RyR from internal SR stores binds to troponin-C to cause contraction through actin-myosin filament crossbridge formation; (4) Ca^{2+} is transported out of the cardiomyocyte through NCX and PMCA or back into internal stores through SERCA and MCU (Bers, 2002; Lou et al., 2012) (**Figure 2**). The function of SERCA is tightly regulated by PLN. In its dephosphorylated form, PLN inhibits SERCA2a but when its phosphorylated at Ser10, Ser16 or Thr17, the inhibition of SERCA2 is relieved (Mattiazzi et al., 2005). Such is the importance of PLN-mediated SERCA2a regulation that PLN ablation induces a hypercontractile cardiac phenotype (Luo et al., 1994). Ca^{2+} homeostasis is also maintained through additional Ca^{2+} channels located on the plasma membrane (**Figure 2**). The transient receptor potential channels (TRP) are a large family of non-selective cation permeable channels which, depending on the family, permit the influx of Ca^{2+}, along with Mg^{2+}, Zn^{2+}, and Na^+(Falcon et al., 2019). The TRP family can be further divided into subfamilies, including TRP-canonical (TRPC), TRP vallinoid-related (TRPV), and TRP melastatin-related (TRPM) (Freichel et al., 2017). The ECC Ca^{2+} cycle is tightly regulated by protein kinases and accessory proteins which modify the activity and expression of ECC Ca^{2+} handling proteins. Functional changes to proteins involved in ECC and Ca^{2+} homeostasis can impair contractility and contribute to cardiac dysfunction. Furthermore, changes to Ca^{2+} handling can also impair cardiac conductivity, causing fatal arrhythmias. Altered Ca^{2+} homeostasis can result in abnormal automaticity, triggered activity, and can provide a substrate for re-entry arrhythmias (Landstrom et al., 2017). The contributions these Ca^{2+} handling proteins make to the pathophysiology of cardiac hypertrophy, HF, and cardiac arrhythmias are discussed in detail later in this review.

Current Therapeutic Approaches Targeting HF and Cardiac Arrhythmia and Their Impact on Ca^{2+}-Handling Proteins

Treatment of HF and cardiac arrhythmias can be surgical (including implantation of a pacemaker or implantable cardioverter defibrillator) and/or pharmacological. Primary drug-based therapies for these disorders include targeting (1) the RAAS signaling system, (2) β-adrenergic hyperactivation, and (3) aberrant ion channel activation (Ca^{2+}, Na^+, and K^+). As the focus of this review concerns how Ca^{2+} handling proteins present a novel therapeutic approach, we discuss the current

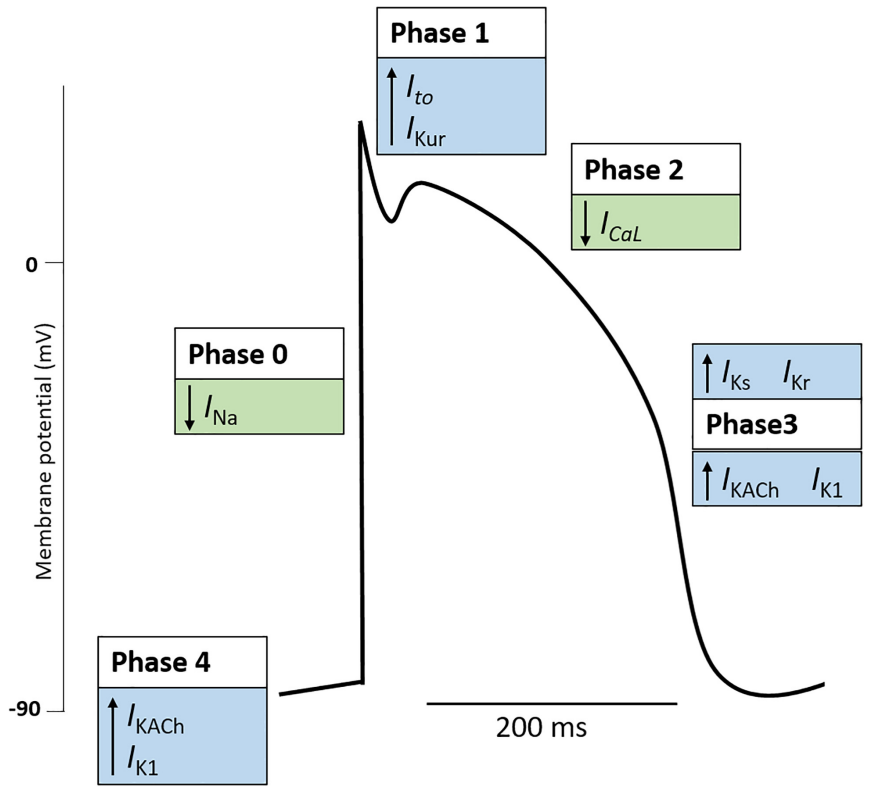

FIGURE 1 | The cardiac action potential. The cardiac action potential represents the electrical activity of a cardiomyocyte during cardiac contraction and is governed by changes in outward (blue boxes) and inward (green boxes) cardiac ion currents. Generally, the cardiac action potential is divided into five Phases. (Phase 4: Resting) The resting membrane potential is stable (∼–90 mV) and maintained by outward leak of K^+ (I_{KACh}, I_{K1}). Here the Na^+ and Ca^+ channels are closed. (Phase 0: Upstroke) An action potential at a neighboring cardiomyocyte initiates a rise in membrane potential. When the membrane potential reaches the threshold potential (∼70 mV), Na^+ channels open, resulting in a rapid influx of Na^+ and the generation on the inward Na^+ current (I_{Na}). Na^+ channels become inactivated soon after opening (Phase 1: Early repolarization). Some K^+ channels transiently open causing an outward K^+ current (I_{to}, I_{Kur}). This results in a period of rapid repolarization. (Phase 2: Plateau phase) L-type Ca^{2+} channels are open to create a small, constant inward Ca^{2+} current (I_{CaL}) which triggers excitation contraction coupling resulting in cardiomyocyte contraction. K^+ currents remain active, although the two currents are electrically balanced and maintain a plateau. (Phase 3: Repolarization) Ca^{2+} channels become gradually inactivated and the outflow of K^+ exceeds the Ca^{2+} inflow. K^+ currents (I_{Ks}, I_{Kr}, I_{KACh}, I_{K1}) repolarize the cell and the resting membrane potential is restored. Note, the figure represents the typical ventricular cardiac action potential. The action potential of atrial cells and pacemaker cells (those found in the sinus node, atrioventricular node, and Purkinje fibers) differ. K^+, potassium; Na^+, sodium; Ca^{2+}, calcium; I_{KACh}, muscarinic-gated K^+ current; I_{K1}, inward rectifier K^+ current; I_{Na}, Na^+ current; I_{to}, transient outward K^+ current; I_{Kur}, delayed rectifier K^+ current; I_{CaL}, L-type Ca^{2+} current; I_{Ks}, delayed rectifier (slow) K^+ current; I_{kr}, delayed rectifier (fast) K^+ current.

pharmacological therapies mentioned above in brief, including any known impact they have on Ca^{2+} handling in the heart.

The Renin–Angiotensin–Aldosterone System

Renin–angiotensin–aldosterone signaling is elevated in patients with HF and reduced ejection fraction (HFrEF, ejection fraction < 40%) (Watkins et al., 1976) and in advanced HF, the levels of plasma renin activity and aldosterone are increased (Dzau et al., 1981). Furthermore, aldosterone secretion is enhanced in response to ANG-II signaling and its receptor is upregulated in cardiomyocytes from HFrEF patients (Yoshida et al., 2005). Aldosterone alone is pro-hypertrophic, pro-fibrotic and pro-inflammatory (Pinilla-Vera et al., 2019). Increased neurohormonal signaling can activate the MAPK which, in turn, upregulates pro-hypertrophic gene transcription (Zhang et al., 2003; Nakamura and Sadoshima, 2018). The MAPK signaling cascade comprises four main 'typical' branches; ERK1/2, JNK, p38 and ERK5, all with distinct upstream regulators (Rose et al., 2010) and activation of the ERK1/2 signaling cascade may determine whether concentric or eccentric cardiomyocyte growth and remodeling occurs (Bueno et al., 2000; Lorenz et al., 2009; Kehat et al., 2011). Activation of RAAS can also promote cardiac arrhythmias including AF and ventricular tachyarrhythmias, partly due to the formation of a pro-arrhythmia substrate in cardiac hypertrophy and HF. In addition, RAAS is also known to directly affect cardiac ion channels. Angiotensin and aldosterone have been shown to attenuate the transient outward K^+ current (I_{to}) and enhance I_{CaL}, impacting AP duration and repolarization. Whilst oxidative stress triggered by RAAS activation is reported to affect cardiac ion currents and several Ca^{2+} handling proteins (Iravanian and Dudley, 2008).

The maladaptive effects associated with over-activation of the RAAS is one of main focuses of current therapeutics; both ACEI and ARBs are prescribed to patients with HF to

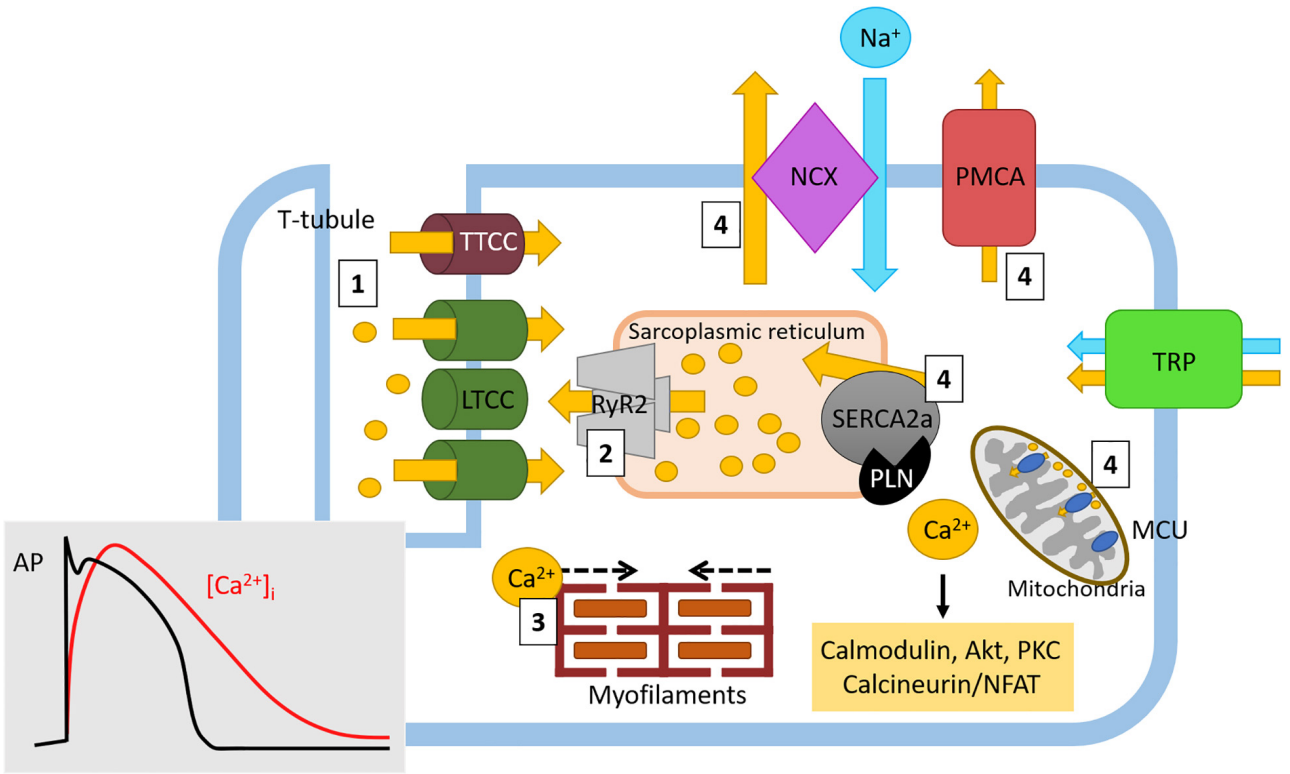

FIGURE 2 | Physiological Ca^{2+} cycling in cardiomyocytes. Ca^{2+} cycling in cardiomyocytes generates cardiac contraction through excitation-contraction coupling. Briefly, (1) Ca^{2+} (yellow circles and arrows) rapidly enters the cell through LTCC where it causes (2) Ca^{2+}-induced Ca^{2+} release from Ca^{2+} stores in the sarcoplasmic reticulum. During these early stages of ECC, intracellular Ca^{2+} ($[Ca^{2+}]_i$) levels rapidly increase (red line, insert) following the onset of the cardiac action potential and cardiomyocyte depolarization (and black line, insert). (3) The amplified Ca^{2+} signal then induces actin-myosin myofilament crossbridge formation, resulting in cardiac contraction. Following this action, as the cardiac action potential enters the plateau phase (black line), the inward $[Ca^{2+}]_i$ levels begin to slowly decrease (red line). (4) Ca^{2+} is either returned to internal stores through SR-located SERCA2a and mitochondrial MCU or to the extracellular space through NCX (in exchange for $3Na^+$, blue circle and arrow) and PMCA. Here, as cardiac repolarization occurs (black line) the levels of $[Ca^{2+}]_i$ return to baseline (red line) in order to return membrane polarization to baseline. Free Ca^{2+} can also drive intracellular signaling (yellow box) which can influence gene transcription. Ca^{2+} homeostasis is also maintained by the TRP channel family of proteins. Ca^{2+}, calcium; Na^+, sodium; LTCC, L-type Ca^{2+} channel; TTCC, T-type Ca^{2+} channel; NCX, sodium calcium exchanger; PMCA, plasma membrane Ca^{2+} ATPase; TRP, transient receptor potential (canonical, vallinoid-related, melastatin-related), RyR, ryanodine receptor; SERCA, sarco/endoplasmic reticulum Ca^{2+}-ATPase; PLN, phospholamban; MCU, mitochondrial Ca^{2+} uniporter.

help improve cardiac function and survival (McMurray, 2004; Demers et al., 2005). Several clinical trials have shown that ACEI and ARBs reduce mortality in patients with HFrEF (Kjekshus et al., 1992; Maggioni et al., 2002; McMurray et al., 2003). In addition, further inhibition of RAAS is achieved through aldosterone antagonism. Aldosterone receptor blockade with an agent such as eplerenone has been shown to reduce the risk of death and hospitalization events in patients with HFrEF (Pitt et al., 2003; Zannad et al., 2011). However, the absolute beneficial use of aldosterone agonists in patients with HF and preserved ejection fraction (HFpEF, ejection fraction > 50%) is still yet to be determined (Pitt et al., 2014). Studies have also aimed to dissect the use of RAAS inhibitors in patients with cardiac arrhythmias (Iravanian and Dudley, 2008). ACEI and ARBs have been shown to reduce the recurrence rate in patients with existing AF (Madrid et al., 2002; Ueng et al., 2003), and reduce the incidence of new onset AF in hypertensive (Wachtell et al., 2005)- and post-MI (Pedersen et al., 1999) patients. Treatment with ACEI has also been associated with a reduced risk of sudden cardiac death in HF patients (Heart Outcomes Prevention Evaluation Study Investigator, Yusuf et al., 2000).

The β-Adrenergic Pathway

In HF, elevated sympathetic activity increases blood catecholamines; an increase which inversely correlates with survival (Lymperopoulos et al., 2013). The initial elevation in sympathetic activation is beneficial as cardiac contractility is enhanced to maintain function; however, chronic activation of β-adrenergic receptors (β-AR) promotes cardiac dysfunction through increased cardiomyocyte hypertrophy (Lohse et al., 2003). Catecholamine binding to β-AR activates AC and subsequently leads to an increase in cAMP levels; cAMP activates PKA which phosphorylates proteins associated with Ca^{2+} handling, including LTCC (Schroder et al., 1998), RyR2 (Wehrens et al., 2006), and PLN (Antos et al., 2001; Nakamura and Sadoshima, 2018), together culminating in increased levels of cytosolic Ca^{2+} (Port and Bristow, 2001;

Nakamura and Sadoshima, 2018). In addition to phosphorylation of key Ca^{2+} handling proteins, β-AR signaling also results in the *s*-nitrosylation of many Ca^{2+} handling proteins in cardiomyocytes, such as PLN and cardiac troponin C (Irie et al., 2015). Furthermore, activation of β-AR is the primary mechanism underlying sympathetic control of heart rhythm, with many of the cardiac ionic currents responsive to β-adrenergic stimulation (Gardner et al., 2016). Unsurprisingly, enhanced adrenergic activity has been identified in arrhythmic conditions, including AF, and results in enhanced automaticity and triggered activity (Workman, 2010; Antzelevitch and Burashnikov, 2011).

Therapeutic targeting of this excessive β-adrenergic response is achieved using β-blockers. β-blockers are deployed to improve cardiac function, reduce incidence of arrhythmias, and decrease mortality associated with HF by diminishing the hyperactivity of the β-adrenergic pathway. Improvements in mortality rates in patients with HFrEF have been recorded, irrespective of the type of β-blocker (Chatterjee et al., 2013; Pinilla-Vera et al., 2019), and large randomized trials have provided further evidence of the advantageous effects of single β-blockers agents in the treatment of HFrEF (CIBIS-II Investigators and Committees, 1999; Tepper, 1999; Packer et al., 2002). Furthermore, a meta-analysis of all clinical trials involving the use of β-blockers in HFpEF patients suggested the use of β-blockers may reduce mortality by 22% (Fukuta et al., 2017). Interestingly, through their mechanism of action, β-blockers also inhibit PKA hyperphosphorylation of the RyR2 channel in both human and animal models of HF (Reiken et al., 2001, 2003); the proposed mechanism by which β-blockers improve cardiac function in HF is by preventing PKA hyperphosphorylation of RyR2 Ser2808 and subsequent receptor destabilization (Shan et al., 2010). β-blockers also display multiple antiarrhythmic effects including a lowering of heart rate, a decrease in SAN/AVN automaticity and re-entry events, and a reduction in afterdepolarizations. Notably, β-blockers are used for the treatment of sinus and supraventricular tachycardias and in rate control of AF and ventricular tachyarrhythmias (Lei et al., 2018). In addition, β-blockers are also used to treat some patients with LQTS, thus reducing the risk of adverse cardiac events; although it is reported that some β-blockers are more effective than others (Chockalingam et al., 2012; Abu-Zeitone et al., 2014). Patients with CPVT are prescribed β1/β2-blockers such as nadolol which, when compared to β1-selective blockers, reduces the severity and incidence of ventricular arrhythmias (Leren et al., 2016).

Ion Channel Blockers; Ca^{2+}, Na^{+}, and K^{+}

The voltage activated LTCC is a multi-subunit protein which, under basal conditions, provides the primary entry point for rapid Ca^{2+} influx. During HF, increased phosphorylation of LTCCs may result in redistribution of LTCCs and increased channel open probability (Schroder et al., 1998; Sanchez-Alonso et al., 2016) which can lead to increased Ca^{2+} influx, a phenomenon implicated in both hypertrophy and HF (Richard et al., 1998). Changes in LTCC dynamics have also been associated with the development of arrhythmias, and numerous LTCC mutations have been identified in primary arrhythmic disorders such as LQTS and Brugada syndrome (Grant, 2009). The LTCC is the primary target of Ca^{2+} channel blockers which are currently extensively used to treat hypertension and certain arrhythmic disorders, but are used with caution in HF. Inhibiting the LTCC with amlodipine prevents adverse cardiac remodeling in a mouse model of TAC-induced pressure overload hypertrophy (Liao et al., 2005). However, cardiac-specific knockdown of LTCC has the opposing effect and results in pathological hypertrophy partly due to a compensatory increase in Ca^{2+} leak from the SR via RyR2 (Goonasekera et al., 2012).

Ca^{2+} channel blockers (non-dihydropyridines and dihydropyridines) are generally not prescribed to patients with HFrEF, except for amlodipine. Due to their negative inotropic effects, clinical studies have demonstrated that non-dihydropyridines increase mortality rates and incidence of late-onset HF (The Danish Study Group on Verapamil in Myocardial Infarction, 1990; Goldstein et al., 1991) and should be avoided to prevent further depression of cardiac function. However, amlodipine (a dihydropyridine) does not affect mortality so can be used to treat HFrEF patients with angina and/or hypertension (Packer et al., 1996). On the other hand, both classes of Ca^{2+} channel blockers have no adverse effects on mortality or HF hospitalization in patients with HFpEF (Patel et al., 2014); although, non-dihydropyridines tend only to be considered when β-blockers alone are unsuccessful (Godfraind, 2017).

Ca^{2+} channel blockers are currently approved antiarrhythmic agents used to treat arrhythmias arising from SAN and AVN dysfunction; the AP generated by these areas of the heart are strongly dependent on Ca^{2+} entry (Lei et al., 2018). The non-dihydropyridines Ca^{2+} channel blockers used for the treatment of arrhythmias (supraventricular arrhythmias, ventricular tachycardias occurring in the absence of structural heart disease, and AF) include phenylalkylamines and benzothiazepines (for example, verapamil, and diltiazem, respectively) (January et al., 2014; Lei et al., 2018). However, as noted above, non-dihydropyridines should not be used in patients with decompensated HF. In addition, non-dihydropyridines should be avoided in patients with AF combined with pre-excitation (a condition in which the ventricles activate too early) as treatment may increase the risk of ventricular fibrillation (January et al., 2014). There is evidence that combining Ca^{2+} channel blockers with other pharmacological approaches can enhance the treatment of arrhythmic conditions. For example, in patients with CPVT, the addition verapamil to existing β-blocker therapy was shown to reduce the incidence of exercise-induced arrhythmias when compared to β-blocker therapy alone (Rosso et al., 2007).

Na^{+} channel blockers target the voltage-gated Na^{+} channel, $Na_v1.5$, which drives the inward Na^{+} current responsible for the rapid depolarization at the start of the cardiac AP (Lei et al., 2018). The aim of Na^{+} channel blockers is therefore to reduce the rate of the AP upstroke and reduce AP conduction in the atria, ventricle, and Purkinje fiber tissue (where $Na_v1.5$ is preferentially expressed). Class I Na^{+} channel blockers are further subclassified based on their molecular properties and interaction with the $Na_v1.5$ (Lei et al., 2018;

Li et al., 2019). Class Ia (quinidine, ajmaline, disopyramide) and Ib (lidocaine, mexiletine) Na^+ channel blockers are used to treat patients with sustained ventricular tachycardia and ventricular fibrillation. In addition, quinidine has been indicated for short QT syndrome and Brugada syndrome and mexiletine suggested for the treatment of premature ventricular complexes, LQT3, and ventricular arrhythmias after MI (Al-Khatib et al., 2018; Lei et al., 2018). Class Ic agents (flecainide, propafenone) are used for ventricular tachycardia, premature ventricular complexes, and AF, with flecainide also having a role in the treatment of CPVT (January et al., 2014; Al-Khatib et al., 2018). However, Class Ic agents should not be used in patients with underlying structural heart disease (January et al., 2014). Ranolazine, a Class Id agent, is used to treat ventricular tachycardia and differs from Class Ia-Ic agents by inhibiting the late Na^+ current (Al-Khatib et al., 2018; Lei et al., 2018). Despite Na^+ channel blockers being identified as an effective antiarrhythmic treatment; they have also been shown to be proarrhythmic. The Cardiac Arrhythmia Suppression Trial (CAST) in the late 1980s studied the effect of Na^+ channel blockers on patients with ventricular ectopic activity up to 2 years following a MI. The study revealed a higher rate of death in patients receiving flecainide or encainide compared to the placebo group (Cardiac Arrhythmia Suppression Trial I., 1989). Na^+ channel blockers are therefore generally limited to patients who do not have structural heart disease.

The Class III K^+ channel blockers work by binding to K^+ channels involved in Phase 3 repolarization, and thus delay repolarization and increase AP duration (Lei et al., 2018). Class IIIa K^+ blockers can be divided based on their K^+ channel target. Non-selective K^+ channel blockers (ambasilide, amiodarone, dronedarone) and $K_v11.1$ blockers (dofetilide, ibutilide, sotalol) have been indicated for the treatment of ventricular tachycardia in patients with structural heart disease or with remote MI, tachyarrhythmias in patients with Wolff-Parkinson-White syndrome, rate control in AF [with amiodarone the most effective antiarrhythmic drug for maintenance of sinus rhythm in patients with persistent or paroxysmal AF (January et al., 2014)], ventricular fibrillation and premature ventricular contraction, and supraventricular tachyarrhythmias (January et al., 2014; Al-Khatib et al., 2018; Lei et al., 2018). Another type of K^+ channel blocker which targets $K_v1.5$ (vernakalant) has been suggested for the treatment of AF (Lei et al., 2018). Similar to Na^+ channel blockers, K^+ blockers can exhibit proarrhythmic effects. QT interval prolongation caused by K^+ channel blockers has been shown to predispose patients to ventricular arrhythmias and TdP (McCauley et al., 2016). Due to the AP prolongation effect, K^+ channel blockers should not be given to patients with LQTS, those being treated with QT-prolonging drugs, or with comorbidities associated with an increased risk for TdP (Dan et al., 2018). In addition, co-administration of amiodarone with other cardiac therapeutics including β-blockers, can result in bradycardia and atrioventricular block (Dan et al., 2018). As well as K^+ channel blockers, Class IIIb drugs are metabolically dependent K^+ channel openers and target $K_{ir}6.2$ channels (although these have not been indicated in the treatment of arrhythmias) (Lei et al., 2018). A recent updated classification determined a Class IIIc group made up of transmitter dependent K^+ channel blockers with BMS 914392 currently under review for the management of AF (Lei et al., 2018).

PATHOLOGICAL CARDIAC HYPERTROPHY AND HEART FAILURE

Cardiac hypertrophy occurs under both physiological and pathological conditions. Hypertrophy itself is an adaptive cardiac response which arises due to either pressure- or volume-cardiac overload. Typically, in physiological hypertrophy, the increase in cardiomyocyte size is initially due to the addition of sarcomeres in parallel (eccentric hypertrophy) which increases both ventricular volume and relative wall thickness, resulting in increased contractility which preserves cardiac output (Nakamura and Sadoshima, 2018). Conversely, in pathological hypertrophy cardiomyocytes are added in series (concentric hypertrophy) in order to compensate for the increased cardiac stress, this type of hypertrophy results in maintained or reduced ventricle volume but an increased relative wall thickness (Sawada and Kawamura, 1991; Lazzeroni et al., 2016; Nakamura and Sadoshima, 2018). Furthermore, persistent maladaptive remodeling can eventually lead to ventricular dilatation (eccentric hypertrophy), contractile dysfunction and impaired cardiac output (Sawada and Kawamura, 1991; Lazzeroni et al., 2016; Nakamura and Sadoshima, 2018).

It is now widely believed that each form of hypertrophy is regulated by distinct molecular mechanisms that drive the differing cardiac phenotypes and overall prognosis. Despite the activation of initial compensatory hypertrophic mechanisms, maladaptive remodeling occurs when the following processes occur: cell death (apoptosis, necrosis, autophagy), deposition of fibrosis throughout the myocardium, impaired mitochondrial function and regulation, dysregulation of Ca^{2+}-handling proteins, re-expression of fetal genes, changes to sarcomere structure and rarefaction of the cardiac microvasculature (Nakamura and Sadoshima, 2018). Chronic maladaptive remodeling witnessed during the pathological response to hypertrophy often develops into HF with the diagnosis of HF itself rapidly becoming a universal healthcare and financial burden. HF is an end-stage CVD which frequently occurs secondary to many different aetiologies (Ziaeian and Fonarow, 2016). Physiologically, HF can be defined as (1) insufficient cardiac output to meet metabolic demands or (2) adequate cardiac output with increased left ventricular filling pressure through activation of compensatory neurohormonal pathways (Ponikowski et al., 2016). HF can be further classified into one of three subtypes: HFpEF, HFrEF or HFmrEF) (Ponikowski et al., 2016; Rastogi et al., 2017). These subclassifications are divided based on quantitation of ejection fraction; HFrEF $< 40\%$, HFmrEF $> 40\%$ but $< 50\%$ and HFpEF $> 50\%$ (Ponikowski et al., 2016; Ziaeian and Fonarow, 2016; Rastogi et al., 2017).

The presence of altered Ca^{2+} transients in HF has been well-documented since the late 1980s. These early studies were amongst the first to show that cardiomyocytes isolated from the failing human heart exhibit reduced Ca^{2+} transient amplitudes,

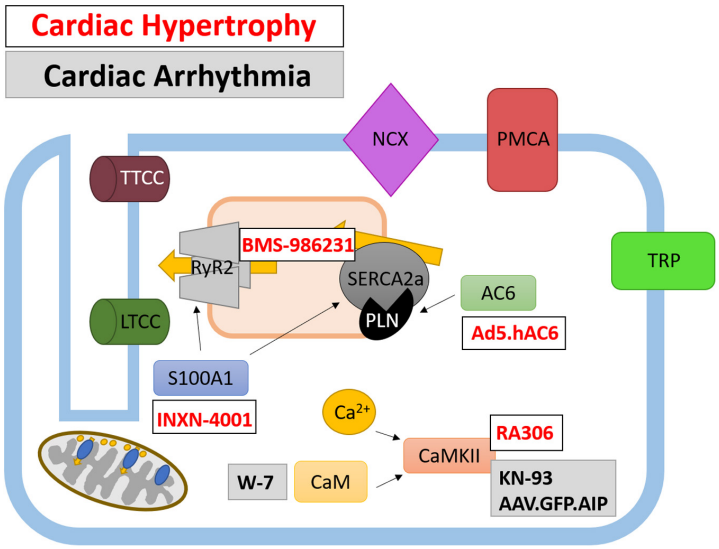

FIGURE 3 | Therapeutically targeted Ca^{2+}-handling proteins and their function in cardiomyocytes. Ca^{2+} handling proteins are extensively involved in intracellular signaling and the regulation of Ca^{2+}-channels and pumps, as such their modulation presents a different avenue for therapeutic targeting. Both current and potential therapeutics are shown for cardiac hypertrophy (white box, red text) and cardiac arrhythmias (gray box, black text).

fewer actin-myosin crossbridge formations, a slower rate of Ca^{2+} removal and increased resting intracellular Ca^{2+} when compared to healthy cardiomyocytes (Gwathmey et al., 1987, 1991; Beuckelmann et al., 1992; Hasenfuss et al., 1993). In broad terms, the failing cardiomyocyte shows impaired Ca^{2+} cycling, Ca^{2+} release from the SR and Ca^{2+} removal. Therefore, altering Ca^{2+} in HF through modulation of Ca^{2+} handling proteins has long been investigated as a therapeutic target.

CALCIUM HANDLING PROTEINS IN CARDIAC HYPERTROPHY AND HF AND THEIR POTENTIAL AS NOVEL THERAPEUTIC TARGETS

The National Institute of Clinical Excellence (NICE, United Kingdom) and other regulatory bodies such as the European Society of Cardiology recommends ACEIs and β-blockers as first-line treatment for HF (Al-Mohammad et al., 2010; Ponikowski et al., 2016); however, dysregulation of Ca^{2+} handling proteins occurs exclusively during pathological hypertrophy (and not physiological hypertrophy) which suggests altered Ca^{2+} cycling and signaling precedes Ca^{2+} dysregulation observed in HF. The following section of this review will focus on how proteins associated with Ca^{2+}-handling, encompassing Ca^{2+} signaling proteins and Ca^{2+} channels and pumps, are altered in cardiac hypertrophy and HF.

Ca^{2+} Homeostasis and Signaling in Hypertrophy and HF

Given the importance of Ca^{2+}-dependent signaling pathways in the development of hypertrophy and HF, there is scope for developing therapies which target their aberrant expression and activity. Three such potential targets are calmodulin (CaM), calcineurin and CaMKII which are all activated following the release of Ca^{2+} from internal stores. CaMKII signaling is upregulated in human HF (Anderson, 2009). Evidence from animal studies suggests that CaMKII-δ is important in the cardiac stress response as CaMKII-δ null mice show no overt cardiac phenotype under physiological conditions but have an attenuated response to pressure-overload induced hypertrophy (Backs et al., 2009; Ling et al., 2009). CaMKII-δ may influence cardiac hypertrophy through two distinct mechanisms which are mediated by different splice variants; CaMKII-δ_C regulates phosphorylation of RyR and PLN resulting in increased Ca^{2+} spark frequency and decreased SR Ca^{2+} content whereas both CaMKII-δ_C and CaMKII-δ_B variants mediate pro-hypertrophic gene transcription (Zhang et al., 2007). Despite this data to suggest CaMKII plays an important role in HF, no clinically available compounds are currently in clinical trials. However, a recently developed, novel ATP-competitive CaMKII-δ and CaMKII-γ inhibitor, RA306, has shown potential in animal studies (Beauverger et al., 2020) (**Figure 3** and **Table 1**). RA306 prevented phosphorylation of PLN (Thr17) *in vitro* and *in vivo* following stimulation with isoproterenol (Beauverger et al., 2020). Furthermore, twice-daily RA306 treatment was sufficient to increase ejection fraction in a mouse model of dilated cardiomyopathy; importantly, the study used aged mice with advanced cardiac disease to demonstrate the 'curative' ability of RA306 (Beauverger et al., 2020).

The use of gene therapy to treat CVD has garnered much attention in recent years and has been used as a tool to alter expression of a wide variety of Ca^{2+}-handling proteins. Recent work has been undertaken to trial a triple gene plasmid construct INXN-4001 in patients with an outpatient left ventricular assist

TABLE 1 | Therapeutic targeting of Ca^{2+}-handling proteins in cardiac hypertrophy, HF and arrhythmia.

Target	Pre-clinical	FDA approved	Clinical trial identifier	Status	Results
S100A1	INXN-4001		NCT03409627	A	N/A
CaM	W-7		Pre-clinical	N/A	N/A
CaMKII	RA306		Pre-clinical	N/A	N/A
	KN-93		Pre-clinical	N/A	N/A
	AAV.GFP.AIP		Pre-clinical	N/A	N/A
AC6	Ad5.hAC6		NCT00787059	C	Safe, tolerable (Hammond et al., 2016)
			NCT03360448	W	N/A
PLN	BMS-986231		NCT03016325	C	Safe, well-tolerated; adverse effects included headaches (Cowart et al., 2019)
			NCT02157506	C	Increased treatment-emergent adverse events in treatment group (>55% in all three regimes vs. 25% in placebo)
			NCT03016325	C	None posted
			NCT03357731	C	None posted
			NCT03730961	C	None posted

*For each therapy listed in **Figure 3**, their status as either pre-clinical or FDA-approved is listed in the table. In addition, any clinical trial information available for the therapies listed in the table is also presented, where NCT denotes the number given to clinical trials on clinicaltrials.gov. Therapies which have yet to enter registered clinical trials are shown as pre-clinical. A brief description on the in human safety and tolerability of each therapy is also shown where available. A, active; C, completed; N/A, not applicable; W, withdrawn.*

device [clinicaltrials.gov Identifier NCT03409627] (**Figure 3** and **Table 1**). Plasmid INXN-4001 contains human VEGF165, S100A1 and stromal cell-derived factor 1; expression of these three proteins has been designed to target fibrosis, angiogenesis and impaired cardiac contractility (Jaruga-Killeen et al., 2019). To date there are no reported adverse cardiac-specific safety effects after one infusion of INXN-4001 (Jaruga-Killeen et al., 2019). Of interest to this review is the expression of constitutively active S100A1 protein within the INXN-4001 plasmid. S100A1 is a Ca^{2+} binding protein which controls Ca^{2+}-dependent networks in cardiomyocytes through, for example, modulation of RyR2 and SERCA2a activity (Ritterhoff and Most, 2012). S100A1 protein levels are reduced in cardiomyocytes from both human and animal model-derived failing myocardium and levels of reduced S100A1 are associated with poorer contractile function (Du et al., 2002; Most et al., 2006). Adenoviral-based delivery of S100A1 is able to rescue cardiac function in mouse, rat, and pig models of MI-induced HF (Most et al., 2004; Pleger et al., 2005, 2007, 2011; Kraus et al., 2009). Importantly, S100A1 gene transfer alone can restore Ca^{2+} homeostasis in acute and chronic models of HF (Most et al., 2004; Pleger et al., 2005, 2007, 2011; Kraus et al., 2009). However, gene therapy using S100A1 alone has not yet been developed for use in clinical trials.

Gene therapy has also been utilized to overexpress AC6 (Kieserman et al., 2019) (**Figure 3** and **Table 1**). The primary role of AC6 is to catalyze the conversion of ATP to cAMP; however, AC6 can also downregulate the expression of PLN, independently of cAMP concentration (Gao et al., 2004). Adenoviral transfer of AC6 ($Ad.AC_{VI}$) in a porcine model of congestive HF successfully improved LV function (Lai et al., 2004). The promising outcome of $Ad.AC_{VI}$ treatment in a large animal models of HF led to its development for a first in man clinical trial (Ad5.hAC6, also known as RT-100), beginning in 2010 (Hammond et al., 2016; Penny et al., 2018). Results from this placebo-controlled, randomized clinical trial of 56 HFrEF patients confirmed the safety of Ad5.hAC6 [clinicaltrials.gov Identifier NCT00787059] (Hammond et al., 2016). Furthermore, patients receiving the two highest doses (out of five possible different doses) of Ad5.hAC6 showed an acute improvement in EF, assessed 4 weeks post-viral delivery (Hammond et al., 2016). The promising results from this Phase II clinical trial paved the way for the 'FLOURISH' trial, a Phase III follow-up [clinicaltrials.gov Identifier NCT03360448] (Penny et al., 2018). However, the FLOURISH study was withdrawn prior to patient recruitment owing to a change of clinical development plans. Therefore, the clinical benefit of Ad5.hAC6 for the treatment of HF still requires investigation in a large, multi-centre clinical trial.

Ca^{2+} Handling Proteins During Hypertrophy and HF; Ca^{2+} Channels, Pumps and Exchangers

LTCC

Currently, LTCC Ca^{2+} blockers are used with caution in patients with HF; however, there may be some therapeutic potential in targeting a subset of LTCC which have been shown to specifically localize to caveolae and do not present as 'typical' LTCC which reside on T-tubules (Makarewich et al., 2012). Within caveolae membrane invaginations, Ca^{2+} entry through LTCC may activate pro-hypertrophic calcineurin/NFAT signaling without contributing to ECC (Makarewich et al., 2012). Interestingly, the calcineurin/NFAT signaling axis only contributes to pathological and not physiological hypertrophy (Wilkins et al., 2004). Inhibition of LTCC with channel blocking Rem proteins specifically targeted to Cav-3 caveolae membranes attenuates the inward Ca^{2+} current and prevents pro-hypertrophic gene activation without affecting contractility of feline cardiomyocytes (Makarewich et al., 2012). However,

these findings were not replicated a murine model of cardiac hypertrophy *in vivo* (Correll et al., 2017). Therefore, the direct contribution of LTCC to the development of cardiac hypertrophy remains inconclusive and requires further investigation in different pre-clinical models of HF.

SERCA2

In failing human cardiomyocytes and in animal models of hypertrophy and HF, the levels of SERCA2 are reduced (Komuro et al., 1989; Nagai et al., 1989; Mercadier et al., 1990; Lipskaia et al., 2014). Downregulation of SERCA2 and therefore a reduction in SERCA2 activity are concordantly associated with both systolic and diastolic dysfunction (Periasamy et al., 1999). The importance of SERCA2 signaling is evidenced by knockout mouse studies. Cardiomyocyte-specific deletion of SERCA2 in adult mice leads to diastolic dysfunction under basal conditions (Andersson et al., 2009). Furthermore, an important feature of Ca^{2+} dysregulation during cardiac hypertrophy is SR Ca^{2+} leak and at the molecular level, cardiomyocyte loss of SERCA2 results in changes to SR Ca^{2+} handling, characterized by slower cytosolic Ca^{2+} removal, reduced SR content and impaired Ca^{2+} transient magnitude (Andersson et al., 2009; Louch et al., 2010; Li et al., 2012). SERCA2 activity could also be affected in HF due to changes in the phosphorylation status of PLN (Schwinger et al., 1995; Mattiazzi and Kranias, 2014). The reduction in phosphorylation of PLN is partly due to increased activity of calcineurin and protein phosphatase 1, as shown in both human HF and animal models (Neumann et al., 1997; Munch et al., 2002). However, more recent data suggests direct post-transcriptional modifications of SERCA2a contribute to its decreased activity (Kranias and Hajjar, 2012). In HF, SERCA2 can undergo either 'stimulatory' modification by glutathionylation on C674 (Adachi et al., 2004) and/or SUMOylation on K480 and K585 (Kho et al., 2011), and 'inhibitory' acetylation of K492 (Gorski et al., 2019). These modifications to SERCA2a and its regulatory proteins provides more scope for enhancing SERCA2 activity in HF patients.

Restoring SERCA2a protein expression levels has been shown by numerous groups to improve cardiac metabolism, including a reduced incidence of arrhythmia and increased coronary blood flow (Hayward et al., 2015; Hulot et al., 2016). However, the benefits of administering SERCA2a were shown to be diminished in a myocardium with a limited energy supply (Pinz et al., 2011), suggesting increasing SERCA2 levels may only be beneficial in non-ischemic tissue. In humans, directly restoring SERCA2 levels has been achieved using gene transfer. Adeno-associated virus1.SERCA2a (AAV1.SERCA2a) gene transfer successfully restored the Ca^{2+} transient and contraction in isolated failing human cardiomyocytes (del Monte et al., 1999) and in animal models of HF, SERCA2a gene transfer was shown to increase survival and improve cardiac hemodynamics and function (del Monte et al., 2001, 2004; Kawase et al., 2008) (**Figure 4** and **Table 2**). Given that SERCA2a gene transfer improved outcome in animal models of HF, AAV1.SERCA2a was administered in Phase I and Phase II clinical trials [ClincalTrials.gov identifiers NCT00534703 and NCT00454818] (Jessup et al., 2011; Zsebo et al., 2014; Greenberg et al., 2016). The results of the initial Phase I and IIa trials suggested that AAV1.SERCA2a treatment reduced the number of cardiac events in HF patients (Jaski et al., 2009; Jessup et al., 2011); however, larger Phase IIb clinical trials failed to show improvement in any primary or secondary endpoints, leading to their early termination (Hulot et al., 2017). The failure of these clinical trials suggests the dosage and delivery method of AAV1.SERCA2a may require optimizing (Hulot et al., 2016) [SERCA2a gene therapy in HF has been extensively reviewed elsewhere (Samuel et al., 2018)]. Despite the lack of promising results for AAV1.SERCA2a, clinical trials are underway for istaroxime, a dual functional luso-inotropic agent which both stimulates SERCA2a and inhibits Na^{+}/K^{+} ATPase (Micheletti et al., 2002) (**Figure 4** and **Table 2**). Istaroxime increases Ca^{2+} uptake into the SR by relieving PLN-mediated inhibition of SERCA2a through cAMP/PKA-depending mechanism (Ferrandi et al., 2013). In animal models of HF, intravenous istaroxime improved cardiac function without causing any arrhythmic events (Micheletti et al., 2007; Sabbah et al., 2007). Phase I-II clinical trials demonstrated the safety of istaroxime in HF patients and showed beneficial effects on cardiac contractility (Ghali et al., 2007). The follow-up Phase IIa clinical trial, 'HORIZON-HF,' showed a reduction in diastolic stiffness and increase in contractility in HFrEF patients receiving istaroxime when compared to placebo (Shah et al., 2009). Additional clinical trials for istaroxime are on-going [ClincalTrials.gov identifiers NCT02617446 and NCT02477449].

Focus for novel SERCA2 therapeutics has also extended to SERCA2 post-translational modifications and mediators of SERCA2 expression. Gene-transfer of SUMO1 and S100A1 which both promote SERCA2 activity were shown to improve cardiac function in rodent and porcine models of HF (Most et al., 2004; Kho et al., 2011; Pleger et al., 2011; Tilemann et al., 2013). Moreover, a small-molecule SUMO1 activator, termed N106, has recently been developed which, through activating the SUMO-activating enzyme, leads to the SUMOylation of SERCA2 (Kho et al., 2015). In addition, microRNA's upregulated in human HF also provide a novel therapeutic target as they can be inhibited using anti-*miR*'s. One such microRNA, microRNA-25, is upregulated in human HF and application of anti-*miR-25* following TAC improved survival and function by restoring SERCA2 activity (Wahlquist et al., 2014). However, none of these SERCA2 modifying mechanisms have been investigated in the clinical setting. SERCA2a and its regulator PLN can be modified by nitroxyl (HNO/NO^{-}), the single electron reduced form of nitric oxide (Paolocci et al., 2001; Farah et al., 2018). HNO readily converts negatively charged thiol groups of proteins, such as cysteine, to disulfide residues; a feature which is reversible (Fukuto, 2019; Pinilla-Vera et al., 2019). HNO modifies cysteine residues on SERCA2a and PLN (and RyR2) which enhances Ca^{2+} cycling through reduced PLN-mediated SERCA2a inhibition (Froehlich et al., 2008; Farah et al., 2018). The original HNO donor used in proof-of-principal experiments, Angeli's salt, is not stable at room temperature, therefore, first- and second-generation HNO donors have been developed with more favorable drug-like properties. One such second-generation HNO derivative to have undergone clinical testing is BMS-986231 (**Figure 3** and **Table 1**). To date, there

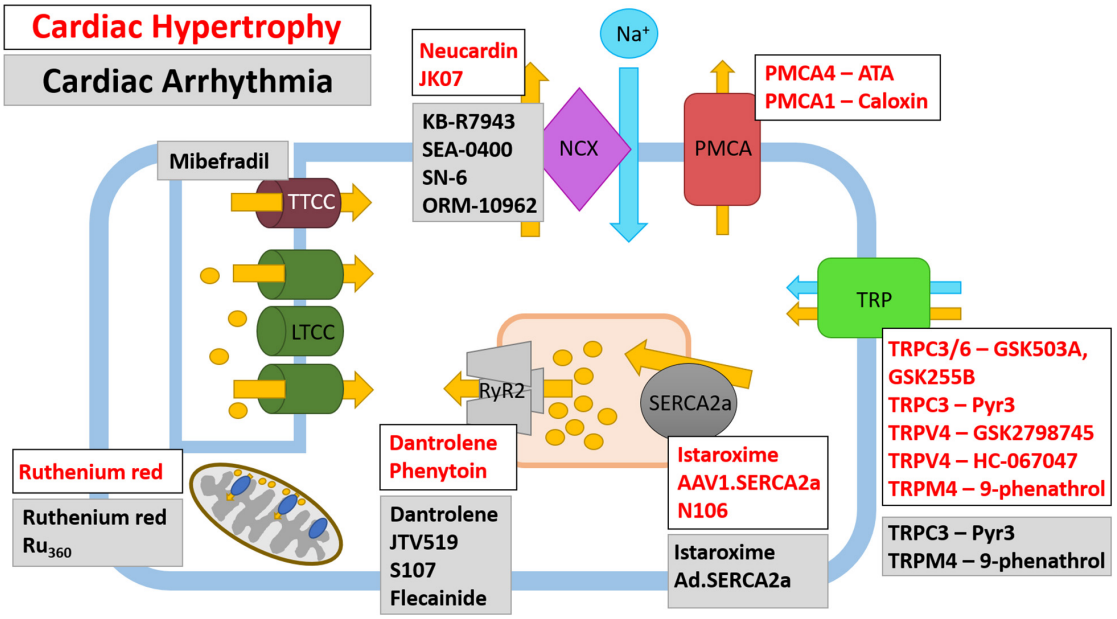

FIGURE 4 | Therapeutic targeting of Ca^{2+} ion channels and pumps in cardiac hypertrophy and cardiac arrhythmia. Ca^{2+} ion channels and Ca^{2+} pumps have been the subject of pharmacological and gene therapy intervention; however, not all therapies have been translated from pre-clinical studies into human trials. Both current and potential therapeutics and their Ca^{2+} ion channel or Ca^{2+} pump target are shown for cardiac hypertrophy (white box, red text) and cardiac arrhythmias (gray box, black text), note there are some agents which have been tested in models of HF and arrhythmia. The LTCC are currently targeted by Ca^{2+} channel blockers which are prescribed to patients with CVD, as such, these are not shown on the schematic.

have been eight completed different clinical trials utilizing BMS-986231. Results from a Phase I clinical trial showed that BMS-986231 was well tolerated but that nearly half of healthy volunteers receiving BMS-986231 reported headaches; however, the authors noted that owing to BMS-986231 vasodilatory effects, the presence of headaches was not unexpected (Cowart et al., 2019) [clinicaltrials.gov identifier NCT03016325]. In a separate placebo-controlled, double-blind Phase IIa study, 34 patients were randomly assigned to receive one infusion of BMS-986231 (Tita et al., 2017) [clinicaltrials.gov identifier NCT02157506]. The results from this Phase IIa clinical trial also suggest BMS-986231 is safe and in HFrEF patients, exhibits a favorable hemodynamic profile (Tita et al., 2017). The success of these early Phase I and II clinical trials have led to the development of three further clinical trials to determine the effect of BMS-986231 on (1) symptomatic hypotension in HFrEF patients, (2) cardiac systolic and diastolic function in HFrEF patients, and (3) salt and water-handling in patients with HFrEF and HFmrEF (EF < 45%) [clinicaltrials.gov identifier(s) NCT03016325, NCT03357731, and NCT03730961, respectively] (Felker et al., 2019). To date, these studies have completed recruitment and are on-going.

NCX

Depending on the membrane potential and intracellular Ca^{2+} and Na^{+} gradients, NCX1 can act in 'forward' (Ca^{2+} ion out, 3 Na^{+} ions in) or 'reverse' (Ca^{2+} ion in, 3 Na^{+} ions out) mode. In a failing cardiomyocyte, NCX1 has been shown to operate in reverse mode which results in Ca^{2+} entry and a repolarizing current (Mattiello et al., 1998). Furthermore, elevated intracellular Ca^{2+} seen after I/R injury is caused by NCX1 operating in 'reverse' mode (Piper et al., 1996; Inserte et al., 2002; Imahashi et al., 2005). NCX1 is upregulated in human and murine models of HF (Hasenfuss et al., 1999; Menick et al., 2007) and over-expression of NCX is sufficient to impair cardiomyocyte function *in vitro* (Schillinger et al., 2000). However, as the function of NCX is also affected by Na^{+}, and intracellular Na^{+} is increased in both human HF and models of HF (Bers and Despa, 2006), Ca^{2+} extrusion through NCX could be impaired due to Na^{+}-loading observed in end stage HF (Louch et al., 2010; Li et al., 2012). Interestingly, following TAC there is an increase in NCX expression but no change in SERCA2a; however, when TAC progresses into HF, there is a downregulation in SERCA2 expression (Wang et al., 2001). Therefore, in HF there is a change in the NCX/SERCA2 ratio which has been implicated in impaired cardiac contraction and conduction (Pogwizd et al., 2001).

Historically, digoxin has been used to inhibit NCX; however, there is no improvement in mortality of patients receiving digoxin (Campbell and MacDonald, 2003; Goldhaber and Hamilton, 2010). It was recently observed that an increase in NCX1 seen in an animal model of HF could be attenuated by neuroglin-1β (Wang et al., 2019) (**Figure 4**). Neuroglin-1β has been extensively explored as a therapeutic option in HF and expression of recombinant human neuroglin-1β (rhNRG-1/also known as Neucardin) has undergone successful clinical trials; however, its full mechanism of action has not yet been determined (Galindo et al., 2014). Neuroglin-1β is a growth factor which, along with its receptors ErbB2-4, is critical for the cardiac response to stress (Lemmens et al., 2004; Galindo et al., 2014;

TABLE 2 | Therapeutic targeting of Ca^{2+}-channels and pumps in cardiac hypertrophy, HF and cardiac arrhythmia.

Target	Pre-clinical	FDA approved	Clinical trial identifier	Status	Results
NCX	Neucardin		NCT01251406	C	None posted
			NCT01541202	T	N/A
			NCT03388593	R	N/A
	JK07		NCT04210375	NYR	N/A
	KB-R7943		Pre-clinical	N/A	N/A
	SEA-0400		Pre-clinical	N/A	N/A
	SN-6		Pre-clinical	N/A	N/A
	ORM-10962		Pre-clinical	N/A	N/A
PMCA4	ATA		Pre-clinical	N/A	N/A
	Caloxin 1B1		Pre-clinical	N/A	N/A
PMCA1	Caloxin 1B3		Pre-clinical	N/A	N/A
RyR2		Dantrolene	jRCTs61180059	R	N/A
		Phenytoin	Pre-clinical for HF	N/A	N/A
	JTV519		NCT00626652	C	None posted
	S107		Pre-clinical	N/A	N/A
		Flecainide	NCT01117454	C	Used with β-blockers, no safety concerns (Kannankeril et al., 2017)
SERCA2a	Istaroxime		NCT02617446	U	N/A
			NCT02477449	U	N/A
	AAV1.SERCA2a		NCT00534703	T	Only 5 participants, trial terminated early
			NCT00454818	C	No safety concerns in 3-year follow-up (Zsebo et al., 2014)
	N106		Pre-clinical	N/A	N/A
	Ad.SERCA2a		Pre-clinical	N/A	N/A
TRPC3	Pyr3		Pre-clinical	N/A	N/A
TRPC3/C6	GSK2332255B GSK2833503A		Pre-clinical	N/A	N/A
TRPV4	GSK2798745		NCT02497937	C	1 (/11) incident of a serious adverse event in treatment group
			NCT02119260	C	Safe, well-tolerated (Goyal et al., 2019)
	HC-067047		Pre-clinical	N/A	N/A
TRPM4	9-phenanthrol		Pre-clinical	N/A	N/A
TTCC		Mibefradil*			Initially safe (Bursztyn et al., 1997; Kobrin et al., 1997) but later withdrawn due to interference with metabolism of other medicines
MCU	Ruthenium red		Pre-clinical	N/A	N/A
	Ru_{360}		Pre-clinical	N/A	N/A

*Each therapy listed in **Figure 4** is listed as having either pre-clinical or FDA-approved status. Any clinical trial information available, either through publication or as results published, is also presented. Clinical trials accessed through clinicaltrials.gov have an NCT number whereas those obtained through the Japan Registry of Clinical Trials are denoted by a jRCTs number. *Mibefradil was withdrawn from the market following FDA approval. C, completed; N/A, not applicable; NYR, not yet recruiting; R, recruiting; T, terminated; U, unknown.*

Wang et al., 2019). Following pressure-overload induced cardiac hypertrophy, the expression of ErbB2 and B4 are increased during the cardiac compensation phase and reduced following the transition into HF (Rohrbach et al., 1999). Similarly, in the left ventricle of human failing myocardium, the expression of ErbB2 and B4 is reduced (Rohrbach et al., 2005). Animal models of hypertrophic- and ischemia-induced HF have been used extensively to show the benefit of recombinant neuroglin-1β (Galindo et al., 2014). Treatment with neuroglin-1β for 7 days was sufficient to prevent ventricular remodeling following volume-overload induced cardiac hypertrophy (Wang et al., 2019). At the molecular level, neuroglin-1β partially prevented the decrease in SERCA2a, LTCC and increase in NCX1 associated with HF (Wang et al., 2019). Therefore, neuroglin-1β may confer its cardioprotective effects through regulation of Ca^{2+}-handling protein expression. Given the promising effects of recombinant neuroglin-1β treatment in animal models of HF, Phase II and III clinical trials were approved to determine the safety and efficacy of daily infusions of Neucardin (Galindo et al., 2014). The first Phase II clinical trials successfully demonstrated the safety, tolerability and efficacy of rhNRG-1 in patients with chronic HF (Gao et al., 2010; Jabbour et al., 2011) [clinicaltrials.gov identifier NCT01251406 and NCT01541202]. Following on from these early Phase II clinical trials, large-scale, multi-centre

Phase III clinical trials have begun recruiting patients to determine the effect of Neucardin on all-cause mortality after 1 year [clinicaltrials.gov NCT03388593]. Furthermore, a Phase I clinical trial has recently been accepted to test the safety, tolerability and immunogenicity of the drug JK07 in HFrEF patients; JK07 is a human immunoglobulin IG1 monoclonal antibody containing an active polypeptide fragment of neuroglin-1 [clinicaltrials.gov identifier NCT04210375] (**Figure 4** and **Table 2**). Future studies should aim to determine whether neuroglin-1β mediates NCX1, SERCA2a and LTCC channel expression in other animal models of HF and whether the efficacious effects of Neucardin in clinical trials is partly due to altered Ca^{2+} dynamics.

RyR2

There is a general consensus that SR-located RyR2 contributes to Ca^{2+} leak during HF which can cause (1) cardiac arrhythmias, (2) reduced Ca^{2+} SR content, (3) systolic dysfunction, and (4) altered cardiac energetics (Bers, 2014). The function of RyR2, the major cardiac isoform of the RyR, is tightly regulated though changes to its phosphorylation status, Ca^{2+} activation and inactivation sites and post-translational modifications (Roe et al., 2015). RyR2 channel gating is regulated by accessory proteins whilst its tetrameric confirmation is stabilized by FK506-binding protein-12.6 (FKBP12.6). Disassociation of FKBP12.6 from RyR2 is observed in some models of HF and is achieved through PKA-mediated hyperphosphorylation of RyR2 at Ser2808 (Marx et al., 2000). One study has demonstrated that transgenic mice with an absent PKA phosphorylation site on RyR2 are protected against MI-induced HF (Wehrens et al., 2006); however, others have shown that CaMKII-mediated RyR2 phosphorylation leads to altered Ca^{2+} sparks as opposed to PKA-mediated phosphorylation (Li et al., 2002; Guo et al., 2006). Such is the importance of CaMKII-mediated phosphorylation of RyR2 that it has been shown to promote the transition from hypertrophy into HF (Ling et al., 2009; Respress et al., 2012).

Changes to Ca^{2+} transfer between the SR and mitochondria impedes mitochondrial function in cardiomyocytes (Fernandez-Sanz et al., 2014; Ruiz-Meana et al., 2019), potentially contributing to cardiomyocyte deterioration in HF. Recently, a novel mechanism of RyR2 hyperglycation was shown to increase Ca^{2+} leak from the SR in cardiomyocytes of aged mice (Ruiz-Meana et al., 2019). Aging alone results in advanced glycation of RyR2, leading to increased SR Ca^{2+} leak, mitochondrial Ca^{2+} overload and mitochondrial dysfunction, independently of cardiac disease (Ruiz-Meana et al., 2019). Importantly, hyperglycation of RyR2 and increased mitochondrial Ca^{2+} was prevalent in atrial appendages from aged patients (75 years or above) and absent in young patients (Ruiz-Meana et al., 2019). Preventing the glycation of RyR2 by inhibiting dicarbonyl intermediaries or stimulating their detoxification may provide a preventative measure to attenuate mitochondrial damage associated with aged, failing cardiomyocytes.

RyR2 can be inhibited by dantrolene sodium, a derivative of the hydantoin class of compounds (Maxwell et al., 2012). Application of dantrolene normalizes the diastolic Ca^{2+} leak seen in HF; however, owing to its hepatotoxic side-effect, dantrolene is not suitable for long-term use (Durham et al., 1984) (**Figure 4** and **Table 2**). Despite this, the 'SHO-IN' clinical trial seeks to determine the safety and efficacy of dantrolene on patients with chronic HF [Japanese Registry of Clinical Trials identifier 61180059] (Kobayashi et al., 2020). Recent work has shown that phenytoin, a member of the same class of hydantoin compounds, shares the same RyR2 inhibitory effects as dantrolene (Ashna et al., 2020). *In vitro* application of phenytoin to RyR2 channels isolated from failing human hearts shows that phenytoin reversibly inhibits RyR2 which subsequently inhibits diastolic cytoplasmic, but not systolic, Ca^{2+} release (Ashna et al., 2020). Interestingly, phenytoin is currently used clinically as a Na^{+} channel blocker to treat epilepsy, therefore there is scope to determine the potential therapeutic use of phenytoin in HF (**Figure 4**). Designing novel therapeutic targets for RyR2 may, in future, involve RyR2 accessory proteins which modulate its function. TRIC-A and B are SR-located K^{+} channels known to participate in ECC (Yazawa et al., 2007; Yamazaki et al., 2009b; Yang et al., 2016); both TRIC-A and TRIC-B knockout mice exhibit Ca^{2+} overload in the SR (Yamazaki et al., 2009a; Zhao et al., 2010). TRIC-A, but not TRIC-B, physically associates with RyR2 to enhance RyR2-dependent Ca^{2+} efflux from the SR; however, there is still a limited understanding of the function of TRIC-A-dependent RyR2 modulation under pathological conditions (Zhou et al., 2020).

TRP Channels

When compared to a healthy myocardium, TRPC1, C5, M4, and M7 are upregulated and TRPC4 and V2 are downregulated in the failing human heart (Dragun et al., 2019), suggesting each TRP channel may differentially contribute to CVD [reviewed extensively elsewhere (Falcon et al., 2019; Hof et al., 2019)]. Interestingly, in neonatal rat cardiomyocytes, stimulation with hypertrophy-inducing agents leads to the upregulation and subsequent activation of TRPC1 (Ohba et al., 2007) and C5 (Sunggip et al., 2018). Furthermore, in mouse models, global deletion of *Trpc1* attenuates pressure-overload induced hypertrophy through reduced activation of the calcineurin/NFAT pathway (Ohba et al., 2007; Seth et al., 2009). In addition to TRPC1 and C5, TRPC3 (Brenner and Dolmetsch, 2007) and C7 (Satoh et al., 2007) are also upregulated in hypertrophy-stimulated cardiomyocytes and TRPC6 overexpression induces cardiac hypertrophy in mice (Kuwahara et al., 2006). TRPC3 and C6 have been successfully co-targeted with the thiazole inhibitors GSK2332255B (GSK255B) and GSK2833503A (GSK503A), respectively (Washburn et al., 2013) (**Figure 4** and **Table 2**). When these inhibitors were co-administered following pressure-overload induced hypertrophy in mice, both cardiomyocyte hypertrophy and cardiac fibrosis were reduced (Seo et al., 2014). Mechanistically, blockade of TRPC3 reduces phosphorylation of Ca^{2+}-handling proteins in mouse embryonic stem cell-derived cardiomyocytes (Qi et al., 2016), which may alter downstream Ca^{2+}-mediated signaling. More specifically, TRPC3 can be exclusively inhibited by Pyr-3 (Kiyonaka et al., 2009) (**Figure 4** and **Table 2**). Pyr-3 inhibition of TRPC3 attenuates NFAT-mediated transcription and can prevent hypertrophy *in vitro* in ANG-II stimulated neonatal rat cardiomyocytes and

in vivo following pressure overload-induced hypertrophy in mice (Kiyonaka et al., 2009). Other studies have also shown TRPC1 and TRPC3-C6 upregulation in failing human hearts when compared to non-failing myocardium (Bush et al., 2006; Morine et al., 2016). Interestingly, the same TRPC channels are also upregulated in the border zone of rats hearts after left anterior descending coronary artery ligation-induced MI (Dominguez-Rodriguez et al., 2018). Therefore, it appears that the TRPC family of channels contribute to the cardiac HF phenotype; however, more research is required in order to determine the functional effect of each upregulated TRPC channel in order to progress pre-clinical studies.

The TRPV family have also been extensively investigated; however, as mentioned above, there is no detectable upregulation of TRPV family members in the failing human myocardium (Dragun et al., 2019). Despite this, there is promising data to suggest blockade of TRPV4 may prove beneficial in HF patients; the pulmonary endothelial-localized TRPV4 channel has been shown to play a role in pulmonary venous pressure-induced formation of pulmonary oedema in HF (Thorneloe et al., 2012). In support of this, TRPV4 is upregulated in human lungs derived from patients with congestive HF (Thorneloe et al., 2012). As such, TRPV4 channel blockade with the first in class orally active pharmaceutic GSK2798745 successfully prevents the formation of and reverses established pulmonary oedema in acute and chronic HF models (Thorneloe et al., 2012) (**Figure 4** and **Table 2**). The positive data obtained from TRPV4 inhibition in animal models led to a Phase I clinical trial to investigate the safety and efficacy of inhibiting TRPV4 with GSK2798745 (Goyal et al., 2019). Results of this first in man trial has shown there are no adverse effects or safety issues in both healthy volunteers and patients with mild to moderate HF (Goyal et al., 2019) [clinicaltrials.gov identifiers NCT02497937 and NCT02119260]. In addition, TRPV4 is activated in the murine model of I/R injury (Dong et al., 2017). Mechanistically, activation of TRPV4 following I/R leads to increased Ca^{2+} influx and generation of ROS (Wu et al., 2017). Therefore, chemical inhibition of TRPV4 with the selective antagonist HC-067047 prevents aberrant TRPV4 activation which leads to a reduction in infarct size and improved cardiac function following I/R injury (Dong et al., 2017). Furthermore, both TRPV1 and V2 contribute to the inflammatory response following MI; however, mice harboring a global deletion of TRPV1 show an exacerbated inflammatory response 3- and 7-days post-MI whereas mice with a global knockout of TRPV2 show improved cardiac recovery following MI due to a reduction in peri-infarct macrophages (Huang et al., 2009; Entin-Meer et al., 2017; Falcon et al., 2019).

Some of the TRPM and TRPP channels exhibit the highest levels of expression in basal ventricular myocytes, amongst these are TRPM7, M1 and M4 and TRPP1 and P2 (Chevalier et al., 2018). As mentioned, both TRPM4 and M7 levels are elevated in the failing human ventricle myocardium (Dragun et al., 2019); however, TRPM7 mRNA was shown to be reduced in the left ventricle of patients with ischemic cardiomyopathy (Ortega et al., 2016), therefore the underlying cause of HF may influence the expression pattern of TRP channels. TRPM7 is expressed in the SAN and has a known role in modulation of cardiac automaticity (Sah et al., 2013a,b); however, TRMP7 also promotes cardiomyocyte proliferation during early cardiogenesis (Sah et al., 2013a,b). TRMP7 kinase dead mice exhibit significant cardiac hypertrophy and upregulation of pro-inflammatory mediators, driven by a Mg^{2+}- but not a Ca^{2+}-sensitive mechanism (Rios et al., 2020). Therefore, TRPM4 may provide a better option to therapeutically target Ca^{2+} mishandling. Interestingly, despite the upregulation of TRPM4 in failing human hearts, the channel itself is impermeable to Ca^{2+}; however, it is both Ca^{2+}- and voltage-activated (Nilius et al., 2003, 2005; Wang et al., 2018). TRMP4 expression is upregulated by 50-fold in spontaneously hypertensive rats when compared to controls (Guinamard et al., 2006). Furthermore, global deletion of *Trpm4* causes eccentric cardiac hypertrophy with aging which is caused by neonatal cardiomyocyte hyperplasia (Demion et al., 2014). In a cardiomyocyte-specific *Trpm4* knockout mouse ($Trpm^{cko}$), induction of cardiac hypertrophy with ANG-II resulted in increased hypertrophy in $Trpm4^{cko}$ mice when compared to controls (Kecskes et al., 2015). TRPM4 activity can be exclusively inhibited by 9-phenanthrol (Guinamard et al., 2014). Most studies using 9-phenanthrol have aimed to determine the contribution of TRMP4 to smooth muscle cell contraction (Guinamard et al., 2014); however, application of 9-phenanthrol to isolated rat hearts in a model of I/R injury reduces infarct size and improves contractility (Wang J. et al., 2013).

PMCAs

The PMCAs are rapidly emerging as potential signaling mediators (Armesilla et al., 2004; Oceandy et al., 2007; Cartwright et al., 2011; Stafford et al., 2017); however, to date, only a role for PMCA4 has been elucidated in a mouse model of TAC-induced pressure-overload hypertrophy. In the study by Mohamed et al. (2016), global knockout of *Atp2b4* was shown to attenuate the pressure-overload response; however, the anti-hypertrophic effects of PMCA4 knockout could only be replicated in fibroblast-specific and not in cardiomyocyte-specific knockout mouse models (Mohamed et al., 2016; Stafford et al., 2017). Non-myocyte cells such as cardiac fibroblasts and endothelial cells account for around 70% of total cardiac cells (Pinto et al., 2016), and are able to secrete factors which can influence adjacent cardiomyocyte signaling. Interestingly, fibroblast-specific deletion of PMCA4 leads to significant upregulation of secreted frizzled related protein 2 which is thought to confer cardioprotective properties by inhibiting the Wnt pathway in neighboring cells (Mohamed et al., 2016). Despite this role for PMCA4 in cardiac hypertrophy, there is no evidence that *human* ATP2B4 is associated with CVD; genome-wide association studies (GWAS) have to date been unable to associate SNPs within ATP2B4 with any CVD (Tabara et al., 2010).

In contrast to GWAS data for *ATP2B4*, SNPs located in *ATP2B1,* the gene encoding PMCA1, have been strongly associated with CVDs, including hypertension, coronary artery disease and MI (Tabara et al., 2010; Takeuchi et al., 2010; Wang Y. et al., 2013; Xu et al., 2016; Jamshidi et al., 2018; Sombie et al., 2019). The association of *ATP2B1* with hypertension has been

shown in numerous studies across different ethnic groups; to date, there are at least six different SNPs within *ATP2B1* which are associated with elevated blood pressure (Tabara et al., 2010; Takeuchi et al., 2010; Wang Y. et al., 2013; Xu et al., 2016; Jamshidi et al., 2018; Sombie et al., 2019). In mice, vascular smooth muscle cell-specific PMCA1 knockout mice exhibit elevated blood pressure (Kobayashi et al., 2012). Mechanistically, loss of PMCA1 from vascular smooth muscle cells leads to enhanced expression of LTCC and increased Ca^{2+} concentration which may affect smooth muscle cell stiffness and subsequently, vascular tone (Okuyama et al., 2018; Zhu et al., 2019). Furthermore, PMCA1 global heterozygous mice have increased hypertension with aging, which is preceded by vascular remodeling (Little et al., 2017). Taken together, PMCA1 appears to play a functional role in the development of hypertension through modulation of Ca^{2+}. Whilst more research is required to determine the contribution of PMCA1 to hypertrophy and HF, there is scope to therapeutically target PMCA1 as a modulator of hypertension to prevent CVD (Little et al., 2016).

The PMCAs are typical ATPases and therefore present a suitable novel therapeutic target (**Figure 4** and **Table 2**). ATPases have been clinically targeted to treat hypotension and some cardiac arrhythmias; ouabain inhibits Na^+/K^+-ATPase and omeprazole inhibits H^+/K^+-ATPase. Therapeutically, the two main cardiac isoforms of PMCA have been successfully targeted *in vitro*; the caloxins, a class of PMCA inhibitors, show differential specificity for each PMCA isoform (Pande et al., 2011). Caloxin 1B3 shows increased specificity for PMCA1 over PMCA4 and results in increased Ca^{2+} in endothelial cells (Szewczyk et al., 2010; Pande et al., 2011), whereas caloxin 1B1 is predominantly PMCA4-isoform specific (Pande et al., 2006). PMCA4 has also been successfully targeted with aurintricarboxylic acid (Mohamed et al., 2013a). Application of aurintricarboxylic acid *in vivo* was able to prevent and also reverse hypertrophy in the murine TAC model of pressure overload (Mohamed et al., 2013b), suggesting inhibition of PMCA4 may provide an interesting therapeutic target.

MCU

Ca^{2+} is also required for effective mitochondrial function. Mitochondrial Ca^{2+} cycling is achieved through the inner mitochondrial membrane located MCU (**Figure 2**). Mitochondria are abundant in cardiomyocytes owing to their function in the synthesis of ATP (Kwong, 2017). In the process of ATP generation, mitochondria utilize Ca^{2+} to activate pyruvate dehydrogenase, ATP synthase and other enzymes involved in the redox reaction, as such $[Ca^{2+}]$ in the inner matrix is tightly regulated by MCU (Kwong, 2017). MCU levels are elevated in the failing human heart and in animal models of HF (Zaglia et al., 2017; Yu et al., 2018). Under pathological conditions, overload of mitochondrial Ca^{2+} is associated with reduced cell viability, as well as apoptotic and autophagic cell death (Pinton et al., 2008). Interestingly, recent work suggests MCU is dispensable for normal cardiac function; cardiomyocyte-specific $Mcu^{-/-}$ mice show no overt phenotype under basal conditions, suggesting MCU is not required for maintaining cardiac homeostasis (Luongo et al., 2015). Furthermore, $Mcu^{-/-}$ mice do not experience mitochondrial Ca^{2+} overload following I/R injury which protects them against cell death and adverse cardiac remodeling (Luongo et al., 2015). Similarly, following TAC-induced pathological cardiac hypertrophy, mice treated with the MCU chemical inhibitor RR show improved survival, cardiac function and maintained mitochondrial integrity (Yu et al., 2018) (**Figure 4** and **Table 2**). Treatment of isoprenaline stressed H9C2 cells with RR *in vitro* confirmed its ability to increase both autophagy and mitophagy (Yu et al., 2018). Taken together, inhibition or depletion of MCU appears beneficial for attenuating the pathological response to ischemic and hypertrophy stimuli. However, the use of RR has been shown to interfere with Ca^{2+} flux through mitochondrial-located RyR1 and membrane bound LTCC (Beutner et al., 2001). Therefore, developing more specific inhibitors of MCU to combat HF offers an alternative to targeting the 'typical' Ca^{2+}-handling proteins.

CARDIAC ARRHYTHMIAS

Cardiac arrhythmias are a class of conditions describing abnormalities in the heart's normal rhythm. Arrhythmias are a leading cause of morbidity and mortality, and can lead to stroke, deterioration of ventricular function, and sudden cardiac death (Kass and Clancy, 2006). Arrhythmic events can vary in terms of speed, rhythm, duration and location in the heart, and can present in numerous ways. The main types of arrhythmia include bradycardias (slow but regular heart rhythms) and tachycardias (faster than normal heart rates), including supraventricular tachycardias (tachycardia originating in the atria). Other common arrhythmias are AF (an irregular, often fast heart rhythm) and heart block (the heart beats slower than normal due to a delay in conduction) (Keating and Sanguinetti, 2001; Kass and Clancy, 2006).

Arrhythmogenesis is complex and multifactorial. Numerous genetic mutations have been shown underlie primary arrhythmia disorders, such as LQTS and CPVT. Within these conditions, the underlying genetic defect determines the arrhythmia phenotype, including the physiological triggers which incite arrhythmic events in these patients (Wilde and Bezzina, 2005). In addition, pathological and physiological factors can influence cardiac electrical remodeling, and therefore trigger arrhythmia development, including HF, hypertension, and coronary heart disease. For example, HF can result in structural and hemodynamic dysfunction, electrical remodeling (including those impacting Ca^{2+} handling), and metabolic changes which pre-dispose the development of arrhythmias (Masarone et al., 2017). Furthermore, susceptibility to these acquired arrhythmic disorders can be influenced by genetic factors (Wilde and Bezzina, 2005).

Calcium Handling Proteins in Arrhythmia Development and Their Potential as Novel Therapeutic Targets

Calcium handling in the myocardium is key to the generation and control of the heartbeat. Intracellular Ca^{2+} remodeling has been identified as a major factor in the development of arrhythmias

and current approved therapies for arrhythmic disorders include Ca^{2+} channel blockers (Deo et al., 2017). Advancements in human genetic studies have highlighted mutations in Ca^{2+} handling proteins, as well as Ca^{2+} channels, that can result in the development of arrhythmias. In addition, remodeling of Ca^{2+} handling proteins has been identified in patients with acquired arrhythmic conditions (Landstrom et al., 2017). Therefore, Ca^{2+} handling proteins are promising therapeutic targets for the treatment of arrhythmic disorders. In the following section, we will discuss the current research aimed at targeting Ca^{2+} handling proteins in arrhythmia development.

The Role of Ca^{2+} in Arrhythmia Development

The mechanisms underlying arrhythmia development are generally divided into three categories: automaticity, triggered activity, and re-entry (Antzelevitch and Burashnikov, 2011). The role of Ca^{2+} in the generation of arrhythmias has been previously extensively reviewed (see Antzelevitch and Burashnikov, 2011; Kistamas et al., 2020). Automaticity is the ability of a cell to spontaneously depolarize and generate an AP. Under normal conditions, automaticity is restricted to the cardiac conduction system, specifically the SAN pacemaker cells which initiate cardiac contraction (Antzelevitch and Burashnikov, 2011). Abnormal automaticity occurs when the automaticity of the SAN is altered or when other cells begin to fire spontaneously. Spontaneous beating of the SAN is regulated by a coupled system of the surface membrane clock (inactivation and deactivation of cardiac ion channels) and the intracellular Ca^{2+} clock (rhythmic SR Ca^{2+} release) (Joung et al., 2011). Unsurprisingly, malfunction of both clocks has been associated with arrhythmia development. In relation to Ca^{2+} handling, Ca^{2+} clock remodeling (unresponsiveness to β-adrenergic stimulation and downregulation of RyR2) has been identified in SAN dysfunction (Joung et al., 2011). In addition, triggered oxidation and activation of CaMKII has been shown to result in SAN cell death which may contribute to SAN dysfunction (Huke and Knollmann, 2011).

Triggered activity refers to voltage oscillations termed afterdepolarizations which are often Ca^{2+}-mediated. Early afterdepolarizations (EADs) occur during the plateau phase of the cardiac AP and are associated with LQTS and ventricular tachyarrhythmias (associated with HF) (Landstrom et al., 2017). They are triggered by a reduction in repolarization reserve as a result of an increase in an inward current or a decrease in an outward current (Huang et al., 2018). A main contributor to EAD initiation is an increase in L-type Ca^{2+} current (I_{CaL}) which drives the EAD upstroke. This can occur due to a reactivation of the current during the repolarization phase caused by a reduction in the outward IK current or by CaMKII-mediated phosphorylation of I_{CaL} (Weiss et al., 2010; Landstrom et al., 2017). In addition, increased NCX current (I_{NCX}) can contribute to EAD. Spontaneous Ca^{2+} release events either prior to the completion of repolarization or during the initial phase of EADs can cause an increase in I_{NCX} activity which may delay repolarization and allow I_{CaL} to reactivate (Zhong et al., 2018).

Delayed afterdepolarizations (DADs) typically occur after repolarization and are caused by Ca^{2+} overload driving spontaneous Ca^{2+} release from the SR (Fink et al., 2011). Ca^{2+} release from the SR activates NCX (Ca^{2+}-sensitive Cl^{-}- and non-specific ion currents can also be activated) leading to depolarization of the membrane. If the excitation threshold is reached, I_{Na} becomes activated and an AP is triggered (Fink et al., 2011). An increase in Ca^{2+} influx or a decrease in Ca^{2+} efflux can lead to an increase in SR Ca^{2+} content and drive the Ca^{2+} waves that activate NCX. The SR threshold for Ca^{2+} waves is thought to be dependent on the properties of RyR, with the opening of RyR decreasing the threshold for Ca^{2+} release (Venetucci et al., 2008). Elevated Ca^{2+} levels increase the open probability of RyR, making them more sensitive to stochastic Ca^{2+} release, ultimately leading to Ca^{2+} release (Fink et al., 2011). Phosphorylation of RyR at the PKA site or the CaMKII site can also increase RyR calcium sensitivity and open probability (Wehrens et al., 2004a). Modulation of RyR has been attributed to arrhythmias associated with HF and CPVT (caused by an underlying RyR mutation) (Venetucci et al., 2008).

Re-entry underlies the formation of arrhythmias due to abnormal impulse conduction. Here an electrical impulse fails to terminate and instead re-excites the myocardium. For re-entry to occur there must be an abnormal electrical circuit, slow conduction and a unidirectional block (Antzelevitch and Burashnikov, 2011). Changes to Ca^{2+} handling can cause cardiac tissue to become vulnerable to re-entry arrhythmias by increasing the dispersion of refractoriness, leading to unidirectional conduction block, and slowing of conduction (Weiss et al., 2011). Subthreshold EADs and DADs cause electrical homogeneity by increasing dispersion of refractoriness and dispersion of excitability, respectively (Landstrom et al., 2017; Kistamas et al., 2020). In addition, cardiac alternans can act as a substrate from the initiation of re-entry and can arise due to Ca^{2+} cycling dysfunction. Cardiac alternans present as beat to beat variations in Ca^{2+} transient amplitude (Ca^{2+} alternans), AP duration (APD alternans), or contraction amplitude (mechanical alternans) (Kistamas et al., 2020). Changes in the level of SR Ca^{2+} content, reduced SERCA activity, and changes in the refractoriness have been proposed as mechanisms for the generation of Ca^{2+}-derived alternans. DADs can also result in Ca^{2+} alternans and subsequent APD alternans (Kistamas et al., 2020).

Ca^{2+}-Handling Proteins in Arrhythmia Development; Ca^{2+} Channels, Pumps and Exchangers

RyR2

Abnormal RyR2-mediated Ca^{2+} release from the SR can lead to both atrial and ventricular arrhythmias, some primary arrhythmia disorders including CPVT and forms of acquired arrhythmias associated with heart disease (AF during HF) (McCauley and Wehrens, 2011). To diminish arrhythmic events, therapies have been developed to reduce and stabilize abnormal RyR activity, in order to inhibit diastolic SR Ca^{2+} release whilst maintaining the normal SR Ca^{2+} release during systole.

Dantrolene sodium is an approved muscle relaxant which is used for the treatment of malignant hyperthermia, caused by mutations in the skeletal RyR (RyR1) (McCauley and Wehrens, 2011). Dantrolene binds to the N-terminal of RyR1 to stabilize the inter-domain interactions required for the closed state of the RyR Ca^{2+} channel (Kobayashi et al., 2005). Further studies have shown dantrolene binds to RyR2 in a similar manner to improve the function of the receptor, suggesting the use of dantrolene in the treatment of arrhythmias (**Figure 4**) (Kobayashi et al., 2009). In a study using a knock-in mouse model carrying a human CPVT-RyR2 mutation (R2475S), dantrolene inhibited CPVT-related tachycardia (Kobayashi et al., 2010). Furthermore, in a cohort of CPVT-1 patients, dantrolene had an anti-arrhythmic effect, and reduced the number of premature ventricular complexes. This anti-arrhythmic response was also evident in induced pluripotent stem cell derived CPVT1 cardiomyocytes (Penttinen et al., 2015). In addition to CPVT, dantrolene has been shown to prevent the occurrence of DADs in failing cardiomyocytes isolated from a canine model (Kobayashi et al., 2009) and have a protective effect against arrhythmic events in animal models of I/R (Balam Ortiz et al., 1999; Boys et al., 2010). Together the data suggest dantrolene is a promising therapy to attenuate Ca^{2+}-mediated arrhythmias associated with HF. An early Phase I clinical trial aimed to assess the feasibility of intravenous delivery of dantrolene to reduce ventricular arrhythmias in patients with structural heart disease [clinicaltrials.gov identifier NCT04134845]. While no results have yet been posted, the study highlights the potential of RyR2 inhibition for the treatment of arrhythmias.

JTV519 (also known as K201) is a 1,4-Benzothiazepines derivative initially identified to suppress sudden cardiac cell death associated with Ca^{2+} overload (Kaneko et al., 2009). Further studies identified RyR2 as a target of JTV519, with JTV519 having a protective effect in models of AF as a result of the restoration of RyR function (**Figure 4** and **Table 2**) (Kumagai et al., 2003; Vest et al., 2005). PKA hyperphosphorylation of RyR2 and a reduction in the RyR2 channel-stabilizing subunit calstabin2 has been identified in AF. In a canine model of AF, treatment with JTV519 restored calstabin2 levels, stabilizing the closed state of RyR2 and reducing Ca^{2+} leak (Vest et al., 2005). A Phase 2 clinical trial evaluated the effects of JTV519 on sinus rhythm restoration in patients with AF [clinicaltrials.gov identifier NCT00626652], although no data is available. In terms of ventricular arrhythmias, a study using a calstabin2 global heterozygous knockout found pre-treatment with JTV519 prevented exercise-induced ventricular arrhythmias and sudden cardiac death associated with depletion of calstabin2. In the same study, JTV519 had no effect on calstabin2 knockout mice highlighting the requirement of calstabin2 for the antiarrhythmic effect of JTV519 (Wehrens et al., 2004b). Another 1,4-Benzothiazepines derivative is S107 which, like JTV519, can enhance RyR2 and calstabin2 binding to stabilize RyR2. S107 has been shown to be more specific than JTV519, with the latter known to interact with other cardiac ion channels including LTCC (Andersson and Marks, 2010). In a mouse model, S107 increased the binding of calstabin2 to RyRs carrying a CPVT mutation (R2474S) and inhibited associated arrhythmias (**Figure 4**) (Lehnart et al., 2008). The antiarrhythmic effect of S107 was further identified using a human induced pluripotent stem cell model of CPVT (Sasaki et al., 2016).

Flecainide is a trifluoroethoxybenzamide approved for the treatment of AF and/or supraventricular tachycardia. Importantly, flecainide is not recommended to patients with underling structural heart disease as the drug can be pro-arrhythmic in this environment (Andrikopoulos et al., 2015). While flecainide is classed as a type IC antiarrhythmic drug (a Na^{+} channel blocker) it is worth noting here the drugs ability to inhibit RyR2 action by reducing the duration of channel opening (**Figure 4**). Through this role as an RyR inhibitor, flecainide has been shown, in a mouse model of CPVT, to prevent ventricular tachycardia by suppressing spontaneous Ca^{2+} release. In addition, flecainide prevented exercise-induced ventricular arrhythmias in two patients carrying a CPVT-linked RyR mutation who were refectory to conventional therapy (Watanabe et al., 2009).

NCX

NCX has been identified to have a dual role in arrhythmogenesis. When Na^{+} levels are high, NCX acts in the reverse model to bring Ca^{2+} into the cell which can result in Ca^{2+} overload. When acting in the forward mode, the inward current formed during Ca^{2+} release can result in DADs (Antoons and Sipido, 2008). Increased NCX activity has been shown to underlie arrhythmogenesis in numerous conditions including HF and AF, making NCX inhibition an attractive arrhythmia treatment.

First generation NCX blockers such as aprinidine and bepridil displayed anti-arrhythmic effects. However, these NCX blockers lacked selectivity and were suggested to only have modest NCX blocking effects at therapeutic concentrations (Hobai and O'Rourke, 2004). KB-R7943 was the first NCX blocker with reported mode-selectivity, shown to be a more specific blocker of NCX in the reverse mode (Elias et al., 2001). Animal studies have shown KB-R7943 to be protective against Ca^{2+} overload and able to suppress reoxygenation-induced arrhythmias (**Figure 4**) (Ladilov et al., 1999; Mukai et al., 2000). In addition, KB-R7943 suppressed afterdepolarizations and ventricular tachyarrhythmias in a rabbit MI mode l (Chang et al., 2015). Paradoxically, this study also found KB-R7943 to enhance the inducibility of arrhythmias in this model (Chang et al., 2015), with another study showing KB-R7943 had no effect on I/R arrhythmias (Miyamoto et al., 2002). Further studies have also shown KB-R7943 to inhibit the LTCC current and various K^{+} currents, which brings into question the use of the drug in the treatment of arrhythmias (Tanaka et al., 2002).

SEA-0400 has been described as the most potent and selective NCX inhibitor compared to KB-R7943 (Tanaka et al., 2002). Like KB-R7943, SEA-0400 has been suggested to have a higher potency for the forward NCX mode (Lee et al., 2004) and has been shown to have a cardioprotective and antiarrhythmic effect, although results vary in different models (**Figure 4**). In a rat model of myocardial I/R injury, SEA-0400 improved cardiac function, and reduced the incidence of ventricular fibrillation and mortality (Takahashi et al., 2003). In contrast, however, the drug had no effect on the incidence of ventricular tachycardia and fibrillation in a larger animal model of I/R injury

(Nagasawa et al., 2005). This study also investigated arrhythmias induced by digitalis. Here, SEA-0400 reduced the incidence of induced tachyarrhythmias although 2/8 animals experienced AV block and cardiac standstill (Nagasawa et al., 2005). This differential arrhythmic effect may be dependent on the expression levels of NCX. A study found SEA-0400 to be antiarrhythmic in mouse models with increased NCX expression, such as HF and AF, but in conditions with reduced NCX expression, SEA-0400 was found to increase Ca^{2+} transient amplitude and spontaneous Ca^{2+} transients, ultimately acting proarrhythmic (Bogeholz et al., 2017). These findings suggest that in clinical conditions in which NCX function is reduced, such as diabetic cardiomyopathy, further NCX inhibition could trigger arrhythmias by reducing NCX function below the level required for balanced Ca^{2+} dynamics (Bogeholz et al., 2017).

The antiarrhythmic benefits of blocking NCX with KB-R7943 and SEA-0700 has driven further studies to identify novel NCX inhibitors including SN-6 and ORM-10962 (**Figure 4** and **Table 2**). While SN-6 has been shown to have cardioprotective effects, the potential of the benzyloxyphenyl derivative in treating HF-associated arrhythmias is hindered by its ability to also increase diastolic Ca^{2+} and block I_{Ca} (Gandhi et al., 2013). ORM-10962 is a potent NCX blocker which can inhibit both forward and reverse NCX currents and which has no significant effect on other cardiac ion currents. The drug has been shown to attenuate digoxin-induced DAD in isolated ventricular Purkinje fibers but had no effect on arrhythmias related to I/R injury (Kohajda et al., 2016). The contrasting effects of NCX blockers on arrhythmogenesis under different conditions highlights the need for further studies to explore the use of NCX blockers.

Interestingly, another therapeutic approach has been to stimulate the forward mode of NCX to reduce cytosolic Ca^{2+} and attenuate Ca^{2+} overload. Heparin oligosaccharides have been shown to directly interact with NCX and accelerate its activity (de Godoy et al., 2018). In a model of I/R, trisulfated heparin disaccharide and low molecular weight heparins had a significant antiarrhythmic effect, as a result of increased NCX forward activity. While it is worth nothing that both agents are known to target LTCC and Na^+ channels, the mechanism of NCX acceleration appears to be a promising antiarrhythmic target (de Godoy et al., 2018).

SERCA

SERCA and its inhibitory protein PLN have been identified as important regulators of cardiac contractility and therefore potential antiarrhythmic targets (Antoons and Sipido, 2008). Impaired SERCA activity in HF results in dysregulation of systolic and diastolic function which can lead to cardiac arrhythmias. Increasing SERCA activity is a way of improving cardiac function in HF. In terms of arrhythmogenesis an increase in SERCA activity could theoretically result in Ca^{2+} overload and ultimately be arrhythmogenic (Antoons and Sipido, 2008). Encouragingly however, studies focusing on HF have found an increase in SERCA2 expression to be antiarrhythmic. In pre-clinical models of HF, increased SERCA2 expression through adenoviral delivery (Ad.SERCA2a) improved intracellular Ca^{2+} handling, restored contractility and attenuated ventricular arrhythmias (**Figure 4**) (del Monte et al., 2004; Lyon et al., 2011; Cutler et al., 2012). Other direct therapies to activate SERCA2 or inhibit PLN binding have been studied. Istaroxime, a Na^+/K^+ ATPase inhibitor which also stimulates SERCA, has been shown to have a moderate antiarrhythmic effect (**Figure 4**) (Bossu et al., 2018). Several clinical trials have assessed istaroxime in HF, highlighting the promise of the drug in cardiac disorders. However, it is worth noting is not known if higher doses of istaroxime could stimulate further arrhythmic episodes through Na^+/K^+ ATPase inhibition (Bossu et al., 2018).

T-Type Ca^{2+} Channel

As previously described, LTCC blockers are an approved treatment strategy for some arrhythmic conditions. The T-type Ca^{2+} channel has been also investigated as an antiarrhythmic target. T-type Ca^{2+} channels are localized in the pacemaker regions of the heart (the SAN, AVN and Purkinje fibers) where they are thought to contribute to SAN pacemaker activity and atrioventricular conduction (Mangoni et al., 2006). Inactivation of T-type Ca^{2+} channels results in bradycardia and delayed atrioventricular conduction, highlighting the importance of the channel in cardiac rhythm (Mangoni et al., 2006). Several studies have investigated the effect of blocking T-type Ca^{2+} channels with mibefradil, a tetralol derivative which inhibits T-type Ca^{2+} channels but is also known to block I_{CaL}. Treatment with mibefradil results in a dose-dependent decrease in heart rate (Brogden and Markham, 1997), and prevention of ischemic-induced ventricular fibrillation (**Figure 4**) (Billman and Hamlin, 1996). However, the drug has been reported to result in toxicity, inducing TdP due to QT_c prolongation (Glaser et al., 2001).

CaMKII

CaMKII dysfunction is a common hallmark of many cardiac pathologies including HF. CaMKII-mediated arrhythmias have been identified in HF, AF, reperfusion injury, and genetic arrhythmic conditions including LQTS. Changes in CaMKII expression can influence the function of key cardiac ion channels and result in arrhythmogenesis (Mustroph et al., 2017). CaMKII-mediated hyperphosphorylation of RyR2 leads to spontaneous Ca^{2+} release events which can be proarrhythmic in disease conditions associated with Ca^{2+} leak. CaMKII can also drive Ca^{2+} overload through phosphorylation of $Na_v1.5$ and subsequent reduction in NCX-mediated Ca^{2+} extrusion. In addition, an increase in CaMKII activity can result in prolonged repolarization through an increase in I_{CaL}, an increase in Na^+ influx, and reduced I_K function (Mustroph et al., 2017). This makes the inhibition of CaMKII is a promising antiarrhythmic approach.

KN-93, a CaMKII inhibitor, which works by binding directly to Ca^{2+}/CaM, disrupts the ability of Ca^{2+}/CaM to interact with CaMKII and activate the kinase (Wong et al., 2019). Inhibition of CaMKII by KN-93 has been shown to be antiarrhythmic in several models (**Figure 3**). In a $RyR2^{R4496C\pm}$ knock-in mouse model of CPVT, KN-93 prevented catecholamine-induced sustained ventricular tachyarrhythmias (Liu et al., 2011). Further studies using induced pluripotent stem cells generated from a CPVT patient carrying a RyR2 mutation, showed KN-93 to

drastically reduce DADs induced by catecholaminergic stress as well as stabilize Ca^{2+} activation under β-adrenergic stimulation to a pattern seen in normal tissue (Di Pasquale et al., 2013). CaMKII inhibition by KN-93 was also shown to reduce the incidence of stress-induced ventricular tachycardia in a junction knock-out mouse model which presents with a phenotype similar to CPVT (RyR2 channels display CaMKII-dependent hyperphosphorylation). Here, KN-93 also reduced the number of spontaneous Ca^{2+} aftertransients and aftercontractions under stress conditions (Tzimas et al., 2015). It is worth noting that in relation to CPVT, AAV-mediated delivery of a CaMKII peptide inhibitor (autocamtide-2-related inhibitory peptide, AIP) has been shown to suppress ventricular arrhythmias induced by either β-adrenergic stimulation or programmed ventricular pacing. AAV-GFP-AIP delivery also suppressed abnormal Ca^{2+} release events in induced pluripotent stem cells derived from two patients with two distinct CPVT pathogenic mutations (Bezzerides et al., 2019). The advantage of using a gene therapy approach over classic CaMKII blockers, including KN-93, is that it allows for cardiomyocyte-specific CaMKII inhibition with limited extracardiac effects.

In addition to CPVT, KN-93 has been shown to be effective in several other models of cardiac arrhythmias. Increased CaMKII-dependent SR Ca^{2+} leak is a hallmark of AF. Diastolic SR Ca^{2+} release via leaky RyR2 is hypothesized to contribute to arrhythmogenesis. In $Ryr^{2R176Q/+}$ mice (exhibiting a gain-of-function defect in RyR), CaMKII inhibition prevented arrhythmias induced by rapid atrial pacing (Chelu et al., 2009). Studies have also indicated that KN-93 is effective at reversing the diastolic Ca^{2+} leak and attenuating the frequency of spontaneous Ca^{2+} transients in aged atrial murine myocytes (Guo et al., 2014), which is an important finding given that aging is associated with an increase risk of AF. Finally, CaMKII is also activated in HF and has been linked to HF-associated arrhythmias. In hypertrophic mice, KN-93 suppressed isoproterenol-induced ventricular arrhythmias and reduced isoproterenol-induced QT_c prolongation (Feng et al., 2017). Furthermore, KN-93 significantly reduced arrhythmia inducibility and slowed initiation of ventricular tachycardia in a rabbit model of HF (Hoeker et al., 2016), strengthening the notion that CaMKII inhibition may have antiarrhythmic effects in the failing human heart.

W-7 has been identified as a CaMKII inhibitor; as a CaM antagonist it inhibits the Ca^{2+}/CaM dependent activation of CaMKII thereby acting as an upstream blocker of CaMKII (Mazur et al., 1999). In a mouse model of cardiac hypertrophy (in which CaMKII expression levels were increased), inhibition of CaMKII activation by W-7 and KN-93 suppressed polymorphic ventricular arrhythmias (**Figure 3**). Here, W-7 was found to prolong AP duration to a greater extent than that of KN-93 (Kirchhof et al., 2004). W-7 has been shown to suppress TdP induction, without affecting QT duration or heart rate (Gbadebo et al., 2002; Pu et al., 2005). In a canine model of chronic AV block (associated with compensated hypertrophy and an increased risk of TdP) W-7 suppressed drug-induced TdP and shortened AP duration. Additional *in vitro* experiments found W-7 attenuated the dofetilide-induced enhanced CaMKII phosphorylation (Bourgonje et al., 2012).

TRP

Transient receptor potential channels may prove to be suitable therapeutic targets for arrhythmic disorders as a number of these channels have been implicated in arrhythmogenesis and they exhibit specific expression patterns in the cardiac conduction system (Hof et al., 2019). Within the SAN, TRP channels have been identified to contribute to both the membrane and Ca^{2+} clock (Hof et al., 2019). TRPC isoforms 1, 2, 3, 4, 6 and 7 have been detected in the mouse SAN, and treatment with the broad TRP channel inhibitor SKF-96365 results in reduced Ca^{2+} influx and a reduction in the spontaneous pacemaker rate (Ju et al., 2007). Store-operated Ca^{2+} entry (SOCE) describes the influx of Ca^{2+} into the cell when Ca^{2+} levels within the SR become depleted, a process which has been implicated in arrhythmia development (Bonilla et al., 2019). TRPC channels have been identified at store-operated transmembrane Ca^{2+} channels (Bonilla et al., 2019). With TRPC3 being the only TRPC channel to be located at the plasma membrane of pacemaker cells, it has been suggested that this channel is the main isoform to be involved in SOCE in the SAN (Hof et al., 2019). Spontaneous AP events via SOCE-activation were found to be reduced in a TRPC3 knockout mouse model (Ju et al., 2015), while excessive activation of TRPC3 has been shown to result in Ca^{2+} overload and arrhythmias. Under normal conditions, TRPC3 is understood to mediate Ca^{2+} and Na^{+} entry near NCX1, thereby promoting the forward mode of NCX and driving diastolic depolarization (Doleschal et al., 2015; Hof et al., 2019). However, when TRPC activation is increased, Ca^{2+} overload and spatial uncoupling between TRPC3 and NCX1 occurs, resulting in arrhythmogenesis (Doleschal et al., 2015). This evidence therefore suggests that TRPC3 contributes to SAN pacemaking through the stimulation of the Ca^{2+} clock via SOCE, activation of CaMKII and phosphorylation of Ca^{2+} handling proteins (including PLN and RyR2), and via TRPC3-NCX dynamics (Hof et al., 2019).

TRPC3 expression is upregulated in the atria of AF patients, and in numerous animal models of AF (Harada et al., 2012; Zhao et al., 2013), conversely, when TRPC3 expression is deleted, in a TRPC3 knockout mouse model, pacing-induced AF was significantly reduced (Ju et al., 2015). Further studies have suggested TRPC3 overexpression in AF mediates cardiac fibroblast proliferation and differentiation via the regulation of Ca^{2+} influx and downstream Ca^{2+}-mediated signaling (Harada et al., 2012). In a canine model of AF, treatment with the selective TRPC3 blocker Pyr-3 reduced atrial fibroblast proliferation and therefore the development of an AF substrate (**Figure 4**) (Harada et al., 2012). TRPC3 has also been linked to other arrhythmia conditions in addition to AF. Its activation by GSK1702934A has been shown to influence cardiac contractility and favor rhythmic instability (Doleschal et al., 2015), and in a TRPC3 overexpression mouse model, GSK1702934A resulted in arrhythmic events including paired ventricular beats, and episodes of atrial tachycardia, ventricular tachycardia and cardiac alternans (Doleschal et al., 2015). TRPC3 overexpressing hearts

were also more susceptible to ANG-II-stimulated arrhythmic events which included atrial or ventricular tachycardia. The interaction between TRPC3 and NCX1 is believed to drive the increased contractility and arrhythmogenesis upon TRPC3 activation (Doleschal et al., 2015). Therefore, inhibiting TRPC3 may be a potential therapeutic approach for arrhythmias arising due to sinus node dysfunction and AF. Pyr-3 has been identified as a selective inhibitor of TRPC3 and has been shown to efficiently suppress physiological events associated with TRPC3, including atrial fibroblast proliferation as highlighted above (Kiyonaka et al., 2009; Harada et al., 2012).

Studies have identified TRPM4 to be involved in SAN pacemaking through modulation of diastolic depolarization, suggesting that therapeutically targeting TRPM4 channels may be useful for heart rate modulation (Hof et al., 2019). Inhibition of TRPM4 by 9-phenanthrol reduced spontaneous AP in isolated mouse and rat atrial preparations and resulted in a frequency-dependent reduction of right atria beating rate (**Figure 4** and **Table 2**). Similar results were evident in rabbit SAN pacemaker cells where inhibition of TRPM4 reduced the diastolic depolarization slope (Hof et al., 2013). The study suggested that TRPM4 may act as a rate accelerator channel in the SAN that becomes activated when heart rate decreases to provide protection against bradycardia (Hof et al., 2013). In addition to TRPM4, TRPM7 has also been detected in the mouse SAN (Hof et al., 2019) and is required for maintaining cardiac automaticity. Deletion of TRPM7 *in vitro* slows spontaneous Ca^{2+} transient frequency and disrupts cardiac automaticity, while *in vivo* a loss-of-function zebrafish model displayed a slowing of heart rate (Sah et al., 2013b). In addition, the study of two mouse models of TRPM7 deletion has revealed a role for TRPM7 SAN function: (1) a cardiomyocyte-specific deletion of TRPM7 resulted in sinus pauses and (2) an inducible SAN/AVN TRPM7 knock-out drove atrioventricular block. These phenotypes were associated with a reduction in diastolic depolarization due to a downregulation of HCN4, and I_f, as a result of TRPM7 deletion (Sah et al., 2013b).

Both TRPM4 and TRPM7 are also expressed in human atrial cells (Hof et al., 2019). Small animal studies have identified that these TRP channels contribute to the atrial AP (Simard et al., 2013), with inhibition of TRPM4 by 9-phenanthrol leading to a shortening of the atrial AP duration, suggesting it may be a potential target for pharmacological approaches against atrial arrhythmias (Simard et al., 2013). It is proposed that TRPM7 channels are involved in fibrogenesis in human AF, and TRPM7 protein expression is upregulated in atrial specimens from AF patients (Zhang et al., 2012). In terms of ventricle conduction, studies using a knockout TRPM4 mouse model found that its loss increased β-adrenergic inotropic response, with $TRPM4^{-/-}$ ventricular myocytes displaying a faster repolarization phase and a shorter AP waveform compared to controls (Mathar et al., 2014). The study concluded that TRPM4 reduces the driving force of Ca^{2+} influx, and subsequently contractile force, with the action of TRPM4 specifically important during β-adrenergic stimulation when there is an increase in the Ca^{2+} current. TRPM4 channels have also been identified in Purkinje fibers, with mRNA expression most abundant in the Purkinje fibers compared to the atria, ventricle and septum (Hof et al., 2019). Inhibition of TRPM4 by 9-phenanthrol was identified to shorten the AP of Purkinje fibers isolated from rabbit hearts with no effect on ventricle AP, suggesting TRPM4 is specifically involved in Purkinje fiber AP regulation (Hof et al., 2016).

The clinical importance of TRPM4 in cardiac conduction has been highlighted by studies that have identified TRPM4 mutations in numerous arrhythmic conditions including progressive cardiac bundle branch disease (Kruse et al., 2009), Brugada syndrome (Liu et al., 2013), LQT syndrome (Hof et al., 2017), atrioventricular and right bundle branch block (Stallmeyer et al., 2012), chronic heart block (Bianchi et al., 2018), and ventricular fibrillation (Bianchi et al., 2018). Furthermore, the cardiac phenotype of TRPM4 knockout mice included conduction block with PR ad QRS lengthening and Luciani-Wenckebach atrioventricular block (Demion et al., 2014). Interestingly, the mutations identified in familial arrhythmic conditions included loss- and gain- of function mutations, which suggests targets may have to be specific for the underlying mutation.

As highlighted in the studies above, 9-phenanthrol is a commonly used inhibitor of TRPM4 (**Figure 4** and **Table 2**). The phenanthrene-derivative has been shown to be a specific inhibitor of TRPM4 channels in numerous tissues in the body (Guinamard et al., 2014). Within cardiomyocytes it is worth noting that 9-phenanthrol has been shown to modulate intracellular Ca^{2+} oscillation in HL-1 cells derived from mouse atrial cardiomyocytes, resulting in a transient increase in intracellular Ca^{2+} levels (most likely from mitochondrial Ca^{2+} stores). The study suggested this may be due to a feedback mechanism from inhibition of TRPM4 since it is known to be activated by Ca^{2+} (Burt et al., 2013). While 9-phenanthrol is a strong TRPM4 inhibitor for *in vitro* and *ex vivo* studies, the use of the agent *in vivo* is limited due low solubility and possible toxicity (Guinamard et al., 2014). In terms of TRPM7, pharmacological agents driving specific TRPM7 inhibition within the heart are lacking. TRPM7 is also one of several TRP channels which display broad tissue expression, suggesting targeting of this channel may result in off-target effects (Hof et al., 2019). Despite this, TRPM7 remains a potential therapeutic target for a range of conditions, including cardiac arrhythmias.

In addition to TRPC and TRPM channels, further TRP channels have been implicated in cardiac rhythm. Increased gene expression of various TRP channels (including TRPM, TRPC, TRPV, and TRPP) have been identified in leukocytes of patients with non-valvular AF (Duzen et al., 2017). TRPV channels have been linked to atrial inotropy related to ROS-mediated signaling (Odnoshivkina et al., 2015), and in a porcine model, depletion of TRPV1 afferent fibers resulted in a reduction in ventricular arrhythmic events associated with MI (Yoshie et al., 2020). A study has shown that TRPA1 may be a novel therapeutic target for increasing inotropic and lusitropic states in the heart, having demonstrated that stimulation of TRPA1 in isolated murine cardiomyocytes resulted in activation of CaMKII-dependent signaling and an increase in peak intracellular Ca^{2+} levels, driving an increase in cardiomyocyte contractile function (Andrei et al., 2017). Finally, in a zebrafish model, mutations in PKD2 (which encodes for TRPP2) resulted in atrioventricular

block, with isolated hearts displaying impaired intracellular Ca^{2+} cycling and Ca^{2+} alternans (Paavola et al., 2013).

MCU

It has been suggested that cardiac mitochondria influence arrhythmia development through the regulation of cytoplasmic Ca^{2+} fluxes achieved via the uptake of Ca^{2+} through MCU (Brown and O'Rourke, 2010). Much of the work focused on targeting MCU as a potential therapeutic approach to arrhythmogenesis has focused on HF models. A study utilizing a knockout MCU mouse model found, in a non-ischemic HF setting, MCU knockout mice display a shorter AP duration and fewer incidences of EADs and ventricular fibrillation when compared to control animals (Xie et al., 2018). Use of the MCU blocker RR was found to reduce the incidence of ventricular fibrillation in an I/R rat model (**Figure 4** and **Table 2**) (de et al., 2006). However, RR has off-target effects related to Ca^{2+} dynamics, including SR Ca^{2+} release and LTCC (Brown and O'Rourke, 2010). Ru_{360}, an RR analog, has been shown to be a more specific MCU inhibitor and able to suppress ventricular fibrillation associated with I/R (**Figure 4** and **Table 2**) (de et al., 2006). Both Ruthenium compounds have also been shown to convert pacing-induced ventricular fibrillation to ventricular tachycardia in isolated rat hearts, highlighting the role of MCU in arrhythmia development (Kawahara et al., 2003). It is worth noting that while Ru_{360} had no effect on left ventricle pressure, at high concentrations RR reduced left ventricle pressure amplitude (Kawahara et al., 2003).

DISCUSSION

Ca^{2+} plays a critical role in maintaining cardiac physiology and changes to the proteins which are involved in Ca^{2+} handling underly numerous cardiac diseases. Targeting Ca^{2+} dysregulation in HF and arrhythmias has long been investigated as a potential therapeutic target and, as is evident from this review, there is considerable current research investigating targeting proteins associated with Ca^{2+} handling, including RyR2, NCX, SERCA, and TRP channels, as a therapeutic approach for cardiomyopathy, HF and arrhythmias. The pathogenic remodeling of these Ca^{2+} handling proteins has been shown to differ dependent on the underlying pathological mechanism, suggesting a "personalized" approach to targeting Ca^{2+} handling proteins may be required for specific cardiac conditions. Furthermore, while several therapeutics targeting Ca^{2+} have progressed to clinical trials, several are still in early preclinical stages, demonstrating the need for further research in this area. Altogether, targeting Ca^{2+} handling is a promising approach to developing novel and effective therapies for key cardiovascular disorders.

AUTHOR CONTRIBUTIONS

EC, CW, and AN contributed conceptually to the manuscript. AN and CW drafted the manuscript. AN contributed the section concerning cardiac hypertrophy and heart failure, and the tables. CW contributed the section regarding cardiac arrhythmias. Both AN and CW contributed to the introduction, the current therapeutic approaches, the discussion, the figures, and the abstract. All authors reviewed the manuscript prior to submission.

FUNDING

This study was supported by the British Heart Foundation (FS/13/56/30645) and the Medical Research Council (G1002082).

REFERENCES

Abu-Zeitone, A., Peterson, D. R., Polonsky, B., McNitt, S., and Moss, A. J. (2014). Efficacy of different beta-blockers in the treatment of long QT syndrome. *J. Am. Coll. Cardiol.* 64, 1352–1358. doi: 10.1016/j.jacc.2014.05.068

Adachi, T., Weisbrod, R. M., Pimentel, D. R., Ying, J., Sharov, V. S., Schoneich, C., et al. (2004). S-Glutathiolation by peroxynitrite activates SERCA during arterial relaxation by nitric oxide. *Nat. Med.* 10, 1200–1207. doi: 10.1038/nm1119

Al-Khatib, S. M., Stevenson, W. G., Ackerman, M. J., Bryant, W. J., Callans, D. J., Curtis, A. B., et al. (2018). 2017 AHA/ACC/HRS Guideline for Management of Patients With Ventricular Arrhythmias and the prevention of sudden cardiac death: executive summary: a report of the American College of Cardiology/American Heart Association task force on clinical practice guidelines and the heart rhythm society. *J. Am. Coll. Cardiol.* 72, 1677–1749.

Al-Mohammad, A., Mant, J., Laramee, P., Swain, S., and Chronic Heart Failure Guideline Development G. (2010). Diagnosis and management of adults with chronic heart failure: summary of updated NICE guidance. *BMJ* 341:c4130. doi: 10.1136/bmj.c4130

Anderson, M. E. (2009). CaMKII and a failing strategy for growth in heart. *J. Clin. Invest.* 119, 1082–1085. doi: 10.1172/jci39262

Andersson, D. C., and Marks, A. R. (2010). Fixing ryanodine receptor Ca leak - a novel therapeutic strategy for contractile failure in heart and skeletal muscle. *Drug Discov. Today Dis. Mech.* 7, e151–e157. doi: 10.1016/j.ddmec.2010.09.009

Andersson, K. B., Birkeland, J. A., Finsen, A. V., Louch, W. E., Sjaastad, I., Wang, Y., et al. (2009). Moderate heart dysfunction in mice with inducible cardiomyocyte-specific excision of the Serca2 gene. *J. Mol. Cell Cardiol.* 47, 180–187. doi: 10.1016/j.yjmcc.2009.03.013

Andrei, S. R., Ghosh, M., Sinharoy, P., Dey, S., Bratz, I. N., and Damron, D. S. (2017). TRPA1 ion channel stimulation enhances cardiomyocyte contractile function via a CaMKII-dependent pathway. *Channels* 11, 587–603. doi: 10.1080/19336950.2017.1365206

Andrikopoulos, G. K., Pastromas, S., and Tzeis, S. (2015). Flecainide: current status and perspectives in arrhythmia management. *World J. Cardiol.* 7, 76–85.

Antoons, G., and Sipido, K. R. (2008). Targeting calcium handling in arrhythmias. *Europace* 10, 1364–1369. doi: 10.1093/europace/eun271

Antos, C. L., Frey, N., Marx, S. O., Reiken, S., Gaburjakova, M., Richardson, J. A., et al. (2001). Dilated cardiomyopathy and sudden death resulting from constitutive activation of protein kinase a. *Circ. Res.* 89, 997–1004. doi: 10.1161/hh2301.100003

Antzelevitch, C., and Burashnikov, A. (2011). Overview of Basic Mechanisms of Cardiac Arrhythmia. *Card Electrophysiol. Clin.* 3, 23–45. doi: 10.1016/j.ccep.2010.10.012

Armesilla, A. L., Williams, J. C., Buch, M. H., Pickard, A., Emerson, M., Cartwright, E. J., et al. (2004). Novel functional interaction between the plasma membrane Ca2+ pump 4b and the proapoptotic tumor suppressor Ras-associated factor 1 (RASSF1). *J. Biol. Chem.* 279, 31318–31328. doi: 10.1074/jbc.m307557200

Ashna, A., van Helden, D. F., Dos Remedios, C., Molenaar, P., and Laver, D. R. (2020). Phenytoin Reduces Activity of Cardiac Ryanodine Receptor 2; A Potential Mechanism for Its Cardioprotective Action. *Mol. Pharmacol.* 97, 250–258. doi: 10.1124/mol.119.117721

Backs, J., Backs, T., Neef, S., Kreusser, M. M., Lehmann, L. H., Patrick, D. M., et al. (2009). The delta isoform of CaM kinase II is required for pathological cardiac hypertrophy and remodeling after pressure overload. *Proc. Natl. Acad. Sci. U.S.A.* 106, 2342–2347. doi: 10.1073/pnas.0813013106

Balam Ortiz, E. O., Carvajal, K., and Cruz, D. (1999). [Protective effect of dantrolene in post-ischemic reperfusion myocardial damage]. *Arch. Inst. Cardiol. Mex.* 69, 311–319.

Beauverger, P., Ozoux, M. L., Begis, G., Glenat, V., Briand, V., Philippo, M. C., et al. (2020). Reversion of cardiac dysfunction by a novel orally available calcium/calmodulin-dependent protein kinase II inhibitor. RA306, in a genetic model of dilated cardiomyopathy. *Cardiovasc. Res.* 116, 329–338.

Bers, D. M. (2002). Cardiac excitation-contraction coupling. *Nature* 415, 198–205.

Bers, D. M. (2014). Cardiac sarcoplasmic reticulum calcium leak: basis and roles in cardiac dysfunction. *Annu. Rev. Physiol.* 76, 107–127. doi: 10.1146/annurev-physiol-020911-153308

Bers, D. M., and Despa, S. (2006). Cardiac myocytes Ca2+ and Na+ regulation in normal and failing hearts. *J. Pharmacol. Sci.* 100, 315–322. doi: 10.1254/jphs.cpj06001x

Beuckelmann, D. J., Nabauer, M., and Erdmann, E. (1992). Intracellular calcium handling in isolated ventricular myocytes from patients with terminal heart failure. *Circulation* 85, 1046–1055. doi: 10.1161/01.cir.85.3.1046

Beutner, G., Sharma, V. K., Giovannucci, D. R., Yule, D. I., and Sheu, S. S. (2001). Identification of a ryanodine receptor in rat heart mitochondria. *J. Biol. Chem.* 276, 21482–21488. doi: 10.1074/jbc.m101486200

Bezzerides, V. J., Caballero, A., Wang, S., Ai, Y., Hylind, R. J., Lu, F., et al. (2019). Gene Therapy for Catecholaminergic Polymorphic Ventricular Tachycardia by Inhibition of Ca(2+)/Calmodulin-Dependent Kinase II. *Circulation* 140, 405–419. doi: 10.1161/circulationaha.118.038514

Bianchi, B., Ozhathil, L. C., Medeiros-Domingo, A., Gollob, M. H., and Abriel, H. (2018). Four TRPM4 cation channel mutations found in cardiac conduction diseases lead to altered protein stability. *Front. Physiol.* 9:177. doi: 10.3389/fphys.2018.00177

Billman, G. E., and Hamlin, R. L. (1996). The effects of mibefradil, a novel calcium channel antagonist on ventricular arrhythmias induced by myocardial ischemia and programmed electrical stimulation. *J. Pharmacol. Exp. Ther.* 277, 1517–1526.

Bogeholz, N., Schulte, J. S., Kaese, S., Bauer, B. K., Pauls, P., Dechering, D. G., et al. (2017). The Effects of SEA0400 on Ca(2+) Transient Amplitude and Proarrhythmia Depend on the Na(+)/Ca(2+) exchanger expression level in murine models. *Front. Pharmacol.* 8:649. doi: 10.3389/fphar.2017.00649

Bonilla, I. M., Belevych, A. E., Baine, S., Stepanov, A., Mezache, L., Bodnar, T., et al. (2019). Enhancement of Cardiac Store Operated Calcium Entry (SOCE) within Novel Intercalated Disk Microdomains in Arrhythmic Disease. *Sci. Rep.* 9:10179.

Bossu, A., Kostense, A., Beekman, H. D. M., Houtman, M. J. C., van der Heyden, M. A. G., and Vos, M. A. (2018). Istaroxime, a positive inotropic agent devoid of proarrhythmic properties in sensitive chronic atrioventricular block dogs. *Pharmacol. Res.* 133, 132–140. doi: 10.1016/j.phrs.2018.05.001

Bourgonje, V. J., Schoenmakers, M., Beekman, J. D., van der Nagel, R., Houtman, M. J., Miedema, L. F., et al. (2012). Relevance of calmodulin/CaMKII activation for arrhythmogenesis in the AV block dog. *Heart Rhythm.* 9, 1875–1883.

Boyett, M. R. (2009). 'And the beat goes on.' The cardiac conduction system: the wiring system of the heart. *Exp. Physiol.* 94, 1035–1049. doi: 10.1113/expphysiol.2009.046920

Boys, J. A., Toledo, A. H., Anaya-Prado, R., Lopez-Neblina, F., and Toledo-Pereyra, L. H. (2010). Effects of dantrolene on ischemia-reperfusion injury in animal models: a review of outcomes in heart, brain, liver, and kidney. *J. Investig. Med.* 58, 875–882. doi: 10.2310/jim.0b013e3181e5d719

Brenner, J. S., and Dolmetsch, R. E. (2007). TrpC3 regulates hypertrophy-associated gene expression without affecting myocyte beating or cell size. *PLoS One* 2:e802. doi: 10.1371/journal.pone.0000802

Brogden, R. N., and Markham, A. (1997). Mibefradil. A review of its pharmacodynamic and pharmacokinetic properties, and therapeutic efficacy in the management of hypertension and angina pectoris. *Drugs* 54, 774–793. doi: 10.2165/00003495-199754050-00010

Brown, D. A., and O'Rourke, B. (2010). Cardiac mitochondria and arrhythmias. *Cardiovasc. Res.* 88, 241–249. doi: 10.1093/cvr/cvq231

Bueno, O. F., De Windt, L. J., Tymitz, K. M., Witt, S. A., Kimball, T. R., Klevitsky, R., et al. (2000). The MEK1-ERK1/2 signaling pathway promotes compensated cardiac hypertrophy in transgenic mice. *EMBO J.* 19, 6341–6350. doi: 10.1093/emboj/19.23.6341

Bursztyn, M., Kadr, H., Tilvis, R., Martina, B., Oigman, W., Talberg, J., et al. (1997). Mibefradil, a novel calcium antagonist, in elderly patients with hypertension: favorable hemodynamics and pharmacokinetics. *Am. Heart J.* 134, 238–247. doi: 10.1016/s0002-8703(97)70130-3

Burt, R., Graves, B. M., Gao, M., Li, C., Williams, D. L., Fregoso, S. P., et al. (2013). 9-Phenanthrol and flufenamic acid inhibit calcium oscillations in HL-1 mouse cardiomyocytes. *Cell Calcium* 54, 193–201. doi: 10.1016/j.ceca.2013.06.003

Bush, E. W., Hood, D. B., Papst, P. J., Chapo, J. A., Minobe, W., Bristow, M. R., et al. (2006). Canonical transient receptor potential channels promote cardiomyocyte hypertrophy through activation of calcineurin signaling. *J. Biol. Chem.* 281, 33487–33496. doi: 10.1074/jbc.m605536200

Campbell, T. J., and MacDonald, P. S. (2003). Digoxin in heart failure and cardiac arrhythmias. *Med. J. Aust.* 179, 98–102. doi: 10.5694/j.1326-5377.2003.tb05445.x

Cardiac Arrhythmia Suppression Trial I. (1989). Preliminary report: effect of encainide and flecainide on mortality in a randomized trial of arrhythmia suppression after myocardial infarction. *N. Engl. J. Med.* 321, 406–412. doi: 10.1056/nejm198908103210629

Cartwright, E. J., Oceandy, D., Austin, C., and Neyses, L. (2011). Ca2+ signalling in cardiovascular disease: the role of the plasma membrane calcium pumps. *Sci. China-Life Sci.* 54, 691–698. doi: 10.1007/s11427-011-4199-1

Chang, P. C., Wo, H. T., Lee, H. L., Wen, M. S., and Chou, C. C. (2015). Paradoxical effects of KB-R7943 on arrhythmogenicity in a chronic myocardial infarction rabbit model. *J. Cardiol.* 66, 80–87. doi: 10.1016/j.jjcc.2014.08.002

Chatterjee, S., Biondi-Zoccai, G., Abbate, A., D'Ascenzo, F., Castagno, D., Van Tassell, B., et al. (2013). Benefits of beta blockers in patients with heart failure and reduced ejection fraction: network meta-analysis. *BMJ* 346:f55.

Chelu, M. G., Sarma, S., Sood, S., Wang, S., van Oort, R. J., Skapura, D. G., et al. (2009). Calmodulin kinase II-mediated sarcoplasmic reticulum Ca2+ leak promotes atrial fibrillation in mice. *J. Clin. Invest.* 119, 1940–1951.

Chevalier, M., Vermij, S. H., Wyler, K., Gillet, L., Keller, I., and Abriel, H. (2018). Transcriptomic analyses of murine ventricular cardiomyocytes. *Sci. Data* 5:180170.

Chockalingam, P., Crotti, L., Girardengo, G., Johnson, J. N., Harris, K. M., van der Heijden, J. F., et al. (2012). Not all beta-blockers are equal in the management of long QT syndrome types 1 and 2: higher recurrence of events under metoprolol. *J. Am. Coll. Cardiol.* 60, 2092–2099.

CIBIS-II Investigators and Committees (1999). The Cardiac Insufficiency Bisoprolol Study II (CIBIS-II): a randomised trial. *Lancet* 353, 9–13 doi: 10.1016/s0140-6736(98)11181-9

Collaborators GBDCoD. (2018). Global, regional, and national age-sex-specific mortality for 282 causes of death in 195 countries and territories, 1980-2017: a systematic analysis for the Global Burden of Disease Study 2017. *Lancet* 392, 1736–1788.

Correll, R. N., Makarewich, C. A., Zhang, H., Zhang, C., Sargent, M. A., York, A. J., et al. (2017). Caveolae-localized L-type Ca2+ channels do not contribute to function or hypertrophic signalling in the mouse heart. *Cardiovasc. Res.* 113, 749–759. doi: 10.1093/cvr/cvx046

Cowart, D., Venuti, R. P., Lynch, K., Guptill, J. T., Noveck, R. J., and Foo, S. Y. (2019). A Phase 1 Randomized Study of Single Intravenous Infusions of the Novel Nitroxyl Donor BMS-986231 in Healthy Volunteers. *J. Clin. Pharmacol.* 59, 717–730. doi: 10.1002/jcph.1364

Cutler, M. J., Wan, X., Plummer, B. N., Liu, H., Deschenes, I., Laurita, K. R., et al. (2012). Targeted sarcoplasmic reticulum Ca2+ ATPase 2a gene delivery to restore electrical stability in the failing heart. *Circulation* 126, 2095–2104. doi: 10.1161/circulationaha.111.071480

Dan, G. A., Martinez-Rubio, A., Agewall, S., Boriani, G., Borggrefe, M., Gaita, F., et al. (2018). Antiarrhythmic drugs-clinical use and clinical decision making: a consensus document from the European Heart Rhythm Association (EHRA) and European Society of Cardiology (ESC) Working Group on Cardiovascular

Pharmacology, endorsed by the Heart Rhythm Society (HRS), Asia-Pacific Heart Rhythm Society (APHRS) and International Society of Cardiovascular Pharmacotherapy (ISCP). *Europace* 20, 731an–732an.

de Godoy, C. M. G., Vasques, E. R., Caricati-Neto, A., Tavares, J. G. P., Alves, B. J., Duarte, J., et al. (2018). Heparin oligosaccharides have antiarrhythmic effect by accelerating the sodium-calcium exchanger. *Front. Cardiovasc. Med.* 5:67. doi: 10.3389/fcvm.2018.00067

de, J., Garcia-Rivas, G., Carvajal, K., Correa, F., and Zazueta, C. (2006). Ru360, a specific mitochondrial calcium uptake inhibitor, improves cardiac post-ischaemic functional recovery in rats in vivo. *Br. J. Pharmacol.* 149, 829–837. doi: 10.1038/sj.bjp.0706932

del Monte, F., Harding, S. E., Schmidt, U., Matsui, T., Kang, Z. B., Dec, G. W., et al. (1999). Restoration of contractile function in isolated cardiomyocytes from failing human hearts by gene transfer of SERCA2a. *Circulation* 100, 2308–2311. doi: 10.1161/01.cir.100.23.2308

del Monte, F., Lebeche, D., Guerrero, J. L., Tsuji, T., Doye, A. A., Gwathmey, J. K., et al. (2004). Abrogation of ventricular arrhythmias in a model of ischemia and reperfusion by targeting myocardial calcium cycling. *Proc. Natl. Acad. Sci. U.S.A.* 101, 5622–5627. doi: 10.1073/pnas.0305778101

del Monte, F., Williams, E., Lebeche, D., Schmidt, U., Rosenzweig, A., Gwathmey, J. K., et al. (2001). Improvement in survival and cardiac metabolism after gene transfer of sarcoplasmic reticulum Ca(2+)-ATPase in a rat model of heart failure. *Circulation* 104, 1424–1429. doi: 10.1161/hc3601.095574

Demers, C., Mody, A., Teo, K. K., and McKelvie, R. S. (2005). ACE inhibitors in heart failure: what more do we need to know? *Am. J. Cardiovasc. Drugs* 5, 351–359. doi: 10.2165/00129784-200505060-00002

Demion, M., Thireau, J., Gueffier, M., Finan, A., Khoueiry, Z., Cassan, C., et al. (2014). Trpm4 gene invalidation leads to cardiac hypertrophy and electrophysiological alterations. *PLoS One* 9:e115256. doi: 10.1371/journal.pone.0115256

Deo, M., Weinberg, S. H., and Boyle, P. M. (2017). Calcium Dynamics and Cardiac Arrhythmia. *Clin. Med. Insights Cardiol.* 11:1179546817739523.

Di Pasquale, E., Lodola, F., Miragoli, M., Denegri, M., Avelino-Cruz, J. E., Buonocore, M., et al. (2013). CaMKII inhibition rectifies arrhythmic phenotype in a patient-specific model of catecholaminergic polymorphic ventricular tachycardia. *Cell Death Dis.* 4:e843. doi: 10.1038/cddis.2013.369

Doleschal, B., Primessnig, U., Wolkart, G., Wolf, S., Schernthaner, M., Lichtenegger, M., et al. (2015). TRPC3 contributes to regulation of cardiac contractility and arrhythmogenesis by dynamic interaction with NCX1. *Cardiovasc. Res.* 106, 163–173. doi: 10.1093/cvr/cvv022

Dominguez-Rodriguez, A., Mayoral-Gonzalez, I., Avila-Medina, J., de Rojas-de Pedro, E. S., Calderon-Sanchez, E., Diaz, I., et al. (2018). Urocortin-2 Prevents Dysregulation of Ca(2+) homeostasis and improves early cardiac remodeling after ischemia and reperfusion. *Front. Physiol.* 9:813. doi: 10.3389/fphys.2018.00813

Dong, Q., Li, J., Wu, Q. F., Zhao, N., Qian, C., Ding, D., et al. (2017). Blockage of transient receptor potential vanilloid 4 alleviates myocardial ischemia/reperfusion injury in mice. *Sci. Rep.* 7:42678.

Dragun, M., Gazova, A., Kyselovic, J., Hulman, M., and Matus, M. (2019). TRP channels expression profile in human end-stage heart failure. *Medicina* 55:380. doi: 10.3390/medicina55070380

Du, X. J., Cole, T. J., Tenis, N., Gao, X. M., Kontgen, F., Kemp, B. E., et al. (2002). Impaired cardiac contractility response to hemodynamic stress in S100A1-deficient mice. *Mol. Cell Biol.* 22, 2821–2829. doi: 10.1128/mcb.22.8.2821-2829.2002

Durham, J. A., Gandolfi, A. J., and Bentley, J. B. (1984). Hepatotoxicological evaluation of dantrolene sodium. *Drug Chem. Toxicol.* 7, 23–40. doi: 10.3109/01480548409014171

Duzen, I. V., Yavuz, F., Vuruskan, E., Saracoglu, E., Poyraz, F., Goksuluk, H., et al. (2017). Leukocyte TRP channel gene expressions in patients with non-valvular atrial fibrillation. *Sci. Rep.* 7:9272.

Dzau, V. J., Colucci, W. S., Hollenberg, N. K., and Williams, G. H. (1981). Relation of the renin-angiotensin-aldosterone system to clinical state in congestive heart failure. *Circulation* 63, 645–651. doi: 10.1161/01.cir.63.3.645

Elias, C. L., Lukas, A., Shurraw, S., Scott, J., Omelchenko, A., Gross, G. J., et al. (2001). Inhibition of Na+/Ca2+ exchange by KB-R7943: transport mode selectivity and antiarrhythmic consequences. *Am. J. Physiol. Heart Circ. Physiol.* 281, H1334–H1345.

Entin-Meer, M., Cohen, L., Hertzberg-Bigelman, E., Levy, R., Ben-Shoshan, J., and Keren, G. (2017). TRPV2 knockout mice demonstrate an improved cardiac performance following myocardial infarction due to attenuated activity of peri-infarct macrophages. *PLoS One* 12:e0177132. doi: 10.1371/journal.pone.0177132

Falcon, D., Galeano-Otero, I., Calderon-Sanchez, E., Del Toro, R., Martin-Bornez, M., Rosado, J. A., et al. (2019). TRP channels: current perspectives in the adverse cardiac remodeling. *Front. Physiol.* 10:159. doi: 10.3389/fphys.2019.00159

Farah, C., Michel, L. Y. M., and Balligand, J. L. (2018). Nitric oxide signalling in cardiovascular health and disease. *Nat. Rev. Cardiol.* 15, 292–316. doi: 10.1038/nrcardio.2017.224

Felker, G. M., Borentain, M., Cleland, J. G., DeSouza, M. M., Kessler, P. D., O'Connor, C. M., et al. (2019). Rationale and design for the development of a novel nitroxyl donor in patients with acute heart failure. *Eur. J. Heart Fail.* 21, 1022–1031. doi: 10.1002/ejhf.1504

Feng, Y., Cheng, J., Wei, B., and Wang, Y. (2017). CaMKII inhibition reduces isoproterenol-induced ischemia and arrhythmias in hypertrophic mice. *Oncotarget* 8, 17504–17509. doi: 10.18632/oncotarget.15099

Fernandez-Sanz, C., Ruiz-Meana, M., Miro-Casas, E., Nunez, E., Castellano, J., Loureiro, M., et al. (2014). Defective sarcoplasmic reticulum-mitochondria calcium exchange in aged mouse myocardium. *Cell Death Dis.* 5:e1573. doi: 10.1038/cddis.2014.526

Ferrandi, M., Barassi, P., Tadini-Buoninsegni, F., Bartolommei, G., Molinari, I., Tripodi, M. G., et al. (2013). Istaroxime stimulates SERCA2a and accelerates calcium cycling in heart failure by relieving phospholamban inhibition. *Br. J. Pharmacol.* 169, 1849–1861. doi: 10.1111/bph.12278

Fink, M., Noble, P. J., and Noble, D. (2011). Ca(2)(+)-induced delayed afterdepolarizations are triggered by dyadic subspace Ca2(2)(+) affirming that increasing SERCA reduces aftercontractions. *Am. J. Physiol. Heart Circ. Physiol.* 301, H921–H935.

Freichel, M., Berlin, M., Schurger, A., Mathar, I., Bacmeister, L., Medert, R., et al. (2017). "TRP Channels in the Heart," in *Neurobiology of TRP Channels*, ed. T. L. R. Emir (Boca Raton, FL: CRC Press), 149–185.

Froehlich, J. P., Mahaney, J. E., Keceli, G., Pavlos, C. M., Goldstein, R., Redwood, A. J., et al. (2008). Phospholamban thiols play a central role in activation of the cardiac muscle sarcoplasmic reticulum calcium pump by nitroxyl. *Biochemistry* 47, 13150–13152. doi: 10.1021/bi801925p

Fukuta, H., Goto, T., Wakami, K., and Ohte, N. (2017). The effect of beta-blockers on mortality in heart failure with preserved ejection fraction: a meta-analysis of observational cohort and randomized controlled studies. *Int. J. Cardiol.* 228, 4–10. doi: 10.1016/j.ijcard.2016.11.239

Fukuto, J. M. (2019). A recent history of nitroxyl chemistry, pharmacology and therapeutic potential. *Br. J. Pharmacol.* 176, 135–146. doi: 10.1111/bph.14384

Galindo, C. L., Ryzhov, S., and Sawyer, D. B. (2014). Neuregulin as a heart failure therapy and mediator of reverse remodeling. *Curr. Heart Fail Rep.* 11, 40–49. doi: 10.1007/s11897-013-0176-2

Gandhi, A., Siedlecka, U., Shah, A. P., Navaratnarajah, M., Yacoub, M. H., and Terracciano, C. M. (2013). The effect of SN-6, a novel sodium-calcium exchange inhibitor, on contractility and calcium handling in isolated failing rat ventricular myocytes. *Cardiovasc. Ther.* 31, e115–e124. doi: 10.1111/1755-5922.12045

Gao, M. H., Tang, T., Guo, T., Sun, S. Q., Feramisco, J. R., and Hammond, H. K. (2004). Adenylyl cyclase type VI gene transfer reduces phospholamban expression in cardiac myocytes via activating transcription factor 3. *J. Biol. Chem.* 279, 38797–38802. doi: 10.1074/jbc.m405701200

Gao, R., Zhang, J., Cheng, L., Wu, X., Dong, W., Yang, X., et al. (2010). A Phase II, randomized, double-blind, multicenter, based on standard therapy, placebo-controlled study of the efficacy and safety of recombinant human neuregulin-1 in patients with chronic heart failure. *J. Am. Coll. Cardiol.* 55, 1907–1914. doi: 10.1016/j.jacc.2009.12.044

Gardner, R. T., Ripplinger, C. M., Myles, R. C., and Habecker, B. A. (2016). Molecular mechanisms of sympathetic remodeling and arrhythmias. *Circ. Arrhythm. Electrophysiol.* 9:e001359.

Gbadebo, T. D., Trimble, R. W., Khoo, M. S., Temple, J., Roden, D. M., and Anderson, M. E. (2002). Calmodulin inhibitor W-7 unmasks a novel electrocardiographic parameter that predicts initiation of torsade de pointes. *Circulation* 105, 770–774. doi: 10.1161/hc0602.103724

Ghali, J. K., Smith, W. B., Torre-Amione, G., Haynos, W., Rayburn, B. K., Amato, A., et al. (2007). A phase 1-2 dose-escalating study evaluating the safety and tolerability of istaroxime and specific effects on electrocardiographic and hemodynamic parameters in patients with chronic heart failure with reduced systolic function. *Am. J. Cardiol.* 99, 47A–56A.

Glaser, S., Steinbach, M., Opitz, C., Wruck, U., and Kleber, F. X. (2001). Torsades de pointes caused by Mibefradil. *Eur. J. Heart Fail.* 3, 627–630. doi: 10.1016/s1388-9842(01)00159-3

Godfraind, T. (2017). Discovery and development of calcium channel blockers. *Front. Pharmacol.* 8:286. doi: 10.3389/fphar.2017.00286

Goldhaber, J. I., and Hamilton, M. A. (2010). Role of inotropic agents in the treatment of heart failure. *Circulation* 121, 1655–1660. doi: 10.1161/circulationaha.109.899294

Goldstein, R. E., Boccuzzi, S. J., Cruess, D., and Nattel, S. (1991). Diltiazem increases late-onset congestive heart failure in postinfarction patients with early reduction in ejection fraction. The Adverse Experience Committee; and the Multicenter Diltiazem Postinfarction Research Group. *Circulation* 83, 52–60. doi: 10.1161/01.cir.83.1.52

Goonasekera, S. A., Hammer, K., Auger-Messier, M., Bodi, I., Chen, X., Zhang, H., et al. (2012). Decreased cardiac L-type Ca(2)(+) channel activity induces hypertrophy and heart failure in mice. *J. Clin. Invest.* 122, 280–290. doi: 10.1172/jci58227

Gorski, P. A., Jang, S. P., Jeong, D., Lee, A., Lee, P., Oh, J. G., et al. (2019). Role of SIRT1 in Modulating Acetylation of the Sarco-Endoplasmic Reticulum Ca(2+)-ATPase in Heart Failure. *Circ. Res.* 124, e63–e80.

Goyal, N., Skrdla, P., Schroyer, R., Kumar, S., Fernando, D., Oughton, A., et al. (2019). Clinical Pharmacokinetics, Safety, and Tolerability of a Novel, First-in-Class TRPV4 Ion Channel Inhibitor, GSK2798745, in Healthy and Heart Failure Subjects. *Am. J. Cardiovasc. Drugs* 19, 335–342. doi: 10.1007/s40256-018-00320-6

Grant, A. O. (2009). Cardiac ion channels. *Circ. Arrhythm. Electrophysiol.* 2, 185–194.

Greenberg, B., Butler, J., Felker, G. M., Ponikowski, P., Voors, A. A., Desai, A. S., et al. (2016). Calcium upregulation by percutaneous administration of gene therapy in patients with cardiac disease (CUPID 2): a randomised, multinational, double-blind, placebo-controlled, phase 2b trial. *Lancet* 387, 1178–1186. doi: 10.1016/s0140-6736(16)00082-9

Guinamard, R., Demion, M., Magaud, C., Potreau, D., and Bois, P. (2006). Functional expression of the TRPM4 cationic current in ventricular cardiomyocytes from spontaneously hypertensive rats. *Hypertension* 48, 587–594. doi: 10.1161/01.hyp.0000237864.65019.a5

Guinamard, R., Hof, T., and Del Negro, C. A. (2014). The TRPM4 channel inhibitor 9-phenanthrol. *Br. J. Pharmacol.* 171, 1600–1613. doi: 10.1111/bph.12582

Guo, T., Zhang, T., Mestril, R., and Bers, D. M. (2006). Ca2+/Calmodulin-dependent protein kinase II phosphorylation of ryanodine receptor does affect calcium sparks in mouse ventricular myocytes. *Circ. Res.* 99, 398–406. doi: 10.1161/01.res.0000236756.06252.13

Guo, X., Yuan, S., Liu, Z., and Fang, Q. (2014). Oxidation- and CaMKII-mediated sarcoplasmic reticulum Ca(2+) leak triggers atrial fibrillation in aging. *J. Cardiovasc. Electrophysiol.* 25, 645–652. doi: 10.1111/jce.12395

Gwathmey, J. K., Copelas, L., MacKinnon, R., Schoen, F. J., Feldman, M. D., Grossman, W., et al. (1987). Abnormal intracellular calcium handling in myocardium from patients with end-stage heart failure. *Circ. Res.* 61, 70–76. doi: 10.1161/01.res.61.1.70

Gwathmey, J. K., Warren, S. E., Briggs, G. M., Copelas, L., Feldman, M. D., Phillips, P. J., et al. (1991). Diastolic dysfunction in hypertrophic cardiomyopathy. *Effect on active force generation during systole. J. Clin. Invest.* 87, 1023–1031. doi: 10.1172/jci115061

Hammond, H. K., Penny, W. F., Traverse, J. H., Henry, T. D., Watkins, M. W., Yancy, C. W., et al. (2016). Intracoronary gene transfer of adenylyl cyclase 6 in patients with heart failure: a randomized clinical trial. *JAMA Cardiol.* 1, 163–171.

Harada, M., Luo, X., Qi, X. Y., Tadevosyan, A., Maguy, A., Ordog, B., et al. (2012). Transient receptor potential canonical-3 channel-dependent fibroblast regulation in atrial fibrillation. *Circulation* 126, 2051–2064. doi: 10.1161/circulationaha.112.121830

Hasenfuss, G., Pieske, B., Holubarsch, C., Alpert, N. R., and Just, H. (1993). Excitation-contraction coupling and contractile protein function in failing and nonfailing human myocardium. *Adv. Exp. Med. Biol.* 346, 91–100. doi: 10.1007/978-1-4615-2946-0_9

Hasenfuss, G., Schillinger, W., Lehnart, S. E., Preuss, M., Pieske, B., Maier, L. S., et al. (1999). Relationship between Na+-Ca2+-exchanger protein levels and diastolic function of failing human myocardium. *Circulation* 99, 641–648. doi: 10.1161/01.cir.99.5.641

Hayward, C., Banner, N. R., Morley-Smith, A., Lyon, A. R., and Harding, S. E. (2015). The current and future landscape of SERCA gene therapy for heart failure: a clinical perspective. *Hum. Gene Ther.* 26, 293–304. doi: 10.1089/hum.2015.018

Heart Outcomes Prevention Evaluation Study Investigator, Yusuf, S., Sleight, P., Pogue, J., Bosch, J., Davies, R., et al. (2000). Effects of an angiotensin-converting-enzyme inhibitor, ramipril, on cardiovascular events in high-risk patients. *N. Engl. J. Med.* 342, 145–153. doi: 10.1056/nejm200001203420301

Hobai, I. A., and O'Rourke, B. (2004). The potential of Na+/Ca2+ exchange blockers in the treatment of cardiac disease. *Expert Opin. Invest. Drugs* 13, 653–664. doi: 10.1517/13543784.13.6.653

Hoeker, G. S., Hanafy, M. A., Oster, R. A., Bers, D. M., and Pogwizd, S. M. (2016). Reduced Arrhythmia Inducibility With Calcium/Calmodulin-dependent Protein Kinase II Inhibition in Heart Failure Rabbits. *J. Cardiovasc. Pharmacol.* 67, 260–265. doi: 10.1097/fjc.0000000000000343

Hof, T., Chaigne, S., Recalde, A., Salle, L., Brette, F., and Guinamard, R. (2019). Transient receptor potential channels in cardiac health and disease. *Nat. Rev. Cardiol.* 16, 344–360. doi: 10.1038/s41569-018-0145-2

Hof, T., Liu, H., Salle, L., Schott, J. J., Ducreux, C., Millat, G., et al. (2017). TRPM4 non-selective cation channel variants in long QT syndrome. *BMC Med. Genet.* 18:31. doi: 10.1186/s12881-017-0397-4

Hof, T., Salle, L., Coulbault, L., Richer, R., Alexandre, J., Rouet, R., et al. (2016). TRPM4 non-selective cation channels influence action potentials in rabbit Purkinje fibres. *J. Physiol.* 594, 295–306. doi: 10.1113/jp271347

Hof, T., Simard, C., Rouet, R., Salle, L., and Guinamard, R. (2013). Implication of the TRPM4 nonselective cation channel in mammalian sinus rhythm. *Heart Rhythm.* 10, 1683–1689. doi: 10.1016/j.hrthm.2013.08.014

Huang, W., Rubinstein, J., Prieto, A. R., Thang, L. V., and Wang, D. H. (2009). Transient receptor potential vanilloid gene deletion exacerbates inflammation and atypical cardiac remodeling after myocardial infarction. *Hypertension* 53, 243–250. doi: 10.1161/hypertensionaha.108.118349

Huang, X., Song, Z., and Qu, Z. (2018). Determinants of early afterdepolarization properties in ventricular myocyte models. *PLoS Comput. Biol.* 14:e1006382. doi: 10.1371/journal.pcbi.1006382

Huke, S., and Knollmann, B. C. (2011). Oxidized CaMKII: a "heart stopper" for the sinus node? *J. Clin. Invest.* 121, 2975–2977. doi: 10.1172/jci58389

Hulot, J. S., Ishikawa, K., and Hajjar, R. J. (2016). Gene therapy for the treatment of heart failure: promise postponed. *Eur. Heart J.* 37, 1651–1658. doi: 10.1093/eurheartj/ehw019

Hulot, J. S., Salem, J. E., Redheuil, A., Collet, J. P., Varnous, S., Jourdain, P., et al. (2017). Effect of intracoronary administration of AAV1/SERCA2a on ventricular remodelling in patients with advanced systolic heart failure: results from the AGENT-HF randomized phase 2 trial. *Eur. J. Heart Fail* 19, 1534–1541. doi: 10.1002/ejhf.826

Imahashi, K., Pott, C., Goldhaber, J. I., Steenbergen, C., Philipson, K. D., and Murphy, E. (2005). Cardiac-specific ablation of the Na+-Ca2+ exchanger confers protection against ischemia/reperfusion injury. *Circ. Res.* 97, 916–921. doi: 10.1161/01.res.0000187456.06162.cb

Inserte, J., Garcia-Dorado, D., Ruiz-Meana, M., Padilla, F., Barrabes, J. A., Pina, P., et al. (2002). Effect of inhibition of Na(+)/Ca(2+) exchanger at the time of myocardial reperfusion on hypercontracture and cell death. *Cardiovasc. Res.* 55, 739–748. doi: 10.1016/s0008-6363(02)00461-3

Iravanian, S., and Dudley, S. C. Jr. (2008). The renin-angiotensin-aldosterone system (RAAS) and cardiac arrhythmias. *Heart Rhythm.* 5, S12–S17.

Irie, T., Sips, P. Y., Kai, S., Kida, K., Ikeda, K., Hirai, S., et al. (2015). S-Nitrosylation of calcium-handling proteins in cardiac adrenergic signaling and hypertrophy. *Circ. Res.* 117, 793–803. doi: 10.1161/circresaha.115.307157

Jabbour, A., Hayward, C. S., Keogh, A. M., Kotlyar, E., McCrohon, J. A., England, J. F., et al. (2011). Parenteral administration of recombinant human neuregulin-1 to patients with stable chronic heart failure produces favourable acute and

chronic haemodynamic responses. *Eur. J. Heart Fail.* 13, 83–92. doi: 10.1093/eurjhf/hfq152

Jamshidi, J., Asnaashari, A., Alipoor, R., Mohammadi, S., Roostaei, S., Samadian, M. M., et al. (2018). ATP2B1 rs2681472 and STK39 rs35929607 polymorphisms and risk of Hypertension in Iranian Population. *Med. J. Islam. Repub. Iran.* 32:14.

January, C. T., Wann, L. S., Alpert, J. S., Calkins, H., Cigarroa, J. E., Cleveland, J. C. Jr., et al. (2014). 2014 AHA/ACC/HRS guideline for the management of patients with atrial fibrillation: a report of the American College of Cardiology/American Heart Association Task Force on practice guidelines and the Heart Rhythm Society. *Circulation* 130, e199–e267.

Jaruga-Killeen, E., Bull, D. A., Lotun, K., Henry, T. D., Egnaczyk, G., Reed, T. D., et al. (2019). Abstract 16296: Safety of First in Human Triple-Gene Therapy Candidate for Heart Failure Patients. *Circulation* 140, A16296–A16296.

Jaski, B. E., Jessup, M. L., Mancini, D. M., Cappola, T. P., Pauly, D. F., Greenberg, B., et al. (2009). Calcium upregulation by percutaneous administration of gene therapy in cardiac disease (CUPID Trial), a first-in-human phase 1/2 clinical trial. *J. Card. Fail* 15, 171–181. doi: 10.1016/j.cardfail.2009.01.013

Jessup, M., Greenberg, B., Mancini, D., Cappola, T., Pauly, D. F., Jaski, B., et al. (2011). Calcium Upregulation by Percutaneous Administration of Gene Therapy in Cardiac Disease (CUPID): a phase 2 trial of intracoronary gene therapy of sarcoplasmic reticulum Ca2+-ATPase in patients with advanced heart failure. *Circulation* 124, 304–313. doi: 10.1161/circulationaha.111.022889

Joung, B., Chen, P. S., and Lin, S. F. (2011). The role of the calcium and the voltage clocks in sinoatrial node dysfunction. *Yonsei Med. J.* 52, 211–219.

Ju, Y. K., Chu, Y., Chaulet, H., Lai, D., Gervasio, O. L., Graham, R. M., et al. (2007). Store-operated Ca2+ influx and expression of TRPC genes in mouse sinoatrial node. *Circ. Res.* 100, 1605–1614. doi: 10.1161/circresaha.107.152181

Ju, Y. K., Lee, B. H., Trajanovska, S., Hao, G., Allen, D. G., Lei, M., et al. (2015). The involvement of TRPC3 channels in sinoatrial arrhythmias. *Front. Physiol.* 6:86. doi: 10.3389/fphys.2015.00086

Kaneko, N., Matsuda, R., Hata, Y., and Shimamoto, K. (2009). Pharmacological characteristics and clinical applications of K201. *Curr. Clin. Pharmacol.* 4, 126–131. doi: 10.2174/157488409788184972

Kannankeril, P. J., Moore, J. P., Cerrone, M., Priori, S. G., Kertesz, N. J., Ro, P. S., et al. (2017). Efficacy of flecainide in the treatment of catecholaminergic polymorphic ventricular tachycardia: a randomized clinical trial. *JAMA Cardiol.* 2, 759–766.

Kannel, W. B., Dawber, T. R., Kagan, A., Revotskie, N., and Stokes, J. III (1961). Factors of risk in the development of coronary heart disease–six year follow-up experience. The Framingham Study. *Ann. Intern. Med.* 55, 33–50.

Kass, R. S., and Clancy, C. E. (2006). *Basis and Treatment of Cardiac Arrhythmias*. Berlin: Springer.

Kawahara, K., Takase, M., and Yamauchi, Y. (2003). Ruthenium red-induced transition from ventricular fibrillation to tachycardia in isolated rat hearts: possible involvement of changes in mitochondrial calcium uptake. *Cardiovasc. Pathol.* 12, 311–321. doi: 10.1016/s1054-8807(03)00090-5

Kawase, Y., Ly, H. Q., Prunier, F., Lebeche, D., Shi, Y., Jin, H., et al. (2008). Reversal of cardiac dysfunction after long-term expression of SERCA2a by gene transfer in a pre-clinical model of heart failure. *J. Am. Coll. Cardiol.* 51, 1112–1119. doi: 10.1016/j.jacc.2007.12.014

Keating, M. T., and Sanguinetti, M. C. (2001). Molecular and cellular mechanisms of cardiac arrhythmias. *Cell* 104, 569–580. doi: 10.1016/s0092-8674(01)00243-4

Kecskes, M., Jacobs, G., Kerselaers, S., Syam, N., Menigoz, A., Vangheluwe, P., et al. (2015). The Ca(2+)-activated cation channel TRPM4 is a negative regulator of angiotensin II-induced cardiac hypertrophy. *Basic Res. Cardiol.* 110:43.

Kehat, I., Davis, J., Tiburcy, M., Accornero, F., Saba-El-Leil, M. K., Maillet, M., et al. (2011). Extracellular signal-regulated kinases 1 and 2 regulate the balance between eccentric and concentric cardiac growth. *Circ. Res.* 108, 176–183. doi: 10.1161/circresaha.110.231514

Kho, C., Lee, A., Jeong, D., Oh, J. G., Chaanine, A. H., Kizana, E., et al. (2011). SUMO1-dependent modulation of SERCA2a in heart failure. *Nature* 477, 601–605. doi: 10.1038/nature10407

Kho, C., Lee, A., Jeong, D., Oh, J. G., Gorski, P. A., Fish, K., et al. (2015). Small-molecule activation of SERCA2a SUMOylation for the treatment of heart failure. *Nat. Commun.* 6:7229.

Khot, U. N., Khot, M. B., Bajzer, C. T., Sapp, S. K., Ohman, E. M., Brener, S. J., et al. (2003). Prevalence of conventional risk factors in patients with coronary heart disease. *JAMA* 290, 898–904.

Kieserman, J. M., Myers, V. D., Dubey, P., Cheung, J. Y., and Feldman, A. M. (2019). Current landscape of heart failure gene therapy. *J. Am. Heart Assoc.* 8:e012239.

Kirchhof, P., Fabritz, L., Kilic, A., Begrow, F., Breithardt, G., and Kuhn, M. (2004). Ventricular arrhythmias, increased cardiac calmodulin kinase II expression, and altered repolarization kinetics in ANP receptor deficient mice. *J. Mol. Cell Cardiol.* 36, 691–700. doi: 10.1016/j.yjmcc.2004.03.007

Kistamas, K., Veress, R., Horvath, B., Banyasz, T., Nanasi, P. P., and Eisner, D. A. (2020). Calcium handling defects and cardiac arrhythmia syndromes. *Front Pharmacol.* 11:72. doi: 10.3389/fphar.2020.00072

Kiyonaka, S., Kato, K., Nishida, M., Mio, K., Numaga, T., Sawaguchi, Y., et al. (2009). Selective and direct inhibition of TRPC3 channels underlies biological activities of a pyrazole compound. *Proc. Natl. Acad. Sci. U.S.A.* 106, 5400–5405. doi: 10.1073/pnas.0808793106

Kjekshus, J., Swedberg, K., and Snapinn, S. (1992). Effects of enalapril on long-term mortality in severe congestive heart failure. CONSENSUS Trial Group. *Am. J. Cardiol.* 69, 103–107. doi: 10.1016/0002-9149(92)90683-p

Kobayashi, S., Bannister, M. L., Gangopadhyay, J. P., Hamada, T., Parness, J., and Ikemoto, N. (2005). Dantrolene stabilizes domain interactions within the ryanodine receptor. *J. Biol. Chem.* 280, 6580–6587. doi: 10.1074/jbc.m408375200

Kobayashi, S., Wakeyama, T., Ono, S., Ikeda, Y., Omura, M., Oda, T., et al. (2020). A multicenter, randomized, double-blind, controlled study to evaluate the efficacy and safety of dantrolene on ventricular arrhythmia as well as mortality and morbidity in patients with chronic heart failure (SHO-IN trial): rationale and design. *J. Cardiol.* 75, 454–461. doi: 10.1016/j.jjcc.2019.08.020

Kobayashi, S., Yano, M., Suetomi, T., Ono, M., Tateishi, H., Mochizuki, M., et al. (2009). Dantrolene, a therapeutic agent for malignant hyperthermia, markedly improves the function of failing cardiomyocytes by stabilizing interdomain interactions within the ryanodine receptor. *J. Am. Coll. Cardiol.* 53, 1993–2005. doi: 10.1016/j.jacc.2009.01.065

Kobayashi, S., Yano, M., Uchinoumi, H., Suetomi, T., Susa, T., Ono, M., et al. (2010). Dantrolene, a therapeutic agent for malignant hyperthermia, inhibits catecholaminergic polymorphic ventricular tachycardia in a RyR2(R2474S/+) knock-in mouse model. *Circ. J.* 74, 2579–2584. doi: 10.1253/circj.cj-10-0680

Kobayashi, Y., Hirawa, N., Tabara, Y., Muraoka, H., Fujita, M., Miyazaki, N., et al. (2012). Mice Lacking Hypertension Candidate Gene ATP2B1 in Vascular Smooth Muscle Cells Show Significant Blood Pressure Elevation. *Hypertension* 59, 854–U213.

Kobrin, I., Charlon, V., Lindberg, E., and Pordy, R. (1997). Safety of mibefradil, a new once-a-day, selective T-type calcium channel antagonist. *Am. J. Cardiol.* 80, 40C–46C. doi: 10.1016/s0002-9149(97)00569-9

Kohajda, Z., Farkas-Morvay, N., Jost, N., Nagy, N., Geramipour, A., Horvath, A., et al. (2016). The effect of a novel highly selective inhibitor of the sodium/calcium exchanger (NCX) on cardiac arrhythmias in in vitro and in vivo experiments. *PLoS One* 11:e0166041. doi: 10.1371/journal.pone.0166041

Komuro, I., Kurabayashi, M., Shibazaki, Y., Takaku, F., and Yazaki, Y. (1989). Molecular cloning and characterization of a Ca2+ + Mg2+-dependent adenosine triphosphatase from rat cardiac sarcoplasmic reticulum. Regulation of its expression by pressure overload and developmental stage. *J. Clin. Invest.* 83, 1102–1108. doi: 10.1172/jci113989

Kranias, E. G., and Hajjar, R. J. (2012). Modulation of cardiac contractility by the phospholamban/SERCA2a regulatome. *Circ. Res.* 110, 1646–1660. doi: 10.1161/circresaha.111.259754

Kraus, C., Rohde, D., Weidenhammer, C., Qiu, G., Pleger, S. T., Voelkers, M., et al. (2009). S100A1 in cardiovascular health and disease: closing the gap between basic science and clinical therapy. *J. Mol. Cell Cardiol.* 47, 445–455. doi: 10.1016/j.yjmcc.2009.06.003

Kruse, M., Schulze-Bahr, E., Corfield, V., Beckmann, A., Stallmeyer, B., Kurtbay, G., et al. (2009). Impaired endocytosis of the ion channel TRPM4 is associated with human progressive familial heart block type I. *J. Clin. Invest.* 119, 2737–2744. doi: 10.1172/jci38292

Kumagai, K., Nakashima, H., Gondo, N., and Saku, K. (2003). Antiarrhythmic effects of JTV-519, a novel cardioprotective drug, on atrial fibrillation/flutter

in a canine sterile pericarditis model. *J. Cardiovasc. Electrophysiol.* 14, 880–884. doi: 10.1046/j.1540-8167.2003.03050.x

Kuwahara, K., Wang, Y., McAnally, J., Richardson, J. A., Bassel-Duby, R., Hill, J. A., et al. (2006). TRPC6 fulfills a calcineurin signaling circuit during pathologic cardiac remodeling. *J. Clin. Invest.* 116, 3114–3126. doi: 10.1172/jci27702

Kwong, J. Q. (2017). The mitochondrial calcium uniporter in the heart: energetics and beyond. *J. Physiol.* 595, 3743–3751. doi: 10.1113/jp273059

Ladilov, Y., Haffner, S., Balser-Schafer, C., Maxeiner, H., and Piper, H. M. (1999). Cardioprotective effects of KB-R7943: a novel inhibitor of the reverse mode of Na+/Ca2+ exchanger. *Am. J. Physiol.* 276, H1868–H1876.

Lai, N. C., Roth, D. M., Gao, M. H., Tang, T., Dalton, N., Lai, Y. Y., et al. (2004). Intracoronary adenovirus encoding adenylyl cyclase VI increases left ventricular function in heart failure. *Circulation* 110, 330–336. doi: 10.1161/01.cir.0000136033.21777.4d

Landstrom, A. P., Dobrev, D., and Wehrens, X. H. T. (2017). Calcium Signaling and Cardiac Arrhythmias. *Circ. Res.* 120, 1969–1993. doi: 10.1161/circresaha.117.310083

Lazzeroni, D., Rimoldi, O., and Camici, P. G. (2016). From Left Ventricular Hypertrophy to Dysfunction and Failure. *Circ. J.* 80, 555–564. doi: 10.1253/circj.cj-16-0062

Lee, C., Visen, N. S., Dhalla, N. S., Le, H. D., Isaac, M., Choptiany, P., et al. (2004). Inhibitory profile of SEA0400 [2-[4-[(2,5-difluorophenyl)methoxy]phenoxy]-5-ethoxyaniline] assessed on the cardiac Na+-Ca2+ exchanger. NCX1.1. *J. Pharmacol. Exp. Ther.* 311, 748–757. doi: 10.1124/jpet.104.070805

Lehnart, S. E., Mongillo, M., Bellinger, A., Lindegger, N., Chen, B. X., Hsueh, W., et al. (2008). Leaky Ca2+ release channel/ryanodine receptor 2 causes seizures and sudden cardiac death in mice. *J. Clin. Invest.* 118, 2230–2245.

Lei, M., Wu, L., Terrar, D. A., and Huang, C. L. (2018). Modernized Classification of Cardiac Antiarrhythmic Drugs. *Circulation* 138, 1879–1896. doi: 10.1161/circulationaha.118.035455

Lemmens, K., Fransen, P., Sys, S. U., Brutsaert, D. L., and De Keulenaer, G. W. (2004). Neuregulin-1 induces a negative inotropic effect in cardiac muscle: role of nitric oxide synthase. *Circulation* 109, 324–326. doi: 10.1161/01.cir.0000114521.88547.5e

Leren, I. S., Saberniak, J., Majid, E., Haland, T. F., Edvardsen, T., and Haugaa, K. H. (2016). Nadolol decreases the incidence and severity of ventricular arrhythmias during exercise stress testing compared with beta1-selective beta-blockers in patients with catecholaminergic polymorphic ventricular tachycardia. *Heart Rhythm.* 13, 433–440. doi: 10.1016/j.hrthm.2015.09.029

Li, L., Louch, W. E., Niederer, S. A., Aronsen, J. M., Christensen, G., Sejersted, O. M., et al. (2012). Sodium accumulation in SERCA knockout-induced heart failure. *Biophys. J.* 102, 2039–2048. doi: 10.1016/j.bpj.2012.03.045

Li, Y., Kranias, E. G., Mignery, G. A., and Bers, D. M. (2002). Protein kinase A phosphorylation of the ryanodine receptor does not affect calcium sparks in mouse ventricular myocytes. *Circ. Res.* 90, 309–316. doi: 10.1161/hh0302.105660

Li, Z. M., Chen, L. X., and Li, H. (2019). Voltage-gated Sodium Channels and Blockers: An Overview and Where Will They Go? *Curr. Med. Sci.* 39, 863–873. doi: 10.1007/s11596-019-2117-0

Liao, Y., Asakura, M., Takashima, S., Kato, H., Asano, Y., Shintani, Y., et al. (2005). Amlodipine ameliorates myocardial hypertrophy by inhibiting EGFR phosphorylation. *Biochem. Biophys. Res. Commun.* 327, 1083–1087. doi: 10.1016/j.bbrc.2004.12.112

Ling, H., Zhang, T., Pereira, L., Means, C. K., Cheng, H., Gu, Y., et al. (2009). Requirement for Ca2+/calmodulin-dependent kinase II in the transition from pressure overload-induced cardiac hypertrophy to heart failure in mice. *J. Clin. Invest.* 119, 1230–1240. doi: 10.1172/jci38022

Lipskaia, L., Keuylian, Z., Blirando, K., Mougenot, N., Jacquet, A., Rouxel, C., et al. (2014). Expression of sarco (endo) plasmic reticulum calcium ATPase (SERCA) system in normal mouse cardiovascular tissues, heart failure and atherosclerosis. *Biochim. Biophys. Acta* 1843, 2705–2718. doi: 10.1016/j.bbamcr.2014.08.002

Little, R., Cartwright, E. J., Neyses, L., and Austin, C. (2016). Plasma membrane calcium ATPases (PMCAs) as potential targets for the treatment of essential hypertension. *Pharmacol. Therapeut.* 159, 23–34. doi: 10.1016/j.pharmthera.2016.01.013

Little, R., Zi, M., Hammad, S. K., Nguyen, L., Njegic, A., Kurusamy, S., et al. (2017). Reduced expression of PMCA1 is associated with increased blood pressure with age which is preceded by remodelling of resistance arteries. *Aging Cell* 16, 1104–1113. doi: 10.1111/acel.12637

Liu, H., Chatel, S., Simard, C., Syam, N., Salle, L., Probst, V., et al. (2013). Molecular genetics and functional anomalies in a series of 248 Brugada cases with 11 mutations in the TRPM4 channel. *PLoS One* 8:e54131. doi: 10.1371/journal.pone.0054131

Liu, N., Ruan, Y., Denegri, M., Bachetti, T., Li, Y., Colombi, B., et al. (2011). Calmodulin kinase II inhibition prevents arrhythmias in RyR2(R4496C+/-) mice with catecholaminergic polymorphic ventricular tachycardia. *J. Mol. Cell Cardiol.* 50, 214–222. doi: 10.1016/j.yjmcc.2010.10.001

Lohse, M. J., Engelhardt, S., and Eschenhagen, T. (2003). What is the role of beta-adrenergic signaling in heart failure? *Circ. Res.* 93, 896–906. doi: 10.1161/01.res.0000102042.83024.ca

Lorenz, K., Schmitt, J. P., Vidal, M., and Lohse, M. J. (2009). Cardiac hypertrophy: targeting Raf/MEK/ERK1/2-signaling. *Int. J. Biochem. Cell Biol.* 41, 2351–2355. doi: 10.1016/j.biocel.2009.08.002

Lou, Q., Janardhan, A., and Efimov, I. R. (2012). Remodeling of calcium handling in human heart failure. *Adv. Exp. Med. Biol.* 740, 1145–1174. doi: 10.1007/978-94-007-2888-2_52

Louch, W. E., Hougen, K., Mork, H. K., Swift, F., Aronsen, J. M., Sjaastad, I., et al. (2010). Sodium accumulation promotes diastolic dysfunction in end-stage heart failure following Serca2 knockout. *J. Physiol.* 588, 465–478. doi: 10.1113/jphysiol.2009.183517

Luo, W., Grupp, I. L., Harrer, J., Ponniah, S., Grupp, G., Duffy, J. J., et al. (1994). Targeted ablation of the phospholamban gene is associated with markedly enhanced myocardial contractility and loss of beta-agonist stimulation. *Circ. Res.* 75, 401–409. doi: 10.1161/01.res.75.3.401

Luongo, T. S., Lambert, J. P., Yuan, A., Zhang, X., Gross, P., Song, J., et al. (2015). The Mitochondrial Calcium Uniporter Matches Energetic Supply with Cardiac Workload during Stress and Modulates Permeability Transition. *Cell Rep.* 12, 23–34. doi: 10.1016/j.celrep.2015.06.017

Lymperopoulos, A., Rengo, G., and Koch, W. J. (2013). Adrenergic nervous system in heart failure: pathophysiology and therapy. *Circ. Res.* 113, 739–753. doi: 10.1161/circresaha.113.300308

Lyon, A. R., Bannister, M. L., Collins, T., Pearce, E., Sepehripour, A. H., Dubb, S. S., et al. (2011). SERCA2a gene transfer decreases sarcoplasmic reticulum calcium leak and reduces ventricular arrhythmias in a model of chronic heart failure. *Circ. Arrhythm. Electrophysiol.* 4, 362–372. doi: 10.1161/circep.110.961615

Madrid, A. H., Bueno, M. G., Rebollo, J. M., Marin, I., Pena, G., Bernal, E., et al. (2002). Use of irbesartan to maintain sinus rhythm in patients with long-lasting persistent atrial fibrillation: a prospective and randomized study. *Circulation* 106, 331–336. doi: 10.1161/01.cir.0000022665.18619.83

Maggioni, A. P., Anand, I., Gottlieb, S. O., Latini, R., Tognoni, G., Cohn, J. N., et al. (2002). Effects of valsartan on morbidity and mortality in patients with heart failure not receiving angiotensin-converting enzyme inhibitors. *J. Am. Coll. Cardiol.* 40, 1414–1421. doi: 10.1016/s0735-1097(02)02304-5

Makarewich, C. A., Correll, R. N., Gao, H., Zhang, H., Yang, B., Berretta, R. M., et al. (2012). A caveolae-targeted L-type Ca(2)+ channel antagonist inhibits hypertrophic signaling without reducing cardiac contractility. *Circ. Res.* 110, 669–674. doi: 10.1161/circresaha.111.264028

Mangoni, M. E., Traboulsie, A., Leoni, A. L., Couette, B., Marger, L., Le Quang, K., et al. (2006). Bradycardia and slowing of the atrioventricular conduction in mice lacking CaV3.1/*alpha*1G T-type calcium channels. *Circ. Res.* 98, 1422–1430. doi: 10.1161/01.res.0000225862.14314.49

Marx, S. O., Reiken, S., Hisamatsu, Y., Jayaraman, T., Burkhoff, D., Rosemblit, N., et al. (2000). PKA phosphorylation dissociates FKBP12.6 from the calcium release channel (ryanodine receptor): defective regulation in failing hearts. *Cell* 101, 365–376. doi: 10.1016/s0092-8674(00)80847-8

Masarone, D., Limongelli, G., Rubino, M., Valente, F., Vastarella, R., Ammendola, E., et al. (2017). Management of arrhythmias in heart failure. *J. Cardiovasc. Dev. Dis.* 4:3. doi: 10.1007/978-3-642-75326-8_1

Mathar, I., Kecskes, M., Van der Mieren, G., Jacobs, G., Camacho Londono, J. E., Uhl, S., et al. (2014). Increased beta-adrenergic inotropy in ventricular myocardium from Trpm4-/- mice. *Circ. Res.* 114, 283–294. doi: 10.1161/circresaha.114.302835

Mattiazzi, A., and Kranias, E. G. (2014). The role of CaMKII regulation of phospholamban activity in heart disease. *Front. Pharmacol.* 5:5. doi: 10.3389/fphar.2014.00005

Mattiazzi, A., Mundina-Weilenmann, C., Guoxiang, C., Vittone, L., and Kranias, E. (2005). Role of phospholamban phosphorylation on Thr17 in cardiac physiological and pathological conditions. *Cardiovasc. Res.* 68, 366–375. doi: 10.1016/j.cardiores.2005.08.010

Mattiello, J. A., Margulies, K. B., Jeevanandam, V., and Houser, S. R. (1998). Contribution of reverse-mode sodium-calcium exchange to contractions in failing human left ventricular myocytes. *Cardiovasc. Res.* 37, 424–431. doi: 10.1016/s0008-6363(97)00271-x

Maxwell, J. T., Domeier, T. L., and Blatter, L. A. (2012). Dantrolene prevents arrhythmogenic Ca2+ release in heart failure. *Am. J. Physiol. Heart Circ. Physiol.* 302, H953–H963.

Mazur, A., Roden, D. M., and Anderson, M. E. (1999). Systemic administration of calmodulin antagonist W-7 or protein kinase A inhibitor H-8 prevents torsade de pointes in rabbits. *Circulation* 100, 2437–2442. doi: 10.1161/01.cir.100.24.2437

McCauley, M. D., and Wehrens, X. H. (2011). Targeting ryanodine receptors for anti-arrhythmic therapy. *Acta Pharmacol. Sin.* 32, 749–757. doi: 10.1038/aps.2011.44

McCauley, M., Vallabhajosyula, S., and Darbar, D. (2016). Proarrhythmic and torsadogenic effects of potassium channel blockers in patients. *Card Electrophysiol. Clin.* 8, 481–493. doi: 10.1016/j.ccep.2016.02.009

McMurray, J. J. (2004). Angiotensin inhibition in heart failure. *J. Renin. Angiotensin. Aldosterone Syst.* 5(Suppl. 1), S17–S22.

McMurray, J. J., Ostergren, J., Swedberg, K., Granger, C. B., Held, P., Michelson, E. L., et al. (2003). Effects of candesartan in patients with chronic heart failure and reduced left-ventricular systolic function taking angiotensin-converting-enzyme inhibitors: the CHARM-Added trial. *Lancet* 362, 767–771. doi: 10.1016/s0140-6736(03)14283-3

Menick, D. R., Renaud, L., Buchholz, A., Muller, J. G., Zhou, H., Kappler, C. S., et al. (2007). Regulation of Ncx1 gene expression in the normal and hypertrophic heart. *Ann. N. Y. Acad. Sci.* 1099, 195–203. doi: 10.1196/annals.1387.058

Mercadier, J. J., Lompre, A. M., Duc, P., Boheler, K. R., Fraysse, J. B., Wisnewsky, C., et al. (1990). Altered sarcoplasmic reticulum Ca2(+)-ATPase gene expression in the human ventricle during end-stage heart failure. *J. Clin. Invest.* 85, 305–309. doi: 10.1172/jci114429

Micheletti, R., Mattera, G. G., Rocchetti, M., Schiavone, A., Loi, M. F., Zaza, A., et al. (2002). Pharmacological profile of the novel inotropic agent (E,Z)-3-((2-aminoethoxy)imino)androstane-6,17-dione hydrochloride (PST2744). *J. Pharmacol. Exp. Ther.* 303, 592–600. doi: 10.1124/jpet.102.038331

Micheletti, R., Palazzo, F., Barassi, P., Giacalone, G., Ferrandi, M., Schiavone, A., et al. (2007). Istaroxime, a stimulator of sarcoplasmic reticulum calcium adenosine triphosphatase isoform 2a activity, as a novel therapeutic approach to heart failure. *Am. J. Cardiol.* 99, 24A–32A.

Miyamoto, S., Zhu, B. M., Kamiya, K., Nagasawa, Y., and Hashimoto, K. (2002). KB-R7943, a Na+/Ca2+ exchange inhibitor, does not suppress ischemia/reperfusion arrhythmias nor digitalis arrhythmias in dogs. *Jpn. J. Pharmacol.* 90, 229–235. doi: 10.1254/jjp.90.229

Mohamed, T. M. A., Abou-Leisa, R., Stafford, N., Maqsood, A., Zi, M., Prehar, S., et al. (2016). The plasma membrane calcium ATPase 4 signalling in cardiac fibroblasts mediates cardiomyocyte hypertrophy. *Nat. Commun.* 7:11074.

Mohamed, T. M., Abou-Leisa, R., Baudoin, F., Stafford, N., Neyses, L., Cartwright, E. J., et al. (2013a). Development and characterization of a novel fluorescent indicator protein PMCA4-GCaMP2 in cardiomyocytes. *J. Mol. Cell Cardiol.* 63, 57–68. doi: 10.1016/j.yjmcc.2013.07.007

Mohamed, T. M., Zakeri, S. A., Baudoin, F., Wolf, M., Oceandy, D., Cartwright, E. J., et al. (2013b). Optimisation and validation of a high throughput screening compatible assay to identify inhibitors of the plasma membrane calcium ATPase pump–a novel therapeutic target for contraception and malaria. *J. Pharm. Pharm. Sci.* 16, 217–230.

Monfredi, O., Dobrzynski, H., Mondal, T., Boyett, M. R., and Morris, G. M. (2010). The anatomy and physiology of the sinoatrial node–a contemporary review. *Pacing Clin. Electrophysiol.* 33, 1392–1406. doi: 10.1111/j.1540-8159.2010.02838.x

Morine, K. J., Paruchuri, V., Qiao, X., Aronovitz, M., Huggins, G. S., DeNofrio, D., et al. (2016). Endoglin selectively modulates transient receptor potential channel expression in left and right heart failure. *Cardiovasc. Pathol.* 25, 478–482. doi: 10.1016/j.carpath.2016.08.004

Most, P., Pleger, S. T., Volkers, M., Heidt, B., Boerries, M., Weichenhan, D., et al. (2004). Cardiac adenoviral S100A1 gene delivery rescues failing myocardium. *J. Clin. Invest.* 114, 1550–1563. doi: 10.1172/jci21454

Most, P., Seifert, H., Gao, E., Funakoshi, H., Volkers, M., Heierhorst, J., et al. (2006). Cardiac S100A1 protein levels determine contractile performance and propensity toward heart failure after myocardial infarction. *Circulation* 114, 1258–1268. doi: 10.1161/circulationaha.106.622415

Mukai, M., Terada, H., Sugiyama, S., Satoh, H., and Hayashi, H. (2000). Effects of a selective inhibitor of Na+/Ca2+ exchange, KB-R7943, on reoxygenation-induced injuries in guinea pig papillary muscles. *J. Cardiovasc. Pharmacol.* 35, 121–128. doi: 10.1097/00005344-200001000-00016

Munch, G., Bolck, B., Karczewski, P., and Schwinger, R. H. (2002). Evidence for calcineurin-mediated regulation of SERCA 2a activity in human myocardium. *J. Mol. Cell Cardiol.* 34, 321–334. doi: 10.1006/jmcc.2001.1515

Mustroph, J., Neef, S., and Maier, L. S. (2017). CaMKII as a target for arrhythmia suppression. *Pharmacol. Ther.* 176, 22–31. doi: 10.1016/j.pharmthera.2016.10.006

Nagai, R., Zarain-Herzberg, A., Brandl, C. J., Fujii, J., Tada, M., MacLennan, D. H., et al. (1989). Regulation of myocardial Ca2+-ATPase and phospholamban mRNA expression in response to pressure overload and thyroid hormone. *Proc. Natl. Acad. Sci. U.S.A.* 86, 2966–2970. doi: 10.1073/pnas.86.8.2966

Nagasawa, Y., Zhu, B. M., Chen, J., Kamiya, K., Miyamoto, S., and Hashimoto, K. (2005). Effects of SEA0400, a Na+/Ca2+ exchange inhibitor, on ventricular arrhythmias in the in vivo dogs. *Eur. J. Pharmacol.* 506, 249–255. doi: 10.1016/j.ejphar.2004.11.011

Nakamura, M., and Sadoshima, J. (2018). Mechanisms of physiological and pathological cardiac hypertrophy. *Nat. Rev. Cardiol.* 15, 387–407. doi: 10.1038/s41569-018-0007-y

Neumann, J., Eschenhagen, T., Jones, L. R., Linck, B., Schmitz, W., Scholz, H., et al. (1997). Increased expression of cardiac phosphatases in patients with end-stage heart failure. *J. Mol. Cell Cardiol.* 29, 265–272. doi: 10.1006/jmcc.1996.0271

Nilius, B., Prenen, J., Droogmans, G., Voets, T., Vennekens, R., Freichel, M., et al. (2003). Voltage dependence of the Ca2+-activated cation channel TRPM4. *J. Biol. Chem.* 278, 30813–30820. doi: 10.1074/jbc.m305127200

Nilius, B., Prenen, J., Tang, J., Wang, C., Owsianik, G., Janssens, A., et al. (2005). Regulation of the Ca2+ sensitivity of the nonselective cation channel TRPM4. *J. Biol. Chem.* 280, 6423–6433. doi: 10.1074/jbc.m411089200

Oceandy, D., Cartwright, E. J., Emerson, M., Prehar, S., Baudoin, F. M., Zi, M., et al. (2007). Neuronal nitric oxide synthase signaling in the heart is regulated by the sarcolemmal calcium pump 4b. *Circulation* 115, 483–492. doi: 10.1161/circulationaha.106.643791

Odnoshivkina, U. G., Sytchev, V. I., Nurullin, L. F., Giniatullin, A. R., Zefirov, A. L., and Petrov, A. M. (2015). beta2-adrenoceptor agonist-evoked reactive oxygen species generation in mouse atria: implication in delayed inotropic effect. *Eur. J. Pharmacol.* 765, 140–153. doi: 10.1016/j.ejphar.2015.08.020

Ohba, T., Watanabe, H., Murakami, M., Takahashi, Y., Iino, K., Kuromitsu, S., et al. (2007). Upregulation of TRPC1 in the development of cardiac hypertrophy. *J. Mol. Cell Cardiol.* 42, 498–507. doi: 10.1016/j.yjmcc.2006.10.020

Okuyama, Y., Hirawa, N., Fujita, M., Fujiwara, A., Ehara, Y., Yatsu, K., et al. (2018). The effects of anti-hypertensive drugs and the mechanism of hypertension in vascular smooth muscle cell-specific ATP2B1 knockout mice. *Hypertens. Res.* 41, 80–87. doi: 10.1038/hr.2017.92

Ortega, A., Rosello-Lleti, E., Tarazon, E., Gil-Cayuela, C., Lago, F., Gonzalez-Juanatey, J. R., et al. (2016). TRPM7 is down-regulated in both left atria and left ventricle of ischaemic cardiomyopathy patients and highly related to changes in ventricular function. *ESC Heart Fail.* 3, 220–224. doi: 10.1002/ehf2.12085

Paavola, J., Schliffke, S., Rossetti, S., Kuo, I. Y., Yuan, S., Sun, Z., et al. (2013). Polycystin-2 mutations lead to impaired calcium cycling in the heart and predispose to dilated cardiomyopathy. *J. Mol. Cell Cardiol.* 58, 199–208. doi: 10.1016/j.yjmcc.2013.01.015

Packer, M., Fowler, M. B., Roecker, E. B., Coats, A. J., Katus, H. A., Krum, H., et al. (2002). Effect of carvedilol on the morbidity of patients with severe chronic heart failure: results of the carvedilol prospective randomized cumulative survival (COPERNICUS) study. *Circulation* 106, 2194–2199. doi: 10.1161/01.cir.0000035653.72855.bf

Packer, M., O'Connor, C. M., Ghali, J. K., Pressler, M. L., Carson, P. E., Belkin, R. N., et al. (1996). Effect of amlodipine on morbidity and mortality in severe chronic

heart failure. Prospective Randomized Amlodipine Survival Evaluation Study Group. *N. Engl. J. Med.* 335, 1107–1114.

Pande, J., Mallhi, K. K., Sawh, A., Szewczyk, M. M., Simpson, F., and Grover, A. K. (2006). Aortic smooth muscle and endothelial plasma membrane Ca2+ pump isoforms are inhibited differently by the extracellular inhibitor caloxin 1b1. *Am. J. Physiol. Cell Physiol.* 290, C1341–C1349.

Pande, J., Szewczyk, M. M., and Grover, A. K. (2011). Allosteric inhibitors of plasma membrane Ca pumps: Invention and applications of caloxins. *World J. Biol. Chem.* 2, 39–47.

Paolocci, N., Saavedra, W. F., Miranda, K. M., Martignani, C., Isoda, T., Hare, J. M., et al. (2001). Nitroxyl anion exerts redox-sensitive positive cardiac inotropy in vivo by calcitonin gene-related peptide signaling. *Proc. Natl. Acad. Sci. U.S.A.* 98, 10463–10468. doi: 10.1073/pnas.181191198

Patel, K., Fonarow, G. C., Ahmed, M., Morgan, C., Kilgore, M., Love, T. E., et al. (2014). Calcium channel blockers and outcomes in older patients with heart failure and preserved ejection fraction. *Circ. Heart Fail.* 7, 945–952. doi: 10.1161/circheartfailure.114.001301

Pedersen, O. D., Bagger, H., Kober, L., and Torp-Pedersen, C. (1999). Trandolapril reduces the incidence of atrial fibrillation after acute myocardial infarction in patients with left ventricular dysfunction. *Circulation* 100, 376–380. doi: 10.1161/01.cir.100.4.376

Penny, W. F., Henry, T. D., Watkins, M. W., Patel, A. N., and Hammond, H. K. (2018). Design of a Phase 3 trial of intracoronary administration of human adenovirus 5 encoding human adenylyl cyclase type 6 (RT-100) gene transfer in patients with heart failure with reduced left ventricular ejection fraction: The FLOURISH Clinical Trial. *Am. Heart J.* 201, 111–116. doi: 10.1016/j.ahj.2018.04.005

Penttinen, K., Swan, H., Vanninen, S., Paavola, J., Lahtinen, A. M., Kontula, K., et al. (2015). Antiarrhythmic effects of dantrolene in patients with catecholaminergic polymorphic ventricular tachycardia and replication of the responses using iPSC Models. *PLoS One* 10:e0125366. doi: 10.1371/journal.pone.0125366

Periasamy, M., Reed, T. D., Liu, L. H., Ji, Y., Loukianov, E., Paul, R. J., et al. (1999). Impaired cardiac performance in heterozygous mice with a null mutation in the sarco(endo)plasmic reticulum Ca2+-ATPase isoform 2 (SERCA2) gene. *J. Biol. Chem.* 274, 2556–2562. doi: 10.1074/jbc.274.4.2556

Pinilla-Vera, M., Hahn, V. S., and Kass, D. A. (2019). Leveraging signaling pathways to treat heart failure with reduced ejection fraction. *Circ. Res.* 124, 1618–1632. doi: 10.1161/circresaha.119.313682

Pinto, A. R., Ilinykh, A., Ivey, M. J., Kuwabara, J. T., D'Antoni, M. L., Debuque, R., et al. (2016). Revisiting cardiac cellular composition. *Circ. Res.* 118, 400–409. doi: 10.1161/circresaha.115.307778

Pinton, P., Giorgi, C., Siviero, R., Zecchini, E., and Rizzuto, R. (2008). Calcium and apoptosis: ER-mitochondria Ca2+ transfer in the control of apoptosis. *Oncogene* 27, 6407–6418. doi: 10.1038/onc.2008.308

Pinz, I., Tian, R., Belke, D., Swanson, E., Dillmann, W., and Ingwall, J. S. (2011). Compromised myocardial energetics in hypertrophied mouse hearts diminish the beneficial effect of overexpressing SERCA2a. *J. Biol. Chem.* 286, 10163–10168. doi: 10.1074/jbc.m110.210757

Piper, H. M., Balser, C., Ladilov, Y. V., Schafer, M., Siegmund, B., Ruiz-Meana, M., et al. (1996). The role of Na+/H+ exchange in ischemia-reperfusion. *Basic Res. Cardiol.* 91, 191–202.

Pitt, B., Pfeffer, M. A., Assmann, S. F., Boineau, R., Anand, I. S., Claggett, B., et al. (2014). Spironolactone for heart failure with preserved ejection fraction. *N. Engl. J. Med.* 370, 1383–1392.

Pitt, B., Remme, W., Zannad, F., Neaton, J., Martinez, F., Roniker, B., et al. (2003). Eplerenone, a selective aldosterone blocker, in patients with left ventricular dysfunction after myocardial infarction. *N. Engl. J. Med.* 348, 1309–1321. doi: 10.1056/nejmoa030207

Pleger, S. T., Most, P., Boucher, M., Soltys, S., Chuprun, J. K., Pleger, W., et al. (2007). Stable myocardial-specific AAV6-S100A1 gene therapy results in chronic functional heart failure rescue. *Circulation* 115, 2506–2515. doi: 10.1161/circulationaha.106.671701

Pleger, S. T., Remppis, A., Heidt, B., Volkers, M., Chuprun, J. K., Kuhn, M., et al. (2005). S100A1 gene therapy preserves in vivo cardiac function after myocardial infarction. *Mol. Ther.* 12, 1120–1129. doi: 10.1016/j.ymthe.2005.08.002

Pleger, S. T., Shan, C., Ksienzyk, J., Bekeredjian, R., Boekstegers, P., Hinkel, R., et al. (2011). Cardiac AAV9-S100A1 gene therapy rescues post-ischemic heart failure in a preclinical large animal model. *Sci. Transl. Med.* 3:92ra64. doi: 10.1126/scitranslmed.3002097

Pogwizd, S. M., Schlotthauer, K., Li, L., Yuan, W., and Bers, D. M. (2001). Arrhythmogenesis and contractile dysfunction in heart failure: Roles of sodium-calcium exchange, inward rectifier potassium current, and residual beta-adrenergic responsiveness. *Circ. Res.* 88, 1159–1167. doi: 10.1161/hh1101.091193

Ponikowski, P., Voors, A. A., Anker, S. D., Bueno, H., Cleland, J. G., Coats, A. J., et al. (2016). 2016 ESC Guidelines for the diagnosis and treatment of acute and chronic heart failure: The Task Force for the diagnosis and treatment of acute and chronic heart failure of the European Society of Cardiology (ESC). Developed with the special contribution of the Heart Failure Association (HFA) of the ESC. *Eur. J. Heart Fail.* 18, 891–975.

Port, J. D., and Bristow, M. R. (2001). Altered beta-adrenergic receptor gene regulation and signaling in chronic heart failure. *J. Mol. Cell Cardiol.* 33, 887–905. doi: 10.1006/jmcc.2001.1358

Pu, J., Zhang, C. T., Bai, R., Liu, N., Li, Y., and Wang, L. (2005). [Calmodulin antagonist inhibits torsade de pointes induced by d-sotalol in an isolated rabbit heart model]. *Zhonghua Xin Xue Guan Bing Za Zhi.* 33, 364–368.

Qi, Z., Wong, C. K., Suen, C. H., Wang, J., Long, C., Sauer, H., et al. (2016). TRPC3 regulates the automaticity of embryonic stem cell-derived cardiomyocytes. *Int. J. Cardiol.* 203, 169–181. doi: 10.1016/j.ijcard.2015.10.018

Ramza, B. M., Tan, R. C., Osaka, T., and Joyner, R. W. (1990). Cellular mechanism of the functional refractory period in ventricular muscle. *Circ. Res.* 66, 147–162. doi: 10.1161/01.res.66.1.147

Rastogi, A., Novak, E., Platts, A. E., and Mann, D. L. (2017). Epidemiology, pathophysiology and clinical outcomes for heart failure patients with a mid-range ejection fraction. *Eur. J. Heart Fail* 19, 1597–1605. doi: 10.1002/ejhf.879

Reiken, S., Gaburjakova, M., Gaburjakova, J., He, K. L., Prieto, A., Becker, E., et al. (2001). beta-adrenergic receptor blockers restore cardiac calcium release channel (ryanodine receptor) structure and function in heart failure. *Circulation* 104, 2843–2848. doi: 10.1161/hc4701.099578

Reiken, S., Wehrens, X. H., Vest, J. A., Barbone, A., Klotz, S., Mancini, D., et al. (2003). Beta-blockers restore calcium release channel function and improve cardiac muscle performance in human heart failure. *Circulation* 107, 2459–2466. doi: 10.1161/01.cir.0000068316.53218.49

Respress, J. L., van Oort, R. J., Li, N., Rolim, N., Dixit, S. S., deAlmeida, A., et al. (2012). Role of RyR2 phosphorylation at S2814 during heart failure progression. *Circ. Res.* 110, 1474–1483. doi: 10.1161/circresaha.112.268094

Richard, S., Leclercq, F., Lemaire, S., Piot, C., and Nargeot, J. (1998). Ca2+ currents in compensated hypertrophy and heart failure. *Cardiovasc. Res.* 37, 300–311. doi: 10.1016/s0008-6363(97)00273-3

Rios, F. J., Zou, Z. G., Harvey, A. P., Harvey, K. Y., Nosalski, R., Anyfanti, P., et al. (2020). Chanzyme TRPM7 protects against cardiovascular inflammation and fibrosis. *Cardiovasc. Res.* 116, 721–735. doi: 10.1093/cvr/cvz164

Ritterhoff, J., and Most, P. (2012). Targeting S100A1 in heart failure. *Gene Ther.* 19, 613–621. doi: 10.1038/gt.2012.8

Roe, A. T., Frisk, M., and Louch, W. E. (2015). Targeting cardiomyocyte Ca2+ homeostasis in heart failure. *Curr. Pharm. Des.* 21, 431–448. doi: 10.2174/1381612821041412041241 29

Rohrbach, S., Niemann, B., Silber, R. E., and Holtz, J. (2005). Neuregulin receptors erbB2 and erbB4 in failing human myocardium – depressed expression and attenuated activation. *Basic Res Cardiol.* 100, 240–249. doi: 10.1007/s00395-005-0514-4

Rohrbach, S., Yan, X., Weinberg, E. O., Hasan, F., Bartunek, J., Marchionni, M. A., et al. (1999). Neuregulin in cardiac hypertrophy in rats with aortic stenosis. Differential expression of erbB2 and erbB4 receptors. *Circulation* 100, 407–412. doi: 10.1161/01.cir.100.4.407

Rose, B. A., Force, T., and Wang, Y. (2010). Mitogen-activated protein kinase signaling in the heart: angels versus demons in a heart-breaking tale. *Physiol. Rev.* 90, 1507–1546. doi: 10.1152/physrev.00054.2009

Rosso, R., Kalman, J. M., Rogowski, O., Diamant, S., Birger, A., Biner, S., et al. (2007). Calcium channel blockers and beta-blockers versus beta-blockers alone for preventing exercise-induced arrhythmias in catecholaminergic polymorphic ventricular tachycardia. *Heart Rhythm.* 4, 1149–1154. doi: 10.1016/j.hrthm.2007.05.017

Roth, G. A., Johnson, C., Abajobir, A., Abd-Allah, F., Abera, S. F., Abyu, G., et al. (2017). Global, Regional, and National Burden of Cardiovascular Diseases for 10 Causes, 1990 to 2015. *J. Am. Coll. Cardiol.* 70, 1–25.

Ruiz-Meana, M., Minguet, M., Bou-Teen, D., Miro-Casas, E., Castans, C., Castellano, J., et al. (2019). Ryanodine receptor glycation favors mitochondrial damage in the senescent heart. *Circulation* 139, 949–964. doi: 10.1161/circulationaha.118.035869

Sabbah, H. N., Imai, M., Cowart, D., Amato, A., Carminati, P., and Gheorghiade, M. (2007). Hemodynamic properties of a new-generation positive luso-inotropic agent for the acute treatment of advanced heart failure. *Am. J. Cardiol.* 99, 41A–46A.

Sah, R., Mesirca, P., Mason, X., Gibson, W., Bates-Withers, C., Van den Boogert, M., et al. (2013a). Timing of myocardial trpm7 deletion during cardiogenesis variably disrupts adult ventricular function, conduction, and repolarization. *Circulation* 128, 101–114. doi: 10.1161/circulationaha.112.000768

Sah, R., Mesirca, P., Van den Boogert, M., Rosen, J., Mably, J., Mangoni, M. E., et al. (2013b). Ion channel-kinase TRPM7 is required for maintaining cardiac automaticity. *Proc. Natl. Acad. Sci. U.S.A.* 110, E3037–E3046.

Samuel, T. J., Rosenberry, R. P., Lee, S., and Pan, Z. (2018). Correcting calcium dysregulation in chronic heart failure using SERCA2a gene therapy. *Int. J. Mol. Sci.* 19:1086. doi: 10.3390/ijms19041086

Sanchez-Alonso, J. L., Bhargava, A., O'Hara, T., Glukhov, A. V., Schobesberger, S., Bhogal, N., et al. (2016). Microdomain-Specific Modulation of L-type calcium channels leads to triggered ventricular arrhythmia in heart failure. *Circ. Res.* 119, 944–955. doi: 10.1161/circresaha.116.308698

Sasaki, K., Makiyama, T., Yoshida, Y., Wuriyanghai, Y., Kamakura, T., Nishiuchi, S., et al. (2016). Patient-Specific Human Induced Pluripotent Stem Cell Model Assessed with Electrical Pacing Validates S107 as a potential therapeutic agent for catecholaminergic polymorphic ventricular tachycardia. *PLoS One* 11:e0164795. doi: 10.1371/journal.pone.0164795

Satoh, S., Tanaka, H., Ueda, Y., Oyama, J., Sugano, M., Sumimoto, H., et al. (2007). Transient receptor potential (TRP) protein 7 acts as a G protein-activated Ca2+ channel mediating angiotensin II-induced myocardial apoptosis. *Mol. Cell Biochem.* 294, 205–215. doi: 10.1007/s11010-006-9261-0

Sawada, K. I., and Kawamura, K. (1991). Architecture of myocardial cells in human cardiac ventricles with concentric and eccentric hypertrophy as demonstrated by quantitative scanning electron microscopy. *Heart Vessels* 6, 129–142. doi: 10.1007/bf02058278

Schillinger, W., Janssen, P. M., Emami, S., Henderson, S. A., Ross, R. S., Teucher, N., et al. (2000). Impaired contractile performance of cultured rabbit ventricular myocytes after adenoviral gene transfer of Na(+)-Ca(2+) exchanger. *Circ. Res.* 87, 581–587. doi: 10.1161/01.res.87.7.581

Schroder, F., Handrock, R., Beuckelmann, D. J., Hirt, S., Hullin, R., Priebe, L., et al. (1998). Increased availability and open probability of single L-type calcium channels from failing compared with nonfailing human ventricle. *Circulation* 98, 969–976. doi: 10.1161/01.cir.98.10.969

Schwinger, R. H., Bohm, M., Schmidt, U., Karczewski, P., Bavendiek, U., Flesch, M., et al. (1995). Unchanged protein levels of SERCA II and phospholamban but reduced Ca2+ uptake and Ca(2+)-ATPase activity of cardiac sarcoplasmic reticulum from dilated cardiomyopathy patients compared with patients with nonfailing hearts. *Circulation* 92, 3220–3228. doi: 10.1161/01.cir.92.11.3220

Seo, K., Rainer, P. P., Shalkey Hahn, V., Lee, D. I., Jo, S. H., Andersen, A., et al. (2014). Combined TRPC3 and TRPC6 blockade by selective small-molecule or genetic deletion inhibits pathological cardiac hypertrophy. *Proc. Natl. Acad. Sci. U.S.A.* 111, 1551–1556. doi: 10.1073/pnas.1308963111

Seth, M., Zhang, Z. S., Mao, L., Graham, V., Burch, J., Stiber, J., et al. (2009). TRPC1 channels are critical for hypertrophic signaling in the heart. *Circ. Res.* 105, 1023–1030. doi: 10.1161/circresaha.109.206581

Shah, S. J., Blair, J. E., Filippatos, G. S., Macarie, C., Ruzyllo, W., Korewicki, J., et al. (2009). Effects of istaroxime on diastolic stiffness in acute heart failure syndromes: results from the Hemodynamic, Echocardiographic, and Neurohormonal Effects of Istaroxime, a Novel Intravenous Inotropic and Lusitropic Agent: a Randomized Controlled Trial in Patients Hospitalized with Heart Failure (HORIZON-HF) trial. *Am. Heart J.* 157, 1035–1041. doi: 10.1016/j.ahj.2009.03.007

Shan, J., Betzenhauser, M. J., Kushnir, A., Reiken, S., Meli, A. C., Wronska, A., et al. (2010). Role of chronic ryanodine receptor phosphorylation in heart failure and beta-adrenergic receptor blockade in mice. *J. Clin. Invest.* 120, 4375–4387. doi: 10.1172/jci37649

Simard, C., Hof, T., Keddache, Z., Launay, P., and Guinamard, R. (2013). The TRPM4 non-selective cation channel contributes to the mammalian atrial action potential. *J. Mol. Cell Cardiol.* 59, 11–19. doi: 10.1016/j.yjmcc.2013.01.019

Sombie, H. K., Kologo, J. K., Tchelougou, D., Ouedraogo, S. Y., Ouattara, A. K., Compaore, T. R., et al. (2019). Positive association between ATP2B1 rs17249754 and essential hypertension: a case-control study in Burkina Faso. West Africa. *BMC Cardiovasc. Disord.* 19:155. doi: 10.1186/s12872-019-1136-x

Stafford, N., Wilson, C., Oceandy, D., Neyses, L., and Cartwright, E. J. (2017). The Plasma Membrane Calcium ATPases and Their Role as Major New Players in Human Disease. *Physiol. Rev.* 97, 1089–1125. doi: 10.1152/physrev.00028.2016

Stallmeyer, B., Zumhagen, S., Denjoy, I., Duthoit, G., Hebert, J. L., Ferrer, X., et al. (2012). Mutational spectrum in the Ca(2+)–activated cation channel gene TRPM4 in patients with cardiac conductance disturbances. *Hum. Mutat.* 33, 109–117. doi: 10.1002/humu.21599

Sunggip, C., Shimoda, K., Oda, S., Tanaka, T., Nishiyama, K., Mangmool, S., et al. (2018). TRPC5-eNOS axis negatively regulates ATP-induced cardiomyocyte hypertrophy. *Front. Pharmacol.* 9:523. doi: 10.3389/fphar.2018.00523

Szewczyk, M. M., Pande, J., Akolkar, G., and Grover, A. K. (2010). Caloxin 1b3: a novel plasma membrane Ca(2+)-pump isoform 1 selective inhibitor that increases cytosolic Ca(2+) in endothelial cells. *Cell Calcium* 48, 352–357. doi: 10.1016/j.ceca.2010.10.008

Tabara, Y., Kohara, K., Kita, Y., Hirawa, N., Katsuya, T., Ohkubo, T., et al. (2010). Common variants in the ATP2B1 gene are associated with susceptibility to hypertension: the Japanese Millennium Genome Project. *Hypertension* 56, 973–980. doi: 10.1161/hypertensionaha.110.153429

Takahashi, K., Takahashi, T., Suzuki, T., Onishi, M., Tanaka, Y., Hamano-Takahashi, A., et al. (2003). Protective effects of SEA0400, a novel and selective inhibitor of the Na+/Ca2+ exchanger, on myocardial ischemia-reperfusion injuries. *Eur. J. Pharmacol.* 458, 155–162. doi: 10.1016/s0014-2999(02)02732-2

Takeuchi, F., Isono, M., Katsuya, T., Yamamoto, K., Yokota, M., Sugiyama, T., et al. (2010). Blood Pressure and Hypertension Are Associated With 7 Loci in the Japanese Population. *Circulation* 121, 2302–U140.

Tanaka, H., Nishimaru, K., Aikawa, T., Hirayama, W., Tanaka, Y., and Shigenobu, K. (2002). Effect of SEA0400, a novel inhibitor of sodium-calcium exchanger, on myocardial ionic currents. *Br. J. Pharmacol.* 135, 1096–1100. doi: 10.1038/sj.bjp.0704574

Tepper, D. (1999). Frontiers in congestive heart failure: Effect of Metoprolol CR/XL in chronic heart failure: Metoprolol CR/XL Randomised Intervention Trial in Congestive Heart Failure (MERIT-HF). *Congest. Heart Fail.* 5, 184–185.

The Danish Study Group on Verapamil in Myocardial Infarction (1990).. Effect of verapamil on mortality and major events after acute myocardial infarction (the Danish Verapamil Infarction Trial II–DAVIT II). *Am. J. Cardiol.* 66, 779–785 doi: 10.1016/0002-9149(90)90351-z

Thorneloe, K. S., Cheung, M., Bao, W., Alsaid, H., Lenhard, S., Jian, M. Y., et al. (2012). An orally active TRPV4 channel blocker prevents and resolves pulmonary edema induced by heart failure. *Sci. Transl. Med.* 4:159ra148. doi: 10.1126/scitranslmed.3004276

Tilemann, L., Lee, A., Ishikawa, K., Aguero, J., Rapti, K., Santos-Gallego, C., et al. (2013). SUMO-1 gene transfer improves cardiac function in a large-animal model of heart failure. *Sci Transl. Med.* 5:211ra159. doi: 10.1126/scitranslmed.3006487

Tita, C., Gilbert, E. M., Van Bakel, A. B., Grzybowski, J., Haas, G. J., Jarrah, M., et al. (2017). A Phase 2a dose-escalation study of the safety, tolerability, pharmacokinetics and haemodynamic effects of BMS-986231 in hospitalized patients with heart failure with reduced ejection fraction. *Eur. J. Heart Fail.* 19, 1321–1332. doi: 10.1002/ejhf.897

Tzimas, C., Terrovitis, J., Lehnart, S. E., Kranias, E. G., and Sanoudou, D. (2015). Calcium/calmodulin-dependent protein kinase II (CaMKII) inhibition ameliorates arrhythmias elicited by junctin ablation under stress conditions. *Heart Rhythm.* 12, 1599–1610. doi: 10.1016/j.hrthm.2015.03.043

Ueng, K. C., Tsai, T. P., Yu, W. C., Tsai, C. F., Lin, M. C., Chan, K. C., et al. (2003). Use of enalapril to facilitate sinus rhythm maintenance after external cardioversion of long-standing persistent atrial fibrillation. Results of a

prospective and controlled study. *Eur. Heart J.* 24, 2090–2098. doi: 10.1016/j.ehj.2003.08.014

Venetucci, L. A., Trafford, A. W., O'Neill, S. C., and Eisner, D. A. (2008). The sarcoplasmic reticulum and arrhythmogenic calcium release. *Cardiovasc. Res.* 77, 285–292. doi: 10.1093/cvr/cvm009

Vest, J. A., Wehrens, X. H., Reiken, S. R., Lehnart, S. E., Dobrev, D., Chandra, P., et al. (2005). Defective cardiac ryanodine receptor regulation during atrial fibrillation. *Circulation* 111, 2025–2032. doi: 10.1161/01.cir.0000162461.67140.4c

Wachtell, K., Lehto, M., Gerdts, E., Olsen, M. H., Hornestam, B., Dahlof, B., et al. (2005). Angiotensin II receptor blockade reduces new-onset atrial fibrillation and subsequent stroke compared to atenolol: the Losartan Intervention For End Point Reduction in Hypertension (LIFE) study. *J. Am. Coll. Cardiol.* 45, 712–719. doi: 10.1016/j.jacc.2004.10.068

Wahlquist, C., Jeong, D., Rojas-Munoz, A., Kho, C., Lee, A., Mitsuyama, S., et al. (2014). Inhibition of miR-25 improves cardiac contractility in the failing heart. *Nature* 508, 531–535. doi: 10.1038/nature13073

Wang, C., Naruse, K., and Takahashi, K. (2018). Role of the TRPM4 channel in cardiovascular physiology and pathophysiology. *Cells* 7:62. doi: 10.3390/cells7060062

Wang, J., Takahashi, K., Piao, H., Qu, P., and Naruse, K. (2013). 9-Phenanthrol, a TRPM4 inhibitor, protects isolated rat hearts from ischemia-reperfusion injury. *PLoS One* 8:e70587. doi: 10.1371/journal.pone.0070587

Wang, X., Zhuo, X., Gao, J., Liu, H., Lin, F., and Ma, A. (2019). Neuregulin-1beta partially improves cardiac function in volume-overload heart failure through regulation of abnormal calcium handling. *Front. Pharmacol.* 10:616. doi: 10.3389/fphar.2019.00616

Wang, Y., Zhang, Y., Li, Y., Zhou, X., Wang, X., Gao, P., et al. (2013). Common variants in the ATP2B1 gene are associated with hypertension and arterial stiffness in Chinese population. *Mol. Biol. Rep.* 40, 1867–1873. doi: 10.1007/s11033-012-2242-3

Wang, Z., Nolan, B., Kutschke, W., and Hill, J. A. (2001). Na+-Ca2+ exchanger remodeling in pressure overload cardiac hypertrophy. *J. Biol. Chem.* 276, 17706–17711. doi: 10.1074/jbc.m100544200

Washburn, D. G., Holt, D. A., Dodson, J., McAtee, J. J., Terrell, L. R., Barton, L., et al. (2013). The discovery of potent blockers of the canonical transient receptor channels. TRPC3 and TRPC6, based on an anilino-thiazole pharmacophore. *Bioorg. Med. Chem. Lett.* 23, 4979–4984. doi: 10.1016/j.bmcl.2013.06.047

Watanabe, H., Chopra, N., Laver, D., Hwang, H. S., Davies, S. S., Roach, D. E., et al. (2009). Flecainide prevents catecholaminergic polymorphic ventricular tachycardia in mice and humans. *Nat. Med.* 15, 380–383. doi: 10.1038/nm.1942

Watkins, L. Jr., Burton, J. A., Haber, E., Cant, J. R., Smith, F. W., and Barger, A. C. (1976). The renin-angiotensin-aldosterone system in congestive failure in conscious dogs. *J. Clin. Invest.* 57, 1606–1617.

Wehrens, X. H., Lehnart, S. E., Reiken, S. R., Deng, S. X., Vest, J. A., Cervantes, D., et al. (2004b). Protection from cardiac arrhythmia through ryanodine receptor-stabilizing protein calstabin2. *Science* 304, 292–296. doi: 10.1126/science.1094301

Wehrens, X. H., Lehnart, S. E., Reiken, S. R., and Marks, A. R. (2004a). Ca2+/calmodulin-dependent protein kinase II phosphorylation regulates the cardiac ryanodine receptor. *Circ. Res.* 94, e61–e70.

Wehrens, X. H., Lehnart, S. E., Reiken, S., Vest, J. A., Wronska, A., and Marks, A. R. (2006). Ryanodine receptor/calcium release channel PKA phosphorylation: a critical mediator of heart failure progression. *Proc. Natl. Acad. Sci. U.S.A.* 103, 511–518. doi: 10.1073/pnas.0510113103

Weiss, J. N., Garfinkel, A., Karagueuzian, H. S., Chen, P. S., and Qu, Z. (2010). Early afterdepolarizations and cardiac arrhythmias. *Heart Rhythm.* 7, 1891–1899. doi: 10.1016/j.hrthm.2010.09.017

Weiss, J. N., Nivala, M., Garfinkel, A., and Qu, Z. (2011). Alternans and arrhythmias: from cell to heart. *Circ. Res.* 108, 98–112. doi: 10.1161/circresaha.110.223586

Wilde, A. A., and Bezzina, C. R. (2005). Genetics of cardiac arrhythmias. *Heart* 91, 1352–1358. doi: 10.1136/hrt.2004.046334

Wilkins, B. J., Dai, Y. S., Bueno, O. F., Parsons, S. A., Xu, J., Plank, D. M., et al. (2004). Calcineurin/NFAT coupling participates in pathological, but not physiological, cardiac hypertrophy. *Circ. Res.* 94, 110–118. doi: 10.1161/01.res.0000109415.17511.18

Wong, M. H., Samal, A. B., Lee, M., Vlach, J., Novikov, N., Niedziela-Majka, A., et al. (2019). The KN-93 Molecule Inhibits Calcium/Calmodulin-Dependent Protein Kinase II (CaMKII) Activity by Binding to Ca(2+)/CaM. *J. Mol. Biol.* 431, 1440–1459. doi: 10.1016/j.jmb.2019.02.001

Workman, A. J. (2010). Cardiac adrenergic control and atrial fibrillation. *Naunyn Schmiedebergs Arch. Pharmacol.* 381, 235–249. doi: 10.1007/s00210-009-0474-0

Wu, Q. F., Qian, C., Zhao, N., Dong, Q., Li, J., Wang, B. B., et al. (2017). Activation of transient receptor potential vanilloid 4 involves in hypoxia/reoxygenation injury in cardiomyocytes. *Cell Death Dis.* 8:e2828. doi: 10.1038/cddis.2017.227

Xie, A., Song, Z., Liu, H., Zhou, A., Shi, G., Wang, Q., et al. (2018). Mitochondrial Ca(2+) influx contributes to arrhythmic risk in nonischemic cardiomyopathy. *J Am Heart Assoc.* 7:e007805.

Xu, J., Qian, H. X., Hu, S. P., Liu, L. Y., Zhou, M., Feng, M., et al. (2016). Gender-Specific Association of ATP2B1 Variants with Susceptibility to Essential Hypertension in the Han Chinese Population. *Biomed. Res. Int.* 2016:1910565.

Yamazaki, D., Komazaki, S., Nakanishi, H., Mishima, A., Nishi, M., Yazawa, M., et al. (2009a). Essential role of the TRIC-B channel in Ca2+ handling of alveolar epithelial cells and in perinatal lung maturation. *Development* 136, 2355–2361. doi: 10.1242/dev.036798

Yamazaki, D., Yamazaki, T., and Takeshima, H. (2009b). New molecular components supporting ryanodine receptor-mediated Ca(2+) release: roles of junctophilin and TRIC channel in embryonic cardiomyocytes. *Pharmacol. Ther.* 121, 265–272. doi: 10.1016/j.pharmthera.2008.11.004

Yang, H., Hu, M., Guo, J., Ou, X., Cai, T., and Liu, Z. (2016). Pore architecture of TRIC channels and insights into their gating mechanism. *Nature* 538, 537–541. doi: 10.1038/nature19767

Yazawa, M., Ferrante, C., Feng, J., Mio, K., Ogura, T., Zhang, M., et al. (2007). TRIC channels are essential for Ca2+ handling in intracellular stores. *Nature* 448, 78–82. doi: 10.1038/nature05928

Yoshida, M., Ma, J., Tomita, T., Morikawa, N., Tanaka, N., Masamura, K., et al. (2005). Mineralocorticoid receptor is overexpressed in cardiomyocytes of patients with congestive heart failure. *Congest. Heart Fail.* 11, 12–16. doi: 10.1111/j.1527-5299.2005.03722.x

Yoshie, K., Rajendran, P. S., Massoud, L., Mistry, J., Swid, M. A., Wu, X., et al. (2020). Cardiac TRPV1 afferent signaling promotes arrhythmogenic ventricular remodeling after myocardial infarction. *JCI Insight* 5:e124477.

Yu, Z., Chen, R., Li, M., Yu, Y., Liang, Y., Han, F., et al. (2018). Mitochondrial calcium uniporter inhibition provides cardioprotection in pressure overload-induced heart failure through autophagy enhancement. *Int. J. Cardiol.* 271, 161–168. doi: 10.1016/j.ijcard.2018.05.054

Zaglia, T., Ceriotti, P., Campo, A., Borile, G., Armani, A., Carullo, P., et al. (2017). Content of mitochondrial calcium uniporter (MCU) in cardiomyocytes is regulated by microRNA-1 in physiologic and pathologic hypertrophy. *Proc. Natl. Acad. Sci. U.S.A.* 114, E9006–E9015.

Zannad, F., McMurray, J. J., Krum, H., van Veldhuisen, D. J., Swedberg, K., Shi, H., et al. (2011). Eplerenone in patients with systolic heart failure and mild symptoms. *N. Engl. J. Med.* 364, 11–21.

Zhang, T., Kohlhaas, M., Backs, J., Mishra, S., Phillips, W., Dybkova, N., et al. (2007). CaMKIIdelta isoforms differentially affect calcium handling but similarly regulate HDAC/MEF2 transcriptional responses. *J. Biol. Chem.* 282, 35078–35087. doi: 10.1074/jbc.m707083200

Zhang, W., Elimban, V., Nijjar, M. S., Gupta, S. K., and Dhalla, N. S. (2003). Role of mitogen-activated protein kinase in cardiac hypertrophy and heart failure. *Exp. Clin. Cardiol.* 8, 173–183.

Zhang, Y. H., Sun, H. Y., Chen, K. H., Du, X. L., Liu, B., Cheng, L. C., et al. (2012). Evidence for functional expression of TRPM7 channels in human atrial myocytes. *Basic Res. Cardiol.* 107:282.

Zhao, J., Wang, X., Hang, P., Yun, F., Zhao, H., Xu, W., et al. (2013). Valsartan inhibits transient receptor potential canonical-3 channel in canine atrial fibrillation. *Int. J. Cardiol.* 168, 4417–4418. doi: 10.1016/j.ijcard.2013.05.029

Zhao, X., Yamazaki, D., Park, K. H., Komazaki, S., Tjondrokoesoemo, A., Nishi, M., et al. (2010). Ca2+ overload and sarcoplasmic reticulum instability in tric-a null skeletal muscle. *J. Biol. Chem.* 285, 37370–37376.

Zhong, M., Rees, C. M., Terentyev, D., Choi, B. R., Koren, G., and Karma, A. (2018). NCX-mediated subcellular Ca(2+) dynamics underlying early afterdepolarizations in LQT2 cardiomyocytes. *Biophys. J.* 115, 1019–1032. doi: 10.1016/j.bpj.2018.08.004

Zhou, X., Park, K. H., Yamazaki, D., Lin, P. H., Nishi, M., Ma, Z., et al. (2020). TRIC-A channel maintains store calcium handling by interacting with type 2 ryanodine receptor in cardiac muscle. *Circ. Res.* 126, 417–435. doi: 10.1161/circresaha.119.316241

Zhu, Y., Qu, J., He, L., Zhang, F., Zhou, Z., Yang, S., et al. (2019). Calcium in vascular smooth muscle cell elasticity and adhesion: novel insights into the mechanism of action. *Front. Physiol.* 10:852. doi: 10.3389/fphys.2019.00852

Ziaeian, B., and Fonarow, G. C. (2016). Epidemiology and aetiology of heart failure. *Nat. Rev. Cardiol.* 13, 368–378.

Zsebo, K., Yaroshinsky, A., Rudy, J. J., Wagner, K., Greenberg, B., Jessup, M., et al. (2014). Long-term effects of AAV1/SERCA2a gene transfer in patients with severe heart failure: analysis of recurrent cardiovascular events and mortality. *Circ. Res.* 114, 101–108. doi: 10.1161/circresaha.113.302421

Conflict of Interest: The authors declare that the research was conducted in the absence of any commercial or financial relationships that could be construed as a potential conflict of interest.

Copyright © 2020 Njegic, Wilson and Cartwright. This is an open-access article distributed under the terms of the Creative Commons Attribution License (CC BY). The use, distribution or reproduction in other forums is permitted, provided the original author(s) and the copyright owner(s) are credited and that the original publication in this journal is cited, in accordance with accepted academic practice. No use, distribution or reproduction is permitted which does not comply with these terms.

frontiers in Physiology

REVIEW
published: 15 September 2020
doi: 10.3389/fphys.2020.568632

Repurposing Antidiabetic Drugs for Cardiovascular Disease

*Mario Schubert, Sinah Hansen, Julian Leefmann and Kaomei Guan**

Institute of Pharmacology and Toxicology, Technische Universität Dresden, Dresden, Germany

Metabolic diseases and diabetes represent an increasing global challenge for human health care. As associated with a strongly elevated risk of developing atherosclerosis, kidney failure and death from myocardial infarction or stroke, the treatment of diabetes requires a more effective approach than lowering blood glucose levels. This review summarizes the evidence for the cardioprotective benefits induced by antidiabetic agents, including sodium-glucose cotransporter 2 inhibitor (SGLT2i) and glucagon-like peptide-1 receptor agonist (GLP1-RA), along with sometimes conversely discussed effects of dipeptidyl peptidase-4 inhibitor (DPP4i) and metformin in patients with high cardiovascular risk with or without type 2 diabetes. Moreover, the proposed mechanisms of the different drugs are described based on the results of preclinical studies. Recent cardiovascular outcome trials unexpectedly confirmed a beneficial effect of GLP-1RA and SGLT2i in type 2 diabetes patients with high cardiovascular risk and with standard care, which was independent of glycaemic control. These results triggered a plethora of studies to clarify the underlying mechanisms and the relevance of these effects. Taken together, the available data strongly highlight the potential of repurposing the original antidiabetics GLP1-RA and SGLT2i to improve cardiovascular outcome even in non-diabetic patients with cardiovascular diseases.

Keywords: SGLT2 inhibitor, GLP1 receptor agonist, dipeptidyl peptidase-4 inhibitor, metformin, cardiovascular outcome trials, drug repurposing

OPEN ACCESS

Edited by:
Ying Mei Zhang,
Fudan University, China

Reviewed by:
Felipe Ignacio Paredes,
Emory University, United States
Antigone Lazou,
Aristotle University of Thessaloniki, Greece

***Correspondence:**
Kaomei Guan
kaomei.guan@tu-dresden.de

Specialty section:
This article was submitted to Clinical and Translational Physiology, a section of the journal Frontiers in Physiology

Received: *01 June 2020*
Accepted: *25 August 2020*
Published: *15 September 2020*

Citation:
Schubert M, Hansen S, Leefmann J and Guan K (2020) Repurposing Antidiabetic Drugs for Cardiovascular Disease. Front. Physiol. 11:568632. doi: 10.3389/fphys.2020.568632

INTRODUCTION

With the global health problem of overweight and obesity, the prevalence of type 2 diabetes mellitus (T2D) and cardiovascular disease (CVD) is drastically increasing. Diabetes is a major risk factor for the development of micro- and macrovascular complications, including coronary artery disease (CAD), chronic kidney disease (CKD), blindness and stroke (Cosentino et al., 2020). Each of the three individual cardiovascular risk factors, diabetes, a recent heart attack or stroke, leads to a shortened life expectancy. With a combination of these diseases, life expectancy drops significantly further (Emerging Risk Factors Collaboration et al., 2015). Moreover, the clinical observations over the last decade have emphasized the tight correlation between heart failure (HF) and diabetes, which is revealed by the highly elevated risk (2–5 times) of death from heart disease in diabetic patients and the high prevalence (∼30–40%) of a pre-diabetic or diabetic disease in patients with HF (Cosentino et al., 2020).

HF represents a manifold disease, which is diagnosed based on the ejection fraction (EF), the presence of signs or symptoms such as reduced exercise capability or angina pectoris, structural changes in the heart, or the elevated levels of natriuretic peptides, especially brain natriuretic

peptide (BNP)/N-terminal pro-brain natriuretic peptide (NT-proBNP) (Cosentino et al., 2020). In light of these criteria, HF is classified to HF with reduced (HFrEF), moderately reduced (HFmrEF), or preserved EF (HFpEF). So far, the treatment strategies for HF in diabetic patients are comparable to non-diabetic patients, despite the presence of additional risk factors including development of atherosclerosis and CKD as well as increased bodyweight or hyperglycaemia. Recommended as first-line therapy for HFrEF are angiotensin converting enzyme inhibitors (ACEi) or β-blockers (BB) and, if necessary, mineralocorticoid receptor antagonists (MRA). Alternatively, angiotensin receptor blockers (ARB) or valsartan/sacubitril, an ARB-neprilysin inhibitor (ARNI) combination, can be used in case of ACEi intolerance (Cosentino et al., 2020). However, the application of these drugs in diabetic HF may lead to complications. BB reduce all-cause mortality and hospitalization in HFrEF patients with congestive HF after myocardial infarction (MI), but their long-term use in T2D patients with CAD was associated with increased all-cause mortality, compared to non-diabetic individuals (Tsujimoto et al., 2017, 2018). Furthermore, the combination of BB and diuretics to treat hypertension favors the development/new-onset of T2D (Cosentino et al., 2020). ACEi or ARB treatment may have beneficial effects on the prevention of T2D in HFrEF patients and protect against kidney damage in patients with hypertension. The use of ARNI in T2D patients with HFrEF had a more favorable effect, which was shown to reduce the risk of cardiovascular death and hypertensive HF, and was associated with improved insulin sensitivity and efficient reduction of glycated hemoglobin (HbA1c) levels (Seferovic et al., 2017). In contrast to these proven medical approaches for HFrEF, no specific therapies are available for HFpEF, although overall survival of these patients is comparable to HFrEF (Bhatia et al., 2006). The high prevalence of HFpEF in patients with T2D is reflected in the diagnosis of HF in 161 of 581 T2D patients (age $\geq$ 60) with previously unknown HF. Of these patients, 133 patients (82%) were diagnosed with HFpEF (Boonman-de Winter et al., 2012; Cosentino et al., 2020).

A critical aspect for the development and progression of CVD and HF in diabetes is the lowering of impaired blood glucose levels. In patients with T2D, a HbA1c level outside the target range ($\geq$ 7.0%) was the strongest predictor of stroke and acute MI (Rawshani et al., 2018). Epidemiologic studies have demonstrated that a 1% increase of HbA1c levels leads to a 15–18% increased risk for cardiovascular events in T2D patients (Erqou et al., 2013). Clinical trials were performed to examine intensified glucose-lowering therapy in patients with T2D, but the results revealed either no effect or a tendency to worsen the cardiovascular outcome (Erqou et al., 2013). Until 2008, the requirements for diabetes medication were limited to the effectiveness in lowering HbA1c levels and short-term safety in patients (Harrington et al., 2018). However, the signs of adverse cardiovascular events associated with the use of thiazolidinediones, for example, rosiglitazone, led to the initiation of specifically designed cardiovascular outcome trials (CVOTs) (Home et al., 2009; Harrington et al., 2018). The completed CVOTs have evaluated the cardiovascular safety of dipeptidyl-peptidase 4 inhibitors (DPP4i), glucagon-like peptide-1 receptor agonists (GLP1-RA) and sodium-glucose transporter 2 inhibitors (SGLT2i) in T2D patients at risk for HF. Importantly, these drugs were evaluated in patients already receiving standard care with proven benefit for cardiovascular outcome including statins, ACEi, ARB, BB, and glucose-lowering medication such as metformin (**Table 1**). The Food and Drug Administration (FDA) pretended a maximal hazard ratio (HR) of 1.3 (upper 95% confidence interval, CI) for T2D medications as the primary outcome of three-point major adverse cardiovascular events (3P-MACE), a composite of cardiovascular death, non-fatal MI, and non-fatal stroke (Home et al., 2009).

In this review, we summarize the results from clinical studies evaluating the cardioprotective potential of glucose-lowering drugs including metformin, DPP4i, GLP1-RA, and SGLT2i. While broad evidences confirm the safety of glucose-lowering agents from these classes except saxagliptin, several clinical trials strongly indicate drug-specific, beneficial effects of SGLT2i and GLP1-RA on cardiovascular outcome in T2D patients with high cardiovascular risk. Recently reported benefits in non-diabetic patients with cardiovascular diseases further suggest the repurposing of these drugs to improve cardiovascular outcome in non-diabetic patients (**Table 2**). These findings are highly relevant for everyday clinical practice, considering the prevalence of CVD in diabetic patients and the need for specific therapies for the majority of patients with HFpEF. The clinical data further point toward different cardioprotective mechanisms of SGLT2i and GLP1-RA but leave many questions unanswered. Here, we discuss different hypotheses and potential mechanisms for cardioprotection based on the results from experimental studies, which provide the evidence for direct drug effects on the heart independent of glucose management and not restricted to patients with T2D.

METFORMIN IN CARDIOVASCULAR DISEASE

Metformin was introduced into the pharmaceutical market in 1995 and belongs to the biguanide class, of which several compounds were retracted from the market because of the severe side effect lactic acidosis (Harrington et al., 2018). The FDA classified HF as a contraindication to metformin therapy up to 2006, which stands against broad evidence from clinical trials (Eurich et al., 2013; Retwinski et al., 2018). Today, a broad evidence has proven the beneficial effect of metformin as a gold standard for the therapy of T2D, due to its good tolerability, weight-lowering effect and low risk of hypoglycaemia (Apovian et al., 2019; Han et al., 2019). Different studies revealed that lactic acidosis is barely occurring with metformin (reviewed in Misbin, 2004).

The antidiabetic mechanism of metformin is dependent on the inhibition of gluconeogenesis and glucose output in the liver (Foretz et al., 2019). Recent studies demonstrated that the increased release of glucagon-like peptide-1 (GLP1) from enterocytes and enteroendocrine cells in the intestine

TABLE 1 | Cardiovascular outcomes of randomized multicentre clinical trials in T2D patients.

Study	Patient no/follow up	Patient history	Comparison	Parameter	HR (95% CI)
Metformin					
UKPDS34 (UKPDS Group, 1998; Holman et al., 2008)	753/10.7 years	T2D, no HF or MI	Metformin vs. diet	T2D-EP*	0.68 (0.53–0.87)
				All-cause mortality	0.64 (0.45–0.91)
				MI	0.61 (0.41–0.89)
			Intensive therapy# vs. diet	T2D-EP*	0.93 (0.77–1.12)
				All-cause mortality	0.92 (0.71–1.18)
				MI	0.79 (0.60–1.05)
SAVOR TIMI 53 (Bergmark et al., 2019): *Post hoc* analysis	12,156/2.1 years	T2D, CVD HF history (21% metformin vs. 11% non-metformin)	Metformin vs. never taken metformin	All-cause mortality	0.75 (0.59–0.95)
				3P-MACE	0.92 (0.76–1.11)
				CV death	0.68 (0.51–0.91)
				MI	1.23 (0.92–1.65)
	2447 pairs of patients§ /2.1 years	T2D, CVD HF history (16% both groups)	Metformin vs. never taken metformin	All-cause mortality	0.73 (0.59–0.91)
				3P-MACE	0.92 (0.78–1.10)
				CV death	0.77 (0.59–0.99)
				MI	1.24 (0.95–1.62)
GLP1 receptor agonists					
LEADER (Marso et al., 2016b)	9,340/3.8 years	T2D, CVD (81%) HF history (18%)	Liraglutide vs. placebo	All-cause mortality	0.85 (0.74–0.97)
				3P-MACE	0.87 (0.78–0.97)
				CV death	0.78 (0.66–0.93)
				MI	0.86 (0.73–1.00)
				HHF	0.87 (0.73–1.05)
SUSTAIN-6 (Marso et al., 2016a)	3,297/2 years	T2D, CVD (83%) HF history (24%)	Semaglutide (subcutaneous) vs. placebo	All-cause mortality	1.05 (0.74–1.50)
				3P-MACE	0.74 (0.58–0.95)
				CV death	0.98 (0.65–0.93)
				MI	0.81 (0.57–1.16)
				HHF	1.11 (0.77–1.61)
PIONEER 6 (Husain et al., 2019)	3,183/1.3 years	T2D, CVD (85%) HF history (12%)	Semaglutide (oral) vs. placebo	All-cause mortality	0.51 (0.31–0.84)
				3P-MACE	0.79 (0.57–1.11)
				CV death	0.49 (0.27–0.92)
				MI	1.18 (0.73–1.90)
				HHF	0.86 (0.48–1.44)
Harmony Outcomes (Hernandez et al., 2018)	9,463/1.5 years	T2D, CVD (100%) HF history (20%)	Albiglutide vs. placebo	All-cause mortality	0.95 (0.79–1.16)
				3P-MACE	0.78 (0.68–0.90)
				CV death	0.93 (0.73–1.19)
				MI	0.75 (0.61–0.90)
				HHF	0.71 (0.53–0.94)
REWIND (Gerstein et al., 2019)	9,901/5.4 years	T2D, CVD (31%) HF history (9%)	Dulaglutide vs. placebo	All-cause mortality	0.90 (0.80–1.01)
				3-P MACE	0.88 (0.79–0.99)
				CV death	0.91 (0.78–1.06)
				MI	0.96 (0.79–1.15)
				HHF	0.93 (0.77–1.12)
EXSCEL (Holman et al., 2017)	14,752/3.2 years	T2D, CVD (73%) HF history (16%)	Exenatide vs. placebo	All-cause mortality	0.86 (0.77–0.97)
				3P-MACE	0.91 (0.83–1.00)
				CV death	0.88 (0.76–1.02)
				MI	0.97 (0.85–1.10)
				HHF	0.94 (0.78–1.13)
Elixa (Pfeffer et al., 2015)	6,068/2 years	T2D, CVD (100%) HF history (22%)	Lixisenatide vs. placebo	All-cause mortality	0.94 (0.78–1.13)
				3P-MACE	1.02 (0.89–1.17)
				CV death	0.98 (0.78–1.22)
				MI	1.03 (0.87–1.22)
				HHF	0.96 (0.75–1.23)
DPP4 inhibitors					
Carmelina (Rosenstock et al., 2019)	6,979/2.2 years	T2D, CVD (57%)	Linagliptin vs. placebo	All-cause mortality	0.98 (0.84–1.13)
				3P-MACE	1.02 (0.89–1.17)
				CV death	0.96 (0.81–1.14)
				MI	1.12 (0.90–1.40)
				HHF	0.90 (0.74–1.08)

(Continued)

TABLE 1 | Continued

Study	Patient no/follow up	Patient history	Comparison	Parameter	HR (95% CI)
Tecos (Green et al., 2015)	14,671/3.0 years	T2D, CVD (100%)	Sitagliptin vs. placebo	All-cause mortality	1.01 (0.90–1.14)
				3P-MACE	0.99 (0.89–1.11)
				CV death	1.03 (0.89–1.19)
				MI	0.95 (0.81–1.11)
				HHF	1.00 (0.83–1.20)
Savor timi 53 (Scirica et al., 2013)	16,492/2.1 years	T2D, CVD (78%)	Saxagliptin vs. placebo	All-cause mortality	1.11 (0.96–1.27)
				3P-MACE	1.00 (0.89–1.12)
				CV death	1.03 (0.87–1.22)
				MI	0.95 (0.80–1.12)
				HHF	1.27 (1.07–1.51)
Examine (White et al., 2013; Zannad et al., 2015)	5,380/1.5 years	T2D, CVD (100%), acute coronary event within 15-90 days	Alogliptin vs. placebo	All-cause mortality	0.80 (0.62–1.03)
				3P-MACE	0.96 ($\leq$ 1.16)
				CV death	0.85 (0.66–1.10)
				MI	1.10 (0.88–1.37)
				HHF	1.19 (0.90–1.58)
SGLT2 inhibitors					
Empareg-outcome (Zinman et al., 2015)	7,020/3.1 years	T2D, CVD (100%), HF (10%)	Empagliflozin vs. placebo	All-cause mortality	0.68 (0.57–0.82)
				3P-MACE	0.86 (0.74–0.99)
				CV death	0.62 (0.49–0.77)
				MI	0.87 (0.70–1.09)
				HHF	0.65 (0.50–0.85)
Canvas (Neal et al., 2017)	10,142/3.6 years	T2D, CVD (66%), HF (14%)	Canagliflozin vs. placebo	All-cause mortality	0.87 (0.74–1.01)
				3P-MACE	0.86 (0.75–0.97)
				CV death	0.87 (0.72–1.06)
				MI	0.89 (0.73–1.09)
				HHF	0.67 (0.52–0.87)
Declare-timi 58 (Wiviott et al., 2019)	17,160/4.2 years	T2D, CVD (41%), HF (10%)	Dapagliflozin vs. placebo	All-cause mortality	0.93 (0.82–1.04)
				3P-MACE	0.93 (0.84–1.03)
				CV death	0.98 (0.82–1.17)
				MI	0.89 (0.77–1.01)
				HHF	0.73 (0.61–0.88)
Credence (Perkovic et al., 2019)	4,401/2.6 years	T2D, CKD (GFR 30 to $\leq$ 90 mL/min per 1.73 m^2)	Canagliflozin vs. placebo	All-cause mortality	0.83 (0.68–1.02)
				3P-MACE	0.80 (0.67–0.90)
				CV death	0.78 (0.61–1.00)
				HHF	0.61 (0.47–0.80)

**T2D endpoint (T2D-EP, diabetes related endpoint): sudden death, death from hypo- or hyperglycaemia, fatal or nonfatal myocardial infarction, angina, heart failure, stroke, renal failure, amputation, vitreous hemorrhage, retinopathy requiring photocoagulation, blindness in one eye, or cataract extraction. #Intensive therapy: therapy with chloropropamide, glibenclamide, insulin. §Propensity matched patients (2,447 patients with metformin vs. 2,447 patients never taken metformin). 3P-MACE, 3-point major adverse cardiovascular events; CI, confidence interval; CKD, chronic kidney disease; CV death, cardiovascular death; CVD, cardiovascular disease; HHF, hospitalization for heart failure; HF, heart failure; HR, hazard ratio; MI, myocardial infarction; T2D, type 2 diabetes mellitus.*

is an important mechanism for the glucose-lowering effect of metformin (Glossmann and Lutz, 2019). An immunometabolism-based beneficial effect of metformin may also contribute to the improved outcome in non-diabetic HF patients (Rena and Lang, 2018). Apart from its effect on diabetes and the heart, metformin treatment was shown to extend the lifespan in mice, highlighting a potential anti-aging effect of the drug (Martin-Montalvo et al., 2013). However, this effect was not found in other species (Glossmann and Lutz, 2019). Further results for a potential anti-aging effect of metformin may be expected from the Targeting Aging with Metformin (TAME) trial, which specifically investigates the effect of metformin on the onset of aging-related diseases (MI, congestive HF, stroke, cancer, dementia, death), however, the trial was not yet listed in ClinicalTrials.gov as of May 2020.

Cardiovascular Outcome of Metformin in Patients With Diabetes

The UKPDS34 trial represents the most important study for the clinical efficacy of metformin, which enrolled overweight (body mass index, BMI $\geq$ 25 kg/m^2) patients with newly diagnosed T2D for conventional diet change and therapy with metformin or other intensive glucose-lowering medications (UKPDS Group, 1998). Patients with a recent MI, HF or angina pectoris were excluded. The trial revealed a 36% reduced rate of all-cause mortality and 39% lower incidence of MI in

TABLE 2 | Cardiovascular outcomes in patients without T2D.

Study	Patient no/follow up	Patient history	Comparison	Parameter	Outcome difference (95% CI)
Metformin					
Met-remodel (Mohan et al., 2019)	68/12 months	LVH, CAD with insulin resistance or prediabetes	Metformin (12 months) vs. placebo	LVEF (%)	−0.21 (−4.30–3.88)
				LV mass (g)	−4.4 (−7.4 to −1.4)
				NT-proBNP (pg/mL)	305 (−273 to 884)
Camera (Preiss et al., 2014)	173/1.5 years	CAD	Metformin (1.5 years) vs. placebo	cIMT progression (mm/year)	0.007 (−0.006 to 0.020)
GIPS-III RCT (Lexis et al., 2014; Hartman et al., 2017)	379/2 years	STEMI, primary PCI	Metformin (4 months) vs. placebo	LVEF (%)	−1.71 (−3.73 to 0.31)
				NT-proBNP	No change
				MACE (HR)	1.84 (0.68–4.97)
MetCAB (El Messaoudi et al., 2015)	111/24 h	CABG surgery	Metformin (3 days before surgery) vs. placebo	Troponin I (%)	12.3 (−12.4 to 44.1)
				Arrhythmia	No change
				Days in Intensive Care Unit	No change
GLP1-RA					
NCT02001363 (Chen et al., 2015; Huang et al., 2017)	92/3 months	STEMI, T2D: 20% in liraglutide, 16% in control	Liraglutide, 30 min before PCI, total 7 days	LVEF (WMD, %)	4.60 (0.84–8.36)
				MACE* (HR)	0.52 (0.21–1.27)
				Infarct size (% LV)	−6.20 (−9.81 to −2.59)
NCT02001363 (Chen et al., 2016b; Huang et al., 2017)	90/3 months	NSTEMI, T2D: 20% in liraglutide, 28% in control	Liraglutide 7 days prior PCI vs. placebo	LVEF (WMD, %)	5.10 (2.58–7.62)
				MACE* (HR)	0.56 (0.20–1.53)
Kyhl et al. (Kyhl et al., 2016; Huang et al., 2017)	334/5.2 years	STEMI 7–11% diabetes	Exenatide i.v. injection	LVEF (WMD, %)	0.00 (−2.42 to 2.42)
				MACE* (HR)	0.89 (0.61–1.28)
NCT01254123 (Roos et al., 2016; Huang et al., 2017)	91/4 months	STEMI	Exenatide 30 min before PCI, followed by 20μg/day for 3 days	LVEF (WMD, %)	−1.20 (−4.74 to 2.34)
				MACE* (HR)	1.17 (0.17–7.93)
				Infarct size (% LV)	−1.80 (−5.79 to 2.19)
Live (Jorsal et al., 2017)	241 total, 167 w/o T2D/24 weeks	HFrEF LVEF ≤ 45%	Liraglutide (24 weeks) vs. placebo	LVEF (%)	−0.80 (−2.1 to 0.5)
				NT-proBNP (pg/mL)	−140 (−317 to 37)
Fight (Margulies et al., 2016)	300 total, 41% w/o T2D/180 days	HFrEF LVEF ≤ 40%, HHF in last 14 days	Liraglutide (180 days) vs. placebo	CV death (HR)	1.10 (0.57–2.14)
				HHF (HR)	1.30 (0.89–1.88)
				LVEF (%)	−0.1 (−2.3 to 2.1)
SGLT2 inhibitors					
DAPA-HF (McMurray et al., 2019)	2,605 w/o T2D of 4,744 total	HFrEF: LVEF ≤ 40%, NYHA class II-IV, NT-proBNP ≥ 600 pg/mL (≥400 pg/mL with prev. HHF)	Dapagliflozin vs. placebo	Prim. outcome# no T2D (HR)	0.73 (0.60–0.88)
				Prim. outcome# total (HR)	0.74 (0.65–0.85)
				CV death (HR)	0.82 (0.69–0.98)
				HHF (HR)	0.70 (0.59–0.83)

**MACE defined as death due to all causes, cardiac death, heart failure, re-myocardial infarction, repeated revascularization, and stroke. #Primary outcome: composite of worsening heart failure (hospitalization or an urgent visit resulting in intravenous therapy for heart failure) or cardiovascular death. CAD, coronary artery disease, including previous myocardial infarction/unstable angina and/or previous revascularization by either percutaneous coronary intervention (PCI) or coronary artery bypass graft (CABG) surgery; CI, confidence interval; cIMT, carotid intima-media thickness; HFrEF, heart failure with reduced ejection fraction; HHF, hospitalization for heart failure; HR, hazard rate; LV, left ventricular; LVEF, left ventricular ejection fraction; LVH, left ventricular hypertrophy; MACE, major adverse cardiovascular events; NSTEMI, non-ST-elevation myocardial infarction; NT-proBNP, N-terminal pro-brain natriuretic peptide; NYHA, New York Heart Association; STEMI, ST-elevation myocardial infarction; WMD, weighted mean difference.*

patients treated with metformin compared to conventional diet change therapy (**Table 1**). In comparison to other intensive glucose-lowering groups treated with insulin, chlorpropamide or glibenclamide, metformin was superior with respect to diabetes-related endpoints (sudden death, death from hypo- or hyperglycaemia, fatal or non-fatal MI, angina, HF, stroke, renal failure, amputation, vitreous hemorrhage, retinopathy requiring photocoagulation, blindness in one eye, or cataract extraction), all-cause mortality and stroke. In addition, metformin treatment was associated with a lower, but non-significant, risk of MI events compared to other intensive glucose-lowering therapies. The beneficial effects of metformin on diabetes-related endpoints, MI and all-cause death were still present after 10-year follow-up without attempts to maintain the previously assigned therapy (Holman et al., 2008). Notably, no differences in HbA1c were remaining between metformin and other groups after 10-year follow-up. In T2D patients with a history of CAD, treatment with metformin, compared to glipizide, was

associated with lowered re-occurrence of major cardiovascular events (MI, stroke, coronary angioplasty, coronary artery bypass graft, cardiovascular death, and death from any cause) (Hong et al., 2013).

The REMOVAL trial, a double-blind, randomized, placebo-controlled study, investigated the effect of metformin on the reduction of insulin requirements and the progression of CAD in T1D patients (Petrie et al., 2017). The maximal carotid intima-media thickness (cIMT, a correlative parameter for atherosclerosis) was significantly reduced in patients treated with metformin, but only trends toward lower mean cIMT progression and insulin requirements were observed. Metformin treatment for 3 years led to the reduction of bodyweight and LDL cholesterol as well as the increase of the estimated glomerular filtration rate (eGFR) in the patients (Petrie et al., 2017). Lowering of HbA1c was initially observed after 3 months, but no differences were remaining 12 months after treatment (Petrie et al., 2017). These findings indicate a use of metformin to improve CVD risk management in both T1D and T2D, but do not support a beneficial effect on glycaemic control in T1D patients.

A limiting aspect for the evaluation of metformin on cardiovascular outcome in T2D patients represents the reproducibility as well as the number and size of specific clinical trials (Boussageon et al., 2016). Critiques of the UKPDS34 trial include the lack of a double-blind design, and no placebo treatment in the control group. In addition, some meta-analyses could not confirm the cardioprotective effect of metformin in T2D patients, although including data from the UKPDS34 trial (Griffin et al., 2017; Harrington et al., 2018). These uncertainties may have contributed to the relatively high proportion of T2D patients without metformin treatment at baseline (up to 34%) in the CVOTs performed for DPP4i, GLP1-RA, and SGLT2i (**Table 1**). The re-analysis of the CVOT data with respect to metformin would provide randomized, placebo-controlled evidence. In the *post hoc* analysis of the SAVOR TIMI 53 trial (Saxagliptin and Cardiovascular Outcomes in Patients With Type 2 Diabetes Mellitus), patients (n = 12,156) with T2D and high cardiovascular risk were classified as ever versus never taking metformin during the trial period. Metformin use was associated with lower rates of all-cause mortality and cardiovascular death but not lower rates of 3P-MACE (Bergmark et al., 2019). In the propensity score-matched analysis (2,447 pairs of patients), similar results were obtained. This observation was most apparent in patients without prior HF or moderate to severe CKD. Supporting evidence for the beneficial effect of metformin for the treatment of T2D is further provided by comprehensive meta-analyses of 25 studies in addition to the SAVOR TIMI 53 covering data from 815,639 patients, showing a reduction of all-cause mortality by 26% (vs. various comparators including sulfonylureas, SU) (Bergmark et al., 2019). In another meta-analysis including 40 studies with total 1,066,408 patients, a reduction of all-cause mortality by 33% (vs. placebo) was reported (Han et al., 2019). Moreover, Han et al. confirmed that metformin reduced the rate of cardiovascular death (19%) and the incidence of cardiovascular events (17%) compared to non-metformin therapy, and lowered the incidence of cardiovascular events (19%) in comparison to SU monotherapy.

Metformin in Patients Without Diabetes

The already mentioned meta-analysis by Han et al. included the use of metformin in non-diabetic patients, but did not reveal a reduction in cardiovascular events (HR: 0.92; 95% CI: 0.28–3.0; I^2 69%) (Han et al., 2019). Evidence for a positive effect of metformin in a non-diabetic population with CAD is provided by the MET-REMODEL trial. This study evaluated the effect of metformin (2,000 mg daily) on left ventricular (LV) hypertrophy (LVH) in pre- or non-diabetic patients (n = 68) with insulin resistance and CAD, in addition to standard medication (Mohan et al., 2019). Metformin treatment for 12 months led to the reduction in LV mass, bodyweight, subcutaneous adipose tissue, blood pressure and NT-proBNP levels (**Table 2**). Importantly, the reduction in LV mass is unlikely caused by the reduction of blood glucose level (Rajagopalan and Rashid, 2019). However, most studies in non-diabetic patients reported that metformin treatment had no or only moderately lowering effects on HbA1c levels (Lexis et al., 2014; Preiss et al., 2014; Griffin et al., 2018; Mohan et al., 2019).

Notably, some studies investigating the effect of metformin on atherosclerosis in non-diabetic patients show different results. The CAMERA study (n = 173 patients) examined the effect of metformin (1,700 mg daily) over 18 months in patients with CAD and mean BMI < 30 kg/m^2 but without diabetes, who were treated with statins (Preiss et al., 2014). Atherosclerosis progression was measured by cIMT, carotid plaque score, and other surrogate markers of CVD and T2D. The trial confirmed the reduction of bodyweight, waist circumference, body fat, level of insulin and tissue plasminogen activator as well as moderately lowered HbA1c for patients treated with metformin, compared to placebo. However, several surrogate markers of cardiovascular disease, including primary outcome cIMT, and carotid score, and secondary outcome cholesterol levels (HDL, non-HDL), triglycerides, C-reactive protein (CRP), and fasting glucose were not affected by metformin. These data are different from those reported in T2D patients, showing reductions in cIMT and total cholesterol levels by metformin in two previous studies (Katakami et al., 2004; Meaney et al., 2008). In the study by Katakami et al. (2004) these changes appear to be independent of the glucose-lowering effect, as fasting glycaemia was comparable between the group treated with metformin and the control group. The effect might be attributed to the absence of statin treatment in the study population (Lexis and van der Horst, 2014).

The GIPS-III trial evaluated the effect of 4-month metformin (1,000 mg daily) treatment on LVEF in patients without diabetes (n = 380). Treatment was initiated at the time of hospitalization in patients with ST-elevation MI (STEMI), who underwent primary percutaneous coronary intervention (PCI). Metformin had no influence on the LV function, NT-proBNP levels or MACE during the 4-month study period (Lexis et al., 2014) as well as after 2-year follow-up (Hartman et al., 2017). In the MetCAB trial (n = 111 patients), metformin was applied for 3 days before coronary artery bypass surgery in non-diabetic patients (El Messaoudi

et al., 2015). The results revealed that short-term metformin pre-treatment, although safe, did not seem to be an effective strategy to reduce periprocedural myocardial injury.

Taken together, these studies underline the efficacy of standard care for non-diabetic patients. Based on the available data, it appears that further metformin medication may induce a relatively small benefit for cardiovascular outcome in non-diabetic patients. Therefore, further evidence is needed to clarify whether metformin has cardiovascular benefit in non-diabetes patients with high cardiovascular risk. The VA-IMPACT (Investigation of Metformin in Pre-Diabetes on Atherosclerotic Cardiovascular OuTcomes, NCT02915198), a randomized, placebo-controlled and double-blind study with a total of 7,868 pre-diabetic patients with established CAD will expand our knowledge. The completion of the study is expected for 2024.

GLUCAGON-LIKE PEPTIDE-1-MEDIATED CARDIOPROTECTION

During the last years, clinical trials provided strong evidence for a cardioprotective effect of GLP1-RA in T2D patients (**Table 1**). GLP1 is a peptide hormone secreted by the intestine in response to food intake. Through its incretin-like activity, the peptide potentiates insulin secretion while inhibiting glucagon release (Drucker, 2018). GLP1 served as a lead structure for the development of stabilized variants of GLP1-RA to overcome the short plasma half-life of the peptide for therapeutic application (Nauck and Meier, 2019). The effect of GLP1-RA on insulin levels is glucose dependent, which strongly limits the risk of hypoglycaemia (Meloni et al., 2013). In addition, GLP1-RA induce weight loss through the reduction of food intake which is relevant for risk reduction in overweight patients (Drucker, 2018). Liraglutide, a GLP1-RA, has been approved for treatment of T2D in 2009 by the European Medicines Agency (EMA), and in 2010 by the FDA and for the treatment of obesity in 2014 (FDA) and 2015 (EMA) (Iepsen et al., 2015). Liraglutide requires daily injection, whereas prolonged half-life and once-weekly dosing was achieved for newer analogs albiglutide, dulaglutide, and semaglutide. Semaglutide is further available as an orally-available formulation (Jensen et al., 2017). In all GLP1-RA CVOTs, the cardiovascular safety was confirmed, and positive outcomes were observed based on the reduction in either 3P-MACE, cardiovascular mortality, or all-cause mortality, albeit to varying degrees for different GLP1-RA (**Table 1**).

Effect of GLP1-RA on Cardiovascular Events in Patients With T2D

Seven CVOTs were performed for the GLP1-RA liraglutide (LEADER; Marso et al., 2016b), semaglutide (SUSTAIN-6; Marso et al., 2016a, PIONEER 6; Husain et al., 2019), albiglutide (Harmony Outcomes; Hernandez et al., 2018), dulaglutide (REWIND; Gerstein et al., 2019), lixisenatide (ELIXA; Pfeffer et al., 2015), and exenatide (EXSCEL; Holman et al., 2017; **Table 1**). A comprehensive meta-analysis integrating the data from all trials was performed by Kristensen et al. (2019), covering a total number of 56,004 patients. The analysis underlined the positive effect of GLP1-RA on cardiovascular outcome by a 12% reduction in all-cause mortality and cardiovascular death, a reduction in hospitalization due to heart failure (HHF) by 9% as well as a 16% reduction in fatal/non-fatal stroke.

Liraglutide is the first GLP1-RA showing a significant reduction in all-cause mortality (15%) and cardiovascular mortality (22%) in the LEADER trial. The LEADER trial is a randomized, placebo-controlled, double-blind study with 9,340 T2D patients, of which 81% had established CVD. The cardioprotective effect of liraglutide in T2D patients compared to all comparator groups with respect to MACE, acute MI, all-cause mortality, and cardiovascular death was proven in a separate meta-analysis including the data from LEADER and six other studies, but with most patients from the LEADER trial (9,340 of 14,608 total patients) (Duan et al., 2019). Notably, subgroup analysis confirmed a significant reduction in MACE with liraglutide versus placebo, but only a beneficial trend versus other comparators (glibenclamide, rosiglitazone, glimepiride, sitagliptin, total 4,170 patients, HR: 0.58; 95% CI: 0.29–1.16; $P = 0.122$).

A major challenge of most GLP1-RA in clinical practice is their need for subcutaneous application, an issue that has been addressed with the development of oral semaglutide. The placebo-controlled trials of oral semaglutide (PIONEER 6) and subcutaneous semaglutide (SUSTAIN-6) revealed that subcutaneous semaglutide induced a greater reduction of 3P-MACE incidence, whereas the oral form led to remarkably stronger reduction in cardiovascular death (Marso et al., 2016a; Husain et al., 2019; Kristensen et al., 2019). Harmony Outcomes and REWIND investigated the effects of albiglutide and dulaglutide, respectively, and reported the reduction of 3P-MACE incidence consistent with the benefits of liraglutide and subcutaneous semaglutide (Hernandez et al., 2018; Gerstein et al., 2019).

In the EXCSEL trial assessing the cardiovascular outcome of exenatide long-acting release, 14,752 patients (73% of enrolled patients had previous CVD) were followed for a median of 3.2 years. Exenatide treatment was associated with a nominally lower rate of 3P-MACE (HR: 0.91; 95% CI: 0.83–1.00; P = 0.06), cardiovascular death (HR: 0.88; 95% CI: 0.76–1.02; P = 0.096), and all-cause mortality (HR: 0.86; 95% CI: 0.77–0.97; $P = 0.016$) (Holman et al., 2017). A meta-analysis of 16 trials comparing the outcome of exenatide to placebo or other active comparators (different DPP4i, other GLP1-RA or insulin) including the data of EXCSEL (total of 22,003 patients) revealed no significant difference in the rate of cardiovascular events between the groups (Bonora et al., 2019). However, separate analysis of the data excluding the EXCSEL study revealed a non-significant trend toward lower rate of cardiovascular events (HR: 0.80; 95% CI: 0.40–1.63) and all-cause mortality (HR: 0.75; 95% CI: 0.30–1.84).

It is worthy to mention that differences in the results were observed among trials of different GLP1-RA. A stronger cardiovascular benefit was induced by liraglutide, semaglutide, albiglutide and dulaglutide, which are highly homologous with

endogenous human GLP1, compared to the structurally distinct exendin-based agonists exenatide and lixisenatide (**Table 1**; Kristensen et al., 2019). A critical aspect that limits the direct comparability of the data represents also the variation in the study populations as well as drug dosing and kinetics of the different agonists, especially with respect to the short half-time of lixisenatide (Standl, 2019). Moreover, the cardiovascular benefit may be restricted to patients with established CVD, because it could not be shown in a meta-analysis of GLP1-RA trials for patients with multiple risk factors but without established CVD (Zelniker et al., 2019b). Only 73% of patients had established CVD at baseline in the EXCSEL trial whereas 81, 83, and 100% of the population in LEADER, SUSTAIN-6, and Harmony Outcomes, respectively, were in secondary prevention. Based on the slight, non-significant risk reduction of 5% for 3P-MACE in T2D patients at cardiovascular risk without former event, the preventive value of GLP1-RA is discussed for this group of patients (Kristensen et al., 2019). Head-to-head trials comparing the drugs in the same study population directly are required to clarify these differences (Drucker, 2018).

Some results obtained in the recent CVOTs provide the evidence that the reductions in HbA1c, blood pressure and bodyweight alone are not sufficient to explain the cardiovascular effects of GLP1-RA (Drucker, 2018). Especially, whereas no major difference in blood pressure, bodyweight, or renal function between the albiglutide and placebo groups was observed over time in the Harmony Outcomes trial, albiglutide was superior to placebo with respect to 3P-MACE and the risk of atherothrombotic events in T2D patients with high cardiovascular risk (Zweck and Roden, 2019). Hypotheses for the cardioprotective activity of GLP1-RA include an anti-inflammatory pathway, the decrease of blood sugar and lipids as well as prevention of hypertension or reduced atherosclerosis (Reed et al., 2018).

Cardiovascular Effect of GLP1-RA in Patients Without T2D

Although GLP1-RA are cardioprotective in patients with T2D and high cardiovascular risk, recent studies showed that GLP1 levels were increased in patients with acute MI and were correlated with an adverse outcome and early events (Kahles et al., 2020). Different trials investigated the potential of liraglutide (Chen et al., 2015, 2016a,b) and exenatide (Kyhl et al., 2016; Roos et al., 2016) as a medication in patients presenting with non-ST-elevation MI (NSTEMI) and STEMI (**Table 2**). A meta-analysis of trials enrolling acute MI patients with PCI (<26% T2D patients) confirmed the reduction in infarct size and improvement in LVEF by treatment with GLP1-RA compared to placebo (Huang et al., 2017). A non-significant trend towards lower rates of MACE (HR: 0.72; 95% CI: 0.58–1.06) was found for GLP1-RA treatment. Interestingly, the improvement of LVEF and the reduction in MACE was consistently observed in patients treated with liraglutide, but absent or much less evident in trials with exenatide. These results point towards a cardioprotective effect of GLP1-RA, especially liraglutide, to improve clinical outcome in patients with acute MI. As seen in the CVOTs, the findings for an application of GLP1-RA in T2D patients with acute MI seem to vary between different agonists.

Two smaller trials testing liraglutide in patients with LVEF < 45% with and without T2D did not reveal a benefit on cardiovascular events, although a reduction of bodyweight and improved glycaemic control was observed (Margulies et al., 2016; Jorsal et al., 2017). Notably, both studies reported an increased rate of serious cardiac adverse events in the group treated with liraglutide. This may be due to increased blood pressure and heart rate reported in different studies after injection of GLP1-RA (Drucker, 2018; Standl, 2019). Based on these findings, the use of GLP1-RA is contraindicated in patients with chronic HF.

DPP4 INHIBITORS (GLIPTINS) IN CARDIOVASCULAR DISEASE

DPP4i represent a class of antidiabetics, which are frequently used in combination with metformin to improve glycaemic control in T2D patients. DPP4 is an abundantly expressed transmembrane-spanning exopeptidase. The antidiabetic activity of DPP4i has been attributed to the role of DPP4 in the cleavage and thus the inactivation of the incretins GLP1 and GIP. However, the physiological consequences of DPP4 inhibition are very complex. DPP4 is involved in the cleavage of a variety of peptides including incretins, cytokines, growth factors and neuropeptides. Thereby, the enzyme affects multiple processes in different tissue, which are involved in sympathetic activation, inflammatory processes and regulation of the immune system (Makrilakis, 2019). In addition, DPP4 also exists in a cleaved, soluble form (sDPP4) (Makrilakis, 2019). The activity of circulating sDPP4 was shown to correlate with poor cardiovascular outcome and reduced LVEF in HF patients and animal models, suggesting a protective effect and an improved cardiovascular outcome of DPP4 inhibition (dos Santos et al., 2013).

Effect of DPP4i on Cardiovascular Outcome in Patients With T2D

All clinical studies carried out with DPP4i confirmed the cardiovascular safety of the substances sitagliptin (Green et al., 2015), alogliptin (White et al., 2013; Zannad et al., 2015), linagliptin (Rosenstock et al., 2019), and saxagliptin (Scirica et al., 2013), however, the drugs showed only a neutral effect with regard to cardiovascular risk in T2D patients with a history of CVD (**Table 1**). The results of CARMELINA and TECOS did not show beneficial effects of linagliptin and sitagliptin on cardiovascular outcome for the treatment of T2D patients with increased risk for cardiovascular events (Green et al., 2015; Rosenstock et al., 2019). Conflicting results were observed for the DPP4i saxagliptin. In the SAVOR trial, saxagliptin had also no effect on the 3P-MACE although the treatment improved glycaemic control (lower fasting glucose and HbA1c levels) (Scirica et al., 2013). Notably, the rate of HHF was increased in patients treated with saxagliptin. Adverse events were occurring directly after initiation of the treatment, persisted at 12 months and were most pronounced in patients with impaired kidney

function (eGFR < 60 mL/min per1.73 m^2), prior HF, and elevated baseline levels of NT-proBNP (Scirica et al., 2014). These results suggest the contraindication of saxagliptin for patients with high risk.

The EXAMINE trial investigated the effect of alogliptin in T2D patients after acute coronary disease, MI or unstable angina hospitalization within the previous 15–90 days and reported no effect of alogliptin on 3P-MACE (White et al., 2013). A *post hoc* analysis assessed HHF in the EXAMINE trial, in which about 60% of the patients at baseline had a history of HF before the acute coronary syndrome event. Patients with a history of HF at baseline had higher baseline BNP concentrations and lower eGFR values than patients without a HF history (Zannad et al., 2015). The risk of 3P-MACE and HHF was similar for alogliptin and placebo in the whole cohort (White et al., 2013; Zannad et al., 2015). Subgroup analysis showed that alogliptin did not lead to more new HHF or worse outcome for existing HF in patients with the comorbidity of HF. In those patients without a HF history, a slightly increased risk of cardiovascular death and HHF was observed in the alogliptin group. Further analysis based on the BNP levels revealed that the increased HHF rate by alogliptin was observed in the quartile of patients with highest BNP levels (>173.8 pg/mL), importantly, the rate of cardiovascular death was reduced in these patients, suggesting the influence of possible mortality bias. Based on all available data, alogliptin is not associated with increased risk of HF outcomes in T2D patients with recent acute coronary events.

Seen in the broad context of all clinical trials of linagliptin, alogliptin, and sitagliptin, the increased HHF observed with saxagliptin in the SAVOR TIMI 53 trial is likely a compound-specific, rather than a general class effect (Home, 2019). Conclusions about the class-specific effects of DPP4i should be done carefully, due to the structural variations of different DPP4i and the resulting differences in the selectivity toward DPP8 and DPP9 (Riche and Davis, 2015). These differences may lead to altered adverse effect profiles which must be considered for each chemical entity.

Application of DPP4i in Patients Without Diabetes

Based on their mechanism of action and the influence of DPP4 inhibition on a variety of different peptide hormones, the class of DPP4i could be expected to affect the metabolism of patients similar to GLP1-RA independently of the presence of diabetes. However, evidence of the effect of DPP4i in non-diabetic patients is rare, and to our best knowledge, no reports have been published on the cardiovascular outcome of DPP4i in patients without diabetes.

Single studies confirmed the reduction of postprandial triglyceride-rich lipoprotein (TRL) apoB48 levels and increased levels of GLP1 in healthy individuals after a single dose of sitagliptin (Xiao et al., 2014). Levels of hepatic apoB100, plasma triglyceride, blood glucose and insulin were not significantly altered. Notably, sitagliptin treatment of T2D patients for 6 weeks led to reduced postprandial plasma levels of apoB100, apoB48, triglyceride, VLDL and glucose (Tremblay et al., 2011). Based on the cleavage of BNP by DPP4, it has been speculated that DPP4i may be beneficial for HF associated with increased pressure load by improving vasodilation and protective cardiac cGMP signaling of BNP (Lambeir et al., 2008). However, in the context of the CVOT results in T2D patients, these expectations were not met as no benefit of DPP4i was observed in addition to standard care (**Table 1**).

SGLT2 INHIBITORS (GLIFLOZINS) IN CARDIOVASCULAR DISEASE

Different SGLT2 inhibitors including canagliflozin, dapagliflozin, empagliflozin, and ertugliflozin are approved for the therapy of T2D and have been recently evaluated for their cardiovascular risk profile in clinical trials (Zinman et al., 2015; Neal et al., 2017; Wiviott et al., 2019). SGLT2i act on the renal proximal tube to block the reabsorption of glucose. By this mechanism, the drugs lead to increased urinary glucose excretion, reduced blood glucose levels, and reduction of plasma volume and sodium load (Verma, 2019; Santos-Ferreira et al., 2020). Unexpectedly, SGLT2i induced a 35–40% risk reduction in cardiovascular death in patients already receiving optimal secondary prevention strategies for heart disease (**Table 1**). These findings encouraged the re-evaluation for the recommendation of SGLT2i as a first-line treatment for T2D patients with risk for heart disease. Moreover, new trials and experimental studies were initiated to investigate the efficacy of SGLT2i to treat HF in the absence of diabetes (McMurray et al., 2019) and the mechanisms behind the strong cardioprotective effect.

SGLT2i in Patients With T2D

Different CVOTs including EMPAREG-OUTCOME (Zinman et al., 2015), CANVAS (Neal et al., 2017), and DECLARE-TIMI 58 (Wiviott et al., 2019) have been performed to evaluate the cardiovascular risk of empagliflozin, canagliflozin, and dapagliflozin, respectively, in T2D patients with CVD. In these trials, treatment with SGLT2i was performed on top of standard care therapy and led to a lower rate of all-cause mortality as well as remarkable improvement in the cardiovascular outcome (**Table 1**).

The meta-analysis of all three trials by Zelniker et al. (2019a) (total of 34,322 patients) confirmed an 11% reduction in 3P-MACE for the overall population and a 14% reduction in patients with atherosclerotic cardiovascular disease (ASCVD). The MACE reduction in ASCVD patients was mainly driven by the lowered incidence of cardiovascular death and MI, but not through the reduction of stroke events. Moreover, a 23% reduced rate of the composite of HHF and cardiovascular death was observed in patients treated with SGLT2i independent of the presence of ASCVD. Interestingly, no effect on 3P-MACE was found for canagliflozin (66% of patients had a history of CVD) and dapagliflozin (41% of patients had a history of ASCVD) whereas a significantly lower rate was observed for empagliflozin in EMPAREG-OUTCOME trial (more than 99% of patients had established CVD). These findings strongly support the high efficacy of SGLT2i in T2D patients with

established CVD. The broader entry criteria in DECLARE-TIMI 58 and CANVAS resulted in the inclusion of T2D patients with a history of MI and thus, these trials provide information for the use of SGLT2i as secondary prevention (**Table 1**). Importantly, the beneficial effect of all three SGLT2i on the composite outcome of HHF and cardiovascular death was present in patients with a history of HF, which highlights the potential of SGLT2i as a secondary prevention therapy for heart disease (Zelniker et al., 2019a). Analysis of the cardioprotective effect of dapagliflozin and canagliflozin in relation to heart function revealed that the lowered HHF rates were consistently present for patients with HFpEF or HFrEF, while the benefit on cardiovascular death and all-cause mortality was restricted to HFrEF patients (Figtree et al., 2019; Kato et al., 2019). In addition to clinical trials, data observed from population-based studies confirmed the reduced rates of HHF and all-cause mortality with the SGLT2i therapy compared to other glucose-lowering drugs (reviewed in Santos-Ferreira et al., 2020).

Importantly, the results from EMPAREG-OUTCOME, DECLARE-TIMI 58, and CANVAS further demonstrate the positive effect of SGLT2i on kidney function. Treatment with SGLT2i was associated with a 45% reduction of the progression of renal disease (composite of worsening renal function, end-stage renal disease, and renal death), independent of the presence of ASCVD (Zelniker et al., 2019b). This benefit was observed in patients over a broad range of basal eGFR (60 to $>$ 90 mL/min per 1.73 m^2) but was most pronounced in patients with preserved renal function (eGFR $\geq$ 90 mL/min per 1.73 m^2). The cardiorenal-protective effect of SGLT2i was further highlighted in the CREDENCE trial to assess the renal outcomes of canagliflozin in T2D patients (total 4,401) with albuminuric CKD and GFR of 30 to $<$ 90 mL/min per 1.73 m^2 (Perkovic et al., 2019). This trial revealed a 34% risk reduction (HR 0.66; 95% CI: 0.54–0.86) of the renal-specific composite of end-stage kidney disease, a doubling of the creatinine level, or death from renal causes (Perkovic et al., 2019). In addition, the results of CREDENCE confirmed the cardioprotective effect of canagliflozin by observing a 20% risk reduction of 3P-MACE and 39% reduction of HHF (Perkovic et al., 2019).

These results provide evidence for the SGLT2i use in a broader population of T2D patients, irrespective of ASCVD, kidney disease or HF and as a first-line therapy after metformin in most patients with T2D (Verma et al., 2019). Further trials are ongoing to examine the potential of empagliflozin in T2D patients with HFpEF including EMPERIAL-Preserved (NCT03448406) and EMPEROR-Preserved (NCT03057951). Overall, EMPAREG-OUTCOME, CANVAS, CREDENCE, and DECLARE-TIMI 58 trials, as well as several observation studies of population data confirm the significant cardiovascular benefit of T2D patients from the SGLT2i therapy. Moreover, the positive effect on multiple cardiovascular risk factors in addition to glycaemic control, such as improved kidney function, and reduction in bodyweight as well as systolic and diastolic blood pressure, highlight the great potential of SGLT2i in the therapy of T2D patients at high cardiovascular risk.

SGLT2i in Patients Without T2D

Since glucose levels were comparably managed by standard care in the control and SGLT2i treatment groups in the CVOTs, speculations became evident for a diabetes-independent positive effect. These results encourage investigations for the repurposing of SGLT2i for the treatment of patients with CVD in the absence of diabetes (Petrie, 2019). This issue was addressed in the DAPA-HF trial which enrolled 4,744 patients with HFrEF (LVEF $<$ 40%) already receiving standard care medication including ACEi, ARB, BB, and MRA (McMurray et al., 2019). About half of the patients in the trial had no diabetes. Treatment with dapagliflozin in comparison to placebo led to a 26% risk reduction in the primary outcomes including an unplanned HHF, an intravenous therapy for HF or cardiovascular death. Importantly, this effect was similarly observed for patients with T2D and without diabetes with respective risk reductions of 25 and 27% (McMurray et al., 2019). The data further suggest that dapagliflozin improves the primary outcome in patients taking ARNI at baseline, which is known to be more efficient than RAAS inhibition alone, as shown by reducing the incidence of cardiovascular death and HHF in HF patients. Further trials for empagliflozin were initiated in patients with HFrEF and with or without diabetes, including EMPIRE-HF (NCT03198585) and EMPEROR-Reduced (NCT03057977). Although the data of these trials are required to draw final conclusions, the findings of DAPA-HF indicate a remarkable potential of SGLT2i to improve the efficacy of current HF treatments in non-diabetic patients.

IMPLICATIONS FOR THE CHOICE OF THE ANTIDIABETIC DRUGS

As T2D is strongly associated with increased risk for development of atherosclerosis, CKD, and HF, treatment of T2D requires a more effective approach and should not exclusively be glucose lowering. The data observed in recent clinical trials confirm the great potential of the antidiabetic drugs SGLT2i and GLP1-RA in terms of reducing cardiovascular events and preventing the progression of kidney disease.

GLP1-RA cause substantial bodyweight reduction, blood pressure reduction, and a reduction in atherosclerosis and inflammation. Since these are all prevalent in patients with HFpEF or obesity, GLP1-RA could benefit these groups of patients. The greatest cardiovascular risk reduction of GLP1-RA (liraglutide, semaglutide) was observed in obese patients with BMI $>$ 30 kg/m^2. Some evidences suggest a beneficial effect of the GLP1-RA liraglutide on the clinical outcome in patients with acute MI. Although the data from the LIVE and FIGHT trials of GLP1-RA in HFrEF so far are discouraging, future studies should focus on GLP1-RA in patients with HFpEF. Nephroprotection has been observed in two GLP1-RA (liraglutide and semaglutide) CVOTs, therefore, treatment with GLP1-RA liraglutide and semaglutide is associated with a lower risk of renal endpoints, and should be considered for diabetic patients if eGFR is $>$ 30 mL/min per 1.73 m^2 (Cosentino et al., 2020).

SGLT2i have been proven to be very useful to reduce cardiovascular risk in T2D patients, beside the reduction of bodyweight and blood pressure. The strong benefits of SGLT2i in preventing HF in patients with T2D have been established in the clinical CVOTs, as discussed above. Especially, results obtained with SGLT2i in patients with established HFrEF but without T2D strongly suggest the repurposing of this class of drugs for HF patients without diabetes. New results from the ongoing trials EMPIRE-HF (NCT03198585) and EMPEROR-Reduced (NCT03057977) for empagliflozin in patients with HFrEF with and without diabetes will provide us a wealth of new evidence. Moreover, positive renal outcomes were observed in the CREDENCE trial for canagliflozin in T2D patients with an eGFR of 30–90 mL/min per 1.73 m^2. As the results of ongoing trials evaluating SGLT2i in patients with CKD (DAPA-CKD, EMPA-Kidney) are expected with great interest, the correlation indicated by the common incidence of T2D, HF and CKD may hint to the question whether the improvement in kidney function may play a direct role in cardioprotection. If the beneficial effects of SGLT2i in non-diabetic patients can be confirmed, they may become important for the prevention of HF in patients with established CKD (Herrington et al., 2018).

The combined use of SGLT2i and GLP1-RA to further improve the cardiovascular outcome of patients with high cardiovascular risk has been investigated in several studies. Treatment of obese, non-diabetic patients with exenatide and dapagliflozin for 52 weeks reduced bodyweight, total adipose tissue volume, LDL cholesterol, triglycerides, systolic blood pressure and the proportion of patients with pre-diabetes (Lundkvist et al., 2017). In a trial with T2D patients, the influence of liraglutide-empagliflozin combination therapy was compared to monotherapy with liraglutide, empagliflozin or insulin as add-on to metformin (Ikonomidis et al., 2020). All treatments led to reductions in HbA1c, total cholesterol, LDL cholesterol and triglycerides. The combination of empagliflozin and liraglutide was associated with the most favorable effects on myocardial functional markers (global longitudinal and radial strains, myocardial work index) and metabolic parameters (BMI, endothelial glycocalyx thickness, central systolic blood pressure) (Ikonomidis et al., 2020).

The benefit of short-term (12–30 weeks) SGLT2i/GLP1-RA combination therapy in patients with T2D was further confirmed in a meta-analysis (1,913 patients) of seven trials, which revealed the greater reduction in HbA1c, bodyweight and systolic blood pressure compared to GLP1-RA or SGLT2i therapy (Mantsiou et al., 2020). However, conclusions on cardiovascular outcome and mortality are not available so far due to the rare number of cardiovascular events and the duration of the trials. Long-term data (104 weeks) are only available from the DURATION-8 trial, which confirmed the beneficial effect of dapagliflozin/exenatide treatment on HbA1c, bodyweight and systolic blood pressure (Mantsiou et al., 2020). A limitation is the use of different SGLT2i/GLP1-RA combinations in each of these studies, especially with respect to the different benefits of GLP1-RA observed in the CVOTs (**Table 1**).

These studies underline the potential of the SGLT2i/GLP1-RA combination therapy in patients with high cardiovascular risk. However, whether this is associated with improved cardiovascular outcome in terms of all-cause mortality or incidence of cardiovascular events (3C-MACE, CV death, MI, stroke, HHF) needs to be further investigated.

Although all clinical studies carried out with the DPP4i confirmed their cardiovascular safety, only a neutral effect on the reduction of cardiovascular risk was observed in T2D patients with a history of CVD. A critical question is why no cardioprotective outcomes were observed for DPP4i in clinical trials compared to GLP1-RA although the baseline characteristics of the study populations for GLP1-RA and DPP4i were similar (**Table 1**). Trials included T2D patients with CVD and eGFR in the range of 71–80 mL/min per 1.73 m^2, indicating mildly impaired kidney function (EXAMINE, TECOS, Harmony Outcomes, ELIXA). An important aspect might be the difference in the effectively reached GLP1-RA levels and the duration of agonist availability in both therapies. Treatment with DPP4i leads to modest increase in endogenous GLP1 plasma levels (2–3-folds) although the enzyme activity is up to 90% reduced. In contrast, application of a synthetic GLP1-RA results in a remarkably higher plasma concentration of the GLP1-RA (8–10 folds) and a prolonged effect due to the improved half-life of the peptides (Gallwitz, 2019). It is important to note the large variations in plasma stability of the chemically modified GLP1-RA, which could be a reason for the lack of cardiovascular benefit on MACE or cardiovascular death with the short-acting agonist lixisenatide (3 hour plasma half-life) in the ELIXA trial, in contrast to liraglutide (11–15 h plasma half-life) in the LEADER study (Bolli and Owens, 2014). Furthermore, an altered GLP1 receptor (GLP1R) activation by the chemically modified GLP1-RA in comparison to native GLP1 may affect the outcomes. *In vitro* studies demonstrated an increased receptor residence time of lixisenatide, liraglutide, dulaglutide and semaglutide in comparison to the native GLP1 as well as small changes in receptor downstream signaling (Jones et al., 2018). Apart from degradation of GLP1, other factors could be involved in the DPP4i-induced blood glucose-lowering effect. This is indicated by results showing that DPP4i lead to anti-hyperglycaemic effects even in mice lacking GLP1R, and that GLP1R antagonism only results in partial inhibition of DPP4i effect (Aulinger et al., 2014). These findings may hint toward different outcomes with DPP4i and GLP1-RA due to different mechanisms of action. Therefore, DPP4i may be second-choice medication behind GLP1-RA and SGLT2i. However, the excellent safety profile of DPP4i, mostly applied in combination with further medication such as metformin, sulfonylurea or thiazolidinediones (with the advantage of DPP4i to induce less weight gain), makes this class of drugs an important treatment option in T2D, especially in patients with CKD or metformin intolerance (Makrilakis, 2019). DPP4i can be used in patients with severe renal impairment (eGFR $<$ 30 mL/min per 1.73 m^2), especially, linagliptin and vildagliptin (Russo et al., 2013), when metformin was associated with increased mortality in patients with eGFR $<$ 30 mL/min per 1.73 m^2.

Although clinical trials (**Table 1**) and more recent meta-analyses (Bergmark et al., 2019; Han et al., 2019) provide evidence for a cardioprotective effect of metformin on the

cardiovascular outcome in T2D patients, the available data are less comprehensive compared to DPP4i, GLP1-RA, and SGLT2i (Harrington et al., 2018). The justifiable advantage of metformin is the long experience with the drug in clinical practice, its proven safety and its beneficial influence on a variety of different risk factors in T2D patients, including the reduction of bodyweight, cholesterol levels and all-cause mortality in addition to blood glucose-lowering (Meaney et al., 2008; Herrington et al., 2018). However, due to the exciting CVOT data for GLP1-RA and SGLT2i, metformin as first-line medical therapy for T2D patients with ASCVD is now under review because the evidence of cardiovascular benefit appears weak (Harrington et al., 2018).

MECHANISMS OF CARDIOPROTECTION OF THE ANTIDIABETIC DRUGS

On a molecular level, insulin resistance causes substantial changes in the energy metabolism in cardiomyocytes, leading to the loss of substrate flexibility and increased fatty acid (FA) oxidation (Garcia-Ropero et al., 2019). This is accompanied with lipid accumulation, impaired mitochondrial membrane potential and reduced ATP production (**Figure 1**). These processes not only affect cellular energy levels, but also are accompanied with cardiac fibrosis, myocardial stiffness, inflammation, apoptosis, which finally lead to impaired structural organization and the decrease in heart function (Johnson et al., 2016; Hopf et al., 2018; Peng et al., 2019). Over the years, this comprehensive dysregulation manifests clinically as arrhythmia and HFpEF, which may develop into HFrEF.

Clinical data strongly suggest that SGLT2i and GLP1-RA induce cardioprotection through different mechanisms. This becomes evident by the gradual divergence of the event curves for both drug classes, with a direct risk reduction after initiation of treatment with SGLT2i, whereas GLP1-RA show effects at later time points (Cosentino et al., 2020). The fast incidence of cardioprotection observed for SGLT2i was discussed to be induced by volume reduction, an increase of haematopoiesis and erythropoietin or the occurrence of ketone bodies and resulting switch in cardiac energy metabolism (Garcia-Ropero et al., 2019; Santos-Ferreira et al., 2020). These changes were observed directly with the initiation of the treatment, resulted in a reduced cardiac workload, blood pressure as well as reduced ventricular filling pressures and went in line with the direct onset of cardiovascular benefits (Verma et al., 2019). These recently emphasized cardioprotective effects of antidiabetics lead to the investigation of their mechanisms in different animal models *in vivo* including diabetic, MI and ischemia-reperfusion injury (IRI) models and cardiac cell types *in vitro* (**Table 3**). Whether SGLT2i, GLP1-RA, DPP4i, and metformin, in addition to their blood glucose-lowering mechanisms, act directly on the cells of the heart is still under debate. Animal models for diabetic heart disease include *db/db* mice as well as obesity and diabetes induced by high-fat diet or streptozotocin (STZ)-induced insulin deficiency (**Table 3**). In cellular models, the diabetes-associated metabolic imbalance and insulin resistance is induced by cultivation under high-glucose conditions (> 25 mM) or high FA levels (**Table 3**). The type of animal model or the culture conditions for the modeling of diabetic cardiomyopathy *in vitro* are highly relevant to the results and conclusions. As an example, Ramirez et al. demonstrated the beneficial effect of sitagliptin in diabetic, non-obese, non-hypertonic Goto-Kakizaki (GK) Wistar rats by improving glucose metabolism and downregulation of FA metabolism (Ramirez et al., 2018). The results from the animal studies could be reproduced *in vitro* in cardiomyocytes treated with high-FA medium, but not under high-glucose conditions. Thus, it may be difficult to directly compare the effects observed with different compounds under different experimental conditions. Another limitation, especially for the work with isolated cells from rat or mice, is the short incubation time of 12–24 h, which raises a question whether the short-time cultivations of the cells are suitable to recapitulate a disease phenotype that is established over the time course of 5–10 years.

Many reports for the different classes of antidiabetics highlight the similar cellular effects of metformin, GLP1-RA, DPP4i, and SGLT2i on the heart, which contribute to cardioprotection (**Figure 2**). Treatment with all compounds was associated with reduced fibrosis, arrhythmia and apoptosis, demonstrating a beneficial effect of all these antidiabetics on the heart (**Table 3**). Moreover, application of all four classes lead to reduced infarct size and improved heart function in animal models of MI or IRI even in non-diabetic animals. In line with these findings, a reduction in inflammation and lipid accumulation as well as improved autophagy and glucose uptake have been described for metformin, GLP1-RA, SGLT2i, and DPP4i. On a molecular level, compounds from all four classes have been shown to increase the activity of adenosine monophosphate-activated protein kinase (AMPK), one of the central regulators of cellular metabolism (He et al., 2013; Noyan-Ashraf et al., 2013; Balteau et al., 2014; Ye et al., 2017; Ramirez et al., 2018; Yang et al., 2019). The critical role of this activation step in the beneficial effect of metformin, GLP1-RA and SGLT2i was confirmed in studies using specific AMPK inhibitors (Noyan-Ashraf et al., 2013; Ye et al., 2017; Yang et al., 2019), suggesting that the common activation of AMPK represents a key event for cardioprotection of the compounds and that the cardioprotective effects are at least partly independent of blood glucose lowering. From a clinical perspective, the detailed investigation of the underlying mechanisms may be an important rational basis for the specific combination of antidiabetic classes. For example, it is known that metformin stimulates autophagy via activating AMPK and sirtuin-1 (SIRT1) and by this way, may contribute to the cardioprotective effects seen in experimental models of HF (Gundewar et al., 2009). Recent studies revealed that SGLT2i may exert cardioprotective effects by stimulating autophagy (Levine et al., 2015), which may involve the activation of AMPK and SIRT1 (Packer, 2020). The overlap in the mechanism of action between metformin and SGLT2i may be the reason for the reduced cardioprotective effects of SGLT2i in patients with metformin treatment at baseline, when compared to the non-metformin group (Packer, 2020).

Based on the robust cardioprotective effect of GLP1-RA and SGLT2i in clinical studies, understanding their molecular mechanisms is of particular importance. Common effects

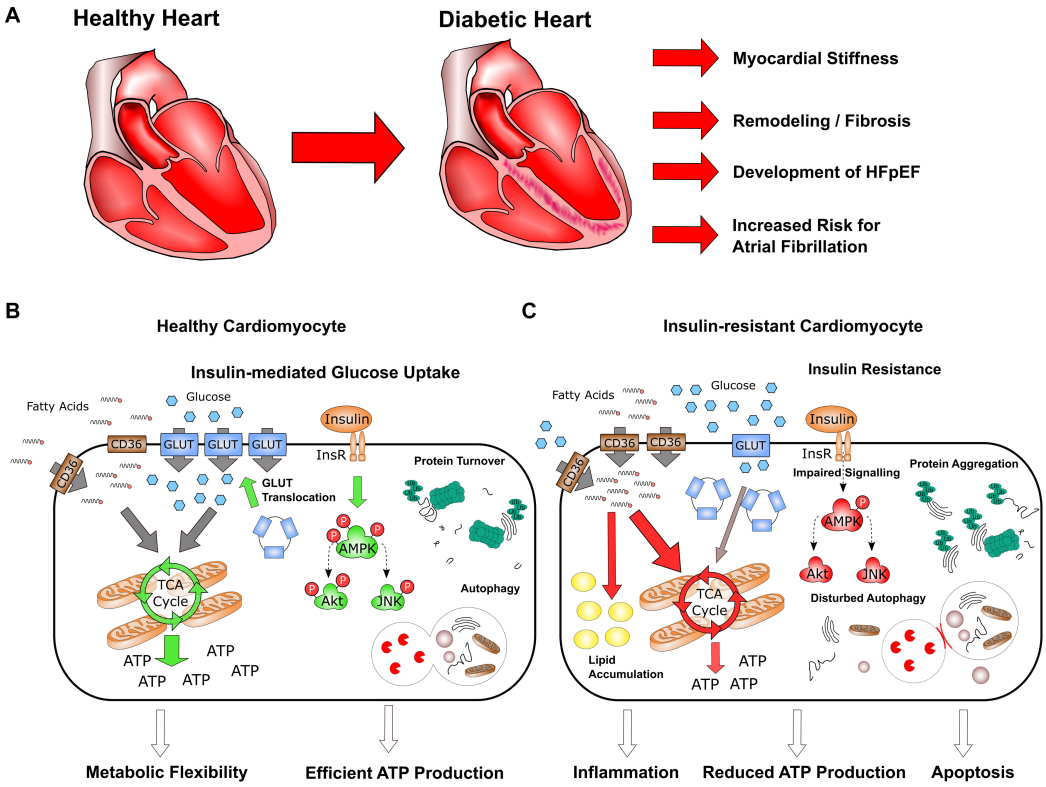

FIGURE 1 | Characteristics of heart failure in diabetes. **(A)** Long-time diabetes is associated with structural remodeling, fibrosis and increased myocardial stiffness in the heart, which lead to the development of HFpEF as well as increased risk for atrial fibrillation. **(B,C)** On the cellular level, insulin-mediated glucose uptake in healthy cardiomyocytes is of key importance for metabolic flexibility and efficient ATP production **(B)**; insulin resistance strongly impairs metabolism and homeostasis in cardiomyocytes, resulting in reduced ATP production and increased inflammation and apoptosis **(C)**.

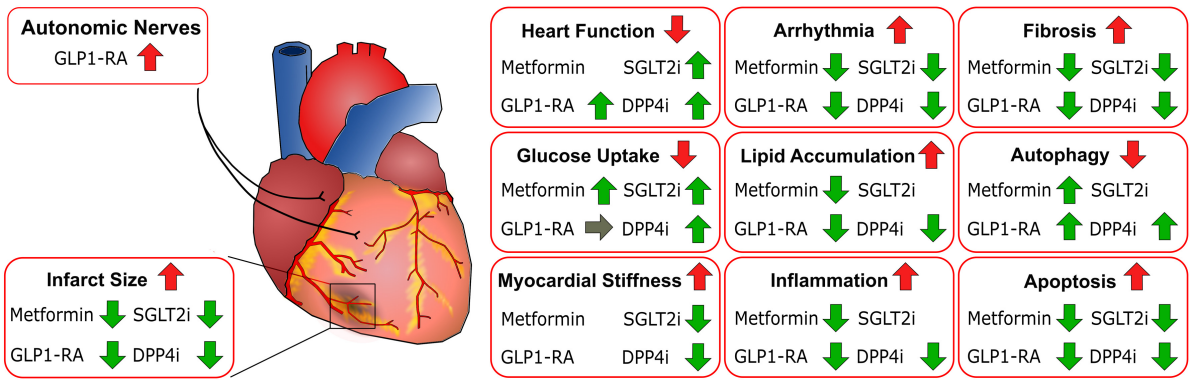

FIGURE 2 | Similar cellular effects of metformin, GLP1-RA, DPP4i, and SGLT2i contributing to cardioprotection. Effects of different drug classes on the heart or cardiac cells in animals and cellular models of diabetes or myocardial infarction. Red arrows indicate the state of the respective aspect under disease conditions. Green arrows indicate the effects observed for treatment.

of GLP1-RA and SGLT2i include the above-mentioned activation of AMPK and reduction of ROS by increased expression of redox-enzymes catalase and superoxide-dismutase SOD2 (Balteau et al., 2014; Andreadou et al., 2017; Mizuno et al., 2018). However, differences between SGLT2i and GLP1-RA are evident in the activation of several downstream signaling pathways. Treatment with SGLT2i led to an activation of STAT3 and reduced levels of IL-6 and inducible NO synthase (iNOS) in the myocardium of mice after ischemia-reperfusion (Andreadou et al., 2017). Furthermore, SGLT2i were shown to improve mitochondrial function, as demonstrated for empagliflozin in mouse MI models (Mizuno

TABLE 3 | Experimental studies to investigate cardioprotective mechanisms of metformin, GLP1-RA, DPP4i, and SGLT2i.

Treatment	Model	Treatment-induced effects	References
Animal models			
Diabetes			
Metformin, 4 months	STZ-induced diabetic mice	Reduced autophagy, apoptosis, and fibrosis Reduced Inflammation, **AMPK activation**	He et al., 2013; Yang et al., 2019
Metformin, 3 months	Diabetic GK rats	Reduced fibrosis, and arrhythmia	Fu et al., 2018
GLP1-RA – liraglutide, 2 months	STZ-induced, HFD Wistar rats	Improved heart function, reduced fibrosis	Ji et al., 2014
GLP1-RA – liraglutide, 1 week	HFD induced obese, insulin resistant mice	Reduced fibrosis, and inflammation, AMPK activation, activation of RISK pathway (Akt, GSK3β,Erk1/2), increased eNOS expression	Noyan-Ashraf et al., 2013
DPP4i – sitagliptin, 3 months	STZ induced, HFD Wistar rats	Improved cardiac function, reduced fibrosis, lipid accumulation, inflammation, apoptosis, and arrhythmia	Liu et al., 2015
DPP4i – sitagliptin, 5 months	Diabetic GK rats	Improved insulin sensitivity, and diastolic function, increased glucose uptake, AMPK activation	Ramirez et al., 2018
SGLT2i – empagliflozin, 2 weeks	*db/db* mice	Increased cardiac ATP production and glucose oxidation, improved cardiac function	Verma et al., 2018
SGLT2i – dapagliflozin	BTBR *ob/ob* mice	Improved cardiac function, reduced inflammation, fibrosis, and apoptosis	Ye et al., 2017
Myocardial infarction/ischemia-reperfusion injury			
Metformin	C57BL/6 mice	Reduced infarct size, improved cardiac output	Calvert et al., 2008
GLP1-RA – liraglutide, 1 week before MI	C57BL/6 mice	Reduced infarct size, improved cardiac output	Noyan-Ashraf et al., 2009
DPP4i – linagliptin, 1 week before MI	C57BL/6J mice, *db/db* mice	Reduced infarct size, inflammation, fibrosis marker, and apoptosis, improved cardiac output	Birnbaum et al., 2019
SGLT2i – dapagliflozin, 4 weeks before IRI	HFD induced pre-diabetic, obese rats	Reduced apoptosis, ROS, arrhythmia susceptibility, improved heart function	Tanajak et al., 2018
SGLT2i – empagliflozin, 6 weeks before IRI	C57BL/6 mice, HFD	Reduced infarct size, STAT3 activation, independent on Akt, eNOS, Erk1/2, GSK3β	Andreadou et al., 2017
Direct cellular/tissue effects			
Metformin, 1 mM	H9c2 cells, high glucose condition	Reduced autophagy, apoptosis, and fibrosis	He et al., 2013
Metformin, 1 μM	H9c2 cells, high glucose condition	Increased glucose uptake, reduced FA uptake	Johnson et al., 2016
GLP1-RA – liraglutide, 100 nM	H9c2 cells, high glucose condition	Reduced ROS, and apoptosis, improved autophagy	Yu et al., 2018
GLP1-RA – GLP1, 25 nM	Neonatal rat CMs, high fatty-acid medium	Reduced lipid accumulation, and apoptosis	Ying et al., 2015
GLP1-RA – GLP1, 100 nM	Isolated rat CMs, high glucose medium	Reduced ROS, no effect on glucose uptake or glycolysis	Balteau et al., 2014
DPP4i – sitagliptin	H9c2 cells, high glucose conditions	Improved autophagy	Zhou et al., 2018
DPP4i – linagliptin	Human CMs and fibroblasts	Reduced inflammasome activation	Birnbaum et al., 2019
SGLT2i – empagliflozin, 0.5–1 μM	Isolated human trabeculae from T2D patients	Reduction of diastolic stiffness, improvement of diastolic function	Pabel et al., 2018
SGLT2i – empagliflozin, 1 μM	Isolated CMs of HF patients	Increased glucose uptake	Mustroph et al., 2019
SGLT2i – dapagliflozin, 0.5 μM	Mouse cardiac fibroblasts, lipopolysaccharide stimulation	Reduced inflammation markers, AMPK activation	Ye et al., 2017

AMPK, adenosine monophosphate-activated protein kinase; CMs, cardiomyocytes; FA, fatty acid; GK, Goto-Kakizaki; HFD, high-fat diet; IRI, ischemia-reperfusion injury; MI, myocardial infarction; ROS, reactive oxygen species; STZ, streptozotocin.

et al., 2018) and by dapagliflozin treatment in pre-diabetic rats after ischemia-reperfusion (Tanajak et al., 2018). The *in vitro* studies showed the prevention of TNFα-induced increases in ROS levels and reductions of NO levels by empagliflozin and dapagliflozin, suggesting an important role of endothelial cells for the cardioprotective effect of SGLT2i (Uthman et al., 2019).

The cardioprotective activity of GLP1-RA may involve activation of the reperfusion injury survival kinase (RISK) pathway, which is characterized by activation of the prosurvival kinases phosphatidylinositol-3-OH kinase (PI3K)-Akt and p42/p44 extracellular signal-regulated kinases (Erk1/2) (Rowlands et al., 2018). Liraglutide has been shown to increase phosphorylation of Akt, GSK3β and Erk1/2 in obese, insulin resistant mice (Noyan-Ashraf et al., 2013). In particular, empagliflozin had no effect on the phosphorylation of Akt, GSK3β, and Erk1/2 after ischemia-reperfusion in mice (Andreadou et al., 2017) or Akt- and Erk1/2-activation in *db/db* mice (Habibi et al., 2017). Further mechanisms for the cardioprotection effect of GLP1-RA include beneficial effects on the pathogenesis of arrhythmias and coronary function by increasing cardiac

connexin-43 and eNOS levels, as demonstrated by liraglutide in high-fat diet (HFD)-induced insulin-resistant mice (Noyan-Ashraf et al., 2013).

The molecular mechanisms by which cardioprotection can be achieved could vary from drug to drug. Several studies demonstrate that treatment with metformin and DPP4i increases glucose uptake and shifts energy production toward glycolysis by inhibition of key players for FA metabolism as, for example, PDK4, PPARG and CPT1 (**Table 3** and **Figure 2**). Limited data are available for the effect of SGLT2i on cardiac metabolism (Mustroph et al., 2018), and GLP1-RA treatment was not associated with increased glucose uptake in cellular models (Balteau et al., 2014). In addition, beneficial effects on myocardial stiffness have been reported for SGLT2i and DPP4i, accompanied by increasing the phosphorylation of titin which is impaired in diabetic patients (Hamdani et al., 2014; Pabel et al., 2018). Interestingly, metformin was shown to increase phosphorylation of titin (Hopf et al., 2018) but it has not been studied whether metformin reduces cardiac stiffness (**Figure 2**). These aspects require further investigation to draw general conclusions. Ideally, compounds of the different classes should be examined in parallel in the same model system.

DIRECT CARDIAC EFFECTS QUESTION THE MOLECULAR TARGET

Experimental studies using isolated cardiac cells or cardiac cell lines provide strong evidence for a direct effect of SGLT2i, GLP1-RA, metformin, and DPP4i on the heart (**Table 3**). Pabel et al. (2018) demonstrated the direct effect of empagliflozin by immediately reducing the passive stiffness of trabeculae isolated from human end-stage HF patients and improving the diastolic function in mice models directly after injection. These results provide a mechanistic aspect for the early improvement of cardiovascular outcomes with SGLT2i in the clinical studies. A general issue of the *in-vitro* studies represents the concentration of the drug in the experiment, which may strongly exceed the present concentrations *in vivo*.

An ongoing debate about the molecular target of the antidiabetics is not only for newer agents SGLT2i and GLP1-RA, but also for DPP4i or the widely used metformin. Several studies failed to detect SGLT2 in different heart cells (Mustroph et al., 2018; Packer, 2020). An off-target effect of SGLT2i on SGLT1 is also questionable based on the high selectivity of the compounds as well as experiments using phlorizin, a dual SGLT1/2 inhibitor, which could not induce the effects observed with dapagliflozin in isolated cardiac fibroblasts (Ye et al., 2017; Pabel et al., 2018). The observation that SGLT2i reduce cytosolic Na^+ and Ca^{2+} levels and inhibit the sodium-hydrogen exchanger (NHE) in mouse cardiomyocytes, which are known to be increased in diabetic cardiomyopathy and HF (Baartscheer et al., 2017; Uthman et al., 2018), suggests that the cardioprotective effect of SGLT2i might be due to the direct inhibition of cardiac NHE flux and the reduction of cytosolic Na^+ and Ca^{2+} levels. Molecular docking studies using a homology model of a bacterial protein structure further suggested a direct binding of SGLT2i to NHE-1 (Uthman et al., 2018). However, this interaction has never been proven using binding assays or site-directed mutagenesis of the putative binding site. Furthermore, reduced bulk cytosolic Ca^{2+} levels by empagliflozin were not observed in human cardiomyocytes (Pabel et al., 2018). Taken together, although a direct effect on the heart has been proven, the molecular target of SGLT2i has not been identified. Off-target effects on SGLT1 and direct binding of SGLT2i to NHE-1 are questionable but the regulation of Na^+, H^+, and Ca^{2+} in cardiomyocytes and in specific microdomains may contribute to cardioprotective effects of SGLT2i (Pabel et al., 2018). Of note, the increase in haematocrit and levels of erythropoietin through treatment with SGLT2i were recently discussed to trigger autophagy and reduce reactive oxygen species (ROS) in the heart and thus may represent another indirect effect contributing to cardioprotection (Packer, 2020).

With respect to the target of GLP1-RA, the GLP1R expression is highly relevant. GLP1R is primarily detected in the atria (Ussher et al., 2014). Although detection of GLP1R was shown on mRNA level in ventricles, it is unclear which cardiac cell type expresses functional GLP1R (Ang et al., 2018). Furthermore, GLP1R expression was not found in rat ventricular cardiomyocytes (Wang et al., 2020), but in H9c2 cells (Chang et al., 2018). Ussher et al. provided strong evidence that the cardioprotective effect of GLP1-RA is independent of GLP1R expression in cardiomyocytes (Ussher et al., 2014). Protective effects of liraglutide in a MI model were still present in cardiomyocyte-specific knockout (KO) of GLP1R. Interestingly, cardiomyocyte-specific GLP1R-KO animals showed a lower basal heart rate while liraglutide-induced increase in heart rate was still present (Ussher et al., 2014). In line with these findings, injection of GLP1 increases heart rate and blood pressure in rodents, which has also been reported in some, but not all human trials (Drucker, 2018). This activity of GLP1-RA was linked to direct effects on autonomic nerves (**Figure 2**). In addition, a recent study in rats indicates an effect of exendin-4 on the ventricular action potential via GLP1R activation on parasympathetic neurons (Ang et al., 2018). In this study, exendin-4 had opposite effects to the stimulation of β-adrenergic receptor, likely through an indirect mechanism mediated by released acetylcholine and nitric oxide, which lead to a reduction of arrhythmia. These findings provide first evidence for the involvement of different processes in the cardioprotective effect of GLP1-RA. However, although the presence of GLP1R in cardiomyocytes seems dispensable for the cardioprotective effect of liraglutide, it is still unclear whether these receptors may be important in other cardiac cell types including endothelial cells, macrophages or fibroblasts, or if other off-target effects may exist.

Further questions arise for the class of DPP4i. The membrane-bound form of the enzyme could not be found in the heart. The broad evidence for cardioprotective effects in pre-clinical studies, especially the effects observed using cell culture models of cardiomyocytes or cardiac fibroblasts, stands in contrast to the lack of efficacy in the CVOTs (**Tables 1**, **3**). Relevant factors to this issue may include species differences, bioavailability of the compounds or the presence of other medication in patients. Importantly, this discrepancy of DPP4i effects may be

mechanism-based, because the influence of DPP4 inhibition is, at least partly, indirect and through an increase of the plasma levels of a variety of peptides including GLP1, GIP, neuropeptide Y, peptide YY, gastric inhibitory peptide, or stromal cell-derived factor 1 (SDF-1). An involvement of these indirect downstream effects on the outcome is highlighted by experiments showing that the beneficial effects of saxagliptin in diabetic rats could be prevented by the SDF-1 antagonist plerixafor (Connelly et al., 2016). Moreover, the structural differences of the compounds within the class of DPP4i are relevant for the treatment effect. Saxagliptin, but not sitagliptin, was shown to affect CaMKII/PLB phosphorylation in cardiomyocytes through off-target inhibition of DPP9, which leads to prolonged action potential duration and may trigger arrhythmic events (Koyani et al., 2018). These results indicate that off-target activities of DPP4i on other DPPs may contribute to the different outcome of DPP4i in the clinical trials.

Questions about the molecular target also remain for metformin although it is used in clinical practice since about 25 years. It is widely proven that metformin treatment induces phosphorylation and activation of AMPK (Glossmann and Lutz, 2019). Mechanistically, this has been linked to the ability of metformin to inhibit the activity of mitochondrial complex 1 (MC-1) in the respiratory chain, resulting in an increased AMP/ATP ratio, which triggers AMPK phosphorylation (Glossmann and Lutz, 2019; Soukas et al., 2019). However, the inhibition of MC-1 requires metformin at millimolar concentrations and is therefore critically discussed to fully explain the effects of the drug (Zhang et al., 2016; Soukas et al., 2019). Growing evidence suggests the involvement of other targets including fructose-1,6-bisphosphatase, mechanistic target of rapamycin (mTOR) or mitochondrial glycerol phosphate-dehydrogenase, which are also involved in cellular energy metabolism (Soukas et al., 2019). More recently, an experimental study suggests that the prokineticin (PK) 2/PK receptor (PKR) pathway plays a crucial role in the pathogenesis of diabetic cardiomyopathy and that metformin prevents diabetes-induced glucose and lipid metabolism dysfunction, cardiomyocyte apoptosis, fibrosis, and cardiac insufficiency by stimulating PK2/PKR and the downstream AKT/GSK3β pathway (Yang et al., 2020).

Taken together, although cardioprotective effects were demonstrated for SGLT2i, GLP1-RA, DPP4i, and metformin, the direct targets of the drugs remain elusive and require further investigation. In the future, it is worth to establish novel model systems of diabetic cardiomyopathy, for example, by using induced pluripotent stem cell (iPSC)-derived cardiomyocytes, to investigate the direct effects of the antidiabetics on human cardiomyocytes. The iPSC-based system needs to overcome the challenges of the limited maturity of iPSC-derived cardiomyocytes, but allows long-time cultures to study disease progression in human cells. This may provide sufficient throughput to test different drugs in parallel (Kolanowski et al., 2017). Despite the variety of approaches to model cardiomyopathy hinders the direct comparison of the different drug classes, important information about the cellular pathways involved in cardioprotection could be identified.

CONCLUSION

Until recently, T2D and HF were managed independently in clinical practice. The clinical trials clearly confirmed the safety of metformin, GLP1-RA, DPP4i, and SGLT2i (except saxagliptin) for T2D patients at high risk of CVD. The CVOTs demonstrated the cardioprotective effects of GLP1-RA and SGLT2i in T2D patients at high risk of CVD, which strongly encourages clinicians to consider modern T2D therapy in addition to lowering blood glucose levels. Taking into account the baseline characteristics of the patient, especially renal function, atherosclerotic disease or HF, the antidiabetic therapy should be selected in a personalized manner to achieve the best cardiovascular outcome. Moreover, there is an urgent need for further clinical and basic research to decipher and understand the molecular mechanisms of the glucose level-independent cardiovascular benefit observed in the CVOTs.

AUTHOR CONTRIBUTIONS

MS, SH, JL, and KG conducted a review of the literature and wrote the first draft of the review. KG contributed to conception and design of the article and finalized the review. All authors read and approved the final manuscript.

FUNDING

This study was supported by the Deutsche Forschungsgemeinschaft (DFG, German Research Foundation) – Project Number 288034826 – IRTG 2251: "Immunological and Cellular Strategies in Metabolic Disease" and by the Free State of Saxony and the European Union EFRE (SAB projects "HERMES" and "PhenoCor") to KG. MS was supported by the MeDDrive START grant from the Medical Faculty at TU Dresden. We acknowledge the support of the Open Access Funding by the Publication Fund of the TU Dresden.

REFERENCES

Andreadou, I., Efentakis, P., Balafas, E., Togliatto, G., Davos, C. H., Varela, A., et al. (2017). Empagliflozin limits myocardial infarction in vivo and cell death in vitro: role of STAT3, mitochondria, and redox aspects. *Front. Physiol.* 8:1077. doi: 10.3389/fphys.2017.01077

Ang, R., Mastitskaya, S., Hosford, P. S., Basalay, M., Specterman, M., Aziz, Q., et al. (2018). Modulation of cardiac ventricular excitability by GLP-1 (Glucagon-Like Peptide-1). *Circ. Arrhythm. Electrophysiol.* 11:e006740. doi: 10.1161/CIRCEP.118.006740

Apovian, C. M., Okemah, J., and O'Neil, P. M. (2019). Body weight considerations in the management of Type 2 diabetes. *Adv. Ther.* 36, 44–58. doi: 10.1007/s12325-018-0824-8

Aulinger, B. A., Bedorf, A., Kutscherauer, G., de Heer, J., Holst, J. J., Goke, B., et al. (2014). Defining the role of GLP-1 in the enteroinsulinar axis in type 2 diabetes

using DPP-4 inhibition and GLP-1 receptor blockade. *Diabetes Metab. Res. Rev.* 63, 1079–1092. doi: 10.2337/db13-1455

Baartscheer, A., Schumacher, C. A., Wust, R. C., Fiolet, J. W., Stienen, G. J., Coronel, R., et al. (2017). Empagliflozin decreases myocardial cytoplasmic Na(+) through inhibition of the cardiac Na(+)/H(+) exchanger in rats and rabbits. *Diabetologia* 60, 568–573. doi: 10.1007/s00125-016-4134-x

Balteau, M., Van Steenbergen, A., Timmermans, A. D., Dessy, C., Behets-Wydemans, G., Tajeddine, N., et al. (2014). AMPK activation by glucagon-like peptide-1 prevents NADPH oxidase activation induced by hyperglycemia in adult cardiomyocytes. *Am. J. Physiol. Heart Circ. Physiol.* 307, H1120–H1133. doi: 10.1152/ajpheart.00210.2014

Bergmark, B. A., Bhatt, D. L., McGuire, D. K., Cahn, A., Mosenzon, O., Steg, P. G., et al. (2019). Metformin use and clinical outcomes among patients with diabetes mellitus with or without heart failure or kidney dysfunction: observations from the SAVOR-TIMI 53 TRIAL. *Circulation* 140, 1004–1014. doi: 10.1161/CIRCULATIONAHA.119.040144

Bhatia, R. S., Tu, J. V., Lee, D. S., Austin, P. C., Fang, J., Haouzi, A., et al. (2006). Outcome of heart failure with preserved ejection fraction in a population-based study. *N. Engl. J. Med.* 355, 260–269. doi: 10.1056/NEJMoa051530

Birnbaum, Y., Tran, D., Bajaj, M., and Ye, Y. (2019). DPP-4 inhibition by linagliptin prevents cardiac dysfunction and inflammation by targeting the Nlrp3/ASC inflammasome. *Basic Res. Cardiol.* 114:35. doi: 10.1007/s00395-019-0743-0

Bolli, G. B., and Owens, D. R. (2014). Lixisenatide, a novel GLP-1 receptor agonist: efficacy, safety and clinical implications for type 2 diabetes mellitus. *Diabetes. Obes. Metab.* 16, 588–601. doi: 10.1111/dom.12253

Bonora, B. M., Avogaro, A., and Fadini, G. P. (2019). Effects of exenatide long-acting release on cardiovascular events and mortality in patients with type 2 diabetes: a systematic review and meta-analysis of randomized controlled trials. *Acta Diabetol.* 56, 1051–1060. doi: 10.1007/s00592-019-01347-0

Boonman-de Winter, L. J., Rutten, F. H., Cramer, M. J., Landman, M. J., Liem, A. H., Rutten, G. E., et al. (2012). High prevalence of previously unknown heart failure and left ventricular dysfunction in patients with type 2 diabetes. *Diabetologia* 55, 2154–2162. doi: 10.1007/s00125-012-2579-0

Boussageon, R., Gueyffier, F., and Cornu, C. (2016). Metformin as firstline treatment for type 2 diabetes: are we sure? *BMJ* 352:h6748. doi: 10.1136/bmj.h6748

Calvert, J. W., Gundewar, S., Jha, S., Greer, J. J., Bestermann, W. H., Tian, R., et al. (2008). Acute metformin therapy confers cardioprotection against myocardial infarction via AMPK-eNOS-mediated signaling. *Diabetes Metab. Res. Rev.* 57, 696–705. doi: 10.2337/db07-1098

Chang, G., Liu, J., Qin, S., Jiang, Y., Zhang, P., Yu, H., et al. (2018). Cardioprotection by exenatide: A novel mechanism via improving mitochondrial function involving the GLP-1 receptor/cAMP/PKA pathway. *Int. J. Mol. Med.* 41, 1693–1703. doi: 10.3892/ijmm.2017.3318

Chen, W. R., Chen, Y. D., Tian, F., Yang, N., Cheng, L. Q., Hu, S. Y., et al. (2016a). Effects of liraglutide on reperfusion injury in patients with ST-segment-elevation myocardial infarction. *Circ. Cardiovasc. Imaging* 9:5146. doi: 10.1161/CIRCIMAGING.116.005146

Chen, W. R., Shen, X. Q., Zhang, Y., Chen, Y. D., Hu, S. Y., Qian, G., et al. (2016b). Effects of liraglutide on left ventricular function in patients with non-ST-segment elevation myocardial infarction. *Endocrine* 52, 516–526. doi: 10.1007/s12020-015-0798-0

Chen, W. R., Hu, S. Y., Chen, Y. D., Zhang, Y., Qian, G., Wang, J., et al. (2015). Effects of liraglutide on left ventricular function in patients with ST-segment elevation myocardial infarction undergoing primary percutaneous coronary intervention. *Am. Heart. J.* 170, 845–854. doi: 10.1016/j.ahj.2015.07.014

Connelly, K. A., Advani, A., Zhang, Y., Advani, S. L., Kabir, G., Abadeh, A., et al. (2016). Dipeptidyl peptidase-4 inhibition improves cardiac function in experimental myocardial infarction: role of stromal cell-derived factor-1alpha. *J. Diabetes* 8, 63–75. doi: 10.1111/1753-0407.12258

Cosentino, F., Grant, P. J., Aboyans, V., Bailey, C. J., Ceriello, A., Delgado, V., et al. (2020). 2019 ESC Guidelines on diabetes, pre-diabetes, and cardiovascular diseases developed in collaboration with the EASD. *Eur. Heart J.* 41, 255–323. doi: 10.1093/eurheartj/ehz486

dos Santos, L., Salles, T. A., Arruda-Junior, D. F., Campos, L. C., Pereira, A. C., Barreto, A. L., et al. (2013). Circulating dipeptidyl peptidase IV activity correlates with cardiac dysfunction in human and experimental heart failure. *Circ. Heart Fail* 6, 1029–1038. doi: 10.1161/CIRCHEARTFAILURE.112.000057

Drucker, D. J. (2018). Mechanisms of action and therapeutic application of glucagon-like peptide-1. *Cell Metab.* 27, 740–756. doi: 10.1016/j.cmet.2018.03.001

Duan, C. M., Wan, T. F., Wang, Y., and Yang, Q. W. (2019). Cardiovascular outcomes of liraglutide in patients with type 2 diabetes: a systematic review and meta-analysis. *Medicine* 98:e17860. doi: 10.1097/MD.0000000000017860

El Messaoudi, S., Nederlof, R., Zuurbier, C. J., van Swieten, H. A., Pickkers, P., Noyez, L., et al. (2015). Effect of metformin pretreatment on myocardial injury during coronary artery bypass surgery in patients without diabetes (MetCAB): a double-blind, randomised controlled trial. *Lancet Diabetes Endocrinol.* 3, 615–623. doi: 10.1016/S2213-8587(15)00121-7

Emerging Risk Factors Collaboration, Di Angelantonio, E., Kaptoge, S., Wormser, D., Willeit, P., Butterworth, A. S., et al. (2015). Association of cardiometabolic multimorbidity with mortality. *JAMA* 314, 52–60. doi: 10.1001/jama.2015.7008

Erqou, S., Lee, C. T., Suffoletto, M., Echouffo-Tcheugui, J. B., de Boer, R. A., van Melle, J. P., et al. (2013). Association between glycated haemoglobin and the risk of congestive heart failure in diabetes mellitus: systematic review and meta-analysis. *Eur. J. Heart Fail.* 15, 185–193. doi: 10.1093/eurjhf/hfs156

Eurich, D. T., Weir, D. L., Majumdar, S. R., Tsuyuki, R. T., Johnson, J. A., Tjosvold, L., et al. (2013). Comparative safety and effectiveness of metformin in patients with diabetes mellitus and heart failure: systematic review of observational studies involving 34,000 patients. *Circ. Heart Fail* 6, 395–402. doi: 10.1161/CIRCHEARTFAILURE.112.000162

Figtree, G. A., Radholm, K., Barrett, T. D., Perkovic, V., Mahaffey, K. W., de Zeeuw, D., et al. (2019). Effects of canagliflozin on heart failure outcomes associated with preserved and reduced ejection fraction in Type 2 diabetes mellitus. *Circulation* 139, 2591–2593. doi: 10.1161/CIRCULATIONAHA.119.040057

Foretz, M., Guigas, B., and Viollet, B. (2019). Understanding the glucoregulatory mechanisms of metformin in type 2 diabetes mellitus. *Nat. Rev. Endocrinol.* 15, 569–589. doi: 10.1038/s41574-019-0242-2

Fu, X., Pan, Y., Cao, Q., Li, B., Wang, S., Du, H., et al. (2018). Metformin restores electrophysiology of small conductance calcium-activated potassium channels in the atrium of GK diabetic rats. *BMC Cardiovasc. Disord.* 18:63. doi: 10.1186/s12872-018-0805-5

Gallwitz, B. (2019). Clinical use of DPP-4 inhibitors. *Front. Endocrinol.* 10:389. doi: 10.3389/fendo.2019.00389

Garcia-Ropero, A., Santos-Gallego, C. G., Zafar, M. U., and Badimon, J. J. (2019). Metabolism of the failing heart and the impact of SGLT2 inhibitors. *Expert. Opin. Drug Metab. Toxicol.* 15, 275–285. doi: 10.1080/17425255.2019.1588886

Gerstein, H. C., Colhoun, H. M., Dagenais, G. R., Diaz, R., Lakshmanan, M., Pais, P., et al. (2019). Dulaglutide and cardiovascular outcomes in type 2 diabetes (REWIND): a double-blind, randomised placebo-controlled trial. *Lancet* 394, 121–130. doi: 10.1016/S0140-6736(19)31149-3

Glossmann, H. H., and Lutz, O. M. D. (2019). Metformin and aging: a review. *Gerontology* 65, 581–590. doi: 10.1159/000502257

Green, J. B., Bethel, M. A., Armstrong, P. W., Buse, J. B., Engel, S. S., Garg, J., et al. (2015). Effect of sitagliptin on cardiovascular outcomes in Type 2 diabetes. *N. Engl. J. Med.* 373, 232–242. doi: 10.1056/NEJMoa1501352

Griffin, S. J., Bethel, M. A., Holman, R. R., Khunti, K., Wareham, N., Brierley, G., et al. (2018). Metformin in non-diabetic hyperglycaemia: the GLINT feasibility RCT. *Health Technol. Assess.* 22, 1–64. doi: 10.3310/hta22180

Griffin, S. J., Leaver, J. K., and Irving, G. J. (2017). Impact of metformin on cardiovascular disease: a meta-analysis of randomised trials among people with type 2 diabetes. *Diabetologia* 60, 1620–1629. doi: 10.1007/s00125-017-4337-9

Gundewar, S., Calvert, J. W., Jha, S., Toedt-Pingel, I., Ji, S. Y., Nunez, D., et al. (2009). Activation of AMP-activated protein kinase by metformin improves left ventricular function and survival in heart failure. *Circ. Res.* 104, 403–411. doi: 10.1161/CIRCRESAHA.108.190918

Habibi, J., Aroor, A. R., Sowers, J. R., Jia, G., Hayden, M. R., Garro, M., et al. (2017). Sodium glucose transporter 2 (SGLT2) inhibition with empagliflozin improves cardiac diastolic function in a female rodent model of diabetes. *Cardiovasc. Diabetol.* 16:9. doi: 10.1186/s12933-016-0489-z

Hamdani, N., Hervent, A. S., Vandekerckhove, L., Matheeussen, V., Demolder, M., Baerts, L., et al. (2014). Left ventricular diastolic dysfunction and myocardial stiffness in diabetic mice is attenuated by inhibition of dipeptidyl peptidase 4. *Cardiovasc. Res.* 104, 423–431. doi: 10.1093/cvr/cvu223

Han, Y., Xie, H., Liu, Y., Gao, P., Yang, X., and Shen, Z. (2019). Effect of metformin on all-cause and cardiovascular mortality in patients with coronary

artery diseases: a systematic review and an updated meta-analysis. *Cardiovasc. Diabetol.* 18:96. doi: 10.1186/s12933-019-0900-7

Harrington, J. L., de Albuquerque Rocha, N., Patel, K. V., Verma, S., and McGuire, D. K. (2018). Should metformin remain first-line medical therapy for patients with Type 2 diabetes mellitus and atherosclerotic cardiovascular disease? An alternative approach. *Curr. Diab. Rep.* 18:64. doi: 10.1007/s11892-018-1035-z

Hartman, M. H. T., Prins, J. K. B., Schurer, R. A. J., Lipsic, E., Lexis, C. P. H., van der Horst-Schrivers, A. N. A., et al. (2017). Two-year follow-up of 4 months metformin treatment vs. placebo in ST-elevation myocardial infarction: data from the GIPS-III RCT. *Clin. Res. Cardiol.* 106, 939–946. doi: 10.1007/s00392-017-1140-z

He, C., Zhu, H., Li, H., Zou, M. H., and Xie, Z. (2013). Dissociation of Bcl-2-Beclin1 complex by activated AMPK enhances cardiac autophagy and protects against cardiomyocyte apoptosis in diabetes. *Diabetes Metab. Res. Rev.* 62, 1270–1281. doi: 10.2337/db12-0533

Hernandez, A. F., Green, J. B., Janmohamed, S., D'Agostino, R. B. Sr., Granger, C. B., Jones, N. P., et al. (2018). Albiglutide and cardiovascular outcomes in patients with type 2 diabetes and cardiovascular disease (Harmony Outcomes): a double-blind, randomised placebo-controlled trial. *Lancet* 392, 1519–1529. doi: 10.1016/S0140-6736(18)32261-X

Herrington, W. G., Preiss, D., Haynes, R., von Eynatten, M., Staplin, N., Hauske, S. J., et al. (2018). The potential for improving cardio-renal outcomes by sodium-glucose co-transporter-2 inhibition in people with chronic kidney disease: a rationale for the EMPA-KIDNEY study. *Clin. Kidney J.* 11, 749–761. doi: 10.1093/ckj/sfy090

Holman, R. R., Bethel, M. A., Mentz, R. J., Thompson, V. P., Lokhnygina, Y., Buse, J. B., et al. (2017). Effects of once-weekly exenatide on cardiovascular outcomes in Type 2 diabetes. *N. Engl. J. Med.* 377, 1228–1239. doi: 10.1056/NEJMoa1612917

Holman, R. R., Paul, S. K., Bethel, M. A., Matthews, D. R., and Neil, H. A. (2008). 10-year follow-up of intensive glucose control in type 2 diabetes. *N. Engl. J. Med.* 359, 1577–1589. doi: 10.1056/NEJMoa0806470

Home, P. (2019). Cardiovascular outcome trials of glucose-lowering medications: an update. *Diabetologia* 62, 357–369. doi: 10.1007/s00125-018-4801-1

Home, P. D., Pocock, S. J., Beck-Nielsen, H., Curtis, P. S., Gomis, R., Hanefeld, M., et al. (2009). Rosiglitazone evaluated for cardiovascular outcomes in oral agent combination therapy for type 2 diabetes (RECORD): a multicentre, randomised, open-label trial. *Lancet* 373, 2125–2135. doi: 10.1016/S0140-6736(09)60953-3

Hong, J., Zhang, Y., Lai, S., Lv, A., Su, Q., Dong, Y., et al. (2013). Effects of metformin versus glipizide on cardiovascular outcomes in patients with type 2 diabetes and coronary artery disease. *Diabetes Care* 36, 1304–1311. doi: 10.2337/dc12-0719

Hopf, A. E., Andresen, C., Kotter, S., Isic, M., Ulrich, K., Sahin, S., et al. (2018). Diabetes-induced cardiomyocyte passive stiffening is caused by impaired insulin-dependent titin modification and can be modulated by Neuregulin-1. *Circ. Res.* 123, 342–355. doi: 10.1161/CIRCRESAHA.117.312166

Huang, M., Wei, R., Wang, Y., Su, T., Li, Q., Yang, X., et al. (2017). Protective effect of glucagon-like peptide-1 agents on reperfusion injury for acute myocardial infarction: a meta-analysis of randomized controlled trials. *Ann. Med.* 49, 552–561. doi: 10.1080/07853890.2017.1306653

Husain, M., Birkenfeld, A. L., Donsmark, M., Dungan, K., Eliaschewitz, F. G., Franco, D. R., et al. (2019). Oral semaglutide and cardiovascular outcomes in patients with Type 2 diabetes. *N. Engl. J. Med.* 381, 841–851. doi: 10.1056/NEJMoa1901118

Iepsen, E. W., Torekov, S. S., and Holst, J. J. (2015). Liraglutide for Type 2 diabetes and obesity: a 2015 update. *Expert. Rev. Cardiovasc. Ther.* 13, 753–767. doi: 10.1586/14779072.2015.1054810

Ikonomidis, I., Pavlidis, G., Thymis, J., Birba, D., Kalogeris, A., Kousathana, F., et al. (2020). Effects of Glucagon-like peptide-1 receptor agonists, sodium-glucose cotransporter-2 inhibitors, and their combination on endothelial glycocalyx, arterial function, and myocardial work index in patients with Type 2 diabetes mellitus after 12-month treatment. *J. Am. Heart Assoc.* 9:e015716. doi: 10.1161/JAHA.119.015716

Jensen, L., Helleberg, H., Roffel, A., van Lier, J. J., Bjornsdottir, I., Pedersen, P. J., et al. (2017). Absorption, metabolism and excretion of the GLP-1 analogue semaglutide in humans and nonclinical species. *Eur. J. Pharm. Sci.* 104, 31–41. doi: 10.1016/j.ejps.2017.03.020

Ji, Y., Zhao, Z., Cai, T., Yang, P., and Cheng, M. (2014). Liraglutide alleviates diabetic cardiomyopathy by blocking CHOP-triggered apoptosis via the inhibition of the IRE-alpha pathway. *Mol. Med. Rep.* 9, 1254–1258. doi: 10.3892/mmr.2014.1956

Johnson, R., Dludla, P., Joubert, E., February, F., Mazibuko, S., Ghoor, S., et al. (2016). Aspalathin, a dihydrochalcone C-glucoside, protects H9c2 cardiomyocytes against high glucose induced shifts in substrate preference and apoptosis. *Mol. Nutr. Food Res.* 60, 922–934. doi: 10.1002/mnfr.201500656

Jones, B., Buenaventura, T., Kanda, N., Chabosseau, P., Owen, B. M., Scott, R., et al. (2018). Targeting GLP-1 receptor trafficking to improve agonist efficacy. *Nat. Commun.* 9:1602. doi: 10.1038/s41467-018-03941-2

Jorsal, A., Kistorp, C., Holmager, P., Tougaard, R. S., Nielsen, R., Hanselmann, A., et al. (2017). Effect of liraglutide, a glucagon-like peptide-1 analogue, on left ventricular function in stable chronic heart failure patients with and without diabetes (LIVE)-a multicentre, double-blind, randomised, placebo-controlled trial. *Eur. J. Heart Fail.* 19, 69–77. doi: 10.1002/ejhf.657

Kahles, F., Ruckbeil, M. V., Mertens, R. W., Foldenauer, A. C., Arrivas, M. C., Moellmann, J., et al. (2020). Glucagon-like peptide 1 levels predict cardiovascular risk in patients with acute myocardial infarction. *Eur. Heart J.* 41, 882–889. doi: 10.1093/eurheartj/ehz728

Katakami, N., Yamasaki, Y., Hayaishi-Okano, R., Ohtoshi, K., Kaneto, H., Matsuhisa, M., et al. (2004). Metformin or gliclazide, rather than glibenclamide, attenuate progression of carotid intima-media thickness in subjects with type 2 diabetes. *Diabetologia* 47, 1906–1913. doi: 10.1007/s00125-004-1547-8

Kato, E. T., Silverman, M. G., Mosenzon, O., Zelniker, T. A., Cahn, A., Furtado, R. H. M., et al. (2019). Effect of dapagliflozin on heart failure and mortality in Type 2 diabetes mellitus. *Circulation* 139, 2528–2536. doi: 10.1161/CIRCULATIONAHA.119.040130

Kolanowski, T. J., Antos, C. L., and Guan, K. (2017). Making human cardiomyocytes up to date: derivation, maturation state and perspectives. *Int. J. Cardiol.* 241, 379–386. doi: 10.1016/j.ijcard.2017.03.099

Koyani, C. N., Trummer, C., Shrestha, N., Scheruebel, S., Bourgeois, B., Plastira, I., et al. (2018). Saxagliptin but not sitagliptin inhibits CaMKII and PKC via DPP9 inhibition in cardiomyocytes. *Front. Physiol.* 9:1622. doi: 10.3389/fphys.2018.01622

Kristensen, S. L., Rorth, R., Jhund, P. S., Docherty, K. F., Sattar, N., Preiss, D., et al. (2019). Cardiovascular, mortality, and kidney outcomes with GLP-1 receptor agonists in patients with type 2 diabetes: a systematic review and meta-analysis of cardiovascular outcome trials. *Lancet Diabetes Endocrinol.* 7, 776–785. doi: 10.1016/S2213-8587(19)30249-9

Kyhl, K., Lonborg, J., Vejlstrup, N., Kelbaek, H., Helqvist, S., Holmvang, L., et al. (2016). A post hoc analysis of long-term prognosis after exenatide treatment in patients with ST-segment elevation myocardial infarction. *EuroIntervention* 12, 449–455. doi: 10.4244/EIJV12I4A78

Lambeir, A. M., Scharpe, S., and De Meester, I. (2008). DPP4 inhibitors for diabetes–what next? *Biochem. Pharmacol.* 76, 1637–1643. doi: 10.1016/j.bcp.2008.07.029

Levine, B., Packer, M., and Codogno, P. (2015). Development of autophagy inducers in clinical medicine. *J. Clin. Invest.* 125, 14–24. doi: 10.1172/JCI73938

Lexis, C. P., and van der Horst, I. C. (2014). Metformin for cardiovascular disease: promise still unproven. *Lancet Diabetes Endocrinol.* 2, 94–95. doi: 10.1016/S2213-8587(13)70171-2

Lexis, C. P., van der Horst, I. C., Lipsic, E., Wieringa, W. G., de Boer, R. A., van den Heuvel, A. F., et al. (2014). Effect of metformin on left ventricular function after acute myocardial infarction in patients without diabetes: the GIPS-III randomized clinical trial. *JAMA* 311, 1526–1535. doi: 10.1001/jama.2014.3315

Liu, Y. S., Huang, Z. W., Wang, L., Liu, X. X., Wang, Y. M., Zhang, Y., et al. (2015). Sitagliptin alleviated myocardial remodeling of the left ventricle and improved cardiac diastolic dysfunction in diabetic rats. *J. Pharmacol. Sci.* 127, 260–274. doi: 10.1016/j.jphs.2014.12.007

Lundkvist, P., Pereira, M. J., Katsogiannos, P., Sjostrom, C. D., Johnsson, E., and Eriksson, J. W. (2017). Dapagliflozin once daily plus exenatide once weekly in obese adults without diabetes: Sustained reductions in body weight, glycaemia and blood pressure over 1 year. *Diabetes Obes. Metab.* 19, 1276–1288. doi: 10.1111/dom.12954

Makrilakis, K. (2019). The role of DPP-4 inhibitors in the treatment algorithm of Type 2 diabetes mellitus: when to select, what to expect. *Int. J. Environ. Res. Public Health* 16:2720. doi: 10.3390/ijerph16152720

Mantsiou, C., Karagiannis, T., Kakotrichi, P., Malandris, K., Avgerinos, I., Liakos, A., et al. (2020). Glucagon-like peptide-1 receptor agonists and sodium-glucose co-transporter-2 inhibitors as combination therapy for type 2 diabetes: a systematic review and meta-analysis. *Diabetes Obes. Metab.* doi: 10.1111/dom.14108 [Epub ahead of print].

Margulies, K. B., Hernandez, A. F., Redfield, M. M., Givertz, M. M., Oliveira, G. H., Cole, R., et al. (2016). Effects of liraglutide on clinical stability among patients with advanced heart failure and reduced ejection fraction: a randomized clinical trial. *JAMA* 316, 500–508. doi: 10.1001/jama.2016.10260

Marso, S. P., Bain, S. C., Consoli, A., Eliaschewitz, F. G., Jodar, E., Leiter, L. A., et al. (2016a). Semaglutide and cardiovascular outcomes in patients with Type 2 diabetes. *N. Engl. J. Med.* 375, 1834–1844. doi: 10.1056/NEJMoa1607141

Marso, S. P., Daniels, G. H., Brown-Frandsen, K., Kristensen, P., Mann, J. F., Nauck, M. A., et al. (2016b). Liraglutide and cardiovascular outcomes in Type 2 diabetes. *N. Engl. J. Med.* 375, 311–322. doi: 10.1056/NEJMoa1603827

Martin-Montalvo, A., Mercken, E. M., Mitchell, S. J., Palacios, H. H., Mote, P. L., Scheibye-Knudsen, M., et al. (2013). Metformin improves healthspan and lifespan in mice. *Nat. Commun.* 4:2192. doi: 10.1038/ncomms3192

McMurray, J. J. V., Solomon, S. D., Inzucchi, S. E., Kober, L., Kosiborod, M. N., Martinez, F. A., et al. (2019). Dapagliflozin in patients with heart failure and reduced ejection fraction. *N. Engl. J. Med.* 381, 1995–2008. doi: 10.1056/NEJMoa1911303

Meaney, E., Vela, A., Samaniego, V., Meaney, A., Asbun, J., Zempoalteca, J. C., et al. (2008). Metformin, arterial function, intima-media thickness and nitroxidation in metabolic syndrome: the mefisto study. *Clin. Exp. Pharmacol. Physiol.* 35, 895–903. doi: 10.1111/j.1440-1681.2008.04920.x

Meloni, A. R., DeYoung, M. B., Lowe, C., and Parkes, D. G. (2013). GLP-1 receptor activated insulin secretion from pancreatic beta-cells: mechanism and glucose dependence. *Diabetes Obes. Metab.* 15, 15–27. doi: 10.1111/j.1463-1326.2012.01663.x

Misbin, R. I. (2004). The phantom of lactic acidosis due to metformin in patients with diabetes. *Diabetes Care* 27, 1791–1793. doi: 10.2337/diacare.27.7.1791

Mizuno, M., Kuno, A., Yano, T., Miki, T., Oshima, H., Sato, T., et al. (2018). Empagliflozin normalizes the size and number of mitochondria and prevents reduction in mitochondrial size after myocardial infarction in diabetic hearts. *Physiol. Rep.* 6:e13741. doi: 10.14814/phy2.13741

Mohan, M., Al-Talabany, S., McKinnie, A., Mordi, I. R., Singh, J. S. S., Gandy, S. J., et al. (2019). A randomized controlled trial of metformin on left ventricular hypertrophy in patients with coronary artery disease without diabetes: the MET-REMODEL trial. *Eur. Heart J.* 40, 3409–3417. doi: 10.1093/eurheartj/ehz203

Mustroph, J., Lucht, C. M., Wagemann, O., Sowa, T., Hammer, K. P., Sag, C. M., et al. (2019). Empagliflozin enhances human and murine cardiomyocyte glucose uptake by increased expression of GLUT1. *Diabetologia* 62, 726–729. doi: 10.1007/s00125-019-4819-z

Mustroph, J., Wagemann, O., Lucht, C. M., Trum, M., Hammer, K. P., Sag, C. M., et al. (2018). Empagliflozin reduces Ca/calmodulin-dependent kinase II activity in isolated ventricular cardiomyocytes. *ESC Heart Fail* 5, 642–648. doi: 10.1002/ehf2.12336

Nauck, M. A., and Meier, J. J. (2019). MANAGEMENT OF ENDOCRINE DISEASE: are all GLP-1 agonists equal in the treatment of type 2 diabetes? *Eur. J. Endocrinol.* 181, R211–R234. doi: 10.1530/EJE-19-0566

Neal, B., Perkovic, V., Mahaffey, K. W., de Zeeuw, D., Fulcher, G., Erondu, N., et al. (2017). Canagliflozin and cardiovascular and renal events in Type 2 diabetes. *N. Engl. J. Med.* 377, 644–657. doi: 10.1056/NEJMoa1611925

Noyan-Ashraf, M. H., Momen, M. A., Ban, K., Sadi, A. M., Zhou, Y. Q., Riazi, A. M., et al. (2009). GLP-1R agonist liraglutide activates cytoprotective pathways and improves outcomes after experimental myocardial infarction in mice. *Diabetes Metab. Res. Rev.* 58, 975–983. doi: 10.2337/db08-1193

Noyan-Ashraf, M. H., Shikatani, E. A., Schuiki, I., Mukovozov, I., Wu, J., Li, R. K., et al. (2013). A glucagon-like peptide-1 analog reverses the molecular pathology and cardiac dysfunction of a mouse model of obesity. *Circulation* 127, 74–85. doi: 10.1161/CIRCULATIONAHA.112.091215

Pabel, S., Wagner, S., Bollenberg, H., Bengel, P., Kovacs, A., Schach, C., et al. (2018). Empagliflozin directly improves diastolic function in human heart failure. *Eur. J. Heart Fail.* 20, 1690–1700. doi: 10.1002/ejhf.1328

Packer, M. (2020). Autophagy stimulation and intracellular sodium reduction as mediators of the cardioprotective effect of sodium-glucose cotransporter 2 inhibitors. *Eur. J. Heart Fail.* 22, 618–628. doi: 10.1002/ejhf.1732

Peng, S., Wang, Y., Zhou, Y., Ma, T., Wang, Y., Li, J., et al. (2019). Rare ginsenosides ameliorate lipid overload-induced myocardial insulin resistance via modulating metabolic flexibility. *Phytomedicine* 58:152745. doi: 10.1016/j.phymed.2018.11.006

Perkovic, V., Jardine, M. J., Neal, B., Bompoint, S., Heerspink, H. J. L., Charytan, D. M., et al. (2019). Canagliflozin and renal outcomes in Type 2 diabetes and nephropathy. *N. Engl. J. Med.* 380, 2295–2306. doi: 10.1056/NEJMoa1811744

Petrie, J. R., Chaturvedi, N., Ford, I., Brouwers, M., Greenlaw, N., Tillin, T., et al. (2017). Cardiovascular and metabolic effects of metformin in patients with type 1 diabetes (REMOVAL): a double-blind, randomised, placebo-controlled trial. *Lancet Diabetes Endocrinol.* 5, 597–609. doi: 10.1016/S2213-8587(17)30194-8

Petrie, M. C. (2019). Sodium glucose cotransporter 2 inhibitors: searching for mechanisms in the wake of large, positive cardiovascular outcomes trials. *Circulation* 140, 1703–1705. doi: 10.1161/CIRCULATIONAHA.119.043487

Pfeffer, M. A., Claggett, B., Diaz, R., Dickstein, K., Gerstein, H. C., Kober, L. V., et al. (2015). Lixisenatide in patients with Type 2 diabetes and acute coronary syndrome. *N. Engl. J. Med.* 373, 2247–2257. doi: 10.1056/NEJMoa1509225

Preiss, D., Lloyd, S. M., Ford, I., McMurray, J. J., Holman, R. R., Welsh, P., et al. (2014). Metformin for non-diabetic patients with coronary heart disease (the CAMERA study): a randomised controlled trial. *Lancet Diabetes Endocrinol.* 2, 116–124. doi: 10.1016/S2213-8587(13)70152-9

Rajagopalan, S., and Rashid, I. (2019). Regression therapy for cardiovascular disease. *Eur. Heart J.* 40, 3418–3420. doi: 10.1093/eurheartj/ehz481

Ramirez, E., Picatoste, B., Gonzalez-Bris, A., Oteo, M., Cruz, F., Caro-Vadillo, A., et al. (2018). Sitagliptin improved glucose assimilation in detriment of fatty-acid utilization in experimental type-II diabetes: role of GLP-1 isoforms in Glut4 receptor trafficking. *Cardiovasc. Diabetol.* 17:12. doi: 10.1186/s12933-017-0643-2

Rawshani, A., Rawshani, A., Franzen, S., Sattar, N., Eliasson, B., Svensson, A. M., et al. (2018). Risk factors, mortality, and cardiovascular outcomes in patients with Type 2 diabetes. *N. Engl. J. Med.* 379, 633–644. doi: 10.1056/NEJMoa1800256

Reed, J., Kanamarlapudi, V., and Bain, S. (2018). Mechanism of cardiovascular disease benefit of glucagon-like peptide 1 agonists. *Cardiovasc. Endocrinol. Metab.* 7, 18–23. doi: 10.1097/XCE.0000000000000147

Rena, G., and Lang, C. C. (2018). Repurposing metformin for cardiovascular disease. *Circulation* 137, 422–424. doi: 10.1161/CIRCULATIONAHA.117.031735

Retwinski, A., Kosmalski, M., Crespo-Leiro, M., Maggioni, A., Opolski, G., Ponikowski, P., et al. (2018). The influence of metformin and the presence of type 2 diabetes mellitus on mortality and hospitalisation in patients with heart failure. *Kardiol. Pol.* 76, 1336–1343. doi: 10.5603/KP.a2018.0127

Riche, D. M., and Davis, C. (2015). EXAMINE: targeting risk and treatment in diabetes. *Lancet* 386, 1443–1444. doi: 10.1016/S0140-6736(15)00406-7

Roos, S. T., Timmers, L., Biesbroek, P. S., Nijveldt, R., Kamp, O., van Rossum, A. C., et al. (2016). No benefit of additional treatment with exenatide in patients with an acute myocardial infarction. *Int. J. Cardiol.* 220, 809–814. doi: 10.1016/j.ijcard.2016.06.283

Rosenstock, J., Perkovic, V., Johansen, O. E., Cooper, M. E., Kahn, S. E., Marx, N., et al. (2019). Effect of linagliptin vs placebo on major cardiovascular events in adults with Type 2 diabetes and high cardiovascular and renal risk: the CARMELINA randomized clinical trial. *JAMA* 321, 69–79. doi: 10.1001/jama.2018.18269

Rowlands, J., Heng, J., Newsholme, P., and Carlessi, R. (2018). Pleiotropic effects of GLP-1 and analogs on cell signaling, metabolism, and function. *Front. Endocrinol.* 9:672. doi: 10.3389/fendo.2018.00672

Russo, E., Penno, G., and Del Prato, S. (2013). Managing diabetic patients with moderate or severe renal impairment using DPP-4 inhibitors: focus on vildagliptin. *Diabetes Metab. Syndr. Obes.* 6, 161–170. doi: 10.2147/DMSO.S28951

Santos-Ferreira, D., Goncalves-Teixeira, P., and Fontes-Carvalho, R. (2020). SGLT-2 inhibitors in heart failure and Type-2 diabetes: hitting two birds with one stone? *Cardiology* 145, 311–320. doi: 10.1159/000504694

Scirica, B. M., Bhatt, D. L., Braunwald, E., Steg, P. G., Davidson, J., Hirshberg, B., et al. (2013). Saxagliptin and cardiovascular outcomes in patients with type 2 diabetes mellitus. *N. Engl. J. Med.* 369, 1317–1326. doi: 10.1056/NEJMoa1307684

Scirica, B. M., Braunwald, E., Raz, I., Cavender, M. A., Morrow, D. A., Jarolim, P., et al. (2014). Heart failure, saxagliptin, and diabetes mellitus: observations from the SAVOR-TIMI 53 randomized trial. *Circulation* 130, 1579–1588. doi: 10.1161/CIRCULATIONAHA.114.010389

Seferovic, J. P., Claggett, B., Seidelmann, S. B., Seely, E. W., Packer, M., Zile, M. R., et al. (2017). Effect of sacubitril/valsartan versus enalapril on glycaemic control in patients with heart failure and diabetes: a post-hoc analysis from the PARADIGM-HF trial. *Lancet Diabetes Endocrinol.* 5, 333–340. doi: 10.1016/S2213-8587(17)30087-6

Soukas, A. A., Hao, H., and Wu, L. (2019). Metformin as anti-aging therapy: is it for everyone? *Trends Endocrinol. Metab.* 30, 745–755. doi: 10.1016/j.tem.2019.07.015

Standl, E. (2019). GLP-1 receptor agonists and cardiovascular outcomes: an updated synthesis. *Lancet Diabetes Endocrinol.* 7, 741–743. doi: 10.1016/S2213-8587(19)30267-0

Tanajak, P., Sa-Nguanmoo, P., Sivasinprasasn, S., Thummasorn, S., Siri-Angkul, N., Chattipakorn, S. C., et al. (2018). Cardioprotection of dapagliflozin and vildagliptin in rats with cardiac ischemia-reperfusion injury. *J. Endocrinol.* 236, 69–84. doi: 10.1530/JOE-17-0457

Tremblay, A. J., Lamarche, B., Deacon, C. F., Weisnagel, S. J., and Couture, P. (2011). Effect of sitagliptin therapy on postprandial lipoprotein levels in patients with type 2 diabetes. *Diabetes. Obes. Metab.* 13, 366–373. doi: 10.1111/j.1463-1326.2011.01362.x

Tsujimoto, T., Kajio, H., Shapiro, M. F., and Sugiyama, T. (2018). Risk of all-cause mortality in diabetic patients taking beta-blockers. *Mayo Clin. Proc.* 93, 409–418. doi: 10.1016/j.mayocp.2017.11.019

Tsujimoto, T., Sugiyama, T., Shapiro, M. F., Noda, M., and Kajio, H. (2017). Risk of cardiovascular events in patients with diabetes mellitus on beta-blockers. *Hypertension* 70, 103–110. doi: 10.1161/HYPERTENSIONAHA.117.09259

UKPDS Group (1998). Effect of intensive blood-glucose control with metformin on complications in overweight patients with type 2 diabetes (UKPDS 34). UK prospective diabetes study (UKPDS) Group. *Lancet* 352, 854–865. doi: 10.1016/s0140-6736(98)07037-8

Ussher, J. R., Baggio, L. L., Campbell, J. E., Mulvihill, E. E., Kim, M., Kabir, M. G., et al. (2014). Inactivation of the cardiomyocyte glucagon-like peptide-1 receptor (GLP-1R) unmasks cardiomyocyte-independent GLP-1R-mediated cardioprotection. *Mol. Metab.* 3, 507–517. doi: 10.1016/j.molmet.2014.04.009

Uthman, L., Baartscheer, A., Bleijlevens, B., Schumacher, C. A., Fiolet, J. W. T., Koeman, A., et al. (2018). Class effects of SGLT2 inhibitors in mouse cardiomyocytes and hearts: inhibition of Na(+)/H(+) exchanger, lowering of cytosolic Na(+) and vasodilation. *Diabetologia* 61, 722–726. doi: 10.1007/s00125-017-4509-7

Uthman, L., Homayr, A., Juni, R. P., Spin, E. L., Kerindongo, R., Boomsma, M., et al. (2019). Empagliflozin and dapagliflozin reduce ROS generation and restore NO bioavailability in tumor necrosis factor alpha-stimulated human coronary arterial endothelial cells. *Cell Physiol. Biochem.* 53, 865–886. doi: 10.33594/000000178

Verma, S. (2019). Potential mechanisms of sodium-glucose co-transporter 2 inhibitor-related cardiovascular benefits. *Am. J. Cardiol.* 124(Suppl. 1), S36–S44. doi: 10.1016/j.amjcard.2019.10.028

Verma, S., Juni, P., and Mazer, C. D. (2019). Pump, pipes, and filter: do SGLT2 inhibitors cover it all? *Lancet* 393, 3–5. doi: 10.1016/S0140-6736(18)32824-1

Verma, S., Rawat, S., Ho, K. L., Wagg, C. S., Zhang, L., Teoh, H., et al. (2018). Empagliflozin increases cardiac energy production in diabetes: novel translational insights into the heart failure benefits of SGLT2 inhibitors. *JACC Basic Transl. Sci.* 3, 575–587. doi: 10.1016/j.jacbts.2018.07.006

Wang, D., Jiang, L., Feng, B., He, N., Zhang, Y., and Ye, H. (2020). Protective effects of glucagon-like peptide-1 on cardiac remodeling by inhibiting oxidative stress through mammalian target of rapamycin complex 1/p70 ribosomal protein S6 kinase pathway in diabetes mellitus. *J. Diabetes Investig.* 11, 39–51. doi: 10.1111/jdi.13098

White, W. B., Cannon, C. P., Heller, S. R., Nissen, S. E., Bergenstal, R. M., Bakris, G. L., et al. (2013). Alogliptin after acute coronary syndrome in patients with type 2 diabetes. *N. Engl. J. Med.* 369, 1327–1335. doi: 10.1056/NEJMoa1305889

Wiviott, S. D., Raz, I., Bonaca, M. P., Mosenzon, O., Kato, E. T., Cahn, A., et al. (2019). Dapagliflozin and cardiovascular outcomes in Type 2 diabetes. *N. Engl. J. Med.* 380, 347–357. doi: 10.1056/NEJMoa1812389

Xiao, C., Dash, S., Morgantini, C., Patterson, B. W., and Lewis, G. F. (2014). Sitagliptin, a DPP-4 inhibitor, acutely inhibits intestinal lipoprotein particle secretion in healthy humans. *Diabetes Metab. Res. Rev.* 63, 2394–2401. doi: 10.2337/db13-1654

Yang, F., Qin, Y., Wang, Y., Meng, S., Xian, H., Che, H., et al. (2019). Metformin inhibits the NLRP3 inflammasome via AMPK/mTOR-dependent effects in diabetic cardiomyopathy. *Int. J. Biol. Sci.* 15, 1010–1019. doi: 10.7150/ijbs.29680

Yang, Z., Wang, M., Zhang, Y., Cai, F., Jiang, B., Zha, W., et al. (2020). Metformin ameliorates diabetic cardiomyopathy by activating the PK2/PKR pathway. *Front. Physiol.* 11:425. doi: 10.3389/fphys.2020.00425

Ye, Y., Bajaj, M., Yang, H. C., Perez-Polo, J. R., and Birnbaum, Y. (2017). SGLT-2 inhibition with dapagliflozin reduces the activation of the Nlrp3/ASC inflammasome and attenuates the development of diabetic cardiomyopathy in mice with Type 2 diabetes. Further augmentation of the effects with saxagliptin, a DPP4 inhibitor. *Cardiovasc. Drugs Ther.* 31, 119–132. doi: 10.1007/s10557-017-6725-2

Ying, Y., Zhu, H., Liang, Z., Ma, X., and Li, S. (2015). GLP1 protects cardiomyocytes from palmitate-induced apoptosis via Akt/GSK3b/b-catenin pathway. *J. Mol. Endocrinol.* 55, 245–262. doi: 10.1530/JME-15-0155

Yu, W., Zha, W., and Ren, J. (2018). Exendin-4 and liraglutide attenuate glucose toxicity-induced cardiac injury through mTOR/ULK1-dependent autophagy. *Oxid. Med. Cell Longev.* 2018:5396806. doi: 10.1155/2018/5396806

Zannad, F., Cannon, C. P., Cushman, W. C., Bakris, G. L., Menon, V., Perez, A. T., et al. (2015). Heart failure and mortality outcomes in patients with type 2 diabetes taking alogliptin versus placebo in EXAMINE: a multicentre, randomised, double-blind trial. *Lancet* 385, 2067–2076. doi: 10.1016/S0140-6736(14)62225-X

Zelniker, T. A., Wiviott, S. D., Raz, I., Im, K., Goodrich, E. L., Bonaca, M. P., et al. (2019a). SGLT2 inhibitors for primary and secondary prevention of cardiovascular and renal outcomes in type 2 diabetes: a systematic review and meta-analysis of cardiovascular outcome trials. *Lancet* 393, 31–39. doi: 10.1016/S0140-6736(18)32590-X

Zelniker, T. A., Wiviott, S. D., Raz, I., Im, K., Goodrich, E. L., Furtado, R. H. M., et al. (2019b). Comparison of the effects of glucagon-like peptide receptor agonists and sodium-glucose cotransporter 2 inhibitors for prevention of major adverse cardiovascular and renal outcomes in Type 2 diabetes mellitus. *Circulation* 139, 2022–2031. doi: 10.1161/CIRCULATIONAHA.118.038868

Zhang, C. S., Li, M., Ma, T., Zong, Y., Cui, J., Feng, J. W., et al. (2016). Metformin activates AMPK through the lysosomal pathway. *Cell Metab.* 24, 521–522. doi: 10.1016/j.cmet.2016.09.003

Zhou, Y., Wang, H., Man, F., Guo, Z., Xu, J., Yan, W., et al. (2018). Sitagliptin protects cardiac function by reducing nitroxidative stress and promoting autophagy in zucker diabetic Fatty (ZDF) rats. *Cardiovasc. Drugs Ther.* 32, 541–552. doi: 10.1007/s10557-018-6831-9

Zinman, B., Wanner, C., Lachin, J. M., Fitchett, D., Bluhmki, E., Hantel, S., et al. (2015). Empagliflozin, cardiovascular outcomes, and mortality in Type 2 diabetes. *N. Engl. J. Med.* 373, 2117–2128. doi: 10.1056/NEJMoa1504720

Zweck, E., and Roden, M. (2019). GLP-1 receptor agonists and cardiovascular disease: drug-specific or class effects? *Lancet Diabetes Endocrinol.* 7, 89–90. doi: 10.1016/S2213-8587(18)30351-6

Conflict of Interest: The authors declare that the research was conducted in the absence of any commercial or financial relationships that could be construed as a potential conflict of interest.

Copyright © 2020 Schubert, Hansen, Leefmann and Guan. This is an open-access article distributed under the terms of the Creative Commons Attribution License (CC BY). The use, distribution or reproduction in other forums is permitted, provided the original author(s) and the copyright owner(s) are credited and that the original publication in this journal is cited, in accordance with accepted academic practice. No use, distribution or reproduction is permitted which does not comply with these terms.

frontiers in Physiology

ORIGINAL RESEARCH
published: 15 September 2020
doi: 10.3389/fphys.2020.01104

Circulating Ceramide: A New Cardiometabolic Biomarker in Patients With Comorbid Acute Coronary Syndrome and Type 2 Diabetes Mellitus

*Ruihua Cao[1], Zhiyi Fang[2], Sulei Li[1], Mengqi Xu[1], Jibin Zhang[2], Dong Han[1], Wenchao Hu[2], Liqiu Yan[2], Yabin Wang[1], Li Fan[1] and Feng Cao[2]**

[1] Department of Cardiology, The Second Medical Centre, Chinese PLA General Hospital, National Clinical Research Center for Geriatric Diseases, Beijing, China, [2] The Second Medical Centre, Chinese PLA General Hospital, National Clinical Research Center for Geriatric Diseases, Beijing, China

OPEN ACCESS

Edited by:
Xin Wang,
University of Manchester,
United Kingdom

Reviewed by:
Jun Ren,
University of Washington,
United States
Xu Yan,
Victoria University, Australia

***Correspondence:**
Feng Cao
fengcao8828@163.com

Specialty section:
This article was submitted to Clinical and Translational Physiology, a section of the journal Frontiers in Physiology

Received: 31 May 2020
Accepted: 10 August 2020
Published: 15 September 2020

Citation:
Cao R, Fang Z, Li S, Xu M, Zhang J, Han D, Hu W, Yan L, Wang Y, Fan L and Cao F (2020) Circulating Ceramide: A New Cardiometabolic Biomarker in Patients With Comorbid Acute Coronary Syndrome and Type 2 Diabetes Mellitus. Front. Physiol. 11:1104. doi: 10.3389/fphys.2020.01104

Aims: This study investigated the association of circulating ceramides in patients with comorbid acute coronary syndrome and type 2 diabetes mellitus (ACS-DM).

Methods: A total of 761 patients with coronary heart disease who were admitted to the Department of Cardiology at the Chinese PLA General Hospital from March to August 2018 were enrolled in this study. Of these 761 patients, 282 were diagnosed with acute coronary syndrome (ACS). We selected 65 patients with ACS-DM (ACS-DM group; mean age 64.88 years; 38 men) and 65 patients with ACS but without any comorbidities (ACS group; mean age 64.68 years; 38 men); the two groups were matched by age and sex. We determined four circulating ceramides in 130 plasma samples: Cer(d18:1/16:0), Cer(d18:1/18:0), Cer(d18:1/24:1), and Cer(d18:1/24:0). The ceramides in plasma samples from patients with ACS and those from patients with ACS-DM were compared. Pearson correlation coefficients between individual ceramides and traditional cardiovascular risk factors for the whole study population were calculated. Multiple logistic regression models were used to evaluate the relativity between the ceramide and ACS-DM.

Results: Compared with the ACS group, the levels of Cer(d18:1/16:0), Cer(d18:1/18:0), and Cer(d18:1/24:1) and their ratios to Cer(d18:1/24:0) were higher in the ACS-DM group and Cer(d18:1/24:0) was lower in the ACS-DM group ($P < 0.05$). Correlation analysis demonstrated mild-to-moderate correlations of ceramide and traditional cardiovascular risk factors. There were relatively strong correlations of Cer(d18:1/18:0) and Cer(d18:1/24:1) with C-reactive protein, blood lipids, fasting blood glucose, and glycated hemoglobin A_1c. In multiple logistic regression models, Cer(d18:1/18:0) [odds ratio (OR) 2.396; 95% confidence interval (CI) 1.103–5.205; $P = 0.027$], Cer(d18:1/24:1) (OR 2.826; 95% CI 1.158–6.896; $P = 0.023$), Cer(d18:1/18:0)/Cer(d18:1/24:0) (OR 2.242; 95% CI 1.103–4.555; $P = 0.026$), and Cer(d18:1/24:1)/Cer(d18:1/24:0) (OR 2.673; 95% CI 1.225–5.836; $P = 0.014$) were positively correlated with ACS-DM,

and Cer(d18:1/24:0) (OR 0.200; 95% CI 0.051–0.778; P = 0.020) was negatively correlated with ACS-DM.

Conclusion: Circulating ceramides are positively correlated with the risk of ACS-DM comorbidity. These results give a new insight into the pathogenesis of ACS-DM comorbidity and could provide new options for risk estimation.

Keywords: ceramide, acute coronary syndrome with type 2 diabetes mellitus, comorbidity, cardiometabolic diseases, risk factors

INTRODUCTION

The serum concentration of lipids is used to assess the risk of atherosclerotic heart disease. The level of low-density lipoprotein cholesterol (LDL-C) is closely related to atherosclerosis and acute coronary events. Previous studies have indicated that distinct ceramide species are closely related to cardiovascular death in patients with coronary heart disease (CHD). Ceramide molecules Cer(d18:1/16:0), which is abbreviated to Cer16:0; Cer(d18:1/18:0), which is abbreviated to Cer18:0; Cer(d18:1/24:1), which is abbreviated to Cer24:1; and their ratios to Cer(d18:1/24:0), which is abbreviated to Cer24:0, have been investigated as new risk stratification factors in patients with CHD (Meeusen et al., 2017; Peterson et al., 2018). In patients with CHD, a high level of Cer16:0, low level of Cer24:0, and a high Cer16:0/Cer24:0 ratio in plasma are related directly to cardiovascular mortality (Tarasov et al., 2014; Laaksonen et al., 2016). Accumulating evidence has shown that ceramides are closely related to the pathological process of type 2 diabetes mellitus (DM) and its complications (Galadari et al., 2013; Muilwijk et al., 2020).

Coronary heart disease is the main cause of mortality worldwide, resulting in more than 7 million deaths every year. Acute coronary syndrome (ACS) is a severe type of CHD associated with substantial mortality. DM is the main risk factor contributing to CHD, being regarded as having an equivalent risk to CHD (Juutilainen et al., 2005). Over 425 million people worldwide have DM. The number of adults in China with DM has reached 114 million, and China remains the country with the largest number of patients with DM (Cho et al., 2018). Cardiovascular events in patients with CHD and DM are five to six times higher than in patients with CHD alone (Høfsten et al., 2009).

Coronary heart disease and DM are both metabolic diseases and have mutual pathological mechanisms, but the pathological mechanism of the comorbidity is still unclear. Abnormal glucose and lipid metabolism is the pathological basis of many metabolic diseases. The pathophysiological alterations related to DM promote the development of CHD, the important driving mechanisms of which include oxidative stress, alterations in calcium metabolism, the inflammatory response, endothelial dysfunction, and autophagy (Yahagi et al., 2016; Zhang et al., 2018). Although our understanding of the pathogenesis of this comorbidity is increasing, the incidence of cardiovascular death in patients with acute coronary syndrome and type 2 diabetes mellitus (ACS-DM) remains high, and there is a lack of more effective risk stratification and prediction biomarkers for patients with ACS-DM.

It is not known whether the levels of ceramides are higher in patients with comorbid ACS-DM. Therefore, we measured the plasma concentrations of ceramides in patients with ACS-DM to ascertain if they could be novel cardiometabolic biomarkers for ACS-DM.

MATERIALS AND METHODS

Ethics Approval of the Research Protocol

This study was approved by the ethics committee of the PLA General Hospital. All patients gave written informed consent.

Participants

A total of 761 patients with CHD were admitted to the Cardiology Department of PLA General Hospital from March to August 2018. The inclusion criteria were: (i) patients aged 18 years or older and diagnosed as having ACS according to the ACS diagnostic criteria and (ii) patients had a complete clinical data record. According to the inclusion criteria, 401 adult patients were enrolled in the study. The exclusion criteria were: chronic heart failure, acute cerebrovascular disease, moderate-to-severe renal dysfunction (estimated glomerular filtration rate (eGFR) $<$ 60 mL/min/1.73 m^2), prolonged bedridden status, mental illness, and malignant tumor. Considering the effect of disease on ceramide levels, 45 patients with chronic heart failure and 12 patients with acute cerebrovascular disease were excluded. After excluding another 62 patients with moderate-to-severe renal dysfunction, 282 participants with ACS were enrolled in the study. Among these, there were 65 patients with ACS-DM, who were selected as the experimental group (ACS-DM group), and 65 patients with only ACS (ACS group), who were selected as the control group after matching for age and sex with patients with ACS-DM. According to a previous study (Yao et al., 2019), ceramide levels were associated with ACS with an odds ratio (OR) of 3.0. According to the sample size calculation formula for a paired case–control study, the sample size required was calculated to be 56 patients by using PASS software (proportioning, two related proportions; tests for two correlated proportions, McNemar test and OR). Consequently, 65 patients in each group met the sample size requirements; therefore, 130 patients were finally selected as the study cohort. Among them, 65 patients (mean age 64.88 years, range 34–84 years; 38 men) were in the ACS-DM group, and 65 patients

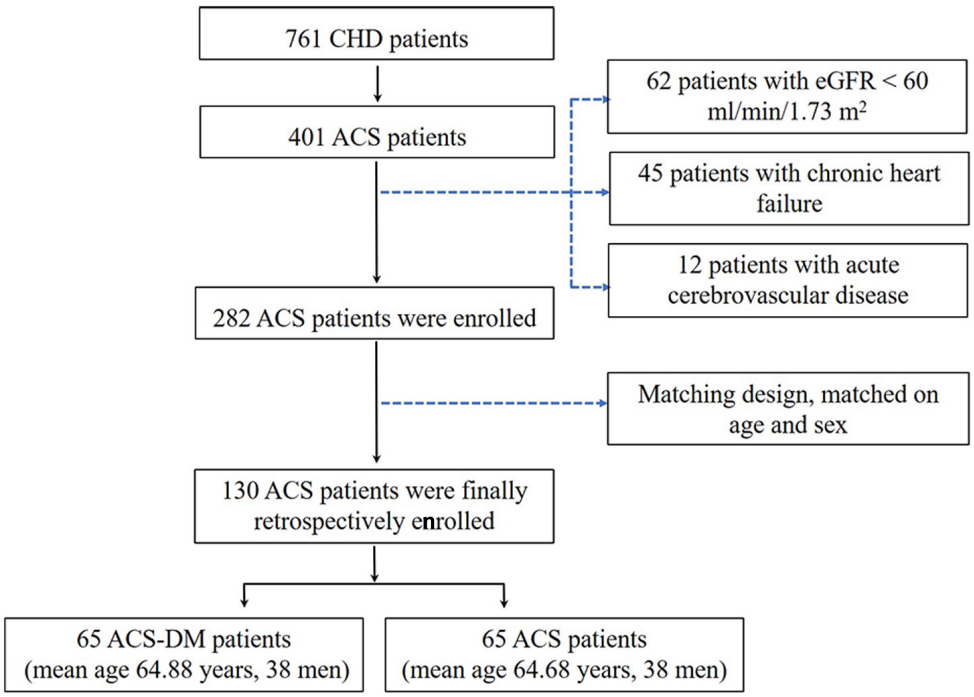

FIGURE 1 | Study frame diagram. ACS, acute coronary syndrome; CHD, coronary heart disease; eGFR, estimated glomerular filtration rate.

(mean age 64.68 years, range 34–86 years; 38 men) were in the ACS group (**Figure 1**).

Data Collection

Patients' demographic characteristics, lifestyle information, and medication use were obtained by review of medical records. The definition of "smoking" is having smoked more than 1 cigarette per day for over 1 year. Patients' body mass index (BMI) was also calculated, and blood pressure was measured using the right arm of seated participants by mercury sphygmomanometer.

Variable Biomarkers Determination

Blood samples were obtained with EDTA anticoagulation between 6:00 and 7:00 after patients fasted overnight. Samples were stored at 4°C for less than 1 h, and then the plasma samples were frozen at −80°C. Concentrations of fasting blood glucose (FBG), uric acid, blood lipid, and C-reactive protein (CRP) were measured by enzymatic assays (Roche Diagnostics, Mannheim, Germany). The glycated hemoglobin A_1c (HbA_1c) level was tested using high-performance liquid chromatography. The concentration of creatinine was determined by an enzymatic assay (Roche Diagnostics) on an autoanalyzer (7600; Hitachi, Tokyo, Japan). N-terminal pro-type-B natriuretic peptide (NT-proBNP) was measured by an electro-chemiluminescence immunoassay (Roche Diagnostics). The concentration of high-sensitivity cardiac troponin T (hs-cTnT) was measured on an E170 autoanalyzer (Modular Analytics; Roche Diagnostics) (Xiao et al., 2017).

Quantification of Ceramides

The levels of ceramides were determined from the available plasma samples (n = 130). We used liquid chromatography–tandem mass spectrometry (LC-MS/MS) to quantitatively and simultaneously measure the four circulating ceramides in human plasma (Kauhanen et al., 2016). In short, the deuterated internal standards were added to 10 μL plasma: D7-Cer16:0, D7-Cer18:0, D7-Cer24:0, and D7-Cer24:1. The plasma levels of Cer16:0, Cer18:0, Cer24:0, and Cer24:1 were quantified on a Triple Quad™ 3200 (Sciex, Framingham, MA, United States). A 5 μL sample was added, then the ceramide was separated on an Acquity UPLC I-Class column (Waters, Milford, MA, United States) using a 5 min gradient. Quantification was evaluated by calibration line samples containing known amounts of synthetic Cer16:0, Cer18:0, Cer24:0, and Cer24:1 and the deuterated standards. We calculated and plotted the peak area ratios of ceramides to the corresponding deuterated form according to the added ceramide concentration. According to the measured peak area ratios, the plasma concentration of ceramides was calculated by the individual fitting linear regression equation. The final concentration of ceramide is expressed in μmol/L.

Definition of Variables

ACS refers to unstable angina (UA), non-ST elevated myocardial infarction (NSTEMI), and ST elevated myocardial infarction (STEMI). The diagnostic criteria for ACS are according to a comprehensive examination of clinical characteristics, including biomarkers of myocardial injury and an electrocardiogram

(ECG). Unstable angina is defined as ischemic symptoms without increased biomarkers but with transient changes on the ECG. Myocardial infarction (MI) refers to myocardial necrosis during acute myocardial ischemia. The difference between STEMI and NSTEMI is whether the ST segment is elevated or not on the ECG (Anderson et al., 2007; Levine et al., 2016).

Hypertension was defined as systolic blood pressure (SBP) ≥ 140 mmHg, diastolic blood pressure (DBP) ≥ 90 mmHg, or taking antihypertensive medication. The diagnostic criteria of DM were FBG ≥ 7.0 mmol/L, HbA_1c ≥ 6.5%, non-fasting glucose ≥ 11.1 mmol/L, or taking antihyperglycemic medication (Cosentino et al., 2020). The eGFR was calculated using eGFR (mL/min/1.73 m^2) = 175 × plasma creatinine$^{-1.234}$ × age$^{-0.179}$ × 0.79 (if female) (Ma et al., 2006).

Statistical Analyses

Continuous variables were expressed as the mean ± standard deviation or median, and categorical variables were expressed as percentages. Differences in risk factors at baseline and clinical characteristics between patients with ACS and those with ACS-DM were compared by Chi-squared test or Student's *t*-test. Continuous variables in the skewness distribution were compared with the Wilcoxon rank sum test. Pearson correlation coefficients between individual ceramides and traditional cardiovascular risk factors for the whole study population were calculated. Multiple logistic regression analysis was used to assess the relationship between the concentration of ceramide and the risk of ACS-DM. The ceramide concentration was logarithm transformed. The basic model was adjusted for age and sex. The multi-model was further adjusted for smoking, BMI, hypertension, SBP, uric acid, triglycerides (TG), high-density lipoprotein cholesterol (HDL-C), LDL-C, CRP, HbA_1c, and lipid-lowering medication. The multi-model + hs-cTnT was further adjusted for hs-cTnT based on the multi-model. The receiver operating characteristic (ROC) curve was used to assess the accuracy of the ceramide concentration for the prediction of ACS-DM; the discrimination was assessed with the area under curve (AUC).

Analyses were implemented with SPSS 23.0 (IBM, NY, United States). $P < 0.05$ was regarded as significant.

RESULTS

Clinical Characteristics at Baseline

A total of 130 patients were enrolled in this study. The characteristics of the patients according to disease status (ACS group and ACS-DM group) are summarized in **Table 1**. Higher plasma levels of glucose, uric acid, TG, and CRP and lower levels of DBP and HDL-C were associated with ACS-DM. The proportion of patients with MI between the ACS group and the ACS-DM group did not differ, but the levels of hs-cTnT were higher in the ACS-DM group. Compared with the ACS group, the levels of Cer16:0, Cer18:0, and Cer24:1 and their ratios to Cer24:0 in the ACS-DM group were higher, whereas the level of Cer24:0 was lower (**Figure 2**).

TABLE 1 | Clinical characteristics of the subjects categorized by disease status.

Characteristic	ACS group (*n* = 65)	ACS-DM group (*n* = 65)	*P*-value
Demographic			
Age (years)	64.68 ± 10.17	64.88 ± 10.71	0.913
Male, *n* (%)	38 (58.5)	38 (58.5)	1.000
BMI (kg/m^2)	25.32 ± 3.80	25.16 ± 3.70	0.817
Smoking, *n* (%)	33(50.8)	34(52.3)	0.861
MI, *n* (%)	32(49.2)	33(50.8)	0.861
Stroke, *n* (%)	8(12.3)	12(18.5)	0.331
Family history of CHD, *n* (%)	8(12.3)	15(23.1)	0.108
Hypertension, *n* (%)	41(63.1)	49(75.4)	0.128
Lipid-lowering medication, *n* (%)	49 (75.4)	51 (78.5)	0.677
Antihypertensive medication, *n* (%)	44 (67.7)	48 (73.8)	0.441
Systolic BP (mmHg)	133.0 ± 21.2	131.9 ± 19.2	0.755
Diastolic BP (mmHg)	76.5 ± 12.2	71.5 ± 10.7	0.014
Laboratory value			
TC (mmol/L)	3.80 ± 1.04	3.94 ± 1.22	0.484
TG (mmol/L)	1.22 ± 0.56	1.78 ± 1.07	< 0.001
HDL-C (mmol/L)	1.14 ± 0.27	1.00 ± 0.29	0.005
LDL-C (mmol/L)	2.37 ± 1.01	2.45 ± 1.06	0.652
FBG (mmol/L)	5.49 ± 0.70	10.75 ± 4.68	< 0.001
HbA_1c (%)	5.74 ± 0.42	7.70 ± 1.56	< 0.001
Uric acid (μmol/L)	324.11 ± 97.56	363.61 ± 116.06	0.038
CRP (mg/dL)	0.81 (0.01, 9.28)	1.64 (0.01, 16.00)	0.023
hs-cTnT (ng/mL)	1.494 (0.003, 31.490)	3.223 (0.005, 57.240)	0.019
NT-proBNP (pg/mL)	2490.2 (35.8, 35 000.0)	2833.4 (21.3, 35 000.0)	0.766
eGFR (mL/min/1.73 m^2)	95.3 ± 28.6	100.2 ± 76.3	0.739

Values are reported as n (%), mean ± SD, or median (interquartile range). BMI, body mass index; MI, myocardial infarction; CHD, coronary heart disease; BP, blood pressure; TC, total cholesterol; TG, triglyceride; HDL-C, high-density lipoprotein cholesterol; LDL-C, low-density lipoprotein cholesterol; FBG, fasting blood glucose; HbA_1c, glycated hemoglobin A_1c; CRP, C-reactive protein; hs-cTnT, high-sensitivity cardiac troponin T; NT-proBNP, N-terminal pro-type-B natriuretic peptide; eGFR, estimated glomerular filtration rate.

Subgroup Analyses

According to whether or not they had MI, patients were divided into the UA and MI subgroups and circulating ceramides in patients with ACS and those with ACS-DM were compared. In the UA subgroup, the levels of Cer18:0, Cer24:1, and Cer16:0/Cer24:0 in patients with ACS-DM were higher (n = 32) than those in patients with ACS (n = 33) ($P < 0.05$). In the MI subgroup, compared with patients with ACS (n = 32), the levels of Cer24:1, Cer16:0/Cer24:0, Cer18:0/Cer24:0, and Cer24:1/Cer24:0 were higher in patients with ACS-DM (n = 33), and the levels of Cer24:0 were lower in patients with ACS-DM ($P < 0.05$) (**Figure 3**).

Correlation of Ceramides and Traditional Cardiovascular Risk Factors

The Pearson correlation coefficients for the levels of individual ceramides and those for traditional cardiovascular risk factors for the whole study population were calculated. Correlation

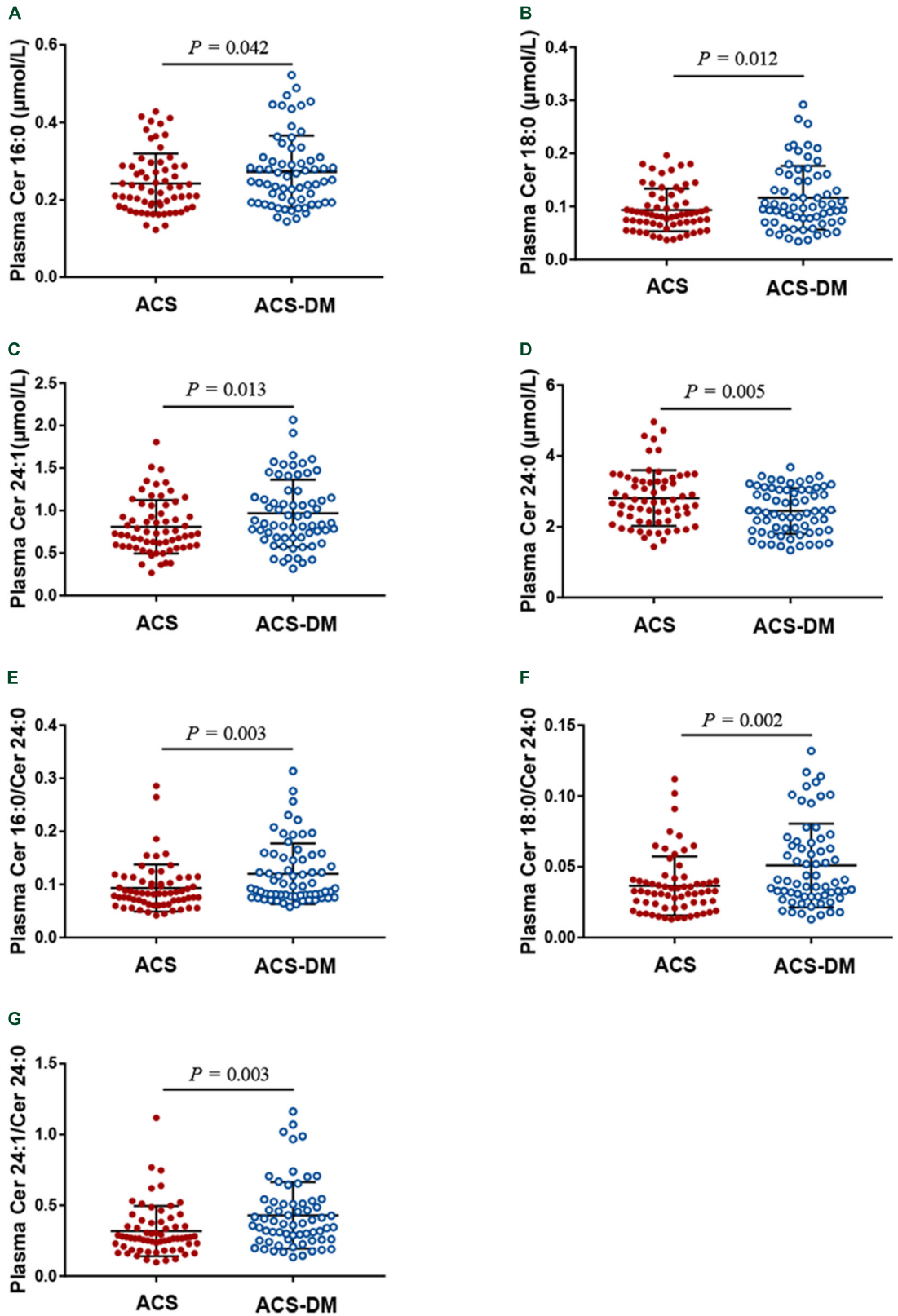

FIGURE 2 | (A–G) A comparison of the levels of ceramides in patients with acute coronary syndrome (ACS) and those with comorbid acute coronary syndrome and type 2 diabetes mellitus (ACS-DM).

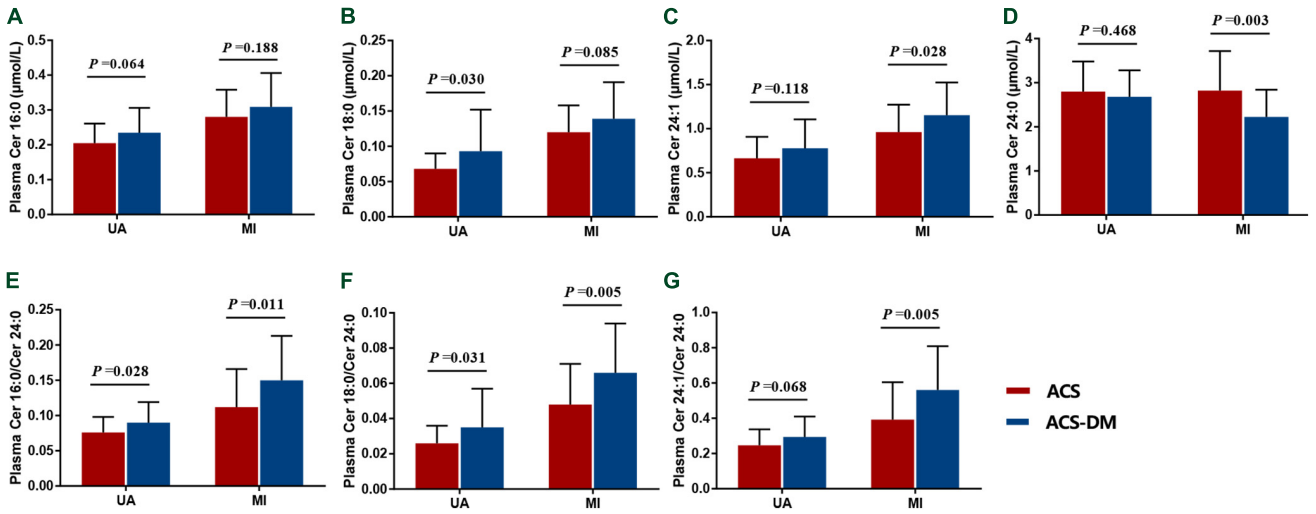

FIGURE 3 | (A–G) Subgroup analysis of the levels of ceramides in patients with acute coronary syndrome (ACS) compared with those with comorbid acute coronary syndrome and type 2 diabetes mellitus (ACS-DM). MI, myocardial infarction; UA, unstable angina.

analysis demonstrated that the levels of ceramides and their ratios had a mild-to-moderate correlation with those of traditional cardiovascular risk factors. Of note was the relatively strong correlation of Cer18:0 and Cer24:1 with the levels of CRP, blood lipids, FBG, HbA_1c, and hs-cTnT (**Table 2**).

Relationship Between Ceramides and the ACS-DM Group

Stepwise multiple logistic regression analysis revealed that the ceramide levels are significantly related to ACS-DM. In the basic model and the multi-model, the relationship between the ceramide level and the ACS-DM group was significant ($P < 0.05$). In the multi-model + hs-cTnT, Cer(d18:1/18:0) [OR 2.396; 95% confidence interval (CI) 1.103–5.205; $P = 0.027$], Cer(d18:1/24:1) (OR 2.826; 95% CI 1.158–6.896; $P = 0.023$), Cer(d18:1/18:0)/Cer(d18:1/24:0) (OR 2.242; 95% CI 1.103–4.555; $P = 0.026$), and Cer(d18:1/24:1)/Cer(d18:1/24:0) (OR 2.673; 95% CI 1.225–5.836; $P = 0.014$) were positively correlated with ACS-DM and Cer(d18:1/24:0) (OR 0.200; 95% CI 0.051–0.778; $P = 0.020$) was negatively correlated with ACS-DM, whereas the association of Cer16:0 and Cer16:0/Cer24:0 with ACS-DM disappeared. The significance of the ceramide levels in the adjusted models (basic model, multi-model, and multi-model + hs-cTnT) is presented in **Table 3**.

Analyses of ROC Curves on Ceramide Levels in Patients With ACS-DM

Analyses of ROC curves indicated that the level of ceramides (except for Cer16:0 and Cer16:0/Cer24:0) had reasonable accuracy for the prediction of ACS-DM (**Figures 4A,B**).

DISCUSSION

We demonstrated in patients with ACS-DM and patients with ACS matched by age and sex that ceramides were associated with patients with ACS-DM independent of sex, age, or other risk factors of vascular disease. The levels of Cer18:0 and Cer24:1 and the ratios to Cer24:0 had reasonable accuracy for ACS-DM prediction. Cer18:0 and

TABLE 2 | Spearman rank correlation coefficients between ceramides and traditional cardiovascular risk factors for the whole study population (n = 130).

	Age	TC	TG	HDL-C	LDL-C	CRP	FBG	HbA_1c	NT-proBNP	hs-cTnT
Cer(d18:1/16:0)	n.s.	0.401**	0.280**	−0.176	0.432**	0.349**	0.315**	0.235**	0.438**	0.440**
Cer(d18:1/18:0)	n.s.	0.340**	0.285**	−0.212*	0.395**	0.361**	0.306**	0.255**	0.390**	0.496**
Cer(d18:1/24:1)	n.s.	0.317**	0.280**	−0.277**	0.357**	0.370**	0.363**	0.300**	0.415**	0.414**
Cer(d18:1/24:0)	−0.307**	0.266**	0.203*	n.s.	0.276**	−0.260**	−0.200*	n.s.	−0.286**	−0.186*
Cer(d18:1/16:0)/Cer(d18:1/24:0)	0.224*	n.s.	n.s.	−0.217*	n.s.	0.431**	0.370**	0.240**	0.556**	0.455**
Cer(d18:1/18:0)/Cer(d18:1/24:0)	n.s.	n.s.	n.s.	−0.245**	0.204*	0.417**	0.341**	0.246**	0.475**	0.494**
Cer(d18:1/24:1)/Cer(d18:1/24:0)	n.s.	n.s.	n.s.	−0.273**	n.s.	0.420**	0.388**	0.289**	0.498**	0.429**

**P-value for comparison <0.05, **P-value for comparison <0.01. Non-significant correlation (P > 0.05) is marked with n.s. TC, total cholesterol; TG, triglyceride; HDL-C, high-density lipoprotein cholesterol; LDL-C, low-density lipoprotein cholesterol; CRP, C-reactive protein; FBG, fasting blood glucose; HbA_1c, glycated hemoglobin A_1c; NT-proBNP, N-terminal pro-type-B natriuretic peptide; hs-cTnT, high-sensitivity cardiac troponin T.*

TABLE 3 | Association between plasma ceramides and the risk of ACS-DM.

	Model	OR	95% CI	*P*-value
Cer(d18:1/16:0)	Basic	3.214	1.038–9.955	0.043
	Multi	3.167	1.017–9.863	0.047
	Multi + hs-cTnT	0.397	0.051–3.120	0.380
Cer(d18:1/18:0)	Basic	2.270	1.063–4.847	0.034
	Multi	2.227	1.040–4.771	0.039
	Multi + hs-cTnT	2.396	1.103–5.205	0.027
Cer(d18:1/24:1)	Basic	2.741	1.135–6.616	0.025
	Multi	2.698	1.115–6.530	0.028
	Multi + hs-cTnT	2.826	1.158–6.896	0.023
Cer(d18:1/24:0)	Basic	0.191	0.052–0.698	0.012
	Multi	0.187	0.050–0.708	0.014
	Multi + hs-cTnT	0.200	0.051–0.778	0.020
Cer(d18:1/16:0) /Cer(d18:1/24:0)	Basic	4.614	1.785–11.924	0.002
	Multi	4.084	1.486–11.219	0.006
	Multi + hs-cTnT	1.531	0.295–7.940	0.612
Cer(d18:1/18:0) /Cer(d18:1/24:0)	Basic	2.825	1.438–5.550	0.003
	Multi	2.425	1.153–5.101	0.020
	Multi + hs-cTnT	2.242	1.103–4.555	0.026
Cer(d18:1/24:1) /Cer(d18:1/24:0)	Basic	3.263	1.544–6.897	0.002
	Multi	2.824	1.307–6.100	0.008
	Multi + hs-cTnT	2.673	1.225–5.836	0.014

The table shows the OR and 95% CI of the incidence of comorbid acute coronary syndrome and type 2 diabetes mellitus (ACS-DM) associated with an increase in plasma log-transformed ceramides. The ORs were estimated from analyses using logistic regression. The basic model was adjusted for age and sex. The multi-model was futher adjusted for hypertension, smoking, BMI, systolic BP, uric acid, TG, HDL-C, LDL-C, CRP, HbA1c, lipid-lowering medication. OR, odds ratio; CI, confidence interval; Cer, Ceramide; hs-cTnT, highly sensitive cardiac troponin T; BMI, body mass index; BP, blood pressure; TG, triglycerides; HDL-C, high-density lipoprotein cholesterol; LDL-C, low-density lipoprotein cholesterol; CRP, C-reactive protein; HbA$_1$c, glycated hemoglobin A$_1$c.

Cer24:1 and their ratios to Cer24:0 were positively correlated with ACS-DM, and Cer24:0 was negatively correlated with ACS-DM. These results suggest that ceramides could be new biomarkers of ACS-DM.

Recent studies have demonstrated that ceramides are associated with an atherosclerotic process (Bismuth et al., 2008). Elevated levels of ceramides are also related to multiple cardiovascular risk factors, such as hypertension (Mielke et al., 2019), heart failure (Lemaitre et al., 2019), and DM (Neeland et al., 2018). Increases in levels of ceramides are predictive of cardiovascular events and are also independently correlated with adverse cardiovascular events in patients with and without CHD. The predictive value of ceramides is better than that of LDL-C levels (Meeusen et al., 2018). Gierens et al. explained the potential cause of this phenomenon. They confirmed that interleukin-6 (IL-6) enhances LDL receptor activity in the liver during the inflammatory response, subsequently increasing the elimination of circulating LDL-C. Thus, the acute inflammatory response in patients with ACS may increase the clearance of LDL-C, leading to a decrease in the circulating LDL-C concentration and affecting the accuracy of risk prediction (Lubrano et al., 2015). Determination of ceramide levels using a high-throughput methodology such as LC-MS/MS is efficient and convenient. Accurate quantification of ceramides can be achieved by isotope-labeled standards, enabling ceramides to be new potential predictors of cardiovascular events. Long-chain ceramides have the effect of promoting apoptosis, and very-long-chain ceramides (Cer24;0) have an anti-apoptotic effect (Grösch et al., 2012). Consistent with the present study, long-chain species (Cer16:0 and Cer18:0) increased cardiovascular risk, and very-long-chain (Cer24:0) species were cardioprotective. Also, in patients with established CHD, Cer24:0 appears to be cardioprotective, and the increase in Cer24:0/Cer24:1 can lower the risk of cardiovascular events in patients with or without DM (Menuz et al., 2009). Our results are consistent with these studies.

Our study demonstrated that the levels of Cer16:0, Cer18:0, and Cer24:1 and their ratios to Cer24:0 in patients with ACS-DM were higher than those in patients with ACS. The levels of Cer24:0, Cer18:0/Cer24:0, and Cer24:1/Cer24:0 had a relatively strong correlation with ACS-DM. The levels of Cer18:0 and Cer24:1 were associated with the levels of CRP, blood lipids, FBG, and HbA$_1$c; these results are consistent with a previous study

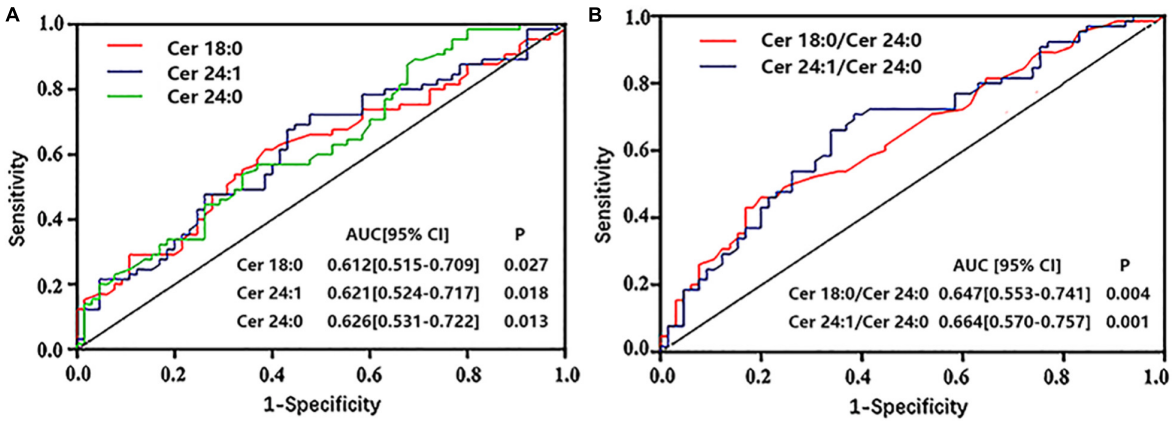

FIGURE 4 | (A,B) Receiver operator characteristic (ROC) curves of ceramides to predict comorbid acute coronary syndrome and type 2 diabetes mellitus. ROC analysis was performed to determine the sensitivity and specificity of the value. AUC, area under the curve; CI, confidence interval.

(Havulinna et al., 2016). Cer18:0 and Cer24:1 may be the main risk factors and pathogenic factors for ACS-DM. The Cer24:0 level was negatively correlated with ACS-DM and appeared to have a protective effect in patients with ACS-DM.

Ceramides are complex sphingolipids widely expressed in cells and lipoproteins. The increase in ceramide content in LDL promotes the atherosclerotic process of the vascular wall (Li et al., 2014). Ceramides are involved in biological processes that may influence atherosclerosis and cardiovascular events, including oxidative stress apoptosis, endothelial dysfunction, inflammation, lipotoxicity, and insulin resistance (Alessenko et al., 2018). The inflammatory cytokines interferon-γ and IL-6 promote ceramide synthesis. Ceramides participate in endothelial damage and platelet activation (Marathe et al., 1998). Ceramides are associated with vulnerable atherosclerotic plaques and participate in the process of atherosclerosis, including lipoprotein aggregation and uptake, the inflammatory response, endothelial damage, and apoptosis. They also inhibit the production of apolipoprotein E in macrophages and lead to cholesterol accumulation in macrophage-derived foam cells (Lucic et al., 2007). The levels of ceramides increased with accumulated lipid loading and inflammation in patients with DM, and ceramides can directly regulate β-cell apoptosis and induce insulin resistance (Kayser et al., 2019). Circulating leptin levels were significantly increased in insulin resistance, which is associated with cardiac dysfunction (Ren and Relling, 2006). The potential toxicity of ceramides and their ability to inhibit contraction in cardiomyocytes are related to exposure time (Relling et al., 2003). Several studies have demonstrated that different ceramide species have different effects. For instance, cell experiments have shown that Cer16:0 can promote apoptosis, while Cer24:0 appears to protect against apoptosis. Evidence is also accumulating on the functions of ceramides with different chain lengths. Increases in Cer16:0 but not Cer24:0 are involved in insulin resistance. C2 ceramide reduced the damage to cardiac function caused by a high glucose concentration (Colligan et al., 2002). In brief, ceramides have a mutual pathologic mechanism in patients with ACS and those with DM that increases the risk of cardiovascular events. Ceramides may be potential targets for the treatment of CHD in patients with DM.

LIMITATIONS

There were four main limitations to this study. First, our study was an observational study, unable to establish a causal relationship between ceramides and ACS-DM. Because of this, it is unclear whether cardiovascular risk treatment based on ceramides would improve clinical benefits. Second, although a paired design was used to reduce confounding factors, the sample size was relatively small. The possibility of residual confounding from imprecisely measured or unmeasured variables cannot be ruled out. Third, our study cohort comprised primarily a Chinese Han population. Therefore, it is necessary to conduct further research on an ethnically more diverse population. Fourth, the AUC showed that the individual discriminative power of ceramides was low for ACS-DM detection (AUC < 0.70). Therefore, our observations need to be further confirmed in longitudinal studies with a larger sample.

CONCLUSION

In conclusion, circulating ceramides are positively correlated with the risk of ACS-DM comorbidity. However, longitudinal follow-up studies are still needed to evaluate the causal relationship between ceramides and comorbid ACS-DM. The results of this study demonstrated new insights into the pathogenesis of comorbid ACS-DM. Circulating ceramides may provide new options for risk evaluation as novel biomarkers of cardiometabolic diseases.

DATA AVAILABILITY STATEMENT

The raw data supporting the conclusions of this article will be made available by the authors, without undue reservation.

ETHICS STATEMENT

The studies involving human participants were reviewed and approved by The ethics committee of Chinese PLA General Hospital (Beijing, China). The patients/participants provided their written informed consent to participate in this study.

AUTHOR CONTRIBUTIONS

FC designed the experiments. RC, ZF, SL, MX, JZ, DH, WH, and LY performed the experiments. RC, ZF, and LY analyzed the data. RC prepared the manuscript. RC, YW, and LF supervised data collection. All authors have contributed to the study and approved the manuscript.

FUNDING

This work was supported by the National Key R&D Program of China (2016YFC1300300 and 2016YFA0100903), the Key Project of Chinese Military Health Care Projects (18BJZ32), the National Natural Science Foundation of China (81530058), and the Science Foundation of the PLA General Hospital (2018XXFC-9).

ACKNOWLEDGMENTS

We would like to thank the Department of Laboratory Medicine of the PLA General Hospital for their help in biomarker detection.

REFERENCES

Alessenko, A. V., Lebedev, ÀÒ, and Kurochkin, I. N. (2018). The role of sphingolipids in cardiovascular pathologies. *Biomed. Khim.* 64, 487–495. doi: 10.18097/PBMC20186406487

Anderson, J. L., Adams, C. D., Antman, E. M., Bridges, C. R., Califf, R. M., Casey, D. E. Jr., et al. (2007). ACC/AHA 2007 guidelines for the management of patients with unstable angina/non-ST-elevation myocardial infarction: a report of the american college of cardiology/american heart association task force on practice guidelines (Writing committee to revise the 2002 guidelines for the management of patients with unstable angina/non-ST-elevation myocardial infarction) developed in collaboration with the american college of emergency physicians, the society for cardiovascular angiography and interventions, and the society of thoracic surgeons endorsed by the American association of cardiovascular and pulmonary rehabilitation and the society for academic emergency medicine. *J. Am. Coll. Cardiol.* 50, e1–e157. doi: 10.1016/j.jacc.2007.02.013

Bismuth, J., Lin, P., Yao, Q., and Chen, C. (2008). Ceramide: a common pathway for atherosclerosis? *Atherosclerosis* 196, 497–504. doi: 10.1016/j.atherosclerosis.2007.09.018

Cho, N. H., Shaw, J. E., Karuranga, S., Huang, Y., da Rocha Fernandes, J. D., Ohlrogge, A. W., et al. (2018). IDF diabetes atlas: global estimates of diabetes prevalence for 2017 and projections for 2045. *Diabetes Res. Clin. Pract.* 138, 271–281. doi: 10.1016/j.diabres.2018.02.023

Colligan, P. B., Relling, D. P., and Ren, J. (2002). Ceramide attenuates high glucose-induced cardiac contractile abnormalities in cultured adult rat ventricular myocytes. *Cell. Mol. Biol.* 48, OL251-7.

Cosentino, F., Grant, P. J., Aboyans, V., Bailey, C. J., Ceriello, A., Delgado, V., et al. (2020). 2019 ESC Guidelines on diabetes, pre-diabetes, and cardiovascular diseases developed in collaboration with the EASD. *Eur. Heart J.* 41, 255–323. doi: 10.1093/eurheartj/ehz486

Galadari, S., Rahman, A., Pallichankandy, S., Galadari, A., and Thayyullathil, F. (2013). Role of ceramide in diabetes mellitus: evidence and mechanisms. *Lipids Health Dis.* 12:98. doi: 10.1186/1476-511x-12-98

Grösch, S., Schiffmann, S., and Geisslinger, G. (2012). Chain length-specific properties of ceramides. *Prog. Lipid Res.* 51, 50–62. doi: 10.1016/j.plipres.2011.11.001

Havulinna, A. S., Sysi-Aho, M., Hilvo, M., Kauhanen, D., Hurme, R., Ekroos, K., et al. (2016). Circulating ceramides predict cardiovascular outcomes in the population-based FINRISK 2002 cohort. *Arterioscler. Thromb. Vasc. Biol.* 36, 2424–2430. doi: 10.1161/ATVBAHA.116.307497

Høfsten, D. E., Løgstrup, B. B., Møller, J. E., Pellikka, P. A., and Egstrup, K. (2009). Abnormal glucose metabolism in acute myocardial infarction: influence on left ventricular function and prognosis. *JACC Cardiovasc. Imaging* 2, 592–599. doi: 10.1016/j.jcmg.2009.03.007

Juutilainen, A., Lehto, S., Ronnemaa, T., Pyorala, K., and Laakso, M. (2005). Type 2 diabetes as a "Coronary Heart Disease Equivalent": an 18-year prospective population-based study in Finnish subjects. *Diabetes Care* 28, 2901–2907. doi: 10.2337/diacare.28.12.2901

Kauhanen, D., Sysi-Aho, M., Koistinen, K. M., Laaksonen, R., Sinisalo, J., and Ekroos, K. (2016). Development and validation of a high-throughput LC-MS/MS assay for routine measurement of molecular ceramides. *Anal. Bioanal. Chem.* 408, 3475–3483. doi: 10.1007/s00216-016-9425-z

Kayser, B. D., Prifti, E., Lhomme, M., Belda, E., Dao, M. C., Aron-Wisnewsky, J., et al. (2019). Elevated serum ceramides are linked with obesity-associated gut dysbiosis and impaired glucose metabolism. *Metabolomics* 15:140. doi: 10.1007/s11306-019-1596-0

Laaksonen, R., Ekroos, K., Sysi-Aho, M., Hilvo, M., Vihervaara, T., Kauhanen, D., et al. (2016). Plasma ceramides predict cardiovascular death in patients with stable coronary artery disease and acute coronary syndromes beyond LDL-cholesterol. *Eur. Heart. J.* 37, 1967–1976. doi: 10.1093/eurheartj/ehw148

Lemaitre, R. N., Jensen, P. N., Hoofnagle, A., McKnight, B., Fretts, A. M., King, I. B., et al. (2019). Circ. *Heart Fail.* 12, e005708. doi: 10.1161/CIRCHEARTFAILURE.118.005708

Levine, G. N., Bates, E. R., Bittl, J. A., Brindis, R. G., Fihn, S. D., Fleisher, L. A., et al. (2016). 2016 ACC/AHA guideline focused update on duration of dual antiplatelet therapy in patients with coronary artery disease: a report of the american college of cardiology/american heart association task force on clinical practice guidelines: an update of the 2011 ACCF/AHA/SCAI guideline for percutaneous coronary intervention, 2011 ACCF/AHA guideline for coronary artery bypass graft surgery, 2012 ACC/AHA/ACP/AATS/PCNA/SCAI/STS guideline for the diagnosis and management of patients with stable ischemic heart disease, 2013 ACCF/AHA guideline for the management of ST-elevation myocardial infarction, 2014 AHA/ACC guideline for the management of patients with non-ST-elevation acute coronary syndromes, and 2014 ACC/AHA guideline on perioperative cardiovascular evaluation and management of patients undergoing noncardiac surgery. *Circulation* 134, e123–e155. doi: 10.1161/CIR.0000000000000404

Li, W., Yang, X., Xing, S., Bian, F., Yao, W., Bai, X., et al. (2014). Endogenous ceramide contributes to the transcytosis of oxLDL across endothelial cells and promotes its subendothelial retention in vascular wall. *Oxid. Med. Cell. Longev.* 2014:823071. doi: 10.1155/2014/823071

Lubrano, V., Gabriele, M., Puntoni, M. R., Longo, V., and Pucci, L. (2015). Relationship among IL-6, LDL cholesterol and lipid peroxidation. *Cell. Mol. Biol. Lett.* 20, 310–322. doi: 10.1515/cmble-2015-0020

Lucic, D., Huang, Z. H., Gu, D., Subbaiah, P. V., and Mazzone, T. (2007). Cellular sphingolipids regulate macrophage apolipoprotein E secretion. *Biochemistry* 46, 11196–11204. doi: 10.1021/bi701106v

Ma, Y. C., Zuo, L., Chen, J. H., Luo, Q., Yu, X. Q., Li, Y., et al. (2006). Modified glomerular filtration rate estimating equation for Chinese patients with chronic kidney disease. *J. Am. Soc. Nephrol.* 17, 2937–2944. doi: 10.1681/ASN.2006040368

Marathe, S., Schissel, S. L., Yellin, M. J., Beatini, N., Mintzer, R., Williams, K. J., et al. (1998). Human vascular endothelial cells are a rich and regulatable source of secretory sphingomyelinase. Implications for early atherogenesis and ceramide-mediated cell signaling. *J. Biol. Chem.* 273, 4081–4088. doi: 10.1074/jbc.273.7.4081

Meeusen, J. W., Donato, L. J., Bryant, S. C., Baudhuin, L. M., Berger, P. B., and Jaffe, A. S. (2018). Plasma Ceramides. *Arterioscler. Thromb. Vasc. Biol.* 38, 1933–1939. doi: 10.1161/ATVBAHA.118.311199

Meeusen, J. W., Donato, L. J., and Jaffe, A. S. (2017). Lipid biomarkers for risk assessment in acute coronary syndromes. *Curr. Cardiol. Rep.* 19:48. doi: 10.1007/s11886-017-0863-9

Menuz, V., Howell, K. S., Gentina, S., Epstein, S., Riezman, I., Fornallaz-Mulhauser, M., et al. (2009). Protection of *C. elegans* from anoxia by HYL-2 ceramide synthase. *Science* 324, 381–384. doi: 10.1126/science.1168532

Mielke, M. M., Syrjanen, J. A., Bui, H. H., Petersen, R. C., Knopman, D. S., Jack, C. R. Jr., et al. (2019). Elevated plasma ceramides are associated with higher white matter hyperintensity volume-brief Report. *Arterioscler. Thromb. Vasc. Biol.* 39, 2431–2436. doi: 10.1161/ATVBAHA.119.313099

Muilwijk, M., Goorden, S. M. I., Celis-Morales, C., Hof, M. H., Ghauharali-van der Vlugt, K., Beers-Stet, F. S., et al. (2020). Contributions of amino acid, acylcarnitine and sphingolipid profiles to type 2 diabetes risk among South-Asian Surinamese and Dutch adults. *BMJ Open Diabetes Res. Care* 8:e001003. doi: 10.1136/bmjdrc-2019-001003

Neeland, I. J., Singh, S., McGuire, D. K., Vega, G. L., Roddy, T., Reilly, D. F., et al. (2018). Relation of plasma ceramides to visceral adiposity, insulin resistance and the development of type 2 diabetes mellitus: the dallas heart study. *Diabetologia* 61, 2570–2579. doi: 10.1007/s00125-018-4720-1

Peterson, L. R., Xanthakis, V., Duncan, M. S., Gross, S., Friedrich, N., Völzke, H., et al. (2018). Ceramide remodeling and risk of cardiovascular events and mortality. *J. Am. Heart Assoc.* 7:e007931. doi: 10.1161/jaha.117.007931

Relling, D. P., Hintz, K. K., and Ren, J. (2003). Acute exposure of ceramide enhances cardiac contractile function in isolated ventricular myocytes. *Br. J. Pharmacol.* 140, 1163–1168. doi: 10.1038/sj.bjp.0705510

Ren, J., and Relling, D. P. (2006). Leptin-induced suppression of cardiomyocyte contraction is amplified by ceramide. *Peptides* 27, 1415–1419. doi: 10.1016/j.peptides.2005.11.022

Tarasov, K., Ekroos, K., Suoniemi, M., Kauhanen, D., Sylvänne, T., Hurme, R., et al. (2014). Molecular lipids identify cardiovascular risk and are efficiently lowered by simvastatin and PCSK9 deficiency. *J. Clin. Endocrinol. Metab.* 99, E45–E52. doi: 10.1210/jc.2013-2559

Xiao, W., Cao, R., Liu, Y., Wang, F., Bai, Y., Wu, H., et al. (2017). Association of high-sensitivity cardiac troponin T with mortality and cardiovascular events in a community-based prospective study in Beijing. *BMJ Open* 7:e013431. doi: 10.1136/bmjopen-2016-013431

Yahagi, K., Kolodgie, F. D., Lutter, C., Mori, H., Romero, M. E., Finn, A. V., et al. (2016). Pathology of human coronary and carotid artery atherosclerosis and vascular calcification in diabetes mellitus. *Arterioscler. Thromb. Vasc. Biol.* 37, 191–204. doi: 10.1161/atvbaha.116.306256

Yao, K., Wang, Y., Xu, D., Liu, X., Shen, C., Hu, W., et al. (2019). Effect of combined testing of ceramides with high-sensitive troponin T on the detection of acute coronary syndrome in patients with chest pain in China: a prospective observational study. *BMJ Open* 9:e028211. doi: 10.1136/bmjopen-2018-028211

Zhang, Y., Whaley-Connell, A. T., Sowers, J. R., and Ren, J. (2018). Autophagy as an emerging target in cardiorenal metabolic disease: from pathophysiology to management. *Pharmacol. Ther.* 191, 1–22. doi: 10.1016/j.pharmthera.2018.06.004

Conflict of Interest: The authors declare that the research was conducted in the absence of any commercial or financial relationships that could be construed as a potential conflict of interest.

Copyright © 2020 Cao, Fang, Li, Xu, Zhang, Han, Hu, Yan, Wang, Fan and Cao. This is an open-access article distributed under the terms of the Creative Commons Attribution License (CC BY). The use, distribution or reproduction in other forums is permitted, provided the original author(s) and the copyright owner(s) are credited and that the original publication in this journal is cited, in accordance with accepted academic practice. No use, distribution or reproduction is permitted which does not comply with these terms.

frontiers in Physiology

ORIGINAL RESEARCH
published: 30 September 2020
doi: 10.3389/fphys.2020.566410

Angiotensin II Decreases Endothelial Nitric Oxide Synthase Phosphorylation *via* AT_1R Nox/ROS/PP2A Pathway

Jing Ding[1,2†], Min Yu[1,2†], Juncai Jiang[1,2], Yanbei Luo[1,2], Qian Zhang[1,2], Shengnan Wang[3], Fei Yang[4], Alei Wang[1,2], Lingxiao Wang[1,2], Mei Zhuang[5], Shan Wu[6], Qifang Zhang[7], Yong Xia[8] and Deqin Lu[1,2]**

[1]Department of Pathophysiology, Guizhou Medical University, Guiyang, China, [2]Guizhou Provincial Key Laboratory of Pathogenesis and Drug Research on Common Chronic Diseases, Guizhou Medical University, Guiyang, China, [3]Department of Pathology, The Second Clinical Medical School of Inner Mongolia University for the Nationalities, Yakeshi, China, [4]Department of Cardiology, The Second Provincial People's Hospital of Gansu, Lanzhou, China, [5]Department of Cardiology, Affiliated Hospital of Guizhou Medical University, Guiyang, China, [6]Department of Neurology, Affiliated Hospital of Guizhou Medical University, Guiyang, China, [7]Key Laboratory of Medical Molecular Biology, Guizhou Medical University, Guiyang, China, [8]Davis Heart and Lung Research Institute, The Ohio State University College of Medicine, Columbus, OH, United States

OPEN ACCESS

Edited by:
Jun Ren,
University of Washington,
United States

Reviewed by:
Si Jin,
Huazhong University of Science and Technology, China
Thiago Bruder Do Nascimento,
University of Pittsburgh,
United States

***Correspondence:**
Deqin Lu
dqlu91@hotmail.com
Yong Xia
yong.xia@osumc.edu

†These authors have contributed equally to this work

Specialty section:
This article was submitted to Vascular Physiology, a section of the journal Frontiers in Physiology

Received: 03 June 2020
Accepted: 08 September 2020
Published: 30 September 2020

Citation:
Ding J, Yu M, Jiang J, Luo Y, Zhang Q, Wang S, Yang F, Wang A, Wang L, Zhuang M, Wu S, Zhang Q, Xia Y and Lu D (2020) Angiotensin II Decreases Endothelial Nitric Oxide Synthase Phosphorylation via AT_1R Nox/ROS/PP2A Pathway. Front. Physiol. 11:566410. doi: 10.3389/fphys.2020.566410

Increasing evidences suggest that angiotensin (Ang) II participates in the pathogenesis of endothelial dysfunction (ED) through multiple signaling pathways, including angiotensin type 1 receptor (AT_1R) mediated NADPH oxidase (Nox)/reactive oxygen species (ROS) signal transduction. However, the detailed mechanism is not completely understood. In this study, we reported that AngII/AT_1R-mediated activated protein phosphatase 2A (PP2A) downregulated endothelial nitric oxide synthase (eNOS) phosphorylation *via* Nox/ROS pathway. AngII treatment reduced the levels of phosphorylation of eNOS Ser1177 and nitric oxide (NO) content along with phosphorylation of PP2Ac (PP2A catalytic subunit) Tyr307, meanwhile increased the PP2A activity and ROS production in human umbilical vein endothelial cells (HUVECs). These changes could be impeded by AT_1R antagonist candesartan (CAN). The pretreatment of 10^{-8} M PP2A inhibitor okadaic acid (OA) reversed the levels of eNOS Ser1177 and NO content. Similar effects of AngII on PP2A and eNOS were also observed in the mesenteric arteries of Sprague-Dawley rats subjected to AngII infusion *via* osmotic minipumps for 2 weeks. We found that the PP2A activity was increased, but the levels of PP2Ac Tyr307 and eNOS Ser1177 as well as NO content were decreased in the mesenteric arteries. The pretreatments of antioxidant N-acetylcysteine (NAC) and apocynin (APO) abolished the drop of the levels of PP2Ac Tyr307 and eNOS Ser1177 induced by AngII in HUVECs. The knockdown of p22phox by small interfering RNA (siRNA) gave rise to decrement of ROS production and increment of the levels of PP2Ac Tyr307 and eNOS Ser1177. These results indicated that AngII/AT_1R pathway activated PP2A by downregulating its catalytic subunit Tyr307 phosphorylation, which relies on the Nox activation and ROS production. In summary, our findings indicate that AngII downregulates PP2A catalytic subunit Tyr307 phosphorylation to activate PP2A *via* AT_1R-mediated Nox/ROS signaling pathway. The activated PP2A further decreases levels of eNOS Ser1177 phosphorylation and NO content leading to endothelial dysfunction.

Keywords: angiotensin II, angiotensin II type 1 receptor, protein phosphatase 2A, endothelial nitric oxide synthase, NADPH oxidase

INTRODUCTION

Angiotensin (Ang) II is a key component of the renin–angiotensin system and participates in cardiovascular disease (CVD) *via* its specific AngII type 1 receptor (AT_1R; Tassone et al., 2013; Ding et al., 2016). Although numerous studies have shown that AngII/AT_1R regulates the physiological and pathological cardiovascular systems, the exact mechanisms involved remain unclear.

Nitric oxide (NO) is the primary endothelium-derived relaxing factor, which is synthesized by the endothelial nitric oxide synthase (eNOS) that plays a pivotal role in regulating endothelium-dependent vessel dilation (Zhao et al., 2015). Altered eNOS/NO function is a common feature of endothelial dysfunction (ED), and the mechanism underlying ED may be related to decreased eNOS activity accompanied by reduced NO production and bioavailability (Lovren and Verma, 2013; Godo and Shimokawa, 2017). Regulation of eNOS activity is complex and involves a variety of mechanisms, such as phosphorylation/dephosphorylation, which is important for post-translational regulation of eNOS. Phosphorylation of eNOS at serine 1177 site (Ser1177), which activates eNOS, was shown to determine eNOS activity regulation in response to various physiological and pathological stimuli (Searles, 2006; Fleming, 2009).

Previous studies have confirmed that activation of AngII/AT_1R downregulates phosphorylation of eNOS Ser1177 and leads to ED in human umbilical vein endothelial cells (HUVECs; Tassone et al., 2013). Protein phosphatase 2A (PP2A) is the major enzyme that dephosphorylates eNOS Ser1177, and increased PP2A protein expression or enzyme activity resulted in dephosphorylation of eNOS at Ser1177 (Mount et al., 2007; Zhang et al., 2012). Studies have shown that AngII upregulates PP2A activity (Everett et al., 2001; Liu et al., 2015; Li et al., 2016). However, it is not completely clear how the AngII/AT_1R pathway activates PP2A.

The increased reactive oxygen species (ROS) production (oxidative stress) has been demonstrated to contribute in ED. It is well-established that AngII/AT_1R can activate NADPH oxidase (Nox) and promote the production of ROS (Liu et al., 2016). The superoxide derived from Nox is a significant stimulator of PP2A (Han et al., 2010). However, it is still unclear whether the AngII/AT_1R pathway can activate PP2A *via* Nox. Therefore, the aim of the present study was to determine the role of Nox/ROS in AngII/AT_1R-induced PP2A activation to explore the mechanism of endothelial dysfunction induced by AngII.

MATERIALS AND METHODS

Materials

Fetal bovine serum (FBS; Biological Industries, CT, United States), 0.25% trypsin, high-glucose Dulbecco's modified Eagle's medium (DMEM), and cyan-streptomycin were all purchased from HyClone (UT, United States). *N*-acetylcysteine (NAC), apocynin (APO), and AngII were purchased from Sigma-Aldrich (St. Louis, MO, United States). Candesartan (CAN) was purchased from Selleck (Houston, TX, United States). Antibodies against eNOS and eNOS Ser1177 (Millipore, Billerica, MA, United States), PP2Ac Tyr307, p22phox, and PP2A Cα were purchased from Santa Cruz Biotechnology. NO assay kit for HUVECs (DAF-FM DA) and for tissues (Griess reaction), and okadaic acid (OA) was purchased from Beyotime Biotechnology (Shanghai, China). Primary antibody against β-tubulin and secondary antibodies were purchased from PMK Biotechnology (Wuhan, China). ROS assay kit was purchased from Nanjing Jiancheng Bioengineering Institute. siRNA targeting p22phox was purchased from Santa Cruz Biotechnology.

Cell Cultures

Human umbilical vein endothelial cells were isolated from the umbilical cords of newborns born at the Affiliated Hospital of Guizhou Medical University. Written informed consent was obtained from all participants prior to being included in the study. The study was approved by the Ethics Committees of Guizhou Medical University. HUVECs were isolated as described previously (Hastie et al., 2016; Luo et al., 2019). Isolated HUVECs were seeded and cultured in 6 cm cell culture dishes with using culture medium containing 20% FBS. Expression of factor VIII-related antigen and CD34 was measured using immunohistochemical assay for cell characterization. HUVECs were cultured in 10% FBS in high-glucose DMEM at 37°C in a 5% CO_2 incubator. When cells reached 70–80% confluence, the medium was replaced with fresh medium for subsequent treatments. HUVECs were used for experiments at passages 4–8.

Cell Experiments

In order to determine the concentration and duration of AngII, HUVECs were incubated with AngII for 12 h at concentrations of 10^{-5}, 10^{-6}, 10^{-7}, and 10^{-8} M, and in the presence of AngII at the concentration of 10^{-7} M for 6, 12, 24, or 36 h.

Candesartan (CAN) is an angiotensin receptor antagonist that can specifically block the binding of AngII to its specific type 1 receptor. *N*-acetylcysteine (NAC) is a thiol compound, as a donor of cysteine leading to replenishment of glutathione and thus can be used as a reactive oxygen scavenging agent (Aldini et al., 2018). Apocynin (APO) predominantly acts as an antioxidant in endothelial cells and vascular smooth muscle cells (Heumüller et al., 2008). Okadaic acid is a lipophilic natural compound originally isolated from the marine black sponges *Halichondria okadaii* and *Halichondria melanodocia* and is the most widely used inhibitor of PP2A and PP1, with IC50 values of 2×10^{-10} and 2×10^{-8} M (Dounay and Forsyth, 2002). According to the reports, in the present study, CAN pretreated HUVECs 3 h before the AngII at concentrations of 10^{-6} M to block the binding of AngII to AT_1R (Wang et al., 2015); NAC and APO pretreated, respectively, 1 h before the AngII at concentrations of 10^{-3} M (Kadowaki et al., 2015) and 2×10^{-5} M (Qin et al., 2017) to reduce ROS content; and

Abbreviations: AngII, Angiotensin II; PP2A, Protein phosphatase 2A; AT_1R, Angiotensin type 1 receptor; Nox, NADPH oxidase; ROS, Reactive oxygen species; HUVECs, Human umbilical vein endothelial cells; CAN, Candesartan; NAC, N-acetylcysteine; APO, Apocynin; OA, Okadaic acid; siRNA, Small interfering RNA; ED, Endothelial dysfunction; NO, Nitric oxide; eNOS, Endothelial nitric oxide synthase; CVD, Cardiovascular disease.

OA was added to HUVECs 1 h before the AngII at concentration of 10^{-8} M to inhibit PP2A enzyme activity (Chao et al., 2014).

Animal Studies

All animal procedures were conducted in accordance with the guidelines issued by the Guizhou Medical University Animal Care and Use Committee. Forty-eight male Sprague–Dawley rats weighing 160–200 g were provided by the Experimental Animal Center of Guizhou Medical University [animal certificate number: SCXK (QIAN) 2012-0001] and subjected to adaptive feeding for 1 week. The rats were randomly divided into four groups: Control, AngII, AngII + CAN, and CAN, $n = 12$ in each group. All rats had an osmotic minipump (Alzet model 2002, Alza, Vacaville, CA, United States) implanted subcutaneously in the back of the neck as follows. After intraperitoneal injection of 3% sodium pentobarbital (1 ml/kg body weight), rats were fixed in the prone position on an operating table. A surgical scalpel was then used to make a 1-cm incision behind the ear, over the shoulder that was perpendicular to the tail. A vascular clamp was used to make a subcutaneous pocket for the osmotic minipump. The minipump was inserted gently, the skin incision was sutured, and then mopirocin ointment (Baiduobang) was applied to the incisions for 3 days to prevent infection. Rats in the AngII and the AngII + CAN groups were received AngII *via* the minipump continuously for 2 weeks, whereas rats in the Control and CAN groups were infused with normal saline. The average infusion rate was 500 ng/kg/min. CAN was administered after the minipump implantation by gavage at a dose of 10 mg/kg/day during the AngII infusion. Systolic blood pressure was measured by tail cuff plethysmography with the aid of a computerized system (BP600A, Techman Soft, Chengdu, China) on days 3, 7, and 14 after implantion of the pump.

Western Blot Analysis

Western blot analysis was performed to measure protein expression. Briefly, radio-immunoprecipitation assay (RIPA) lysis buffer was used to collect total protein from HUVECs and mesenteric arteries. One 6-cm-dish of cells were lysed with 150 μl of RIPA lysis buffer, and 0.1 grams of mesenteric arterial tissue were lysed with 100 μl of RIPA lysis buffer, lysed on ice for 45 min, and then centrifuged at 12,000 *g* at 4°C for 25 min. The supernatants were collected, and protein concentrations were determined. Next, proteins were separated by 10% sodium dodecyl sulfate polyacrylamide gel electrophoresis and then transferred onto transfer membranes (Millipore). After blocking with 5% nonfat milk for 60 min at room temperature, the membranes were incubated with targeted primary antibodies overnight at 4°C. After washing in tris-buffered saline with Tween-20 (TBST), the membranes were incubated with horseradish peroxidase-conjugated secondary antibodies for 1 h at room temperature. After washing the membranes three times in TBST, protein bands were detected using enhanced chemiluminescence reagents (Bio-Rad). Densitometric analysis was conducted using Bio-Rad software.

NO Measurement

Human umbilical vein endothelial cells were seeded in six-well plates at the appropriate densities. The cells were treated when they reached 70–80% confluence. HUVECs were then washed with phosphate-buffered saline (PBS) and incubated with 10 μM diaminofluorescein-FM diacetate (DAF-FM DA; NO-sensitive fluorescent dye) without phenol red at 37°C in 5% CO_2 for 30 min. Measurement of NO production was performed using an Olympus microscope (IX71, Japan). The mean fluorescence intensity values were analyzed using ImageJ software.

The content of NO in mesenteric arteries was determined using the Griess method according to the instruction of the manufacturer. Briefly, tissues were lysed on ice and then centrifuged at 14,000 *g* at 4°C for 5 min. The supernatants were collected, and protein concentrations were determined by BCA method. The standard $NaNO_2$ and samples were added to a 96-well plate (50 μl/well), respectively. After adding Griess Reagents I and II sequentially (50 μl of each reagent/well), the absorbance was determined at 540 nm in wavelength.

PP2A Activity Assay

PP2A activity was measured using a V2460 kit from Promega (Madison, WI, United States) as previously reported (Sun et al., 2012). One 6-cm-dish of cells and 0.1 grams of mesenteric arterial tissue were lysed with 300 μl of precooled phosphatase storage buffer, lysed on ice for 30 min, and then centrifuged at 4°C and 12,000 rpm for 25 min to remove the supernatant. As per the manufacturer's instructions, 250 μl of supernatant was added to the column. The filtrate was collected as the sample to be tested, and the phosphate content of the sample was measured after the reaction using the optical density value at 600 nm. The enzyme activity of PP2A in each sample was calculated based on a standard curve.

Measurement of Intracellular ROS

Intracellular ROS production was measured using the ROS-sensitive detection probe 2,7-dichlorodihydrofluorescein diacetate (DCFH-DA). HUVECs were cultured in six-well plates and treated with the appropriate drugs when they reached 60–70% confluence. The following day, the cells were cocultured with 5 μM DCFH-DA in the dark at 37°C in 5% CO_2 for 30 min. The cells were then washed three times with PBS and observed under an Olympus microscope. The mean fluorescence intensity values were analyzed using ImageJ software.

p22phox Small Interfering RNA Transfection

HUVECs were seeded in six-well plates and cultured until they reached 40–50% confluence. Prior to transfection, culture medium containing 10% FBS was replaced with serum-free culture medium without antibiotics, and the cells were serum-starved for 2 h. A transfection reagent (Santa Cruz, CA, United States) was used to perform transfection of small interfering RNA (siRNA; Santa Cruz, CA, United States) p22phox gene into HUVECs, which was performed in six-well plates. The final concentration of p22phox or scrambled siRNA was 80 pmol per well. After transfection for 6 h, the medium was replaced with fresh serum-free culture medium without antibiotics.

Statistical Analysis

Data were analyzed using SPSS version 17.0 statistical software, and were expressed as mean ± SD. Homogeneity of variance test was used to compare samples from multiple groups. A one-way ANOVA or two-way ANOVA was used for comparisons among groups. Values of $p < 0.05$ were considered to indicate statistically significance.

RESULTS

AngII Induced eNOS Ser1177 Dephosphorylation Resulting in a Reduction in NO Production *via* AT_1R

We investigated the effects of AngII/AT_1R on phosphorylation of eNOS Ser1177 and production of NO in cultured HUVECs and AngII-infusion rats. In cultured HUVECs, after incubation with AngII at concentrations of 10^{-5}, 10^{-6}, 10^{-7}, and 10^{-8} M for 12 h or at a concentration of 10^{-7} M for 6, 12, and 24, and 36 h, the phosphorylation levels of eNOS Ser1177 were significantly lower than those in the Control group (**Figures 1A–D**). Based on these results, treatment with 10^{-7} M AngII for 12 h was used for subsequent experiments. CAN, AT_1R antagonist, abolished AngII-induced decrease of eNOS Ser1177 phosphorylation (**Figures 1E,F**). There were no statistically significant differences in total eNOS protein expression levels among the groups. To clarify the effect of AngII on NO generation, we used DAF-FM DA fluorescent probe to measure the NO content in HUVECs. The results showed that the NO production of the AngII group was lower than that of the Control group, and blocking AT_1R with CAN reversed the production of NO (**Figures 1G,H**).

In AngII-infusion rats, the systolic blood pressure increased significantly after 3 days, reached the highest value at day 7, and remained at stable level until 14 days. Treatment the rats with CAN markedly reduced the systolic blood pressure in AngII-infusion group (**Table 1**). Next, we measured protein expression levels of eNOS and eNOS Ser1177 in the mesenteric arteries of rats at day 14. AngII infusion decreased the levels of phosphorylation of eNOS Ser1177, and CAN abolished the effect of AngII. There were no statistically significant differences in eNOS protein expression levels among the groups (**Figures 1I,J**). AngII infusion reduced the NO production, which could be reversed by CAN (**Figure 1K**). The alterations of the levels of eNOS protein expression, eNOS Ser1177 phosphorylation and NO content were consistent with those of in HUVECs. These results demonstrated that AngII dephosphorylates eNOS Ser1177 leading to a reduction in NO production *via* AT_1R pathway.

AngII/AT_1R Pathway Downregulates the Phosphorylation of eNOS Ser1177 and Reduces the Production of NO by Activating PP2A

It was reported that PP2A can dephosphorylate eNOS Ser1177 and decrease eNOS activity (Mount et al., 2007; Zhang et al., 2012). Therefore, we examined the activity of PP2A both *in vitro* and *in vivo*. As expected, the activity of PP2A was significantly increased both in the AngII-treated HUVECs and mesenteric arteries of AngII-infusion rats, pretreatment with CAN reduced the activity of PP2A (**Figures 2A,B**). To further clarify the role of PP2A in AngII-induced eNOS/NO dysfunction, 10^{-8} M PP1/PP2A inhibitor OA were used to pretreat HUVECs, according to the report that OA at concentration of 10^{-8} M inhibits PP2A enzyme activity (Chao et al., 2014). The results demonstrated that pretreatment with OA reversed the effect of AngII on phosphorylation of eNOS Ser1177 and generation of NO (**Figures 2C–F**). These findings indicated that AngII/AT_1R activated PP2A resulting in dephosphorylation of eNOS Ser1177, decreased eNOS enzyme activity, and reduced NO production.

Activation of the AngII/AT_1R Pathway Upregulates PP2Ac Tyr307 Phosphorylation to Activate PP2A by Promoting ROS Generation

Post-translational phosphorylation modulation of PP2A catalytic subunit, for instance, phosphorylation of PP2Ac Tyr307 reduces its activity (Ishii et al., 2017). Therefore, we measured the phosphorylation level of PP2Ac Tyr307. The results showed that AngII treatment significantly decreased phosphorylation of PP2Ac Tyr307, which could be prevented by pretreatment with CAN both *in vitro* and *in vivo* (**Figures 3A–D**). There were no statistically significant differences in the PP2A catalytic subunit α protein (PP2ACα) expression among the groups. Accordingly, AngII may activate PP2A by reducing the phosphorylation level of PP2Ac Tyr307.

AngII is one of the most common oxidative stress-induced factors. Therefore, we speculated that AngII/AT_1R activated PP2A may be related to the increased production of ROS. We used the DCFH-DA fluorescent probe to measure the content of intracellular ROS. The results showed that the ROS production was higher in the AngII group than that in the Control group, and CAN treatment decreased the production of ROS (**Figures 3E,F**). To clarify the effect of ROS on AngII/AT_1R-induced PP2A activation, we pretreated HUVECs with the antioxidants NAC and APO. The data showed that NAC and APO restored the levels of PP2Ac Tyr307 and eNOS Ser1177 phosphorylation (**Figures 3G–J**). Taken together, these data suggest that activation of the AngII/AT_1R pathway promotes the production of ROS, which activates PP2A by downregulating the phosphorylation of PP2Ac Tyr307, leading to eNOS Ser1177 dephosphorylation.

Effects of Nox on AngII/AT_1R-Induced PP2A Activation

NADPH oxidase is the main source of ROS in endothelial cells exposed to AngII (Cat et al., 2013). There have been reports suggest that the p22phox subunit is critical for the activation of Noxs except Nox5 and duox1/2 (Petry et al., 2010), and AngII increased the expression of p22phox and induced oxidative stress in the lungs and hearts of mice with hypoxia-induced pulmonary hypertension (Zhang et al., 2019). Therefore, we measured the protein expression level of p22phox

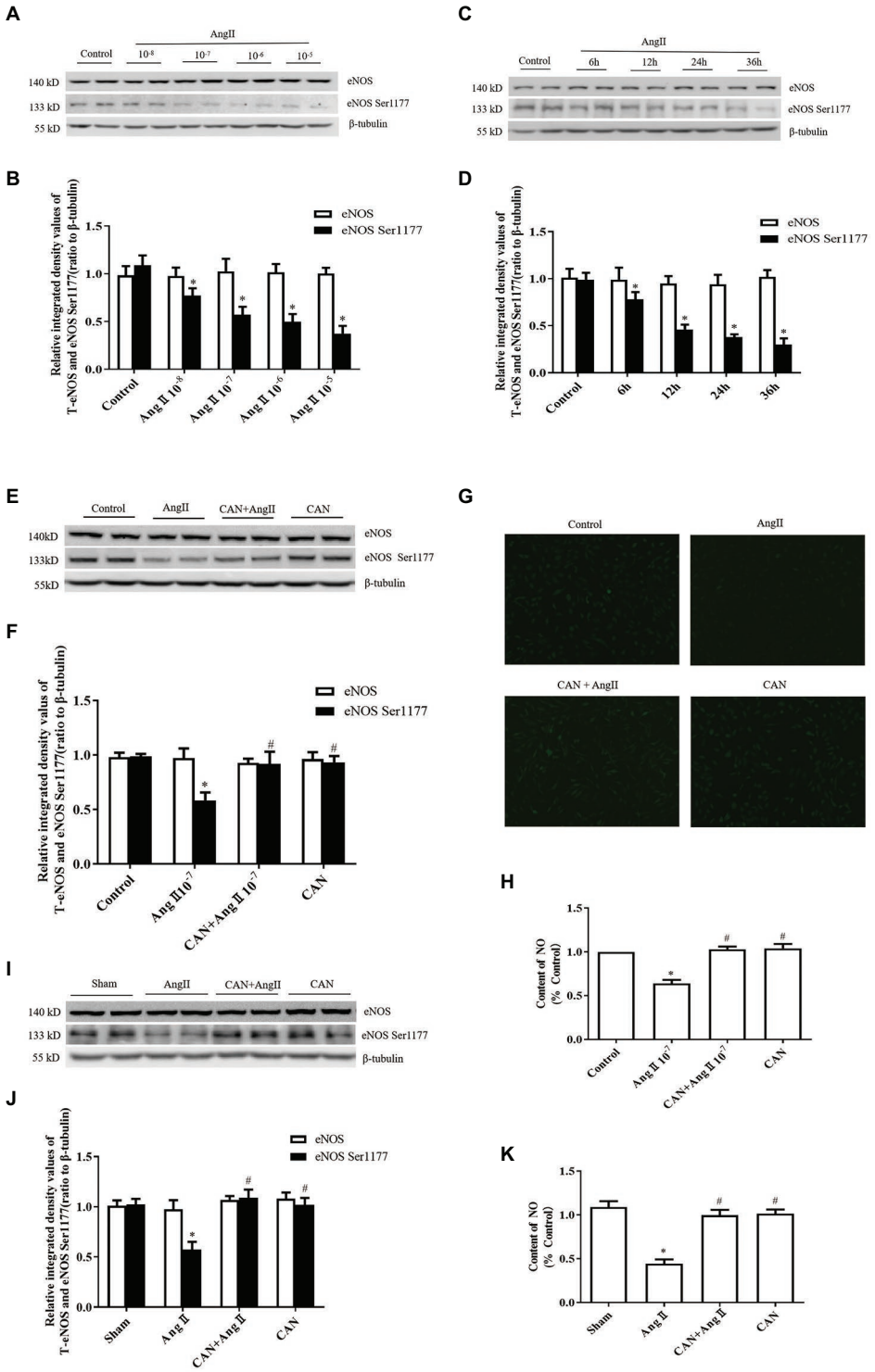

FIGURE 1 | Effects of the angiotensin II (AngII)/angiotensin type 1 receptor (AT_1R) pathway on endothelial nitric oxide synthase (eNOS) Ser1177 phosphorylation and nitric oxide (NO) production. **(A,B)** AngII downregulated phosphorylation levels of eNOS Ser1177 in a dose-dependent manner. Human umbilical vein endothelial cells (HUVECs) were treated with the indicated concentrations of AngII for 12 h, and phosphorylation levels of eNOS Ser1177 were detected by Western Blot analysis (n = 6 independent experiments). **(C,D)** AngII downregulated phosphorylation levels of eNOS Ser1177 in a time-dependent manner. HUVECs were treated with 10^{-7} M AngII for the indicated time, and phosphorylation levels of eNOS Ser1177 were detected by Western Blot analysis (n = 6 independent experiments).

(Continued)

FIGURE 1 | (E,F) Candesartan (CAN) remarkably inhibited AngII-mediated downregulation of eNOS Ser1177 in HUVECs. HUVECs were pretreated with CAN (10^{-6} M, 3 h) and then stimulated with AngII (10^{-7} M, 12 h), and phosphorylation levels of eNOS Ser1177 were detected by Western Blot analysis (n = 6 independent experiments). **(G,H)** CAN blocked AngII-mediated (10^{-7} M, 12 h) downregulation of NO production in HUVECs. HUVECs were incubated with DAF-FM DA (10 μmol/L) for 30 min. The representative images were captured with a fluorescence microscope (200× magnification; n = 4 independent experiments). **(I,J)** AngII reduced levels of eNOS Ser1177 phosphorylation in rat mesenteric arteries, whereas the AT_1R antagonist, CAN, blocked AngII-mediated downregulation of eNOS Ser1177 phosphorylation (n = 6 rats per group). Rats received AngII infusion *via* osmotic minipumps for 2 weeks. CAN was administered after minipump implantation by gavage at a dose of 10 mg/kg/day during the AngII infusion period. **(K)** The content of NO in rat mesenteric arteries of AngII-infused rats. The content of NO was decreased in the mesenteric arteries of AngII-infused rats. CAN blocked AngII-induced downregulation of NO production (n = 3 rats per group). $^{*}p < 0.05$ vs. Control or Sham group; $^{\#}p < 0.05$ vs. AngII group.

TABLE 1 | Systolic blood pressure in each group of rats.

Group	Before pump implanted (mmHg)	Day 3 after pump implanted (mmHg)	Day 7 after pump implanted (mmHg)	Day 14 after pump implanted (mmHg)
Sham (n = 12)	89.39 ± 3.09	86.80 ± 2.14	88.39 ± 3.03	87.27 ± 2.54
AngII (n = 12)	84.77 ± 2.81	125.12 ± 3.59$^{*\#}$	150.66 ± 5.05$^{*\#\triangle}$	153.86 ± 2.21$^{*\#\triangle}$
CAN + AngII (n = 12)	87.21 ± 2.62	89.69 ± 4.22$^{\blacktriangle}$	91.61 ± 4.33$^{\blacktriangle}$	95.50 ± 3.39$^{\blacktriangle}$
CAN (n = 12)	88.69 ± 1.66	86.05 ± 2.08	87.46 ± 4.17	89.00 ± 4.86

Effects of AngII infusion on the systolic blood pressure in each group rats. Data are presented as mean ± SD.
$^{*}p < 0.05$ *vs. Sham group.*
$^{\#}p < 0.05$ *vs. before pump implanted.*
$^{\triangle}p < 0.05$ *vs. 3 days after pump implanted.*
$^{\blacktriangle}p < 0.05$ *vs. AngII group.*

in HUVECs. The results showed that AngII treatment augmented p22phox protein expression and CAN pretreatment blocked this effect of AngII (**Figures 4A,B**).

To further confirm the roles of Nox, HUVECs were transfected with p22phox siRNA. After p22phox gene silencing by p22phox siRNA, the amount of ROS decreased significantly (**Figure 4C**). Western blot analysis revealed that knockdown of p22phox protein expression by p22phox siRNA obviously upregulated the phosphorylation levels of PP2Ac Tyr307 and eNOS Ser1177. Moreover, p22phox knockdown almost abolished the effects of AngII on PP2Ac Tyr307 and eNOS Ser1177 phosphorylation in the HUVECs (**Figures 4D–F**).

DISCUSSION

Endothelial dysfunction is considered the basis of CVD, and eNOS/NO dysfunction is a common feature of ED (Godo and Shimokawa, 2017). NO is considered central to mediating the diverse action carried out by the endothelium and plays a pivotal role in regulating endothelium-dependent dilatation. Under physiological conditions, eNOS is the predominant source of NO in endothelial cells (Bonetti et al., 2003; Zhao et al., 2015). AngII is a key component of the renin–angiotensin system and regulates physiological and pathological cardiovascular functions mainly *via* its specific receptors (Tassone et al., 2013; Ding et al., 2016). Several studies have demonstrated that AngII contributes to the pathogenesis of ED by decreasing eNOS activity and NO bioavailability. It is reported that treatment of human aortic endothelial cells with AngII downregulates the phosphorylation of eNOS Ser1177, decreases eNOS activity and NO production by downregulating the expression of PGC-1α (Li et al., 2016). The previous study shows that AngII decreases eNOS activity and total NO content by upregulating SIRT3 expression in HUVECs (Liu et al., 2015). eNOS enzyme activity is regulated by various mechanisms, including protein post-translation phosphorylation. The eNOS phosphorylation site at serine 1177 near the carboxyl terminal is the center of eNOS activity regulation, phosphorylation at this site significantly upregulates eNOS activity, and PP2A is the major phosphatase that dephosphorylates eNOS leading to a decrease in eNOS activity and NO production (Searles, 2006; Fleming, 2009). However, the precise molecular mechanisms under which AngII activates PP2A to drop the levels of eNOS Ser1177 phosphoryation are remained unknown. In the present study, we demonstrated that AngII downregulates eNOS Ser1177 phosphorylation by activating PP2A *via* the AT_1R/Nox/ROS signaling pathway.

PP2A is a highly conserved serine/threonine phosphatase that exists across species as a dephosphorylation protein (Janssens and Goris, 2001). It is composed of structural subunit A, regulatory subunit B, and catalytic subunit C. PP2A regulates several important cellular processes, such as cell cycle, apoptosis, cell metabolism, and migration, *via* dephosphorylation of intracellular proteins (Apostolidis et al., 2016; Wlodarchak and Xing, 2016). Studies have shown that PP2A is activated in CVD, and that activated PP2A could lead to ED *via* dephosphorylation of eNOS or Akt (Zhang et al., 2012; Etwebi et al., 2018; Schnelle et al., 2019). AngII/AT_1R can enhance the activity of PP2A in cardiomyocytes (Everett et al., 2001) as well as HUVECs (Luo et al., 2019). In the present study, we observed that AngII/AT_1R pathway activation increased PP2A enzyme activity and reduced phosphorylation of eNOS Ser1177 and the content of NO both *in vitro* and *in vivo*; PP2A inhibition (by OA) reversed the phosphorylation of eNOS Ser1177 *in vitro*. These results suggested that AngII/AT_1R downregulates phosphorylation of eNOS Ser1177 by activating PP2A.

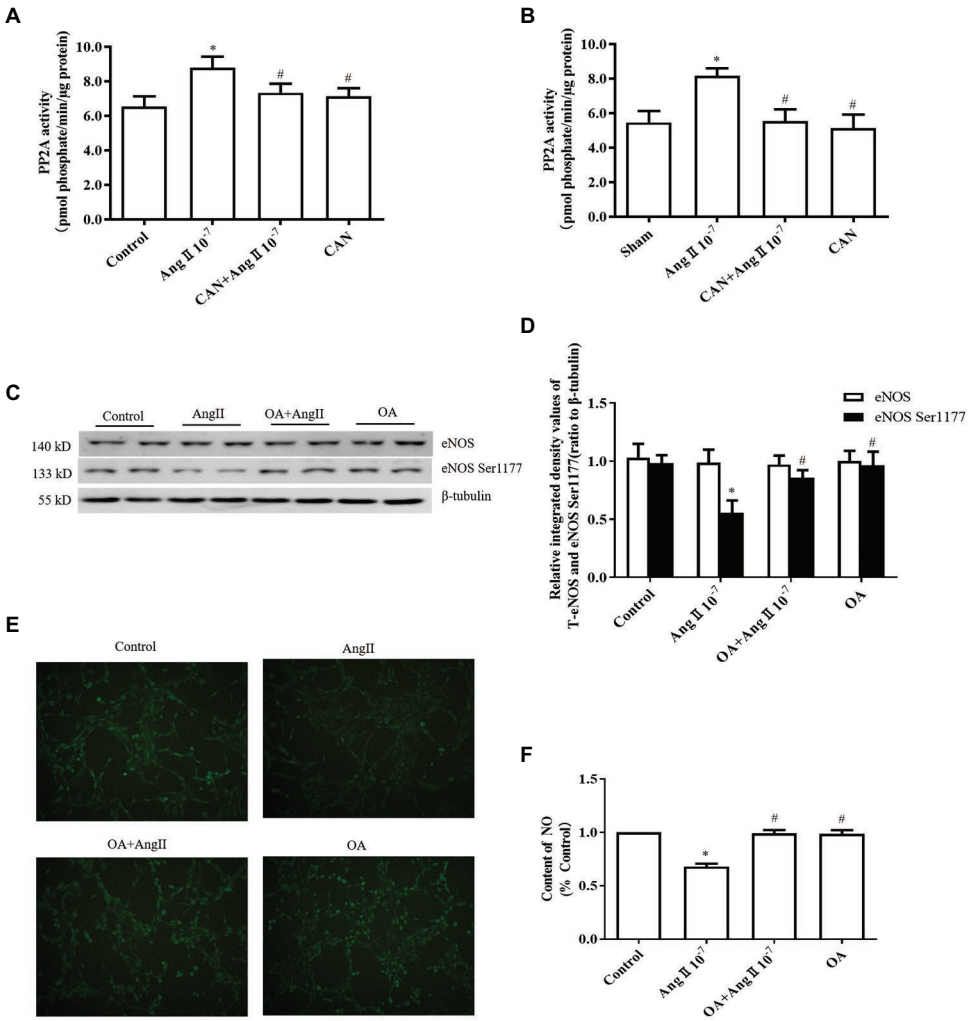

FIGURE 2 | The AngII/AT_1R pathway reduces the levels of eNOS Ser1177 phosphorylation and NO production by activating protein phosphatase 2A (PP2A). **(A)** AngII augmented PP2A activity, while CAN blocked AngII-mediated enhancement of PP2A activity. HUVECs were pretreated with 10^{-6} M CAN for 3 h or not, then stimulated with 10^{-7} M AngII for 12 h (n = 4 independent experiments). **(B)** PP2A activity was increased in the mesenteric arteries of AngII-infused rats. CAN blocked AngII-induced upregulation of PP2A activity (n = 3 rats per group). **(C,D)** PP2A inhibitor (OA) blocked the effect of AngII on eNOS Ser1177 *in vitro*. HUVECs were pretreated with 10^{-8} M OA for 1 h or not, then stimulated with 10^{-7} M AngII for 12 h (n = 6 independent experiments). **(E,F)** OA blocked AngII-induced downregulation of NO production in HUVECs (200× magnification; n = 4 independent experiments). $^{*}p < 0.05$ vs. Control or Sham group; $^{\#}p < 0.05$ vs. AngII group.

There are several mechanisms involved in the modulation of PP2A activity, including enzyme assembly, subunit post-translational modification, inhibitors, and protein interactions. The PP2A catalytic subunit, PP2Ac, can be modified by phosphorylation, methylation, and acetylation (Lambrecht et al., 2013; Hung et al., 2016). We previously reported that AngII/AT_1R activates PP2A by reducing endogenous phosphatase 2A inhibitor 2 (I_2^{PP2A}; Luo et al., 2019). Phosphorylation of the PP2Ac at Tyr307 site inactivates PP2A; therefore, phosphorylation level of PP2Ac Tyr307 is considered to be the indicators of PP2A activity (Brautigan, 1995; Ishii et al., 2017). In the present study, we found that the phosphorylation level of PP2Ac Tyr307 decreased and PP2A activity increased after AngII treatment accompanied by the decline in the levels of eNOS Ser1177 and NO generation. All of these changes were reversed by OA *in vitro*. These results suggest that downregulation of PP2Ac Tyr307 phosphorylation is one of mechanisms by which the AngII/AT_1R pathway increases PP2A activity. However, the molecular mechanisms involved in AngII-induced PP2A activation were needed to further explore.

Oxidative stress is an established cause of ED, and has been well recognized in the pathogenesis of CVD. The NADPH oxidase system is one of the main sources of ROS. There are seven known members of the Nox family: Nox1, Nox2, Nox3, Nox4, Nox5, Duox1, and Duox2. The main isoforms of Nox in endothelial cells are Nox1, Nox2, Nox4, and Nox5 and are the major sources of endothelial cell-derived ROS (Touyz et al., 2011; Wingler et al., 2011; Cat et al., 2013).

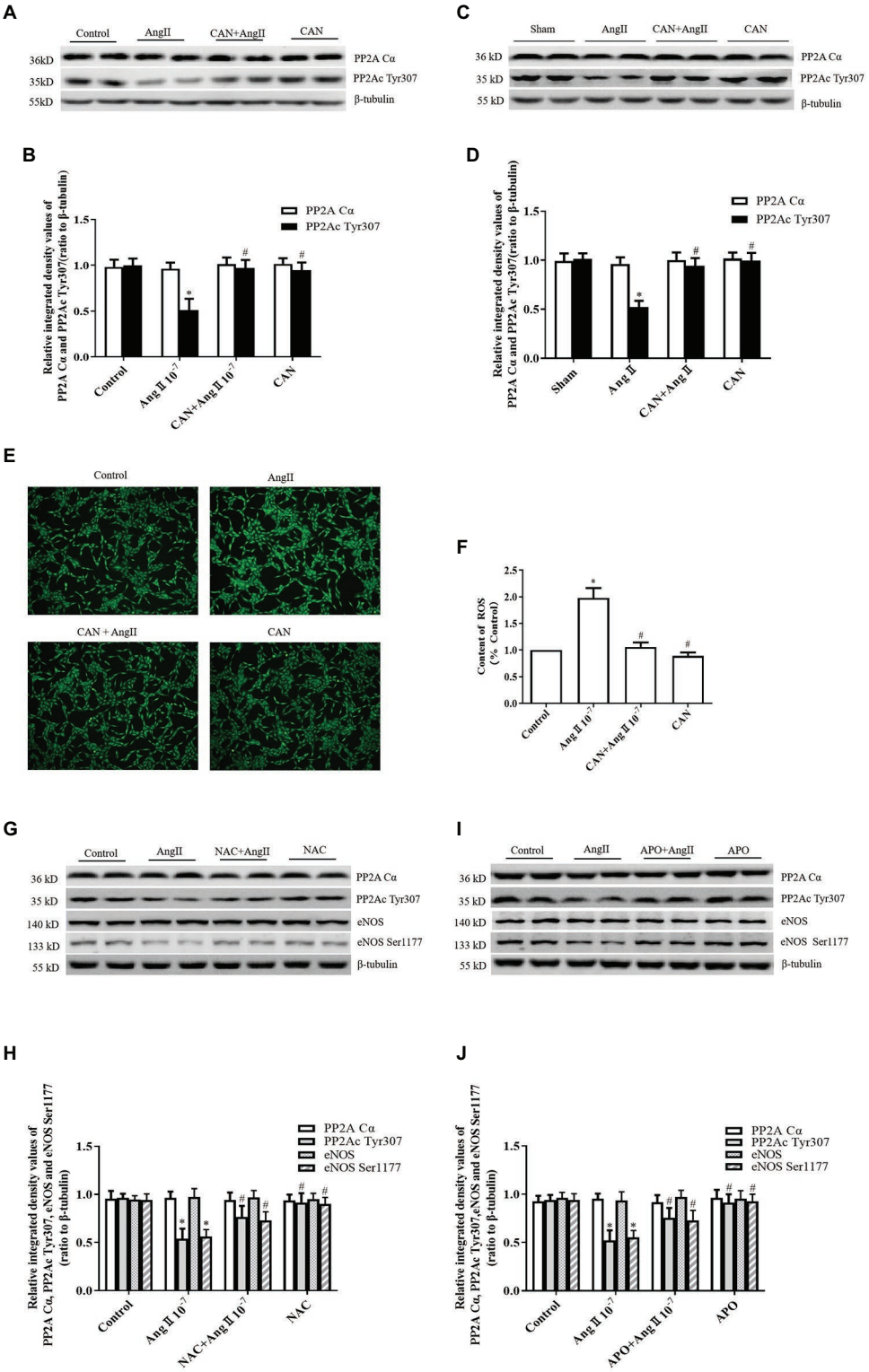

FIGURE 3 | AngII/AT_1R pathway downregulates PP2Ac Tyr307 phosphorylation, which is related with ROS generation. **(A,B)** CAN blocked AngII-mediated downregulation of PP2Ac Tyr307 phosphorylation in HUVECs. HUVECs were pretreated with 10^{-6} M CAN for 3 h or not, then stimulated with 10^{-7} M AngII for 12 h (n = 6 independent experiments). **(C,D)** CAN blocked AngII-mediated downregulation of PP2Ac Tyr307 phosphorylation in rat mesenteric arteries (n = 6 rats per group).

(Continued)

FIGURE 3 | (E,F) ROS content was enhanced by AngII (10^{-7} M, 12 h) and abolished by pretreatment with CAN (10^{-6} M, 3 h). HUVECs were incubated with DCFH-DA (5 μmol/L) for 30 min, and ROS content was measure. The representative images shown were captured using a fluorescence microscope (100× magnification; $n = 4$ independent experiments). Pretreatment with the antioxidant, **(G,H)** N-acetylcysteine (NAC; 10^{-3} M, 1 h) and **(I,J)** Apocynin (APO; 2×10^{-5} M, 1 h), inhibited AngII/AT_1R-mediated downregulation of PP2Ac Tyr307 and eNOS Ser1177 ($n = 6$ independent experiments). $^{*}p < 0.05$ vs. Control or Sham group; $^{\#}p < 0.05$ vs. AngII group.

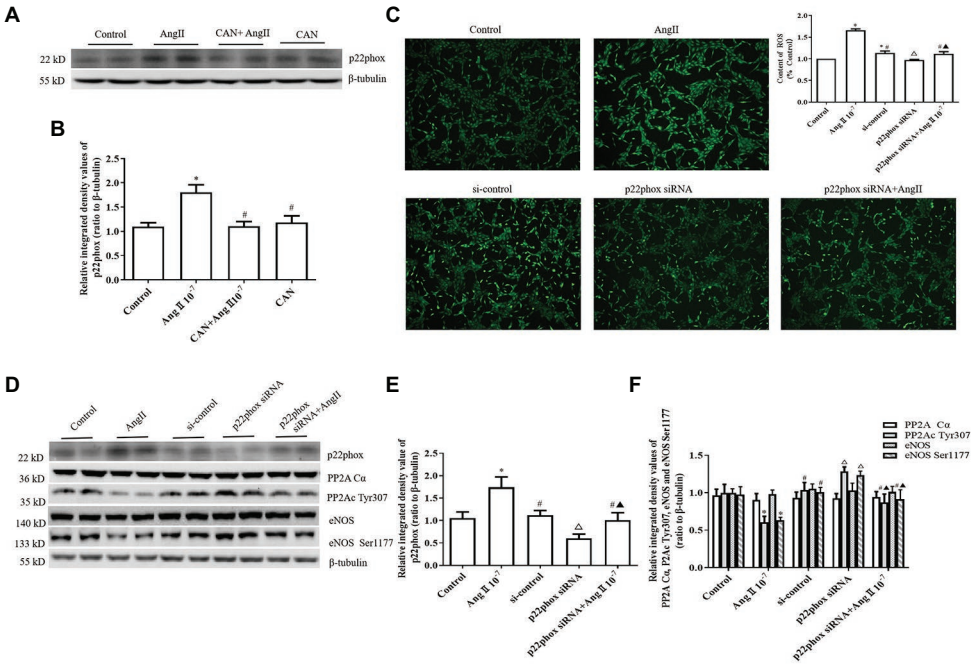

FIGURE 4 | AngII downregulating the levels of PP2Ac Tyr307 phosphorylation is dependent on NADPH oxidase (Nox) activation and ROS production in HUVECs. **(A,B)** AngII (10^{-7} M, 12 h) augments p22phox protein expression and pretreatment with CAN (10^{-6} M, for 3 h) blocked the effect of AngII ($n = 6$ independent experiments). **(C)** Silencing of p22phox protein expression by siRNA abrogated AngII-mediated increase of ROS (100× magnification; $n = 4$ independent experiments). **(D–F)** Knockdown of p22phox protein by siRNA reversed the downregulation of PP2Ac Tyr307 and eNOS Ser1177 ($n = 6$ independent experiments). HUVECs were transfected with control siRNA or p22phox-specific siRNA for 24 h, then treated with 10^{-7} M AngII for 12 h. Levels of PP2Ac Tyr307 and eNOS Ser1177 were determined by Western blot analysis. $^{*}p < 0.05$ vs. Control group; $^{\#}p < 0.05$ vs. AngII group; $^{\triangle}p < 0.05$ vs. si-control group; $^{\blacktriangle}p < 0.05$ vs. p22phox siRNA group.

It has been confirmed that AngII activates Nox and promotes the production of ROS (Qiu et al., 2015; Liu et al., 2016; Zhang et al., 2019). It is believed to increase ROS production *via* the Nox families by increasing their protein expression as well as their catalytic activity (Zhang et al., 2019).

ROS leads to endothelial cell damage through multiple pathways, including activation of proinflammatory signaling pathways, depletion of antioxidants and signaling molecules, and oxidation of macromolecules (Valko et al., 2007; Incalza et al., 2018). In addition, ROS results in the uncoupling of eNOS, which leads to the reduction of NO production and bioavailability in endothelial cells (Drummond and Sobey, 2014) and cardiomyocytes (Roe et al., 2013). NO is the key molecule to regulate the biological function of endothelium. The reduced NO bioavailability is a significant mechanism of ROS induced endothelial damage. eNOS is the main source of endothelial NO. eNOS oxidizes the terminal guanidine nitrogen atom of L-arginine by using electrons from NADPH to produce NO when the substrate (L-arginine) and co-substrate (tetrahydrobiopterin, flavin adenine mononucleotide, flavin adenine dinucleotide, and NADPH) are sufficient. The eNOS protein is a homodimer, and dimerization is necessary for NO production. Uncoupled eNOS is unable to deliver electrons between two monomers, then electrons from NADPH can be captured by oxygen and produced superoxide anion (O_2^-; Bonetti et al., 2003; Roe and Ren, 2012; Zhao et al., 2015). Whether ROS activates a protein phosphatase to reduce the eNOS enzyme activity through post-translation phosphorylation modulation is an important purpose of this study.

Previous studies have shown that PP2A is a target molecule of Nox-derived ROS (Nagata et al., 2006; Menden et al., 2013). Therefore, we hypothesized that activation of PP2A by AngII/AT_1R may be related to Nox/ROS activation. Our study confirmed that AngII/AT_1R notably increased ROS formation and p22phox protein expression in HUVECs, and the effect of AngII on PP2Ac Tyr307 and eNOS Ser1177 phosphorylation was eliminated after ROS reducing by NAC and APO. Nox enzyme complex comprises of membrane bound subunits (p91phox and p22phox) and cytoplasmic subunits (p47phox, p67phox, p40phox, and Rac). Phosphorylated cytoplasmic subunits form a complex and translocate to the membrane to dock with the membrane subunits (Panday et al., 2015). p22phox is one of the two

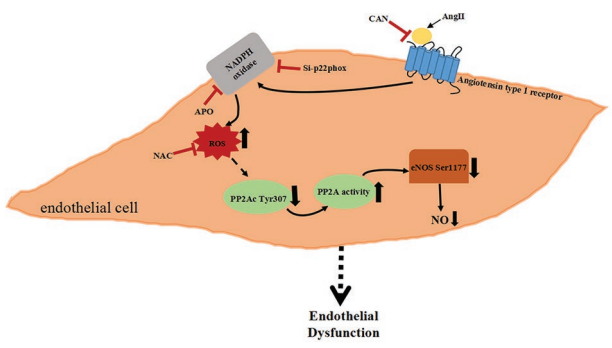

FIGURE 5 | Schematic diagram of AngII-activated PP2A downregulate eNOS phosphorylation *via* the Nox/ROS signaling pathway.

membrane subunits, and regulates the activity of Nox. Therefore, we further verified the effect of Nox/ROS on PP2A activation by knocking down p22phox gene expression *in vitro*. After p22phox gene silencing, the ROS production reduced significantly, and the AngII-induced dephosphorylation of PP2Ac Tyr307 and eNOS Ser1177 decreased. Accordingly, we believe that AngII/AT_1R activates PP2A by downregulating the phosphorylation of PP2Ac Tyr307 leading to the losses of eNOS Ser1177 phosphorylation and NO production at least in part through the Nox/ROS signaling pathway. However, the mechanism by which Nox/ROS causes the downregulation of PP2Ac Tyr307 is not well understood, and it may be related to the tyrosine protein kinases (Fedida-Metula et al., 2012; Xiong et al., 2013), which need to be confirmed in the next work.

In summary, the present study demonstrates that AngII binding to its specific type 1 receptor activates PP2A through Nox/ROS signal pathway, which leads to eNOS/NO dysfunction. The increased Nox membrane subunit p22phox protein expression causing excessive ROS activates a certain signaling pathway to decrease the phosphorylation of PP2Ac Tyr307 further increase the activity of PP2A. PP2A dephosphorylated eNOS Ser1177 and reduced NO production, which may be another significant mechanism of AngII induced ED (**Figure 5**).

DATA AVAILABILITY STATEMENT

All data included in this study are available upon by contact with the corresponding authors.

ETHICS STATEMENT

The studies involving human participants were reviewed and approved by The Ethics Committee of Guizhou Medical University. Written informed consent to participate in this study was provided by the participants' legal guardian/next of kin. The animal study was reviewed and approved by Guizhou Medical University Animal Care and Use Committee.

AUTHOR CONTRIBUTIONS

JD has performed all experiments and revised the manuscript. MY has performed all experiments, analyzed all data, and drafted the manuscript. JJ performed the animal experiments. YL helped with *in vitro* experiments and data analysis. SW and FY helped with collection of the data. QZ helped with the Western blotting analysis. AW and LW helped with the NO measurement. MZ helped with the data analysis and revised the manuscript. QZ made the statistical charts. SW and YX revised the manuscript. DL designed the study, supervised all experiments, and responsible for critically revising the manuscript. All authors contributed to the article and approved the submitted version.

FUNDING

This work was supported by the National Natural Science Foundation of China (30871003 and 31460267), the Key Social Development Project of Guizhou Provincial Science and Technology Department [grant SY (2013) 3019], the Cooperation Project of Guizhou Provincial Science and Technology Department and Guizhou Medical University [grant LH (2014)7088]. YX was supported by an ADA grant (1-19-IBS-142).

REFERENCES

Aldini, G., Altomare, A., Baron, G., Vistoli, G., Carini, M., Borsani, L., et al. (2018). N-Acetylcysteine as an antioxidant and disulphide breaking agent: the reasons why. *Free Radic. Res.* 52, 751–762. doi: 10.1080/10715762.2018.1468564

Apostolidis, S., Rodríguez-Rodríguez, N., Suárez-Fueyo, A., Dioufa, N., Ozcan, E., Crispín, J., et al. (2016). Phosphatase PP2A is requisite for the function of regulatory T cells. *Nat. Immunol.* 17, 556–564. doi: 10.1038/ni.3390

Bonetti, P., Lerman, L., and Lerman, A. (2003). Endothelial dysfunction a marker of atherosclerotic risk. *Arterioscler. Thromb. Vasc. Biol.* 23, 168–175. doi: 10.1161/01.atv.0000051384.43104.fc

Brautigan, D. L. (1995). Flicking the switches: phosphorylation of serine/threonine protein phosphatases. *Semin. Cancer Biol.* 6, 211–217. doi: 10.1006/scbi.1995.0028

Cat, A. N. D., Montezano, A., Burger, D., and Touyz, R. (2013). Angiotensin II, NADPH oxidase, and redox signaling in the vasculature. *Antioxid. Redox Signal.* 19, 1110–1120. doi: 10.1089/ars.2012.4641

Chao, C. Y., Lii, C. K., Ye, S. Y., Li, C. C., Lu, C. Y., Lin, A. H., et al. (2014). Docosahexaenoic acid inhibits vascular endothelial growth factor (VEGF)-induced cell migration via the GPR120/PP2A/ERK1/2/eNOS signaling pathway in human umbilical vein endothelial cells. *J. Agric. Food Chem.* 62, 4152–4158. doi: 10.1021/jf5007165

Ding, Y., Chen, J., Cui, G., Wei, Y., Lu, C., Wang, L., et al. (2016). Pathophysiological role of osteopontin and angiotensin II in atherosclerosis. *Biochem. Biophys. Res. Commun.* 471, 5–9. doi: 10.1016/j.bbrc.2016.01.142

Dounay, A. B., and Forsyth, C. J. (2002). Okadaic acid: the archetypal serine/threonine protein phosphatase inhibitor. *Curr. Med. Chem.* 9, 1939–1980. doi: 10.2174/0929867023368791

Drummond, G. R., and Sobey, C. G. (2014). Endothelial NADPH oxidases: which NOX to target in vascular disease? *Trends Endocrinol. Metab.* 25, 452–463. doi: 10.1016/j.tem.2014.06.012

Etwebi, Z., Landesberg, G., Preston, K., Eguchi, S., and Scalia, R. (2018). Mechanistic role of the calcium-dependent protease calpain in the endothelial dysfunction induced by MPO (myeloperoxidase). *Hypertension* 71, 761–770. doi: 10.1161/HYPERTENSIONAHA.117.10305

Everett, A. D., Stoops, T. D., Nairn, A. C., and Brautigan, D. (2001). Angiotensin II regulates phosphorylation of translation elongation factor-2 in cardiac myocytes. *Am. J. Physiol. Heart Circ. Physiol.* 281, 161–167. doi: 10.1152/ajpheart.2001.281.1.H161

Fedida-Metula, S., Feldman, B., Koshelev, V., Levin-Gromiko, U., Voronov, E., and Fishman, D. (2012). Lipid rafts couple store-operated Ca^{2+} entry to constitutive activation of PKB/Akt in a Ca^{2+}/calmodulin-, Src- and PP2A-mediated pathway and promote melanoma tumor growth. *Carcinogenesis* 33, 740–750. doi: 10.1093/carcin/bgs021

Fleming, I. (2009). Molecular mechanisms underlying the activation of eNOS. *Pflugers Arch.* 459, 793–806. doi: 10.1007/s00424-009-0767-7

Godo, S., and Shimokawa, H. (2017). Endothelial functions. *Arterioscler. Thromb. Vasc. Biol.* 37, 108–114. doi: 10.1161/ATVBAHA.117.309813

Han, M., Pendem, S., Teh, S., Sukumaran, D., Wu, F., and Wilson, J. (2010). Ascorbate protects endothelial barrier function during septic insult: role of protein phosphatase type 2A. *Free Radic. Biol. Med.* 48, 128–135. doi: 10.1016/j.freeradbiomed.2009.10.034

Hastie, R., Tong, S., Hannan, N., Brownfoot, F., Cannon, P., and Kaitu'u-Lino, T. (2016). Epidermal growth factor rescues endothelial dysfunction in primary human tissues in vitro. *Reprod. Sci.* 24, 1245–1252. doi: 10.1016/j.freeradbiomed.2009.10.034

Heumüller, S., Wind, S., Barbosa-Sicard, E., Schmidt, H. H., Busse, R., Schröder, K., et al. (2008). Apocynin is not an inhibitor of vascular NADPH oxidases but an antioxidant. *Hypertension* 51, 211–217. doi: 10.1161/HYPERTENSIONAHA.107.100214

Hung, M., Wang, C., Chen, Y., Chu, P., Hsiao, Y., Tai, W., et al. (2016). SET antagonist enhances the chemosensitivity of non-small cell lung cancer cells by reactivating protein phosphatase 2A. *Oncotarget* 7, 638–655. doi: 10.18632/oncotarget.6313

Incalza, M. A., D'Oria, R., Natalicchio, A., Perrini, S., Laviola, L., and Giorgino, F. (2018). Oxidative stress and reactive oxygen species in endothelial dysfunction associated with cardiovascular and metabolic diseases. *Vascul. Pharmacol.* 100, 1–19. doi: 10.1016/j.vph.2017.05.005

Ishii, Y., Kuroda, K., Matsushita, K., Yokoo, Y., Takasu, S., Kijima, A., et al. (2017). Phosphorylation of protein phosphatase 2A facilitated an early stage of chemical carcinogenesis. *Toxicol. Appl. Pharmacol.* 336, 75–83. doi: 10.1016/j.taap.2017.10.009

Janssens, V., and Goris, J. (2001). Protein phosphatase 2A: a highly regulated family of serine/threonine phosphatases implicated in cell growth and signalling. *Biochem. J.* 353, 417–439. doi: 10.1042/0264-6021:3530417

Kadowaki, D., Anraku, M., Sakaya, M., Hirata, S., Maruyama, T., and Otagiri, M. (2015). Olmesartan protects endothelial cells against oxidative stress-mediated cellular injury. *Clin. Exp. Nephrol.* 19, 1007–1014. doi: 10.1007/s10157-015-1111-5

Lambrecht, C., Haesen, D., Sents, W., Ivanova, E., and Janssens, V. (2013). Structure, regulation, and pharmacological modulation of PP2A phosphatases. *Methods Mol. Biol.* 1053, 283–305. doi: 10.1007/978-1-62703-562-0_17

Li, J., Geng, X., and Cong, X. (2016). PGC-1α ameliorates angiotensinII-induced eNOS dysfunction in human aortic endothelial cells. *Vascul. Pharmacol.* 83, 90–97. doi: 10.1016/j.vph.2016.05.005

Liu, H., Chen, T., Li, N., Wang, S., and Bu, P. (2015). Role of SIRT3 in angiotensin II-induced human umbilical vein endothelial cells dysfunction. *BMC Cardiovasc. Disord.* 15:81. doi: 10.1186/s12872-015-0075-4

Liu, X., Gao, R., Li, M., Si, C., He, Y., Wang, M., et al. (2016). The ROS derived mitochondrial respirstion not from NADPH oxidase plays key role in celastrol against angiotensin II-mediated HepG2 cell proliferation. *Apoptosis* 21, 1315–1326. doi: 10.1007/s10495-016-1294-6

Lovren, F., and Verma, S. (2013). Evolving role of microparticles in the pathophysiology of endothelial dysfunction. *Clin. Chem.* 59, 1166–1174. doi: 10.1373/clinchem.2012.199711

Luo, Y., Zhang, Q., Ding, J., Yu, M., Jiang, J., Yang, F., et al. (2019). Roles of I2PP2A in the downregulation of eNOS Ser1177 phosphorylation by angiotensin II-activated PP2A. *Biochem. Biophys. Res. Commun.* 516, 613–618. doi: 10.1016/j.bbrc.2019.06.063

Menden, H., Tate, E., Hogg, N., and Sampath, V. (2013). LPS-mediated endothelial activation in pulmonaryendothelial cells: role of Nox2-dependent IKK-β phosphorylation. *Am. J. Physiol. Lung Cell Mol. Physiol.* 304, 445–455. doi: 10.1152/ajplung.00261.2012

Mount, P., Kemp, B., and Power, D. (2007). Regulation of endothelial and myocardial NO synthesis by multi-site eNOS phosphorylation. *J. Mol. Cell Cardiol.* 42, 271–279. doi: 10.1016/j.yjmcc.2006.05.023

Nagata, D., Takahashi, M., Sawai, K., Tagami, T., Usui, T., Shimatsu, A., et al. (2006). Molecular mechanism of the inhibitory effect of aldosterone on endothelial NO synthase activity. *Hypertension* 48, 165–171. doi: 10.1161/01.HYP.0000226054.53527.bb

Panday, A., Sahoo, M. K., Osorio, D., and Batra, S. (2015). NADPH oxidases: an overview from structure to innate immunity-associated pathologies. *Cell. Mol. Immunol.* 12, 5–23. doi: 10.1038/cmi.2014.89

Petry, A., Weitnauer, M., and Görlach, A. (2010). Receptor activation of NADPH oxidases. *Antioxid. Redox Signal.* 13, 467–487. doi: 10.1089/ars.2009.3026

Qin, Y. Y., Li, M., Feng, X., Wang, J., Cao, L., Shen, X. K., et al. (2017). Combined NADPH and the NOX inhibitor apocynin provides greater anti-inflammatory and neuroprotective effects in a mouse model of stroke. *Free Radic. Biol. Med.* 104, 333–345. doi: 10.1016/j.freeradbiomed.2017.01.03

Qiu, Y., Tao, L., Lei, C., Wang, J., Yang, P., Li, Q., et al. (2015). Downregulating p22phox ameliorates inflammatory response in angiotensin II-induced oxidative stress by regulating MAPK and NF-κB pathways in ARPE-19 cells. *Sci. Rep.* 5:14362. doi: 10.1038/srep14362

Roe, N. D., He, E. Y., Wu, Z., and Ren, J. (2013). Folic acid reverses nitric oxide synthase uncoupling and prevents cardiac dysfunction in insulin resistance: role of Ca^{2+}/calmodulin-activated protein kinase II. *Free Radic. Biol. Med.* 65, 234–243. doi: 10.1016/j.freeradbiomed.2013.06.042

Roe, N. D., and Ren, J. (2012). Nitric oxide synthase uncoupling: a therapeutic target in cardiovascular diseases. *Vascul. Pharmacol.* 57, 168–172. doi: 10.1016/j.vph.2012.02.004

Schnelle, M., Sawyer, I., Anilkumar, N., Mohamed, B. A., Richards, D. A., Toischer, K., et al. (2019). NADPH oxidase-4 promotes eccentric cardiac hypertrophy in response to volume overload. *Cardiovasc. Res.* cvz331. doi: 10.1093/cvr/cvz331 (in press).

Searles, C. (2006). Transcriptional and posttranscriptional regulation of endothelial nitric oxide synthase expression. *Am. J. Physiol. Cell Physiol.* 291, C803–C816. doi: 10.1152/ajpcell.00457.2005

Sun, X., Wei, Y., Xiong, Y., Wang, X., Xie, A., Wang, X., et al. (2012). Synaptic released zinc promotes tau hyperphosphorylation by inhibition of protein phosphatase 2A (PP2A). *J. Biol. Chem.* 287, 11174–11182. doi: 10.1074/jbc.M111.309070

Tassone, E. J., Sciacqua, A., Andreozzi, F., Presta, I., Perticone, M., Carnevale, D., et al. (2013). Angiotensin (1-7) counteracts the negative effect of angiotensinIIon insulin signalling in HUVECs. *Cardiovasc. Res.* 99, 129–136. doi: 10.1093/cvr/cvt065

Touyz, R., Briones, A., Sedeek, M., Burge, D., and Montezano, A. (2011). NOX isoforms and reactive oxygen species in vascular health. *Mol. Interv.* 11, 27–35. doi: 10.1124/mi.11.1.5

Valko, M., Leibfritz, D., Moncol, J., Cronin, M. T., Mazur, M., and Telser, J. (2007). Free radicals and antioxidants in normal physiological functions and human disease. *Int. J. Biochem. Cell Biol.* 39, 44–84. doi: 10.1016/j.biocel.2006.07.001

Wang, C., Qian, X., Sun, X., and Chang, Q. (2015). Angiotensin II increases matrix metalloproteinase 2 expression in human aortic smooth muscle cells via AT1R and ERK1/2. *Exp. Biol. Med.* 240, 1564–1571. doi: 10.1177/1535370215576312

Wingler, K., Hermans, J. J., Schiffers, P., Moens, A., Paul, M., and Schmidt, H. H. (2011). NOX1, 2, 4, 5: counting out oxidative stress. *Br. J. Pharmacol.* 164, 866–883. doi: 10.1111/j.1476-5381.2011.01249.x

Wlodarchak, N., and Xing, Y. (2016). PP2A as a master regulator of the cell cycle. *Crit. Rev. Biochem. Mol. Biol.* 51, 162–184. doi: 10.3109/10409238.2016.1143913

Xiong, Y., Jing, X. P., Zhou, X. W., Wang, X. L., Yang, Y., Sun, X. Y., et al. (2013). Zinc induces protein phosphatase 2A inactivation and tau hyperphosphorylation through Src dependent PP2A (tyrosine 307) phosphorylation. *Neurobiol. Aging* 34, 745–756. doi: 10.1016/j.neurobiolaging.2012.07.003

Zhang, Q., Holland, W., Wilson, L., Tanner, J., Kearns, D., Cahoon, J., et al. (2012). Ceramide mediates vascular dysfunction in diet-induced obesity by PP2A-mediated dephosphorylation of the eNOS-Akt complex. *Diabetes* 61, 1848–1859. doi: 10.2337/db11-1399

Zhang, Z., Trautz, B., Kračun, D., Vogel, F., Weitnauer, M., Hochkogler, K., et al. (2019). Stabilization of p22phox by hypoxia promotes pulmonary hypertension. *Antioxid. Redox Signal.* 30, 56–73. doi: 10.1089/ars.2017.7482

Zhao, Y., Vanhoutte, P. M., and Leung, S. W. (2015). Vascular nitric oxide: beyond eNOS. *J. Pharmacol.* 129, 83–94. doi: 10.1016/j.jphs.2015.09.002

Conflict of Interest: The authors declare that the research was conducted in the absence of any commercial or financial relationships that could be construed as a potential conflict of interest.

Copyright © 2020 Ding, Yu, Jiang, Luo, Zhang, Wang, Yang, Wang, Wang, Zhuang, Wu, Zhang, Xia and Lu. This is an open-access article distributed under the terms of the Creative Commons Attribution License (CC BY). The use, distribution or reproduction in other forums is permitted, provided the original author(s) and the copyright owner(s) are credited and that the original publication in this journal is cited, in accordance with accepted academic practice. No use, distribution or reproduction is permitted which does not comply with these terms.

frontiers in Physiology

ORIGINAL RESEARCH
published: 22 October 2020
doi: 10.3389/fphys.2020.579712

Disruption of STAT6 Signal Promotes Cardiac Fibrosis Through the Mobilization and Transformation of CD11b$^+$ Immature Myeloid Cells

Weiwei Zhang[1†], Baoling Zhu[1,2†], Suling Ding[1], Xiangfei Wang[1,2], Jian Wu[1,2], Xiaowei Zhu[1,2], Yunzeng Zou[1,2], Junbo Ge[1,2], Minghong Tong[3] and Xiangdong Yang[1,2*]*

[1] Shanghai Institute of Cardiovascular Diseases, Zhongshan Hospital, Fudan University, Shanghai, China, [2] Department of Cardiology, Zhongshan Hospital, Fudan University, Shanghai, China, [3] Division of Clinical Laboratory, TongRen Hospital, Shanghai Jiao Tong University School of Medicine, Shanghai, China

OPEN ACCESS

Edited by:
Jun Ren,
University of Washington,
United States

Reviewed by:
Han Xiao,
Peking University Third Hospital,
China
Xiaoxiang Yan,
Shanghai Jiao Tong University, China

***Correspondence:**
Xiangdong Yang
yang.xiangdong@zs-hospital.sh.cn;
yangxiangdong_zs@163.com
Minghong Tong
tmh0944@shtrhospital.com

[†] These authors have contributed equally to this work

Specialty section:
This article was submitted to Clinical and Translational Physiology, a section of the journal Frontiers in Physiology

Received: 03 July 2020
Accepted: 16 September 2020
Published: 22 October 2020

Citation:
Zhang W, Zhu B, Ding S, Wang X, Wu J, Zhu X, Zou Y, Ge J, Tong M and Yang X (2020) Disruption of STAT6 Signal Promotes Cardiac Fibrosis Through the Mobilization and Transformation of CD11b$^+$ Immature Myeloid Cells. Front. Physiol. 11:579712. doi: 10.3389/fphys.2020.579712

Cardiac fibrosis is an important pathological basis of various cardiovascular diseases. The roles of STAT6 signal in allergy, immune regulation, tumorigenesis, and renal fibrosis have been documented. However, the function and mechanism of STAT6 signal in sympathetic overactivation-induced cardiac fibrosis have not been fully elucidated. This study explores the novel role of STAT6 signal in isoproterenol (ISO)–induced cardiac fibrosis through the regulation of inflammatory response and the differentiation of macrophages from immature myeloid cells. The expression levels of STAT6, β1-adrenergic receptor (β1-AR), and inflammatory factors [interleukin α (IL-1α), IL-6, IL-18, and transforming growth factor β (TGF-β)] in CD11b$^+$ myeloid cells were analyzed with a microarray study. The levels of IL-6 and TGF-β1 in the CD11b$^+$ myeloid cells–derived macrophages were detected with reverse transcriptase–polymerase chain reaction (RT-PCR). STAT6–knockout (KO) and WT mice were used to establish a murine cardiac fibrosis model by ISO injection. Cardiac fibroblasts were isolated from the hearts of newborn STAT6-KO and WT mice, and STAT6 expression was measured by Western blotting and RT-PCR after ISO stimulation, while α-smooth muscle actin (α-SMA) expression was detected by immunofluorescence and immunohistochemistry staining. Cardiac function and pathological characteristics were examined by echocardiography and immunohistochemistry staining, respectively. Immunohistochemistry staining with anti-CD11b was performed to detect the infiltration of CD11b$^+$ myeloid cells in heart tissue. Flow cytometry analysis was used to measure the percentages of CD11b$^+$ myeloid cells and CD11b$^+$Ly6C$^+$ macrophages in the peripheral blood. The results showed that STAT6 was highly expressed in CD11b$^+$ myeloid cells located in injured hearts, and STAT6 expression in cardiac fibroblasts was down-regulated after ISO treatment. STAT6 deficiency further aggravated ISO-induced increased expression of α-SMA in cardiac fibroblasts, myocardial fibrosis, and cardiac dysfunction. The activation of ISO/β1-AR signal aggravated cardiac inflammatory infiltration, promoted CD11b$^+$ myeloid cell mobilization, and enhanced CD11b$^+$Ly6C$^{+/low}$ macrophage differentiation, which was further exacerbated by STAT6 deficiency. Furthermore, β1-AR mRNA

expression significantly increased in splenic CD11b$^+$ myeloid cells compared to their bone marrow–derived controls, and STAT6 deficiency promoted β1-AR expression in an MI-induced sensitive cardiac fibrosis mouse model. The spleen-derived CD11b$^+$ myeloid cells of STAT6-KO mice produced more IL-1α, IL-18, and TGF-β than their WT counterparts. Taken together, these results suggest that STAT6 signal plays a critical role in ISO-induced β1-AR overactivation and systemic inflammatory cascades, contributing to cardiac fibrogenesis. STAT6 should be a promising cardioprotective target against myocardial fibrosis and heart failure after β1-AR overactivation–induced myocardial injury.

Keywords: cardiac fibrosis, STAT6, isoproterenol, β-adrenergic receptor, inflammatory, CD11b$^+$ myeloid cells, macrophages

INTRODUCTION

The proliferation of fibroblasts and collagen secretion are crucial for the repair of cardiomyocytes after acute ischemic injury due to the poor regenerative abilities of cardiomyocytes. However, cardiac fibrosis post–acute myocardial ischemic injury is a double-edged sword. On the one hand, fibroblasts can repair the structural damage caused by myocardial necrosis. On the other hand, the excessive proliferation of myofibroblasts and the release of inflammatory cytokines aggravate the pathological remodeling of myocardium. It is well known that the pathological features of cardiac remodeling induced by hypertension are cardiomyocyte hypertrophy and cardiac interstitial fibrosis (Cuspidi et al., 2020; Ruan et al., 2018).

Chronic overactivation of the sympathetic nervous system by stimulation of β-adrenergic receptors (β-ARs) has been demonstrated to play a critical role in the development of hypertension and cardiac fibrosis (Alemasi et al., 2019), whereas cardiac sympathetic afferent denervation could suppress deleterious cardiac remodeling and improve cardiovascular dysfunction (Wang et al., 2014). By stimulating β-ARs, catecholamine overload leads to cardiac remodeling (Morishige et al., 2019). Isoproterenol (ISO) is a nonspecific β-AR agonist, and low-dose continuous injection of ISO may contribute to sustained β-AR stimulation in cardiomyocytes. A recent study revealed that acute β-AR overactivation by single-dose ISO injection could trigger interleukin 18 (IL-18)–dependent cytokine cascades, macrophage infiltration, and cardiac remodeling (Xiao et al., 2018). N-propargyl caffeate amide was reported to prevent cardiac fibrosis induced by myocardial infarction (MI) by enhancing pro-resolving macrophage polarization (Cheng et al., 2020). These studies highlight the critical role of innate immune cells in cardiovascular diseases caused by sympathetic dysfunction. However, more investigation is needed in order to understand the mechanisms behind this effect.

Histamine is a biogenic amine that has variable roles in allergies, inflammation, and gastric acid secretion and has also been linked to immune responses and tumorigenesis (Yang et al., 2011). Histidine decarboxylase (HDC) is the unique enzyme responsible for the conversion of L-histidine to histamine. Our previous studies demonstrated that histamine deficiency in HDC knockout (HDC-KO) mice could promote myocardial injury and cardiac fibrosis through aggravating macrophage dysfunction and cardiomyocyte apoptosis post-MI (Deng et al., 2015). The STAT6 signal was identified to mediate the effect of histamine on macrophage differentiation from CD11b$^+$Gr-1$^+$ immature myeloid cells (Xu et al., 2017). Furthermore, aggravated cardiac fibrogenesis was also examined in STAT6-KO mice (Chen et al., 2017). STAT6 has been found to be essential for the regulation of immune response and allergic response (Haase et al., 2020; Nam et al., 2020). Activation of the sympathetic nervous system has been demonstrated in acute MI (Graham et al., 2004; Hogarth et al., 2009; Hogarth et al., 2006). However, the roles and mechanisms of the β-AR signaling pathway in innate immune cell activation and myocardial fibrosis have not been fully elucidated.

The role of STAT6 and β-AR signals in cardiac fibrosis has not yet been characterized. To address this question, the expression levels of β1-AR mRNA were analyzed in CD11b$^+$ myeloid cells directly isolated from the spleen and bone marrow of mice with MI-induced cardiac fibrosis. Furthermore, the activation of immune subsets in the peripheral blood and injured hearts of mice with ISO treatment was analyzed by flow cytometry analysis and histopathological study, respectively. STAT6-KO mice were also used to establish an ISO-induced cardiac fibrosis model and to investigate the effects of STAT6 deficiency on macrophage activation and fibroblast proliferation. We identified a higher level of β1-AR mRNA expressed in the spleen-derived CD11b$^+$ myeloid cells compared to the bone marrow–derived counterparts. Overactivation of the β1-AR signal by ISO stimulation aggravated cardiac fibrosis mainly through the regulation of inflammatory infiltration, myeloid immune cell mobilization, and macrophage differentiation in STAT6 deficiency mice.

MATERIALS AND METHODS

Animals

Male HDC-enhanced green fluorescent protein (EGFP), HDC-KO, STAT6-KO, and wild-type (WT) mice (Balb/C background, 10 weeks old) were purchased from the Model Animal Research Center of Nanjing University. All mice were housed in the SPF (specific pathogen–free) environment at 25°C with a 12-h

bright/dark alternation and allowed free access to water and food. All animal experiments were reviewed and approved by the Animal Ethics Committee of Fudan University. Our study was performed in accordance with the Guidelines for the Care and Use of Laboratory Animals, which was published by the US National Institutes of Health (NIH Publication, 8th edition, 2011).

ISO-Induced Cardiac Fibrosis Model Establishment

ISO (Sigma–Aldrich, United States) was formulated in saline prior to use. The mice were divided into six groups as follows: (i) WT + ISO 1 week: daily administration of ISO (5 mg/kg per day) for 1 week; (ii) WT + ISO 4 weeks: daily administration of ISO (5 mg/kg per day) for 4 weeks; (iii) WT control: daily subcutaneous administration of saline (same volume as ISO group) for 4 weeks; (iv) STAT6-KO + ISO 1 week: daily administration of ISO (5 mg/kg per day) for 1 week; (v) STAT6-KO + ISO 4 weeks: daily administration of ISO (5 mg/kg per day) for 4 weeks; (vi) STAT6-KO control: daily subcutaneous administration of saline for 4 weeks. Mice were euthanized approximately 24 h after the last injection.

Echocardiography

The echocardiography was performed using a high-resolution small animal ultrasound system VisualSonics Vevo770 (VISUALSONIC, Canada). Mice were anesthetized under 2% isoflurane concentrations, and parastolic left ventricular long-axis view was captured. The following parameters of left ventricular ejection fraction (EF%) and left ventricular fractional shortening (FS%) were selected to evaluate cardiac function. EF% and FS% were calculated by the Simpson method as previously reported (Heinen et al., 2018). Each parameter took the mean value of three consecutive cardiac cycles.

Flow Cytometry Analysis

Approximately 24 h after the last injection, mice were euthanized. The peripheral blood was collected and made into single-cell suspension. Erythrocyte lysate was used to get rid of red blood cells. Then cells were centrifuged and resuspended with 1 × phosphate-buffered saline (PBS). APC-CD11b (Biolegend, 101212), Gr-1-PerCP-Cy5.5 (BD, 552093), and Ly6C-PE (BD, 560592) fluorescent antibodies were used to incubate and stain cells for 45 min at 4°C. After washing, cells were resuspended with 300 μL PBS. The data were collected using a LSRII flow cytometer (BD Biosciences) and analyzed using FlowJo v7 software (Tree Star, Inc.).

Histology and Immunohistochemistry Staining

After mice euthanasia, the heart was perfused with cold PBS and fixed with 10% neutral-buffered formalin at 4°C overnight. Then, the heart was embedded in paraffin and cut into 5-μm-thick coronal slides for further procedures. Sirius red staining and Masson staining were used to detect cardiac fibrosis; hematoxylin and eosin (HE) staining was used for morphology and inflammatory analysis, and immunohistochemistry staining was used to test the expression of α-SMA (Abcam, ab5694) and CD11b (BD, 553308) in heart tissues. The heart sections were captured with a light microscopy (Leica, Germany). Image-Pro-Plus 6 software was used to measure the area of anti-CD11b staining, collagen, and heart, respectively. The ratio of anti-CD11b staining area to heart area was used to evaluate cardiac $CD11b^+$ infiltration; the ratio of collagen area to heart area was used to evaluate cardiac fibrosis.

Cell Culture and Treatment

Primary cardiac fibroblasts were isolated from newborn (days 0–2) mice as described previously (Sawaki et al., 2018). Then, fibroblasts were collected and cultured in Dulbecco modified eagle medium supplemented with 10% fetal bovine serum (Sigma–Aldrich, United States) and 1% penicillin-streptomycin in a humidified environment at 37°C with 5% CO_2. Generation 2–4 fibroblasts were used in this study. Fibroblasts were cultured at densities of less than 80% confluency in a six-well culture plate, and the serum-free medium was used for at least 24 h before ISO treatment. Then the cells were stimulated by ISO and harvested after 24 h of continuous stimulation. In control groups, fibroblasts were given an equal volume of PBS instead. The mRNA and protein expression were measured with polymerase chain reaction (PCR) and Western blotting, respectively.

Bone marrow–derived cells were isolated from the femur bones of WT and STAT6-KO mice and made into single-cell suspensions, and the FACS lysing solution (BD) was used to lyse red blood cells. $CD11b^+$ cells were then sorted by magnetic beads. $CD11b^+$ cells were cultured in six-well culture plates (approximately 2.5 million cells/well) with RPMI-1640 medium (Hyclone) supplemented with 10% fetal bovine serum (Sigma–Aldrich, United StatesA) and 1% penicillin-streptomycin in a humidified environment (37°C at 5% CO_2 concentration). The cells were induced to differentiate into macrophages with macrophage colony-stimulating factor (M-CSF, PeproTech, 100 ng/mL) for 5–7 days, and the liquid medium was changed every 2 days. After the last change of the culture medium, the macrophages were cultured in serum-free medium for 24 h. Then, the macrophages were stimulated with ISO for 15 min and collected with Trizol for the subsequent detection of inflammatory factors mRNA expression.

Immunofluorescence Staining

Cardiac fibroblasts were isolated from STAT6-KO and WT mice hearts and cultured as above. Cardiac fibroblasts were fixed with 4% (vol/vol) paraformaldehyde for 20 min, permeabilized with 0.2% TritonX-100 for 20 min, and blocked with 5% bovine serum albumin for 1 h at room temperature. Then samples were incubated with anti–α-SMA antibody (Abcam, ab5694) at 1:200 overnight at 4°C. After washing three times with 1 × PBS, cells were incubated with Alexa Flour 594–conjugated donkey anti–rabbit immunoglobulin G (1:400) for 1 h at room temperature in a dark environment. After washing, DAPI (Beyotime Biotechnology, China) was used to stain nuclei. The method of immunofluorescence for frozen section was similar to

our previous study (Chen et al., 2017). The immunofluorescence staining method for heart and spleen tissues is as similar as above. All photographs were taken with a fluorescence microscope (Leica, Germany).

Quantitative Real-Time PCR

Total RNA was extracted by TRIzol reagent (Invitrogen, Waltham, MA, United States) for mRNA quantification. Then 1 μg of RNA was reverse transcribed with a PrimeScript RT reagent Kit with gDNA Eraser (Takara, Japan). The gene expression level of STAT6 was quantified by SYBR Premix Ex Taq (Takara, Japan). Data analysis was performed with an Applied Biosystems Prism7500 sequence detection system. Based on the sequences that were available in NCBI database, gene primers of β-actin, GAPDH, STAT6, IL-6, and transforming growth factor β (TGF-β) were designed by Sangon Biotech (Shanghai, China), which is shown in detail in the **Table 1**. After the expression of β-actin or GAPDH was normalized, the fold change of STAT6, IL-6, and TGF-β1 expression was calculated according to the ΔΔ cycle time (Ct) method.

Western Blotting

Cardiac fibroblasts were lysed on ice with RIPA lysis buffer (Beyotime Biotechnology, China) supplemented with protease and phosphatase inhibitors for protein extraction. The protein concentrations were measured by BCA protein assay kit (Beyotime Biotechnology, China). Proteins were loaded onto 10% sodium dodecyl sulfate–polyacrylamide gel electrophoresis and were blotted onto the polyvinylidene fluoride membrane. These membranes were incubated with 5% nonfat dry milk to block proteins for 1 h. Next, membranes were incubated and stained with primary antibodies overnight at 4°C. The primary antibodies were diluted for 1:1,000 and 1:5,000 for anti-STAT6 (Abcam, ab44718) and anti-GAPDH (Abcam, ab8245), respectively. On the next day, membranes were washed with 1 × TBST (Tris-buffered saline + Tween 20) for three times and were then incubated with second antibodies labeled by horseradish peroxidase for 2 h. Membranes were washed with 1 × TBST for three times and were quantified by scanning densitometries.

Microarray Performance and Analysis

Differentially expressed genes of $CD11b^+$ myeloid cells in the spleen and bone marrow of WT, HDC-KO, and STAT6-KO mice (five mice in each group) were examined by microarray analysis (Agilent Mouse 4x44K Gene Expression Microarrays). Total RNA was extracted from $CD11b^+$ cells (10 million cells) isolated from the spleen and bone marrow of MI and control mice for microarray studies. The sample preparation and chip data analysis of Gene Expression Microarrays were described in detail in our previous article (Xu et al., 2017). The microarray data have been deposited in the GEO (Gene Expression Omnibus) database (accession number: GSE154733). Basic analysis was performed with Genespring software. Then, according to the threshold (fold change >2.0 and $P < 0.05$), differentially expressed genes were selected out.

Statistical Methods

GraphPad Prism software was used for statistical analysis, and data were expressed with $\bar{x} \pm s$. Student t test was used to compare data between two groups, and one-way analysis of variance (ANOVA) was used to compare data among multiple groups. When two factors were involved, data were statistically analyzed by the two-way ANOVA analysis. $P < 0.05$ was considered to be statistically significant.

RESULTS

β1-AR Expression Increased in the Splenic $CD11b^+$ Myeloid Cells in HDC-KO Mice With MI

Our previous studies have shown that HDC-KO mice are sensitive models of cardiac fibrosis after MI and that histamine deficiency inhibits the expression of STAT6 signal in $CD11b^+Ly6C^+$ macrophages (Xu et al., 2017; Chen et al., 2017). By microarray analysis, the data showed the downregulation of STAT1, STAT2, STAT3, STAT4, and STAT6 mRNA in the spleen-derived $CD11b^+$ cells after MI-1wk compared to sham group (**Figure 1A**). Furthermore, we also observed a higher level expression of β1-AR mRNA in the spleen-derived $CD11b^+$ cells than that of bone marrow–derived $CD11b^+$ cells (**Figure 1B**). The expression of β1-AR decreased in the spleen-derived $CD11b^+$ cells of WT mice both 1 week and 4 weeks after MI (**Figure 1C**). Interestingly, we found significant upregulation of β1-AR in the spleen-derived $CD11b^+$ cells of HDC-KO mice at 1 week and 4 weeks after MI compared to WT mice (**Figure 1D**). A similar result was examined in the bone marrow–derived $CD11b^+$ cells of HDC-KO mice at 4 weeks after MI compared to WT mice (**Figure 1E**). Taken together, these data not only confirm that the spleen is the main cellular source of $CD11b^+$ myeloid cells in the early stage of MI, but also suggest that the β-AR–related sympathetic signal and the STAT6 signal are involved in the activation of $CD11b^+$ immune cells and cardiac fibrogenesis after MI.

STAT6 Was Highly Expressed in $CD11b^+$ Myeloid Cells Infiltrated Into Mouse Heart

HDC-EGFP transgenic mice provide a very convenient tool for tracing GFP-expressing $CD11b^+$ myeloid immune cells *in vivo* (Yang et al., 2011). FACS data showed that about 40–50% of bone marrow cells, 3–5% of spleen cells, and 10% to 20% of blood cells were GFP^+ and thus expressing HDC (**Figures 2A,B**). Furthermore, FACS data revealed that the majority of GFP^+ cells expressed myeloid cell marker CD11b (90–95%) including $CD11b^+Gr\text{-}1^+$ granulocytic cells and $CD11b^+Gr\text{-}1^-$ monocytic cells (**Figures 2A,C**). In this study, we examined the expression of GFP and STAT6 in the hearts of HDC-EGFP mice with ISO treatment (three times I.P). The results of immunostaining with anti-STAT6 showed that the expression levels of STAT6 and GFP-expressing myeloid cells increased in the injured hearts of HDC-EGFP

TABLE 1 | Primers for RT-PCR.

Gene	Forward primer	Reverse primer
β-Actin	ACGTTGACATCCGTAAAGACC	ACACAGAGTACTTGCGCTCA
GAPDH	GACATCAAGAAGGTGGTGAAGCAG	ATACCAG GAAATG AGCTTG ACAAA
STAT6	CTCTGTGG G GCCTAATTTCCA	GCATCTGAACCGACCAGGAAC
IL-6	CCAAGAGGTGAGTGCTTCCC	CTGTTGTTCAGACTCTCTCCCT
TGF-βI	TCTGCATTGCACTTATGCTGA	AAAGGGCGATCTAGTGATGGA

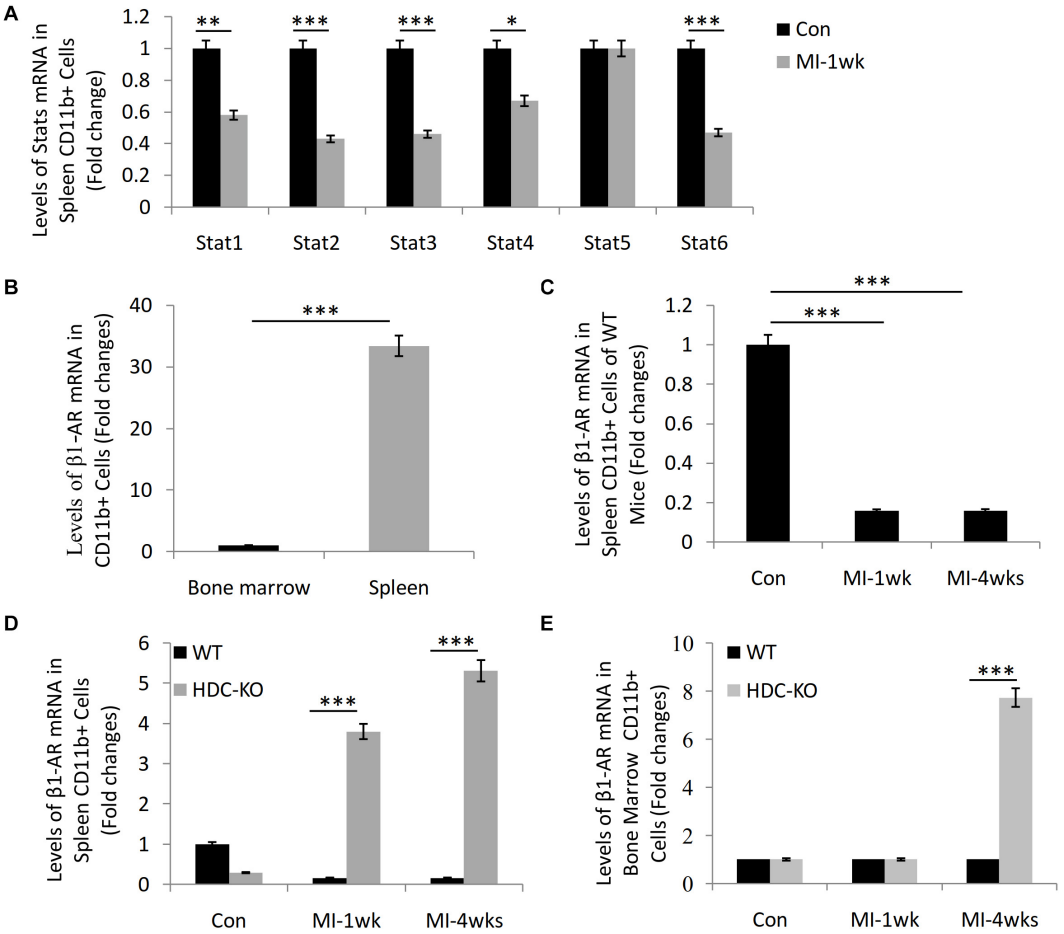

FIGURE 1 | Microarray study data showing STAT6 and β1-AR expression in CD11b$^+$ myeloid cells of mice with MI. **(A)** The mRNA levels of STAT1, STAT2, STAT3, STAT4, STAT5, and STAT6 in the splenic CD11b$^+$ cells isolated from WT mice 1 week after MI. **(B)** The expression of β1-AR in bone marrow and spleen-derived CD11b$^+$ cells of WT mice. **(C)** The expression of β1-AR in spleen-derived CD11b$^+$ cells of WT mice after MI. **(D)** The expression of β1-AR in spleen-derived CD11b$^+$ cells of HDC-KO and WT mice after MI. **(E)** The expression of β1-AR in bone marrow–derived CD11b$^+$ cells of HDC-KO and WT mice after MI. ***$P < 0.001$, **$P < 0.01$, *$P < 0.05$. $n = 5$ per group.

mice after ISO stimulation; the colocalization results showed that STAT6 was highly expressed in GFP$^+$ myeloid cells and cardiac interstitial cells instead of cardiomyocytes (**Figure 2D**). Furthermore, the result of coimmunostaining with anti-STAT6 (red) and anti-CD11b (green) confirmed a high level expression of STAT6 protein in CD11b$^+$ myeloid cells (**Figure 2E**). Spleen tissue was used as a positive control because of high level expression of STAT6 in lymphocytes and CD11b$^+$ cells (data not shown). Thus, these results suggest that the STAT6 signaling pathway is involved in the expression and function of CD11b$^+$ myeloid cells in stress-induced myocardial injury and repair.

STAT6 Expression Decreased in ISO-Treated Fibroblasts and STAT6 Deficiency Promoted Cardiac Fibroblast Transdifferentiation

To further investigate the link between ISO and STAT6 expression, we isolated and cultured the cardiac fibroblasts from

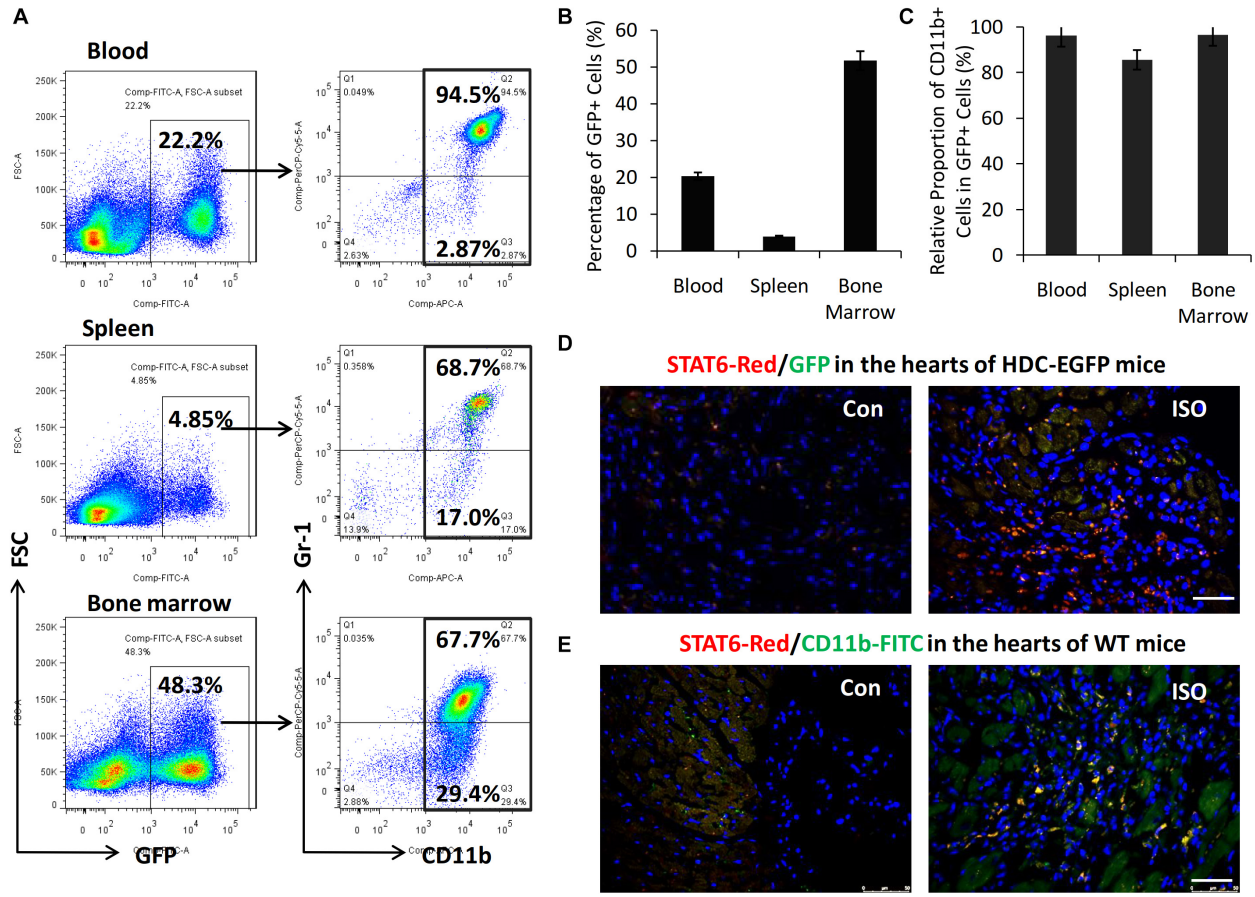

FIGURE 2 | High level expression of STAT6 in CD11b$^+$ myeloid cells in mouse heart. **(A)** Representative FACS graphs show the percentage of CD11b$^+$GFP$^+$ cells in the blood, spleen, and bone marrow of HDC-EGFP mice. **(B)** Quantitative analysis of percentage of GFP$^+$ cells in the blood, spleen, and bone marrow of HDC-EGFP mice. **(C)** Quantitative analysis of the relative proportion of CD11b$^+$ myeloid cells in total GFP$^+$ cells in the blood, spleen, and bone marrow of HDC-EGFP mice. **(D)** The expression of STAT6 (red) in the injured hearts of HDC-EGFP mice after ISO stimulation. Scale bar, 50 μm. **(E)** The expression of STAT6 (red) its colocalization with CD11b$^+$ (green). Scale bar, 50 μm. n = 5–6 per group.

neonatal mice *in vitro*. The result of quantitative PCR showed that STAT6 mRNA expression was significantly downregulated in cardiac fibroblasts following ISO treatment (**Figure 3A**). Western blotting data further confirmed that ISO remarkably reduced the expression of STAT6 protein (**Figure 3B**).

Next, to investigate the role of STAT6 in ISO-induced cardiac myofibroblasts transdifferentiation, we stained α-SMA (a canonical marker of myofibroblasts) *in vivo* and *in vitro*. Immunofluorescence staining with anti–α-SMA showed that the expression of α-SMA in cardiac fibroblasts was significantly up-regulated upon ISO stimulation, and more α-SMA$^+$ myofibroblasts proliferated and accumulated in the hearts of STAT6-KO mice compared with that of WT mice (**Figure 3C**). The expression of α-SMA in cardiac tissue was detected by immunohistochemical staining. The results confirmed that the hearts of STAT6-KO mice exhibited abundant positively α-SMA–labeled cells than that of WT mice by ISO administration (**Figures 3D,E**). These data demonstrate that the STAT6 signaling pathway has a close relationship with ISO-induced cardiac fibrosis, and STAT6 deficiency aggravates ISO-induced cardiac α-SMA$^+$ myofibroblasts differentiation and proliferation in mice.

STAT6 Deficiency Aggravated ISO-Induced Cardiac Dysfunction and Fibrosis in Mice

We sought to explore the role of STAT6 signal in ISO-induced cardiac fibrosis. Age- and gender-matched STAT6 and WT mice were treated with ISO injection for 4 weeks. The ratio of heart weight to body weight (HW/BW) increased in STAT6-KO and WT mice with ISO compared to control groups; a significant upward shift of the HW/BW ratio was examined in ISO-treated STAT6-KO mice compared to ISO-treated WT mice (**Figure 4A**). Furthermore, HE staining data showed that the ventricular cavity was enlarged in response to persistent ISO stimulation and that the hearts of STAT6-KO + ISO mice were significantly bigger than those of WT + ISO mice (**Figure 4B**). Echocardiography was performed to evaluate the left ventricular systolic function (**Figure 4C**). Cardiac function parameters (EF% and FS%) of

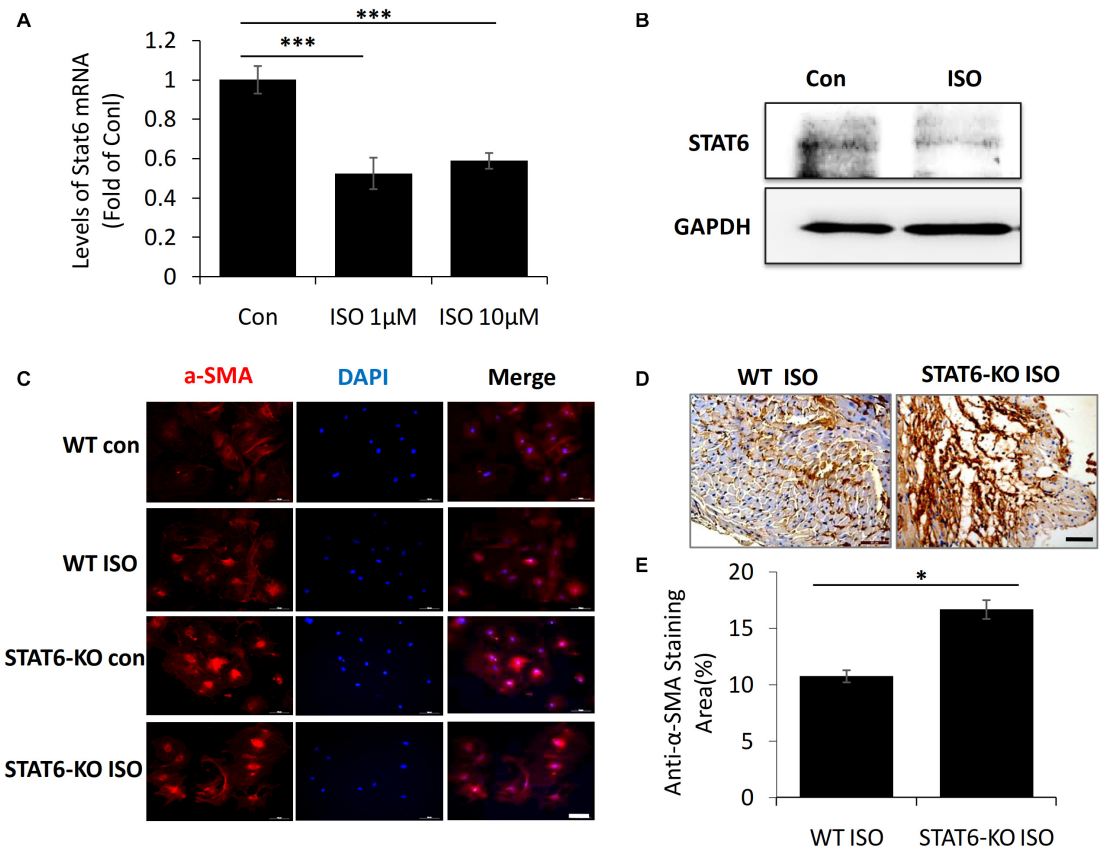

FIGURE 3 | The expression of STAT6 and α-SMA expression in cardiac fibroblasts upon ISO stimulation. **(A)** The mRNA level of STAT6 expression by RT-PCR (n = 3). **(B)** The protein level of STAT6 expression by Western blotting. **(C)** Representative images of immunofluorescence staining for α-SMA in isolated cardiac fibroblasts upon ISO treatment. Scale bar, 100 μm, n = 3. **(D)** Representative images of immunohistochemical staining for α-SMA in heart tissue after ISO treatment for 4 weeks. Scale bar, 50 μm, n = 6. **(E)** Quantitative analysis of anti–α-SMA area (%) with immunohistochemical staining in heart tissue after ISO treatment for 4 weeks (n = 6). ***P < 0.001, *P < 0.05.

ISO mice were significantly lower than those of control mice, reflecting the impairment of cardiac function. What's more, EF% and FS% of STAT6-KO + ISO mice were significantly lower than those of WT + ISO mice (**Figures 4D,E**). The results of Sirius red staining (**Figures 4F,G**) and Masson staining (**Figures 4H,I**) showed that the hearts of ISO mice produced more interstitial collagen than those of control mice and that STAT6 deficiency significantly increased collagen accumulation after ISO stimulation compared to WT controls. Taken together, these data demonstrate that the STAT6 signal plays a critical role in ISO-induced cardiac dysfunction and that its deficiency promotes cardiac fibrosis.

STAT6 Knockout Promoted CD11b$^+$ Myeloid Cells Mobilization, CD11b$^+$Ly6C$^+$ Macrophage Differentiation, and Aggravated ISO-Induced Cardiac Inflammation

Given that ISO treatment could induce inflammatory reaction in the hearts of mice, we sought to investigate the effects of STAT6-KO on the expression of immune cells in the development of ISO-induced cardiac fibrosis. HE staining showed that the number of infiltrated immune cells significantly increased in the hearts of STAT6-KO + ISO mice compared to those of WT + ISO mice; concurrently, we also found that STAT6-KO did not significantly increase the immune cells in the hearts without ISO stimulation (**Figure 5A**). We further examined the expression of CD11b in cardiac tissue by immunohistochemical staining, which showed that STAT6-KO significantly increased the infiltration of CD11b$^+$ myeloid cells in the injured hearts caused by ISO (**Figure 5B**). What's more, FACS data showed that after ISO treatment, the percentage of CD11b$^+$Gr1$^+$ myeloid cells increased in the peripheral blood of STAT6-KO mice compared to WT mice with ISO treatment (**Figures 5C,D**). Additionally, FACS data showed that the percentage of CD11b$^+$ly6C$^+$ monocytes/macrophages increased in the peripheral blood of STAT6-KO + ISO mice than that of WT + ISO mice (**Figures 5E,F**). These results suggest that STAT6 deficiency mediates a crucial role in ISO-induced inflammatory storm, which is characterized by aggravating cardiac inflammatory infiltration, increasing CD11b$^+$ myeloid cell mobilization, and promoting CD11b$^+$ly6C$^+$ macrophage differentiation.

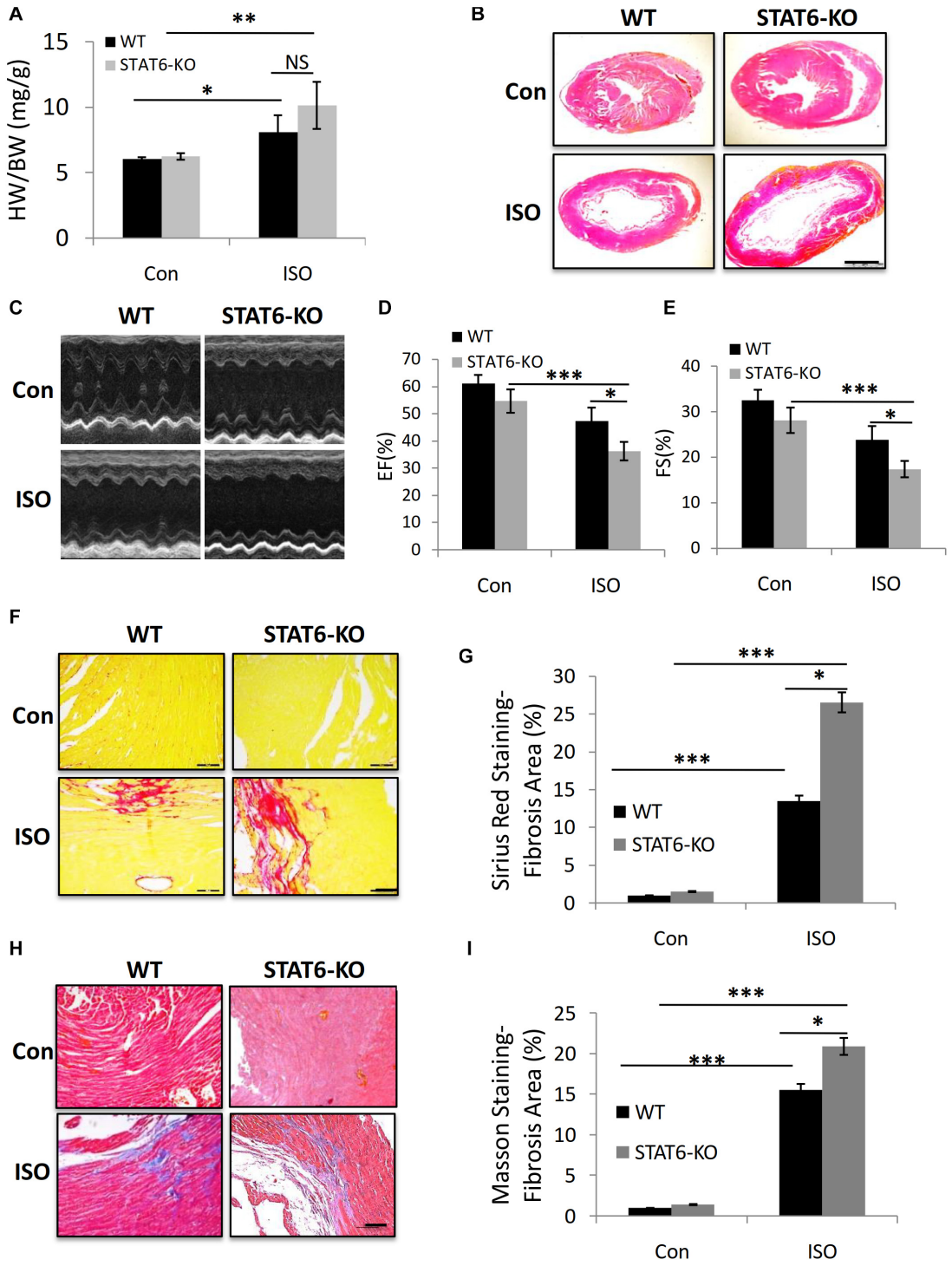

FIGURE 4 | The impact of STAT6 deficiency on ISO-induced cardiac dysfunction and fibrosis in mice. **(A)** The HW/BW ratio of mice. **(B)** Representative HE staining images of heart. Scale bar, 1,000 μm. **(C)** Representative parasternal long-axis view echocardiographic M-mode images after ISO treatment for 4 weeks. **(D)** Quantitative analysis of EF (%) after ISO treatment for 4 weeks. **(E)** Quantitative analysis of FS (%) after ISO treatment for 4 weeks. **(F)** Representative micrographs of Sirius red staining. Scale bar, 100 μm. **(G)** Quantitative analysis of fibrosis area (%) with Sirius red staining. **(H)** Representative micrographs of Masson staining. Scale bar, 100 μm. **(I)** Quantitative analysis of fibrosis area (%) with Masson staining. ***$P < 0.001$, **$P < 0.01$, *$P < 0.05$. $n = 6$–8 per group.

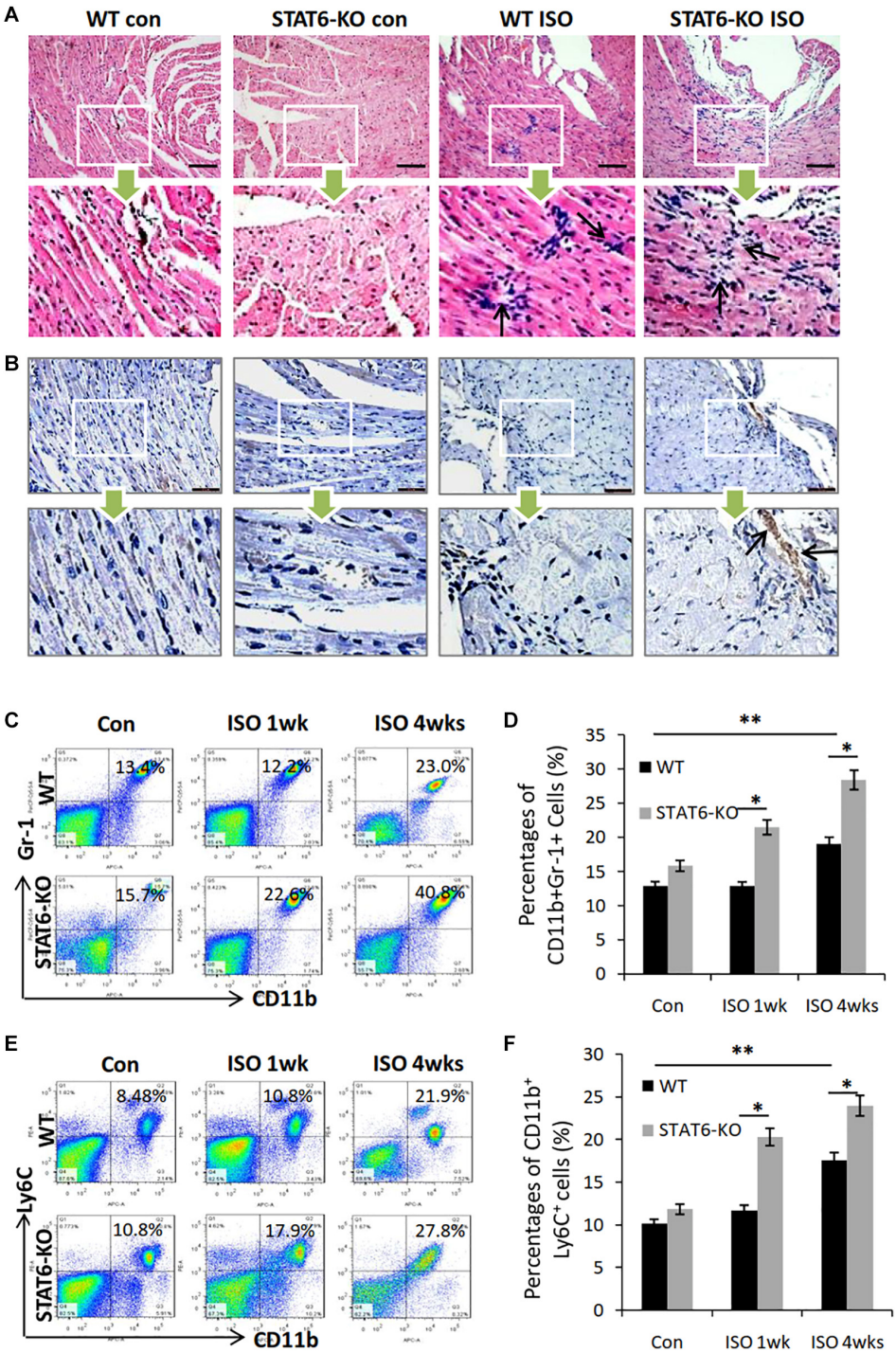

FIGURE 5 | The impact of ISO and STAT6 signal on systemic and cardiac inflammatory responses. **(A)** Representative HE staining images of heart sections, and the black arrows refer to the infiltrated inflammatory cells. Scale bar, 100 μm. **(B)** Representative images of immunohistochemical staining for CD11b in hearts, and the black arrows refer to the infiltrated $CD11b^+$ cells. Scale bar, 50 μm. **(C)** Representative FACS graphs show the percentage of $CD11b^+Gr\text{-}1^+$ myeloid cells following ISO treatment. **(D)** Quantitative analysis of percentage of $CD11b^+Gr\text{-}1^+$ myeloid cells. **(E)** Representative FACS graphs show the percentage of $CD11b^+Ly6C^+$ myeloid cells following ISO treatment. **(F)** Quantitative analysis of percentage of $CD11b^+Ly6C^+$ macrophages. $^{***}P < 0.001$, $^{**}P < 0.01$, $^{*}P < 0.05$. $n = 6$–8 per group.

STAT6 Deficiency Promoted the Expression of β1-AR and Inflammatory Factors in Splenic CD11b$^+$ Cells and Myeloid Cell–Derived Macrophages

The microarray data revealed that the level of β1-AR expression in the spleen-derived CD11b$^+$ cells of STAT6-KO mice was significantly higher than that of WT mice in a sensitive myocardial fibrosis model induced by MI (**Figure 6A**). Furthermore, we analyzed the effect of STAT6-KO on the expression of a series of inflammatory factors (IL-1α, IL-6, IL-18, and TGF-β), which had been proved to promote inflammation and participate in cytokine storms. Results showed that the expression levels of IL-1α, IL-18, and TGF-β in STAT6-KO splenic CD11b$^+$ cells were significantly higher than their WT counterparts, while there was no significant difference in IL-6 expression between the two genotypes of splenic CD11b$^+$ cells (**Figure 6B**). Besides, the bone marrow cells were isolated from STAT6-KO and WT mice and induced macrophage differentiation. The result of reverse transcriptase (RT)–PCR showed that STAT6-KO significantly increased the mRNA expression of IL-6 and TGF-β1 in macrophages after ISO treatment (**Figures 6C,D**). Thus, these results imply that STAT6 deficiency promotes ISO-induced cardiac fibrosis associated with the upregulation of β1-AR in splenic CD11b$^+$ cells and the increasing of inflammatory cytokines in CD11b$^+$ myeloid cells and macrophages.

DISCUSSION

In the present study, we show the first evidence that the disruption of the STAT6 signal aggravates ISO-induced adverse cardiac fibrosis, which mechanisms involve a series of events, including cardiomyocyte injury, β1-AR expression up-regulation, increased CD11b$^+$ myeloid cell mobilization, increased macrophages differentiation, and collagen deposition aggravation in response to ISO stimulation. Taken together, these results provide novel evidence that STAT6 signal is a potential target for the treatment of myocardial fibrosis and heart failure after ISO-induced myocardial injury.

The sympathetic–catecholamine system is involved in the regulation of multiple cardiovascular physiological activities through adrenergic receptor (Winter et al., 2018; Schinner et al., 2017). β-AR is a member of the superfamily of G protein–coupled receptors, which are also called seven-transmembrane receptors (Vassilatis et al., 2003). There are three β-AR subtypes, β1-AR, β2-AR, and β3-AR. Among them, β1-AR is the predominant subtype of adrenergic receptor in heart tissue, which plays a pivotal role in mediating cardiac function (Chottova and Slavikova, 2011). After

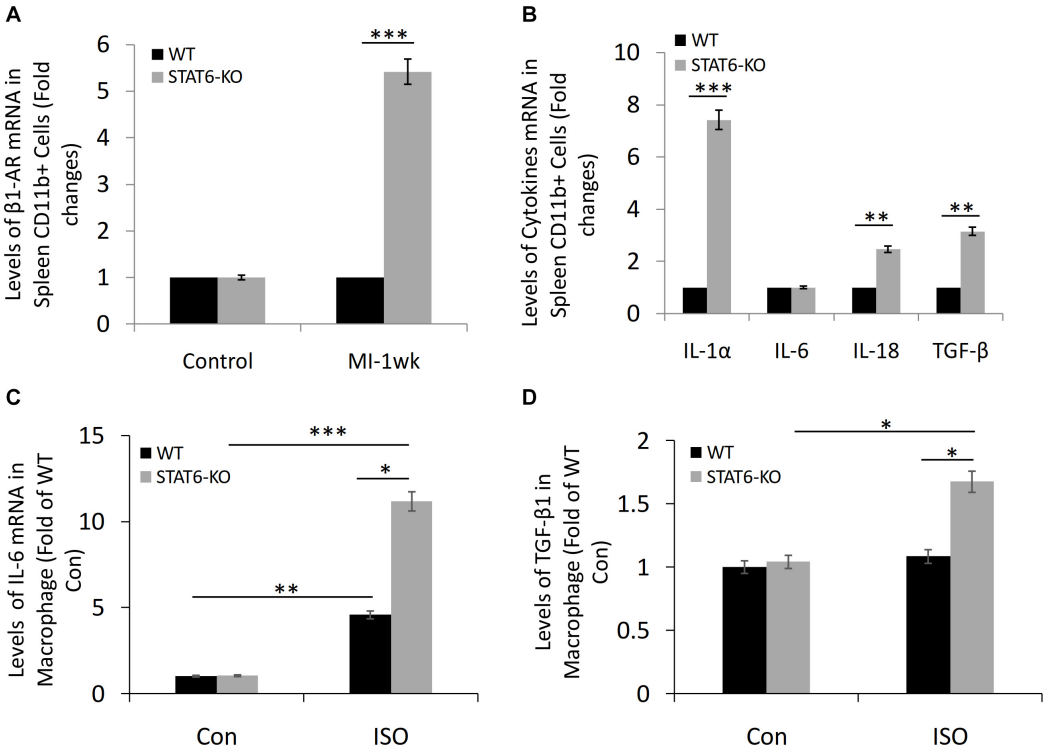

FIGURE 6 | The expression of β1-AR, IL-1α, IL-6, IL-18, and TGF-β in CD11b$^+$ cells and macrophages of STAT6-KO and WT mice. **(A)** Microarray study data showing the expression of β1-AR in spleen-derived CD11b$^+$ cells of STAT6-KO and WT mice after MI (n = 5 per group). **(B)** Microarray study data showing the expression of inflammatory factors in spleen-derived CD11b$^+$ cells of STAT6-KO and WT mice (n = 5 per group). **(C)** The mRNA level of IL-6 expression in the CD11b$^+$ myeloid cell–derived macrophages by RT-PCR (n = 3). **(D)** The mRNA level of TGF-β1 expression in the CD11b$^+$ myeloid cell–derived macrophages by RT-PCR (n = 3). ***P < 0.001, **P < 0.01, and *P < 0.05.

β1-AR activation, the classical Gs-AC-cAMP-PKA signaling cascade is activated. It is also noteworthy that β1-AR is closely related to excessive sympathetic stimulation and cardiac fibrosis. Previous studies have indicated that β1-AR transgenic overexpression mice show increased cardiac interstitial fibrosis, and altered calcium handling is responsible for these detrimental effects of β1-AR signaling (Engelhardt et al., 2004). Accumulating evidences have indicated that ISO, a nonselective β-AR agonist, can induce cardiac hypertrophy and fibrosis by activating multiple signaling pathways to regulate the expression of extracellular matrix, oxidative stress response, and inflammatory response and ultimately affect cardiac function (Tang et al., 2018; Wang M. et al., 2019). In this study, we provide a new perspective to explain the effect of ISO on myocardial fibrogenesis. By a microarray study, we identified higher-level expression of β1-AR mRNA in $CD11b^+$ myeloid cells directly isolated from the spleen, main extramedullary immune cell reservoir in the development of cardiac fibrosis of WT mice post-MI. Using the established HDC-KO mouse model sensitive to myocardial fibrosis, we further confirmed the increased expression of β1-AR mRNA in spleen and bone marrow–derived $CD11b^+$ cells from HDC-KO mice compared to WT controls.

STAT6 signal has previously been demonstrated to mediate the effects of histamine on the protection of MI-induced myocardial injury and on the differentiation of macrophages from bone marrow–derived $CD11b^+$ myeloid cells with granulocyte M-CSF incubation (Xu et al., 2017; Chen et al., 2017). Thus, these data highlight that STAT6 signaling pathway plays a key role in the regulation of inflammatory immune response in ischemic myocardial injury and fibrosis. However, the roles of STAT6 signal in myocardial injury and fibrosis caused by ISO/β1-AR–induced sympathetic nervous system hyperactivity are not fully clarified.

The STAT family consists of seven members (STAT1, 2, 3, 4, 5A, 5B, and 6) in mammals, which exists in the cytoplasm and can be transported into the nucleus after activation and binds to DNA (Wang and Levy, 2012). Among them, STAT6 plays a central role in immune regulation, cell proliferation, and apoptosis (Wang J. et al., 2019; Wang L. et al., 2019). In the current study, we confirmed that STAT6 was highly expressed in $CD11b^+$ myeloid cells and cardiac fibroblasts than in cardiomyocytes. We found STAT6 deficiency increased β1-AR expression and aggravated ISO-induced cardiac fibrosis, with abnormal immune response, consistent with our previous study that STAT6 deficiency promotes the proliferation and differentiation of $CD11b^+Gr\text{-}1^+$ immature myeloid cells in the blood and bone marrow of MI mice. $CD11b^+Gr\text{-}1^+$ immature myeloid cells consist of $CD11b^+Ly6G^+$ granulocytic subset and $CD11b^+Ly6C^+$ monocytic subset. A previous study indicated that the expression of STAT6 signal was down-regulated during the differentiation of tumor-associated neutrophils from $CD11b^+Gr\text{-}1^+$ IMCs of HDC-KO mice (Yang et al., 2011). In this study, we found that STAT6 deficiency promoted the mobilization of $CD11b^+$ IMCs and $CD11b^+Ly6C^+$ macrophage differentiation upon β-AR stimulation. Macrophages, as one of the most important antigen-presenting cells, play a pivotal role in the development of cardiac fibrosis. Macrophages potentially lead to angiotensin II–induced cardiac fibrosis when recruited into the heart from the spleen (Wang et al., 2017). Further, cardiac macrophages are responsible for impaired myocardial relaxation and aggravated myocardial stiffness while diastolic dysfunction develops (Hulsmans et al., 2018). It is known that β-ARs are expressed on the surface of macrophages in most tissues, and macrophage mechanotype and function can be regulated through β-AR by stress hormone signal (Kim et al., 2019). In this study, the data demonstrated that STAT6 deficiency promotes macrophage differentiation from $CD11b^+$ IMCs and recruits them into the injured hearts after chronic stimulation of β-AR, which in turn aggravated cardiac fibrosis. Moreover, the microarray data showed that STAT6 gene knockout (KO) leads to an significant upsurge of a series of key cytokines (IL-1α, IL-18, and TGF-β), which served an important role in cytokine storm and immunopathological damage process (Huang et al., 2005; Yao et al., 2020). Furthermore, the expression of IL-6 and TGF-β1 in the $CD11b^+$ myeloid cell–derived macrophages increased significantly with ISO stimulation, which could be further promoted by STAT6 deficiency.

In clinical settings, hypertensive heart diseases are major health problems worldwide and possess cardiac fibrosis that significantly reduces cardiac function. It is noteworthy that β-blockers are widely used to improve cardiac function in the failing heart and reverse cardiac remodeling (Cleland et al., 2018). However, besides mediating pathological cardiac remodeling, β-AR signal pathways also take part in normal cardiac physiological activity, which consists of positive chronotropic, dromotropic, and inotropic effects. So when β-blockers alleviate the pathological function, it also antagonizes the normal physiological effects, which is harmful to patients. Over the past years, more and more evidence has accumulated indicating that long-acting β-blockers can lead to some detrimental effects (Woron et al., 2019). In addition to β-blockers, anti–TGF-β antibodies have also been considered as potential antifibrotic agents (Kuwahara et al., 2002). Nevertheless, it is found that anti–TGF-β administration before or after coronary artery ligation contributes to increased mortality and worsened left ventricular remodeling in mice with MI, and ECM remodeling may be related to these detrimental effects (Frantz et al., 2008). Therefore, rationally designed antifibrotic therapies need to be explored and discovered to curb these problems. In this regard, STAT6 could confer cardioprotection in β-AR–mediated cardiac fibrosis chronically stimulated with catecholamine. As a novel antifibrotic strategy, STAT6 signal target does not interfere and damage the normal physiological function of β-AR, and no increased mortality has been found in mice. Thus, STAT6 signal could be a safe, promising, and viable candidate drug target against ISO-induced cardiac fibrosis.

DATA AVAILABILITY STATEMENT

The microarray data has been deposited in the GEO (Gene Expression Omnibus) database (accession number: GSE154733).

ETHICS STATEMENT

The animal study was reviewed and approved by Animal Ethics Committee of Fudan University.

AUTHOR CONTRIBUTIONS

WZ, BZ, MT, and XY participated in the study design, experiment operation, and manuscript preparation. SD and XZ contributed to the animal experiments and statistical analysis. XW and JW helped with the collection and analysis of echocardiography. YZ and JG provided the suggestions for study design and helped with revision of the manuscript. All authors discussed and approved the manuscript.

FUNDING

This work was supported by the National Key Research and Development Plan (2016YFC1101102), the National Natural Science Foundation of China (81521001 and 91439121), the Basic Research Project of Shanghai Committee of Science and Technology (19JC1411400), and the Laboratory Animal Science Foundation of Shanghai Committee of Science and Technology (19140902000).

ACKNOWLEDGMENTS

We would like to thank Jinmiao Chen, Zhiwei Zhang, JianguoJia, Bingyu Li, and Sanli Qian for their technical support and helpful contribution.

REFERENCES

Alemasi, A., Cao, N., An, X., Wu, J., Gu, H., Yu, H., et al. (2019). Exercise Attenuates Acute beta-Adrenergic Overactivation-Induced Cardiac Fibrosis by Modulating Cytokines. *J. Cardiovasc. Transl. Res.* 12, 528–538. doi: 10.1007/s12265-019-09894-1

Chen, J., Hong, T., Ding, S., Deng, L., Abudupataer, M., Zhang, W., et al. (2017). Aggravated myocardial infarction-induced cardiac remodeling and heart failure in histamine-deficient mice. *J. Sci. Rep.* 7:44007.

Cheng, Y., Luo, D., Zhao, Y., and Rong, J. (2020). N-Propargyl caffeate amide (PACA) prevents cardiac fibrosis in experimental myocardial infarction by promoting pro-resolving macrophage polarization. *J. Aging* 12, 5384–5398. doi: 10.18632/aging.102959

Chottova, D. M., and Slavikova, J. (2011). [Adrenergic regulation of the mammalian heart. *Cesk. Fysiol.* 60, 14–19.

Cleland, J. G. F., Bunting, K. V., Flather, M. D., Altman, D. G., Holmes, J., and Coats, A. J. S. (2018). Beta-blockers for heart failure with reduced, mid-range, and preserved ejection fraction: an individual patient-level analysis of double-blind randomized trials. *Eur. Heart J.* 39, 26–35. doi: 10.1093/eurheartj/ehx564

Cuspidi, C., Facchetti, R., Quarti-Trevano, F., Dell'oro, R., Tadic, M., Grassi, G., et al. (2020). Left ventricular hypertrophy in isolated and dual masked hypertension. *J. Clin. Hypertens* 22, 673–677. doi: 10.1111/jch.13808

Deng, L., Hong, T., Lin, J., Ding, S., Huang, Z., Chen, J., et al. (2015). Histamine deficiency exacerbates myocardial injury in acute myocardial infarction through impaired macrophage infiltration and increased cardiomyocyte apoptosis. *Sci. Rep.* 5:13131.

Engelhardt, S., Hein, L., Dyachenkow, V., Kranias, E. G., Isenberg, G., and Lohse, M. J. (2004). Altered calcium handling is critically involved in the cardiotoxic effects of chronic beta-adrenergic stimulation. *Circulation* 109, 1154–1160. doi: 10.1161/01.cir.0000117254.68497.39

Frantz, S., Hu, K., Adamek, A., Wolf, J., Sallam, A., Maier, S. K., et al. (2008). Transforming growth factor beta inhibition increases mortality and left ventricular dilatation after myocardial infarction. *Basic Res. Cardiol.* 103, 485–492. doi: 10.1007/s00395-008-0739-7

Graham, L. N., Smith, P. A., Stoker, J. B., Mackintosh, A. F., and Mary, D. A. (2004). Sympathetic neural hyperactivity and its normalization following unstable angina and acute myocardial infarction. *Clin. Sci.* 106, 605–611. doi: 10.1042/cs20030376

Haase, P., Mokada-Gopal, L., Radtke, D., and Voehringer, D. (2020). Modulation of the humoral immune response by constitutively active STAT6 expression in murine B cells. *Eur. J. Immunol.* 50, 558–567. doi: 10.1002/eji.201948313

Heinen, A., Raupach, A., Behmenburg, F., Holscher, N., Flogel, U., Kelm, M., et al. (2018). Echocardiographic Analysis of Cardiac Function after Infarction in Mice: Validation of Single-Plane Long-Axis View Measurements and the Bi-Plane Simpson Method. *Ultrasound. Med. Biol.* 44, 1544–1555. doi: 10.1016/j.ultrasmedbio.2018.03.020

Hogarth, A. J., Graham, L. N., Mary, D. A., and Greenwood, J. P. (2009). Gender differences in sympathetic neural activation following uncomplicated acute myocardial infarction. *Eur. Heart. J.* 30, 1764–1770. doi: 10.1093/eurheartj/ehp188

Hogarth, A. J., Mackintosh, A. F., and Mary, D. A. (2006). The sympathetic drive after acute myocardial infarction in hypertensive patients. *Am. J. Hypertens* 19, 1070–1076. doi: 10.1016/j.amjhyper.2006.03.015

Huang, K. J., Su, I. J., Theron, M., Wu, Y. C., Lai, S. K., Liu, C. C., et al. (2005). An interferon-gamma-related cytokine storm in SARS patients. *J. Med. Virol.* 75, 185–194. doi: 10.1002/jmv.20255

Hulsmans, M., Sager, H. B., Roh, J. D., Valero-Munoz, M., Houstis, N. E., and Iwamoto, Y. (2018). Cardiac macrophages promote diastolic dysfunction. *J. Exp. Med.* 215, 423–440.

Kim, T. H., Ly, C., Christodoulides, A., Nowell, C. J., Gunning, P. W., Sloan, E. K., et al. (2019). Stress hormone signaling through beta-adrenergic receptors regulates macrophage mechanotype and function. *FASEB J.* 33, 3997–4006. doi: 10.1096/fj.201801429rr

Kuwahara, F., Kai, H., Tokuda, K., Kai, M., Takeshita, A., Egashira, K., et al. (2002). Transforming growth factor-beta function blocking prevents myocardial fibrosis and diastolic dysfunction in pressure-overloaded rats. *Circulation* 106, 130–135. doi: 10.1161/01.cir.0000020689.12472.e0

Morishige, S., Takahashi-Yanaga, F., Ishikane, S., Arioka, M., Igawa, K., Kuroo, A., et al. (2019). 2,5-Dimethylcelecoxib prevents isoprenaline-induced cardiomyocyte hypertrophy and cardiac fibroblast activation by inhibiting Akt-mediated GSK-3 phosphorylation. *Biochem. Pharmacol.* 168, 82–90. doi: 10.1016/j.bcp.2019.06.018

Nam, Y. K., Jin, S. C., Kim, M. H., Choi, Y., Lee, Y. B., and Yang, W. M. (2020). Banhahubak-Tang Tablet, a Standardized Medicine Attenuates Allergic Asthma via Inhibition of Janus Kinase 1 (JAK1)/ Signal Transducer and Activator of Transcription 6 (STAT6) Signal Pathway. *Molecules* 25:1100436.

Ruan, C. C., Kong, L. R., Chen, X. H., Ma, Y., Pan, X. X., Zhang, Z. B., et al. (2018). A2A Receptor Activation Attenuates Hypertensive Cardiac Remodeling via Promoting Brown Adipose Tissue-Derived FGF21. *Cell Metab.* 28, 476–489e5.

Sawaki, D., Czibik, G., Pini, M., Ternacle, J., Suffee, N., and Mercedes, R. (2018). Visceral Adipose Tissue Drives Cardiac Aging Through Modulation of Fibroblast Senescence by Osteopontin Production. *Circulation* 138, 809–822. doi: 10.1161/circulationaha.117.031358

Schinner, C., Vielmuth, F., Rotzer, V., Hiermaier, M., Radeva, M. Y., and Co, T. K. (2017). Adrenergic Signaling Strengthens Cardiac Myocyte Cohesion. *Circ. Res.* 120, 1305–1317. doi: 10.1161/circresaha.116.309631

Tang, Y., Guo, M., Ma, X. Y., Sun, W. P., Hao, M. H., and Zhu, H. Y. (2018). Oltipraz attenuates the progression of heart failure in rats through inhibiting oxidative stress and inflammatory response. *Eur. Rev. Med. Pharmacol. Sci.* 22, 8918–8923.

Vassilatis, D. K., Hohmann, J. G., Zeng, H., Li, F., Ranchalis, J. E., and Mortrud, M. T. (2003). The G protein-coupled receptor repertoires of human and mouse. *Proc. Natl. Acad. Sci. U S A* 100, 4903–4908.

Wang, H. J., Wang, W., Cornish, K. G., Rozanski, G. J., and Zucker, I. H. (2014). Cardiac sympathetic afferent denervation attenuates cardiac remodeling and improves cardiovascular dysfunction in rats with heart failure. *Hypertension* 64, 745–755. doi: 10.1161/hypertensionaha.114.03699

Wang, J., Shen, Y., Li, C., Liu, C., Wang, Z. H., Li, Y. S., et al. (2019). IL-37 attenuates allergic process via STAT6/STAT3 pathways in murine allergic rhinitis. *Int. Immunopharmacol.* 69, 27–33. doi: 10.1016/j.intimp.2019.01.013

Wang, L., Shen, S., Xiao, H., Ding, F., Wang, M., Li, G., et al. (2019). ARHGAP24 inhibits cell proliferation and cell cycle progression and induces apoptosis of lung cancer via a STAT6-WWP2-P27 axis. *Carcinogenesis* 1, 711–721. doi: 10.1093/carcin/bgz144

Wang, M., Qian, L., Li, J., Ming, H., Fang, L., Li, Y., et al. (2019). GHSR Deficiency Exacerbates Cardiac Fibrosis: Role in Macrophage Inflammasome Activation and Myofibroblast Differentiation. *Cardiovasc. Res.* 2:cvz318.

Wang, N. P., Erskine, J., Zhang, W. W., Zheng, R. H., Zhang, L. H., Duron, G., et al. (2017). Recruitment of macrophages from the spleen contributes to myocardial fibrosis and hypertension induced by angiotensin II. *J. Renin. Angiotensin. Aldosterone Syst.* 18:1470320317706653.

Wang, Y., and Levy, D. E. (2012). Comparative evolutionary genomics of the STAT family of transcription factors. *JAKSTAT* 1, 23–33. doi: 10.4161/jkst.19418

Winter, J., Bishop, M. J., Wilder, C. D. E., O'shea, C., Pavlovic, D., and Shattock, M. J. (2018). Sympathetic Nervous Regulation of Calcium and Action Potential Alternans in the Intact Heart. *Front. Physiol.* 9:16. doi: 10.3389/fphys.2018.00016

Woron, J., Siwek, M., and Gorostowicz, A. (2019). Adverse effects of interactions between antidepressants and medications used in treatment of cardiovascular disorders. *Psychiatr. Pol.* 53, 977–995. doi: 10.12740/pp/onlinefirst/96286

Xiao, H., Li, H., Wang, J. J., Zhang, J. S., Shen, J., and An, X. B. (2018). IL-18 cleavage triggers cardiac inflammation and fibrosis upon beta-adrenergic insult. *Eur. Heart J.* 39, 60–69. doi: 10.1093/eurheartj/ehx261

Xu, L., Cheng, D., Huang, Z., Ding, S., Zhang, W., Tan, H., et al. (2017). Histamine promotes the differentiation of macrophages from CD11b(+) myeloid cells and formation of foam cells through a Stat6-dependent pathway. *Atherosclerosis* 263, 42–52. doi: 10.1016/j.atherosclerosis.2017.05.024

Yang, X. D., Ai, W., Asfaha, S., Bhagat, G., Friedman, R. A., Jin, G., et al. (2011). Histamine deficiency promotes inflammation-associated carcinogenesis through reduced myeloid maturation and accumulation of CD11b+Ly6G+ immature myeloid cells. *Nat. Med.* 17, 87–95. doi: 10.1038/nm.2278

Yao, Z., Zheng, Z., Wu, K., and Junhua, Z. (2020). Immune environment modulation in pneumonia patients caused by coronavirus: SARS-CoV, MERS-CoV and SARS-CoV-2. *Aging* 12, 7639–7651. doi: 10.18632/aging.103101

Conflict of Interest: The authors declare that the research was conducted in the absence of any commercial or financial relationships that could be construed as a potential conflict of interest.

Copyright © 2020 Zhang, Zhu, Ding, Wang, Wu, Zhu, Zou, Ge, Tong and Yang. This is an open-access article distributed under the terms of the Creative Commons Attribution License (CC BY). The use, distribution or reproduction in other forums is permitted, provided the original author(s) and the copyright owner(s) are credited and that the original publication in this journal is cited, in accordance with accepted academic practice. No use, distribution or reproduction is permitted which does not comply with these terms.

frontiers in Physiology

MINI REVIEW
published: 29 October 2020
doi: 10.3389/fphys.2020.567899

Drug Discovery and Development of Novel Therapeutics for Inhibiting TMAO in Models of Atherosclerosis and Diabetes

*Ian Steinke[1], Nila Ghanei[1], Manoj Govindarajulu[1], Sieun Yoo[2], Juming Zhong[2] and Rajesh H. Amin[1]**

[1] Drug Discovery and Development, Auburn University, Auburn, AL, United States, [2] Department of Anatomy, Physiology and Pharmacology, Auburn University, Auburn, AL, United States

Diabetes mellitus exists as a comorbidity with congestive heart failure (CHF). However, the exact molecular signaling mechanism linking CHF as the major form of mortality from diabetes remains unknown. Type 2 diabetic patients display abnormally high levels of metabolic products associated with gut dysbiosis. One such metabolite, trimethylamine N-oxide (TMAO), has been observed to be directly related with increased incidence of cardiovascular diseases (CVD) in human patients. TMAO a gut-liver metabolite, comes from the metabolic degenerative product trimethylamine (TMA) that is produced from gut microbial metabolism. Elevated levels of TMAO in diabetics and obese patients are observed to have a direct correlation with increased risk for major adverse cardiovascular events. The pro-atherogenic effect of TMAO is attributed to enhancing inflammatory pathways with cholesterol and bile acid dysregulation, promoting foam cell formation. Recent studies have revealed several potential therapeutic strategies for reducing TMAO levels and will be the central focus for the current review. However, few have focused on developing rational drug therapeutics and may be due to the gaps in knowledge for understanding the mechanism by which microbial TMA producing enzymes and hepatic flavin-containing monoxygenase (FMO) can work together in preventing elevation of TMAO levels. Therefore, it is critical to understand the advantages of developing a novel rational drug design strategy that manipulates FMO production of TMAO and TMA production by microbial enzymes. This review will focus on the inspection of FMO manipulation, as well as gut microbiota dysbiosis and its influence on metabolic disorders including cardiovascular disease and describe novel potential pharmacological therapeutic development.

Keywords: FMO3, TMA, CVD, T2D, TMAO, dysbiosis, atherosclerosis, microbiome

OPEN ACCESS

Edited by:
Jun Ren,
University of Washington,
United States

Reviewed by:
Yi Sun,
University of Alabama at Birmingham,
United States
Ne Natalie Wu,
Fudan University, China

***Correspondence:**
Rajesh H. Amin
rha0003@auburn.edu

Specialty section:
This article was submitted to Clinical and Translational Physiology, a section of the journal Frontiers in Physiology

Received: *30 May 2020*
Accepted: *23 September 2020*
Published: *29 October 2020*

Citation:
Steinke I, Ghanei N, Govindarajulu M, Yoo S, Zhong J and Amin RH (2020) Drug Discovery and Development of Novel Therapeutics for Inhibiting TMAO in Models of Atherosclerosis and Diabetes. Front. Physiol. 11:567899. doi: 10.3389/fphys.2020.567899

INTRODUCTION

Heart disease is the leading cause of death in the United States today. Furthermore, diabetic patients are twice as likely to develop cardiovascular disease (CVD). Most recent reports on diabetes mellitus from the Center for Disease Control and Prevention estimate that 9.1% of the population in the United States of adults 18 years and older have been diagnosed, where type 2 diabetes (T2D) mellitus is being attributed to approximately 95% of these cases (Centers for Disease Control and Prevention, 2018).

In patients with diabetes mellitus, primarily T2D, atherosclerotic CVD predominates as the leading cause of mortality (Booth et al., 2006; Wang et al., 2016). CVD is characterized by inflammation induced atherosclerotic complications, resulting from an increase of lipid particles to the endothelial cells causing foam cell and the resultant plaque formation (Libby, 2006). T2D develops out of metabolic disorder, characterized by insulin resistance and reduced insulin secretion leading to chronically elevated blood glucose levels.

Other comorbidities associated with T2D are hypertension, dyslipidemia, and renal insufficiency (Iglay et al., 2016). Further increasing CVD pathology are T2D related risk factors that include decreased high-density lipoprotein (HDL) cholesterol, increased low-density lipoprotein (LDL) cholesterol, hyperlipidemia, hyperinsulinemia, and an increase of reactive oxygen species (ROS) in the blood (Ding and Triggle, 2005).

As T2D progresses, hyperinsulinemia, hyperglycemia, and oxidized LDL culminates in endothelial cell dysfunction and apoptosis (Ding and Triggle, 2005). This decrease in the proper functioning of endothelial cell walls coupled with glycated hemoglobin causes a reduction in blood flow to the vasculature, increasing blood pressure and risk of ischemic damage (Hosseini-Beheshti and Grau, 2019). In the final progression of atherosclerosis, plaque formations become unstable and rupture, dislodging from the endothelial cell wall, resulting in myocardial infarction, and stroke (Bennett et al., 2016).

Complicating CVD in T2D patients is the common association of combined hyperlipidemia, a pro-atherogenic lipid disorder, characterized by high levels of LDL, triglycerides (TGs), and decreased levels of HDL (Athyros et al., 2002). Improper metabolic utilization of dietary fatty acids can cause increasingly higher levels of LDL and TGs in the blood, coupled with ROS, that can initiate or exacerbate plaque formation in the endothelial membrane (Bai et al., 2015).

Current pharmacological therapies for T2D, when in conjunction with CVD, attempt to reduce associated risks through tight glycemic control, dietary changes, and statin drugs. However, statistical evidence shows no significant correlation in lowering the risk of CVD with these treatments alone when considering T2D patients (Leon and Maddox, 2015). Even when intensive lifestyle changes are implemented and T2D symptoms are reduced, the cardiovascular outcome remains unchanged (Pi-Sunyer, 2014; Ferrannini and DeFronzo, 2015).

Conversely, therapies that seek to lower LDL via clearance upon upregulation of LDL receptors have shown statistical significance in cardiovascular risk reduction (Silverman et al., 2016). These findings show promise in the ability to reorganize the levels of HDL and LDL in circulation, yet many therapies are unable to improve energy regulation through glucose metabolism and insulin resistance in unison with cholesterol.

This review will examine different metabolic pathways involved in dysbiosis and efforts to ameliorate the downstream physiological consequences. In addition to, an examination of how modulating enzymatic activity directly involved with formation of the biomarker trimethylamine N-oxide (TMAO) may improve health outcomes in patients with CVD and/or T2D.

GUT MICROBIOMES ROLE IN THE TMA/TMAO PATHWAY

Recent research has intensified in the area of the gut microbiome and its implication in various disease pathologies exhibiting the significant role bacteria play in metabolic homeostasis (Sung et al., 2017). There exists a vast array of bacteria in the human digestive system that can facilitate metabolism, immune health, and secondary energy scavenging based upon the host's dietary intake (Simon and Gorbach, 1986). Due to the diversity and adaptability of the gut microbiome, changes in diet can quickly and dramatically influence the species of bacteria present; thus, altering the concentration and effect of bacterial metabolites that can influence the host metabolism (Arora and Bäckhed, 2016). Furthermore, the potential of the gut microbiome to metabolize dietary compounds is so profound that it equals that of the liver and is capable of being classified as an organ (Sommer and Bäckhed, 2013), demonstrating a propensity to influence host absorption of undesirable compounds. Bacteria respond quickly to dietary changes by an increase or decrease in the number of their species based upon the dietary source available (Rachel et al., 2015). Major changes in gut microbiome taxa are influenced most significantly by high carbohydrate and high protein diets but show no significant change in response to high lipid content (Holmes et al., 2017). These changes in the microbiota can have a dramatic impact on intestinal permeability and alter cardiovascular outcomes through inflammatory pathways (Sandek et al., 2012).

Along with microbial induced inflammatory effects, degradation of the mucosal membrane leads to infiltration of the epithelial membrane by other endotoxins, pro-inflammatory cytokines, and potentially harmful bacterial metabolites (Murphy et al., 2015). Crosstalk distribution of gut microbiota has been illustrated in the pathology of diabetes, obesity, CVD and metabolic syndrome (Lau and Vaziri, 2019). The major metabolites that are produced by beneficial gut microbiota are short chain fatty acids (SCFAs) such as butyrate, acetate, and propionate. These SCFAs are essential to maintain intestinal health, insulin, glucose, and lipid homeostasis (Lau and Vaziri, 2019). Recent research showed the proatherogenic contribution of microbial metabolites such as increased trimethylamine (TMA) and decreased SCFAs in CVD (Liu et al., 2019; Tang et al., 2019).

Moreover, structural and functional intestinal alterations arising from a lack of diversity in the microbiome have shown a correlation with increased heart failure related risk and incidence (Luedde et al., 2017). Marques et al. (2017) implied increases in phyla Bacteroidetes and Proteobacteria and decreases in phyla Firmicutes and Fusobacteria strains with changes in their related metabolites, like TMA to TMAO, with relation to chronic heart disease. Primarily two different species of bacteria (Firmicutes and Proteobacteria) have been identified as being responsible for the metabolism of choline to produce TMA (Velasquez et al., 2016).

In addition, there exists links between microbiota dysbiosis and vascular tone resulting in blood pressure regulation by

regulating cardiac and renal early growth response 1 protein (Egr1) and the renin-angiotensin system (Marques et al., 2017). Marques and colleagues observed in apparent mineralocorticoid excess mouse models that were fed a high fiber diet with a SCFA acetate supplement, Egr1, markers of hypertension and heart failure, were decreased in comparison to these mice fed with a control diet (Marques et al., 2017). Egr1's role of being a master regulator of kidney, renal fibrosis and regulation of the renin-angiotensin system further validates the role dysbiosis can have by propagating host inflammatory responses through dietary intake and reorganization of commensal bacteria. Along these lines, the dysbiosis of the gut microbiome may have significant impact through the different bacterial metabolites and production of SCFAs toward intestinal mucosal barrier protection and excretory pathways. To add to this SCFA propionate has been observed to modulate blood pressure via Gpr41, which is a SCFA receptor expressed in smooth muscle cells of small vessels, exhibiting a vasodilatory effect and influencing the secretion of renin in the modulation of blood pressure (Pluznick et al., 2013).

Wang et al. (2015) demonstrated that there is a positive correlation between the TMAO pathway and progression of heart failure. Treatment in mice with 3,3-dimethyl-1-butanol (DMB), a choline mimetic, displayed potential therapeutic effects in CVD via inhibition of microbial cleavage of choline consequently decreasing circulating levels of TMAO. DMB is found in balsamic vinegar, olive oil, grape seed oil, and red wines, and has been observed to decrease macrophage-foam cell formation and aortic root atherosclerotic lesion development through the inhibition of the bacterial enzyme TMA lyase CutC/D in ApoE knockout mice (Wang et al., 2015; Velasquez et al., 2016). Other inhibitors such as meldonium, an analog of carnitine, has also shown to display anti-atherosclerotic activity by preventing bacterial TMA formation via competitive inhibition of bacterial carnitine palmitoyltransferase-1 (CPT1) (Velasquez et al., 2016).

Trimethylamine N-oxide has been associated as an independent risk factor, aside from genetic predisposition and environmental factors, for CVD and atherosclerosis (Mohammadi et al., 2016). Kamo et al. (2017) illustrated that patients with HF have higher plasma levels of TMAO than control subjects and show a positive correlation with increased incidence of mortality. Foods such as meat, eggs, and salt-water fish contain high levels of specific TMA containing nutrients, i.e., phosphatidylcholine, choline, and carnitine. Recent research has revealed that inhibition of specific bacterial enzymes, containing TMA lyase, can attenuate the CVD (Craciun et al., 2014). TMA is known to be a toxic gaseous compound that causes corrosion and necrosis of mucosal membranes. TMA is also a known inhibitor of acetylcholine esterase, blocking the ability of cholinergic neurons to return to their resting potential. TMA is rapidly absorbed in the intestines and progresses into the liver where it is metabolized by human flavin-containing monooxygenase isoform-3 enzyme (FMO3) into TMAO where it is readily excreted in the urine (Janeiro et al., 2018). Despite TMA's known toxic effect, it is TMAO that has become commonly accepted as a biomarker of CVD (Barrea et al., 2018). Higher levels of circulating TMAO is of primary concern since greater than 90% of dietary TMA is excreted in the urine through this metabolic form, as demonstrated in the case of 167 healthy individuals (Al-Waiz et al., 1987). Moreover, TMAO levels are associated with an increased risk of major cardiovascular events in patients with diabetes (Zhu et al., 2016). However controversy exists as to whether TMAO influences the progression of CVD disease or acts as a bystander of dysbiosis and pro-inflammatory pathways when examining CVD and T2D patients (Landfald et al., 2017; Lau and Vaziri, 2019). Non-lethal inhibition of bacteria in this pathway, has shown potential value as a therapeutic target. Mechanistically, dietary choline supplementation was shown to increase foam cell formation, promoting atherosclerotic complications in Apoe knockout mice (Wang et al., 2011). Furthermore, non-lethal inhibition of TMA lyase using DMB demonstrated a decrease in foam cell formation in Apoe knockout mice resulting in decreasing in circulating TMAO levels in the blood and cardiovascular complications (Wang et al., 2015). These results reinforce the viability of TMA lyase as a potential therapeutic target to alleviate symptoms related to thrombotic events and ischemic damage.

Trimethylamine N-oxide has been shown to induce endoplasmic reticulum (ER) stress through the elevation of ER-HSP70 isoform (Mohammadi et al., 2016), and by directly binding to ER stress kinase PERK whereby its activation lead to induction of FoxO1 (Chen et al., 2019). Other findings have observed that TMAO promotes foam cell formation by upregulating macrophage scavenger receptors, resulting in the development of atherosclerosis (Shih et al., 2019). SR-A1, and multiple scavenger receptors such as LOX-1, CD36, and SR-A1, contribute to the development of atherosclerosis by enhancing the uptake of cholesterol with lipoprotein modification. Wang et al. (2011) reported that increased TMAO levels enforced macrophages to accumulate cholesterol by inducing SR-A1 as a scavenger receptor. In addition, Mohammadi et al. (2016) showed that TMAO-induced upregulation of SR-A1 at mRNA and protein levels, contributed to the development of ER stress as well as lipid-laden macrophage activation in atherosclerosis (Hotamisligil, 2010).

Elevated levels of TMAO have also been observed to inhibit mitochondrial electron transport, thus leading to mitochondrial uncoupling and ROS formation in vascular endothelial cells (Hotamisligil, 2010). In addition, increased plasma levels of TMAO positively correlate with the aggregation of blood platelet thrombosis (Tilg, 2016). Recent research with isotope-labeled phosphatidylcholine illustrated the direct correlation between increased serum TMAO and extent of coronary atherosclerotic plaque development (Tilg, 2016; Zhu et al., 2016). **Figure 1** provides an overview for the microbiomes contribution to the TMA/TMAO pathway and eventual disease progression from dietary intake to atherosclerotic complications.

INHIBITION OF TMA LYASE CutC/D

Trimethylamine lyase is a bacterial enzyme that is known to cleave dietary choline during an anaerobic process releasing TMA and acetyl aldehyde in the process. Recent reports have built

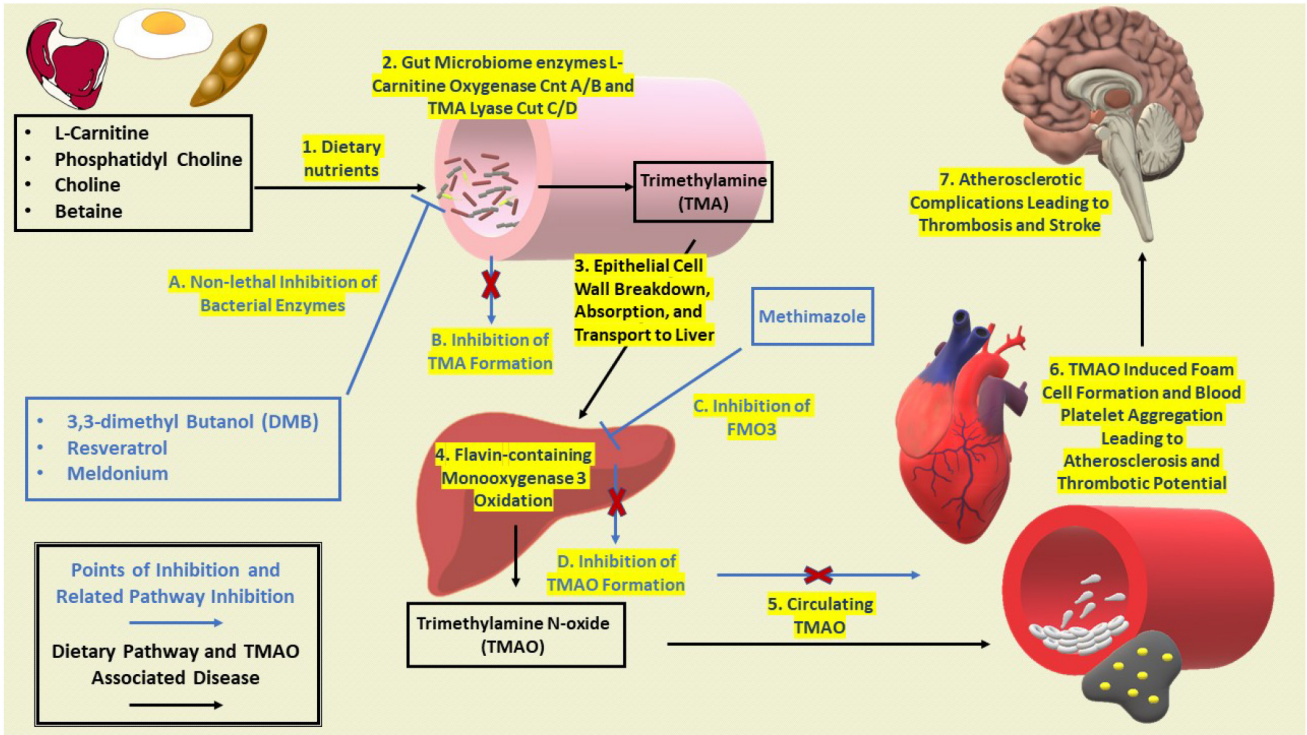

FIGURE 1 | Development of dysbiosis and propagation of CVD and T2D with potential points of inhibition. Excess nutrients begin to influence dysbiosis of the gut microbiome to produce bacterial metabolite TMA. TMA lyase CutC/D as a main enzyme for inhibition as it is the most prominently expressed in bacterial communities (Rath et al., 2017). General progression of dysbiosis leads to further infiltration of unwanted bacterial by products leading to increased expression of FMO3 and elevated levels of TMAO. As circulating levels of TMAO begin to increase, pathologies related to CVD and T2D, reverse cholesterol transport is inhibited leading to lipid laden macrophages and increased blood platelet aggregation. Continued atherosclerotic complications then promote thrombotic events and stroke in the brain.

DMB analogs to inhibit TMA formation by inhibiting CutC/D lyase. **Figures 2A,B** shows a representation for describing mechanistically how choline binds to CutC/D choline lyase. Choline is shown to interact with CutC/D via hydrogen bonding at the Cys 771 and Glu 773 sites of CutC/D, along with aromatic hydrogen bonds to Phe 677. When choline binds to TMA lyase, the active site residues engulf choline, whereby choline can stabilize the active site allowing the enzymatic reaction to proceed. Mechanistically the aromatic hydrogen bonding of the quaternary amine in choline with Phe 677 provides additional stabilization of the active site and provides improved chemical reactivity. In addition, TMA is formed by the Cys 771 promoting cleavage of choline through a radical exchange with the alpha carbon to form alcohol in the formation of acetaldehyde and TMA (Bodea et al., 2016).

Another study has shown that mechanistically DMB prevents the catalytic activity required from the substrate choline's quaternary ammonium motif, thus providing a structure that can competitively bind but not exhibit reactivity, thus effectively inhibiting choline from being cleaved to TMA as illustrated in **Figure 1** (Craciun et al., 2014). These findings are highly significant for development of novel compounds to prevent atherosclerosis in patients with western diets, as non-lethal inhibition promotes reorganization of the gut microbiome without drastically reducing the numbers of beneficial bacteria.

Trimethylamine lyase is also of important to consider, as strictly inhibiting FMO3, can lead to an increase in circulating TMA levels causing an unpleasant "fishy" smell in a condition that is known as Trimethylaminuria (Mitchell and Smith, 2001). To avoid this consequence and promote reorganization of the gut microbiome non-lethal inhibition of TMA lyase must be factored into the drug design of any potential therapeutics.

INHIBITION OF FMO3

Of the major oxidative drug metabolizing enzymes in the body the Cytochrome P-450 (CYP450) family exists as the most prominently expressed, existing in over fifty isoforms, class of enzymes for first step biotransformation of xenobiotic compounds (Srinivas, 2017). More recent research has begun to shed light on the importance of another major oxidative drug metabolizing class of enzymes known as flavin-containing monooxygenases (FMO). FMO's have distinct differences in function and substrate activity compared to the CYP450 class of enzymes resulting in different disease pathologies that may be accompanied with FMO expression or inhibition (Cashman and Zhang, 2006). FMO's exist in five isoforms, with a sixth FMO existing as a pseudogene, this family of genes are conserved across all phyla and

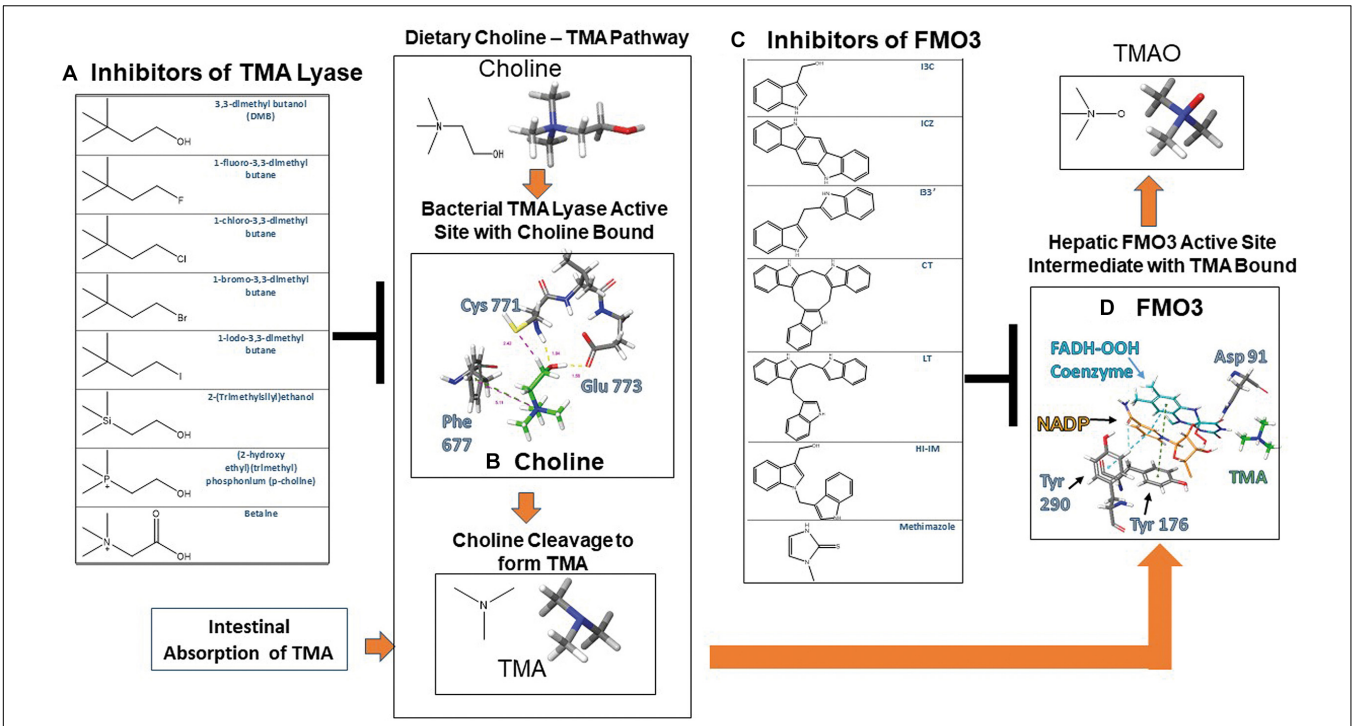

FIGURE 2 | Crystallographic active sites of TMA lyase CutC/D and FMO3 with chemical structures of current known inhibitors. **(A)** Chemical structures of substrates and inhibitors of TMA lyase (Wang et al., 2015). **(B)** Choline bound to TMA lyase showing key binding interactions with active site amino acid residues that occur upon activation PDB 5AOU. **(C)** Chemical structures of dietary indole condensation products shown to be FMO3 inhibitors (Cashman et al., 1999). **(D)** Reactive enzymatic intermediates and key interactions with active site amino acid residues with TMA bound to FMO3 PDB 2GV8.

are characterized by their unique structural and functional differences (Ziegler, 1993).

Functional characterization of FMO3 is best understood when examining the polymorphisms that are commonly associated with the enzyme. Single nucleotide changes can have profound effects on the structure and function of FMO3, often leading to Trimethylaminuria (Arseculeratne et al., 2007). Genomic analysis of these polymorphisms indicate key amino acid residues that are integral in the performance of these enzymes when metabolizing specific analytes such as TMA (Motika et al., 2009). Further interpretation of genetic variants has shown specific preferences for xenobiotic substrates providing insight into the preferable substrate models that can be used as a potential therapeutic by reducing expression of FMO3 (Borbas et al., 2006).

Located on the endoplasmic reticulum, FMO's can oxygenate a wide variety of soft nucleophilic xenobiotics such as heteroatoms containing nitrogen, sulfur, boronic acids, selenium, and phosphorous functional groups (Ziegler, 1993). FMO's require a FAD prosthetic group and NADPH cofactor for enzymatic activation. Molecular oxygen and NADPH react with FAD to form the activated 4α-hydroperoxy flavin (FAD-OOH) intermediate that reacts with the nucleophilic substrate converting it to its respective oxide form (Phillips and Shephard, 2008). Nucleophilic substrate accessibility to the FMO active site is primarily limited by steric bulk preventing access to the activated 4α-hydroperoxy flavin intermediate (Hines et al., 1994). In **Figure 2B** TMA can be seen binding in the FMO3 active site with the intermediate $NADP^+$ and FAD-OOH. TMA is located at the entrance for nucleophilic substrates to enter the enzymatic cycle and become oxygenated.

Crystallographic data shows coordination of FAD, NADPH, and amino acid Asparagine 91 (Asp 91) as the main focal point at which substrate metabolism occurs. By mapping out the surrounding enzyme binding site *in silico* key structural features can be identified and mechanistic action can be better understood to further aid with drug design (Eswaramoorthy et al., 2006). Crystal structures with methimazole, a known competitive inhibitor (Nace et al., 1997), bound to FMO3 gives further binding information about the possible mechanism of inhibition and help to further drug design of novel therapeutics. Methimazole forms strong pi–pi interactions with the cofactor FAD and is capable of hydrogen boding to the Asp 91 residue in the same location as NADPH and its intermediate $NADP^+$ seen in **Figure 2D**, leading to inhibition of the enzymatic reaction by blocking NADPH from entering the catalytic site (Gao et al., 2018).

Clinical trials using dietary indoles coming from Brussel sprouts have shown efficacy in lowering the relative ratio of TMAO to TMA through inhibition of FMO3. This research discovered that acid condensation products of dietary indoles that can be observed in **Figure 2C** are the main culprit in the results observed, providing chemical structures

with known function and structural characterization shown in **Figure 2C** (Cashman et al., 1999). Docking studies show that these dietary indoles bind to residues specific for NADPH, similarly to methimazole, and are capable of competitive inhibition of enzymatic activity.

In male diabetic Sprague-Dawley rat models treated with streptozotocin, increased FMO activity and was thus positively correlated with increasing blood glucose levels. However insulin treatment returned FMO activity to normal (non-diabetic) levels. Conversely, insulin treatment had no effect on FMO activity in non-diabetic rats (Borbás et al., 2006). In regards to other forms of FMO, the potentiation of liver injury by thioacetamide, in diabetic rats, due to induced CYP2E1, showed that inhibition of FMO1 using indole-3-carbinol, potentiated liver damage. This study demonstrated that a potential mechanism by which FMO1 inactivates potentially harmful metabolites, and how FMO1 activity increases with increasing blood glucose levels (Wang et al., 2000).

cDNA analysis of biopsied liver tissues from T2D patients have also shown that genes associated with stress defense such as FMO5 and superoxide dismutase 2 are down-regulated when compared to the non-diabetic patients (Takamura et al., 2004). Thus, FMO's have become an attractive target for drug design and therapeutics due to their ability to metabolize or activate prodrugs and their complex involvement in regulating metabolic function in associated disorders such as T2D and CVD.

Flavin-containing monooxygenase 3's primary expression has been observed in the liver where it is the primary site for TMA metabolism to TMAO for the purpose of increased solubility and improved renal clearance as observed in **Figure 1** (Ayesh and Smith, 1990; Fennema et al., 2016). FMO3 has also demonstrated a significant role in reverse cholesterol transport (RCT), cholesterol absorption in the small intestine, and bile acid formation in FMO3 knockout mice. This result is most likely due to TMAO's ability to inhibit macrophage RCT contributing to increased plaque formation and an increased risk of CVD (Warrier et al., 2015). In obese-insulin resistant mice, FMO3 was shown to have increased expression contributing to higher levels of circulating TMAO and correlating positively with insulin resistance in human populations during clinical trials (Randrianarisoa et al., 2016).

In patients with chronic kidney disease, elevated levels of TMAO contributed significantly to the development of renal fibrosis resulting in poor mortality outcomes (Tang et al., 2015). These results in connection with other reports demonstrate that TMAO is a significant factor in platelet aggregation, due to promoting Ca^{2+} efflux and vascular smooth muscle cell activation. Further these results also demonstrate the significance that TMAO has on propagating diseases through a variety of metabolic pathways (Zhu et al., 2016).

While FMO3 has garnered the most attention, other FMO enzymes demonstrate potential for therapeutic intervention as well. While FMO5 shows expression in the small intestines, kidneys, lungs, and liver (Overby et al., 1995; Cashman and Zhang, 2006) expression in the small intestines and liver is of the greatest interest for CVD related therapeutics. However, FMO5 differs significantly in substrate catalytic activity and shows low affinity for similar substrates seen in FMO3 (Zhang et al., 2007). While expression of FMO5 in the small intestines is independent of the bacteria present, there is evidence to suggest that a high fat diet does influence FMO5 expression in the small intestines, but this was tissue specific as an increase in FMO5 liver expression was not observed (Scott et al., 2017).

CONCLUSION

Even though compounds such as DMB and dietary indoles have shown promise as a therapeutic intervention for CVD and T2D there is still much that can be improved upon in their chemical structures. DMB has only been shown to be effective as a non-lethal inhibitor of bacteria and inhibiting TMAO levels, however it has yet to be demonstrated that any improvements in glucose homeostasis or insulin sensitivity would be observed.

Dietary indoles, while effective at inhibiting FMO3 activity and reducing TMAO levels, (Cashman et al., 1999) have inherent problems with specificity as indoles have shown to be effective serotonin agonists with the significant ability to permeate the blood brain barrier, eliciting potentially harmful psychotropic effects (Chen et al., 2016; Zajdel et al., 2016). Combining the structural features of these chemical compounds into one drug design that is capable of specific sites of action holds promise that significant advancements can be made to attenuate the effects of CVD and T2D in one efficient drug therapy.

No current therapeutics target both bacterial and human metabolism in a way that can reduce systemic inflammation, reorganize cholesterol levels, and improve energy regulation to reduce the effects of aging and dietary overload that is characteristic of patients with CVD and T2D. By combining these targets into one therapeutic, it might be possible to modulate crosstalk in the gut-liver-heart axis, effectively controlling the succeeding cascade of events that play out in rescuing further development of complications that arise in T2D and CVD.

AUTHOR CONTRIBUTIONS

IS and NG drafted and finalized the manuscript with support from RA. RA provided the basis for the review and guidance throughout the manuscript development. MG, SY, and JZ involved in subject discussion, formation of material, and manuscript revision. All authors contributed to the article and approved the submitted version.

FUNDING

The current manuscript was supported by the Presidential Award for Interdisciplinary Research to Dr. Amin.

REFERENCES

Al-Waiz, M., Ayesh, R., Mitchell, S. C., Idle, J. R., and Smith, R. L. (1987). A Genetic polymorphism of the N-oxidation of trimethylamine in humans. *Clin. Pharmacol. Therap.* 42, 588–594. doi: 10.1038/clpt.1987.201

Arora, T., and Bäckhed, F. (2016). The gut microbiota and metabolic disease: current understanding and future perspectives. *J. Intern. Med.* 280, 339–349. doi: 10.1111/joim.12508

Arseculeratne, G., Wong, A. K. C., Goudie, D. R., and Ferguson, J. (2007). Trimethylaminuria (Fish-Odor syndrome): a case report. *Archiv. Dermatol.* 143, 81–84.

Athyros, V. G., Papageorgiou, A. A., Athyrou, V. V., Demitriadis, D. S., and Kontopoulos, A. G. (2002). Atorvastatin and micronized fenofibrate alone and in combination in Type 2 diabetes with combined hyperlipidemia. *Diabetes Care* 25, 1198–1202. doi: 10.2337/diacare.25.7.1198

Ayesh, R., and Smith, R. L. (1990). Genetic polymorphism of trimethylamine N-oxidation. *Pharmacol. Therap.* 45, 387–401. doi: 10.1016/0163-7258(90)90074-c

Bai, J., Zheng, S., Jiang, D., Han, T., Li, Y., Zhang, Y., et al. (2015). Oxidative stress contributes to abnormal glucose metabolism and insulin sensitivity in two hyperlipidemia models. *Intern. J. Clin. Exper. Pathol.* 8, 13193–13200.

Barrea, L., Annunziata, G., Muscogiuri, G., Di Somma, C., Laudisio, D., Maisto, M., et al. (2018). Trimethylamine-N-oxide (TMAO) as novel potential biomarker of early predictors of metabolic syndrome. *Nutrients* 10:1971. doi: 10.3390/nu10121971

Bennett, M. R., Sinha, S., and Owens, G. K. (2016). Vascular smooth muscle cells in atherosclerosis. *Circ. Res.* 118, 692–702.

Bodea, S., Funk, M. A., Emily, P., Balskus, L., and Catherine, L. D. (2016). Molecular basis of C–N bond cleavage by the glycyl radical enzyme Choline Trimethylamine-Lyase. *Cell Chem. Biol.* 23, 1206–1216. doi: 10.1016/j.chembiol.2016.07.020

Booth, G. L., Kapral, M. K., Fung, K., and Tu, J. V. (2006). Relation between age and cardiovascular disease in men and women with diabetes compared with non-diabetic people: a population-based retrospective cohort study. *Lancet* 368, 29–36. doi: 10.1016/s0140-6736(06)68967-8

Borbás, T., Benkő, B., Dalmadi, B., Szabó, I., and Tihanyi, K. (2006). Insulin in flavin-containing monooxygenase regulation: flavin-containing monooxygenase and cytochrome P450 activities in experimental diabetes. *Eur. J. Pharmaceut. Sci.* 28, 51–58.

Borbas, T., Zhang, J., Cerny, M. A., Liko, I., and Cashman, J. R. (2006). Investigation of structure and function of a catalytically efficient variant of the human flavin-containing monooxygenase form 3. *Drug Metab. Dispos.* 34, 1995–2002. doi: 10.1124/dmd.106.010827

Cashman, J. R., and Zhang, J. (2006). Human flavin-containing monooxygenases. *Ann. Rev. Pharmacol. Toxicol.* 46, 65–100.

Cashman, J. R., Xiong, Y., Lin, J., Verhagen, H., van Poppel, G., van Bladeren, P. J., et al. (1999). In vitro and in vivo inhibition of human flavin-containing monooxygenase form 3 (FMO3) in the presence of dietary indoles. *Biochem. Pharmacol.* 58, 1047–1055. doi: 10.1016/s0006-2952(99)00166-5

Centers for Disease Control and Prevention (2018). *U.S. Diabetes Surveillance System*. Atlanta: Centers for Disease Control and Prevention.

Chen, J., Tao, L.-X., Xiao, W., Ji, S.-S., Wang, J.-R., Li, X.-W., et al. (2016). Design, synthesis and biological evaluation of novel chiral oxazino-indoles as potential and selective neuroprotective agents against Aβ25–35-induced neuronal damage. *Bioorgan. Med. Chem. Lett.* 26, 3765–3769. doi: 10.1016/j.bmcl.2016.05.061

Chen, S., Henderson, A., Petriello, M. C., Romano, K. A., Gearing, M., Miao, J., et al. (2019). Trimethylamine N-oxide binds and activates PERK to promote metabolic dysfunction. *Cell Metab.* 30, 1141–1151.e5.

Craciun, S., Marks, J. A., and Balskus, E. P. (2014). Characterization of choline Trimethylamine-Lyase Expands the chemistry of glycyl radical enzymes. *ACS Chem. Biol.* 9, 1408–1413. doi: 10.1021/cb500113p

Ding, H., and Triggle, C. R. (2005). Endothelial cell dysfunction and the vascular complications associated with type 2 diabetes: assessing the health of the endothelium. *Vasc. Health Risk Manag.* 1, 55–71. doi: 10.2147/vhrm.1.1.55.58939

Eswaramoorthy, S., Bonanno, J. B., Burley, S. K., and Swaminathan, S. (2006). Mechanism of action of a flavin-containing monooxygenase. *Proc. Natl. Acad. Sci. U.S.A.* 103, 9832–9837.

Fennema, D., Phillips, I. R., and Shephard, E. A. (2016). Trimethylamine and Trimethylamine N-Oxide, a Flavin-containing monooxygenase 3 (FMO3)-mediated host-microbiome metabolic axis implicated in health and disease. 44, 1839–1850. doi: 10.1124/dmd.116.070615

Ferrannini, E., and DeFronzo, R. A. (2015). Impact of glucose-lowering drugs on cardiovascular disease in type 2 diabetes. *Eur. Heart J.* 36, 2288–2296. doi: 10.1093/eurheartj/ehv239

Gao, C., Catucci, G., Gilardi, G., and Sadeghi, S. J. (2018). Binding of methimazole and NADP (H) to human FMO3: in vitro and in silico studies. *Intern. J. Biol. Macromol.* 118, 460–468. doi: 10.1016/j.ijbiomac.2018.06.104

Hines, R. N., Cashman, J. R., Philpot, R. M., Williams, D. E., and Ziegler, D. M. (1994). The mammalian flavin-containing monooxygenases: molecular characterization and regulation of expression. *Toxicol. Appl. Pharmacol.* 125, 1–6. doi: 10.1006/taap.1994.1042

Holmes, A. J., Chew, Y. V., Colakoglu, F., Cliff, J. B., Klaassens, E., Read, M. N., et al. (2017). Diet-microbiome interactions in health are controlled by intestinal nitrogen source constraints. *Cell Metab.* 25, 140–151. doi: 10.1016/j.cmet.2016.10.021

Hosseini-Beheshti, E., and Grau, G. E. R. (2019). Extracellular vesicles and microvascular pathology: decoding the active dialogue. *Microcirculation* 26:e12485. doi: 10.1111/micc.12485

Hotamisligil, G. S. (2010). Endoplasmic reticulum stress and atherosclerosis. *Nat. Med.* 16:396.

Iglay, K., Hannachi, H., Joseph Howie, P., Xu, J., Li, X., Engel, S. S., et al. (2016). Prevalence and co-prevalence of comorbidities among patients with type 2 diabetes mellitus. *Curr. Med. Res. Opin.* 32, 1243–1252. doi: 10.1185/03007995.2016.1168291

Janeiro, M., Ramírez, M., Milagro, F., Martínez, J., and Solas, M. (2018). Implication of trimethylamine N-Oxide (TMAO) in disease: potential biomarker or new therapeutic target. *Nutrients* 10:1398. doi: 10.3390/nu10101398

Kamo, T., Akazawa, H., Suda, W., Saga-Kamo, A., Shimizu, Y., Yagi, H., et al. (2017). Dysbiosis and compositional alterations with aging in the gut microbiota of patients with heart failure. *PLoS One* 12:e0174099. doi: 10.1371/journal.pone.0174099

Landfald, B., Valeur, J., Berstad, A., and Raa, J. (2017). Microbial trimethylamine-N-oxide as a disease marker: something fishy? *Microb. Ecol. Health Dis.* 28:1327309. doi: 10.1080/16512235.2017.1327309

Lau, W. L., and Vaziri, N. D. (2019). Gut microbial short-chain fatty acids and the risk of diabetes. *Nat. Rev. Nephrol.* 15, 389–390. doi: 10.1038/s41581-019-0142-7

Leon, B. M., and Maddox, T. M. (2015). Diabetes and cardiovascular disease: epidemiology, biological mechanisms, treatment recommendations and future research. *World J. Diabetes* 6, 1246–1258. doi: 10.4239/wjd.v6.i13.1246

Libby, P. (2006). Inflammation and cardiovascular disease mechanisms. *Am. J. Clin. Nutr.* 83, 456S–460S.

Liu, L., He, X., and Feng, Y. (2019). Coronary heart disease and intestinal microbiota. *Coron. Artery Dis.* 30, 384–389. doi: 10.1097/mca.0000000000000758

Luedde, M., Winkler, T., Heinsen, F.-A., Rühlemann, M. C., Spehlmann, M. E., Bajrovic, A., et al. (2017). Heart failure is associated with depletion of core intestinal microbiota. *ESC Heart Fail.* 4, 282–290. doi: 10.1002/ehf2.12155

Marques, F. Z., Nelson, E., Chu, P.-Y., Horlock, D., Fiedler, A., Ziemann, M., et al. (2017). High-fiber diet and acetate supplementation change the gut microbiota and prevent the development of hypertension and heart failure in hypertensive mice. *Circulation* 135, 964–977. doi: 10.1161/circulationaha.116.024545

Mitchell, S. C., and Smith, R. L. (2001). Trimethylaminuria: the fish malodor syndrome. *Drug Metab. Disposit.* 29, 517–521.

Mohammadi, A., Najar, A. G., Yaghoobi, M. M., Jahani, Y., and Vahabzadeh, Z. (2016). Trimethylamine-N-oxide treatment induces changes in the ATP-binding cassette transporter A1 and scavenger receptor A1 in murine macrophage J774A. 1 cells. *Inflammation* 39, 393–404. doi: 10.1007/s10753-015-0261-7

Motika, M. S., Zhang, J., Zheng, X., Riedler, K., and Cashman, J. R. (2009). Novel variants of the human flavin-containing monooxygenase 3 (FMO3) gene

associated with trimethylaminuria. *Mol. Genet. Metab.* 97, 128–135. doi: 10.1016/j.ymgme.2009.02.006

Murphy, E. A., Velazquez, K. T., and Herbert, K. M. (2015). Influence of high-fat diet on gut microbiota: a driving force for chronic disease risk. *Curr. Opin. Clin. Nutr. Metab. Care* 18, 515–520. doi: 10.1097/mco.0000000000000209

Nace, C. G., Genter, M. B., Sayre, L. M., and Crofton, K. M. (1997). Effect of Methimazole, an FMO Substrate and Competitive Inhibitor, on the Neurotoxicity of 3,3'-Iminodipropionitrile in Male Rats1. *Toxicol. Sci.* 37, 131–140. doi: 10.1006/faat.1997.2307

Overby, L. H., Buckpitt, A. R., Lawton, M. P., Attaasafoadjei, E., Schulze, J., and Philpot, R. M. (1995). Characterization of flavin-containing monooxygenase-5 (FMO5) cloned from human and guinea-pig: evidence that the unique catalytic properties of FMO5 are not confined to the rabbit ortholog. *Archiv. Biochem. Biophys.* 317, 275–284. doi: 10.1006/abbi.1995.1163

Phillips, I. R., and Shephard, E. A. (2008). Flavin-containing monooxygenases: mutations, disease and drug response. *Trends Pharmacol. Sci.* 29, 294–301. doi: 10.1016/j.tips.2008.03.004

Pi-Sunyer, X. (2014). The look AHEAD trial: a review and discussion of its outcomes. *Curr. Nutr. Rep.* 3, 387–391. doi: 10.1007/s13668-014-0099-x

Pluznick, J. L., Protzko, R. J., Gevorgyan, H., Peterlin, Z., Sipos, A., and Han, J. (2013). Olfactory receptor responding to gut microbiota-derived signals plays a role in renin secretion and blood pressure regulation. *Proc. Natl. Acad. Sci. U.S.A.* 110, 4410–4415. doi: 10.1073/pnas.1215927110

Rachel, N., Carmody, G. K, Gerber, J. M., Luevano, D. M., Gatti, L. S., Svenson, K. L., et al. (2015). Diet dominates host genotype in shaping the murine gut microbiota. *Cell Host Microb.* 17, 72–84. doi: 10.1016/j.chom.2014.11.010

Randrianarisoa, E., Lehn-Stefan, A., Wang, X., Hoene, M., Peter, A., Heinzmann, S. S., et al. (2016). Relationship of Serum Trimethylamine N-Oxide (TMAO) Levels with early *Atherosclerosis* in humans. *Sci. Rep.* 6:26745.

Rath, S., Heidrich, B., Pieper, D. H., and Vital, M. (2017). Uncovering the trimethylamine-producing bacteria of the human gut microbiota. *Microbiome* 5:54.

Sandek, A., Bjarnason, I., Volk, H.-D., Crane, R., Meddings, J. B., Niebauer, J., et al. (2012). Studies on bacterial endotoxin and intestinal absorption function in patients with chronic heart failure. *Intern. J. Cardiol.* 157, 80–85. doi: 10.1016/j.ijcard.2010.12.016

Scott, F., Gonzalez Malagon, S. G., O'Brien, B. A., Fennema, D., Veeravalli, S., Coveney, C. R., et al. (2017). Identification of flavin-containing monooxygenase 5 (FMO5) as a regulator of glucose homeostasis and a potential sensor of gut bacteria. *Drug Metab. Dispos.* 45, 982–989. doi: 10.1124/dmd.117.076612

Shih, D. M., Zhu, W., Schugar, R. C., Meng, Y., Jia, X., Miikeda, A., et al. (2019). Genetic deficiency of Flavin-containing monooxygenase 3 (Fmo3) protects against thrombosis but has only a minor effect on plasma lipid levels—brief report. *Thromb. Biol.* 39, 1045–1054. doi: 10.1161/atvbaha.119.312592

Silverman, M. G., Ference, B. A., Im, K., Wiviott, S. D., Giugliano, R. P., Grundy, S. M., et al. (2016). Association between lowering LDL-C and cardiovascular risk reduction among different therapeutic interventions: a systematic review and meta-analysis. *JAMA* 316, 1289–1297. doi: 10.1001/jama.2016.13985

Simon, G. L., and Gorbach, S. L. (1986). The human intestinal microflora. *Digest. Dis. Sci.* 31, 147–162.

Sommer, F., and Bäckhed, F. (2013). The gut microbiota — masters of host development and physiology. *Nat. Rev. Microbiol.* 11, 227–238. doi: 10.1038/nrmicro2974

Srinivas, M. (2017). Cytochrome P450 enzymes, drug transporters and their role in pharmacokinetic drug-drug interactions of Xenobiotics: a comprehensive review. *Open J. Chem.* 3, 1–11.

Sung, M. M., Kim, T. T., Denou, E., Soltys, C.-L. M., Hamza, S. M., Byrne, N. J., et al. (2017). Improved glucose homeostasis in obese mice treated with resveratrol is associated with alterations in the gut microbiome. *Diabetes* 66, 418–425. doi: 10.2337/db16-0680

Takamura, T., Sakurai, M., Ota, T., Ando, H., Honda, M., and Kaneko, S. (2004). Genes for systemic vascular complications are differentially expressed in the livers of Type 2 diabetic patients. *Diabetologia* 47, 638–647. doi: 10.1007/s00125-004-1366-y

Tang, W. H., Wang, Z., Kennedy, D. J., Wu, Y., Buffa, J. A., Agatisa-Boyle, B., et al. (2015). Gut microbiota-dependent trimethylamine N-oxide (TMAO) pathway contributes to both development of renal insufficiency and mortality risk in chronic kidney disease. *Circ. Res.* 116, 448–455. doi: 10.1161/circresaha.116.305360

Tang, W. W., Li, D. Y., and Hazen, S. L. (2019). Dietary metabolism, the gut microbiome, and heart failure. *Nat. Rev. Cardiol.* 16, 137–154. doi: 10.1038/s41569-018-0108-7

Tilg, H. (2016). A gut feeling about thrombosis. *New Engl. J. Med.* 374, 2494–2496. doi: 10.1056/nejmcibr1604458

Velasquez, M., Ramezani, A., Manal, A., and Raj, D. (2016). Trimethylamine N-oxide: the good, the bad and the unknown. *Toxins* 8:326. doi: 10.3390/toxins8110326

Wang, C. C. L., Hess, C. N., Hiatt, W. R., and Goldfine, A. B. (2016). Clinical update: cardiovascular disease in diabetes mellitus. *Circulation* 133, 2459–2502. doi: 10.1161/circulationaha.116.022194

Wang, T., Shankar, K., Ronis, M. J., and Mehendale, H. M. (2000). Potentiation of thioacetamide liver injury in diabetic rats is due to induced CYP2E1. *J. Pharmacol. Exp. Ther.* 294, 473–479.

Wang, Z., Klipfell, E., Bennett, B. J., Koeth, R., Levison, B. S., DuGar, B., et al. (2011). Gut flora metabolism of phosphatidylcholine promotes cardiovascular disease. *Nature* 472:57. doi: 10.1038/nature09922

Wang, Z., Roberts, A. B., Buffa, J. A., Levison, B. S., Zhu, W., Org, E., et al. (2015). Non-lethal inhibition of gut microbial trimethylamine production for the treatment of atherosclerosis. *Cell* 163, 1585–1595. doi: 10.1016/j.cell.2015.11.055

Warrier, M., Shih, D. M., Burrows, A. C., Ferguson, D., Gromovsky, A. D., Brown, A. L., et al. (2015). The TMAO-generating enzyme flavin monooxygenase 3 is a central regulator of cholesterol balance. *Cell Rep.* 10, 326–338. doi: 10.1016/j.celrep.2014.12.036

Zajdel, P., Marciniec, K., Satała, G., Canale, V., Kos, T., Partyka, A., et al. (2016). N1-Azinylsulfonyl-1H-indoles: 5-HT6 receptor antagonists with procognitive and antidepressant-like properties. *ACS Med. Chem. Lett.* 7, 618–622. doi: 10.1021/acsmedchemlett.6b00056

Zhang, J., Cerny, M. A., Lawson, M., Mosadeghi, R., and Cashman, J. R. (2007). Functional activity of the mouse flavin-containing monooxygenase forms 1, 3, and 5. *J. Biochem. Mol. Toxicol.* 21, 206–215. doi: 10.1002/jbt.20176

Zhu, W., Gregory, J. C., Org, E., Buffa, J. A., Gupta, N., Wang, Z., et al. (2016). Gut microbial metabolite TMAO enhances platelet hyperreactivity and thrombosis risk. *Cell* 165, 111–124. doi: 10.1016/j.cell.2016.02.011

Ziegler, D. M. (1993). Recent studies on the structure and function of multisubstrate flavin-containing monooxygenases. *Annu. Rev. Pharmacol. Toxicol.* 33, 179–199. doi: 10.1146/annurev.pa.33.040193.001143

Conflict of Interest: The authors declare that the research was conducted in the absence of any commercial or financial relationships that could be construed as a potential conflict of interest.

Copyright © 2020 Steinke, Ghanei, Govindarajulu, Yoo, Zhong and Amin. This is an open-access article distributed under the terms of the Creative Commons Attribution License (CC BY). The use, distribution or reproduction in other forums is permitted, provided the original author(s) and the copyright owner(s) are credited and that the original publication in this journal is cited, in accordance with accepted academic practice. No use, distribution or reproduction is permitted which does not comply with these terms.

frontiers in Physiology

REVIEW
published: 05 November 2020
doi: 10.3389/fphys.2020.580811

Unraveling the Mystery of Cold Stress-Induced Myocardial Injury

*Xue Kong, Haitao Liu, Xiaole He, Yang Sun and Wei Ge**

Department of General Practice, Xijing Hospital, Fourth Military Medical University, Xi'an, China

Exposure to low ambient temperature imposes great challenge to human health. Epidemiological evidence has noted significantly elevated emergency admission and mortality rate in cold climate in many regions, in particular, adverse events in cardiovascular system. Cold stress is becoming one of the important risk factors for cardiovascular death. Through recent advance in echocardiography and myocardial histological techniques, both clinical and experimental experiments have unveiled that cold stress triggers a variety of pathological and pathophysiological injuries, including ventricular wall thickening, cardiac hypertrophy, elevated blood pressure, decreased cardiac function, and myocardial interstitial fibrosis. In order to examine the potential mechanism of action behind cold stress-induced cardiovascular anomalies, ample biochemical and molecular biological experiments have been conducted to denote a role for mitochondrial injury, intracellular Ca^{2+} dysregulation, generation of reactive oxygen species (ROS) and other superoxide, altered gene and protein profiles for apoptosis and autophagy, and increased adrenergic receptor sensitivity in cold stress-induced cardiovascular anomalies. These findings suggest that cold stress may damage the myocardium through mitochondrial injury, apoptosis, autophagy, metabolism, oxidative stress, and neuroendocrine pathways. Although the precise nature remains elusive for cold stress-induced cardiovascular dysfunction, endothelin ($ET\text{-}_A$) receptor, endoplasmic reticulum (ER) stress, transient receptor potential vanilloid, mitochondrial-related protein including NRFs and UCP-2, ROS, Nrf2-Keap1 signaling pathway, Bcl-2/Bax, and lipoprotein lipase (LPL) signaling may all play a pivotal role. For myocardial injury evoked by cold stress, more comprehensive and in-depth mechanisms are warranted to better define the potential therapeutic options for cold stress-associated cardiovascular diseases.

Keywords: cold stress, hypothermia, myocardial injury, cardiac function, mechanism, molecular pathways

OPEN ACCESS

Edited by:
Jun Ren,
University of Washington,
United States

Reviewed by:
Howard Prentice,
Florida Atlantic University,
United States
Asli Ceylan,
Ankara Yıldırım Beyazıt University,
Turkey

***Correspondence:**
Wei Ge
geweidr@fmmu.edu.cn

Specialty section:
This article was submitted to Clinical and Translational Physiology, a section of the journal Frontiers in Physiology

Received: *07 July 2020*
Accepted: *05 October 2020*
Published: *05 November 2020*

Citation:
Kong X, Liu H, He X, Sun Y and Ge W (2020) Unraveling the Mystery of Cold Stress-Induced Myocardial Injury. Front. Physiol. 11:580811. doi: 10.3389/fphys.2020.580811

INTRODUCTION

Sustained exposure to cold climate is one of the main risk factors that adversely affect human health. Numerous epidemiological studies, including Asia, Europe, and the America, have noted a tight correlation between cold climate and increased cardiovascular mortality (Keatinge, 1997; Mercer, 2003; Ogawa et al., 2007; Berko et al., 2014; Zhou et al., 2014). Moreover, cold weather also leads to an increase in the number of patients admitted to the emergency department (Baumgartner et al., 2008; Chen et al., 2019). Ample clinical and epidemiological studies have confirmed that cold weather is associated with increased adverse cardiovascular events (Keatinge, 1997; Stewart et al., 2002; Medina-Ramón et al., 2006; Cheng and Su, 2010; Ikäheimo, 2018). These findings indicate

that cold stress can be considered as an independent risk factor for cardiovascular events. However, mechanisms responsible for adverse cardiac changes induced by cold stress remain unclear. Over the past decades, cold stress was noted to trigger a series of pathophysiological changes in cardiac function. These studies have revealed possible molecular pathways associated with cold stress-induced cardiovascular events and potential treatment options for cold stress-induced myocardial injury.

In this review, we summarized pathophysiological changes in myocardial injury induced by cold stress. We will further summarize specific molecular pathways that play an important role in cold stress-induced cardiovascular anomalies and provide a more comprehensive understanding of myocardial injury induced by cold stress.

MYOCARDIAL PATHOPHYSIOLOGICAL CHANGES INDUCED BY COLD STRESS

Cardiac Structure and Function

Animal experiments reveal that cold exposure does not cause overt changes in body weight or size (Bello Roufai et al., 2007; Zhang et al., 2012b; Jiang et al., 2013; Matsubara et al., 2016). Nonetheless, cold exposure is associated with significant alterations in heart weight (Fregly et al., 1989; Bello Roufai et al., 2007; Cheng and Hauton, 2008; Yin et al., 2015; Matsubara et al., 2016; Liang et al., 2017), left ventricular (LV) wall thickness (Bello Roufai et al., 2007; Templeman et al., 2010; Zhang et al., 2012b; Liang et al., 2017), LV end-diastolic (LV EDD; Cheng and Hauton, 2008; Zhang et al., 2012b; Jiang et al., 2013), and LV mass (Zhang et al., 2012b). A transverse mice heart section showed that compared with the control group, cold stress significantly thickened the LV wall. In another study, histological staining sections revealed increased cardiomyocyte area following cold exposure, which was consistent with increased LV mass, wall thickness, EDD, and heart weight (Zhang et al., 2012b; Yin et al., 2015; Nagasawa et al., 2016; Liang et al., 2017). These changes indicate that cold stress leads to changes in cardiac structure and cardiac hypertrophy. However, scientists have observed that cold exposure does not affect LV wall thickness, LV mass (Zhang et al., 2012a; Jiang et al., 2013), and LV EDD (Zhang et al., 2012a). These differences may be related to the extent and duration of cold stress in different experiments. Evaluation of cardiac function using echocardiography has indicated that cold stress decreases in ejection fraction and shortening fraction of mouse hearts, leading to dampened LV function (Zhang et al., 2012b; Jiang et al., 2013; Yin et al., 2015; Cong et al., 2018).

Fibrosis and Cardiomyocyte Injury

Masson trichrome staining revealed overt fibrosis in cold stress-exposed mouse heart, demonstrating that cold exposure prompted overt interstitial fibrosis in the heart (Zhang et al., 2012a,b; Yin et al., 2015; Nagasawa et al., 2016; Liang et al., 2017; Cong et al., 2018). Myocardial hypertrophy is often characterized by myocardial ultrastructural damage. Further observation of murine cardiomyocytes using transmission electron microscope depicted that cold stress led to sarcomere loss, myofibril disarray, and myofilament breakage. Besides, a high number of altered mitochondria was observed with different degrees of alterations such as swelling, vacuolation, autophagy, and a decrease in the number as well as disruption of cristae with formation of large vesicles, indicating significant degenerative changes (Bombig et al., 2003; Daud et al., 2009; Yin et al., 2015; Liang et al., 2017; Wang Z. et al., 2020). Vacuolar degeneration, eosinophilic degeneration, increased macrophage infiltration (Nagasawa et al., 2016; Cong et al., 2018), and nuclear shrinkage has also been reported to occur in cardiomyocytes (Meneghini et al., 2009).

Experimental observations have confirmed that cold stress induces cardiomyocyte injury, overt interstitial fibrosis, mitochondrial damage, and inflammation of the heart.

MECHANISM OF MYOCARDIAL INJURY INDUCED BY COLD STRESS

Oxidative Stress

Changes in oxidative stress products, antioxidant defense enzymes, and non-enzymatic antioxidants in myocardium have been observed in nearly all cold stress studies. Research has revealed that cold stress may cause an increase in the metabolic rate and increased production of reactive oxygen species (ROS), such as hydrogen peroxide (H_2O_2), hydroxyl radicals (HO), and superoxide anion radicals ($O_2^{-}\cdot$), which cause lipid peroxidation (Selman et al., 2000). At the same time, the body produces enzymatic Cu, Zn-superoxide dismutase (SOD-1), catalase (CAT), selenium-dependent glutathione peroxidase (Se-GSH-Px), and non-enzymatic antioxidants, such as reduced glutathione (GSH) to neutralize excessive ROS. Therefore, the damage caused by cold to the myocardium may be caused by an imbalance between oxidants and antioxidants in the body (Sahin and Gümüşlü, 2004).

Experimental findings have shown that sustained cold exposure promotes ROS production (Zhang et al., 2012a,b; Jain et al., 2013; Jiang et al., 2013; Wang et al., 2013), carbonyl formation, and generation of superoxide (O_2^{-}; Jiang et al., 2013) in the myocardium. 3′-Nitrotyrosine (3′-NT) and 4-hydroxynonenal (4-HNE) represent two markers for myocardial oxidative stress (Asselin et al., 2013). These markers are elevated with sustained cold exposure (Cong et al., 2018). More studies have found that cold exposure combined with hypoxia causes a significant increase in the level of malondialdehyde (MDA), a marker of oxidative stress (Jain et al., 2013). Cold stress has also been reported to cause an increase in the production of superoxide in myocardial tissue slices, and the activity of NADPH oxidase in LV tissue homogenate increases significantly (Nagasawa et al., 2016). Furthermore, other studies have found that cold combined with hypoxia causes a double increase in free radicals in the myocardium. The hypoxia-inducible factor (HIF-1α) is considered a key marker of cell response to hypoxia and plays a vital regulatory role in facilitating oxygen transport in tissues (Semenza, 2004). When there is cold climate and poor oxygenation in the environment, hypoxia-inducible factor expression is overtly upregulated (Zhang et al., 2012a; Jain et al., 2013). These results indicate that collectively,

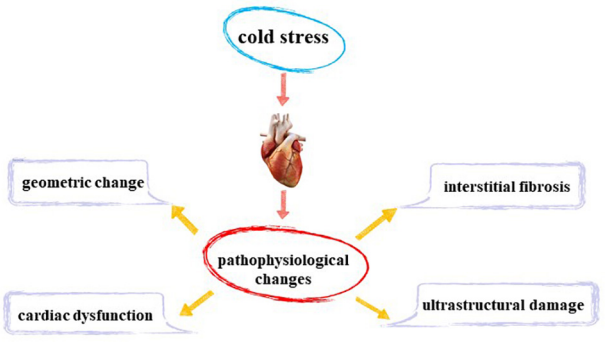

FIGURE 1 | Myocardial pathophysiological changes induced by cold stress.

acute hypothermia and hypoxia significantly intensifies free radical-mediated physiological response in the myocardium. Some studies have revealed the role of oxidative stress in myocardial injury caused by cold stress through antioxidants. Metallothionein, a low molecular weight heavy metal-chelating antioxidant (Yang et al., 2019), significantly improves ROS overproduction, myocardial fibrosis, and myocardial contraction dysfunction caused by cold stress (Zhang et al., 2012a).

Besides pro-oxidation products, levels and activities of various antioxidant enzymes are also altered in response to cold stress. Experimental studies have shown that sustained cold exposure decreases levels of GSH and GSH/GSSG ratio not only in the myocardium (Zhang et al., 2012a; Jiang et al., 2013) but also in nearly all tissues (Kaushik and Kaur, 2003; Sahin and Gümüşlü, 2004). Western blotting analysis also demonstrated that levels of superoxide dismutase SOD-1 and Mn-superoxide dismutase (SOD-2) in mice decreases after 2 weeks of cold exposure. The expression of SOD-1 and SOD-2 mRNA in LV myocardium, detected by real-time RT-PCR, also indicated similar changes as observed with protein expression (Cong et al., 2018). In terms of antioxidant enzyme activity, SOD-1 and CAT activities have been shown to significantly decrease in the heart due to cold stress (Kaushik and Kaur, 2003; Sahin and Gümüşlü, 2004). The reason for this phenomenon may be that SOD-1 catalyzes the production of a large amount of H_2O_2, resulting in product inhibition. However, other studies noted an upregulated CAT and Se-GSH-Px activities in the myocardium following cold stress (Sahin and Gümüşlü, 2004). These results revealed that cold stress provokes an imbalance between oxidative stress and antioxidant defense, leading to myocardial injury. An independent study conducted in humans revealed a significant increase in the activities of Se-GSH-px, GSH, and CAT in erythrocytes from short track skaters exposed to prolonged cold environment, which may represent a protective mechanism against ROS damage (Hong et al., 2008; Cong et al., 2018). Therefore, myocardial injury induced by cold stress may be caused by an imbalance between oxidation and antioxidation and thus elimination by antioxidants.

To explore specific pathways and mechanisms of oxidative stress in myocardial injury induced by cold stress, ample experimental studies have been conducted. Nrf2 is a cell sensor protein with an important role in antioxidation, while Keap1 initiates its autophagy degradation (Tonelli et al., 2018). Cold stress has been reported to reduce protein expression of Nrf2 and keap1. Similar trends were noted in mRNA expression of these two genes (Cong et al., 2018). Oxidative stress changes amino acid residues in Keap1 structure, resulting in dysfunction (Cui et al., 2015; Barančík et al., 2016). These findings imply that myocardial oxidative stress injury provoked by cold stress develops likely through the Nrf2-Keap1 signaling pathway.

Autophagy

Autophagy plays an important role in many physiological and pathological processes, including regulating the degradation of macromolecular substances, organelles, and nutrients, which are positively correlated with cold exposure (Williams et al., 2010; Nemchenko et al., 2011). Autophagy plays a vital role in the quality control of organelles and intracellular proteins, and autophagy products, such as amino acids and fatty acids, provide raw materials for the synthesis of adenosine 5′-triphosphate (ATP), proteins, and organelles. At the same time, autophagy also plays an important role in regulating intracellular secretion and transportation and was initially (Kroemer, 2015) considered a nonspecific degradation process, although specific autophagy degradation was recently noted. Mitophagy is a specific autophagy that clears damaged mitochondria and plays an important role in mitochondrial quality control (Shirakabe et al., 2016). Mitochondrial quality control of cardiomyocytes is very critical for heart function because mitochondria of cardiomyocytes produce a large amount of ATP daily to maintain the heart's blood-pumping function. In a normal physiological state, mitochondria function is consistent with energy demand of the heart, to maintain normal heart function (Saito and Sadoshima, 2015; Nirwane and Majumdar, 2018). Therefore, cardiac autophagy is one of the important ways of maintaining cardiac homeostasis, and in some cases, autophagy activation can protect the heart. However, when the external injury persists, excessive autophagy is also considered to be related to the pathological changes of the heart (Delbridge et al., 2017). Autophagy results include adaptation, apoptosis, and necrosis. When autophagy is activated by various stresses, adaptation occurs in most cases, which limits cell dysfunction and causes cell death; however, in some cases, it results in apoptosis and necrosis (Sciarretta et al., 2018). Autophagy can resist heart injury under various pathological conditions by eliminating misfolded proteins, damaged organelles, dysfunctional mitochondria, and inhibiting oxidative stress, and can alleviate systolic dysfunction and cardiac structural remodeling during hemodynamic overload, to maintain the normal structure and function of the heart (Nakai et al., 2007; Maejima et al., 2013; Ikeda et al., 2015; Yin et al., 2020).

Excessive accumulation of PTEN-induced putative kinase 1 (PINK1) protein phosphorylates Parkinson's disease protein 2 (Parkin) protein and initiates the formation of mitochondrial autophagy (Yamano et al., 2016). Compared with the control group, proteins related to mitochondrial autophagy, PINK1, and phosphorylation level of Parkin were reported to be significantly

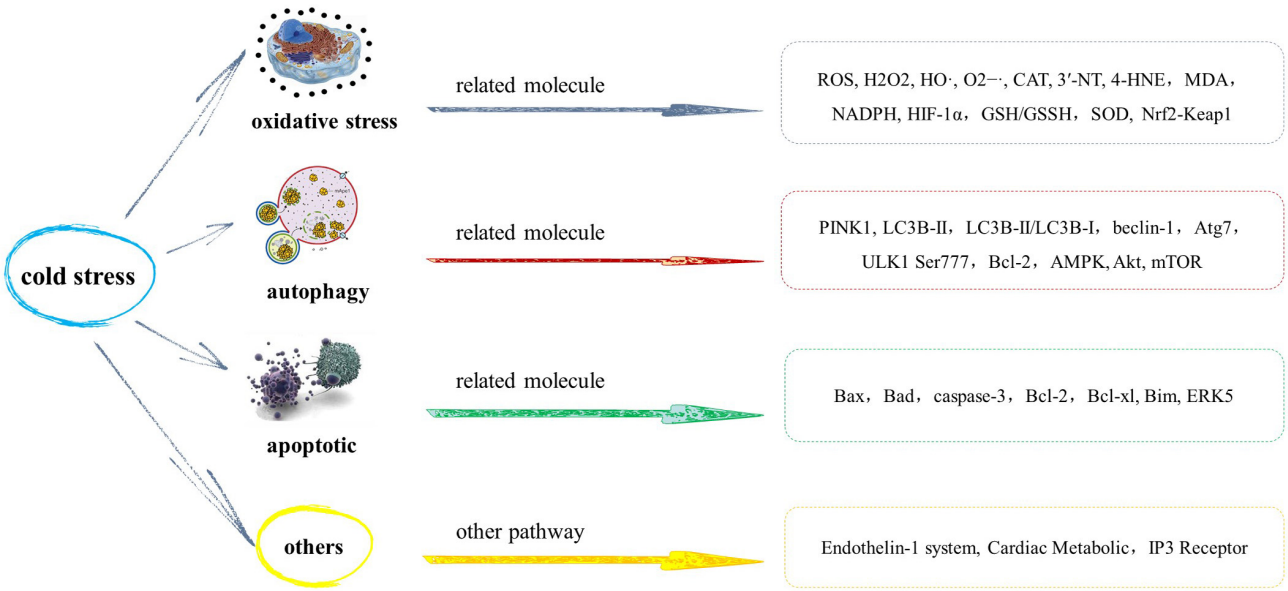

FIGURE 2 | Mechanism of myocardial injury induced by cold stress.

increased during cold exposure (Wang Z. et al., 2020). Studies have found that cold exposure significantly upregulates the levels of essential protein markers of autophagy including LC3B-II, LC3B-II/LC3B-I ratio, and beclin-1, Atg7, and ULK1 Ser777 phosphorylation, indicating facilitated autophagy following cold exposure. A large number of LC3+ puncta have been observed in the myocardial slices of murine after cold exposure by fluorescence immunohistochemistry. Western blot and fluorescence immunohistochemistry showed that inhibition of autophagy significantly alleviated an increase in LC3+ puncta induced by cold exposure. Furthermore, inhibition of autophagy can significantly reduce the abnormal mechanical function of myocardial cells caused by cold compared with normal conditions (Jiang et al., 2013). These results indicate that autophagy plays a significant role in myocardial contraction induced by cold stress. The BH3 domain of Bcl-2 binds to beclin-1, and the conformation of beclin-1 may be altered by phosphorylation in the BH3 domain, resulting in the release of beclin-1 from the complex and induction of autophagy (Qi et al., 2011). Immunoprecipitation results found that the amount of Bcl-2 that immunoprecipitated with beclin-1 was significantly decreased in mice exposed to low temperatures. This indicates that cold stress can trigger the dissociation of between Bcl-2 and beclin-1, leading to autophagy (Jiang et al., 2013). It was reported earlier that cold exposure significantly augmented pressure overload-induced phosphorylation of AMP-dependent protein kinase (AMPK; Lu and Xu, 2013), which serves as a positive regulator of autophagy (Shaw, 2009). All these findings showed a possible role of autophagy induction in cold stress-induced changes in the myocardial. Akt and mammalian target of rapamycin (mTOR) are two proteins that inhibit autophagy. Assessment of signaling mechanisms involved in autophagy regulation revealed that cold exposure-induced autophagy is related to inhibition of the phosphorylation of the two proteins (Williams et al., 2010; Nemchenko et al., 2011; Xu and Ren, 2012). Autophagy is strictly regulated by upstream mediators, and both Atg (autophagy-related gene) family and mTOR kinase can inhibit autophagy (Ren et al., 2008; Williams et al., 2010). The phosphorylation level of Akt and mTOR is also reported to decrease after cold stress exposure. mTOR is the main inhibitor of autophagy and plays a key role in the regulation of autophagy, while Akt is the most important upstream activator of mTOR autophagy (Jiang et al., 2013). Therefore, reduced phosphorylation of Akt and mTOR further reveals their signaling role in cold stress-induced regulation of myocardial autophagy.

Apoptotic

Through staining to detect apoptosis rate of cardiomyocytes *in vitro*, cold stress was found to significantly increase the apoptosis rate (L'Ecuyer et al., 2012; Zhang et al., 2012a,b; Wang et al., 2013; Yin et al., 2015; Liang et al., 2017). Apoptosis-related proteins include proapoptotic proteins and antiapoptotic proteins. The proapoptotic proteins include Bax, Bad, and caspase-3, while Bcl-2 belongs to antiapoptotic protein (Delbridge et al., 2016; Pereira et al., 2018). The expression of Bax and Bad was reported to be increased, and the expression of Bcl-2 decreased after 2 weeks of cold exposure (Yin et al., 2015; Liang et al., 2017; Cong et al., 2018; Wang Z. et al., 2020). The mRNA expression in Bax and Bad was significantly elevated in the cold exposed groups, while the expression of mRNA in Bcl-2 decreased (Cong et al., 2018). The protein and gene detection results are consistent, and cold exposure promotes cardiomyocyte apoptosis by decreasing Bcl-2/Bax levels. The production and activity of caspase-3 were also found to be significantly elevated in cardiomyocytes in cold-stressed mice (Zhang et al., 2012b; Yin et al., 2015).

However, some studies have differing results, although cold exposure is reported to lead to an increase in apoptosis and an increase in the expression of the proapoptotic protein Bax in the cold-exposed group. However, there is no significant change in Bcl-xl; hence, Bcl-xl dose not participate in cold-induced myocardial apoptosis (Lai et al., 2009; Zhang et al., 2012a). Bcl-xl is a member of the antiapoptotic protein Bcl-2 family, a transmembrane molecule in the mitochondria (Lai et al., 2009). Bim, which is widely expressed in different organs, is an important proapoptotic protein and belongs to the Bcl-2 family (Czabotar et al., 2013). Hypothermal stimulation induces increased Bim expression in cardiomyocytes and extracellular signal-regulated kinase 5 (ERK5) knockdown, which can further promote increased Bim expression. Further studies have reported that knocking down Bim can attenuate hypothermia stimulation-induced apoptosis, while knocking down ERK5 can increase hypothermia stimulation-induced apoptosis. These results suggest that the expression of proapoptotic protein Bim in the myocardium may be regulated by ERK5. ERK5 has an antiapoptotic effect and is the upstream regulator of Bim (Wang et al., 2013).

Others

In addition to the pathways discussed above, some other pathways also play a role in myocardial injury caused by cold stress.

Endothelin-1 System

Endothelin (ET)-1 is a vasoconstrictor peptide secreted by vascular endothelial cells, which play an important role in maintaining vascular tension. It is one of the most effective endogenous vasoconstrictors and an important participant in coronary atherosclerotic heart disease and myocardial infarction (Skovsted et al., 2017). It is reported that ET-1 is a local hormone whose secretion varies according to changes in the surrounding environment. Cold exposure increases the secretion of ET in plasma and increase in ET-1 in the heart tissue (Chen and Sun, 2006; Barton and Yanagisawa, 2008; Wang D. et al., 2020). ET-1 plays an important role in the regulation of cardiac growth, myocardial contractility, and hemodynamics, and also leads to pathological myocardial hypertrophy by activating phosphoinositide 3-kinases (PI3Ks)/Akt pathway related to myocardial contractility and mitogen-activated protein kinase (MAPK)/extracellular signal-regulated kinases (ERK1/2) pathway related to cell hypertrophy (Drawnel et al., 2013; Takano et al., 2020). The effect of ET-1 on myocardial contractility and arrhythmia causes pathological remodeling of the heart (Drawnel et al., 2013). The knockout of the ET-1 receptor significantly counteracts cardiac hypertrophy and contractile dysfunction induced by cold. It was noted that knockout of ET-1 receptor causes a decrease in temperature-sensor protein in conjunction with dampened mitochondrial function (Zhang et al., 2012b).

The temperature sensor protein transient receptor potential vanilloid (TRPV1) receptor is an important protein that maintains myocardial contraction. TRPV1 acts as a major cold sensor to prevent nociceptive cold stimulation (Karashima et al., 2009). Cold stress causes changes in the structure and function of the heart, such as LV hypertrophy and decreased contractility, and TRPV1 agonists can significantly alleviate these adverse changes. TRPV1 antagonist stimulates a decrease in myocardial contractile function induced by cold stress. Consistent with this finding, knockout ET-1 receptors reverse downregulation of TRPV1, thereby improving cardiac hypertrophy and dysfunction induced by cold (Zhang et al., 2012b). These results show that TRPV1 plays a significant role in the changes of heart injury caused by cold stress.

Glycogen synthase kinase-3β (GSK3β) is a signal molecule that regulates the geometry of the myocardium, the integrity of the mitochondrial structure, and the survival of cardiomyocytes (Cheng et al., 2011). PGC1α and UCP2 are proteins responsible for mitochondrial oxidative phosphorylation and biogenesis (Finck and Kelly, 2006; Rey et al., 2010). Cold is reported to upregulate UCP2, downregulate PGC1α, and enhance GSK3β phosphorylation. In addition, knockout of the ET-1 receptor eliminates these protein changes caused by cold, and besides, knockout of the ET-1 receptor significantly alleviates cold-induced damage to heart structure and function (Zhang et al., 2012b).

Cold increases the level of ET-1 in plasma and myocardial tissue, and ET-1 plays an important role in the regulation of cardiac physiological and pathological function. The ET system also plays an important role in the governance of myocardial homeostasis, which may be involved in cold stress-provoked cardiovascular defect.

Cardiac Metabolism

The heart is an organ necessitating high-energy consumption, in particular, continuous energy demand is continuous. This energy is derived from nutrients in plasma (Lopaschuk et al., 2010). Short-chain hydroxy acyl-coenzyme A dehydrogenase (SCHAD) is a key transcriptional regulator of fatty acid catabolism enzymes and plays a regulatory role in cardiac metabolic remodeling (Brown et al., 1995; Aoyama et al., 1998). Chronic cold stress has been found to reduce the activity of SCHAD in the left ventricle by one third (Templeman et al., 2010). Previous studies have found that chronic cold stress does not affect oxygen supply to the heart, since brown adipose tissue has a higher demand for fatty acids, and this changes the amount of energy provided to the heart (Kayar and Banchero, 1985; Hauton et al., 2009). Therefore, myocardial hypertrophy caused by cold stress causes a decrease in the heart fatty acid oxidation ability, which further leads to a series of subsequent myocardial injuries (Templeman et al., 2010).

Chronic cold stress aggravates abnormal glucose and lipid metabolism in metabolic syndrome model animals. Glucocorticoid receptor (GR) antagonists alleviate metabolic abnormalities caused by cold stress (Nagasawa et al., 2016). GR widely exists in the myocardium and blood vessel walls (Walker, 2007), and glucocorticoids have a certain immunosuppressive effect. This indicates that the glucocorticoid-GR signaling pathway is involved in the heart injury of metabolic syndrome mice induced by cold stress. However, there is no available data on GR pathway changes in the heart of normal mice after cold stress; therefore, it is impossible to infer whether the

heart of people with metabolic diseases is more vulnerable to damage by the cold.

IP3 Receptor

Inositol 1,4,5-trisphosphate (IP3) is the second messenger involved in G protein-coupled receptor-mediated signal transduction. Extracellular signals, such as growth factors and neurotransmitters, stimulate the formation of IP3 by activating G protein-coupled receptors. The IP3 functions by opening the Ca^{2+} channel and binding to the IP3 receptor on the sarcoplasmic reticulum (SR) and nuclear envelope, resulting in release of Ca^{2+} from the intracellular pool (Berridge, 2016). Under normal physiological conditions, IP3 receptors respond to the needs of the cells under precise regulation *in vivo* and closely control a variety of Ca-dependent physiological processes. The IP3/Ca^{2+} signaling pathway regulates many cellular physiological processes and plays a key role in the development of many diseases (Berridge, 2016; Prole and Taylor, 2019; Ivanova et al., 2020). There are three types of IP3 receptor isoforms, IP3R1, IP3R2, and IP3R3. Their distribution in the heart is significantly different, and they have different physiological characteristics and functions. IP3R1 is mainly distributed in the cardiac ganglia, IP3R2 is mainly distributed in cardiomyocytes, and IP3R3 is distributed in the atrial cell junction and plays an important role in atrial excitation–contraction coupling. The action of ET-1 on IP3R3 enhances the release of Ca^{2+} and spreads to the whole cell, thus enhancing the contractile force (García et al., 2004; Slavikova et al., 2006; Berridge, 2016). The regulation of Ca^{2+} release by IP3 plays an important role in the development of myocardial hypertrophy (Nakayama et al., 2010). In cardiomyocytes, an increase in the expression of IP3R3 is stimulated by various factors, and the ectopic calcium released induces the expression of the hypertrophy gene and promotes arrhythmia (Drawnel et al., 2012; Berridge, 2016). IP3-mediated plasma membrane calcium signal transduction regulates the contraction of atrial myocytes and participates in the arrhythmogenic effect of ET-1, and this may be the ionic basis for ET-1 stimulation of cardiomyocytes to enhance automaticity. Atrial arrhythmia is the most common arrhythmia caused by abnormal IP3/Ca^{2+} signal pathway. Similarly, IP3 plays a similar role in the sinoatrial node (Drawnel et al., 2013; Hohendanner et al., 2015). IP3R2 integrates the contractile Ca^{2+} signal to generate the nuclear Ca^{2+} signal, which activates the transcriptional events that cause hypertrophy (Berridge, 2016). Previous studies found that after 28 days of cold exposure, the mRNA and protein level of IP3R1 increased significantly, the mRNA level of IP3R2 significantly increased, but its protein expression showed an increasing trend, but with no significant difference (Krizanova et al., 2008). Besides, the expression of the IP3R1 mRNA gene in the left atrium was significantly upregulated after cold exposure for 7 days (Krizanova et al., 2005). These results are consistent with the finding that Ca^{2+} of mice cardiomyocytes increased significantly after cold exposure (Zhang et al., 2012a). These results suggest that the IP3/Ca^{2+} signaling pathway plays a role in heart injury caused by cold exposure. Cold stress upregulates the IP3 receptor in cardiomyocytes and causes the release of intracellular Ca^{2+}, leading to arrhythmia and myocardial hypertrophy through the IP3/Ca^{2+} signaling pathway, and finally leads to cardiac geometric remodeling.

SUMMARY

Existing experimental data on myocardial injury caused by cold stress showed that cold stress can lead to oxidative stress injury, promote autophagy and apoptosis. Cardiomyocytes are vigorous aerobic cells that produce a series of ROS, including O_2^-, H_2O_2, HO_2, and OH, etc. At an appropriate concentration, ROS maintains the normal physiological function of cells, including activation of transcription factors and promotion of normal differentiation and proliferation of cells. However, when the concentration of ROS is too high, it causes oxidative stress, which leads to cell dysfunction and apoptosis (Wang et al., 2013). When cardiomyocytes are in a hypothermal environment, various subcellular changes take place in the cells. Hypothermia can cause damage to mitochondrial biological function, and the degree of damage is proportional to an increase in ROS in the myocardium (Camara et al., 2004). Mitochondria and apoptosis are closely related, since a decrease in mitochondrial transmembrane potential ($\Delta\Psi m$) induces apoptosis, and this process is irreversible. Further, this leads to a series of subsequent pathophysiological processes. For example, it triggers cell apoptosis by uncoupling the respiratory chain and oxidative phosphorylation to stop ATP synthesis, or disrupt the mitochondrial membrane permeability, and open the mitochondrial permeability transition pore (Wang et al., 2013). Previous studies have found that cardiomyocyte apoptosis induced by pressure overload can lead to cardiac hypertrophy, and apoptosis may be involved in the pathological process of cardiac remodeling (Teiger et al., 1996). Myocardial fiber is ubiquitous in many cardiovascular diseases, which results in an imbalance between collagen synthesis and metabolism. It was noted that cold stress causes myocardial fibrosis. Autophagy is an important catabolic system, which plays an essential role in maintaining cellular physiological function. Studies have shown that autophagy plays an important role in myocardial fibrosis (Shimizu and Minamino, 2016; Lu et al., 2018). In addition to the aforementioned pathways, the ET system also plays an important role in myocardial injury caused by cold stress. ET-1 is one of the most important endogenous vasoconstrictors, which regulates the cardiovascular system and myocardial contractility, affecting cardiac remodeling, and so on. Cold stress causes an increase in ET-1 secretion, which leads to myocardial hypertrophy, cardiac systolic dysfunction, and so on. GSK3 proteins related to the regulation of myocardial geometry and TRPV1 proteins related to cold receptors are involved in this process. Metabolic disorders can lead to oxidative stress and damage to multiple organs throughout the body (Wu and Ren, 2006; Li et al., 2007). Cardiac metabolic disorders and IP3-mediated Ca^{2+} disorders also play an important role in myocardial damage, as well as in cardiac geometric remodeling and ultimately cardiac dysfunction (Xu et al., 2020). In conclusion, the myocardial injury caused by cold

is a multipathway and multimolecular process, and a variety of measures can be taken to prevent and treat the myocardial injury caused by cold stress.

AUTHOR CONTRIBUTIONS

XK and HL searched the articles and retrieved the information from the included studies. XK drafted this article. XH and YS put forward some amendments to the article. WG supervised the whole process of this review. All authors contributed to the article and approved the submitted version.

FUNDING

This study was supported by grants of the Major Science and Technology Project of Shaanxi Province (2017ZDXMSF023), and Xijing Hospital Discipline Promotion Program (XJZT18MDT21, XJGX15Y44, and XJZT19Z18).

REFERENCES

Aoyama, T., Peters, J. M., Iritani, N., Nakajima, T., Furihata, K., Hashimoto, T., et al. (1998). Altered constitutive expression of fatty acid-metabolizing enzymes in mice lacking the peroxisome proliferator-activated receptor alpha (PPARalpha). *J. Biol. Chem.* 273, 5678–5684. doi: 10.1074/jbc.273.10.5678

Asselin, C., Ducharme, A., Ntimbane, T., Ruiz, M., Fortier, A., Guertin, M., et al. (2013). Circulating levels of linoleic acid and HDL-cholesterol are major determinants of 4-hydroxynonenal protein adducts in patients with heart failure. *Redox Biol.* 2, 148–155. doi: 10.1016/j.redox.2013.12.009

Barančík, M., Grešová, L., Barteková, M., and Dovinová, I. (2016). Nrf2 as a key player of redox regulation in cardiovascular diseases. *Physiol. Res.* 65(Suppl. 1), S1–S10. doi: 10.33549/physiolres.933403

Barton, M., and Yanagisawa, M. (2008). Endothelin: 20 years from discovery to therapy. *Can. J. Physiol. Pharmacol.* 86, 485–498. doi: 10.1139/Y08-059

Baumgartner, E. A., Belson, M., Rubin, C., and Patel, M. (2008). Hypothermia and other cold-related morbidity emergency department visits: United States, 1995-2004. *Wild Environ. Med.* 19, 233–237. doi: 10.1580/07-WEME-OR-104.1

Bello Roufai, M., Li, H., and Sun, Z. (2007). Heart-specific inhibition of protooncogene c-myc attenuates cold-induced cardiac hypertrophy. *Gene Ther.* 14, 1406–1416. doi: 10.1038/sj.gt.3302995

Berko, J., Ingram, D. D., Saha, S., and Parker, J. D. (2014). Deaths attributed to heat, cold, and other weather events in the United States, 2006-2010. *Natl. Health Stat. Rep.* 76, 1–15.

Berridge, M. J. (2016). The inositol trisphosphate/calcium signaling pathway in health and disease. *Physiol. Rev.* 96, 1261–1296. doi: 10.1152/physrev.00006.2016

Bombig, M. T., Ferreira, C., Mora, O., Soares, J. D., Povoa, R., Luna, F. B., et al. (2003). Pravastatin protection from cold stress in myocardium of rats. *Jpn. Heart J.* 44, 243–255. doi: 10.1536/jhj.44.243

Brown, N. F., Weis, B. C., Husti, J. E., Foster, D. W., and McGarry, J. D. (1995). Mitochondrial carnitine palmitoyltransferase I isoform switching in the developing rat heart. *J. Biol. Chem.* 270, 8952–8957. doi: 10.1074/jbc.270.15.8952

Camara, A. K. S., Riess, M. L., Kevin, L. G., Novalija, E., and Stowe, D. F. (2004). Hypothermia augments reactive oxygen species detected in the guinea pig isolated perfused heart. *Am. J. Physiol. Heart Circ. Physiol.* 286, H1289–H1299. doi: 10.1152/ajpheart.00811.2003

Chen, G., and Sun, Z. (2006). Effects of chronic cold exposure on the endothelin system. *J. Appl. Physiol. (1985)* 100, 1719–1726. doi: 10.1152/japplphysiol.01407.2005

Chen, T., Du, X. L., Chan, W., and Zhang, K. (2019). Impacts of cold weather on emergency hospital admission in Texas, 2004-2013. *Environ. Res.* 169, 139–146. doi: 10.1016/j.envres.2018.10.031

Cheng, H., Woodgett, J., Maamari, M., and Force, T. (2011). Targeting GSK-3 family members in the heart: a very sharp double-edged sword. *J Mol Cell Cardiol.* 51, 607–613. doi: 10.1016/j.yjmcc.2010.11.020

Cheng, X., and Su, H. (2010). Effects of climatic temperature stress on cardiovascular diseases. *Eur. J. Intern. Med.* 21, 164–167. doi: 10.1016/j.ejim.2010.03.001

Cheng, Y., and Hauton, D. (2008). Cold acclimation induces physiological cardiac hypertrophy and increases assimilation of triacylglycerol metabolism through lipoprotein lipase. *Biochim. Biophys. Acta Mol. Cell Biol. Lipids* 1781, 618–626. doi: 10.1016/j.bbalip.2008.07.006

Cong, P., Liu, Y., Liu, N., Zhang, Y., Tong, C., Shi, L., et al. (2018). Cold exposure induced oxidative stress and apoptosis in the myocardium by inhibiting the Nrf2-Keap1 signaling pathway. *BMC Cardiovasc. Disord.* 18:36. doi: 10.1186/s12872-018-0748-x

Cui, G., Luk, S. C. W., Li, R. A., Chan, K. K. K., Lei, S. W., Wang, L., et al. (2015). Cytoprotection of baicalein against oxidative stress-induced cardiomyocytes injury through the Nrf2/Keap1 pathway. *J. Cardiovasc. Pharmacol.* 65, 39–46. doi: 10.1097/FJC.0000000000000161

Czabotar, P. E., Westphal, D., Dewson, G., Ma, S., Hockings, C., Fairlie, W. D., et al. (2013). Bax crystal structures reveal how BH3 domains activate Bax and nucleate its oligomerization to induce apoptosis. *Cell* 152, 519–531. doi: 10.1016/j.cell.2012.12.031

Daud, F. V., Murad, N., Meneghini, A., Ferreira, M., Ferreira Filho, C., Abreu, L. C. D., et al. (2009). Fluoxetine effects on mitochondrial ultrastructure of right ventricle in rats exposed to cold stress. *Rev. Bras. Cir. Cardiovasc.* 24, 173–179. doi: 10.1590/s0102-76382009000200013

Delbridge, A. R., Grabow, S., Strasser, A., and Vaux, D. L. (2016). Thirty years of BCL-2: translating cell death discoveries into novel cancer therapies. *Nat. Rev. Cancer* 16, 99–109. doi: 10.1038/nrc.2015.17

Delbridge, L., Mellor, K. M., Taylor, D. J., and Gottlieb, R. A. (2017). Myocardial stress and autophagy: mechanisms and potential therapies. *Nat. Rev. Cardiol.* 14, 412–425. doi: 10.1038/nrcardio.2017.35

Drawnel, F. M., Archer, C. R., and Roderick, H. L. (2013). The role of the paracrine/autocrine mediator endothelin-1 in regulation of cardiac contractility and growth. *Br. J. Pharmacol.* 168, 296–317. doi: 10.1111/j.1476-5381.2012.02195.x

Drawnel, F. M., Wachten, D., Molkentin, J. D., Maillet, M., Aronsen, J. M., Swift, F., et al. (2012). Mutual antagonism between IP (3) RII and miRNA-133a regulates calcium signals and cardiac hypertrophy. *J. Cell Biol.* 199, 783–798. doi: 10.1083/jcb.201111095

Finck, B. N., and Kelly, D. P. (2006). PGC-1 coactivators: inducible regulators of energy metabolism in health and disease. *J. Clin. Invest.* 116, 615–622. doi: 10.1172/JCI27794

Fregly, M. J., Kikta, D. C., Threatte, R. M., Torres, J. L., and Barney, C. C. (1989). Development of hypertension in rats during chronic exposure to cold. *J. Appl. Physiol. (1985)* 66, 741–749. doi: 10.1152/jappl.1989.66.2.741

García, K. D., Shah, T., and García, J. (2004). I mmunolocalization of type 2 inositol 1,4,5-trisphosphate receptors in cardiac myocytes from newborn mice. *Am. J. Physiol. Cell Physiol.* 287, C1048–C1057. doi: 10.1152/ajpcell.00004.2004

Hauton, D., Coney, A. M., and Egginton, S. (2009). Both substrate availability and utilisation contribute to the defence of core temperature in response to acute cold. *Comp. Biochem. Physiol. A Mol. Integr. Physiol.* 154, 514–522. doi: 10.1016/j.cbpa.2009.08.008

Hohendanner, F., Walther, S., Maxwell, J. T., Kettlewell, S., Awad, S., Smith, G. L., et al. (2015). Inositol-1,4,5-trisphosphate induced Ca2+ release and excitation-contraction coupling in atrial myocytes from normal and failing hearts. *J. Physiol.* 593, 1459–1477. doi: 10.1113/jphysiol.2014.283226

Hong, J. H., Kim, K. J., Suzuki, K., Lee, I., Waseda, U., Consolidated, R. I. F. A., et al. (2008). Effect of cold acclimation on antioxidant status in cold acclimated skaters. *J. Physiol. Anthropol.* 27, 255–262. doi: 10.2114/jpa2.27.255

Ikäheimo, T. M. (2018). Cardiovascular diseases, cold exposure and exercise. *Temperature* 5, 123–146. doi: 10.1080/23328940.2017.1414014

Ikeda, Y., Shirakabe, A., Maejima, Y., Zhai, P., Sciarretta, S., Toli, J., et al. (2015). Endogenous Drp1 mediates mitochondrial autophagy and protects the heart against energy stress. *Circ. Res.* 116, 264–278. doi: 10.1161/CIRCRESAHA.116.303356

Ivanova, H., Vervliet, T., Monaco, G., Terry, L. E., Rosa, N., Baker, M. R., et al. (2020). Bcl-2-protein family as modulators of IP (3) receptors and other organellar Ca (2+) channels. *Cold Spring Harb. Perspect. Biol.* 12:a035089. doi: 10.1101/cshperspect.a035089

Jain, K., Suryakumar, G., Prasad, R., Singh, S. N., and Ganju, L. (2013). Myocardial ER chaperone activation and protein degradation occurs due to synergistic, not individual, cold and hypoxic stress. *Biochimie* 95, 1897–1908. doi: 10.1016/j.biochi.2013.06.018

Jiang, S., Guo, R., Zhang, Y., Zou, Y., and Ren, J. (2013). Heavy metal scavenger metallothionein mitigates deep hypothermia-induced myocardial contractile anomalies: role of autophagy. *Am. J. Physiol. Endocrinol. Metab.* 304, E74–E86. doi: 10.1152/ajpendo.00176.2012

Karashima, Y., Talavera, K., Everaerts, W., Janssens, A., Kwan, K. Y., Vennekens, R., et al. (2009). TRPA1 acts as a cold sensor in vitro and in vivo. *Proc. Natl. Acad. Sci. U.S.A.* 106, 1273–1278. doi: 10.1073/pnas.0808487106

Kaushik, S., and Kaur, J. (2003). Chronic cold exposure affects the antioxidant defense system in various rat tissues. *Clin. Chim. Acta* 333, 69–77. doi: 10.1016/s0009-8981(03)00171-2

Kayar, S. R., and Banchero, N. (1985). Volume overload hypertrophy elicited by cold and its effects on myocardial capillarity. *Respir. Physiol.* 59, 1–14. doi: 10.1016/0034-5687(85)90013-1

Keatinge, W. R. (1997). Cold exposure and winter mortality from ischaemic heart disease, cerebrovascular disease, respiratory disease, and all causes in warm and cold regions of Europe. *Lancet* 349, 1341–1346. doi: 10.1016/s0140-6736(96)12338-2

Krizanova, O., Holotnakova, T., Jurkovicova, D., Polakova, E., Zahradnikova, A., Lacinova, L., et al. (2008). Type 1 and 2 IP3 receptors respond differently to catecholamines and stress. *Ann. N. Y. Acad. Sci.* 1148, 331–337. doi: 10.1196/annals.1410.023

Krizanova, O., Kvetnansky, R., and Jurkovicova, D. (2005). Effect of two distinct stressors on gene expression of the type 1 IP3 receptors. *Gen. Physiol. Biophys.* 24, 237–246.

Kroemer, G. (2015). Autophagy: a druggable process that is deregulated in aging and human disease. *J. Clin. Invest.* 125, 1–4. doi: 10.1172/JCI78652

Lai, K., Sanderson, J. E., and Yu, C. (2009). High dose norepinephrine-induced apoptosis in cultured rat cardiac fibroblast. *Int. J. Cardiol.* 136, 33–39. doi: 10.1016/j.ijcard.2008.04.022

L'Ecuyer, T. J., Aggarwal, S., Zhang, J. P., and Van der Heide, R. S. (2012). Effect of hypothermia on doxorubicin-induced cardiac myoblast signaling and cell death. *Cardiovasc. Pathol.* 21, 96–104. doi: 10.1016/j.carpath.2011.02.001

Li, Q., Wu, S., Li, S. Y., Lopez, F. L., Du, M., Kajstura, J., et al. (2007). Cardiac-specific overexpression of insulin-like growth factor 1 attenuates aging-associated cardiac diastolic contractile dysfunction and protein damage. *Am. J. Physiol. Heart Circ. Physiol.* 292, H1398–H1403. doi: 10.1152/ajpheart.01036.2006

Liang, J., Yin, K., Cao, X., Han, Z., Huang, Q., Zhang, L., et al. (2017). Attenuation of low ambient temperature-induced myocardial hypertrophy by atorvastatin via promoting Bcl-2 expression. *Cell Physiol. Biochem.* 41, 286–295. doi: 10.1159/000456111

Lopaschuk, G. D., Ussher, J. R., Folmes, C. D., Jaswal, J. S., and Stanley, W. C. (2010). Myocardial fatty acid metabolism in health and disease. *Physiol. Rev.* 90, 207–258. doi: 10.1152/physrev.00015.2009

Lu, C., Yang, Y., Zhu, Y., Lv, S., and Zhang, J. (2018). An intervention target for myocardial fibrosis: autophagy. *Biomed. Res. Int.* 2018:6215916. doi: 10.1155/2018/6215916

Lu, S., and Xu, D. (2013). Cold stress accentuates pressure overload-induced cardiac hypertrophy and contractile dysfunction: role of TRPV1/AMPK-mediated autophagy. *Biochem. Biophys. Res. Commun.* 442, 8–15. doi: 10.1016/j.bbrc.2013.10.128

Maejima, Y., Kyoi, S., Zhai, P., Liu, T., Li, H., Ivessa, A., et al. (2013). Mst1 inhibits autophagy by promoting the interaction between Beclin1 and Bcl-2. *Nat. Med.* 19, 1478–1488. doi: 10.1038/nm.3322

Matsubara, T., Shimamoto, S., Ijiri, D., Ohtsuka, A., Kanai, Y., and Hirabayashi, M. (2016). The effects of acute cold exposure on morphology and gene expression in the heart of neonatal chicks. *J. Comp. Physiol. B* 186, 363–372. doi: 10.1007/s00360-015-0957-x

Medina-Ramón, M., Zanobetti, A., Cavanagh, D. P., and Schwartz, J. (2006). Extreme temperatures and mortality: assessing effect modification by personal characteristics and specific cause of death in a multi-city case-only analysis. *Environ. Health Perspect.* 114, 1331–1336. doi: 10.1289/ehp.9074

Meneghini, A., Ferreira, C., Abreu, L. C. D., Valenti, V. E., Ferreira, M., Filho, C., et al. (2009). Memantine prevents cardiomyocytes nuclear size reduction in the left ventricle of rats exposed to cold stress. *Clinics* 64, 921–926. doi: 10.1590/S1807-59322009000900014

Mercer, J. B. (2003). Cold–an underrated risk factor for health. *Environ. Res.* 92, 8–13. doi: 10.1016/s0013-9351(02)00009-9

Nagasawa, K., Matsuura, N., Takeshita, Y., Ito, S., Sano, Y., Yamada, Y., et al. (2016). Attenuation of cold stress-induced exacerbation of cardiac and adipose tissue pathology and metabolic disorders in a rat model of metabolic syndrome by the glucocorticoid receptor antagonist RU486. *Nutr. Diabetes* 6:e207. doi: 10.1038/nutd.2016.14

Nakai, A., Yamaguchi, O., Takeda, T., Higuchi, Y., Hikoso, S., Taniike, M., et al. (2007). The role of autophagy in cardiomyocytes in the basal state and in response to hemodynamic stress. *Nat. Med.* 13, 619–624. doi: 10.1038/nm1574

Nakayama, H., Bodi, I., Maillet, M., DeSantiago, J., Domeier, T. L., Mikoshiba, K., et al. (2010). The IP3 receptor regulates cardiac hypertrophy in response to select stimuli. *Circ. Res.* 107, 659–666. doi: 10.1161/CIRCRESAHA.110.220038

Nemchenko, A., Chiong, M., Turer, A., Lavandero, S., and Hill, J. A. (2011). Autophagy as a therapeutic target in cardiovascular disease. *J. Mol. Cell. Cardiol.* 51, 584–593. doi: 10.1016/j.yjmcc.2011.06.010

Nirwane, A., and Majumdar, A. (2018). Understanding mitochondrial biogenesis through energy sensing pathways and its translation in cardio-metabolic health. *Arch. Physiol. Biochem.* 124, 194–206. doi: 10.1080/13813455.2017.1391847

Ogawa, M., Tanaka, F., Onoda, T., Ohsawa, M., Itai, K., Sakai, T., et al. (2007). A community based epidemiological and clinical study of hospitalization of patients with congestive heart failure in Northern Iwate, Japan. *Circ. J.* 71, 455–459. doi: 10.1253/circj.71.455

Pereira, R. M., Mekary, R. A., Da, C. R. K., Anaruma, C. P., Ropelle, E. R., Da, S. A., et al. (2018). Protective molecular mechanisms of clusterin against apoptosis in cardiomyocytes. *Heart Fail. Rev.* 23, 123–129. doi: 10.1007/s10741-017-9654-z

Prole, D. L., and Taylor, C. W. (2019). Structure and Function of IP (3) Receptors. *Cold Spring Harb. Perspect. Biol.* 11:a035063. doi: 10.1101/cshperspect.a035063

Qi, Z., Yang, W., Liu, Y., Cui, T., Gao, H., Duan, C., et al. (2011). Loss of PINK1 function decreases PP2A activity and promotes autophagy in dopaminergic cells and a murine model. *Neurochem. Int.* 59, 572–581. doi: 10.1016/j.neuint.2011.03.023

Ren, J., Privratsky, J. R., Yang, X., Dong, F., and Carlson, E. C. (2008). Metallothionein alleviates glutathione depletion-induced oxidative cardiomyopathy in murine hearts. *Crit. Care Med.* 36, 2106–2116. doi: 10.1097/CCM.0b013e31817bf925

Rey, B., Roussel, D., Romestaing, C., Belouze, M., Rouanet, J. L., Desplanches, D., et al. (2010). Up-regulation of avian uncoupling protein in cold-acclimated and hyperthyroid ducklings prevents reactive oxygen species production by skeletal muscle mitochondria. *BMC Physiol.* 10:5. doi: 10.1186/1472-6793-10-5

Sahin, E., and Gümüşlü, S. (2004). Cold-stress-induced modulation of antioxidant defence: role of stressed conditions in tissue injury followed by protein oxidation and lipid peroxidation. *Int. J. Biometeorol.* 48, 165–171. doi: 10.1007/s00484-004-0205-7

Saito, T., and Sadoshima, J. (2015). Molecular mechanisms of mitochondrial autophagy/mitophagy in the heart. *Circ. Res.* 116, 1477–1490. doi: 10.1161/CIRCRESAHA.116.303790

Sciarretta, S., Maejima, Y., Zablocki, D., and Sadoshima, J. (2018). The role of autophagy in the heart. *Annu. Rev. Physiol.* 80, 1–26. doi: 10.1146/annurev-physiol-021317-121427

Selman, C., McLaren, J. S., Himanka, M. J., and Speakman, J. R. (2000). Effect of long-term cold exposure on antioxidant enzyme activities in a small mammal. *Free Radic. Biol. Med.* 28, 1279–1285. doi: 10.1016/s0891-5849(00)00263-x

Semenza, G. L. (2004). O2-regulated gene expression: transcriptional control of cardiorespiratory physiology by HIF-1. *J. Appl. Physiol. (1985).* 96, 1172–1173. doi: 10.1152/japplphysiol.00770.2003

Shaw, R. J. (2009). LKB1 and AMP-activated protein kinase control of mTOR signalling and growth. *Acta Physiol. (Oxf.)* 196, 65–80. doi: 10.1111/j.1748-1716.2009.01972.x

Shimizu, I., and Minamino, T. (2016). Physiological and pathological cardiac hypertrophy. *J. Mol. Cell Cardiol.* 97, 245–262. doi: 10.1016/j.yjmcc.2016.06.001

Shirakabe, A., Fritzky, L., Saito, T., Zhai, P., Miyamoto, S., Gustafsson, ÅB., et al. (2016). Evaluating mitochondrial autophagy in the mouse heart. *J. Mol. Cell Cardiol.* 92, 134–139. doi: 10.1016/j.yjmcc.2016.02.007

Skovsted, G. F., Kruse, L. S., Berchtold, L. A., Grell, A. S., Warfvinge, K., and Edvinsson, L. (2017). Myocardial ischemia-reperfusion enhances transcriptional expression of endothelin-1 and vasoconstrictor ETB receptors via the protein kinase MEK-ERK1/2 signaling pathway in rat. *PLoS One.* 12:e174119. doi: 10.1371/journal.pone.0174119

Slavikova, J., Dvorakova, M., Reischig, J., Palkovits, M., Ondrias, K., Tarabova, B., et al. (2006). IP3 type 1 receptors in the heart: their predominance in atrial walls with ganglion cells. *Life Sci.* 78, 1598–1602. doi: 10.1016/j.lfs.2005.07.012

Stewart, S., McIntyre, K., Capewell, S., and McMurray, J. J. V. (2002). Heart failure in a cold climate. Seasonal variation in heart failure-related morbidity and mortality. *J. Am. Coll. Cardiol.* 39, 760–766. doi: 10.1016/s0735-1097(02)01685-6

Takano, A., Senger, N., and Barreto-Chaves, M. (2020). The endocrinological component and signaling pathways associated to cardiac hypertrophy. *Mol. Cell Endocrinol.* doi: 10.1016/j.mce.2020.110972 [Epub ahead of print].

Teiger, E., Than, V. D., Richard, L., Wisnewsky, C., Tea, B. S., Gaboury, L., et al. (1996). Apoptosis in pressure overload-induced heart hypertrophy in the rat. *J. Clin. Invest.* 97, 2891–2897. doi: 10.1172/JCI118747

Templeman, N. M., Beaudry, J. L., Le Moine, C. M. R., and McClelland, G. B. (2010). Chronic hypoxia- and cold-induced changes in cardiac enzyme and gene expression in CD-1 mice. *BBA Gen. Subjects* 1800, 1248–1255. doi: 10.1016/j.bbagen.2010.08.004

Tonelli, C., Chio, I., and Tuveson, D. A. (2018). Transcriptional regulation by Nrf2. *Antioxid. Redox Signal.* 29, 1727–1745. doi: 10.1089/ars.2017.7342

Walker, B. R. (2007). Glucocorticoids and cardiovascular disease. *Eur. J. Endocrinol.* 157, 545–559. doi: 10.1530/EJE-07-0455

Wang, D., Cheng, X., Fang, H., Ren, Y., Li, X., Ren, W., et al. (2020). Effect of cold stress on ovarian & uterine microcirculation in rats and the role of endothelin system. *Reprod. Biol. Endocrinol.* 18:29. doi: 10.1186/s12958-020-00584-1

Wang, Y., Zhou, J., Liang, C., Hong, K., Cheng, X., and Wu, Z. (2013). ERK5 knock down aggravates detrimental effects of hypothermal stimulation on cardiomyocytes via Bim upregulation. *Environ. Toxicol. Phar.* 36, 724–731. doi: 10.1016/j.etap.2013.06.012

Wang, Z., Xu, J. H., Mou, J. J., Kong, X. T., Zou, J. W., Xue, H. L., et al. (2020). Novel ultrastructural findings on cardiac mitochondria of huddling Brandt's voles in mild cold environment. *Comp. Biochem. Physiol. A Mol. Integr. Physiol.* 249:110766. doi: 10.1016/j.cbpa.2020.110766

Williams, B., Kabbage, M., Britt, R., and Dickman, M. B. (2010). AtBAG7, an Arabidopsis Bcl-2-associated athanogene, resides in the endoplasmic reticulum and is involved in the unfolded protein response. *Proc. Natl. Acad. Sci. U.S.A.* 107, 6088–6093. doi: 10.1073/pnas.0912670107

Wu, S., and Ren, J. (2006). Benfotiamine alleviates diabetes-induced cerebral oxidative damage independent of advanced glycation end-product, tissue factor and TNF-alpha. *Neurosci. Lett.* 394, 158–162. doi: 10.1016/j.neulet.2005.10.022

Xu, H. X., Cui, S. M., Zhang, Y. M., and Ren, J. (2020). Mitochondrial Ca2+ regulation in the etiology of heart failure: physiological and pathophysiological implications. *Acta Pharmacol. Sin.* 41, 1301–1309. doi: 10.1038/s41401-020-0476-5

Xu, X., and Ren, J. (2012). Unmasking the janus faces of autophagy in obesity-associated insulin resistance and cardiac dysfunction. *Clin. Exp. Pharmacol. Physiol.* 39, 200–208. doi: 10.1111/j.1440-1681.2011.05638.x

Yamano, K., Matsuda, N., and Tanaka, K. (2016). The ubiquitin signal and autophagy: an orchestrated dance leading to mitochondrial degradation. *EMBO Rep.* 17, 300–316. doi: 10.15252/embr.201541486

Yang, L., Ma, J., Tan, Y., Zheng, Q., Dong, M., Guo, W., et al. (2019). Cardiac-specific overexpression of metallothionein attenuates L-NAME-induced myocardial contractile anomalies and apoptosis. *J. Cell Mol. Med.* 23, 4640–4652. doi: 10.1111/jcmm.14375

Yin, K., Zhao, L., Feng, D., Ma, W., Liu, Y., Wang, Y., et al. (2015). Resveratrol attenuated low ambient temperature-induced myocardial hypertrophy via inhibiting cardiomyocyte apoptosis. *Cell Physiol. Biochem.* 35, 2451–2462. doi: 10.1159/000374045

Yin, Z., Ding, G., Chen, X., Qin, X., Haixia, X., Zeng, B., et al. (2020). Beclin1 haploinsufficiency rescues low ambient temperature-induced cardiac remodeling and contractile dysfunction through inhibition of ferroptosis and mitochondrial injury. *Metabolism* doi: 10.1016/j.metabol.2020.154397 [Epub ahead of print].

Zhang, Y., Hu, N., Hua, Y., Richmond, K. L., Dong, F., and Ren, J. (2012a). Cardiac overexpression of metallothionein rescues cold exposure-induced myocardial contractile dysfunction through attenuation of cardiac fibrosis despite cardiomyocyte mechanical anomalies. *Free Radic. Bio Med.* 53, 194–207. doi: 10.1016/j.freeradbiomed.2012.04.005

Zhang, Y., Li, L., Hua, Y., Nunn, J. M., Dong, F., Yanagisawa, M., et al. (2012b). Cardiac-specific knockout of ETA receptor mitigates low ambient temperature-induced cardiac hypertrophy and contractile dysfunction. *J. Mol. Cell Biol.* 4, 97–107. doi: 10.1093/jmcb/mjs002

Zhou, M. G., Wang, L. J., Liu, T., Zhang, Y. H., Lin, H. L., Luo, Y., et al. (2014). Health impact of the 2008 cold spell on mortality in subtropical China: the climate and health impact national assessment study (CHINAs). *Environ. Health* 13:60. doi: 10.1186/1476-069X-13-60

Conflict of Interest: The authors declare that the research was conducted in the absence of any commercial or financial relationships that could be construed as a potential conflict of interest.

Copyright © 2020 Kong, Liu, He, Sun and Ge. This is an open-access article distributed under the terms of the Creative Commons Attribution License (CC BY). The use, distribution or reproduction in other forums is permitted, provided the original author(s) and the copyright owner(s) are credited and that the original publication in this journal is cited, in accordance with accepted academic practice. No use, distribution or reproduction is permitted which does not comply with these terms.

frontiers in Pharmacology

REVIEW
published: 26 November 2020
doi: 10.3389/fphar.2020.567582

Functioning of Long Noncoding RNAs Expressed in Macrophage in the Development of Atherosclerosis

Xirui Ma, Huifang Liu and Fengling Chen**

Department of Endocrinology and Metabolism, Shanghai Ninth People's Hospital, Shanghai Jiao Tong University School of Medicine, Shanghai, China

Chronic inflammation is part of the pathological process during atherosclerosis (AS). Due to the abundance of monocytes/macrophages within the arterial plaque, monocytes/macrophages have become a critical cellular target in AS studies. In recent decades, a number of long noncoding RNAs (lncRNAs) have been found to exert regulatory roles on the macrophage metabolism and macrophage plasticity, consequently promoting or suppressing atherosclerotic inflammation. In this review, we provide a comprehensive overview of lncRNAs in macrophage biology, highlighting the potential role of lncRNAs in AS based on recent findings, with the aim to identify disease biomarkers and future therapeutic interventions for AS.

Keywords: long noncoding RNA, atherosclerosis, macrophage, kappa B, foam cell macrophage

OPEN ACCESS

Edited by:
Xin Wang,
University of Manchester,
United Kingdom

Reviewed by:
Jason Hellmann,
University of Louisville, United States
Yuhuang Li,
Technical University of Munich,
Germany

****Correspondence:***
Huifang Liu
Lhf_404@163.com
Fengling Chen
Chenfl1101@126.com

Specialty section:
This article was submitted to Cardiovascular and Smooth Muscle Pharmacology, a section of the journal Frontiers in Pharmacology

Received: *30 May 2020*
Accepted: *22 September 2020*
Published: *26 November 2020*

Citation:
Ma X, Liu H and Chen F (2020) Functioning of Long Noncoding RNAs Expressed in Macrophage in the Development of Atherosclerosis. Front. Pharmacol. 11:567582. doi: 10.3389/fphar.2020.567582

INTRODUCTION

Atherosclerosis (AS) is a multifaceted chronic inflammatory disease characterized by the formation of atherosclerotic plaques predominantly at branch points of arteries and bifurcations due to the disturbed laminar flow at these sites (Shapouri-Moghaddam et al., 2018). Atherosclerotic plaques consist of lipids, foam cells, calcified sites, and necrotic cores (Donaldson et al., 2018; Moore et al., 2013; Shapouri-Moghaddam et al., 2018; Tabas and Bornfeldt, 2016). Monocytes and macrophages are dynamically involved in the initiation and development of AS and ultimately contribute to plaque rupture. An altered metabolism dictates macrophage activities and subsequent AS progression (Koelwyn et al., 2018).

During early atherogenic stages, apolipoprotein B-lipoproteins accumulated in the intima initiate an early inflammatory response and formation of fatty streak lesions (Williams and Tabas, 1995; Moore and Tabas, 2011; Liu et al., 2014). The inflammatory response progresses through various modifications in the endothelium, such as oxidation (causing altered expression of adhesion molecules and elevating secretion of chemokines) (Moore and Tabas, 2011). Activated endothelial cells produce monocyte chemoattractant protein-1 (MCP-1). On monocytes, MCP-1 can interact with cognate chemokine receptors and promote monocyte migration in a specific direction (Moore and Tabas, 2011). Later, the recruited monocytes are tethered and roll along the endothelium. The interaction between P-selectin glycoprotein ligand-1 molecules on monocytes and endothelial selectins further triggers firm adhesions (Mestas and Ley, 2008). After entering the intima, monocytes gradually differentiate into macrophages and internalize native and modified lipoproteins (Johnson and Newby, 2009; Paulson et al., 2010). Atherosclerosis is a nonresolving inflammatory condition characterized by monocytes continually entering the intima and lesion plaques and constantly differentiating into macrophages (Moore and Tabas, 2011).

Lipid uptake, cholesterol esterification, and efflux are three distinct processes of a normal cholesterol metabolism in macrophages (Chistiakov et al., 2017). Disturbances of the cholesterol metabolism are a key contributor to AS, resulting in the accumulation of lipids in macrophages and the formation of "foam cells" (Crowther, 2005; Maguire et al., 2019). In the early plaque, uptake of modified low-density lipoprotein (LDL) (Kunjathoor et al., 2002), phagocytosis of matrix-retained LPs, and pinocytosis of fluid native LDL contribute to foam cell formation (Tabas et al., 1993; Kruth et al., 2005; Moore and Tabas, 2011). Key scavenger receptors such as the CD36, SR-A class, and lectin-like ox-LDL receptor-1 play regulatory roles on cholesterol uptake and the formation of foam cells (Moore and Freeman, uhu2006).

In advanced AS lesions, macrophage apoptosis, incomplete clearance, and defective phagocytosis of apoptotic macrophages give rise to necrotic cores, which exacerbate inflammation, incite thrombosis, and increase inner stress on the fibrous plaques (Virmani et al., 2002; Tabas, 2010). Notably, thinning of the fibrous cap and necrotic core size increments are critical features of vulnerable plaques. The sites on the shoulder of necrotic cores are vulnerable to rupture. Functions and biological mechanisms of all lncRNAs we discussed below are summarized in **Table 1**.

LONG NONCODING RNAS

Long noncoding RNAs (lncRNAs) are defined as a large class of non-protein-coding transcripts. They consist of more than 200 nucleotides in length. Knowledge on the biological function of lncRNAs has been expanding with new publications in the fields of epigenetic activity regulation (McHugh et al., 2015), *cis*- (Engreitz et al., 2016) and *trans*- (Atianand et al., 2016) gene transcription regulations, protein translation (Carrieri et al., 2012), RNA (Hansen et al., 2013) or protein "sponging," (Tichon et al., 2016), and nuclear/cytoplasmic "shuttling" (Yap et al., 2018; Maguire and Xiao, 2020).

In accordance with the positional association between lncRNAs and protein-coding genes (Gao et al., 2020), the lncRNAs can be classified as exonic sense, anti-sense, intronic sense, bidirectional (enhancer), and intergenic sense classes (Derrien et al., 2012). At the transcriptional level, lncRNAs can also be divided into four models (signals, decoys, guides, or scaffolds) to regulate gene expression (Chang, 2011; Mathy and Chen, 2017; Wang and Chang, 2011).

LONG NONCODING RNAS IN MACROPHAGE DIFFERENTIATION

Monocyte chemotaxis is triggered by chemokines or cytokines released from cells in damaged tissue or infection areas and stimulates monocytes to migrate to pathologic sites and begin differentiation into macrophages. These macrophages effectively take infections under control and remove dead cells and debris for tissue repair and wound healing. On the other hand, macrophages are involved in the inflammatory tissue damage caused by inflammatory diseases (Moore and Tabas, 2011).

In the development of AS, MCP-1 secreted by endothelial cells is a potent chemokine for monocyte migration involved in the initiation of the inflammatory response (Panee, 2012). MCP-1 attracts monocytes in the circulation, triggering migration via its interaction with the membrane CC chemokine receptor 2 on monocytes. Under normal blood flow conditions, monocytes can firmly adhere to the vascular endothelium through interactions with MCP-1, IL-8, or CXC ligand-8 (Melgarejo et al., 2009, Shapouri-Moghaddam et al., 2018; Moghaddam et al., 2018). After entering the intima, phagocytic monocyte-derived macrophages start to internalize native and modified lipoproteins (Johnson and Newby, 2009; Paulson et al., 2010; Moore and Tabas, 2011).

Long noncoding monocytic RNA (lnc-MC) and miR-199a-5p, both PU.1-regulated noncoding RNAs, work together during human monocyte/macrophage differentiation. The dominant transcription factor PU.1 commits the monocytic lineage during hematopoiesis and promotes the maturation of monocytes/macrophages (Anderson et al., 1998; Lin et al., 2014). PU.1 transcriptionally regulates lnc-MC. Increased expression of lnc-MC reinforces the role of PU.1 by sequestering and soaking upmiR-199a-5p, relieving the suppression on the expression of activin A receptor type 1B, an important regulator of monocyte/macrophage differentiation. This suggests that lnc-MC acts as an antagonist of miR-199a-5p and strengthens the role of PU.1 in cell differentiation (Chen et al., 2015).

LONG NONCODING RNAS IN MACROPHAGE PHENOTYPIC SWITCHING

Plasticity and polarization are hallmarks of macrophages (Wang L. X. et al., 2019). Phenotype switching of macrophages, in response to cues from the local microenvironment, is necessary for a diversity of indispensable functions during host defense responses and tissue repair (Koelwyn et al., 2018). Reciprocal skewing of macrophage polarization is modulated by many intricate factors like the daily dietary intakes and transcriptional factors (Chinetti-Gbaguidi and Staels, 2011). Macrophages can be broadly categorized into two types: M1 and M2 phenotypes. Classically, M1-activated macrophages enhance the production of pro-inflammatory cytokines (TNF, IL-6, IL-1β, IL-12, and IL-23 in humans) and lower the secretion of IL-10 (Verreck et al., 2004), whereas M2 macrophages are characterized by their improved endocytic clearance capacity that can protect local tissues from detrimental inflammatory damages and eliminate inflammation (Mantovani et al., 2004; Chinetti-Gbaguidi and Staels, 2011). Therefore, metabolic reprogramming in macrophages has a direct influence on cell functions and energy homeostasis (Koelwyn et al., 2018). In AS, both macrophage phenotypes are present in fibrous caps of established lesions (Anderson et al., 2002), with a predominance of M1 over M2 in progressing atherosclerotic lesions (Khallou-Laschet et al., 2010; Chinetti-Gbaguidi and Staels, 2011; Khallou et al., 2010). TCONS_00019715 was the first reported lncRNA expressed in human macrophages with

phenotype switching functions. The expression level of TCONS_00019715 in macrophages was drastically induced by IFN-γ + LPS stimulation, and it underwent a strong reduction after IL-4 treatment. Knockdown of TCONS_00019715 reduced the expression of M1 markers in IFN-γ + LPS-stimulated macrophages, and it elevated the M2 phenotype markers in IL-4-stimulated ones. PAK1 (p21-activated kinase 1), an important protein-coding gene associated with TCONS_00019715, has been speculated to mediate TCONS_00019715's macrophage polarization effects (Huang Z. et al., 2016). The myocardial infarction–associated transcript 2 (Mirt2) is another lncRNA that has been proved to affect macrophage phenotypic switching. It can block the expression of the M1 polarization and has anti-inflammatory functions through its control of NF-κB activation (Du et al., 2017). Detailed information about the function of Mirt2 will be covered in a later section.

LONG NONCODING RNAS IN MACROPHAGE APOPTOSIS

Macrophage apoptosis occurs during the atherosclerotic plaque development process. Apoptosis in the early stages is protective because it cleans up macrophage foam cells residing inside the plaque lesions (Shapouri-Moghaddam et al., 2018).

LincRNA-p21 has been shown to modulate cell proliferation and apoptosis in AS. In apolipoprotein E–deficient (ApoE$^{-/-}$) mice with atherosclerotic plaques, lincRNA-p21 expression was dramatically reduced at the transcription level. Small interfering RNA–induced lincRNA-p21 inhibition greatly increased the total number of RAW274.7 and HA-VSMC cells. P53 could transcriptionally target lincRNA-p21. In the mouse carotid artery injury model, blockade of lncRNA-p21 dysregulated many p53 downstream targets, leading to neointimal hyperplasia and enhanced cell proliferation with reduced apoptosis (Wu et al., 2014).

Cytoplasmic lncRNA CERNA1 can stabilize atherosclerotic plaques by promoting an important apoptosis inhibitor named apoptosis inhibitor 5 (API5). API5 is capable of inhibiting apoptosis of VSMCs and anti-inflammatory macrophages in apolipoprotein E$^{-/-}$ (Apo E$^{-/-}$) mice (Lu et al., 2019).

In a most recent study, an lncRNA associated with the progression and intervention of AS named RAPIA was increasingly expressed in advanced atherosclerotic sites and in macrophages. Blockade of RAPIA greatly attenuated the development of advanced AS in ApoE$^{-/-}$ mice (Sun et al., 2020). RAPIA exerted a regulatory role by targeting miR-183-5p in macrophages. miR-183-5p contains two binding sites for RAPIA. As RAPIA binds to miRNA-183-5p, miRNA loses its ability to inhibit proliferation or to promote macrophage apoptosis. Interestingly, suppression of RAPIA has atheroprotective effects in ApoE$^{-/-}$ mice fed with a high-fat diet which is similar to those of atorvastatin on advanced atherosclerotic plaques, by attenuating lipid accumulation, decreasing plaque size, increasing collagen content, and decreasing macrophage accumulation in advanced atherosclerotic plaques. Therefore, repressing RAPIA expression may be an alternative treatment for advanced atherosclerotic lesions, especially in patients resistant or intolerant to statins (Sun et al., 2020).

LONG NONCODING RNAS IN MACROPHAGE PYROPTOSIS

Pyroptosis is a programmed cell death of macrophages controlled by the NF-κB pathway (Bergsbaken et al., 2009; Sunami et al., 2012; Shen et al., 2014; Sheng et al., 2014). It causes cell lysis. Inflammatory responses can be induced upon cytosolic content release to the extracellular space (Xu et al., 2018). However, this type of cell death, once mislabeled as apoptosis, is attributable to the involvement of caspase 1 (Shi et al., 2017). Pyroptosis can be induced in macrophages in lesions by ox-LDL and cholesterol crystal–triggered increases in NLRP3 inflammasome and caspase 1, leading to AS progression. In advanced atherosclerotic lesions, the formation of necrotic cores and unstable plaques may be attributed to macrophage pyroptosis (Xu et al., 2018).

MALAT1 in diabetic AS has been reported to participate in macrophage pyroptosis after sinapic acid (SA) treatment. Gain- and loss-of-function approaches have demonstrated that in normal macrophages, MALAT1 shows a modestly beneficial effect against pyroptosis. Chronic low-dose SA treatment could block the inflammasome activation, macrophage pyroptosis, and the systemic inflammatory response by mediating MALAT1 (Yong et al., 2018).

LONG NONCODING RNAS IN MACROPHAGE DURING ATHEROSCLEROTIC INFLAMMATION

Many studies have shown that lncRNAs affect the expression profiles of inflammatory pathways in different diseases. For example, in response to LPS stimulation, LIN28B-AS1 (Xie Z. et al., 2019) and Mirt2 (Du et al., 2017) associate with pro- and anti-atherosclerotic inflammation factors in macrophages through NF-κB. Mathy's review provided detailed information about lncRNAs' classification and functions in transcriptional control (Mathy and Chen, 2017). In this review, we focused on the functions and effects of individual lncRNAs in the context of atherosclerotic inflammation.

The canonical NF-κB signaling is critical for regulation of innate and adaptive immune responses and is involved in cell proliferation and apoptosis, migration, and invasion (Taniguchi and Karin, 2018). The activation of NF-κB is induced by inflammatory chemokines, notably LPS, TNF-α, IL-1, and many toll-like receptors (TLRs) (Qin et al., 2005; Mathy and Chen, 2017). Under inactive conditions, IκBα sequesters cytoplasmic p50-p65 dimers, hindering the translocation of p50-p65 dimers to the nucleus. After receiving activating signals, IκBα is phosphorylated by a IκB kinase complex and get degraded into free NF-κB dimers. Free NF-κB dimers translocate to the nucleus, where they interact with specific

DNA-binding sites to augment transcription and expression of different genes (Baker and Ghosh, 2010; Hayden and Ghosh, 2014; Mitchell and Carmody, 2018).

A number of studies have mentioned lncRNAs' diverse regulatory roles in inflammatory diseases, including AS, by controlling NF-κB–regulated transcription in both the cytosol and nucleus.

TOLL-LIKE RECEPTOR LIGATION-STIMULATED LONG NONCODING RNAS

In response to LPS stimulation, lncRNA-Mirt2 (Du et al., 2017), LINC00305, LIN28B-AS1 (Zhang et al., 2017), and MALAT1 (Zhao et al., 2016) show remarkable effects on the progression of AS through NF-κB–dependent mechanisms. LINC00305 is a pro-inflammatory agent during AS progression. In Zhang's work, LINC00305 in the cytosol interacted with the transmembrane protein lipocalin-1 interacting membrane receptor (LIMR) and promoted the expression of inflammatory genes in human THP-1 cells. Notably, LINC00305 has been associated with LPS-stimulated inflammation by targeting the transmembrane receptor LIMR. The inflammation promotor in LPS shock, aryl-hydrocarbon receptor repressor (AHRR), is a binding partner of LIMR (Brandstätter et al., 2016) that tends to enhance NF-κB activity when cotransfected with LIMR. LINC00305-LIMR interaction strengthened LIMR–AHRR binding and promoted AHRR nuclear localization in addition to promoting NF-κB activation, which in turn inhibited the downstream aryl-hydrocarbon receptor signaling (Zhang et al., 2017).

In the nucleus, a novel insulin-like growth factor 2 mRNA-binding protein 1 (IGF2BP1)–binding lncRNA (LIN28B-AS1) has been associated with pro-inflammatory activity. TLR4 ligation activates canonical NF-κB pathways, followed by release and activation of p65-p52 heterodimers. The p65–p52 heterodimers then shuttle to the nucleus and enhance pro-inflammatory responses, including facilitating gene transcriptions of IL-6, IL-1β, and TNF-α by interacting with IGF2BP1 (Perkins, 2007; Rahman and McFadden, 2011; Xie J. et al., 2019). It is noteworthy that LIN28B–AS1–IGF2BP1 binding is essential for IGF2BP1–p65–p52 complex formation, because nuclear LIN28B-AS1 could interact with IGF2BP1 and assemble the IGF2BP1-p65-p52 complex in THP-1 cells (Xie Z. et al., 2019).

Unlike LIN28B-AS1, anti-inflammatory lncRNA-Mirt2 regulates inflammation by blocking the NF-κB signaling in the cytosol. Mirt2 expression was potently up-regulated in response to LPS. LPS-triggered signaling pathways required the adaptor protein myeloid differentiation marker 88 (MyD88) and toll-interleukin-1 receptor domain–containing adaptor-inducing IFNβ (TRIF) (Kawai and Akira, 2010). The TLR4-MyD88 binding at the membrane contributed to recruiting and phosphorylating IL-1 receptor associated kinase 1 (IRAK1) and IRAK4 that promote oligomerization and ubiquitination of TNF receptor-associated factor 6 (TRAF6) (Hirotani et al., 2005; Skaug et al., 2009). However, Mirt2 can bind to TRAF6 in the cytosol and attenuate oligomerization and its Lys63 (K63)-linked ubiquitination, which restricts MyD88-dependent NF-κB and MAPK activation and TRAF6-mediated M1 polarization of macrophages. In addition to repressing macrophage inflammation, exotic Mirt2 expression remarkably facilitates IL-4–stimulated expression of multiple M2 markers, including Arg1, CD206, and Ym1, suggesting Mirt2 participates in M2 polarization. But the underlying mechanism remains unclear, and more studies are needed to gain a deeper understanding of the mechanism by which Mirt2 facilitates M2 polarization (Du et al., 2017).

Several findings have confirmed MALAT1 as a key controller of inflammation. Following LPS treatment, NF-κB–dependent enhancement of MALAT1 expression initiates a negative feedback loop. In human THP-1 cells, nuclear NF-κB triggered the transcription of MALAT1, and after that, MALAT1 interacted with the p50/p65 complex sequestering NF-κB and repressing its DNA-binding activity, which subsequently led to transcription of inflammatory cytokines TNF-α, IL-6, and IL-1β. MALAT1 knockdown enhanced the binding ability of p65 to TNF-α and IL-6 promoters (Zhao et al., 2016).

OX-LDL-STIMULATED LONG NONCODING RNAS

In addition to responding to TLR4 ligation, MALAT1 facilitates ox-LDL–induced inflammation by controlling CD36 expression. CD36 on the membrane of macrophages is a key scavenger receptor participating in lipid uptake and forming foam cells, and it has a strong affinity for ox-LDL (Tarhda et al., 2013; Chistiakov et al., 2017). Ox-LDL stimulation initiates MALAT1 transcription via NF-κB. *ß*-catenin is a transcription factor for CD36 expression, and *ß*-catenin gets recruited to the binding site on the CD36 promotor by the enhanced expression of MALAT1 that facilitates lipid uptake in macrophages (Huangfu et al., 2018).

SNHG16, an ox-LDL-sensitive long noncoding small nucleolar RNA, was found to be highly expressed in patients with AS. In an *in vitro* study, exogenous SNHG16 expression augmented production of pro-inflammatory cytokines by activating NF-κB signaling cascades. Conversely, SNHG16 knockdown resulted in inhibited IKKβ expression, IκBα phosphorylation, and p65 phosphorylation. Functionally, SNHG16 gets released into the cytoplasm in response to ox-LDL; then, SNHG16 acting as a sponge binds directly to and absorbs miR-17-5p to abolish the inhibitory effect of miR-17=5p on NF-κB activation. A SNHG16/miR-17-5p/NF-κB signaling axis promoting an inflammatory response in AS may exist (An al., 2019).

LINC01140 mediates ox-LDL–induced inflammation and plays a protective role on inflammation (He et al., 2020). After ox-LDL stimulation, LINC01140 becomes down-regulated in macrophage-differentiated THP1 cells, whereas p53 mRNA and miR-23b are up-regulated. The expression of inflammation factors, such as MCP-1, TNF-α, and IL-1β, is repressed potently when p53 is down-regulated. The

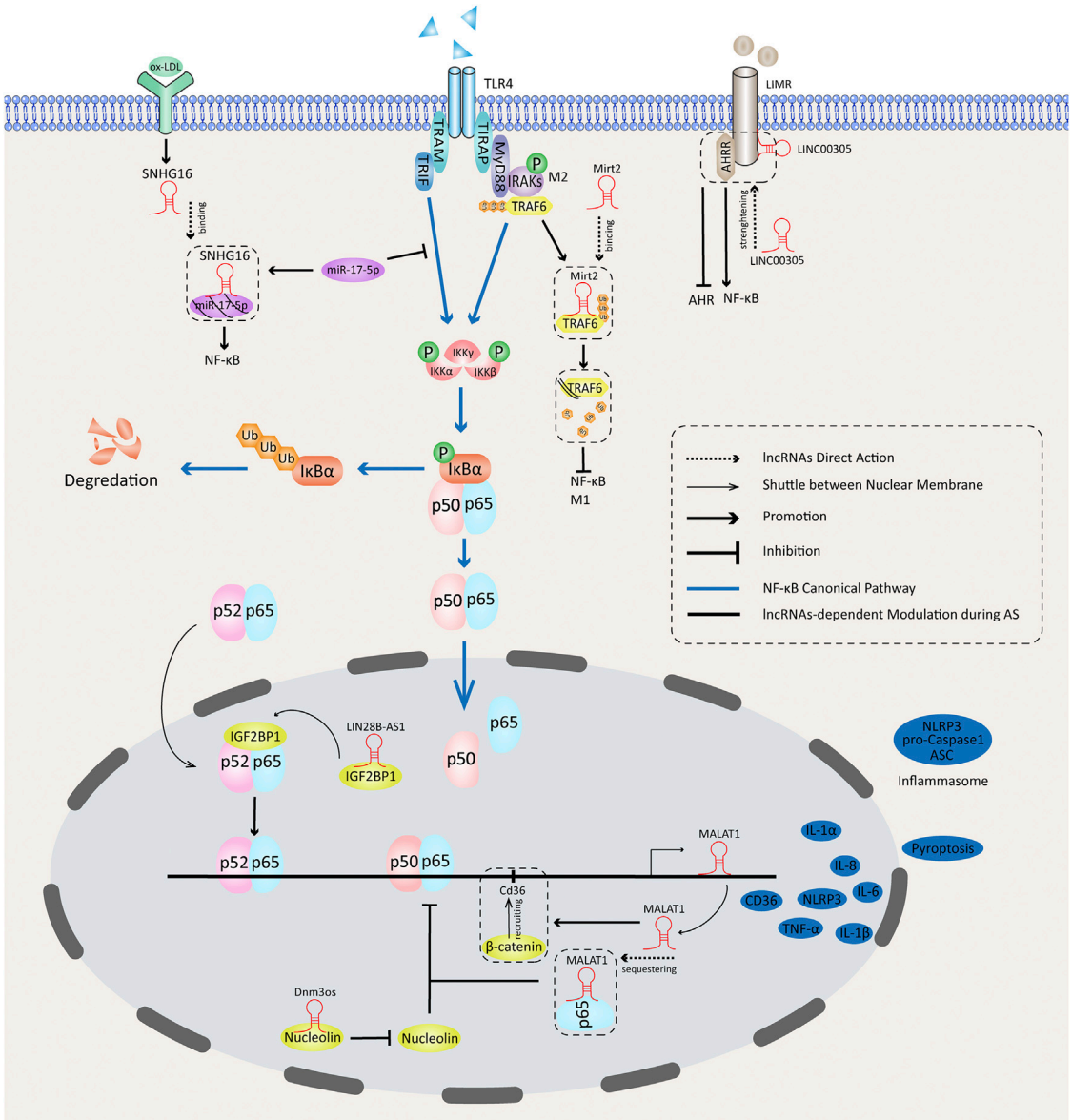

FIGURE 1 | Functions of NF-κB–dependent lncRNAs in atherosclerotic inflammation.

association between p53 and the LINC01140 promoters was shown using a luciferase reporter assay. After transfecting cells with a p53-overexpression vector (pcDNA-p53), LINC01140 expression was repressed and miR-23b expression was enhanced (He et al., 2020).

HIGH GLUCOSE AND PALMITIC ACID-STIMULATED LONG NONCODING RNAS

High glucose (HG) and palmitic acid (PA) can activate the lncRNA dynamin 3 opposite strand (Dnm3os) promotor and enhance pro-inflammatory actions by targeting nucleolin. Gene overexpression and knockdown experiments identified Dnm3os as a pro-inflammatory molecule under diabetic conditions. For instance, PA significantly induces the expression of IL-6, TNF, Nos2, and Cd36 in RAW264.7 cells transfected with a Dnm3os expression vector. RNA pull-down assays identified a close interaction between Dnm3os and nucleolin. Nucleolin is a nuclear RNA-binding protein in macrophages (Cong et al., 2011) that can regulate chromatin structure and exert an atheroprotective function. HG and PA substantially decrease the nucleolin protein level. Silencing nucleolin increased the gene expression of inflammatory factors induced by Dnm3os, including that of IL-6 and histone H3K9-acetylation at their promoters (Das et al., 2018).

In addition to activating lncRNAs through NF-κB, lincRNA-EPS, for example, is a nuclear repressor for inflammation that controls the expression of immune response genes (IRGs). Under an endotoxin challenge, lincRNA-EPS–deficient mice displayed exacerbated inflammatory responses and lethality. Gain-of-function and rescue approaches showed that lincRNA-EPS overexpression effectively limited IRG expression. lincRNA-EPS localizing at regulatory sites of IRGs interacts with hnRNPL via a CANACA motif to control nucleosome positioning and repress IRG transcriptions (Atianand et al., 2016).

On the other hand, lncRNA uc.48+ modulates P2X7R-mediated diabetic immune and inflammatory responses in RAW264.7 macrophages. P2X7R is protein of the P2X7 receptor and ERK pathway (Ponnusamy et al., 2011; Zanin et al., 2015). HG and free fatty acid (FFA) RAW264.7 cell treatments promoted the expression of uc.48+. Increased expression of uc.48+ in response to HG and FFAs augmented the inflammatory cytokine secretion, ROS formation, and ERK signaling via P2X7R activation (Wu et al., 2018).

Figure 1 summarizes the NF-κB–associated activities of lncRNAs during AS in macrophages. lncRNAs regulate the expression of NF-κB in both cytosols and nuclei. They can promote or inhibit translocation of NF-κB dimers to the nucleus by controlling the phosphorylation of the IKK complex and IκBα. NF-κB–dependent gene transcriptions are functionally affected by lncRNAs in the nucleus, partially through assembly of functional nuclear proteins complexes. MALAT1 can be expressed through an NF-κB pathway, and it affects the transcriptions of NF-κB–dependent inflammatory genes.

LONG NONCODING RNAS IN MACROPHAGE CHOLESTEROL METABOLISM

Lipid uptake and foam cell formation depend on activation of scavenger receptors, including the type A scavenger receptor (SRA) and the type B CD36 in the macrophages (Kunjathoor et al., 2002). Following lipid uptake, lipid droplets bud off the endoplasmic reticulum (ER) into the cytoplasm. The accumulation of free cholesterol (FC) requires re-esterification by the enzyme acyl-cholesterol transferase 1 (ACAT-1) in cells. Excessive FC can be stored in the form of cholesterol esters (CE) (McLaren et al., 2011; Maguire et al., 2019). Furthermore, the efflux of cholesterol can potentially keep cells from foaming. Cholesterol efflux depends mainly on several membrane transporters, such as the ATP-binding cassette transporter 1 (ABCA1) and the ATP-binding cassette subfamily G member-1 (ABCG1); and SR-B1, PPAR, and liver X receptor α (LXLRα) are key transcriptional factors for this process (Maguire et al., 2019). Notably, ABCA1, ABCG1, and SR-B1 control the removal of cholesterol and phospholipids out of macrophages by directing lipid droplets to apolipoprotein A1 and high-density lipoprotein (HDL) (Moore and Tabas, 2011; Maguire et al., 2019). Dysregulation of cholesterol homeostasis in macrophages results in lipid uptake disturbances, foam cell formation, and the progression of AS. LncRNAs in macrophages have been demonstrated to manage cholesterol loading and foam cell formation. **Figure 2** shows a summary of these findings.

Generally, lncRNAs serve as miRNA sponges. Several studies have identified the intricate interplay between lncRNAs and microRNAs in macrophages that significantly affect the cell cholesterol metabolism and lead to foam cell formation and AS development. For example, nuclear-enriched abundant transcript 1 (NEAT1) (Chen et al., 2018; Wang L. et al., 2019) and growth arrest–specific transcript 5 (GAS5) (Ye et al., 2018) are involved in oxidative stress, lipid uptake, and inflammation by targeting miRNAs and may cause exacerbation of atherogenesis. However, RP5-833A20.1 (Hu et al., 2015), the cholesterol homeostasis regulator of miRNA expression (CHROME) (Hennessy et al., 2019), and the H19-imprinted maternally expressed transcript (H19) (Han et al., 2018) can reverse cholesterol metabolism disturbances and alleviate the inflammatory response.

GAS5 is capable of mediating macrophage polarization (Chi et al., 2019; Sun et al., 2017), apoptosis (Chen et al., 2017), and inflammation (Ye et al., 2018). GAS5 is found abundantly in atherosclerotic plaques after ox-LDL treatment. In THP-1 cells, enrichment of GAS5 suppressed the miR-211 expression, aggravating the inflammatory response and stimulating the expression of MMP, whose production in foam cells exacerbates proteolytic rupture of extracellular matrix components in plaque lesions. These findings support the role of GAS5 as a contributor of plaque destabilization in AS (Ye et al., 2018).

The nuclear lncRNA NEAT1 is a pro-atherosclerotic agent shown to serve as a sponge for downstream miR-128 (Chen et al., 2018) and miR-342-3p (Wang et al., 2019) targets. NEAT1 triggered an inflammatory response and oxidative stress by suppressing miR-128 in RAW264.7 cells after ox-LDL stimulation. Down-regulating NEAT1 repressed not only cell proliferation, inflammation, and the oxidative stress process but also inhibited CD36 expression, foam cell formation, and apoptosis (Chen et al., 2018). In addition, the NEAT1-miR-342-3p pathway modulates inflammation and lipid uptake. In THP-1 cells, lipid uptake was inhibited by NEAT1 silencing plus miR-34-3p mimics treatment. Because of this, NEAT1 blockade could suppress the ox-LDL–induced apoptosis and inflammation via miR-342-3p curbing (Wang et al., 2019).

Another nuclear lncRNA RP5-833A20.1 is anti-atherosclerotic. The expression of RP5-833A20.1 under ox-LDL or ac-LDL treatment weakens the expression of nuclear factor IA (NFIA) in THP-1-derived foam cells. In an ApoE$^{-/-}$ mice model, NFIA overexpression enhanced HDL cholesterol (HDL-C), decreased the production of LDL cholesterol (LDL-C) and very LDL cholesterol (VLDL-C), and reduced the secretion of inflammatory cytokines in plasma. Meanwhile, NFIA promoted reverse cholesterol transport across cell membranes by stimulating ABCA1 and ABCG1 expression. ABCA1 and ABCG1 can deliver cholesterol across cell membranes (Stefulj et al., 2009) and may enable AS regression. Overexpressing RP5-

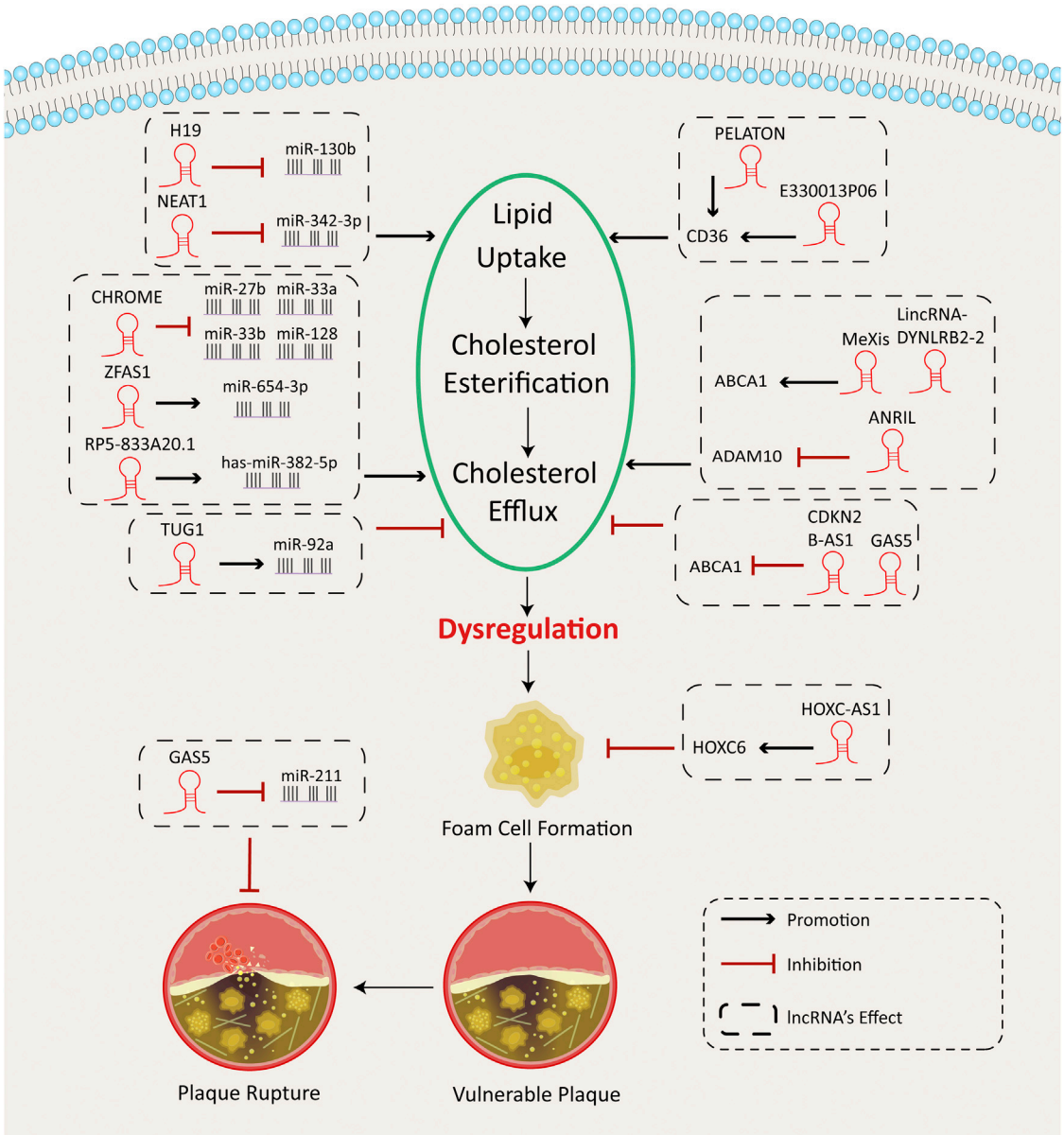

FIGURE 2 | Cholesterol metabolism functions of lncRNAs in macrophages.

833A20.1 and hsa-miR-382-5p mimics *in vitro* effectively down-regulated the expression of ABCA1 and ABCG1 but elevated the expression of SRA1, CD36, and NF-κB. As a result of this, lncRNA RP5-833A20.1 can stimulate cholesterol efflux in human macrophages and relieve the inflammatory response via the RP5-833A20.1- has-miR-382-5p pathway (Hu et al., 2015).

Furthermore, CHROME levels in the plasma and atherosclerotic plaques of patients with coronary artery disease (CAD) are elevated. Cells expressing wild-type CHROME *in vitro* inhibit the expression of miRNAs, such as miR-27b, miR-33a, miR-33b, and miR-128; these miRNAs suppress cholesterol efflux and prohibit HDL biogenesis.

CHROME derepresses these collective target genes through its miRNA interactions, which further affects cholesterol transport. Cells lacking CHROME express lower levels of ABCA1, cannot efflux cholesterol, and present reduced formation of nascent HDL particles in response to activating sterol-activated liver X receptor (LXR), leading to reduced expression of genes involved in the response to cholesterol excess in human hepatocytes and macrophages (Hennessy et al., 2019).

H19 participates in many pathological processes, including tumorigenesis (Ghafouri-Fard et al., 2020), cerebral ischemia-reperfusion injury (Wang et al., 2017), and acute myocardial infarction (Yu and Dong, 2018). H19 is highly expressed, while miR-130b is down-regulated in blood samples of patients with

TABLE 1 | Summary of atherosclerosis-related lncRNAs expressed in macrophage.

lncRNA	Full name	Location	Stimulus	Cells	Function	Mechanism	Reference
Macrophage differentiation							
Lnc-MC	Long noncoding monocytic RNA	Cytoplasm	Pam3CSK4	Macrophage HL-60	Monocyte/macrophage differentiation	Sequestering and soaking up miR-199a-5p to release the expression of ACVR1B	Chen et al. (2015)
Macrophage phenotypic switching							
TCONS_00019715	—	—	IFN-α LPS	Macrophage	Macrophage polarization	Reducing M1 elevating M2 may be through regulating PAK1	Huang Z. et al. (2016)
Mirt2	Myocardial infraction-associated transcript 2	Cytoplasm	LPS	Macrophage	Macrophage polarization and anti-inflammation	Blocking the MyD88-mediated MAPK and NF-κB activities to inhibit M1 polarization	Du et al. (2017)
Macrophage apoptosis							
CERNA1	—	Cytoplasm and nucleus	Ox-LDL	Vascular smooth muscle cells and macrophage	Atherosclerotic plaque stabilization	Increasing API5 to inhibit apoptosis of VSMCs and anti-inflammatory macrophages	Lu et al. (2019)
RAPIA	LncRNA associated with the progression and intervention of atherosclerosis	Cytoplasm	—	Macrophage	Macrophage proliferation and apoptosis	Binding to miRNA-183-5p to promote proliferation and promote apoptosis of macrophages	Sun et al. (2020)
Macrophage pyroptosis							
MALAT1	Metastasis-associated lung adenocarcinoma transcript 1	Nucleus	Low-dose sinapic acid	Macrophage	Macrophage pyroptosis	Chronic low-dose SA treatment could block the function of MALAT1-dependent NLRP3 inflammasome, consequently inhibit pyroptosis, and systemic inflammatory response	Yong et al. (2018)
Atherosclerotic inflammation							
Mirt2	Myocardial infraction-associated transcript 2	Cytoplasm	LPS	Macrophage	Macrophage polarization and anti-inflammation	Blocking the MyD88-mediated MAPK and NF-κB activities to inhibit M1 polarization	Du et al. (2017)
LINC00305	—	Cytoplasm	LPS	Macrophage	Pro-inflammation	Binding to LIMR then promoted nuclear localization of AHRR to activate NF-κB	Zhang et al. (2017)
LIN28B-AS1	—	Nucleus	LPS	Macrophage and monocyte	Pro-inflammation	Increasing IGF2BP1-p65-p52 association to activate NF-κB signaling	Xie Z. et al. (2019)
MALAT1	Metastasis-associated lung adenocarcinoma transcript 1	Nucleus	LPS	Macrophage	Decreased transcription of inflammatory cytokines	Interacting with NF-κB p50/p65 dimmers to sequester NF-κB and decrease cytokine transcription	Zhao et al. (2016)
SNHG16	Small nucleolar RNA host gene 16	Cytoplasm	Ox-LDL	Macrophage	Cell proliferation and pro-inflammation	Binding to and absorbed miR-17-5p to release the activity of NF-κB pathway	An et al. (2019)
LINC01140	—	—	Ox-LDL	Macrophage	Anti-inflammation	Binding to miR-23b in order to down-regulate p53 and decrease the expression of inflammation factors	He et al. (2020)
Dnm3os	Dynamin 3 opposite strand	Nucleus	PA and HG	Macrophage	Pro-inflammation	Decreasing nucleolin protein levels to increase inflammatory gene expression	Das et al. (2018)

(Continued on following page)

TABLE 1 | (*Continued*) Summary of atherosclerosis-related lncRNAs expressed in macrophage.

lncRNA	Full name	Location	Stimulus	Cells	Function	Mechanism	Reference
lincRNA-EPS	LincRNA erythroid prosurvival	Nucleus	Pam3CSK4	Macrophage	Anti-inflammation	Controlling nucleosome positioning and repressing transcription expression of inflammatory cytokines by targeting hnRNPL	Atianand et al. (2016)
uc.48+	—	—	HG and FFAs	Macrophage	Pro-inflammation and promote immune response	Evoking P2X7R-mediated cytokine production, ROS activity, and reaction of the ERK pathway	Wu et al. (2018)
Macrophage cholesterol metabolism							
NEAT1	Nuclear-enriched abundant transcript 1	Nucleus	Ox-LDL	Macrophage	Inflammation and oxidative stress	Sponging and inhibiting miR-128 to trigger inflammation and oxidative stress and to increase CD36	Chen et al. (2018)
			Ox-LDL	Macrophage	Inflammation and lipid uptake	Inducing ox-LDL-induced apoptosis and inflammation via targeting miR-342-3p	Wang L. et al. (2019)
GAS5	Growth arrest–specific transcript 5	Cytoplasm	Ox-LDL	Macrophage	Atherosclerotic plaque destabilization	Suppressing the miR-211 expression to aggravate inflammatory response and the expression of MMP exacerbating plaque rupture	Ye et al. (2018)
		Nucleus	Ox-LDL	Macrophage	Pro-atherosclerotic	Promoting atherosclerosis development through targeting EZH2-mediated ABCA1 transcription	Meng et al. (2020)
RP5-833A20.1	—	Nucleus	Ox-LDL and Ac-LDL	Macrophage-derived foam cells	Anti-atherosclerotic	Reducing cholesterol efflux and alleviating inflammatory responses via RP5-833A20.1-has-miR-382-5p pathway	Hu et al. (2015)
ZFAS1	Zinc finger NFX1-type containing 1 antisense RNA 1	Cytoplasm	Ox-LDL	Macrophage-derived foam cells	Anti-atherosclerotic	Ameliorating inflammation and reducing cholesterol efflux by targeting miR-654-3p-ADAM10/RAB22A axis	Tang et al. (2020)
CHROME	Cholesterol homeostasis regulator of miRNA expression	Cytoplasm	LXR agonist (GW3965	Hepatocytes and macrophage	Anti-atherosclerotic	Interacting with microRNAs to curb their repression on cholesterol efflux and HDL biogenesis	Hennessy et al. (2019)
H19	H19-imprinted maternally expressed transcript	Nucleus	Ox-LDL	Macrophage	Anti-atherosclerotic	Regulating adipogenesis and inflammation by inhibiting miR-130b	Han et al. (2018)
PELATON/LINC01272	Plaque-enriched lncRNA in atherosclerotic and inflammatory bowel macrophage regulation	Nucleus	—	Macrophage	Regulator of phagocytosis	Inducing CD36 expression to promote phagocytosis, ROS production, and ox-LDL uptake	Hung et al. (2019)
TUG1	Taurine up-regulated gene 1	—	Ox-LDL	Macrophage	Pro-atherosclerotic	Dysregulating high-density lipoprotein metabolism and cholesterol efflux through inhibiting miR-92a and improving FXR1	Yang and Li (2020)
E330013P06	—	—	HG PA	Macrophage	Pro-atherogenic	Increasing inflammatory genes along with foam cell formation through up-regulating CD36 expression	Reddy et al. (2014)
lincRNA-DYNLRB2-2/LINC01228	—	—	Ox-LDL	Macrophage	Anti-atherosclerotic	Up-regulating GPR 119 and ABCA1 by the GLP1-R signaling pathway	Hu et al. (2014)

(Continued on following page)

TABLE 1 | (*Continued*) Summary of atherosclerosis-related lncRNAs expressed in macrophage.

lncRNA	Full name	Location	Stimulus	Cells	Function	Mechanism	Reference
MeXis	Macrophage-expressed LXR-induced sequence	Nucleus	GW3965	Macrophage	Anti-atherosclerotic	Promoting LXR-mediated Abca1 expression and cholesterol efflux	Sallam et al. (2018)
HOXC-AS1	HOXC cluster and antisense RNA 1	—	Ox-LDL	Macrophage	Regulation of cholesterol accumulation	Suppressing lipid accumulation by increasing HOXC6 expression	Huang C. et al. (2016)
CDKN2B-AS1/ANRIL	Cyclin-dependent kinase inhibitor 2B antisense noncoding RNA	Nucleus	Ox-LDL	Macrophage	Pro-atherosclerotic	Assembling an RNA–DNA triplex in the promoter region of CDKN2B to recruit EZH2 and CTCF, then increase histone methylation, then adversely affect EZH2-mediated gene transcription	Ou et al. (2020)
					Anti-atherosclerotic	Binding to DNMT1 to improve methylation of ADAM10 promoter to suppress inflammation and cytokine production, and promote cholesterol efflux	Li et al. (2019)

AS. This suggests that in ox-LDL stimulated RAW264.7 cells, H19 participates in adipogenesis and the inflammatory response by inhibiting the activity of miR-130b. miR-130b is a target for H19; H19-induced miR-130b expression after ox-LDL treatment stimulates anti-inflammatory cytokine production and decreases pro-inflammatory cytokine levels. Knocking down H19 using shRNAs alleviated lipid metabolism disturbances and decreased the inflammatory response by mitigating lipid accumulation and promoting the lipid metabolism (Han et al., 2018). H19 is also a regulator of hepatic inflammation during cholestasis that secretes exosome cargos in cholangiocytes (Li et al., 2020).

The plaque-enriched lncRNA in atherosclerotic and inflammatory bowel macrophage regulation (PELATON) lncRNA is a potential regulator of macrophage phagocytosis. After being confirmed by *in situ* hybridization, PELATON was enriched in unstable human atherosclerotic plaques with a necrotic core and plaque shoulders and colocalized with the M1 marker CD68. Knocking down PELATON in monocyte-derived macrophages markedly reduced the cell phagocytotic performance by reducing the CD36 mRNA (Hung et al., 2019). lncRNA E330013P06 (E33) also caused foam cell formation by up-regulating CD36 expression. Under type 2 diabetic (T2D) conditions, HG and PA treatment of macrophages greatly up-regulates the expression of E33. Exogenous expression of E33 highly induces inflammation by increasing inflammatory expression of Nos2, Il6, and Ptgs2 genes, along with foam cell formation through up-regulation of CD36 expression, resulting in pro-atherogenic macrophages responses (Reddy et al., 2014).

The pro-atherosclerotic taurine up-regulated gene 1 (TUG1) can worsen AS via the miR-92a/FXR1 axis (Yang and Li, 2020). TUG1 overexpression increases plaque size and enhances macrophage recruitment to the plaque area by targeting apolipoprotein (apo) M in ApoE$^{-/-}$mice. Generally, ApoM is a critical lipocalin for delivering lipid sphingosine-1-phosphate (S1P). ApoM delivers S1P to its S1P receptors on endothelial cells. The anti-atherosclerotic ApoM can regulate high-density lipoprotein metabolism, protecting against oxidation and mediating CE (Christoffersen et al., 2011; Nádró et al., 2018). TUG1 was found to down-regulate ApoM levels via miR-92a inhibition and FXR1 stimulation in mouse liver NCTC 1469 cells. In RAW264.7 cells, TUG1 overexpression significantly decreased ABCA1 and ABCG1 expressions, which consequently slowed down the CE rate (Yang and Li, 2020).

In recent studies, GAS5 (Meng et al., 2020) and cyclin-dependent kinase inhibitor 2B antisense noncoding RNA (CDKN2B-AS1, also known as ANRIL) (Ou et al., 2020) showed an important role on AS development through its EZH2-mediated ABCA1 transcription targeting. In Meng's work, GAS5 stimulated lipid accumulation and prevented cholesterol efflux by regulating ABCA1 in macrophage-derived foam cells (Meng et al., 2020).

By recruiting zeste homolog 2 (EZH2), one of the enzymatic factors of the polycomb repressive complex (Lu et al., 2018), to the promotor region of ABCA1, GAS5 transcriptionally represses its target genes (Shi et al., 2018). Knocking down GAS5 can greatly reverse cholesterol transportation and decrease lipid accumulation

by alleviating the EZH2-dependent transcriptional inhibition of ABCA1. EZH2 enhances the triple methylation of lysine 27 (H3K27) in the promoter region of ABCA1. GAS5 transcriptionally inhibits ABCA1 by binding to the EZH2 enhancer. EZH2 can promote AS progression by efficiently blocking ABCA1 transcription in AS (Lv et al., 2016).

Similarly, the lncRNA CDKN2B-AS1 promotes cholesterol uptake and accumulation and inhibits macrophage reverse cholesterol transport (mRCT) in macrophage-derived foam cells (Ou et al., 2020). The detrimental effects of CDKN2B knockdown on atherosclerotic lesions could be reversed by sh-CDKN2B-AS1 in an *in vivo* mouse model. Mechanically, CDKN2B-AS1 can package an RNA–DNA triplex in the CDKN2B promoter region. This triplex can recruit EZH2 and CTCF to the promoter region of CDKN2B to increase histone methylation, which then adversely affects CDKN2B transcription (Ou et al., 2020).

In contrast, LincRNA-DYNLRB2-2, macrophage-expressed LXR-induced sequence (MeXis), HOXC cluster antisense RNA 1 (HOXC-AS1), and ANRIL are anti-atherogenic molecules that modulate cholesterol efflux and cholesterol accumulation. Among them, LincRNA-DYNLRB2-2 (Hu et al., 2014) and MeXis (Hennessy et al., 2019) both target ABCA1 to regulate the cholesterol metabolism. The ox-LDL–induced increased lincRNA-DYNLRB2-2 expression in THP-1 macrophage–derived foam cells ameliorates inflammation by up-regulating G protein–coupled receptor 119 (GPR119), meanwhile improving ABCA1-regulated cholesterol efflux via a glucagon-like peptide 1 receptor (GLP-1R) signaling pathway. GPR119 is an anti-inflammatory regulator that induces ABCA1 expression and can be controlled by GLP-1R–mediated signaling cascades. By inducing the expression of ABCA1, GPR119 promotes cellular cholesterol efflux through apoA-I. Therefore, lincRNA-DYNLRB2-2 prevents atherosclerotic plaque formation by repressing expression of inflammation and adhesion molecules and increasing cholesterol efflux (Hu et al., 2014). MeXis is an amplifier of the critical cholesterol efflux gene Abca1, whose transcription is mediated by LXR. In response to LXR signaling, MeXis expression induction in macrophages promotes the expression of Abca1 and consequently improves cholesterol efflux. MeXis knockout in the bone marrow of mice represses Abca1 and inflammatory gene expression, causing an impaired cell response to cholesterol overload and plaque development. The LXR-MeXis-Abca1 axis may reverse cholesterol delivery and play a protective role on AS development (Sallam et al., 2018; Xie Y. et al., 2019). Additionally, ANRIL could serve as a biomarker candidate of AS that is up-regulated in atherosclerotic plaques and in patients' plasma (Hao et al., 2016). ANRIL also reduces inflammation and promotes cholesterol efflux by blocking ADAM10 expression. ADAM10 can shed or cleave several molecules on cell surface–like adhesion molecules and cytokines (van der Vorst et al., 2018). As a result of this, ANRIL suppresses the cytokine production and inflammation induced by AS, and it promotes cholesterol efflux (Li et al., 2019).

Moreover, the oncogenic LncRNA zinc finger NFX1-type containing one antisense RNA 1 (ZFAS1) is a viable target to ameliorate the development of AS because it reduces the cholesterol efflux rate and facilitates inflammation (Tang et al., 2020). In THP-1 macrophage-induced macrophages, overexpressing ZFAS1 promotes inflammatory responses and blocks cholesterol efflux. ZFAS1 is an upstream factor for miR-654-3p, which can target and suppress the expression of ADAM10 and RAB22A. In short, ZFAS1 can positively mediate the expression of ADAM10 and RAB22A by sponging miR-654-3p (Tang et al., 2020).

Lipid uptake, cholesterol esterification, and efflux are the main processes for the macrophage lipid metabolism. Disturbance of these processes leads to lipid accumulation and finally causes foam cell formation. lncRNAs participate in macrophage lipid metabolism and atherosclerotic plaque formation by targeting microRNAs or controlling the gene expression of important lipid metabolic enzymes or proteins.

HOXC cluster antisense RNA 1 (HOXC-AS1) exerts an inhibitory effect on ox-LDL–mediated cholesterol accumulation by improving homeobox C6 (HOXC6) expression in human THP-1 cells. HOX genes have significant regulatory effects on the cardiovascular system through vasculature function regulation (Miano et al., 1996). HOXC-AS1 and HOXC6 are both down-regulated in human atherosclerotic plaques. Lentivirus-mediated overexpression of HOXC-AS1 promoted the expression of HOXC6 and blocked ox-LDL–induced foam cell formation and disruption of cholesterol homeostasis in THP-1 cells. Ox-LDL could repress HOXC6 expression by reducing HOXC-AS1, partly suppressing Ox-LDL–mediated cholesterol accumulation to prevent AS (Huang C. et al., 2016).

Dysregulated lipid metabolism in macrophages is a potential cause of the foam cell formation, which speeds up the progress of AS. Several lncRNAs mentioned above play important roles during this process.

LONG NONCODING RNAS AS POTENTIAL BIOMARKERS AND THERAPEUTIC PERSPECTIVES

Among the noncoding RNAs, many miRNAs have been identified as disease biomarkers for a variety of cardiovascular diseases (CVDs) (Indolfi et al., 2019). Advances in the field of lncRNAs have provided evidence that these molecules display specific characteristics that make them attractive as prospective therapeutic targets to be exploited for clinical use (Indolfi et al., 2019). The expression profiles of lncRNAs have revealed individual lncRNAs or clusters of lncRNAs within plaque lesions. These molecules are potential biomarker candidates and can be seen as prospective therapeutic targets during AS progression (Fasolo et al., 2019; Indolfi et al., 2019).

On the one hand, as potential biomarkers, some "sponge" lncRNAs are more robust than miRNAs. LncRNAs can be upstream targets of miRNAs. For example, the macrophage anti-atherosclerotic lncRNA ZFAS1 serves as sponge that binds to miR-654-3p and improves the expression of ADAM10 and RAB22A (Tang et al., 2020). Moreover, some lncRNAs "sponges" are capable of interacting with more than one miRNA. CHROME can exert regulatory roles on cholesterol efflux and reverses cholesterol transport by reducing the expression of four miRNAs, namely, miR-27b, miR-33a, miR-33b, and miR-128 (Hennessy et al., 2019). Several miRNAs are

regulated by a single lncRNA; therefore, targeting such lncRNAs can be convenient (Indolfi et al., 2019).

On the other hand, lncRNAs can be biomarkers to predict different AS stages. RAPIA, for instance, is highly expressed in advanced atherosclerotic sites in mice models. The high level of RAPIA expression in atherosclerotic plaques may predict the occurrence of advanced AS (Sun et al., 2020). Suppression of RAPIA showed similar effects to those of atorvastatin on advanced atherosclerotic plaques by attenuating lipid accumulation and decreasing plaque size in advanced atherosclerotic plaques of mice models. RAPIA has been seen as a promising therapeutic target for treating advanced atherosclerotic lesions, especially in patients resistant or intolerant to statins.

LncRNAs offer the promise of a noninvasive diagnostic tool to manage AS. These molecules can be detected in the patients' sera and are considered attractive disease biomarker candidates (Zeng et al., 2018). ANRIL is a potential AS biomarker as it was found to increase in human atherosclerotic plaques and plasma (Hao et al., 2016). In a clinical study, GAS5 was specifically down-regulated in the sera of patients with CAD (Yin et al., 2017): GAS5 expression was greatly down-regulated in patients with CAD compared to its levels in normal controls and in patients with diabetes mellitus (the expression levels of GAS5 were decreased only in patients with CAD) (Indolfi et al., 2019). The expression of CHROME was also found to be high in the sera of patients with CAD and atherosclerotic plaques (Hennessy et al., 2019). Thus, significant high levels of these candidate lncRNAs in the blood may be predictors of CAD.

FUTURE PERSPECTIVES AND CONCLUSION

As Koelwyn stated, identifying the changing patterns of metabolism in monocytes and macrophages during early atherogenesis and figuring out at which point these processes become maladaptive and progress to the next stage are important. The progression of advanced AS can trigger acute cardiovascular diseases, like heart attack and stroke. Understanding the changing metabolism of macrophages across all stages of AS development is urgent, as is identifying the timing of early foam cell lesion formations, the progression to advanced plaques, and the rupture of vulnerable plaques (Koelwyn et al., 2018). Several lines of evidence have suggested that lncRNAs could be involved in regulating macrophage inflammation, macrophage cholesterol loading, macrophage differentiation, polarization, and apoptosis during the development of AS. Additionally, lncRNAs are promising candidates for AS biomarkers and potential therapeutic targets, like ANRIL, which was found to be greatly increased in patients' plasma (Hao et al., 2016), or the fact that blocking RAPPIA can partially mimic the effect of atorvastatin (Sun et al., 2020). We believe macrophage-related lncRNAs provide a novel and unique perspective to investigate the crossroads between chronic inflammation and AS. Future studies need to provide insights into the lncRNAs' functions in macrophages and explain how they function in the development of AS.

AUTHOR CONTRIBUTIONS

XM designed the review, gathered the data, drafted the initial manuscript, and revised the manuscript. FC and HL conceptualized and designed the review, coordinated, supervised, and critically reviewed the manuscript for important intellectual content. All authors approved the final manuscript as submitted and agreed to be accountable for all aspects of the work.

FUNDING

The National Natural Science Foundation of China, No. 81670735 to FC. The National Natural Science Foundation of China, No. 81400802 and Outstanding Youth Training Project from Shanghai Ninth People's Hospital the National Natural Science Foundation of China, jyyq 08201607 to HL.

REFERENCES

An, J. H., Chen, Z. Y., Ma, Q. L., Wang, H. J., Zhang, J. Q., and Shi, F. W. (2019). LncRNA SNHG16 promoted proliferation and inflammatory response of macrophages through miR-17-5p/NF-κB signaling pathway in patients with atherosclerosis. *Eur. Rev. Med. Pharmacol. Sci.* 23, 8665–8677. doi:10.26355/eurrev_201910_19184

Anderson, C. F., Gerber, J. S., and Mosser, D. M. (2002). Modulating macrophage function with IgG immune complexes. *J. Endotoxin Res.* 8, 477–481. doi:10.1179/09680510212500111810.1177/09680519020080060501

Anderson, K. L., Smith, K. A., Conners, K., McKercher, S. R., Maki, R. A., and Torbett, B. E. (1998). Myeloid development is selectively disrupted in PU.1 null mice. *Blood* 91, 3702–3710. doi:10.1182/blood.v91.10.3702

Atianand, M. K., Hu, W., Satpathy, A. T., Shen, Y., Ricci, E. P., Alvarez-Dominguez, J. R., et al. (2016). A long noncoding RNA lincRNA-EPS acts as a transcriptional brake to restrain inflammation. *Cell* 165, 1672–1685. doi:10.1016/j.cell.2016.05.075

Baker, R., and Ghosh, S. (2010). Direct activation of protein kinases by ubiquitin. *J. Mol. Cell Biol.* 2, 20–22. doi:10.1093/jmcb/mjp029

Bergsbaken, T., Fink, S. L., and Cookson, B. T. (2009). Pyroptosis: host cell death and inflammation. *Nat. Rev. Microbiol.* 7, 99–109. doi:10.1038/nrmicro2070

Brandstätter, O., Schanz, O., Vorac, J., König, J., Mori, T., Maruyama, T., et al. (2016). Balancing intestinal and systemic inflammation through cell type-specific expression of the aryl hydrocarbon receptor repressor. *Sci. Rep.* 6, 26091. doi:10.1038/srep26091

Carrieri, C., Cimatti, L., Biagioli, M., Beugnet, A., Zucchelli, S., Fedele, S., et al. (2012). Long non-coding antisense RNA controls Uchl1 translation through an embedded SINEB2 repeat. *Nature* 491, 454–457. doi:10.1038/nature11508

Chen, D. D., Hui, L. L., Zhang, X. C., and Chang, Q. (2018). NEAT1 contributes to ox-LDL-induced inflammation and oxidative stress in macrophages through inhibiting miR-128. *J. Cell. Biochem.* 120, 2493. doi:10.1002/jcb.27541

Chen, L., Yang, W., Guo, Y., Chen, W., Zheng, P., Zeng, J., et al. (2017) Exosomal lncRNA GAS5 regulates the apoptosis of macrophages and vascular endothelial cells in atherosclerosis. *PLoS One* 12 e0185406. doi:10.1371/journal.pone.0185406

Chen, M.-T., Lin, H.-S., Shen, C., Ma, Y.-N., Wang, F., Zhao, H.-L., et al. (2015). The PU.1-Regulated long noncoding RNA lnc-MC controls human monocyte/macrophage differentiation through interaction with MicroRNA-199a-5p. *Mol. Cell Biol.* 35, 3212–3224. doi:10.1128/MCB.00429-15

Chi, X., Ding, B., Zhang, L., Zhang, J., Wang, J., and Zhang, W. (2019). lncRNA GAS5 promotes M1 macrophage polarization via miR-455-5p/SOCS3 pathway in childhood pneumonia. *J. Cell. Physiol.* 234, 13242–13251. doi:10.1002/jcp.27996

Chinetti-Gbaguidi, G., and Staels, B. (2011). Macrophage polarization in metabolic disorders. *Curr. Opin. Lipidol.* 22, 365–372. doi:10.1097/MOL.0b013e32834a77b4

Chistiakov, D. A., Melnichenko, A. A., Myasoedova, V. A., Grechko, A. V., and Orekhov, A. N. (2017). Mechanisms of foam cell formation in atherosclerosis. *J. Mol. Med.* 95, 1153–1165. doi:10.1007/s00109-017-1575-8

Christoffersen, C., Obinata, H., Kumaraswamy, S. B., Galvani, S., Ahnström, J., Sevvana, M., et al. (2011). Endothelium-protective sphingosine-1-phosphate provided by HDL-associated apolipoprotein M. *Proc. Natl. Acad. Sci. U.S.A.* 108, 9613–9618. doi:10.1073/pnas.1103187108

Cong, R., Das, S., and Bouvet, P. (2011). "The multiple properties and functions of nucleolin" in *The nucleolus*. Editor M. O. J. Olson (New York, NY: Springer New York), 185–212.

Crowther, M. A. (2005). Pathogenesis of atherosclerosis. *Hematol. Am. Soc. Hematol. Educ. Progr.* 2005, 436–441. doi:10.1182/asheducation-2005.1.436

Das, S., Reddy, M. A., Senapati, P., Stapleton, K., Lanting, L., Wang, M., et al. (2018). Diabetes mellitus-induced long noncoding RNA Dnm3os regulates macrophage functions and inflammation via nuclear mechanisms. *Arterioscler. Thromb. Vascu. Biol.* 38, 1806–1820. doi:10.1161/atvbaha.117.310663

Derrien, T., Johnson, R., Bussotti, G., Tanzer, A., Djebali, S., Tilgner, H., et al. (2012). The GENCODE v7 catalog of human long noncoding RNAs: analysis of their gene structure, evolution, and expression. *Genome Res.* 22, 1775–1789. doi:10.1101/gr.132159.111

Donaldson, C. J., Lao, K. H., and Zeng, L. (2018). The salient role of microRNAs in atherogenesis. *J. Mol. Cell. Cardiol.* 122, 98–113. doi:10.1016/j.yjmcc.2018.08.004

Du, M., Yuan, L., Tan, X., Huang, D., Wang, X., Zheng, Z., et al. (2017). The LPS-inducible lncRNA Mirt2 is a negative regulator of inflammation. *Nat. Commun.* 8, 2049. doi:10.1038/s41467-017-02229-1

Engreitz, J. M., Haines, J. E., Perez, E. M., Munson, G., Chen, J., Kane, M., et al. (2016). Local regulation of gene expression by lncRNA promoters, transcription and splicing. *Nature* 539, 452–455. doi:10.1038/nature20149

Fasolo, F., Di Gregoli, K., Maegdefessel, L., and Johnson, J. L. (2019). Non-coding RNAs in cardiovascular cell biology and atherosclerosis. *Cardiovasc. Res.* 115, 1732–1756. doi:10.1093/cvr/cvz203

Gao, J., Wang, F., Wu, P., Chen, Y., and Jia, Y. (2020). Aberrant LncRNA expression in leukemia. *J. Cancer* 11, 4284–4296. doi:10.7150/jca.42093

Ghafouri-Fard, S., Esmaeili, M., and Taheri, M. (2020). H19 lncRNA: roles in tumorigenesis. *Biomed. Pharmacother.* 123, 109774. doi:10.1016/j.biopha.2019.109774

Han, Y., Ma, J., Wang, J., and Wang, L. (2018). Silencing of H19 inhibits the adipogenesis and inflammation response in ox-LDL-treated Raw264.7 cells by up-regulating miR-130b. *Mol. Immunol.* 93, 107–114. doi:10.1016/j.molimm.2017.11.017

Hansen, T. B., Jensen, T. I., Clausen, B. H., Bramsen, J. B., Finsen, B., Damgaard, C. K., et al. (2013). Natural RNA circles function as efficient microRNA sponges. *Nature* 495, 384–388. doi:10.1038/nature11993

Hao, L., Hongming, Z., and Junbo, G. (2016). Long noncoding RNA: recent updates in atherosclerosis. *Int. J. Biol. Sci.* 12, 898–910. doi:10.7150/ijbs.14430

Hayden, M. S., and Ghosh, S. (2014). Regulation of NF-κB by TNF family cytokines. *Semin. Immunol.* 26, 253–266. doi:10.1016/j.smim.2014.05.004

He, L., Zhao, X., and He, L. (2020). LINC01140 alleviates the oxidized low-density lipoprotein-induced inflammatory response in macrophages via suppressing miR-23b. *Inflammation* 43, 66–73. doi:10.1007/s10753-019-01094-y

Hennessy, E. J., van Solingen, C., Scacalossi, K. R., Ouimet, M., Afonso, M. S., Prins, J., et al. (2019). The long noncoding RNA CHROME regulates cholesterol homeostasis in primates. *Nat. Metab.* 1, 98–110. doi:10.1038/s42255-018-0004-9

Hirotani, T., Yamamoto, M., Kumagai, Y., Uematsu, S., Kawase, I., Takeuchi, O., et al. (2005). Regulation of lipopolysaccharide-inducible genes by MyD88 and Toll/IL-1 domain containing adaptor inducing IFN-β. *Biochem. Biophys. Res. Commun.* 328, 383–392. doi:10.1016/j.bbrc.2004.12.184

Hu, Y.-W., Yang, J.-Y., Ma, X., Chen, Z.-P., Hu, Y.-R., Zhao, J.-Y., et al. (2014). A lincRNA-DYNLRB2-2/GPR119/GLP-1R/ABCA1-dependent signal transduction pathway is essential for the regulation of cholesterol homeostasis. *J. Lipid Res.* 55, 681–697. doi:10.1194/jlr.M044669

Hu, Y.-W., Zhao, J.-Y., Li, S.-F., Huang, J.-L., Qiu, Y.-R., Ma, X., et al. (2015). RP5-833A20.1/miR-382-5p/NFIA-dependent signal transduction pathway contributes to the regulation of cholesterol homeostasis and inflammatory reaction. *Arterioscler. Thromb. Vasc. Biol.* 35, 87–101. doi:10.1161/ATVBAHA.114.304296

Huang, C., Hu, Y.-W., Zhao, J.-J., Ma, X., Zhang, Y., Guo, F.-X., et al. (2016). Long noncoding RNA HOXC-AS1 suppresses ox-LDL-induced cholesterol accumulation through promoting HOXC6 expression in THP-1 macrophages. *DNA Cell Biol.* 35, 722–729. doi:10.1089/dna.2016.3422

Huang, Z., Luo, Q., Yao, F., Qing, C., Ye, J., Deng, Y., et al. (2016). Identification of differentially expressed long non-coding RNAs in polarized macrophages. *Sci. Rep.* 6, 19705. doi:10.1038/srep19705

Huangfu, N., Xu, Z., Zheng, W., Wang, Y., Cheng, J., and Chen, X. (2018). LncRNA MALAT1 regulates oxLDL-induced CD36 expression via activating β-catenin. *Biochem. Biophys. Res. Commun.* 495, 2111–2117. doi:10.1016/j.bbrc.2017.12.086

Hung, J., Scanlon, J. P., Mahmoud, A. D., Rodor, J., Ballantyne, M., Fontaine, M. A. C., et al. (2019). Novel plaque enriched long noncoding RNA in atherosclerotic macrophage regulation (PELATON). *Arterioscler. Thromb. Vasc. Biol.* 40, 697. doi:10.1161/ATVBAHA.119.313430

Indolfi, C., Iaconetti, C., Gareri, C., Polimeni, A., and De Rosa, S. (2019). Non-coding RNAs in vascular remodeling and restenosis. *Vasc. Pharmacol.* 114, 49–63. doi:10.1016/j.vph.2018.10.006

Johnson, J. L., and Newby, A. C. (2009). Macrophage heterogeneity in atherosclerotic plaques. *Curr. Opin. Lipidol.* 20, 370–378. doi:10.1097/MOL.0b013e3283309848

Kawai, T., and Akira, S. (2010). The role of pattern-recognition receptors in innate immunity: update on Toll-like receptors. *Nat. Immunol.* 11, 373–384. doi:10.1038/ni.1863

Khallou-Laschet, J., Varthaman, A., Fornasa, G., Compain, C., Gaston, A.-T., Clement, M., et al. (2010). Macrophage plasticity in experimental atherosclerosis. *PloS One* 5, e8852. doi:10.1371/journal.pone.0008852

Koelwyn, G. J., Corr, E. M., Erbay, E., and Moore, K. J. (2018). Regulation of macrophage immunometabolism in atherosclerosis. *Nat. Immunol.* 19, 526–537. doi:10.1038/s41590-018-0113-3

Kruth, H. S., Jones, N. L., Huang, W., Zhao, B., Ishii, I., Chang, J., et al. (2005). Macropinocytosis is the endocytic pathway that mediates macrophage foam cell formation with native low density lipoprotein. *J. Biol. Chem.* 280, 2352–2360. doi:10.1074/jbc.M407167200

Kunjathoor, V. V., Febbraio, M., Podrez, E. A., Moore, K. J., Andersson, L., Koehn, S., et al. (2002). Scavenger receptors class A-I/II and CD36 are the principal receptors responsible for the uptake of modified low density lipoprotein leading to lipid loading in macrophages. *J. Biol. Chem.* 277, 49982–49988. doi:10.1074/jbc.M209649200

Li, H., Han, S., Sun, Q., Yao, Y., Li, S., Yuan, C., et al. (2019). Long non-coding RNA CDKN2B-AS1 reduces inflammatory response and promotes cholesterol efflux in atherosclerosis by inhibiting ADAM10 expression. *Aging (Albany NY)* 11, 1695–1715. doi:10.18632/aging.101863

Li, X., Liu, R., Wang, Y., Zhu, W., Zhao, D., Wang, X., et al. (2020). Cholangiocyte-derived exosomal lncRNA H19 promotes macrophage activation and hepatic inflammation under cholestatic conditions, *Cells* 9, 190. doi:10.3390/cells9010190

Lin, H.-S., Gong, J.-N., Su, R., Chen, M.-T., Song, L., Shen, C., et al. (2014). miR-199a-5p inhibits monocyte/macrophage differentiation by targeting the activin A type 1B receptor gene and finally reducing C/EBPα expression. *J. Leukoc. Biol.* 96, 1023–1035. doi:10.1189/jlb.1A0514-240R

Liu, Y.-C., Zou, X.-B., Chai, Y.-F., and Yao, Y.-M. (2014). Macrophage polarization in inflammatory diseases. *Int. J. Biol. Sci.* 10, 520–529. doi:10.7150/ijbs.8879

Lu, J., Ji, H., Tang, H., and Xu, Z. (2018). microRNA-124a suppresses PHF19 over-expression, EZH2 hyper-activation, and aberrant cell proliferation in human glioma. *Biochem. Biophys. Res. Commun.* 503, 1610–1617. doi:10.1016/j.bbrc.2018.07.089

Lu, W., He, X., Su, L., and Miao, J. (2019). Long noncoding RNA-CERNA1 stabilized atherosclerotic plaques in apolipoprotein E−/− mice. *J. Cardiovasc. Trans. Res.* 12, 425–434. doi:10.1007/s12265-019-09883-4

Lv, Y.-C., Tang, Y.-Y., Zhang, P., Wan, W., Yao, F., He, P.-P., et al. (2016). Histone methyltransferase enhancer of zeste homolog 2-mediated ABCA1 promoter

DNA methylation contributes to the progression of atherosclerosis. *PLoS One.* 11, e0157265. doi:10.1371/journal.pone.0157265

Maguire, E. M., Pearce, S. W. A., and Xiao, Q. (2019). Foam cell formation: a new target for fighting atherosclerosis and cardiovascular disease. *Vasc. Pharmacol.* 112, 54–71. doi:10.1016/j.vph.2018.08.002

Maguire, E. M., and Xiao, Q. (2020). Noncoding RNAs in vascular smooth muscle cell function and neointimal hyperplasia. *FEBS J.* [Epub ahead of print] doi:10.1111/febs.15357

Mantovani, A., Sica, A., Sozzani, S., Allavena, P., Vecchi, A., and Locati, M. (2004). The chemokine system in diverse forms of macrophage activation and polarization. *Trends Immunol.* 25, 677–686. doi:10.1016/j.it.2004.09.015

Mathy, N. W., and Chen, X.-M. (2017). Long non-coding RNAs (lncRNAs) and their transcriptional control of inflammatory responses. *J. Biol. Chem.* 292, 12375–12382. doi:10.1074/jbc.R116.760884

McHugh, C. A., Chen, C.-K., Chow, A., Surka, C. F., Tran, C., McDonel, P., et al. (2015). The Xist lncRNA interacts directly with SHARP to silence transcription through HDAC3. *Nature* 521, 232–236. doi:10.1038/nature14443

McLaren, J. E., Michael, D. R., Ashlin, T. G., and Ramji, D. P. (2011). Cytokines, macrophage lipid metabolism and foam cells: implications for cardiovascular disease therapy. *Prog. Lipid Res.* 50, 331–347. doi:10.1016/j.plipres.2011.04.002

Melgarejo, E., Medina, M. Á., Sánchez-Jiménez, F., and Urdiales, J. L. (2009). Monocyte chemoattractant protein-1: a key mediator in inflammatory processes. *Int. J. Biochem. Cell Biol.* 41, 998–1001. doi:10.1016/j.biocel.2008.07.018

Meng, X.-D., Yao, H.-H., Wang, L.-M., Yu, M., Shi, S., Yuan, Z.-X., et al. (2020). Knockdown of GAS5 inhibits atherosclerosis progression via reducing EZH2-mediated ABCA1 transcription in ApoE(-/-) mice. *Mol. Ther. Nucleic Acids* 19, 84–96. doi:10.1016/j.omtn.2019.10.034

Mestas, J., and Ley, K. (2008). Monocyte-endothelial cell interactions in the development of atherosclerosis. *Trends Cardiovasc. Med.* 18, 228–232. doi:10.1016/j.tcm.2008.11.004

Miano, J. M., Firulli, A. B., Olson, E. N., Hara, P., Giachelli, C. M., and Schwartz, S. M. (1996). Restricted expression of homeobox genes distinguishes fetal from adult human smooth muscle cells. *Proc. Natl. Acad. Sci. U.S.A.* 93, 900–905. doi:10.1073/pnas.93.2.900

Mitchell, J. P., and Carmody, R. J. (2018). NF-κB and the transcriptional control of inflammation. *Int. Rev. Cell Mol. Biol.* 335, 41–84. doi:10.1016/bs.ircmb.2017.07.007

Moore, K. J., and Freeman, M. W. (2006). Scavenger receptors in atherosclerosis: beyond lipid uptake. *Arterioscler. Thromb. Vasc. Biol.* 26, 1702–1711. doi:10.1161/01.Atv.0000229218.97976.43

Moore, K. J., Sheedy, F. J., and Fisher, E. A. (2013). . *Nat. Rev. Immunol.* 13, 709–721. doi:10.1038/nri3520

Moore, K. J., and Tabas, I. (2011). Macrophages in the pathogenesis of atherosclerosis. *Cell* 145, 341–355. doi:10.1016/j.cell.2011.04.005

Nádró, B., Juhász, L., Szentpéteri, A., Páll, D., Paragh, G., and Harangi, M. (2018). The role of apolipoprotein M and sphingosine 1-phosphate axis in the prevention of atherosclerosis]. *Orv. Hetil.* 159, 168–175. [in Hu]. doi:10.1556/650.2018.30980

Ou, M., Li, X., Zhao, S., Cui, S., and Tu, J. (2020). Long non-coding RNA CDKN2B-AS1 contributes to atherosclerotic plaque formation by forming RNA-DNA triplex in the CDKN2B promoter. *EBioMedicine* 55, 102694. doi:10.1016/j.ebiom.2020.102694

Panee, J. (2012). Monocyte chemoattractant protein 1 (MCP-1) in obesity and diabetes. *Cytokine* 60, 1–12. doi:10.1016/j.cyto.2012.06.018

Paulson, K. E., Zhu, S.-N., Chen, M., Nurmohamed, S., Jongstra-Bilen, J., and Cybulsky, M. I. (2010). Resident intimal dendritic cells accumulate lipid and contribute to the initiation of atherosclerosis. *Circ. Res.* 106, 383–390. doi:10.1161/circresaha.109.210781

Perkins, N. D. (2007). Integrating cell-signalling pathways with NF-κB and IKK function. *Nat. Rev. Mol. Cell Biol.* 8, 49–62. doi:10.1038/nrm2083

Ponnusamy, M., Liu, N., Gong, R., Yan, H., and Zhuang, S. (2011). ERK pathway mediates P2X7 expression and cell death in renal interstitial fibroblasts exposed to necrotic renal epithelial cells. *Am. J. Physiol. Ren. Physiol.* 301, F650–F659. doi:10.1152/ajprenal.00215.2011

Qin, H., Wilson, C. A., Lee, S. J., Zhao, X., and Benveniste, E. N. (2005). LPS induces CD40 gene expression through the activation of NF-κB and STAT-1α in macrophages and microglia. *Blood* 106, 3114–3122. doi:10.1182/blood-2005-02-0759

Rahman, M. M., and McFadden, G. (2011). Modulation of NF-κB signalling by microbial pathogens. *Nat. Rev. Microbiol.* 9, 291–306. doi:10.1038/nrmicro2539

Reddy, M. A., Chen, Z., Park, J. T., Wang, M., Lanting, L., Zhang, Q., et al. (2014). Regulation of inflammatory phenotype in macrophages by a diabetes-induced long noncoding RNA. *Diabetes* 63, 4249–4261. doi:10.2337/db14-0298

Sallam, T., Jones, M., Thomas, B. J., Wu, X., Gilliland, T., Qian, K., et al. (2018). Transcriptional regulation of macrophage cholesterol efflux and atherogenesis by a long noncoding RNA. *Nat. Med.* 24, 304–312. doi:10.1038/nm.4479

Shapouri-Moghaddam, A., Mohammadian, S., Vazini, H., Taghadosi, M., Esmaeili, S.-A., Mardani, F., et al. (2018). Macrophage plasticity, polarization, and function in health and disease. *J. Cell. Physiol.* 233, 6425–6440. doi:10.1002/jcp.26429

Shen, H., Sheng, L., Chen, Z., Jiang, L., Su, H., Yin, L., et al. (2014). Mouse hepatocyte overexpression of NF-κB-inducing kinase (NIK) triggers fatal macrophage-dependent liver injury and fibrosis. *Hepatology* 60, 2065–2076. doi:10.1002/hep.27348

Shi, J., Gao, W., and Shao, F. (2017). Pyroptosis: gasdermin-mediated programmed necrotic cell death. *Trends Biochem. Sci.* 42, 245–254. doi:10.1016/j.tibs.2016.10.004

Shi, X., Liu, Z., Feng, X., Hua, F., Hu, X., et al. (2018). Long noncoding RNA PCAT6 functions as an oncogene by binding to EZH2 and suppressing LATS2 in non-small-cell lung cancer. *EBioMedicine* 37, 177–187. doi:10.1016/j.ebiom.2018.10.004

Skaug, B., Jiang, X., and Chen, Z. J. (2009). The role of ubiquitin in NF-κB regulatory pathways. *Annu. Rev. Biochem.* 78, 769–796. doi:10.1146/annurev.biochem.78.070907.102750

Stefulj, J., Panzenboeck, U., Becker, T., Hirschmugl, B., Schweinzer, C., Lang, I., et al. (2009). Human endothelial cells of the placental barrier efficiently deliver cholesterol to the fetal circulation via ABCA1 and ABCG1. *Circ. Res.* 104, 600–608. doi:10.1161/circresaha.108.185066

Sun, C., Fu, Y., Gu, X., Xi, X., Peng, X., Wang, C., et al. (2020). Macrophage-enriched lncRNA RAPIA: a novel therapeutic target for atherosclerosis. *Arterioscler. Thromb. Vasc. Biol.* 40, 1464–1478. doi:10.1161/ATVBAHA.119.313749

Sun, D., Yu, Z., Fang, X., Liu, M., Pu, Y., Shao, Q., et al. (2017). Lnc RNA GAS 5 inhibits microglial M2 polarization and exacerbates demyelination. *EMBO Rep.* 18, 1801–1816. doi:10.15252/embr.201643668

Sunami, Y., Leithäuser, F., Gul, S., Fiedler, K., Güldiken, N., Espenlaub, S., et al. (2012). Hepatic activation of IKK/NFκB signaling induces liver fibrosis via macrophage-mediated chronic inflammation. *Hepatology* 56, 1117–1128. doi:10.1002/hep.25711

Tabas, I. (2010). Macrophage death and defective inflammation resolution in atherosclerosis. *Nat. Rev. Immunol.* 10, 36–46. doi:10.1038/nri2675

Tabas, I., and Bornfeldt, K. E. (2016). Macrophage phenotype and function in different stages of atherosclerosis. *Circ. Res.* 118, 653–667. doi:10.1161/circresaha.115.306256

Tabas, I., Li, Y., Brocia, R. W., Xu, S. W., Swenson, T. L., and Williams, K. J. (1993). Lipoprotein lipase and sphingomyelinase synergistically enhance the association of atherogenic lipoproteins with smooth muscle cells and extracellular matrix. A possible mechanism for low density lipoprotein and lipoprotein(a) retention and macrophage foam cell formation. *J. Biol. Chem.* 268, 20419–20432.

Tang, X., Yin, R., Shi, H., Wang, X., Shen, D., Wang, X., et al. (2020). LncRNA ZFAS1 confers inflammatory responses and reduces cholesterol efflux in atherosclerosis through regulating miR-654-3p-ADAM10/RAB22A axis. *Int. J. Cardiol.* 315, 72–80. doi:10.1016/j.ijcard.2020.03.056

Taniguchi, K., and Karin, M. (2018). NF-κB, inflammation, immunity and cancer: coming of age. *Nat. Rev. Immunol.* 18, 309–324. doi:10.1038/nri.2017.142

Tarhda, Z., Semlali, O., Kettani, A., Moussa, A., Abumrad, N. A., and Ibrahimi, A. (2013). Three dimensional structure prediction of fatty acid binding site on human transmembrane receptor CD36. *Bioinf. Biol. Insights* 7, 369–373. doi:10.4137/bbi.S12276

Tichon, A., Gil, N., Lubelsky, Y., Havkin Solomon, T., Lemze, D., Itzkovitz, S., et al. (2016). A conserved abundant cytoplasmic long noncoding RNA modulates repression by pumilio proteins in human cells. *Nat. Commun.* 7, 12209. doi:10.1038/ncomms12209

van der Vorst, E., Weber, C., and Donners, M. (2018). A disintegrin and metalloproteases (ADAMs) in cardiovascular, metabolic and inflammatory

diseases: aspects for theranostic approaches. *Thromb. Haemostasis* 118, 1167–1175. doi:10.1055/s-0038-1660479

Verreck, F. A. W., de Boer, T., Langenberg, D. M. L., Hoeve, M. A., Kramer, M., Vaisberg, E., et al. (2004). Human IL-23-producing type 1 macrophages promote but IL-10-producing type 2 macrophages subvert immunity to (myco)bacteria. *Proc. Natl. Acad. Sci. U.S.A.* 101, 4560–4565. doi:10.1073/pnas.0400983101

Virmani, R., Burke, A. P., Kolodgie, F. D., and Farb, A. (2002). Vulnerable plaque: the pathology of unstable coronary lesions. *J. Intervent. Cardiol.* 15, 439–446. doi:10.1111/j.1540-8183.2002.tb01087.x

Wang, J., Cao, B., Han, D., Sun, M., and Feng, J. (2017). Long non-coding RNA H19 induces cerebral ischemia reperfusion injury via activation of autophagy. *Ae&D* 8, 71–84. doi:10.14336/ad.2016.0530

Wang, K. C., and Chang, H. Y. (2011). Molecular mechanisms of long noncoding RNAs. *Mol. Cell* 43, 904–914. doi:10.1016/j.molcel.2011.08.018

Wang, L., Xia, J.-W., Ke, Z.-P., and Zhang, B.-H. (2019). Blockade of NEAT1 represses inflammation response and lipid uptake via modulating miR-342-3p in human macrophages THP-1 cells. *J. Cell. Physiol.* 234, 5319–5326. doi:10.1002/jcp.27340

Wang, L. X., Zhang, S. X., Wu, H. J., Rong, X. I., and Guo, J. (2019). M2b macrophage polarization and its roles in diseases. *J. Leukoc. Biol.* 106, 345–358. doi:10.1002/JLB.3RU1018-378RR

Williams, K. J., and Tabas, I. (1995). The response-to-retention hypothesis of early atherogenesis. *Arterioscler. Thromb. Vasc. Biol.* 15, 551–561. doi:10.1161/01.atv.15.5.551

Wu, G., Cai, J., Han, Y., Chen, J., Huang, Z.-P., Chen, C., et al. (2014). LincRNA-p21 regulates neointima formation, vascular smooth muscle cell proliferation, apoptosis, and atherosclerosis by enhancing p53 activity. *Circulation* 130, 1452–1465. doi:10.1161/CIRCULATIONAHA.114.011675

Wu, H., Wen, F., Jiang, M., Liu, Q., and Nie, Y. (2018). LncRNA uc.48+ is involved in the diabetic immune and inflammatory responses mediated by P2X7 receptor in RAW264.7 macrophages. *Int. J. Mol. Med.* 42, 1152–1160. doi:10.3892/ijmm.2018.3661

Xie, J., Li, Q., Zhu, X.-h., Gao, Y., and Zhao, W.-h. (2019). IGF2BP1 promotes LPS-induced NFκB activation and pro-inflammatory cytokines production in human macrophages and monocytes. *Biochem. Biophys. Res. Commun.* 513, 820–826. doi:10.1016/j.bbrc.2019.03.206

Xie, Y., Wang, M., Tian, J., Li, X., Yang, M., Zhang, K., et al. (2019). Long non-coding RNA expressed in macrophage co-varies with the inflammatory phenotype during macrophage development and polarization. *J. Cell Mol. Med.* 23, 6530–6542. doi:10.1111/jcmm.14557

Xie, Z., Zhang, H., Wang, J., Li, Z., Qiu, C., and Sun, K. (2019). LIN28B-AS1-IGF2BP1 association is required for LPS-induced NFκB activation and pro-inflammatory responses in human macrophages and monocytes. *Biochem. Biophys. Res. Commun.* 519, 525–532. doi:10.1016/j.bbrc.2019.09.012

Xu, Y.-J., Zheng, L., Hu, Y.-W., and Wang, Q. (2018). Pyroptosis and its relationship to atherosclerosis. *Clin. Chim. Acta* 476, 28–37. doi:10.1016/j.cca.2017.11.005

Yang, L., and Li, T. (2020). LncRNA TUG1 regulates ApoM to promote atherosclerosis progression through miR-92a/FXR1 axis. *J. Cell Mol. Med.* 24, 8836. doi:10.1111/jcmm.15521

Yap, K., Mukhina, S., Zhang, G., Tan, J. S. C., Ong, H. S., and Makeyev, E. V. (2018). A short tandem repeat-enriched RNA assembles a nuclear compartment to control alternative splicing and promote cell survival. *Mol. Cell* 72, 525–540.e13. doi:10.1016/j.molcel.2018.08.041

Ye, J., Wang, C., Wang, D., and Yuan, H. (2018). LncRBA GSA5, up-regulated by ox-LDL, aggravates inflammatory response and MMP expression in THP-1 macrophages by acting like a sponge for miR-221. *Exp. Cell Res.* 369, 348–355. doi:10.1016/j.yexcr.2018.05.039

Yin, Q., Wu, A., and Liu, M. (2017). Plasma Long Non-Coding RNA (lncRNA) GAS5 is a New Biomarker for Coronary Artery Disease. *Med. Sci. Monit.* 23, 6042–6048. doi:10.12659/msm.907118

Yong, H., Hong, Q., Xing, P., Yigang, F., Hongyan, T., and Jie, G. (2018). Low-dose sinapic acid abates the pyroptosis of macrophages by downregulation of lncRNA-MALAT1 in rats with diabetic atherosclerosis. *J. Cardiovasc. Pharmacol.* 71 104–112.

Yu, B.-y., and Dong, B. (2018). LncRNA H19 regulates cardiomyocyte apoptosis and acute myocardial infarction by targeting miR-29b. *Int. J. Cardiol.* 271, 25. doi:10.1016/j.ijcard.2018.04.108

Zanin, R. F., Bergamin, L. S., Morrone, F. B., Coutinho-Silva, R., de Souza Wyse, A. T., and Battastini, A. M. O. (2015). Pathological concentrations of homocysteine increases IL-1β production in macrophages in a P2X7, NF-κB, and erk-dependent manner. *Purinergic Signal.* 11, 463–470. doi:10.1007/s11302-015-9464-5

Zeng, Y., Ren, K., Zhu, X., Zheng, Z., and Yi, G. (2018). Long noncoding RNAs: advances in lipid metabolism. *Adv. Clin. Chem.* 87, 1–36. doi:10.1016/bs.acc.2018.07.001

Zhang, D.-D., Wang, W.-T., Xiong, J., Xie, X.-M., Cui, S.-S., Zhao, Z.-G., et al. (2017). Long noncoding RNA LINC00305 promotes inflammation by activating the AHRR-NF-κB pathway in human monocytes. *Sci. Rep.* 7, 46204. doi:10.1038/srep46204

Zhao, G., Su, Z., Song, D., Mao, Y., and Mao, X. (2016). The long noncoding RNA MALAT1 regulates the lipopolysaccharide-induced inflammatory response through its interaction with NF-κB. *FEBS Lett.* 590, 2884–2895. doi:10.1002/1873-3468.12315

Conflict of Interest: The authors declare that the research was conducted in the absence of any commercial or financial relationships that could be construed as a potential conflict of interest.

Copyright © 2020 Ma, Liu and Chen.. This is an open-access article distributed under the terms of the Creative Commons Attribution License (CC BY). The use, distribution or reproduction in other forums is permitted, provided the original author(s) and the copyright owner(s) are credited and that the original publication in this journal is cited, in accordance with accepted academic practice. No use, distribution or reproduction is permitted which does not comply with these terms.

frontiers in Pharmacology

ORIGINAL RESEARCH
published: 12 April 2021
doi: 10.3389/fphar.2020.574656

The Cardioprotective Mechanism of Phenylaminoethyl Selenides (PAESe) Against Doxorubicin-Induced Cardiotoxicity Involves Frataxin

Xiaoyu Fu[1], Mathew Eggert[1], Sieun Yoo[2], Nikhil Patel[1], Juming Zhong[2], Ian Steinke[1], Manoj Govindarajulu[1], Emine Akyuz Turumtay[3], Shravanthi Mouli[1], Peter Panizzi[1†], Ronald Beyers[4,5], Thomas Denney[4,5], Robert Arnold[1†] and Rajesh H. Amin[1*†]*

[1]Department of Drug, Discovery and Development, Harrison School of Pharmacy, Auburn University, Alabama, AL, United States, [2]Department of Anatomy, Physiology and Pharmacology, College of Veterinary Medicine, Auburn University, Auburn, AL, United States, [3]Department of Chemistry, Recep Tayyip Erdogan University, Rize, Turkey, [4]Department of Electrical and Computer Engineering, Auburn University, Auburn, AL, United States, [5]Auburn University M.R.I. Research Center, Auburn, AL, United States

Doxorubicin (DOX) is an anthracycline cancer chemotherapeutic that exhibits cumulative dose-limiting cardiotoxicity and limits its clinical utility. DOX treatment results in the development of morbid cardiac hypertrophy that progresses to congestive heart failure and death. Recent evidence suggests that during the development of DOX mediated cardiac hypertrophy, mitochondrial energetics are severely compromised, thus priming the cardiomyocyte for failure. To mitigate cumulative dose (5 mg/kg, QIW x 4 weeks with 2 weeks recovery) dependent DOX, mediated cardiac hypertrophy, we applied an orally active selenium based compound termed phenylaminoethyl selenides (PAESe) (QIW 10 mg/kg x 5) to our animal model and observed that PAESe attenuates DOX-mediated cardiac hypertrophy in athymic mice, as observed by MRI analysis. Mechanistically, we demonstrated that DOX impedes the stability of the iron-sulfur cluster biogenesis protein Frataxin (FXN) (0.5 fold), resulting in enhanced mitochondrial free iron accumulation (2.5 fold) and reduced aconitase activity (0.4 fold). Our findings further indicate that PAESe prevented the reduction of FXN levels and the ensuing elevation of mitochondrial free iron levels. PAESe has been shown to have anti-oxidative properties in part, by regeneration of glutathione levels. Therefore, we observed that PAESe can mitigate DOX mediated cardiac hypertrophy by enhancing glutathione activity (0.4 fold) and inhibiting ROS formation (1.8 fold). Lastly, we observed that DOX significantly reduced cellular respiration (basal (5%) and uncoupled (10%)) in H9C2 cardiomyoblasts and that PAESe protects against the DOX-mediated attenuation of cellular respiration. In conclusion, the current study determined the protective mechanism of PAESe against DOX mediated myocardial damage and that FXN is implicitly involved in DOX-mediated cardiotoxicity.

Keywords: doxorubicin, phenylaminoethyl selenides, frataxin, cardiomyopathy, cardiotoxicity, glutathione, mitochondrial metabolism

OPEN ACCESS

Edited by:
Jun Ren,
University of Washington,
United States

Reviewed by:
Lei Xi,
Virginia Commonwealth University,
United States
Qiangrong Liang,
New York Institute of Technology,
United States

****Correspondence:***
Robert Arnold
rda0007@auburn.edu
Rajesh H. Amin
rha0003@auburn.edu

†ORCID:
Robert D. Arnold
orcid.org//0000-0001-6143-3991
Peter Panizzi
orcid.org/0000-0003-0141-8807
Rajesh H. Amin
orcid.org/0000-0001-8741-0018

Specialty section:
This article was submitted to Cardiovascular and Smooth Muscle Pharmacology, a section of the journal Frontiers in Pharmacology

Received: *25 June 2020*
Accepted: *09 September 2020*
Published: *12 April 2021*

Citation:
Fu X, Eggert M, Yoo S, Patel N, Zhong J, Steinke I, Govindarajulu M, Turumtay EA, Mouli S, Panizzi P, Beyers R, Denney T, Arnold R and Amin RH (2021) The Cardioprotective Mechanism of Phenylaminoethyl Selenides (PAESe) Against Doxorubicin-Induced Cardiotoxicity Involves Frataxin. Front. Pharmacol. 11:574656. doi: 10.3389/fphar.2020.574656

INTRODUCTION

Doxorubicin (DOX) is an anthracycline cancer chemotherapeutic agent that is used widely for the treatment of multiples cancers, including prostate, breast, lung, bone, and leukemias (Kuerer et al., 1999; Khan and Denmeade, 2000; Neville-Webbe et al., 2005). However, DOX use is also associated with the development of drug resistance and several adverse effects (Cersosimo and Hong, 1986; Lipshultz et al., 1991; Solem et al., 1996; Tada et al., 2002), including cumulative dose-dependent cardiotoxicity that leads to cardiac failure (CF) and has been reported to be one of most significant challenges associated with its clinical efficacy (Arola et al., 2000). Therefore, reducing DOX-induced toxicity without dampening its anti-cancer activity is critical to optimizing its use and effectively treating different cancers.

It has been well established that energy starvation plays an important role in the mechanism underlying DOX-induced cardiac failure (Ashour et al., 2012). Altered mitochondrial bioenergetics has attracted attention among researchers due to its association with reduced ATP generation and heart failure (Rajamanickam et al., 1979; Wang et al., 1999; Tokarska-Schlattner et al., 2006; Berthiaume and Wallace, 2007; Xu et al., 2020). For example, cardiac hypertrophy is associated with changes in mitochondrial morphology and numbers (Rajamanickam et al., 1979; Ong and Hausenloy, 2010). Furthermore, studies demonstrated that DOX-induced cardiomyopathy and the eventual cardiotoxicity was caused by mitochondrial iron accumulation (Kwok and Richardson, 2004; Mouli et al., 2015). Frataxin is a mitochondrial iron-sulfur cluster biogenesis protein and plays an important role in regulating mitochondrial energetics and cellular metabolism (Koutnikova et al., 1997). Patient's with Friedreich's Ataxia (FRDA) display an autosomal recessive mutation in the frataxin gene on chromosome nine and display symptoms such as ataxia, diabetes, limb failure, and severe cardiomyopathy (Durr et al., 1996; Campuzano et al., 1997). Previous reports from our lab have determined that DOX-induced cardiotoxicity was associated with attenuation of FXN. (Mouli et al., 2015). Furthermore, overexpression of FXN offered significant cardioprotection against DOX exposure (Mouli et al., 2015).

In the current study, we explored the novel application of a selenium-containing compound, phenylaminoethyl selenides (PAESe), as a potential therapeutic agent for reducing DOX-induced cardiotoxicity. Previous reports have shown that PAESe has antihypertensive and antioxidant activity (Herman et al., 1988; Pollock et al., 1988; Kang et al., 2011). Glutathione peroxidase, a cellular reductant, and well-known glutathione (GSH) replenisher was found to be directly involved and required in the redox cycling of PAESe antioxidant activity (De Silva et al., 2004; Cowan et al., 2011). Recently, we demonstrated that PAESe reduced DOX-induced cardiotoxicity in athymic mice with human prostate cancer xenografts by increasing cell viability and reducing reactive oxidant species (ROS) generation without diminishing the antitumor activity of DOX treatments (Kang et al., 2011; Cowan et al., 2011).

Based on a mechanistic understanding of Frataxin and the descriptive observations related to PAESe's cardio-protective activity, we hypothesize that PAESe protects against DOX-induced cardiotoxicity through stabilizing mitochondrial bioenergetic metabolism and mitigating the attenuation of frataxin expression through antioxidant mechanisms by recycling GSH. Here we describe the molecular basis for the observed cardioprotective activity of PAESe against DOX-induced cardiotoxicity.

METHODS AND MATERIALS

Animals

Juvenile NCr athymic (*nu/nu*) mice were obtained from Taconic (Tarrytown, NY) and maintained according to an approved Institutional Animal Care Use Committee protocol at Auburn University. Mice were housed in a controlled environment (23°C; 12:12-h light-dark cycle) with *ad libitum* access to water and standard chow diet. Juvenile (6–8 week old) mice were randomly divided into four groups, saline (control), DOX, DOX + PAESe, PAESe. Mice received weekly tail vein injections of saline, DOX (QIW 5 mg/kg in saline x 5) for a cumulative dose of 25 mg/kg of DOX, PAESe in saline (10 mg/kg), or DOX + PAESe (QIW 10 mg/kg x 5) over four weeks followed by two weeks of recovery with no treatment. At two weeks after the last dose, hearts were surgically removed immediately after exsanguination, snap-frozen in liquid nitrogen, and stored at −80°C for further use.

MRI Measurements of Cardiac Parameters

Magnetic resonance imaging (MRI) was completed at the AU-MRI Research Center. Cardiac volumetric functional parameters for left ventricular (LV) end-diastolic (E.D.) volume, end-systolic (ES) volume, ejection fraction (EF), ejection volume (EV), and LV mass were calculated using Matlab (Mathworks, Natick, MA) and bull's eye graphing. Wall thickness was calculated as the radial distance between the endo- and epicardial contours and wall thickening as percent change from the end-diastolic (ED) wall thickness to end-systolic (ES) wall thickness. Both endo- and epicardial contours were traced on the short-axis (SA), and images that were acquired were at the E.D. and E.S. phases. The values attained from the areas defined by these contours included the associated per-slice E.D. volume (EDV), E.S. volume (ESV), LV ejection fraction (LVEF), LV ejection volume (LVEV), and thus allowing the LV mass to be calculated; where LV mass = LV volume * 1.055 g/cm^3. The sum of the individual S.A. slice parameters provided whole-LV volumetric parameters.

Cell Cultures

Rat-derived embryonic ventricular cardiomyoblast (H9C2) cells were purchased from ATCC (CRL-1446) and cultured according to the manufactures recommendations. In brief, cells were grown in DMEM supplemented with 10% (v/v) fetal bovine serum and 1% (v/v) Pen-Strep. Before drug treatment, cells were counted and plated with equivalent numbers of cells (density) based upon plate size into several 100 or 150 mm^2 plastic cell culture plates for drug treatment.

Drug Treatment *In Vitro*

DOX was purchased from Sigma-Aldrich (St. Louis, MO), and phenylaminoethyl selenide (PAESe) was synthesized and provided by Dr. Sheldon May (Georgia Tech). DOX and PAESe were reconstituted in DMSO. Cells were treated with complete DMEM media containing the desired concentration of drugs for 24 h. In this study, cells were treated with or without DOX (10 μm) for 24 h, followed by incubation with or without PAESe (1 μM) for an additional 24 h.

Western Immunoblot

Heart tissue lysates were homogenized using a polytron tissue disruptor in cell lysis buffer (Cell Signaling Technologies cat. #9803) with protease cocktail inhibitor (Thermo Sci. cat. #87786). Proteins were extracted from H9C2 cardiomyoblasts and heart tissue with cell lysis buffer and supplemented with protease cocktail inhibitor. Proteins were standardized using a Nanodrop (Thermo Scientific). Changes in FXN levels were measured by western analysis as described previously using FXN (1:1,000, SantaCruz, cat. #25830) antibody (Mouli et al., 2015; Nanayakkara et al., 2015). Briefly, protein lysates were denatured, resolved and blotted on a nitrocellulose membrane. The blots were stained with primary antibodies, FXN (1:1,000, Santa Cruz, cat. #25830) and α-tubulin (1:2,000, DSHBY, cat. #12G10), washed with Tris-buffered saline-Tween and incubated with a secondary - horseradish peroxidase-conjugated antibody (1:2,000, Rockland) for 1 h. Blots were visualized with chemiluminescence reagent (Millipore) and imaged on a Bio-Rad gel dock system. Protein bands were analyzed using Quantity One software (BioRad) or ImageJ software and standardized to α-tubulin.

Gene Expression

Changes in markers (gene expression) associated with ventricular size enlargement were measured by real-time PCR analysis. Total R.N.A. was extracted from animal tissues and cultured H9C2 cardiomyocytes with or without DOX using Trizol (Invitrogen) following the recommended protocol from Invitrogen. Briefly, heart tissues were crushed in liquid nitrogen with mortar and pestle into a fine powder. Trizol was then added to each sample and combined with 0.1 ml chloroform into each tube. Partition containing R.N.A. was isolated by centrifugation (12,000 g for 15 min at 4°C). The upper aqueous phase containing R.N.A. was isolated and combined with isopropanol, centrifuged again at 12,000 g for 10 min at 4°C. R.N.A. pellet was washed with 75% ethanol, and then centrifuge at 7,500 g for 5 min at 4°C. R.N.A. pellets were then air-dried and reconstituted into RNAse free water. cDNA was synthesized from R.N.A. using a first strand OneScript cDNA synthesis kit (A.B.M.).

Markers of cardiac hypertrophy were detected by qPCR analysis using a BrightGreen 2X qPCR MasterMix (A.B.M.). Sequences of probes for β-MHC are as follows: Forward 5′-AAG GAG GAG TTT GGG CGA GTC AAA-3′ and reverse 5′-TGC ATC CGC CAA GTT GTC TTG TTC-3'. Sequences of probes for A.N.P. are as follows: Forward 5′-AGA CAG CAA ACA TCA GAT CGT GCC-3′ and reverse 5′-ATC TGT GTT GGA CAC CGC ACT GTA-3'. Sequences of probes for β-Actin are as follows: Forward 5′-TTG CTG ACA GGA TGC AGA AGG AGA-3′ and reverse 5′-ACT CCT GCT TGC TGA TCC ACA TCT-3'. Data analysis was conducted using ΔΔCt method (Zhang et al., 2013; Pabinger et al., 2014).

Aconitase Assay

Aconitase activity was measured using Aconitase Assay Kit (Cayman chemicals, cat. #705502). Mechanistically, aconitase catalyzes the isomerization of citrate to isocitrate, which is then converted to α-ketoglutarate by isocitrate dehydrogenase. Cells were grown in 150 mm^2 plates and treated with or without DOX (10 μM) for 24 h, followed by incubation of PAESe (1 μM). Aconitase enzyme activity was monitored from isolated mitochondria and based on assay protocol by measuring the change in absorbance at 340 nm that is associated with the formation of NADPH using a Cytation 5 (BioTek) multimodal imaging reader. Values were standardized by protein concentrations, as measured by Nanodrop (Thermo).

Cardiac Troponin Assay (cTnI)

Cardiac troponin-I (cTnI) is a component of the troponin complex that regulates cardiac muscle contraction. After cardiac injury, cTnI is released into the circulation. The current ELISA measures troponin expressed specifically in cardiomyocytes and therefore it is an excellent biomarker of cardiac injury. ELISA for mouse cTnI was purchased from Life Diagnostics (Cat # CTNI-1-HS). Briefly, cTnI was measured from serum samples (100 μL). Values were determined from samples by the endpoint method, where plates are measured at 450 nm after 5 min at room temperature using a Cytation five multimodal imaging reader. Concentrations of cTnI from measured samples were based upon given concentration curve of mouse cTnI from the ELISA kit. Final values were represented as per ml of blood.

Glutathione Assay

Glutathione peroxidase activity was measured using a Glutathione Peroxidase Assay Kit (Cayman Chemical). Cells were grown in 150 mm^2 plates and treated with or without DOX (10 μM) for 24 h, followed by incubation of PAESe (1 μM). Briefly, heart tissue samples from mice were washed with PBS and then snap-frozen and ground to a powder with liquid nitrogen using a mortar and pestle (as per instructions form the kit). Tissue and cell pellets were reconstituted in MES buffer (supplied in kit). Values were standardized by protein concentrations, as determined by Nanodrop (Thermo). Glutathione peroxidase activity from samples was determined by the endpoint method, where plates are read at 405–414 nm after 25 min at room temperature using a Cytation five multimodal imaging reader.

Mitochondrial Respiration

Cellular respiration was measured as previously described (Koves et al., 2005). Following DOX (10 μM) with or without PAESe (1 μM) treatment, H9C2 cells were washed in PBS, trypsinized and centrifuged at 800 g for 3 min. Cellular particulate pellets were then washed and resuspended in 400 μL PBS containing 10 mM glucose, 10 mM HEPES, 0.2% B.S.A. and pH 7.45 and

maintained at 37°C. After that, 300 μL of glucose supplemented PBS was added to the oximeter chamber (Hansatech Instruments, Pentney, United Kingdom) and equilibrated for approximately 1 min after which, 350 μL of the cell suspension solution was added. The basal respiration rate was then recorded for approximately 5 min. Subsequently, 6 μM FCCP (OXPHOS uncoupler) was added, and respiration was monitored for an additional 2 min. Basal (coupled) and maximal (uncoupled) respiration rates were normalized to protein concentrations from cells (50 μL of aliquot) remaining in supplemented PBS.

Mitochondrial Membrane Potential Assay

The mitochondrial membrane potential was measured utilizing tetramethylrhodamine ethyl ester, TMRE (Biotium, cat. #70016), a positively charged red-orange dye that accumulates in active mitochondria. H9C2 cells treated with or without DOX (10 μM) plus or minus PAESe (1 μM) were plated in a 12 well plate, and mitochondrial membrane potential was determined. Depolarized or inactive mitochondria have reduced membrane potential and therefore fail to sequester TMRE. The cells were stained according to the manufacture's protocol, and the signals were measured (ex/em at 548/575 nm) using a Cytation five multimodal imaging reader.

ATP Assay

The ATP levels were quantified based on a protocol using the ATPlite luminescence ATP detection assay system (PerkinElmer, no. 6016941). H9C2 cells were plated based upon a standardized cell number using a hemocytometer. Cells were then treated with increasing concentrations of DOX (1–50 μM) with or without PAESe (1 μM). Briefly, the bioluminescence represents the reaction between D-luciferin and ATP and was proportional to the ATP concentrations. The luminescence was measured using Glomax luminometer (Promega). Values were standardized to total protein concentrations per well.

Mitochondrial Iron Detection: Ferrozine Colorimetric Assay

Iron detection was performed using a Ferrozine colorimetric assay, which is based upon previously published technique for detection and quantification of free iron by forming a colorimetric complex (Riemer et al., 2004; Nanayakkara et al., 2015). Cultured H9C2 cardiomyocytes were treated with or without DOX (10 μM) for 24 h, followed by incubation with or without PAESe (1 μM). Mitochondrial and cytosolic fractions were isolated from ventricular lysate and H9C2 cell lines and lyzed with NaOH lysis buffer for 45 min. Cellular fractions were then incubated with H.C.L./$KMnO_4$ for 2 h at 60°C, which enhanced the detection of iron in the samples. Absorbance was read at 550 nm and standardized to total protein concentrations.

ROS Measurement

Mitochondrial reactive oxygen species (ROS) was measured using mitochondrial specific dihydrorhodamine (DHR) assay (Biotium). DHR is a ROS indicator that accumulates in the mitochondria and is oxidized to form the charged cationic rhodamine 123, where it exhibits a green fluorescence (505/534 nm). The cells were seeded in a 24-well plate and stained according to the manufacturer's protocol. Briefly, cells were treated with or without DOX (10 μM) for 24 h, followed by incubation of PAESe (1 μM). Fluorescence intensity was detected using a Cytation five multimodal image reader, and analysis was accomplished using Gen5 software and ImageJ software per treatment from four independent sets of experiments. The total fluorescence values were obtained by comparisons of densitometric values to the total area.

Statistical Analysis

Statistical comparisons between groups were determined using paired Student's t-test, and one-way ANOVA was applied to analyze for multiple groups. Data were reported as means ± S.E.M. A p-value ≤0.05 was considered to be a significant difference between groups. All experiments were accomplished with a minimal of N = 3 replicates in three independent experiments.

RESULTS

PAESe Mitigates from the Development of Ventricular Enlargement and Impaired Cardiac Performance (Figure 1)

Chronic administration of DOX at clinically relevant concentrations is known to induce cardiomyopathy, which eventually progresses the heart towards failure (Wang et al., 1998; Karagiannis et al., 2010). The impact of PAESe on chronic DOX (5 mg/kg, QIW x 4 weeks with 2 weeks recovery) mediated changes in cardiac architecture and performance as evaluated in mice using MRI. Following DOX treatment, MRI imaging and analysis revealed an increase in the left ventricular mass (1B) [t (6) = 3.450; $p < 0.05$]. Bull's eye maps were used to illustrate changes in ventricular mass by computational analyses of the cardiac architecture. DOX treatment resulted in an enlargement in the anterolateral segment of the left ventricle by evaluation of changes associated with the left ventricular segmented regions (**Figures 1A,B**). Further MRI analysis measured significant changes in cardiac output in DOX treated mice when compared to control mice [t (10) = 2.914; $p = 0.0155$]. Further that PAESe protected against the reduced cardiac output mediated by DOX [t (10) = 2.691; $p = 0.0227$]. However, mice treated with DOX plus PAESe did not show enlargement in the anterolateral and lateral regions of the heart (**Figures 1C,D**). However, the addition of PAESe to DOX treatment appeared to protect against this observed increase (non-significant) in mean LV mass [t (6) = 1.787; $p = 0.124$]. Markers associated with cardiac hypertrophy including atrial natriuretic peptide (A.N.P.) (~4 fold) [t (6) = 4.296; $p = 0.005$] and beta-myosin heavy chain (β-MHC) (~3.5 fold) [t (6) = 2.418; $p = 0.052$] were also evaluated following DOX treatment when compared to control mice (**Figures 1D,E**). Together, these data reveal an increase in the size of the left ventricle from mice treated with DOX when compared to

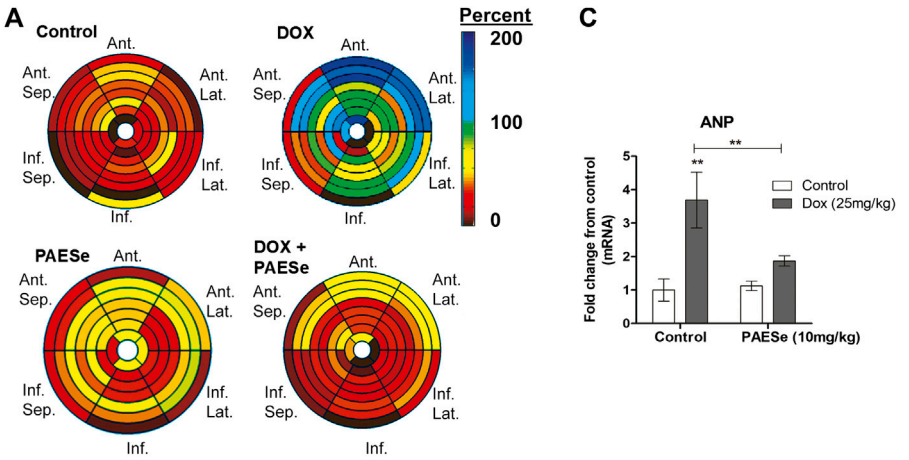

B

Group	Control	DOX	PAESe	DOX+PAESe
Heart rate (beats/min)	415 ± (71)	405 ± (30)	433 ± (26)	410 ± (30)
End Diastolic volume (ul)	58.1 ± (7.9)	78.0 ± (5.9)	54.0 ± (5.4)	61.7 ± (8.1)
End Systolic Volume (ul)	20.4 ± (5.9)	35.7 ± (6.9)	17.8 ± (5.9)	20.8 ± (7.7)
Ejection Volume (%)	64.9 ± (5.3)	54.2± (5.4)	67.0 ± (3.8)	66.0 ± (7.9)
Cardiac Output (ml/min)	15.8 ± (1.8)	12.8 ± (1.0)*	14.2 ± (1.4)	16.8 ± (1.1)#
Left ventricular mass	95.4 ± (3.1)	110 ± (8)*	86.0 ± (6.5)	99.9 ± (8.3)#
Cardiac Troponin I ng/ml of blood	0.452 ± (.071)	1.34 ± (0.211)**	0.584 ± (0.068)	0.722 ± (0.15)#

FIGURE 1 | PAESe protects against DOX-induced cardiac hypertrophy. **(A,B)** PAESe reduces DOX mediated changes in cardiac architecture and performance in athymic mice as determined from MRI analysis. 16 segment model of the LV portion of the Bull's eye plot from MRI scans show the anterio-lateral geometry of the left ventricle (LV) in DOX treated mice (Ant, Anterior; sep, septum; Lat, Lateral; Inf, Inferior). Further MRI the analysis revealed an increase in left ventricular mass index, the effects of DOX on cardiac performance revealed a reduced end-diastolic volume and end-systolic volume, as well as reduced heart rate, ejection volume and overall cardiac output. Measurements of cardiac troponin (cTnI) from serum samples revealed the presences of cardiotoxicity and that PAEse offered cardioprotection against Dox mediated cardiotoxicity. **(C,D)** Measurements of changes in markers for cardiac hypertrophy (ANP and β-MHC) as measured by qRT-PCR analysis in athymic mice treated with Doxorubicin (DOX) (5 mg/kg, one dose per week for 5 weeks, 2 weeks recovery). Values were based on ΔΔct values, which were standardized to β-actin expression. Statistical differences were determined by a student t-test, and comparisons were analyzed based on SEM where n = 4 animals per group. Values are represented as mean ± S.E.M. and were analyzed by student t-test where N = 4 animals per group. *; $p < 0.05$. **;$p < 0.001$

control mice. To further test that PAESe confers protection on cardiac performance in DOX treated mice, we observed by MRI analysis, reduced end-diastolic and end-systolic volumes, as well as reduced heart rate, ejection volume, and overall cardiac output (**Figure 1B**). These data together suggest that PAESe protects the heart against the chronic regimen of DOX that induces compensatory ventricular hypertrophy and potentially progresses to cardiac decompensation. However, DOX also induces cardiotoxicity and therfore we measured circulating levels of cardiac troponin. We observed a significant increase after 2 weeks recovery from cumulative dosing of DOX [t (10) = 3.954; $p = 0.0027$]. We also observed that PAESe reduced DOX mediated increase in cTnI levels in circulation [t (10) = 2.397; $p = 0.0381$]. In **Figure 2**, our *in vitro* findingsobserved that DOX (10 μM) induces an increase in H9C2 cardiomyoblast size [t (6) = 4.240; $p = 0.0280$]. Further that PAESe protected against DOX mediated increase in H9C2 cardiomyoblast size [t (8) = 1.974; $p = 0.838$] as measured by surface area (2A) and gene expression studies (**Figures 3C,D**) [ANP (t (8) = 12.68; $p = 0.0001$)], [MHCβ (t (8) = 3.405; $p = 0.0093$)].

PAESe Mitigates DOX-Induced Cardiotoxicity by Increasing Frataxin Expression Levels (Figure 3)

In the current study, we observed a significant reduction in FXN protein expression in ventricles of hearts from DOX treated athymic mice when compared to our control-treated athymic mice (**Figures 2A,B**) [t (4) = 3.309; $p = 0.0297$]. Furthermore, that PAESe abrogated the deleterious effect of DOX on FXN expression (**Figures 2A,B**) [t (4) = 3.037; $p = 0.385$]. These findings were confirmed in H9C2 cells after exposure to 10 μM DOX, resulting in a significant decrease in both forms of FXN (mitochondrial (18 kDa) and cytosolic (24 and 32 kDa))

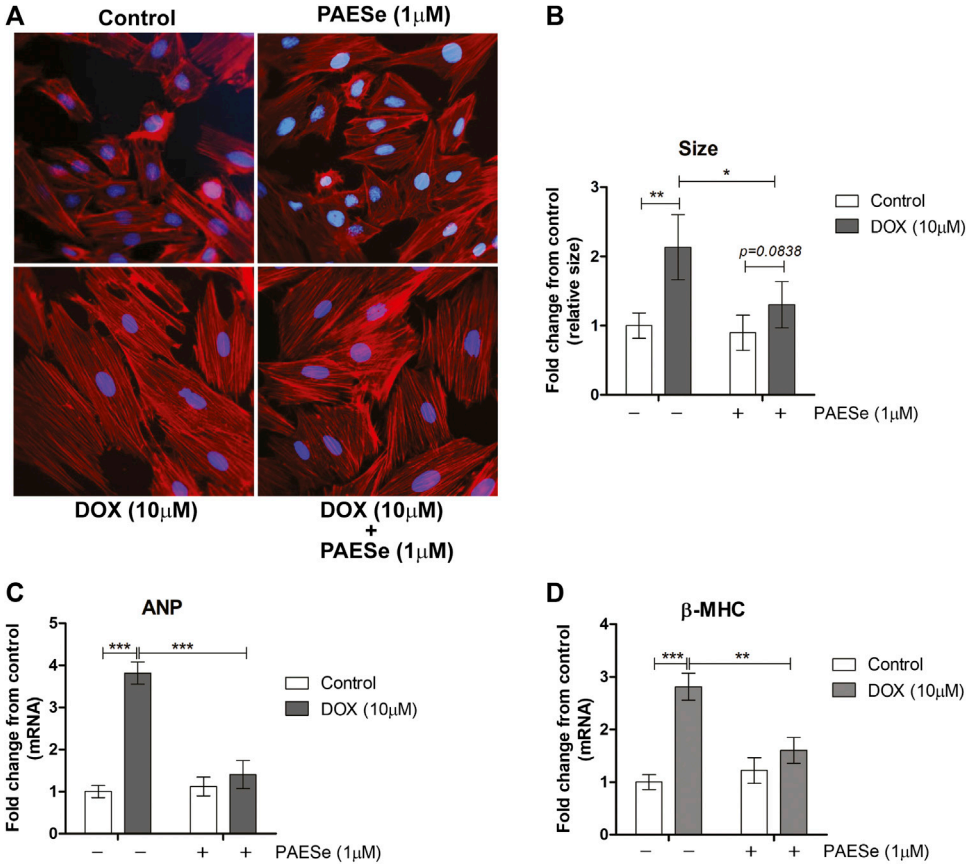

FIGURE 2 | PAESe protects against DOX-induced cardiac hypertrophy in H9C2 cardiomyoblasts. **(A)** Representative phalloidin fluorescence imaging displays protective effects by PAESe (1 μM) against DOX (10 μM) mediated hypertrophy in H9C2 cell as demonstrated by fold change in size by treatment. **(B)** Graphical measurement of morphometric measurements from panel **A**. (**C**,**D**) ANP and β-MHC mRNA expression were evaluated by two-step qPCR analysis from cells treated with DOX (10 μM) with and without PAESe (1 μM) for 24 h. Data are represented as fold change from control and in the case for qPCR analysis standardized to β-actin. Indicated above are the mean ± S.E.M. of the replicates, N = 4 individual experiments, **; $p < 0.001$, ***; $p < 0.0001$, ###; $p < 0.00001$.

after 24 h (**Figure 3B**). However, PAESe was observed to preserve the reduction of FXN by increased concentrations of DOX (**Figures 2C,D**). To further understand the role of FXN in the cellular signaling events leading to cardiac hypertrophy, we constructed Frataxin overexpressing (FXN-OE) H9C2 cardiomyocyte cell lines which have been previously described (Nanayakkara et al., 2015). In the current study, we observed minimal reduction in response to DOX (10 μM) after 24 h (**Figures 2E,F**). Our results suggest that increasing DOX concentrations leads to reduced expression FXN. However, these findings were not replicated in our FXN-OE cells.

DOX Mediated Reduction in Frataxin Attenuates Mitochondrial Iron Homeostasis (Figure 4)

FRDA fibroblasts and yeast mutants (ΔYFH1) display attenuated levels of FXN expression. As a result, both cells display elevated mitochondrial iron accumulation (Cavadini et al., 2000; Huang et al., 2009; Chen et al., 2013). Therefore, we postulated that reduced FXN expression by DOX alters the sub-cellular iron distribution and thereby leads to an increase in mitochondrial iron accumulation. Furthermore, PAESe inhibits the reduction of FXN, resulting in preventing the elevation of mitochondrial iron accumulation. Our DOX treated mice displayed elevated mitochondrial iron accumulation (~2.2 fold increase) and conversely reduced cytosolic iron levels when compared to control mice, as demonstrated by results from our Ferrozine colorimetric iron assay (**Figure 4A**) [t (10) = 13.34; $p = 0.0001$]. Most importantly, we observed that the co-administration of PAESe with DOX in our animal studies prevented the accumulation of iron in the mitochondria [t (10) = 8.254; $p = 0.0001$]. To examine this at a cellular level, we observed that DOX-induced a significant increase in mitochondrial iron accumulation in H9C2 cardiomyoblasts (**Figure 4B**), [t (9) = 17.25; $p = 0.0001$]. Furthermore, we demonstrated that PAESe treatment inhibited DOX-mediated increases in iron accumulation [t (9) = 11.80; $p = 0.0001$]. These results support the hypothesis that PAESe protects against DOX-mediated cellular iron dyshomeostasis, and FXN expression is involved

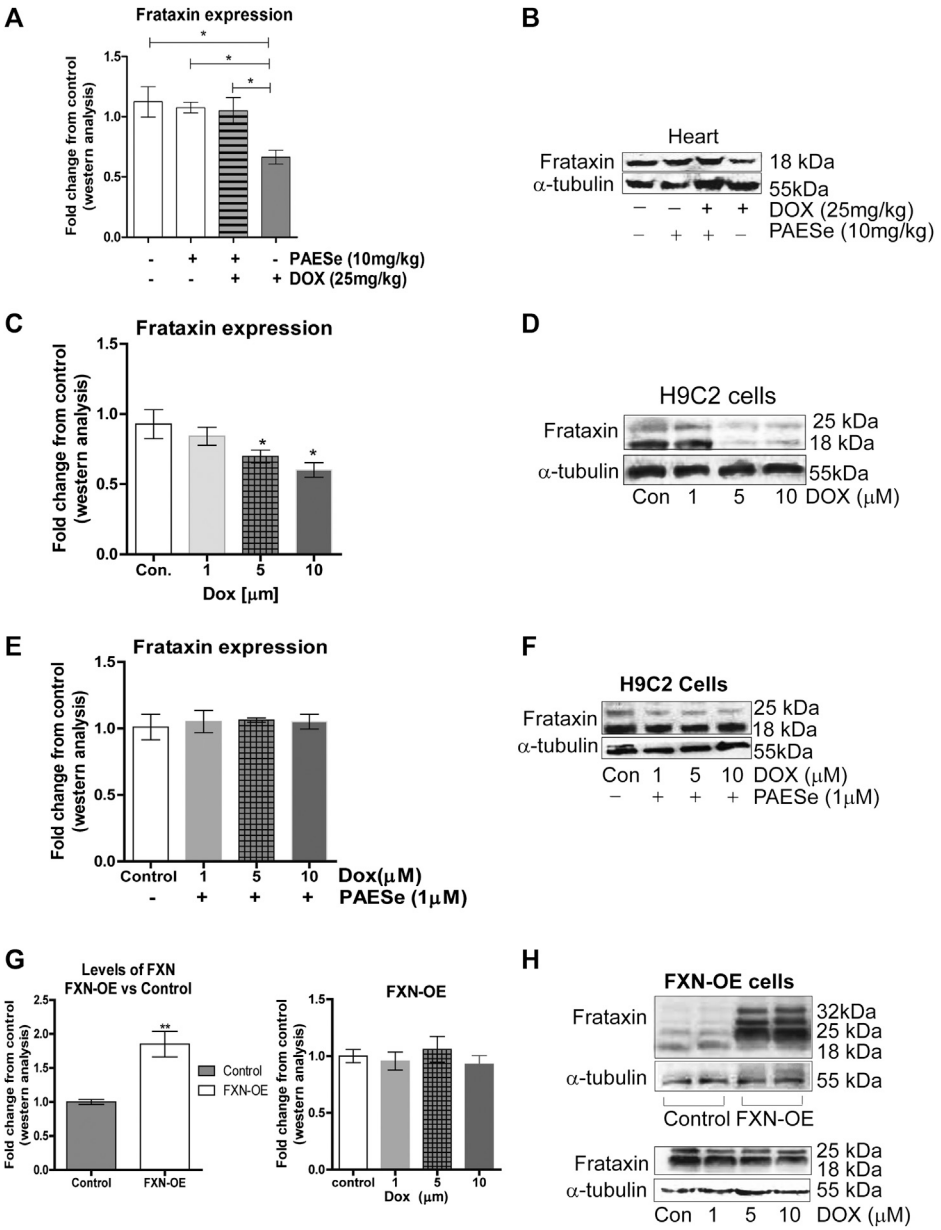

FIGURE 3 | PAESe prevents DOX-mediated reduction of frataxin expression. **(A,B)** Western blot analysis of frataxin expression levels from heart tissue from cumulative dosing of DOX (25 mg/kg) ± PAESe (50 mg/kg/dose) as described in the methods section. Animals were administered drugs once a week (Q.I.W.), and the dosing stopped at the 4th weeks. (*$p < 0.05$; **$p < 0.001$, ***$p < 0.0001$; Mean ± SEM, n = 3x4) **(C,D)** Western blot on H9C2 and **(E–H)** Frataxin over expressing (OE) H9C2 cardiomyobalsts cell lines. Both H9C2 and Frataxin overexpressing cells were treated with drug for 24 h as control (media), DOX (1 μm, 5 μm, or 10 μm) with or without PAESe (1 μM). (*$p < 0.05$,**$p < 0.001$, ***$p < 0.0001$ vs Control; Mean ± SEM, N = 3).

in the protective mechanism underlying PAESe's role in preventing mitochondrial iron overload.

PAESe Attenuates DOX Mediated ROS formation and Maintains Mitochondrial Membrane Potential (Figures 5, 6)

Previous reports confirm that DOX, induced mitochondrial iron accumulation, enhances R.O.S. formation, and oxidative stress in cardiomyocytes (Mouli et al., 2015). Therefore, the maintenance of iron homeostasis in mitochondria is vital for cell survival. Based on our observations, that PAESe mediates mitochondrial iron homeostasis in the presence of DOX by preventing alterations in the expression of Frataxin. We observed that H9C2 cardiomyoblasts treated with increasing concentrations of DOX elevated mitochondrial ROS formation (**Figures 5A,B**) [t (10) = 63.46; p = 0.0001]. Furthermore, PAESe protected against the DOX-mediated increase in ROS formation [t (10) = 14; p = 0.0001].

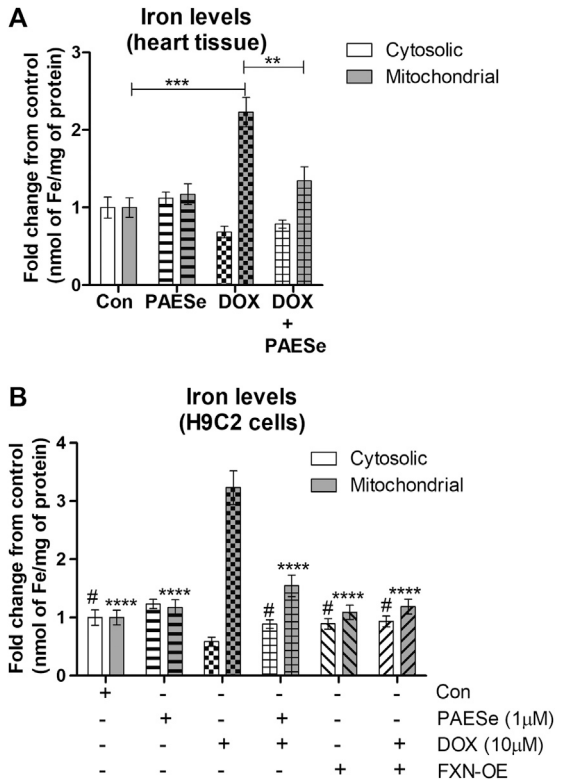

FIGURE 4 | PAESe protects against DOX mediated mitochondrial iron accumulation. **(A)** Ferrozine assay from heart tissue. Mitochondrial and cytosolic fractions were partitioned from heart tissues collected from control and drug-treated nude mice that were imaged by MRI in **Figure 1**. Groups were divided as the following: Control (saline), DOX (25 mg/kg/Dose), PAESe (10 mg/kg/dose) and DOX + PAESe (25 mg/kg/dose+50 mg/kg/dose) as indicated in the methods section. Animals were administered drugs once a week (Q.I.W.), and the dosing stopped at the 4th week, followed by two weeks of recovery. (*$p < 0.05$,**$p < 0.001$, ***$p < 0.0001$; Mean ± SEM, n = 4 mice per group). Mitochondrial and cytosolic iron levels were measured by Ferrozine colorimetric assay. **(B)** Free iron ($Fe^{2+/3+}$ was measured by a Ferrozine colorimetric assay based upon a previously published technique (Riemer et al., 2004), from mitochondrial and cytosolic H9C2 subcellular fractions. Cells were treated with DOX (10 μM) with or without PAESe (1 μM) for 24 h (*$p < 0.05$,**$p < 0.001$, ***$p < 0.0001$ vs Control; Mean ± SEM, N = 4).

To further explore this mechanism, we demonstrated that PAESe inhibited DOX-mediated reductions in glutathione peroxidase (GSHPx) activity in mice hearts (**Figure 5C**), [t (4) = 13.01; p = 0.0002] and H9C2 cardiomyoblasts [t (4) = 10.37; p = 0.0005]. Selenium is an vital element of selenocysteine, the active site of GSHPx (Ursini and Bindoli, 1987; Gladyshev et al., 1996). GSHPx is an antioxidant enzyme that reduces oxidant-induced DNA damage and lipid peroxidation. Further reduced levels of GSHPx is highly correlated with the initiation and progression of malignancy (Sundstrom et al., 1984; Ursini and Bindoli, 1987). The ability of PAESe to replenish the cellular anti-oxidative capacity with glutathione is to effectively improve mitochondrial iron homeostatic levels, which are in excess (Kang et al., 2011; Kang et al., 2015).

PAESe Improves Mitochondrial Bioenergetics (Figure 6)

Previous reports have observed reduced mitochondrial respiration in FXN lacking cellular models, including fibroblasts isolated from FRDA patients (Bradley et al., 2000; Vorgerd et al., 2000; Mühlenhoff et al., 2002). Our DOX treated H9C2 cardiomyoblasts displayed reduced FXN expression levels and increased mitochondrial ROS formation. We then tested that PAESe ameliorates DOX impaired aconitase activity and ATP levels and also improved cellular respiration. (**Figure 6A**) Our results indicate that PAESe improved aconitase activity that was altered by DOX [t (6) = 5.483; p = 00.15] and (t [6) = 4.279; p = 0.0052]. We observed a dose-dependent reduction in the ATP in our H9C2 cardiomyoblasts after DOX treatment. However, PAESe prevented the DOX-induced reduction in ATP levels in H9C2 cardiomyoblast cells (**Figure 6B**), (t (10) = 4.988, p = 0.0005 (5 μM), (t (10) = 3.413; p = 0.0066 (10 μM), (t (10) = 2.735, p = 0.0210 (20 μM), (t (10) = 4.032, p = 0.0024 (50 μM). We also observed that Dox (10 μm for 24 h) significantly impaired cellular respiration (**Figure 6C**) [basal (t (4) = 6.1155; p = 0.0036)] and [uncoupled (t (4) = 4.720; p = 0.0092)]. Furthermore, we also observed that PAESe conferred protection against DOX-mediated reduction in reduction in basal oxygen consumption rates [basal (t (4) = 3.089; p = 0.0366)] and [uncoupled (t (4) = 3.358;p = 0.0284)]. These findings are in line with our previously published work, where we observed similarly reduced oxygen consumption rates in FRDA fibroblasts and cells with FXN knockdown. Our working model (**Figure 7A**), describes together how PAESe regenerates glutathione and protects Frataxin from damage associated from doxorubicin.

DISCUSSION

Cardiotoxicity associated with anthracycline therapy develops as a progressive form of cardiomyopathy after the termination of the dosage regimen. Previously, we have demonstrated that administration of DOX (5 mg/kg) to athymic mice resulted in significant toxicity, reducing the median survival rates mice by 50% after 8 weeks of dosing (Kang et al., 2014). Acute dosing in the clinical setting induces the development of ventricular conduction abnormalities, including ST and T wave abnormalities, prolonged QT interval, and ventricular arrhythmias (Rudzinski et al., 2007). However, anthracycline dosing regimens are regarded as chronic due to their cumulative and dose-dependent impact on the heart over time. Further, the onset of cardiomyopathy from chronic dosing appears only after cessation of anthracycline therapy (Grenier and Lipshultz, 1998; Lipshultz et al., 2008; Fadol and Lech, 2011; Liang et al., 2020). However, the mechanisms associated with the development of DOX-mediated cardiotoxicity are unclear and complicated.

To better understand the mechanisms that are involved in the development of cardiotoxicity, we determined parameters of cardiac function after cumulative dosing of 25 mg/kg of DOX. Our dosing regimen is analogous to other studies that investigate the effects of similar chronic dosing on the myocardial architecture. As determined by our MRI analysis, we observed

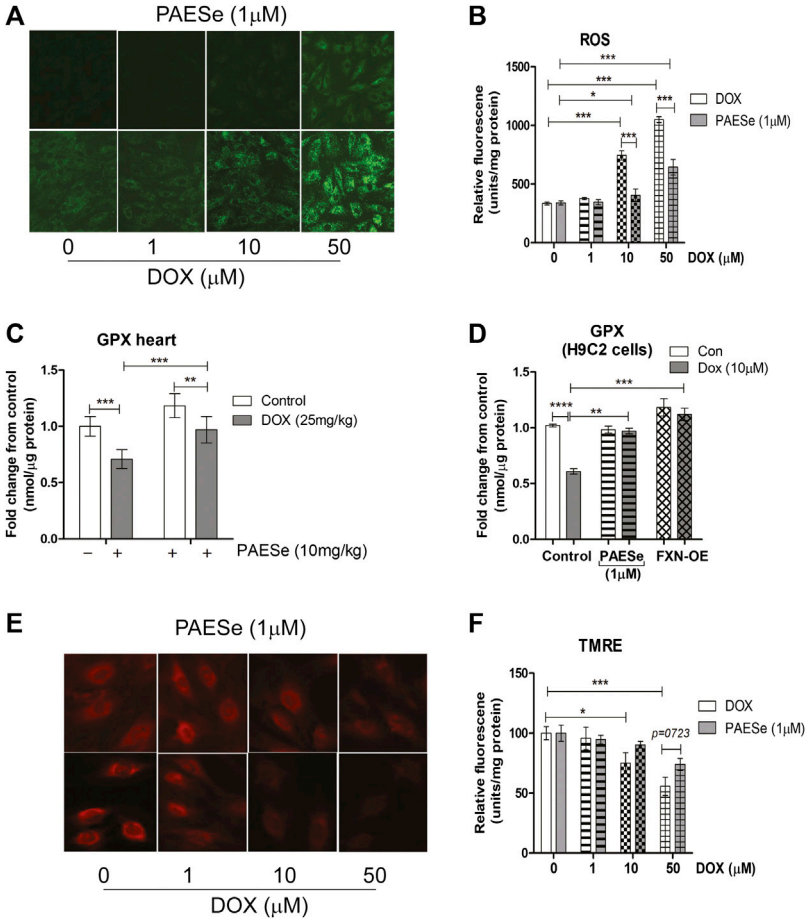

FIGURE 5 | PAESe protects against DOX mediated mitochondrial ROS formation. **(A,B)** Fluorescence images of mitochondrial ROS formation (green) in increasing concentrations of DOX (0–50 μM) treated H9C2 cells with or without PAESe (1 μM) and graphical representation of ROS levels in H9C2 cardiomyoblasts. **(C)** Glutathione peroxidase activity, mitochondrial heart lysate from DOX treated athymic mice with and without PAESe (cumulative dosing of (DOX 25 mg/kg) ± PAESe (50 mg/kg/dose). **(D)** In addition, GPx activity was measured in isolated mitochondria from H9C2 cells treated with DOX (10 μM) or PAESe (1 μM) treated and non-treated H9C2 and FXN-OE cardiomyoblasts. **(E,F)** Mitochondrial membrane potential ($\Delta\psi_m$) determined by TMRE (2 μM) immunofluorescence in DOX treated (1–50 μM) H9C2 cells with and without PAESe (1 μM) for 24 h where N = 4 independent experiments and are represented as mean ± S.E.M. and analysis was accomplished by student t-test with post-hoc analysis for significances between groups and within groups based upon averages from the assays. *;$p < 0.05$ **; $p < 0.001$, ***; $p < 0.0001$.

enlargement in the anterolateral and lateral segments of the left ventricle and reduced hemodynamic performance suggesting a compensatory state that potentially can progress to heart failure over time. To further explain the consequent cardiac related pathological condition of Dox treatment in our mice, we observed elevated cardiac troponin levels in circulation, thus suggesting cardiotoxicity. These results are in line with other reports in DOX treated athymic mice, where similar cumulative dosing regimen (25 mg/kg) induced an increase in cTnI levels (Sonowal et al., 2017). These findings helps to explain the reduced ejection volumes and reduced cardiac outputs in our mice.

The effects of DOX on the development of cardiac hypertrophy at the subcellular level can be studied in parallel with the impact on the dysregulation mitochondrial respiration, membrane potential and ROS levels. Mitochondrial damage has been reported to be a major target for DOX-mediated cardiomyopathy (Jarreta et al., 2000; Lev et al., 2004). DOX induces free oxygen radical production in the heart, which is a contributing factor for the disruption of mitochondrial bioenergetics (Keizer et al., 1990; Cadenas and Davies, 2000; Carvalho et al., 2014). However, alternative mechanisms associated with DOX cardiotoxicity may also contribute to the dysregulation of mitochondrial dynamics. Therefore, identifying the molecular and cellular targets that are altered by DOX in the mitochondria will help develop novel therapeutics to circumvent the adverse cardiogenic effects of DOX in cancer patients. The present study elucidated a potential mechanism by which DOX exposure induces a compensatory hypertrophic cardiac hypertrophy by implicating FXN as a crucial mediator in this process. Our previous reports have observed that reduced FXN levels induce an increase in mitochondrial iron accumulation and the subsequent ROS formation and H9C2 cell enlargement. Further, that by chelating this iron, using pyridoxal isonicotinol hydrazine (PIH) the DOX mediated H9C2

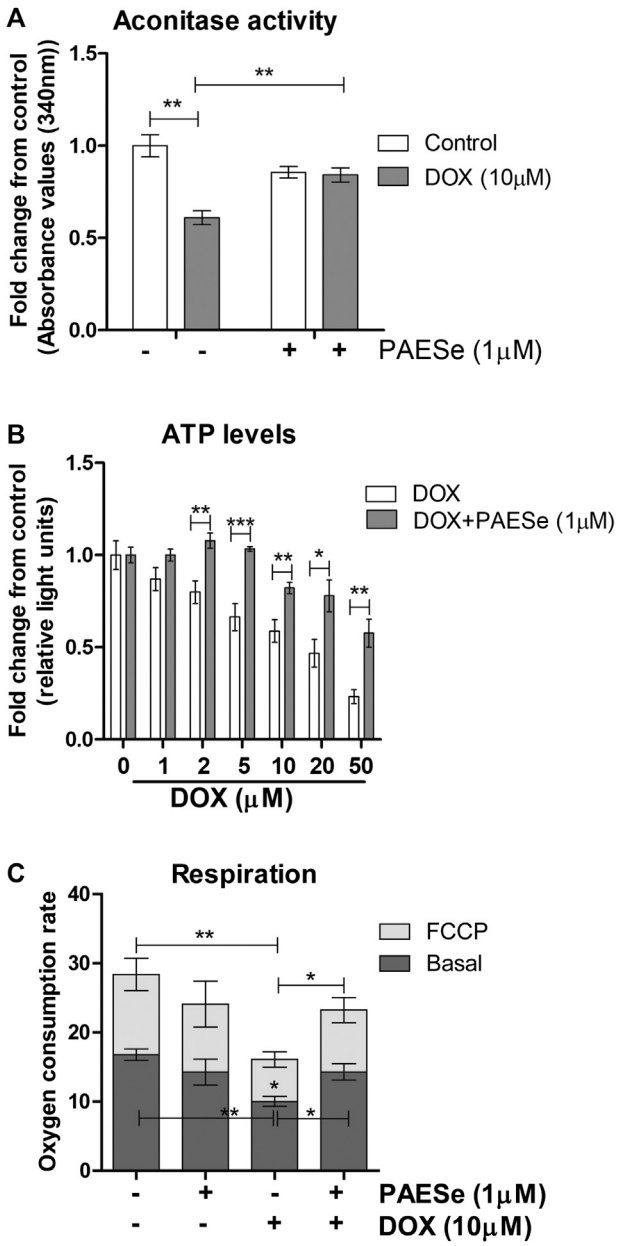

FIGURE 6 | PAESe protects against DOX-mediated attenuation of mitochondrial bioenergetics. **(A)** H9C2 cells were treated as following; control (media), DOX (10 μm), PAESe (1 μM), and DOX (10 μM) + PAESe (1 μM). Mitochondrial isolations were extracted from cells for aconitase activity assay. Values were standardized to total protein concentrations, based upon on a standard curve of enzyme activity from the kit, and compared to control levels. **(B)** ATP levels were measured from H9C2 cardiomyoblasts treated with increasing concentrations of DOX (0–50 μM), for 24 h treated with and without PAESe (1 μm) (N = 4 independent experiments with three repetitions and values are based upon averages ± SEM. **(C)** Mitochondrial respiration (basal and uncoupled (FCCP)) in H9C2 cardiomyoblasts were measured following DOX (10 μm) with our without PAESe (1 μm) for 24 h. Values were normalized to total protein levels. The mitochondrial complex activity was decoupled by adding Trifluorocarbonylcyanide (FCCP; 6 μM), where N = 4 independent experiments. (*$p < 0.05$,**$p < 0.001$, ***$p < 0.0001$; Mean ± SEM, N = 4 independent experiments with N = 3 repetitions per group).

cardiomyocyte enlargement was significantly reduced (Mouli et al., 2015).

PAESe is a phenylaminoalkyl selenide is a strong antioxidant that scavenges reactive oxygen species while also serving as an antihypertensive activity agent (May et al., 1987; May et al., 1997; May and Pollock, 1998). Furthermore, PAESe mechanistically serves as a selenoxide product that is recycled back to its selenide form by cellular reductants including ascorbate and glutathione (May et al., 1987; May et al., 1997; May and Pollock, 1998). In addition, we have observed that PAESe is stable *in vitro*, displays very low toxicity *in vivo* (rats and mice), and displays no complicating side effects. Recently, we demonstrated that PAESe exhibits cardio-protective effects against anthracyclin-mediated cardiotoxicity *in vitro* cell culture as well as *in vivo* antitumor activity (Kang et al., 2011). However, the exact mechanism (s) is not known; furthermore, mitochondrial damage exists as an underlying factor in the progression of cardiomyopathy to heart failure (Koutnikova et al., 1998; Jarreta et al., 2000; Lev et al., 2004; Rudzinski et al., 2007; Schmitz et al., 2012; Bayeva et al., 2013). Clinical findings support the notion that human patients with FRDA display reduced FXN levels, develop life-threatening hypertrophic cardiomyopathy (Jauslin et al., 2002). In close agreement with this, our *in vivo* and *in vitro* models with DOX have demonstrated a significant reduction in FXN expression (Mouli et al., 2015). Furthermore, that PAESe prevents DOX mediated cardiac hypertrophy via reducing the increase in mitochondrial free iron accumulation (Kang et al., 2015). However, our findings indicate that progressive damage to FXN induced by DOX was central in mediating mitochondrial iron overload. Our hypothesis was confirmed by our previous findings in FXN-KD cardiomyocyte cell lines, which displayed a similar increase in mitochondrial iron, as found in DOX treated cardiomyocytes (Mouli et al., 2015). However, our FXN-OE cardiomyocytes demonstrated stable iron homeostasis in the mitochondria in the presence of DOX and prevented the deleterious effects of DOX on the mitochondrial iron utilization pathways. Furthermore, we previously observed insignificant amounts of ROS production in FXN-OE cell lines after DOX treatment (Mouli et al., 2015). Importantly, our previously published study linked increased mitochondrial iron levels following DOX treatment to increased ROS production that resulted in mitochondrial injury, including reduced mitochondrial membrane potential ($\Delta\Psi_m$) (Mouli et al., 2015). Conversely, the use of the iron chelator, PIH was observed to help maintain mitochondrial $\Delta\Psi_m$ in H9C2 cells treated with DOX. Thus confirming that mitochondrial iron overload with the formation of mitochondrial ROS. Maintenance of mitochondrial $\Delta\Psi_m$ in cardiomyocytes is vital to maintain the high energy requirements for viability and function and attenuation of $\Delta\Psi_m$ induces injury to cardiomyocytes Gladyshev et al., 1996. We assessed $\Delta\Psi_m$ in cardiomyoblasts using the fluorescent probe TMRE. Interestingly, FXN-OE cells treated with DOX were protected from the adverse impact of DOX on $\Delta\Psi_m$. In the present study, we observed that PAESe preserved the normal (lower) mitochondrial $\Delta\Psi_m$, (**Figures**

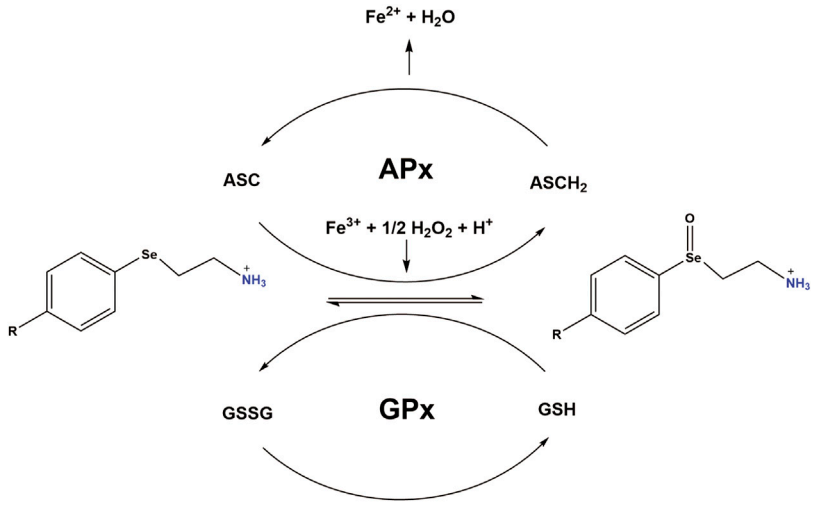

FIGURE 7 | Working model: PAESe is oxidized to its selenoxide PAESe(O) form via dopamine-β-monooxygenase. Reduced Ascorbate ($ASCH_2$) reduces PAESe(O) back to the reduced form generating oxidized ascorbate (ASC) in the process. ASC is then capable of reacting with PAESe and hydrogen peroxide to reduce Fe^{3+} back to Fe^{2+}. Catalytic regeneration of PAESe is also enhanced via Glutathione Peroxidase (GPx) reduction with glutathione (GSH), yielding glutathione disulfide (GSSG). Regeneration of PAESe enables mitochondrial ROS formation to be ameliorated at a much faster rate compared to normal physiological conditions, allowing for potent free radical scavenging and enhanced mitochondrial function. The working model is adapted from a figure by May et al. (May and Pollock, 1998).

5D,E). However, our study had some deficits, including our animal model. We chose to use an athymic mouse model for our studies. This model lacks the T-cell immunity and thus are immunocompromized in many ways. In this manner, our model investigated the direct impact of DOX on the cardiomyocytes. Our goals were to determine the mechanism by which PAESe protects the heart against DOX mediated cardiotoxicity. We acknowledge that the immune system also has a major impact on the inflammation, hypertrophy and development of compensatory myocardial damage to DOX. Future work will investigate whether PAESe protects from DOX mediated cardio toxicity in a model, where the impact of the full immune system is involved, including potential T cell mediated immune damage to the heart.

Our data suggest that DOX induces an increase in mitochondrial ROS formation resulting in early ubiquitination of FXN protein by activating E3 ligase at the current DOX as inferred by other studies demonstrating mechanisms for FXN turnover in FRDA patients (Landré et al., 2014; Rufini et al., 2014). These hypotheses will be explored in detail in our future studies. Reports from FRDA models, have demonstrated severe mitochondrial energy deficits as demonstrated by reduced oxidative capacity due to depleted FXN levels and impaired Fe-S cluster enzyme activities, diminished respiratory function, and reduced ATP levels (Thierbach et al., 2005; González-Cabo and Palau, 2013). Similar events were observed in our DOX treated cardiomyocytes, which displayed a severe reduction in the activities of iron-sulfur containing enzyme aconitase, as well as ATP production and oxygen consumption levels. Further, we observed that by reducing the deleterious effects of DOX on FXN by PAESe, we preserve mitochondrial bioenergetics. Under stress, glutathione reductase maintains the physiological GSH/GSSG balance in an NADPH dependent fashion (Lushchak, 2012). Earlier reports have demonstrated that FXN deficient and FRDA cells can be affiliated with the deficiency of glutathione pool (GSH/GSSG), which serves as a free radical scavenger and co-factor for various mitochondrial antioxidants (Jauslin et al., 2002; Auchère et al., 2008). In line with these findings, we observed that PAESe prevented the DOX-mediated reduction of glutathione peroxidase enzyme activity (a requirement for glutathione replenishment). Previously we have confirmed that PAESe replenishes glutathione levels and FADH2 levels (Mouli et al., 2015).

Mechanistically, PAESe is oxidized to its selenoxide PAESe (O) form via dopamine-β-monooxygenase. Reduced ascorbate reduces the oxidized PAESe back to the reduced form resulting in the generation of oxidized ascorbate in the process. Ascorbate is then capable of reacting with PAESe and hydrogen peroxide to reduce Fe^{3+} back to Fe^{2+}, resulting in lowering reactive oxygen species associated with iron. This source of ROS was confirmed in our previously published reports where the iron chelator pyridoxal isonicotinoyl hydrazine (PIH), was shown to reduce mitochondrial free iron levels and mitochondrial ROS levels. We have observed that catalytic regeneration of PAESe is also enhanced via Glutathione Peroxidase (GPx) reduction with glutathione (GSH) yielding glutathione disulfide (GSSG) (**Figure 7**). In addition, regeneration of PAESe enables mitochondrial ROS formation to be ameliorated at a much faster rate compared to normal physiological conditions, allowing for potent free radical scavenging and enhanced mitochondrial function. To implicate FXN in the signaling mechanism, as previously reported, our FXN-overexpressing (OE) cardiomyoblasts were protected from the unfavorable effects of DOX in the mitochondria and may be due to elevated anti-oxidative defenses (Mouli et al., 2015). Therefore these findings, taken together, suggest that PAESe offered

protection against DOX-mediated adverse effects by significantly improving the mitochondrial energy flux and anti-oxidative capacity, thereby preserving the mitochondrial bioenergetics.

Our H9C2 cardiomyocytes treated with DOX displayed extensive ROS, which was prevented by PAESe. We have previously shown that the consequence of DOX on reducing FXN expression is to induce mitochondrial iron overload and thus enhance mitochondrial ROS formation via the Fenton reaction. Previously we confirmed these findings with the utilization of a mitochondria specific iron chelator, PIH. The consequences of these findings in PAESe treated cells on mitochondrial activity resulted in the preservation of the mitochondrial membrane potential against DOX insult. Lastly, our PAESe in a similar manner to FXN-OE cardiomyocytes (Mouli et al., 2015) demonstrated reduced cardiac hypertrophy in response to DOX treatment. These findings indicate that PAESe protected against DOX-induced iron overload, thus indicating a potential therapeutic mechanism towards mitigating the development of DOX mediated cardiac hypertrophy, as seen by our MRI data.

In summary, our findings indicate that FXN plays a significant role in the development of DOX mediated myocardial iron overload and that PAESe protects FXN from the impaired mitochondrial bioenergetics leading to progression of de-compensatory cardiomyopathy. Further that PAESe was found to be protective against DOX mediated mitochondrial dysfunction and the ensuing cardiac hypertrophy. Our future work will focus on determining how PAESe can prevent myocardial iron accumulation in chronic usage of DOX administration at extended time points following completion of DOX therapy. Second, we are currently developing the FXN overexpressing mouse model to understand better and justify the role of FXN in the DOX mediated damage to the mitochondria. Our FXN overexpressing mouse model will further help decipher the role of FXN in the development of DOX mediated cardiomyopathy.

DATA AVAILABILITY STATEMENT

The raw data supporting the conclusions of this article will be made available by the authors, without undue reservation.

ETHICS STATEMENT

The animal study was reviewed and approved by Auburn University Institutional Animal Care and Use Committee which is accredited by AAALAC.

AUTHOR CONTRIBUTIONS

XF, MT, SY, NP, IS, MG, ET, SM, and RA worked on cell culture and animal work. XF, MT, RB, TD, RA, and RHA worked on animal work and imaging, data analysis. XF, RB, JZ, PP, RA, and RHA contributed to manuscript preparation.

ACKNOWLEDGMENTS

We would like to thank the support from the Auburn University Research Initiative in Cancer (AURIC)-Major (RA/RDA/PP) and Seed Grant (RA/RDA) Awards, as well as a Graduate Fellowship (ME), and the Tubitak Bideb-2219 International Post Doctoral Research Fellowship Programme (ET).

REFERENCES

Arola, O. J., Saraste, A., Pulkki, K., Kallajoki, M., Parvinen, M., and Voipio-Pulkki, L. M. (2000). Acute doxorubicin cardiotoxicity involves cardiomyocyte apoptosis. *Canc. Res.* 60, 1789–1792.

Ashour, A. E., Sayed-Ahmed, M. M., Abd-Allah, A. R., Korashy, H. M., Maayah, Z. H., Alkhalidi, H., et al. (2012). Metformin rescues the myocardium from doxorubicin-induced energy starvation and mitochondrial damage in rats. *Oxid. Med. Cell Longev.* 2012, 434195. doi:10.1155/2012/434195

Auchère, F., Santos, R., Planamente, S., Lesuisse, E., and Camadro, J. M. (2008). Glutathione-dependent redox status of frataxin-deficient cells in a yeast model of Friedreich's ataxia. *Hum. Mol. Genet.* 17, 2790–2802. doi:10.1093/hmg/ddn178

Bayeva, M., Gheorghiade, M., and Ardehali, H. (2013). Mitochondria as a therapeutic target in heart failure. *J. Am. Coll. Cardiol.* 61, 599–610. doi:10.1016/j.jacc.2012.08.1021

Berthiaume, J. M., and Wallace, K. B. (2007). Adriamycin-induced oxidative mitochondrial cardiotoxicity. *Cell Biol. Toxicol.* 23, 15–25. doi:10.1007/s10565-006-0140-y

Bradley, J. L., Blake, J. C., Chamberlain, S., Thomas, P. K., Cooper, J. M., and Schapira, A. H. (2000). Clinical, biochemical and molecular genetic correlations in Friedreich's ataxia. *Hum. Mol. Genet.* 9, 275–282. doi:10.1093/hmg/9.2.275

Cadenas, E., and Davies, K. J. (2000). Mitochondrial free radical generation, oxidative stress, and aging. *Free Radic. Biol. Med.* 29, 222–230. doi:10.1016/s0891-5849(00)00317-8

Campuzano, V., Montermini, L., Lutz, Y., Cova, L., Hindelang, C., Jiralerspong, S., et al. (1997). Frataxin is reduced in Friedreich ataxia patients and is associated with mitochondrial membranes. *Hum. Mol. Genet.* 6, 1771–1780. doi:10.1093/hmg/6.11.1771

Carvalho, F. S., Burgeiro, A., Garcia, R., Moreno, A. J., Carvalho, R. A., and Oliveira, P. J. (2014). Doxorubicin-induced cardiotoxicity: from bioenergetic failure and cell death to cardiomyopathy. *Med. Res. Rev.* 34, 106–135. doi:10.1002/med.21280

Cavadini, P., Gellera, C., Patel, P. I., and Isaya, G. (2000). Human frataxin maintains mitochondrial iron homeostasis in *Saccharomyces cerevisiae*. *Hum. Mol. Genet.* 9, 2523–2530. doi:10.1093/hmg/9.17.2523

Cersosimo, R. J., and Hong, W. K. (1986). Epirubicin: a review of the pharmacology, clinical activity, and adverse effects of an adriamycin analogue. *J. Clin. Oncol.* 4, 425–439. doi:10.1200/JCO.1986.4.3.425

Chen, W. D., Gong, W. T., Ye, Z. Q., Lin, Y., and Ning, G. L. (2013). FRET-based ratiometric fluorescent probes for selective Fe3+ sensing and their applications in mitochondria. *Dalton Trans.* 42, 10093–10096. doi:10.1039/c3dt50832c

Cowan, E. A., Oldham, C. D., and May, S. W. (2011). Identification of a thioselenurane intermediate in the reaction between phenylaminoalkyl selenoxides and glutathione. *Arch. Biochem. Biophys.* 506, 201–207. doi:10.1016/j.abb.2010.11.007

De Silva, V., Woznichak, M. M., Burns, K. L., Grant, K. B., and May, S. W. (2004). Selenium redox cycling in the protective effects of organoselenides against oxidant-induced DNA damage. *J. Am. Chem. Soc.* 126, 2409–2413. doi:10.1021/ja037294j

Dürr, A., Cossee, M., Agid, Y., Campuzano, V., Mignard, C., Penet, C., et al. (1996). Clinical and genetic abnormalities in patients with Friedreich's ataxia. *N. Engl. J. Med.* 335, 1169–1175. doi:10.1056/NEJM199610173351601

Fadol, A., and Lech, T. (2011). Cardiovascular adverse events associated with cancer therapy. *J. Adv. Pract. Onc.* 2, 229–242. doi:10.6004/jadpro.2011.2.4.2

Gladyshev, V. N., Jeang, K. T., and Stadtman, T. C. (1996). Selenocysteine, identified as the penultimate C-terminal residue in human T-cell thioredoxin reductase, corresponds to TGA in the human placental gene. *Proc. Natl. Acad. Sci. U.S.A.* 93, 6146–6151. doi:10.1073/pnas.93.12.6146

González-Cabo, P., and Palau, F. (2013). Mitochondrial pathophysiology in Friedreich's ataxia. *J. Neurochem.* 126, 53–64. doi:10.1111/jnc.12303

Grenier, M. A., and Lipshultz, S. E. (1998). "Epidemiology of anthracycline cardiotoxicity in children and adults. *Semin. Oncol.* 25, 72–85.

Herman, H. H., Pollock, S. H., Fowler, L. C., and May, S. W. (1988). Demonstration of the potent antihypertensive activity of phenyl-2-aminoethyl sulfides. *J. Cardiovasc. Pharmacol.* 11, 501–510. doi:10.1097/00005344-198805000-00001

Huang, M. L., Becker, E. M., Whitnall, M., Suryo Rahmanto, Y., Ponka, P., and Richardson, D. R. (2009). Elucidation of the mechanism of mitochondrial iron loading in Friedreich's ataxia by analysis of a mouse mutant. *Proc. Natl. Acad. Sci. U.S.A.* 106, 16381–16386. doi:10.1073/pnas.0906784106

Jarreta, D., Orús, J., Barrientos, A., Miró, O., Roig, E., Heras, M., et al. (2000). Mitochondrial function in heart muscle from patients with idiopathic dilated cardiomyopathy. *Cardiovasc. Res.* 45, 860–865. doi:10.1016/s0008-6363(99)00388-0

Jauslin, M. L., Wirth, T., Meier, T., and Schoumacher, F. (2002). A cellular model for Friedreich Ataxia reveals small-molecule glutathione peroxidase mimetics as novel treatment strategy. *Hum. Mol. Genet.* 11, 3055–3063. doi:10.1093/hmg/11.24.3055

Kang, J. Y., Costyn, L. J., Nagy, T., Cowan, E. A., Oldham, C. D., May, S. W., et al. (2011). The antioxidant phenylaminoethyl selenide reduces doxorubicin-induced cardiotoxicity in a xenograft model of human prostate cancer. *Arch. Biochem. Biophys.* 515, 112–119. doi:10.1016/j.abb.2011.08.008

Kang, J. Y., Eggert, M., Mouli, S., Aljuffali, I., Fu, X., Nie, B., et al. (2015). Pharmacokinetics, antitumor and cardioprotective effects of liposome-encapsulated phenylaminoethyl selenide in human prostate cancer rodent models. *Pharm. Res.* 32, 852–862. doi:10.1007/s11095-014-1501-5

Kang, J. Y., Eggert, M., Mouli, S., Aljuffali, I., Fu, X., Nie, B., et al. (2014). Pharmacokinetics, antitumor and cardioprotective effects of liposome-encapsulated phenylaminoethyl selenide in human prostate cancer rodent models. *Pharm. Res.*, 1–11.

Karagiannis, T. C., Lin, A. J., Ververis, K., Chang, L., Tang, M. M., Okabe, J., et al. (2010). Trichostatin A accentuates doxorubicin-induced hypertrophy in cardiac myocytes. *Aging (Albany NY)* 2, 659. doi:10.18632/aging.100203

Keizer, H., Pinedo, H., Schuurhuis, G., and Joenje, H. (1990). Doxorubicin (adriamycin): a critical review of free radical-dependent mechanisms of cytotoxicity. *Pharmacol. Ther.* 47, 219–231. doi:10.1016/0163-7258(90)90088-j

Khan, S. R., and Denmeade, S. R. (2000). *In vivo* activity of a PSA-activated doxorubicin prodrug against PSA-producing human prostate cancer xenografts. *Prostate* 45, 80–83. doi:10.1002/1097-0045(20000915)45:1<80::aid-pros10>3.0.co;2-q

Koutnikova, H., Campuzano, V., Foury, F., Dollé, P., Cazzalini, O., and Koenig, M. (1997). Studies of human, mouse and yeast homologues indicate a mitochondrial function for frataxin. *Nat. Genet.* 16, 345–351. doi:10.1038/ng0897-345

Koutnikova, H., Campuzano, V., and Koenig, M. (1998). Maturation of wild-type and mutated frataxin by the mitochondrial processing peptidase. *Hum. Mol. Genet.* 7, 1485–1489. doi:10.1093/hmg/7.9.1485

Koves, T. R., Li, P., An, J., Akimoto, T., Slentz, D., Ilkayeva, O., et al. (2005). Peroxisome proliferator-activated receptor-gamma co-activator 1alpha-mediated metabolic remodeling of skeletal myocytes mimics exercise training and reverses lipid-induced mitochondrial inefficiency. *J. Biol. Chem.* 280, 33588–33598. doi:10.1074/jbc.M507621200

Kuerer, H. M., Newman, L. A., Smith, T. L., Ames, F. C., Hunt, K. K., Dhingra, K., et al. (1999). Clinical course of breast cancer patients with complete pathologic primary tumor and axillary lymph node response to doxorubicin-based neoadjuvant chemotherapy. *J. Clin. Oncol.* 17, 460–469. doi:10.1200/JCO.1999.17.2.460

Kwok, J. C., and Richardson, D. R. (2004). Examination of the mechanism(s) involved in doxorubicin-mediated iron accumulation in ferritin: studies using metabolic inhibitors, protein synthesis inhibitors, and lysosomotropic agents. *Mol. Pharmacol.* 65, 181–195. doi:10.1124/mol.65.1.181

Landré, V., Rotblat, B., Melino, S., Bernassola, F., and Melino, G. (2014). Screening for E3-Ubiquitin ligase inhibitors: challenges and opportunities. *Oncotarget* 5, 7988–8013. doi:10.18632/oncotarget.2431

Lev, D., Nissenkorn, A., Leshinsky-Silver, E., Sadeh, M., Zeharia, A., Garty, B. Z., et al. (2004). Clinical presentations of mitochondrial cardiomyopathies. *Pediatr. Cardiol.* 25, 443–450. doi:10.1007/s00246-003-0490-7

Liang, X., Wang, S., Wang, L., Ceylan, A. F., Ren, J., and Zhang, Y. (2020). Mitophagy inhibitor liensinine suppresses doxorubicin-induced cardiotoxicity through inhibition of Drp1-mediated maladaptive mitochondrial fission. *Pharmacol. Res.* 157, 104846. doi:10.1016/j.phrs.2020.104846

Lipshultz, S. E., Alvarez, J. A., and Scully, R. E. (2008). Anthracycline associated cardiotoxicity in survivors of childhood cancer. *Heart* 94, 525–533. doi:10.1136/hrt.2007.136093

Lipshultz, S. E., Colan, S. D., Gelber, R. D., Perez-Atayde, A. R., Sallan, S. E., and Sanders, S. P. (1991). Late cardiac effects of doxorubicin therapy for acute lymphoblastic leukemia in childhood. *N. Engl. J. Med.* 324, 808–815. doi:10.1056/NEJM199103213241205

Lushchak, V. I. (2012). Glutathione homeostasis and functions: potential targets for medical interventions. *J. Amino Acids* 2012, 736837. doi:10.1155/2012/736837

May, S. W., Herman, H. H., Roberts, S. F., and Ciccarello, M. C. (1987). Ascorbate depletion as a consequence of product recycling during dopamine beta-monooxygenase catalyzed selenoxidation. *Biochemistry* 26, 1626–1633. doi:10.1021/bi00380a021

May, S. W., and Pollock, S. H. (1998). Selenium-based antihypertensives. Rationale and potential. *Drugs* 56, 959–964. doi:10.2165/00003495-199856060-00001

May, S. W., Wang, L., Gill-Woznichak, M. M., Browner, R. F., Ogonowski, A. A., Smith, J. B., et al. (1997). An orally active selenium-based antihypertensive agent with restricted CNS permeability. *J. Pharmacol. Exp. Therapeut.* 283, 470–477.

Mouli, S., Nanayakkara, G., Alalasmari, A., Eldoumani, H., Fu, X., Berlin, A., et al. (2015). The role of frataxin in doxorubicin-mediated cardiac hypertrophy. *Am. J. Physiol. Heart Circ. Physiol.* 309, H844–H859. doi:10.1152/ajpheart.00182.2015

Mühlenhoff, U., Richhardt, N., Ristow, M., Kispal, G., and Lill, R. (2002). The yeast frataxin homolog Yfh1p plays a specific role in the maturation of cellular Fe/S proteins. *Hum. Mol. Genet.* 11, 2025–2036. doi:10.1093/hmg/11.17.2025

Nanayakkara, G., Alasmari, A., Mouli, S., Eldoumani, H., Quindry, J., Mcginnis, G., et al. (2015). Cardioprotective HIF-1α-frataxin signaling against ischemia-reperfusion injury. *Am. J. Physiol. Heart Circ. Physiol.* 309, H867–H879. doi:10.1152/ajpheart.00875.2014

Neville-Webbe, H. L., Rostami-Hodjegan, A., Evans, C. A., Coleman, R. E., and Holen, I. (2005). Sequence- and schedule-dependent enhancement of zoledronic acid induced apoptosis by doxorubicin in breast and prostate cancer cells. *Int. J. Canc.* 113, 364–371. doi:10.1002/ijc.20602

Ong, S. B., and Hausenloy, D. J. (2010). Mitochondrial morphology and cardiovascular disease. *Cardiovasc. Res.* 88, 16–29. doi:10.1093/cvr/cvq237

Pabinger, S., Rodiger, S., Kriegner, A., Vierlinger, K., and Weinhausel, A. (2014). A survey of tools for the analysis of quantitative PCR (qPCR) data. *Biomol. Detect Quantif.* 1, 23–33. doi:10.1016/j.bdq.2014.08.002

Pollock, S. H., Herman, H. H., Fowler, L. C., Edwards, A. S., Evans, C. O., and May, S. W. (1988). Demonstration of the antihypertensive activity of phenyl-2-aminoethyl selenide. *J. Pharmacol. Exp. Therapeut.* 246, 227–234.

Rajamanickam, C., Merten, S., Kwiatkowska-Patzer, B., Chuang, C. H., Zak, R., and Rabinowitz, M. (1979). Changes in mitochondrial DNA in cardiac hypertrophy in the rat. *Circ. Res.* 45, 505–515. doi:10.1161/01.res.45.4.505

Riemer, J., Hoepken, H. H., Czerwinska, H., Robinson, S. R., and Dringen, R. (2004). Colorimetric ferrozine-based assay for the quantitation of iron in cultured cells. *Anal. Biochem.* 331, 370–375. doi:10.1016/j.ab.2004.03.049

Rudzinski, T., Ciesielczyk, M., Religa, W., Bednarkiewicz, Z., and Krzeminska-Pakula, M. (2007). Doxorubicin-induced ventricular arrhythmia treated by implantation of an automatic cardioverter-defibrillator. *Europace* 9, 278–280. doi:10.1093/europace/eum033

Rufini, A., Cavallo, F., Fortuni, S., De Martino, G., Incani, O., Di Venere, A., et al. (2014). Highly specific ubiquitin-competing molecules effectively promote frataxin accumulation and partially rescue the aconitase defect in Friedreich ataxia cells. *Neurobiol. Dis.* 75, 91–99. doi:10.1016/j.nbd.2014.12.011

Schmitz, K. H., Prosnitz, R. G., Schwartz, A. L., and Carver, J. R. (2012). Prospective surveillance and management of cardiac toxicity and health in breast cancer survivors. *Cancer* 118, 2270–2276. doi:10.1002/cncr.27462

Solem, L. E., Heller, L. J., and Wallace, K. B. (1996). Dose-dependent increase in sensitivity to calcium-induced mitochondrial dysfunction and cardiomyocyte cell injury by doxorubicin. *J. Mol. Cell. Cardiol.* 28, 1023–1032. doi:10.1006/jmcc.1996.0095

Sonowal, H., Pal, P. B., Wen, J. J., Awasthi, S., Ramana, K. V., and Srivastava, S. K. (2017). Aldose reductase inhibitor increases doxorubicin-sensitivity of colon cancer cells and decreases cardiotoxicity. *Sci. Rep.* 7, 3182. doi:10.1038/s41598-017-03284-w

Sundström, H., Korpela, H., Viinikka, L., and Kauppila, A. (1984). Serum selenium and glutathione peroxidase, and plasma lipid peroxides in uterine, ovarian or vulvar cancer, and their responses to antioxidants in patients with ovarian cancer. *Canc. Lett.* 24, 1–10. doi:10.1016/0304-3835(84)90073-9

Tada, Y., Wada, M., Migita, T., Nagayama, J., Hinoshita, E., Mochida, Y., et al. (2002). Increased expression of multidrug resistance-associated proteins in bladder cancer during clinical course and drug resistance to doxorubicin. *Int. J. Canc.* 98, 630–635. doi:10.1002/ijc.10246

Thierbach, R., Schulz, T. J., Isken, F., Voigt, A., Mietzner, B., Drewes, G., et al. (2005). Targeted disruption of hepatic frataxin expression causes impaired mitochondrial function, decreased life span and tumor growth in mice. *Hum. Mol. Genet.* 14, 3857–3864. doi:10.1093/hmg/ddi410

Tokarska-Schlattner, M., Zaugg, M., Zuppinger, C., Wallimann, T., and Schlattner, U. (2006). New insights into doxorubicin-induced cardiotoxicity: the critical role of cellular energetics. *J. Mol. Cell. Cardiol.* 41, 389–405. doi:10.1016/j.yjmcc.2006.06.009

Ursini, F., and Bindoli, A. (1987). The role of selenium peroxidases in the protection against oxidative damage of membranes. *Chem. Phys. Lipids* 44, 255–276. doi:10.1016/0009-3084(87)90053-3

Vorgerd, M., Schöls, L., Hardt, C., Ristow, M., Epplen, J., and Zange, J. (2000). Mitochondrial impairment of human muscle in Friedreich ataxia *in vivo*. *Neuromuscul. Disord.* 10, 430–435. doi:10.1016/s0960-8966(00)00108-5

Wang, J., Wilhelmsson, H., Graff, C., Li, H., Oldfors, A., Rustin, P., et al. (1999). Dilated cardiomyopathy and atrioventricular conduction blocks induced by heart-specific inactivation of mitochondrial DNA gene expression. *Nat. Genet.* 21, 133–137. doi:10.1038/5089

Wang, Y., Huang, S., Sah, V. P., Ross, J., Brown, J. H., Han, J., et al. (1998). Cardiac muscle cell hypertrophy and apoptosis induced by distinct members of the p38 mitogen-activated protein kinase family. *J. Biol. Chem.* 273, 2161–2168. doi:10.1074/jbc.273.4.2161

Xu, H., Yu, W., Sun, S., Li, C., Zhang, Y., and Ren, J. (2020). Luteolin attenuates doxorubicin-induced cardiotoxicity through promoting mitochondrial autophagy. *Front. Physiol.* 11, 113. doi:10.3389/fphys.2020.00113

Zhang, J. D., Ruschhaupt, M., and Biczok, R. (2013). *ddCt method for qRT–PCR data analysis*.

Conflict of Interest: The authors declare that the research was conducted in the absence of any commercial or financial relationships that could be construed as a potential conflict of interest.

Copyright © 2021 Fu, Eggert, Yoo, Patel, Zhong, Steinke, Govindarajulu, Turumtay, Mouli, Panizzi, Beyers, Denney, Arnold and Amin. This is an open-access article distributed under the terms of the Creative Commons Attribution License (CC BY). The use, distribution or reproduction in other forums is permitted, provided the original author(s) and the copyright owner(s) are credited and that the original publication in this journal is cited, in accordance with accepted academic practice. No use, distribution or reproduction is permitted which does not comply with these terms.

frontiers in Cardiovascular Medicine

ORIGINAL RESEARCH
published: 21 April 2021
doi: 10.3389/fcvm.2021.655009

Early Passive Leg Movement Prevents Against the Development of Heart Failure With Preserved Ejection Fraction in Rats

*Jian Liu[1,2†], Xi-xin Ji[1†], Yang Fu[1†], Wen-chao Zhang[1], Hui-fang Ji[1], Jian-wei Liu[1], Xiao-shu Cheng[1] and Yi-Fei Dong[1]**

[1] Department of Cardiovascular Medicine, The Second Affiliated Hospital of Nanchang University, Nanchang, China, [2] The First People's Hospital of Yongkang, Yongkang, China

OPEN ACCESS

Edited by:
Jun Ren,
University of Washington,
United States

Reviewed by:
Jing-Song Ou,
The First Affiliated Hospital of Sun Yat-Sen University, China
Ne Natalie Wu,
Fudan University, China
Muralikrishnan Dhanasekaran,
Auburn University, United States

***Correspondence:**
Yi-Fei Dong
yf_dong66@126.com

[†] These authors have contributed equally to this work

Specialty section:
This article was submitted to Cardiovascular Therapeutics, a section of the journal Frontiers in Cardiovascular Medicine

Received: 18 January 2021
Accepted: 26 March 2021
Published: 21 April 2021

Citation:
Liu J, Ji X-x, Fu Y, Zhang W-c, Ji H-f, Liu J-w, Cheng X-s and Dong Y-F (2021) Early Passive Leg Movement Prevents Against the Development of Heart Failure With Preserved Ejection Fraction in Rats. Front. Cardiovasc. Med. 8:655009. doi: 10.3389/fcvm.2021.655009

Exercising was reported by several studies to bring great benefits to heart failure with preserved ejection fraction (HFpEF), which reduced the hospitalization and the mortality of heart failure. However, the underlying mechanism of exercising on HFpEF remains unclear. In the present study, we designed and constructed a device that can perform early passive leg movement (ePLM) in rats and further observed whether treatment of ePLM exerts protective effects on HFpEF of rats. Rats were fed with high salt feed to establish an animal model of pre-clinical diastolic dysfunction (PDD), which would eventually develop into HFpEF, and then treated rats with ePLM. We conducted several experiments to evaluate the conditions of heart and blood vessel. The results show that diastolic functions of heart and blood vessel in rats were significantly improved by treatment of ePLM. We also found that pathological injuries of heart and blood vessel were ameliorated after treatment of ePLM. Moreover, treatment of ePLM decreased the protein levels of Collagen type I, Collagen type III, MMP2, and MMP9 in heart and blood vessel, indicating that cardiac and vascular fibrosis were reduced apparently by treatment of ePLM. Further investigation suggested that treatment of ePLM probably inhibit the activation of TGF-β1/Smad3 signaling pathway as well as promote the activation of Akt/eNOS signaling pathway in high salt diet induced HFpEF. In conclusion, treatment of ePLM alleviated high salt diet induced HFpEF by inhibiting fibrosis *via* suppressing TGF-β1/Smad3 signaling pathway as well as activating Akt/eNOS signaling pathway, implicating treatment of ePLM as a promising novel non-pharmacological approach for HFpEF.

Keywords: heart failure with perserved ejection fraction, pre-clinical diastolic dysfunction, early passive leg movement, cardiac fibrosis, vascular fibrosis

INTRODUCTION

Heart failure with preserved ejection fraction (HFpEF), occupied about 50% of heart failure population, was defined as a peculiar heart failure, which displays diastolic dysfunction but maintains a normal ejection fraction (1, 2). HFpEF is a chronic disease and deteriorates gradually with aging (3). The pathological changes in tissues of heart and blood vessel serve as the major

mechanisms to the disease (4, 5). Several studies have reported that HFpEF resulted in a large number of morbidity and mortality (6). While there was no effective therapeutic methods to improve the prognosis of HFpEF to date (7). Recently, a novel study named PARALLAX trial show that sacubitril/valsartan can ameliorate the outcome of HFpEF, but it needs more investigations to confirm the theory (8). According to these situations, it is necessary to find new therapeutic methods for HFpEF.

Pre-clinical diastolic dysfunction (PDD) is the early stage of cardiac dysfunction, which do not have typical heart failure symptoms and signs, and can only be diagnosed by some auxiliary examinations like echocardiography (9). PDD show a high morbidity of about 27.4% among normal population (10). Several studies suggested that PDD mainly develop into HFpEF (11). Therefore, treatment of PDD might prevent against the development of HFpEF.

Researchers of TOPCAT trial reported that the HFpEF patients who took more exercises had a better prognosis compared to the HFpEF patients who just took little exercises, as evidenced by the facts that the adverse incident risk, hospitalization rate of heart failure, and all-cause mortality rate were lower in the HFpEF patients who took more exercises than the HFpEF patients who just took little exercises (12). Several studies confirmed the conclusion that the HFpEF patients benefit a lot from exercise training (13). These results revealed that exercise training can act as a novel non-pharmacological approach for HFpEF. Instrumental assisted passive movements serve as a simple and effective exercise training (14). Thus, we designed and constructed a device of early passive leg movement (ePLM) to treat rats with PDD and evaluated whether treatment of ePLM can improve the prognosis of HFpEF in rats, and further explored the potential mechanisms.

MATERIALS AND METHODS

Materials

Male Dahl/Salt Sensitive (Dahl/SS) rats (6 weeks old, 150–200 g) were purchased from Beijing Charles River Laboratory Animal Co., Ltd. (Beijing, China). High salt feed (8% NaCl) and Low salt feed (0.3% NaCl) that used to constructed the animal model were obtained from Beijing keao xieli Feed Co., Ltd. (Beijing, China). Passive leg movement device on rats, which was applied for a patent (No. ZL201821187645.0, China), was designed and constructed for treating rats. The working principle of this device is that the rats were anesthetized by continuous inhaling isoflurane at a supine position in the device and then turn on the switch to make an early passive leg movement (ePLM) by the device (**Supplementary Figure 1**). The antibodies applied to the present study are as follows: Collagen type I antibody (Cat. No. 14695-1-AP; Proteintech), Collagen type III antibody (Cat. No. 22734-1-AP; Proteintech), MMP2 antibody (Cat. No. ab97779; Abcam), MMP9 antibody (Cat. No. ab58803; Abcam), TGF-β1 antibody (Cat. No. 21898-1-AP; Proteintech), p-Smad3 antibody (Cat. No. CST-9510S; Cell Signaling Technology), Smad3 antibody (Cat. No. CST-5678S; Cell Signaling Technology), SOD-1 antibody (Cat. No. ab51254; Abcam), p-Akt antibody (Cat. No. ab38449; Abcam), Akt antibody (Cat. No. ab8805; Abcam), p-eNOS antibody (Cat. No. CST-9570; Cell Signaling Technology), eNOS antibody (Cat. No. CST-32027; Cell Signaling Technology), GAPDH antibody (Cat. No. ab8245; Abcam), Tubulin antibody (Cat. No. ab7291; Abcam). The enzyme-linked immunosorbent assay (ELISA) kits for measurement of NT-ProBNP in serum of rats was purchased from Elabscience Biotechnology Co., Ltd. (Wuhan, China). All other reagents used in this study are common and can be acquired easily.

Animal Model

The treatments in rats were performed in accordance with the guidelines of the Animal Care and Use Committee of the Second Affiliated Hospital of Nanchang University (China). In the present study, a total number of 48 male Dahl/SS rats were used for experimental operations. Rats were group-housed in the Animal Center of Jiangxi Medicine of Nanchang University within a 12-h light/dark cycle, with ambient temperature maintaining at $23 \pm 2^{\circ}$C and relative humidity at $50 \pm 10\%$.

In order to adapt the housing conditions, rats first were fed with Low salt feed (0.3% NaCl) for 7 days before any experimental operations. Then the rats were roughly and randomly divided into two groups and given different treatments: (1) Normal group (NS, $n = 12$): The rats in this group were fed with Low salt feed (0.3% NaCl) consistently until sacrificed. (2) High Salt group (HS, $n = 36$): The rats in this group were fed with High salt feed (8% NaCl). After 5 weeks feeding, all rats were gathered together for measurements of echocardiography and blood pressure analysis to evaluate the cardiac function, and we successfully constructed an animal model of PDD in High Salt group (**Table 1**). Next, the rats of High Salt group were further divided into three groups randomly with different treatments for 8 weeks: (1) High Salt group (HS, $n = 12$): Treatments on rats were as before. (2) Early Passive Leg Movement group (HS+ePLM, $n = 12$): Apart from feeding with High salt feed (8% NaCl), the rats were given treatment of ePLM with a passive leg movement device in the condition that rats were anesthetized *via* continuous inhaling isoflurane, with exercise time of 5 days per week, 20 min per day, and 120 revolutions per minute. (3) Isoflurane group (HS+ISO): The treatments of this group were approximately same to the ePLM group except not giving treatment of ePLM. Rats were anesthetized by continuous inhaling isoflurane at a supine position to eliminate the influence of posture and isoflurane and reduce the variables. With 8 weeks treatments, we saw a typical HFpEF in rats of HS group *via* various measurements like echocardiography.

Blood Pressure and Echocardiography Analyses

Blood pressure and heart rate analyses were conducted by a device named BP-2010E non-invasive rat tail sphygmomanometer (Softron, Japan). The working principle of this device is to measure the tail arterial pulse of rats, and a waveform of blood pressure can be obtained automatically. Rats were bound in a board, with a transducer attaching in 3 cm of rats tail root. The blood pressure and heart rate were obtained

TABLE 1 | Echocardiographic data and blood pressure of rats were measured in 12 weeks old.

Parameters	NS	HS
BW (g)	313.71 ± 10.70	297.00 ± 14.13
HR (bmp)	374.03 ± 12.27	389.35 ± 23.04
SBP (mmHg)	119.53 ± 8.31	172.23 ± 5.79*
LVID-d (mm)	5.89 ± 0.86	6.30 ± 0.77
IVS-d (mm)	1.83 ± 0.13	2.28 ± 0.14*
LVPW-d (mm)	1.81 ± 0.18	2.15 ± 0.17*
EF (%)	78.28 ± 9.63	71.86 ± 7.39
FS (%)	48.59 ± 9.36	41.34 ± 5.71
E/A	1.88 ± 0.12	3.21 ± 0.07*
LV mass corrected	612.05 ± 126.10	853.92 ± 117.50*

*Variables were expressed as means ± SD. NS, Normal group; HS, High Salt group; BW, body weight; HR, heart rate; SBP, systolic blood pressure; LVID-d, left ventricular internal dimensions at the end-diastole; IVS-d, interventricular septum thickness at the end-diastole; LVPW-d, left ventricular posterior wall thickness at the end-diastole; EF, ejection fraction; FS, fractional shortening; E/A, maximum peak blood flow velocity at early phase of diastole/maximum peak blood flow velocity at the end of diastole; LVmass corrected, left ventricular mass corrected. *P < 0.05 vs. NS group.*

from the device automatically. We repeated for about 6 times to get a mean value that was used for the final analysis. The operations were performed at two periods of 12 weeks old and 20 weeks old of rats.

Echocardiography was used to assess the function of heart through a device named Vevo770 (VisualSonics, Toronto, Canada), which was equipped with a 30 Hz transducer. First, rats were anesthetized by continuous administration of 2–3% isoflurane and bound in a heating board in a supine position, with the rats hair in chest being cleaned by a razor. Then we applied a short-axis view of the M-mode ultrasound to measuring left ventricle internal dimensions at the end of diastole (LVID-d), left ventricular posterior wall thickness at end of diastole (LVPW-d), interventricular septum thickness at end of diastole (IVS-d), left ventricular mass corrected, left ventricular ejection fraction (EF%), and left ventricular fractional shortening (FS%). Furthermore, four-chamber view of the color Doppler ultrasound was used for measuring maximum peak blood flow velocity at early phase of diastole (E) and maximum peak blood flow velocity at the end of diastole (A) in mitral orifice. Rats were conducted at 12 weeks old and 20 weeks old and the final analysis adopted average values of 6 repeated detections.

Hemodynamics Analysis

Before sacrificed, the rats were used to measure the blood flow parameters *via* carotid artery, such as left ventricular end-diastolic pressure (LVEDP), maximum left ventricular pressure decreasing rate (–dp/dtmax), and maximum left ventricular pressure increasing rate (+dp/dtmax). The device named Multichannel biological recorder (Chengdu Instrument Company, Sichuan), which connected with artery cannula and blood pressure transducer, were available for the experimental operations. First, we used 3% pentobarbital sodium (60 mg/kg) to anesthetize rats through intraperitoneal injection, with rats fixing on a heating board in a supine position. Next, the right carotid artery was isolated, which was ligated of the distal end and shut down of the proximal end of the artery. Then we made a V-shaped incision in the middle of right carotid artery. Finally, the artery cannula was inserted into the left ventricular and the blood flow parameters were collected for final analysis. Since these experimental operations, rats were sacrificed under 3% pentobarbital sodium anesthesia (60 mg/kg) and tissues were collected immediately for further experiments.

Vascular Diastolic Function Analysis

After rats were sacrificed, the thoracic aorta was isolated immediately and used for detecting the vascular diastolic function. DMT620 (Softron, Japan) and Krebs-Henseleit solution were available in this process. We used acetylcholine (Ach) and sodium nitroprusside (SNP) to measure endothelium-dependent or endothelium-independent vasodilation of thoracic aorta. The detailed experimental procedures were in accordance with the previous study.

Enzyme-Linked Immunosorbent Assay Analysis

The NT-ProBNP level in serum was detected through a specific ELISA kit of NT-ProBNP (MultiSciences Biotech Co., Ltd., Wuhan, China), which was in accordance to the instructions of ELISAkit.

H and E and Masson Staining Analyses

The tissues of heart and aorta were isolated from rats and washed carefully in ice-cold saline for three times at least. One portion of heart and aorta were put into 4% formaldehyde solution separately for about 1 h and cut into 5-μm sections at various depths to conducted the procedures of H&E and Masson staining according to the instructions of kits. The "heart injury score" was evaluated by apoptosis, contraction band necrosis, neutrophilic infiltration, intramuscular bleeding, rupture, edema and ischemia (15).

Reactive Oxygen Species Staining Analysis

The tissues of aorta were fixed on 4% formaldehyde solution and frozen in −80°C refrigerator. Then, the frozen tissues were incubated with Dihydroethidium (DHE) for 30 min at 37°C. Next, the tissues were washed out for three times with PBS. Finally, we applied a fluorescence microscope to observing the fluorescence image and the fluorescence intensity of DHE was used for final analysis. The remaining tissues of heart and aorta were stored at −80°C refrigerator and was used to further investigate the molecular mechanisms.

Western Blotting Analysis

A specific protein extraction kit (Cat. No. P0013B, Beyotime Biotechnology, Jiangsu, China) was available to extract total proteins from rats tissues of heart and aorta. The proteins concentration was measured by BCA protein assay kit (Cat. No. P0012, Beyotime Biotechnology, Jiangsu, China). Then, we used 10% sodium dodecyl sulfate–polyacrylamide gel electrophoresis (SDS-PAGE) to divide the total proteins into various target

proteins, and the target proteins were transferred to PVDF membranes (Millipore, Bedford, MA, USA) quickly. Afterwards, the PVDF membranes that contain target proteins were incubated with certain primary antibodies for more than 12 h at 4°C before incubation with certain secondary antibodies such as goat anti-rabbit IgG or goat anti-mouse IgG (ZSGB-Bio, Peking, China, 1:5000). The primary antibodies available in this study were as follows: Collagen type I antibody (1:1000), Collagen type III antibody (1:1000), MMP2 antibody (1:1000), MMP9 antibody (1:1000), TGF-β1 antibody (1:1000), p-Smad3 antibody (1:500), Smad3 antibody (1:1000), SOD-1 antibody (1:1000), p-Akt antibody (1:1000), Akt antibody (1:1000), p-eNOS antibody (1:500), eNOS antibody (1:1000), GAPDH antibody (1:1000), Tubulin antibody (1:1000). Finally, we applied an enhanced chemiluminescence (ECL) detection kit to measuring the target proteins band through an ECL scanner (Thermo Fisher Scientific). Image Lab 4.0.1 software was used in the present study to analyze the results and all target proteins measurements were repeated at least three times.

Statistical Analysis

GraphPad Prism 7.0 software (GraphPad Software Inc., San Diego, CA, U.S.) was used for statistical analysis. The Student's *t*-test was used for the comparisons between two groups, while the one-way ANOVA for the comparisons of multiple groups. Experimental data were expressed as the means ± standard deviations (SD) ($n = 12$). *P*-values < 0.05 represented statistically difference. *P*-values < 0.01 and *P*-values < 0.001 indicated statistically significant difference.

RESULTS

High Salt Diet Induced Pre-clinical Diastolic Dysfunction of Heart in Rats

After 5 weeks high salt diet, we successfully constructed an animal model of PDD in rats, as evidenced by some measurement indexes (**Table 1**). First, systolic blood pressure (SBP) of rats in the HS group show a significant changes ($P < 0.05$) compared to the NS group, with SBP increasing apparently. Yet there were no obvious differences in heart rates (HR) and body weight (BW) between the two groups. Echocardiography analysis revealed that cardiac diastolic function was damaged by high salt diet. Despite the fact that ejection fraction (EF%) and fractional shortening (FS%) as well as left ventricle internal dimensions at the end of diastole (LVID-d) displayed few differences between the two groups, we found that left ventricular posterior wall thickness at end of diastole (LVPW-d), interventricular septum thickness at end of diastole (IVS-d), maximum peak blood flow velocity at early phase of diastole/maximum peak blood flow velocity at the end of diastole (E/A) and left ventricular mass corrected (LV mass corrected) in the HS group increased significantly ($P < 0.05$) in contrast to the NS group. These results show that cardiac diastolic function was damaged while cardiac systolic function remained normal, indicating that the animal model of PDD was constructed by high salt diet.

High Salt Diet Further Promoted the Development of PDD and Eventually Resulted in Heart Failure With Preserved Ejection Fraction

Continuously fed with high salt feed for 8 weeks, rats with 20 weeks old were evaluated through some measurement parameters. The results show that PDD further developed into HFpEF in the HS group. SBP and BW in the HS group show a significant changes ($P < 0.001$) compared to the NS group, while HR in the HS group had little differences in contrast to the NS group (**Figures 1B–D**). LVPW-d, IVS-d, and LV mass corrected, which were detected by the M-mode ultrasound, increased significantly ($P < 0.01$) in the HS group despite of no significant differences in LVID-d, EF%, and FS% between the two groups (**Figures 1H–N**). Furthermore, the color Doppler ultrasound was used to assess the value of E/A ratio, and we found a significant increasing ($P < 0.001$) of this indices in the HS group compare with the NS group (**Figure 1O**). In addition, we also measured the indices like left ventricular end-diastolic pressure (LVEDP), maximum left ventricular pressure decreasing rate (−dp/dtmax) and maximum left ventricular pressure increasing rate (+dp/dtmax). The results show that there was no significant differences in +dp/dtmax of the two groups, while LVEDP and −dp/dtmax displayed a obvious changes ($P < 0.001$) between the two groups, with LVEDP increasing while −dp/dtmax reducing in the HS group in contrast to the NS group (**Figures 1P–R**). All the data demonstrated that we successfully constructed an animal model of HFpEF by fed with high salt feed. The data also proved the fact that PDD can develop into HFpEF through high salt diet.

Treatment of Early Passive Leg Movement Alleviated Deterioration of Cardiac Diastolic Function of HFpEF

HFpEF is a chronic disease and deteriorates gradually following aging, with cardiac diastolic dysfunction being a typical symptom. In the present study, we treated rats in 12 weeks old with ePLM to assess whether treatment of ePLM prevents against the development of PDD into HFpEF and the animal treatment protocols are summarized in **Figure 1A**. We obtained a positive result that treatment of ePLM exerted a protective role in deterioration of cardiac diastolic function of HFpEF. First, general parameters like SBP, HR, Heart weight (HW), and HW/BW did not see significant improvements through treatment of ePLM (**Figures 1B–F**). While others such as BW and Lung weight (LW)/BW acquired obvious improvements ($P < 0.05$) with treatment of ePLM (**Figures 1D,G**). Unfortunately, we did not find apparent improvements by treatment of ePLM according to the data collected in the M-mode ultrasound analysis. Parameters like EF%, FS%, LVID-d, LVPW-d, LV mass corrected, and IVS-d did not have apparent changes in the groups of HS group, HS+ePLM group and HS+ISO group (**Figures 1H–N**). But the color Doppler ultrasound and hemodynamics analyses show a amazing result. Ratio of E/A, −dp/dtmax, and LVEDP revealed significant improvements ($P < 0.05$) through treatment of ePLM despite of no obvious changes in +dp/dtmax (**Figures 1O–R**). In addition, we observed from

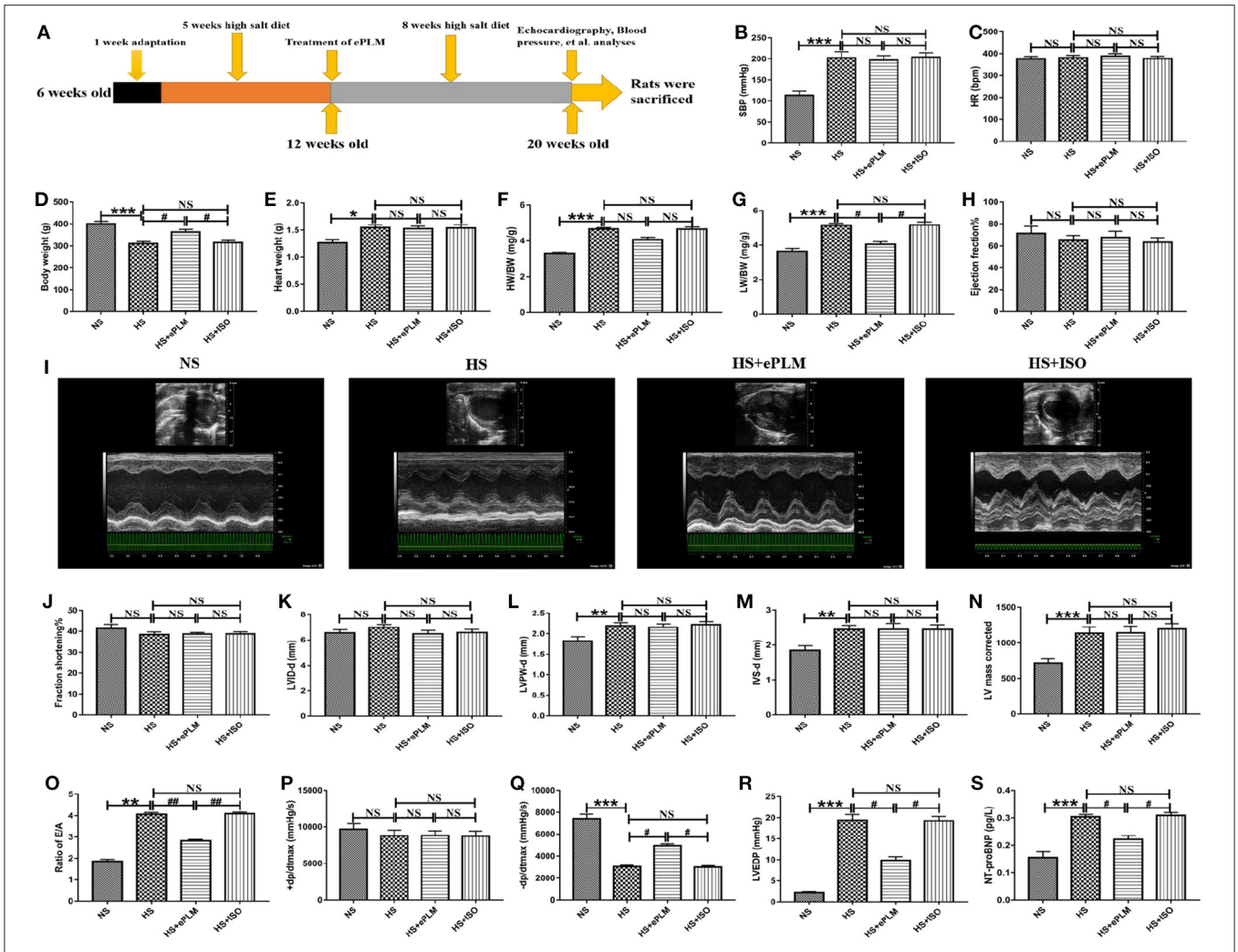

FIGURE 1 | Cardiac diastolic function of HFpEF was improved by treatment of ePLM. **(A)** Overview of animal treatment protocols used in the present study ($n = 12$ each group). **(B–G)** Different parameters like SBP, HR, BW, HW, HW/BW, and LW/BW were obtained *via* many measurements to assess the general conditions of rats. **(H–O)** Parameters like EF, FS, LVID-d, LVPW-d, IVS-d, LVmass corrected and E/A ratio were investigated by echocardiography analysis. **(P–R)** Hemodynamics analysis was performed and parameters like +dp/dtmax, −dp/dtmax and LVEDP were collected. **(S)** ELISA analysis of NT-ProBNP level in serum of rats. $^{*}P < 0.05$, $^{**}P < 0.01$, $^{***}P < 0.001$, $^{\#}P < 0.05$, and $^{\#\#}P < 0.01$ means statistic significance; NS means no statistic significance. All data represent the mean ± SD of at least three experiments.

the ELISA analysis that NT-proBNP level decreased significantly ($P < 0.05$) in the HS+ePLM group compared to the HS group and the HS+ISO group, suggesting that treatment of ePLM can alleviate the development of HFpEF (**Figure 1S**). We concluded from these data that treatment of ePLM can alleviate deterioration of cardiac diastolic function of HFpEF, but cannot reverse the cardiac remodeling, indicating that treatment of ePLM might act as a novel effective precaution approach for HFpEF.

Treatment of Early Passive Leg Movement Alleviated Pathological Injury in Heart Tissue of HFpEF

Pathological injury in heart tissue is a typical feature of HFpEF. In the present study, we evaluated the pathological changes in heart tissue through H&E and Masson staining analyses. First, the result of H&E staining analysis show a significant improvement ($P < 0.05$) with treatment of ePLM in the HS+ePLM group compared with the HS group and the HS+ISO group (**Figures 2A,C**). Similar to the result of H&E staining analysis, the fibrotic area detected by Masson staining analysis reduced obviously ($P < 0.05$) in the HS+ePLM group in contrast to the HS group and the HS+ISO group (**Figures 2B,D**). The results suggested that treatment of ePLM can alleviate pathological injury in heart tissue of HFpEF, indicating treatment of ePLM being a novel non-pharmacological approach for HFpEF.

Treatment of Early Passive Leg Movement Inhibited Cardiac Fibrosis of HFpEF

In order to explore the mechanism of treatment of ePLM in HFpEF, we conducted western blotting analysis to measure the protein level in heart tissue. First, the protein level of fibrotic

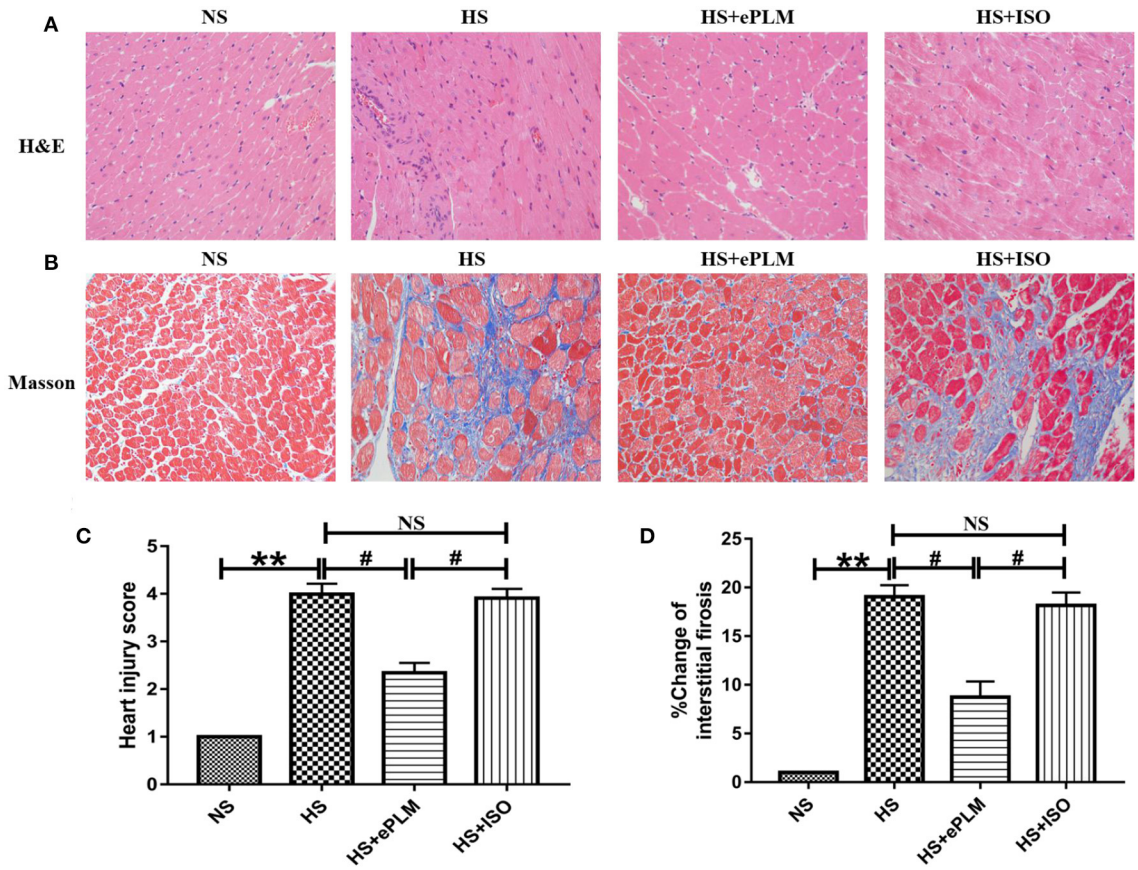

FIGURE 2 | Pathological injuries in heart of rats were significantly improved by treatment of ePLM. **(A,C)** H&E staining of heart tissues and heart injury score. **(B,D)** Massion staining analysis was performed to evaluate the area of cardiac fibrosis ($n = 12$ each group). $^{**}P < 0.01$ and $^{\#}P < 0.05$ means statistic significance; NS means no statistic significance. All data represent the mean ± SD of at least three experiments.

factor (Collagen type I) increased significantly ($P < 0.01$) in heart tissues of the HS group and the HS+ISO group compared to the NS group, while this effect was significantly inhibited ($P < 0.01$) by treatment of ePLM in the HS+ePLM group (**Figures 3A,B**). The proteins of MMP2 and MMP9 exert an important role in maintaining the balance of extracellular matrix and participate in the process of fibrosis. In the present study, we observed that the protein expression levels of pro-fibrotic genes (MMP2 and MMP9) increased significantly ($P < 0.01$) in heart tissues of the HS group and the HS+ISO group compared with the NS group, while the effect was significantly inhibited ($P < 0.05$) by treatment of ePLM in the HS+ePLM group (**Figures 3A–D**). The changes of the protein levels (Collagen I, MMP2, and MMP9) suggested that high salt diet and ePLM had a significant influence on cardiac fibrosis, with high salt diet inducing cardiac fibrosis while treatment of ePLM inhibiting cardiac fibrosis. The TGF-β1/Smad3 signaling pathway exerts an important role in the process of fibrosis. Thus, we further investigated the protein levels of TGF-β1 and p-Smad3 by the western blotting analysis. High salt diet upregulated the expression of TGF-β1 and the ratio of p-Smad3 to total Smad3, while the effect was inhibited by treatment of ePLM (**Figures 3A–F**), indicating that the TGF-β1/Smad3 signaling pathway might participate in the beneficial effect of treatment of ePLM on high salt diet-induced cardiac fibrosis. Akt/eNOS signaling pathway has been reported by several studies to be associated crucially with fibrosis. Therefore, we also measured the protein levels of p-Akt and p-eNOS. The results show that the protein levels of p-Akt and p-eNOS reduced significantly ($P < 0.01$) in heart tissues of the HS group and the HS+ISO group compared to the NS group, while this effect was significantly inhibited ($P < 0.05$) by treatment of ePLM in the HS+ePLM group (**Figures 3G–I**), suggesting that Akt/eNOS signaling pathway might also play an important role in the process of cardiac fibrosis.

Treatment of Early Passive Leg Movement Alleviated the Injury of Blood Vessel in HFpEF

It is well-known that the injury of blood vessel is a typical pathological change to HFpEF. Alleviating blood vessel injury can improve the prognosis of HFpEF. Thus, we also evaluated the function of blood vessel in HFpEF through vascular diastolic function analysis in the present study. Acetylcholine (Ach)

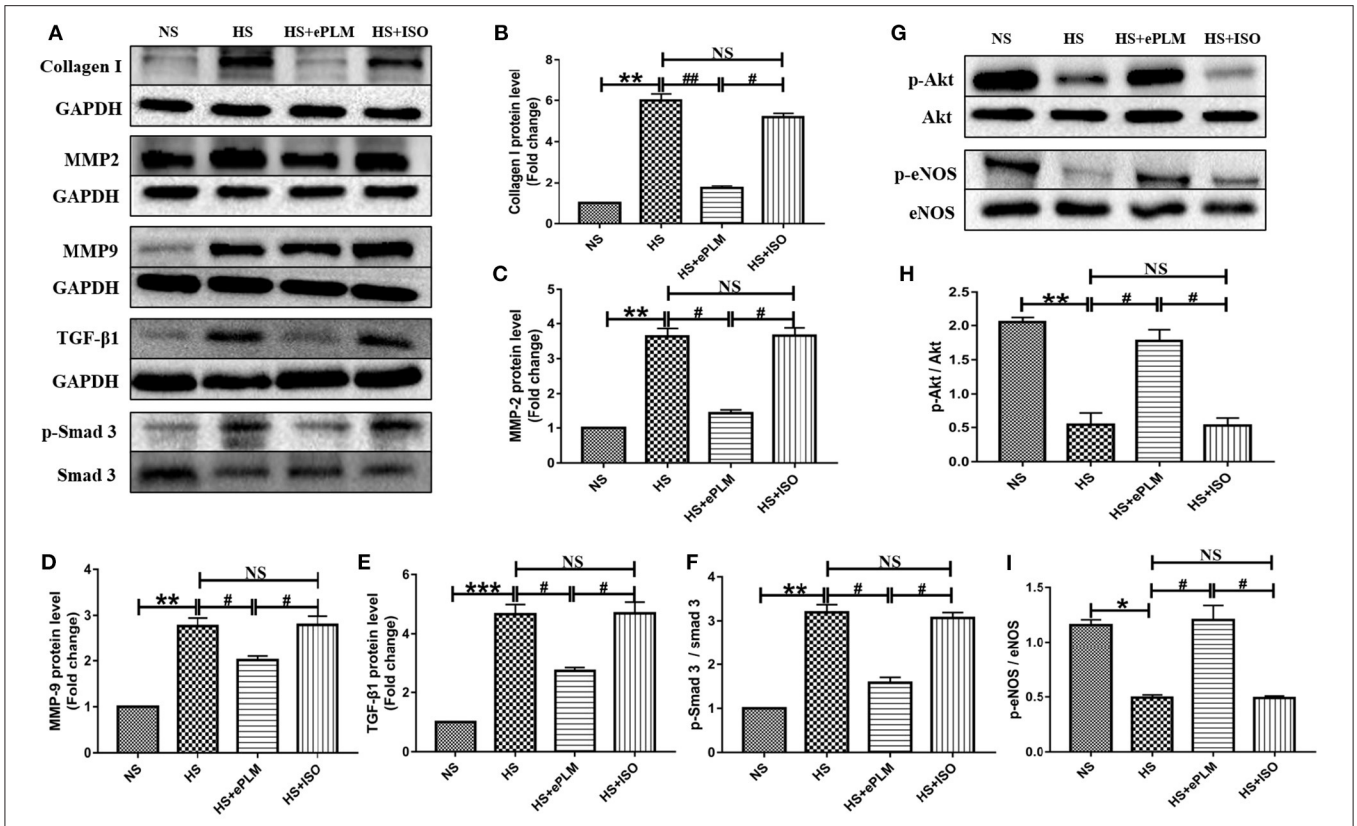

FIGURE 3 | Treatment of ePLM can inhibit cardiac fibrosis *via* TGF-β1/Smad3 and Akt/eNOS signaling pathways potentially. **(A,G)** Western blotting analysis of protein levels in rats heart tissues ($n = 12$ each group). **(B–D)** Statistical analyses of protein levels (Collagen I, MMP2, and MMP9). **(E,F)** The protein levels of TGF-β1/Smad3 signaling pathway (TGF-β1 and p-Smad3). **(H,I)** The protein levels of Akt/eNOS signaling pathway (p-Akt and p-eNOS). $^{*}P < 0.05$, $^{**}P < 0.01$, $^{***}P < 0.001$, $^{\#}P < 0.05$, and $^{\#\#}P < 0.01$ means statistic significance; NS means no statistic significance. All data represent the mean ± SD of at least three experiments.

was used to measure endothelium-dependent vasodilation and sodium nitroprusside (SNP) was used to measure endothelium-independent vasodilation. The results show that endothelium-dependent vasodilation was damaged seriously ($P < 0.05$) by the high salt diet in the HS group and the HS+ISO group compared to the NS group, while this effect was inhibited significantly ($P < 0.05$) through the treatment of ePLM in the HS+ePLM group (**Figure 4A**). However, treatment of ePLM only improved endothelium-independent vasodilation dysfunction in a certain degree (**Figure 4B**). In summary, treatment of ePLM improved the vascular diastolic dysfunction of HFpEF. We further detected the pathological changes of blood vessel through H&E and Masson staining analyses. H&E staining analysis show that arterial wall thickness increased significantly ($P < 0.05$) in the HS group and the HS+ISO group compared with the NS group, while this effect was inhibited significantly ($P < 0.05$) by treatment of ePLM in the HS+ePLM group (**Figures 4C,F**). Masson staining analysis show that the fibrotic area increased significantly ($P < 0.05$) in the HS group and the HS+ISO group compared to the NS group, while reduced significantly ($P < 0.05$) in the HS+ePLM group (**Figures 4D,G**). In addition, we also measured the changes of reactive oxygen species (ROS) by DHE staining, the result show that the level of ROS increased significantly ($P < 0.05$) in the HS group and the HS+ISO group in contrast to the NS group, while reduced significantly ($P < 0.05$) in the HS+ePLM group (**Figures 4E,H**). All these data suggested that treatment of ePLM alleviated the injury of blood vessel in HFpEF.

Treatment of Early Passive Leg Movement Inhibited Vascular Fibrosis of HFpEF

Vascular fibrosis serves as an important part of HFpEF. Thus, we conducted western blotting analysis to measure the protein levels in blood vessel. The protein levels of fibrotic factors (Collagen type I and Collagen type III) increased significantly ($P < 0.01$) in blood vessel of the HS group and the HS+ISO group compared to the NS group, while this effect was significantly inhibited ($P < 0.01$) by treatment of ePLM in the HS+ePLM group (**Figures 5A–E**). Moreover, the protein levels of pro-fibrotic genes (MMP2 and MMP9) increased significantly ($P < 0.01$) in blood vessel of the HS group and the HS+ISO group compared with the NS group, while the effect was significantly inhibited ($P < 0.01$) by treatment of ePLM in the HS+ePLM group (**Figures 5A–G**). The results show that high salt diet and treatment of ePLM had a significant influence in vascular fibrosis, with high salt diet inducing vascular fibrosis while treatment

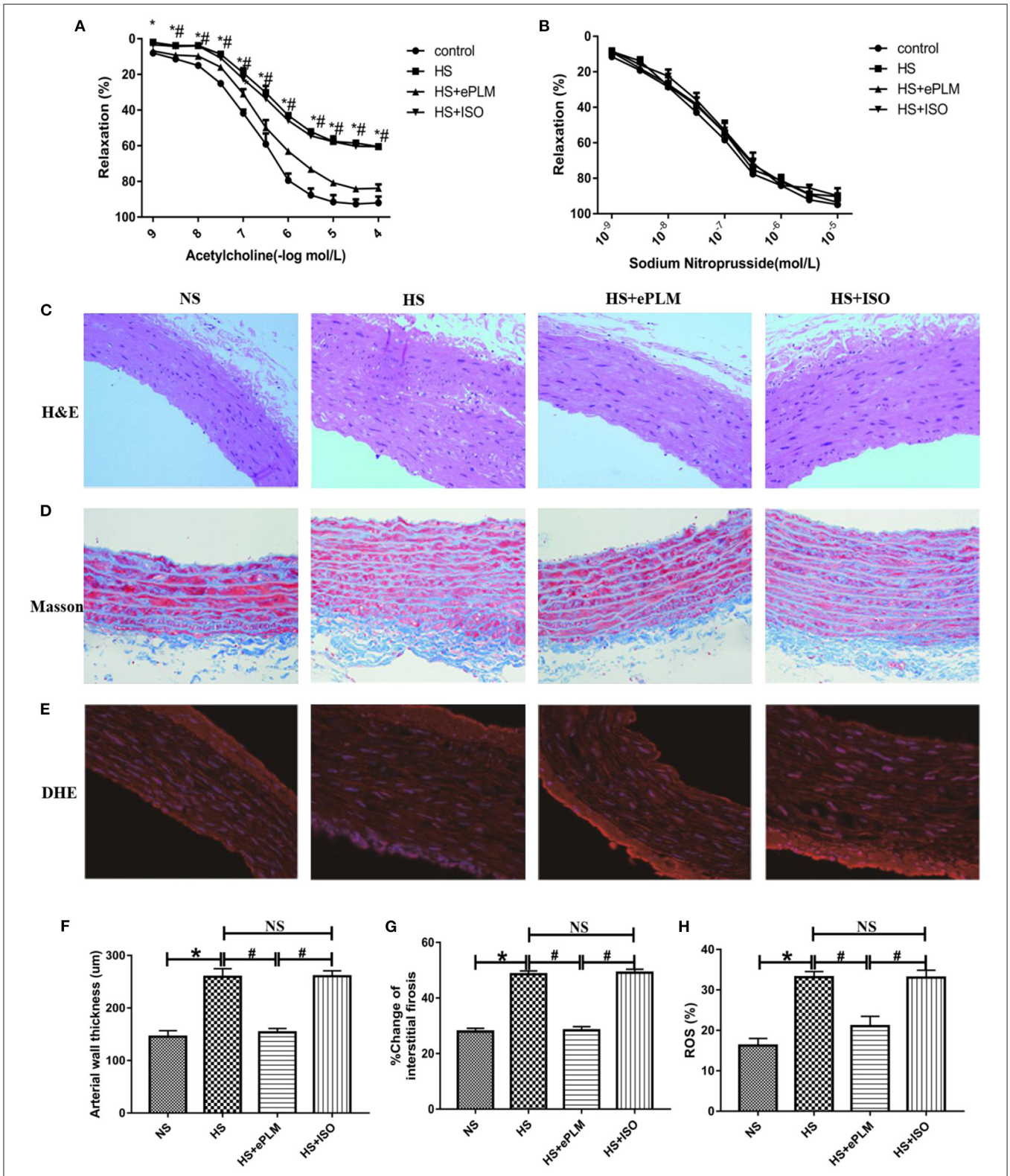

FIGURE 4 | Treatment of ePLM alleviated the injury of blood vessel in HFpEF. **(A,B)** Endothelium-dependent vasodilation and endothelium-independent vasodilation were detected *via* vascular diastolic function analysis by using acetylcholine (Ach) and sodium nitroprusside (SNP) ($n = 12$ each group). **(C,F)** H&E staining of blood vessel and measurement of arterial wall thickness. **(D,G)** Massion staining analysis was conducted to evaluate the area of vascular fibrosis. **(E,H)** The level of ROS was measured by DHE staining. $^{*}P < 0.05$ and $^{\#}P < 0.05$ means statistic significance; NS means no statistic significance. All data represent the mean ± SD of at least three experiments.

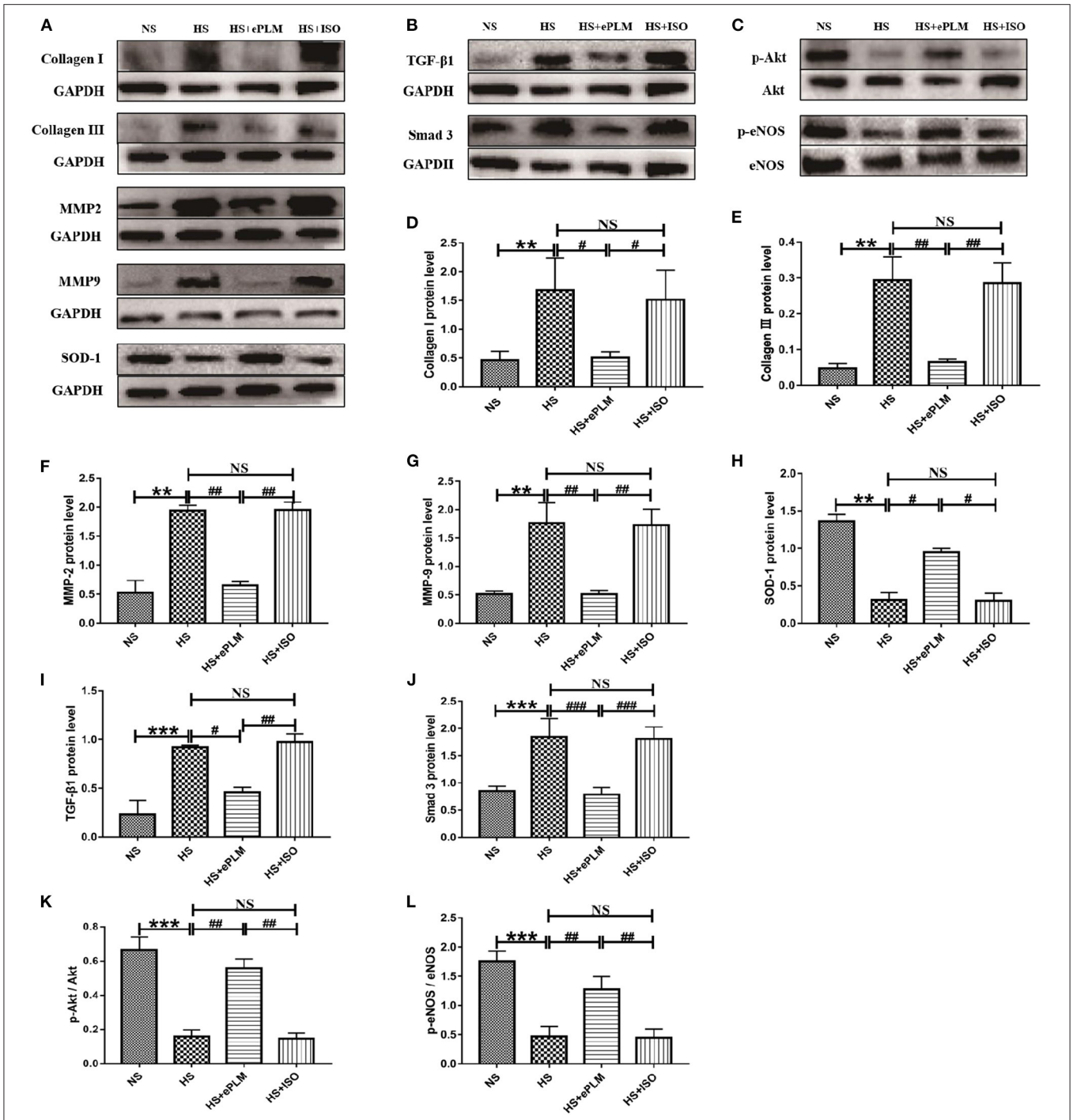

FIGURE 5 | Treatment of ePLM inhibited vascular fibrosis *via* TGF-β1/Smad3 and Akt/eNOS signaling pathways potentially. **(A–C)** Western blotting analysis of protein levels in blood vessel of rats ($n = 12$ each group). **(D–G)** Statistical analyses of protein levels (Collagen I, Collagen III, MMP2, and MMP9). **(H)** The protein level of antioxidant SOD-1. **(I,J)** The protein levels of TGF-β1/Smad3 signaling pathway (TGF-β1 and Smad3). **(K,L)** The protein levels of Akt/eNOS signaling pathway (p-Akt and p-eNOS). $^{**}P < 0.01$, $^{***}P < 0.001$, $^{\#}P < 0.05$, $^{\#\#}P < 0.01$, and $^{\#\#\#}P < 0.001$ means statistic significance; NS means no statistic significance. All data represent the mean ± SD of at least three experiments.

of ePLM inhibiting vascular fibrosis. The protein of SOD-1 exerts a function of anti-oxidation. In this study, we found that the level of SOD-1 increased significantly ($P < 0.05$) by treatment of ePLM (**Figures 5A,H**). We also investigated the protein levels of TGF-β1 and Smad3 and found that high salt diet upregulated the expression of TGF-β1 and Smad3, while

the effect was inhibited by treatment of ePLM (**Figures 5B,I,J**), indicating that the TGF-β1/Smad3 signaling pathway might participate in the protective effect of treatment of ePLM on high salt diet-induced vascular fibrosis. In addition, we measured the protein levels of p-Akt and p-eNOS and the results show that the protein levels of p-Akt and p-eNOS reduced significantly ($P < 0.01$) in blood vessel of the HS group and the HS+ISO group compared to the NS group, while this effect was significantly inhibited ($P < 0.01$) by treatment of ePLM in the HS+ePLM group (**Figures 5C–L**), suggesting that Akt/eNOS signaling pathway might also play an important role in the process of vascular fibrosis.

DISCUSSION

In the present study, we first successfully constructed an animal model of PDD in rats at 12 weeks old, and PDD eventually developed into HFpEF through high salt diet. Then we treated rats in period of PDD with early passive leg movement (ePLM) to evaluate its effect on HFpEF. The study show that treatment of ePLM exerted a protective effect on HFpEF, implicating that treatment of ePLM as a promising novel non-pharmacological approach for HFpEF.

It is reported that mitochondrial homeostasis serves as an important role in the progression of heart failure (16). Further studies concluded that overload of Ca^{2+} in mitochondrion will open the mitochondrial permeability transition pore (mPTP) and contribute to mitochondrial swelling, which will result in injury of mitochondrion, apoptosis, cardiac remodeling, and ultimately development into heart failure (17). HFpEF is a severe and chronic disease and belongs to heart failure, which results in numerous deaths of patients (6). However, there was no effective therapeutic approaches to improve the prognosis of HFpEF to date (7). Although a study recently reported that sacubitril/valsartan might ameliorate the outcome of HFpEF, but it needs more investigations to comfirm the theory (8). Thus, its urgent to explore novel therapeutic approaches for HFpEF. Several studies have reported that patients of HFpEF benefited a lot from exercising, with enhancing sport ability and improving living quality, which indicated that exercising might serve as a more promising novel non-pharmacological approach for HFpEF (13). Exercising also show a good security and effectiveness to the patients with a poor physical conditions (18). Instrumental assisted passive movement was proved as a simple and effective method of exercising (14). So our team designed and constructed a device of ePLM to pretreat rats in the period of PDD, which eventually developed into HFpEF, to evaluate the effect of treatment of ePLM on HFpEF.

Cardiac diastolic dysfunction is a typical symptom of HFpEF (2). In our study, we confirmed the theory by the findings that parameters like LVPW-d, IVS-d, LV mass corrected, E/A ratio, and LVEDP increased significantly while –dp/dtmax reduced in the HS group in contrast to the NS group. After treatment of ePLM, the condition of cardiac diastolic function was significantly improved, evidenced by the fact that ratio of E/A, –dp/dtmax, and LVEDP revealed a obvious improvement, despite of no apparent changes in LVPW-d, IVS-d, LV mass corrected, and +dp/dtmax. Consistent with the fact that NT-ProBNP serves as a strong predictive factor of heart failure events in patients with HFpEF (19), we discovered that the level of NT-ProBNP in rats serum with HFpEF decreased significantly by the treatment of ePLM. We also found that pathological injuries in heart were ameliorated after treatment of ePLM. All these data collected from the study suggested that treatment of ePLM might serve as a novel therapeutic approach for HFpEF. We further explored the molecular mechanism of treatment of ePLM through western blotting analysis. The proteins of MMP2 and MMP9 exert an important role in maintaining the balance of extracellular matrix and participate in the process of fibrosis (20). We found in this study that the protein levels of fibrotic factor (Collagen type I) and pro-fibrotic genes (MMP2 and MMP9) reduced obviously by treatment of ePLM. TGF-β1/Smad3 signaling pathway has been reported to play an important role on the development of cardiac fibrosis (21). Thus, we supposed that TGF-β1/Smad3 signaling pathway might be involved in the anti-fibrotic role of treatment of ePLM in cardiac fibrosis induced by the high salt diet. Our findings show that treatment of ePLM markedly suppressed the activation of TGF-β1/Smad3 signaling pathway during the progression of the high salt diet induced cardiac fibrosis, suggesting that this signaling pathway might be involved in the cardioprotective effects of treatment of ePLM in HFpEF. Akt/eNOS signaling pathway also has been reported to be associated crucially with fibrosis (22). Therefore, we also detected the protein levels of p-Akt and p-eNOS. The results show that the protein levels of p-Akt and p-eNOS increased significantly in heart tissues by treatment of ePLM, suggesting that Akt/eNOS signaling pathway might also play an important role in the process of cardiac fibrosis with HFpEF.

It is reported that the injury of blood vessel acts as a major part in pathological injuries of HFpEF (23). Thus, alleviating blood vessel injury might prevent against the development of HFpEF. In the present study, we observed that treatment of ePLM improved the vascular diastolic dysfunction of HFpEF through vascular diastolic function analysis. We further measured the pathological changes of blood vessel by H&E and Masson staining and discovered that pathological injuries in blood vessel of HFpEF were apparently improved by treatment of ePLM. Reactive oxygen species (ROS) are a kind of single electron reductive products that contain oxygens, which usually lead to bad effects of blood vessel like increasing vascular thickness or inhibiting release of NO (24). We detected the level of ROS by DHE staining and found that treatment of ePLM significantly reduced the level of ROS in blood vessel with HFpEF. We also measured the level of SOD-1 by western blotting analysis, with SOD-1 exerting a function of anti-oxidation (25), and observed that treatment of ePLM apparently increased the level of SOD-1 in blood vessel with HFpEF, suggesting that treatment of ePLM might balance the redox reaction to ameliorate blood vessel injury. All these data suggested that treatment of ePLM alleviated the injury of blood vessel in

HFpEF. We further investigated the molecular mechanism of treatment of ePLM in blood vessel with HFpEF. The pro-fibrotic protein levels of Collagen type I, Collagen type III, MMP2, and MMP9 reduced significantly after treatment of ePLM, indicating that treatment of ePLM inhibited vascular fibrosis in HFpEF. TGF-β1/Smad3 signaling pathway and Akt/eNOS signaling pathway in blood vessel were also detected in this study and we obtained a similar result to heart tissues, suggesting that TGF-β1/Smad3 signaling pathway and Akt/eNOS signaling pathway both play an important role in the process of alleviating vascular fibrosis by treatment of ePLM in HFpEF.

However, there were some limitations in the present study. First, HFpEF is a complex chronic disease which include a series of pathological changes in tissues like lung and kidney (26). While our study only evaluated two tissues of heart and blood vessel of HFpEF, so it needs more investigations in HFpEF to further confirmed the effect of treatment of ePLM. And an *in vitro* experiment was also needed to be designed and conducted for comprehensively verifying the results.

In summary, the present study suggested that treatment of ePLM prevents against the development of HFpEF in rats. Improving cardiac and vascular injuries might be the major protective mechanisms of treatment of ePLM. Such protective abilities may derive from the inhibition of cardiac and vascular fibrosis by suppressing TGF-β1/Smad3 signaling pathway as well as activating Akt/eNOS signaling pathway. Thus, our findings implied that treatment of ePLM may serve as a more promising novel non-pharmacological approach for HFpEF.

DATA AVAILABILITY STATEMENT

The raw data supporting the conclusions of this article will be made available by the authors, without undue reservation.

ETHICS STATEMENT

The animal study was reviewed and approved by The Animal Care and Use Committee of the Second Affiliated Hospital of Nanchang University (China).

AUTHOR CONTRIBUTIONS

Y-FD designed and funded the experiment. JL, X-xJ, and YF conducted the study and accomplished the paper. W-cZ, H-fJ, J-wL, and X-sC offered some assistance to the experiment. All authors contributed to the article and approved the submitted version.

FUNDING

This study was funded by National Natural Science Foundation of China (81960088 and 81460071), and Innovation driven 5511 project platform and talent team project, Jiangxi, China (20165BCB18020).

SUPPLEMENTARY MATERIAL

The Supplementary Material for this article can be found online at: https://www.frontiersin.org/articles/10.3389/fcvm.2021.655009/full#supplementary-material

REFERENCES

1. Bhatia RS, Tu JV, Lee DS, Austin PC, Fang J, Haouzi A, et al. Outcome of heart failure with preserved ejection fraction in a population-based study. *N Engl J Med*. (2006) 355:260–9. doi: 10.1056/NEJMoa051530
2. Hogg K, Swedberg K, McMurray J. Heart failure with preserved left ventricular systolic function; epidemiology, clinical characteristics, and prognosis. *J Am Coll Cardiol*. (2004) 43:317–27. doi: 10.1016/j.jacc.2003.07.046
3. Cheng S, Xanthakis V, Sullivan LM, Lieb W, Massaro J, Aragam J, et al. Correlates of echocardiographic indices of cardiac remodeling over the adult life course: longitudinal observations from the Framingham Heart Study. *Circulation*. (2010) 122:570–8. doi: 10.1161/CIRCULATIONAHA.110.937821
4. Mohammed SF, Hussain S, Mirzoyev SA, Edwards WD, Maleszewski JJ, Redfield MM. Coronary microvascular rarefaction and myocardial fibrosis in heart failure with preserved ejection fraction. *Circulation*. (2015) 131:550–9. doi: 10.1161/CIRCULATIONAHA.114.009625
5. Maréchaux S, Samson R, Belle EV, Breyne J, Monte JD, Dédrie C, et al. Vascular and microvascular endothelial function in heart failure with preserved ejection fraction. *J Card Fail*. (2016) 22:3–11. doi: 10.1016/j.cardfail.2015.09.003
6. Makaya MT, Hamaguchi S, Kinugawa S, Yokota T, Goto D, Yokoshiki H, et al. Characteristics and outcomes of hospitalized patients with heart failure and reduced vs. preserved ejection fraction: report from the Japanese Cardiac Registry of Heart Failure in Cardiology (JCARE-CARD). *Circ J*. (2009) 73:1893–900. doi: 10.1253/circj.cj-09-0254
7. Aurigemma GP, Gaasch WH. Clinical practice. Diastolic heart failure. *N Engl J Med*. (2004) 351:1097–105. doi: 10.1056/NEJMcp022709
8. Wachter R, Shah SJ, Cowie MR, Szecsödy P, Shi V, Ibram G, et al. Angiotensin receptor neprilysin inhibition compared with individualized medical therapy for comorbidities in patients with heart failure and preserved ejection fraction—the PARALLAX trial. *ESC Heart Fail*. (2020) 7:856–64. doi: 10.1002/ehf2.12694
9. Jessup M, Abraham WT, Casey DE, Feldman AM, Francis GS, Ganiats TG, et al. 2009 focused update: ACCF/AHA guidelines for the diagnosis and management of heart failure in adults: a report of the American College of Cardiology Foundation/American Heart Association Task Force on Practice Guidelines: developed in collaboration with the International Society for Heart and Lung Transplantation. *Circulation*. (2009) 119:1977–2016. doi: 10.1161/CIRCULATIONAHA.109.192064
10. Redfield MM, Jacobsen SJ, Burnett, JC, Jr., Mahoney DW, Bailey KR, Rodeheffer RJ, et al. Burden of systolic and diastolic ventricular dysfunction in the community: appreciating the scope of the heart failure epidemic. *JAMA*. (2003) 289:194–202. doi: 10.1001/jama.289.2.194
11. From AM, Scott CG, Chen HH. The development of heart failure in patients with diabetes mellitus and pre-clinical diastolic dysfunction a population-based study. *J Am Coll Cardiol*. (2010) 55:300–5. doi: 10.1016/j.jacc.2009.12.003
12. Hegde SM, Claggett B, Shah AM, Lewis EF, Anand I, Shah SJ, et al. Physical activity and prognosis in the TOPCAT trial (treatment of preserved cardiac function heart failure with an aldosterone antagonist). *Circulation*. (2017) 136:982–92. doi: 10.1161/CIRCULATIONAHA.117.028002

13. Taylor RS, Davies EJ, Dalal HM, Davis R, Doherty P, Cooper C, et al. (2012). Effects of exercise training for heart failure with preserved ejection fraction: a systematic review and meta-analysis of comparative studies. *Int J Cardiol*. 162:6–13. doi: 10.1016/j.ijcard.2012.05.070
14. Ozasa N, Morimoto T, Bao B, Kimura T. Effects of machine-assisted cycling on exercise capacity and endothelial function in elderly patients with heart failure. *Circ J*. (2012) 76:1889–94. doi: 10.1253/circj.cj-11-1113
15. Braun CK, Kalbitz M, Halbgebauer R, Eisele P, Messerer DAC, Weckbach S, et al. Early structural changes of the heart after experimental polytrauma and hemorrhagic shock. *PLoS ONE*. (2017) 12:e0187327. doi: 10.1371/journal.pone.0187327
16. Wu NN, Zhang Y, Ren J. Mitophagy, mitochondrial dynamics, and homeostasis in cardiovascular aging. *Oxid Med Cell Longev*. (2019) 2019:9825061. doi: 10.1155/2019/9825061
17. Xu HX, Cui SM, Zhang YM, Ren J. Mitochondrial Ca2+ regulation in the etiology of heart failure: physiological and pathophysiological implications. *Acta Pharmacol Sin*. (2020) 41:1301–9. doi: 10.1038/s41401-020-0476-5
18. Owen A, Croucher L. Effect of an exercise programme for elderly patients with heart failure. *Eur J Heart Fail*. (2000) 2:65–70. doi: 10.1016/s1388-9842(99)00067-7
19. Cunningham JW, Vaduganathan M, Claggett BL, Zile MR, Anand IS, Packer M, et al. Effects of sacubitril/valsartan on N-terminal pro-B-type natriuretic peptide in heart failure with preserved ejection fraction. *JACC Heart Fail*. (2020) 8:372–81. doi: 10.1016/j.jchf.2020.03.002
20. Martos R, Baugh J, Ledwidge M, O'Loughlin C, Conlon C, Patle A, et al. Diastolic heart failure: evidence of increased myocardial collagen turnover linked to diastolic dysfunction. *Circulation*. (2007) 115:888–95. doi: 10.1161/CIRCULATIONAHA.106.638569
21. Hu H, Fu Y, Li M, Xia H, Liu Y, Sun X, et al. Interleukin-35 pretreatment attenuates lipopolysaccharide-induced heart injury by inhibition of inflammation, apoptosis and fibrotic reactions. *Int Immunopharmacol*. (2020) 86:106725. doi: 10.1016/j.intimp.2020.106725
22. Chong E, Chang SL, Hsiao YW, Singhal R, Liu SH, Leha T, et al. Resveratrol, a red wine antioxidant, reduces atrial fibrillation susceptibility in the failing heart by PI3K/AKT/eNOS signaling pathway activation. *Heart Rhythm*. (2015) 12:1046–56. doi: 10.1016/j.hrthm.2015.01.044
23. Lee JF, Barrett-O'Keefe Z, Garten RS, Nelson AD, Ryan JJ, Nativi JN, et al. Evidence of microvascular dysfunction in heart failure with preserved ejection fraction. *Heart*. (2016) 102:278–84. doi: 10.1136/heartjnl-2015-308403
24. Wei EP, Kontos HA, Christman CW, DeWitt DS, Povlishock JT. Superoxide generation and reversal of acetylcholine-induced cerebral arteriolar dilation after acute hypertension. *Circ Res*. (1985) 57:781–7. doi: 10.1161/01.res.57.5.781
25. Faraci FM, Didion SP. Vascular protection: superoxide dismutase isoforms in the vessel wall. *Arterioscler Thromb Vasc Biol*. (2004) 24:1367–73. doi: 10.1161/01.ATV.0000133604.20182.cf
26. Shah SJ, Kitzman DW, Borlaug BA, Heerebeek LV, Zile MR, Kass DA, et al. Phenotype-specific treatment of heart failure with preserved ejection fraction: a multiorgan roadmap. *Circulation*. (2016) 134:73–90. doi: 10.1161/CIRCULATIONAHA.116.021884

Conflict of Interest: The authors declare that the research was conducted in the absence of any commercial or financial relationships that could be construed as a potential conflict of interest.

Copyright © 2021 Liu, Ji, Fu, Zhang, Ji, Liu, Cheng and Dong. This is an open-access article distributed under the terms of the Creative Commons Attribution License (CC BY). The use, distribution or reproduction in other forums is permitted, provided the original author(s) and the copyright owner(s) are credited and that the original publication in this journal is cited, in accordance with accepted academic practice. No use, distribution or reproduction is permitted which does not comply with these terms.

frontiers in Cardiovascular Medicine

REVIEW
published: 16 June 2021
doi: 10.3389/fcvm.2021.633013

Heat Shock Proteins: Potential Modulators and Candidate Biomarkers of Peripartum Cardiomyopathy

*Graham Chakafana[1,2], Timothy F. Spracklen[1,2], Stephen Kamuli[1,2], Tawanda Zininga[3], Addmore Shonhai[4], Ntobeko A. B. Ntusi[1,2,5] and Karen Sliwa[1,2]**

[1] Department of Medicine, Faculty of Health Sciences, Cape Heart Institute, University of Cape Town, Cape Town, South Africa, [2] Division of Cardiology, Department of Medicine, Faculty of Health Sciences, University of Cape Town, Cape Town, South Africa, [3] Department of Biochemistry, Stellenbosch University, Stellenbosch, South Africa, [4] Department of Biochemistry, University of Venda, Thohoyandou, South Africa, [5] Cape Universities Body Imaging Centre, Faculty of Health Sciences, University of Cape Town, Cape Town, South Africa

OPEN ACCESS

Edited by:
Jun Ren,
University of Washington,
United States

Reviewed by:
Tom Van Agtmael,
University of Glasgow,
United Kingdom
Tilman Grune,
German Institute of Human Nutrition
Potsdam-Rehbruecke (DIfE), Germany

***Correspondence:**
Karen Sliwa
karen.sliwa-hahnle@uct.ac.za

Specialty section:
This article was submitted to
Cardiovascular Therapeutics,
a section of the journal
Frontiers in Cardiovascular Medicine

Received: 24 November 2020
Accepted: 06 May 2021
Published: 16 June 2021

Citation:
Chakafana G, Spracklen TF, Kamuli S, Zininga T, Shonhai A, Ntusi NAB and Sliwa K (2021) Heat Shock Proteins: Potential Modulators and Candidate Biomarkers of Peripartum Cardiomyopathy.
Front. Cardiovasc. Med. 8:633013.
doi: 10.3389/fcvm.2021.633013

Peripartum cardiomyopathy (PPCM) is a potentially life-threatening condition in which heart failure and systolic dysfunction occur late in pregnancy or within months following delivery. To date, no reliable biomarkers or therapeutic interventions for the condition exist, thus necessitating an urgent need for identification of novel PPCM drug targets and candidate biomarkers. Leads for novel treatments and biomarkers are therefore being investigated worldwide. Pregnancy is generally accompanied by dramatic hemodynamic changes, including a reduced afterload and a 50% increase in cardiac output. These increased cardiac stresses during pregnancy potentially impair protein folding processes within the cardiac tissue. The accumulation of misfolded proteins results in increased toxicity and cardiac insults that trigger heart failure. Under stress conditions, molecular chaperones such as heat shock proteins (Hsps) play crucial roles in maintaining cellular proteostasis. Here, we critically assess the potential role of Hsps in PPCM. We further predict specific associations between the Hsp types Hsp70, Hsp90 and small Hsps with several proteins implicated in PPCM pathophysiology. Furthermore, we explore the possibility of select Hsps as novel candidate PPCM biomarkers and drug targets. A better understanding of how these Hsps modulate PPCM pathogenesis holds promise in improving treatment, prognosis and management of the condition, and possibly other forms of acute heart failure.

Keywords: heat shock protein, stress, cardiomyopathy, pregnancy, biomarkers, drug targets

INTRODUCTION

Protein folding processes are fundamental in the maintenance of cardiac tissue integrity (1). The metabolic and mechanical demands of the heart, such as its continuous contractile activities, place a burden for robust protein quality control systems (2). Several cardiovascular diseases such as ischemic heart disease and heart failure (HF) are characterised by increased mechanical and oxidative pressures which trigger an accumulation of misfolded proteins in cardiomyocytes. Misfolded proteins are toxic to cardiomyocytes, potentially causing cardiac insults that lead to

HF (3). Under ensuing stress conditions, protein folding processes which typically occur in the sarcoplasmic reticulum, sarcomeres and mitochondria, are crucial in maintaining cardiac muscle integrity (4). Molecular chaperones such as heat shock proteins (Hsps) are an important class of proteins involved in the maintenance of proteostasis in various cell types under both normal and stress conditions. Here, we review the potential involvement of Hsps in peripartum cardiomyopathy (PPCM). Notably, the additional cardiac stress associated with pregnancy may further induce unique protein folding pathways in PPCM. Using bioinformatics tools, we further propose novel interactions (between proteins involved in PPCM pathogenesis and Hsps) which can be targeted toward drug interventions. Currently, echocardiography is the principal diagnostic tool for PPCM, as no reliable biomarkers exist. In this review, we also critically assess the potential of Hsps as candidate PPCM biomarkers.

PATHOPHYSIOLOGY AND MOLECULAR PATHWAYS OF PPCM

PPCM is a common and devastating disease that is associated with the unexpected loss of maternal cardiac function in the period surrounding parturition i.e., toward the end of pregnancy or within months following delivery (5). PPCM is characterised by a decreased left ventricular ejection fraction (LVEF) that is <45% in patients without prior cardiac disease (6). Generally, PPCM presents as congestive HF and systolic dysfunction, with typical symptoms including dyspnoea, fatigue, palpitations, oedema and chest pain (5). Although 90% of PPCM cases present after parturition, in rare cases disease onset has also been reported in the second trimester (7, 8). With a reported incidence ranging from 1:100 to 1:10,000 deliveries (9, 10), the frequency of PPCM appears to be influenced by ethnicity, with individuals of African origin at greater risk of developing the disease (10, 11). Other risk factors for PPCM include preeclampsia, multiparity, maternal age and multiple pregnancies.

Although the pathophysiology of PPCM is not entirely understood, several mechanisms of disease have been suggested. These include malnutrition, viral infection, autoimmunity and increased haemodynamic strain, although their roles in PPCM have proved nebulous (12). Current evidence, however, strongly suggests that PPCM may be driven by a pathological imbalance of pro- and anti-angiogenic hormones, as well as genetic factors. Two main pathways underlying disease pathogenesis have accrued from studies of mouse models of PPCM, as well as observations in human patients. These are reviewed in more detail elsewhere (12), but both involve the creation of a profoundly vasculotoxic environment through imbalances in angiogenic hormones.

The first pathway is characterised by increased expression of the pituitary hormone prolactin (PRL) which, in conditions of high oxidative stress, ultimately leads to cardiomyocyte apoptosis and cardiac dysfunction. The post translational processing of PRL is complex and the full length 23 kDa protein may be cleaved by peptidases (such as Cathepsin D) into a smaller 16 kDa variant. The 16 kDa PRL variant is a potent anti-angiogenic factor which acts as a vasoinhibin which can also cause vascular dropout, global systolic dysfunction and cardiac endothelial apoptosis. A murine PPCM model demonstrated that cardiac-specific deletion of the *STAT3* gene caused increased oxidative stress through reduced MnSOD expression (13). Further investigation also revealed an increase in cathepsin D activity and a corresponding increase in 16 kDa PRL levels (13). Altogether, this implies a vital role of STAT3 in cardioprotection during pregnancy, suggesting that dysregulation of STAT3 may also underlie PPCM. Recently, inhibition of Notch1/Hes1 has been found to induce PPCM through suppression of STAT3 activation, as well as increasing cathepsin D expression (14). Another protein involved in PPCM pathophysiology, Akt, is highly activated during pregnancy and promotes cardiac hypertrophy, and was shown to be activated by both PRL and interferon-γ (IFNγ) (15).

The second PPCM pathophysiology pathway involves the increased placental secretion of soluble Fms-like tyrosine kinase 1 (sFlt1) into the maternal system. Precisely why sFlt1 is secreted by the placenta is unclear, but both sFlt1 and membrane bound Flt1 are decoy receptors for vascular endothelial growth factors (VEGFs). VEGFA and VEGFB are proangiogenic factors and important mediators of cardiac homeostasis, but the binding of sFlt1 inhibits their activity (16). VEGF expression is driven by PGC-1α, and suppression of this in murine hearts led to PPCM and an increased susceptibility to sFlt1-induced cardiomyopathy (17). In this study, excessively high sFlt1 levels were able to cause cardiomyopathy, even in mice without the PGC1-1α deletion or pregnancy, indicating that excess sFlt1 alone can induce cardiac dysfunction. This emphasises the sensitivity of the heart to angiogenic imbalance as a result of placental sFlt1, that may occur during pregnancy. Synchtiotrophoblasts of the placenta secrete copious amounts of sFlt1 and as such, plasma levels of the protein rise exponentially toward birth (18). Most of the free VEGF in maternal circulation is thus neutralised by sFlt1 during pregnancy. More so, elevated sFlt1 have been described in women with PPCM (17), and have been directly correlated with disease severity and the occurrence of adverse clinical events (19). Notably, higher sFlt1 levels have been reported in twin pregnancies, another risk factor for PPCM (20, 21), possibly as a result of the larger placenta (22).

CARDIAC MECHANICAL STRESS DURING PREGNANCY

Pregnancy is accompanied by dramatic hemodynamic changes, including reduced resistance during systole (afterload) and a 50% increase in cardiac output and blood volume (23). Furthermore, foetal microchimeric cells may reduce cardiac function resulting in increased cardiac mechanical stress during pregnancy (24, 25). It is however worth noting that most of these changes typically occur early in gestation, many months before PPCM typically presents (**Figure 1**). These changes trigger homeostatic and structural remodelling of cardiovascular tissues. Whereas, hemodynamic changes of pregnancy peak in the second trimester, hormonal changes of pregnancy are most drastic in

the third trimester and early postpartum (**Figure 1**) (26). These changes also coincide with the presentation of PPCM. As such, the vasculotoxic hormonal changes that occur during and after parturition act as a trigger for PPCM. Indeed, several studies have demonstrated that PPCM is triggered by the rapidly changing environment of late gestation thus inducing vasculopathy in susceptible women (13, 27, 28). This is supported by the fact that hormones that likely trigger PPCM (PRL and sFlt1) are mostly at their peak in late pregnancy and postpartum. In addition, unlike other forms of cardiomyopathy, cardiac function is usually restored upon a drop in these hormones which comes with delivery. Apart from sFlt1, the placenta also secretes several other hormones which may result in maternal stress during pregnancy. Despite these cardiac demands associated with pregnancy, there is a need for protein quality control to be maintained in the cardiomyocytes.

CARDIOMYOCYTE PROTEOSTASIS AND POTENTIAL ROLES OF Hsps IN PPCM

The robust maintenance of proteostasis in cardiomyocytes is crucial in ensuring the integrity of cardiac tissue. An accumulation of misfolded and unfolded proteins results in the formation of aggregates which are usually cytotoxic. The heart is constantly exposed to mechanical stresses associated with its continuous contractile activities, as well as chemical stresses induced by free radicals and hormones. In PPCM, pregnancy further burdens cardiac tissue, as the heart readjust to the needs of the developing foetus. Stress supresses the cell's capacity to maintain proteostasis thus compromising the ability of proteins to attain native conformation. Cellular stress can lead to protein misfolding or unfolding, leading to proteins that are unable to carry out their normal functions (29). Such stresses typically impair protein folding, potentially resulting in the formation of functionally impaired and toxic protein aggregates that trigger cardiac insults. Under the ensuing stress conditions, molecular chaperones such as Hsps likely facilitate cardiomyocyte proteostasis. Generally, Hsps perform a myriad of housekeeping and stress-protective roles in cells to maintain proteostasis (**Figure 2**) (30). We propose that Hsps are particularly important in PPCM since the heart is further burdened by pregnancy related stresses that may impair optimal protein folding processes in the cardiomyocytes.

Hsps can generally be classified into seven families, based on structural and functional features (**Table 1**). Broadly, Hsps function to facilitate the correct folding and assembly of polypeptides, thus preventing the formation of misfolded or incorrectly assembled proteins (44). Hsps also play an important role in the suppression or inhibition of polypeptide aggregation in cells (45). When a nascent polypeptide chain exits the ribosome or an organellar import pore, or when a labile native protein becomes transiently heat denatured, it may transiently unfold and expose hydrophobic segments to the aqueous environment (31). Depending on the intensity and duration of the stress as well as the degree of hydrophobic exposure, the misfolded monomers may clamp together through intermolecular hydrophobic associations to form aggregates (46). Hsps of the "holdase" class (such as small Hsps (sHsps), Hsp40, Hsp70, and Hsp110) can bind to the exposed hydrophobic residues on the surface of misfolded polypeptides to prevent the formation of aggregates (47).

The roles of Hsps in several cardiovascular conditions such as HF and dilated cardiomyopathy (DCM) have been reported (**Table 1**). The Hsp70 family of molecular chaperones is a central hub for the maintenance of proteostasis in cells (48). Hsp70s are actively involved in almost every stage of a protein's life course (**Figure 2**). Thus, Hsp70s facilitate folding of nascent peptides emerging at the ribosomes (49), protein trafficking and translocation across membranes (50). In addition, Hsp70s facilitate the refolding of misfolded protein (31, 51), and also channelling misfolded proteins which are beyond repair toward degradation (52, 53). In order for Hsp70s to function efficiently, they depend on assistance from functional networks formed with members of several co-chaperones which include Carboxyl terminus of HSC70-interacting protein (CHIP), Bcl-2 associated athanogene 3 (BAG3) and Hsp70-Hsp90 organising protein (Hop) (2). Additionally, Hsp70 also forms functional networks with Hsp40 (54), Hsp90 (55), and sHsps (56). Protein folding by Hsp70 is tightly controlled by J-domain proteins (Hsp40) and nucleotide exchange factors (NEFs) such as BAG3. The co-ordinated action of Hsp70 and Hsp90 facilitates the folding of most structural and signalling proteins (**Figure 2**). In fact, Hsp70 has been described as a promiscuous chaperone that is capable of binding virtually any peptide sequence (57).

Hsps also play crucial roles in the ubiquitin proteasome system (UPS) which is the main proteolytic system in eukaryotic cells facilitating the degradation of misfolded proteins. It has previously been established that the constitutively expressed Hsp70 (Hsc70) is required for ubiquitylation of several proteasome substrates (58). Furthermore, the majority of E3 ligase complexes of the UPS pathway have been shown to cooperate with Hsps (59). Hsps also function as escort factors that either deliver or dock the Ub-protein conjugates to the proteasome thus preventing the formation of ubiquitylated protein aggregates (**Figure 3A**) (53). Functional co-operations of Hsp70 could be pivotal in maintaining cardiomyocyte proteostasis during pregnancy-induced stress. The co-chaperone CHIP (a ubiquitin ligase) is ubiquitously expressed, although it is prominently expressed in striated muscle such as cardiac tissue (2). Functionally, CHIP co-operates with Hsp70 to ubiquitinate misfolded proteins that cannot be repaired, targeting them for protein degradation by the proteasome (**Figure 3A**) (60). Previous studies have implicated CHIP in cardiac disease. In a murine model, genetic knockout of CHIP resulted in exaggerated cardiac hypertrophy, as evidenced by increased heart weights, wall thickness and cardiomyocyte size following exercise or pressure overload (61, 62). Genetic knockout of CHIP was also associated with a dramatic decline in cardiac function in response to pressure overload (63). Due to its ability to regulate Hsp70 chaperone activity, CHIP may also be an important determinant in modulating Hsp70-chaperoned proteins in the cardiomyocyte.

The interaction of Hsp70 with another co-chaperone, BAG3, is also critical for cardiac muscle development and

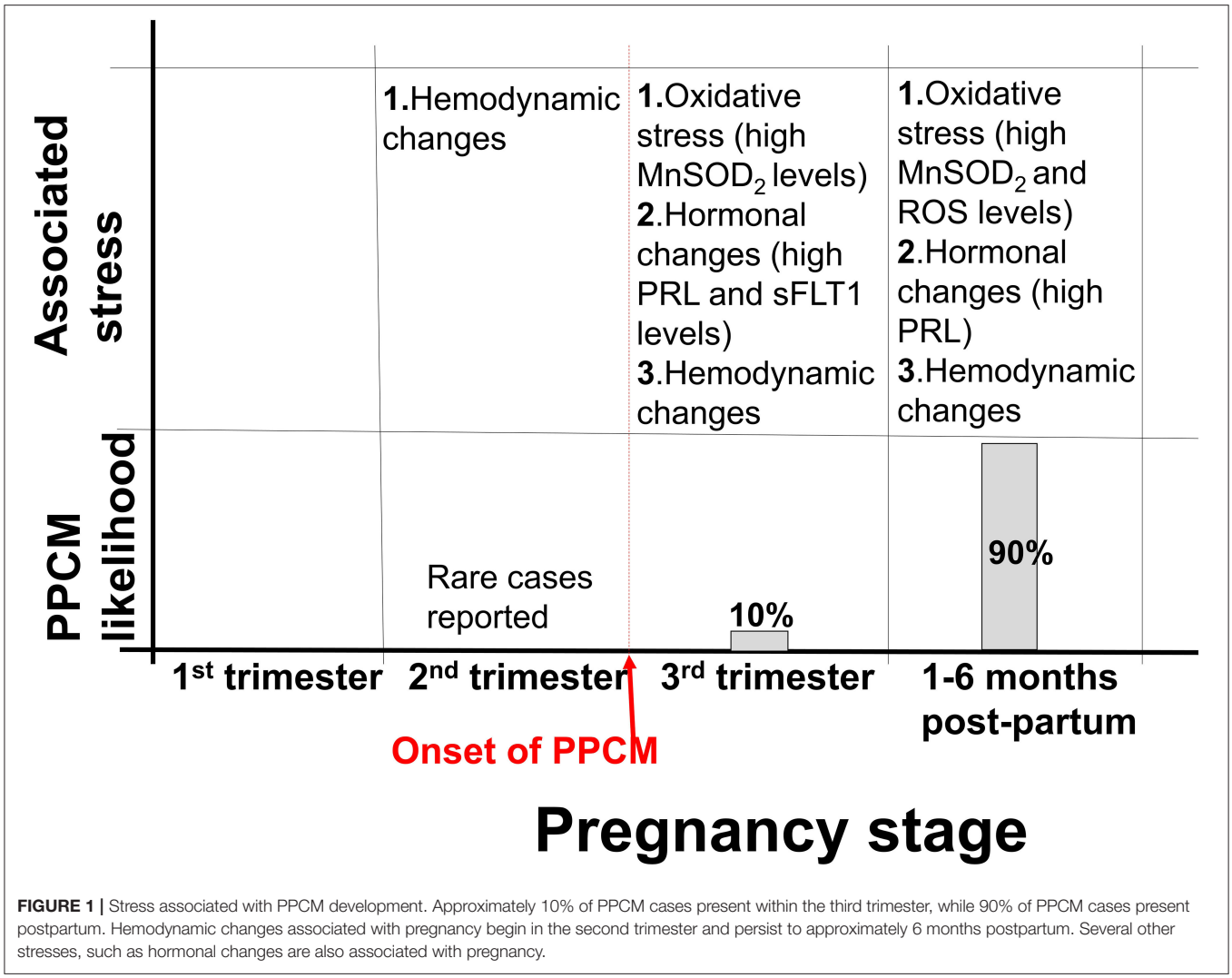

FIGURE 1 | Stress associated with PPCM development. Approximately 10% of PPCM cases present within the third trimester, while 90% of PPCM cases present postpartum. Hemodynamic changes associated with pregnancy begin in the second trimester and persist to approximately 6 months postpartum. Several other stresses, such as hormonal changes are also associated with pregnancy.

vascular disease pathogenesis (64). BAG3 is generally involved in a range of cellular functions which include protein folding, apoptosis, autophagy as well as CMA/chaperone-assisted selective autophagy (CASA) to the UPS (2). BAG3 not only forms functional co-operations with Hsp70, but also with sHsps such as HspB5, HspB6 and HspB8 (65, 66). sHSPs act in concert with Hsp70 to facilitate protein refolding (**Figure 3B**) (67, 68). Since sHSPS lack ATP-dependent enzymatic activity that is necessary for active protein refolding, BAG3 facilitates the formation of a BAG3-sHsp-Hsp70 complex through which protein refolding can occur. The direct involvement of BAG3 in cardiac disease has previously been reported in ΔBAG3 mice that were observed to develop cardiomyopathy and non-inflammatory myofibrillar myopathy (MFM) (64).

In the heart, Hsp70 is induced by several factors which include steroid hormones (e.g., vasopressin), free radicals, drugs, probiotic derived proteins, physical exercise and environmental changes (69, 70). Elevated Hsp70 expression results in reduced myocardial infarction (71). In addition, Hsp70 levels are also thought to correlate with a timecourse of cardioprotection (36). Furthermore, high Hsp70 levels are linked with a decrease in cardiac apoptosis (33, 72). As such, high Hsp70 levels have been reported to confer improvement in the recovery of post ischemia reperfusion injury (73). Wei et al. (74) demonstrated high Hsp70 expression levels in hearts showing failure due to cardiomyopathy (arrhythmogenic cardiomyopathy, DCM) and ischemia. The degradation of misfolded proteins is important for the constant turnover of sarcomeric proteins required for correct function and regulation of cardiac mass (75). In addition, Hsp70 co-operates with CHIP and BAG1 to control the degradation of myosin and sarcomeric proteins (76). Given these roles of Hsp70 in cardiac function, it is tempting to speculate implications of the chaperone in PPCM. This hypothesis may need experimental validation.

Hsp90 is a unique molecular chaperone which possesses the ability to bind target proteins that are in a near native state in order to mediate the final stages of folding (77). In addition, Hsp90 is specialised to facilitate the folding of specific, defined

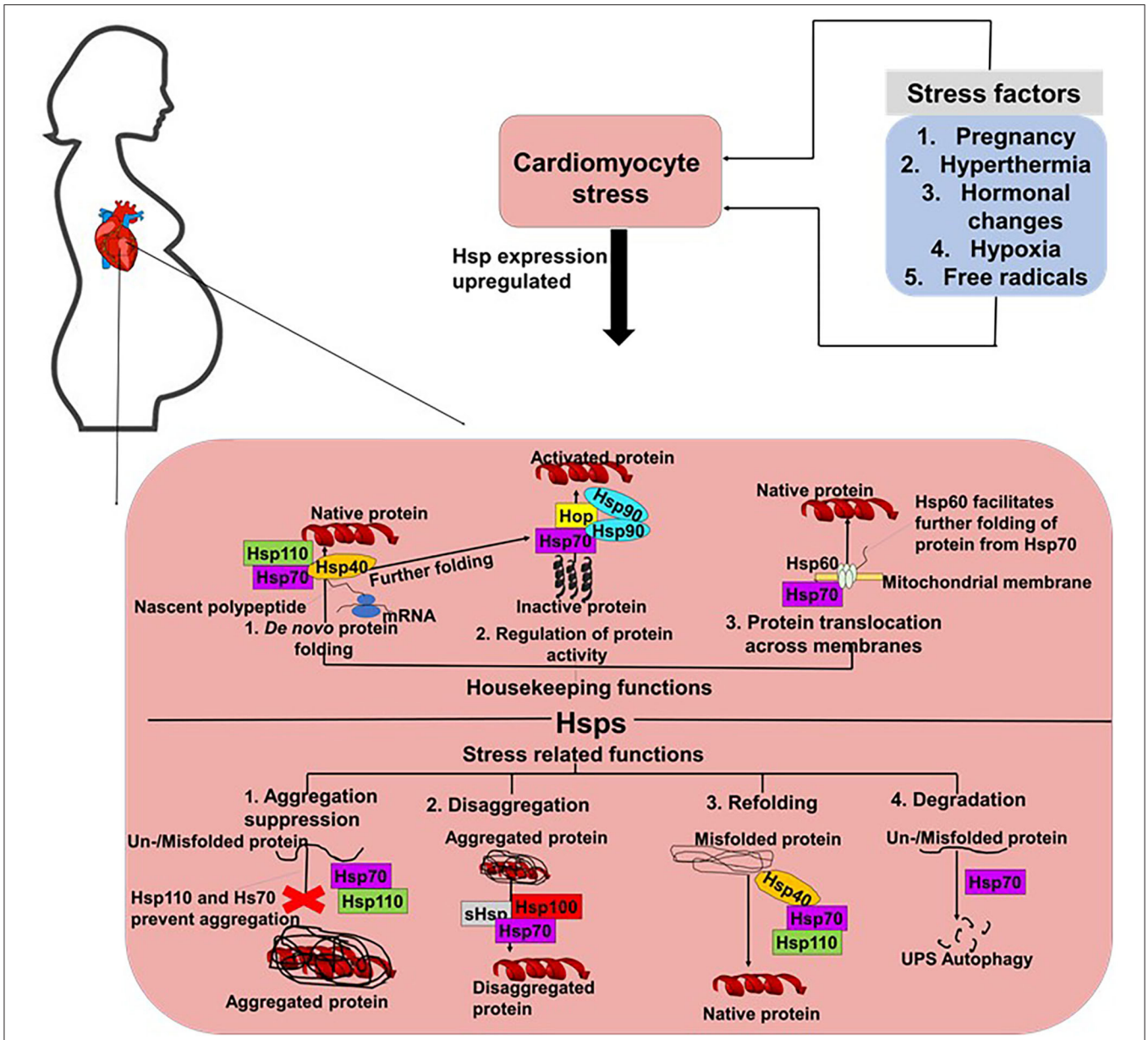

FIGURE 2 | Proposed roles of Hsps in PPCM. In cells, Hsp70s perform both housekeeping and stress response related roles. Hsp70s co-operate with various co-chaperones such as Hsp40 and Hsp110 to facilitate the *de novo* folding of polypeptides from the ribosome to facilitate their folding into their native conformations. Hsp70s also co-operate with Hsp90 and Hop to activate proteins. Hsp70s also form partnerships with Hsp60 to facilitate the translocation of proteins across membranes. Under stress conditions, Hsp70s prevent the formation of aggregates and also facilitate the degradation of misfolded/unfolded proteins.

sets of client proteins such as steroid hormone receptors, TLR innate immunity receptors, RNA polymerases and PI3-kinase-related kinases (PIKKs) (78). As such, Hsp90 modulates cell signalling, genome maintenance and assembly of transcriptional and translational apparatuses in cells (36). Together with Hsp70, Hsp90 plays key roles in protein folding as they facilitate the folding, maturation and activation of virtually all proteins in the cell (50, 57). While Hsp70 generally binds to nascent polypeptide chains at the ribosome, Hsp90 binds a more specialised clientome that includes steroid hormones and kinases. Hop acts as an adaptor protein to enable Hsp70-Hsp90 interaction through their C-terminal sequences (**Figure 3C**) (79, 80). As such, Hop enables the transfer of client proteins such as kinases, nuclear receptors like the steroid hormone receptors (SHR) and transcription factors between the chaperones Hsp70 and Hsp90 for folding, assembly and activation (**Figure 2**) (81, 82).

Hsp90 also plays an active role in protein quality control by directing misfolded proteins toward the UPS for degradation (83). Hsp90 possesses anti-apoptotic effects on hypoxia-mediated cardiomyocyte damage (84). An Hsp90 client, ErBB2, was shown

TABLE 1 | Major Hsp families and cardiovascular roles.

Protein family	Localisation	CVD implication	Stress inducers	References
Hsp110	Cytosol, ER	ND* (General role: Protein aggregation suppression; Possess holdase function)		(31)
Hsp100	Mitochondrion	ND* (General role: Dis-assembly of quaternary structure of polypeptide complexes and are required for thermotolerance)		(32)
Hsp90	Myocyte	1. Hsp90 antibody levels rise 16-fold under stress (potential CVD biomarker?) 2. Hsp90 supports Akt signalling (elevated Hsp90 and Akt levels have been reported in hypoxia challenged cardiomyocytes) 3. Hsp90 possesses anti-apoptotic effects on hypoxia-mediated cardiomyocyte damage 4. Cardiac Hsp90 supports protein maturation and has roles in the development of mutation-related cardiac arrhythmia 5. Hsp90 regulates angiotensin II-induced cardiac hypertrophy	Ischemia ROS	(33, 34)
Hsp70	Myocyte cells	1. Specific role in myocardial protection from chronic ischemia 2. Participates in myocardial adaptive processes to chronic repetitive ischemia (high tissue levels of Hsp72 have been reported in myocardial hibernation) 3. High Hsp70 expression levels were correlated to HF progression (potential HF biomarker)	Ischemia and mechanical stress, steroid hormones, drugs, physical exercise	(35, 36)
Hsp60	Endothelial cells Myocyte surface	1. Ischemic myocardial damage 2. Thought to participate in inflammatory processes (activates autoimmune response. High Hsp60 expression elicits an autoimmune response that can trigger further vascular/ myocardial damage) 3. High Hsp60 levels reported in coronary artery disease patients 4. Serum Hsp60 was related to the severity of CHF and associated with a high risk for late stage cardiac events in CHF patients	Biochemical or infective insults; hyperthermia	(37–40)
Hsp40	Cytosol, membranes, ER	1. Co-chaperone of Hsp70; Host cell modifications 2. Associated with development of fatal DCM	Ischemia and mechanical stress	(41)
sHsps		1. High expression levels during cardiac hypertrophy 2. Cardioprotection (Hsp27 has a cardioprotective effect in cases of infarction) 3. Overexpression of Hsp27 results in reduction in cell apoptosis in cardiac tissue 4. High Hsp25 expression improved survival of cardiomyopathy patients and the heart resistance against toxicity	Hypertrophic stimuli, including aortic banding, angiotensin II infusion	(42, 43)

ND, not determined.

to be linked to the development of HF in a murine model (85). Mice lacking cardiac specific ErBB2 developed HF characterised by left ventricular (LV) dilation, wall thinning and decreased systolic function (85). Due to its large clientome, we speculate a likelihood of Hsp90 in chaperoning several other proteins involved in PPCM pathogenesis. We therefore sought to predict the interaction and roles of Hsp90, Hsp70 and sHsps in PPCM using bioinformatics.

PREDICTED ASSOCIATIONS BETWEEN MAJOR Hsp FAMILIES AND THE PPCM PROTEOME

Using STRING analysis, we predicted the associations of several proteins currently known to be involved in PPCM pathophysiology with members of the Hsp70, Hsp90 and sHsp family members (**Table 2** and **Figure 4**). Although the actual implications of such interactions are at present unknown, experimental validation may provide insights into candidate drug design or biomarker discovery. These Hsps and PPCM protein associations are described in the following sections.

Akt

Akt is a protein kinase and a key component of the ubiquitous PI3K/Akt signalling pathway. Activated Akt promotes cellular survival, proliferation and growth. In the heart, Akt signalling induces both pathological hypertrophy and physiological hypertrophy (for example, during pregnancy) (86). However, Akt appears to have an exacerbatory effect in PPCM (15), possibly by aggravating an underlying angiogenic imbalance. Select Hsp70 (HspA4, HspA5, HspA9), Hsp90 (Hsp90AB1), and sHsps (HspB1) are predicted to interact with Akt (**Table 2**).

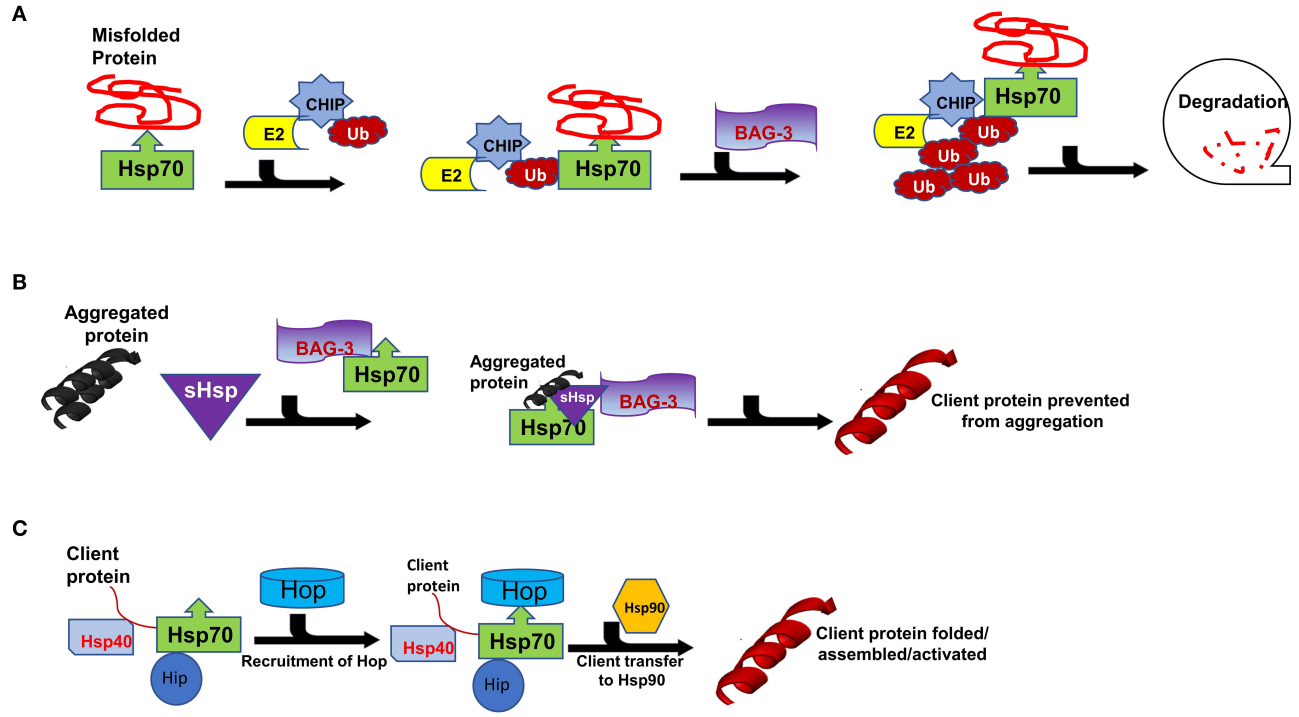

FIGURE 3 | Interaction of Carboxyl terminus of HSC70-interacting protein (CHIP) with binding partners for protein quality control. Hsp70 functions with co-chaperones CHIP, BAG3 and Hop in maintain cellular proteostasis. **(A)** The CHIP pathway involves the association of CHIP with Ub, E2, BAG3, Bcl-2-associated athanogene 3 and Hsp70 to facilitate degradation. **(B)** Formation of sHSPs-BAG3-HSP70 complex to prevent aggregation of proteins thus forming insoluble substrates in the cardiomyocytes. **(C)** Hsp70-Hsp90 Organising Protein (Hop) adaptor properties to link Heat shock protein 70 (Hsp70) with Heat shock protein 90 for client substrates transfer.

HspA4 (a non-canonical Hsp70 member), HspA5 (an Hsp of the endoplasmic reticulum (ER) also referred to as Grp78), and HspA9 (a mitochondrial Hsp also referred to as Grp75) (**Figure 4**) have been demonstrated to activate Akt in cancer models (87–90). Interestingly, Akt has also been shown to phosphorylate HspA5 (91) and regulate its expression (92), thus suggesting a possible feedback loop in which Akt and Hsp70 proteins positively regulate each other. This may be protective in cellular conditions such as oxidative stress and ER stress, which induce HspA9 and HspA5, respectively (89, 90). Since these Hsp70 isoforms are predicted to bind and possibly activate Akt, it is possible that HspA4, HspA5, and HspA9 play decisive roles in PPCM pathogenesis. HspA5/Akt interaction has been demonstrated as essential for cardiac development, function, and stress response. The loss of HspA5 in cardiomyocytes leaves them vulnerable to apoptosis following oxidative and ER stresses through suppressed Akt signalling (93), while upregulation of HspA5 attenuated ischaemia/reperfusion-induced cardiac damage by stimulating Akt activity (94, 95). Recently, ER stressors and ischaemia were also shown to increase the secretion of HspA5 by cardiomyocytes (96), indicating an extracellular cardioprotective role of this Hsp by activating Akt signalling.

Hsp90 proteins and sHsps are also predicted to interact with Akt (**Figure 4**). Similar to Hsp70s, these also appear to be involved in the stabilisation and activation of Akt kinase activity (97–100). Hsp90AB1/HspB1 interaction with Akt may have cardioprotective effects against a range of cardiac insults (101–105). While the activation of Akt by Hsps is generally beneficial in response to several cardiac insults, Akt stimulation is detrimental in the case of PPCM (15). As PPCM is characterised by oxidative and other stresses (**Figure 2**), the induction of Hsp70s, Hsp90s and sHsps during PPCM is highly probable, as is the subsequent stimulation of the Akt signalling pathway, although more research will be needed to confirm this hypothesis.

STAT3

Contrary to Akt, STAT3 activation may inhibit PPCM (13). Although no interactions between Hsp70s and STAT3 were observed, members of the Hsp90 and sHsp families are predicted to interact with STAT3 (**Figure 4**). The role of Hsp90 and the small HspB1 (Hsp27) in STAT3 signalling has recently been reviewed in detail (106), with these Hsps acting as key chaperones at numerous stages of the STAT3 pathway, including phosphorylation, activation and nuclear localisation of STAT3, as well as limiting its proteasomal degradation. It is therefore plausible that Hsp90 promotes STAT3 activation which may reverse the progression to fulminant PPCM. Therapeutic interventions that promote elevated Hsp90 expression levels in the cardiomyocytes may therefore prove beneficiual to PPCM patients. Further research is however needed to ascertain the functions of Hsps in modulating these pathways.

TABLE 2 | STRING interactions between heat shock and PPCM proteins.

Protein	Hsps involved	Role in PPCM pathology
Akt	HspA4, HspA5, HspA9, Hsp90, sHsps	Accelerates inflammation and fibrosis postpartum, through an unknown mechanism
CCL2	HspA4	Initiates inflammatory process, triggered by IFNγ or PRL
ERBB4	Hsp90	Cardiomyocyte survival; suppression during PPCM triggers cellular apoptosis
Flt1	Hsp90	Excess of soluble form (sFlt1) triggers angiogenic imbalance and PPCM, associated with adverse outcomes in PPCM patients
HES1	HspA4, Hsp90	Activation of cardioprotective STAT3 signalling
IFNγ	HspA1A, Hsp90	Continuously high IFNγ serum levels are associated with increased inflammatory status and adverse outcomes in PPCM patients
MMP	HspA13	MMPs can cleave PRL to its 16 kDa variant. High MMP levels have been detected in murine PPCM experiments
MnSOD	HspA4, HspA5	Responsible for organ specific antioxidant defence mechanisms in the peripartum phase. Generally cardiac MnSOD levels are high, although these are reduced in PPCM patients
NF-κB	HspA1L, Hsp90	Transcription factor activated by 16 kDa PRL, inducing apoptosis and antiangiogenic effects
NOTCH1	Hsp90	Activation of cardioprotective STAT3 signalling
STAT3	Hsp90, sHsps	Cardioprotective signaling
VEGF	HspA4	Crucial for blood vessel formation and homeostasis (VEGF A). Also drives trans-endothelial transport of fatty acids in the cardiomyocytes (VEGF B)

Other Interactions

Several other interactions were observed between Hsps and proteins in the PPCM pathway (**Table 2**), although the functional and biochemical roles of these remain to be determined. For instance, excess sFlt1 and reduced VEGF levels are key components of the angiogenic imbalance that characterises PPCM. While an interaction between Hsp90 and Flt1 was observed, current knowledge has only implicated Hsp90 in the maintenance of membrane-bound Flt1 in endothelial cells (107); interaction with the soluble form of the protein is unknown. However, because inhibition of Hsp90 could reduce levels of Flt1 (107), the role of Hsps in the stabilisation or folding of Flt1 may be worth exploring, especially in the context of placentally-derived sFlt1. We also predicted association of HspA4 with VEGFA. It has previously been demonstrated that HspA4 has a stabilising effect on *VEGFA* mRNA in cancer cells (108). It is conceivable that HspA4 suppresses aggregation of VEGFA under stress conditions, keeping the protein in a folding competent form, as has been demonstrated with other Hsp70 isoforms (56).

The Role of Hsps in Buffering Mutations

PPCM has been demonstrated to have a genetic basis, in at least a subset of patients (109–111). It is notable that molecular chaperones play a key role in the translation of genetic variation, by silencing or potentiating mutations (112). Hsp90, in particular, may potentiate mutations by assisting the folding and function of the mutant proteins, allowing them to have immediate phenotypic consequences (113). Alternatively, Hsp90 can silence mutations so that they have no phenotypic manifestation, although these buffering effects can be overwhelmed by environmental stresses (113). The implications of this are that Hsp90, or other Hsps, can buffer genetic mutations in a manner that is dependent on the environmental conditions. This may explain, in part, why the same mutations can cause DCM in some individuals, and PPCM in others.

The modulation of mutations by Hsps has also been described in Fanconi Anaemia, where Hsp70 was found to bind to inactive mutant proteins with severe phenotypic effects (114). The roles of Hsps in the buffering of cardiomyopathy-causing mutations is largely unknown, although heritable cardiomyopathies including DCM and hypertrophic cardiomyopathy (HCM) may be characterised by dysfunction of the UPS and other protein quality control mechanisms (115, 116). DCM- and HCM-causing mutations typically occur as truncations of genes encoding the sarcomeric proteins titin and cMyBP-C, respectively, and mutations in both have been described in PPCM patients, as well as other sarcomeric gene mutations (109–111, 117). Notably, these truncated protein products are not incorporated into the sarcomeres of mutation carriers (118, 119), although in the case of titin this haploinsufficiency has been attributed to mRNA degradation by nonsense-mediated decay (120). The role of Hsps in the buffering of truncating PPCM-causing mutations remains to be determined.

The Role of Hsps in the PPCM Inflammasome

In addition to their proteostatic roles, Hsps may also act as "chaperokines" which present antigens to the immune system. Hsp70, Hsp90 and sHps are secreted under stress conditions, where they can have pro- or anti-inflammatory effects [reviewed in (121)]. As myocardial inflammation is thought to be a key contributor to PPCM pathogenesis (12), the immunomodulatory effects of Hsps may be of interest. Indeed, several studies have

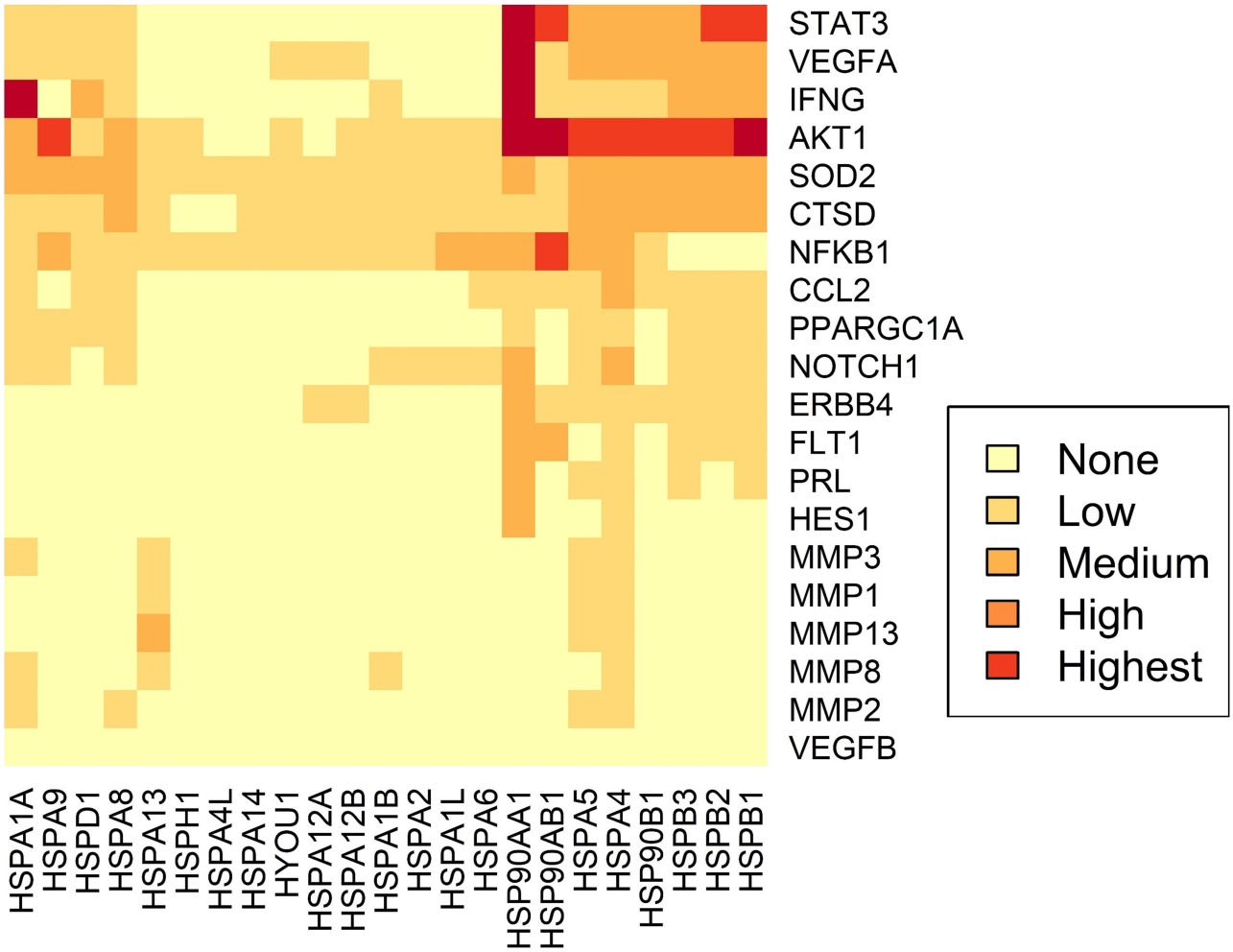

FIGURE 4 | Predicted interactome of several Hsps with PPCM proteins. The heat map shows the interaction of PPCM pathogenesis proteins with Hsp70, Hsp90 and sHsp group members.

demonstrated potential roles of Hsps in cardiac inflammatory pathways in response to myocarditis (122, 123) and myocardial injury (discussed below).

Extracellular Hsp70 can induce cardiomyocyte inflammation and cell death, in contrast with the pro-survival role of intracellular Hsp70 (124). Increased levels of circulating Hsp70 have been reported in models of acute myocardial infarction, autoimmune myocarditis and left ventricular dysfunction, all in association with elevated inflammatory markers and worse outcomes (37, 125, 126). Up-regulation of Hsp70 by treatment with Melusin in a mouse model of myocardial infarction was shown to reduce inflammatory cell infiltrates in the myocardium and improve cardiac function (127). The roles of Hsp90, Hsp60 and sHsps in cardiac inflammatory responses has also been demonstrated. Hsp90 has been shown to have cardioprotective effects in ischaemic pre- and post-conditioning by suppression of immune responses (128, 129). On the other hand, HspB1 may down-regulate leukocyte recruitment and cardiac inflammation (130). Hsp60 appears to induce cardiac inflammation and cytokine production (131, 132). It is therefore plausible that the level of circulating Hsps may promote or suppress cardiac inflammation, although it is unclear at this stage whether Hsp induction in PPCM would be beneficial or detrimental to recovery of cardiac function.

TARGETING Hsps TOWARD NOVEL PPCM THERAPY

To date, no disease-specific interventions for PPCM exist. As is the case with other cardiomyopathies, PPCM management is primarily focused on managing volume status, neutralising neurohormonal maladaptive responses, and preventing complications (133). One of the most used PPCM treatments is bromocriptine which functions by suppressing PRL production postpartum. A small proof-of-concept randomised trial of bromocriptine in 20 women with PPCM in Africa demonstrated improvements in mortality and LVEF at 6 months (134). Those observations were confirmed in a multi-center randomized

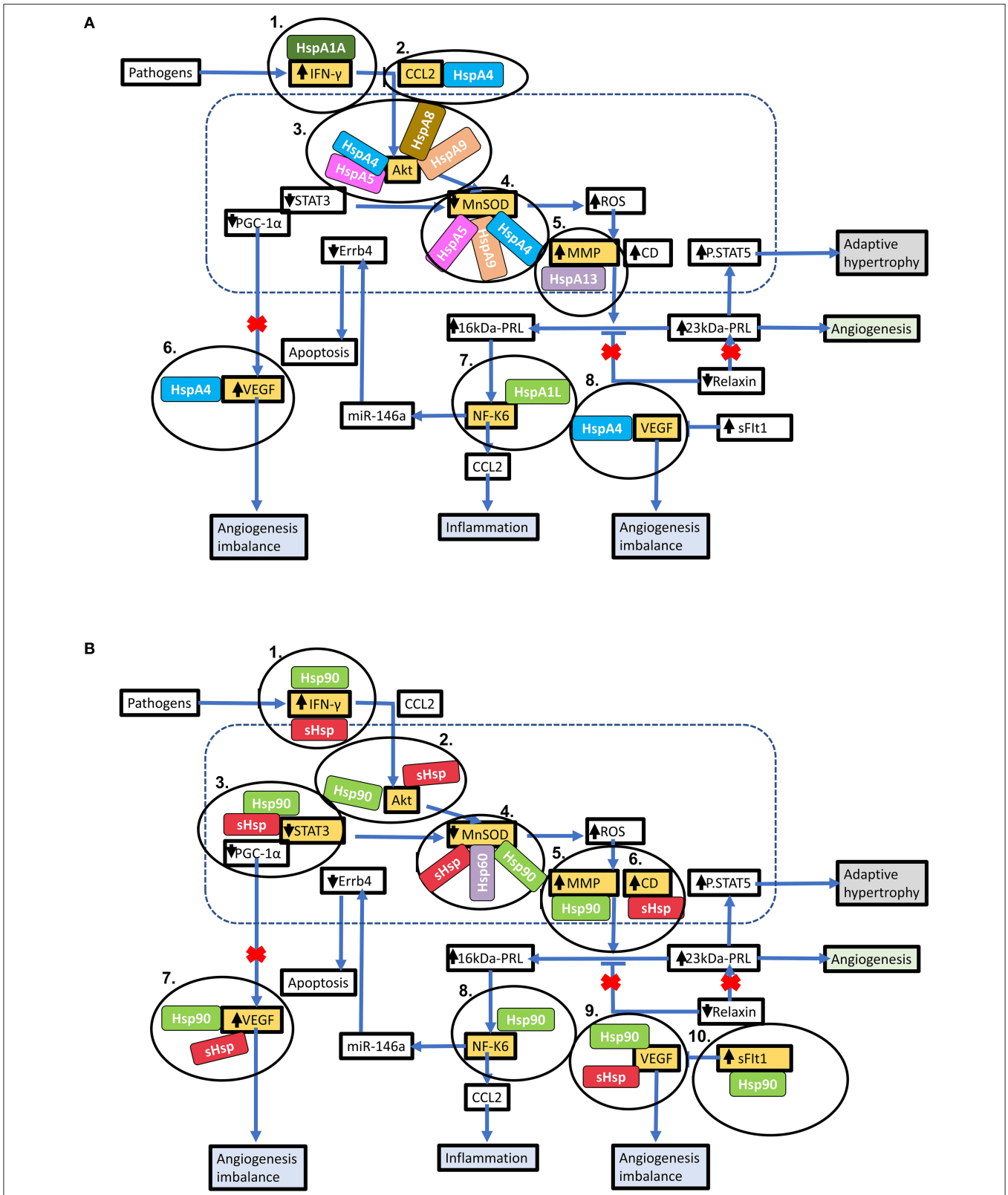

FIGURE 5 | Key stages in the PPCM pathophysiology pathway which are modulated by Hsps. Hsps interact with several proteins involved in the PPCM pathophysiological pathway. **(A)** Several Hsp70 isoforms interact with various proteins involved in PPCM pathogenesis. **(B)** The stages within the PPCM pathophysiology pathway where Hsp90 and sHsps interact with PPCM proteins are shown. Targeting these stages may be crucial in novel PPCM interventions.

TABLE 3 | Hsp-centred drug modulation strategies in novel PPCM drug design.

Drug molecule	Mechanism of action	Possible cardiac implication
(i) Hsp expression enhancing drugs		
Geranylgeranyl-Acetone	Induces Hsp70 and HspB8 expression	Cardioprotective effects have been reported in cardiomyopathy modes
Simvastain	Induces HspB1, Hsp70 and Hsp90 expression	Improves cardiac function and symptoms in DCM patients
(ii) Hsp functionality inhibitors		
Polymixin B	Inhibits Hsp90 and Hsp70 (NBD) chaperone function	May reduce inflammatory effects of Hsps on cardiac tissue
EGCG	Inhibits Hsp70 and Hsp90 expression by inhibiting the promoter activity of the respective chaperones	May reduce inflammatory effects of Hsps on cardiac tissue
Colistin sulphate	Inhibits Hsp90 and Hsp70 (NBD) chaperone function	May reduce inflammatory effects of Hsps on cardiac tissue

study (135). Based on these data the 2018 ESC Guidelines for the management of cardiovascular diseases during pregnancy states that bromocriptine may be considered in women with newly diagnosed PPCM (5). However, more research in this area is needed. As such, there is an urgent need for the identification of novel PPCM drug targets in the design of novel therapeutic interventions.

Hsps have previously been suggested as druggable candidates in human disease models (136). Several Hsps, such as Hsp70 and Hsp90 members, show great potential as drug targets in several cancers. For instance, the proteasome inhibitor, Bortezomib, has been used in anticancer therapy where it exerts antitumor effects by upregulating Hsp60 and Hsp90 on the surface of cancer cells (137). Attention is currently being drawn toward Hsp-directed therapies as candidates for novel cardiovascular disease therapies. A study recently demonstrated that blocking Hsp70 activity could be therapeutically beneficial in HF treatment (138). Given its ATP-dependent nature, Hsp70 is also amenable to inhibition using ATP-mimicking drugs. Interestingly, predictions from our STRING analysis revealed several stages which can potentially be modulated by Hsp70 (**Figure 5A**).

Hsp-centred drug modulation strategies may be centred around one of the following strategies; (i) boosting Hsp expression and (ii) inhibition of Hsp functionality. Each of these possible strategies is assessed in detail (**Table 3**). Inhibition would generally involve the development of small molecule inhibitors that target the functional domains of the Hsps thus disrupting their chaperone function. The direct inhibition of Hsps, resulting in the subsequent disruption of key protein-associations can be an efficacious way to modulate protein fate. Small molecule inhibitors such as polymyxin B and colistin sulphate possess great potential in this regard, as they have been successfully used to inhibit the activity Hsp70 *in vitro* (139). These two compounds are directed toward the nucleotide-binding domain, thus lowering the basal ATPase activity of the Hsp70. Designing domain specific inhibitory compounds may prove useful in Hsp70-targeted PPCM therapy. Since Hsp70 functions in co-operation with several other proteins involved in the pathophysiology of PPCM, selective targeting of cardiac Hsp70 may become a decisive step in inhibiting PPCM pathology. An alternative strategy worth exploring in designing novel PPCM therapy involves targeting heat shock factors (e.g., HSF1) which are responsible for modulation of Hsp expression. Although the generally high sequence and structural conservation of Hsp70 may be a snag in targeted inhibition, specific signature motifs in individual Hsp70 family members may be targeted toward this. Particularly, we predicted the association of several PPCM pathophysiology proteins with HspA4 (**Figure 5A**). HspA4 belongs to the Hsp110 family of chaperones, which are a specialised subclass of Hsp70s functionally and structurally distinguished from the canonical Hsp70s (56). This makes HspA4 amenable to selective targeting by inhibitors since it is unique from the more conserved canonical Hsp70s.

Prospects of targeting co-chaperones that are crucial for Hsp70 function also exist. The Hsp70 co-chaperone, CHIP, has been shown to play a crucial role in regulating intracellular protein signalling as evidenced by an increase in Akt phosphorylation which in turn leads to activation of the Akt signalling pathway leading to cardiac hypertrophy (63, 140). CHIP-directed therapies may potentially disrupt Hsp70 activity in turn causing detrimental downstream effects on Akt signalling within cardiomyocytes (**Figure 6**). Another Hsp70 co-chaperone, BAG3, may also be a crucial PPCM drug target. Disruption of the BAG3-sHsp-Hsp70 complex has previously been shown to be associated with DCM and non-inflammatory MFM (141–143). The specific roles of BAG3 in PPCM pathophysiology are however yet to be validated. BAG3 mutations have however been proposed to be associated with PPCM. Thus, enhancing BAG3 expression in PPCM patients may possibly offer cardioprotection by augmenting cardiomyocyte proteostasis. As such, it may therefore be generally hypothesised that these co-chaperones may act as decisive players in Hsp-modulated proteostasis within the cardiomyocyte and may thus act as PPCM drug targets.

Hsp90 also serves as an attractive candidate for novel PPCM drug interventions given that it is predicted to modulate the PPCM pathogenesis pathway (**Figure 5B**) via its interaction with AKT and NFKB1 (**Figure 6**). It is well-established that Hsp90 plays important functions in regulating client proteins into their active conformations. As such, Hsp90 possibly activates AKT triggering a cascade of events that leads to PPCM. Furthermore, Hsp90 is predicted to interact with NFKB which is associated with cardiac inflammation in PPCM. Hsp90 thus likely plays decisive

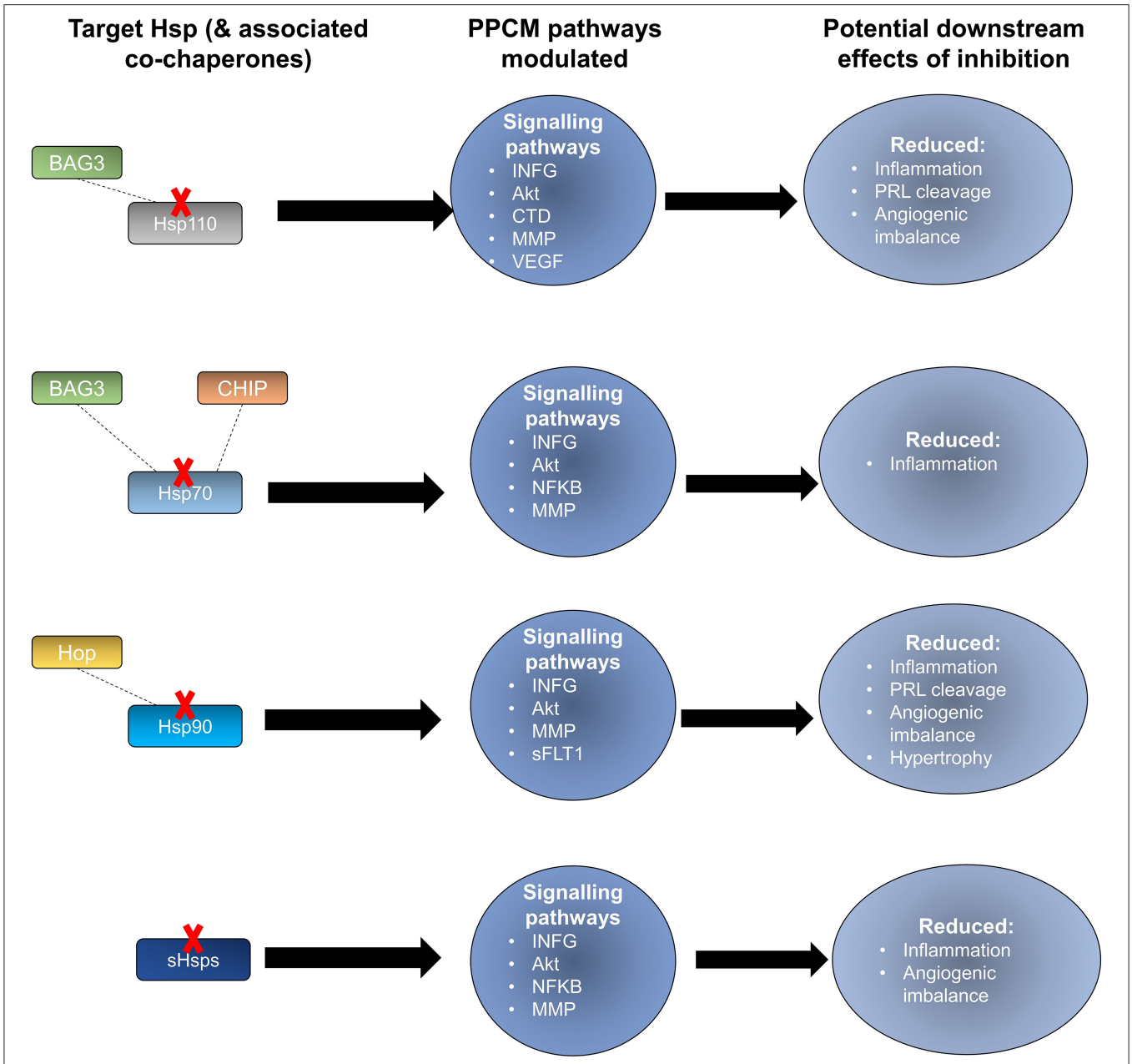

FIGURE 6 | Potential effects of Hsp-directed inhibition in PPCM therapy. Targeting the Hsp types sHsp, Hsp110, Hsp90, and Hsp70 has the potential to disrupt key signalling pathways that are important in PPCM pathophysiology.

roles in PPCM pathophysiology via AKT and NFKB signalling. Consequently, Hsp90-inhibiting directed therapies may prove beneficial in novel PPCM therapies. To date, several classes of Hsp90-targeting small molecule inhibitors have been proposed for disrupting Hsp90 chaperone function. The majority of these compete with ATP for binding onto the N-terminal domain (NTD) ultimately keeping the chaperone in an inhibitor-bound conformation that abrogates its function (144). Currently, the following natural and synthetic Hsp90-targeting drugs, such as ansamycin and derivatives of purine, resorcinol, benzamide, and tricyclic imidapyridines have been described in several disease models such as cancer [reviewed in (145)]. However, the potential of Hsp90-targeting drugs in PPCM is yet to be explored.

Hsps AS CANDIDATE PPCM BIOMARKERS

Despite the importance of early diagnosis for full cardiac recovery in PPCM patients, physicians are often faced with the difficulty of distinguishing between peripartum discomfort in healthy women and the pathological PPCM symptoms. PPCM diagnosis thus relies on a high index of suspicion. A thorough history

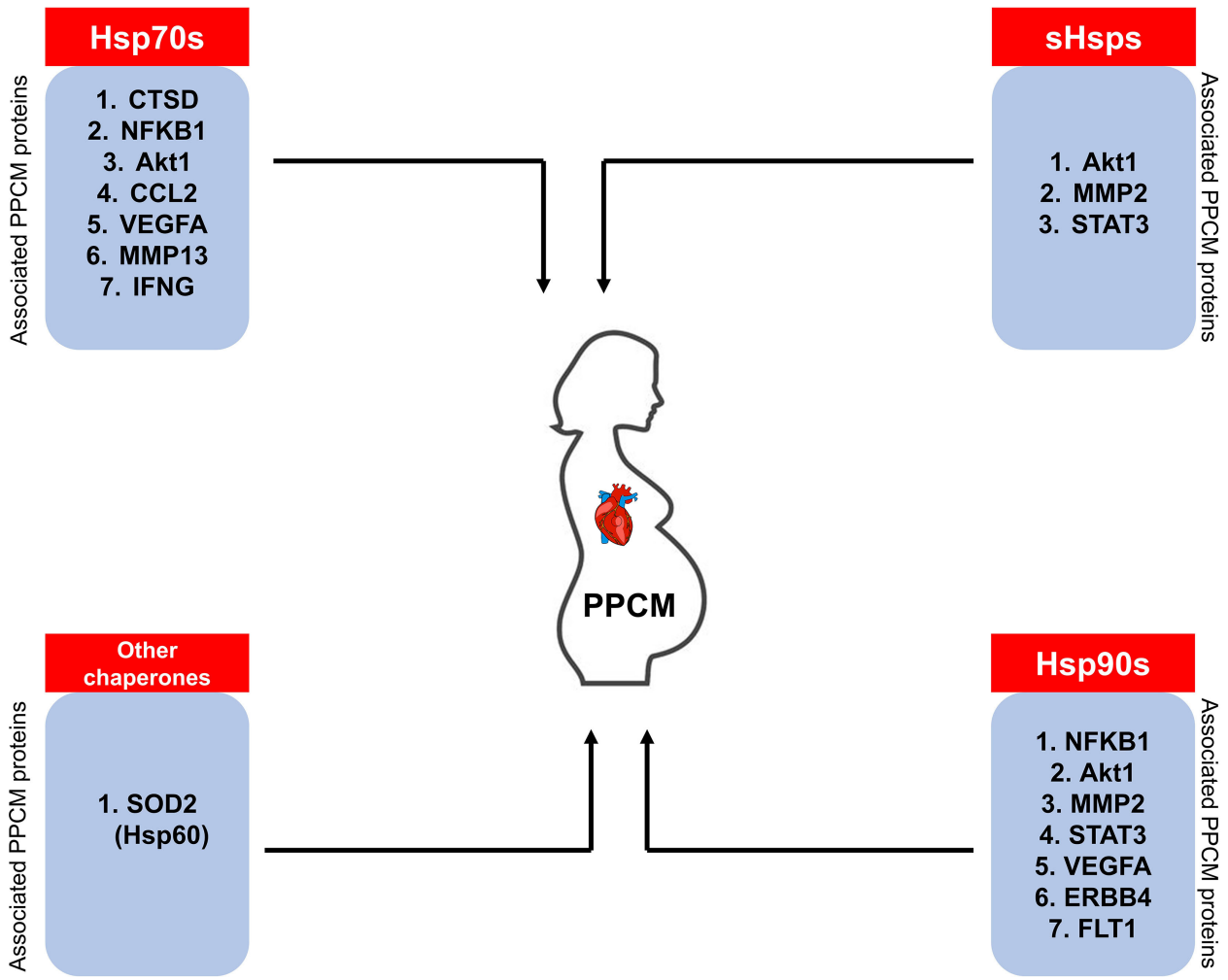

FIGURE 7 | Hsps as potential PPCM biomarkers. The Hsps (sHsps, Hsp60, Hsp70, Hsp90) predicted to associate with PPCM pathogenesis proteins may be used as candidate biomarkers.

of the onset of symptoms combined with a comprehensive echocardiography report confirming <45% LVEF are important diagnostic determinants. Currently, the only clinically confirmed PPCM biomarker is the brain natriuretic peptide NT (proBNP) which is however not specific for PPCM diagnosis (12, 146). Since Hsps are triggered by stress, we hypothesise that Hsp expression is upregulated to allow the chaperones to form functional partnerships with markers of inflammation in PPCM patients. It is important to monitor Hsp expression levels through the progression of PPCM as this presents a basis for the potential use of Hsps as biomarkers. Indeed, STRING analysis predicts the interaction of Hsp70, Hsp90, sHsps, and Hsp60 with several PPCM pathophysiology proteins (**Figure 7**). The prospects of Hsps as PPCM biomarkers either individually or in a panel with the already established proBNP marker is promising.

At present, some Hsps have been proposed as biomarkers in cardiovascular disease. A study by Giannessi and colleagues (37) demonstrated that circulating Hsp60 and HspA1A levels correlate with LV dysfunction severity. Interestingly, the same study also established that HspA1A protein levels are significantly correlated with BNP levels. Hsp70 and Hsp60 activation and inflammation markers, such as IL6 are also correlated with the extent of cardiac and microvascular dysfunction in patients with angiographically normal coronary arteries (37). Hsps have also been reported to mediate coronary endothelial dysfunction and produce microvascular damage in response to metabolic or infective insults (147). The potential of Hsp60 as a potential diagnostic or prognostic marker of heart disease has also been investigated. Veres et al. (148) noted the increased risk of heart disease when Hsp60 expression is upregulated. Also, elevated Hsp60 concentrations are positively associated with the severity of coronary arterial disease and ischemic heart disease in a dose-dependent fashion (149). Hsp70 levels were found to be significantly higher in HF and myocardial infarction, potentially implicating the protein's role as a CVD biomarker (150, 151). To date, not many proteomics-based studies have been conducted to assess the expression levels of stress proteins in PPCM. Nonetheless, the exacerbated

stress associated with PPCM may trigger a unique chaperone response which may be studied toward biomarker design. Therefore, it may also be necessary to validate the role of other Hsp families such as the Hsp110 and Hsp40 members to determine their specific roles in PPCM. Recently, Hsp110 family members have been demonstrated to play important roles in cancers (152, 153). As such, the differential expression of Hsps in PPCM patients may lay a foundation toward novel biomarker identification.

Hsp70 may serve as an important diagnostic or prognostic biomarker of PPCM since Hsp70 expression levels are correlated with traditional injury markers such as AST, ALT, γGT and bilirubin in HF patients (154). Furthermore, a study by Baba et al. (155) predicted that worse outcomes correlate with increased Hsp70 levels after heart transplantation. Although similar studies have not yet been applied to PPCM at present, they are worth exploring. Given that there are 13 different Hsp70 isoforms which are subtly distinguished from each other by unique signature motifs, the Hsp70 family members are promising PPCM biomarkers. sHSPs have also been proposed as biomarkers of congestive HF. It has been demonstrated that Hsp20, Hsp27, and Hsp32 expression correlates to disease (156). The Hsp70 co-chaperone, BAG3 is also an attractive potential PPCM biomarker. Increased BAG3 levels were observed in sera of patients with end stage HF, purporting that BAG3 is released by cardiomyocytes as a stress response (157–159). As such, BAG3 may be a useful biomarker to monitor HF progression. The aggravated stress conditions associated with PPCM potentially trigger upregulated Hsp-expression to maintain proteostasis and alleviate the effects of cardiotoxicity. We therefore hypothesise an Hsp expression profile that is unique from other forms of cardiomyopathy toward the identification of novel PPCM biomarkers of diagnosis or prognosis. Indeed, while in HF several studies have focused on the potential role of Hsp60 and Hsp70, there is need to investigate the role of co-chaperones and other Hsps (e.g., Hsp40 and Hsp110) as PPCM biomarkers.

CONCLUSION

The involvement of Hsps in protein quality control systems has been reported in several cardiovascular disorders such as ischaemic heart disease and HF. Given the exaggerated cardiac stress associated with pregnancy, Hsps likely play crucial roles in PPCM pathophysiology. Here, we predicted associations between proteins involved in PPCM pathogenesis and sHsp, Hsp70 as well as Hsp90. Furthermore, Hsps and their respective co-chaperones hold promise as novel candidate PPCM biomarkers. However, fundamental research is needed in this regard to experimentally validate the utility of Hsps as PPCM biomarkers. These associations could also pave the way for the development of novel Hsp-targeted therapeutic PPCM drug interventions.

AUTHOR CONTRIBUTIONS

GC, TS, and SK wrote the draft, the original idea was conceived by GC and KS. Critical feedback was provided by TZ, AS, NN, and KS. All authors contributed to the article and approved the submitted version.

FUNDING

GC is a recipient of the UCT Faculty of Health Sciences, URC grant. TS acknowledges funding received from the South African Medical Research Council. NN gratefully acknowledges support from the South African Medical Research Council, the NRF and the Lily and Ernst Hausmann Trust.

REFERENCES

1. Willis MS, Schisler JC, Portbury AL, Patterson C. Build it up-Tear it down: protein quality control in the cardiac sarcomere. *Cardiovasc Res.* (2009) 81:439–48. doi: 10.1093/cvr/cvn289
2. Ranek MJ, Stachowski MJ, Kirk JA, Willis MS. The role of heat shock proteins and co-chaperones in heart failure. *Philos Trans R Soc Lond B Biol Sci.* (2018) 373:20160530. doi: 10.1098/rstb.2016.0530
3. McLendon PM, Robbins J. Proteotoxicity and cardiac dysfunction. *Circ Res.* (2015) 116:1863–82. doi: 10.1161/CIRCRESAHA.116.305372
4. Bennett PM, Ehler E, Wilson AJ. Sarcoplasmic reticulum is an intermediary of mitochondrial and myofibrillar growth at the intercalated disc. *J Muscle Res Cell Motil.* (2016) 37:55–69. doi: 10.1007/s10974-016-9444-6
5. Bauersachs J, Konig T, van der Meer P, Petrie MC, Hilfiker-Kleiner D, Mbakwem A, et al. Pathophysiology, diagnosis and management of peripartum cardiomyopathy: a position statement from the Heart Failure Association of the European Society of Cardiology Study Group on peripartum cardiomyopathy. *Eur J Heart Fail.* (2019) 21:827–43. doi: 10.1002/ejhf.1493
6. Sliwa K, Hilfiker-Kleiner D, Petrie MC, Mebazaa A, Pieske B, Buchmann E, et al. Current state of knowledge on aetiology, diagnosis, management, and therapy of peripartum cardiomyopathy: a position statement from the Heart Failure Association of the European Society of Cardiology Working Group on peripartum cardiomyopathy. *Eur J Heart Fail.* (2010) 12:767–78. doi: 10.1093/eurjhf/hfq120
7. Arany Z. Understanding peripartum cardiomyopathy. *Annu Rev Med.* (2018) 69:165–76. doi: 10.1146/annurev-med-041316-090545
8. Shaikh N. An obstetric emergency called peripartum cardiomyopathy! *J Emerg Trauma Shock.* (2010) 3:39–42. doi: 10.4103/0974-2700.break58664
9. Ersbøll AS, Johansen M, Damm P, Rasmussen S, Vejlstrup NG, Gustafsson F. Peripartum cardiomyopathy in Denmark: a retrospective, population-based study of incidence, management and outcome. *Eur J Heart Fail.* (2017) 19:1712–20. doi: 10.1002/ejhf.882
10. Karaye KM, Ishaq NA, Sa'idu H, Balarabe SA, Talle MA, Isa MS, et al. Incidence, clinical characteristics, and risk factors of peripartum cardiomyopathy in Nigeria: results from the PEACE Registry. *ESC Heart Fail.* (2020) 7:235–43. doi: 10.1002/ehf2.12562
11. Kolte D, Khera S, Aronow WS, Palaniswamy C, Mujib M, Ahn C, et al. Temporal trends in incidence and outcomes of peripartum cardiomyopathy in the United States: a nationwide population-based study. *J Am Heart Assoc.* (2014) 3:e001056. doi: 10.1161/JAHA.114.001056
12. Azibani F, Sliwa K. Peripartum cardiomyopathy: an update. *Curr Heart Fail Rep.* (2018) 15:297–306. doi: 10.1007/s11897-018-0404-x
13. Hilfiker-Kleiner D, Kaminski K, Podewski E, Bonda T, Schaefer A, Sliwa K, et al. A cathepsin D-cleaved 16 kDa form of prolactin mediates postpartum cardiomyopathy. *Cell.* (2007) 128:589–600. doi: 10.1016/j.cell.2006.12.036

14. Zhu R-R, Chen Q, Liu Z-B, Ruan H-G, Wu Q-C, Zhou X-L. Inhibition of the Notch1 pathway induces peripartum cardiomyopathy. *J Cell Mol Med.* (2020) 24:7907–14. doi: 10.1111/jcmm.15423
15. Ricke-Hoch M, Bultmann I, Stapel B, Condorelli G, Rinas U, Sliwa K, et al. Opposing roles of Akt and STAT3 in the protection of the maternal heart from peripartum stress. *Cardiovasc Res.* (2014) 101:587–96. doi: 10.1093/cvr/cvu010
16. Fischer C, Mazzone M, Jonckx B, Carmeliet P. FLT1 and its ligands VEGFB and PlGF: drug targets for anti-angiogenic therapy? *Nat Rev Cancer.* (2008) 8:924–56. doi: 10.1038/nrc2524
17. Patten IS, Rana S, Shahul S, Rowe GC, Jang C, Liu L, et al. Cardiac angiogenic imbalance leads to peripartum cardiomyopathy. *Nature.* (2012) 485:333–8. doi: 10.1038/nature11040
18. Maynard SE, Min JY, Merchan J, Lim KH, Li J, Mondal S, et al. Excess placental soluble fms-like tyrosine kinase 1 (sFlt1) may contribute to endothelial dysfunction, hypertension, and proteinuria in preeclampsia. *J Clin Invest.* (2003) 111:649–58. doi: 10.1172/JCI17189
19. Damp J, Givertz MM, Semigran M, Alharethi R, Ewald G, Felker GM, et al. Relaxin-2 and soluble Flt1 levels in peripartum cardiomyopathy: results of the multicenter IPAC study. *JACC Heart Fail.* (2016) 4:380–8. doi: 10.1016/j.jchf.2016.01.004
20. Ntusi NBA, Badri M, Gumedze F, Sliwa K, Mayosi BM. Pregnancy-associated heart failure: a comparison of clinical presentation and outcome between hypertensive heart failure of pregnancy and idiopathic peripartum cardiomyopathy. *PLoS ONE.* (2015) 10:e0133466. doi: 10.1371/journal.pone.0133466
21. Barasa A, Rosengren A, Sandström TZ, Ladfors L, Schaufelberger M. Heart failure in late pregnancy and postpartum: incidence and long-term mortality in Sweden from 1997 to 2010. *J Card Fail.* (2017) 23:370–8. doi: 10.1016/j.cardfail.2016.12.011
22. Faupel-Badger JM, McElrath TF, Lauria M, Houghton LC, Lim KH, Parry S, et al. Maternal circulating angiogenic factors in twin and singleton pregnancies. *Am J Obstet Gynecol.* (2015) 212:636.e1-8. doi: 10.1016/j.ajog.2014.11.035
23. Hall ME, George EM, Granger JP. The heart during pregnancy. *Rev Esp Cardiol.* (2011) 64:1045–50. doi: 10.1016/j.rec.2011.07.008
24. Kara RJ, Bolli P, Karakikes I, Matsunaga I, Tripodi J, Tanweer O, et al. Fetal cells traffic to injured maternal myocardium and undergo cardiac differentiation. *Circ Res.* (2012) 110:82–93. doi: 10.1161/CIRCRESAHA.111.249037
25. Boddy AM, Fortunato A, Wilson Sayres M, Aktipis A. Fetal microchimerism and maternal health: a review and evolutionary analysis of cooperation and conflict beyond the womb. *Bioessays.* (2015) 37:1106–18. doi: 10.1002/bies.201500059
26. Kodogo V, Azibani F, Sliwa K. Role of pregnancy hormones and hormonal interaction on the maternal cardiovascular system: a literature review. *Clin Res Cardiol.* (2019) 108:831–46. doi: 10.1007/s00392-019-01441-x
27. Halkein J, Tabruyn SP, Ricke-Hoch M, Haghikia A, Nguyen NQ, Scherr M, et al. MicroRNA-146a is a therapeutic target and biomarker for peripartum cardiomyopathy. *J Clin Invest.* (2013) 123:2143–54. doi: 10.1172/JCI64365
28. Bajou K, Herkenne S, Thijssen VL, D'Amico S, Nguyen NQ, Bouché A, et al. PAI-1 mediates the antiangiogenic and profibrolytic effects of 16K prolactin. *Nat Med.* (2014) 2014:741–7. doi: 10.1038/nm.3552
29. Basaiawmoit RV, Rattan SI. Cellular stress and protein misfolding during aging. *Methods Mol Biol.* (2010) 648:107–17. doi: 10.1007/978-1-60761-756-3_7
30. Lindquist S. The heat-shock response. *Ann Rev Biochem.* (1986) 55:1151–91. doi: 10.1146/annurev.bi.55.070186.005443
31. Mattoo RU, Sharma SK, Priya S, Finka A, Goloubinoff P. Hsp110 is a bona fide chaperone using ATP to unfold stable misfolded polypeptides and reciprocally collaborate with Hsp70 to solubilize protein aggregates. *J Biol Chem.* (2013) 288:21399–411. doi: 10.1074/jbc.M113.479253
32. Glover JR, Lindquist S. Hsp104, Hsp70, and Hsp40: a novel chaperone system that rescues previously aggregated proteins. *Cell.* (1998) 94:73–82. doi: 10.1016/S0092-8674(00)81223-4
33. Zhao Y, Wang W, Qian L. Hsp70 may protect cardiomyocytes from stress-induced injury by inhibiting Fas-mediated apoptosis. *Cell Stress Chaperones.* (2007) 12:83–95. doi: 10.1379/CSC-231R.1
34. Datta R, Bansal T, Rana S, Datta K, Chaudhuri RD, Chawla-Sarkar M, et al. Myocyte-derived Hsp90 modulates collagen upregulation via biphasic activation of STAT-3 in fibroblasts during cardiac hypertrophy. *Mol Biol Cell.* (2017) 37:e00611–16. doi: 10.1128/MCB.00611-16
35. Biasucci LM, Liuzzo G, Ciervo A, Petrucca A, Piro M, Angiolillo DJ, et al. Antibody response to chlamydial heat shock protein 60 is strongly associated with acute coronary syndromes. *Circulation.* (2003) 107:3015–7. doi: 10.1161/01.CIR.0000078632.76653.6C
36. Li Q, Shi M, Li B. Anandamide enhances expression of heat shock protein 72 to protect against ischemia-reperfusion injury in rat heart. *J Physiol Sci.* (2013) 63:47–53. doi: 10.1007/s12576-012-0228-5
37. Giannessi D, Colotti C, Maltinti M, Del Ry S, Prontera C, Turchi S, et al. Circulating heat shock proteins and inflammatory markers in patients with idiopathic left ventricular dysfunction: their relationships with myocardial and microvascular impairment. *Cell Stress Chaperones.* (2007) 12:265–74. doi: 10.1379/CSC-272.1
38. Dybdahl B, Slørdahl SA, Waage A, Kierulf P, Espevik T, Sundan A. Myocardial ischaemia and the inflammatory response: release of heat shock protein 70 after myocardial infarction. *Heart.* (2005) 91:299–304. doi: 10.1136/hrt.2003.028092
39. Kanwar JR, Shen WP, Kanwar RK, Berg RW, Krissansen GW. Effects of survivin antagonists on growth of established tumors and B7-1 immunogene therapy. *J Natl Cancer Inst.* (2001) 93:1541–52. doi: 10.1093/jnci/93.20.1541
40. Xu Q, Schett G, Perschinka H, Mayr M, Egger G, Oberhollenzer F, et al. Serum soluble heat shock protein 60 is elevated in subjects with atherosclerosis in a general population. *Circulation.* (2000) 102:14–20. doi: 10.1161/01.CIR.102.1.14
41. Hayashi M, Imanaka-Yoshida K, Yoshida T, Wood M, Fearns C, Tatake RJ, et al. A crucial role of mitochondrial Hsp40 in preventing dilated cardiomyopathy. *Nat Med.* (2006) 12:128–32. doi: 10.1038/nm1327
42. Zhu Y, Ma T, Wang X. Gene transfer of heat-shock protein 20 protects against ischemia/reperfusion injury in rat hearts. *Acta Pharmacol Sin.* (2005) 26:1193–200. doi: 10.1111/j.1745-7254.2005.00139.x
43. Krishnamurthy K, Vedam K, Kanagasabai R, Druhan LJ, Ilangovan G. Heat shock factor-1 knockout induces multidrug resistance gene, MDR1b, and enhances P-glycoprotein (ABCB1)-based drug extrusion in the heart. *Proc Natl Acad Sci USA.* (2012) 109:9023–8. doi: 10.1073/pnas.1200731109
44. Zügel U, Kaufmann SH. Role of heat shock proteins in protection from and pathogenesis of infectious diseases. *Clin Microbiol Rev.* (1999) 12:19–39. doi: 10.1128/CMR.12.1.19
45. Zininga T, Makumire S, Gitau GW, Njunge JM, Pooe OJ, Klimek H, et al. Plasmodium falciparum Hop (PfHop) interacts with the Hsp70 chaperone in a nucleotide-dependent fashion and exhibits ligand selectivity. *PLoS ONE.* (2015) 10:e0135326. doi: 10.1371/journal.pone.0135326
46. Marinko JT, Huang H, Penn WD, Capra JA, Schlebach JP, Sanders CR. Folding and misfolding of human membrane proteins in health and disease: from single molecules to cellular proteostasis. *Chem Rev.* (2019) 119:5537–606. doi: 10.1021/acs.chemrev.8b00532
47. Welch WJ. How cells respond to stress. *Sci Am.* (1993) 268:56–64. doi: 10.1038/scientificamerican0593-56
48. Calloni G, Chen T, Schermann SM, Chang HC, Genevaux P, Agostini F, et al. DnaK functions as a central hub in the *E. coli* chaperone network. *Cell Rep.* (2012) 1:251–64. doi: 10.1016/j.celrep.2011.12.007
49. Szabo A, Langer T, Schröder H, Flanagan J, Bukau B, Hartl FU. The ATP hydrolysis-dependent reaction cycle of the *Escherichia coli* Hsp70 system DnaK, DnaJ, and GrpE. *Proc Natl Acad Sci USA.* (1994) 91:10345–9. doi: 10.1073/pnas.91.22.10345
50. Rosenzweig R, Sekhar A, Nagesh J, Kay LE. Promiscuous binding by Hsp70 results in conformational heterogeneity and fuzzy chaperone-substrate ensembles. *Elife.* (2017) 6:e28030. doi: 10.7554/eLife.28030.025
51. Goloubinoff P, De Los Rios P. The mechanism of Hsp70 chaperones: (entropic) pulling the models together. *Trends Biochem Sci.* (2007) 32:372–80. doi: 10.1016/j.tibs.2007.06.008
52. Kampinga HH, Craig EA. The HSP70 chaperone machinery: J proteins as drivers of functional specificity. *Nat Rev Mol Cell Biol.* (2010) 11:579–92. doi: 10.1038/nrm2941

53. Shiber A, Ravid T. Chaperoning proteins for destruction: diverse roles of Hsp70 chaperones and their co-chaperones in targeting misfolded proteins to the proteasome. *Biomolecules.* (2014) 4:704–24. doi: 10.3390/biom4030704
54. Alderson TR, Kim JH, Markley JL. Dynamical structures of Hsp70 and Hsp70-Hsp40 complexes. *Structure.* (2016) 24:1014–30. doi: 10.1016/j.str.2016.05.011
55. Genest O, Reidy M, Street TO, Hoskins JR, Camberg JL, Agard DA, et al. Uncovering a region of heat shock protein 90 important for client binding in *E. coli* and chaperone function in yeast. *Mol Cell.* (2013) 49:464–73. doi: 10.1016/j.molcel.2012.11.017
56. Zwirowski S, Kłosowska A, Obuchowski I, Nillegoda NB, Piróg A, Zietkiewicz S, et al. Hsp70 displaces small heat shock proteins from aggregates to initiate protein refolding. *EMBO J.* (2017) 36:783–96. doi: 10.15252/embj.201593378
57. Rosenzweig R, Nillegoda NB, Mayer MP, Bukau B. The Hsp70 chaperone network. *Nat Rev Mol Cell Biol.* (2019) 20:665–80. doi: 10.1038/s41580-019-0133-3
58. Bercovich B, Stancovski I, Mayer A, Blumenfeld N, Laszlo A, Schwartz AL, et al. Ubiquitin-dependent degradation of certain protein substrates in vitro requires the molecular chaperone Hsc70. *J Biol Chem.* (1997) 272:9002–10. doi: 10.1074/jbc.272.14.9002
59. Kriegenburg F, Ellgaard L, Hartmann-Petersen R. Molecular chaperones in targeting misfolded proteins for ubiquitin-dependent degradation. *FEBS J.* (2012) 279:532–42. doi: 10.1111/j.1742-4658.2011.08456.x
60. McLellan AJ, Frydman J. Molecular chaperones and the art of recognizing a lost cause. *Nat Cell Biol.* (2001) 3:E51–3. doi: 10.1038/35055162
61. Schisler JC, Rubel CE, Zhang C, Lockyer P, Cyr DM, Patterson C. CHIP protects against cardiac pressure overload through regulation of AMPK. *J Clin Invest.* (2013) 123:3588–99. doi: 10.1172/JCI69080
62. Willis MS, Min JN, Wang S, McDonough H, Lockyer P, Wadosky KM, et al. Carboxyl terminus of Hsp70-interacting protein (CHIP) is required to modulate cardiac hypertrophy and attenuate autophagy during exercise. *Cell Biochem Funct.* (2013) 31:724–35. doi: 10.1002/cbf.2962
63. McMullen JR, Izumo S. Role of the insulin-like growth factor 1 (IGF1)/phosphoinositide-3-kinase (PI3K) pathway mediating physiological cardiac hypertrophy. *Novartis Found Symp.* (2006) 274:90–111. doi: 10.1002/0470029331.ch7
64. Homma S, Iwasaki M, Shelton GD, Engvall E, Reed JC, Takayama S. BAG3 deficiency results in fulminant myopathy and early lethality. *Am J Pathol.* (2006) 169:761–73. doi: 10.2353/ajpath.2006.060250
65. Fuchs M, Poirier DJ, Seguin SJ, Lambert H, Carra S, Charette SJ, et al. Identification of the key structural motifs involved in HspB8/HspB6-Bag3 interaction. *Biochem J.* (2009) 425:245–55. doi: 10.1042/BJ20090907
66. Rauch JN, Tse E, Freilich R, Mok S-A, Makley LN, Southworth DR, et al. BAG3 is a modular, scaffolding protein that physically links heat shock protein 70 (Hsp70) to the small heat shock proteins. *J Mol Biol.* (2017) 429:128–41. doi: 10.1016/j.jmb.2016.11.013
67. Giffard RG, Macario AJL, de Macario EC. The future of molecular chaperones and beyond. *J Clin Invest.* (2013) 123:3206–8. doi: 10.1172/JCI70799
68. Mymrikov EV, Daake M, Richter B, Haslbeck M, Buchner J. The chaperone activity and substrate spectrum of human small heat shock proteins. *J Biol Chem.* (2017) 292:672–84. doi: 10.1074/jbc.M116.760413
69. Moalic JM, Bauters C, Himbert D, Bercovici J, Mouas C, Guicheney P, et al. Phenylephrine, vasopressin and angiotensin II as determinants of proto-oncogene and heat-shock protein gene expression in adult rat heart and aorta. *J Hypertens.* (1989) 7:195–201. doi: 10.1097/00004872-198903000-00005
70. Kukreja RC, Kontos MC, Loesser KE, Batra SK, Qian YZ, Gbur CJJ, et al. Oxidant stress increases heat shock protein 70 mRNA in isolated perfused rat heart. *Am J Physiol.* (1994) 267:H2213–9. doi: 10.1152/ajpheart.1994.267.6.H2213
71. Marber MS, Latchman DS, Walker JM, Yellon DM. Cardiac stress protein elevation 24 hours after brief ischemia or heat stress is associated with resistance to myocardial infarction. *Circulation.* (1993) 88:1264–72. doi: 10.1161/01.CIR.88.3.1264
72. Shinohara T, Takahashi N, Ooie T, Ichinose M, Hara M, Yonemochi H, et al. Estrogen inhibits hyperthermia-induced expression of heat-shock protein 72 and cardioprotection against ischemia/reperfusion injury in female rat heart. *J Mol Cell Cardiol.* (2004) 37:1053–61. doi: 10.1016/j.yjmcc.2004.09.006
73. Qian YZ, Bernardo NL, Nayeem MA, Chelliah J, Kukreja RC. Induction of 72-kDa heat shock protein does not produce second window of ischemic preconditioning in rat heart. *Am J Physiol.* (1999) 276:H224–34. doi: 10.1152/ajpheart.1999.276.1.H224
74. Wei J, Tong J, Yu L, Zhang J. EMF protects cardiomyocytes against hypoxia-induced injury via heat shock protein 70 activation. *Chem Biol Interact.* (2016) 248:8–17. doi: 10.1016/j.cbi.2016.02.003
75. Tarone G, Brancaccio M. Keep your heart in shape: molecular chaperone networks for treating heart disease. *Cardiovasc Res.* (2014) 102:346–61. doi: 10.1093/cvr/cvu049
76. Ficker E, Dennis AT, Wang L, Brown AM. Role of the cytosolic chaperones Hsp70 and Hsp90 in maturation of the cardiac potassium channel HERG. *Circ Res.* (2003) 92:e87–100. doi: 10.1161/01.RES.0000079028.31393.15
77. Young JC, Moarefi I, Hartl FU. Hsp90: a specialized but essential protein-folding tool. *J Cell Biol.* (2001) 154:267–73. doi: 10.1083/jcb.200104079
78. Kakihara Y, Houry WA. The R2TP complex: discovery and functions. *Biochim Biophys Acta.* (2012) 1823:101–7. doi: 10.1016/j.bbamcr.2011.08.016
79. Scheufler C, Brinker A, Bourenkov G, Pegoraro S, Moroder L, Bartunik H, et al. Structure of TPR domain-peptide complexes: critical elements in the assembly of the Hsp70-Hsp90 multichaperone machine. *Cell.* (2000) 101:199–210. doi: 10.1016/S0092-8674(00)80830-2
80. Schmid AB, Lagleder S, Gräwert MA, Röhl A, Hagn F, Wandinger SK, et al. The architecture of functional modules in the Hsp90 co-chaperone Sti1/Hop. *EMBO J.* (2012) 31:1506–17. doi: 10.1038/emboj.2011.472
81. Pratt WB, Morishima Y, Osawa Y. The Hsp90 chaperone machinery regulates signaling by modulating ligand binding clefts. *J Biol Chem.* (2008) 283:22885–9. doi: 10.1074/jbc.R800023200
82. Taipale M, Krykbaeva I, Koeva M, Kayatekin C, Westover KD, Karras GI, et al. Quantitative analysis of HSP90-client interactions reveals principles of substrate recognition. *Cell.* (2012) 150:987–1001. doi: 10.1016/j.cell.2012.06.047
83. Gamerdinger M, Hajieva P, Kaya AM, Wolfrum U, Hartl FU, Behl C. Protein quality control during aging involves recruitment of the macroautophagy pathway by BAG3. *EMBO J.* (2009) 28:899–901. doi: 10.1038/emboj.2009.29
84. Wang W, Peng Y, Wang Y, Zhao X, Yuan Z. Anti-apoptotic effect of heat shock protein 90 on hypoxia-mediated cardiomyocyte damage is mediated via the phosphatidylinositol 3-kinase/AKT pathway. *Clin Exp Pharmacol Physiol.* (2009) 36:899–903. doi: 10.1111/j.1440-1681.2009.05167.x
85. Negro A, Brar BK, Lee K-F. Essential roles of Her2/erbB2 in cardiac development and function. *Recent Prog Horm Res.* (2004) 59:1–12. doi: 10.1210/rp.59.1.1
86. Shimizu I, Minamino T. Physiological and pathological cardiac hypertrophy. *J Mol Cell Cardiol.* (2016) 97:245–62. doi: 10.1016/j.yjmcc.2016.06.001
87. Choi DW, Lim MS, Lee JW, Chun W, Lee SH, Nam YH, et al. The cytotoxicity of kahweol in HT-29 human colorectal cancer cells is mediated by apoptosis and suppression of Heat Shock Protein 70 expression. *Biomol Ther.* (2015) 23:128–33. doi: 10.4062/biomolther.2014.133
88. Fu Y, Wey S, Wang M, Ye R, Liao C-P, Roy-Burman P, et al. Pten null prostate tumorigenesis and AKT activation are blocked by targeted knockout of ER chaperone GRP78/BiP in prostate epithelium. *Proc Natl Acad Sci USA.* (2008) 105:19444–9. doi: 10.1073/pnas.0807691105
89. Guo W, Yan L, Yang L, Liu X, E Q, Gao P, et al. Targeting GRP75 improves HSP90 inhibitor efficacy by enhancing p53-mediated apoptosis in hepatocellular carcinoma. *PLoS ONE.* (2014) 9:e85766. doi: 10.1371/journal.pone.0085766
90. Yung HW, Charnock-Jones DS, Burton GJ. Regulation of AKT phosphorylation at Ser473 and Thr308 by endoplasmic reticulum stress modulates substrate specificity in a severity dependent manner. *PLoS ONE.* (2011) 6:e17894. doi: 10.1371/journal.pone.0017894
91. Barati MT, Rane MJ, Klein JB, McLeish KR. A proteomic screen identified stress-induced chaperone proteins as targets of Akt phosphorylation in mesangial cells. *J Proteome Res.* (2006) 5:1636–46. doi: 10.1021/pr0502469
92. Gray MJ, Mhawech-Fauceglia P, Yoo E, Yang W, Wu E, Lee AS, et al. AKT inhibition mitigates GRP78 (glucose-regulated protein) expression and contribution to chemoresistance in endometrial cancers. *Int J Cancer.* (2013) 133:21–30. doi: 10.1002/ijc.27994

93. Wang X, Bi X, Zhang G, Deng Y, Luo X, Xu L, et al. Glucose-regulated protein 78 is essential for cardiac myocyte survival. *Cell Death Differ.* (2018) 25:2181–94. doi: 10.1038/s41418-018-0109-4
94. Bi X, Zhang G, Wang X, Nguyen C, May HI, Li X, et al. Endoplasmic reticulum chaperone GRP78 protects heart from ischemia/reperfusion injury through Akt activation. *Circ Res.* (2018) 122:1545–54. doi: 10.1161/CIRCRESAHA.117.312641
95. Petrovski G, Das S, Juhasz B, Kertesz A, Tosaki A, Das DK. Cardioprotection by endoplasmic reticulum stress-induced autophagy. *Antioxid Redox Signal.* (2011) 14:2191–200. doi: 10.1089/ars.2010.3486
96. Blackwood EA, Thuerauf DJ, Stastna M, Stephens H, Sand Z, Pentoney A, et al. Proteomic analysis of the cardiac myocyte secretome reveals extracellular protective functions for the ER stress response. *J Mol Cell Cardiol.* (2020) 143:132–44. doi: 10.1016/j.yjmcc.2020.04.012
97. Basso AD, Solit DB, Chiosis G, Giri B, Tsichlis P, Rosen N. Akt forms an intracellular complex with heat shock protein 90 (Hsp90) and Cdc37 and is destabilized by inhibitors of Hsp90 function. *J Biol Chem.* (2002) 277:39858–66. doi: 10.1074/jbc.M206322200
98. Sato S, Fujita N, Tsuruo T. Modulation of Akt kinase activity by binding to Hsp90. *Proc Natl Acad Sci USA.* (2000) 97:10832–7. doi: 10.1073/pnas.170276797
99. Rane MJ, Pan Y, Singh S, Powell DW, Wu R, Cummins T, et al. Heat shock protein 27 controls apoptosis by regulating Akt activation. *J Biol Chem.* (2003) 278:27828–35. doi: 10.1074/jbc.M303417200
100. Wu R, Kausar H, Johnson P, Montoya-Durango DE, Merchant M, Rane MJ. Hsp27 regulates Akt activation and polymorphonuclear leukocyte apoptosis by scaffolding MK2 to Akt signal complex. *J Biol Chem.* (2007) 282:21598–608. doi: 10.1074/jbc.M611316200
101. Liu L, Zhang X, Jiang S, Ding Z, Ding G, Huang J, et al. Heat shock protein 27 regulates oxidative stress-induced apoptosis in cardiomyocytes: mechanisms via reactive oxygen species generation and Akt activation. *Chin Med J.* (2007) 120:2271–7. doi: 10.1097/00029330-200712020-00023
102. You W, Min X, Zhang X, Qian B, Pang S, Ding Z, et al. Cardiac-specific expression of heat shock protein 27 attenuated endotoxin-induced cardiac dysfunction and mortality in mice through a PI3K/Akt-dependent mechanism. *Shock.* (2009) 32:108–17. doi: 10.1097/SHK.0b013e318199165d
103. Penna C, Brancaccio M, Tullio F, Rubinetto C, Perrelli M-G, Angotti C, et al. Overexpression of the muscle-specific protein, melusin, protects from cardiac ischemia/reperfusion injury. *Basic Res Cardiol.* (2014) 109:418. doi: 10.1007/s00395-014-0418-9
104. Ke X, Chen J, Peng L, Zhang W, Yang Y, Liao X, et al. Heat shock protein 90/Akt pathway participates in the cardioprotective effect of exogenous hydrogen sulfide against high glucose-induced injury to H9c2 cells. *Int J Mol Med.* (2017) 39:1001–10. doi: 10.3892/ijmm.2017.2891
105. Zhang X-H, Wu J-X, Sha J-Z, Yang B, Sun J-R, Bao E-D. Heat shock protein 90 relieves heat stress damage of myocardial cells by regulating Akt and PKM2 signaling in vivo. *Int J Mol Med.* (2020) 45:1888–908. doi: 10.3892/ijmm.2020.4560
106. Jego G, Hermetet F, Girodon F, Garrido C. Chaperoning STAT3/5 by heat shock proteins: interest of their targeting in cancer therapy. *Cancers.* (2019) 12:21. doi: 10.3390/cancers12010021
107. Sanderson S, Valenti M, Gowan S, Patterson L, Ahmad Z, Workman P, et al. Benzoquinone ansamycin heat shock protein 90 inhibitors modulate multiple functions required for tumor angiogenesis. *Mol Cancer Ther.* (2006) 5:522–32. doi: 10.1158/1535-7163.MCT-05-0439
108. Kishor A, Tandukar B, Ly YV, Toth EA, Suarez Y, Brewer G, et al. Hsp70 is a novel posttranscriptional regulator of gene expression that binds and stabilizes selected mRNAs containing AU-rich elements. *Mol Cell Biol.* (2013) 33:71–84. doi: 10.1128/MCB.01275-12
109. Morales A, Painter T, Li R, Siegfried JD, Li D, Norton N, et al. Rare variant mutations in pregnancy-associated or peripartum cardiomyopathy. *Circulation.* (2010) 121:2176–82. doi: 10.1161/CIRCULATIONAHA.109.931220
110. van Spaendonck-Zwarts KY, Posafalvi A, van den Berg MP, Hilfiker-Kleiner D, Bollen IA, Sliwa K, et al. Titin gene mutations are common in families with both peripartum cardiomyopathy and dilated cardiomyopathy. *Eur Heart J.* (2014) 35:2165–73. doi: 10.1093/eurheartj/ehu050
111. Ware JS, Li J, Mazaika E, Yasso CM, DeSouza T, Cappola TP, et al. Shared genetic predisposition in peripartum and dilated cardiomyopathies. *N Engl J Med.* (2016) 374:233–41. doi: 10.1056/NEJMoa1505517
112. Jarosz DF, Taipale M, Lindquist S. Protein homeostasis and the phenotypic manifestation of genetic diversity: principles and mechanisms. *Annu Rev Genet.* (2010) 44:189–216. doi: 10.1146/annurev.genet.40.110405.090412
113. Zabinsky RA, Mason GA, Queitsch C, Jarosz DF. It's not magic - Hsp90 and its effects on genetic and epigenetic variation. *Semin Cell Dev Biol.* (2019) 88:21–35. doi: 10.1016/j.semcdb.2018.05.015
114. Karras GI, Yi S, Sahni N, Fischer M, Xie J, Vidal M, et al. HSP90 shapes the consequences of human genetic variation. *Cell.* (2017) 168:856–66. doi: 10.1016/j.cell.2017.01.023
115. Dorsch LM, Schuldt M, dos Remedios CG, Schinkel AFL, de Jong PL, Michels M, et al. Protein quality control activation and microtubule remodeling in hypertrophic cardiomyopathy. *Cells.* (2019) 8:741. doi: 10.3390/cells8070741
116. Schlossarek S, Frey N, Carrier L. Ubiquitin-proteasome system and hereditary cardiomyopathies. *J Mol Cell Cardiol.* (2014) 71:25–31. doi: 10.1016/j.yjmcc.2013.12.016
117. Moller DV, Andersen PS, Hedley P, Ersboll MK, Bundgaard H, Moolman-Smook J, et al. The role of sarcomere gene mutations in patients with idiopathic dilated cardiomyopathy. *Eur J Hum Genet.* (2009) 17:1241–9. doi: 10.1038/ejhg.2009.34
118. Glazier AA, Hafeez N, Mellacheruvu D, Basrur V, Nesvizhskii AI, Lee LM, et al. HSC70 is a chaperone for wild-type and mutant cardiac myosin binding protein C. *JCI Insight.* (2018) 3:e99319. doi: 10.1172/jci.insight.99319
119. Parbhudayal RY, Garra AR, Götte MJW, Michels M, Pei J, Harakalova M, et al. Variable cardiac myosin binding protein-C expression in the myofilaments due to MYBPC3 mutations in hypertrophic cardiomyopathy. *J Mol Cell Cardiol.* (2018) 123:59–63. doi: 10.1016/j.yjmcc.2018.08.023
120. Tharp CA, Haywood ME, Sbaizero O, Taylor MRG, Mestroni L. The giant protein Titin's role in cardiomyopathy: genetic, transcriptional, and post-translational modifications of TTN and their contribution to cardiac disease. *Front Physiol.* (2019) 10:1436. doi: 10.3389/fphys.2019.01436
121. Zininga T, Ramatsui L, Shonhai A. Heat shock proteins as immunomodulants. *Molecules.* (2018) 23:2846. doi: 10.3390/molecules23112846
122. Qiu Y, Ye X, Hanson PJ, Zhang HM, Zong J, Cho B, et al. Hsp70-1: upregulation via selective phosphorylation of heat shock factor 1 during coxsackieviral infection and promotion of viral replication via the AU-rich element. *Cell Mol Life Sci.* (2016) 73:1067–84. doi: 10.1007/s00018-015-2036-6
123. Wang Y, Zhao S, Chen Y, Wang T, Dong C, Wo X, et al. The capsid protein VP1 of Coxsackievirus B induces cell cycle arrest by up-regulating Heat shock protein 70. *Front Microbiol.* (2019) 10:1633. doi: 10.3389/fmicb.2019.01633
124. Mathur S, Walley KR, Wang Y, Indrambarya T, Boyd JH. Extracellular heat shock protein 70 induces cardiomyocyte inflammation and contractile dysfunction via TLR2. *Circ J.* (2011) 75:2445–52. doi: 10.1253/circj.CJ-11-0194
125. Sanzen Y, Ito M, Ohta Y, Yoshida Y, Kawada T, Sato H, et al. Functional proteomic analysis of experimental autoimmune myocarditis-induced chronic heart failure in the rat. *Biol Pharm Bull.* (2010) 33:477–86. doi: 10.1248/bpb.33.477
126. Satoh M, Shimoda Y, Akatsu T, Ishikawa Y, Minami Y, Nakamura M. Elevated circulating levels of heat shock protein 70 are related to systemic inflammatory reaction through monocyte Toll signal in patients with heart failure after acute myocardial infarction. *Eur J Heart Fail.* (2006) 8:810–5. doi: 10.1016/j.ejheart.2006.03.004
127. Unsöld B, Kaul A, Sbroggiò M, Schubert C, Regitz-Zagrosek V, Brancaccio M, et al. Melusin protects from cardiac rupture and improves functional remodelling after myocardial infarction. *Cardiovasc Res.* (2014) 101:97–107. doi: 10.1093/cvr/cvt235
128. Wang DX, Huang Z, Li QJ, Zhong GQ, He Y, Huang WQ, et al. Involvement of HSP90 in ischemic postconditioning-induced cardioprotection by inhibition of the complement system, JNK and inflammation. *Acta Cir Bras.* (2020) 35:e202000105. doi: 10.1590/s0102-865020200010000005

129. Zhang XY, Huang Z, Li QJ, Zhong GQ, Meng JJ, Wang DX, et al. Role of HSP90 in suppressing TLR4-mediated inflammation in ischemic postconditioning. *Clin Hemorheol Microcirc.* (2020) 76:51–62. doi: 10.3233/CH-200840
130. Wang Y, Liu J, Kong Q, Cheng H, Tu F, Yu P, et al. Cardiomyocyte-specific deficiency of HSPB1 worsens cardiac dysfunction by activating NFκB-mediated leucocyte recruitment after myocardial infarction. *Cardiovasc Res.* (2019) 115:154–67. doi: 10.1093/cvr/cvy163
131. Li Y, Si R, Feng Y, Chen HH, Zou L, Wang E, et al. Myocardial ischemia activates an injurious innate immune signaling via cardiac heat shock protein 60 and toll-like receptor 4. *J Biol Chem.* (2011) 286:31308–19. doi: 10.1074/jbc.M111.246124
132. Tian J, Guo X, Liu XM, Liu L, Weng QF, Dong SJ, et al. Extracellular HSP60 induces inflammation through activating and up-regulating TLRs in cardiomyocytes. *Cardiovasc Res.* (2013) 98:391–401. doi: 10.1093/cvr/cvt047
133. Arany Z, Elkayam U. Peripartum cardiomyopathy. *Circulation.* (2016) 133:1397–409. doi: 10.1161/CIRCULATIONAHA.115.020491
134. Sliwa K, Blauwet L, Tibazarwa K, Libhaber E, Smedema JP, Becker A, et al. Evaluation of bromocriptine in the treatment of acute severe peripartum cardiomyopathy: a proof-of-concept pilot study. *Circulation.* (2010) 121:1465–73. doi: 10.1161/CIRCULATIONAHA.109.901496
135. Hilfiker-Kleiner D, Haghikia A, Berliner D, Vogel-Claussen J, Schwab J, Franke A, et al. Bromocriptine for the treatment of peripartum cardiomyopathy: a multicentre randomised study. *Eur Heart J.* (2017) 38:2671–9. doi: 10.1093/eurheartj/ehx35
136. Zininga T, Shonhai A. Are heat shock proteins druggable candidates? *Am J Biochem Biotechnol.* (2004) 10:209–10. doi: 10.3844/ajbbsp.2014.208.210
137. Chang CL, Hsu YT, Wu CC, Yang YC, Wang C, Wu T-C, et al. Immune mechanism of the antitumor effects generated by bortezomib. *J Immunol.* (2012) 189:3209–20. doi: 10.4049/jimmunol.1103826
138. Liu P, Bao HY, Jin CC, Zhou JC, Hua F, Li K, et al. Targeting extracellular heat shock protein 70 ameliorates doxorubicin-induced heart failure through resolution of Toll-like receptor 2-mediated myocardial inflammation. *J Am Heart Assoc.* (2019) 8:e012338. doi: 10.1161/JAHA.119.012338
139. Zininga T, Pooe OJ, Makhado PB, Ramatsui L, Prinsloo E, Achilonu I, et al. Polymyxin B inhibits the chaperone activity of *Plasmodium falciparum* Hsp70. *Cell Stress Chaperones.* (2017) 22:707–15. doi: 10.1007/s12192-017-0797-6
140. McMullen JR, Shioi T, Huang WY, Zhang L, Tarnavski O, Bisping E, et al. The insulin-like growth factor 1 receptor induces physiological heart growth via the phosphoinositide 3-kinase(p110alpha) pathway. *J Biol Chem.* (2004) 279:4782–93. doi: 10.1074/jbc.M310405200
141. Bova MP, Yaron O, Huang Q, Ding L, Haley DA, Stewart PL, et al. Mutation R120G in alphaB-crystallin, which is linked to a desmin-related myopathy, results in an irregular structure and defective chaperone-like function. *Proc Natl Acad Sci USA.* (1999) 96:6137–42. doi: 10.1073/pnas.96.11.6137
142. Fang X, Bogomolovas J, Wu T, Zhang W, Liu C, Veevers J, et al. Loss-of-function mutations in co-chaperone BAG3 destabilize small HSPs and cause cardiomyopathy. *J Clin Invest.* (2017) 127:3189–200. doi: 10.1172/JCI94310
143. Selcen D, Engel AG. Myofibrillar myopathy caused by novel dominant negative alpha B-crystallin mutations. *Ann Neurol.* (2003) 54:804–10. doi: 10.1002/ana.10767
144. Jhaveri K, Ochiana SO, Dunphy MP, Gerecitano JF, Corben AD, Peter RI, et al. Heat shock protein 90 inhibitors in the treatment of cancer: current status and future directions. *Exp Opin Investig Drugs.* (2014) 23:611–28. doi: 10.1517/13543784.2014.902442
145. Zininga T, Shonhai A. Small molecule inhibitors targeting the heat shock protein system of human obligate protozoan parasites. *Int J Mol Sci.* (2019) 20:5930. doi: 10.3390/ijms20235930
146. Ricke-Hoch M, Hoes MF, Pfeffer TJ, Schlothauer S, Nonhoff J, Haidari S, et al. In peripartum cardiomyopathy plasminogen activator inhibitor-1 is a potential new biomarker with controversial roles. *Cardiovasc Res.* (2019) 116:1875–86. doi: 10.1093/cvr/cvz300
147. Kühl U, Pauschinger M, Noutsias M, Seeberg B, Bock T, Lassner D, et al. High prevalence of viral genomes and multiple viral infections in the myocardium of adults with "idiopathic" left ventricular dysfunction. *Circulation.* (2005) 111:887–93. doi: 10.1161/01.CIR.0000155616.07901.35
148. Veres A, Füst G, Smieja M, McQueen M, Horváth A, Yi Q, et al. Relationship of anti-60 kDa heat shock protein and anti-cholesterol antibodies to cardiovascular events. *Circulation.* (2002) 106:2775–80. doi: 10.1161/01.CIR.0000038890.39298.8D
149. Zhang X, He M, Cheng L, Chen Y, Zhou L, Zeng H, et al. Elevated heat shock protein 60 levels are associated with higher risk of coronary heart disease in Chinese. *Circulation.* (2008) 118:2687–93. doi: 10.1161/CIRCULATIONAHA.108.781856
150. Genth-Zotz S, Bolger AP, Kalra PR, von Haehling S, Doehner W, Coats AJ, et al. Heat shock protein 70 in patients with chronic heart failure: relation to disease severity and survival. *Int J Cardiol.* (2004) 96:397–401. doi: 10.1016/j.ijcard.2003.08.008
151. Comini L, Gaia G, Curello S, Ceconi C, Pasini E, Benigno M, et al. Right heart failure chronically stimulates heat shock protein 72 in heart and liver but not in other tissues. *Cardiovasc Res.* (1996) 31:882–90. doi: 10.1016/S0008-6363(96)00039-9
152. Berthenet K, Bokhari A, Lagrange A, Marcion G, Boudesco C, Causse S, et al. HSP110 promotes colorectal cancer growth through STAT3 activation. *Oncogene.* (2017) 36:2328–36. doi: 10.1038/onc.2016.403
153. Gozzi GJ, Gonzalez D, Boudesco C, Dias AMM, Gotthard G, Uyanik B, et al. Selecting the first chemical molecule inhibitor of HSP110 for colorectal cancer therapy. *Cell Death Differ.* (2020) 27:117–29. doi: 10.1038/s41418-019-0343-4
154. Gombos T, Förhécz Z, Pozsonyi Z, Jánoskuti L, Prohászka Z. Interaction of serum 70-kDa heat shock protein levels and HspA1B (+1267) gene polymorphism with disease severity in patients with chronic heart failure. *Cell Stress Chaperones.* (2008) 13:199–206. doi: 10.1007/s12192-007-0001-5
155. Baba HA, Schmid KW, Schmid C, Blasius S, Heinecke A, Kerber S, et al. Possible relationship between heat shock protein 70, cardiac hemodynamics, and survival in the early period after heart transplantation. *Transplantation.* (1998) 65:799–804. doi: 10.1097/00007890-199803270-00006
156. Dohke T, Wada A, Isono T, Fujii M, Yamamoto T, Tsutamoto T, et al. Proteomic analysis reveals significant alternations of cardiac small heat shock protein expression in congestive heart failure. *J Card Fail.* (2006) 12:77–84. doi: 10.1016/j.cardfail.2005.07.006
157. De Marco M, D'Auria R, Rosati A, Vitulano G, Gigantino A, Citro R, et al. BAG3 protein in advanced-stage heart failure. *JACC Heart Fail.* (2014) 2:673–5. doi: 10.1016/j.jchf.2014.05.012
158. De Marco M, Falco A, Basile A, Rosati A, Festa M, d'Avenia M, et al. Detection of soluble BAG3 and anti-BAG3 antibodies in patients with chronic heart failure. *Cell Death Dis.* (2013) 4:e495. doi: 10.1038/cddis.2013.8
159. Feldman AM, Begay RL, Knezevic T, Myers VD, Slavov D, Zhu W, et al. Decreased levels of BAG3 in a family with a rare variant and in idiopathic dilated cardiomyopathy. *J Cell Physiol.* (2014) 299:1697–702. doi: 10.1002/jcp.24615

Conflict of Interest: The authors declare that the research was conducted in the absence of any commercial or financial relationships that could be construed as a potential conflict of interest.

Copyright © 2021 Chakafana, Spracklen, Kamuli, Zininga, Shonhai, Ntusi and Sliwa. This is an open-access article distributed under the terms of the Creative Commons Attribution License (CC BY). The use, distribution or reproduction in other forums is permitted, provided the original author(s) and the copyright owner(s) are credited and that the original publication in this journal is cited, in accordance with accepted academic practice. No use, distribution or reproduction is permitted which does not comply with these terms.

frontiers in Cardiovascular Medicine

ORIGINAL RESEARCH
published: 08 July 2021
doi: 10.3389/fcvm.2021.630231

Cross-Sectional Survey of Clinical Trials of Stem Cell Therapy for Heart Disease Registered at ClinicalTrials.gov

Rong Yang[1], Yonggang Zhang[2], Xiaoyang Liao[1]*, Ru Guo[1], Yi Yao[1], Chuanying Huang[1] and Li Qi[1]*

[1] Department of International Medical Center/Ward of General Practice, West China Hospital, Sichuan University, Chengdu, China, [2] Department of Periodical Press and National Clinical Research Center for Geriatrics, West China Hospital, Sichuan University, Chengdu, China

OPEN ACCESS

Edited by:
Ying Mei Zhang,
Fudan University, China

Reviewed by:
Suowen Xu,
University of Science and Technology of China, China
Jun Ren,
University of Washington, United States

***Correspondence:**
Yonggang Zhang
jebm_zhang@yahoo.com
Xiaoyang Liao
liaoxiaoyang@wchscu.cn

Specialty section:
This article was submitted to Cardiovascular Therapeutics, a section of the journal Frontiers in Cardiovascular Medicine

Received: 17 November 2020
Accepted: 27 May 2021
Published: 08 July 2021

Citation:
Yang R, Zhang Y, Liao X, Guo R, Yao Y, Huang C and Qi L (2021) Cross-Sectional Survey of Clinical Trials of Stem Cell Therapy for Heart Disease Registered at ClinicalTrials.gov. Front. Cardiovasc. Med. 8:630231. doi: 10.3389/fcvm.2021.630231

Objective: It is important to register clinical trials before their implementation. There is a lack of study to evaluate registered clinical trials of stem cell therapy for heart diseases. Our study used the registration information at ClinicalTrials.gov to provide an overview of the registered trials investigating stem cell therapy for heart diseases.

Methods: We searched ClinicalTrials.gov from inception to October 1, 2020 to identify clinical trials evaluating stem cell therapy for heart diseases. These trials were included in a cross-sectional survey and descriptive analysis. The outcomes included start date, completion date, location, status, study results, funding, phase, study design, conditions, interventions, sex, age, and sample size of those trials, as well as conditions, efficacy, safety and samples of the publications. SPSS 24.0 software was used for the statistical analysis.

Results: A total of 241 trials were included. The registration applications for most trials originated from the United States, and the research start date ranged from 2001 to 2025. More than half of the trials have been completed, but few trials have published results (15.62%). The funding source for 81.12% of trials was recorded as "other" because the specific funding source was not indicated. There were 226 (93.78%) interventional studies and 15 (6.22%) observational studies; among all 241 studies, only 2.90% were phase 4 trials. Most interventional studies used randomized allocation, parallel assignment, and blinding. Of the observational studies, 6 were cohort studies (40.00%) and 73.33% were prospective. The most common disease was coronary artery disease (57.68%) and 98.34% included both male and female participants. The sample size included fewer than 50 patients in 58.51% of trials, and only 18 trials (7.47%) lasted more than 121 months. The registered details were illogical for nine trials (3.8%) that included 0 subjects and two trials (0.8%) that had a duration of 0 months (0.8%). In term of publications of the trials, most of the publications of the trials showed efficacy and safety in stem cell therapy for heart disease.

Conclusion: The clinical trials investigating stem cell therapy for heart diseases registered at ClinicalTrials.gov are mostly interventional studies, and only a few are phase 4 trials. Most trials have a small sample size, and few have a duration of more than 121 months. Most of the completed trials did not publish their results, and some of the registration information was incomplete and illogical.

Keywords: stem cell, heart disease, therapy, cross-sectional survey, ClinicalTrials.gov

INTRODUCTION

Under United States federal law, the National Institutes of Health has been required since 1997 to create public resources providing information about clinical trials regulated by the United States Food and Drug Administration[1]. Clinical trial registration and result publication have multiple benefits. For individuals, this information can help patients understand their condition and the latest treatment plan and progress; for the general public, knowledge about clinical trials can eliminate unnecessary anxiety and better promote population health; for researchers and institutions, this information can reduce unnecessary repeated trials, reduce the risk of bias, and increase the reliability of trial results (1). Therefore, it is important for the progress and results of clinical trials to be announced in a timely and truthful manner.

Cardiomyocytes are terminally differentiated cells that cannot differentiate to repair and remodel the damaged heart (2, 3). In contrast, stem cells have immortal self-renewal ability and can produce at least one type of highly differentiated progeny cell (3). Therefore, stem cell therapy shows potential in damage repair and cure of refractory diseases, such as spinal cord injury (4), nerve pain (5), and immune regulation (6). Stem cell therapy is also a promising treatment for heart diseases. Stem cell therapy effectively improves cardiac ejection fraction and reverse remodeling in heart failure (7), improves the survival rate, exercise capacity, and performance of patients with non-ischemic cardiomyopathy (8), and reduces the onset of refractory angina (9). However, the Efficacy and safety of stem cell therapy for heart diseases are unclarified, with potential risks of tumorigenicity, immunogenicity, and arrhythmia (10). Rigorously designed clinical trials are needed to prove the Efficacy of stem cell therapy in treating heart diseases and improve technology to reduce the related risks. Clinical trial registration is an important step in making these clinical trials open and transparent, reducing redundant research, and identifying future research directions (11). Therefore, we analyzed the characteristics of trials registered at ClinicalTrials.gov that investigated stem cell therapy for heart diseases, aiming to provide a comprehensive overview of this topic for individuals, the public, researchers, and institutions.

METHODS

Platform Selection

ClinicalTrials.gov is a clinical trial database founded in 1997 that is jointly operated by the National Library of Medicine and the United States Food and Drug Administration. Up to now, 216 countries from 50 regions around the world have registered trials at ClinicalTrials.gov. As of October 1, 2020, there were 353,838 trials registered at ClinicalTrials.gov. Therefore, the ClinicalTrials.gov database was selected as the source from which data was collected for the present analysis.

Data Extraction

We performed an advanced search of ClinicalTrials.gov. First, we searched the database for trials that included the PubMed MeSH terms "heart disease" and "stem cell," and performed a radiation search by matching each term with "condition or disease" and "intervention/treatment," respectively. We retrieved relevant trials that were registered from database inception to October 1, 2020. For all retrieved trials, we recorded the unique identification code (NCT number), title, start date, completion date, location, status, study results, funding, phase, study design, conditions, interventions, outcome measures, sex, age, sample size, and uniform resource location (URL). Duplicates and irrelevant trials were eliminated. We also excluded trials in which the heart diseases were relieved by the treatment of diseases in other body systems, such as treating pulmonary fibrosis to reduce pulmonary hypertension and treating kidney disease to improve heart function. If there was unclear or missing information, the researchers entered the URL and NCT number into the database to confirm and supplement this information. After that, we searched articles by NCT numbers for analyzing efficacy and safety of stem cell therapy. All abovementioned steps were independently completed by two researchers. Any controversy was resolved by a third researcher.

Statistical Analysis

Data on the location, start date, status, study results, and funding were recorded to provide a basic overview of the registered trials. Research type, allocation, blinding, and other information were used to describe the study design. Conditions, sex, age, sample size, and study duration were used to show specific research content. Finally, conditions, efficacy, safety and samples were recorded to analyze the articles. Categorical variables were described as frequency and percentage, whereas continuous variables were described as the maximum, minimum, median, and average.

RESULTS

The initial search retrieved 7,064 clinical trials. Among them, 4,878 trials were repeated, and 1,945 were not related to the aims

[1] ClinicalTrials.gov (accessed January 1, 2020).

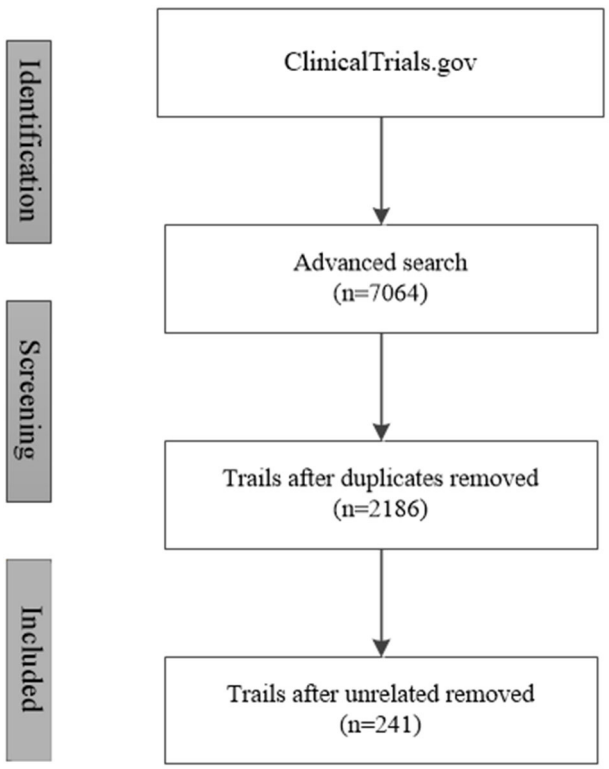

FIGURE 1 | Trial retrieval process.

of the present study. A final total of 241 trials were included (**Figure 1**).

Basic Overview

Location

The 241 included trials were performed in 35 countries. The five most common countries were the United States (67 trials; 27.80%), China (20 trials; 8.30%), Germany (13 trials; 5.39%), Denmark (12 trials; 4.98%), and France (12 trials; 4.98%). Classification in accordance with the continent of origin showed that most trials were conducted in Europe (34.85%) and North America (31.54%), followed by Asia (21.99%), South America (4.15%), and Oceania (0.41%). The location was not stated for 17 trials (7.05%). The distribution of the trial locations is shown in **Table 1**.

TABLE 1 | Location of trials.

	Absolute (n = 241)	Relative (%)
North America	76	31.54%
United States	67	27.80%
Mexico	4	1.66%
Canada	5	2.07%
South America	10	4.15%
Brazil	8	3.32%
Colombia	1	0.41%
Chile	1	0.41%
Asia	53	21.99%
China	20	8.30%
Japan	8	3.32%
Iran	6	2.49%
Korea	5	2.07%
India	4	1.66%
Israel	4	1.66%
Kazakhstan	2	0.83%
Indonesia	2	0.83%
Malaysia	1	0.41%
Singapore	1	0.41%
Europe	84	34.85%
Germany	13	5.39%
Denmark	12	4.98%
France	12	4.98%
Spain	10	4.15%
United Kingdom	6	2.49%
Italy	6	2.49%
Slovenia	5	2.07%
Russian	4	1.66%
Belgium	3	1.24%
Poland	3	1.24%
Greece	2	0.83%
Austria	2	0.83%
Finland	2	0.83%
Ukraine	1	0.41%
Switzerland	1	0.41%
Norway	1	0.41%
Turkey	1	0.41%
Oceania	1	0.41%
Australia	1	0.41%
Unknown	17	7.05%

Start Date

The earliest start date was 2001 and the latest was 2025(not begin), with only one trial started in each of these years. Most trials were started in 2007 (20 trials; 8.30%), followed by 2008 (19 trials; 7.88%), and 2005 and 2013 (each with 18 trials; 7.47%). The distribution of the trial start date is shown in **Table 2**.

Status and Results

The status was "active, not recruiting" for 27 trials (11.20%), "recruiting patients" for 26 (10.79%), "completed" for 101 (41.91%), and "terminated" for 27 (11.20%). Three trials (1.24%) were suspended and 10 (4.15%) were withdrawn; the reasons for trial suspension and withdrawal are listed in **Table 3**. The status of 47 trials (19.50%) was unknown. Among the trials that had been completed or terminated, the results were only available for 20 trials (15.62%).

Funding

Three trials (1.20%) received United States federal funding support, 21 (8.43%) received funding support from the National Institutes of Health, 65 (26.10%) received industrial funding

TABLE 2 | Trial start dates.

Start year	Number of trials (%)
2001	1 (0.41%)
2002	2 (0.83%)
2003	4 (1.66%)
2004	11 (4.56%)
2005	18 (7.47%)
2006	15 (6.22%)
2007	20 (8.30%)
2008	19 (7.88%)
2009	12 (4.98%)
2010	16 (6.64%)
2011	17 (7.05%)
2012	14 (5.81%)
2013	18 (7.47%)
2014	12 (4.98%)
2015	12 (4.98%)
2016	10 (4.15%)
2017	8 (3.32%)
2018	8 (3.32%)
2019	11 (4.56%)
2020	12 (4.98%)
2025	1 (0.41%)

TABLE 3 | Reasons for trial withdrawn.

NCT number	Reasons
NCT02107118	contract issues
NCT01502514	no participants enrolled
NCT01502501	no participants enrolled
NCT00279539	study never started
NCT00346177	funding not obtained and no participants enrolled
NCT00463853	inability to recruit due to administrative difficulties at the site
NCT01458405	unknown
NCT01770613	corporate business decision, may consider different subject population
NCT03272191	company dissolved
NCT01974128	no participants enrolled

support, and 202 (81.12%) received funding from other sources. The funding source was not reported for eight trials (3.21%).

Study Design

Among the 241 included trials, 226 (93.78%) were interventional studies, and 15 (6.22%) were observational studies. Fifty-two trials were phase I clinical trials (21.58%), 64 were phase 2 (26.56%), 18 were phase 3 (7.47%), seven were phase 4 (2.90%), and 49 (20.33%) were phase 1 and phase 2. There were 15 (6.22%) phase 2 and phase 3 trials, and the phase of another 36 trials (14.94%) was not applicable or unknown (**Table 4**).

TABLE 4 | Trial phases.

Phase	Number of trials (%)
Phase 1	52 (21.58%)
Phase 2	64 (26.56%)
Phase 3	18 (7.47%)
Phase 4	7 (2.90%)
Phase 1|Phase 2	49 (20.33%)
Phase 2|Phase 3	15 (6.22%)
Not applicable or unknown	36 (14.94%)

TABLE 5 | Study design of interventional studies.

Study design	Absolute (n = 226)	Relative (%)
Allocation		
Randomized	164	72.57%
Other	61	26.99%
Not applicable	1	0.44%
Blinded		
Single	35	15.49%
Double	32	14.16%
Triple	20	8.85%
Quadruple	40	17.70%
None	98	43.36%
Not applicable or unknown	1	0.44%
Model		
Parallel assignment	147	65.04%
Single group assignment	60	26.55%
Crossover assignment	9	3.98%
Factorial assignment	4	1.77%
Sequential assignment	2	0.88%

Interventional Studies

In the interventional studies, the group allocation was randomized in 164 trials (72.57%), "other" in 61 (26.99%), and not applicable in one (0.4%); 147 trials (65.04%) used parallel assignment, 60 (26.55%) used single-group assignment, nine used crossover assignment, four used factorial assignment, two used sequential assignment, and the assignment in four was not applicable or unknown. A total of 127 interventional trials were blinded (35 were single-blinded, 32 were double-blinded, 20 were triple-blinded, and 40 were quadruple-blinded), 98 were non-blinded, and the blinding in one interventional trial was not applicable or unknown (**Table 5**).

Observational Studies

Among the observational studies, there were six (40.00%) cohort studies, three (20.00%) case-only studies, one (6.67%) case-control study, one (6.67%) family-based study, and two studies (13.33%) classified as "other." Two trials (13.33%) did not provide information on the study design. Eleven observational studies (73.33%) were prospective, one (6.67%) was retrospective, one (6.67%) was cross-sectional, and one (6.67%) was classified as

TABLE 6 | Study design of observational studies.

Study design	Absolute (n = 15)	Relative (%)
Model		
Cohort	6	40.00%
Case-only	3	20.00%
Case-control	1	6.67%
Family-based	1	6.67%
other	2	13.33%
unknown	2	13.33%
Time perspective		
Prospective	11	73.33%
Cross-sectional	1	6.67%
Retrospective	1	6.67%
other	1	6.67%
unknown	2	13.33%

"other"; two trials (13.33%) did not provide this information (**Table 6**).

Specific Research Content

Among the 241 included trials, the most common heart condition was coronary artery disease (139 trials; 57.68%), followed by heart failure (50 trials; 20.75%) and cardiomyopathy (30 trials; 12.45%). Regarding the sex of the participants, most trials (237 trials; 98.34%) included both male and female participants; three trials (1.24%) only included male participants, and one trial did not state the sex of the participants. Most trials included adults and older adults (214 trials; 88.80%); 14 trials only included children, three only included adults, one included children and adults, and nine included children, adults, and older adults.

In terms of the sample size, the median number of registered patients was 40 (range 0–800). The number of enrolled patients was 50 or fewer in 141 trials (58.51%), 50–100 in 51 trials (21.16%), 101–150 in 19 trials (7.88%), 151–200 in 13 trials (5.39%), more than 200 in 14 trials (5.81%), and unknown in three trials.

If the research plan did not report an end-date for the trial, the end-date was set as October 1, 2020. As a result, the research duration ranged from 0 to 218 months; 10 trials ran for 12 months or less, 37 (15.35%) ran for 13–24 months, 37 (15.35%) ran for 25–36 months, 45 (18.67%) ran for 27–48 months, 42 (17.43%) ran for 49–60 months, 51 (21.16%) ran for 61–120 months, 18 (7.47%) ran for more than 121 months, and the duration was recorded as "not applicable" for one trial(**Table 7**).

Publications of Trials

The initial search retrieved 124 publications and finally retained 109 publications from 73 trials, for 13 publications were excluded for protocols, reviews and non-stem cell therapy, and 2 were excluded because of Harvard fraud stem cell investigation (NCT00474461). Among them, trial of NCT00684021 published most articles ($n = 6$), accounting for 5.50%. 68 (63.30%) articles were stem cell therapy for coronary artery disease, followed by heart failure (20 articles, 18.35%), cardiomyopathy (15 articles, 13.76%) and others (5 articles, 4.59%). 92 (84.40%) articles assessed the efficacy of stem cell therapy for heart diseases, in which 74 (67.89%) articles showed effectiveness while 18 (16.51%) showed non- effectiveness. 55 (50.46%) articles assessed the safety of stem cell therapy for heart disease with all of them showed safety. In terms of sample, 37 (33.94%) articles were <50 cases, 31 (28.44%) articles were 50 to 100 cases, 28 (25.69%) were 100–500 cases and 2 (1.83%) were more than 500 cases (**Table 8**).

Furthermore, the articles assessed efficacy and safety in different conditions. In terms of efficacy, 10 (50.00%) articles showed effectiveness in heart failure, 46 (66.67%) showed effectiveness in coronary artery disease and 13 (86.67%) in cardiomyopathy and 5 (100.00%) in others. Fortunately, all

TABLE 7 | Research content.

Characteristics	Absolute (n = 241)	Relative (%)
Conditions		
Heart failure	50	20.75%
Coronary artery disease	139	57.68%
Cardiomyopathy	30	12.45%
Others	22	9.13%
Gender		
All	237	98.34%
Male	3	1.24%
Unknown	1	0.41%
Age group		
Child	14	5.81%
Adult	3	1.24%
Child, adult	1	0.41%
Adult, old adult	214	88.80%
All	9	3.73%
Enrollment (n)		
0–50	141	58.51%
51–100	51	21.16%
101–150	19	7.88%
151–200	13	5.39%
≥200	14	5.81%
Unknown	3	1.24%
Duration (month)		
0–12	10	4.15%
13–24	37	15.35%
25–36	37	15.35%
37–48	45	18.67%
49–60	42	17.43%
61–72	16	6.64%
73–84	20	8.30%
85–96	12	4.98%
97–108	3	1.24%
109–120	0	0.00%
≥121	18	7.47%
Unknown	1	0.41%

TABLE 8 | Publication status of trials.

	Absolute (*n* = 109)	Relative (%)
Conditions		
Heart failure	20	18.35%
Coronary artery disease	69	63.30%
Cardiomyopathy	15	13.76%
Others	5	4.59%
Efficacy		
Yes	74	67.89%
No	18	16.51%
Not assessment	9	8.26%
Not applicable	8	7.34%
Safety		
Yes	55	50.46%
No	0	0.00%
Not assessment	46	42.20%
Not applicable	8	7.34%
Sample		
<50	37	33.94%
50–100	31	28.44%
100–500	28	25.69%
>500	2	1.83%
Not applicable	11	10.09%

TABLE 9 | Efficacy and safety of stem cell therapy for heart disease.

	Heart failure (*n* = 20)	Coronary artery disease (*n* = 69)	Cardiomyopathy (*n* = 15)	Others (*n* = 5)
Efficacy, *n* (%)				
Yes	10 (50.00%)	46 (66.67%)	13 (86.67%)	5 (100.00%)
No	5 (25.00%)	11 (15.94%)	2 (13.33%)	0 (0.00%)
Not assessment	3 (15.00%)	6 (8.70%)	0 (0.00%)	0 (0.00%)
Not applicable	2 (10.00%)	6 (8.70%)	0 (0.00%)	0 (0.00%)
Safety, *n* (%)				
Yes	9 (45.00%)	40 (57.97%)	3 (20.00%)	3 (60.00%)
No	0 (0.00%)	0 (0.00%)	0 (0.00%)	0 (0.00%)
Not assessment	9 (45.00%)	22 (31.88%)	12 (80.00%)	2 (40.00%)
Not applicable	2 (10.00%)	7 (10.14%)	0 (0.00%)	0 (0.00%)

results showed safety of stem cell therapy for heart disease if assessed (**Table 9**).

DISCUSSION

Heart diseases such as coronary artery disease, heart failure, and cardiomyopathy currently cannot be cured in most patients, and the complications of these heart diseases cause a great burden on patients, families, and society (12–14). Stem cell therapy provides hope for curing these heart diseases (15, 16). Because the clinical trial registration platform is a valuable resource for providing research status and tracking, we performed a cross-sectional analysis of the trials registered at ClinicalTrials.gov to comprehensively evaluate the research status of clinical trials investigating stem cell therapy for heart disease. A final total of 241 trials were included. Most trials were carried out in the United States, followed by China, Germany, Denmark, and France; these five countries are all high-ranking countries in terms of gross domestic product (GDP) (17). National GDP is positively correlated with healthcare expenditure, population health status, and life expectancy. Good population health and longer life expectancy also promote the growth of national GDP (18). Most trials were also performed in continents with a high GDP; one-third of clinical trials were conducted in each of Europe and North America. The high proportion of trials from Europe and North America may also reflect the fact that ClinicalTrials.gov is an American database, whereas other platforms are also used (19–21). The most common start date was 2007, followed by 2006–2010, and 2011–2015. Overall, the analysis shows that stem cell therapy for heart disease has attracted an increasing amount of attention in the past 20 years (4).

The present analysis of the status of registered trials evaluating stem cell therapy for heart disease found that 24.9% of trials were suspended, withdrawn, or had an unknown status; this is much higher than the 14.22% (50,301 of 353,838 trials; updated on October 9, 2020) of all trials registered at ClinicalTrials.gov. The main reason for trial withdrawal was failure to enroll patients, as well as company or enterprise decisions. Among the 128 trials that have been completed or terminated, only 20 (15.62%) have published their results on the platform. Although ClinicalTrials.gov requires clinical trials to have clear objectives, maximum transparency, and to publish results as soon as possible within a specified timeframe (22), only a few completed trials evaluating stem cell therapy for heart disease have released the results. This may be because of the relatively short period in which stem cell therapy has been has investigated for heart diseases, and the long duration of some of the related trials. Furthermore, some of the included trials may have also been registered on other platforms and published the results elsewhere. A previous study showed similar results (23).

Previous research has shown that the funding source plays a decisive role in research (24). In the present study, the funding source was listed as "other" for 202 trials (81.12%), and no funding information was listed for eight trials. Insufficient funding sources may also be the reason for the unclear status of a large number of trials and the delay in the release of the results. Therefore, it is necessary to provide more detailed funding sources in clinical trial registration to reduce the production of redundant research (25).

Of the included trials, 226 were interventional studies (93.78%) and 15 (6.22%) were observational studies (6.22%). Most were early clinical trials (phase 1, 2, 3), while only four (2.90%) were phase 4 clinical trials. This is consistent with the current related research publications and the research on stem cell therapy for heart diseases in the past 20 years (26). The current studies are still in the phase of proving the efficacy and safety of stem cell therapy for heart diseases,

providing a basis for future large-scale, long-term studies. The included trials generally had good study designs, with 72.57% of intervention studies using randomized allocation, 65.04% using parallel assignment, and 56.19% using blinding. These designs are conducive to improving study quality and increasing the value of the results (27).

The main heart disease being treated by stem cell therapy was coronary artery disease (57.68%), followed by heart failure (20.75%) and cardiomyopathy (12.45%). This is because animal experiments have found that stem cells can differentiate into cardiomyocytes and coronary blood vessels (28), thereby promoting the recovery of heart structure and function (29). Based on previous animal studies, most of the patients selected for treatment had heart diseases likely to respond to stem cell therapy.

The study population comprised adults and older adults in most clinical trials (88.80%). This may be because of safety considerations, and because coronary heart disease and heart failure mostly occur in middle-aged and older adults (30, 31).

The maximum number of recruited patients was 800, and most trials (58.15%) included 50 or fewer patients. Only 5.81% of trials included more than 200 patients. This shows that there is a lack of large-scale interventional or observational research. Furthermore, some of the registered trials showed enrollment numbers of 0, which is impossible, and three trials did not include patient data. This indicates that the required clinical trial registration information was not provided. There are also problems with incomplete test information and lack of feasibility regarding the registered study duration. For example, the shortest study duration was 0 months, while only 18 trials (7.47%) ran for more than 121 months.

The publications of the trials showed that more article of stem cell therapy for coronary artery disease, which was consistent with the results of trial registered. Moreover, most of them were exploratory, most of the publications reported a conclusion that the stem cell therapy for heart disease was effective and safe. However, the registered details weakened the values of the publications.

This study is a cross-sectional analysis of registered clinical trials investigating stem cell therapy for heart diseases, and it comprehensively demonstrates the current research status of stem cell treatment for heart diseases. The main limitation of this study is that only trials registered at ClinicalTrials.gov were analyzed. Although, we searched the other clinical trials database of China which is a first-level registration agency of the world health organization's international clinical trial registration platform, while there was only 1 registered trial in this field. Another limitation is that subgroup analyses were not performed to determine whether the suspension and withdrawal of trials were dictated by the funding source, and whether the trial duration was related to the research objective and funding source. In addition, the published research results were not compared with the registered trials.

CONCLUSION

This is a cross-sectional study evaluating the registered clinical trials investigating stem cell therapy for heart disease. The clinical trials investigating stem cell therapy for heart diseases registered at ClinicalTrials.gov are mostly interventional studies, with only a few phase 4 trials. Most trials have a small sample size, and few have a duration of more than 121 months. Some registered trials provided incomplete and illogical information, and there were few completed and terminated trials that provided results.

DATA AVAILABILITY STATEMENT

The original contributions presented in the study are included in the article/**Supplementary Material**, further inquiries can be directed to the corresponding author/s.

AUTHOR CONTRIBUTIONS

YZ and XL design the review. RY contributed to manuscript writing, revised, and supervised the project. RG and YY contributed to trials searches and data extraction. CH and LQ contributed to literature searches and to preparing the manuscript draft. All authors approved the manuscript.

FUNDING

This study is supported by the grant of science and technology department of Sichuan province (No. 2020YFSY0014).

ACKNOWLEDGMENTS

We thank Kelly Zammit, from Liwen Bianji, Edanz Editing China (www.liwenbianji.cn/ac), for editing the English text of a draft of this manuscript.

SUPPLEMENTARY MATERIAL

The Supplementary Material for this article can be found online at: https://www.frontiersin.org/articles/10.3389/fcvm.2021.630231/full#supplementary-material

REFERENCES

1. (OD) NOotD. *HHS and NIH take steps to enhance transparency of clinical trial results*. U.S. Department of Health and Human Services (2014). Available online at: https://www.nih.gov/news-events/news-releases/ (accessed November 19, 2014).
2. Bergmann O, Zdunek S, Felker A, Salehpour M, Alkass K, Bernard S, et al. Dynamics of cell generation and turnover in the human heart. *Cell.* (2015) 161:1566–75. doi: 10.1016/j.cell.2015.05.026

3. Xu X, Ren J. Cardiac stem cell regeneration in metabolic syndrome. *Curr Pharm Des.* (2013) 19:4888–92. doi: 10.2174/1381612811319270011
4. Khalid SI, Nunna RS, Maasarani S, Kelly BSR, Sroussi H, Mehta AI, et al. Pharmacologic and cellular therapies in the treatment of traumatic spinal cord injuries: a systematic review. *J Clin Neurosci.* (2020) 79:12–20. doi: 10.1016/j.jocn.2020.07.013
5. Zhang WJ, Zhu JF, Zhu ZM. Transplantation of microencapsulated neural stem cells inhibits neuropathic pain mediated by P2X7 receptor overexpression. *Biochem Biophys Res Commun.* (2020) 533:1219–25. doi: 10.1016/j.bbrc.2020.09.112
6. Chin SP, Mohd-Shahrizal MY, Liyana MZ, Then KY, Cheong SK. High dose of intravenous allogeneic umbilical cord-derived mesenchymal stem cells (CLV-100) infusion displays better immunomodulatory effect among healthy volunteers: a phase 1 clinical study. *Stem Cells Int.* (2020) 2020:8877003. doi: 10.1155/2020/8877003
7. Teerlink JR, Metra M, Filippatos GS, Davison BA, Bartunek J, Terzic A, et al. Benefit of cardiopoietic mesenchymal stem cell therapy on left ventricular remodelling: results from the Congestive Heart Failure Cardiopoietic Regenerative Therapy (CHART-1) study. *Eur J Heart Fail.* (2017) 19:1520–9. doi: 10.1002/ejhf.898
8. Xia L, Zeng L, Pan J, Ding Y. Effects of stem cells on non-ischemic cardiomyopathy: a systematic review and meta-analysis of randomized controlled trials. *Cytotherapy.* (2020) 22:699–711. doi: 10.1016/j.jcyt.2020.06.006
9. Losordo DW, Schatz RA, White CJ, Udelson JE, Veereshwarayya V, Durgin M, et al. Intramyocardial transplantation of autologous CD34+ stem cells for intractable angina: a phase I/IIa double-blind, randomized controlled trial. *Circulation.* (2007) 115:3165–72. doi: 10.1161/CIRCULATIONAHA.106.687376
10. Liew LC, Ho BX, Soh BS. Mending a broken heart: current strategies and limitations of cell-based therapy. *Stem Cell Res Ther.* (2020) 11:138. doi: 10.1186/s13287-020-01648-0
11. Wu T-x, Li Y-p, Yao XJ. Clinical trial registration: to improve the quality of clinical research in China. *Chinese J Evid Based Med.* (2006) 3:153–6.
12. Butler J, Djatche LM, Sawhney B, Chakladar S, Yang L, Brady JE, et al. Clinical and economic burden of chronic heart failure and reduced ejection fraction following a worsening heart failure event. *Adv Ther.* (2020) 37:4015–32. doi: 10.1007/s12325-020-01456-1
13. Ho CY, Day SM, Ashley EA, Michels M, Pereira AC, Jacoby D, et al. Genotype and lifetime burden of disease in hypertrophic cardiomyopathy: insights from the sarcomeric human cardiomyopathy registry (SHaRe). *Circulation.* (2018) 138:1387–98. doi: 10.1161/CIRCULATIONAHA.117.033200
14. Emery C, Torreton E, Briere JB, Evers T, Fagnani F. Economic burden of coronary artery disease or peripheral artery disease in patients at high risk of ischemic events in the French setting: a claims database analysis. *J Med Econ.* (2020) 23:513–20. doi: 10.1080/13696998.2020.1715415
15. Nair N, Gongora E. Stem cell therapy in heart failure: Where do we stand today? *Biochim Biophys Acta Mol Basis Dis.* (2020) 1866:165489. doi: 10.1016/j.bbadis.2019.06.003
16. Tompkins BA, Rieger AC, Florea V, Banerjee MN, Natsumeda M, Nigh ED, et al. Comparison of mesenchymal stem cell efficacy in ischemic versus nonischemic dilated cardiomyopathy. *J Am Heart Assoc.* (2018) 7:e008460. doi: 10.1161/JAHA.117.008460
17. Ge Y, Tang K. Commodity prices and GDP growth. *Int Rev Finan Anal.* (2020) 71:101512. doi: 10.1016/j.irfa.2020.101512
18. Jakovljevic M, Timofeyev Y, Ranabhat CL, Fernandes PO, Teixeira JP, Rancic N, et al. Real GDP growth rates and healthcare spending - comparison between the G7 and the EM7 countries. *Global Health.* (2020) 16:64. doi: 10.1186/s12992-020-00590-3
19. Bhaskar SB. Clinical trial registration: a practical perspective. *Indian J Anaesth.* (2018) 62:10–5. doi: 10.4103/ija.IJA_761_17
20. García-Vello P, Smith E, Elias V, Florez-Pinzon C, Reveiz L. Adherence to clinical trial registration in countries of Latin America and the Caribbean, 2015. *Rev Panam Salud Publica.* (2018) 42:e44. doi: 10.26633/RPSP.2018.44
21. Zhou Q, Chen XY, Yang ZM, Wu YL. The changing landscape of clinical trial and approval processes in China. *Nat Rev Clin Oncol.* (2017) 14:577–83. doi: 10.1038/nrclinonc.2017.10
22. Zarin DA, Tse T, Williams RJ, Carr S. Trial reporting in clinicaltrials.gov—the final rule. *N Engl J Med.* (2016) 375:1998–2004. doi: 10.1056/NEJMsr1611785
23. Chen L, Su Y, Quan L, Zhang Y, Du L. Clinical trials focusing on drug control and prevention of ventilator-associated pneumonia: a comprehensive analysis of trials registered on clinicaltrials.gov. *Front Pharmacol.* (2018) 9:1574. doi: 10.3389/fphar.2018.01574
24. Sertkaya A, Wong HH, Jessup A, Beleche T. Key cost drivers of pharmaceutical clinical trials in the United States. *Clin Trials.* (2016) 13:117–26. doi: 10.1177/1740774515625964
25. Gresham G, Meinert JL, Gresham AG, Meinert CL. Assessment of trends in the design, accrual, and completion of trials registered in clinicaltrials.gov by sponsor type, 2000–2019. *JAMA Netw Open.* (2020) 3:e2014682. doi: 10.1001/jamanetworkopen.2020.14682
26. Sanz-Ruiz R, Fernández-Avilés F. Autologous and allogeneic cardiac stem cell therapy for cardiovascular diseases. *Pharmacol Res.* (2018) 127:92–100. doi: 10.1016/j.phrs.2017.05.024
27. Logullo P, MacCarthy A, Kirtley S, Collins GS. Reporting guideline checklists are not quality evaluation forms: they are guidance for writing. *Health Sci Rep.* (2020) 3:e165. doi: 10.1002/hsr2.165
28. Orlic D, Kajstura J, Chimenti S, Bodine DM, Leri A, Anversa P. Bone marrow stem cells regenerate infarcted myocardium. *Pediatr Transplant.* (2003) 7 (Suppl 3):86–8. doi: 10.1034/j.1399-3046.7.s3.13.x
29. Marvasti TB, Alibhai FJ, Weisel RD, Li RK. CD34(+) Stem cells: promising roles in cardiac repair and regeneration. *Can J Cardiol.* (2019) 35:1311–21. doi: 10.1016/j.cjca.2019.05.037
30. Dharmarajan K, Rich MW. Epidemiology, Pathophysiology, and prognosis of heart failure in older adults. *Heart Fail Clin.* (2017) 13:417–26. doi: 10.1016/j.hfc.2017.02.001
31. Joodi G, Maradey JA, Bogle B, Mirzaei M, Sadaf MI, Pursell I, et al. Coronary artery disease and atherosclerotic risk factors in a population-based study of sudden death. *J Gen Intern Med.* (2020) 35:531–7. doi: 10.1007/s11606-019-05486-6

Conflict of Interest: The authors declare that the research was conducted in the absence of any commercial or financial relationships that could be construed as a potential conflict of interest.

Copyright © 2021 Yang, Zhang, Liao, Guo, Yao, Huang and Qi. This is an open-access article distributed under the terms of the Creative Commons Attribution License (CC BY). The use, distribution or reproduction in other forums is permitted, provided the original author(s) and the copyright owner(s) are credited and that the original publication in this journal is cited, in accordance with accepted academic practice. No use, distribution or reproduction is permitted which does not comply with these terms.

Advantages of publishing in Frontiers

OPEN ACCESS
Articles are free to read for greatest visibility and readership

FAST PUBLICATION
Around 90 days from submission to decision

HIGH QUALITY PEER-REVIEW
Rigorous, collaborative, and constructive peer-review

TRANSPARENT PEER-REVIEW
Editors and reviewers acknowledged by name on published articles

Frontiers
Avenue du Tribunal-Fédéral 34
1005 Lausanne | Switzerland

Visit us: www.frontiersin.org
Contact us: frontiersin.org/about/contact

REPRODUCIBILITY OF RESEARCH
Support open data and methods to enhance research reproducibility

DIGITAL PUBLISHING
Articles designed for optimal readership across devices

FOLLOW US
@frontiersin

IMPACT METRICS
Advanced article metrics track visibility across digital media

EXTENSIVE PROMOTION
Marketing and promotion of impactful research

LOOP RESEARCH NETWORK
Our network increases your article's readership